DEVELOPMENT OF PHOSPHINE LIGANDS FOR EFFICIENT AND CHEMOSELECTIVE PALLADIUM-CATALYSED CROSS-COUPLING REACTIONS

NG SHAN SHAN

PhD

The Hong Kong Polytechnic University

2025

The Hong Kong Polytechnic University

Department of Applied Biology and Chemical Technology

DEVELOPMENT OF PHOSPHINE LIGANDS FOR EFFICIENT AND CHEMOSELECTIVE PALLADIUM-CATALYSED CROSS-COUPLING REACTIONS

Ng Shan Shan

A thesis submitted in partial fulfilment of the requirements for the degree of Doctor of Philosophy

August 2024

Certificate of Originality

I hereby declare that this thesis is my own work and that, to the best of my knowledge and belief, it reproduces no material previously published or written, nor material that has been accepted for the award if any other degree or diploma, except where due acknowledgement has been made in the text.

Ng Shan Shan

Abstract

Design and synthesis of novel phosphine ligands is one of the most enduring and fascinating research areas for chemists. These new designs aim to improve reactions with harsh conditions or achieve challenging goals in transition metal-catalysed reactions. This thesis focuses on the utility of newly synthesised phosphine ligands in Pd-catalysed cross-coupling reactions.

Following a brief introduction to the development of phosphine ligands utilised in palladium catalysis, Chapter 2 discusses the synthesis of sterically hindered biaryls using an indole-amide-based phosphine ligand in Pd-catalysed Suzuki−Miyaura cross-coupling reactions. This method achieves excellent yields in short reaction times, such as 10 minutes, and with extremely low palladium catalyst loadings down to 50 ppm. As these target compounds serve as the fundamental framework for materials science and pharmaceutical agents, this more efficient, milder, and more diverse synthetic route remains alluring.

From Chapter 3 onwards, the thesis explores the unconventional and specific chemoselectivity exhibited by a series of C2-alkylated indole-based phosphine ligands in Pd-catalysed borylation. Polyhalogenated aryl triflates, which have multiple reactive sites, were traditionally believed to follow the reactivity order of C−Br > C−OTf > C−Cl. However, this chapter reports a Pd-catalysed chemoselective borylation reaction with a reactivity order of C−Cl > C−OTf. SelectPhos achieves high reactivity and chemoselectivity through a C−H···Pd interaction involving the methine hydrogen of the C2-alkyl group. This interaction may help stabilise the palladium centre and facilitate the activation of the C−Cl bond. Additionally, the catalyst can perform a one-pot two-step sequence of chemoselective borylation followed by intermolecular Suzuki−Miyaura coupling to synthesise asymmetric biaryls containing triflate moieties, paving the way for the synthesis of complicated terphenyls.

The properties of these ligands form the basis for Chapter 4, where 2-alkylated indole-based phosphine ligands are applied to achieve a reactivity order of C−Br > C−Cl > C−OTf in Suzuki−Miyaura cross-coupling reactions with polyhalogenated aryl triflates. Various bromo(hetero)aryl triflates were successfully coupled with (hetero)arylboronic acids, achieving excellent reactivity and chemoselectivity. This catalyst is active at a remarkably low palladium loading of 0.02 mol%. This system demonstrates a sequential dual functionalisation of bromochloroaryl triflates, laying the groundwork for synthesising triphenyl and its derivatives.

Publications

This thesis partially incorporates and expands upon content from the following co-authored published articles.

1. Gu, C.; Yuen, O. Y.; Ng, S. S.; So, C. M.* Palladium-Catalyzed Chemoselective Amination of Chloro(hetero)aryl Triflates Enabled by Alkyl-Pyrazole-Based Phosphine Ligands. *Adv. Synth. Catal.* **2024**, *366*, 1565−1574, DOI: 10.1002/adsc.202301255.

2. Chen, Z.; Pang, W. H.; Yuen, O. Y.; Ng, S. S.; So, C. M.* Palladium-Catalyzed Chemoselective Phosphorylation of Poly(pseudo)halides: A Route for Organophosphorus Synthesis. *J. Org. Chem.* **2024**, *22*, 16262–16268, DOI: 10.1021/acs.joc.3c02345.

3. Yuen, O. Y.; Ng, S. S.; Pang, W. H.; So, C. M.* Palladium-Catalyzed Chemoselective Suzuki−Miyaura Cross-Coupling Reaction of Poly(pseudo)halogenated Arenes, *J. Organomet. Chem.* **2023**, *1005*, 122983, DOI: 10.1016/j.jorganchem.2023.122983.

4. Miao, W.; Pang, W. H.; Yuen O. Y.; Ng, S. S.; So, C. M.* Palladium-Catalyzed Deuterodehalogenation of Halogenated Aryl Triflates Using Isopropanol-d_8 as the Deuterium Source. *Org. Lett.* **2023**, *25*, 8429−8433, DOI: 10.1021/acs.orglett.3c03281.

5. Ng, S. S.; Pang, W. H.; Yuen, O. Y.; So, C. M.* Recent Advances in the Application of Ligands in Palladium-Catalyzed Chemoselective Coupling Reactions at C−Br, C−OTf, and C−Cl Sites. *Org. Chem. Front.* **2023**, *10*, 4408−4436, DOI: 10.1039/D3QO00640A.

6. Ng, S. S.; Chen, Z.; Yuen, O. Y.; So, C. M.* Palladium-Catalyzed Chemoselective Borylation of (Poly)halogenated Aryl Triflates and Their Application in Consecutive Reactions. *Adv. Synth. Catal.* **2022**, *364*, 1596−1601, DOI: 10.1002/adsc.202200230.

7. Ng, S. S.; Chen, Z.; Yuen, O. Y.; So, C. M.* An Indole-Amide-Based Phosphine Ligand Enabling a General Palladium-Catalyzed Sterically Hindered Suzuki−Miyaura Cross-Coupling Reaction. *Org. Biomol. Chem.* **2022**, *20*, 1373−1378, DOI: 10.1039/D1OB02294F.

8. So, C. M.*; Yuen, O. Y.; Ng, S. S.; Chen, Z. General Chemoselective Suzuki−Miyaura Coupling of Polyhalogenated Aryl Triflates Enabled by an Alkyl-Heteroaryl-Based Phosphine Ligand. *ACS Catal.* **2021**, *11*, 7820−7827, DOI: 10.1021/acscatal.1c02146.

Acknowledgements

I am sincerely grateful to God for accompanying me on this journey over the years, bringing me countless beautiful encounters, and allowing me to arrive here safely — something I could not have imagined a decade ago.

I want to extend my deepest gratitude to my supervisor, Dr. Chau Ming So, for his invaluable guidance and patience over the years. I truly believe that no one else would have granted me the freedom to design and create all the cover art and posters (happy to share them below) while also teaching me so much along the way. Despite his busy schedule, he always took the time to listen to my concerns and provide valuable guidance. I am also deeply grateful to the other members of the research team, especially Dr. On Ying Yuen Bella—without her, the lab might have exploded long ago! In no particular order, I thank Dr. Zicong Chen, Dr. Miao Wang, Ms. Zifang Peng, Mr. Changxue Gu, Mr. Junyu Wu Eddie, Mr. Wai Hang Pang Ernest, and Mr. Chuan Han for their companionship and emotional support in the lab, which allowed me to conduct my research in a joyful atmosphere. I also appreciate the technical and instrumental support provided by the department staff.

I am deeply grateful to Dr. Kwong-chak Cheung, Gary, for welcoming me to this department and for supporting me from the beginning of my undergraduate study until now. My heartfelt thanks go to my dear friends, Ms. Yuen Chui-Ying, Ailsa, Ms. Man Ka Yi, Angela, Ms. Wan Siu Wai, Anna, and Mr. Tang Hok Him, Timothy. Without you all, it would have been impossible to continue working hard while maintaining a healthy balance.

I am also immensely appreciative of the consistent care and support from my closest friends: Ms. Wu Yin Ching, Erin, Ms. Au Yim Man, Niki, Ms. Ng Pui Yu, Yuki, Ms. Ko Wing Sze, Ceci, Ms. Yu Ka Mon, Carmen, Ms. Lam Ying Kwan, Sylvain, Ms. Wong Ho Yi, Holly, Ms. Ho Wan Yin, Shirley, Ms. Tong Wing Ki, Winkie, Ms. Ng Yuen Ling, Venus, Mr. Li An-Che, Zack, and many others. It’s incredible that we have remained connected throughout this amazing journey. You can’t imagine how much love and support I have felt, and it touches me deeply how kind you all have been.

Finally, I want to thank my family for their unwavering support. To my reliable sister, Ms. Ng Lee Lee, and my lovely brother, Mr. Ng Yuk Chuen, thank you for tolerating my quirks and bad temper. I am also thankful to my parents, Mr. Ng Lik Hak and Ms. Ngai Oi Wa, for their consistent challenges to my intelligence—you know your daughter so well.

Published Cover Arts

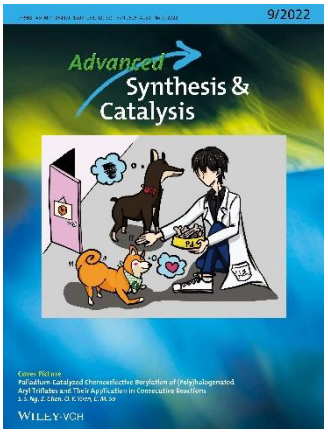

Adv. Synth. Catal. **2022**, *364*, 1507−1620.

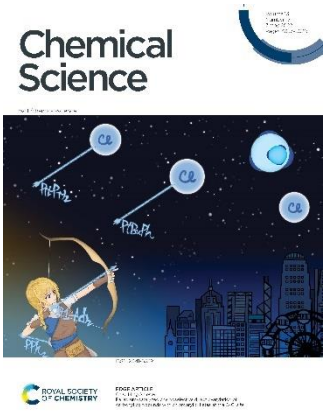

Chem. Sci. **2022**, *13*, 4762−4769.

Chin. J. Chem. **2023**, *41*, 909−914.

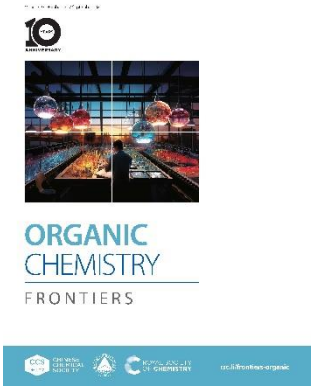

Org. Chem. Front. **2023**, *10*, 4408−4436.

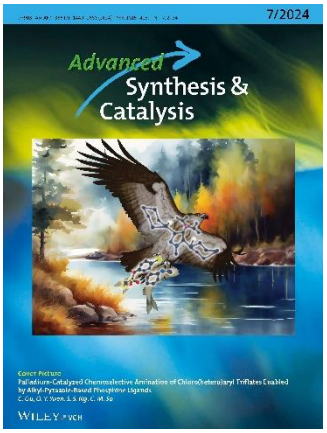

Adv. Synth. Catal. **2024**, *366*, 1449−1668.

Table of Contents

List of Figures

List of Tables

List of Schemes

List of Abbreviations

Abbreviation	Meaning
Ac	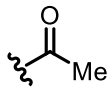 acetyl
acac	acetylacetonate
Ad	adamantyl
APPI	atmospheric pressure photoionisation ionisation
aq.	aqueous
Ar	aryl
B_2eg_2	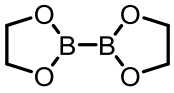 bis(ethylene glycolato)diboron
B_2pin_2	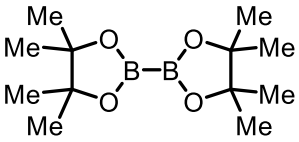 bis(pinacolato)diboron
BDE	bond dissociation energy
BMIDA	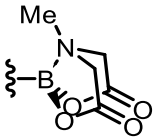 *N*-methyliminodiacetic acid boronate
Bn	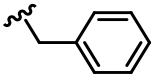 benzyl
Boc	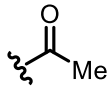 *tert*-butyloxycarbonyl
ChCl	choline chloride
CPME	cyclopentyl methyl ether
Cy	cyclohexyl
dba	dibenzylideneacetone
DCM	dichloromethane
DES	deep eutectic solvent
DFT	density functional theory
DMAc	dimethylacetamide
DMF	dimethylformamide
DMSO	dimethyl sulfoxide
e^-	electron
e.g.	for example
ee	enantiomeric excess
EI	electron ionisation
equiv.	equivalent
ESI	electrospray ionisation
Et	ethyl
et al.	and others

Et_3N	triethylamine
EtOH	ethanol
FID	flame ionisation detector
GC	gas chromatography
Gly	glycerol
Het	hetero
HRMS	high resolution mass spectrum
IMes·HCl	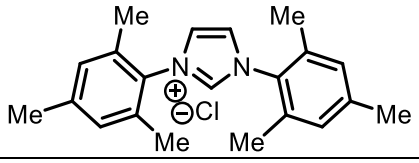
IPA	isopropyl alcohol
IPr·HCl	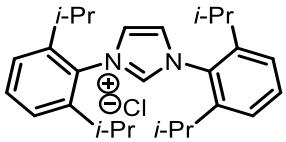
i-Pr	isopropyl
i-Pr_2NEt	Hünig's base
L	ligand
LiTMP	lithium tetramethylpiperidide
m.p.	melting point
m/z	mass-to-charge ratio
m-	*meta*-
Me	methyl
MeCN	acetonitrile
$MeNO_2$	nitromethane
MeOH	methanol
Mes	mesitylene
MPBI	2-[4-(4,5-diphenyl-1*H*-imidazol-2-yl)phenyl]-6-(4-methoxyphenyl)pyridine
MS	mass spectrometer
MTBE	methyl *tert*-butyl ether
$NaBAr^F_4$	sodium tetrakis(3,5-bis(trifluoromethyl)phenyl)borate
n-Amyl	*n*-pentyl
Naph	naphthalene
n-Bu	*n*-butyl
n-BuLi	*n*-butyl lithium
n.d.	not determined
neop	neopentyl
NHC	*N*-Heterocyclic carbene
NMP	*N*-Methyl-2-pyrrolidone
NMR	nuclear magnetic resonance
NSAID	non-steroidal anti-inflammatory drugs
Nu	nucleophile
o-	*ortho*-
OA	oxidative addition
OAc	acetate
OFs	fluorosulfate (OSO_2F)
OMs	mesylate (OSO_2Me)
OTf	triflate (OSO_2CF_3)
OTs	tosylate (OSO_2(*p*-tolyl))
p-	*para*-

PAHs	polycyclic aromatic hydrocarbons
PC	propylene carbonate
Ph	phenyl
ppm	parts per million
QToF	quadrupole time-of-flight
r.t.	room temperature
rac	racemic
t-AmylOH	2-methylbutan-2-ol
t-Bu	*tert*-butyl
t-BuLi	*tert*-butyl lithium
t-BuOH	*tert*-butanol
TBAOH	tetrabutylammonium hydroxide
temp.	temperature
TFA	trifluoroacetate
THF	tetrahydrofuran
TLC	thin layer chromatography
TMB	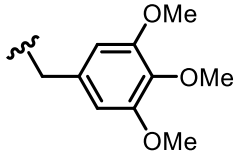 3,4,5-trimethoxylbenzyl
TMEDA	tetramethylethylenediamine
TMS	trimethylsilyl
TOF	turnover frequency
TPGS-750-M	DL-α-tocopherol methoxypolyethylene glycol succinate solution

1. Chapter 1: Introduction

1.1 Background

Phosphine ligands have emerged as one of the most extensively utilised in catalysis, primarily due to their ability to activate metal centres and achieve desired reactivity. When coordinated to metal centres, these ligands significantly enhance catalytic performance compared to the use of metals alone.

The design and synthesis of novel phosphine ligands is a compelling area of chemistry research, driven by the need to enhance the efficiency, selectivity, and versatility of transition metal-catalysed reactions.[1] Phosphine ligands, owing to their tunable steric and electronic properties, play a pivotal role in the modulation of catalytic activity and selectivity in a wide range of chemical transformations. This thesis explores the utility of newly synthesised phosphine ligands in Pd-catalysed cross-coupling reactions, focusing on achieving high reactivity and chemoselectivity.

The field of Pd-catalysed coupling reactions has been an area of intense scientific investigation for several decades. Researchers have dedicated considerable efforts to exploring and advancing the mechanistic underpinnings of these essential organic transformations. Three fundamental steps are at the core of Pd-catalysed coupling reactions: oxidative addition, transmetallation, and reductive elimination (Scheme 1.1).[2]

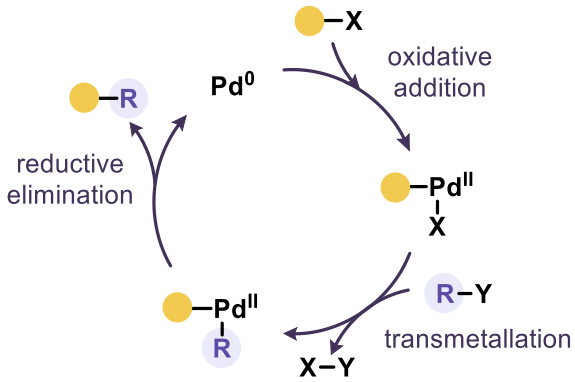

Scheme 1.1 General catalytic cycle of Pd-catalysed coupling reactions

The process begins with an oxidative addition step, wherein an electrophilic species, typically a halide or pseudohalide, binds to the zerovalent and unsaturated palladium(0) catalyst. This results in the generation of an intermediate palladium(II) complex. In the subsequent step, a base, such as an alkoxide or hydroxide, substitutes the halide ligand in the palladium(II) intermediate. Later on, a nucleophilic organometallic species, often an organoboron anion, associates with the palladium(II) complex, forming a new palladium(II) species in a transmetallation step. The final

step in the catalytic cycle involves the reductive elimination of the palladium(II) complex, which releases the desired coupling product and regenerates the active palladium(0) catalyst, completing the cyclic process.[3]

In this thesis, we aim to design and synthesize phosphine ligands to expand the scope and optimize the application of Pd-catalysed transformations, as well as to gain mechanistic insight to elucidate the origins of the ligands.

1.2 The Development of Suzuki−Miyaura Cross-Coupling Reaction

The Suzuki−Miyaura cross-coupling reaction has emerged as one of the most widely utilised tools for carbon-carbon bond formation. This Pd-catalysed transformation offers several distinct advantages compared to other cross-coupling methodologies. Firstly, the starting materials and byproducts associated with Suzuki−Miyaura reactions typically exhibit low toxicity profiles, making them more environmentally friendly. Additionally, milder reaction conditions allow for higher functional group tolerance. Furthermore, organoboron species are commonly employed as coupling partners, both thermally stable and insensitive to oxygen and water, thus enhancing the practical utility of this reaction.[4] As a result of these appealing features, the Suzuki−Miyaura cross-coupling has been the subject of extensive research and development, leading to a vast body of published literature with in-depth investigations into various aspects of the reaction.

The Suzuki−Miyaura cross-coupling reaction was first reported in 1979 by the research team of Suzuki, Miyaura, and Yamada.[5] They demonstrated the successful coupling of alkenyl boranes with alkenyl bromides as their pioneering work, resulting in the formation of coupled products in good yields (Scheme 1.2). A notable feature of the Suzuki−Miyaura cross-coupling reaction is its ability to deliver highly stereospecific and regiospecific coupling products.

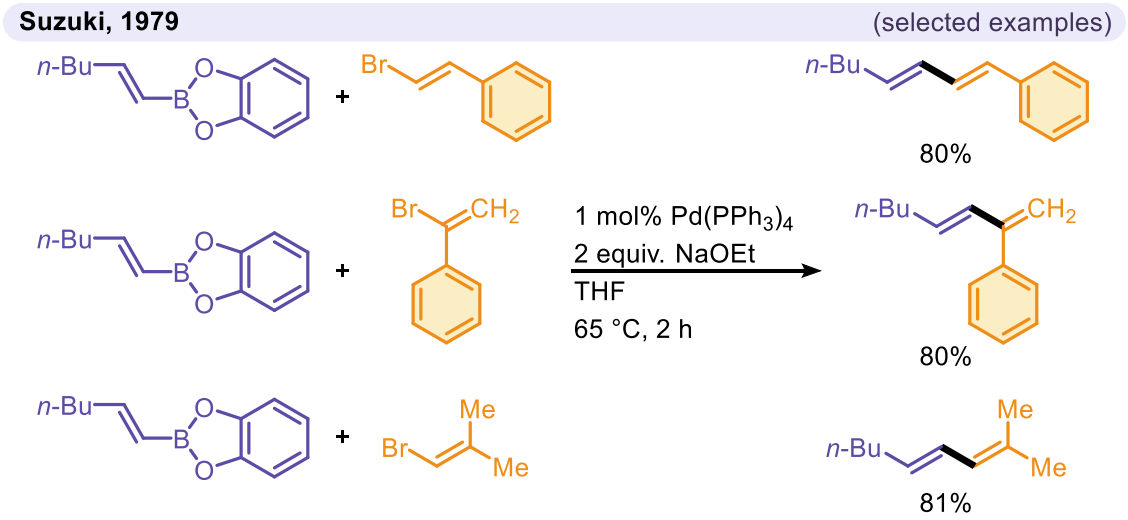

Scheme 1.2 Suzuki−Miyaura cross-coupling of 1-alkenyl boranes and bromides in1979

In 1981, Suzuki and co-workers reported the first examples of coupling reactions involving boronic acids and organic halides. In these pioneering studies, they demonstrated successful coupling reactions between phenylboronic acid and aryl iodides or bromides (Scheme 1.3).[6] These initial findings revealed the potential for broader substrate scope in Suzuki−Miyaura cross-coupling reactions with the ability to readily prepare a diverse range of arylboronic acids, which exhibit stability and tolerance towards a variety of functional groups as well as air stability, opening up new avenues for the development and application of this powerful synthetic method.

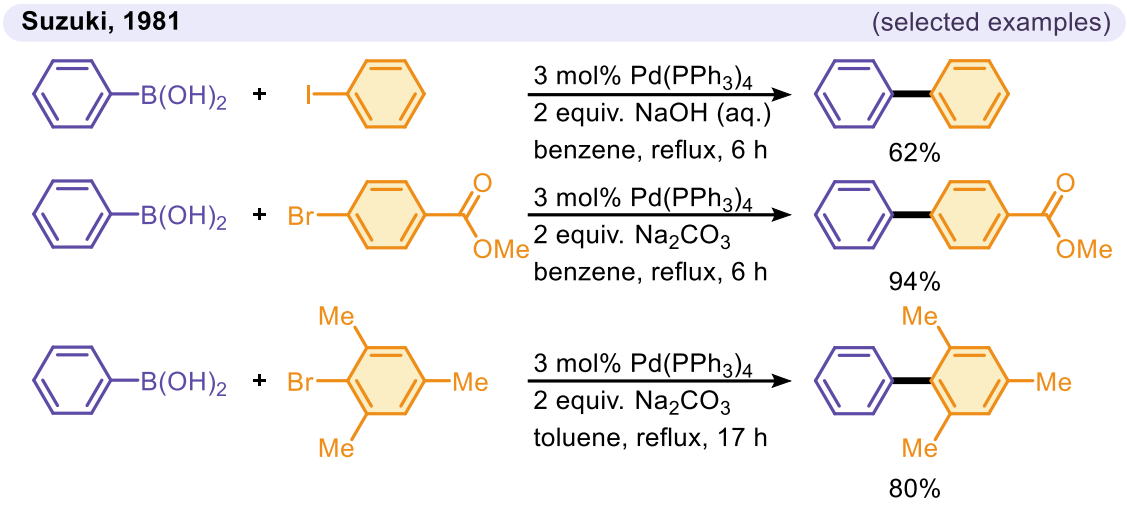

Scheme 1.3 Suzuki−Miyaura cross-coupling of boronic acids and aryl halides in 1981

In 1998, Fu *et al.* developed a general method for the Suzuki−Miyaura cross-coupling of aryl chlorides and arylboronic acids. Their catalyst system, $Pd_2(dba)_3$/P(*t*-Bu)$_3$, efficiently coupled a wide range of substrates, providing the desired biaryl products in excellent yields and leveraging the accessibility of aryl chlorides and the benign nature of organoboron byproducts, was expected to find widespread use in synthetic organic chemistry (Scheme 1.4).[7]

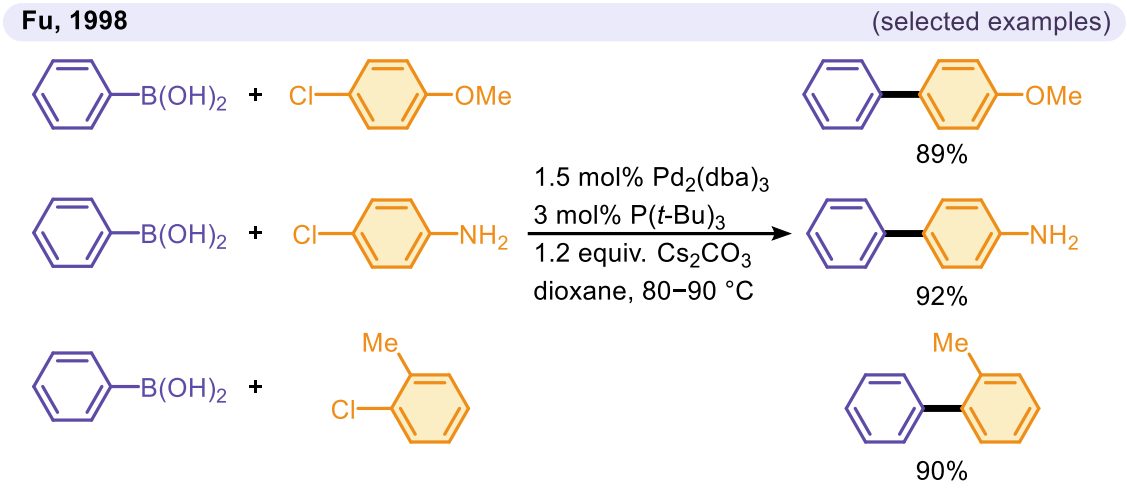

Scheme 1.4 Suzuki−Miyaura cross-coupling using P(*t*-Bu)$_3$ as the ligand

In 1999, Buchwald *et al.* developed a highly active catalyst system for Suzuki−Miyaura cross-coupling of aryl bromides and chlorides using easily prepared CyJohnPhos and *t*-BuJohnPhos (Scheme 1.5). While *t*-BuJohnPhos generally provided faster rates, CyJohnPhos was more effective for hindered substrates and lower catalyst loadings. One example demonstrated the low catalyst loading down to 0.000001 mol% Pd to couple with aryl bromides using *t*-BuJohnPhos (Scheme 1.5). The electron-rich nature of ligands can enhance the oxidative addition rate and hold the palladium in solution, and the steric bulk enhances the reductive elimination rate and

stabilises the palladium centre. The presence of an *o*-biphenyl moiety of these ligands leads to the success of the catalysis by increasing the stability with Pd−arene interactions.[8]

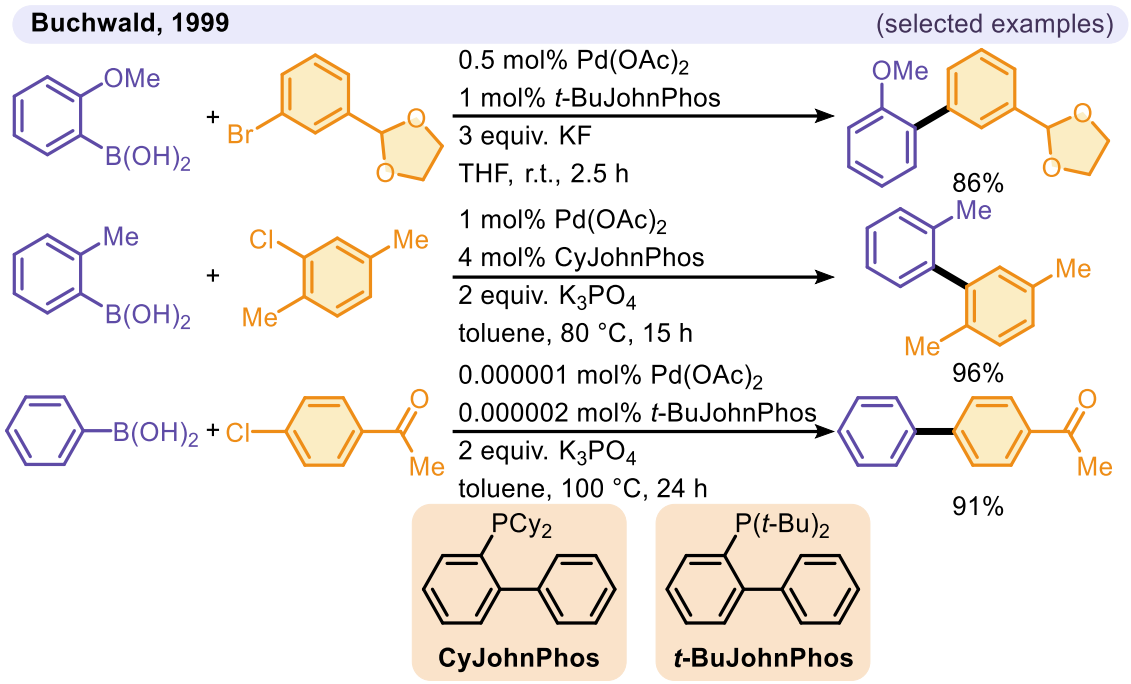

Scheme 1.5 Suzuki−Miyaura cross-coupling using CyJohnPhos and *t*-BuJohnPhos as ligands

In 2003, Molander *et al.* demonstrated the advantages of organotrifluoroborates for Suzuki couplings using $PdCl_2(dppf)\cdot CH_2Cl_2$ as the catalyst or under ligandless conditions (Scheme 1.6). Trifluoroborates are more robust, easily purified, and less prone to protodeboronation against boronic acids or esters used in the reaction. Their protocols enabled the coupling of diverse electron-rich and -poor groups, proving more reactive than their boronic counterparts. Lower catalyst loadings, milder conditions, and open-air reactions yielded results comparable to those of prior boronic acid methods. A key advantage was the ability to use electron-deficient arylborons, though facile protodeboronation of some heteroaryltrifluoroborates was a potential limitation.[9]

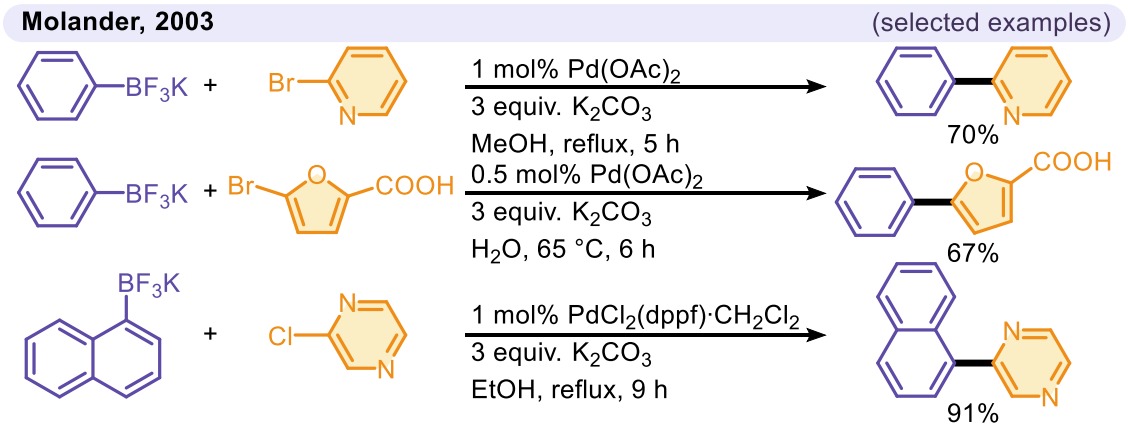

Scheme 1.6 Suzuki−Miyaura cross-coupling using $PdCl_2(dppf)\cdot CH_2Cl_2$ or under ligandless conditions

In 2007, Sajiki and co-workers developed a ligand-free, heterogeneous palladium on carbon (Pd/C) catalysed Suzuki−Miyaura cross-coupling methodology. This approach utilised aryl neopentyl or pinacol boronic esters in combination with aryl bromides or triflates. It could achieve good to high yields under mild reaction conditions at room temperature (Scheme 1.7).[10]

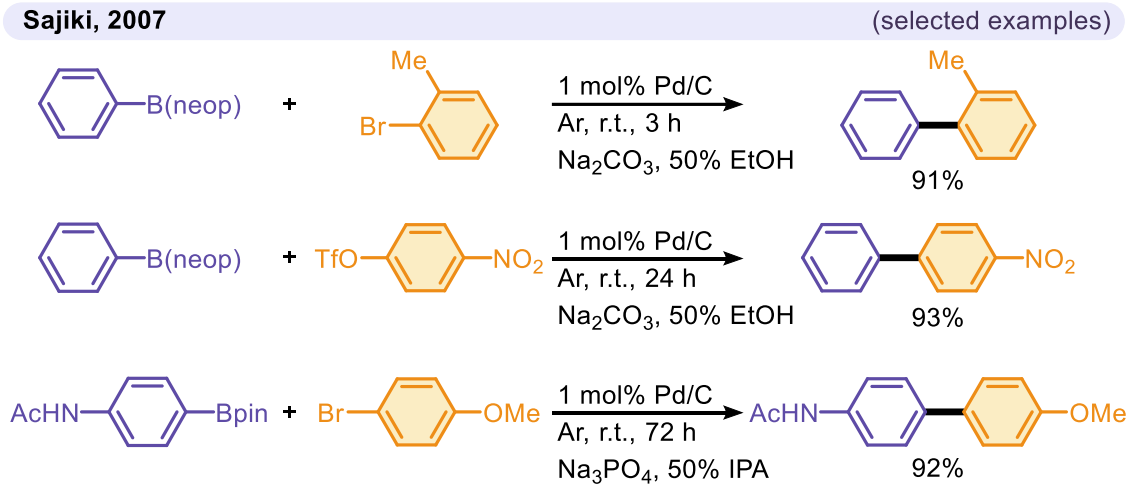

Scheme 1.7 Suzuki−Miyaura cross-coupling of arylboronic esters and (pseudo)halides

In 2007, Wu and co-workers reported on a Pd-catalysed Suzuki−Miyaura cross-coupling methodology that utilised aryl tosylates and potassium aryl trifluoroborates as coupling partners (Scheme 1.8).[11] In a series of reports on employing Buchwald-type dialkylbiarylphosphine ligands in numerous Pd-catalysed cross-coupling reactions, the scope of substrates amenable to Suzuki−Miyaura cross-coupling using these ligands was broad, encompassing aryl bromides, aryl triflates, unactivated aryl chlorides, aryl tosylates, and a range of heteroaryl systems, including hindered substrate combinations and could be carried out at room temperature with low catalyst loadings.[12]

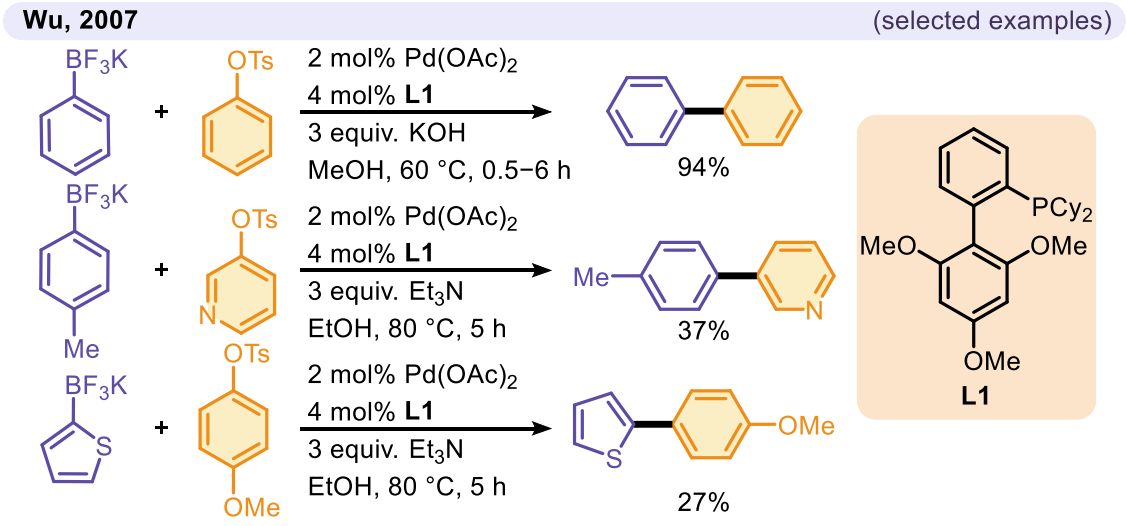

Scheme 1.8 Suzuki−Miyaura cross-coupling of aryl tosylates and potassium aryl trifluoroborates

In 2009, Kwong and co-workers reported the first successful Suzuki−Miyaura cross-coupling reactions of unactivated aryl mesylates (Scheme 1.9). The Pd/CM-Phos catalyst system was active with various mesylate substrates containing some common functional groups. Furthermore, the scope of the organoboron nucleophiles has extended beyond boronic acids to include aryl trifluoroborate salts and boronate esters. They highlighted the simplicity of the ligand synthesis and the ease of modifying the ligand skeleton, which might contribute to further enhancements in the reactivity and versatility of this ligand series in future studies.[13]

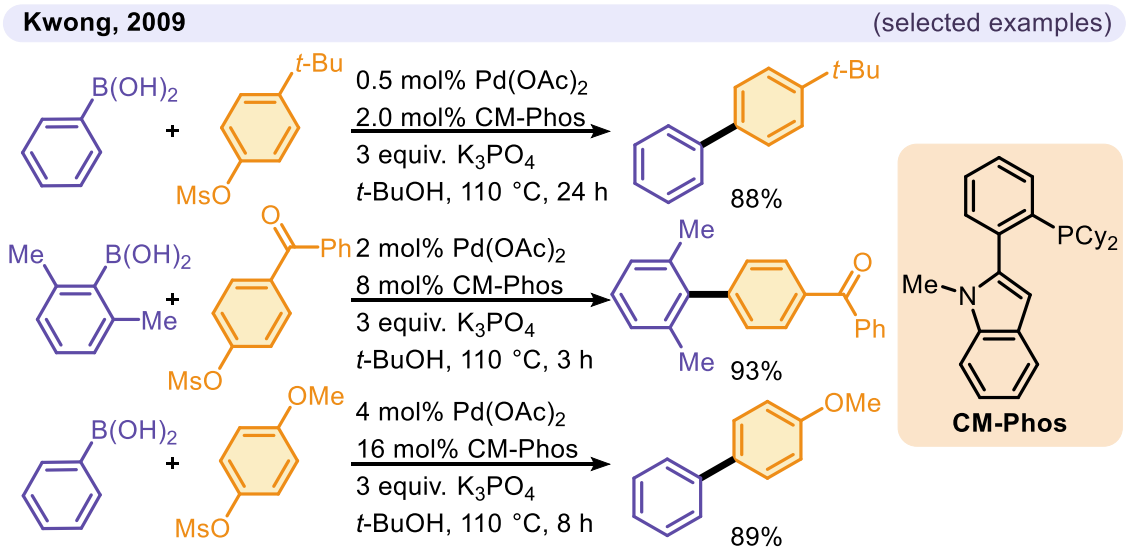

Scheme 1.9 Suzuki−Miyaura cross-coupling of aryl mesylates and arylboronic acids

In 2010, Ackermann and co-workers described the utilisation of a heteroatom-substituted phosphine ligand for Pd-catalysed Suzuki−Miyaura cross-coupling reactions involving sterically hindered substrates. Specifically, they reported that a palladium complex derived from a diaminochlorophosphine ligand enabled the synthesis of challenging tetra-*ortho*-substituted biaryls, among other transformations (Scheme 1.10).[14]

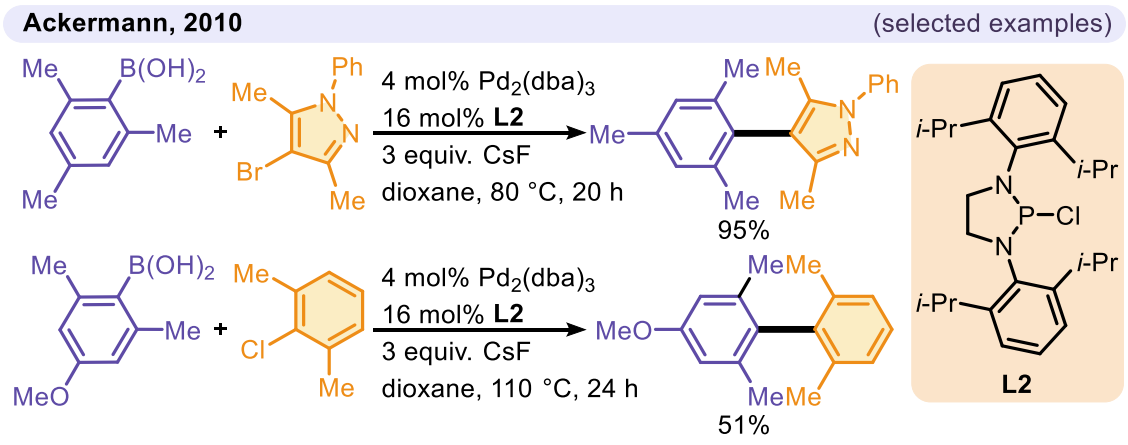

Scheme 1.10 Suzuki−Miyaura cross-coupling of di-*ortho*-substituted aryl halides and arylboronic acids

In 2017, Houk and Newman reported a novel NHC-based palladium catalyst system that enabled Suzuki−Miyaura cross-coupling reactions using aryl esters as the electrophilic coupling partners (Scheme 1.11).[15] This approach allowed the synthesis of various ketone-containing products, contrasted with the known nickel-catalysed reactions of similar esters that typically provided biaryls via C−O bond cleavage. They proposed that the Pd(IPr)(cinammyl)Cl facilitated kinetically feasible oxidative addition onto the C(acyl)−O bond while preventing the formation of a 5-membered transition state that may have favoured C(aryl)−O cleavage. Additionally, the bulky IPr ligand was suggested to suppress decarbonylation of the acyl−Pd intermediate, ultimately enabling the desired direct cross-coupling process.[15]

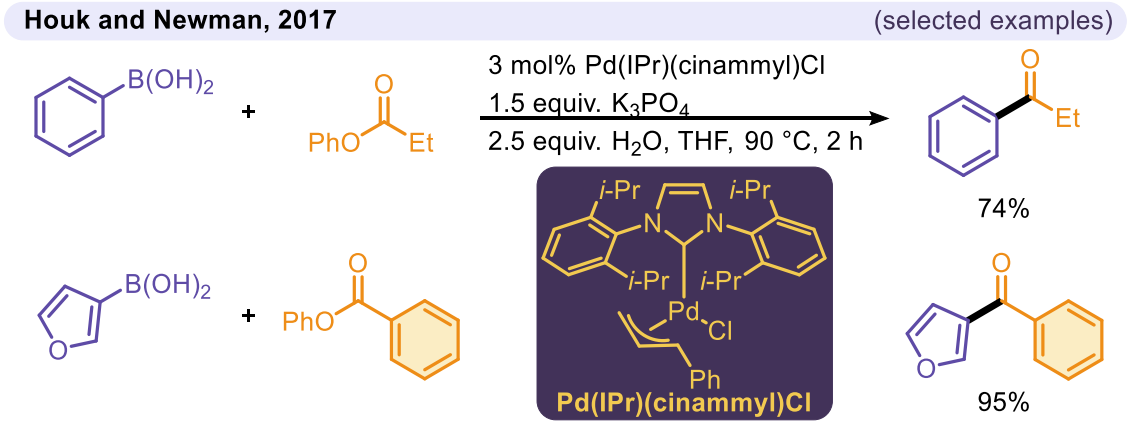

Scheme 1.11 Suzuki−Miyaura cross-coupling reactions of aryl esters and arylboronic acids

In 2019, Lipshutz and co-workers reported a new palladacycle precatalyst that enabled efficient Suzuki−Miyaura couplings in water at just 300 ppm Pd (Scheme 1.12). A key feature was the placement of isopropyl groups on the biaryl skeleton, a substitution pattern not previously explored in such precatalysts. This palladacycle, combined with HandaPhos, was well-suited for the aqueous micellar conditions, allowing valued Suzuki−Miyaura reactions under mild conditions with minimal palladium loading.[16]

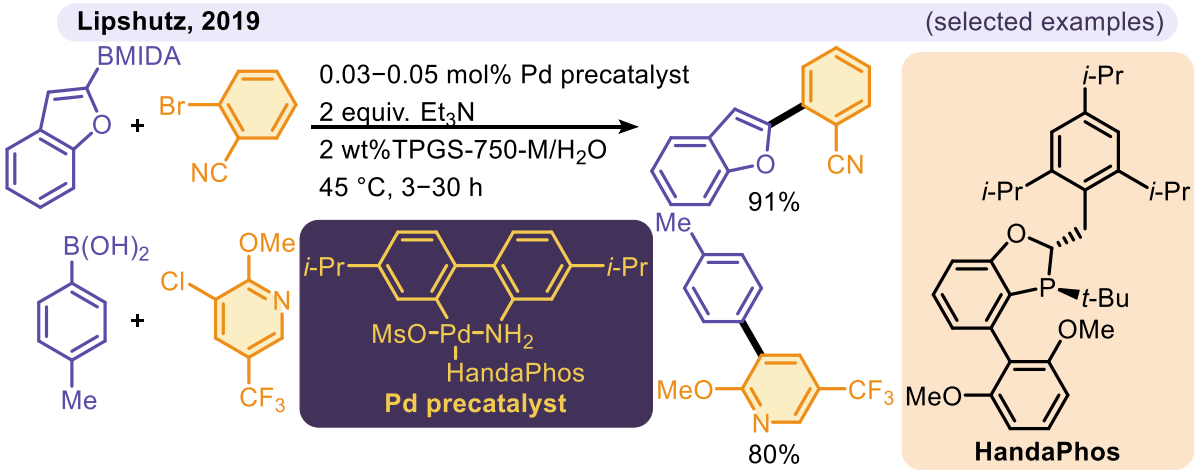

Scheme 1.12 Suzuki−Miyaura cross-coupling reactions using palldacycle prescatalyst

In 2020, Tang *et al.* developed a general, practical, and efficient method for asymmetric Suzuki−Miyaura aryl-aryl cross-coupling. It enabled synthesising a wide range of axially chiral tetra-*ortho*-substituted biaryls in high yields and enantioselectivities (Scheme 1.13). The key was the design of a sterically bulky P-chiral monophosphorus ligand, BaryPhos, which addressed reactivity issues and facilitated a new catalysis mode involving noncovalent interactions to achieve excellent enantioselectivities. Demonstrating a practical example of the enantioselective synthesis of the antitumor agent gossypol can show the potential of broad applications in synthesising chiral ligands, catalysts, materials, natural products and therapeutics (Scheme 1.14).[17]

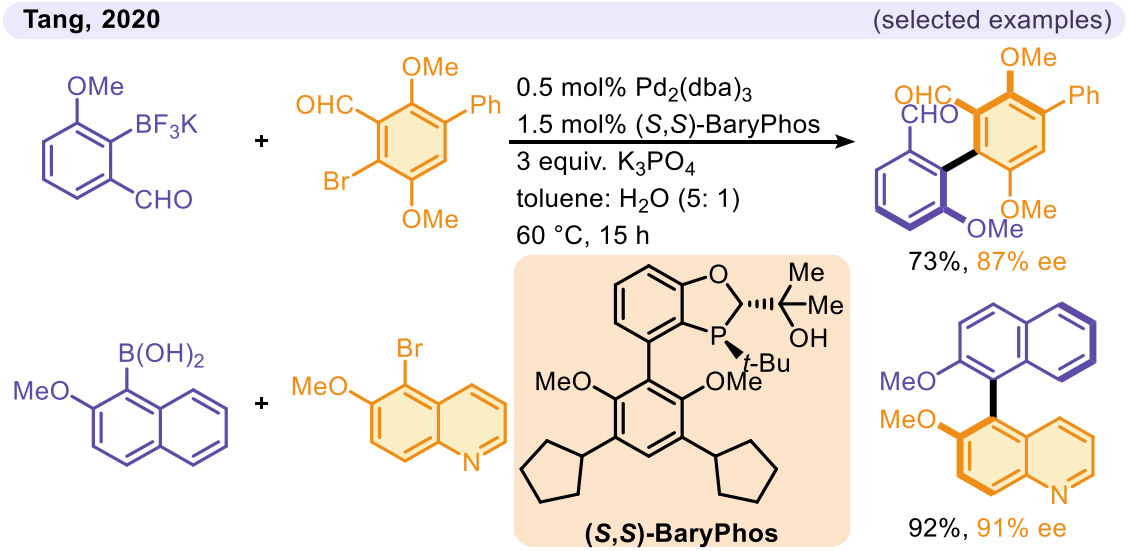

Scheme 1.13 Suzuki−Miyaura cross-coupling reactions using BaryPhos

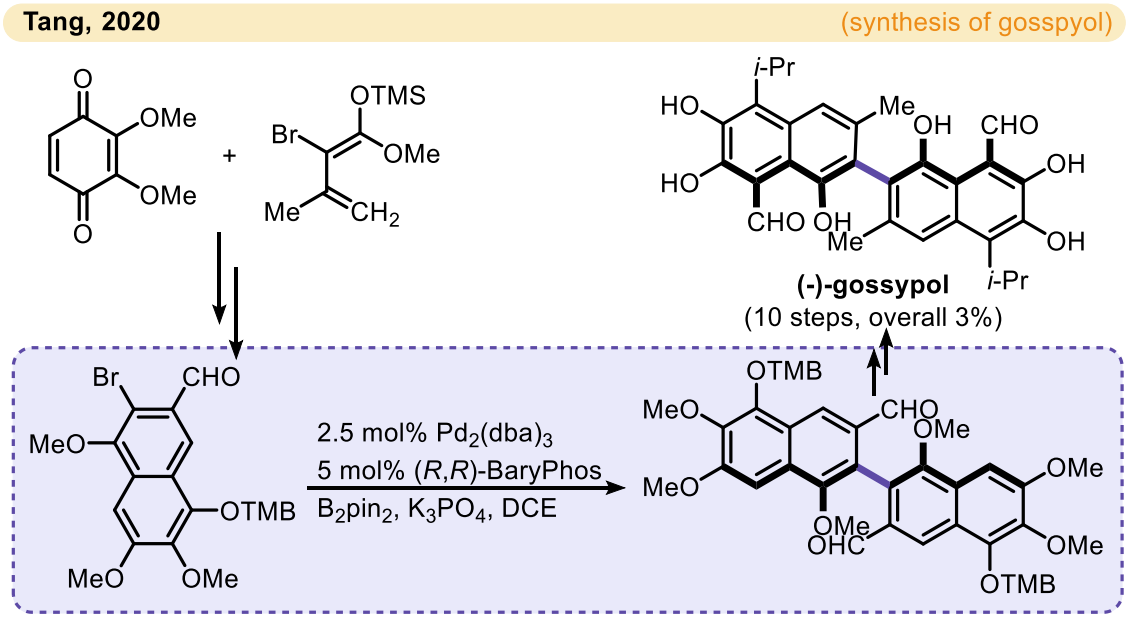

Scheme 1.14 A synthetic route of antitumor agent gossypol

In short, scientists continue to develop more facile, cost-effective, and environmentally benign Suzuki−Miyaura cross-coupling protocols, including identifying economical green catalysts and solvents, minimising transition metal loadings, and expanding the functional group tolerance to accommodate diverse and less reactive coupling partners. These advancements may further expand the synthetic utility and improve the sustainability of these carbon-carbon bond-forming reactions across various scientific and industrial applications.

1.3 The Development of Miyaura Borylation

Organoboron compounds are widely used as coupling partners in Suzuki−Miyaura cross-coupling reactions, serving as an essential reagent for many synthetic and catalytic transformations.[18] While boronic acids are the most common organoboron species employed in these cross-coupling reactions due to their high atom economy and commercial availability, they can be susceptible to protodeboronation if they contain certain functional groups such as vinyl, cyclopropyl, electron-rich heterocycles, or electron-deficient moieties.[19] However, these organoboron compounds are essential structural motifs in many pharmaceutical drugs,[19] including Crizotinib, Etoricoxib, Losartan, Pantoprazole, Roflumilast, and Valsartan (Figure 1.1).[20–23] Consequently, there is a need to develop alternative boron-protecting or boron-masking strategies to enable the effective use of these sensitive organoboron coupling partners in cross-coupling reactions (Figure 1.2).[19]

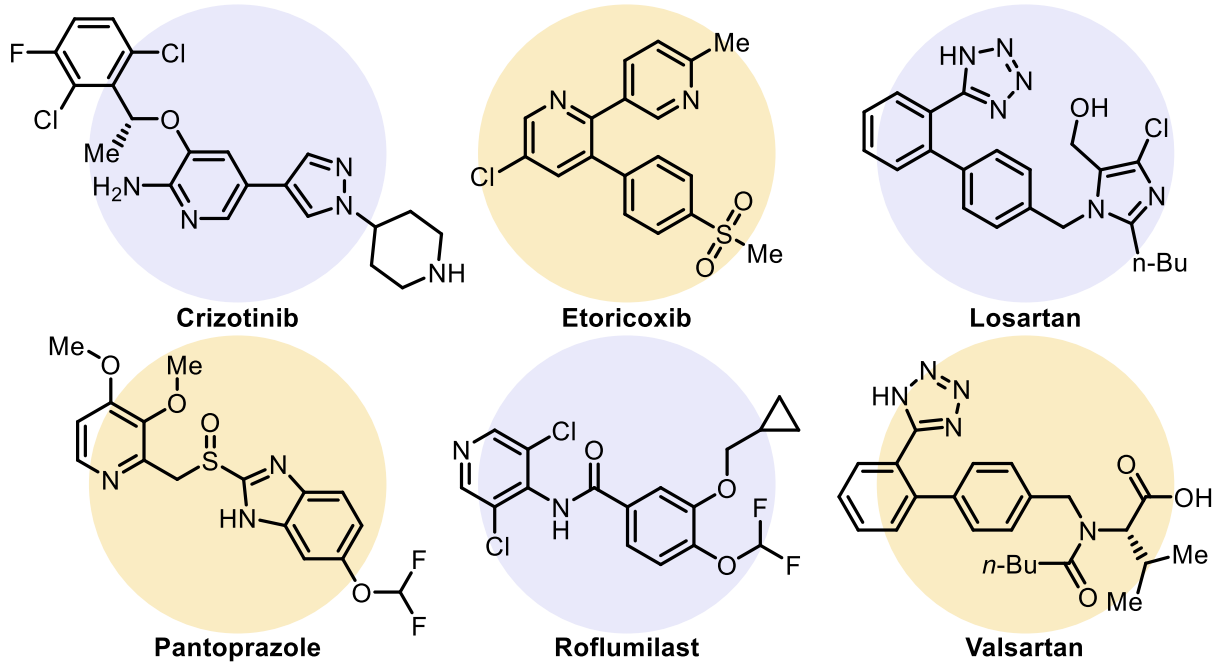

Figure 1.1 Examples of drugs featuring diverse organic structural motifs

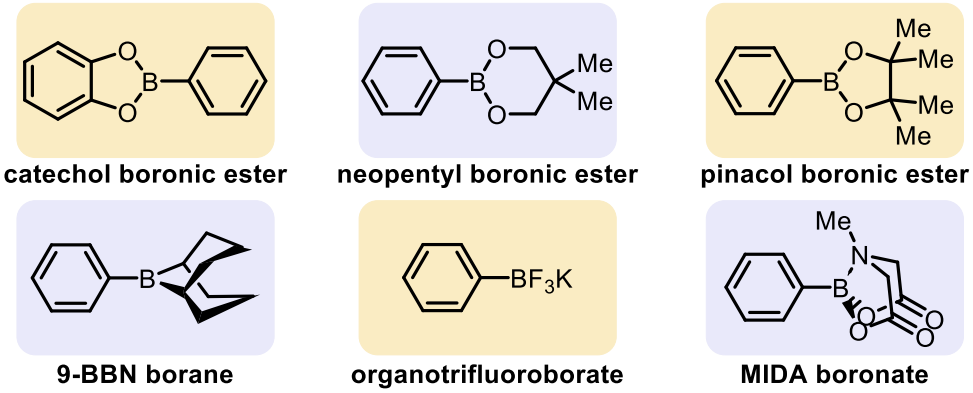

Figure 1.2 Examples of common boron-masking agents

One of the most used classes of organoboron reagents is boronic esters. Boronic esters featuring 6-membered cyclic structures tend to be more thermodynamically stable against their 5-membered ring analogues. Furthermore, methylation of the α-carbon of the diol component can provide additional stabilisation, resulting in comparable stability between neopentyl and pinacol boronic esters.[24] Consequently, boronic esters, particularly pinacol boronic esters, are often preferred over boronic acids in medicinal chemistry and natural product synthesis applications due to their enhanced chemical stability, especially under alkaline reaction conditions.[19]

There are multiple established methods available for the synthesis of boronic esters. One of the most widely employed approaches is the Miyaura borylation, a Pd-catalysed reaction that converts organic halides into pinacol boronic esters.[24] This transformation offers several main advantages. First, it exhibits excellent tolerance of a wide range of functional groups. Second, the required starting materials are readily accessible or even commercially available. Finally, the synthetic procedure and product purification are generally straightforward. As a result, the Miyaura borylation has become a dominant strategy for the facile preparation of pinacol boronic ester building blocks.

The Miyaura borylation, a Pd-catalysed cross-coupling reaction, was first discovered and reported in 1995. This transformation enables the direct preparation of pinacol boronic esters via the coupling of organic halides with bis(pinacolato)diboron.[25] It provided chemists with a convenient method to access organoboron nucleophiles for subsequent use in Suzuki−Miyaura cross-coupling reactions.

The mechanism of the Miyaura borylation is analogous to that of the Suzuki−Miyaura cross-coupling process. However, a potential challenge can arise during the latter stages of the Miyaura borylation, when the concentration of the formed boronic ester product is high. Under these conditions, there is competition between the desired borylation and the competing Suzuki−Miyaura cross-coupling reaction. Fortunately, this issue can be successfully mitigated by carefully selecting a relatively hard Lewis base, which helps to suppress the unwanted side reaction.[26]

In 2000, Masuda *et al.* reported an efficient method for the direct borylation of aryl halides or aryl triflates. This transformation involved the coupling of pinacolborane with the aryl (psuedo)halides in the presence of $PdCl_2$(dppf) along with a base (Scheme 1.15). The choice of base was found to have a significant impact on the product distribution, particularly triethylamine, being particularly effective for selectively promoting the desired boron-carbon bond formation. Importantly, the mild reaction conditions enabled the preparation of arylboronates bearing a diverse array of functional groups, including carbonyl, cyano, and nitro moieties, showcasing the broad functional group tolerance of this direct borylation protocol.[27]

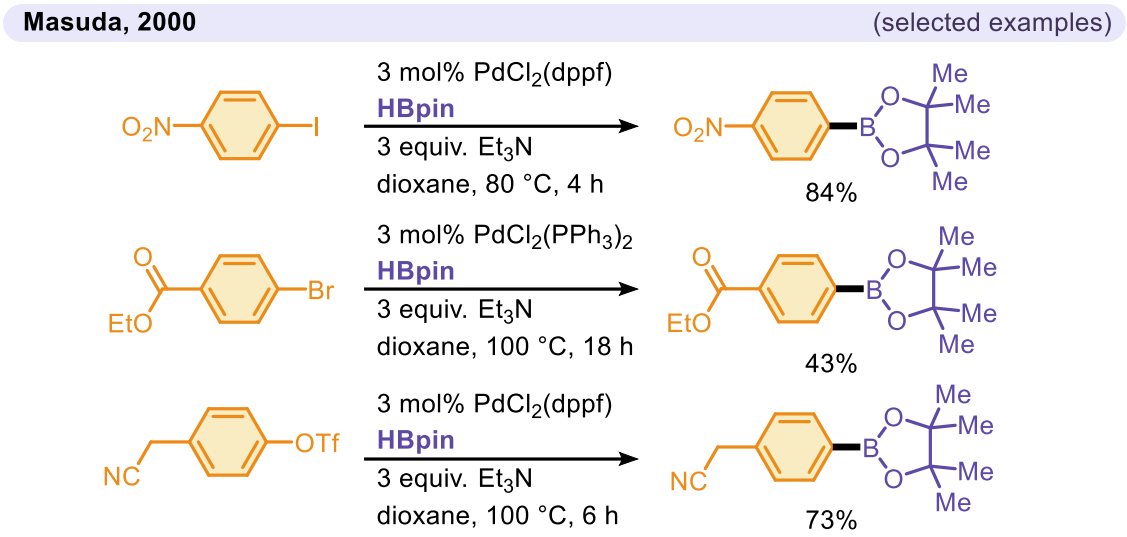

Scheme 1.15 Miyaura borylation of aryl halides or triflates using $PdCl_2(dppf)$

In 2002, Ishiyama and Miyaura reported a Pd-catalysed cross-coupling method for the synthesis of 1-alkenylboronic acid pinacol esters. It involved the reaction of bis(pinacolato)diboron with 1-alkenyl halides or triflates in toluene at 50 °C, using potassium phenoxide and a $PdCl_2(PPh_3)_2/PPh_3$ catalyst system (Scheme 1.16). The borylation was broadly applicable to acyclic and cyclic 1-alkenyl electrophiles, providing the desired products in high yields with complete retention of the alkene geometry. Additionally, the method was utilised in one-pot procedures for the synthesis of unsymmetrical 1,3-dienes.[28]

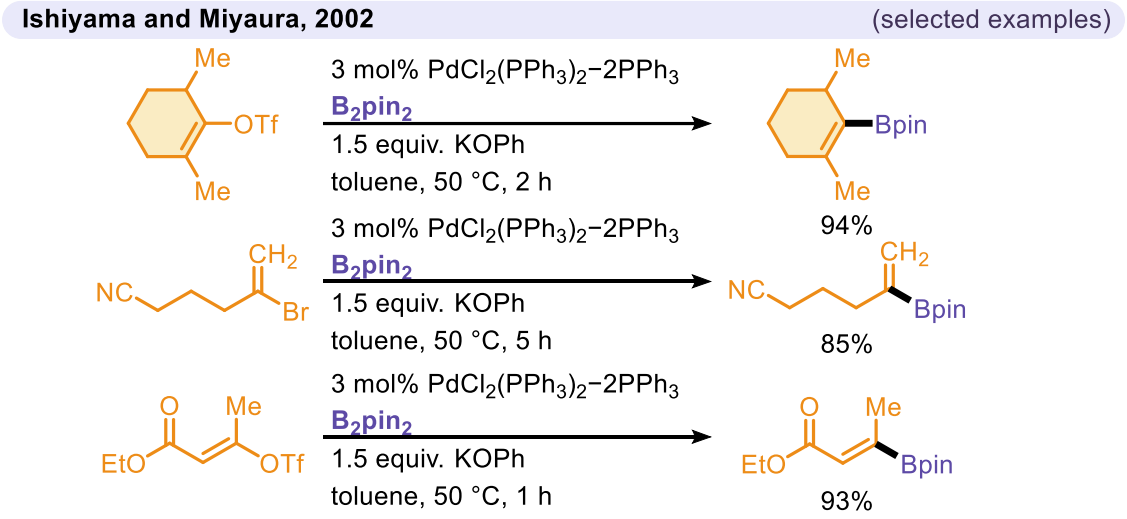

Scheme1.16 Miyaura borylation of 1-alkenyl halides or triflates using $PdCl_2(PPh_3)_2/PPh_3$

In 2007, Buchwald and co-workers developed a Pd-catalysed borylation protocol that allowed symmetrical and unsymmetrical biaryl compound synthesis from aryl chlorides (Scheme 1.17).[29] However, this methodology was not suitable for substrates bearing ketone functionalities, as it led to undesired α-arylation under the reported conditions.

Building on this work, they reported a more general Pd-catalysed borylation using pinacolborane as the boron source in 2008. This approach featured relatively low catalyst loadings and shorter reaction times. It could apply to a broader scope of (hetero)aryl iodides, bromides, and even some (hetero)aryl chlorides, providing the desired borylated products in good yields (Scheme 1.17).[30]

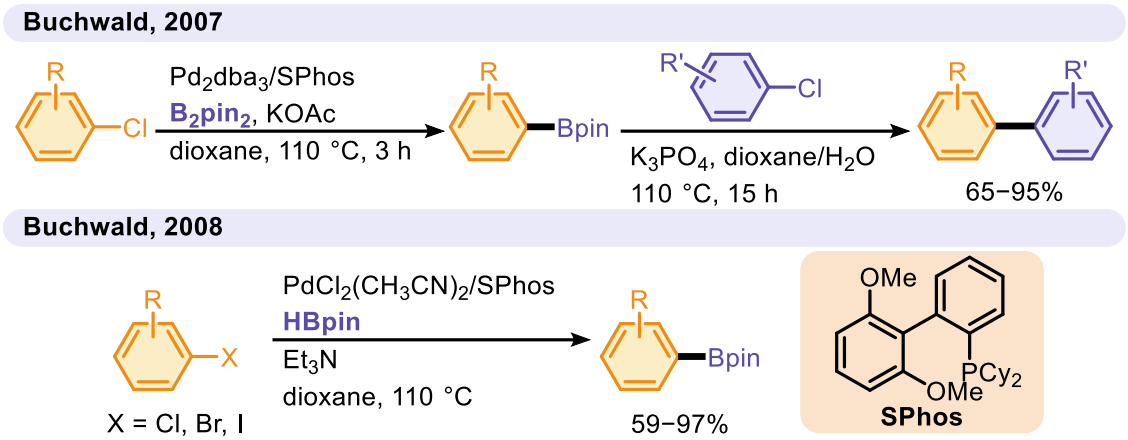

Scheme 1.17 Miyaura borylation of (hetero)aryl halides by Buchwald *et al.*

In 2011, Tang reported the development of a novel biaryl monophosphorus ligand, AntPhos, for Pd-catalysed Miyaura borylation (Scheme 1.18). When AntPhos combined with the Bedford palladium precursor, this ligand system enabled the borylation of sterically hindered aryl bromides with diverse functional groups, even at low catalyst loadings. Remarkably, a turnover number was achieved up to 9000, highlighting the potential for practical applications. Additionally, the BI-DIME ligand was efficient for the borylation of aryl chlorides.[31]

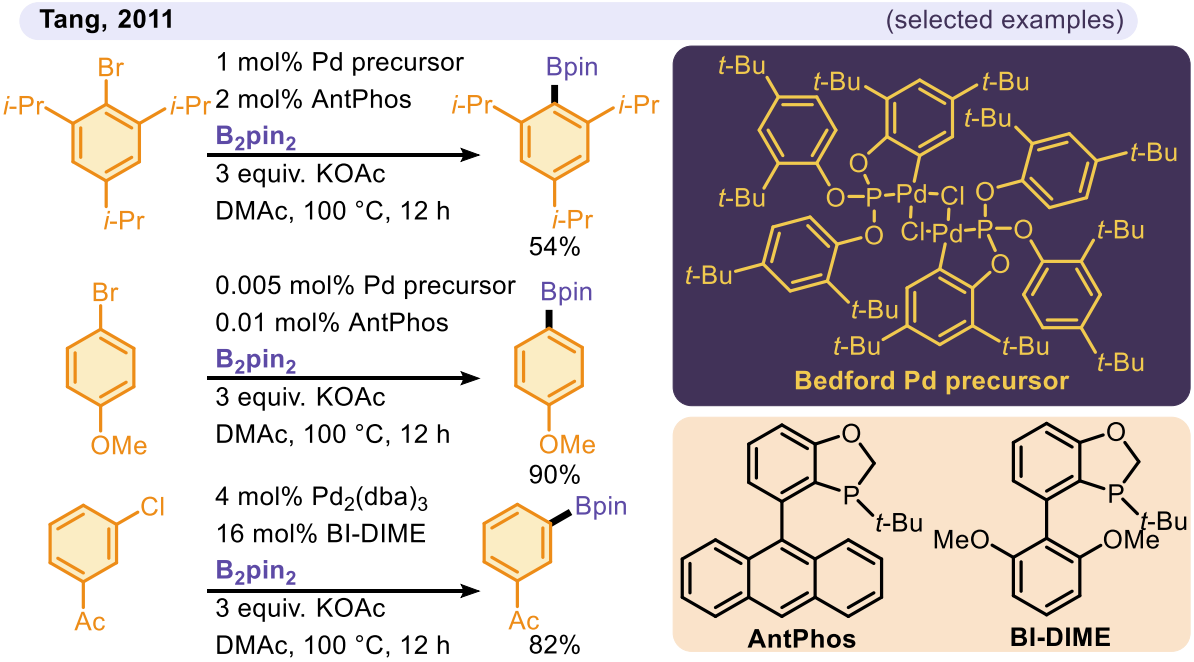

Scheme 1.18 Miyaura borylation of sterically hindered aryl bromides using AntPhos

The synthesis of certain boronic acid derivatives can be streamlined by generating the organoboron species in situ, followed by a Suzuki−Miyaura cross-coupling reaction to furnish the desired coupling product. Along these lines, in 2011, Zhang and co-workers reported a one-pot Pd-catalysed strategy that combined borylation and subsequent Suzuki−Miyaura coupling to prepare 8-arylquinolines (Scheme 1.19).[32] This approach offered increased efficiency and simplicity compared to traditional methods for the synthesis of quinolines bearing (hetero)arene substituents.

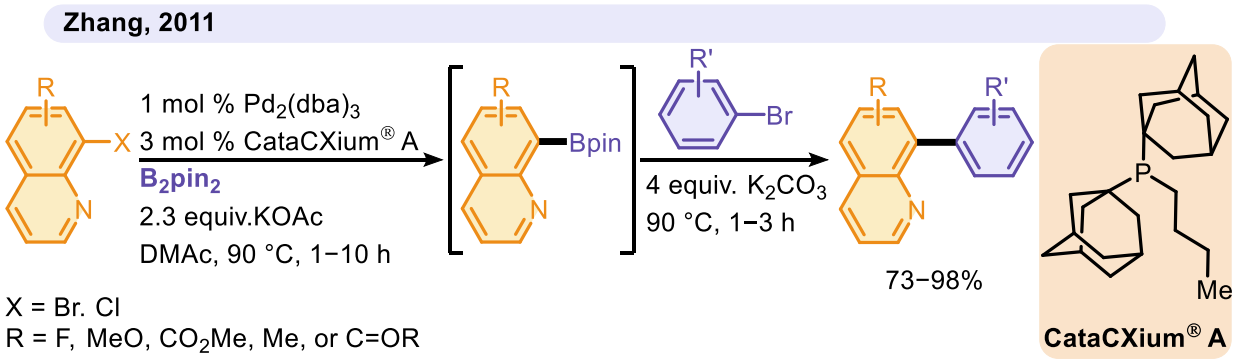

Scheme 1.19 One-pot Pd-catalysed borylation/Suzuki coupling for the preparation of 8-arylquinolines

Heteroaryl and vinyl organoborons are valuable synthetic intermediates for pharmaceuticals, natural products, and functional materials. In 2017, Zou *et al.* reported a Pd-catalysed Miyaura borylation to prepare pyrazine boronic esters, providing a facile approach to access these important building blocks. (Scheme 1.20).[33]

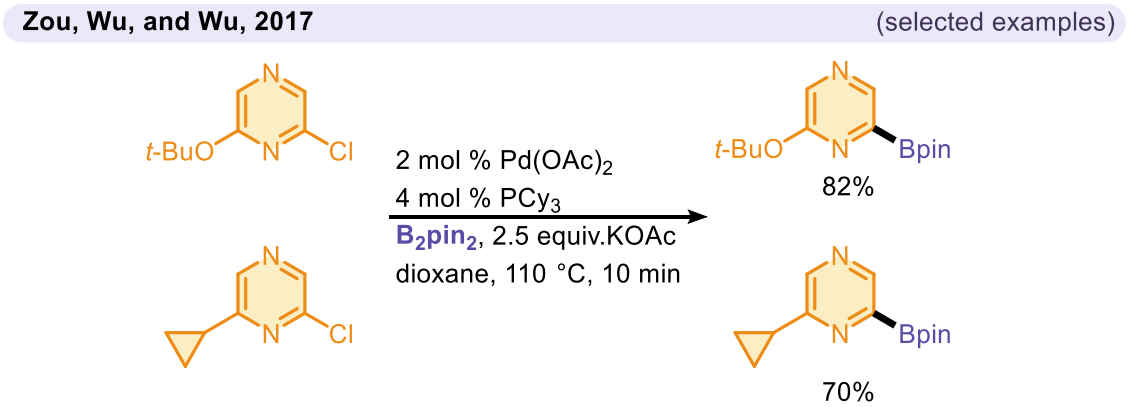

Scheme 1.20 Pd-catalysed Miyaura borylation of pyrazine boronic esters

The one-pot approach to the synthesis of unsymmetrical bi- and triaryls holds significant appeal, as it circumvents the need for expensive, unstable, and commercially unavailable boronic acid starting materials. In this vein, in 2018, Ji and co-workers reported a one-pot, two-step Pd-catalysed protocol involving Miyaura borylation followed by Suzuki−Miyaura coupling of aryl chlorides, which was conducted at room temperature (Scheme 1.21).[34]

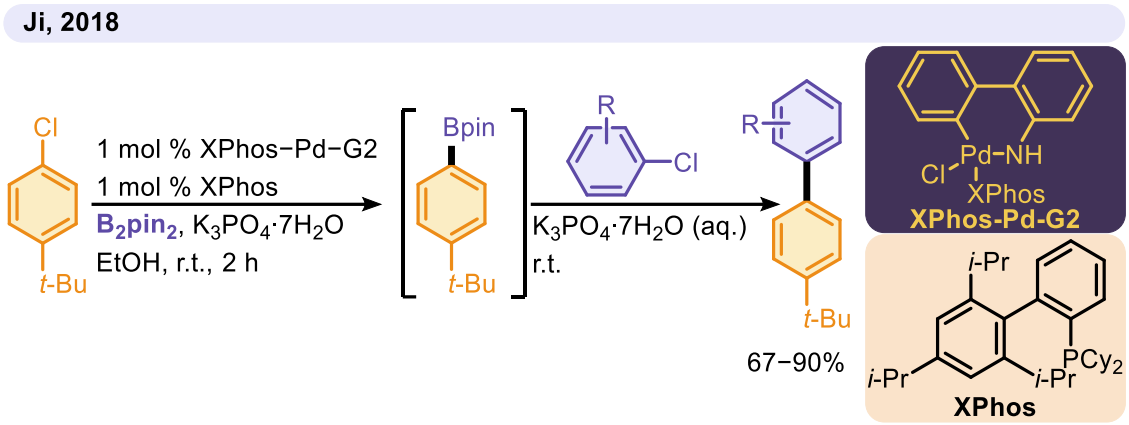

Scheme 1.21 Pd-catalysed borylation/Suzuki–Miyaura coupling of aryl chlorides

Advancements in catalyst design and reaction conditions have enabled the borylation methodology to be more widely adopted in the synthesis of complex natural products (Scheme 1.22),[35] pharmaceutical compounds (Scheme 1.23),[36] and polycyclic materials (Scheme 1.24).[37] Many research groups have successfully demonstrated the utility of borylation reactions in the construction of these important molecular targets, highlighting the growing practical applications of this versatile transformation.

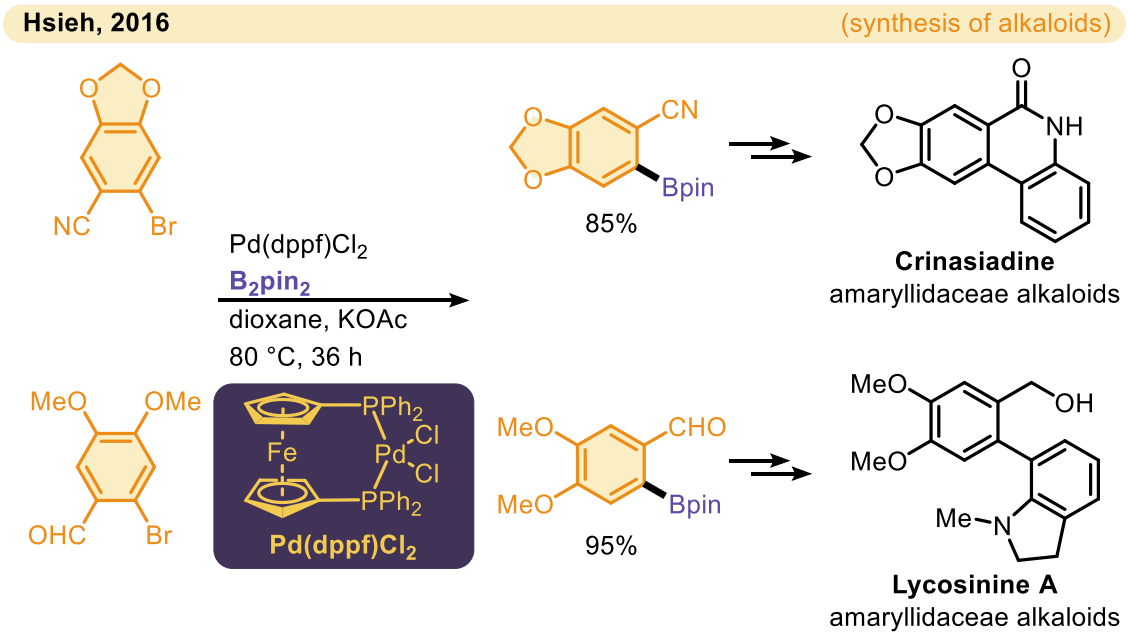

Scheme 1.22 Two examples of borylation application in the synthesis of alkaloids

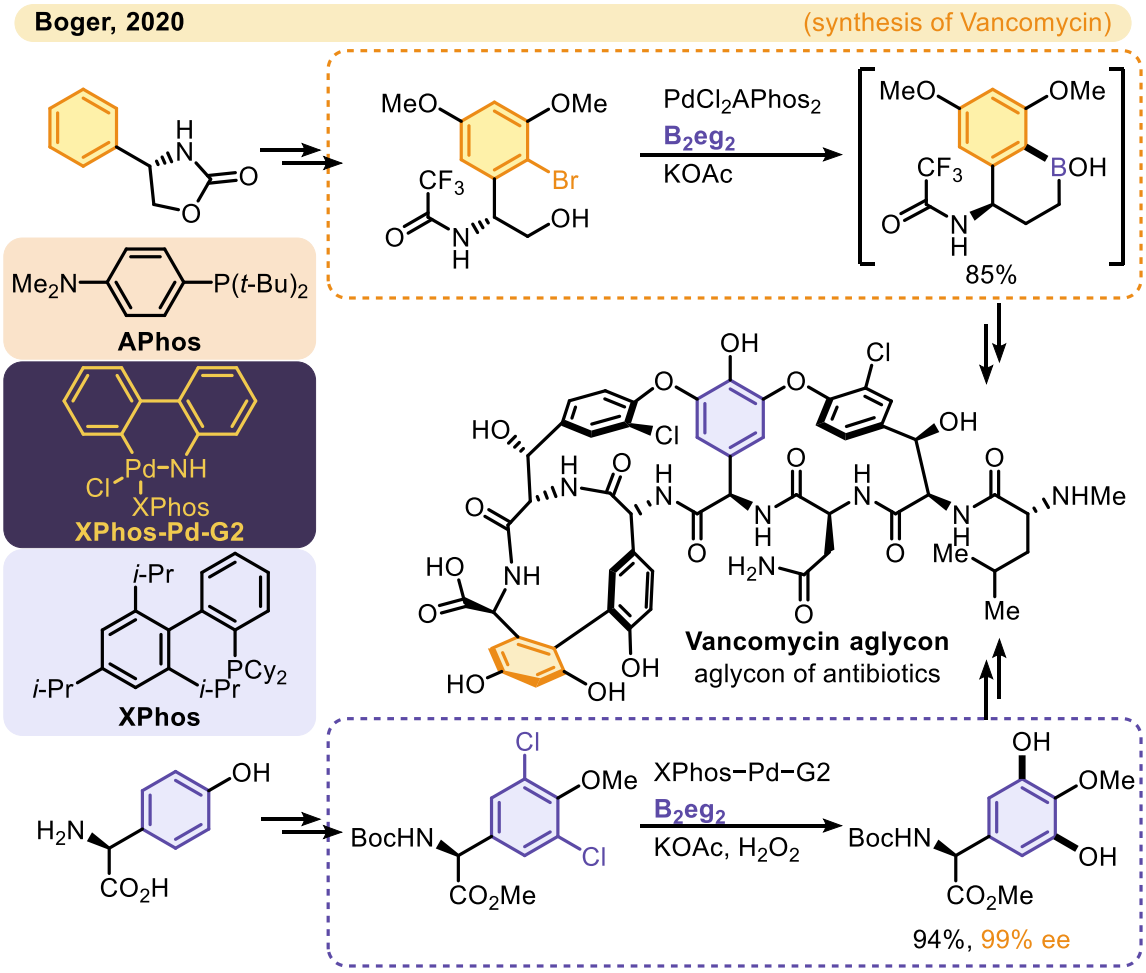

Scheme 1.23 An example of borylation application in the synthesis of medicines

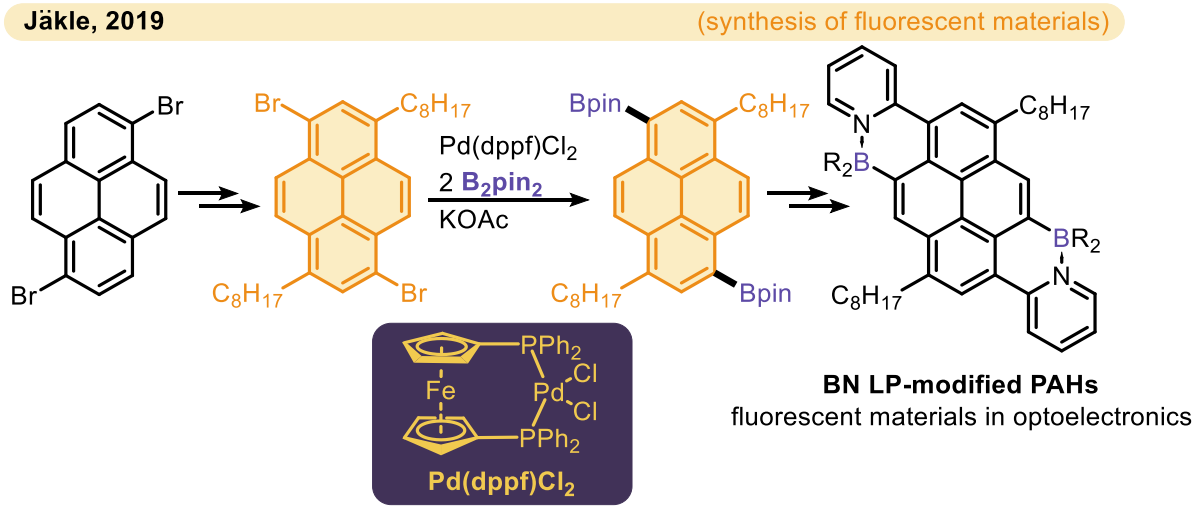

Scheme 1.24 An example of borylation application in the synthesis of materials

In 2022, Kwong and co-workers developed the first general Miyaura borylation of highly sterically hindered aryl chlorides using a homogeneous palladium catalyst system (Scheme 1.25). The key was a strategically designed phosphine ligand with a smaller phosphine head and larger remote steric bulk, in contrast to typical localised steric hindrance. This allowed borylation of even

extremely congested 2,6-diisopropyl aryl chlorides, as well as sterically crowded heteroaryl chlorides, with excellent functional group tolerance and only 0.5 mol% Pd.[38] The success provides a model for designing catalysts for other demanding cross-couplings.

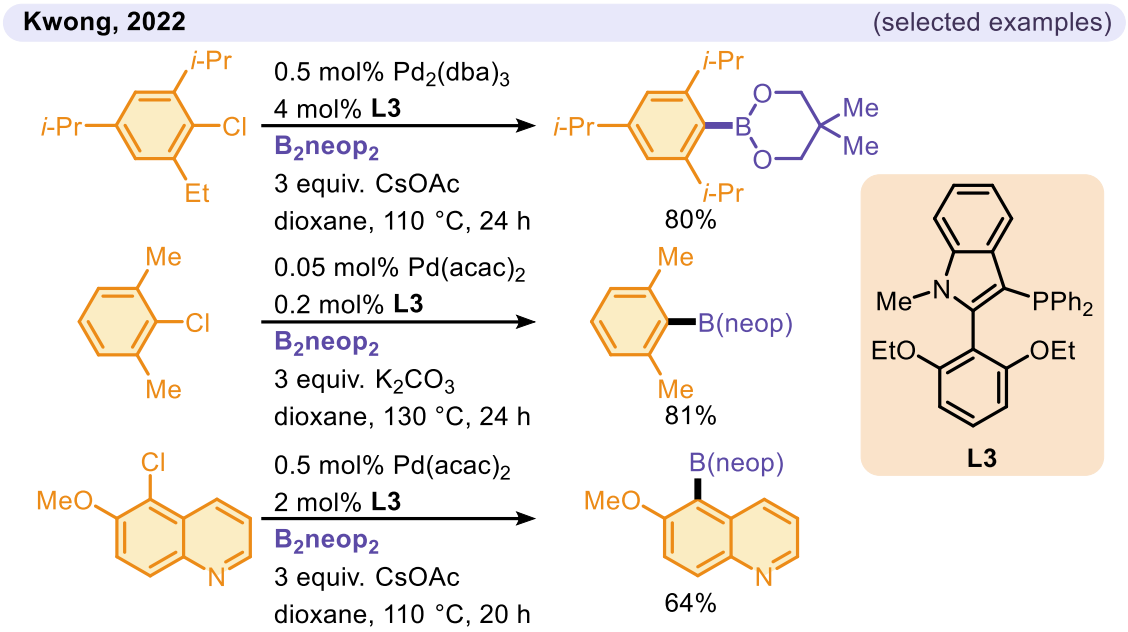

Scheme 1.25 Miyaura borylation of sterically hindered aryl chlorides

In 2024, Zani and Dessì reported the first Pd-catalysed Miyaura borylation of (hetero)aromatic halides and pseudohalides using bis(pinacolato)diboron, conducted in environmentally friendly deep eutectic solvents (DESs). The reactions proceeded smoothly in 1 hour under air, tolerating a range of halides and functional groups, using a Pd_2dba_3/XPhos catalyst system. To avoid purification, they also developed a telescopic borylation/Suzuki−Miyaura coupling for direct bi(hetero)aryl synthesis in DES. Eco-factor and Eco-scale analysis indicated these DES-based protocols offered improvements over traditional volatile organic solvent methods, advantageous for applications in electronics and photovoltaics (Scheme 1.26).[39]

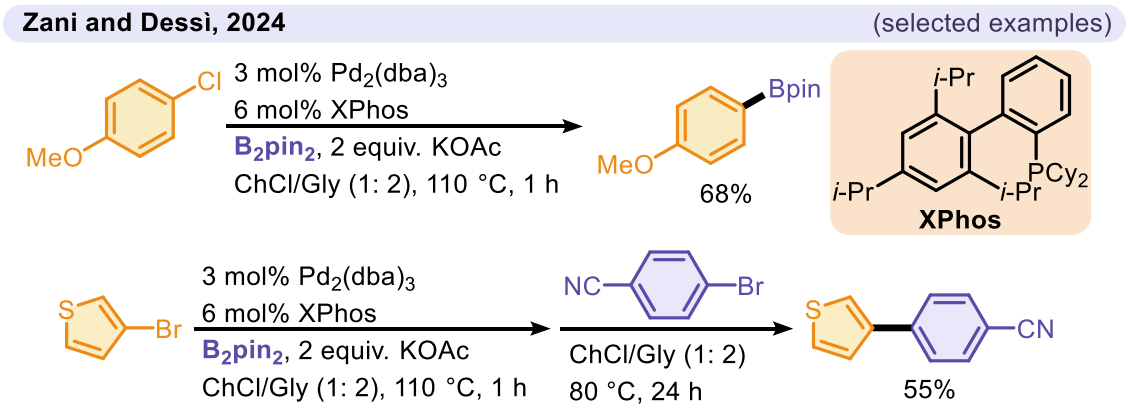

Scheme 1.26 Miyaura borylation of (hetero)aryl halides in deep eutectic solvents

While many boronic acids and esters are commercially available, they often require preparation from arenes or aryl/vinyl halides. Nonetheless, the Pd-catalysed Miyaura borylation of such substrates remains the most popular route to organoboron compounds. Over time, various Miyaura protocols have been developed, employing different palladium catalysts and bases to efficiently convert a range of aromatic halides into boronic esters.

Moreover, the synergy between Miyaura borylation and Suzuki−Miyaura cross-coupling has led researchers to devise one-pot, telescopic procedures. These avoid the need to isolate boronic ester intermediates, providing a more streamlined and sustainable path to the desired (hetero)biaryl products compared to traditional multistep sequences.

1.4 The Development of Chemoselective Cross-Coupling Reactions

Chemoselectivity refers to the selective reaction of one substrate bearing multiple potential reaction sites. There has been renewed interest in developing chemodivergent coupling reactions that can achieve site-selectivity, reacting at a specific site while leaving other sites intact.

The use of multifunctionalised substrates is a widely adopted strategy for synthesising complex molecules. However, this approach can present challenges in separating product mixtures or carrying out subsequent steps, especially when achieving clean selectivity is difficult.

Despite these challenges, there is potential for conducting sequential synthesis by exploiting different substrate reactivities. This can streamline the synthetic pathway and eliminate the need for further functionalisation. Such an approach holds promise for efficient, economical, and environmentally friendly reactions (Scheme 1.27), particularly if a multifunctionalised substrate is utilised in the first step to reduce overall steps.

The ideal scenario involves the substrate reacting selectively at a specific site in a stepwise manner, yielding the desired product without laborious separation. However, accomplishing the chemoselectivity of substrates with multiple electrophilic sites remains a significant challenge.

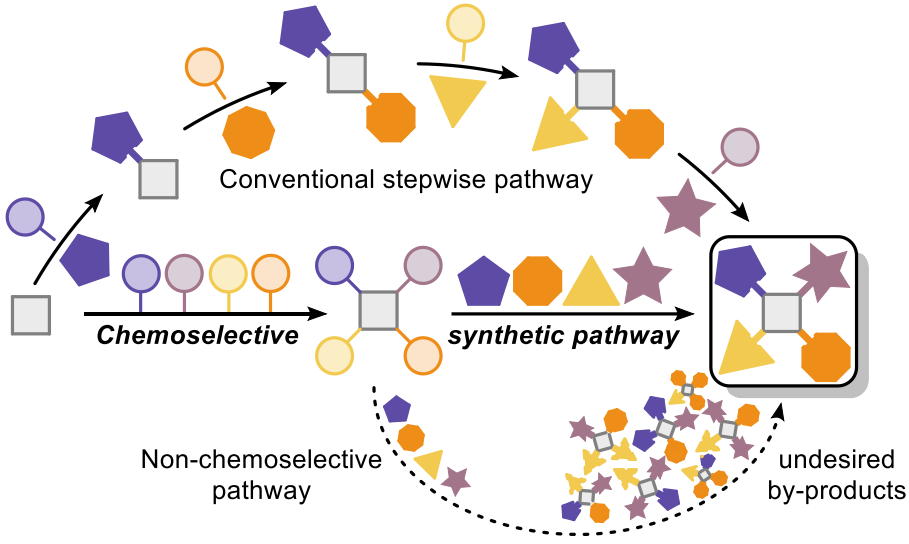

Scheme 1.27 Pathways in synthesising a particular molecule

Palladium-catalysed cross-couplings commonly employ poly(pseudo)halogenated arenes (e.g., I, Br, Cl, OTf) as electrophiles for synthesising complex molecules in iterative or sequential cross-coupling strategies.[40–41] Early studies in the 1970s, such as work by Fitton and Rick, revealed the reactivity sequence of aryl(pseudo)halides in catalyst systems follows the order Ar−I > Ar−Br > Ar−Cl. This suggested the rate-determining step is carbon-halogen bond cleavage, enabling exploration of chemoselectivity between electrophiles.[42] The oxidative addition rates and

bond dissociation energies predominantly determine aryl(pseudo)halide reactivity. Aryl sulfonates exhibit a similar trend, with Ar−OTf > Ar−OTs > Ar−OMs. Depending on the system, Ar−Br reactivity can be comparable to Ar−OTf.[43] Overall, a general chemoselective sequence has been established: Ar−I > Ar−Br ≈ Ar−OTf > Ar−OFs > Ar−Cl > Ar−OTs > Ar−OMs, evolving with new aryl sulfonates and studies (Scheme 1.28).[43–48]

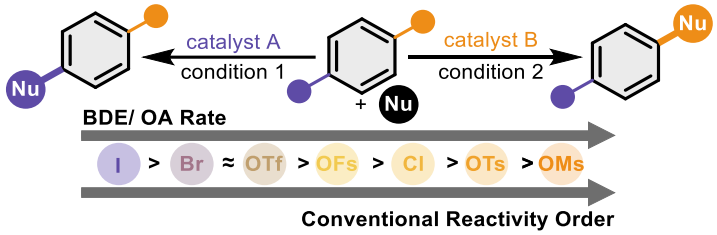

Scheme 1.28 Chemoselective coupling reactions and the reactivity sequence

Appropriate ligand selection is critical for controlling chemoselectivity in coupling reactions. Several studies have reported successful sequential chemoselective couplings exploiting this principle.

For example, Kim *et al.* recently demonstrated an effective sequential Suzuki−Miyaura coupling using bromo-2-sulfonyloxypyridines.[49] The C−Br site underwent selective reaction first, yielding monoarylpyridines. Subsequent coupling then allowed reaction with the remaining sulfonate group, producing unsymmetrical diarylpyridines. This approach proved effective in synthesising the anti-inflammatory drug Etoricoxib (Scheme 1.29). This example highlights catalysts' ability to regulate chemoselectivity and the efficiency of chemoselective cross-coupling procedures. Judicious ligand selection is a crucial tool for achieving desired chemoselectivity, as evidenced by these and other reports of successful sequential chemoselective couplings.

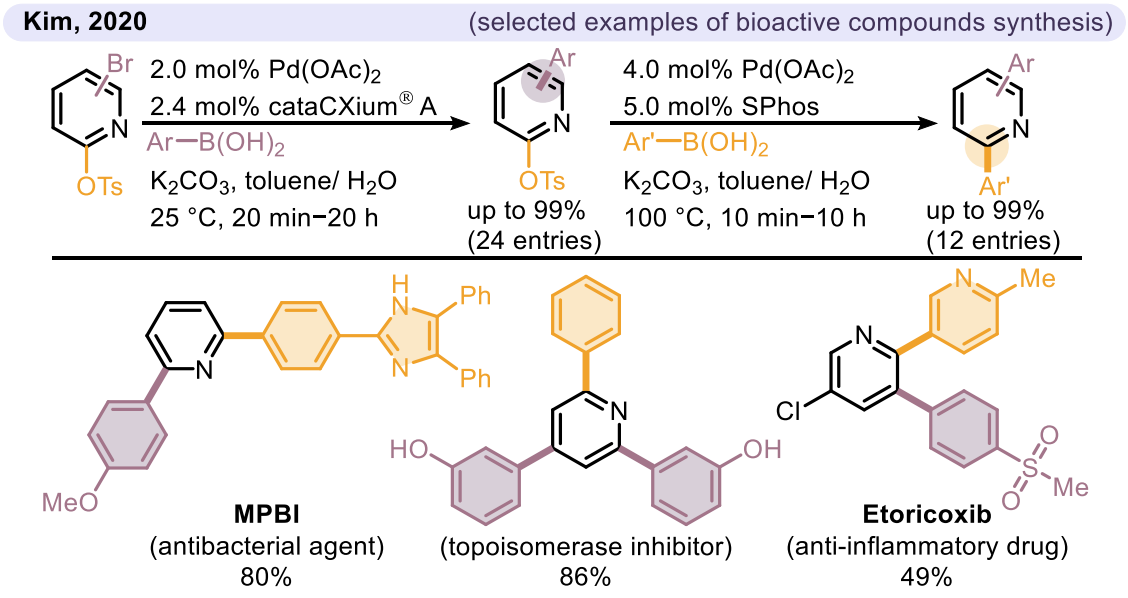

Scheme 1.29 Sequential Suzuki−Miyaura coupling and its applications

In 2016, Sigman *et al.* investigated the mechanistic properties of phosphine ligands in Suzuki−Miyaura couplings, providing insights into their potential applications.[50] Developing this concept further, Neufeldt *et al.* published a 2021 mini-review highlighting examples of chemodivergent couplings between electrophiles, offering valuable insights into factors governing chemoselectivity.[51] More recently, researchers have reported a reversal of the conventional chemoselectivity order in Pd-catalysed couplings of (poly)halogenated aryl triflates. This suggests a need to more thoroughly review ligand design principles and the rationale behind observed ligand activities.[52–55] These studies underscore the importance of understanding ligand properties and their impact on reaction outcomes. Continued investigation of ligand structure-mechanism-selectivity relationships will be crucial for advancing cross-coupling transformations.

In addition to catalysts, solvents, and additives, the intrinsic electronic properties of polyhalogenated heteroarenes can also affect chemoselectivity.[55–59] This section will focus on chemoselective Pd-catalysed couplings of the most common aryl (pseudo)halides: bromides, triflates, and chlorides.

Drawing from a recent mini-review, selected examples will highlight the impacts of ligand properties on chemoselectivity in these transformations.[60] Understanding the impact of ligand properties is crucial for designing efficient and selective Pd-catalysed couplings. The discussed examples will provide valuable insights to guide future advancements in this area.

1.4.1 Triaryl phosphines

Triphenylphosphine (PPh_3) is a widely used ligand in Pd-catalysed reactions due to its low cost, easy handling, and stability. The Pd/PPh_3 system generally exhibits a bias towards activating aryl triflates, enabling either bromo- or *O*-triflyl-selective products, though selectivity may be poor in some cases.

For example, Petrakis found the Pd/PPh_3 system gave a 3: 1 mixture favouring the *O*-triflyl product with 3-bromophenyl triflate.[61] Blum also observed a preference for *O*-triflyl-selective methylation.[62] However, the bromo-selectivity of Pd/PPh_3 can be tuned by adjusting conditions like nucleophile, solvent, and additives (Scheme 1.30).[63–64] These modifications can shift the chemoselectivity to favour the desired bromo-selective product. So, while the Pd/PPh_3 system shows an intrinsic bias towards *O*-triflyl selectivity, its selectivity can be modulated through careful optimisation.

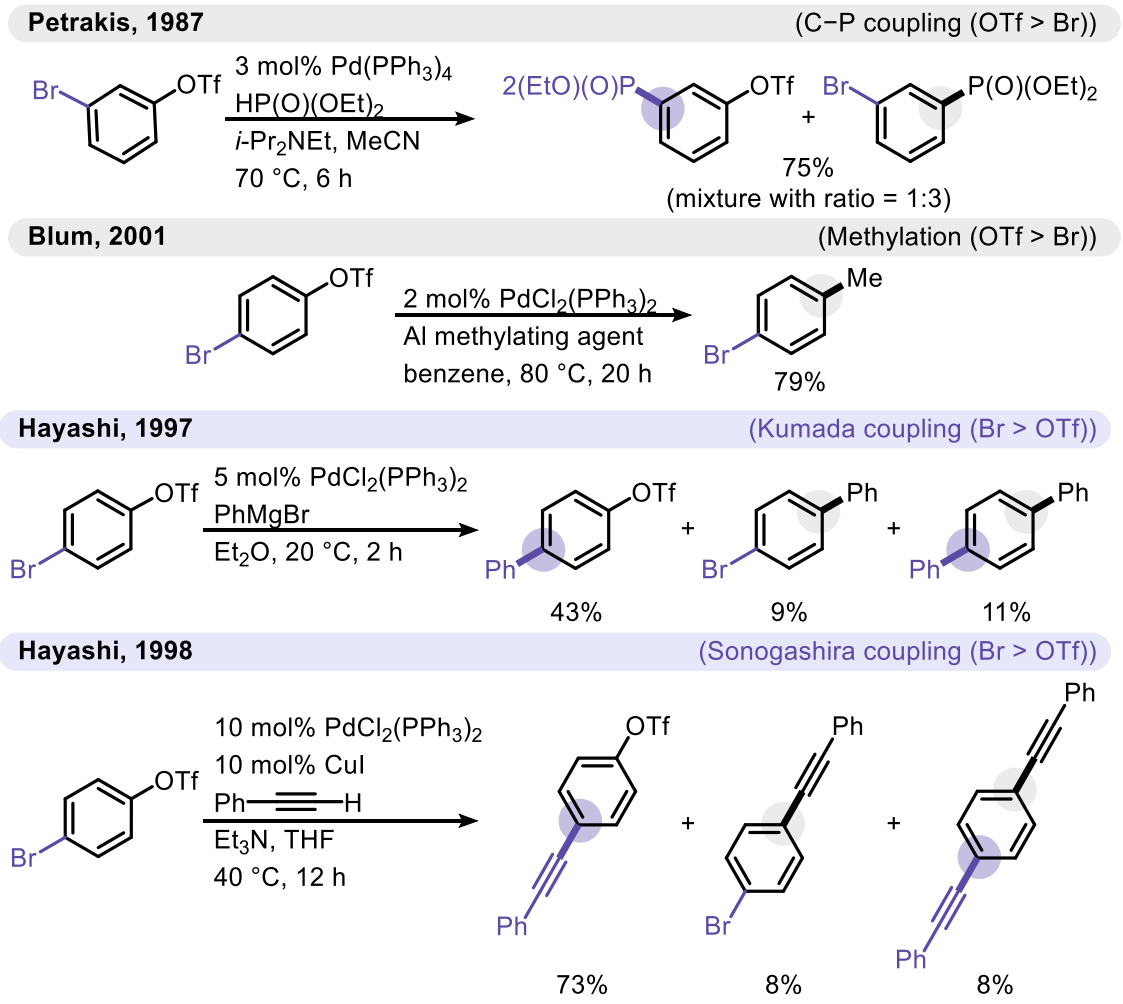

Scheme 1.30 Chemoselective couplings of bromophenyl triflates using PPh_3

Building on previous work, Brown's group found the choice of nucleophile significantly impacted the chemoselectivity of the Pd/PPh_3 system with aryl bromides versus triflates.[65] Using

a boronic acid nucleophile could invert the inherent *O*-triflyl selectivity to favour the bromo-selective product instead. Brown proposed the boronic acid's strong affinity for the bromide anion facilitated activation of the aryl bromide, enabling the Pd/PPh_3 catalyst to preferentially form the bromo-selective product (Scheme 1.31).[65–69] These examples demonstrate how the nucleophile can modulate the chemoselectivity of Pd-catalysed couplings of aryl halides and triflates, in contrast to the typical *O*-triflyl selectivity bias of the Pd/PPh_3 system.

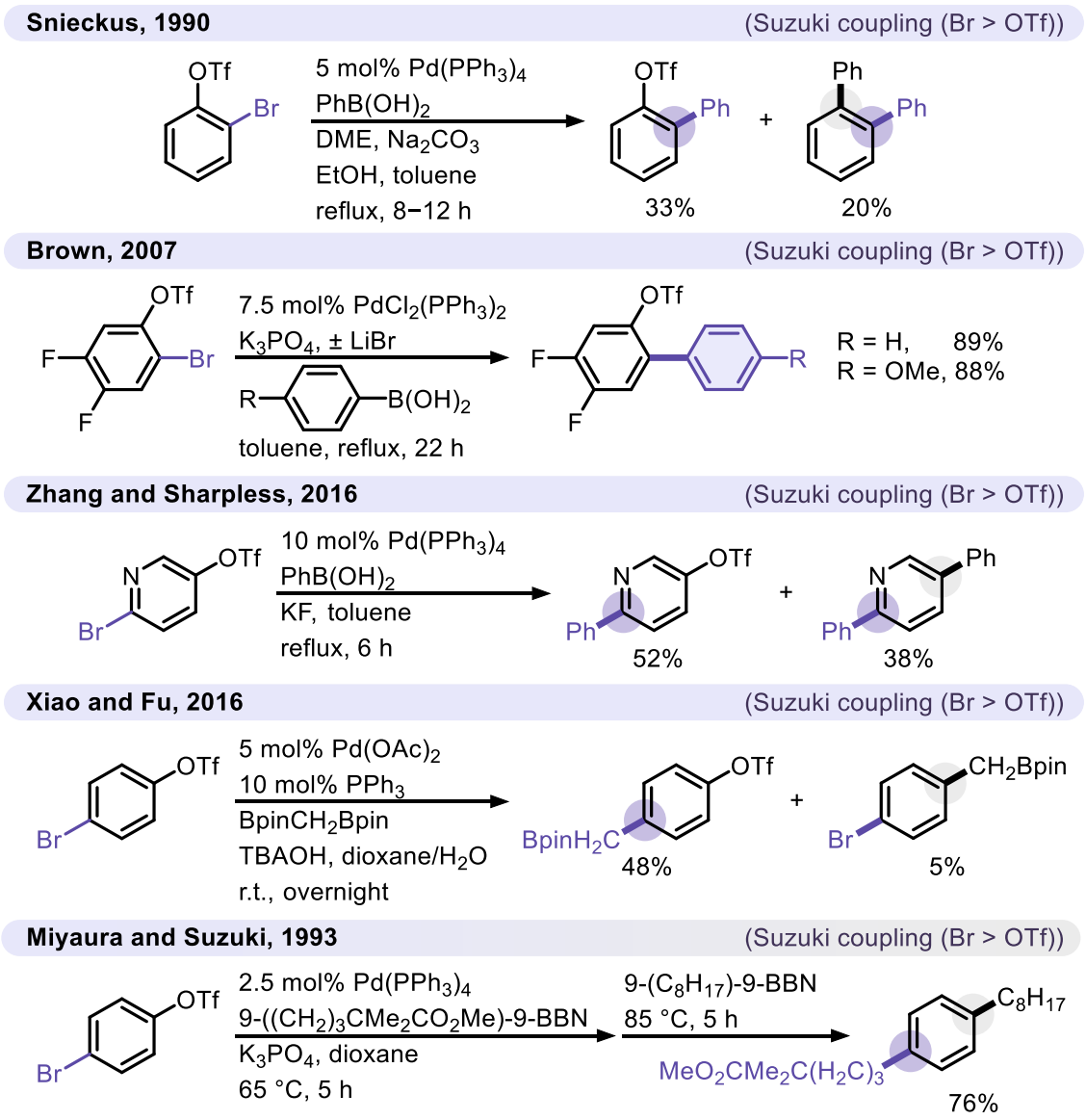

Scheme 1.31 Chemoselective Suzuki−Miyaura coupling of bromoaryl triflates using PPh_3

The Pd/PPh_3 catalyst strongly prefers activating aryl triflates over aryl chlorides. For instance, Huth[70] and Fu[68] found only aryl triflates reacted successfully (Scheme 1.32). This may be because the Pd/PPh_3 system lacks the activity to effectively activate aryl chlorides, resulting in exclusive *O*-triflyl-selectivity. Multiple studies demonstrate this inherent bias.[61–62,71–78] In short, the Pd/PPh_3 catalyst heavily favours aryl triflates over the less reactive aryl chlorides.

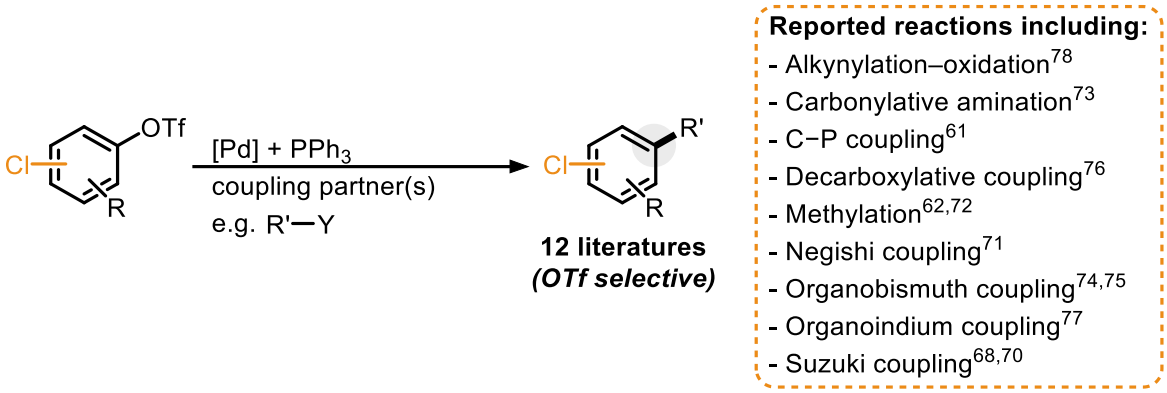

Scheme 1.32 Chemoselective Suzuki–Miyaura coupling of chloroaryl triflates using PPh_3

Solvents and additives can significantly impact chemoselectivity in Pd-catalysed couplings, beyond just substrate effects. Stille reported in 1987 that the Pd/PPh_3 catalyst showed high *O*-triflyl-selectivity for coupling 4-bromophenyl triflate with an organotin in dioxane.[79] However, using DMF with LiCl enhanced both yield and selectivity.[79] Switching to dioxane instead inverted the selectivity to favour the bromo-product (Table 1.1).[79]

Söderberg *et al.* later reconfirmed these solvent effects, though with lower conversions.[80] They proposed polar, strongly coordinating solvents like DMF with LiCl at room temperature promote aryl bromide activation, while polar, weakly coordinating solvents at higher temperatures favour aryl triflates (Table 1.1).[80]

Table 1.1 Stille coupling of bromophenyl triflates with ethenyl tributyltin using PPh_3

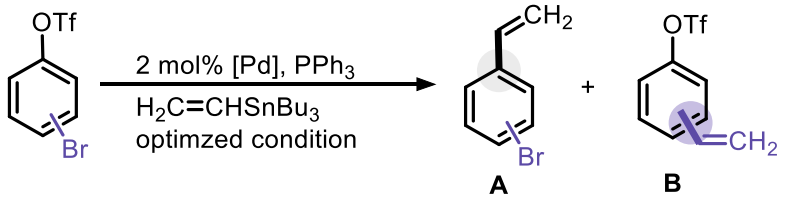

Reference	Br	[Pd]	Solvent	Additive	Temp.	Time	Yield	A: B
Stille, 1987[79]	4-Br	$Pd(PPh_3)_4$	dioxane	LiCl	98 °C	7 h	75%	1: 6
	4-Br	$PdCl_2(PPh_3)_2$	DMF	LiCl	24 °C	18 h	77%	100: 0
	4-Br	$Pd(PPh_3)_4$	dioxane	---	98 °C	2.5 h	77%	1: 33
Söderberg, 2018[80]	4-Br	$Pd(PPh_3)_4$	dioxane	---	reflux	24 h	n.d.	1: >30
	4-Br	$Pd(dba)_2$	dioxane	---	reflux	24 h	30%	1: >30
	3-Br	$Pd(dba)_2$	dioxane	---	reflux	24 h	34%	1: 30
	2-Br	$Pd(dba)_2$	dioxane	---	reflux	24 h	5%	1: >30
	4-Br	$PdCl_2(PPh_3)_2$	DMF	LiCl	24 °C	24 h	n.d.	6.7: 1
	3-Br	$PdCl_2(PPh_3)_2$	DMF	LiCl	24 °C	24 h	---	6.3: 1
	2-Br	$PdCl_2(PPh_3)_2$	DMF	LiCl	24 °C	24 h	n.d.	5.9: 1

Limited examples using other triarylphosphines like P(*o*-tolyl)$_3$ and P(*p*-tolyl)$_3$ have also been reported, showing bromo-selectivity with Pd/P(*o*-tolyl)$_3$ and *O*-triflyl-selectivity with Pd/P(*p*-tolyl)$_3$ (Scheme 1.33).[81–83]

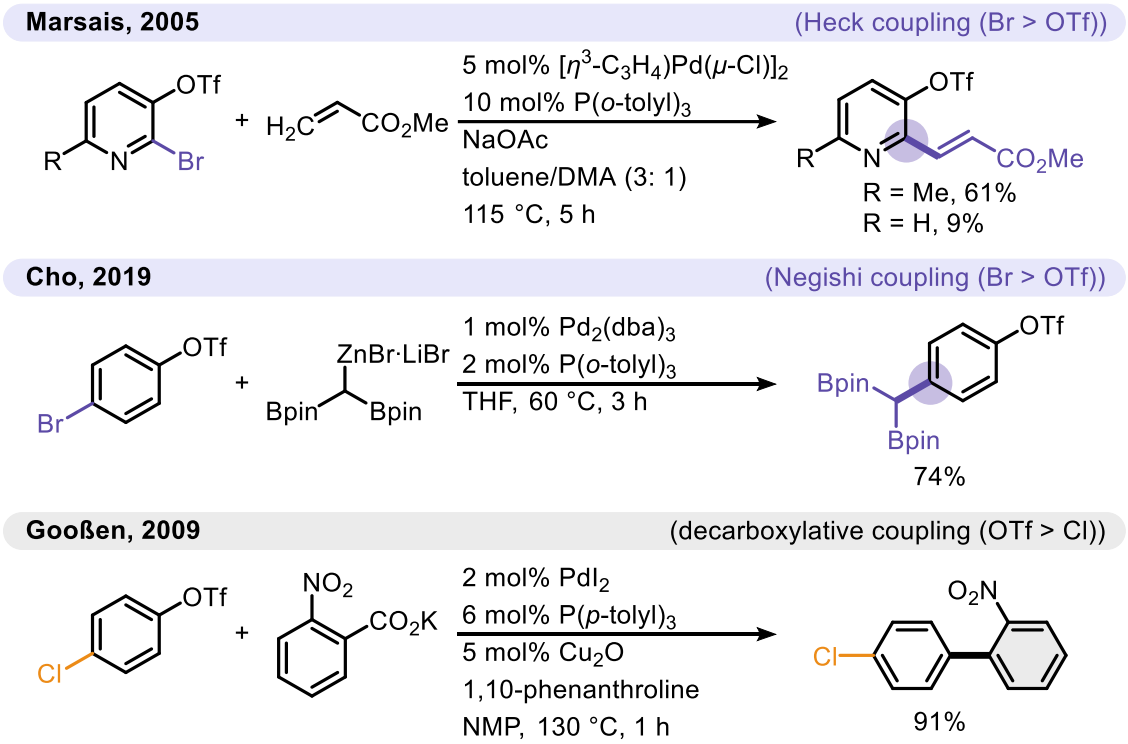

Scheme 1.33 Chemoselective coupling reactions using P(*o*-tolyl)$_3$ or P(*p*-tolyl)$_3$

1.4.2 Trialkyl phosphines

Examples using PCy_3 in chemoselective cross-coupling are less common than those with PPh_3 and P(*t*-Bu)$_3$. However, some key findings have been reported. In 2000, Fu described the first chemoselective Pd/PCy_3-catalysed Suzuki−Miyaura coupling, noting the PCy_3 ligand is less electron-rich and bulky than the more commonly used P(*t*-Bu)$_3$.[84] Interestingly, 4-chlorophenyl triflate gave an *O*-triflyl-selective product with Pd/PCy_3, contrasting the outcome with Pd/P(*t*-Bu)$_3$. This suggests ligand substituents might be feasible to alter chemoselectivity.

Progressing from this basis, Molander *et al.* in 2005 also observed chemoselective Pd/PCy_3-catalysed couplings.[85] With 4-bromophenyl triflate, a bromo-selective product formed, but 4-chlorophenyl triflate gave the *O*-triflyl-selective product — aligning with the typical Br > OTf > Cl reactivity trend (Scheme 1.34).[85]

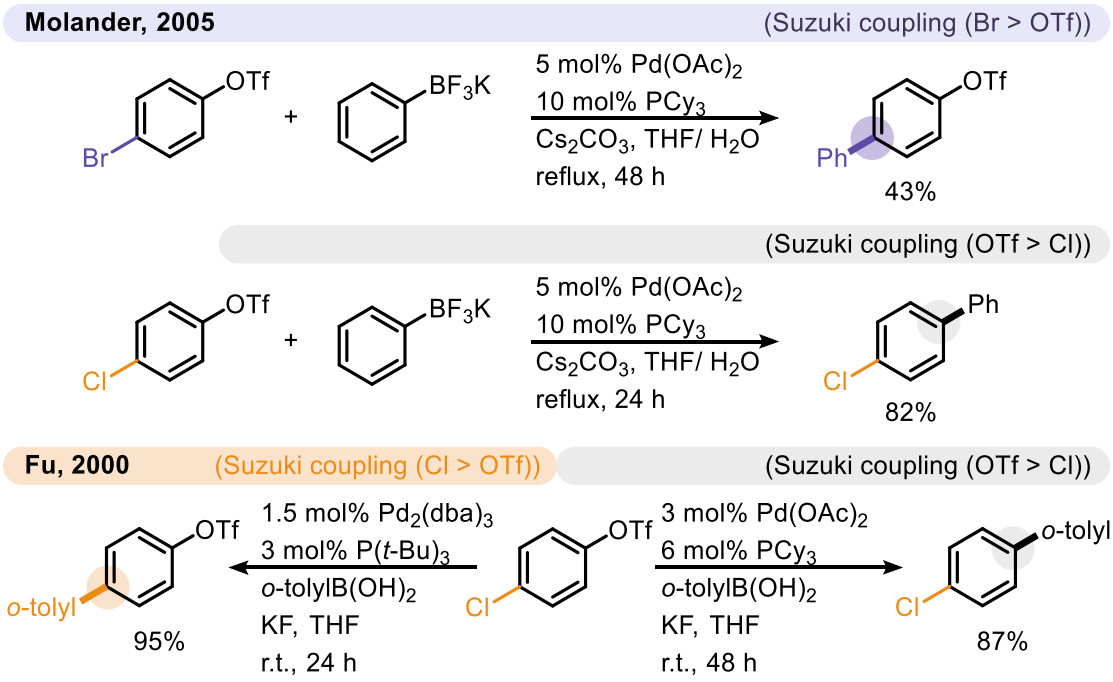

Scheme 1.34 Chemoselective Suzuki−Miyaura coupling of haloaryl triflates using PCy_3

Littke and Fu reported a general Pd/P(*t*-Bu)$_3$-catalysed approach to chemoselective Suzuki−Miyaura couplings in 2000, presenting the first chloro-selective coupling with chloroaryl triflates.[84] Their investigations revealed the chemoselectivity order: I > Br > Cl > OTf.[84] This selectivity trend (e.g., Br > OTf) has been corroborated across diverse coupling reactions like Suzuki−Miyaura,[65] Heck,[86] and carbonylative amination (Table 1.2).[87] The ability to tune chemoselectivity by catalyst and conditions has been a key focus, enabling more selective and efficient cross-couplings. The work by Littke, Fu, and others has laid important groundwork in this area.

Table 1.2 Various chemoselective coupling reactions with bromophenyl triflates using P(*t*-Bu)$_3$

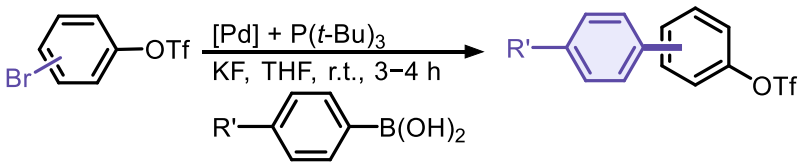

Reference	Br	[Pd]	P(*t*-Bu)$_3$	R'	Yield
Fu, 2000[84]	4-Br	0.5 mol% $Pd_2(dba)_3$	1.2 mol%	H	98%
Brown, 2007[65]	3-Br	1.5 mol% $Pd(dba)_2$	3.6 mol%	H	80%
	3-Br	0.5 mol% $Pd(dba)_2$	1.2 mol%	OMe	76%

Fu, 2001 (Heck coupling (Br > OTf))

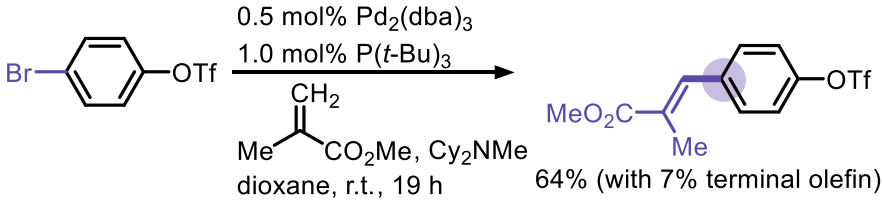

64% (with 7% terminal olefin)

Jiao and Wu, 2017 (carbonylative amination (Br > OTf))

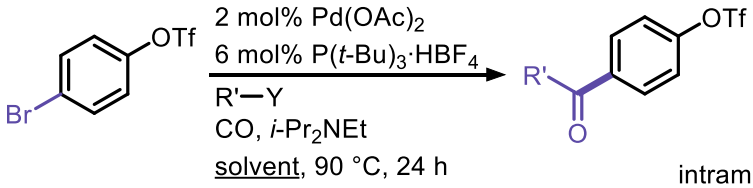

intramolecular competition

Entry	Solvent	R'—Y	Ratio (react at Br: OTf)	Isolated Yield
1	toluene	morpholine	>99: 1	89%
2	DMSO	morpholine	>99: 1	40%
3	toluene	4-$BrPhNH_2$	---	38%

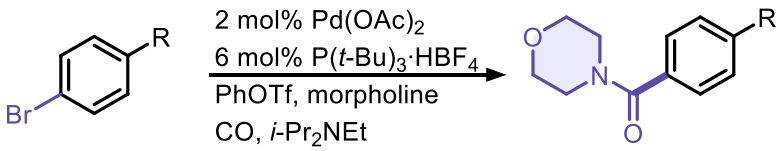

intermolecular competition

Entry	R	Ratio (react at Br: OTf)	Isolated Yield
4	Me	>99: 1	85%
5	Cl	>99: 1	94%

In 2010, Schoenebeck and Houk's DFT study provided insights into the chemoselectivity of Pd-catalysed cross-couplings.[88] Their calculations suggested the ligation state of the palladium catalyst (mono- versus bisligated) was pivotal. For monoligated [Pd(L)] complexes, transition states favoured C−Cl bond activation. However, this contradicted Fu's earlier finding that Pd/PCy_3 selectively coupled at C−OTf.[84]

Further DFT analysis revealed that for bisligated [$Pd(PCy_3)_2$] complexes, the transition state for C−OTf insertion became more accessible, especially accounting for $Pd(L)_2$ dissociation.[89] In

contrast, the [Pd(P(*t*-Bu)$_3$)$_2$] transition state could not be located (Scheme 1.35). Based on these results, Schoenebeck and Houk proposed a "ligation state hypothesis" — monoligated Pd(L) preferentially reacts at C−Cl, while bisligated Pd(L)$_2$ favours C−OTf.[88] This provided key mechanistic insights into the chemoselectivity of these cross-couplings.

Schoenebeck and Houk, 2010

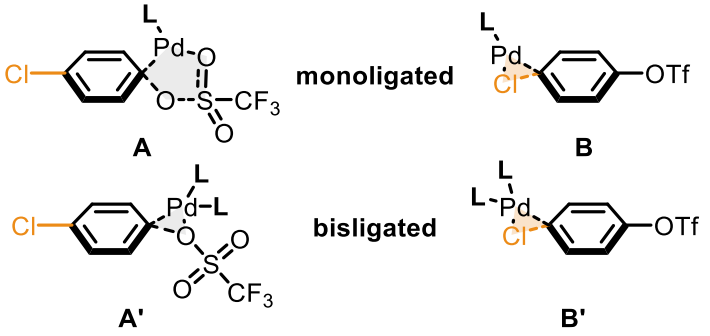

PdL	ΔΔG‡ (B-A)
PdPCy$_3$	-3.6
PdP(*t*-Bu)$_3$	-5.8

PdL$_2$	ΔΔG‡ (B'-A')
Pd(PCy$_3$)$_2$	+4.7
Pd(P(*t*-Bu)$_3$)$_2$	n.d.

Scheme 1.35 DFT studies on monoligated/ bisligated Pd species

In 2016, Sigman *et al.* parameterised phosphine ligands to probe mechanistic pathways and predict chemoselectivity in Pd-catalysed Suzuki−Miyaura couplings.[50] Computational results showed the reaction-product ratios aligned with the parameterised model. Only 6 ligands preferred C−Cl over C−OTf activation, with *tert*-butyl or 1-adamantyl groups being important features (Scheme 1.36).[50] However, *t*-BuJohnPhos showed selectivity for triflates, explained by a hemilabile Pd-arene interaction in the bisligated complex.[12] Overall, the site-selectivity of oxidative addition depended on the phosphine. Sterically bulky ligands favouring monoligated Pd promote C−Cl activation, while other phosphines stabilising bisligated Pd prefer C−OTf coupling.

Sigman, 2016

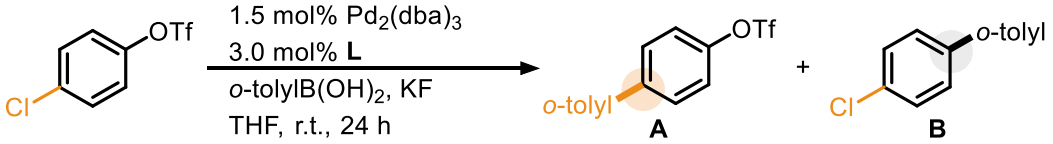

Ligand	ΔΔG‡ (B-A) (kcal/mol)	Ligand	ΔΔG‡ (B-A) (kcal/mol)	Ligand	ΔΔG‡ (B-A) (kcal/mol)
P(*t*-Bu)$_3$	-2.72	P(*i*-Pr)$_3$	1.02	*t*-BuJohnPhos	2.91
P(*t*-Bu)$_2$(*p*-CF$_3$Ph)	-1.46	P(*o*-tolyl)$_3$	1.42	P(*m*-tolyl)$_3$	3.12
P(*n*-Bu)(1-Ad)$_2$	-1.43	PCy$_3$	1.94	CyJohnPhos	3.32
PBn(1-Ad)$_2$	-1.35	PPhCy$_2$	2.08	PPh$_2$Et	3.57
P(*t*-Bu)(*i*-Pr)$_2$	-0.31	PPh$_2$*t*-Bu	2.36	PPh$_2$Me	3.70
P(*t*-Bu)$_2$Ph	-0.26	P(*n*-Bu)$_3$	2.40	PEt$_3$	3.75
P(cyclopentyl)$_3$	0.59	PPh$_3$	2.64	PPhMe$_2$	4.00

negative ΔΔG‡ :reaction at C−Cl is favoured.

positive ΔΔG‡ :reaction at C−OTf is favoured.

Scheme 1.36 Comparison of measured chemoselectivities using different ligands

In 2011, Schoenebeck *et al.* studied the unusual selectivity in Pd/P(*t*-Bu)$_3$-catalysed Suzuki−Miyaura couplings in polar solvents like DMF.[90] They proposed that DMF coordination to Pd promotes C−OTf oxidative addition in a bisligated Pd(P(*t*-Bu)$_3$)(DMF) complex, favouring activation at triflates over chlorides (Table 1.3). This helped explain the contradictory selectivity outcomes observed in these reactions, underscoring the importance of considering ligand-solvent interactions in Pd-catalysed cross-couplings.

Table 1.3 Chemoselective Suzuki−Miyaura coupling chlorophenyl triflates using P(*t*-Bu)$_3$

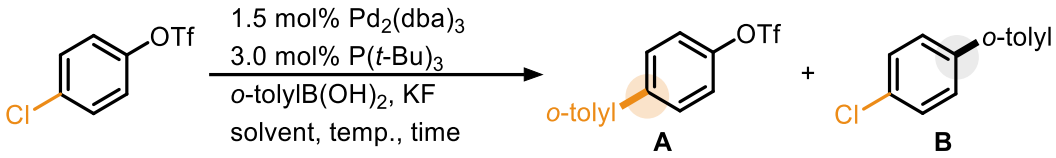

Reference	Solvent	Temp.	Time	A	B
Fu, 2000[84]	THF	r.t.	24 h	95%	---
Schoenebeck, 2011[90]	toluene	70 °C	48 h	70%	0%
	MeCN	r.t.	24 h	3%	74%
	DMF	r.t.	48 h	3%	22%

In 2020, Neufeldt *et al.* further explored the effect of solvents on the Pd/P(*t*-Bu)$_3$-catalysed Suzuki−Miyaura coupling selectivity.[56] Non-polar solvents like toluene and THF favoured C−Cl activation, while some polar solvents like DMSO and MeCN reversed this preference to C−OTf. However, not all polar solvents followed this trend — acetone and IPA still showed chloride selectivity despite their polarity (Table 1.4 and Table 1.5).[56] Neufeldt *et al.* concluded that the reversal of chloride/triflate selectivity is not solely determined by solvent polarity, but rather the specific coordinating ability of the polar solvents towards the palladium catalyst. Their work highlighted the complex interplay between ligands, solvents, and site-selectivity in Pd-catalysed cross-couplings.

Table 1.4 Chemoselective Suzuki−Miyaura coupling in various solvents

Neufeldt, 2020; Neufeldt, 2022

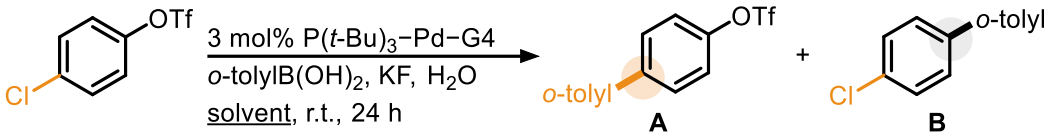

Entry	Solvent	A	B	Entry	Solvent	A	B	Entry	Solvent	A	B
1	dioxane	22%	n.d.	8	acetone	83%	2%	15	$(CH_2)_4SO_2$	44%	11%
2	toluene	76%	n.d.	9	EtOH	71%	n.d.	16	CH_2FCN	4%	10%
3	$CHCl_3$	11%	n.d.	10	MeOH	55%	2%	17	PhCN	9%	62%
4	THF	95%	n.d.	11	$MeNO_2$	84%	2%	18	NMP	9%	37%
5	DCM	65%	n.d.	12	CF_3CH_2OH	82%	1%	19	MeCN	2%	77%
6	$PhCF_3$	42%	n.d.	13	PC	71%	11%	20	DMF	9%	45%
7	IPA	94%	n.d.	14	H_2O	59%	n.d.	21	DMSO	1%	45%

Neufeldt *et al.* conducted a detailed study on the parameters affecting Cl versus OTf selectivity in Pd-catalysed Suzuki−Miyaura couplings in 2022.[58] They found that weakening the solvent's coordinating ability could erode triflate selectivity. For example, changing from strongly coordinating MeCN (1: 39 Cl: OTf) to weakly coordinating CH_2FCN (1: 2.5 Cl: OTf) (Table 1.4).[58] DFT calculations reconfirmed that DMF coordination to Pd/P(*t*-Bu)$_3$ promoted *O*-triflyl selectivity, as observed experimentally. Interestingly, raising the temperature from room temperature to 100 °C inverted the selectivity from triflate-favoured to chloride-favoured. The authors attributed this to changes in both entropic factors and potential transformation of the catalytic intermediate at elevated temperatures (Table 1.5).[58]

Table 1.5 Chemoselective Suzuki−Miyaura coupling under various conditions using P(*t*-Bu)$_3$

Neufeldt, 2020

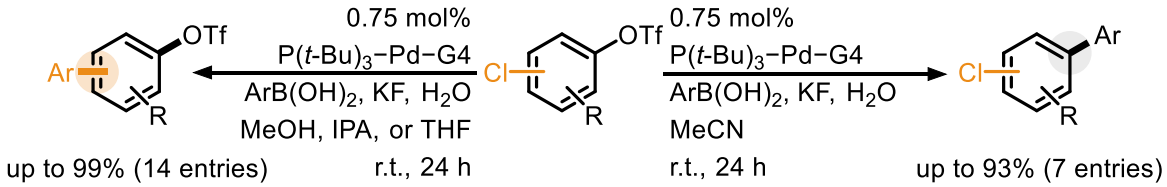

Neufeldt, 2022

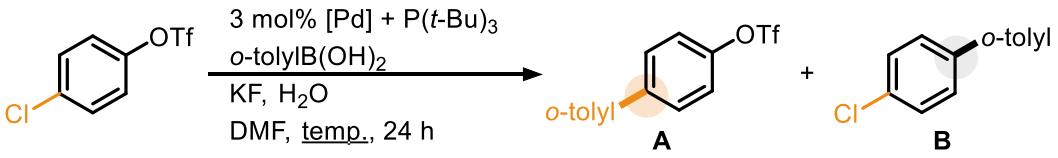

Entry	[Pd] + L	Temp.	A	B
1	3 mol% P(*t*-Bu)$_3$−Pd−G4	r.t.	10%	60%
2	3 mol% P(*t*-Bu)$_3$−Pd−G4	100 °C	21%	30%
3	0.75 mol% $Pd_2(dba)_3$ + 1.5 mol% $Pd(P(t\text{-}Bu)_3)_2$	r.t.	11%	67%
4	0.75 mol% $Pd_2(dba)_3$ + 1.5 mol% $Pd(P(t\text{-}Bu)_3)_2$	100 °C	33%	23%

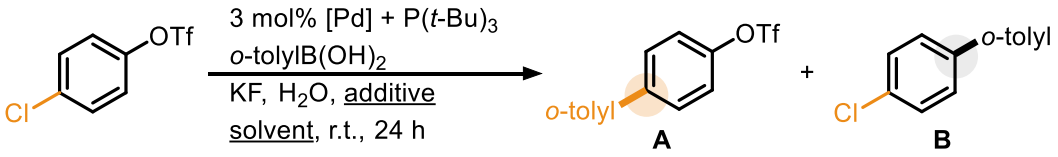

Entry	Solvent	Additive	A	B	Entry	Solvent	Additive	A	B
5	THF	---	74%	<1%	11	PC	---	71%	5%
6	THF	18-Crown-6	1%	76%	12	PC	18-Crown-6	1%	11%
7	THF	*n*-Bu_4NF	<1%	13%	13	IPA	---	87%	1%
8	THF	*n*-Bu_4NCl	4%	69%	14	IPA	18-Crown-6	0%	3%
9	THF	*n*-Bu_4NBr	2%	91%	15	DMF	---	10%	61%
10	THF	*n*-Bu_4NOTf	70%	3%	16	DMF	18-Crown-6	0%	47%

This comprehensive mechanistic study continued to elucidate the complex interplay of solvents, ligands, and conditions governing site-selectivity in Pd cross-couplings. In addition to solvent effects, Neufeldt *et al.* found that anionic additives could also impact Cl/OTf selectivity (Table 1.5).[58]

Previous studies had shown oxidative addition of PhOTf at $[Pd(L)(X)]^-$ with quaternary ammonium halides. DFT suggested $[Pd(P(t\text{-}Bu)_3)(X)]^-$ complexes may govern triflate selectivity in some cases.[58] Neufeldt's team discovered that increasing availability of free fluoride, via additives like crown ethers or quaternary ammonium salts, facilitated triflate activation. This was attributed to a mechanism involving the $[Pd(P(t\text{-}Bu)_3)(X)]^-$ intermediate, where higher "naked" anion concentrations promoted triflate reactivity.[58] This work provided new evidence for the critical role of solvent-ligand interactions in determining site-selectivity in Pd cross-couplings.

In 2002, Littke and Fu reported the use of a palladium/P(*t*-Bu)$_3$ ligand system as a general catalyst system for Stille coupling reactions.[91] They showed this system could achieve excellent yields under mild conditions, including the selective formation of chloro-substituted products using 4-chlorophenyl triflate (Table 1.6). Extending this idea, in 2011, a study by Schoenebeck proposed that using KF or CsF as the base would promote the formation of an anionic palladium intermediate, leading to enhanced selectivity for triflates in the Pd/P(*t*-Bu)$_3$ system (Table 1.6).[90] A similar trend was observed, though the reactions with chlorides exhibited higher reactivity upon heating.[58]

Table 1.6 Chemoselective Stille coupling with various conditions using P(*t*-Bu)$_3$

Fu, 2002 (Stille coupling (Cl > OTf))

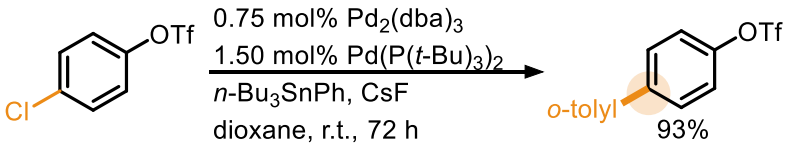

Schoenebeck, 2011

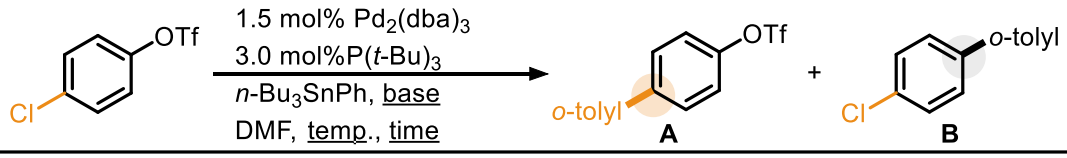

Entry	Base	Temp.	Time	A	B
1	KPF_6	r.t.	38 h	47%	8%
2[a]	KPF_6	100 °C	7 days	88%	9%
3	KF	r.t.	38 h	30%	51%
4[b]	CsF	r.t.	38 h	21%	79%

[a]0.75 mol% $Pd_2(dba)_3$ and 1.5 mol% P(*t*-Bu)$_3$ were used. [b]Me_3SnPh was used.

Neufeldt, 2022

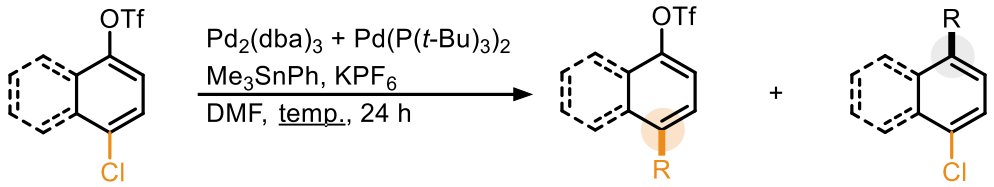

Entry	$Pd_2(dba)_3$	$Pd(P(t\text{-}Bu)_3)_2$	Skeleton	Temp.	A	A'	B	B'
5	0.75 mol%	1.50 mol%	benzene	r.t.	2%	2%	4%	3%
6	0.75 mol%	1.50 mol%	benzene	100 °C	39%	20%	3%	4%
7	1.5 mol%	3.0 mol%	naphthalene	r.t.	1%	3%	9%	42%
8	1.5 mol%	3.0 mol%	naphthalene	100 °C	13%	33%	4%	12%

Previous work had also examined the reactivity of Pd(0)(P(*i*-Pr)(*t*-Bu)$_2$)$_2$ in Suzuki−Miyaura couplings (Table 1.7), finding P(*i*-Pr)(*t*-Bu)$_2$ favoured a monoligated Pd(0) species as the active catalyst, similar to P(*t*-Bu)$_3$.[92] Modulating the ligand equivalents allowed tuning the reactivity, with P(*i*-Pr)(*t*-Bu)$_2$ mimicking the behaviour of both PCy$_3$ and P(*t*-Bu)$_3$ in these cross-coupling reactions.

Table 1.7 Chemoselective Suzuki−Miyaura coupling with various amounts of ligands

Schoenebeck, 2014

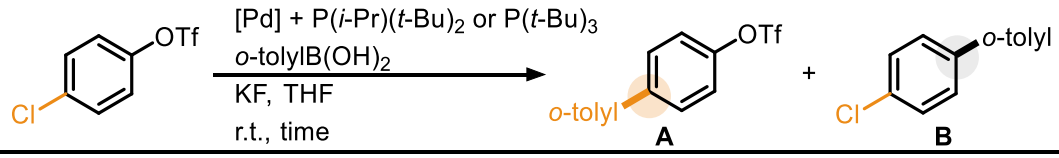

Entry	[Pd] + L	Time	A	B
1	1.5 mol% $Pd(P(i\text{-}Pr)(t\text{-}Bu)_2)_2$	125 h	15%	---
2	1.5 mol% $Pd_2(dba)_3$ + 3 mol% $P(i\text{-}Pr)(t\text{-}Bu)_2$	24 h	86%	---
3	3 mol% $Pd(P(i\text{-}Pr)(t\text{-}Bu)_2)_2$ + 30 mol% $P(i\text{-}Pr)(t\text{-}Bu)_2$	125 h	---	10%
4	1.5 mol% $Pd_2(dba)_3$ + 3 mol% $P(t\text{-}Bu)_3$	169 h	---	5%

In 2024, Qiu *et al.* reported the successful development of a chemoselective C−N coupling reaction involving poly(pseudo)halogenated aromatic hydrocarbons and amines (Scheme 1.37). Using a $PdCl_2/P(t\text{-}Bu)_3/NaBAr^F_4$ catalyst system, the conventional reactivity sequence (Ar−Br ≈ Ar−OTf ≈ Ar−OTs > Ar−Cl) was reversed, yielding the order Ar−Br > Ar−Cl > Ar−OTf/OTs. Under the optimized conditions, 29 coupling reactions were established, demonstrating excellent chemoselectivities.[93]

Qiu, 2024 (selected examples of Buchwald−Hartwig amination ((Cl > OTf))

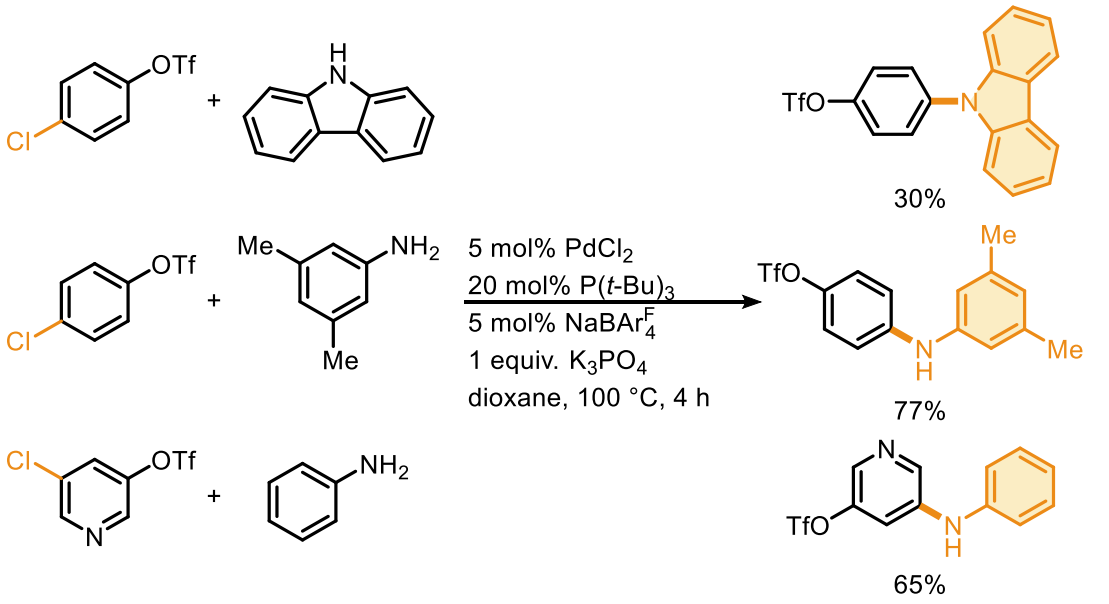

Scheme 1.37 Chemoselective C−N amination of chloroaryl triflates using $P(t\text{-}Bu)_3$

1.4.3 Pd(I) dimers

Moore *et al.* reported using $Pd_2(\mu\text{-2-methylallyl})(\mu\text{-Cl})(P(t\text{-Bu})_3)_2$ as the catalyst for Sonogashira reactions, which selectively yielded bromo-substituted products over aryl triflates, regardless of the steric and electronic properties of the substrates (Scheme 1.38).[94] This selective reactivity was observed across a range of tested substrates, consistently favouring the C−Br bond over other functional groups. Notably, the methodology maintained its effectiveness even when scaled up to the gram scale.

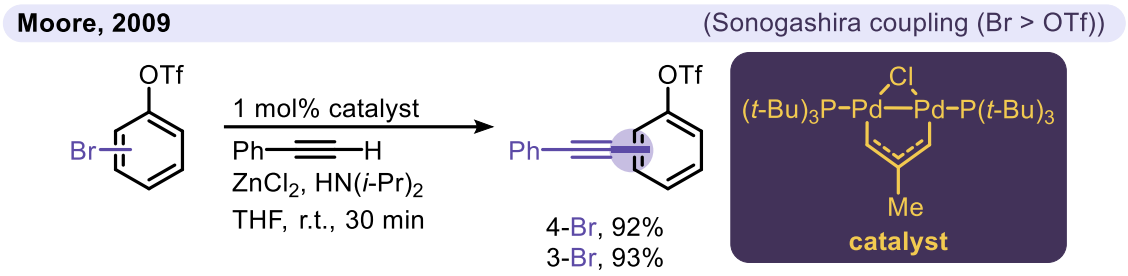

Scheme 1.38 Chemoselective Sonogashira coupling of bromoaryl triflates

Schoenebeck *et al.* reported an improved Pd(I) dimer catalyst system in 2017 that exhibited chemoselective reactivity.[95–96] The catalyst, featuring a Pd−I−Pd bridge and a $P(t\text{-Bu})_3$ ligand, was selectively effective for Negishi and Kumada couplings of aryl bromides over aryl triflates (Scheme 1.39). Computational studies supported the preference for oxidative addition at the C−Br site.

The same group later applied this catalyst to chemoselective alkylation and arylation of aryl triflates, rather than aryl chlorides, in a manner independent of substrate electronics or sterics.[97] The air/moisture-stable Pd(I) dimer enabled rapid, highly selective functionalisation of the three coupling sites in the order C−Br > C−OTf > C−Cl, with excellent yields (Scheme 1.39). This technology provides precise control over selectivity, potentially enabling automated approaches to rapidly access molecular complexity.

Schoenebeck *et al.* also developed a chemoselective C−S bond formation method using this dinuclear Pd(I) dimer catalyst, $[Pd(\mu\text{-I})P(t\text{-Bu})_3]_2$, that avoided generating toxic Pd complexes.[98] This approach enabled thiolations of a wide range of polyhalogenated arenes, even selectively in the presence of C−Br, C−OTf, and C−Cl groups (Scheme 1.39) — a level of chemoselectivity not previously reported. Importantly, this air- and moisture-stable catalyst could be recovered and recycled while retaining high performance. Such chemoselective strategies are valuable for synthesising densely functionalised or complex molecules relevant to pharmaceuticals and materials.

Schoenebeck's Pd(I) dimer catalyst system was also applied to the preparation of vinyl cyclopropanes via Negishi cross-coupling, showcasing its broad chemoselectivity.[99] The installation of cyclopropyl groups can be challenging, but the Pd(I) dimer catalyst selectively activated triflates over chlorides in these transformations (Scheme 1.39).

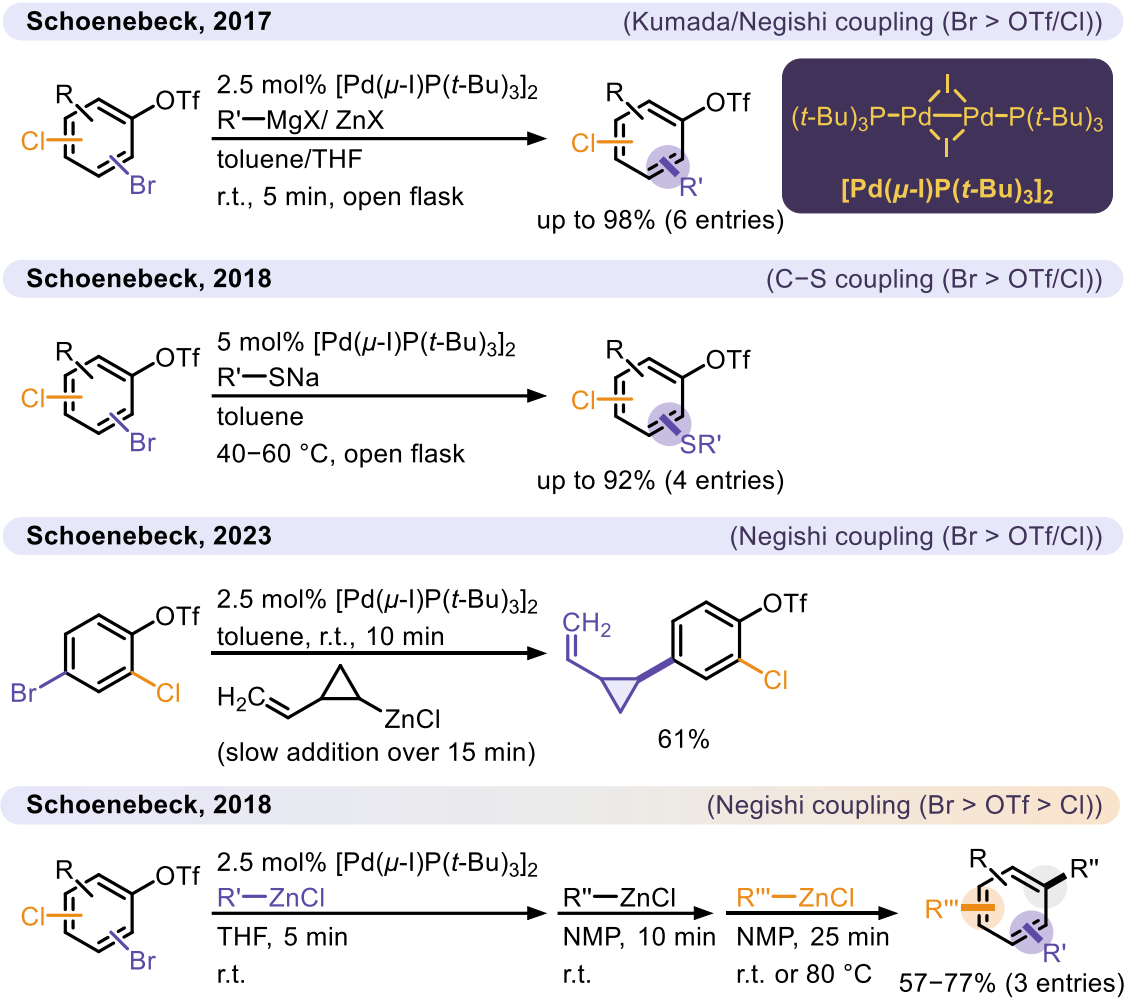

Scheme 1.39 Chemoselectivity of haloaryl triflates in various reactions using [Pd(μ-I)P(*t*-Bu)$_3$]$_2$

In addition to the Kumada,[95–96] Negishi,[95–97] Heck,[100] and C–S bond coupling reactions[98] reported earlier, Schoenebeck's group subsequently developed a method for α-arylation of esters and ketones using their bench-stable Pd(I) dimer catalyst, [Pd(μ-I)P(*t*-Bu)$_3$]$_2$, in 2018.[101] This approach utilised a bulky lithium base in toluene and exhibited a chemoselectivity order of I > Br > OTf > Cl (Scheme 1.40).

Building upon this foundation, in 2020, the same group developed a method to couple sterically hindered bromo-adamantyl arenes using the Pd(I) dimer catalyst, selectively favouring the activation of aryl bromides over triflates (Scheme 1.40).[102] Computational analysis suggested attractive dispersion interactions between the adamantyl and *tert*-butyl groups could offset the steric effects, enabling the desired reactivity.

Schoenebeck, 2017 (Kumada/Negishi coupling (Br > OTf))

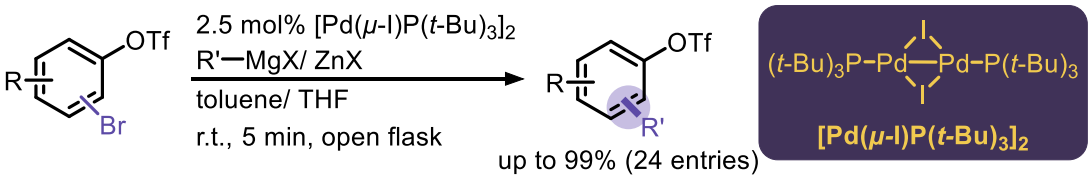

Schoenebeck, 2017 (Heck coupling (Br > OTf))

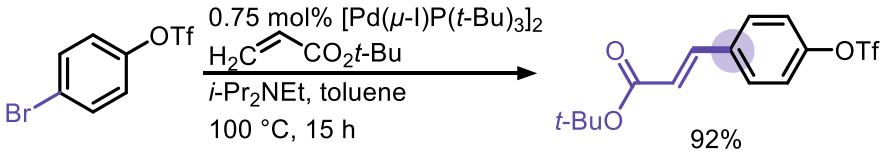

Schoenebeck, 2018 (C–S coupling (Br > OTf))

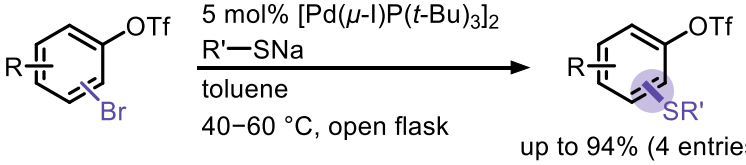

Schoenebeck, 2018 (α-arylation (Br > OTf))

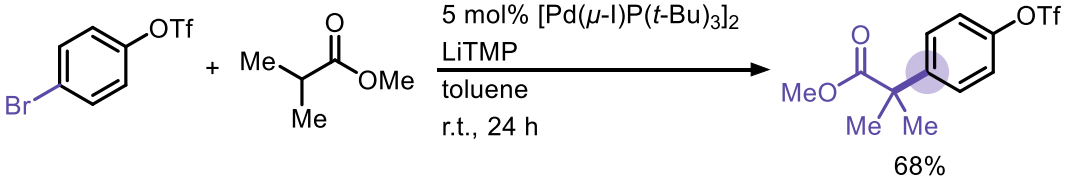

Schoenebeck, 2020 (Negishi coupling (Br > OTf))

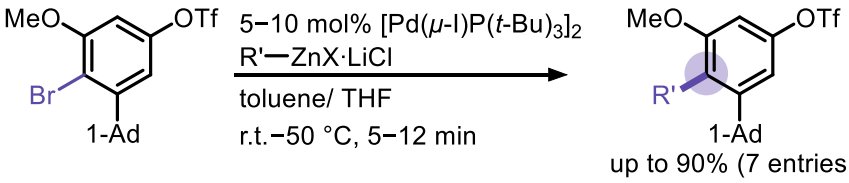

Schoenebeck, 2018 (sequential Negishi coupling (Br > OTf))

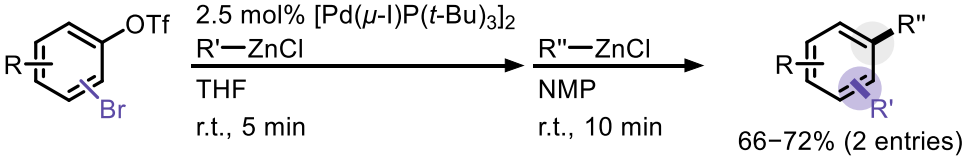

Schoenebeck, 2018 (Negishi coupling (OTf > Cl))

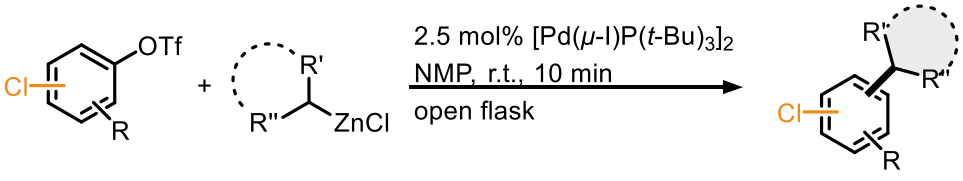

(sequential Negishi coupling (OTf > Cl))

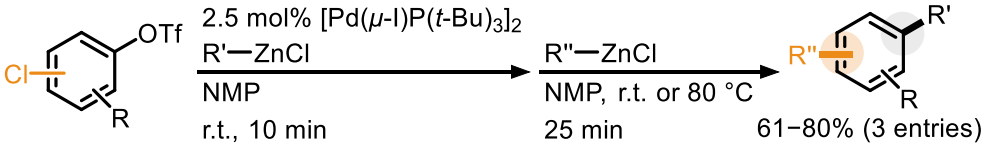

Scheme 1.40 Coupling reactions with haloaryl triflates using [Pd(μ-I)P(*t*-Bu)$_3$]$_2$

Schoenebeck's group developed a new Pd(I) dimer catalyst, [Pd(μ-I)PCy$_2$(*t*-Bu)]$_2$, featuring a PCy$_2$(*t*-Bu) ligand.[103] This catalyst was applied to olefin migration reactions, enabling the synthesis of styrenes and enamines with similar effectiveness and chemoselectivity as the earlier [Pd(μ-I)P(*t*-Bu)$_3$]$_2$ system (Scheme 1.41).

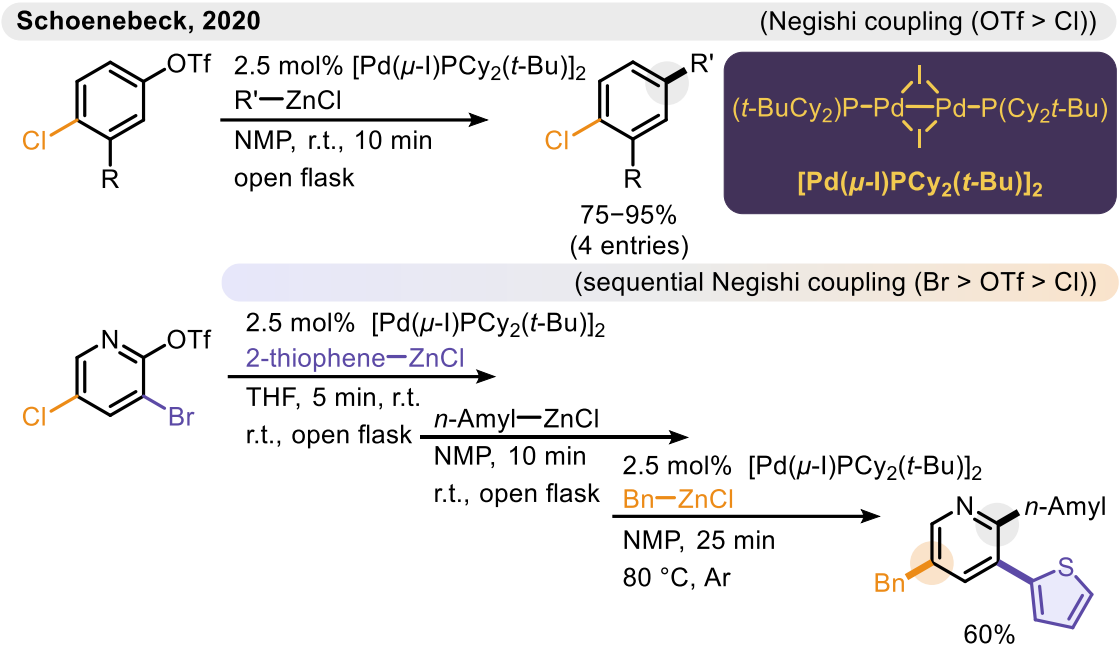

Scheme 1.41 Chemoselective Negishi coupling of haloaryl triflates using [Pd(μ-I)PCy$_2$(*t*-Bu)]$_2$

They also showed that air-stable [Pd(μ-I)PCy$_2$(*t*-Bu)]$_2$ enabled site-selective alkylation of polyhalogenated arenes. Within 10 minutes at room temperature, it selectively activated triflates over other halides, providing excellent branched-to-linear selectivity and up to 94% isolated yields (Scheme 1.42).[104] This rapid chain-walking reactivity was consistent with [Pd(μ-I)PCy$_2$(*t*-Bu)]$_2$'s efficacy in olefin migration.[103] The authors highlighted that subtle ligand modifications can significantly impact the reaction outcome while retaining benefits like air stability and speed.

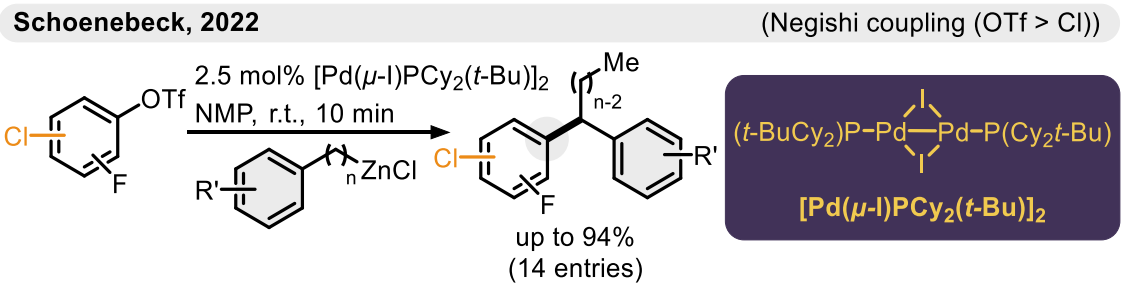

Scheme 1.42 Chemoselective Negishi coupling of chloroaryl triflates using [Pd(μ-I)PCy$_2$(*t*-Bu)]$_2$

1.4.4 Buchwald-type phosphines

Traditionally, aryl triflates have exhibited higher reactivity than aryl chlorides, with some exceptions. Many reports have shown that Buchwald-type ligands display greater selectivity towards triflates over chlorides and bromides. Buchwald-type *ortho*-biaryl phosphine ligands can be modified at the 2,4,6-positions to fine-tune their steric and electronic properties. The bottom aryl ring can also coordinate to the palladium centre via π-interactions, facilitating formation of the active 12e⁻ Pd(L) catalyst.[12]

It has been proposed that Buchwald-type ligands generate Pd(L) species,[105] but these systems predominantly exhibit selectivity for the triflate group. This deviates from computational predictions favouring C−Cl reactivity,[88] as Sigman *et al.* suggested the *ortho*-aryl substituent can obstruct a second coordination site.[106] This leads to selectivities similar to smaller phosphines, regardless of ligand concentration.[50]

Scheme 1.43 demonstrates the clear *O*-triflyl selectivity of palladium-Buchwald systems, which appears highly dominant and independent of solvents, temperatures, or nucleophiles.[107–125]

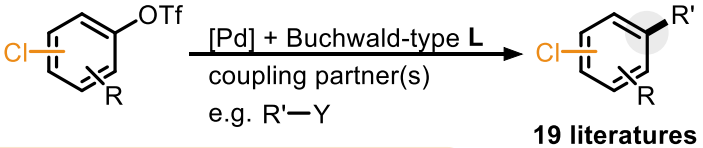

19 literatures
(OTf selective)

Buchwald-type ligands:

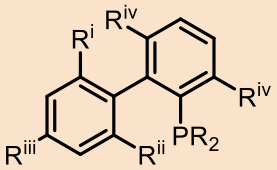

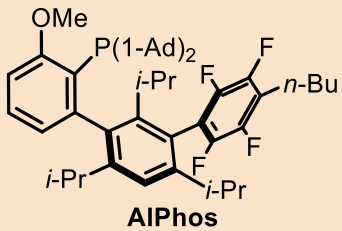

AlPhos

Name	R	R^i	R^{ii}	R^{iii}	R^{iv}
SPhos	Cy	OMe	OMe	H	H
XPhos	Cy	*i*-Pr	*i*-Pr	*i*-Pr	H
PhXPhos	Ph	*i*-Pr	*i*-Pr	*i*-Pr	H
BrettPhos	Cy	*i*-Pr	*i*-Pr	*i*-Pr	OMe
***t*-BuBrettPhos**	*t*-Bu	*i*-Pr	*i*-Pr	*i*-Pr	OMe
DavePhos	Cy	NMe_2	H	H	H
MePhos	Cy	Me	H	H	H
CPhos	Cy	NMe_2	NMe_2	H	H
RuPhos	Cy	O*i*-Pr	O*i*-Pr	H	H

Reported reactions including:
- α-Arylation[108]
- Amination[115,116, 124, 125]
- Arylation-Nef reaction[114]
- Barluenga coupling[110]
- Carboalkoxylation[119]
- Carboamination[118,120,123]
- Carbonylative amination[109]
- Carbonylative Suzuki coupling[107]
- Carboxylation[112,113]
- C–H arylation[117]
- Desulfitative coupling[111]
- Organotitanium coupling[121]
- Suzuki coupling[122]

Scheme 1.43 Chloroaryl triflate couplings using Buchwald-type ligands

Chemoselectivity in cross-coupling of aryl bromides and triflates using Buchwald-type phosphines is rarely reported. However, a few exceptions exist — Chang[107] and Jana[112] used Pd/SPhos and Pd/DavePhos systems to achieve *O*-triflyl-selective carbonylative arylation and

carboxylation (Scheme 1.44). Interestingly, Pospech and Taeufer[126] applied a $Pd_2(dba)_3$/XPhos catalyst system to synthesise *N*,*N*-dimethylanilines from triflates via Buchwald−Hartwig amination. They induced an intramolecular competition using 4-bromoaryl triflate, generating a bromo-activated product unlike prior studies with the same system (Scheme 1.44). These limited examples suggest Buchwald-type ligands typically exhibit high triflate selectivity, but specific cases may tune reactivity to favour alternative pathways, like aryl bromide activation. Further investigation is needed to fully understand chemoselectivity in these systems.

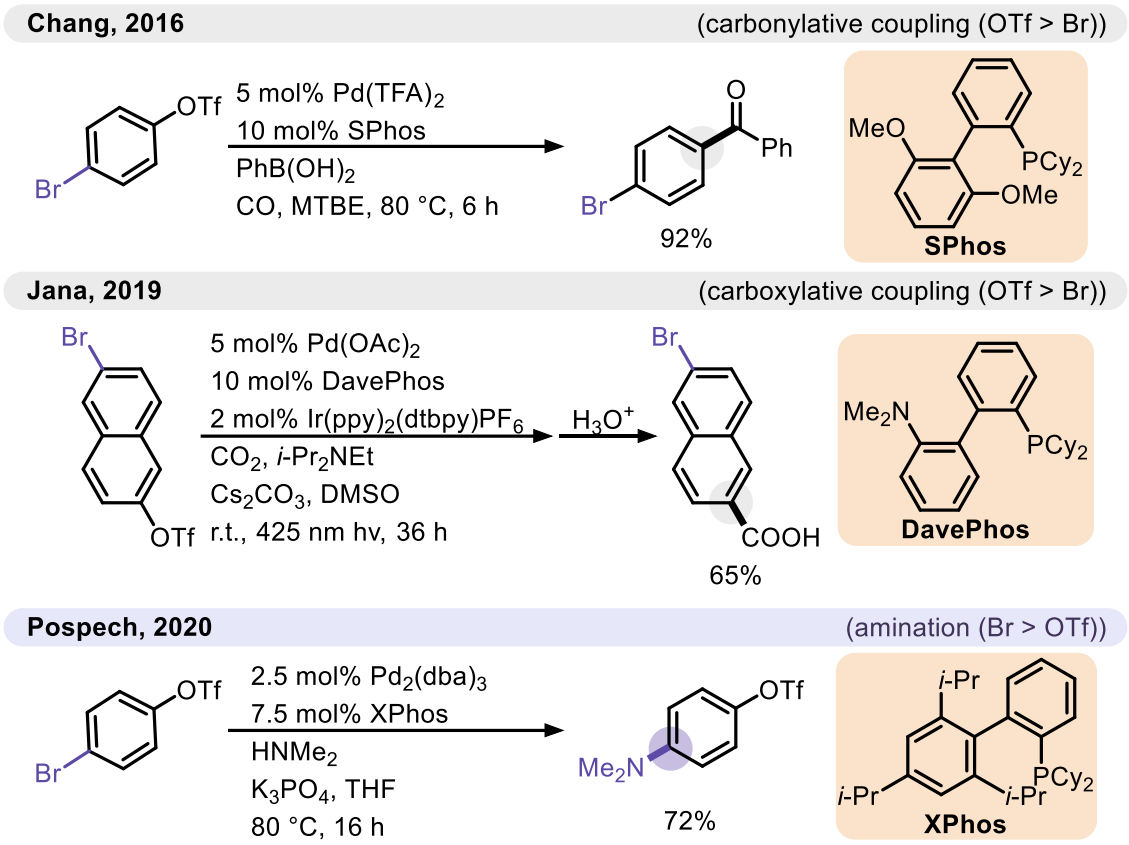

Scheme 1.44 Bromoaryl triflate couplings using Buchwald-type ligands

1.4.5. Bidentate phosphines

In addition to Buchwald-type phosphines, various bidentate phosphine ligands have been explored in palladium cross-coupling, including monophosphines, binaphthyls, ferrocenyls, and others (Figure 1.3). These chelating ligands generate $14e^-$ $Pd(L)_2$ catalysts with similar chemoselectivity as the Buchwald systems.[12]

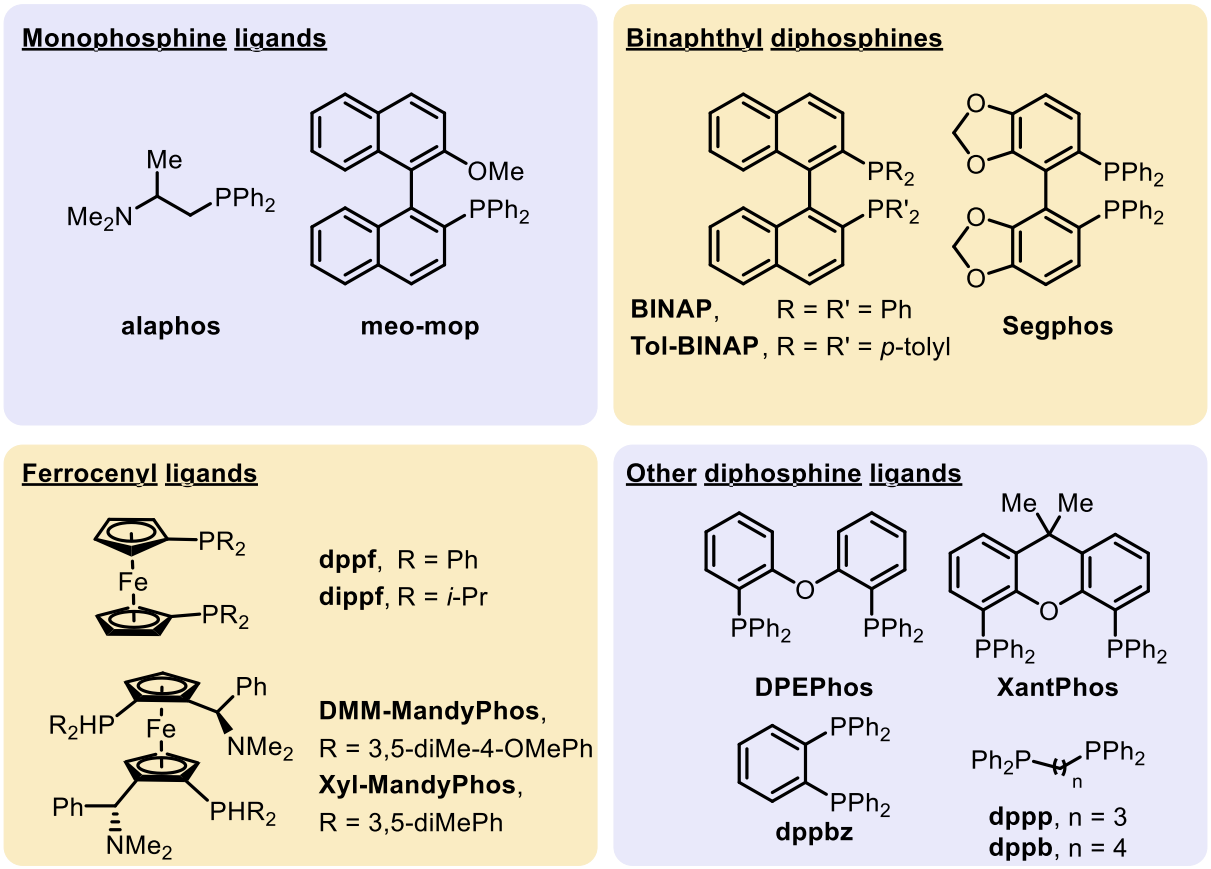

Figure 1.3 Examples of bidentate phosphine ligands

The bidentate phosphine-palladium platform has proven versatile for cross-coupling. 15 examples[63–66,87,98,127–135] demonstrate selectivity for bromoaryl triflates (Scheme 1.45), and over 40 examples[127,129,131–173] show remarkable *O*-triflyl selectivity with chloroaryl triflates (Scheme 1.46). Despite substrate/condition variations, the general trend favours triflate reactivity: C−OTf > C−Br > C−Cl.

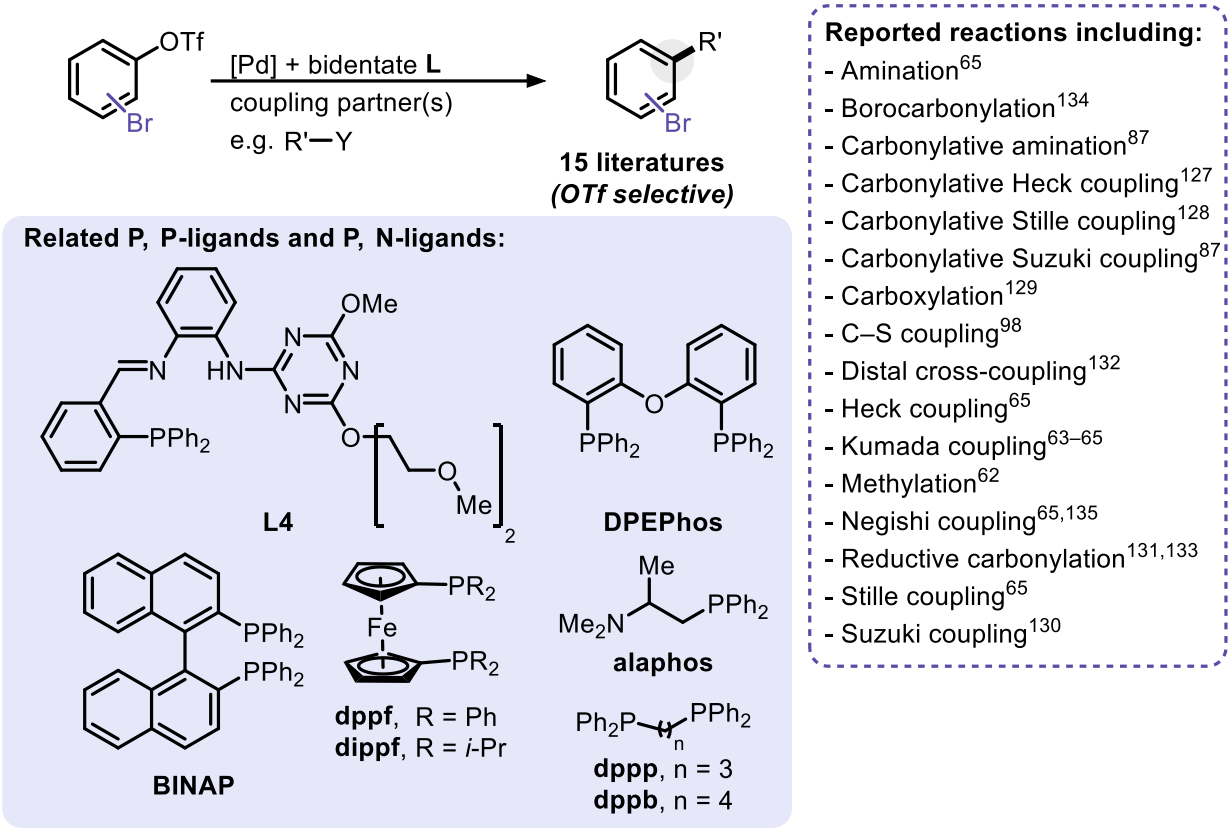

Scheme 1.45 Bromoaryl triflate couplings preferring activation at triflates using bidentate ligands

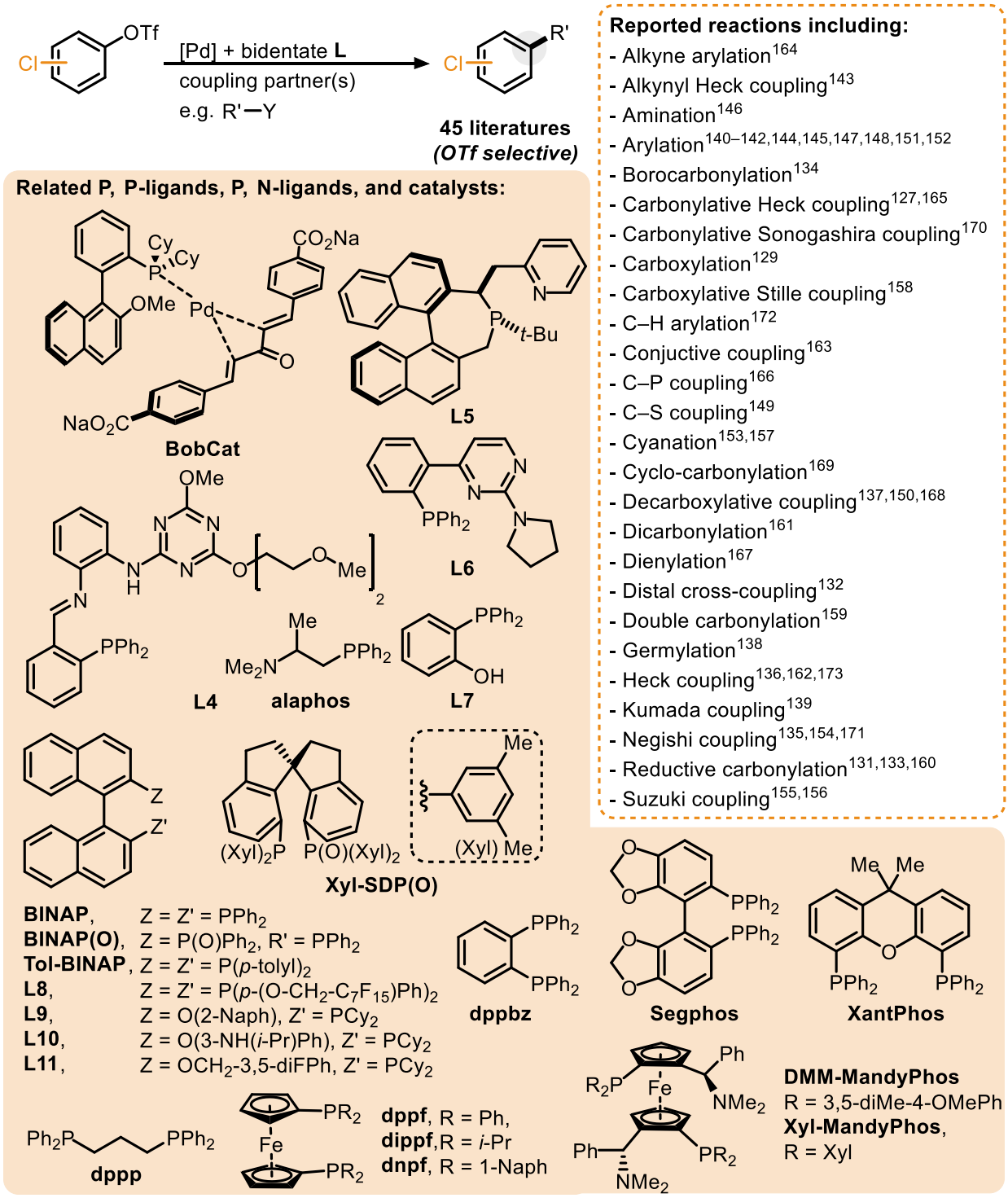

Scheme 1.46 Chloroaryl triflate couplings using bidentate ligands or catalysts

While bidentate phosphine-palladium catalysts generally favour aryl triflates, a few exceptions have been reported. Examples using Pd/BINAP are scarce, but Blum *et al.* achieved selective triflate substitution in a methylation reaction (Scheme 1.45).[62] Similarly, the Pd/dppf system favours triflates in carbonylative couplings (Scheme 1.45).[87,128–131] However, rare cases show selective bromide activation. Hayashi's Pd/(meo-mop) system exhibited 31: 1 (Br: OTf) selectivity in Kumada couplings (Scheme 1.47).[63] Molander[155] and Brown[65] also reported

bromoaryl triflate examples where the boronate coupling partner preferentially activated the bromide (Scheme 1.47). These exceptions indicate bidentate phosphine ligand structure and coupling partners can sometimes override the typical triflate selectivity of these palladium catalysts.

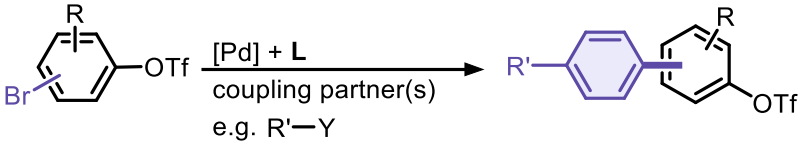

Reference	L	Br	R'—Y	Reaction Type	Yield
Hayashi, 1998[63]	meo-mop	4-Br	PhMgBr	Kumada	62%[a]
					68%[b]
Molander, 2001[155]	dppf	4-Br	$PhCH_2BF_3K$	Suzuki	70%
Brown, 2007[65]	dppp	3-Br	*p*-OMePhB$(OH)_2$	Suzuki	52%
		2-Br (4,5-diF)	PhB$(OH)_2$	Suzuki	78%
Jiao and Wu, 2017[87]	XantPhos	3-Br	morpholine + CO	carbonylative amination	89%
		2-Br			82%
		6-Br (2-OTf naphthyl)			91%
		4-Br	RNH_2 + CO		47−92% (5 entries)

[a]The triflate-substituted product was 2% of the yield. [b]No addition of LiBr,

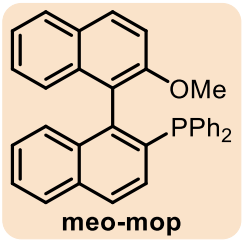

meo-mop

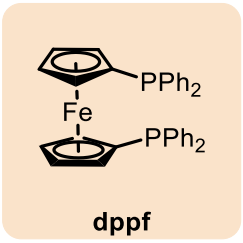

dppf

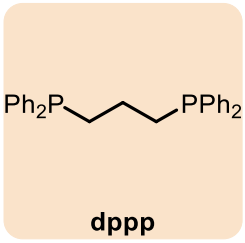

dppp

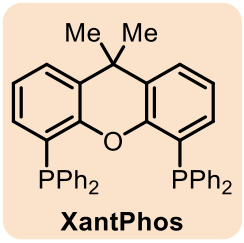

XantPhos

Scheme 1.47 Bromoaryl triflate couplings preferring activation at bromides using bidentate ligands

Prior work has shown that reaction conditions can impact the selectivity between aryl triflates and bromides in palladium catalysis. Ortar *et al.* found that higher temperatures promoted conversion of 4-bromoaryl triflates, eroding the typical triflate preference (Table 1.8).[174] Jiao and Wu further explored the solvent effect using the Pd/dppf catalyst. Polar DMSO gave high triflate selectivity, while less polar dioxane and toluene drastically reduced it (Table 1.8).[87] Interestingly, with the Pd/XantPhos catalyst, the trend reversed, with toluene exhibiting >99: 1 selectivity for the aryl bromide.[87] Mixing polar and non-polar solvents or using highly coordinating DMSO or DMF eliminated selectivity (Table 1.8). These results align with Neufeldt's observation that coordinating solvents can promote triflate activation over chlorides in Suzuki couplings.[56] Controlling temperature and solvent properties appears crucial for optimising chemoselectivity in these transformations.

Table 1.8 Chemoselective couplings of bromoaryl triflates under various conditions using bidentate ligands

Ortar, 1986 (carbonylation (OTf > Br))

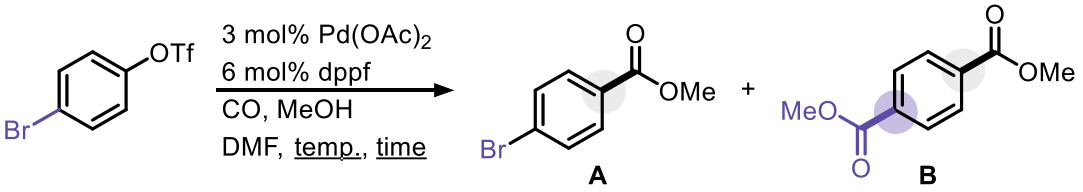

Entry	Temp.	Time	A	B
1	60 °C	1 h	45%	27%
2	40 °C	3.5 h	42%	6%
3	40 °C	20 h	50%	10%

Jiao and Wu, 2017 (carbonylative amination (OTf > Br))

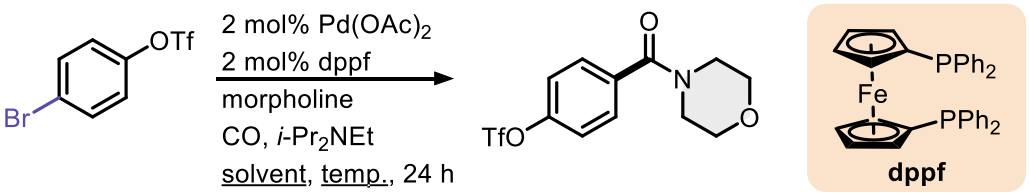

Entry	Solvent	Temp.	Ratio (react at Br: OTf)	Isolated Yield
4	DMSO	90 °C	<1: 99	81%
5	DMSO	110 °C	<1: 99	84%
6	DMF	90 °C	<1: 99	77%
7	NMP	90 °C	<1: 99	---
8	toluene/DMSO (1: 1)	90 °C	<1: 99	68%
9	toluene	90 °C	45: 55	---
10	dioxane	90 °C	31: 69	---

(carbonylative amination (Br > OTf))

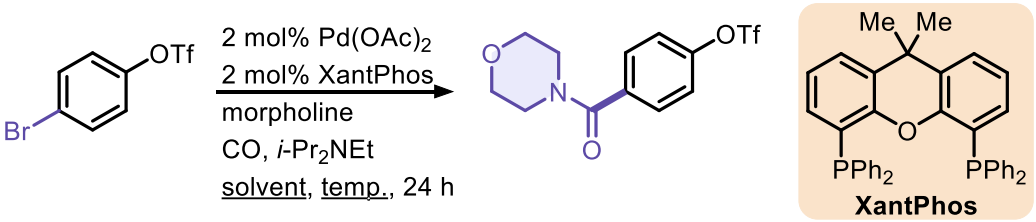

Entry	Solvent	Temp.	Ratio (react at Br: OTf)	Isolated Yield
11	toluene	90 °C	>99: 1	84%
12	toluene	110 °C	>99: 1	86%
13	DMSO	90 °C	50: 50	---
14	DMF	90 °C	58: 42	---
15	toluene/DMSO (1: 1)	90 °C	67: 33	68%

1.4.6 CataCXium® phosphine ligands

CataCXium® phosphine ligands are known for their bulky, electron-rich properties that make them useful in coupling reactions.[175] Ligands like CataCXium® A (*n*-BuP(1-Ad)$_2$) and CataCXium® ABn (BnP(1-Ad)$_2$) have two adamantyl groups and an alkyl substituent on the phosphorus. Jiao and Wu found the Pd/*n*-BuP(1-Ad)$_2$ catalyst exhibited excellent selectivity for aryl bromides over triflates in carbonylative amination and Suzuki−Miyaura reactions, with no difference between toluene and polar DMSO solvents.[87] This bromo-selectivity persisted even with (chloro)aryl bromides and phenyl triflates (Table 1.9).

Table 1.9 Chemoselective carbonylative coupling of bromoaryl triflates using CataCXium® A

Jiao and Wu, 2017 (carbonylative amination (Br > OTf))

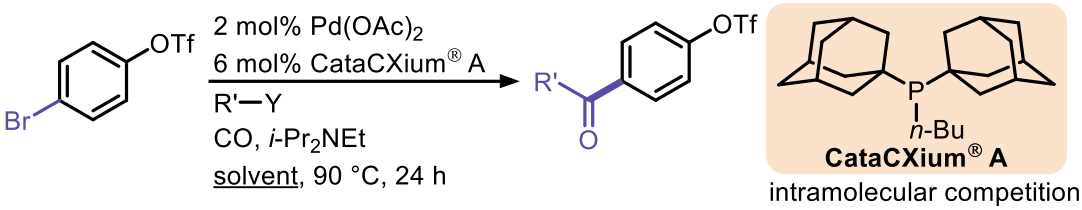

intramolecular competition

Entry	Solvent	R'—Y	Ratio (react at Br: OTf)	Isolated Yield
1	toluene	morpholine	>99: 1	80%
2	DMSO	morpholine	>99: 1	77%
3	toluene	4-BrPhNH$_2$	---	44%
4	toluene	PhB(OH)$_2$	---	75%

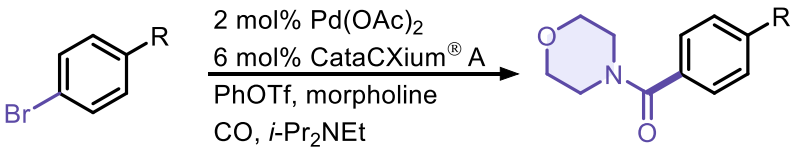

intermolecular competition

Entry	R	Ratio (react at Br: OTf)	Isolated Yield
5	Me	>99: 1	82%
6	Cl	95: 5	---

Other studies report similar selectivity for aryl bromides using CataCXium® ligands. Langer *et al.* showed Pd/CataCXium® A gave higher reactivity and selectivity than Pd/PCy$_3$ in Suzuki couplings of 4-bromo-3-*O*-triflyl-estrones.[176] Hartwig also observed bromide preference with a Pd/CataCXium® PICy catalyst (Scheme 1.48).[177] The ability of bulky, electron-rich CataCXium® phosphines to promote selective activation of aryl bromides makes them valuable for chemoselective cross-coupling.

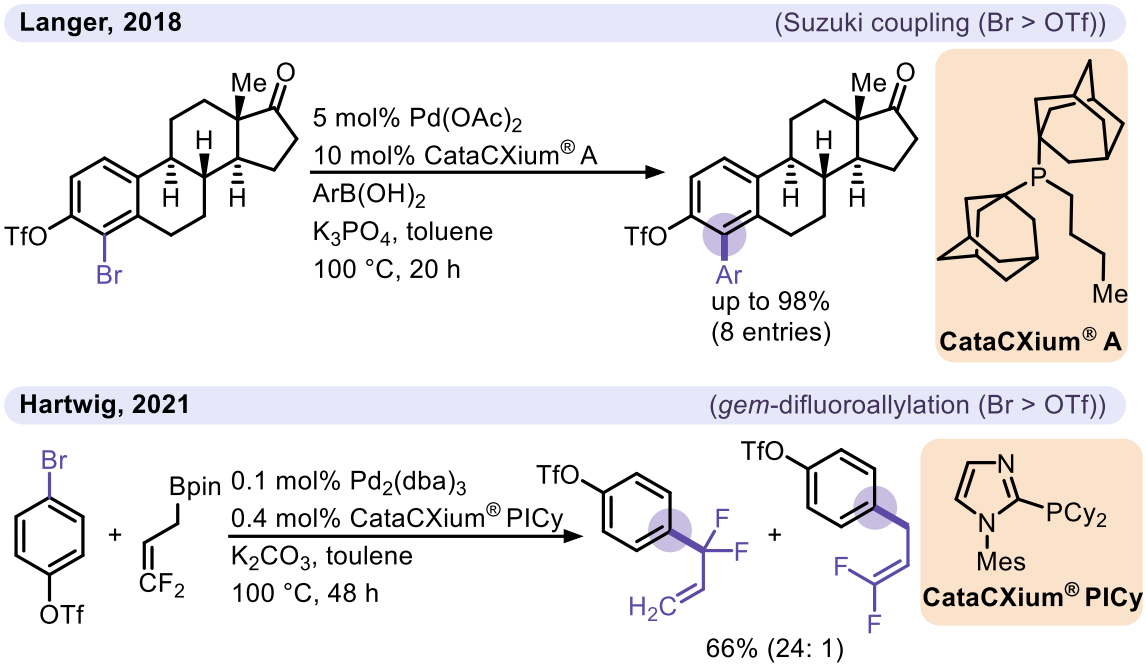

Scheme 1.48 Chemoselective coupling using CataCXium® ligands

1.4.7 Alkyl-based phosphine ligands

In 2021, a research group led by So *et al.* investigated the effect of the ligand-controlled chemoselectivity in palladium-catalysed Suzuki−Miyaura reactions.[53] They discovered a rare chloro-selective reactivity using the Pd/SelectPhos catalyst system (Scheme 1.49). SelectPhos features an indolyl backbone, a phosphine group at the C3 position, and a cyclohexyl ring at the C2 position.The Pd/SelectPhos catalyst system exhibited broad substrate scope, tolerating various boronic acids including electron-rich, electron-poor, functionalised, heteroaromatic, alkenyl, alkyl, and sterically hindered derivatives. It remained highly active even at low loadings of 10 ppm. Additionally, a clear chemoselectivity order was established: Br > Cl > OTf in sequential Suzuki−Miyaura couplings (Scheme 1.49).[53,178]

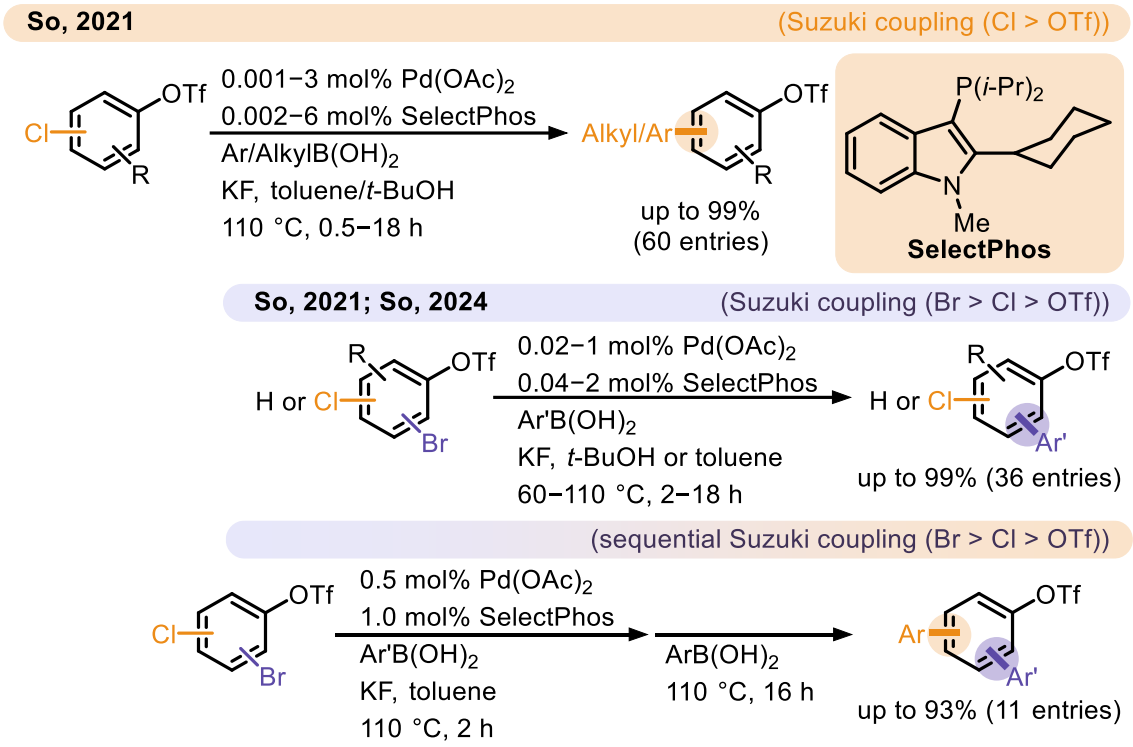

Scheme 1.49 Chemoselective Suzuki−Miyaura coupling of haloaryl triflates using SelectPhos

Crystallographic analysis of the Pd/SelectPhos oxidative addition complex revealed a chloride-bridged dimeric Pd(II) structure with a 1: 1 (Pd: L) ratio. Importantly, a unique interaction was observed between the cyclohexyl methine hydrogen and the palladium centre. DFT calculations showed that, despite the existence of a C−H···Pd interaction, the monoligated Pd/SelectPhos complex still favoured C−Cl bond cleavage over C−O triflate cleavage, in contrast to previous triflate-selective arene hemilabile π-interactions (Scheme 1.50).[53] These results highlighted the importance of ligand design, with the unique C−H···Pd interaction involving SelectPhos' cyclohexyl methine group playing a critical role.

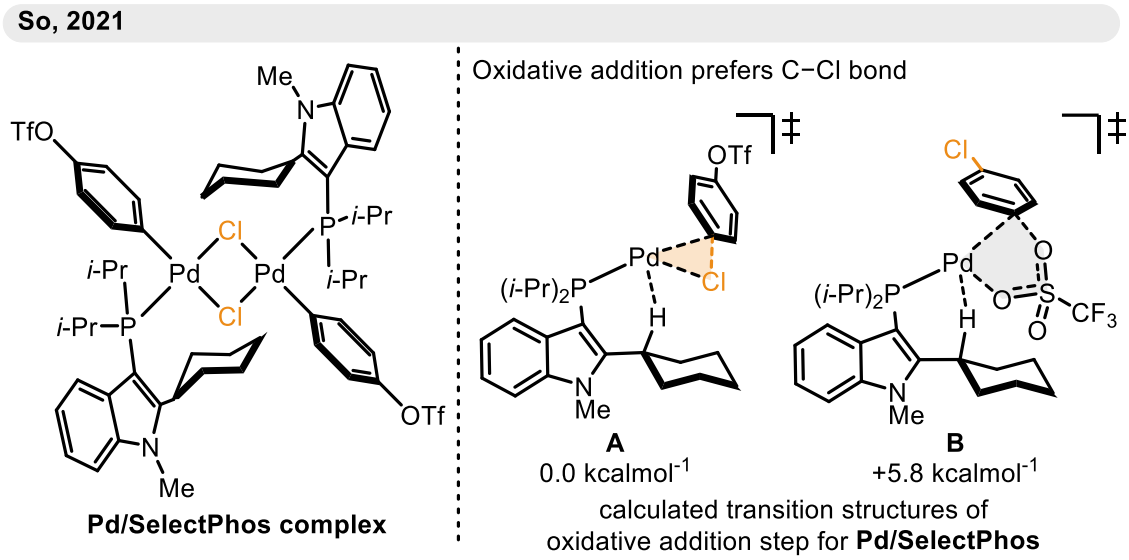

Scheme 1.50 The structure of Pd/SelectPhos and its calculated transition structures

Taking this as a starting point, the same researchers later demonstrated chemoselective borylation of haloaryl triflates using SelectPhos, producing only chloride-coupled products without undesired diborylated products (Scheme 1.51).[179] Importantly, the Pd/SelectPhos catalyst effectively suppressed self-coupling byproducts. The method could be applied to heteroaromatic and electron-deficient substrates, delivering coupled products in up to 95% yield (Scheme 1.51). This catalyst demonstrated high chemoselectivity in intramolecular competition reactions with bromochloroaryl triflates, selectively reacting at the bromide site. Also, it was further applied to chemoselective borylation and Suzuki−Miyaura coupling of chloroaryl triflates in a one-pot, two-step process without requiring additional palladium or ligand, showcasing the versatility of SelectPhos.[179] More details on this will be provided in the subsequent section.

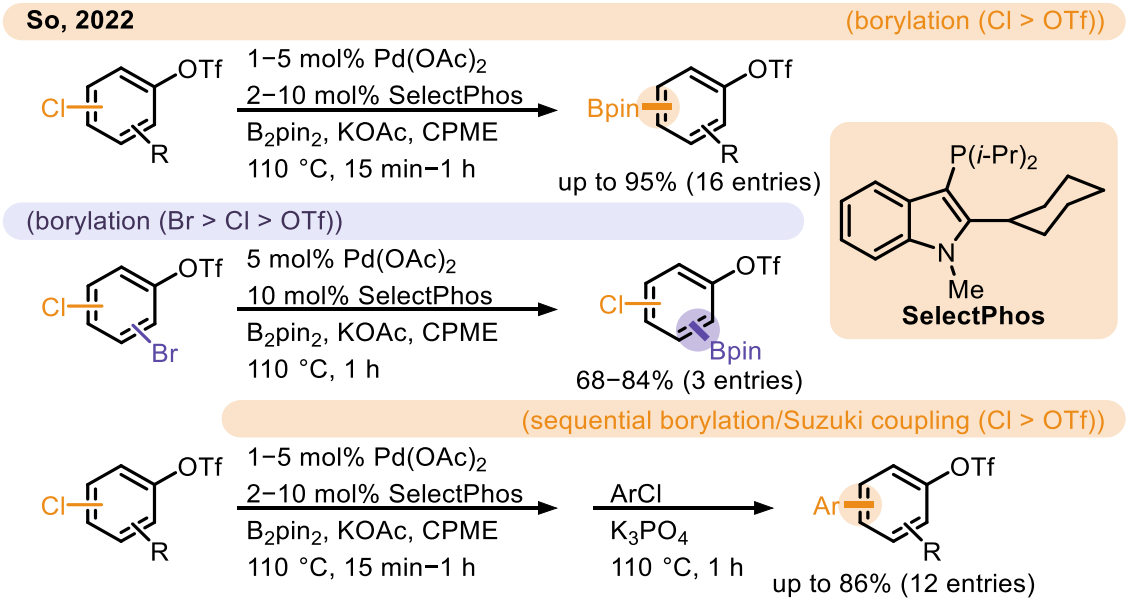

Scheme 1.51 Chemoselective borylation of haloaryl triflates using SelectPhos

So *et al.* later developed a method for α-arylation of carbonyl compounds using chemoselective cross-coupling with chloroaryl triflates, employing either Pd/SelectPhos or Pd/*t*-BuPhSelectPhos catalysts. These systems were able to invert the chemoselectivity, favouring the Ar−Cl bond over the triflate and delivering the desired chloride-substituted products in excellent yields. The scope encompassed a wide range of chloroaryl triflates coupled with oxindoles or other ketones, tolerating both electron-rich and electron-poor substituents (Scheme 1.52).[180]

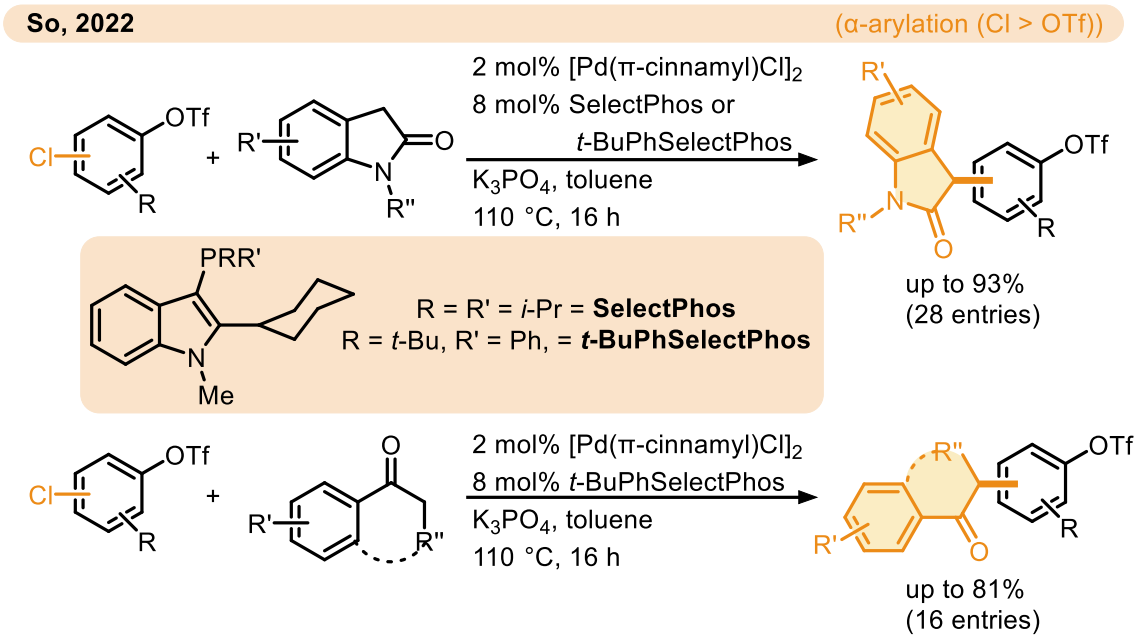

Scheme 1.52 Chemoselective α-arylation of chloroaryl triflates using SelectPhos or *t*-BuPhSelectPhos

The same researchers investigated the effects of the $-PR_2$ module and the C2-alkyl group of alkyl-indolyl-based phosphine ligands on chemoselectivity. They found that the $-PR_2$ moiety with an alkyl group exhibited selectivity towards the Ar−Cl bond, while the $-PPh_2$ ligand (PhSelectPhos) chemoselectively reacted with the Ar−OTf bond. To understand the influence of the $-PPh_2$ group, the authors performed a DFT study on the oxidative addition process for the bisligated Pd(PhSelectPhos)$_2$ complex. The synthetic utility of this catalyst system was demonstrated through the synthesis of the NSAID flurbiprofen from 4-chloro-2-fluorophenyl triflates (Scheme 1.53), highlighting the practical applications of the chemoselective coupling strategies.[180]

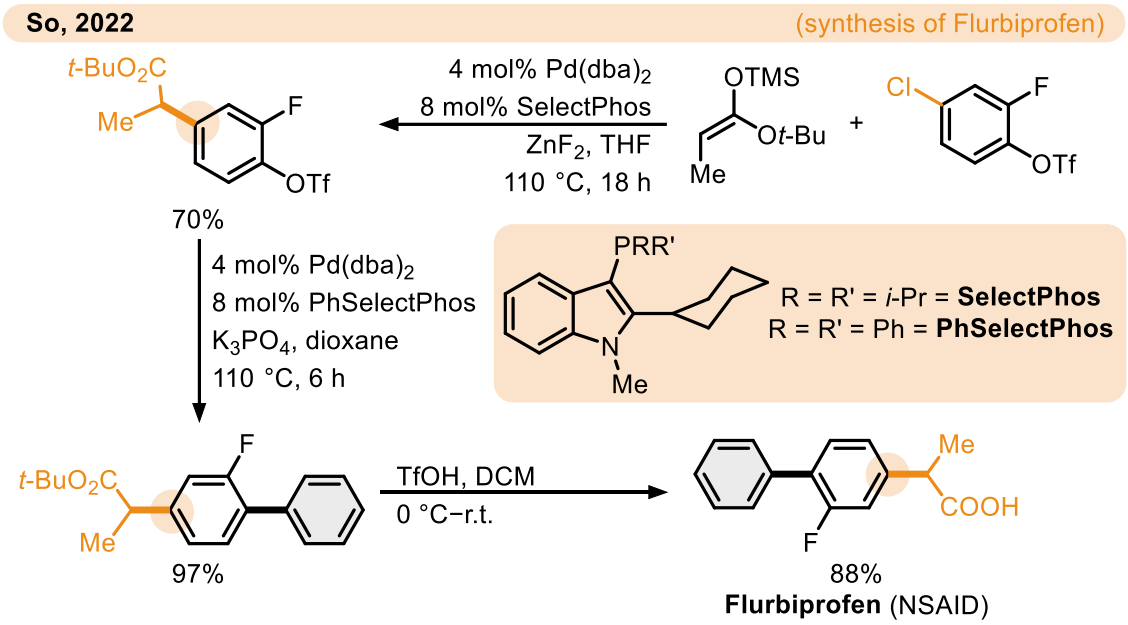

Scheme 1.53 Synthesis of Flubiprofen in a chemoselective approach

So *et al.* reported an inversion of conventional chemoselectivity in the Sonogashira reaction, with the order of reactivity as C−Br > C−Cl > C−OTf. Systematic screening of indolyl ligands showed that the substituent on the phosphine group directly affects the reactivity and chemoselectivity, and the ligand *t*-BuPhSelectPhos exhibited excellent C−Cl chemoselectivity.[181] The chemoselective Sonogashira coupling was applicable to a broad range of chloroaryl triflates and TMS-arylalkynes, coupling the C−Cl bonds at various positions relative to the C−OTf bonds. The method tolerated sterically congested substrates, as well as a variety of electronic and functional group substitutions. The researchers also successfully applied the protocol to polyhalogenated aryl triflates, obtaining excellent C−Br selective products (Scheme 1.54).[181]

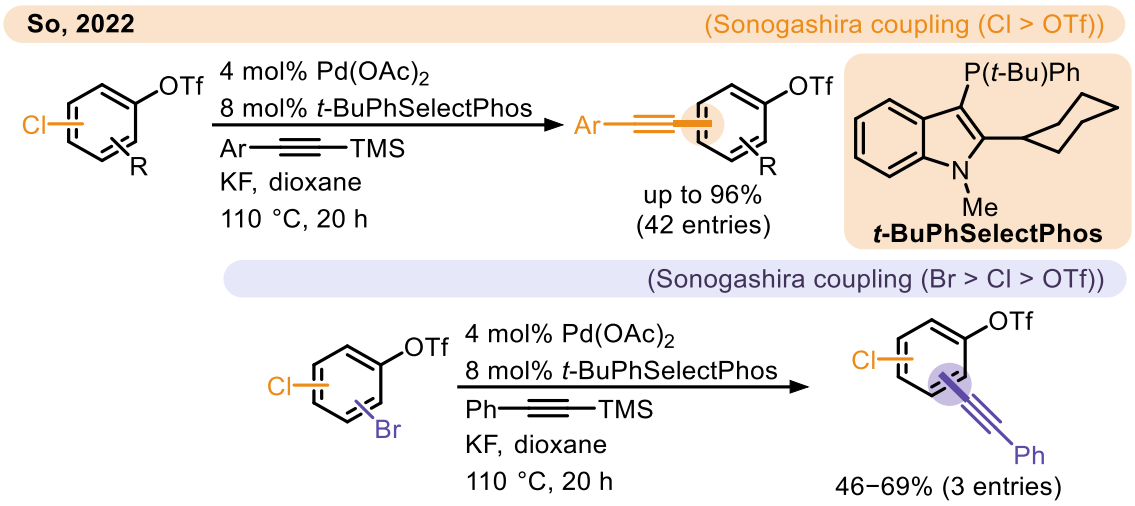

Scheme 1.54 Chemoselective Sonogashira coupling of haloaryl triflates using *t*-BuPhSelectPhos

The synthetic utility of the chemoselective Sonogashira coupling was further demonstrated through its use in the synthesis of polycyclic aromatic hydrocarbons, natural product analogues, and other valuable organic motifs, contributing to the construction of diverse molecular libraries for drug discovery (Scheme 1.55).[181]

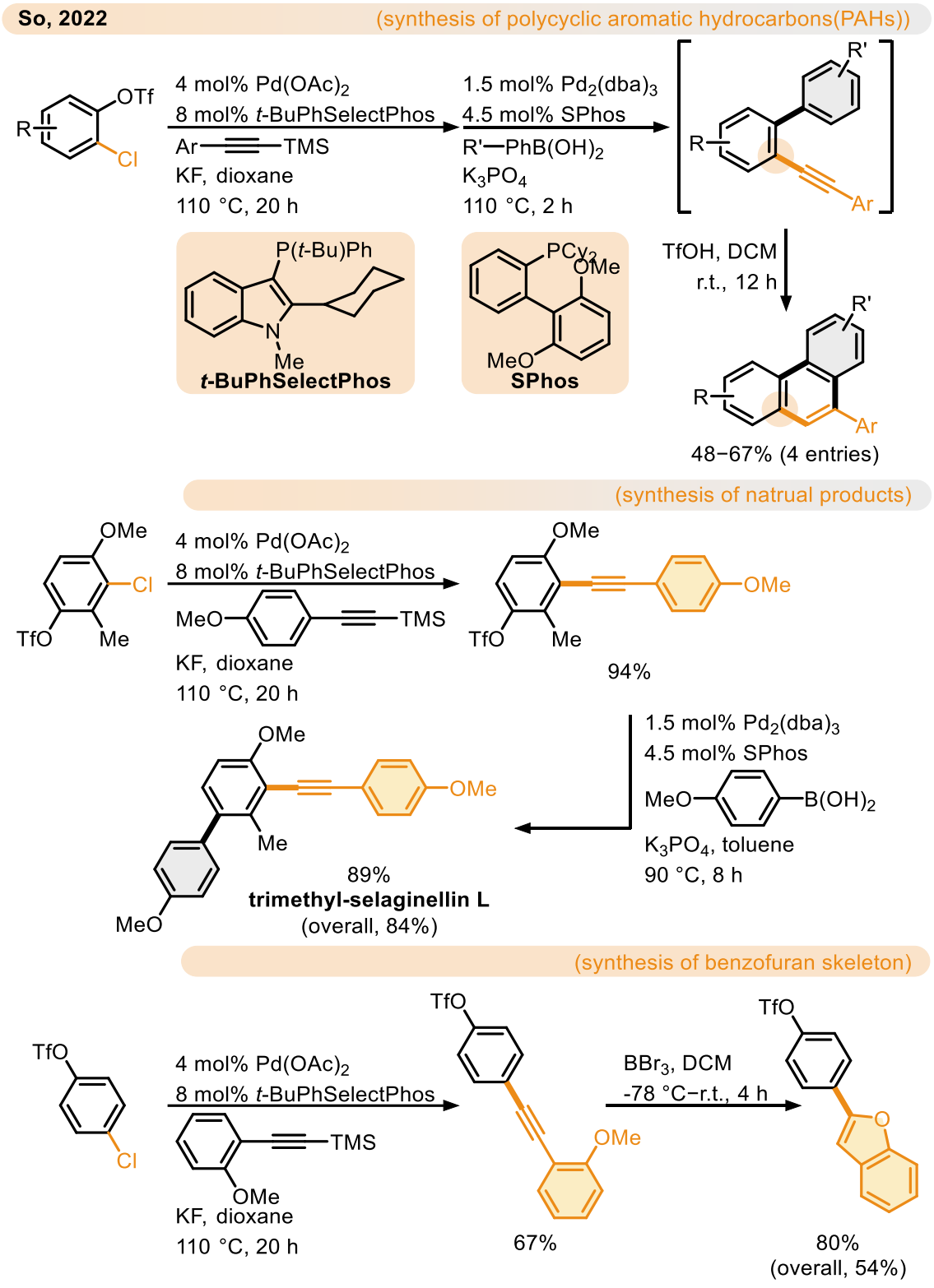

Scheme 1.55 Applications of chemoselective Sonogashira coupling using *t*-BuPhSelectPhos

The desulfinative cross-coupling of aryl sulfinates has emerged as a promising palladium-catalysed C−C bond formation strategy due to its advantages, such as low cost, stability, and broad substrate applicability. However, controlling chemoselectivity between C−Cl and C−OTf sites is challenging, as this reaction typically requires harsh conditions. The same research group found that the *t*-BuPhSelectPhos' methine hydrogen can interact with the palladium centre, stabilizing it and preventing catalyst deactivation at high temperatures and poisoning from SO_2 release. This allows better control over palladium ligation, inverting the typical chemoselectivity order (Scheme 1.56). The substrate scope was explored, revealing a wide range of chloroaryl triflates and *p*-toluenesulfonic acid derivatives with various substituents can be utilized in this chemoselective desulfinative cross-coupling reaction.[182]

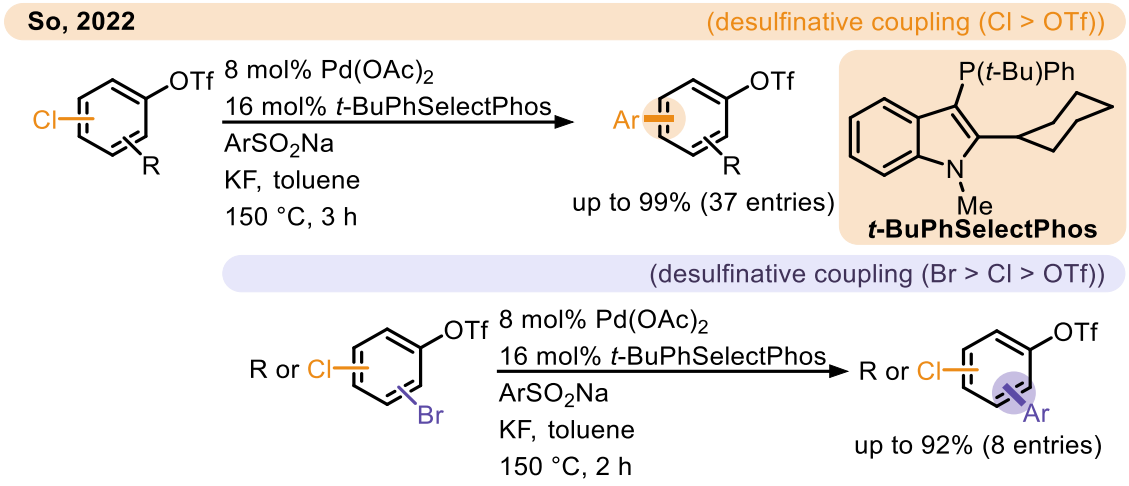

Scheme 1.56 Chemoselective desulfinative coupling of haloaryl triflates using *t*-BuPhSelectPhos

So *et al.* have developed a chemoselective deuterodehalogenation for halogenated aryl triflates, using isopropanol-d_8 as the deuterium source. This method exhibited an unconventional selectivity order of C−Br > C−Cl > C−OTf, and demonstrated a broad substrate scope, tolerating a wide range of functional groups. The team also successfully applied this catalytic system to achieve excellent C−Cl selectivity over C−OTf in the hydrodehalogenation of chloroaryl triflates (Scheme 1.57).[183]

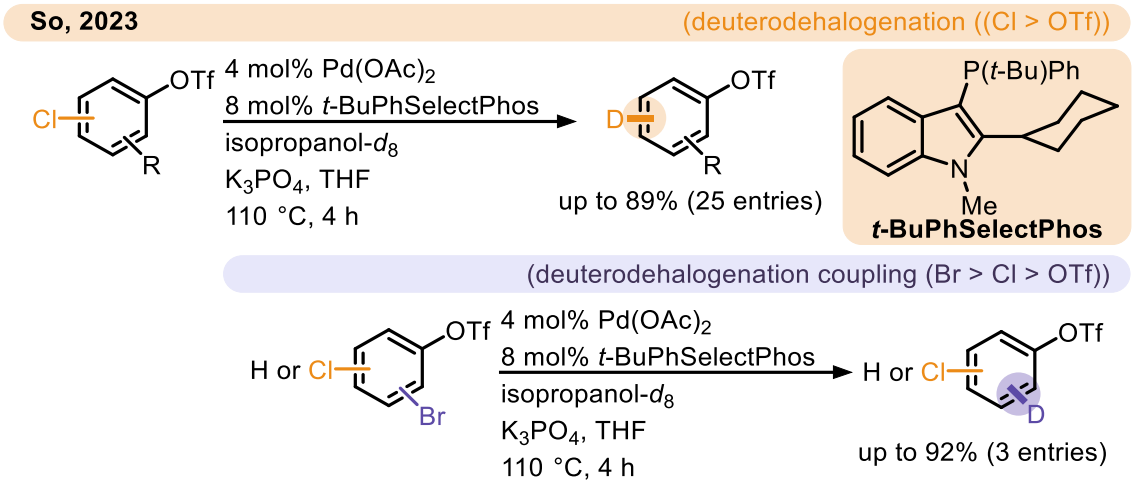

Scheme 1.57 Chemoselective deuterodehalogenation of haloaryl triflates using *t*-BuPhSelectPhos

Additionally, researchers from So's group have recently reported a chemoselective phosphorylation reaction utilizing the Pd/SelectPhos system. This method was able to selectively transform a wide range of chloroaryl and bromoaryl triflates into their corresponding aryl phosphonate products (Scheme 1.58).[184]

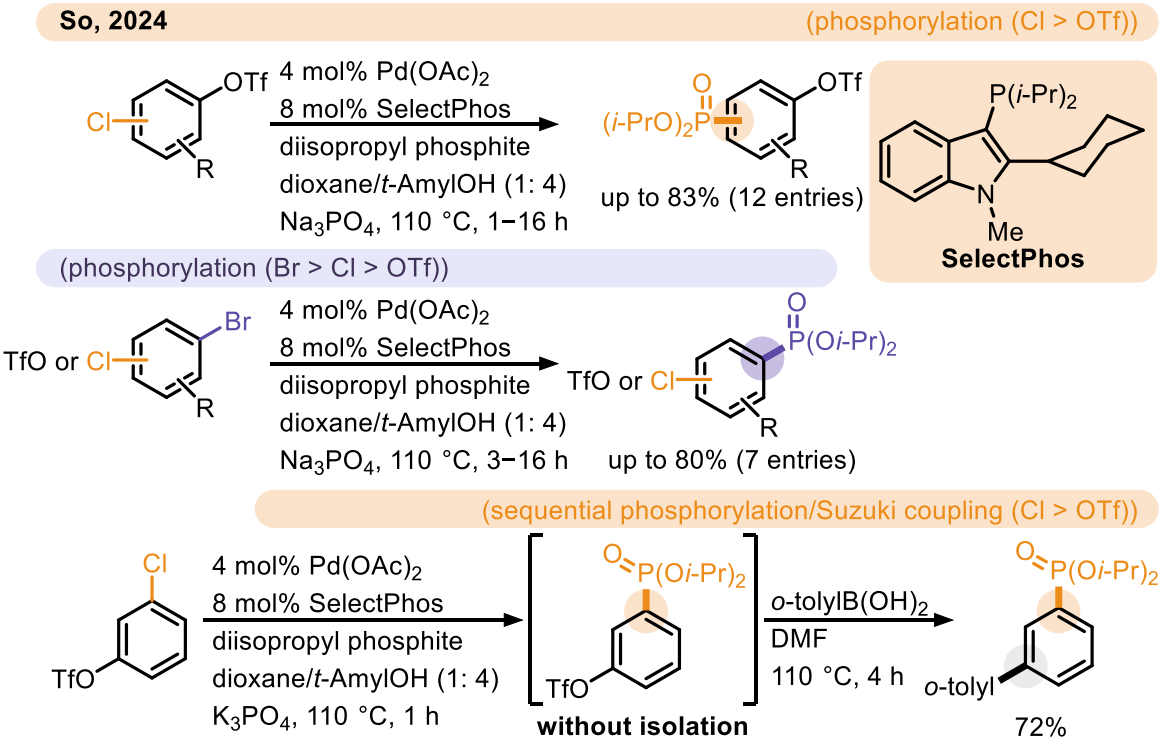

Scheme 1.58 Chemoselective phosphorylation of haloaryl triflates using SelectPhos

In 2024, So *et al.* explored a novel approach for regio- and chemoselective C−H arylation of heterocycles, using innovative pyrazole-alkyl phosphine ligands. These ligands enabled additive-free arylation of various heterocycles under mild conditions, with the key being the different

cycloalkyl ring sizes in the ligand structure (Scheme 1.59).[185] Notable findings included the achieved α/β selectivity and unique chemoselective arylation of C−Cl over C−OTf, facilitating efficient hetero-biaryl synthesis. Experimental and computational evidence suggested the optimally sized ligands may lower the energy barrier in C−H activation, offering potential benefits for sustainable organic synthesis.

In a later study, the same researchers designed new alkyl-pyrazole phosphine ligands, enabling the first palladium-catalysed chemoselective amination of chloro(hetero)aryl triflates in the C−Cl bond (Scheme 1.59).[186] The Pd/BirdPhos system produced new compounds with excellent yield and chemoselectivity, opening possibilities for complex molecules synthesis and providing insights for catalyst design in chemoselective cross-coupling.

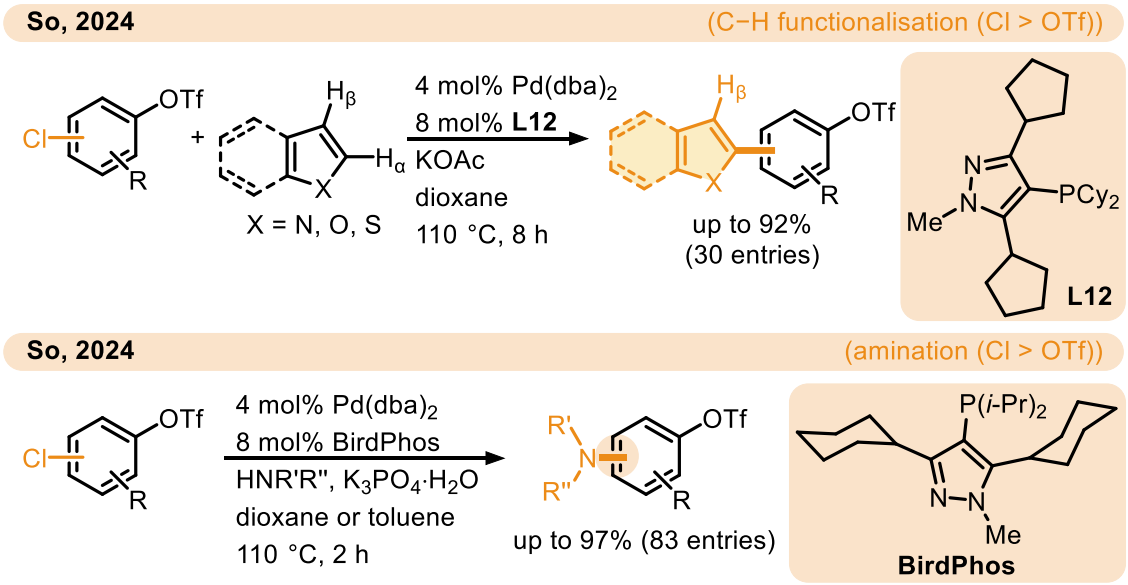

Scheme 1.59 Chemoselective couplings of chloroaryl triflates using alkyl-pyrazole-based phosphine ligands

1.4.8. Ylide-based phosphine ligands

YPhos is a class of ylide-functionalised phosphine ligands developed by Gessner's group. These ligands have been successfully used in palladium- and gold-catalysed reactions, including amination, α-arylation, Negishi coupling, and Suzuki−Miyaura coupling.[187−189] The structure of YPhos consists of a phosphonium group, an ylide group, and an R' substituent. The phosphonium group provides steric demand and secondary interactions with the binding metal, while the ylide group stabilizes electron-deficient, low-valent main-group carbon to enhance the phosphine donor strength. The R' substituent fine-tunes the electronic properties and flexibility of the ligand structure.

Two studies by Gessner and Gooßen investigated the chemoselectivity of YPhos in activating aryl (pseudo)halides in palladium-catalysed cross-coupling reactions. In 2021, the authors developed a method using $Pd_2(dba)_3$ and pinkYPhos for the Negishi coupling of Reformatsky reagents.[190] The study found that the Pd/pinkYPhos system preferentially activates aryl bromides over aryl triflates, and aryl chlorides over aryl triflates (Table 1.10).

Table 1.10 Chemoselective Negishi coupling with Reformatsky reagents using pinkYPhos

Gessner and Gooßen, 2021 (intermolecular competitive Negishi coupling (Br > OTf))

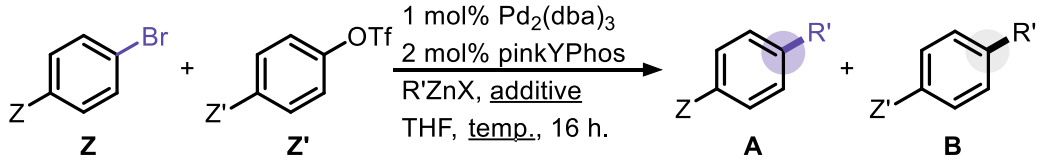

Entry	Z	Z'	R'ZnX	Additive	Temp.	A	B
1	Me	H	EtO_2CCH_2ZnBr	LiCl	0 °C	82%	2%
2	Me	H	*i*-$PrCH_2ZnCl$	$ZnBr_2$	0 °C	96%	n.d.
3	*t*-Bu	Me	PhZnBr	---	r.t.	82%	2%

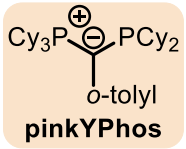

(intermolecular competitive Negishi coupling (Cl > OTf))

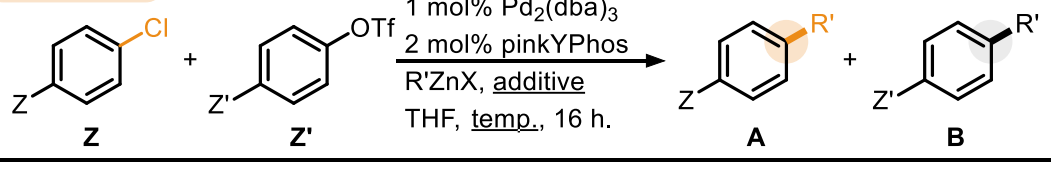

Entry	Z	Z'	R'ZnX	Additive	Temp.	A	B
4	Me	H	EtO_2CCH_2ZnBr	LiCl	r.t.	60%	14%
5	Me	H	*i*-$PrCH_2ZnCl$	---	0 °C	83%	18%
6	*t*-Bu	Me	PhZnBr	---	r.t.	11%	67%

Gessner's group has continued to explore the versatility of YPhos ligands in palladium-catalysed cross-coupling. In 2022, a study found the Pd/keYPhos or Pd/prYPhos catalyst systems

exhibited high reactivity and selectivity towards aryl chlorides.[54] These catalyst systems enabled the coupling of both electron-rich and electron-deficient chloroaryl triflates with electron-rich and electron-deficient arylboronic acids, achieving yields of up to 95% (Scheme 1.60).

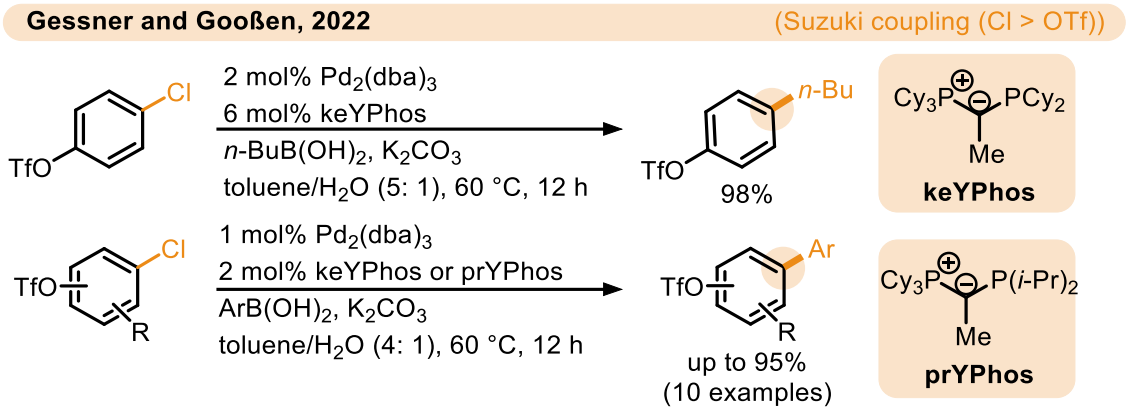

Scheme 1.60 Chemoselective Suzuki−Miyaura coupling of chloroaryl triflates using YPhos

Gessner's group also investigated the chemoselectivity of YPhos in intermolecular competition reactions involving electron-rich and electron-deficient aryl halides and arylboronic acids. Their findings showed that electron-rich arylboronic acids exhibited a selectivity ratio of 4: 1 over electron-deficient arylboronic acids, and a selectivity ratio of 6: 1 for electron-deficient aryl chlorides.[54]

These results underscore the potential of YPhos ligands as valuable tools for the chemoselective activation of chloroaryl triflates in a variety of catalytic transformations. The ligands' ability to discriminate between different electronic profiles of the reactants demonstrates their versatility and utility in selective cross-coupling reactions.

1.4.9. N-Heterocyclic carbene catalysts

N-Heterocyclic carbenes (NHCs) represent another class of ligands commonly employed to form metal complexes in transition metal-catalysed reactions. Organ *et al.* developed a chemoselective Kumada coupling with Pd-PEPPSI-IPent^{Cl}, which exhibited the selectivity order Ar−Br > Ar−OTf or Ar−Cl.[191] They further expanded this to a low-temperature, efficient method for chemoselective Kumada coupling of poly(pseudo)haloalkanes (Scheme 1.61). This method exploited the preference for Ar−Br over Ar−OTf or Ar−Cl, enabling one-pot sequential Kumada and Negishi couplings. The authors attributed the observed chemoselectivity between Ar−Br and Ar−Cl to differences in oxidative addition barriers but did not comment on the selectivity between Ar−OTf and Ar−Cl.[191]

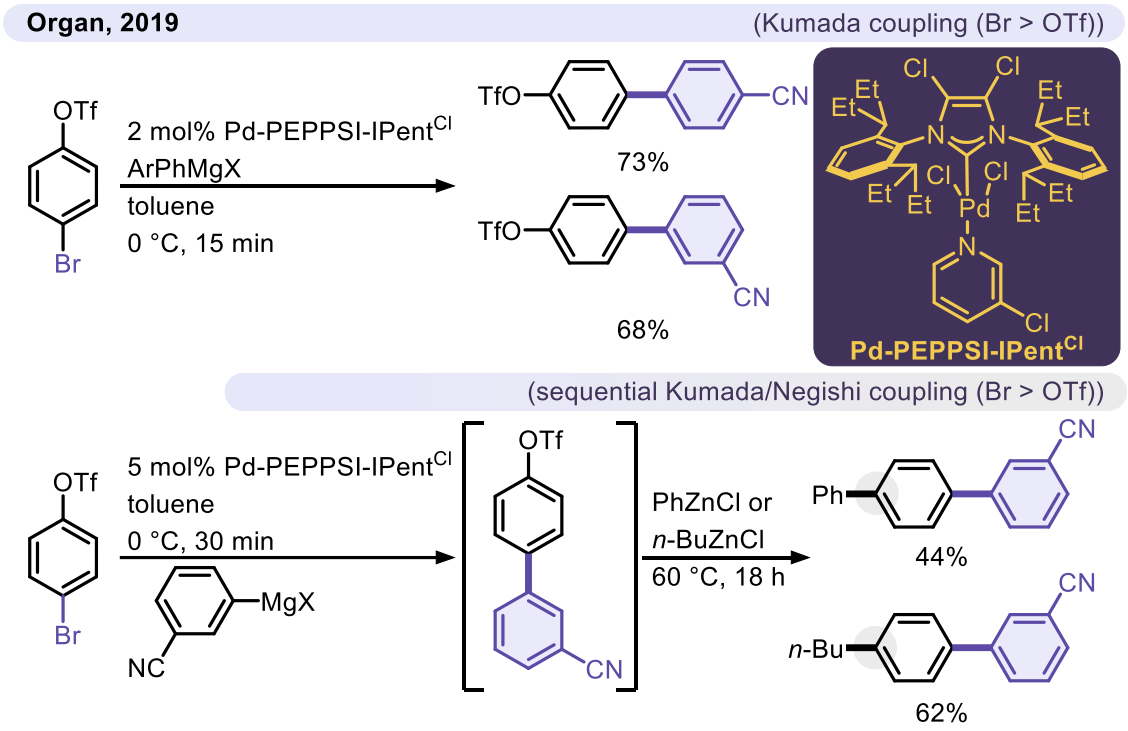

Scheme 1.61 Chemoselective Kumada coupling of bromoaryl triflates using Pd-PEPPSI-IPent^{Cl}

Neufeldt and co-workers introduced a chemoselective Suzuki−Miyaura coupling of chloroaryl triflates using Pd/NHC catalysts. Pd-SIPr complex favoured reaction at the chloride, while Pd-SIMes complex preferred the triflate, giving ≤5% minor/diarylated products.[52] This versatile method addressed limitations of previous Pd/PCy_3 catalyst system, which were ineffective for electron-rich and -deficient arylboronic acids.[97]

In a separate study, Jiang and Shi reported the first palladium-catalysed C(sp^2)−C(sp^3) cross-coupling of aryl chlorides and alkyl zirconium reagents, using [Pd(*i*-Pr)(cin)Cl].[192] One example showed the triflate group was well-tolerated, with the chloride selectively reacting to give the desired product in 40% yield (Scheme 1.62).

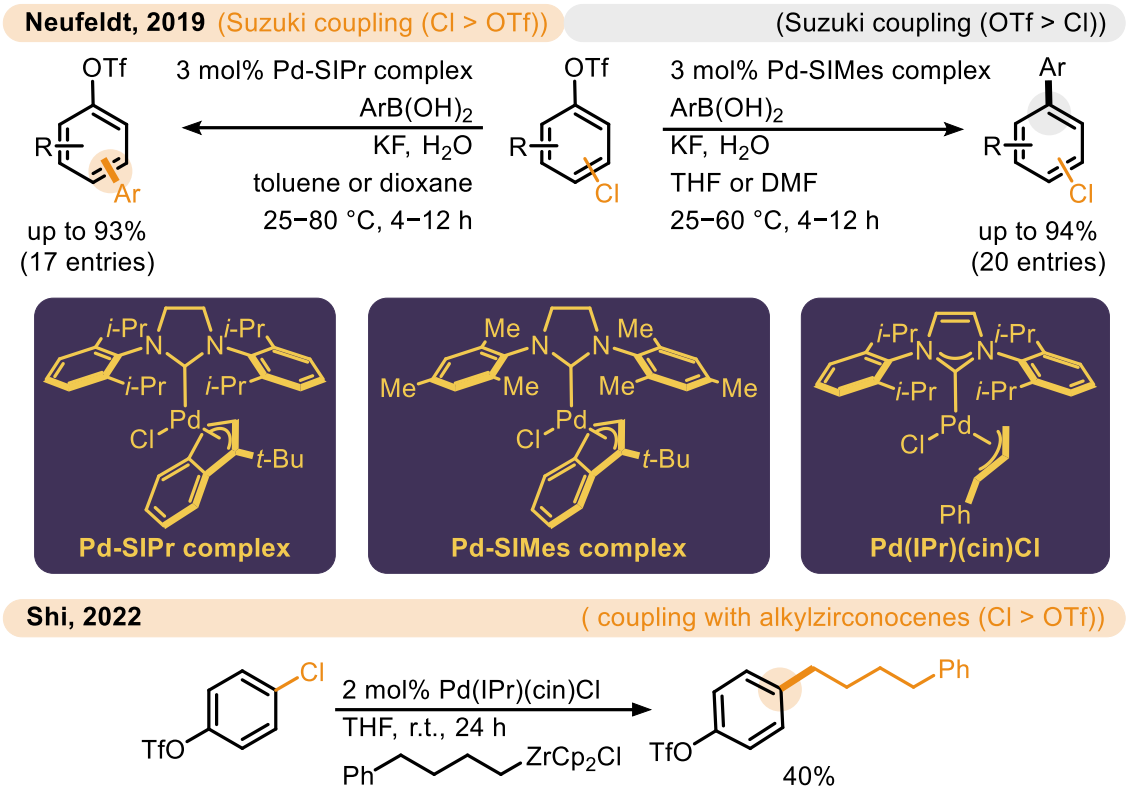

Scheme 1.62 Chemoselective coupling of chloroaryl triflates using NHC catalysts

In summary, the various ligands used in chemoselective palladium catalysis are categorised into 9 groups. By reorganising the reported entries into 7 types of reactions based on their reactivity (Br versus OTf and OTf versus Cl), we can summarize the observed chemoselectivity trends as follows (Table 1.11):

Trialkyl phosphines, Pd(I) dimers, CataCXium series, alkylated heterocyclic based phosphine ligands (SelectPhos and BirdPhos series), Ylide-based phosphines, and NHC catalysts prefer the bromo-site over the OTf-site in all reported palladium catalysis.

In contrast, triaryl phosphines, Buchwald-type phosphines, and bidentate ligands show the opposite preference in some conditions, where the OTf-site is more reactive than the Br-site.

For the chemoselective coupling between OTf-site and Cl-site, the OTf-site is generally more preferred than the Cl-site across all the reactions, except for tri-*tert*-butylphosphine and some newly discovered ligands like CataCXium series, alkylated heterocyclic based phosphine ligands (SelectPhos and BirdPhos series), Ylide-based phosphines, and NHC catalysts.

This comprehensive overview provides valuable insights into the chemoselectivity profiles of various ligand systems, which can inform the rational design and selection of appropriate catalysts for targeted transformations.

Table 1.11 Summary of aforementioned Pd-catalysed chemoselective coupling reactions

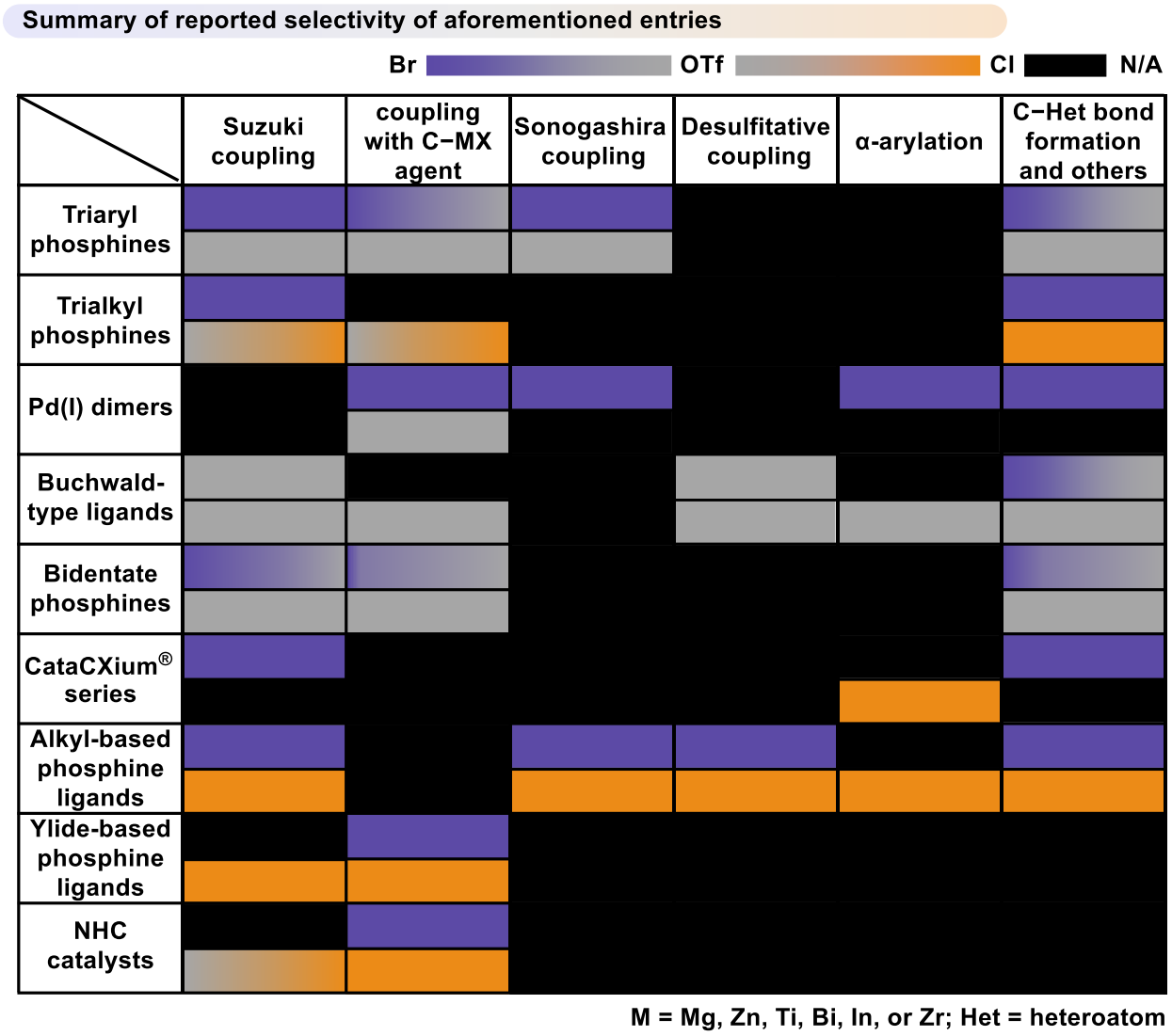

1.5 Research Purpose

Although some ligand architectures appear to be privileged, no single ligand or class of ligands has demonstrated superiority across all applications. Therefore, the development and exploration of ligands for transition metal catalysis remain in high demand. As members of a research group dedicated to synthesizing phosphine ligands, our objective is to rationally design, develop, and synthesize new series of simple and highly effective phosphine ligands with high diversity to address challenging substrate transformations. By strategically introducing novel components into the ligand structure, the reactivity of established catalytic reactions can be enhanced. An improved catalyst has the potential to reduce production costs and conserve materials by enabling the use of less expensive catalysts under milder conditions. This advancement would not only be economically beneficial but also promote environmental sustainability.

The Suzuki−Miyaura cross-coupling reaction, renowned for its utility in synthesising new pharmaceuticals and functional materials, has been extensively studied for several decades. Progress has been made significantly in developing mild, environmentally friendly conditions and tolerance to a wide range of substrates. However, the coupling of sterically hindered aryl halides, particularly *ortho*-substituted substrates, remains a formidable challenge due to spatial hindrance. This steric hindrance restricts the choice of conditions, catalysts, and substrate candidates. Consequently, there is potential for improvement in identifying an effective catalyst for Suzuki coupling of sterically hindered partners while maintaining a broad substrate scope.

In addition to reactivity, selectivity remains a crucial focus for chemists. If a substrate contains multiple reaction sites, it exhibits different selectivity patterns. Three types of selectivity are present: regioselectivity, enantioselectivity, and chemoselectivity. The presence of multi-reactive sites in a substrate can lead to variations in reactivity, which is a leverage in sequential synthesis. However, achieving consistent selectivity is often challenging. Frequently, undesired byproducts with unreacted or multi-site activated components complicate isolation processes and reduce overall product yield. Thus, there is a pressing need to design catalysts that ensure clean selectivity in sequential synthesis. Published examples demonstrate that chemoselectivity can be controlled effectively through careful catalyst design.

Typically, the reactivity follows the order C−I > C−Br ~ C−OTf > C−Cl. However, this order is not absolute when choosing different reaction types, ligands, bases, or solvents. The underlying mechanisms influencing these changes remain under investigation. Further research is needed to develop more reliable methods for achieving chemoselective coupling of different partners.

A C2-alkylated indole-based phosphine ligand, SelectPhos, has been recently synthesised by our research group. Unexpectedly, the methine hydrogen in the C2-cyclohexyl group on the indole ring of the phosphine ligand interacts with the palladium centre, favouring oxidative addition at the C−Cl site over the C−OTf site. This interaction leads to the unusual reactivity order of C−Cl > C−OTf, leaving the typically more reactive OTf moiety in the final product. This thesis demonstrated the chemoselectivity of this ligand in both the Suzuki−Miyaura cross-coupling and borylation. Remarkably, the ligand exhibits an uncommon reactivity order of C−Br > C−Cl > C−OTf with low catalyst loading, enabling sequential transformations in these coupling reactions.

1.6 Organisation of Thesis

The thesis consists of 6 chapters. Chapter 1 covers the background of the research and reviews the development of Suzuki−Miyaura cross-coupling reaction, Miyaura borylation, and Pd-catalysed chemoselective cross-coupling reactions of aryl (pseudo)halides. Chapters 2 and 3 discuss the results of Pd-catalysed Suzuki−Miyaura cross-coupling reactions and Pd-catalysed chemoselective borylation, respectively. Chapter 2 focuses on employing an indole-amide-based phosphine ligand to generate tri-*ortho*-substituted biaryls. Next, Chapter 3 discusses the utility of a C2-alkylated indole-based phosphine ligand, SelectPhos, to achieve an inverted reactivity order in borylation at the C−Cl site over the C−OTf site. Chapter 4 continues to explore the use of SelectPhos in another coupling reaction. Specifically, it demonstrates an unconventional reactivity order: C−Br > C−Cl > C−OTf in the Pd-catalysed Suzuki−Miyaura cross-coupling reaction of bromo(chloro)(hetero)aryl triflates. Chapter 5 concludes the thesis, and Chapter 6 is the appendix of NMR and HRMS spectra for all new compounds mentioned in the thesis.

1.7 References

1. Gillespie, J. A.; Zuidema, E.; van Leeuwen, P. W. N. M.; Kamer, P. C. J. Phosphorus Ligand Effects Homogenous Catalysis and Rational Catalyst Design. In *Phosphorus(III) Ligands in Homogeneous Catalysis: Design and Synthesis*; Kamer, P. C. J., van Leeuwen, P. W. N. M., Eds.; John Wiley & Sons, 2012; pp 1−26.

2. Echavarren, A. M.; Homs, A. Mechanistic Aspects of Metal-Catalyzed C,C- and C,X-Bond Forming Reactions. In *Metal catalyzed cross-coupling reactions and more*, Vol. 1; de Meijere, A.; Bräse, S; Oestreich, M., Eds.; Wiley-VCH, 2014; pp 1−64.

3. Hegedus, L. S.; Söderberg, B. C. G. Synthetic Applications of Complexes Containing Metal−Carbon σ-Bonds. In *Transition Metals in the Synthesis of Complex Organic Molecules*, 3rd ed.; University Science Books, 2010; pp 68−160.

4. Hussain, I.; Capricho, J.; Yawer, M. A. Synthesis of Biaryls via Ligand-Free Suzuki−Miyaura Cross-Coupling Reactions: A Review of Homogeneous and Heterogeneous Catalytic Developments. *Adv. Synth. Catal.* **2016**, *358*, 3320−3349.

5. Miyaura, N.; Yamada K.; Suzuki, A. A New Stereospecific Cross-Coupling by the Palladium-catalyzed Reaction of 1-Alkenylboranes with 1-Alkenyl or 1-Alkynyl Halides. *Tetrahedron Lett.* **1979**, *20*, 3437−3440.

6. Miyaura, N.; Yanagi, T.; Suzuki, A. The Palladium-Catalyzed Cross-Coupling Reaction of Phenylboronic Acid with Haloarenes in the Presence of Bases. *Synth. Commun.* **1981**, *11*, 513−519.

7. Littke, A. F.; Gregory, C. F. A Convenient and General Method for Pd-Catalyzed Suzuki Cross-Couplings of Aryl Chlorides and Arylboronic Acids. *Angew. Chem. Int. Ed.* **1998**, *37*, 3387−3388.

8. Wolfe, J. P.; Singer, R. A.; Yang, B. H.; Buchwald, S. L. Highly Active Palladium Catalysts for Suzuki Coupling Reactions. *J. Am. Chem. Soc.* **1999**, *121*, 9550−9561.

9. Molander, G. A.; Biolatto, B. Palladium-Catalyzed Suzuki−Miyaura Cross-Coupling Reactions of Potassium Aryl- and Heteroaryltrifluoroborates. *J. Org. Chem.* **2003**, *68*, 4302−4314.

10. Kitamura, Y; Sakurai, A.; Udzu, T.; Maegawa, T.; Monguchi, Y.; Sajiki, H. Heterogeneous Pd/C-Catalysed Ligand-Free Suzuki−Miyaura Coupling Reaction Using Aryl Boronic Esters. *Tetrahedron* **2007**, *63*, 10596−10602.

11. Zhang, L.; Meng, T.; Wu, J. Palladium-Catalyzed Suzuki−Miyaura Cross-Couplings of Aryl Tosylates with Potassium Aryltrifluoroborates. *J. Org. Chem.* **2007**, *72*, 9346−9349.

12. Martin, R.; Buchwald, S. L. Palladium-Catalyzed Suzuki−Miyaura Cross-Coupling Reactions Employing Dialkylbiaryl Phosphine Ligands. *Acc. Chem. Res.* **2008**, *41*, 1461−1473.

13. So, C. M.; Lau, C. P.; Kwong, F. Y. A General Palladium-Catalyzed Suzuki−Miyaura Coupling of Aryl Mesylates. *Angew. Chem. Int. Ed.* **2008**, *47*, 8059−8063.

14. Ackermann, L.; Potukuchi, H. K.; Althammer, A.; Born, R.; Mayer, P. Tetra-*ortho*-Substituted Biaryls through Palladium-Catalyzed Suzuki−Miyaura Couplings with a Diaminochlorophosphine Ligand. *Org. Lett.* **2010**, *12*, 1004−1007.

15. Halima, T. B.; Zhang, W.; Yalaoui, I.; Hong, X.; Yang, Y.-F.; Houk, K. N.; Newman, S. G. Palladium-Catalyzed Suzuki−Miyaura Coupling of Aryl Esters. *J. Am. Chem. Soc.* **2017**, *139*, 1311−1318.

16. Takale, B. S.; Thakore, R. R.; Handa, S.; Gallou, F.; Reilly, J.; Lipshutz, B. H. A New, Substituted Palladacycle for Ppm Level Pd-Catalyzed Suzuki−Miyaura Cross Couplings in Water. *Chem. Sci.* **2019**, *10*, 8825−8831.

17. Yang, H.; Sun, J.; Gu, W.; Tang, W. Enantioselective Cross-Coupling for Axially Chiral Tetra-*ortho*-Substituted Biaryls and Asymmetric Synthesis of Gossypol. *J. Am. Chem. Soc.* **2020**, *142*, 8036−8043.

18. Fyfe, J. W.; Watson, A. J. Recent Developments in Organoboron Chemistry: Old Dogs, New Tricks. *Chem* **2017**, *3*, 31−55.

19. Thomas, A. A.; Zahrt, A. F.; Delaney, C. P.; Denmark, S. E. Elucidating the Role of the Boronic Esters in the Suzuki−Miyaura Reaction: Structural, Kinetic, and Computational Investigations. *J. Am. Chem. Soc.* **2018**, *140*, 4401−4416.

20. Markovic, T.; Murray, P. R. D.; Rocke, B. N.; Shavnya, A.; Blakemore, D. C.; Willis, M. C. Heterocyclic Allylsulfones as Latent Heteroaryl Nucleophiles in Palladium-Catalyzed Cross-Coupling Reactions. *J. Am. Chem. Soc.* **2018**, *140*, 15916−15923.

21. Buskes, M. J.; Blanco, M.-J. Impact of Cross-Coupling Reactions in Drug Discovery and Development. *Molecules* **2020**, *25*, 3493.

22. Leroux, F.; Jeschke, P.; Schlosser, M. α-Fluorinated Ethers, Thioethers, and Amines: Anomerically Biased Species. *Chem. Rev.* **2005**, *105*, 827−856.

23. Ghosh, S.; Kumar, A. S.; Mehta, G. N. Convenient Synthesis of Valsartan via a Suzuki Reaction. *J. Chem. Res.* **2010**, *34*, 191−193.

24. Lennox, A. J. J.; Lloyd-Jones, G. C. Selection of Boron Reagents for Suzuki−Miyaura Coupling. *Chem. Soc. Rev.* **2014**, *43*, 412−443.

25. Ishiyama, T.; Murata, M.; Miyaura, N. Palladium(0)-Catalyzed Cross-Coupling Reaction of Alkoxydiboron with Haloarenes: A Direct Procedure for Arylboronic Esters. *J. Org. Chem.* **1995**, *60*, 7508−7510.

26. Murata, M.; Watanabe, S.; Masuda, Y. Novel Palladium(0)-Catalyzed Coupling Reaction of Dialkoxyborane with Aryl Halides: Convenient Synthetic Route to Arylboronates. *J. Org. Chem.* **1997**, *62*, 6458−6459.

27. Murata, M.; Oyama, T.; Watanabe, S.; Masuda, Y. Palladium-Catalyzed Borylation of Aryl Halides or Triflates with Dialkoxyborane: A Novel and Facile Synthetic Route to Arylboronates. *J. Org. Chem.* **2000**, *65*, 164−168.

28. Takagi, J.; Takahashi, K.; Ishiyama, T.; Miyaura, N. Palladium-Catalyzed Cross-Coupling Reaction of Bis(pinacolato)diboron with 1-Alkenyl Halides or Triflates: Convenient Synthesis of Unsymmetrical 1,3-Dienes via the Borylation-Coupling Sequence. *J. Am. Chem. Soc.* **2002**,*124*, 8001−8006.

29. Billingsley, K. L.; Barder, T. E.; Buchwald, S. L. Palladium‐Catalyzed Borylation of Aryl Chlorides: Scope, Applications, and Computational Studies. *Angew. Chem. Int. Ed.* **2007**, *46*, 5359−5363.

30. Billingsley, K. L.; Buchwald, S. L. An Improved System for the Palladium-Catalyzed Borylation of Aryl Halides with Pinacol Borane. *J. Org. Chem.* **2008**, *73*, 5589−5591.

31. Tang, W.; Keshipeddy, S.; Zhang, Y.; Wei, X.; Savoie, J.; Patel, N. D.; Yee, N. K.; Senanayake, C. H. Efficient Monophosphorus Ligands for Palladium-Catalyzed Miyaura Borylation. *Org. Lett.* **2011**, *13*, 1366−1369.

32. Zhang, Y.; Gao, J.; Li, W.; Lee, H.; Lu, B. Z.; Senanayake, C. H. Synthesis of 8-Arylquinolines via One-Pot Pd-Catalyzed Borylation of Quinoline-8-yl Halides and Subsequent Suzuki−Miyaura Coupling. *J. Org. Chem.* **2011**, *76*, 6394−6400.

33. Lu, H.; Wang, S.; Li, J.; Zou, D.; Wu, Y.; Wu, Y. Efficient Synthesis of Pyrazine Boronic Esters via Palladium-Catalyzed Miyaura Borylation. *Tetrahedron Lett.* **2017**, *58*, 839−842.

34. Ji, H.; Wu, L.-Y.; Cai, J.-H.; Li, G.-R.; Gan, N.-N.; Wang, Z.-H. Room-Temperature Borylation and One-Pot Two-Step Borylation/Suzuki−Miyaura Cross-Coupling Reaction of Aryl Chlorides. *RSC Adv.* **2018**, *8*, 13643−13648.

35. Fan-Chiang, T.-T.; Wang, H.-K.; Hsieh, J.-C. Synthesis of Phenanthridine Skeletal Amaryllidaceae Alkaloids. *Tetrahedron* **2016**, *72*, 5640−5645.

36. Moore, M. J.; Qu, S.; Tan, C.; Cai, Y.; Mogi, Y.; Keith, D. J.; Boger, D. L. Next-Generation Total Synthesis of Vancomycin. *J. Am. Chem. Soc.* **2020**, *142*, 16039−16050.

37. Vanga, M.; Lalancette, R. A.; Jäkle, F. Controlling the Optoelectronic Properties of Pyrene by Regioselective Lewis Base-Directed Electrophilic Aromatic Borylation. *Chem. Eur. J.* **2019**, *25*, 10133−10140.

38. Tse, M. H.; Zhong, R.-L.; Kwong, F. Y. Palladium-Catalyzed Miyaura Borylation of Overly Crowded Aryl Chlorides Enabled by a Complementary Localized/Remote Steric Bulk of Ligand Chassis. *ACS Catal.* **2022**, *12*, 3507−3515.

39. D'Amico, F.; Papucci, C.; Franchi, D.; Reginato, G.; Taddei, M.; Mordini, A.; Zani, L.; Dessì, A.; Calamante, M. Pd-Catalyzed Miyaura Borylation and Telescopic Borylation/Suzuki−Miyaura Cross-Coupling Processes in Deep-Eutectic Solvents. *J. Org. Chem.* **2024**, *89*, 6991−7003.

40. Manabe, K.; Ohba, M.; Matsushima, Y. A Repetitive One-Step Method for Oligoarene Synthesis Using Catalyst-Controlled Chemoselective Cross-Coupling. *Org. Lett.* **2011**, *13*, 2436−2439.

41. Dobrounig, P.; Trobe, M.; Breinbauer, R. Sequential and Iterative Pd-Catalyzed Cross-Coupling Reactions in Organic Synthesis. *Monatsh. Chem.* **2017**, *148*, 3−35.

42. Fitton, P.; Rick, E. A. The Addition of Aryl Halides to Tetrakis(triphenylphosphine)palladium(0). *J. Organomet. Chem.* **1971**, *28*, 287−291.

43. Hartwig, J. F. Transition Metal-Catalyzed Coupling Reactions. In *Organotransition Metal Chemistry: From Bonding to Catalysis;* University Science Books, 2010; pp 877−965.

44. Jui, N. T.; Buchwald, S. L. Cascade Palladium Catalysis: A Predictable and Selectable Regiocontrolled Synthesis of *N*-Arylbenzimidazoles. *Angew. Chem. Int. Ed.* **2013**, *52*, 11624−11627.

45. Mendel, M.; Kalvet, I.; Hupperich, D.; Magnin G.; Schoenebeck, F. Site-Selective, Modular Diversification of Polyhalogenated Aryl Fluorosulfates ($ArOSO_2F$) Enabled by an Air-Stable Pd^{I} Dimer. *Angew. Chem. Int. Ed.* **2020**, *59*, 2115−2119.

46. Wu, X.-F. Palladium-Catalyzed Carbonylative Transformation of Aryl Chlorides and Aryl Tosylates. *RSC Adv.* **2016**, *6*, 83831−83837.

47. Ogata, T.; Hartwig, J. F. Palladium-Catalyzed Amination of Aryl and Heteroaryl Tosylates at Room Temperature. *J. Am. Chem. Soc.* **2008**, *130*, 13848−13849.

48. So, C. M.; Kwong, F. Y. Palladium-Catalyzed Cross-Coupling Reactions of Aryl Mesylates. *Chem. Soc. Rev.* **2011**, *40*, 4963−4972.

49. Jeon, Y.-K.; Lee, J.-Y.; Kim, S.-E.; Kim, W.-S. Highly Selective Room-Temperature Suzuki−Miyaura Coupling of Bromo-2-sulfonyloxypyridines for Unsymmetrical Diarylpyridines. *J. Org. Chem.* **2020**, *85*, 7399−7412.

50. Niemeyer, Z. L.; Milo, A.; Hickey, D. P.; Sigman, M. S. Parameterization of Phosphine Ligands Reveals Mechanistic Pathways and Predicts Reaction Outcomes. *Nat. Chem.* **2016**, *8*, 610−617.

51. Reeves, E. K.; Entz, E. D.; Neufeldt, S. R. Chemodivergence between Electrophiles in Cross-Coupling Reactions. *Chem. Eur. J.* **2021**, *27*, 6161−6177.

52. Reeves, E. K.; Humke, J. N.; Neufeldt, S. R. *N*-Heterocyclic Carbene Ligand-Controlled Chemodivergent Suzuki−Miyaura Cross Coupling. *J. Org. Chem.* **2019**, *84*, 11799−11812.

53. So, C. M.; Yuen, O. Y.; Ng, S. S.; Chen, Z. General Chemoselective Suzuki−Miyaura Coupling of Polyhalogenated Aryl Triflates Enabled by an Alkyl-Heteroaryl-Based Phosphine Ligand. *ACS Catal.* **2021**, *11*, 7820−7827.

54. Wei, X.-J.; Xue, B.; Handelmann, J.; Hu, Z.; Darmangeh, H.; Gessner, V. H.; Gooßen, L. J. Ylide-Functionalized Diisopropyl Phosphine (prYPhos): A Ligand for Selective Suzuki−Miyaura Couplings of Aryl Chlorides. *Adv. Synth. Catal.* **2022**, *364*, 3336−3341.

55. Norman, J. P.; Neufeldt, S. R. The Road Less Traveled: Unconventional Site Selectivity in Palladium-Catalyzed Cross-Couplings of Dihalogenated *N*-Heteroarenes. *ACS Catal.* **2022**, *12*, 12014−12026.

56. Reeves, E. K.; Bauman, O. R.; Mitchem, G. B.; Neufeldt, S. R. Solvent Effects on the Selectivity of Palladium-Catalyzed Suzuki−Miyaura Couplings. *Isr. J. Chem.* **2020**, *60*, 406−409.

57. Ibsen, G. M.; Menezes da Silva, V. H.; Pettigrew, J. C.; Neufeldt, S. R. Triflate-Selective Suzuki Cross-Coupling of Chloro- and Bromoaryl Triflates under Ligand-Free Conditions. *Chem. Asian J.* **2023**, *18*, e202300036.

58. Elias, E. K.; Rehbein, S. M.; Neufeldt, S. R. Solvent Coordination to Palladium Can Invert the Selectivity of Oxidative Addition. *Chem. Sci.* **2022**, *13*, 1618−1628.

59. Norman, J. P.; Larson, N. G.; Entz, E. D.; Neufeldt, S. R. Unconventional Site Selectivity in Palladium-Catalyzed Cross-Couplings of Dichloroheteroarenes under Ligand-Controlled and Ligand-Free Systems. *J. Org. Chem.* **2022**, *87*, 7414−7421.

60. Ng, S. S.; Pang, W. H.; Yuen, O. Y.; So, C. M. Recent Advances in the Application of Ligands in Palladium-Catalyzed Chemoselective Coupling Reactions at C−Br, C−OTf, and C−Cl Sites. *Org. Chem. Front.* **2023**, *10*, 4408−4436.

61. Petrakis, K. S.; Nagabhushan, T. L. Palladium-Catalyzed Substitutions of Triflates Derived from Tyrosine-Containing Peptides and Simpler Hydroxyarenes Forming 4-(Diethoxyphosphinyl)phenylalanines and Diethyl Arylphosphonates. *J. Am. Chem. Soc.* **1987**, *109*, 2831−2833.

62. Blum, J.; Katz, J. A.; Jaber, N.; Michman, M.; Schumann, H.; Schutte, S.; Kaufmann, J.; Wassermann, B. C. Palladium-Catalyzed Cross-Methylation of Aryl Triflates by Intramolecularly Stabilized Dialkyl-Aluminum, -Gallium and -Indium Reagents. *J. Mol. Catal. A: Chem.* **2001**, *165*, 97−102.

63. Kamikawa, T.; Hayashi, T. Control of Reactive Site in Palladium-Catalyzed Grignard Cross-Coupling of Arenes Containing Both Bromide and Triflate. *Tetrahedron Lett.* **1997**, *38*, 7087−7090.

64. Kamikawa, T.; Hayashi, T. Dichloro[(2-dimethylamino)propyldiphenylphosphine] palladium(II) ($PdCl_2$(alaphos)): An Efficient Catalyst for Cross-Coupling of Aryl Triflates with Alkynyl Grignard Reagents. *J. Org. Chem.* **1998**, *63*, 8922−8925.

65. Espino, G.; Kurbangalieva, A.; Brown, J. M. Aryl Bromide/Triflate Selectivities Reveal Mechanistic Divergence in Palladium-Catalysed Couplings; The Suzuki−Miyaura Anomaly. *Chem. Commun.* **2007**, 1742−1744.

66. Fu, J.-m.; Snieckus, V. Connections to the Died *ortho* Metalation Strategy. Pd(0)-Catalyzed Cross Coupling of Aryl Boronic Acids with Aryl Triflates. *Tetrahedron Lett.* **1990**, *31*, 1665−1668.

67. Zhang, E.; Tang, J.; Li, S.; Wu, P.; Moses, J. E.; Sharpless, K. B. Chemoselective Synthesis of Polysubstituted Pyridines from Heteroaryl Fluorosulfates. *Chem. Eur. J.* **2016**, *22*, 5692−5697.

68. Cui, L.-C.; Zhang, Z.-Q.; Lu, X.; Xiao, B.; Fu, Y. Pd-Catalyzed Cross-Coupling of 1,1-Diborylalkanes with Aryl Triflates. *RSC Adv.* **2016**, *6*, 51932−51935.

69. Oh-e, T.; Miyaura, N.; Suzuki, A. Palladium-Catalyzed Cross-Coupling Reaction of Organoboron Compounds with Organic Triflates. *J. Org. Chem.* **1993**, *58*, 2201−2208.

70. Huth, A.; Beetz, I.; Schumann, I. Synthesis of Diarylic Compounds by Palladium Catalyzed Reaction of Aromatic Triflates with Boronic Acids. *Tetrahedron* **1989**, *45*, 6679−6682.

71. Orsini, F.; Pelizzoni, F. Pd(0)-Mediated Cross-Coupling of Reformatsky Reagents with Vinyl and Aryl Triflates. *Synth. Commun.* **1987**, *17*, 1389−1402.

72. Hirota, K.; Isobe, Y.; Maki, Y. Palladium-Catalyzed Cross-Coupling Reaction of Trialkylaluminiums with Aryl Triflates: Facile Conversion of a Phenolic Hydroxy Group into an Alkyl Group. *J. Chem. Soc., Perkin Trans. 1* **1989**, 2513−2514.

73. Rahman, O.; Kihlberg, T.; Långström, B. Aryl Triflates and [^{11}C]/(^{13}C)Carbon Monoxide in the Synthesis of ^{11}C-/^{13}C-Amides. *J. Org. Chem.* **2003**, *68*, 3558−3562.

74. Rao, M. L. N.; Banerjee, D.; Jadhav, D. N. Palladium Catalyzed Atom-Efficient Cross-Coupling Reactions of Triarylbismuths with Aryl Iodides and Aryl Triflates. *Tetrahedron Lett.* **2007**, *48*, 6644−6647.

75. Rao, M. L. N.; Jadhav, D. N.; Banerjee, D. A New Palladium Catalyzed Protocol for Atom-Efficient Cross-Coupling Reactions of Triarylbismuths with Aryl Halides and Triflates. *Tetrahedron* **2008**, *64*, 5762−5772.

76. Gooßen, L. J.; Lange, P. P.; Rodríguez, N.; Linder, C. Low-temperature Ag/Pd-Catalyzed Decarboxylative Cross−Coupling of Aryl Triflates with Aromatic Carboxylate Salts. *Chem. Eur. J.* **2010**, *16*, 3906−3909.

77. Park, Y.; Min, J.; Eom, D.; Lee, P. H. Synthesis of Acyl Alkenylindium Reagents and Their Application in the Synthesis of (*Z*)-α,β-Unsaturated Ketones via Palladium-Catalyzed Cross-Coupling Reaction. *Org. Lett.* **2015**, *17*, 3934−3937.

78. Niesobski, P.; Martínez, I. S.; Kustosz, S.; Müller, T. J. J. Sequentially Pd/Cu-Catalyzed Alkynylation-Oxidation Synthesis of 1,2-Diketones and Consecutive One-Pot Generation of Quinoxalines. *Eur. J. Org. Chem.* **2019**, 5214−5218.

79. Echavarren, A. M.; Stille, J. K. Palladium-Catalyzed Coupling of Aryl Triflates with Organostannanes. *J. Am. Chem. Soc.* **1987**, *109*, 5478−5486.

80. Ansari, N. N.; Cummings, M. M.; Söderberg, B. C. G. Chemoselectivity in the Kosugi−Migita−Stille Coupling of Bromophenyl Triflates and Bromo-nitrophenyl Triflates with (Ethenyl)tributyltin. *Tetrahedron* **2018**, *74*, 2547−2560.

81. Robert, N.; Hoarau, C.; Célanire, S.; Ribéreau, P.; Godard, A.; Quéguiner, G.; Marsais, F. Efficient and Fast Heck Vinylation of 2-Bromo-6-methyl Pyridines with Methylacrylate. Application to the Synthesis of 6-Methyl Cyclopenta[*b*]pyridinone. *Tetrahedron* **2005**, *61*, 4569−4576.

82. Lee, H.; Lee, Y.; Cho, S. H. Palladium-Catalyzed Chemoselective Negishi Cross-Coupling of Bis[(pinacolato)boryl]methylzinc Halides with Aryl (Pseudo)Halides. *Org. Lett.* **2019**, *21*, 5912−5916.

83. Gooßen, L. J.; Linder, C.; Rodríguez, N.; Lange, P. P. Biaryl and Aryl Ketone Synthesis via Pd-Catalyzed Decarboxylative Coupling of Carboxylate Salts with Aryl Triflates. *Chem. Eur. J.* **2009**, *15*, 9336−9349.

84. Littke, A. F.; Dai, C.; Fu, G. C. Versatile Catalysts for the Suzuki Cross-Coupling of Arylboronic Acids with Aryl and Vinyl Halides and Triflates under Mild Conditions. *J. Am. Chem. Soc.* **2000**, *122*, 4020−4028.

85. Molander, G. A.; Petrillo, D. E.; Landzberg, N. R.; Rohanna, J. C.; Biolatto, B. Palladium-Catalyzed Suzuki−Miyaura Reactions of Potassium Aryl- and Heteroaryltrifluoroborates with Aryl- and Heteroaryl Triflates. *Synlett* **2005**, 1763−1766.

86. Littke, A. F.; Fu, G. C. A Versatile Catalyst for Heck Reactions of Aryl Chlorides and Aryl Bromides under Mild Conditions. *J. Am. Chem. Soc.* **2001**, *123*, 6989−7000.

87. Shen, C.; Wei, Z.; Jiao, H.; Wu, X.-F. Ligand- and Solvent-Tuned Chemoselective Carbonylation of Bromoaryl Triflates. *Chem. Eur. J.*, **2017**, *23*, 13369−13378.

88. Schoenebeck, F.; Houk, K. N. Ligand-Controlled Regioselectivity in Palladium-Catalyzed Cross Coupling Reactions. *J. Am. Chem. Soc.* **2010**, *132*, 2496−2497.

89. Barrios-Landeros, F.; Hartwig, J. F. Distinct Mechanisms for the Oxidative Addition of Chloro-, Bromo-, and Iodoarenes to a Bisphosphine Palladium(0) Complex with Hindered Ligands. *J. Am. Chem. Soc.* **2005**, *127*, 6944−6945.

90. Proutiere, F.; Schoenebeck, F. Solvent Effect on Palladium-Catalyzed Cross-Coupling Reactions and Implications on the Active Catalytic Species. *Angew. Chem. Int. Ed.* **2011**, *50*, 8192−8195.

91. Littke, A. F.; Schwarz, L.; Fu, G. C. Pd/P(*t*-Bu)$_3$: A Mild and General Catalyst for Stille Reactions of Aryl Chlorides and Aryl Bromides. *J. Am. Chem. Soc.* **2002**, *124*, 6343−6348.

92. Proutiere, F.; Lyngvi, E.; Aufiero, M.; Sanhueza, I. A.; Schoenebeck, F. Combining the Reactivity Properties of PCy$_3$ and P*t*Bu$_3$ into a Single Ligand, P(*i*Pr)(*t*Bu)$_2$. Reaction via Mono- or Bisphosphine Palladium(0) Centers and Palladium(I) Dimer Formation. *Organometallics* **2014**, *33*, 6879−6884.

93. Pu, X.; Zhang, Y.; Su, M.; He, X.; Qiu, L. Palladium-Catalyzed Selective Buchwald−Hartwig C−N Coupling of Chloroaryl Triflates with Amines. *Tetrahedron Lett.* **2024**, *142*,155096.

94. Finke, A. D.; Elleby, E. C.; Boyd, M. J.; Weissman, H.; Moore, J. S. Zinc Chloride-Promoted Aryl Bromide-Alkyne Cross-Coupling Reactions at Room Temperature. *J. Org. Chem.* **2009**, *74*, 8897−8900.

95. Kalvet, I.; Sperger, T.; Scattolin, T.; Magnin, G.; Schoenebeck, F. Palladium(I) Dimer Enabled Extremely Rapid and Chemoselective Alkylation of Aryl Bromides over Triflates and Chlorides in Air. *Angew. Chem. Int. Ed.* **2017**, *56*, 7078−7082.

96. Kalvet, I.; Magnin, G.; Schoenebeck, F. Rapid Room-Temperature, Chemoselective C_{sp^2}−C_{sp^2} Coupling of Poly(pseudo)halogenated Arenes Enabled by Palladium(I) Catalysis in Air. *Angew. Chem. Int. Ed.* **2017**, *56*, 1581−1585.

97. Keaveney, S. T.; Kundu, G.; Schoenebeck, F. Modular Functionalization of Arenes in a Triply Selective Sequence: Rapid C(sp^2) and C(sp^3) Coupling of C−Br, C−OTf, and C−Cl Bonds Enabled by a Single Palladium(I) Dimer. *Angew. Chem. Int. Ed.* **2018**, *57*, 12573−12577.

98. Scattolin, T.; Senol, E.; Yin, G.; Guo, Q.; Schoenebeck, F. Site-Selective C−S Bond Formation at C−Br over C−OTf and C−Cl Enabled by an Air-Stable, Easily Recoverable, and Recyclable Palladium(I) Catalyst. *Angew. Chem. Int. Ed.* **2018**, *57*, 12425−12429.

99. Mendel, M.; Gnägi, L.; Dabranskaya, U.; Schoenebeck, F. Rapid and Modular Access to Vinyl Cyclopropanes Enabled by Air-Stable Palladium(I) Dimer Catalysis. *Angew. Chem. Int. Ed.* **2023**, *62*, e202211167.

100. Sperger, T.; Stirner, C. K.; Schoenebeck, F. Bench-Stable and Recoverable Palladium(I) Dimer as an Efficient Catalyst for Heck Cross-Coupling. *Synthesis* **2017**, *49*, 115−120.

101. Sperger, T.; Schoenebeck, F. α-Arylation of Esters and Ketones Enabled by a Bench-Stable Pd(I) Dimer Catalyst. *Synthesis* **2018**, *50*, 4471−4475.

102. Kalvet, I.; Deckers, K.; Funes-Ardoiz, I.; Magnin, G.; Sperger, T.; Kremer, M.; Schoenebeck, F. Selective *ortho*-Functionalization of Adamantylarenes Enabled by Dispersion and an Air-Stable Palladium(I) Dimer. *Angew. Chem. Int. Ed.* **2020**, *59*, 7721−7725.

103. Kundu, G.; Sperger, T.; Rissanen, K.; Schoenebeck, F. A Next-Generation Air-Stable Palladium(I) Dimer Enables Olefin Migration and Selective C−C Coupling in Air. *Angew. Chem. Int. Ed.* **2020**, *59*, 21930−21934.

104. Kundu, G.; Opincal, F.; Sperger, T.; Schoenebeck, F. Air-Stable Pd^{I} Dimer Enabled Remote Functionalization: Access to Fluorinated 1,1-Diaryl Alkanes with Unprecedented Speed. *Angew. Chem. Int. Ed.* **2022**, *61*, e202113667.

105. Surry, D. S.; Buchwald, S. L. Dialkylbiaryl Phosphines in Pd-Catalyzed Amination: A User's Guide. *Chem. Sci.* **2011**, *2*, 27−50.

106. Barder, T. E.; Walker, S. D.; Martinelli, J. R.; Buchwald, S. L. Catalysts for Suzuki−Miyaura Coupling Processes: Scope and Studies of the Effect of Ligand Structure. *J. Am. Chem. Soc.* **2005**, *127*, 4685−4696.

107. Hao, C. Y.; Wang, D.; Li, Y. W.; Dong, L. L.; Jin, Y.; Zhang, X. R.; Zhu, H. Y.; Chang, S. Carbonylative Coupling of Aryl Tosylates/Triflates with Arylboronic Acids under CO Atmosphere. *RSC Adv.* **2016**, *6*, 86502−86509.

108. Durbin, M. J.; Willis, M. C. Palladium-Catalyzed α-Arylation of Oxindoles. *Org. Lett.* **2008**, *10*, 1413−1415.

109. Odell, L. R.; Sävmarker, J.; Larhed, M. Microwave-Promoted Aminocarbonylation of Aryl Triflates Using $Mo(CO)_6$ as a Solid CO Source. *Tetrahedron Lett.* **2008**, *49*, 6115−6118.

110. Tréguier, B.; Hamze, A.; Provot, O.; Brion, J.-D.; Alami, M. Expeditious Synthesis of 1,1-Diarylethylenes Related to Isocombretastatin A-4(*iso*CA-4) via Palladium-Catalyzed Arylation of *N*-Tosylhydrazones with Aryl Triflates. *Tetrahedron Lett.* **2009**, *50*, 6549−6552.

111. Zhou, C.; Liu, Q.; Li, Y.; Zhang, R.; Fu, X.; Duan, C. Palladium-Catalyzed Desulfitative Arylation by C−O Bond Cleavage of Aryl Triflates with Sodium Arylsulfinates. *J. Org.Chem.* **2012**, *77*, 10468−10472.

112. Bhunia, S. K.; Das, P.; Nandi, S.; Jana, R. Carboxylation of Aryl Triflates with CO_2 Merging Palladium and Visible-Light-Photoredox Catalysts. *Org. Lett.* **2019**, *21*, 4632−4637.

113. Shimomaki, K.; Nakajima, T.; Caner, J.; Toriumi, N.; Iwasawa, N. Palladium-Catalyzed Visible-Light-Driven Carboxylation of Aryl and Alkenyl Triflates by Using Photoredox Catalysts. *Org. Lett.* **2019**, *21*, 4486−4489.

114. He, X.; Hu, S.; Xiao, Y.; Yu, L.; Duan, W. Access to Ketones through Palladium-Catalyzed Cross−Coupling of Phenol Derivatives with Nitroalkanes Followed by Nef Reaction. *Eur. J. Org. Chem.* **2022**, *2022*, 135−139.

115. King, S. M.; Buchwald, S. L. Development of a Method for the *N*-Arylation of Amino Acid Esters with Aryl Triflates. *Org. Lett.* **2016**, *18*, 4128−4131.

116. Onodera, S.; Kochi, T.; Kakiuchi, F. Synthesis of *N*-Arylpyrazoles by Palladium-Catalyzed Coupling of Aryl Triflates with Pyrazole Derivatives. *J. Org. Chem.* **2019**, *84*, 6508−6515.

117. Chang, J. W. W.; Chia, E. Y.; Chai, C. L. L.; Seayad, J. Scope of Direct Arylation of Fluorinated Aromatics with Aryl Sulfonates. *Org. Biomol. Chem.* **2012**, *10*, 2289−2299.

118. Peterson, L. J.; Wolfe, J. P. Palladium-Catalyzed Alkene Carboamination Reactions of Electron-Poor Nitrogen Nucleophiles. *Adv. Synth. Catal.* **2015**, *357*, 2339−2344.

119. Hutt, J. T.; Wolfe, J. P. Synthesis of 2,3-Dihydrobenzofurans via the Palladium Catalyzed Carboalkoxylation of 2-Allylphenols. *Org. Chem. Front.* **2016**, *3*, 1314−1318.

120. Peterson, L. J.; Luo, J.; Wolfe, J. P. Synthesis of Cyclic Guanidines Bearing *N*-Arylsulfonyl and *N*-Cyano Protecting Groups via Pd-Catalyzed Alkene Carboamination Reactions. *Org. Lett.* **2017**, *19*, 2817−2820.

121. Zhang, H. A New Protocol for Synthesizing Diarylmethanes Using a Benzyltitanium Reagent as a Nucleophile. *J. Chem. Res.* **2022**, *46*, DOI: 10.1177/17475198221091941.

122. Murai, N.; Yonaga, M.; Tanaka, K. Palladium-Catalyzed Direct Hydroxymethylation of Aryl Halides and Triflates with Potassium Acetoxymethyltrifluoroborate. *Org. Lett.* **2012**, *14*, 1278−1281.

123. Fornwald, R. M.; Fritz, J. A.; Wolfe, J. P. Influence of Catalyst Structure and Reaction Conditions on *anti*- versus *syn*-Aminopalladation Pathways in Pd-Catalyzed Alkene Carboamination Reactions of *N*-Allylsulfamides. *Chem. Eur. J.* **2014**, *20*, 8782−8790.

124. Dennis, J. M.; White, N. A.; Liu, R. Y.; Buchwald, S. L. Breaking the Base Barrier: An Electron-Deficient Palladium Catalyst Enables the Use of a Common Soluble Base in C−N Coupling. *J. Am. Chem. Soc.* **2018**, *140*, 4721−4725.

125. Dennis, J. M.; White, N. A.; Liu, R. Y.; Buchwald, S. L. Pd-Catalyzed C−N Coupling Reactions Facilitated by Organic Bases: Mechanistic Investigation Leads to Enhanced Reactivity in the Arylation of Weakly Binding Amines. *ACS Catal.* **2019**, *9*, 3822−3830.

126. Taeufer, T.; Pospech, J. Palladium-Catalyzed Synthesis of *N*,*N*-Dimethylanilines via Buchwald−Hartwig Amination of (Hetero)aryl Triflates. *J. Org. Chem.* **2020**, *85*, 7097−7111.

127. Gao, P. S.; Zhang, K.; Yang, M.-M.; Xu, S.; Sun, H.-M.; Zhang, J.-L.; Gao, Z.-W.; Zhang, W.-Q.; Xu, L.-W. A Robust Multifunctional Ligand-Controlled Palladium-Catalyzed Carbonylation Reaction in Water. *Chem. Commun.* **2018**, *54*, 5074−5077.

128. Echavarren, A. M.; Stille, J. K. Palladium-Catalyzed Carbonylative Coupling of Aryl Triflates with Organostannanes. *J. Am. Chem. Soc.* **1988**, *110*, 1557−1565.

129. Lesma, G.; Sacchetti, A.; Silvani, A. Palladium-Catalyzed Hydroxycarbonylation of Aryl and Vinyl Triflates by in situ Generated Carbon Monoxide under Microwave Irradiation. *Synthesis* **2006**, 594−596.

130. Wang, B.; Sun, H.-X.; Sun, Z.-H. A General and Efficient Suzuki−Miyaura Cross-Coupling Protocol Using Weak Base and No Water: The Essential Role of Acetate. *Eur. J. Org. Chem.* **2009**, *2009*, 3688−3692.

131. Dogga, B.; Kumar, C. S. A.; Joseph, J. T. Palladium-Catalyzed Reductive Carbonylation of (Hetero)Aryl Halides and Triflates Using Cobalt Carbonyl as CO Source. *Eur. J. Org. Chem.* **2021**, *2021*, 309−313.

132. Fawcett, A.; Biberger, T.; Aggarwal, V. K. Carbopalladation of C−C σ-Bonds Enabled by Strained Boronate Complexes. *Nat. Chem.* **2019**, *11*, 117−122.

133. Brennfuhrer, A.; Neumann, H.; Beller, M. Palladium-Catalyzed Reductive Carbonylation of Aryl Triflates with Synthesis Gas. *Synlett* **2007**, 2537−2540.

134. Yuan, Y.; Wu, F.-P.; Xu, J.-X.; Wu, X.-F. Four-Component Borocarbonylation of Vinylarenes Enabled by Cooperative Cu/Pd Catalysis: Access to β-Boryl Ketones and β-Boryl Vinyl Esters. *Angew. Chem. Int. Ed.* **2020**, *59*, 17055−17061.

135. Fujita, T.; Ichitsuka, T.; Fuchibe, K.; Ichikawa, J. Facile Synthesis of β,β-Difluorostyrenes via the Negishi Coupling of Thermally Stable 2,2-Difluorovinyl Zinc-TMEDA Complex. *Chem. Lett.* **2011**, *40*, 986−988.

136. Borrajo-Calleja, G. M.; Bizet, V.; Bürgi, T.; Mazet, C. Access to Enantioenriched 2,3- and 2,5-Dihydrofurans with A Fully Substituted C2 Stereocenter by Pd-Catalyzed Asymmetric Intermolecular Heck Reaction. *Chem. Sci.* **2015**, *6*, 4807−4811.

137. Hackenberger, D.; Song, B.; Grünberg, M. F.; Farsadpour, S.; Menges, F.; Kelm, H.; Groß, C.; Wolff, T.; Niedner-Schatteburg, G.; Thiel, W. R.; Gooßen, L. J. Bimetallic Cu/Pd Catalysts with Bridging Aminopyrimidinyl Phosphines for Decarboxylative Cross−Coupling Reactions at Moderate Temperature. *ChemCatChem* **2015**, *7*, 3579−3588.

138. Komami, N.; Matsuoka, K.; Yoshino, T.; Matsunaga, S. Palladium-Catalyzed Germylation of Aryl Bromides and Aryl Triflates Using Hexamethyldigermane. *Synthesis* **2018**, *50*, 2067−2075.

139. Kamikawa, T.; Hayashi, T. Palladium Catalysts for Cross-Coupling of *ortho*-Substituted Aryl Triflates with Grignard Reagents. *Synlett* **1997**, 163−164.

140. Huang, Z.; Lim, L. H.; Chen, Z.; Li, Y.; Zhou, F.; Su, H.; Zhou, J. S. Arene CH−O Hydrogen Bonding: A Stereocontrolling Tool in Palladium-Catalyzed Arylation and Vinylation of Ketones. *Angew. Chem. Int. Ed.* **2013**, *52*, 4906−4911.

141. Huang, Z.; Chen, Z.; Lim, L. H.; Phan-Quang, G. C.; Hirao, H.; Zhou, J. S. Weak Arene C−H···O Hydrogen Bonding in Palladium-Catalyzed Arylation and Vinylation of Lactones. *Angew. Chem. Int. Ed.* **2013**, *52*, 5807−5812.

142. Yang, J.; Zhou, J. S. A General Method for Asymmetric Arylation and Vinylation of Silyl Ketene Acetals. *Org. Chem. Front.* **2014**, *1*, 365−367.

143. Neff, R. K.; Frantz, D. E. Cationic Alkynyl Heck Reaction Toward Substituted Allenes Using BobCat: A New Hybrid Pd(0)-Catalyst Incorporating a Water-Soluble Dba Ligand. *J. Am. Chem. Soc.* **2018**, *140*, 17428−17432.

144. Ozawa, F.; Hayashi, T. Catalytic Asymmetric Arylation of *N*-Substituted 2-Pyrrolines with Aryl Triflates. *J. Organomet. Chem.* **1992**, *428*, 267−277.

145. Ozawa, F.; Kubo, A.; Hayashi, T. Palladium-Catalyzed Asymmetric Arylation of 2,3-Dihydrofuran: 1,8-Bis(dimethylamino)naphthalene as an Efficient Base. *Tetrahedron Lett.* **1992**, *33*, 1485−1488.

146. Wolfe, J. P.; Buchwald, S. L. Palladium-Catalyzed Amination of Aryl Halides and Aryl Triflates: *N*-Hexyl-2-methyl-4-methoxyaniline and *N*-Methyl-*N*,-(4-chlorophenyl)aniline. *Org. Synth.* **2002**, *78*, 23−35.

147. Rabeyrin, C.; Sinou, D. Palladium-Catalyzed Asymmetric Arylation of 2, 3-Dihydrofuran with Aryl Triflates in Water in the Presence of Surfactants. *J. Mol. Catal. A: Chem.* **2004**, *215*, 89−93.

148. Li, H.; Wan, S.-L.; Ding, C.-H.; Xu, B.; Hou, X.-L. Kinetic Resolution of 2-Substituted-2,3-Dihydrofurans by a Palladium-Catalyzed Asymmetric Heck Reaction. *RSC Adv.* **2015**, *5*, 75411−75414.

149. McWilliams, J. C.; Fleitz, F. J.; Zheng, N.; Armstrong, J. D. III Preparation of *n*-Butyl 4-Chlorophenyl Sulfide. *Org. Synth.* **2002**, *79*, 43−51.

150. Gooßen, L. J.; Rodríguez, N.; Linder, C. Decarboxylative Biaryl Synthesis from Aromatic Carboxylates and Aryl Triflates. *J. Am. Chem. Soc.* **2008**, *130*, 15248−15249.

151. Bayardon, J.; Cavazzini, M.; Maillard, D.; Pozzi, G.; Quici, S.; Sinou, D. Chiral Fluorous Phosphorus Ligands Based on the Binaphthyl Skeleton: Synthesis and Applications in Asymmetric Catalysis. *Tetrahedron: Asymmetry* **2003**, *14*, 2215−2224.

152. Jin, Y.; Chen, M.; Ge, S.; Hartwig, J. F. Palladium-Catalyzed, Enantioselective α-Arylation of α-Fluorooxindoles. *Org. Lett.* **2017**, *19*, 1390−1393.

153. Takagi, K.; Sakakibara, Y. Nickel(0) or Palladium(0)-Catalyzed Cyanation of Aryl Triflates. *Chem. Lett.* **1989**, *18*, 1957−1958.

154. Piber, M.; Jensen, A. E.; Rottländer, M.; Knochel, P. New Efficient Nickel- and Palladium-Catalyzed Cross-Coupling Reactions Mediated by Tetrabutylammonium Iodide. *Org. Lett.* **1999**, *1*, 1323−1326.

155. Molander, G. A.; Ito, T. Cross-Coupling Reactions of Potassium Alkyltrifluoroborates with Aryl and 1-Alkenyl Trifluoromethanesulfonates. *Org. Lett.* **2001**, *3*, 393−396.

156. Molander, G. A.; Yun, C.-S. Cross-Coupling Reactions of Primary Alkylboronic Acids with Aryl Triflates and Aryl Halides. *Tetrahedron* **2002**, *58*, 1465−1470.

157. Zhu, Y.-Z.; Cai, C. Palladium-Catalyzed Cyanation of Aryl Triflates. *Synth. Commun.* **2008**, *38*, 2753−2760.

158. Lindh, J.; Fardost, A.; Almeida, M.; Nilsson, P. Convenient Stille Carbonylative Cross-Couplings Using Molybdenum Hexacarbonyl. *Tetrahedron Lett.* **2010**, *51*, 2470−2472.

159. Ying, J.; Le, Z.; Wu, X.-F. Palladium-Catalyzed Double Carbonylative Cyclization of Propargyl Alcohols and Aryl Triflates to Expedite Construction of 4-Aroyl-furan-2(5*H*)-ones. *Org. Chem. Front.* **2020**, *7*, 2757−2760.

160. Konishi, H.; Kumon, M.; Yamaguchi, M.; Manabe, K. Palladium-Catalyzed External-CO-Free Reductive Carbonylation of Aryl Sulfonates. *Tetrahedron* **2020**, *76*, 131639.

161. Wang, S.; Wang, J.-S.; Le, Z.; Ying, J.; Wu, X.-F. Palladium-Catalyzed Carbonylative Synthesis of Aryl Esters from *p*-Benzoquinones and Aryl Triflates. *Org. Biomol. Chem.* **2021**, *19*, 7353−7356.

162. Zou, Y.; Qin, L.; Ren, X.; Lu, Y.; Li, Y.; Zhou, J. S. Selective Arylation and Vinylation at the α Position of Vinylarenes. *Chem. Eur. J.* **2013**, *19*, 3504−3511.

163. Edelstein, E. K.; Namirembe, S.; Morken, J. P. Enantioselective Conjunctive Cross-Coupling of Bis(alkenyl)borates: A General Synthesis of Chiral Allylboron Reagents. *J. Am. Chem. Soc.* **2017**, *139*, 5027−5030.

164. Park, J.-W.; Kang, B.; Dong, V. M. Catalytic Alkyne Arylation Using Traceless Directing Groups. *Angew. Chem. Int. Ed.* **2018**, *57*, 13598−13602.

165. Wu, X.-F.; Neumann, H.; Beller, M. Palladium-Catalyzed Coupling Reactions: Carbonylative Heck Reactions to Give Chalcones. *Angew. Chem. Int. Ed.* **2010**, *49*, 5284−5288.

166. Chen, X.; Wu, H.; Yu, R.; Zhu, H.; Wang, Z. Palladium-Catalyzed C−P(III) Bond Formation by Coupling ArBr/ArOTf with Acylphosphines. *J. Org. Chem.* **2021**, *86*, 8987−8996.

167. Dang, H. T.; Nguyen, V. D.; Pham, H. H.; Arman, H. D.; Larionov, O. V. Highly Stereoselective and Catalytic Desulfitative C−O and C−I Dienylation with Sulfolenes: The Importance of Basic Additives. *Tetrahedron* **2019**, *75*, 3258−3264.

168. Shang, R.; Yang, Z.-W.; Wang, Y.; Zhang, S.-L.; Liu, L. Palladium-Catalyzed Decarboxylative Couplings of 2-(2-Azaaryl)acetates with Aryl Halides and Triflates. *J. Am. Chem. Soc.* **2010**, *132*, 14391−14393.

169. Wu, X.-F.; Sundararaju, B.; Anbarasan, P.; Neumann, H.; Dixneuf, P. H.; Beller, M. A General Cyclocarbonylation of Aryl Bromides and Triflates with Acetylenes: Palladium-Catalyzed Synthesis of 3-Alkylidenefuran-2-ones. *Chem. Eur. J.* **2011**, *17*, 8014−8017.

170. Wu, X.-F.; Sundararaju, B.; Neumann, H.; Dixneuf, P. H.; Beller, M. A General Palladium-Catalyzed Carbonylative Sonogashira Coupling of Aryl Triflates. *Chem. Eur. J.* **2011**, *17*, 106−110.

171. Xia, T.; He, L.; Liu, Y. A.; Hartwig, J. F.; Liao, X. Palladium-Catalyzed Cross-Coupling of Ethyl Bromodifluoroacetate with Aryl Bromides or Triflates and Cross-Coupling of Ethyl Bromofluoroacetate with Aryl Iodides. *Org. Lett.* **2007**, *19*, 2610−2613.

172. Wang, L.; Wang, T.; Cheng, G.-J.; Li, X.; Wei, J.-J.; Guo, B.; Zheng, C.; Chen, G.; Ran, C.; Zheng, C. Direct C−H Arylation of Aldehydes by Merging Photocatalyzed Hydrogen Atom Transfer with Palladium Catalysis. *ACS Catal.* **2020**, *10*, 7543−7551.

173. Hu, J.; Lu, Y.; Li, Y.; Zhou, J. S. Highly Active Catalysts of Bisphosphine Oxides for Asymmetric Heck Reaction. *Chem. Commun.* **2013**, *49*, 9425−9427.

174. Cacchi, S.; Ciattini, P. G.; Morera, E.; Ortar, G. Palladium-Catalyzed Carbonylation of Aryl Triflates. Synthesis of Arenecarboxylic Acid Derivatives from Phenols. *Tetrahedron Lett.* **1986**, *27*, 3931−3934.

175. Fleckenstein, C. A.; Plenio, H. Sterically Demanding Trialkylphosphines for Palladium-Catalyzed Cross Coupling Reactions − Alternatives to P*t*Bu$_3$. *Chem. Soc. Rev.* **2010**, *39*, 694−711.

176. Jopp, S.; Wallaschkowski, T.; Ehlers, P.; Frank, E.; Schneider, G.; Wölfling, J.; Mernyák, E.; Villinger, A.; Langer, P. Chemoselective Suzuki−Miyaura Reactions of 4-Bromo-3-*O*-triflyl-estrone. Synthesis and Atropisomerism of Arylated Estrones. *Tetrahedron* **2018**, *74*, 2825−2836.

177. Sakamoto, S.; Butcher, T. W.; Yang, J. L.; Hartwig, J. F. *gem*-Difluoroallylation of Aryl Halides and Pseudo Halides with Difluoroallylboron Reagents in High Regioselectivity. *Angew. Chem. Int. Ed.* **2021**, *60*, 25746−25752.

178. Yuen, O. Y.; Ng, S. S.; Pang, W. H.; So, C. M. Palladium-Catalyzed Chemoselective Suzuki−Miyaura Cross-Croupling Reaction of Poly(pseudo)halogenated Arenes. *J. Organomet. Chem.* **2024**, *1005*, 122983.

179. Ng, S. S.; Chen, Z.; Yuen, O. Y.; So, C. M. Palladium-Catalyzed Chemoselective Borylation of (Poly)halogenated Aryl Triflates and Their Application in Consecutive Reactions. *Adv. Synth. Catal.* **2022**, *364*, 1596−1601.

180. Chen, Z.; Gu, C.; Yuen, O. Y.; So, C. M. Palladium-Catalyzed Chemoselective Direct α-Arylation of Carbonyl Compounds with Chloroaryl Triflates at the C−Cl Site. *Chem. Sci.* **2022**, *13*, 4762−4769.

181. Wang, M.; So, C. M. Inverting Conventional Chemoselectivity in the Sonogashira Coupling Reaction of Polyhalogenated Aryl Triflates with TMS-Arylalkynes. *Org. Lett.* **2022**, *24*, 681−685.

182. Wang, M.; Yuen, O. Y.; So, C. M. Palladium-Catalyzed Desulfinative Cross−Coupling of Polyhalogenated Aryl Triflates with Aryl Sulfinate Salts: Inversion of Traditional Chemoselectivity. *Chin. J. Chem.* **2023**, *41*, 909−914.

183. Wang, M.; Pang, W. H.; Yuen, O. Y.; Ng, S. S.; So, C. M. Palladium-Catalyzed Deuterodehalogenation of Halogenated Aryl Triflates Using Isopropanol-d_8 as the Deuterium Source. *Org. Lett.* **2023**, *25*, 8429−8433.

184. Chen, Z.; Pang, W. H.; Yuen, O. Y.; Ng, S. S.; So, C. M. Palladium-Catalyzed Chemoselective Phosphorylation of Poly(pseudo)halides: A Route for Organophosphorus Synthesis. *J. Org. Chem.* **2024**, DOI: 10.1021/acs.joc.3c02345.

185. Gu, C.; So, C. M. Regio- and Chemoselective Palladium-Catalyzed Additive-Free Direct C−H Functionalization of Heterocycles with Chloroaryl Triflates Using Pyrazole-Alkyl Phosphine Ligands. *Adv. Sci.* **2024**, *11*, 2309192.

186. Gu, C.; Yuen, O. Y.; Ng, S. S.; So, C. M. Palladium-Catalyzed Chemoselective Amination of Chloro(hetero)aryl Triflates Enabled by Alkyl-Pyrazole-Based Phosphine Ligands, *Adv. Synth. Catal.* **2024**, *366*, 1565−1574.

187. Hu, X.-Q.; Lichte, D.; Rodstein, I.; Weber, P.; Seitz, A.-K.; Scherpf, T.; Gessner, V. H.; Gooßen, L. J. Ylide-Functionalized Phosphine (YPhos)-Palladium Catalysts: Selective Monoarylation of Alkyl Ketones with Aryl Chlorides. *Org. Lett.* **2019**, *21*, 7558−7562.

188. Tappen, J.; Rodstein, I.; McGuire, K.; Großjohann, A.; Löffler, J.; Scherpf, T.; Gessner, V. H. Palladium Complexes Based on Ylide-Functionalized Phosphines (YPhos): Broadly Applicable High-Performance Precatalysts for the Amination of Aryl Halides at Room Temperature. *Chem. Eur. J.* **2020**, *26*, 4281−4288.

189. Lapointe, S.; Sarbajna, A.; Gessner, V. H. Ylide-Substituted Phosphines: A Platform of Strong Donor Ligands for Gold Catalysis and Palladium-Catalyzed Coupling Reactions. *Acc. Chem. Res.* **2022**, *55*, 770−782.

190. Hu, Z.; Wei, X.-J.; Handelmann, J.; Seitz, A.-K.; Rodstein, I.; Gessner, V. H.; Gooßen, L. J. Coupling of Reformatsky Reagents with Aryl Chlorides Enabled by Ylide−Functionalized Phosphine Ligands. *Angew. Chem. Int. Ed.* **2021**, *60*, 6778−6783.

191. Shina, N.; Champagne, P. A.; Rodriguez, M. J.; Lu, Y.; Kopach, M. E.; Mitchell, D.; Organ, M. G. One-Pot Sequential Kumada−Tamao−Corriu Couplings of (Hetero)Aryl Polyhalides in the Presence of Grignard-Sensitive Functional Groups Using Pd-PEPPSI-IPent^{Cl}. *Chem. Eur. J.* **2019**, *25*, 6508−6512.

192. Jiang, B.; Shi, S.-L. Pd-Catalyzed Cross-Coupling of Alkylzirconocenes and Aryl Chlorides. *Chin. J. Chem.* **2022**, *40*, 1813−1820.

2. Chapter 2: An Indole-Amide-Derived Phosphine Ligand Enabling a General Palladium-Catalysed Sterically Hindered Suzuki−Miyaura Cross-Coupling Reaction

2.1 Introduction

The synthesis of biaryl compounds in organic electroluminescent materials, natural products, and bioactive substances often relies on the Suzuki−Miyaura cross-coupling reaction — a widely employed and versatile transformation. These *ortho*-substituted biaryl motifs have practical applications in materials science[1−2] and the pharmaceutical industry,[3−4] such as blue-emitting materials, diospyrol, mastigophorene A, and korupensamine A (Figure 2.1).[5−11] Nonetheless, their preparation can be problematic, especially when utilising relatively inexpensive yet sterically hindered and unreactive aryl chlorides as building blocks.

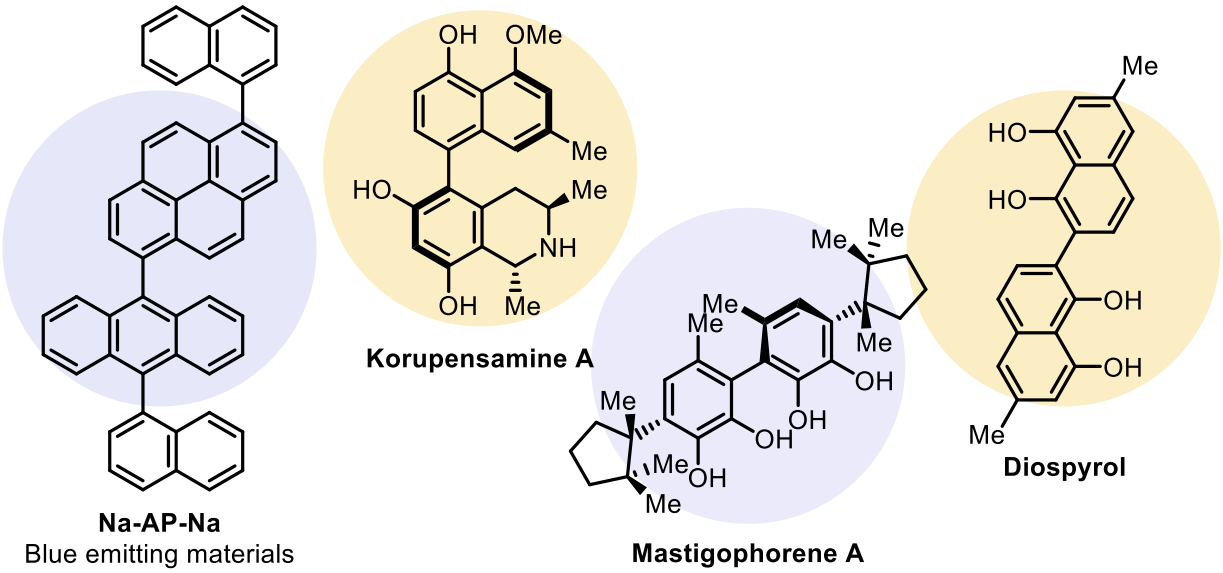

Figure 2.1 Showcasing *ortho*-substituted biaryl frameworks in functional materials, natural products and bioactive compounds

Employing low palladium catalyst loading is appealing to promote cost-effectiveness and reduce toxicity in industrial applications.[12] Catalyst loading can reach up to parts per million levels in the Suzuki coupling of non-sterically hindered aryl chlorides.[13−17] In contrast, constructing tri-*ortho*-substituted biaryls by sterically hindered aryl chlorides remains a significant challenge, requiring high palladium catalyst loading and prolonged reaction times, which might be due to the steric bulk introduced by the substrates, which obstructs their approach to the palladium metal centre.[18−24] Recently, Hoshi *et al.*[25] reported notable progress in this area, achieving the coupling of aryl chlorides bearing two-*ortho*-substituents and *ortho*-substituted arylboronic acids using only 0.025-0.05 mol% $Pd(dba)_2$ associated with CyR-Phos, within 1−17 hours. Developing effective

ligands from the facile preparation of inexpensive and commercially available starting materials is still highly desired to get high-performance catalysts.

Mixed-donor chelating ligands,[26] with both soft and hard donor atoms, have been successfully applied in transition metal catalysis owing to their hemilabile properties.[27] In palladium catalysis, ancillary hard donors (*O*-/*N*-donors) can stabilise metal centres through weak coordination with soft palladium centres.[28] *P*,*O*-ligands have been designed with ancillary acetal, sulfonyl, and amido moieties as a class of hemilabile ligands for cross-coupling reactions[28] and related asymmetric transformations.[29-31] Among these *P*,*O*-ligands, and amido-ligands have received significant attention, possibly due to the coordinating properties of amides and the ease of introducing phosphine motifs based on amide scaffolds.[32] Furthermore, the steric effect provided by ancillary amide groups has been adopted in ligand design for catalysis (e.g., the design of Xing-Phos).[33−34] We envisioned that the utilisation of dynamic steric hindrance, offered by rotatable aromatic tertiary amides, could also facilitate the substrate coordination and reductive elimination process in cross-coupling reactions. Consequently, amido-phosphine ligands demonstrated high efficiency in cross-coupling reactions.[35−40] Therefore, the hemilability and nonrigidity of aromatic amide-derived phosphine ligands prompted us to explore their potential application in Pd-catalysed cross-coupling reactions.

Numerous structures be alternative skeletons for constructing hemilabile ligands with different steric arrangements of *P*,*O*-donors, which are suitable for specific transformations.[28] For instance, benzamide-derived phosphine ligands reported by Dai and Kwong were active in Buchwald−Hartwig amination and Suzuki−Miyaura cross-coupling reactions (Scheme 2.1).[35-38]

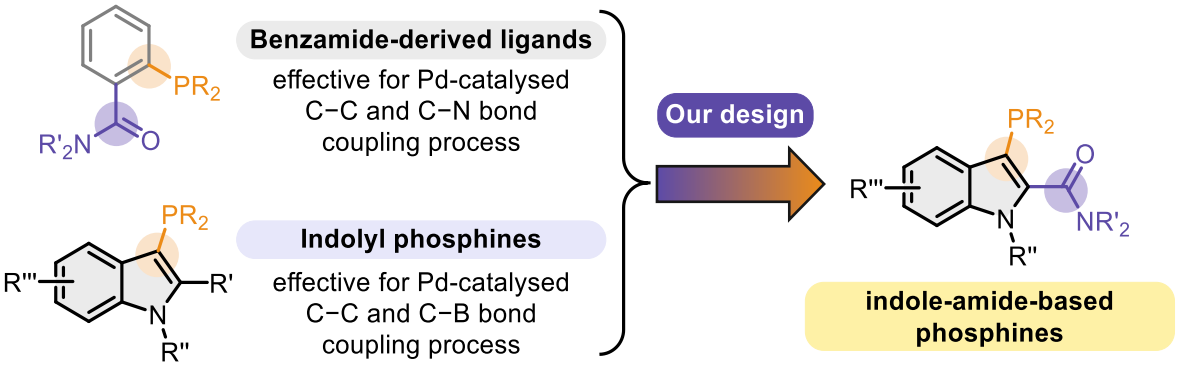

Scheme 2.1 Constructing phosphine ligands based on indole-amide scaffolds

We opted for indole as the skeleton in our design because the electronic-biased heterocyclic core and its bicyclic structure may have a distinct electronic and steric influence on the reaction.[41-49] Furthermore, this indole-based ligand presents the following benefits in modular synthetic processes: (1) readily available indoles and indole carboxylic acids can serve as versatile ligand precursors.; (2) the substituents on the nitrogen atom and the aromatic ring offer additional

electronic tunability; (3) the acidic hydrogen at the C2-position enables facile installation of the amide group through direct deprotonation; and (4) incorporating phosphine motifs at the electron-donating C3-position could enhance the electron density of the phosphine motifs and promote the oxidative process (Scheme 2.2). A series of phosphine ligands with indole-amide-based backbones were prepared and tested in Pd-catalysed cross-coupling reactions (Scheme 2.2), starting with commercially available *N*-substituted indoles or indole-2-carboxylic acids.

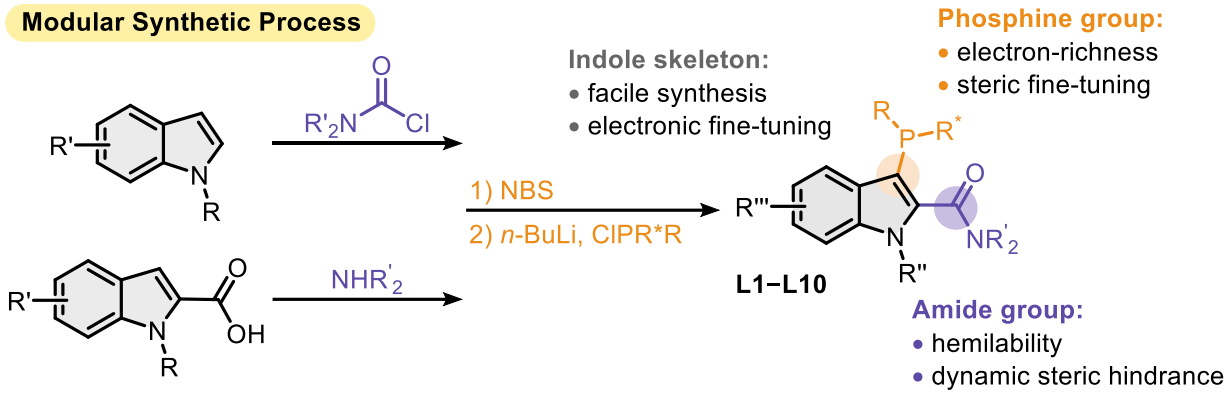

Scheme 2.2 Synthetic routes to indole-amide-based phosphine ligands and their features

2.2 Result and Discussion

2.2.1 Initial screening of ligands

The sterically hindered Suzuki−Miyaura cross-coupling of 2-chlorotoluene **1a** and (2,6-dimethylphenyl)boronic acid **2a** was chosen as the model reaction to evaluate the efficacy of the new indole-amide-based phosphine ligands. The investigation began with ligand screening (Table 2.1), where the newly synthesised indolyl-amide phosphine ligands were tested in this reaction. The steric hindrance offered by the amide group had a significant influence on the catalytic activity (**L1**−**L5**). Pd/**L1** was found to be the most effective catalyst, providing a product yield of 88%. Notably, the product yield dropped significantly when smaller −NMe_2 (**L2**), morpholine (**L3**), and −NPh_2 (**L4**) motifs were used to replace the −N(*i*-Pr)$_2$ (**L1**). Furthermore, bearing a small −NMe_2 group, the derivatives of **L2** did not yield better results by replacing the −PCy_2 group with other phosphine groups (**L8** and **L9**). A similar observation was made for **L3** and **L10**. Interestingly, attempts to enhance the product yield by further increasing the steric bulk of the amide group (**L1** versus **L5**) and replacing the *N*-substituent of the indole backbone (**L1** versus **L6**; **L5** versus **L7**) were unsuccessful. Based on these results, the indole-amide-based phosphine ligand with the electron-donating phosphine motif, the *N*-alkyl amide group, and moderate steric bulk substituent appears to be the most optimal ligand candidate for facilitating the sterically hindered cross-coupling reaction.

A series of previously identified remarkable phosphine ligands were investigated for their efficiency in this reaction. Surprisingly, PPh_3 (**L12**), MorDalPhos (**L23**), and other diphosphine ligands (**L24**−**L27**) were found to be ineffective under these conditions. Similarly, PCy_3 (**L11**), P*t*-Bu_3·HBF_4 (**L13**), CataCXium®A (**L14**), and CataCXium®PInCy (**L15**) did not exhibit enhanced reactivity. Furthermore, Buchwald-type biaryl phosphine ligands (SPhos **L16**, XPhos **L17**, BrettPhos **L18**, and CyJohnPhos **L19**), 2-arylindole phosphine ligands (Andole-Phos **L20**, WK-Phos **L21**), and PhenCar-Phos (**L22**) were also employed in this reaction; however, at most, only moderate yields were obtained within a short time frame. These results emphasize the advantage of the indole-amide-based ligand skeleton in facilitating the sterically hindered Suzuki−Miyaura cross-coupling reaction.

Table 2.1 Screening of ligands for Pd-catalysed Suzuki−Miyaura cross-coupling reaction of 2-chlorotoluene **1a** and (2,6-dimethylphenyl)boronic acid **2a**[a]

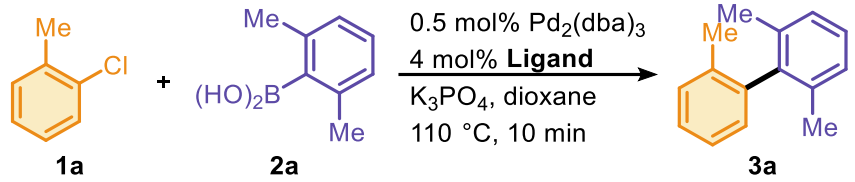

1a **2a** **3a**

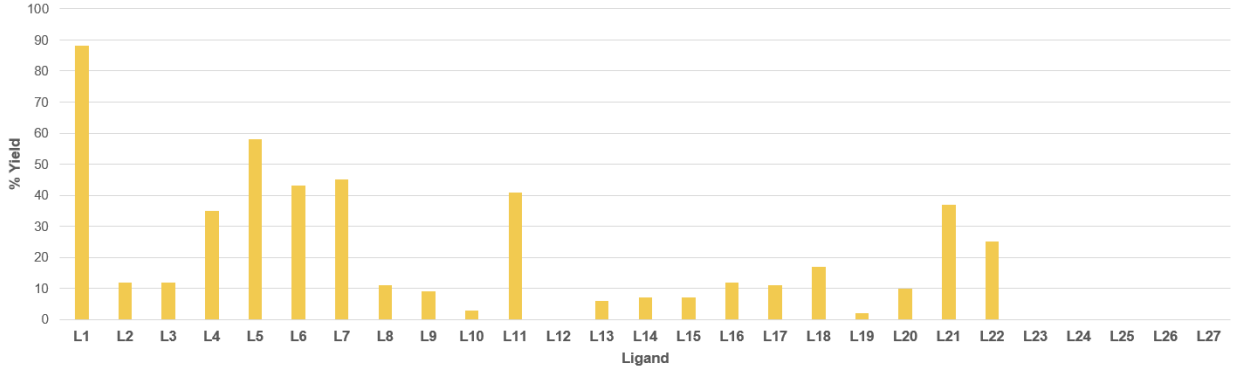

Code	Ligands	Yield of 3a (%)	Code	Ligands	Yield of 3a (%)
L1	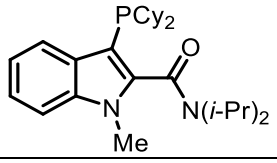	88	**L2**	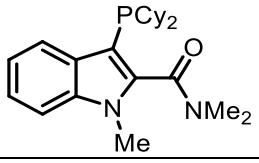	12
L3	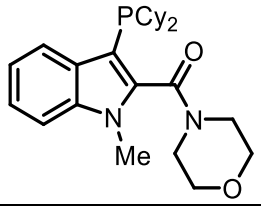	12	**L4**	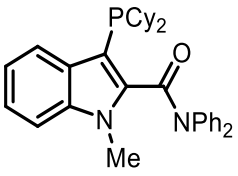	35
L5	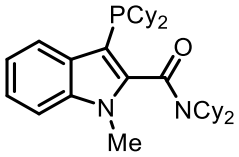	58	**L6**	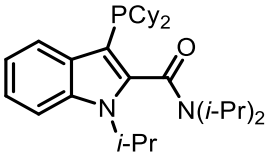	43
L7	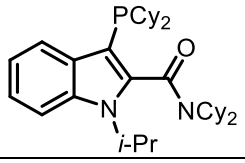	45	**L8**	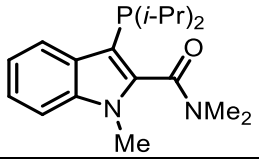	11
L9	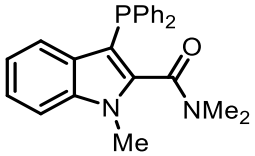	9	**L10**	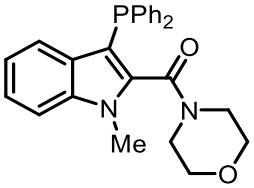	3
L11	PCy_3	41	**L12**	PPh_3	0
L13	P*t*-Bu_3·HBF_4	6	**L14**	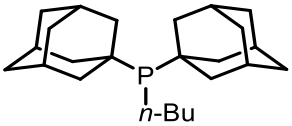 CataCXium®A	7

L15	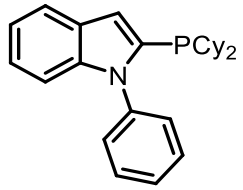 CataCXium®PinCy	7	**L16**	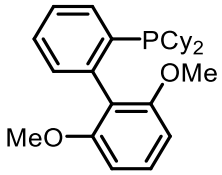 SPhos	12
L17	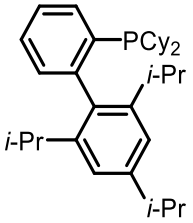 XPhos	11	**L18**	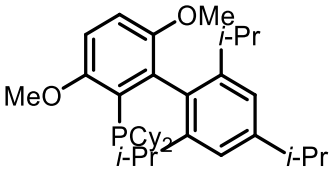 BrettPhos	17
L19	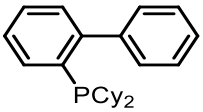 CyJohnPhos	2	**L20**	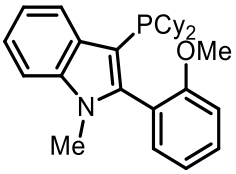 Andole-Phos	10
L21	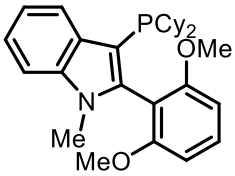 WK-Phos	37	**L22**	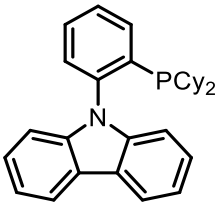 PhenCar-Phos	25
L23	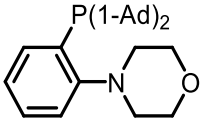 MorDalPhos	0	**L24**[b]	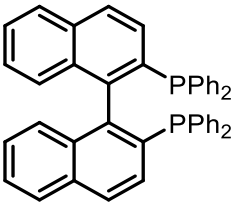 *rac*-BINAP	0
L25[b]	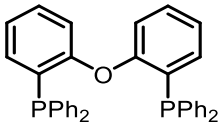 DPEPhos	0	**L26**[b]	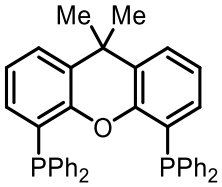 XantPhos	0
L27[b]	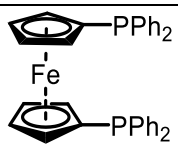 dppf	0			

[a]Reaction conditions: 2-chlorotoluene **1a** (0.50 mmol), (2,6-dimethylphenyl)boronic acid **2a** (1.0 mmol), $Pd_2(dba)_3$ (0.50 mol%), ligand (Pd: L = 1: 4), K_3PO_4 (1.5 mmol), and dioxane (1.5 mL) were stirred under N_2 at 110 °C for 10 minutes. Calibrated GC yields were reported using dodecane as the internal standard. [b]2.0 mol% Ligand (Pd: P = 1: 4) was used instead.

2.2.2 Optimisation of reaction conditions

Subsequently, **L1** was selected as the ligand for further optimisation of the reaction conditions (Table 2.2). An evaluation of the palladium sources revealed that Pd_2dba_3 was the most suitable palladium precursor for this coupling reaction (Table 2.2, entries 1−4). Additionally, a screening of commonly used inorganic bases was conducted (Table 2.2, entries 1 and 5−7), with K_3PO_4 proving to be the superior choice. Regarding the solvent screening, toluene provided better results, achieving a 95% yield, compared to dioxane (Table 2.2, entries 1 and 8−10). In contrast, the use of hexane, a non-polar solvent, led to a low yield (Table 2.2, entry 10).

Table 2.2 Optimisation of reaction conditions for Pd-catalysed Suzuki−Miyaura cross-coupling reaction of 2-chlorotoluene **1a** with (2,6-dimethylphenyl)boronic acid **2a**[a]

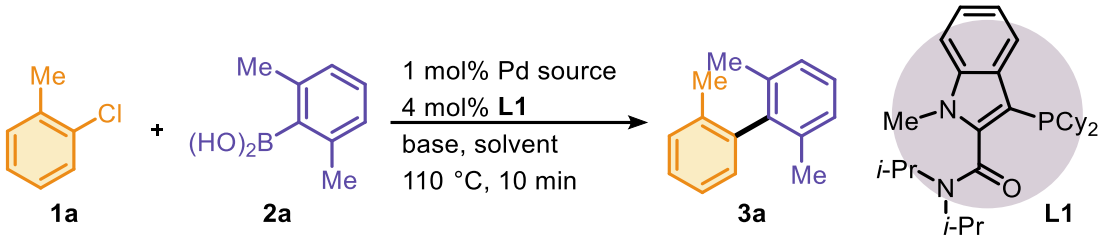

Entry	Pd source	Base	Solvent	Yield (%)[b]
1	$Pd_2(dba)_3$	K_3PO_4	dioxane	88
2	$Pd(OAc)_2$	K_3PO_4	dioxane	31
3	$Pd(dba)_2$	K_3PO_4	dioxane	23
4	$PdCl_2(MeCN)_2$	K_3PO_4	dioxane	26
5	$Pd_2(dba)_3$	$K_3PO_4·H_2O$	dioxane	41
6	$Pd_2(dba)_3$	K_2CO_3	dioxane	4
7	$Pd_2(dba)_3$	Cs_2CO_3	dioxane	62
8	$Pd_2(dba)_3$	K_3PO_4	toluene	95
9	$Pd_2(dba)_3$	K_3PO_4	THF	75
10	$Pd_2(dba)_3$	K_3PO_4	hexane	13

[a]Reaction conditions: 2-chlorotoluene **1a** (0.50 mmol), (2,6-dimethylphenyl)boronic acid **2a** (1.0 mmol), Pd source (1.0 mol% Pd), **L1** (4.0 mol%), base (1.5 mmol), and solvent (1.5 mL) were stirred under N_2 at 110 °C for 10 minutes. [b]Calibrated GC yields were reported using dodecane as the internal standard.

2.2.3 Palladium-catalysed Suzuki−Miyaura coupling of mono-ortho-substituted aryl chlorides with di-ortho-substituted arylboronic acids

The promising results from the initial investigation prompted us to further explore the substrate scope of the reaction (Table 2.3). For the model reaction, the Pd catalyst loading was reduced to just 0.025 mol%, yet a remarkable quantitative product yield was still achieved (Table 2.3, **3a**). During the reaction condition optimisation, the use of dioxane was found to promote the model reaction; however, when other mono-*ortho*-substituted aryl chlorides and di-*ortho*-substituted arylboronic acids were employed, this led to an undesirable increase in the protodeboronated byproducts (e.g., *m*-xylene and mesitylene). To mitigate this issue, we replaced the solvent with a relatively non-polar toluene-hexane mixture (1: 1 ratio) and extended the reaction time to 2 hours, which generally afforded the desired coupling products in up to 99% yields at catalyst loadings of 0.050−0.10 mol% (Table 2.3).

The substrate scope investigation demonstrated the versatility of this optimised protocol. Mono-*ortho*-substituted aryl chlorides bearing a range of electron-rich/-deficient groups, such as methyl (Table 2.3, **3a** and **3c**), methoxy (Table 2.3, **3b**, **3f**, and **3j**), amino (Table 2.3, **3g**), and fluoro (Table 2.3, **3d** and **3e**) groups, were successfully transformed into the corresponding coupling products. Importantly, the reaction also tolerated various functional groups, including ester (Table 2.3, **3i**), aldehyde (Table 2.3, **3k**), and coordinative heterocyclic substrates (Table 2.3, **3h**). Additionally, the arylboronic acid containing a methoxy group was able to couple with 2-chlorotoluene, affording the desired product in good yield (Table 2.3, **3l**). However, the coupling of the more sterically hindered 2-chloromesitylene with 2,6-dimethylphenylboronic acid (5 equiv.) at 110 °C for 2 hours, with an increased catalyst loading of 1.0 mol% Pd, only yielded the tetra-*ortho*-substituted biaryl compound in a modest 22% yield.

Table 2.3 Pd-catalysed Suzuki−Miyaura coupling of mono-*ortho*-substituted aryl chlorides with di-*ortho*-substituted arylboronic acids[a]

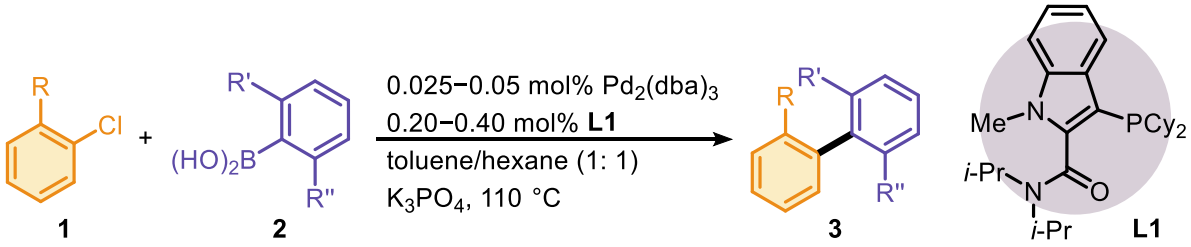

1 **2** **3** **L1**

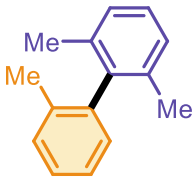

3a, 99%[b]
0.025 mol% [Pd], 1 h

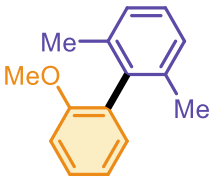

3b, 92%
0.025 mol% [Pd], 2 h

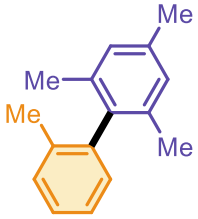

3c, 96%
0.05 mol% [Pd], 2 h

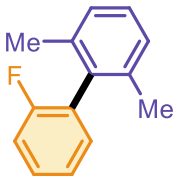

3d, 98%
0.025 mol% [Pd], 2 h

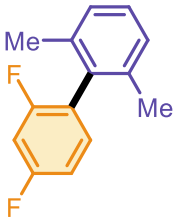

3e, 87%
0.025 mol% [Pd], 2 h

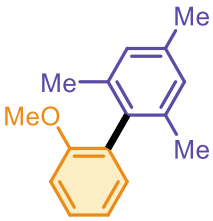

3f, 77%
0.05 mol% [Pd], 2 h

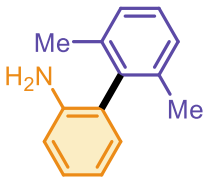

3g, 93%
0.05 mol% [Pd], 2 h

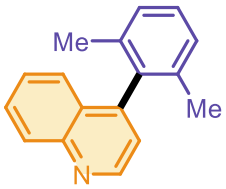

3h, 94%
0.05 mol% [Pd], 2 h

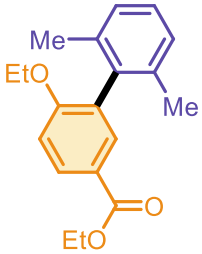

3i, 99%
0.05 mol% [Pd], 2 h

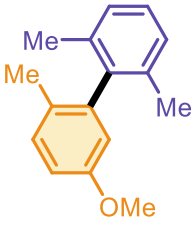

3j, 88%
0.05 mol% [Pd], 2 h

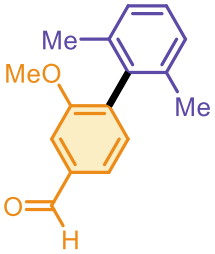

3k, 71%
0.025 mol% [Pd], 2 h

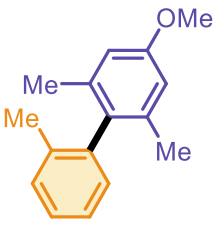

3l, 73%
0.05 mol% [Pd], 2 h

[a]Reaction conditions: mono-*ortho*-substituted aryl chloride (0.50 mmol), di-*ortho*-substituted boronic acid (1.0 mmol), $Pd_2(dba)_3$ (0.025−0.05 mol%), **L1** (0.20−0.40 mol%), Pd: L (1: 4), K_3PO_4 (1.5 mmol), and toluene/hexane (1: 1, 1.5 mL in total) were stirred under N_2 at 110 °C for 1−2 hours. [Pd] was in respect to $Pd_2(dba)_3$. Isolated yields were reported. [b]Dioxane was used instead.

2.2.4 Palladium-catalysed Suzuki−Miyaura coupling of di-ortho-substituted aryl chlorides with mono-ortho-substituted arylboronic acids

The reaction time for the coupling between di-*ortho*-substituted aryl chlorides and mono-*ortho*-substituted arylboronic acids can be further shortened to 30 to 60 minutes, resulting in the same isolated products and excellent yields (Table 2.4, **3a**−**3c**). Good yields were achieved in the conversion of electron-deficient arylboronic acids bearing fluoro or trifluoromethyl group at the *ortho*- or *para*- position (Table 2.4, **3d**, **3e**, and **3m**). This cross-coupling process demonstrated tolerance not only of methyl, methoxy, and fluoro substituents (Table 2.4, **3o**, **3p**, **3q**, **3u**, and **3v**), but also of functional groups such as cyano (Table 2.4, **3s**) and sulfamate (Table 2.4, **3w**) groups. More sterically congested electrophiles were also found to be applicable (Table 2.4, **3t**). Substrates with extended conjugated π-systems were successfully converted into coupled products (Table 2.4, **3q**, **3r**, and **3x**−**3af**). Remarkably, 9-chloroanthracene coupled with 2-tolylboronic acid at a remarkably low 0.05 mol% Pd catalyst loading within just 10 minutes, achieving a record-high turnover frequency (TOF) of 11880 (Table 2.4, **3ab**).

Table 2.4 Pd-catalysed Suzuki−Miyaura coupling of di-*ortho*-substituted aryl chlorides with mono-*ortho*-substituted arylboronic acids[a]

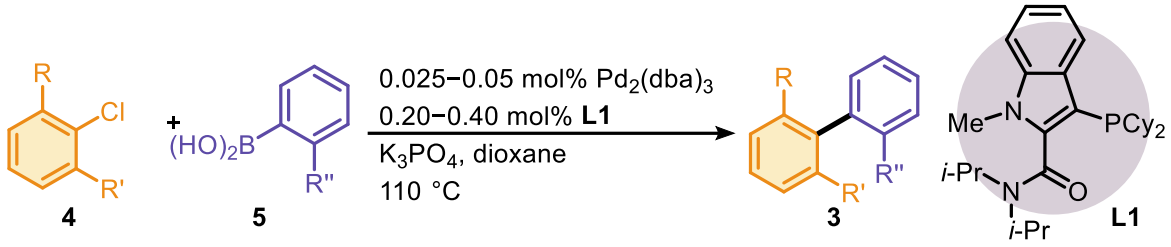

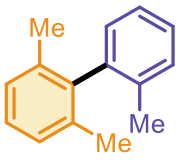

3a, 99%
0.025 mol%[Pd], 30 min
TOF = *3960*

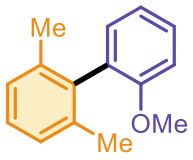

3b, 99%
0.05 mol%[Pd], 60 min
TOF = *990*

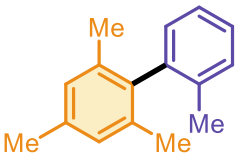

3c, 96%
0.025 mol% [Pd], 30 min
TOF = *3840*

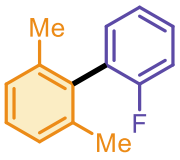

3d, 91%
0.025 mol% [Pd], 30 min
TOF = *3640*

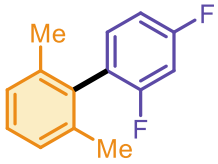

3e, 86%[b]
0.025 mol% [Pd], 30 min
TOF = *3440*

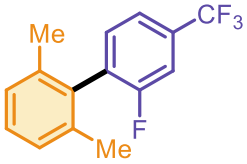

3m, 85%[b]
0.05 mol%[Pd], 60 min
TOF = *850*

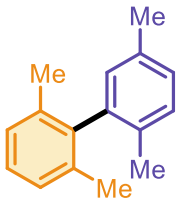

3n, 92%
0.025 mol% [Pd], 30 min
TOF = *3680*

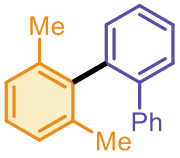

3o, 96%
0.05 mol% [Pd], 60 min
TOF = *960*

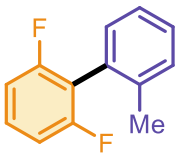

3p, 99%
0.025 mol% [Pd], 30 min
TOF = *3960*

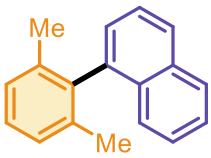

3q, 82%
0.025 mol% [Pd], 30 min
TOF = *3280*

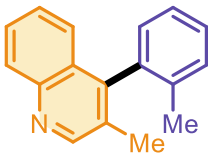

3r, 90%
0.025 mol% [Pd], 30 min
TOF = *3600*

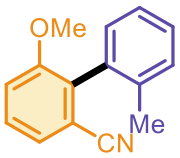

3s, 71%
0.025 mol% [Pd], 60 min
TOF = *1420*

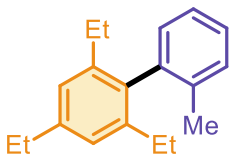

3t, 70%
0.05 mol% [Pd], 60 min
TOF = *700*

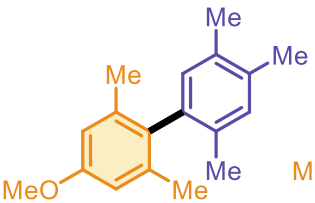

3u, 99%
0.05 mol% [Pd], 60 min
TOF = *990*

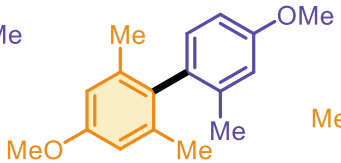

3v, 98%
0.05 mol% [Pd], 60 min
TOF = *980*

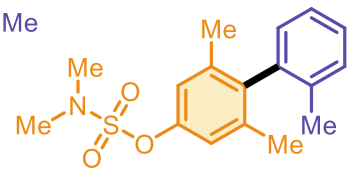

3w, 81%
0.05 mol% [Pd], 60 min
TOF = *810*

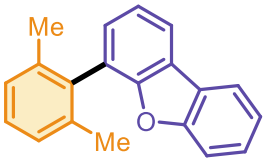

3x, 83%
0.05 mol% [Pd],
30 min
TOF = *1860*

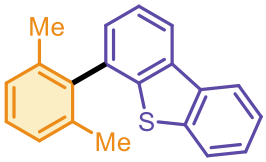

3y, 76%
0.05 mol% [Pd],
60 min
TOF = *760*

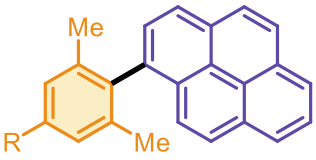

3z, R = Me, 90%
0.025 mol% [Pd],
30 min
TOF = *3600*

3aa, R = OMe, 93%
0.05 mol% [Pd],
30 min
TOF = *1860*

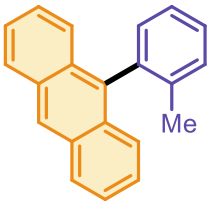

3ab, 99%
0.025 mol% [Pd],
10 min
TOF = *11880*

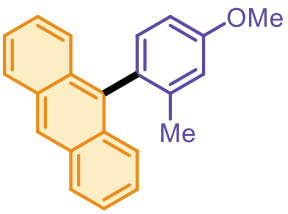

3ac, 92%
0.05 mol% [Pd], 60 min
TOF = 920

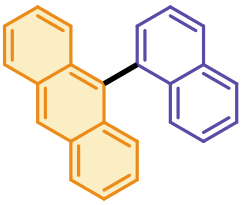

3ad, 94%
0.025 mol% [Pd], 30 min
TOF = *3760*

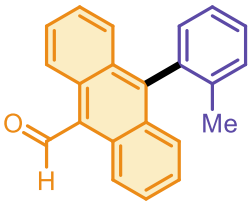

3ae, 97%
0.025 mol% [Pd], 30 min
TOF = *3880*

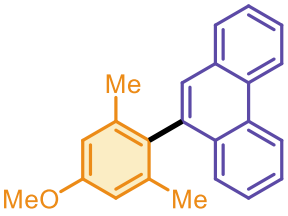

3af, 82%
0.05 mol% [Pd], 30 min
TOF = *1640*

[a]Reaction conditions: di-*ortho*-substituted aryl chloride (0.50 mmol), mono-*ortho*-substituted boronic acid (1.0 mmol), $Pd_2(dba)_3$ (0.025−0.050 mol%), **L1** (0.20−0.40 mol%), Pd: L (1: 4), K_3PO_4 (1.5 mmol), and dioxane (1.5 mL) were stirred under N_2 at 110 °C for 10−60 min. [Pd] was in respect to $Pd_2(dba)_3$. Isolated yields were reported. [b]1.5 mmol of boronic acid was used instead.

2.2.5 Palladium-catalysed Suzuki−Miyaura coupling of sterically hindered aryl chlorides and arylboroxines at ultra-low palladium loading or on a gram scale

Efforts were made to further reduce the catalyst loading to assess the practical feasibility of this transformation (Table 2.5). The catalyst system maintained excellent performance even when the $Pd_2(dba)_3$ loading was decreased to just 25 ppm, using arylboroxine as the nucleophile. This resulted in an impressively high turnover number, ranging from 16,600−19,800. Remarkably, excellent product yields were obtained while minimising the formation of undesired homocoupling and protodeboronated byproducts. 50 ppm of Pd represents the lowest catalyst loading ever reported for the synthesis of tri-*ortho*-substituted biaryls via Suzuki−Miyaura coupling at that time.

Table 2.5 Pd-catalysed Suzuki−Miyaura coupling of di-*ortho*-substituted aryl chlorides with mono-*ortho*-substituted arylboroxines under extremely low Pd loading[a]

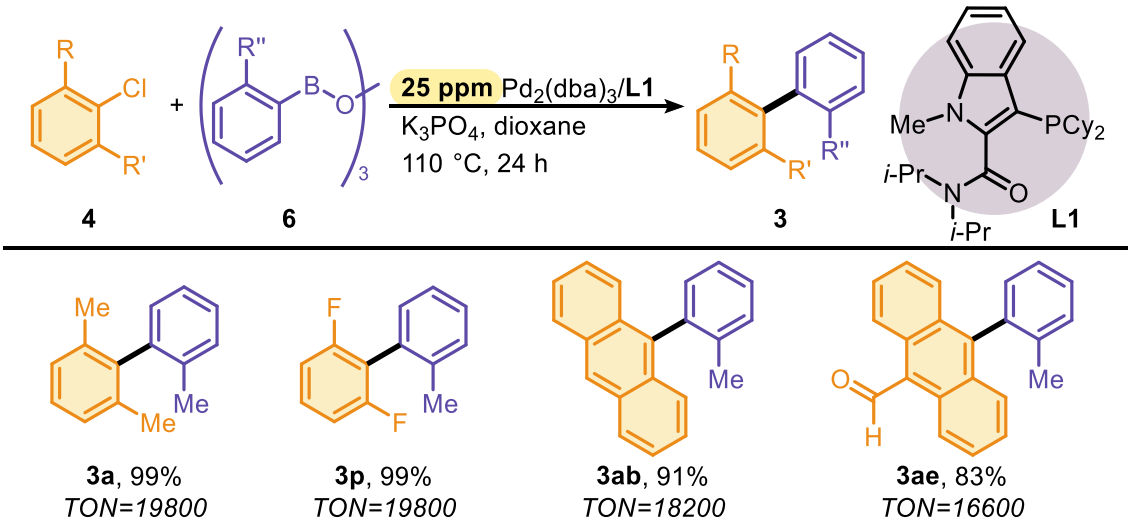

[a]Reaction conditions: di-*ortho*-substituted aryl chloride (0.50 mmol), mono-*ortho*-substituted aryl boroxine (0.30 mmol), $Pd_2(dba)_3$ (0.0025 mol%), **L1** (0.020 mol%), Pd: L (1: 4), K_3PO_4 (1.5 mmol), and dioxane (1.5 mL) were stirred under N_2 at 110 °C for 24 hours. Isolated yields were reported

Additionally, a gram-scale coupling of 2-chloro-1,3-dimethylbenzene and 2-fluorophenylboronic acid was smoothly executed (Scheme 2.3), affording the desired product in an 85% yield.

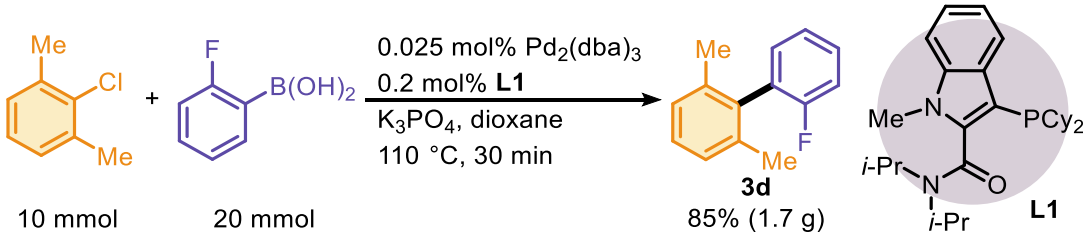

Scheme 2.3 Gram-scale Pd-catalysed Suzuki−Miyaura cross-coupling reaction

*2.2.6 Investigating the ligand effect on the reactivity through the oxidation addition complex **C1***

The oxidative addition complex **C1** was prepared to examine the origin of the ligand effect on the catalytic reactivity towards the coupling reaction. Crystallographic analysis of **C1** revealed a κ^2-*P*,*O*-coordination of **L1** with the palladium, creating a square planar complex, with the oxygen of the amide group bound trans to the aryl ring (Figure 2.2).[50] This finding indicates that the weak *O*-coordination of the amide group stabilised the active species during the intervals between each reaction cycle, prolonging the catalysts' lifespan and potentially accounting for the low catalyst loading needed.

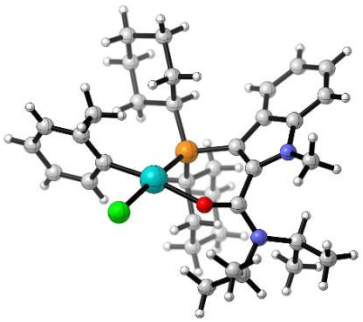

Figure 2.2 X-ray structure of **C1**

Selected distances (Å):

Pd1−P1 = 2.2575(4), Pd1−O1 = 2.1304(12), Pd1−Cl1 = 2.3600(4), and Pd1−C(1) = 1.9815(17).

2.3 Summary

To conclude, a novel family of phosphine ligands featuring an indole-amide-based scaffold was developed and employed in sterically demanding Suzuki−Miyaura cross-coupling reaction. Among these ligands, **L1** exhibited exceptional performance, enabling the reactions to proceed with only 0.050−0.10 mol% Pd catalyst loadings, possibly due to the auxiliary coordination of the amide group. The reactions displayed a high tolerance for various functional groups, allowing for a wide range of substrate combinations and yielding good to excellent products. Furthermore, it was discovered that an extremely low catalyst loading of 0.0050 mol% Pd could successfully facilitate the coupling of sterically hindered aryl chlorides with aryl boroxine. This method is believed to provide an efficient approach for the synthesis of sterically hindered biaryl compounds.

2.4 Experimental Section

2.4.1 General considerations

All reagents were purchased from commercial suppliers and used as received, unless otherwise noted. Suzuki−Miyaura cross-coupling reactions were carried out in a resealable screw-cap Schlenk tube (approximately 20 mL volume) containing a Teflon-coated magnetic stirrer bar (5 mm × 10 mm). Dioxane, toluene, and THF were freshly distilled under nitrogen from sodium or sodium benzophenone ketyl, while hexane was freshly distilled from anhydrous calcium hydride under nitrogen. Water was also freshly distilled under nitrogen.[51] A new bottle of *n*-BuLi was employed, as the concentration of *n*-BuLi from an older bottle may vary, necessitating a titration prior to use. Several starting materials, including 4-chloro-3,5-dimethylanisole,[52] 2-chloro-1,3,5-triethylbenzene,[53] 4-chloro-3,5-dimethylphenyl dimethylsulfamate,[54] 2-chloro-4-methoxytoluene[55] and 4-chloro-3-methoxybenzaldehyde,[56] were synthesised according to literature procedures. Additionally, 2,4,6-tris(2-methylphenyl)boroxine was prepared following published methods.[57] Thin layer chromatography was performed on precoated silica gel 60 F_{254} plates, and column chromatography utilised 230−400 mesh silica gel. Melting points were recorded on an uncorrected Stuart Melting Point SMP30 instrument. NMR spectra were acquired on a Bruker spectrometer, with internal referencing to the residual proton resonance in $CDCl_3$ (δ 7.26 ppm) or tetramethylsilane (TMS, δ 0.00 ppm) for ^{1}H NMR (400 MHz) spectra. ^{13}C NMR (100 MHz) spectra were referenced to the middle peak of $CDCl_3$ (δ 77.0 ppm), and ^{31}P NMR (376 MHz) spectra were referenced externally to 85% H_3PO_4. Coupling constants (J) were reported in Hertz (Hz). Mass spectrometric data, including EI-MS and HRMS, were obtained using HP 5977A MSD, Agilent 6540 ESI-QToF-MS, APPI-QToF-MS, and Waters GCT Premier EI-ToF-MS instruments. GC-MS analysis was performed on an HP 7890B GC system with an HP5MS column, and the reported GC yields were based on authentic samples/dodecane calibration. All yields refer to the isolated products, and literature-reported compounds were characterised by comparison of their NMR spectra to the published data.

2.4.2 Ligand synthesis and characterisation

_N_,_N_-Diisopropyl-1-methyl-1_H_-indole-2-carboxamide (P1)

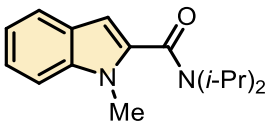

Under a nitrogen atmosphere at room temperature, 1-methylindole (2.50 mL, 20.0 mmol) was dissolved in freshly distilled THF (30 mL). The solution was then cooled to -78 °C, and titrated *t*-BuLi (20 mmol) was added dropwise using a syringe. After the reaction mixture was stirred for 30 minutes at room temperature, *N*,*N*-diisopropylcarbamoyl chloride (3.93 g, 24.0 mmol) was added at -78 °C. The reaction temperature was then increased to room temperature, and the reaction was stirred for 1 hour. The solvent was removed under reduced pressure, and the concentrated mixture was diluted with ethyl acetate and washed with water and brine. The organic layer was dried over Na_2SO_4 and then concentrated. The concentrated mixture was then subjected to column chromatography and eluted with an ethyl acetate/hexane (1: 9 and 2: 8) mixture. The eluent was evaporated to yield *N*,*N*-diisopropyl-1-methyl-1*H*-indole-2-carboxamide as a light-yellow solid (4.62 g, 90%). ^{1}H NMR (400 MHz, $CDCl_3$) δ 1.13−1.70 (br m, 12H), 3.48−4.27 (br m, 2H) superimposed to 3.76 (s, 3H), 6.47 (s, 1H), 7.12 (t, *J* = 7.8 Hz, 1H), 7.23−7.27 (m, 1H), 7.33 (d, *J* = 8.2 Hz, 1H), 7.60 (d, *J* = 7.9 Hz, 1H); ^{13}C NMR (100 MHz, $CDCl_3$) δ 20.8, 30.8, 99.9, 109.6, 120.0, 121.2, 122.5, 126.8, 134.8, 137.1, 163.9. The data obtained align with the information previously reported in the literature.[58]

3-Bromo-_N_,_N_-diisopropyl-1-methyl-1_H_-indole-2-carboxamide (P1')

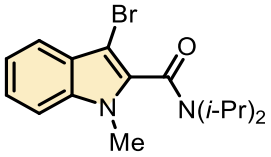

In anhydrous chloroform (25 mL), *N*,*N*-diisopropyl-1-methyl-1*H*-indole-2-carboxamide (4.38 g, 17.0 mmol) was dissolved at room temperature. *N*-Bromosuccinimide (3.02 g, 17.0 mmol) was then added in portions to the solution. After stirring for 30 minutes, water was added to the reaction mixture. The organic layer was washed with water and brine, then concentrated. The concentrated solution was filtered over a pad of silica and eluted with dichloromethane. The eluent was then concentrated, and the solid was subjected to recrystallisation from dichloromethane/hexane. The white solid was collected, washed with hexane, and dried under vacuum to afford 3-bromo-*N*,*N*-diisopropyl-1-methyl-1*H*-indole-2-carboxamide (4.00 g, 70%). The melting point was determined to be 134.9−136.5 °C. ^{1}H NMR (400 MHz, $CDCl_3$) δ 1.11 (d, *J* = 6.7 Hz, 3H), 1.31 (d, *J* = 6.6 Hz, 3H), 1.62 (d, *J* = 6.8 Hz, 6H), 3.56−3.65 (m, 1H), 3.73 (s, 3H), 3.85−3.95 (m, 1H), 7.20−7.24 (m, 1H), 7.29−7.34 (m, 2H), 7.57 (d, *J* = 7.9 Hz, 1H); ^{13}C NMR (100

MHz, $CDCl_3$) δ 20.2, 20.6, 21.1, 21.5, 31.1, 46.4, 51.6, 87.3, 109.7, 119.6, 120.7, 123.2, 126.4, 133.6, 135.9, 162.0; HRMS (ESI): calculated m/z for $C_{16}H_{22}BrN_2O^+$: 337.0910, found 337.0914.

3-(Dicyclohexylphosphanyl)-*N*,*N*-diisopropyl-1-methyl-1*H*-indole-2-carboxamide (L1)

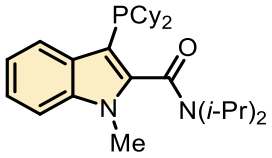

Under a nitrogen atmosphere at room temperature, 3-bromo-*N*,*N*-diisopropyl-1-methyl-1*H*-indole-2-carboxamide (1.00 g, 3.0 mmol) was dissolved in freshly distilled THF (10 mL). The solution was then cooled to -78 °C, and titrated *n*-BuLi (3.3 mmol) was added dropwise using a syringe. After the reaction mixture was stirred for 30 minutes at -78 °C, chlorodicyclohexylphosphine (0.73 mL, 3.3 mmol) was added. The reaction was then allowed to warm to room temperature and stirred overnight. The solvent was removed under reduced pressure, and the solid product was successively washed with ethanol and methanol. The off-white solid was collected by filtration and dried under vacuum to afford 3-(dicyclohexylphosphanyl)-*N*,*N*-diisopropyl-1-methyl-1*H*-indole-2-carboxamide (1.13 g, 83%). The melting point was determined to be 180.4−184.6 °C. ^{1}H NMR (400 MHz, $CDCl_3$) δ 0.93−1.32 (m, 15H), 1.39−1.97 (m, 18H), 2.66−2.74 (m, 1H), 3.52−3.59 (m, 1H), 3.69 (s, 3H), 3.84−3.90 (m, 1H), 7.16 (t, *J* = 7.1 Hz, 1H), 7.26 (t, *J* = 8.1 Hz, 1H), 7.34 (d, *J* = 8.1 Hz, 1H), 7.80 (d, *J* = 8.0 Hz, 1H); ^{13}C NMR (100 MHz, $CDCl_3$) δ 20.0, 20.4, 21.2, 21.4, 21.5, 26.1, 26.6, 27.0, 27.15, 27.24, 27.3, 27.4, 27.5, 27.6, 29.87, 29.89, 30.1, 30.2, 30.8, 31.1, 31.3, 31.6, 31.7, 31.8, 32.0, 35.6, 35.7, 46.0, 51.0, 102.0, 102.2, 109.7, 120.0, 121.8, 122.4, 130.35, 130.43, 137.8, 144.6, 145.1, 163.7; ^{31}P NMR (162 MHz, CD_2Cl_2) δ -17.1; HRMS (ESI): calculated m/z for $C_{28}H_{44}N_2OP^+$: 455.3186, found 455.3185.

***N*,*N*,1-Trimethyl-1*H*-indole-2-carboxamide (P2)**

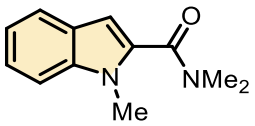

1-Methylindole (6.24 mL, 50.0 mmol) was dissolved in freshly distilled THF (100 mL) under a nitrogen atmosphere at room temperature. The solution was then cooled to -78 °C, and titrated *t*-BuLi (55.0 mmol) was added dropwise using a syringe. After the reaction mixture was stirred for 30 minutes at room temperature, *N*,*N*-dimethylcarbamoyl chloride (5.06 mL, 55.0 mmol) was added. The reaction temperature was then increased to room temperature, and the reaction was stirred for an additional 1 hour. The solvent was removed under reduced pressure, and the concentrated mixture was diluted with ethyl acetate, then washed with water and brine. The organic layer was dried over Na_2SO_4 and concentrated. The concentrated mixture was then subjected to column chromatography, eluting with an ethyl acetate/hexane (1: 9 and 2: 8) mixture.

The eluent was evaporated, and the solid product was generated after the addition of hexane. The light-yellow solid was collected by filtration and dried under vacuum to afford *N*,*N*,1-trimethyl-1*H*-indole-2-carboxamide (5.67 g, 56%). ^{1}H NMR (400 MHz, $CDCl_3$) δ 3.18 (s, 6H), 3.85 (s, 3H), 6.64 (s, 1H), 7.13−7.17 (m, 1H), 7.28−7.32 (m, 1H), 7.37 (d, *J* = 8.4 Hz, 1H), 7.63 (d, *J* = 7.9 Hz, 1H); ^{13}C NMR (100 MHz, $CDCl_3$) δ 31.1, 103.9, 109.8, 120.1, 121.5, 123.2, 126.4, 132.0, 137.8, 164.4. The data obtained align with the information previously reported in the literature.[59]

3-Bromo-*N*,*N*,1-trimethyl-1*H*-indole-2-carboxamide (P2')

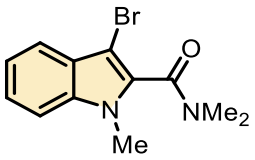

In anhydrous chloroform (25 mL) at 0 °C, *N*,*N*,1-trimethyl-1*H*-indole-2-carboxamide (4.38 g, 2.5 mmol) was treated with *N*-bromosuccinimide (0.51 g, 2.75 mmol) in portions. The reaction mixture was then stirred for 1 hour at room temperature. Water was added to the reaction mixture, and the organic layer was washed with water and brine, then concentrated. The concentrated solution was subjected to column chromatography, eluting with an ethyl acetate/hexane (1: 1) mixture. The eluent was then concentrated under reduced pressure, and the final product was dried under vacuum to afford 3-bromo-*N*,*N*,1-trimethyl-1*H*-indole-2-carboxamide as a brown liquid (0.68 g, 97%). ^{1}H NMR (400 MHz, $CDCl_3$) δ 3.10 (s, 3H), 3.20 (s, 3H), 3.77 (s, 3H), 7.20−7.24 (m, 1H), 7.32−7.34 (m, 2H), 7.56−7.58 (m, 1H); ^{13}C NMR (100 MHz, $CDCl_3$) δ 25.6, 31.4, 34.9, 38.4, 67.9, 90.1, 109.8, 119.8, 120.8, 123.9, 126.3, 131.3, 136.6, 162.8; HRMS (ESI): calculated m/z for $C_{12}H_{13}BrN_2NaO^+$: 303.0103, found 303.0103.

3-(Dicyclohexylphosphanyl)-*N*,*N*,1-trimethyl-1*H*-indole-2-carboxamide (L2)

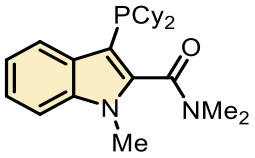

Under a nitrogen atmosphere at room temperature, 3-Bromo-*N*,*N*,1-trimethyl-1*H*-indole-2-carboxamide (0.99 g, 3.27 mmol) was dissolved in freshly distilled THF (10 mL). The solution was then cooled to -78 °C, and titrated *n*-BuLi (3.3 mmol) was added dropwise using a syringe. After the reaction mixture was stirred for 30 minutes at -78 °C, chlorodicyclohexylphosphine (0.79 mL, 3.6 mmol) was added. The reaction was then allowed to warm to room temperature and stirred overnight. The solvent was removed under reduced pressure, and the solid product was successively washed with methanol. The resulting white solid was collected by filtration and dried under vacuum to afford 3-(dicyclohexylphosphanyl)-*N*,*N*,1-trimethyl-1*H*-indole-2-carboxamide (0.30 g, 76%). The melting point was determined to be 204.1−205.7 °C. ^{1}H NMR (400 MHz, $CDCl_3$) δ 0.98−1.97 (m, 21H), 2.61−2.69 (m, 1H), 2.93 (s, 3H), 3.19 (s, 3H), 3.68 (s, 3H), 7.15 (t, *J* = 7.4

Hz, 1H), 7.27 (t, *J* = 7.1Hz, 1H), 7.34 (d, *J* = 8.2 Hz, 1H), 7.80 (d, *J* = 8.0 Hz, 1H); ^{13}C NMR (100 MHz, $CDCl_3$) δ 26.1, 26.5, 26.9, 27.1, 27.2, 27.4, 27.5, 30.0, 30.5, 30.6, 30.9, 31.2, 31.4, 31.6, 31.8, 32.0, 34.7, 35.2, 35.3, 38.7, 103.3, 103.4, 109.9, 120.2, 122.3, 122.5, 130.1, 138.2, 142.8, 143.2, 164.8; ^{31}P NMR (162 MHz, $CDCl_3$) δ -15.2; HRMS (ESI): calculated m/z for $C_{24}H_{36}N_2OP^+$: 399.2560, found 399.2559.

3-(Diisopropylphosphanyl)-*N*,*N*,1-trimethyl-1*H*-indole-2-carboxamide (L8)

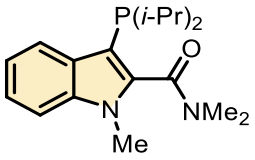

3-Bromo-*N*,*N*,1-trimethyl-1*H*-indole-2-carboxamide (1.61 g, 8.0 mmol) was dissolved in freshly distilled THF (20 mL) at room temperature under a nitrogen atmosphere. The solution was then cooled to -78 °C, and titrated *n*-BuLi (9.6 mmol) was added dropwise using a syringe. After the reaction mixture was stirred for 30 minutes at -78 °C, chlorodiisopropylphosphine (1.53 mL, 9.6 mmol) was added. The reaction was allowed to warm to room temperature and stirred overnight. The solvent was removed under reduced pressure, and the concentrated mixture was dissolved in dichloromethane and filtered through Celite. The solution was then evaporated and subjected to column chromatography, eluting with an ethyl acetate/hexane (2: 8 and 1: 1) mixture. The eluent was evaporated and washed with hexane. The resulting light orange solid was collected by filtration and dried under vacuum to afford 3-(diisopropylphosphanyl)-*N*,*N*,1-trimethyl-1*H*-indole-2-carboxamide (1.6 g, 63%). The melting point was determined to be 159.2−160.1 °C. ^{1}H NMR (400 MHz, C_6D_6) δ 0.95−1.04 (m, 6H), 1.14−1.21 (m, 6H), 2.08−2.15 (m, 1H), 2.45 (s, 3H), 2.73−2.79 (m, 1H), 2.81 (s, 3H), 3.15 (s, 3H), 7.01−7.03 (m, 1H), 7.16−7.23 (m, 2H), 7.81−7.83 (m, 1H); ^{13}C NMR (100 MHz, C_6D_6) δ 20.5, 20.6, 21.3, 21.4, 21.5, 21.67, 21.69, 21.9, 22.6, 22.7, 26.1, 26.2, 30.4, 34.1, 37.9, 38.0, 104.1, 104.2, 110.4, 120.6, 122.6, 122.7, 130.4, 130.5, 138.7, 143.7, 144.1, 164.4; ^{31}P NMR (162 MHz, C_6D_6) δ -5.34; HRMS (ESI): calculated m/z for $C_{18}H_{28}N_2OP^+$: 319.1934, found 319.1936.

3-(Diphenylphosphanyl)-*N*,*N*,1-trimethyl-1*H*-indole-2-carboxamide (L9)

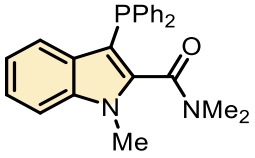

In a solution of 3-bromo-*N*,*N*,1-trimethyl-1*H*-indole-2-carboxamide (2.47 g, 8.8 mmol) in freshly distilled THF (30 mL) under a nitrogen atmosphere at room temperature, the mixture was cooled to -78 °C. Titrated *n*-BuLi (9.68 mmol) was then added dropwise using a syringe. After the reaction mixture was stirred for 30 minutes at -78 °C, chlorodiphenylphosphine (1.95 mL, 10.56 mmol) was added. The reaction was allowed to warm to room temperature and stirred overnight. The

solvent was removed under reduced pressure, and the solid product was successively washed with ethanol. The resulting light orange solid was collected by filtration and dried under vacuum to afford 3-(diphenylphosphanyl)-*N*,*N*,1-trimethyl-1*H*-indole-2-carboxamide (1.88 g, 55%). The melting point was determined to be 178.5−179.5 °C. ^{1}H NMR (400 MHz, $CDCl_3$) δ 2.84 (s, 3H), 3.12 (s, 3H), 3.76 (s, 3H), 6.95 (t, *J* = 7.3 Hz, 1H), 7.11 (d, *J* = 8.0 Hz, 1H), 7.23−7.50 (m, 12H); ^{13}C NMR (100 MHz, $CDCl_3$) δ 31.0, 34.6, 38.69, 38.73, 103.5, 109.9, 120.5, 122.3, 122.8, 127.8, 127.98, 128.03, 128.1, 128.2, 128.3, 129.1, 132.5, 132.6, 132.7, 132.8, 136.7, 136.9, 137.0, 138.3, 141.8, 142.2, 164.1; ^{31}P NMR (162 MHz, $CDCl_3$) δ -29.2; HRMS (ESI): calculated m/z for $C_{24}H_{24}N_2OP^+$: 387.1621, found 387.1624.

(1-Methyl-1*H*-indol-2-yl)(morpholino)methanone (P3)

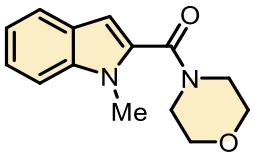

1-Methylindole (6.24 mL, 50.0 mmol) was dissolved in freshly distilled THF (125 mL) at room temperature under a nitrogen atmosphere. The solution was then cooled to -78 °C, and titrated *t*-BuLi (55 mmol) was added dropwise using a syringe. After the reaction mixture was stirred for 30 minutes at room temperature, *N*,*N*-morpholinecarbonyl chloride (7.00 mL, 60.0 mmol) was added at -78 °C. The reaction temperature was then increased to room temperature, and the reaction was stirred for 1 hour. The solvent was removed under reduced pressure, and the concentrated mixture was diluted with ethyl acetate and washed with water and brine. The organic layer was dried over Na_2SO_4 and then concentrated. The concentrated mixture was then subjected to recrystallisation from ethyl acetate/hexane. The resulting solid was collected, washed with hexane, and dried under vacuum to afford (1-methyl-1*H*-indol-2-yl)(morpholino)methanone as a light-yellow solid (8.73 g, 72%). ^{1}H NMR (400 MHz, $CDCl_3$) δ 3.73−3.75 (m, 4H), 3.79−3.82 (m, 4H), 3.86 (s, 3H), 6.60 (s, 1H), 7.14−7.18 (m, 1H), 7.29−7.33 (m, 1H), 7.36−7.38 (m, 1H), 7.63 (d, *J* = 8.0 Hz, 1H); ^{13}C NMR (100 MHz, $CDCl_3$) δ 31.1, 66.9, 103.8, 109.8, 120.3, 121.5, 123.4, 126.2, 131.0, 137.9, 163.1. The data obtained align with the information previously reported in the literature.[60]

(3-Bromo-1-methyl-1*H*-indol-2-yl)(morpholino)methanone (P3')

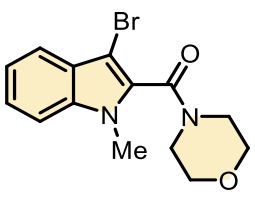

In a solution of (1-methyl-1*H*-indol-2-yl)(morpholino)methanone (7.32 g, 30.0 mmol) in anhydrous chloroform (100 mL), *N*-bromosuccinimide (5.61 g, 31.5 mmol) was added in portions at room temperature. After stirring the reaction mixture for 10 minutes, water was added. The organic layer was then washed with water and brine, and concentrated. The concentrated solution was filtered over a pad of silica and eluted with dichloromethane. The concentrated solution was evaporated to give a solid product, which was subjected to recrystallisation from ethyl acetate/hexane. The resulting white solid was collected and dried under vacuum to afford (3-bromo-1-methyl-1*H*-indol-2-yl)(morpholino)methanone (8.29 g, 86%). The melting point was determined to be 159.4−160.3 °C. ^{1}H NMR (400 MHz, $CDCl_3$) δ 3.40−3.46 (m, 1H), 3.55−3.68 (m, 2H), 3.78 (s, 3H), 3.80−3.89 (m, 5H), 7.19−7.26 (m, 1H), 7.33−7.34 (m, 2H), 7.57 (d, *J* = 8.0 Hz, 1H); ^{13}C NMR (100 MHz, $CDCl_3$) δ 31.4, 42.5, 47.7, 66.8, 67.3, 90.2, 109.8, 119.9, 120.9, 124.2, 126.1, 130.2, 136.7, 161.4; HRMS (ESI): calculated m/z for $C_{14}H_{16}BrN_2O_2^+$: 323.0390, found 323.0389.

(3-(Dicyclohexylphosphanyl)-1-methyl-1*H*-indol-2-yl)(morpholino)methanone (L3)

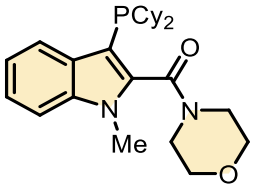

(3-Bromo-1-methyl-1*H*-indol-2-yl)(morpholino)methanone (1.61 g, 5.0 mmol) was dissolved in freshly distilled THF (20 mL) at room temperature under a nitrogen atmosphere. The solution was then cooled to -78 °C, and titrated *n*-BuLi (6.0 mmol) was added dropwise using a syringe. After the reaction mixture was stirred for 30 minutes at -90 °C, chlorodicyclohexylphosphine (1.32 mL, 6.0 mmol) was added. The reaction was then allowed to warm to room temperature and stirred overnight. The solvent was removed under reduced pressure, and the solid product was washed with methanol and collected by filtration. The white solid was subjected to recrystallisation from dichloromethane/methanol, and the off-white solid was collected by filtration and dried under vacuum to afford (3-(dicyclohexylphosphanyl)-1-methyl-1*H*-indol-2-yl)(morpholino)methanone (1.26 g, 57%). The melting point was determined to be 203.1−205.8 °C. ^{1}H NMR (400 MHz, C_6D_6) δ 0.80−1.45 (m, 11H), 1.50−2.04 (m, 10H), 2.73−2.83 (m, 2H), 3.06−3.12 (m, 1H), 3.16−3.33 (m, 5H), 3.45−3.73 (m, 4H), 7.02−7.08 (m, 1H), 7.18−7.22 (m, 2H), 7.90−7.93 (m, 1H); ^{13}C NMR (100 MHz, C_6D_6) δ 26.4, 26.9, 27.2, 27.3, 27.5, 27.55, 27.61, 27.8, 30.4, 30.5, 30.6, 31.0, 31.1, 31.9, 32.1, 32.2, 32.4, 32.5, 36.0, 36.1, 42.2, 47.40, 47.44, 66.7, 67.06, 67.09, 104.0, 104.1, 110.4, 120.9, 122.66, 122.73, 130.66, 130.73, 138.7, 142.8, 143.3, 163.0; ^{31}P NMR (162 MHz, C_6D_6) δ -16.0; HRMS (ESI): calculated m/z for $C_{26}H_{38}N_2O_2P^+$: 441.2665, found 441.2669.

(3-(Diphenylphosphanyl)-1-methyl-1*H*-indol-2-yl)(morpholino)methanone (L10)

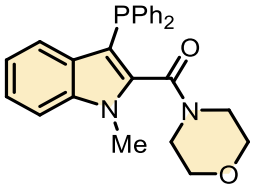

(3-Bromo-1-methyl-1*H*-indol-2-yl)(morpholino)methanone (0.65 g, 2.0 mmol) was dissolved in freshly distilled THF (10 mL) at room temperature under a nitrogen atmosphere. The solution was then cooled to -78 °C, and titrated *n*-BuLi (2.2 mmol) was added dropwise using a syringe. After the reaction mixture was stirred for 30 minutes at -78 °C, chlorodiphenylphosphine (0.44 mL, 2.4 mmol) was added. The reaction was then allowed to warm to room temperature and stirred overnight. The solvent was removed under reduced pressure, and the solid product was washed with methanol and collected by filtration. The white solid was subjected to recrystallisation from dichloromethane/methanol, and the resulting white solid was collected by filtration and dried under vacuum to afford (3-(diphenylphosphanyl)-1-methyl-1*H*-indol-2-yl)(morpholino)methanone (0.59 g, 69%). The melting point was determined to be 155.7−156.8 °C. ^{1}H NMR (400 MHz, $CDCl_3$) δ 3.25−3.34 (m, 3H) 3.45−3.49 (m, 1H), 3.74−3.92 (m, 7H), 6.96 (t, *J* = 7.4 Hz, 1H), 7.05 (d, *J* = 8.0 Hz, 1H), 7.25−7.41 (m, 10H), 7.46−7.50 (m, 2H); ^{13}C NMR (100 MHz, $CDCl_3$) δ 31.2, 42.3, 47.6, 66.7, 66.8, 104.0, 104.1, 110.1, 120.8, 122.5, 123.1, 127.9, 128.18, 128.25, 128.46, 128.52, 128.9, 129.0, 132.3, 132.5, 132.7, 132.8, 136.4, 137.0, 138.5, 141.0, 141.5, 162.9; ^{31}P NMR (162 MHz, $CDCl_3$) δ -29.6; HRMS (ESI): calculated m/z for $C_{26}H_{26}N_2O_2P^+$: 429.1726, found 429.1728.

1-Methyl-*N*,*N*-diphenyl-1*H*-indole-2-carboxamide (P4)

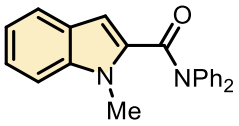

1-Methylindole (2.50 mL, 20.0 mmol) was dissolved in freshly distilled THF (100 mL) at room temperature under a nitrogen atmosphere. The solution was then cooled to -78 °C, and titrated *n*-BuLi (20 mmol) was added dropwise using a syringe. After the reaction mixture was stirred for 30 minutes at room temperature, *N*,*N*-diphenylcarbamoyl chloride (5.56 g, 24.0 mmol) was added at -78 °C. The reaction temperature was then increased to room temperature, and the reaction was stirred for 1 hour. The solvent was removed under reduced pressure, and the concentrated mixture was filtered through a short silica pad, eluting with an ethyl acetate/hexane (2: 8) mixture. The eluent was collected and concentrated under reduced pressure. Hexane (10 mL) was added to the crude product, and the mixture was stirred vigorously to generate a white solid at 0 °C. The solid was collected by filtration and further purified by recrystallisation using ethanol to yield 1-methyl-*N*,*N*-diphenyl-1*H*-indole-2-carboxamide (4.84 g, 74%). The melting point was determined to be 122.1−123.3 °C. ^{1}H NMR (400 MHz, $CDCl_3$) δ 4.07 (s, 3H), 6.30 (s, 1H), 7.11 (t, *J* = 7.2 Hz, 1H), 7.25−7.31 (m, 6H), 7.33−7.41 (m, 6H), 7.48 (d, *J* = 8.0 Hz, 1H); ^{13}C NMR (100 MHz, $CDCl_3$)

δ 31.6, 108.7, 109.8, 120.0, 122.0, 123.9, 125.9, 126.4, 127.2, 129.2, 132.1, 138.1, 143.8, 163.7; HRMS (ESI): calculated m/z for $C_{22}H_{19}N_2O^+$: 327.1492, found 327.1495.

3-Bromo-1-methyl-*N*,*N*-diphenyl-1*H*-indole-2-carboxamide (P4')

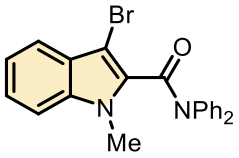

A solution of 1-methyl-*N*,*N*-diphenyl-1*H*-indole-2-carboxamide (1.63 g, 5.0 mmol) in anhydrous chloroform (25 mL) was prepared at room temperature. *N*-Bromosuccinimide (0.89 g, 5.0 mmol) was then added to the solution in portions. After stirring the reaction mixture for 1 hour, water was added. The organic layer was separated, washed with water and brine, and then concentrated. The concentrated solution was filtered over a pad of silica and eluted with dichloromethane. The eluent was then concentrated and dried under vacuum to afford 3-bromo-1-methyl-*N*,*N*-diphenyl-1*H*-indole-2-carboxamide as an off-white solid (1.21 g, 60%). The melting point was determined to be 163.6−164.6 °C. ^{1}H NMR (400 MHz, $CDCl_3$) δ 3.96 (s, 3H), 7.17−7.34 (m, 13H), 7.49 (d, *J* = 8.0 Hz, 1H); ^{13}C NMR (100 MHz, $CDCl_3$) δ 31.5, 91.3, 109.7, 120.0, 120.6, 124.2, 126.1, 126.8, 128.9, 132.1, 136.8, 142.4, 163.0; HRMS (ESI): calculated m/z for $C_{22}H_{18}BrN_2O^+$: 405.0597, found 405.0602.

3-(Dicyclohexylphosphanyl)-1-methyl-*N*,*N*-diphenyl-1*H*-indole-2-carboxamide (L4)

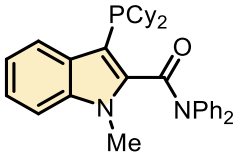

3-Bromo-1-methyl-*N*,*N*-diphenyl-1*H*-indole-2-carboxamide (1.21 g, 3.0 mmol) was dissolved in freshly distilled THF (20 mL) at room temperature under a nitrogen atmosphere. The solution was then cooled to -78 °C in a dry ice/acetone bath. Titrated *n*-BuLi (3.0 mmol) was added dropwise using a syringe. After the reaction mixture was stirred for 30 minutes at -78 °C, chlorodicyclohexylphosphine (0.73 mL, 3.3 mmol) was added. The reaction was allowed to warm to room temperature and stirred overnight. The solvent was removed under reduced pressure, and the solid product was washed with methanol and collected by filtration. The white solid was then subjected to recrystallisation from a dichloromethane/methanol mixture. The purified white solid was collected and dried under vacuum to afford 3-(dicyclohexylphosphanyl)-1-methyl-*N*,*N*-diphenyl-1*H*-indole-2-carboxamide (1.16 g, 74%). The melting point was determined to be 211.2−213.3 °C. ^{1}H NMR (400 MHz, $CDCl_3$) δ 0.96−1.93 (m, 21H), 2.34−2.51 (m, 1H), 3.92 (s, 3H), 7.03−7.14 (m, 6H), 7.26−7.36 (m, 3H), 7.39−7.53 (m, 4H), 7.68 (d, *J* = 8.0 Hz, 1H); ^{13}C NMR (100 MHz, $CDCl_3$) δ 26.2, 26.3, 27.2, 27.4, 28.6, 30.3, 31.5, 32.0, 36.3, 105.3, 109.9, 120.1, 122.6,

122.8, 126.1, 126.7, 127.3, 128.7, 129.2, 130.0, 130.1, 138.4, 143.1, 164.6; ^{31}P NMR (162 MHz, $CDCl_3$) δ -16.9; HRMS (ESI): calculated m/z for $C_{34}H_{40}N_2OP^+$: 523.2873, found 523.2875.

***N*,*N*-Dicyclohexyl-1*H*-indole-2-carboxamide (P5)**

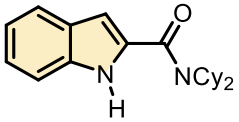

A suspension of 1*H*-indole-2-carboxylic acid (8.05 g, 50.0 mmol) in anhydrous dichloromethane (100 mL) was prepared at room temperature. To this suspension, DMF (5 drops) was added, followed by the addition of oxalyl chloride (6.5 mL, 75 mmol). The reaction mixture was stirred at room temperature for 2 hours. The solvent was then removed under reduced pressure, and the residue was dissolved in anhydrous dichloromethane (100 mL). *N*,*N*-Dicyclohexylamine (29.8 mL, 150 mmol) was added to the solution at 0 °C. The resulting mixture was stirred at room temperature for 30 minutes. The reaction was quenched by the addition of water (200 mL), and the product was extracted with DCM three times. The combined organic layers were washed with water and brine, then dried over anhydrous Na_2SO_4 and concentrated under reduced pressure, yielding a brown oil. Ethanol (30 mL) was added to the brown oil, and the mixture was stirred at 0 °C for 1 hour. A solid product was generated, which was washed with an ethanol/water mixture and dried under vacuum to yield *N*,*N*-dicyclohexyl-1*H*-indole-2-carboxamide (8.74 g, 54%) as a light-yellow solid. The melting point was determined to be 184.6−187.5 °C. ^{1}H NMR (400 MHz, $CDCl_3$) δ 1.14−1.42 (m, 8H), 1.55−2.18 (m, 14H), 6.68 (s, 1H), 7.15 (t, *J* = 7.3 Hz, 1H), 7.25−7.29 (m, 1H), 7.50 (d, *J* = 8.2 Hz, 1H), 7.68 (d, *J* = 8.0 Hz, 1H), 9.89 (s, 1H); ^{13}C NMR (100 MHz, $CDCl_3$) δ 25.3, 26.1, 31.0, 57.8, 103.4. 111.8. 120.1. 121.5. 123.7. 127.4. 131.4. 135.5. 163.1; HRMS (ESI): calculated m/z for $C_{21}H_{29}N_2O^+$: 325.2274, found 325.2277.

***N*,*N*-Dicyclohexyl-1-methyl-1*H*-indole-2-carboxamide (P5')**

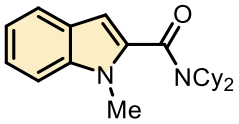

N,*N*-Dicyclohexyl-1*H*-indole-2-carboxamide (5 mmol) was dissolved in 20 mL of THF in a dropping funnel. This solution was then added dropwise to a 20 mL THF solution containing 1.5 equivalents of NaH (60% in mineral oil, 7.5 mmol) at room temperature. The NaH was first washed with dry hexane under a nitrogen atmosphere. The reaction mixture was stirred for 30 minutes at room temperature, after which Me_2SO_4 (5.5 mmol) was added dropwise. The mixture was then stirred at room temperature for 2 hours. The solvent was removed under vacuum, and ethyl acetate and water were added to the mixture. The organic phase was separated and washed with brine several times, then concentrated. The concentrated mixture was applied to a silica pad and eluted with ethyl acetate. The organic solvent was dried over Na_2SO_4 and evaporated under

vacuum to afford *N*,*N*-Dicyclohexyl-1-methyl-1*H*-indole-2-carboxamide (1.39 g, 82%) as a yellow solid. The melting point was determined to be 159.5−161.5 °C. ^{1}H NMR (400 MHz, $CDCl_3$) δ 1.21 (br, 6H), 1.62−1.80 (m, 12H), 2.62 (br, 2H), 3.17 (br, 1H), 3.78−3.87 (m, 4H), 6.48 (s, 1H), 7.13−7.17 (m, 1H), 7.26−7.30 (m, 1H), 7.36 (d, *J* = 8,0 Hz, 1H), 7.63 (d, *J* = 7.9 Hz, 1H); ^{13}C NMR (100 MHz, $CDCl_3$) δ 25.2, 25.9 (br), 30.6 (br), 30.8, 100.0, 109.6, 119.8, 121.3, 122.4, 126.8, 134.8, 137.3, 164.0; HRMS (ESI): calculated for $C_{22}H_{31}N_2O^+$ $[M+H]^+$: 339.2431, found: 339.2434.

3-Bromo-*N*,*N*-dicyclohexyl-1-methyl-1*H*-indole-2-carboxamide (P5'')

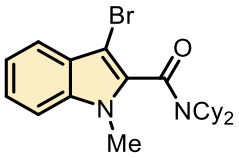

A solution of *N*,*N*-dicyclohexyl-1-methyl-1*H*-indole-2-carboxamide (1.35 g, 4.0 mmol) in anhydrous chloroform (20 mL) was prepared at room temperature. *N*-Bromosuccinimide (0.71 g, 4.0 mmol) was then added to the solution in portions. After stirring the reaction mixture for 30 minutes, water was added. The organic layer was separated, washed with water and brine, and then concentrated. The concentrated solution was subjected to column chromatography, eluting with an ethyl acetate/hexane (1: 4) mixture. The eluent was then concentrated and dried under vacuum to afford 3-bromo-*N*,*N*-dicyclohexyl-1-methyl-1*H*-indole-2-carboxamide (1.31 g, 80%) as a white solid. The melting point was determined to be 158.2−160.0 °C. ^{1}H NMR (400 MHz, $CDCl_3$) δ 1.02−1.18 (m, 3H), 1.26−1.39 (m, 3H), 1.48−1.60 (m, 4H), 1.62−1.79 (m, 5H), 1.84−1.93 (m, 2H), 2.14−2.17 (m, 1H), 2.56−2.90 (m, 2H), 3.12−3.18 (m, 1H), 3.44−3.51 (m, 1H), 3.71 (s, 3H), 7.22 (t, *J* = 7.2 Hz, 1H), 7.29−7.34 (m, 2H), 7.57 (d, *J* = 7.9 Hz, 1H); ^{13}C NMR (100 MHz, $CDCl_3$) δ 25.0, 25.3, 25.4, 25.5, 26.5, 26.6, 29.5, 29.9, 31.1, 31.6, 32.1, 56.6, 60.4, 87.3, 109.7, 119.7, 120.5, 123.1, 126.5, 133.7, 136.0, 162.2; HRMS (ESI): calculated m/z for $C_{22}H_{30}BrN_2O^+$: 417.1536, found 417.1540.

***N*,*N*-Dicyclohexyl-3-(dicyclohexylphosphanyl)-1-methyl-1*H*-indole-2-carboxamide (L5)**

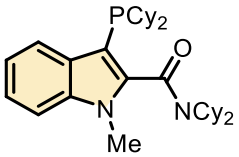

3-Bromo-*N*,*N*-dicyclohexyl-1-methyl-1*H*-indole-2-carboxamide (1.25 g, 3.0 mmol) was dissolved in freshly distilled THF (20 mL) at room temperature under a nitrogen atmosphere. The solution was cooled to -78 °C, and titrated *n*-BuLi (3.3 mmol) was added dropwise using a syringe. After the reaction mixture was stirred for 30 minutes at -78 °C, chlorodicyclohexylphosphine (0.80 mL, 3.6 mmol) was added. The reaction was then allowed to warm to room temperature and stirred overnight. The solvent was removed under reduced pressure, and the solid product was successively washed with methanol. The resulting white solid was collected and dried under

vacuum to afford *N*,*N*-dicyclohexyl-3-(dicyclohexylphosphanyl)-1-methyl-1*H*-indole-2-carboxamide (1.14 g, 72%). The melting point was determined to be 223.9−229.4 °C. ^{1}H NMR (400 MHz, $CDCl_3$) δ 0.95−1.37 (m, 15H), 1.46−1.89 (m, 22H), 1.94−1.97 (m, 1H), 2.20−2.23 (m, 1H), 2.63−2.80 (m, 3H), 3.06−3.11 (m, 1H), 3.26−3.32 (m, 1H), 3.66 (s, 3H), 7.14−7.17 (m, 1H), 7.24−7.28 (m, 1H), 7.34 (d, *J* = 8.1 Hz, 1H), 7.80 (d, *J* = 8.0 Hz, 1H); ^{13}C NMR (100 MHz, $CDCl_3$) δ 25.0, 25.1, 25.2, 25.5, 26.1, 26.5, 26.6, 26.7, 27.1, 27.2, 27.3, 27.36, 27.41, 27.46, 27.5, 27.7, 29.3, 29.7, 29.9, 30.6, 30.7, 30.89, 30.97, 31.03, 31.2, 31.4, 31.5, 31.59, 31.64, 31.8, 32.0, 35.7, 35.8, 56.2, 59.7, 101.9, 102.1, 109.7, 119.9, 121.7, 122.5, 130.5, 130.6, 137.8, 145.0, 145.4, 163.8; ^{31}P NMR (162 MHz, CD_2Cl_2) δ -16.3; HRMS (ESI): calculated m/z for $C_{34}H_{52}N_2OP^+$: 535.3812, found 535.3817.

_N_,_N_-Diisopropyl-1_H_-indole-2-carboxamide (P6)

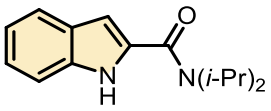

At room temperature, 1*H*-indole-2-carboxylic acid (5.0 g, 31.0 mmol) was suspended in anhydrous chloroform (250 mL) and stirred. DMF (5 drops) was added, followed by oxalyl chloride (4.42 mL, 52.3 mmol). The mixture was then refluxed at 80 °C for 1 hour. The solvent was removed under reduced pressure, and the residue was dissolved in anhydrous chloroform (100 mL). *N*,*N*-Diisopropylamine (100 mmol) was added, and the resulting mixture was stirred at room temperature for 30 minutes. The reaction was then quenched with water (350 mL) and extracted with dichloromethane three times. The combined organic layers were washed with water and brine, then dried over anhydrous Na_2SO_4 and concentrated under reduced pressure. The solid was subjected to recrystallisation from a hot ethanol/water mixture, and the light-yellow solid was washed with the ethanol/water mixture and dried under vacuum, yielding *N*,*N*-diisopropyl-1*H*-indole-2-carboxamide (4.3 g, 56%). ^{1}H NMR (400 MHz, $CDCl_3$) δ 1.40−1.50 (m, 12H), 4.32 (br, 2H), 6.71 (s, 1H), 7.10−7.14 (m, 1H), 7.23−7.27 (m, 1H), 7.42 (d, *J* = 8.2 Hz, 1H), 7.64 (d, *J* = 7.9 Hz, 1H), 9.47 (s, 1H); ^{13}C NMR (100 MHz, $CDCl_3$) δ 21.9, 103.3, 111.6. 120.2. 121.5. 123.8. 127.4. 131.3. 135.3, 162.7. The data obtained align with the information previously reported in the literature.[61]

_N_,_N_-Diisopropyl-1-isopropyl-1_H_-indole-2-carboxamide (P6')

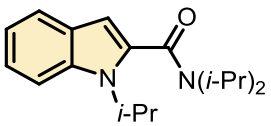

N,*N*-Diisopropyl-1*H*-indole-2-carboxamide (2.4 g, 10 mmol) was dissolved in freshly distilled DMF (100 mL) at room temperature under a nitrogen atmosphere. KOH (5.6 g, 100 mmol) was then added to the reaction mixture and stirred at 0 °C for 15 minutes. 2-Bromopropane (9.4 mL, 100

mmol) was added dropwise at 0 °C, and the reaction mixture was stirred at 0 °C overnight. After the reaction was complete, water was added to the reaction mixture. The mixture was then extracted with dichloromethane, and the organic layer was washed with a large amount of water before being concentrated. The concentrated mixture was subjected to column chromatography and eluted with a 1: 9 mixture of ethyl acetate and hexane. The solution was evaporated, resulting in the formation of a white solid. The final product, *N*,*N*-diisopropyl-1-isopropyl-1*H*-indole-2-carboxamide (1.56 g, 54%), was dried under vacuum. The melting point was determined to be 92.7−93.8 °C. ^{1}H NMR (400 MHz, $CDCl_3$) δ 1.18−1.33 (m, 6H), 1.52−1.64 (m, 6H), 1.70−1.72 (m, 6H), 3.51−3.61 (m, 1H), 4.07−4.28 (m, 1H), 4.71−4.79 (m, 1H), 6.45 (s, 1H), 7.16 (t, *J* = 7.5 Hz, 1H), 7.26 (t, *J* = 7.5 Hz, 1H), 7.57 (d, *J* = 8.4 Hz, 1H), 7.67 (d, *J* = 7.8 Hz, 1H); ^{13}C NMR (100 MHz, $CDCl_3$) δ 20.6, 21.6, 45.9, 48.9, 49.0, 51.0, 99.4, 111.5, 119.6, 121.4, 121.8, 127.7, 134.7, 134.9, 164.7; HRMS: calculated m/z for $C_{18}H_{27}N_2O^+$: 287.2118, found 287.2121.

3-Bromo-*N*,*N*,1-triisopropyl-1*H*-indole-2-carboxamide (P6'')

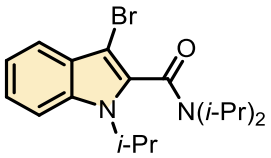

In anhydrous chloroform (10 mL) at 0 °C, *N*,*N*,1-triisopropyl-1*H*-indole-2-carboxamide (0.85 g, 3.0 mmol) was combined with *N*-Bromosuccinimide (0.53 g, 3.0 mmol), which was added in portions. After stirring for 30 minutes, the reaction mixture was concentrated. The concentrated solution was subjected to gel filtration and eluted with a 1: 9 mixture of ethyl acetate and hexane. The solution was then evaporated, resulting in the formation of a white solid. The final product, 3-bromo-*N*,*N*,1-triisopropyl-1H-indole-2-carboxamide (1.06 g, 97%), was dried under vacuum. The melting point was determined to be 89.7−90.7 °C. ^{1}H NMR (400 MHz, $CDCl_3$) δ 1.16 (d, *J* = 6.5 Hz, 3H), 1.35 (d, *J* = 6.4 Hz, 3H), 1.63−1.70 (m, 12H), 3.57−3.65 (m, 1H), 3.92−3.99 (m, 1H), 4.53−4.61 (m, 1H), 7.20−7.30 (m, 2H), 7.55 (d, *J* = 8.2 Hz, 1H), 7.60 (d, *J* = 7.7 Hz, 1H); ^{13}C NMR (100 MHz, $CDCl_3$) δ 20.1, 20.5, 21.0, 21.5, 21.6, 21.9, 46.3, 50.3, 51.5, 87.0, 112.1, 119.9, 120.3, 122.6, 127.5, 133.3, 133.6, 162.4; HRMS: calculated m/z for $C_{18}H_{26}BrN_2O^+$: 365.1223, found 365.1225.

3-(Dicyclohexylphosphanyl)-*N*,*N*,1-triisopropyl-1*H*-indole-2-carboxamide (L6)

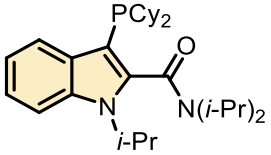

3-Bromo-*N*,*N*,1-triisopropyl-1*H*-indole-2-carboxamide (1.97 g, 5.4 mmol) was dissolved in freshly distilled THF (20 mL) at room temperature under a nitrogen atmosphere. The solution was cooled to -78 °C, and titrated *n*-BuLi (5.4 mmol) was added dropwise using a syringe. After the reaction

mixture was stirred for 30 minutes at -78 °C, chlorodicyclohexylphosphine (1.32 mL, 6.0 mmol) was added. The reaction was allowed to warm to room temperature and stirred overnight. The solvent was then removed under reduced pressure. The resulting solid product was washed with methanol and collected by filtration. The white solid was recrystallised from dichloromethane/methanol, and the collected white solid was dried under vacuum to afford 3-(dicyclohexylphosphanyl)-*N*,*N*,1-triisopropyl-1*H*-indole-2-carboxamide (0.98 g, 38%). The melting point was determined to be 173.7−174.9 °C. ^{1}H NMR (400 MHz, C_6D_6) δ 0.80 (d, *J* = 6.7 Hz, 3H), 0.83−0.91 (m, 1H), 0.94−1.05 (m, 1H), 1.10−1.29 (m, 8H), 1.30−1.40 (m, 10H), 1.42−1.59 (m, 6H), 1.68−1.73 (m, 5H), 1.83−2.08 (m, 5H), 2.72−2.79 (m, 1H), 3.15−3.22 (m, 1H), 3.92−4.02 (m, 1H), 4.43−4.54 (m, 1H), 7.14−7.21 (m, 2H), 7.37 (d, *J* = 8.2 Hz, 1H), 7.96 (d, *J* = 7.6 Hz, 1H); ^{13}C NMR (100 MHz, C_6D_6) δ 20.2, 20.8, 21.2, 21.4, 21.5, 21.6, 26.4, 27.1, 27.4, 27.5, 27.6, 27.7, 27.8, 27.9, 30.60, 30.64, 30.7, 30.8, 31.8, 32.0, 32.6, 32.7, 32.9, 33.1, 36.7, 36.8, 46.1, 49.9, 50.8, 101.9, 113.2, 120.3, 121.9, 123.0, 132.37, 132.44, 136.1, 145.2, 145.7, 164.2; ^{31}P NMR (162 MHz, C_6D_6) δ -19.3; HRMS (ESI): calculated m/z for $C_{30}H_{48}N_2OP^+$: 483.3499, found 483.3502.

_N_,_N_-Dicyclohexyl-1-isopropyl-1_H_-indole-2-carboxamide (P7)

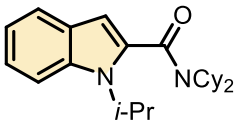

Under a nitrogen atmosphere, *N*,*N*-dicyclohexyl-1*H*-indole-2-carboxamide (6.49 g, 20 mmol) was dissolved in freshly distilled DMF (100 mL) at room temperature. KOH (11.22 g, 200 mmol) was then added to the reaction mixture, and the mixture was kept stirring at 0 °C. 2-Bromopropane (18.78 mL, 200 mmol) diluted in freshly distilled DMF (20 mL) was added dropwise at 0 °C. The reaction mixture was stirred at 0 °C for 24 hours. After the overnight stirring, water was added to the reaction mixture. The mixture was then extracted with dichloromethane, and the organic layer was washed with water and concentrated. Hexane was added, and the mixture was allowed to stir for 10 minutes, resulting in the formation of a white solid. The white solid was filtered and dried under vacuum to afford the final product, *N*,*N*-dicyclohexyl-1-isopropyl-1*H*-indole-2-carboxamide (5.4 g, 74%). The melting point was determined to be 154.8−155.9 °C. ^{1}H NMR (400 MHz, $CDCl_3$) δ 1.10−1.32 (m, 6H), 1.57−1.89 (m, 18H), 2.58−2.81 (m, 2H), 3.05−3.23 (m, 1H), 3.70−3.93 (m, 1H), 4.47−4.77 (m, 1H), 6.40 (s, 1H), 7.14 (t, *J* = 7.2 Hz, 1H), 7.24 (t, *J* = 7.3 Hz, 1H), 7.56 (d, *J* = 8.3 Hz, 1H), 7.65 (d, *J* = 7.8 Hz, 1H); ^{13}C NMR (100 MHz, $CDCl_3$) δ 21.7, 25.1, 26.5, 29.8, 31.4, 49.0, 56.2, 59.9, 99.3, 111.6, 119.5, 121.56, 121.64, 128.0, 135.0, 135.1, 165.0; HRMS (ESI): calculated m/z for $C_{24}H_{35}N_2O^+$: 367.2744, found 367.2747.

3-Bromo-_N_,_N_-dicyclohexyl-1-isopropyl-1_H_-indole-2-carboxamide (P7')

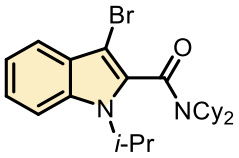

N,*N*-Dicyclohexyl-1-isopropyl-1*H*-indole-2-carboxamide (3.66 g, 10.0 mmol) was dissolved in anhydrous chloroform (30 mL) at room temperature. *N*-Bromosuccinimide (1.77 g, 10.0 mmol) was then added in portions to the solution. After stirring the reaction mixture for 30 minutes, water was added. The organic layer was washed with water and brine, then concentrated. The concentrated solution was filtered over a pad of silica and eluted with dichloromethane. The eluent was then concentrated, and the resulting solid was recrystallised from dichloromethane/hexane. The white solid was collected, washed with hexane, and dried under vacuum to afford 3-bromo-*N*,*N*-dicyclohexyl-1-isopropyl-1*H*-indole-2-carboxamide (1.93 g, 44%). The melting point was determined to be 148.1−149.2 °C. ^{1}H NMR (400 MHz, $CDCl_3$) δ 1.04−1.15 (m, 3H), 1.24−1.39 (m, 3H), 1.53−1.70 (m, 12H), 1.75−1.78 (m, 3H), 1.86−1.95 (m, 2H), 2.22−2.25 (m, 1H), 2.68−2.82 (m, 2H), 3.12−3.18 (m, 1H), 3.45−3.52 (m, 1H), 4.49−4.59 (m, 1H), 7.20−7.29 (m, 2H), 7.55 (d, *J* = 8.2 Hz, 1H), 7.61 (d, *J* = 7.6 Hz, 1H); ^{13}C NMR (100 MHz, $CDCl_3$) δ 21.6, 21.8, 25.1, 25.2, 25.3, 25.5, 26.50, 26.54, 29.3, 29.9, 31.4, 32.2, 50.3, 56.5, 60.5, 86.8, 112.2, 120.0, 120.2, 122.5, 127.7, 133.6, 162.6; HRMS (ESI): calculated m/z for $C_{24}H_{34}BrN_2O^+$: 445.1849, found 445.1848.

_N_,_N_-Dicyclohexyl-3-(dicyclohexylphosphanyl)-1-isopropyl-1_H_-indole-2-carboxamide (L7)

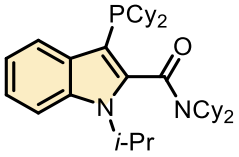

Under a nitrogen atmosphere, 3-Bromo-*N*,*N*-dicyclohexyl-1-isopropyl-1*H*-indole-2-carboxamide (0.89 g, 2.0 mmol) was dissolved in freshly distilled THF (20 mL) at room temperature. The solution was then cooled to -78 °C. Titrated *n*-BuLi (2.2 mmol) was added dropwise using a syringe. After stirring the reaction mixture for 30 minutes at -78 °C, chlorodicyclohexylphosphine (0.53 mL, 2.4 mmol) was added. The reaction was allowed to warm to room temperature and stirred overnight. The solvent was then removed under reduced pressure. The solid product was washed with ethanol, and the resulting white solid was collected and dried under vacuum to afford 3-(dicyclohexylphosphanyl)-*N*,*N*,1-triisopropyl-1*H*-indole-2-carboxamide (0.72 g, 64%). The melting point was determined to be 229.1−230.5 °C. ^{1}H NMR (400 MHz, $CDCl_3$) δ 0.99−1.32 (m, 16H), 1.53−1.75 (m, 22H), 1.81−1.90 (m, 5H), 1.96−1.99 (m, 1H), 2.33−2.36 (m, 1H), 2.61−2.82 (m, 3H), 3.07−3.13 (m, 1H), 3.36−3.42 (m, 1H), 4.44−4.54 (m, 1H), 7.14 (t, *J* = 7.3 Hz, 1H), 7.22 (t, *J* = 7.6 Hz, 1H), 7.60 (d, *J* = 8.2 Hz, 1H), 7.82 (d, *J* = 7.9 Hz, 1H); ^{13}C NMR (100 MHz, $CDCl_3$) δ 21.2, 21.7, 25.1, 25.2, 25.3, 25.6, 26.2, 26.6, 26.7, 27.1, 27.2, 27.4, 27.5, 27.7, 29.1, 29.9, 30.0, 30.6, 30.8, 30.9, 31.3, 31.5, 32.0, 32.3, 32.6, 36.1, 36.2, 49.7, 56.3, 59.7, 112.6, 119.5, 121.1,

122.9, 135.3, 145.5, 164.1; ^{31}P NMR (162 MHz, $CDCl_3$) δ -16.4; HRMS (ESI): calculated m/z for $C_{36}H_{56}N_2OP^+$: 563.4125, found 563.4129.

2.4.3 General procedure for ligand and reaction condition screenings

An array of Schlenk tubes were equipped with Teflon-coated magnetic stir bars (5 mm × 10 mm) and fitted with screw caps. The following reagents were added into each Schlenk tube: Pd source (1.00 mol%, 0.005 mmol), ligand (4.00 mol%, 0.02 mmol), 2,6-dimethylphenyl boronic acid (1.00 mmol), and base (1.50 mmol). The tubes were carefully evacuated and backfilled with nitrogen for three cycles. 2-Chlorotoluene (58.4 μL, 0.50 mmol) was then added by micropipette, followed by the corresponding solvent (1.50 mL) added by syringe. The tubes were placed into a preheated oil bath (110 °C) and stirred for 10 minutes. After the reaction was complete, the tubes were allowed to reach room temperature. Ethyl acetate (~3 mL), dodecane (113 μL, internal standard), and water (~2 mL) were then added. The organic layer was subjected to GC analysis, with the GC yield previously calibrated using an authentic sample/dodecane calibration curve.

2.4.4 General procedure for Suzuki coupling of aryl chlorides

General procedure for Suzuki−Miyaura coupling of aryl chlorides with 0.050−0.10 mol % Pd catalyst loading

Under a nitrogen atmosphere, $Pd_2(dba)_3$ (2.3 mg, 0.0025 mmol) and **L1** (9.1 mg, 0.020 mmol) were charged in either 10 mL of freshly distilled dioxane (0.10 mol% Pd per 1.0 mL Pd complex stock solution) or 5.0 mL of freshly distilled toluene (0.20 mol% Pd per 1.0 mL Pd complex stock solution). Arylboronic acid (1.0 mmol), aryl chloride (if solid, 0.50 mmol), and K_3PO_4 (318 mg, 1.5 mmol) were loaded into an array of Schlenk tubes equipped with Teflon-coated magnetic stir bars (4 mm × 10 mm). The tubes were evacuated and flushed with nitrogen three times. If the aryl chloride was a liquid, it was added by micropipette at this stage. The corresponding volume of the Pd complex stock solution and solvent were then immediately added to the Schlenk tubes by syringes, resulting in a final volume of 1.5 mL per tube. The tubes were placed into a preheated oil bath (110 °C) and stirred for 10 minutes to 2 hours. After the reaction was complete, the reaction tubes were allowed to cool down to room temperature. Before GC or TLC analysis, ethyl acetate (~3.0 mL) and water (~2.0 mL) were added for extraction. The organic layer was separated, and the aqueous layer was washed with ethyl acetate. The filtrate was concentrated under reduced pressure, and the crude products were purified by flash column chromatography on silica gel (230−400 mesh) to afford the desired product.

General procedure for Suzuki−Miyaura coupling of aryl chlorides with 0.0050 mol % Pd catalyst loading

Under a nitrogen atmosphere, $Pd_2(dba)_3$ (2.3 mg, 0.0025 mmol) and **L1** (9.1 mg, 0.020 mmol) were charged in 10 mL of freshly distilled dioxane, resulting in a 0.10 mol% Pd per 1.0 mL Pd complex stock solution. This stock solution was then further diluted by taking 0.50 mL of it and adding 4.5 mL of freshly distilled dioxane, resulting in a 0.010 mol% Pd per 1.0 mL Pd complex stock solution, also under a nitrogen atmosphere. Tri-arylboroxine (0.30 mmol), aryl chloride (if solid, 0.50 mmol), and K_3PO_4 (318 mg, 1.5 mmol) were loaded into an array of Schlenk tubes equipped with Teflon-coated magnetic stir bars (4 mm × 10 mm). The tubes were evacuated and flushed with nitrogen three times. If the aryl chloride was a liquid, it was added by micropipette at this stage. The further diluted stock solution (0.50 mL) and 1.0 mL of freshly distilled dioxane were then immediately added to the Schlenk tubes by syringes, resulting in a final volume of 1.5 mL per tube. The tubes were placed into a preheated oil bath (110 °C) and stirred for 24 hours. After the reaction was complete, the reaction tubes were allowed to reach room temperature. Before GC or TLC analysis, ethyl acetate (~3.0 mL) and water (~2.0 mL) were added. The organic layer was separated, and the aqueous layer was washed with ethyl acetate. The filtrate was concentrated under reduced pressure, and the crude products were purified by flash column chromatography on silica gel (230−400 mesh) to afford the desired product.

General procedure for gram-scale Suzuki−Miyaura coupling of aryl chlorides

In a 100 mL round-bottom Schlenk flask equipped with a Teflon-coated magnetic stir bar (6 mm × 30 mm), $Pd_2(dba)_3$ (2.3 mg, 0.0025 mmol), **L1** (9.1 mg, 0.020 mmol), 2-fluorophenylboronic acid (2.8 g, 20 mmol), and K_3PO_4 (6.4 g, 30 mmol) were added. The flask was evacuated and flushed with nitrogen three times. Afterwards, 2-chloro-1,3-dimethylbenzene (1.4 g, 10 mmol) and dioxane (30 mL) were added to the flask by syringes. The flask was then placed into a preheated oil bath (110 °C) and stirred for 30 minutes. After the reaction was complete, ethyl acetate and water were added to the flask. The mixture was transferred to a separating funnel and subjected to extraction. The combined organic layers were concentrated, and the crude product was purified by column chromatography on silica gel (230−400 mesh) to afford the desired product (1.7 g, 85%).

2.4.5 Characterisation data for coupling products

2,2',6-Trimethyl-1,1'-biphenyl (Table 2.3, 2.4, and 2.5, compound **3a**)[62]

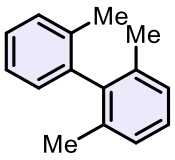

Flash column chromatography was performed using hexane as the eluent (R_f = 0.52). ^{1}H NMR (400 MHz, $CDCl_3$) δ 2.07 (s, 6H), 2.09 (s, 3H), 7.12−7.14 (m, 1H), 7.21−7.23 (m, 2H), 7.26−7.30 (m, 1H), 7.35−7.40 (m, 3H); ^{13}C NMR (100 MHz, $CDCl_3$) δ 19.4, 20.3, 126.0, 126.9, 127.0, 127.2, 128.8, 129.9, 135.5, 135.8, 140.5, 141.0.

2'-Methoxy-2,6-dimethyl-1,1'-biphenyl (Table 2.3 and 2.4, compound **3b**)[63]

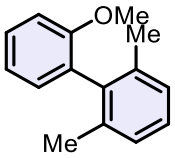

Flash column chromatography was performed using ethyl acetate/hexane (1: 50) as the eluent (R_f = 0.31). ^{1}H NMR (400 MHz, $CDCl_3$) δ 2.20 (s, 6H), 3.87 (s, 3H), 7.13−7.22 (m, 3H), 7.27−7.35 (m, 3H), 7.48−7.52 (m, 1H); ^{13}C NMR (100 MHz, $CDCl_3$) δ 20.4, 55.3, 110.8, 120.6, 126.96, 126.99, 128.3, 129.5, 130.6, 136.5, 138.2, 156.4.

2,2',4,6-Tetramethyl-1,1'-biphenyl (Table 2.3 and 2.4, compound **3c**)[64]

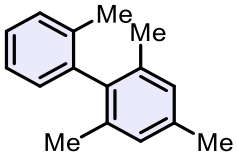

Flash column chromatography was performed using hexane as the eluent (R_f = 0.64). ^{1}H NMR (400 MHz, $CDCl_3$) δ 2.11 (s, 6H), 2.16 (s, 3H), 2.51 (s, 3H), 7.12 (s, 2H), 7.18−7.20 (m, 1H), 7.38−7.43 (m, 3H); ^{13}C NMR (100 MHz, $CDCl_3$) δ 19.4, 20.2, 21.0, 126.0, 126.9, 128.0, 129.1, 129.9, 135.6, 135.8, 136.2, 138.2, 140.5.

2'-Fluoro-2,6-dimethyl-1,1'-biphenyl (Table 2.3, compound **3d**)[63]

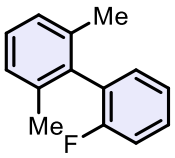

Flash column chromatography was performed using hexane as the eluent (R_f = 0.59). ^{1}H NMR (400 MHz, $CDCl_3$) δ 2.17 (s, 6H), 7.22−7.32 (m, 6H), 7.41−7.46 (m, 1H); ^{13}C NMR (100 MHz, $CDCl_3$) δ 20.4, 115.7 (d, *J* = 22.4 Hz), 124.1 (d, *J* = 3.5 Hz), 127.3, 127.7, 128.0 (d, *J* = 17.7 Hz),

128.9 (d, *J* = 7.9 Hz), 131.3 (d, *J* = 4.0 Hz), 135.3, 136.6, 159.5 (d, *J* = 242.9 Hz); ^{19}F NMR (376 MHz, $CDCl_3$) δ -115.0 (s).

2,4-Difluoro-2',6'-dimethyl-1,1'-biphenyl (Table 2.3, compound **3e**)[65]

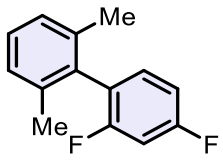

Flash column chromatography was performed using ethyl hexane as the eluent (R_f = 0.50). ^{1}H NMR (400 MHz, $CDCl_3$) δ 2.14 (s, 6H), 6.97−7.05 (m, 2H), 7.15−7.22 (m, 3H), 7.27−7.31 (m, 1H); ^{13}C NMR (100 MHz, $CDCl_3$) δ 20.4, 104.1 (dd, *J* = 25.2 Hz, *J* = 26.2 Hz), 111.4 (dd, *J* = 20.7 Hz, *J* = 3.7 Hz), 124.0 (dd, *J* = 18.1 Hz, *J* = 4.1 Hz), 127.4, 128.0, 131.9 (dd, *J* = 5.4 Hz, *J* = 9.3 Hz), 134.3, 136.8, 159.5 (dd, *J* = 245.5 Hz, *J* = 11.7 Hz), 162.3 (dd, *J* = 246.4 Hz, *J* = 11.4 Hz); ^{19}F NMR (376 MHz, $CDCl_3$) δ -111.6 (m, 1F), -110.5 (m, 1F).

2'-Methoxy-2,4,6-trimethyl-1,1'-biphenyl (Table 2.3, compound **3f**)[66]

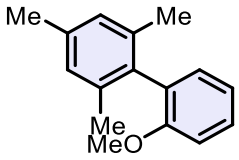

Flash column chromatography was performed using dichloromethane/hexane (1: 20) as the eluent (R_f = 0.31). ^{1}H NMR (400 MHz, $CDCl_3$) δ 2.02 (s, 6H), 2.36 (s, 3H), 3.77 (s, 3H), 6.97−7.08 (m, 5H), 7.34−7.38 (m, 1H); ^{13}C NMR (100 MHz, $CDCl_3$) δ 20.3, 21.1, 55.4, 110.8, 120.6, 127.9, 128.2, 129.5, 130.9, 135.2, 136.4, 136.5, 156.7.

2',6'-Dimethyl-[1,1'-biphenyl]-2-amine (Table 2.3, compound **3g**)[67]

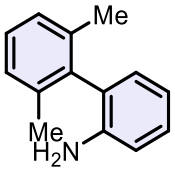

Flash column chromatography was performed using ethyl acetate/hexane (1: 9) as the eluent (R_f = 0.57). ^{1}H NMR (400 MHz, $CDCl_3$) δ 2.08 (s, 6H), 3.40 (br, 2H), 6.79−6.86 (m, 2H), 6.94 (d, *J* = 7.4 Hz, 1H), 7.15−7.22 (m, 4H); ^{13}C NMR (100 MHz, $CDCl_3$) δ 20.2, 115.0, 118.5, 126.1, 127.5, 127.6, 128.1, 129.7, 137.2, 137.8, 143.3.

4-(2,6-Dimethylphenyl)quinoline (Table 2.3, compound **3h**)

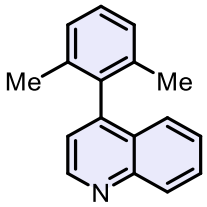

Flash column chromatography was performed using ethyl acetate/hexane (1: 4) as the eluent (R_f = 0.35). The product was obtained as a light-yellow solid. The melting point was determined to be 96.5 − 98.2 °C. ^{1}H NMR (400 MHz, $CDCl_3$) δ 1.92 (s, 6H), 7.19−7.23 (m, 3H), 7.29−7.32 (m, 1H), 7.39−7.43 (m, 2H), 7.72 (t, *J* = 7.5 Hz, 1H), 8.20 (d, *J* = 8.5 Hz, 1H), 8.95 (d, *J* = 4.3 Hz, 1H); ^{13}C NMR (100 MHz, $CDCl_3$) δ 20.1, 121.4, 125.2, 126.7, 127.0, 127.4, 128.0, 129.4, 129.7, 135.9, 136.8, 147.9, 148.4, 150.2; HRMS: calculated m/z for $C_{17}H_{16}N^+$: 234.1277, found 234.1282.

Ethyl 6-ethoxy-2',6'-dimethyl-[1,1'-biphenyl]-3-carboxylate (Table 2.3, compound **3i**)

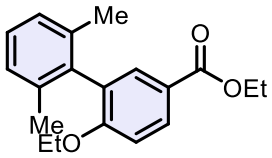

Flash column chromatography was performed using ethyl acetate/hexane (1: 4) as the eluent (R_f = 0.68).The product was obtained as a yellow liquid. ^{1}H NMR (400 MHz, $CDCl_3$) δ 1.27 (t, *J* = 7.0 Hz, 3H), 1.40 (t, *J* = 7.1 Hz, 3H), 2.06 (s, 6H), 4.07−4.12 (m, 2H), 4.35−4.41 (m, 2H), 7.03 (d, *J* = 8.7 Hz, 1H), 7.13−7.15 (m, 2H), 7.18−7.22 (m, 1H), 7.84 (s, 1H), 8.11 (d, *J* = 8.6 Hz, 1H); ^{13}C NMR (100 MHz, $CDCl_3$) δ 14.2, 14.3, 20.2, 60.4, 63.6, 111.0, 122.6, 126.9, 127.0, 129.5, 130.5, 132.3, 136.2, 137.2, 159.4, 166.2; HRMS: calculated m/z for $C_{19}H_{23}O_3^+$: 299.1642, found 299.1645.

5-Methoxy-2,2',6'-trimethyl-1,1'-biphenyl (Table 2.3, compound **3j**)

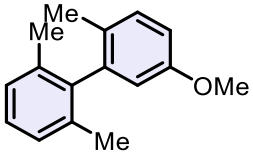

Flash column chromatography was performed using dichloromethane/hexane (1: 20) as the eluent (R_f = 0.37). The product was obtained as a colourless liquid. ^{1}H NMR (400 MHz, $CDCl_3$) δ 2.03 (s, 3H), 2.11 (s, 6H), 3.89 (s, 3H), 6.74 (s, 1H), 6.94 (d, *J* = 8.4 Hz, 1H), 7.22−7.32 (m, 4H); ^{13}C NMR (100 MHz, $CDCl_3$) δ 18.3, 20.2, 55.1, 112.5, 114.0, 126.9, 127.2, 127.5, 130.8, 135.7, 141.0, 141.5, 157.9; HRMS: calculated m/z for $C_{16}H_{18}O$: 226.1352, found 226.1352.

2-Methoxy-2',6'-dimethyl-[1,1'-biphenyl]-4-carbaldehyde (Table 2.3, compound **3k**)

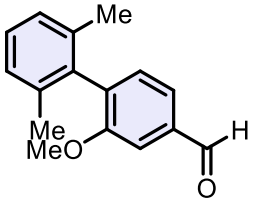

Flash column chromatography was performed using ethyl acetate/hexane (1: 9) as the eluent (R_f = 0.34). The product was obtained as a colourless liquid. ^{1}H NMR (400 MHz, $CDCl_3$) δ 2.05 (s, 6H), 3.86 (s, 3H), 7.16−7.29 (m, 4H), 7.57−7.60 (m, 2H), 10.08 (s, 1H); ^{13}C NMR (100 MHz,

$CDCl_3$) δ 20.2, 55.6, 109.2, 124.4, 127.1, 127.6, 131.2, 135.9, 136.7, 136.9, 137.0, 157.3, 191.8; HRMS: calculated m/z for $C_{16}H_{17}O_2^+$: 241.1223, found 241.1224.

4-Methoxy-2,2',6-trimethyl-1,1'-biphenyl (Table 2.3, compound **3l**)[68]

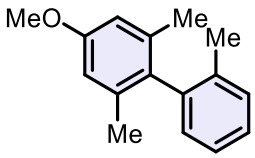

Flash column chromatography was performed using ethyl acetate/hexane (1: 50) as the eluent (R_f = 0.45). ^{1}H NMR (400 MHz, $CDCl_3$) δ 1.97 (s, 6H), 2.02 (s, 3H), 3.87 (s, 3H), 6.72 (s, 2H), 7.05−7.06 (m, 2H), 7.27−7.31 (m, 3H); ^{13}C NMR (100 MHz, $CDCl_3$) δ 19.4, 20.6, 55.0, 112.5, 125.9, 126.9, 129.5, 129.9, 133.7, 136.2, 137.2, 140.3, 158.2.

2-Fluoro-2',6'-dimethyl-4-(trifluoromethyl)-1,1'-biphenyl (Table 2.4, compound **3m**)

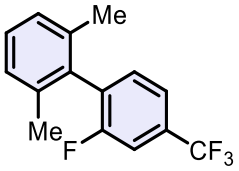

Flash column chromatography was performed using hexane as the eluent (R_f = 0.69). The product was obtained as a colourless liquid. ^{1}H NMR (400 MHz, $CDCl_3$) δ 2.04 (s, 6H), 7.13 (d, *J* = 7.6 Hz, 2H), 7.20−7.28 (m, 2H), 7.45−7.47 (m, 1H), 7.61−7.65 (m, 1H); ^{13}C NMR (100 MHz, $CDCl_3$) δ 20.4, 116.4 (d, *J* = 24.0 Hz), 123.8 (q, *J* = 270.4 Hz), 126.4−126.6 (m), 126.8 (d, *J* = 3.2 Hz), 127.1 (d, *J* = 3.6 Hz), 127.5, 128.4, 128.9−129.1 (m), 133.7, 136.5, 161.4 (d, *J* = 148.3 Hz); ^{19}F NMR (376 MHz, $CDCl_3$) δ -109.4 (s, 1F), -61.8 (s, 3F); HRMS (EI): calculated m/z for $C_{15}H_{12}F_4^+$: 268.0870, found 268.0879.

2,2',5,6'-Tetramethyl-1,1'-biphenyl (Table 2.4, compound **3n**)[63]

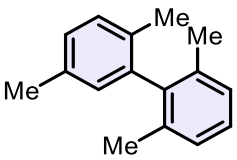

Flash column chromatography was performed using hexane as the eluent (R_f = 0.50). ^{1}H NMR (400 MHz, $CDCl_3$) δ 2.07 (s, 3H), 2.10 (s, 6H), 2.47 (s, 3H), 6.98 (s, 1H), 7.19−7.31 (m, 5H); ^{13}C NMR (100 MHz, $CDCl_3$) δ 18.9, 20.3, 21.0, 126.8, 127.1, 127.7, 129.4, 129.8, 132.3, 135.3, 135.8, 140.4, 141.2.

2,6-Dimethyl-1,1':2',1''-terphenyl (Table 2.4, compound **3o**)[63]

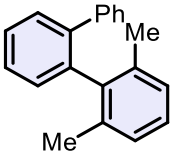

Flash column chromatography was performed using hexane as the eluent (R_f = 0.48). ^{1}H NMR (400 MHz, $CDCl_3$) δ 1.98 (s, 6H), 6.99−7.00 (m, 2H), 7.08−7.22 (m, 7H), 7.41−7.53 (m, 3H); ^{13}C NMR (100 MHz, $CDCl_3$) δ 20.8, 126.5, 126.9, 127.1, 127.3, 127.4, 127.6, 128.8, 130.1, 130.3, 136.1, 138.9, 140.75, 140.78, 141.3.

2,6-Difluoro-2'-methyl-1,1'-biphenyl (Table 2.4 and 2.5, compound **3p**)[69]

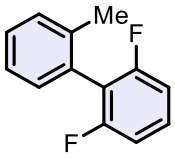

Flash column chromatography was performed using hexane as the eluent (R_f = 0.52). ^{1}H NMR (400 MHz, $CDCl_3$) δ 2.24 (s, 3H), 6.99−7.05 (m, 2H), 7.26−7.40 (m, 5H); ^{13}C NMR (100 MHz, $CDCl_3$) δ 19.7, 111.2−111.4 (m), 117.9−118.3 (m), 125.5, 128.6, 128.8, 129.0−129.2 (m), 130.1, 130.6, 137.3, 160.2 (dd, *J* = 245.9 Hz, *J* = 7.5 Hz); ^{19}F NMR (376 MHz, $CDCl_3$) δ -112.3 (s).

1-(2,6-Dimethylphenyl)naphthalene (Table 2.4, compound **3q**)[70]

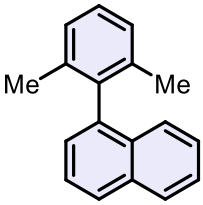

Flash column chromatography was performed using hexane as the eluent (R_f = 0.61). ^{1}H NMR (400 MHz, $CDCl_3$) δ 2.01 (s, 6H), 7.27−7.29 (m, 2H), 7.34−7.38 (m, 2H), 7.43−7.45 (m, 2H), 7.54−7.58 (m, 1H), 7.6−7.65 (m, 1H), 7.94−8.00 (m, 2H); ^{13}C NMR (100 MHz, $CDCl_3$) δ 20.4, 125.4, 125.68, 125.75, 126.0, 126.4, 127.2, 127.25, 127.31, 128.3, 131.7, 133.7, 137.0, 138.7, 139.6.

3-Methyl-4-(*o*-tolyl)quinoline (Table 2.4, compound **3r**)[71]

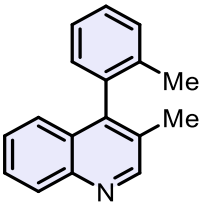

Flash column chromatography was performed using ethyl acetate/hexane (1: 4) as the eluent (R_f = 0.40). ^{1}H NMR (400 MHz, $CDCl_3$) δ 1.92 (s, 3H), 2.17 (s, 3H), 7.06 (d, *J* = 7.4 Hz, 1H), 7.27−7.38 (m, 5H), 7.61 (t, *J* = 7.6 Hz, 1H), 8.14 (d, *J* = 8.4 Hz, 1H), 8.88 (s, 1H); ^{13}C NMR (100 MHz, $CDCl_3$) δ 17.0, 19.3, 125.4, 125.9, 126.4, 127.2, 128.0, 128.07, 128.08, 128.8, 129.3, 130.1, 135.7, 136.2, 145.8, 146.7, 152.5.

6-Methoxy-2'-methyl-[1,1'-biphenyl]-2-carbonitrile (Table 2.4, compound **3s**)[68]

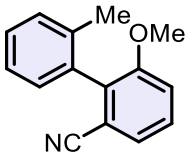

Flash column chromatography was performed using ethyl acetate/hexane (1: 9) as the eluent (R_f = 0.33). ^{1}H NMR (400 MHz, $CDCl_3$) δ 2.12 (s, 3H), 3.78 (s, 3H), 7.18−7.20 (m, 2H), 7.28−7.37 (m, 4H), 7.43 (t, *J* = 8.1 Hz, 1H); ^{13}C NMR (100 MHz, $CDCl_3$) δ 19.5, 55.8, 114.3, 115.0, 117.7, 124.5, 125.7, 128.6, 129.2, 129.6, 129.9, 134.2, 134.6, 136.6, 157.0.

2,4,6-Triethyl-2'-methyl-1,1'-biphenyl (Table 2.4, compound **3t**)[72]

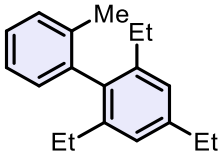

Flash column chromatography was performed using hexane as the eluent (R_f = 0.60). ^{1}H NMR (400 MHz, $CDCl_3$) δ 1.11 (t, *J* = 7.6 Hz, 6H), 1.40 (t, *J* = 7.6 Hz, 3H), 2.07 (s, 3H), 2.24−2.41 (m, 4H), 2.75−2.81 (m, 2H), 7.09 (s, 2H), 7.17−7.21 (m, 1H), 7.28−7.35 (m, 3H); ^{13}C NMR (100 MHz, $CDCl_3$) δ 15.2, 15.4, 19.9, 26.5, 28.7, 125.1, 125.5, 126.9, 129.7, 130.1, 136.3, 137.1, 140.0, 141.7, 143.0.

4'-Methoxy-2,2',4,5,6'-pentamethyl-1,1'-biphenyl (Table 2.4, compound **3u**)

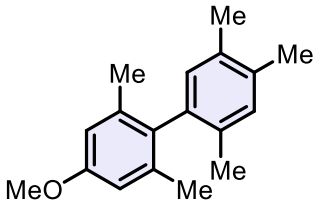

Flash column chromatography was performed using ethyl acetate/hexane (1: 9) as the eluent (R_f = 0.79). The product was obtained as a colourless liquid. ^{1}H NMR (400 MHz, $CDCl_3$) δ 2.00 (s, 3H), 2.04 (s, 6H), 2.33 (s, 3H), 2.36 (s, 3H), 3.89 (s, 3H), 6.76 (s, 2H), 6.87 (s, 1H), 7.13 (s, 1H); ^{13}C NMR (100 MHz, $CDCl_3$) δ 18.8, 19.2, 19.4, 20.7, 54.9, 112.4, 130.6, 131.2, 133.2, 133.7, 133.8, 134.8, 137.3, 137.6, 158.1; HRMS: calculated m/z for $C_{18}H_{23}O^+$: 255.1743, found 255.1744.

4,4'-Dimethoxy-2,2',6-trimethyl-1,1'-biphenyl (Table 2.4, compound **3v**)

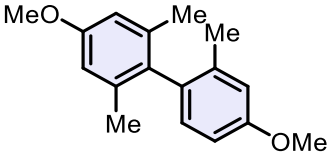

Flash column chromatography was performed using ethyl acetate/hexane (1: 9) as the eluent (R_f = 0.69). The product was obtained as a colourless liquid. ^{1}H NMR (400 MHz, $CDCl_3$) δ 2.00 (s, 6H), 2.01 (s, 3H), 3.86 (s, 3H), 3.87 (s, 3H), 6.73 (s, 2H), 6.83−6.85 (m, 1H), 6.89−6.90 (m, 1H), 6.97 (d, *J* = 8.2 Hz, 1H); ^{13}C NMR (100 MHz, $CDCl_3$) δ 19.7, 20.6, 54.9, 55.0, 111.1, 112.4, 115.3,

130.3, 132.6, 133.3, 137.5, 137.7, 158.1, 158.4; HRMS: calculated m/z for $C_{17}H_{21}O_2^+$: 257.1536, found 257.1536.

2,2',6-Trimethyl-[1,1'-biphenyl]-4-yl dimethylsulfamate (Table 2.4, compound **3w**)

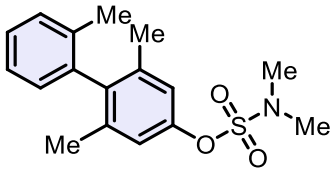

Flash column chromatography was performed using ethyl acetate/hexane (1: 9) as the eluent (R_f = 0.46). The product was obtained as a colourless liquid. ^{1}H NMR (400 MHz, $CDCl_3$) δ 1.99 (s, 9H), 3.05 (s, 6H), 7.00−7.02 (m, 1H), 7.09 (s, 2H), 7.26−7.33 (m, 3H); ^{13}C NMR (100 MHz, $CDCl_3$) δ 19.2, 20.3, 38.7, 119.9, 126.1, 127.2, 128.7, 130.0, 135.4, 137.8, 139.3, 139.5, 148.7; HRMS: calculated m/z for $C_{17}H_{22}NO_3S^+$: 320.1315, found 320.1315.

4-(2,6-Dimethylphenyl)dibenzo[*b,d*]furan (Table 2.4, compound **3x**)

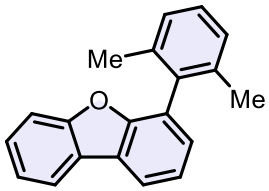

Flash column chromatography was performed using ethyl acetate/hexane (1: 50) as the eluent (R_f = 0.61). The product was obtained as a colourless gel. ^{1}H NMR (400 MHz, $CDCl_3$) δ 2.17 (s, 6H), 7.30−7.45 (m, 5H), 7.49−7.53 (m, 2H), 7.60 (d, *J* = 8.2 Hz, 1H), 8.04−8.09 (m, 2H); ^{13}C NMR (100 MHz, $CDCl_3$) δ 20.5, 111.9, 119.5, 120.6, 122.6, 122.9, 124.3, 124.4, 124.9, 127.1, 127.4, 127.9, 128.2, 135.9, 136.9, 153.6, 156.2; HRMS: calculated m/z for $C_{20}H_{16}O$: 272.1196, found 272.1201.

4-(2,6-Dimethylphenyl)dibenzo[*b,d*]thiophene (Table 2.4, compound **3y**)

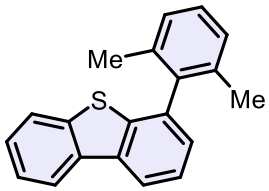

Flash column chromatography was performed using ethyl acetate/hexane (1: 20) as the eluent (R_f = 0.63). The product was obtained as a white solid. The melting point was determined to be 86.9−87.7 °C. ^{1}H NMR (400 MHz, $CDCl_3$) δ 2.16 (s, 6H), 7.28−7.41 (m, 4H), 7.51−7.58 (m, 2H), 7.66 (t, *J* = 7.6 Hz, 1H), 7.87 (d, *J* = 7.3 Hz, 1H), 8.25−8.30 (m, 2H); ^{13}C NMR (100 MHz, $CDCl_3$) δ 20.0, 120.1, 121.7, 122.8, 124.3, 125.0, 126.6, 126.9, 127.5, 128.0, 135.7, 135.97, 136.03, 136.3, 139.4, 139.7, 139.8; HRMS: calculated m/z for $C_{20}H_{16}S$: 288.0973, found 288.0973.

1-Mesitylpyrene (Table 2.4, compound **3z**)

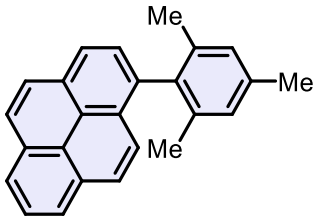

Flash column chromatography was performed using hexane as the eluent (R_f = 0.58). The product was obtained as a white solid. The melting point was determined to be 140.6−141.4 °C. ^{1}H NMR (400 MHz, $CDCl_3$) δ 2.01 (s, 6H), 2.54 (s, 3H), 7.18 (s, 2H), 7.74 (d, *J* = 9.1 Hz, 1H), 7.91 (d, *J* = 7.7 Hz, 1H), 8.03−8.09 (m, 2H), 8.15−8.28 (m, 4H), 8.33 (d, *J* = 7.7 Hz, 1H); ^{13}C NMR (100 MHz, $CDCl_3$) δ 20.6, 21.2, 124.8, 124.9, 125.9, 127.1, 127.3, 127.4, 127.5, 128.2, 128.9, 130.3, 131.1, 131.3, 136.5, 137.0, 137.1; HRMS: calculated m/z for $C_{25}H_{20}$: 320.1565, found 320.1565.

1-(4-Methoxy-2,6-dimethylphenyl)pyrene (Table 2.4, compound **3aa**)[73]

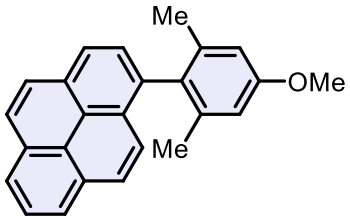

Flash column chromatography was performed using ethyl acetate/hexane (1: 20) as the eluent (R_f = 0.58). ^{1}H NMR (400 MHz, $CDCl_3$) δ 1.96 (s, 6H), 3.95 (s, 3H), 6.87 (s, 2H), 7.68 (d, *J* = 9.2 Hz, 1H), 7.84 (d, *J* = 7.7 Hz, 1H), 7.98−8.05 (m, 2H), 8.11−8.19 (m, 3H), 8.23 (d, *J* = 7.6 Hz, 1H), 8.27 (d, *J* = 7.8 Hz, 1H); ^{13}C NMR (100 MHz, $CDCl_3$) δ 20.9, 55.2, 112.7, 124.86, 124.91, 124.95, 124.97, 125.9, 127.1, 127.4, 127.5, 127.7, 129.3, 130.3, 131.1, 131.3, 132.6, 136.3, 138.5, 158.8.

9-(*o*-Tolyl)anthracene (Table 2.4 and 2.5, compound **3ab**)[74]

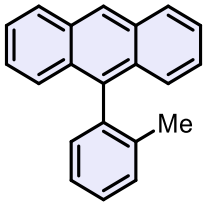

Flash column chromatography was performed using hexane as the eluent (R_f = 0.65). ^{1}H NMR (400 MHz, $CDCl_3$) δ 1.97 (s, 3H), 7.35−7.55 (m, 8H), 7.54−7.64 (m, 2H), 8.11−8.13 (m, 2H), 8.56 (s, 1H); ^{13}C NMR (100 MHz, $CDCl_3$) δ 19.7, 125.1, 125.4, 125.8, 126.4, 126.5, 127.8, 128.4, 129.9, 130.0, 131.2, 131.4, 136.4, 137.8, 138.1.

9-(4-Methoxy-2-methylphenyl)anthracene (Table 2.4, compound **3ac**)[75]

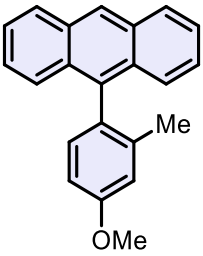

Flash column chromatography was performed using ethyl acetate/hexane (1: 9) as the eluent (R_f = 0.70). ^{1}H NMR (400 MHz, $CDCl_3$) δ 1.87 (s, 3H), 3.95 (s, 3H), 6.95−7.03 (m, 2H), 7.19 (d, *J* = 8.3 Hz, 1H), 7.35−7.38 (m, 2H), 7.46−7.49 (m, 2H), 7.57−7.59 (m, 2H), 8.06−8.08 (m, 2H), 8.50 (s, 1H); ^{13}C NMR (100 MHz, $CDCl_3$) δ 20.0, 55.3, 111.1, 115.4, 125.1, 125.3, 126.2, 126.6, 128.4, 130.35, 130.41, 131.4, 132.1, 136.2, 139.2, 159.2.

9-(Naphthalen-1-yl)anthracene (Table 2.4, compound **3ad**)[76]

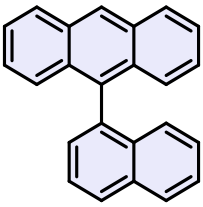

Flash column chromatography was performed using hexane as the eluent (R_f = 0.55). ^{1}H NMR (400 MHz, $CDCl_3$) δ 7.18−7.33 (m, 4H), 7.50−7.62 (m, 6H), 7.76 (t, *J* = 7.5 Hz, 1H), 8.07−8.18 (m, 4H), 8.66 (s, 1H); ^{13}C NMR (100 MHz, $CDCl_3$) δ 125.1, 125.47, 125.51, 125.9, 126.2, 126.5, 126.9, 128.1, 128.2, 128.4, 129.1, 131.0, 131.4, 133.5, 133.7, 134.9, 136.5.

10-(*o*-Tolyl)anthracene-9-carbaldehyde (Table 2.4 and 2.5, compound **3ae**)[68]

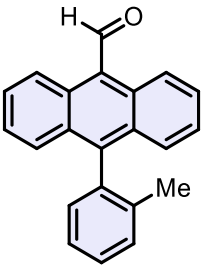

Flash column chromatography was performed using ethyl acetate/hexane (1: 4) as the eluent (R_f = 0.57). ^{1}H NMR (400 MHz, $CDCl_3$) δ 1.85 (s, 3H), 7.22 (d, *J* = 7.4 Hz, 1H), 7.39−7.51 (m, 5H), 7.57−7.60 (m, 2H), 7.65−7.69 (m, 2H), 9.02−9.05 (m, 2H), 11.60 (s, 1H); ^{13}C NMR (100 MHz, $CDCl_3$) δ 19.6, 123.6, 125.0, 125.7, 125.9, 127.5, 128.4, 128.7, 129.6, 130.2, 130.4, 131.7, 137.2, 137.6, 145.2, 193.4.

9-(4-Methoxy-2,6-dimethylphenyl)phenanthrene (Table 2.4, compound **3af**)[77]

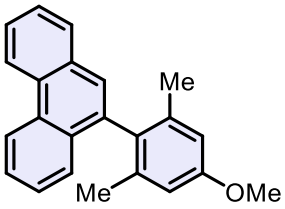

Flash column chromatography was performed using ethyl acetate/hexane (1: 20) as the eluent (R_f = 0.54). ^{1}H NMR (400 MHz, $CDCl_3$) δ 1.97 (s, 6H), 3.90 (s, 3H), 6.79 (s, 2H), 7.44−7.51 (m, 2H), 7.56 (s, 1H), 7.61−7.71 (m, 3H), 7.89 (d, *J* = 7.6 Hz, 1H), 8.77 (m, 2H); ^{13}C NMR (100 MHz, $CDCl_3$) δ 20.7, 55.2, 112.7, 122.6, 122.9, 126.1, 126.36, 126.43, 126.6, 126.7, 127.6, 128.5, 130.0, 130.6, 131.6, 131.98, 132.01, 137.1, 138.5, 158.7.

*2.4.6 Preparation of the oxidative adduct **C1** and its X-ray crystallographic data*

A Schlenk tube (100 mL) equipped with a screw cap and Teflon-coated magnetic stir bar was charged with $Pd(dba)_2$ (0.575 g, 1.0 mmol) and **L1** (0.9080 g, 2.0 mmol). The tube was carefully evacuated and backfilled with nitrogen for three cycles. Subsequently, 2-chlorotoluene (1.89 g, 15.0 mmol) and THF (30 mL) were added to the tube by syringe. The resulting solution was stirred at room temperature for 5 minutes. The tube was then placed into a preheated oil bath (110 °C) and stirred for 14 hours. After the reaction was complete, the reaction tube was allowed to warm to room temperature. The unreacted palladium was filtered through Celite, and the solvent was removed. The crude product was washed successively with hexane, and then recrystallised from DCM and hexane to afford the desired palladium complex **C1** as a grey green solid. A single crystal of **C1** suitable for X-ray diffraction was obtained by vapor diffusion of hexane into a dichloromethane solution containing **C1**.

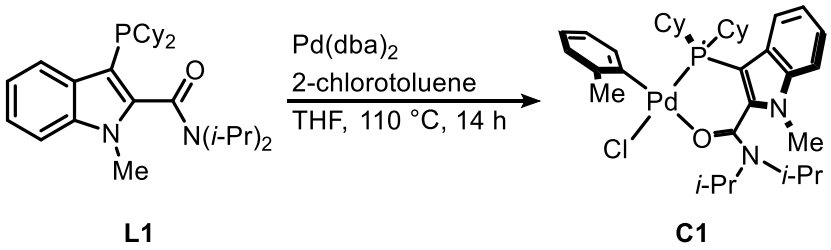

L1 **C1**

Scheme 2.4 Preparation of oxidative addition complex **C1**

Table 2.6 Crystal data and structure refinement for **C1**

Identification code	SCM2105
Empirical formula	C_{36} H_{52} Cl_3 N_2 O P Pd
Formula weight	772.52
Temperature	297(2) K
Wavelength	0.71073 Å
Crystal system, space group	Triclinic, P-1
Unit cell dimensions	a = 11.0002(5) Å α = 93.8303(14)°
	b = 12.8129(5) Å β = 97.7328(14)°
	c = 14.2811(6) Å γ = 110.1124(13)°
Volume	1859.03(14) $Å^3$
Z, Calculated density	2, 1.380 Mg/m^3
Absorption coefficient	0.788 mm^{-1}
F(000)	804
Crystal size	0.68 × 0.36 × 0.28 mm
Theta range for data collection	2.00 to 27.74°
Limiting indices	-14<=h<=14, -16<=k<=16, -18<=l<=18
Reflections collected / unique	96713 / 8667 [R(int) = 0.0230]
Completeness to θ = 27.74	99.1 %
Absorption correction	Semi-empirical from equivalents
Max. and min. transmission	0.8096 and 0.6164
Refinement method	Full-matrix least-squares on F^2
Data / restraints / parameters	8667 / 0 / 403
Goodness-of-fit on F^2	1.050
Final R indices [I>2σ(I)]	R_1 = 0.0256, wR_2 = 0.0647
R indices (all data)	R_1 = 0.0275, wR_2 = 0.0663
Largest diff. peak and hole	0.753 and -0.788 $e.Å^{-3}$

Table 2.7 Atomic coordinates ($\times 10^4$) and equivalent isotropic displacement parameters ($A^2 \times 10^3$) for **C1**

U(eq) is defined as one third of the trace of the orthogonalised U^{ij} tensor.

	x	y	z	U(eq)
P(1)	7107(1)	8403(1)	2740(1)	27(1)
O(1)	5627(1)	6048(1)	1451(1)	38(1)
Pd(1)	7601(1)	6960(1)	2120(1)	29(1)
Cl(1)	8049(1)	5393(1)	1524(1)	47(1)
Cl(2)	7931(1)	4868(1)	4729(1)	123(1)
Cl(3)	8079(2)	3231(1)	3294(1)	146(1)
N(1)	3857(1)	7743(1)	822(1)	32(1)
N(2)	3517(1)	5472(1)	1623(1)	30(1)
C(1)	9449(2)	7606(2)	2778(1)	38(1)
C(2)	9738(2)	7553(2)	3753(2)	47(1)
C(3)	11028(3)	7906(2)	4218(2)	65(1)
C(4)	12032(2)	8328(2)	3718(2)	73(1)
C(5)	11769(2)	8377(2)	2768(2)	67(1)
C(6)	10476(2)	8001(2)	2269(2)	51(1)
C(7)	10252(3)	8005(3)	1209(2)	71(1)
C(8)	6803(2)	8270(1)	3970(1)	31(1)
C(9)	6198(2)	9084(2)	4355(1)	43(1)
C(10)	5926(2)	8892(2)	5364(2)	54(1)
C(11)	5079(2)	7689(2)	5417(2)	58(1)
C(12)	5690(2)	6886(2)	5047(2)	51(1)
C(13)	5951(2)	7059(2)	4038(1)	40(1)
C(14)	8252(2)	9849(1)	2753(1)	36(1)
C(15)	9491(2)	10192(2)	3511(2)	45(1)
C(16)	10366(2)	11396(2)	3468(2)	65(1)
C(17)	10721(3)	11561(3)	2500(3)	88(1)
C(18)	9500(3)	11238(2)	1739(2)	79(1)
C(19)	8599(2)	10032(2)	1765(2)	52(1)
C(20)	5592(2)	8390(1)	2035(1)	29(1)
C(21)	5185(2)	9312(1)	1777(1)	32(1)
C(22)	5540(2)	10447(2)	2126(2)	44(1)
C(23)	4918(2)	11086(2)	1676(2)	54(1)
C(24)	3942(2)	10637(2)	875(2)	54(1)
C(25)	3537(2)	9528(2)	531(1)	44(1)

C(26)	4147(2)	8876(1)	1003(1)	33(1)
C(27)	2993(2)	7051(2)	-26(1)	44(1)
C(28)	4706(2)	7453(1)	1455(1)	28(1)
C(29)	4621(2)	6271(1)	1506(1)	28(1)
C(30)	2300(2)	5661(2)	1792(1)	39(1)
C(31)	2083(2)	5527(2)	2816(2)	59(1)
C(32)	1100(2)	4893(2)	1089(2)	56(1)
C(33)	3501(2)	4306(1)	1674(1)	38(1)
C(34)	4431(3)	4212(2)	2527(2)	61(1)
C(35)	3720(3)	3806(2)	744(2)	57(1)
C(36)	8535(4)	4612(3)	3728(2)	105(1)

Table 2.8 Bond lengths [Å] and angles [°] for **C1**

P(1)−C(20)	1.8214(16)
P(1)−C(8)	1.8396(16)
P(1)−C(14)	1.8453(17)
P(1)−Pd(1)	2.2575(4)
O(1)−C(29)	1.2457(19)
O(1)−Pd(1)	2.1304(12)
Pd(1)−C(1)	1.9815(17)
Pd(1)−Cl(1)	2.3600(4)
Cl(2)−C(36)	1.713(4)
Cl(3)−C(36)	1.710(4)
N(1)−C(28)	1.372(2)
N(1)−C(26)	1.373(2)
N(1)−C(27)	1.458(2)
N(2)−C(29)	1.331(2)
N(2)−C(30)	1.487(2)
N(2)−C(33)	1.494(2)
C(1)−C(6)	1.392(3)
C(1)−C(2)	1.398(3)
C(2)−C(3)	1.387(3)
C(2)−H(2A)	0.9300
C(3)−C(4)	1.370(4)
C(3)−H(3A)	0.9300
C(4)−C(5)	1.359(4)
C(4)−H(4A)	0.9300
C(5)−C(6)	1.404(3)
C(5)−H(5A)	0.9300
C(6)−C(7)	1.501(4)
C(7)−H(7A)	0.9600
C(7)−H(7B)	0.9600
C(7)−H(7C)	0.9600
C(8)−C(9)	1.528(2)
C(8)−C(13)	1.529(2)
C(8)−H(8A)	0.9800
C(9)−C(10)	1.529(3)
C(9)−H(9A)	0.9700
C(9)−H(9B)	0.9700

C(10)−C(11)	1.515(3)
C(10)−H(10A)	0.9700
C(10)−H(10B)	0.9700
C(11)−C(12)	1.514(3)
C(11)−H(11A)	0.9700
C(11)−H(11B)	0.9700
C(12)−C(13)	1.523(3)
C(12)−H(12A)	0.9700
C(12)−H(12B)	0.9700
C(13)−H(13A)	0.9700
C(13)−H(13B)	0.9700
C(14)−C(19)	1.522(3)
C(14)−C(15)	1.533(2)
C(14)−H(14A)	0.9800
C(15)−C(16)	1.522(3)
C(15)−H(15A)	0.9700
C(15)−H(15B)	0.9700
C(16)−C(17)	1.495(4)
C(16)−H(16A)	0.9700
C(16)−H(16B)	0.9700
C(17)−C(18)	1.524(4)
C(17)−H(17A)	0.9700
C(17)−H(17B)	0.9700
C(18)−C(19)	1.528(3)
C(18)−H(18A)	0.9700
C(18)−H(18B)	0.9700
C(19)−H(19A)	0.9700
C(19)−H(19B)	0.9700
C(20)−C(28)	1.387(2)
C(20)−C(21)	1.453(2)
C(21)−C(22)	1.405(2)
C(21)−C(26)	1.406(2)
C(22)−C(23)	1.374(3)
C(22)−H(22A)	0.9300
C(23)−C(24)	1.396(3)
C(23)−H(23A)	0.9300
C(24)−C(25)	1.368(3)

C(24)−H(24A)	0.9300
C(25)−C(26)	1.394(2)
C(25)−H(25A)	0.9300
C(27)−H(27A)	0.9600
C(27)−H(27B)	0.9600
C(27)−H(27C)	0.9600
C(28)−C(29)	1.492(2)
C(30)−C(31)	1.525(3)
C(30)−C(32)	1.528(3)
C(30)−H(30A)	0.9800
C(31)−H(31A)	0.9600
C(31)−H(31B)	0.9600
C(31)−H(31C)	0.9600
C(32)−H(32A)	0.9600
C(32)−H(32B)	0.9600
C(32)−H(32C)	0.9600
C(33)−C(35)	1.520(3)
C(33)−C(34)	1.521(3)
C(33)−H(33A)	0.9800
C(34)−H(34A)	0.9600
C(34)−H(34B)	0.9600
C(34)−H(34C)	0.9600
C(35)−H(35A)	0.9600
C(35)−H(35B)	0.9600
C(35)−H(35C)	0.9600
C(36)−H(36A)	0.9700
C(36)−H(36B)	0.97
C(20)−P(1)−C(8)	106.79(7)
C(20)−P(1)−C(14)	103.43(7)
C(8)−P(1)−C(14)	105.96(8)
C(20)−P(1)−Pd(1)	108.25(5)
C(8)−P(1)−Pd(1)	112.10(5)
C(14)−P(1)−Pd(1)	119.37(6)
C(29)−O(1)−Pd(1)	128.93(10)
C(1)−Pd(1)−O(1)	172.07(6)
C(1)−Pd(1)−P(1)	92.81(5)
O(1)−Pd(1)−P(1)	93.48(3)

C(1)−Pd(1)−Cl(1)	88.16(5)
O(1)−Pd(1)−Cl(1)	85.32(3)
P(1)−Pd(1)−Cl(1)	177.002(17)
C(28)−N(1)−C(26)	108.14(13)
C(28)−N(1)−C(27)	126.79(14)
C(26)−N(1)−C(27)	123.81(14)
C(29)−N(2)−C(30)	124.84(14)
C(29)−N(2)−C(33)	119.06(14)
C(30)−N(2)−C(33)	115.90(13)
C(6)−C(1)−C(2)	119.12(18)
C(6)−C(1)−Pd(1)	121.04(15)
C(2)−C(1)−Pd(1)	119.46(15)
C(3)−C(2)−C(1)	120.9(2)
C(3)−C(2)−H(2A)	119.6
C(1)−C(2)−H(2A)	119.6
C(4)−C(3)−C(2)	119.6(2)
C(4)−C(3)−H(3A)	120.2
C(2)−C(3)−H(3A)	120.2
C(5)−C(4)−C(3)	120.3(2)
C(5)−C(4)−H(4A)	119.9
C(3)−C(4)−H(4A)	119.9
C(4)−C(5)−C(6)	121.7(2)
C(4)−C(5)−H(5A)	119.1
C(6)−C(5)−H(5A)	119.1
C(1)−C(6)−C(5)	118.3(2)
C(1)−C(6)−C(7)	122.48(19)
C(5)−C(6)−C(7)	119.1(2)
C(6)−C(7)−H(7A)	109.5
C(6)−C(7)−H(7B)	109.5
H(7A)−C(7)−H(7B)	109.5
C(6)−C(7)−H(7C)	109.5
H(7A)−C(7)−H(7C)	109.5
H(7B)−C(7)−H(7C)	109.5
C(9)−C(8)−C(13)	110.86(15)
C(9)−C(8)−P(1)	114.35(12)
C(13)−C(8)−P(1)	109.20(11)
C(9)−C(8)−H(8A)	107.4

C(13)−C(8)−H(8A)	107.4
P(1)−C(8)−H(8A)	107.4
C(8)−C(9)−C(10)	111.26(16)
C(8)−C(9)−H(9A)	109.4
C(10)−C(9)−H(9A)	109.4
C(8)−C(9)−H(9B)	109.4
C(10)−C(9)−H(9B)	109.4
H(9A)−C(9)−H(9B)	108
C(11)−C(10)−C(9)	111.86(18)
C(11)−C(10)−H(10A)	109.2
C(9)−C(10)−H(10A)	109.2
C(11)−C(10)−H(10B)	109.2
C(9)−C(10)−H(10B)	109.2
H(10A)−C(10)−H(10B)	107.9
C(12)−C(11)−C(10)	111.07(18)
C(12)−C(11)−H(11A)	109.4
C(10)−C(11)−H(11A)	109.4
C(12)−C(11)−H(11B)	109.4
C(10)−C(11)−H(11B)	109.4
H(11A)−C(11)−H(11B)	108
C(11)−C(12)−C(13)	111.28(17)
C(11)−C(12)−H(12A)	109.4
C(13)−C(12)−H(12A)	109.4
C(11)−C(12)−H(12B)	109.4
C(13)−C(12)−H(12B)	109.4
H(12A)−C(12)−H(12B)	108
C(12)−C(13)−C(8)	111.82(15)
C(12)−C(13)−H(13A)	109.3
C(8)−C(13)−H(13A)	109.3
C(12)−C(13)−H(13B)	109.3
C(8)−C(13)−H(13B)	109.3
H(13A)−C(13)−H(13B)	107.9
C(19)−C(14)−C(15)	111.25(16)
C(19)−C(14)−P(1)	109.91(13)
C(15)−C(14)−P(1)	114.41(12)
C(19)−C(14)−H(14A)	107
C(15)−C(14)−H(14A)	107

P(1)−C(14)−H(14A)	107
C(16)−C(15)−C(14)	110.42(17)
C(16)−C(15)−H(15A)	109.6
C(14)−C(15)−H(15A)	109.6
C(16)−C(15)−H(15B)	109.6
C(14)−C(15)−H(15B)	109.6
H(15A)−C(15)−H(15B)	108.1
C(17)−C(16)−C(15)	111.6(2)
C(17)−C(16)−H(16A)	109.3
C(15)−C(16)−H(16A)	109.3
C(17)−C(16)−H(16B)	109.3
C(15)−C(16)−H(16B)	109.3
H(16A)−C(16)−H(16B)	108
C(16)−C(17)−C(18)	111.3(2)
C(16)−C(17)−H(17A)	109.4
C(18)−C(17)−H(17A)	109.4
C(16)−C(17)−H(17B)	109.4
C(18)−C(17)−H(17B)	109.4
H(17A)−C(17)−H(17B)	108
C(17)−C(18)−C(19)	110.8(2)
C(17)−C(18)−H(18A)	109.5
C(19)−C(18)−H(18A)	109.5
C(17)−C(18)−H(18B)	109.5
C(19)−C(18)−H(18B)	109.5
H(18A)−C(18)−H(18B)	108.1
C(14)−C(19)−C(18)	111.3(2)
C(14)−C(19)−H(19A)	109.4
C(18)−C(19)−H(19A)	109.4
C(14)−C(19)−H(19B)	109.4
C(18)−C(19)−H(19B)	109.4
H(19A)−C(19)−H(19B)	108
C(28)−C(20)−C(21)	105.18(13)
C(28)−C(20)−P(1)	123.30(12)
C(21)−C(20)−P(1)	130.18(12)
C(22)−C(21)−C(26)	117.16(15)
C(22)−C(21)−C(20)	136.09(16)
C(26)−C(21)−C(20)	106.70(14)

C(23)−C(22)−C(21)	119.48(19)
C(23)−C(22)−H(22A)	120.3
C(21)−C(22)−H(22A)	120.3
C(22)−C(23)−C(24)	121.60(19)
C(22)−C(23)−H(23A)	119.2
C(24)−C(23)−H(23A)	119.2
C(25)−C(24)−C(23)	120.83(18)
C(25)−C(24)−H(24A)	119.6
C(23)−C(24)−H(24A)	119.6
C(24)−C(25)−C(26)	117.41(19)
C(24)−C(25)−H(25A)	121.3
C(26)−C(25)−H(25A)	121.3
N(1)−C(26)−C(25)	127.76(16)
N(1)−C(26)−C(21)	108.89(14)
C(25)−C(26)−C(21)	123.35(16)
N(1)−C(27)−H(27A)	109.5
N(1)−C(27)−H(27B)	109.5
H(27A)−C(27)−H(27B)	109.5
N(1)−C(27)−H(27C)	109.5
H(27A)−C(27)−H(27C)	109.5
H(27B)−C(27)−H(27C)	109.5
N(1)−C(28)−C(20)	110.86(14)
N(1)−C(28)−C(29)	122.87(14)
C(20)−C(28)−C(29)	126.24(14)
O(1)−C(29)−N(2)	120.20(14)
O(1)−C(29)−C(28)	117.99(14)
N(2)−C(29)−C(28)	121.80(14)
N(2)−C(30)−C(31)	111.22(16)
N(2)−C(30)−C(32)	111.69(16)
C(31)−C(30)−C(32)	110.88(17)
N(2)−C(30)−H(30A)	107.6
C(31)−C(30)−H(30A)	107.6
C(32)−C(30)−H(30A)	107.6
C(30)−C(31)−H(31A)	109.5
C(30)−C(31)−H(31B)	109.5
H(31A)−C(31)−H(31B)	109.5
C(30)−C(31)−H(31C)	109.5

H(31A)−C(31)−H(31C)	109.5
H(31B)−C(31)−H(31C)	109.5
C(30)−C(32)−H(32A)	109.5
C(30)−C(32)−H(32B)	109.5
H(32A)−C(32)−H(32B)	109.5
C(30)−C(32)−H(32C)	109.5
H(32A)−C(32)−H(32C)	109.5
H(32B)−C(32)−H(32C)	109.5
N(2)−C(33)−C(35)	111.81(15)
N(2)−C(33)−C(34)	113.06(15)
C(35)−C(33)−C(34)	112.16(18)
N(2)−C(33)−H(33A)	106.4
C(35)−C(33)−H(33A)	106.4
C(34)−C(33)−H(33A)	106.4
C(33)−C(34)−H(34A)	109.5
C(33)−C(34)−H(34B)	109.5
H(34A)−C(34)−H(34B)	109.5
C(33)−C(34)−H(34C)	109.5
H(34A)−C(34)−H(34C)	109.5
H(34B)−C(34)−H(34C)	109.5
C(33)−C(35)−H(35A)	109.5
C(33)−C(35)−H(35B)	109.5
H(35A)−C(35)−H(35B)	109.5
C(33)−C(35)−H(35C)	109.5
H(35A)−C(35)−H(35C)	109.5
H(35B)−C(35)−H(35C)	109.5
Cl(3)−C(36)−Cl(2)	115.4(2)
Cl(3)−C(36)−H(36A)	108.4
Cl(2)−C(36)−H(36A)	108.4
Cl(3)−C(36)−H(36B)	108.4
Cl(2)−C(36)−H(36B)	108.4
H(36A)−C(36)−H(36B)	107.5

Symmetry transformations used to generate equivalent atoms:

Table 2.9 Anisotropic displacement parameters ($Å^2 \times 10^3$) for **C1**

The anisotropic displacement factor exponent takes the form: $-2\pi^2[h^2a^{*2}U^{11}+...+2hka^*b^*U^{12}]$

	U^{11}	U^{22}	U^{33}	U^{23}	U^{13}	U^{12}
P(1)	25(1)	26(1)	28(1)	2(1)	3(1)	8(1)
O(1)	27(1)	33(1)	53(1)	-4(1)	4(1)	12(1)
Pd(1)	26(1)	32(1)	29(1)	1(1)	5(1)	12(1)
Cl(1)	45(1)	50(1)	49(1)	-13(1)	1(1)	27(1)
Cl(2)	133(1)	112(1)	115(1)	22(1)	62(1)	16(1)
Cl(3)	221(2)	91(1)	154(1)	31(1)	54(1)	80(1)
N(1)	33(1)	30(1)	31(1)	4(1)	0(1)	12(1)
N(2)	30(1)	27(1)	36(1)	5(1)	7(1)	11(1)
C(1)	30(1)	37(1)	46(1)	-3(1)	1(1)	15(1)
C(2)	48(1)	43(1)	49(1)	-3(1)	-5(1)	21(1)
C(3)	67(2)	60(1)	63(1)	-13(1)	-24(1)	33(1)
C(4)	40(1)	66(2)	104(2)	-21(2)	-15(1)	23(1)
C(5)	34(1)	61(1)	101(2)	-13(1)	11(1)	14(1)
C(6)	35(1)	48(1)	69(1)	-3(1)	14(1)	14(1)
C(7)	62(2)	84(2)	72(2)	11(1)	35(1)	24(1)
C(8)	32(1)	32(1)	28(1)	2(1)	4(1)	11(1)
C(9)	53(1)	39(1)	40(1)	2(1)	14(1)	21(1)
C(10)	71(1)	60(1)	41(1)	1(1)	19(1)	33(1)
C(11)	64(1)	73(2)	47(1)	18(1)	27(1)	28(1)
C(12)	60(1)	49(1)	45(1)	17(1)	18(1)	17(1)
C(13)	47(1)	34(1)	38(1)	6(1)	10(1)	10(1)
C(14)	31(1)	29(1)	43(1)	6(1)	4(1)	6(1)
C(15)	36(1)	36(1)	54(1)	3(1)	-4(1)	5(1)
C(16)	45(1)	40(1)	91(2)	6(1)	-8(1)	-3(1)
C(17)	55(2)	68(2)	117(3)	31(2)	16(2)	-14(1)
C(18)	75(2)	64(2)	83(2)	39(1)	19(2)	0(1)
C(19)	50(1)	51(1)	49(1)	18(1)	11(1)	7(1)
C(20)	28(1)	27(1)	31(1)	3(1)	4(1)	10(1)
C(21)	33(1)	29(1)	36(1)	5(1)	7(1)	13(1)
C(22)	46(1)	32(1)	53(1)	-1(1)	2(1)	16(1)
C(23)	61(1)	32(1)	73(2)	4(1)	7(1)	23(1)
C(24)	59(1)	43(1)	69(1)	17(1)	5(1)	30(1)
C(25)	45(1)	44(1)	47(1)	14(1)	3(1)	21(1)
C(26)	34(1)	32(1)	35(1)	8(1)	7(1)	14(1)

C(27)	46(1)	43(1)	36(1)	1(1)	-7(1)	12(1)
C(28)	28(1)	28(1)	29(1)	4(1)	5(1)	11(1)
C(29)	28(1)	27(1)	27(1)	0(1)	2(1)	10(1)
C(30)	32(1)	39(1)	51(1)	8(1)	16(1)	14(1)
C(31)	59(1)	63(1)	58(1)	6(1)	31(1)	16(1)
C(32)	32(1)	66(1)	68(1)	8(1)	7(1)	14(1)
C(33)	41(1)	26(1)	47(1)	8(1)	7(1)	11(1)
C(34)	81(2)	47(1)	56(1)	19(1)	-1(1)	29(1)
C(35)	76(2)	36(1)	59(1)	-6(1)	6(1)	24(1)
C(36)	136(3)	90(2)	72(2)	18(2)	20(2)	16(2)

Table 2.10 Hydrogen coordinates ($\times 10^4$) and isotropic displacement parameters ($Å^2 \times 10^3$) for **C1**

	x	y	z	U(eq)
H(2A)	9056	7276	4095	57
H(3A)	11210	7856	4865	78
H(4A)	12898	8581	4030	88
H(5A)	12463	8668	2440	81
H(7A)	9382	7999	1002	106
H(7B)	10347	7353	905	106
H(7C)	10883	8666	1044	106
H(8A)	7653	8426	4376	37
H(9A)	5383	8987	3940	51
H(9B)	6793	9846	4359	51
H(10A)	6753	9080	5794	65
H(10B)	5487	9384	5571	65
H(11A)	4972	7590	6072	70
H(11B)	4216	7524	5043	70
H(12A)	5105	6122	5054	61
H(12B)	6510	6998	5462	61
H(13A)	5121	6864	3611	48
H(13B)	6389	6564	3836	48
H(14A)	7780	10348	2898	43
H(15A)	9244	10121	4137	55
H(15B)	9971	9697	3407	55
H(16A)	9913	11894	3630	78
H(16B)	11162	11587	3932	78
H(17A)	11237	11109	2358	106
H(17B)	11256	12340	2493	106
H(18A)	9758	11315	1117	95
H(18B)	9029	11740	1843	95
H(19A)	7799	9863	1308	62
H(19B)	9032	9525	1583	62
H(22A)	6190	10762	2657	53
H(23A)	5153	11835	1910	65
H(24A)	3562	11097	572	65
H(25A)	2879	9221	2	53
H(27A)	2101	6970	12	66
H(27B)	3070	6326	-69	66

H(27C)	3238	7400	-581	66
H(30A)	2413	6435	1689	47
H(31A)	2835	6033	3244	89
H(31B)	1958	4771	2934	89
H(31C)	1318	5692	2914	89
H(32A)	1306	4902	456	84
H(32B)	382	5152	1113	84
H(32C)	858	4144	1255	84
H(33A)	2613	3853	1761	46
H(34A)	4317	4598	3089	91
H(34B)	5321	4540	2423	91
H(34C)	4241	3437	2606	91
H(35A)	3187	3957	220	85
H(35B)	3485	3011	741	85
H(35C)	4629	4133	684	85
H(36A)	8249	4999	3232	126
H(36B)	9486	4931	3869	126

Table 2.11 Torsion angles [°] for **C1**

C(29)−O(1)−Pd(1)−C(1)	137.1(4)
C(29)−O(1)−Pd(1)−P(1)	-5.40(15)
C(29)−O(1)−Pd(1)−Cl(1)	171.84(15)
C(20)−P(1)−Pd(1)−C(1)	162.47(8)
C(8)−P(1)−Pd(1)−C(1)	-80.01(8)
C(14)−P(1)−Pd(1)−C(1)	44.68(9)
C(20)−P(1)−Pd(1)−O(1)	-22.36(7)
C(8)−P(1)−Pd(1)−O(1)	95.17(7)
C(14)−P(1)−Pd(1)−O(1)	-140.14(8)
C(20)−P(1)−Pd(1)−Cl(1)	-88.7(3)
C(8)−P(1)−Pd(1)−Cl(1)	28.8(3)
C(14)−P(1)−Pd(1)−Cl(1)	153.5(3)
O(1)−Pd(1)−C(1)−C(6)	105.8(5)
P(1)−Pd(1)−C(1)−C(6)	-111.65(15)
Cl(1)−Pd(1)−C(1)−C(6)	71.19(15)
O(1)−Pd(1)−C(1)−C(2)	-67.1(5)
P(1)−Pd(1)−C(1)−C(2)	75.40(14)
Cl(1)−Pd(1)−C(1)−C(2)	-101.76(14)
C(6)−C(1)−C(2)−C(3)	1.2(3)
Pd(1)−C(1)−C(2)−C(3)	174.24(16)
C(1)−C(2)−C(3)−C(4)	1.0(3)
C(2)−C(3)−C(4)−C(5)	-1.5(4)
C(3)−C(4)−C(5)−C(6)	-0.2(4)
C(2)−C(1)−C(6)−C(5)	-2.7(3)
Pd(1)−C(1)−C(6)−C(5)	-175.68(16)
C(2)−C(1)−C(6)−C(7)	175.3(2)
Pd(1)−C(1)−C(6)−C(7)	2.4(3)
C(4)−C(5)−C(6)−C(1)	2.3(4)
C(4)−C(5)−C(6)−C(7)	-175.8(2)
C(20)−P(1)−C(8)−C(9)	-49.83(14)
C(14)−P(1)−C(8)−C(9)	59.96(14)
Pd(1)−P(1)−C(8)−C(9)	-168.22(11)
C(20)−P(1)−C(8)−C(13)	75.03(13)
C(14)−P(1)−C(8)−C(13)	-175.18(12)
Pd(1)−P(1)−C(8)−C(13)	-43.37(13)
C(13)−C(8)−C(9)−C(10)	53.8(2)

P(1)−C(8)−C(9)−C(10)	177.81(14)
C(8)−C(9)−C(10)−C(11)	-54.9(2)
C(9)−C(10)−C(11)−C(12)	55.7(3)
C(10)−C(11)−C(12)−C(13)	-55.7(3)
C(11)−C(12)−C(13)−C(8)	55.6(2)
C(9)−C(8)−C(13)−C(12)	-54.5(2)
P(1)−C(8)−C(13)−C(12)	178.63(14)
C(20)−P(1)−C(14)−C(19)	-69.54(15)
C(8)−P(1)−C(14)−C(19)	178.30(13)
Pd(1)−P(1)−C(14)−C(19)	50.71(15)
C(20)−P(1)−C(14)−C(15)	164.47(14)
C(8)−P(1)−C(14)−C(15)	52.31(16)
Pd(1)−P(1)−C(14)−C(15)	-75.28(15)
C(19)−C(14)−C(15)−C(16)	55.0(2)
P(1)−C(14)−C(15)−C(16)	-179.74(17)
C(14)−C(15)−C(16)−C(17)	-56.5(3)
C(15)−C(16)−C(17)−C(18)	57.3(3)
C(16)−C(17)−C(18)−C(19)	-56.1(4)
C(15)−C(14)−C(19)−C(18)	-54.7(3)
P(1)−C(14)−C(19)−C(18)	177.53(18)
C(17)−C(18)−C(19)−C(14)	54.8(3)
C(8)−P(1)−C(20)−C(28)	-101.01(14)
C(14)−P(1)−C(20)−C(28)	147.44(14)
Pd(1)−P(1)−C(20)−C(28)	19.87(15)
C(8)−P(1)−C(20)−C(21)	94.26(16)
C(14)−P(1)−C(20)−C(21)	-17.29(17)
Pd(1)−P(1)−C(20)−C(21)	-144.85(14)
C(28)−C(20)−C(21)−C(22)	172.4(2)
P(1)−C(20)−C(21)−C(22)	-20.7(3)
C(28)−C(20)−C(21)−C(26)	-4.80(18)
P(1)−C(20)−C(21)−C(26)	162.01(13)
C(26)−C(21)−C(22)−C(23)	-3.3(3)
C(20)−C(21)−C(22)−C(23)	179.7(2)
C(21)−C(22)−C(23)−C(24)	-0.3(3)
C(22)−C(23)−C(24)−C(25)	2.4(4)
C(23)−C(24)−C(25)−C(26)	-0.8(3)
C(28)−N(1)−C(26)−C(25)	179.72(18)

C(27)−N(1)−C(26)−C(25)	11.8(3)
C(28)−N(1)−C(26)−C(21)	-1.08(19)
C(27)−N(1)−C(26)−C(21)	-169.03(16)
C(24)−C(25)−C(26)−N(1)	176.05(19)
C(24)−C(25)−C(26)−C(21)	-3.0(3)
C(22)−C(21)−C(26)−N(1)	-174.17(16)
C(20)−C(21)−C(26)−N(1)	3.68(19)
C(22)−C(21)−C(26)−C(25)	5.1(3)
C(20)−C(21)−C(26)−C(25)	-177.08(17)
C(26)−N(1)−C(28)−C(20)	-2.15(19)
C(27)−N(1)−C(28)−C(20)	165.34(16)
C(26)−N(1)−C(28)−C(29)	176.03(14)
C(27)−N(1)−C(28)−C(29)	-16.5(3)
C(21)−C(20)−C(28)−N(1)	4.31(18)
P(1)−C(20)−C(28)−N(1)	-163.65(12)
C(21)−C(20)−C(28)−C(29)	-173.78(15)
P(1)−C(20)−C(28)−C(29)	18.3(2)
Pd(1)−O(1)−C(29)−N(2)	-135.66(13)
Pd(1)−O(1)−C(29)−C(28)	43.2(2)
C(30)−N(2)−C(29)−O(1)	173.76(15)
C(33)−N(2)−C(29)−O(1)	-0.9(2)
C(30)−N(2)−C(29)−C(28)	-5.0(2)
C(33)−N(2)−C(29)−C(28)	-179.70(14)
N(1)−C(28)−C(29)−O(1)	126.73(17)
C(20)−C(28)−C(29)−O(1)	-55.4(2)
N(1)−C(28)−C(29)−N(2)	-54.4(2)
C(20)−C(28)−C(29)−N(2)	123.43(18)
C(29)−N(2)−C(30)−C(31)	-108.07(19)
C(33)−N(2)−C(30)−C(31)	66.7(2)
C(29)−N(2)−C(30)−C(32)	127.47(18)
C(33)−N(2)−C(30)−C(32)	-57.7(2)
C(29)−N(2)−C(33)−C(35)	-64.3(2)
C(30)−N(2)−C(33)−C(35)	120.59(18)
C(29)−N(2)−C(33)−C(34)	63.5(2)
C(30)−N(2)−C(33)−C(34)	-111.68(19)

Symmetry transformations used to generate equivalent atoms:

Table 2.12 Hydrogen bonds for **C1** [Å] and [°]

D−H···A	d(D−H)	d(H···A)	d(D···A)	∠(DHA)
C(27)−H(27B)···Cl(1)#1	0.96	2.74	3.4154(19)	127.8
C(30)−H(30A)···N(1)	0.98	2.42	3.155(2)	131.8
C(32)−H(32B)···Cl(1)#2	0.96	2.82	3.747(2)	162.9
C(34)−H(34B)···O(1)	0.96	2.41	2.919(3)	112.8
C(35)−H(35A)···Cl(1)#1	0.96	2.98	3.932(3)	170.4
C(35)−H(35C)···O(1)	0.96	2.43	2.927(3)	112.2
C(36)−H(36A)··· Cl(1)	0.97	2.52	3.395(4)	150.1

Symmetry transformations used to generate equivalent atoms:

#1 -x+1,-y+1,-z #2 x-1,y,z

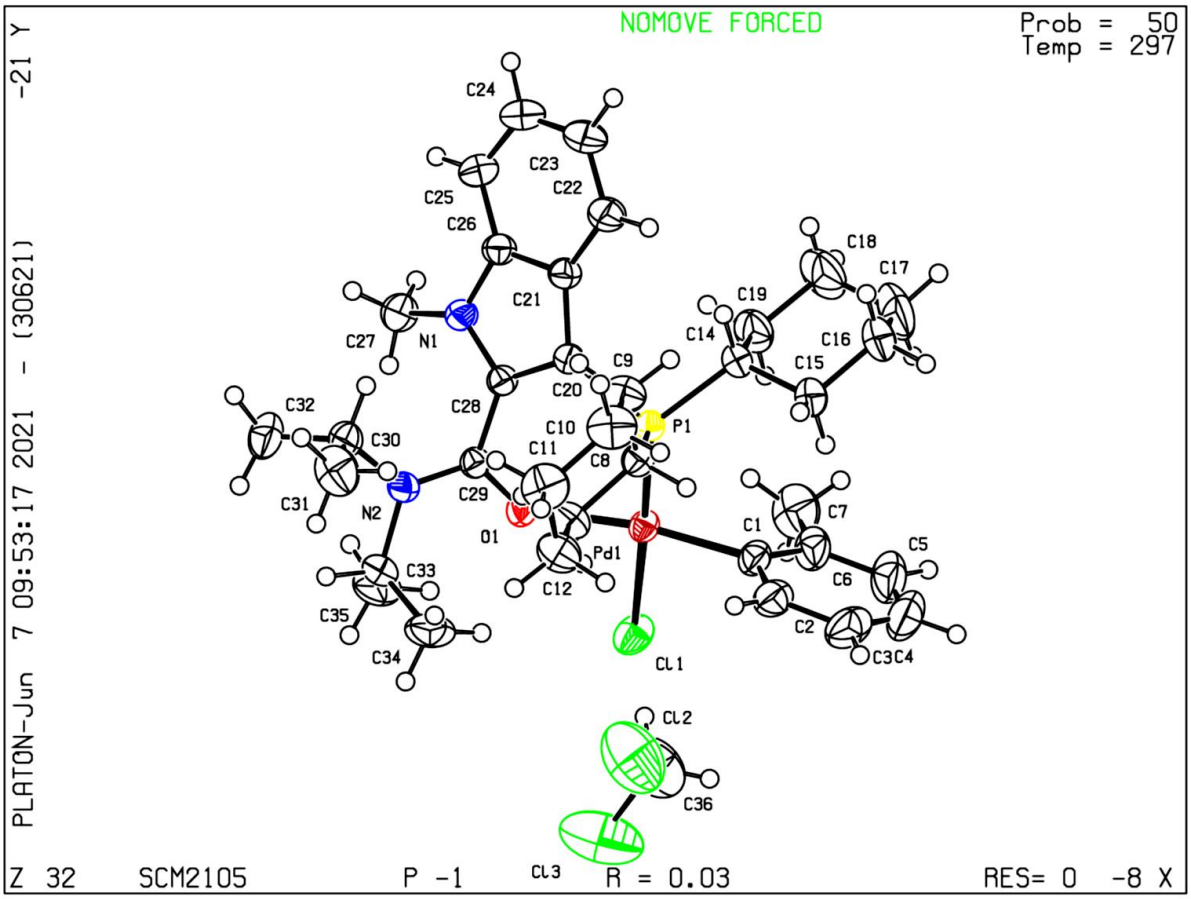

2.5 References

1. Lee, H.; Kim, B.; Kim, S.; Kim, J.; Lee, J.; Shin, H.; Lee, J.-H.; Park, J. Synthesis and Electroluminescence Properties of Highly Efficient Dual Core Chromophores with Side Groups for Blue Emission. *J. Mater. Chem. C* **2014**, *2*, 4737−4747.

2. Zani, L.; Dessì, A.; Franchi, D.; Calamante, M.; Reginato, G.; Mordini, A. Transition Metal-Catalyzed Cross-Coupling Methodologies for the Engineering of Small Molecules with Applications in Organic Electronics and Photovoltaics. *Coord. Chem. Rev.* **2019**, *392*, 177−236.

3. Taheri Kal Koshvandi, A.; Heravi, M. M.; Momeni, T. Current Applications of Suzuki−Miyaura Coupling Reaction in the Total Synthesis of Natural Products: An Update. *Appl. Organomet. Chem.* **2018**, *32*, e4210.

4. Rayadurgam, J.; Sana, S.; Sasikumar, M.; Gu, Q. Palladium Catalyzed C−C and C−N Bond Forming Reactions: An Update on the Synthesis of Pharmaceuticals from 2015−2020. *Org. Chem. Front.* **2021**, *8*, 384−414.

5. Hallock, Y. F.; Manfredi, K. P.; Blunt, J. W.; Cardellina II, J. H.; Schäffer, M.; Gulden, K.-P.; Bringmann, G.; Lee, A. Y.; Clardy, J.; François, G.; Boyd, M. R. Korupensamines AD, Novel Antimalarial Alkaloids from Ancistrocladus Korupensis. *J. Org. Chem.* **1994**, *59*, 6349−6355.

6. Rao, A. V. R.; Gurjar, M. K.; Reddy, K. L.; Rao, A. S. Studies Directed toward the Synthesis of Vancomycin and Related Cyclic Peptides. *Chem. Rev.* **1995**, *95*, 2135−2167.

7. Bringmann, G.; Pokorny, F. The Naphthylisoquinoline Alkaloids. In *The Alkaloids*; Cordell, G. A., Ed.; Vol. 46; Academic Press, 1995; pp 127−271.

8. Nicolaou, K. C.; Boddy, C. N. C.; Bräse, S.; Winssinger, N. Chemistry, Biology, and Medicine of the Glycopeptide Antibiotics. *Angew. Chem. Int. Ed.* **1999**, *38*, 2096−2152.

9. Nicolaou, K. C.; Bulger, P. G.; Sarlah, D. Palladium-Catalyzed Cross-Coupling Reactions in Total Synthesis. *Angew. Chem. Int. Ed.* **2005**, *44*, 4442−4489.

10. Kozlowski, M. C.; Morgan, B. J.; Linton, E. C. Total Synthesis of Chiral Biaryl Natural Products by Asymmetric Biaryl Coupling. *Chem. Soc. Rev.* **2009**, *38*, 3193−3207.

11. Buter, J.; Heijnen, D.; Vila, C.; Hornillos, V.; Otten, E.; Giannerini, M.; Minnaard, A. J.; Feringa, B. L. Palladium-Catalyzed, *tert*-Butyllithium-Mediated Dimerization of Aryl Halides and Its

Application in the Atropselective Total Synthesis of Mastigophorene A. *Angew. Chem. Int. Ed.* **2016**, *55*, 3620−3624.

12. Roy, D.; Uozumi, Y. Recent Advances in Palladium-Catalyzed Cross-Coupling Reactions at Ppm to Ppb Molar Catalyst Loadings. *Adv. Synth. Catal.* **2018**, *360*, 602−625.

13. Zapf, A.; Ehrentraut, A.; Beller, M. A New Highly Efficient Catalyst system for the Coupling of Nonactivated and Deactivated Aryl Chlorides with Arylboronic Acids. *Angew. Chem. Int. Ed.* **2000**, *39*, 4153−4155.

14. Lemo, J.; Heuzé, K.; Astruc, D. Efficient and Recyclable Dendritic Buchwald-Type Catalyst for the Suzuki Reaction. *Chem. Commun.* **2007**, 4351−4353.

15. Yokoyama, N.; Nakayama, Y.; Nara, H.; Sayo, N. Synthesis of Well - Defined Diphenylvinyl(cyclopropyl)phosphine - Palladium Complexes for the Suzuki−Miyaura Reaction and Buchwald−Hartwig Amination. *Adv. Synth. Catal.* **2013**, *355*, 2083−2088.

16. Wong, S. M.; So, C. M.; Chung, K. H.; Lau, C. P.; Kwong, F. Y. An Efficient Class of P, N-Type “PhMezole-phos” Ligands: Applications in Palladium-Catalyzed Suzuki Coupling of Aryl Chlorides. *Eur. J. Org. Chem.* **2012**, 4172−4177.

17. Choy, P. Y.; Yuen, O. Y.; Leung, M. P.; Chow, W. K.; Kwong, F. Y. A Highly Efficient Monophosphine Ligand for Parts per Million Levels Pd-Catalyzed Suzuki−Miyaura Coupling of (Hetero) Aryl Chlorides. *Eur. J. Org. Chem.* **2020**, 2846−2853.

18. Littke, A. F.; Dai, C.; Fu, G. C. Versatile Catalysts for the Suzuki Cross-Coupling of Arylboronic Acids with Aryl and Vinyl Halides and Triflates under Mild Conditions. *J. Am. Chem. Soc.* **2000**, *122*, 4020−4028.

19. Altenhoff, G.; Goddard, R.; Lehmann, C. W.; Glorius, F. An N-Heterocyclic Carbene Ligand with Flexible Steric Bulk Allows Suzuki Cross-Coupling of Sterically Hindered Aryl Chlorides at Room Temperature. *Angew. Chem. Int. Ed.* **2003**, *42*, 3690−3693.

20. Walker, S. D.; Barder, T. E.; Martinelli, J. R.; Buchwald, S. L. A Rationally Designed Universal Catalyst for Suzuki−Miyaura Coupling Processes. *Angew. Chem. Int. Ed.* **2004**, *43*, 1871−1876.

21. Baillie, C.; Zhang, L.; Xiao, J. Ferrocenyl Monophosphine Ligands: Synthesis and Applications in the Suzuki−Miyaura Coupling of Aryl Chlorides. *J. Org. Chem.* **2004**, *69*, 7779−7782.

22. Ackermann, L.; Potukuchi, H. K.; Althammer, A.; Born, R. Mayer, P. Tetra-*ortho*-Substituted Biaryls through Palladium-Catalyzed Suzuki−Miyaura Couplings with a Diaminochlorophosphine Ligand. *Org. Lett.* **2010**, *12*, 1004−1007.

23. Rendón-Nava, D.; Álvarez-Hernández, A.; Rheingold, A. L.; Suárez-Castillo, O. R.; Mendoza-Espinosa, D. Hydroxyl-Functionalized Triazolylidene-Based PEPPSI Complexes: Metallacycle Formation Effect on the Suzuki Coupling Reaction. *Dalton Trans.* **2019**, *48*, 3214−3222.

24. Rendón-Nava, D.; Angeles-Beltrán, D.; Rheingold, A. L.; Mendoza-Espinosa, D. Palladium(II) Complexes of a Neutral CCC-Tris(N-Heterocyclic Carbene) Pincer Ligand: Synthesis and Catalytic Applications. *Organometallics*, **2021**, *40*, 2166−2177.

25. Hoshi, T.; Honma, T.; Mori, A.; Konishi, M.; Sato, T.; Hagiwara, H.; Suzuki, T. An Active, General, and Long-Lived Palladium Catalyst for Cross-Couplings of Deactivated (Hetero)aryl Chlorides and Bromides with Arylboronic Acids. *J. Org. Chem.* **2013**, *78*, 11513−11524.

26. Tannert, R.; Pfaltz, A. Mixed Donor Ligands. In *Phosphorus(III) Ligands in Homogeneous Catalysis: Design and Synthesis*; Kamer, P. C. J., van Leeuwen, P. W. N. M., Eds.; John Wiley & Sons, 2012; pp 233−265.

27. Braunstein, P.; Naud, F. Hemilability of Hybrid Ligands and the Coordination Chemistry of Oxazoline-Based Systems. *Angew. Chem. Int. Ed.* **2001**, *40*, 680−699.

28. Kwong, F. Y.; Chan, A. S. C. Recent Developments on Hemilabile P,O-Type Ligands in Cross-Coupling Reactions. *Synlett* **2008**, 1440−1448.

29. Philipova, I.; Stavrakov, G.; Dimitrov, V. Camphane-Based Phosphino-Carboxamide Ligands as P,O-Chelates in Pd-Catalyzed Enantioselective Allylic Alkylation. *Tetrahedron Asymmetry* **2012**, *23*, 927−930.

30. Huang, D.; Liu, X.; Li, L.; Cai, Y.; Liu, W.; Shi, Y. Enantioselective Bromoaminocyclization of Allyl *N*-Tosylcarbamates Catalyzed by a Chiral Phosphine−$Sc(OTf)_3$ Complex. *J. Am. Chem. Soc.* **2013**, *135*, 8101−8104.

31. Philipova, I.; Stavrakov, G.; Vassilev, N.; Nikolova, R.; Shivachev, B.; Dimitrov, V. Cytisine as a Scaffold for *ortho*-Diphenylphosphinobenzenecarboxamide Ligands for Pd-Catalyzed Asymmetric Allylic Alkylation. *J. Organomet. Chem.* **2015**, *778*, 10−20.

32. Snieckus, V. Directed *Ortho* Metalation. Tertiary Amide and *O*-Carbamate Directors in Synthetic Strategies for Polysubstituted Aromatics. *Chem. Rev.* **1990**, *90*, 879−933.

33. Bai, X.-F.; Song, T.; Xu, Z.; Xia, C.-G.; Huang, W.-S.; Xu, L.-W. Aromatic Amide-Derived Non-Biaryl Atropisomers as Highly Efficient Ligands in Silver-Catalyzed Asymmetric Cycloaddition Reactions. *Angew. Chem. Int. Ed.* **2015**, *54*, 5255−5259.

34. Bai, X.-F.; Zhang, J.; Xia, C.-G.; Xu, J.-X.; Xu, L.-W. *N-tert*-Butanesulfinyl Imine and Aromatic Tertiary Amide Derived Non-Biaryl Atropisomers as Chiral Ligands for Silver-Catalyzed *endo*-Selective [3+2] Cycloaddition of Azomethine Ylides with Maleimides. *Tetrahedron* **2016**, *72*, 2690−2699.

35. Dai, W.-M.; Li, Y.; Zhang, Y.; Lai, K. W.; Wu, J. A Novel Class of Amide-Derived Air-Stable P,O-Ligands for Suzuki Cross-Coupling at Low Catalyst Loading. *Tetrahedron Lett.* **2004**, *45*, 1999−2001

36. Dai, W.-M.; Zhang, Y. A Family of Simple Amide-Derived Air-Stable P,O-Ligands for Suzuki Cross-Coupling of Unactivated Aryl Chlorides. *Tetrahedron Lett.* **2005**, *46*, 1377−1381.

37. Kwong, F. Y.; Lam, W. H.; Yeung, C. H.; Chan, K. S.; Chan, A. S. C. A Simple and Highly Efficient P,O-Type Ligand for Suzuki−Miyaura Cross-Coupling of Aryl Halides. *Chem. Commun.* **2004**, 1922−1923.

38. Chen, G.; Lam, W. H.; Fok, W. S.; Lee, H. W.; Kwong, F. Y. Easily Accessible Benzamide-Derived P,O Ligands (Bphos) for Palladium-Catalyzed Carbon−Nitrogen Bond-Forming Reactions. *Chem. Asian. J.* **2007**, *2*, 306−313.

39. So, C. M.; Yeung, C. C.; Lau, C. P.; Kwong, F. Y. A New Family of Tunable Indolylphosphine Ligands by One-Pot Assembly and Their Applications in Suzuki−Miyaura Coupling of Aryl Chlorides. *J. Org. Chem.* **2008**, *73*, 7803−7806.

40. Wong, S. M.; Choy, P. Y.; Zhao, Q.; Yuen, O. Y.; Yeung, C. C.; So, C. M.; Kwong, F. Y. Design of Benzimidazolyl Phosphines Bearing Alterable *P*,*O* or *P*,*N*-Coordination: Synthesis, Characterization, and Insights into Their Reactivity. *Organometallics* **2021**, *40*, 2265−2271.

41. Lee, H. W.; Lam, F. L.; So, C. M.; Lau, C. P.; Chan, A. S. C.; Kwong, F. Y. Palladium-Catalyzed Cross-Coupling of Aryl Halides Using Organotitanium Nucleophiles. *Angew. Chem. Int. Ed.* **2009**, *48*, 7436−7439.

42. Yeung, P. Y.; Tsang, C. P.; Kwong, F. Y. Efficient Cyanation of Aryl Bromides with $K_4[Fe(CN)_6]$ Catalyzed by a Palladium-Indolylphosphine Complex. *Tetrahedron Lett.* **2011**, *52*, 7038−7041.

43. Chow, W. K.; Yuen, O. Y.; So, C. M.; Wong, W. T.; Kwong, F. Y. Carbon−Boron Bond Cross-Coupling Reaction Catalyzed by $-PPh_2$ Containing Palladium−Indolylphosphine Complexes. *J. Org. Chem.* **2012**, *77*, 3543−3548.

44. Yuen, O. Y.; Wong, S. M.; Chan, K. F.; So, C. M.; Kwong, F. Y. A General Suzuki−Miyaura Coupling of Aryl Chlorides with Potassium Aryltrifluoroborates in Water Catalyzed by an Efficient CPCy Phendole-phos-Palladium Complex. *Synthesis* **2014**, *46*, 2826−2832.

45. Yuen, O. Y.; Charoensak, M.; So, C. M.; Kuhakarn, C.; Kwong, F. Y. A General Direct Arylation of Polyfluoroarenes with Heteroaryl and Aryl Chlorides Catalyzed by Palladium Indolylphosphine Complexes. *Chem. Asian. J.* **2015**, *10*, 857−861.

46. Fu, W. C.; So, C. M.; Chow, W. K.; Yuen O. Y.; Kwong, F. Y. Design of an Indolylphosphine Ligand for Reductive Elimination-Demanding Monoarylation of Acetone Using Aryl Chlorides. *Org. Lett.*, **2015**, *17*, 4612−4615.

47. Yuen, O. Y.; So, C. M.; Man, H. W.; Kwong, F. Y. A General Palladium-Catalyzed Hiyama Cross-Coupling Reaction of Aryl and Heteroaryl Chlorides. *Chem. Eur. J.*, **2016**, *22*, 6471−6476.

48. Yuen, O. Y.; So, C. M. Ligand Control of Palladium-Catalyzed Site-Selective α-and γ-Arylation of α, β-Unsaturated Ketones with (Hetero)aryl Halides. *Angew. Chem. Int. Ed.* **2020** *59*, 23438−23444.

49. So, C. M.; Yuen, O. Y.; Ng, S. S.; Chen, Z. General Chemoselective Suzuki−Miyaura Coupling of Polyhalogenated Aryl Triflates Enabled by an Alkyl-Heteroaryl-Based Phosphine Ligand. *ACS Catal.* **2021**, *11*, 7820−7827.

50. The supplementary crystallographic data for this chapter is available in the CCDC 2123309 entry. This data can be accessed and downloaded free of charge from the website of The Cambridge Crystallographic Data Centre.

51. Armarego, W. L. F.; Perrin, D. D. *Purification of Laboratory Chemicals*, 4th ed.; Butterworth-Heinemann, 1996.

52. Valentina, D.; Maurizio, F.; Angelo, A. Metal-Free Synthesis of Sterically Crowded Biphenyls by Direct Ar−H Substitution in Alkyl Benzenes. *Angew. Chem. Int. Ed.* **2007**, *46*, 6495−6498.

53. Ben-Daniel, R.; de Visser, S. P.; Shaik, S.; Neumann, R. Electrophilic Aromatic Chlorination and Haloperoxidation of Chloride Catalyzed by Polyfluorinated Alcohols: A New Manifestation of Template Catalysis. *J. Am. Chem. Soc.* **2003**, *125*, 12116−12117.

54. Yuen, O. Y.; Leung, M. P.; So, C. M.; Sun, R. W.-Y.; Kwong, F. Y. Palladium-Catalyzed Direct Arylation of Polyfluoroarenes for Accessing Tetra-*ortho*-Substituted Biaryls: Buchwald−type Ligand Having Complementary $-PPh_2$ Moiety Exhibits Better Efficiency. *J. Org. Chem.* **2018**, *83*, 9008−9017.

55. Weiss, M.; Boezio, A.; Boezio, C.; Butler, J. R.; Chu-Moyer, M. Y.; Dimauro, E. F.; Dineen, T.; Graceffa, R.; Guzman-Perez, A.; Huang, H.; Kreiman, C.; La, D.; Marx, I. E.; Milgrim, B. C.; Nguyen, H. N.; Peterson, E.; Romero, K.; Sparling, B. Bicyclic Sulfonamide Compounds as Sodium Channel Inhibitors. PCT Int. Appl., WO 2014201206, December 18, 2014.

56. Kelley, J. L.; Linn, J. A.; Selway, J. W. T. Synthesis and Antirhinovirus Activity of 6-(Dimethylamino)-2-(Trifluoromethyl)-9-(Substituted Benzyl)-9H-Purines. *J. Med. Chem.*, **1989**, *32*, 1757−1763.

57. Alamsetti, S. K.; Persson, A. K. Å.; Jiang T.; Bäckvall, J. -E. Scalable Synthesis of Oxazolones from Propargylic Alcohols through Multistep Palladium(II) Catalysis: β-Selective Oxidative Heck Coupling of Cyclic Sulfonyl Enamides and Aryl Boroxines. *Angew. Chem. Int. Ed.* **2013**, *52*, 13745−13750.

58. Ghinato, S.; Dilauro, G.; Perna, F. M.; Capriati, V.; Blangetti M.; Prandi, C. Directed *ortho*-Metalation−Nucleophilic Acyl Substitution Strategies in Deep Eutectic Solvents: the Organolithium Base Dictates the Chemoselectivity. *Chem. Commun.* **2019**, *55*, 7741−7744.

59. Ong, D. Y.; Yen, Z.; Yoshii, A.; Revillo Imbernon, J.; Takita, R.; Chiba, S. Controlled Reduction of Carboxamides to Alcohols or Amines by Zinc Hydrides. *Angew. Chem. Int. Ed.* **2019**, *58*, 4992−4997.

60. Baba, H.; Moriyama, K.; Togo, H. Preparation of *N*,*N*-Dimethyl Aromatic Amides from Aromatic Aldehydes with Dimethylamine and Iodine Reagents. *Synlett* **2012**, *23*, 1175−1180.

61. Mistry, S. N.; Shonberg, J.; Draper-Joyce, C. J.; Herenbrink, C. K.; Michino, M.; Shi, L.; Christopoulos, A.; Capuano, B.; Scammells, P. J.; Lane, J. R. Discovery of a Novel Class of Negative Allosteric Modulator of the Dopamine D_2 Receptor Through Fragmentation of a Bitopic Ligand. *J. Med. Chem.* **2015**, *58*, 6819−6843.

62. Ouyang, J. S.; Li, Y. F.; Huang, F. D.; Lu, D. D.; Liu, F. S. The Highly Efficient Suzuki−Miyaura Cross-Coupling of (Hetero)aryl Chlorides and (Hetero)arylboronic Acids Catalyzed by “Bulky-yet-Flexible” Palladium−PEPPSI Complexes in Air. *ChemCatChem* **2018**, *10*, 371−375.

63. Zhang, Y.; Zhang, R.; Ni, C.; Zhang, X.; Li, Y.; Lu, Q.; Zhao, Y.; Han, F.; Zeng, Y.; Liu, G. NHC-Pd(II)-Azole Complexes Catalyzed Suzuki−Miyaura Cross-Coupling of Sterically Hindered Aryl Chlorides with Arylboronic Acids. *Tetrahedron Lett.* **2020**, *61*, 151541.

64. Schmid, T. E.; Jones, D. C.; Songis, O.; Diebolt, O.; Frust, M. R. L.; Slawin, A. M. Z.; Cazin, C. S. J. Mixed Phosphine/N-Heterocyclic Carbene Palladium Complexes: Synthesis, Characterization and Catalytic Use in Aqueous Suzuki−Miyaura Reactions. *Dalton Trans.* **2013**, *42*, 7345−7353.

65. Tang, W.; Capacci, A. G.; Wei, X.; Li, W.; White, A.; Patel, N. D.; Krishnamurthy, D.; Yee, N. K.; Senanayake, C. H. A General and Special Catalyst for Suzuki−Miyaura Coupling Processes. *Angew. Chem. Int. Ed.* **2010**, *49*, 5879−5883.

66. Liu, Y.; Peng, H.; Yuan, J.; Yan, M.-Q.; Luo, X.; Wu, Q.-G.; Liu, S.-H.; Chen, J.; Yu, G.-A. An Efficient Indenyl-Derived Phosphine Ligand for the Suzuki−Miyaura Coupling of Sterically Hindered Aryl Halides. *Org. Biomol. Chem.* **2016**, *14*, 4664−4668.

67. Yun, B.-S.; Kim, J.-H.; Kim, S.-Y.; Son, H.-J.; Cho, D. W.; Kang, S. O. Photophysical Properties of Structural Isomers of Homoleptic Ir-Complexes Derived from Xylenyl-Substituted *N*-Heterocyclic Carbene Ligands. *Phys. Chem. Chem. Phys.* **2019**, *21*, 7155−7164.

68. To, S. C.; Kwong, F. Y. Highly Efficient Carbazolyl-Derived Phosphine Ligands: Application to Sterically Hindered Biaryl Couplings. *Chem Commun.* **2011**, *47*, 5079−5081.

69. Yu, S.-B.; Hu, X.-P.; Deng, J.; Huang, J.-D.; Wang, D.-Y.; Duan, Z.-C.; Zheng, Z. Ferrocence-Based Phosphine−Triazine Ligands for Highly Efficient Suzuki−Miyaura Cross-Coupling Reaction of Aryl Chlorides. *Tetrahedron Lett.* **2008**, *49*, 1253−1256.

70. Yadav, M. R.; Nagaoka, M.; Kashihara, M.; Zhong, R.-L.; Miyazaki, T.; Sakaki, S.; Nakao, Y. The Suzuki−Miyaura Coupling of Nitroarenes. *J. Am. Chem. Soc.* **2017**, *139*, 9423−9426.

71. Wei, W.-T.; Cheng, Y.-J.; Hu, Y.; Chen, Y.-Y.; Zhang, X.-J.; Zou, Y.; Yan, M. Concise Synthesis of 4-Arylquinolines via Intramolecular Cyclization of Allylamines and Ketones. *Adv. Synth. Catal.* **2015**, *357*, 3474−3478.

72. Kwong, F. Y.; Choy, P. Y.; Wu, Y.; Yang, Q. Synthesis of Phosphine Ligands Bearing Tunable Linkage: Methods of Their Use in Catalysis. PCT Int. Appl., WO 2017193288, November 16, 2017.

73. Beinhoff, M.; Weigel, W.; Jurczok, M.; Rettig, W.; Modrakowski, C.; Brüdgam, I.; Hans, H.; Schlüter, A. D. Synthesis and Spectroscopic Properties of Arene-Substituted Pyrene Derivatives as Model Compounds for Fluorescent Polarity Probes. *Eur. J. Org. Chem.* **2001**, 3819−3829.

74. Han, B.; Ma, P.; Cong, X.; Chen, H.; Zeng, X. Chromium- and Cobalt-Catalyzed, Regiocontrolled Hydrogenation of Polycyclic Aromatic Hydrocarbons: A Combined Experimental and Theoretical Study. *J. Am. Chem. Soc.* **2019**, *141*, 9018−9026.

75. Fu, Y. H.; Hu, J. Y.; Kido, J.; Takeda, T. Substituted Aromatic Compound, Blue Light-Emitting Material, and Organic EL Element. Jpn. Kokai Tokkyo Koho, JP 2014122212, July 3, 2014.

76. Lu, D.-D.; He, X.-X. Liu, F.-S. Bulky Yet Flexible Pd-PEPPSI-IPentAn for the Synthesis of Sterically Hindered Biaryls in Air. *J. Org. Chem.* **2017**, *82*, 10898−10911.

77. Tu, T.; Sun, Z.; Fang, W.; Xu, M.; Zhou, Y. Robust Acenaphthoimidazolylidene Palladium Complexes: Highly Efficient Catalysts for Suzuki−Miyaura Couplings with Sterically Hindered Substrates. *Org. Lett.* **2012**, *14*, 4250−4253.

3. Chapter 3: Palladium-Catalysed Chemoselective Borylation of Polyhalogenated Triflates and Their Application in Consecutive Reactions

3.1 Introduction

Arylboronates have emerged as widely utilised synthons for the synthesis of pharmaceuticals, agrochemicals, and functional materials.[1–2] Driven by the high demand for this class of attractive compounds due to their reactivity, stability, and cost-effectiveness, a diverse array of methods has been rapidly developed in recent decades.[3–12] Since the pioneering work of Miyaura on the Pd-catalysed borylation reaction,[13] this approach has become a practical means of employing a variety of electrophiles to prepare arylboronates, with a high tolerance for functional groups. Persistent efforts to advance novel ligand designs and further synthetic strategies have expanded the substrate compatibility and the scope of electrophiles for the Pd-catalysed borylation reaction (Scheme 3.1).[14–20]

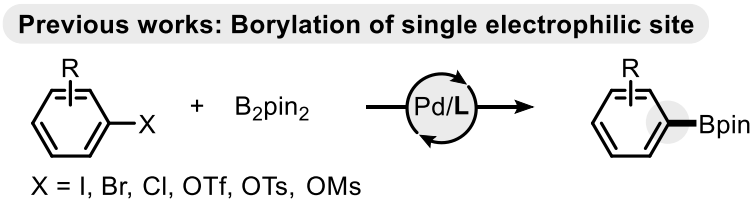

Scheme 3.1 Prior research: Borylation focused on a single electrophilic site

The borylation of arenes featuring multiple electrophilic sites would be a strategically attractive synthetic approach, enabling the targeted electrophile to be selectively converted into a nucleophile and producing a multifunctional synthon with both electrophilic and nucleophilic moieties (Scheme 3.2).

Despite the potential of such an approach, several issues have persisted in achieving a chemoselective borylation reaction. First, it remains challenging to control the borylation process to selectively react at the desired electrophilic site, aligning with the actual synthetic needs. Second, the predominant formation of diborylated products often fails to yield a pure product that activates solely on one side of the aryl (pseudo)halide. Third, the simultaneous presence of electrophilic and nucleophilic sites within the compound may lead to undesired self-coupling reactions of the product.[21] (Scheme 3.2)

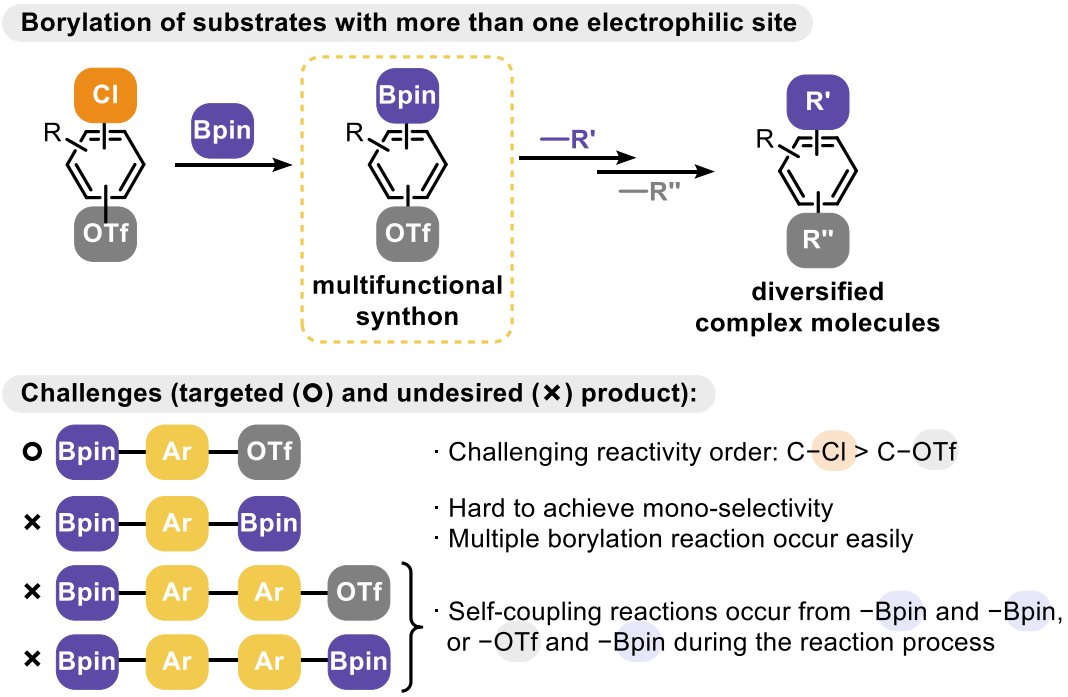

Scheme 3.2 Borylation of substrates with multiple electrophilic sites: Opportunities and challenges

While the potential of chemoselective borylation reactions catalysed by transition metals is recognised, the research efforts in this area have been limited. Nonetheless, a few notable examples have been reported, such as the work by Yoshida *et al.*,[22] who described a copper-catalysed borylation of bromoaryl triflates, demonstrating Ar−Br chemoselectivity (two examples with bis(pinacolato)diboron). Furthermore, Noonan *et al.* have recently introduced a rhodium-catalysed chemoselective borylation strategy targeting the Ar−I bond in bromoiodoarenes.[21] While the available examples have been limited in substrate scope, they have largely adhered to the classical reactivity order, such as Ar−I > Ar−Br[23–25] or Ar−Br > Ar−OTf.[26–27] To the best of our knowledge, there is no prior report of a transition-metal-catalysed chemoselective borylation reaction that can selectively target the C−Cl bond over the C−OTf bond in chloroaryl triflates.

Attaining unconventional chemoselectivity, where the C−Cl bond is preferentially activated over the C−OTf bond, is a highly desirable approach that can facilitate the alteration of reactivity orders to better suit synthetic applications.[28–38] Nonetheless, this remains a paramount challenge. So far, only the research groups of Fu,[32] Neufeldt,[36] and our own[37] have reported the inversion of the typical C−Cl > C−OTf reactivity order in the Suzuki−Miyaura reaction, with a single example also demonstrated in the Stille coupling reaction.[39] In our previous work, we designed and synthesised a novel type of indolyl-based phosphine ligand, and found that the preagostic interaction and steric hindrance offered by the C2-cyclohexyl group enabled Pd-catalysed chemoselective activation of the C−Cl bond in Suzuki−Miyaura reactions involving polyhalogenated aryl triflates and arylboronic acids.[37] Expanding on this, we now report our efforts

in developing the first Pd-catalysed chemoselective C−Cl (over C−OTf) borylation reaction (Scheme 3.3).

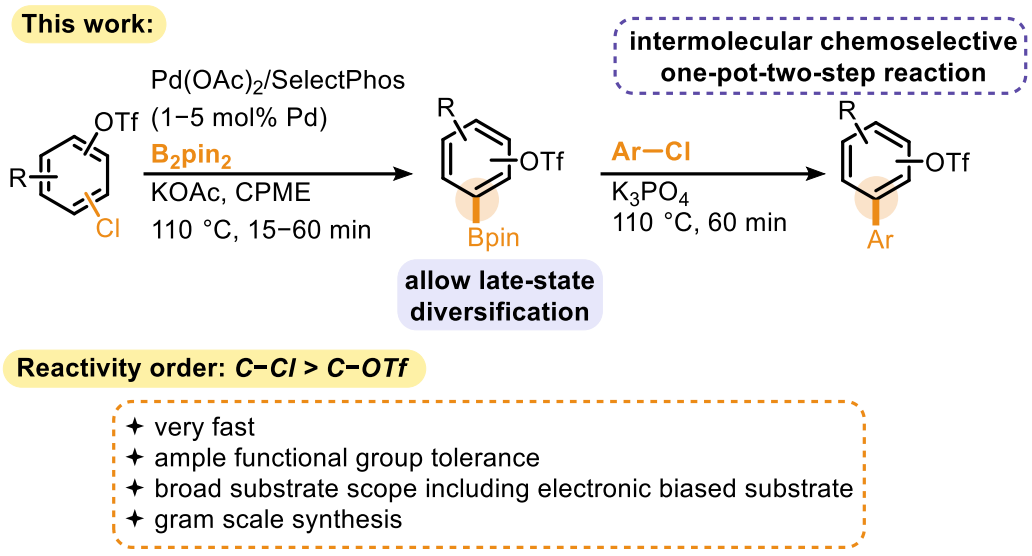

Scheme 3.3 Pioneering Pd-catalysed chemoselective borylation: C−Cl over C−OTf

3.2 Result and Discussion

3.2.1 Initial screening of ligands

We initiated our investigation by employing 4-chlorophenyl triflate **7a** and bis(pinacolato)diboron **8** as the model substrates. An array of commercially available ligands as well as 2-alkyl-indolyl phosphines were explored, with a total of 37 ligands spanning various scaffolds being screened (Table 3.1). Interestingly, the indolyl phosphine ligands featuring a secondary alkyl group at the C2 position (**L1**−**L2**) exhibited an inversion of the common selectivity order, preferentially activating the C−Cl bond and providing the best chemoselectivity and reactivity for the formation of the desired product **9a**.

Among the screened indolyl phosphine ligands, **L1** was a more favourable candidate than **L2**. The former demonstrated excellent chemoselectivity, coupling exclusively at the −Cl site, in contrast to the latter, which produced only trace amounts of the diborylated product **11a**. Ligands bearing a C2 tertiary alkyl group lacking a methine hydrogen (**L3** and **L4**) or a small C2 methyl group (**L5**) exhibited inferior reactivity or poor chemoselectivity, respectively. Additionally, the indolylphosphine ligand with a C2 aryl ring (**L6**) showed selectivity solely for the C−OTf bond, further highlighting the crucial role of the C2 alkyl group of the ligand in this reaction. Among the commercially available phosphine ligands evaluated (**L7**−**L11**), only P*t*-Bu_3 (**L9**), P*t*-Bu_3−Pd−G4 (**L10**), and P(*o*-tolyl)$_3$ (**L11**) demonstrated selective C−Cl activation, though the yields were low. The ligand [Pd(*μ*−I)P*t*-Bu_3]$_2$ (**L12**) proved to be inactive in this reaction. CataCXium®A (**L22**) exhibited C−Cl selectivity but provided a low yield. MorDalphos (**L23**) was found to be ineffective in this catalysis. Ligands with heteroaryl bottom rings (**L13**−**L14**) or aryl bottom rings (**L15**−**L21**) and diphosphine ligands (**L24**−**L35**) followed the general reactivity order of C−OTf > C−Cl. NHC ligands (**L36**−**L37**) showed poor chemoselectivity and reactivity.

Table 3.1 Screening of ligands for Pd-catalysed chemoselective borylation of 4-chlorophenyl triflate **7a** and bis(pinacolato)diboron **8**[a]

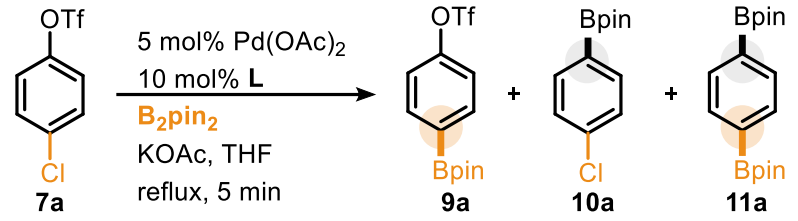

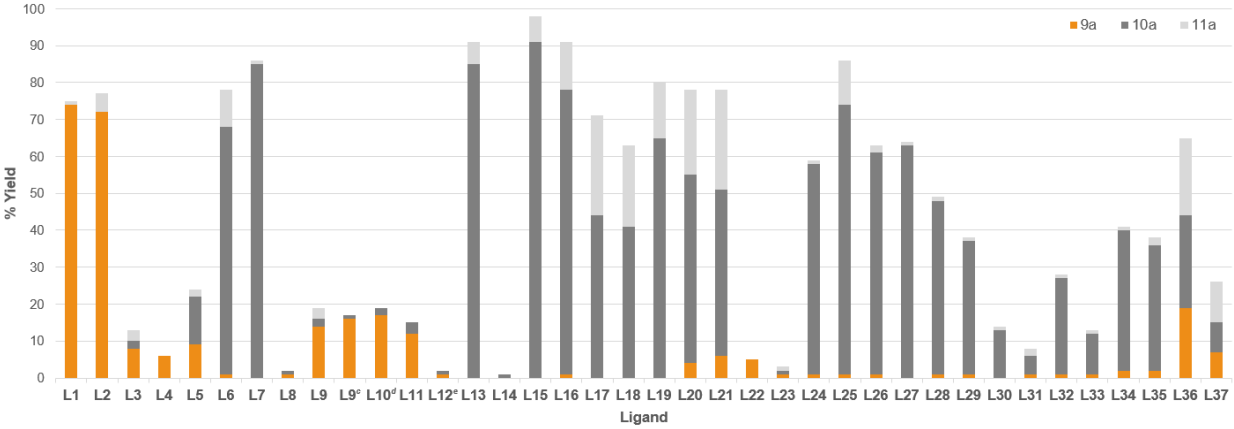

Code	Ligand		Yield of 9a (%)[b]	Yield of 10a (%)[b]	Yield of 11a (%)[b]	Recovery of 7a (%)[b]
L1	SelectPhos	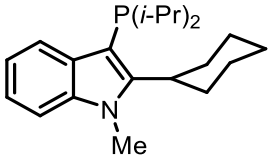	74	0	<1	13
L2	CySelectPhos	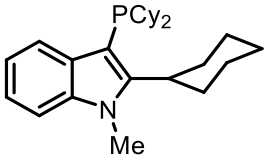	72	0	5	14
L3	2-(adamantan-1-yl)-3-(diphenyl phosphaneyl)-1-methyl-1*H*-indole	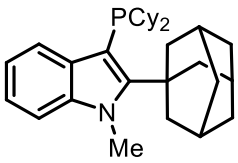	8	2	3	12
L4	2-(*tert*-butyl)-3-(dicyclohexyl phosphaneyl)-1-methyl-1*H*-indole	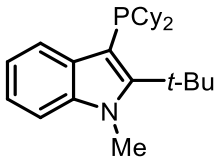	6	0	0	5

L5	3-(dicyclohexyl phosphaneyl)-1,2-dimethyl-1*H*-indole	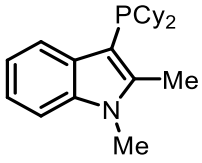	9	13	2	73
L6	*i*-PrPhendolePhos	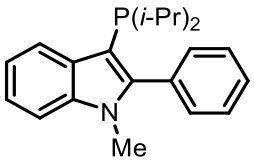	1	67	10	13
L7	triphenyl phosphine	PPh_3	0	85	1	9
L8	tricyclohexyl phosphine	PCy_3	<1	1	0	94
L9 **L9**[c]	tri-*tert*-butylphosphine	$P(t\text{-}Bu)_3$	14 16	2 <1	3 0	12 59
L10[d]	P*t*-Bu_3−Pd−G4	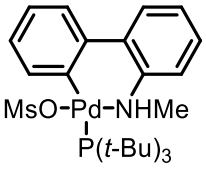	17	2	0	24
L11	tri(*o*-tolyl)phosphine	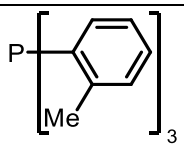	12	3	0	83
L12[e]	[Pd(*μ*−I)P*t*-Bu_3]$_2$	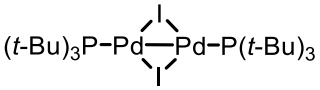	<1	<1	0	94
L13	CM-Phos	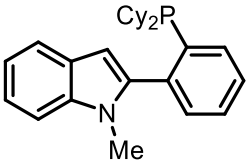	0	85	6	2
L14	PhMezole-Phos	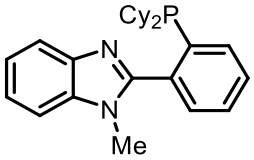	0	<1	0	86
L15	CyJohnPhos	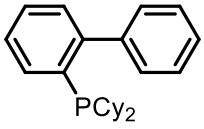	0	91	7	2
L16	DavePhos	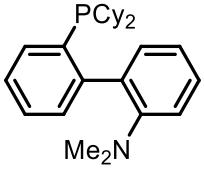	<1	77	13	3

L17	SPhos	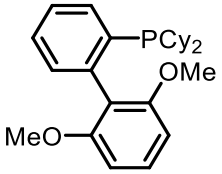	0	44	27	17
L18	RuPhos	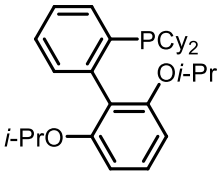	0	41	22	30
L19	XPhos	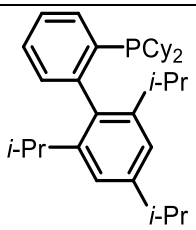	0	65	15	7
L20	CataCXium®PCy	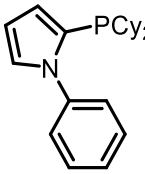	4	51	23	16
L21	CataCXium®PInCy	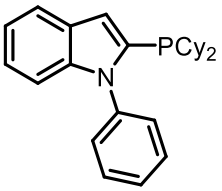	6	45	27	20
L22	CataCXium®A	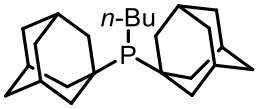	5	0	0	95
L23	MorDalphos	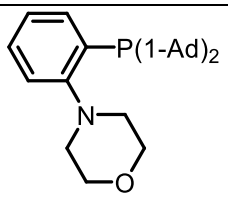	<1	<1	<1	91
L24	dppf	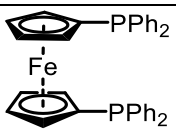	1	57	1	4
L25	dcypf	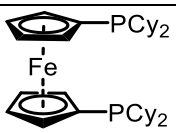	1	73	12	7
L26	DPEPhos	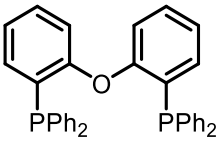	<1	60	2	3

L27	XantPhos	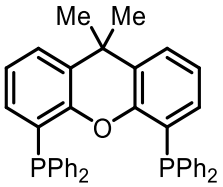	0	63	<1	18
L28	NiXantphos	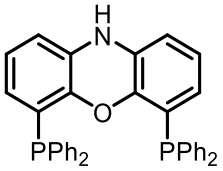	<1	47	1	24
L29	BINAP	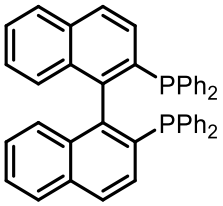	1	36	1	57
L30	dppBz	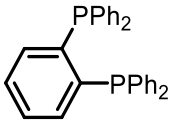	0	13	<1	66
L31	dppm	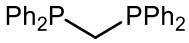	<1	5	2	87
L32	dppe	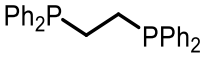	<1	26	<1	56
L33	dppp	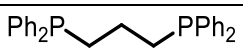	<1	11	<1	72
L34	dppb	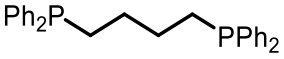	2	38	<1	33
L35	dcype	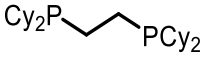	2	34	2	56
L36	IMes·HCl	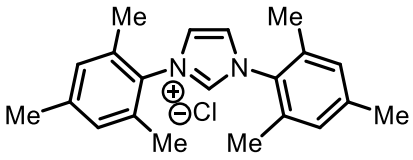	19	25	21	29
L37	IPr·HCl	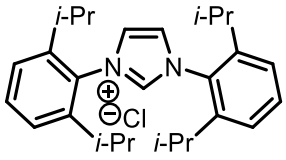	7	8	11	69

[a]Reaction conditions: 4-chlorophenyltriflate (0.20 mmol), B_2pin_2 (0.20 mmol), $Pd(OAc)_2$ (5.0 mol%), ligand (10 mol%), KOAc (0.60 mmol), and THF (0.60 mL) were heated to reflux in a pre-heated oil bath (110 °C) with stirring under N_2 for 5 minutes. [b]Calibrated GC yields were reported using dodecane as an internal standard. [c]$Pd_2(dba)_3$ (2.5 mol%) and *tert*-butylphosphine (P*t*-Bu_3, 5.0 mol%) were used instead, with a Pd: L ratio of 1: 1. [d] P*t*-Bu_3−Pd−G4 (5.0 mol%) was used without $Pd(OAc)_2$. [e]$[Pd(\mu-I)Pt\text{-}Bu_3]_2$ (2.5 mol%) was used without $Pd(OAc)_2$.

3.2.2 Optimisation of reaction conditions

Intrigued by the promising initial ligand screening results, we proceeded to explore other reaction parameters (Table 3.2). A series of palladium sources were evaluated, with both $PdCl_2(MeCN)_2$ and $Pd(OAc)_2$ exhibiting high catalytic activity, in contrast to the relatively lower catalytic performance of $Pd_2(dba)_3$ and $[Pd(\pi\text{-cinnamyl})Cl]_2$ (Table 3.2, entries 1−4). Notably, $Pd(OAc)_2$ demonstrated enhanced selectivity for the C−Cl bond compared to $PdCl_2(MeCN)_2$. Further optimisation efforts focused on the palladium-to-ligand ratio, revealing that a 1: 2 ratio provided the highest yield (Table 3.2, entries 1 and 5−7). Reducing the catalyst loading to 0.2 mol% Pd and extending the reaction time to 30 minutes resulted in a 72% product yield (Table 3.2, entry 9). Solvent screening identified cyclopentyl methyl ether (CPME) as the optimal choice, delivering the desired product with a 94% yield and excellent C−Cl bond chemoselectivity (Table 3.2, entries 11−14). Among the commonly used bases, KOAc was found to be superior to CsF, K_3PO_4, $K_3PO_4{\cdot}H_2O$, and K_2CO_3 (Table 3.2, entries 14−18), because its relatively small size could facilitate in the transmetalation and its moderate basicity and solubility in organic solvents help stabilize reaction intermediates and prevent further coupling of borylated products with aryl (pseudo)halides.

Table 3.2 Optimisation of reaction conditions for Pd-catalysed chemoselective C−Cl (over C−OTf) borylation of 4-chlorophenyl triflate **7a** with bis(pinacolato)diboron **8**[a]

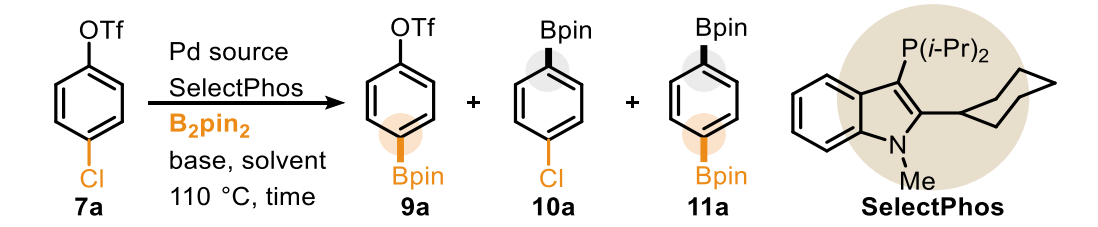

Entry	Pd source (mol%)	Pd: L	Base	Solvent	Time (min)	Yield of 9a (%)[b]	Yield of 10a (%)[b]	Yield of 11a (%)	Recovery of 7a (%)[b]
1	5 mol% $Pd(OAc)_2$	1: 2	KOAc	THF	5	69	<1	<1	27
2	5 mol% $PdCl_2(ACN)_2$	1: 2	KOAc	THF	5	72	<1	4	8
3	2.5 mol% $Pd_2(dba)_3$	1: 2	KOAc	THF	5	32	1	1	58
4	2.5 mol% $[Pd(\pi\text{-cinamyl})Cl]_2$	1: 2	KOAc	THF	5	15	<1	<1	79

5	5 mol% $Pd(OAc)_2$	1:1	KOAc	THF	5	68	1	3	6
6	5 mol% $Pd(OAc)_2$	1:3	KOAc	THF	5	27	<1	<1	61
7	5 mol% $Pd(OAc)_2$	1:4	KOAc	THF	5	8	<1	0	79
8	0.5 mol% $Pd(OAc)_2$	1:2	KOAc	THF	30	89	<1	5	4
9	0.2 mol% $Pd(OAc)_2$	1:2	KOAc	THF	30	72	0	2	10
10	0.1 mol% $Pd(OAc)_2$	1:2	KOAc	THF	30	37	1	2	52
11	0.2 mol% $Pd(OAc)_2$	1:2	KOAc	*t*-BuOH	30	57	0	3	12
12	0.2 mol% $Pd(OAc)_2$	1:2	KOAc	toluene	30	63	0	<1	25
13	0.2 mol% $Pd(OAc)_2$	1:2	KOAc	dioxane	30	53	0	<1	21
14	0.2 mol% $Pd(OAc)_2$	1:2	KOAc	CPME	30	94	0	0	6
15	0.2 mol% $Pd(OAc)_2$	1:2	CsF	CPME	30	15	5	2	61
16	0.2 mol% $Pd(OAc)_2$	1:2	K_3PO_4	CPME	30	20	1	1	67
17	0.2 mol% $Pd(OAc)_2$	1:2	$K_3PO_4 \cdot H_2O$	CPME	30	22	3	2	37
18	0.2 mol% $Pd(OAc)_2$	1:2	K_2CO_3	CPME	30	23	2	2	67

[a]Reaction conditions: 4-chlorophenyltriflate (0.20 mmol), B_2pin_2 (0.20 mmol), $Pd(OAc)_2$, ligand **L1**, base (0.60 mmol), and solvent (0.60 mL) were stirred under N_2 at 110 °C for the indicated time. [b]Calibrated GC yields were reported using dodecane as an internal standard.

3.2.3 Palladium-catalysed chemoselective borylation of polyhalogenated aryl triflates

With the optimised reaction conditions established, a wide range of chloroaryl triflates were examined. These reactions were completed within 60 minutes under a 1−5 mol% palladium catalyst loading and displayed excellent chloro-selectivity (Table 3.3). For instance, *para*- and *meta*-chlorophenyl triflates were directly transformed into their respective products, delivering 95% and 90% yields (Table 3.3, **9a** and **9b**). Notably, the chloro-selectivity was maintained regardless of the presence of additional deactivating (−OMe, −Me, −Bz) or activating (−F) substituents on the aryl triflates (Table 3.3, compounds **9c**−**9f** and **9i**−**9l**). The substrate scope was further expanded to include chloropyridyl triflate and chloroquinolyl triflate, which delivered the desired products in 80% and 60% yields respectively (Table 3.3, **9g** and **9h**). In contrast, when 2-chloro-4-pyridyl triflate was used, only a trace amount of the borylated product at the C−OTf position was detected by GC-MS. Similarly, 4-chloro-2-pyridyl triflate gave a poor yield (~15%) of the borylated product at the C−Cl site, as observed by GC-MS.

The set of substrates utilised demonstrated the broad functional group tolerance of this borylation protocol. Chloroaryl triflates bearing nitrile, aldehyde, and ketone groups were efficiently borylated, providing the corresponding boronic acid pinacol esters in good yields (Table 3.3, **9m**−**9o**). Interestingly, when 3,5-dichlorophenyl triflate was employed as the substrate, smooth diborylation occurred, which could be leveraged for the synthesis of terphenyls or polyphenyls (Table 3.3, **9p**). To further expand the substrate scope, the researchers explored the generality of the C−Br coupling preference. The borylation of poly(pseudo)halogenated arenes displayed complete selectivity, delivering the products resulting from C−Br borylation in good yields, while leaving the C−Cl and C−OTf sites intact (Table 3.3, **9q**−**9s**).

Table 3.3 Pd-catalysed chemoselective borylation of polyhalogenated aryl triflates[a]

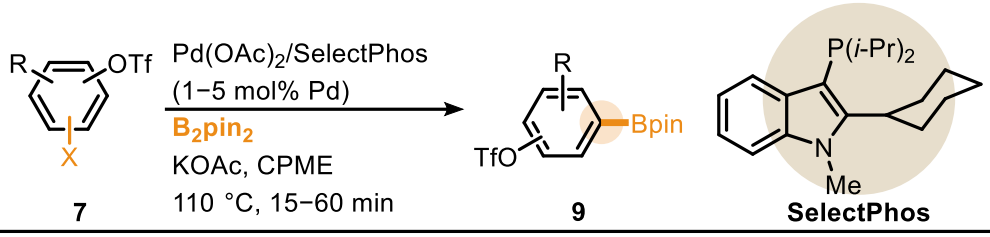

X = Cl (Cl > OTf)

9a
1 mol% Pd, 30 min, 95%, 86%[b,d], 47%[c,d]

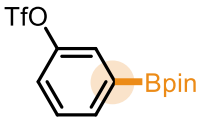

9b
1 mol% Pd, 30 min, 90%

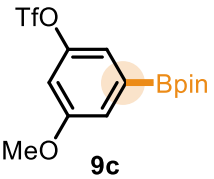

9c
5 mol% Pd, 15 min, 79%

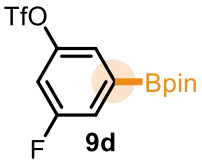

9d
5 mol% Pd, 15 min, 84%

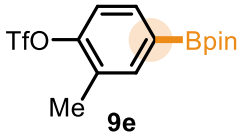

9e
1 mol% Pd, 60 min, 89%

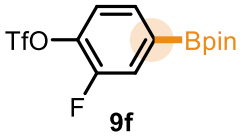

9f
1 mol% Pd, 60 min, 91%

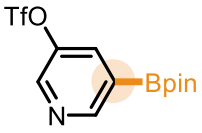

9g
5 mol% Pd, 30 min, 80%

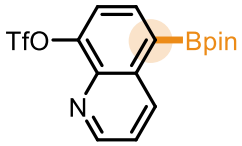

9h
5 mol% Pd, 30 min, 60%

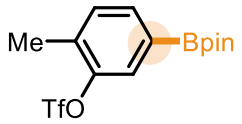

9i
1 mol% Pd, 60 min, 94%

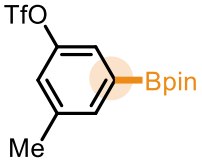

9j
5 mol% Pd, 30 min, 95%

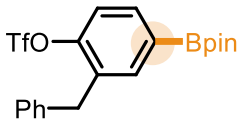

9k
1 mol% Pd, 60 min, 88%

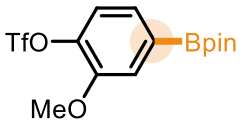

9l
1 mol% Pd, 60 min, 93%

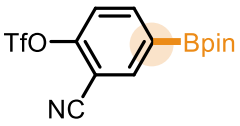

9m
1 mol% Pd, 60 min, 65%[e]

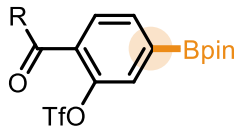

R = H, **9n**
1 mol% Pd, 60 min, 79%
R = Me, **9o**
5 mol% Pd, 15 min, 67%

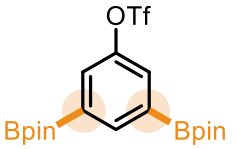

9p
5 mol% Pd, 30 min, 71%[f]

X = Br (Br > Cl > OTf)

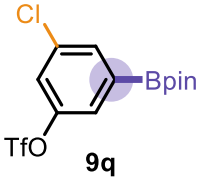

9q
5 mol% Pd, 60 min, 68%[e,g]

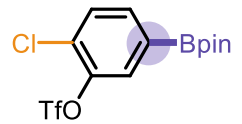

9r
5 mol% Pd, 60 min, 77%[g]

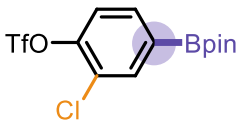

9s
5 mol% Pd, 60 min, 84%[g]

[a]Reaction conditions: polyhalogenated aryl triflate (1.0 mmol), B_2pin_2 (1.0 mmol), $Pd(OAc)_2$, ligand **L1** (Pd: L = 1: 2), KOAc (3.0 mmol) and CPME (3.0 mL) were stirred under N_2 at 110 °C for the indicated time. Isolated yields were reported. A chemoselectivity of 97−100% was observed for all compounds, and the conversion and selectivity ratio of each compound are provided in the latter characterisation section. [b]A Pd: L ratio of 1: 1 was used. [c]The reaction was conducted at 90 °C. [d]Calibrated GC yield was reported using dodecane as an internal standard. [e]>91% chemoselectivity was observed. [f]B_2pin_2 (2.0 mmol) was used instead. [g]Toluene was used as the solvent.

3.2.4 Palladium-catalysed sequential chemoselective borylation and Suzuki−Miyaura coupling

The successful borylation of aryl triflates prompted us to investigate the feasibility of employing the Pd/**L1** system for the chemoselective Suzuki coupling of aryl chlorides. We pursued a one-pot, two-step approach, which could further improve the practical utility of the method and broaden the versatility of the catalyst system. The $Pd(OAc)_2$/ **L1** catalytic approach proved effective in facilitating both the borylation and the subsequent Suzuki cross-coupling reactions.

No additional palladium source or ligand was required for the reaction mixture after the borylation step, as the boronic acid pinacol ester intermediates were not isolated. Substituted chloroaryl triflates underwent successful borylation at the chloro site, and the resulting intermediates were then seamlessly coupled with a second aryl chloride bearing functional groups such as ketones, esters, and aldehydes (Table 3.4, **13a**, **13b**, **13g**, **13h**, and **13k**). Additionally, a variety of heteroaryl chlorides, including 2-picoline, quinoline, and 3-methylbenzo[*b*]thiophene, were reacted with diverse chloroaryl triflates in a one-pot fashion, producing aryl-heteroaryl compounds in 67−80% yield (Table 3.4, **13c**, **13e**, **13f**, and **13i**). The catalyst system also allowed for the use of nonactivated aryl chlorides as cross-coupling partners in the second step (Table 3.4, compounds **13h**, **13j**, and **13l**). Interestingly, this system provided an inversion of the common borylation selectivity order of OTf > Cl and represented the first example of an intermolecular chemoselective Suzuki coupling of aryl chloride with borylated aryl triflates in a sequential manner. Furthermore, the triflate group was preserved after the sequential reactions, enabling further transformation through a cross-coupling approach.

Table 3.4 Chemoselective borylation and Suzuki−Miyaura coupling of chloroaryl triflates in a streamlined one-pot, two-step Pd-catalysed protocol[a]

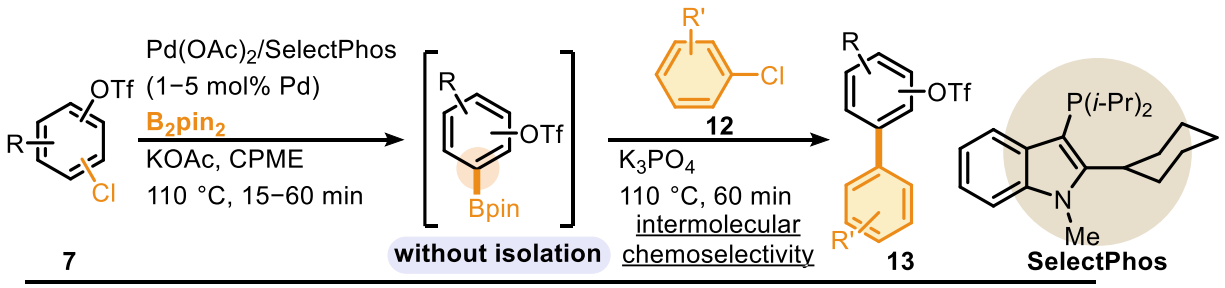

13a
1 mol% Pd, 60 min, 80%

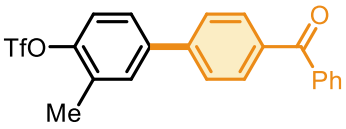

13b
1 mol% Pd, 60 min, 74%

13c
1 mol% Pd, 60 min, 80%

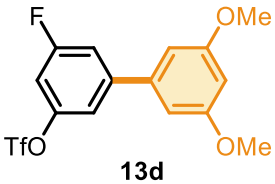

13d
1 mol% Pd, 60 min, 67%

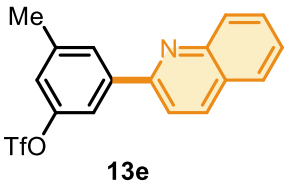

13e
5 mol%, 15 min, 80%

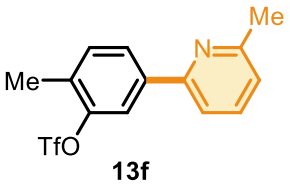

13f
5 mol%, 15 min, 72%

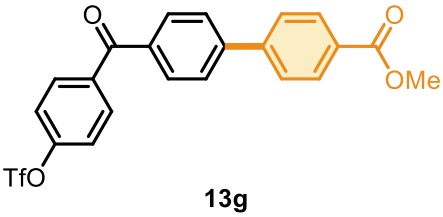

13g
3 mol% Pd, 30 min, 86%

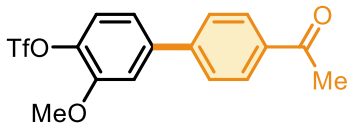

13h
3 mol%, 30 min, 77%

13i
3 mol%, 30 min, 68%

13j
1 mol% Pd, 60 min, 74%

13k
3 mol% Pd, 30 min, 74%

13l
3 mol% Pd, 30 min, 78%

[a]1st Step: Chloroaryl triflate (0.22 mmol), B_2pin_2 (0.22 mmol), $Pd(OAc)_2$, **L1** (Pd: L = 1: 2), KOAc (0.66 mmol), and CPME (0.60 mL) were stirred under N_2 at 110 °C for the specified duration. 2nd Step: Aryl chlorides (0.20 mmol) and K_3PO_4 (0.60 mmol) were added, and the reaction mixture was then stirred under N_2 at 110 °C for 1 hour. Isolated yields were reported.

3.2.5 Gram-scale palladium-catalysed chemoselective borylation

A large-scale reaction was carried out in order to test the practicality of the borylation protocol. This reaction is capable of being scaled up significantly, up to 100 times, to generate the coupling product. The 0.5 mol% Pd catalyst facilitated the smooth coupling of 4-chlorophenyl triflate and 4-chloro-2-methoxyphenyl triflate with bis(pinacolato)diboron, resulting in the desired products in 91% and 74% yields, respectively (Scheme 3.4, **9a** and **9l**).

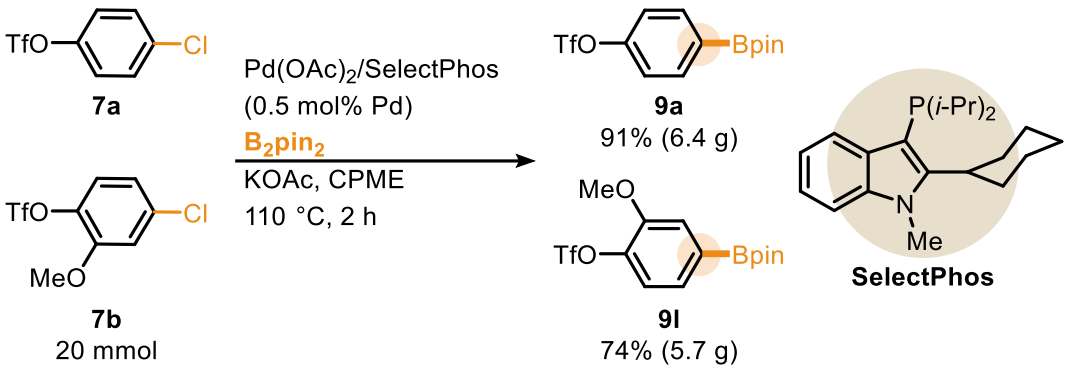

Scheme 3.4 Pd-catalysed chemoselective borylation on a large scale

3.3 Summary

In conclusion, we developed a Pd-catalysed chemoselective borylation of polyhalogenated aryl triflates, which selectively coupled at the chloride group over the triflate. Using a $Pd(OAc)_2$ and SelectPhos (**L1**) catalyst system, we were able to borylate a wide range of polyhalogenated aryl triflates containing sensitive functional groups and heterocycles at the C−Cl site. Furthermore, this catalyst system enabled a one-pot sequential chemoselective borylation and intermolecular Suzuki−Miyaura cross-coupling. We anticipate further advancements in the reactivity, selectivity, and versatility of this ligand series.

3.4 Experimental Section

3.4.1 General considerations

All reagents were purchased from commercial suppliers and used as received, unless otherwise noted. Borylation and Suzuki coupling reactions were carried out in a resealable screw cap Schlenk tube (approximately 20 mL volume) containing a Teflon-coated magnetic stirrer bar (5 mm × 10 mm). Dioxane, CPME, and toluene were freshly distilled from sodium under nitrogen.[40] THF was freshly distilled from sodium benzophenone ketyl under nitrogen.[40] *t*-BuOH was freshly distilled from anhydrous CaH_2 under nitrogen.[40] KF, KOAc, K_3PO_4, $K_3PO_4{\cdot}H_2O$, K_2CO_3, and Na_3PO_4 were purchased from Dieckmann. CsOAc and Cs_2CO_3 were obtained from Energy. $K_3PO4{\cdot}3H_2O$ was purchased from Aladdin. All bases were used as received. $Pd(OAc)_2$, $Pd_2(dba)_3$, $PdCl_2(MeCN)_2$, and $[Pd(\pi\text{-cinnamyl})Cl]_2$ were acquired from Strem. Ligands **L7**−**L10** and **L14**−**L36** were purchased from commercial suppliers. Alkyl-indolyl-based phosphine ligands **L1**−**L5**, and *i*-PrPhendolePhos **L6** were prepared according to the reported literature.[37] CM-Phos **L12** and PhMezole-Phos **L13** were prepared following the literature procedures.[41-42] $[Pd(\mu{-}I)P\textit{t}\text{-}Bu_3]_2$ **L11** was synthesised using a published method.[43] A fresh bottle of *n*-BuLi was used. Thin-layer chromatography was carried out using pre-coated silica gel 60 F_{254} plates. Column chromatography was performed using silica gel (Grace, 60 Å, 40−63 μm). Melting points were measured on an uncorrected Stuart Melting Point SMP30 instrument. NMR spectra were recorded on a Brüker (400 MHz for ^1H, 100 MHz for ^{13}C, 376 MHz for ^{19}F and 162 MHz for ^{31}P) and Jeol JNM-ECZ500R/S1 (200.43 MHz for ^{31}P) spectrometers. Spectra were referenced internally to the residual proton resonance in $CDCl_3$ (δ 7.26 ppm) for ^1H NMR and the middle peak of $CDCl_3$ (δ 77.0 ppm) for ^{13}C NMR. ^{19}F NMR chemical shifts were determined relative to $CFCl_3$ as the external standard, with low field being positive. ^{31}P NMR spectra were referenced to 85% H_3PO_4 externally. Coupling constants (*J*) were reported in Hertz (Hz). EI-MS were recorded on an HP 5977A MSD Mass Spectrometer. HRMS were obtained on an Agilent 6540 ESI-QToF-MS and a Waters GCT Premier EI-ToF-MS. GC-MS analysis was conducted on an HP 7890B GC system using a HP5MS column (30 m × 0.25 mm). The product yields reported were based on the authentic samples/dodecane calibration standard from the HP 7890B GC-FID system. All yields cited refer to the isolated yield of compounds estimated to be greater than 95% pure as determined by capillary gas chromatography (GC) or ^1H NMR. Compounds described in the literature were characterised by comparing their ^1H, ^{13}C, and/or ^{19}F NMR spectra to the previously reported data. The procedures described are representative, and thus the yields may differ from those reported in the tables.

3.4.2 Polyhalogenated aryl triflate synthesis and characterisation

The polyhalogenated aryl triflates were prepared from their corresponding phenols using triflyl chloride in the presence of triethylamine in dry dichloromethane, following a literature procedure.[44]

General procedure

In a nitrogen atmosphere, the corresponding phenol (20 mmol, 1.0 equiv.) was dissolved in freshly distilled dichloromethane (50 mL) at room temperature. Triethylamine (28 mmol, 1.4 equiv.) was then added to the solution. The reaction mixture was cooled to -78 °C using a dry ice/acetone bath, and triflyl chloride (20 mmol, 1.0 equiv.) was added dropwise via syringe. The reaction was allowed to warm to room temperature and stirred for 1 hour. Ethyl acetate and water were then added, and the organic phase was separated. The organic layer was washed several times with water, dried over Na_2SO_4, and concentrated. The crude product was purified by column chromatography, eluting with ethyl acetate/hexane. The desired fractions were collected, and the solvent was removed to give the final product.

The characterisation data for the new polyhalogenated aryl triflates are provided below.

3-Chloro-5-methylphenyl trifluoromethanesulfonate

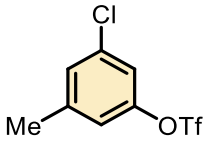

The product was obtained as a colourless liquid in 82% yield (4.49 g). Flash column chromatography was performed using hexane as the eluent (R_f = 0.60). ^{1}H NMR (400 MHz, $CDCl_3$) δ 2.39 (s, 3H), 7.00 (s, 1H), 7.11 (s, 1H), 7.21 (s, 1H); ^{13}C NMR (100 MHz, $CDCl_3$) δ 21.1, 118.7 (q, *J* = 321.4 Hz), 118.9, 120.3, 129.4, 135.1, 142.1, 149.3; ^{19}F NMR (376 MHz, $CDCl_3$) δ -72.9; HRMS (EI): calculated m/z for $C_8H_6ClF_3O_3S^+$ $[M]^+$: 273.9673, found 273.9680.

2-Benzyl-4-chlorophenyl trifluoromethanesulfonate

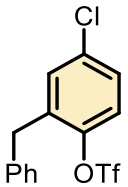

The product was obtained as a colourless liquid in 75% yield (5.26 g). Flash column chromatography was performed using hexane as the eluent (R_f = 0.46). ^{1}H NMR (400 MHz, $CDCl_3$) δ 4.09 (s, 2H), 7.20−7.22 (m, 3H), 7.28−7.33 (m, 3H), 7.36−7.40 (m, 2H); ^{13}C NMR (100 MHz, $CDCl_3$) δ 35.6, 118.5 (q, *J* = 318.2 Hz), 122.6, 127.0, 128.2, 128.8, 129.1, 131.6, 134.1, 136.0,

137.5, 146.1; ^{19}F NMR (376 MHz, $CDCl_3$) δ -73.6; HRMS (EI): calculated m/z for $C_{14}H_{10}ClF_3O_3S^+$ $[M]^+$: 349.9986, found 350.0000.

2-Acetyl-5-chlorophenyl trifluoromethanesulfonate

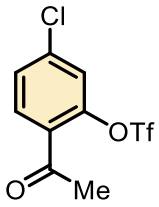

The product was obtained as a light-yellow solid in 16% yield (1.00 g). Flash column chromatography was performed using ethyl acetate/hexane (1: 20) as the eluent (R_f = 0.23). The melting point was determined to be 49.2−50.0 °C. ^{1}H NMR (400 MHz, $CDCl_3$) δ 2.61, (s, 3H), 7.33 (s, 1H), 7.46 (d, *J* = 8.4 Hz, 1H), 7.78 (d, *J* = 8.4 Hz, 1H); ^{13}C NMR (100 MHz, $CDCl_3$) δ 29.3, 118.5 (q, *J* = 318.7 Hz), 123.3, 128.9, 130.3, 131.7, 139.3, 146.9, 195.3; ^{19}F NMR (376 MHz, $CDCl_3$) δ -73.2; HRMS (EI): calculated m/z for $C_9H_6ClF_3O_4S^+$ $[M]^+$: 301.9622, found 301.9625.

3.4.3 General procedure for ligand and reaction condition screenings

General procedure for the initial ligand and reaction condition screening for the chemoselective borylation of 4-chlorophenyl triflate with 5.0 mol% Pd catalyst loading

A Schlenk tube was charged with a Teflon-coated magnetic stir bar (5 mm × 10 mm) and equipped with a screw cap. Pd source (0.010 mmol), ligand (0.010−0.040 mmol, for Pd: L = 1: 1−4), bis(pinacolato)diboron (0.20 mmol), and KOAc (0.60 mmol) were added to the Schlenk tube. The tube was carefully evacuated and flushed with nitrogen (3 cycles). 4-Chlorophenyl triflate (0.20 mmol) and the freshly distilled THF (0.60 mL) were added to the reaction mixture via syringes. The tube was sealed and stirred for 1 minute at room temperature, then magnetically stirred in a preheated oil bath (110 °C) for 5 minutes. The reaction was allowed to reach room temperature. Ethyl acetate (~4.0 mL), dodecane (45.2 μL, internal standard), and water (~2.0 mL) were added, and the organic layer was subjected to GC analysis. The GC yield was previously calibrated by an authentic sample/dodecane calibration curve.

General procedure for the initial reaction condition screening for the chemoselective borylation of 4-chlorophenyl triflate with 0.10−0.50 mol% Pd catalyst loading

A $Pd(OAc)_2$ and ligand **L1** (Pd: L = 1: 2) stock solution was prepared in freshly distilled THF (25 mL) and stirred continuously at room temperature for 1 minute. An array of Schlenk tubes were equipped with magnetic stirrer bars (5 mm × 10 mm) and subjected to cycles of evacuation and nitrogen backfilling (3 cycles). The stock solution (0.20 mol% Pd per 1.0 mL) was then added to the respective Schlenk tubes using syringes. The solvent was removed from the Schlenk tubes under reduced pressure. The tubes were then charged with bis(pinacolato)diboron (0.20 mmol) and bases (0.60 mmol), and the evacuation/backfilling process was repeated (3 cycles). 4-Chlorophenyl triflate (0.20 mmol) and freshly distilled solvent (0.60 mL) were subsequently added to the tubes via syringe. Each tube was sealed and magnetically stirred in a preheated oil bath (110 °C) for 30 minutes. After the reaction period, the tubes were allowed to cool to room temperature. Ethyl acetate (~4.0 mL), dodecane (45.2 μL, internal standard), and water (~2.0 mL) were added. The organic layers were then subjected to GC analysis, using a previously calibrated authentic sample/dodecane calibration curve.

3.4.4 General procedure for borylation of polyhalogenated aryl triflates

$Pd(OAc)_2$ (2.3 mg, 0.010 mmol, 1.0 mol% Pd) or (11.2 mg, 0.050 mmol, 5.0 mol% Pd) and ligand **L1** (6.6 mg, 0.020 mmol, 2.0 mol% **L1** or 33 mg, 0.10 mmol, 10 mol% **L1**) were added to an array of Schlenk tubes equipped with magnetic stirrer bars (5 mm × 10 mm). The Schlenk tubes were then charged with bis(pinacolato)diboron (1.0 mmol), polyhalogenated aryl triflates (1.0 mmol, if solid), and potassium acetate (3.0 mmol). Each tube was evacuated and backfilled with nitrogen for 3 cycles. If polyhalogenated aryl triflates were liquids, they were added to the Schlenk tubes via syringe, along with freshly distilled solvent (3.0 mL). The tubes were then resealed and magnetically stirred in a preheated oil bath (110 °C) for 15 minutes to 1 hour. The crude reaction products were purified by bulb-to-bulb distillation. The distilled product was dissolved in hexane and washed with water 5 times. The organic fraction was then concentrated and dried under vacuum to afford the desired product.

3.4.5 General procedure for one-pot-two-step chemoselective borylation/Suzuki coupling

General procedure for one-pot-two-step chemoselective borylation/Suzuki coupling of chloroaryl triflates with 1.0 mol% Pd catalyst loading

Initially, a stock solution of $Pd(OAc)_2$ (0.020 mmol) and ligand **L1** (0.040 mmol, Pd: L = 1: 2) in freshly distilled THF (10 mL) was prepared with continuous stirring at room temperature for 1 minute. An array of Schlenk tubes were each charged with a magnetic stirrer bar (5 mm × 10 mm) and evacuated and backfilled with nitrogen for 3 cycles. Then, 1.0 mL (1.0 mol% Pd) of the stock solution was added by syringe to each Schlenk tube, and the solvent was removed under reduced pressure. The Schlenk tubes were then charged with chloroaryl triflates (0.22 mmol, if solid), bis(pinacolato)diboron (0.22 mmol), and potassium acetate (0.66 mmol), and again evacuated and backfilled with nitrogen for 3 cycles. If chloroaryl triflates were liquids, they were added to the Schlenk tubes via syringe along with freshly distilled CPME (0.60 mL). The batch of Schlenk tubes was resealed and magnetically stirred in a preheated oil bath (110 °C) for 15 minutes to 1 hour. The reactions were then allowed to reach room temperature. Under a nitrogen atmosphere, aryl chlorides (0.20 mmol) were added to the Schlenk tubes, either by syringe if the aryl chloride was a liquid, or as a solid along with potassium phosphate (0.60 mmol). The batch of Schlenk tubes was resealed and magnetically stirred in the preheated oil bath (110 °C) for 1 hour. After the reactions reached room temperature, ethyl acetate (~4.0 mL) and water (~2.0 mL) were added. The organic layer was subjected to GC analysis, and the aqueous layer was washed with ethyl acetate. The combined organic layers were concentrated, and the crude products were purified by column chromatography on silica gel (230−400 mesh) to afford the desired products.

General procedure for one-pot-two-step chemoselective borylation/Suzuki coupling of chloroaryl triflates with 3.0−5.0 mol% Pd catalyst loading

$Pd(OAc)_2$ (1.3 mg, 0.0060 mmol, 3.0 mol% Pd or 2.2 mg, 0.010 mmol, 5.0 mol% Pd) and ligand **L1** (4.0 mg, 0.012 mmol, 6.0 mol% L or 6.6 mg, 0.020 mmol, 10 mol% L) were added to an array of Schlenk tubes, each containing a magnetic stirrer bar (5 mm × 10 mm). The Pd: L ratio was maintained at 1: 2. The Schlenk tubes were then charged with chloroaryl triflates (0.22 mmol, if solid), bis(pinacolato)diboron (0.22 mmol), and potassium acetate (0.66 mmol), and evacuated and backfilled with nitrogen for 3 cycles. If chloroaryl triflates were liquids, they were added to the Schlenk tubes via syringe along with freshly distilled CPME (0.60 mL). The batch of Schlenk tubes was resealed and magnetically stirred in a preheated oil bath (110 °C) for 15 minutes to 1 hour. The reactions were then allowed to reach room temperature. Under a nitrogen atmosphere, aryl chlorides (0.20 mmol) were added to the Schlenk tubes, either by syringe if the aryl chloride was a liquid, or as a solid along with potassium phosphate (0.60 mmol). The batch of Schlenk tubes was resealed and magnetically stirred in the preheated oil bath (110 °C) for 1 hour. After the reactions reached room temperature, ethyl acetate (~4.0 mL) and water (~2.0 mL) were added.

The organic layer was subjected to GC analysis, and the aqueous layer was washed with ethyl acetate. The combined organic layers were concentrated, and the crude products were purified by column chromatography on silica gel (230−400 mesh) to afford the desired products.

General procedure for gram-scale chemoselective borylation of chloroaryl triflates

In a Schlenk tube equipped with a magnetic stirrer bar (5 mm × 10 mm), $Pd(OAc)_2$ (23 mg, 0.10 mmol), ligand **L1** (66 mg, 0.20 mmol), bis(pinacolato)diboron (20 mmol), and potassium acetate (60 mmol) were added. The Schlenk tube was evacuated and backfilled with nitrogen for 3 cycles. Chloroaryl triflates (20 mmol) were then added to the tube via syringe, along with freshly distilled CPME (60 mL). The sealed Schlenk tube was magnetically stirred in a preheated oil bath (110 °C) for 2 hours. After the reaction reached room temperature, approximately 60 mL of water was added, and the organic layer was subjected to GC analysis. The aqueous layer was washed with dichloromethane, and the combined organic layers were concentrated. The crude products were then purified by bulb-to-bulb distillation. The distilled product was dissolved in hexane and washed with water 5 times. The organic layer was concentrated and dried under vacuum to afford the desired product.

3.4.6 Characterisation data for coupling products

4-(4,4,5,5-Tetramethyl-1,3,2-dioxaborolan-2-yl)phenyl trifluoromethanesulfonate (Table 3.3 and Scheme 3.4, compound **9a**)[45]

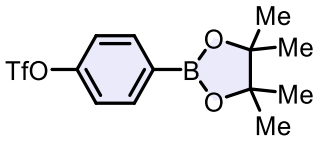

For Table 3.3, the product was obtained in 95% yield (0.950 mmol, 334 mg). The % conversion of starting material = 97%. The % of minor product (reacting C−OTf site): major product (reacting C−Cl site): diborylated product (reacting both C−OTf & C−Cl site) = 0: 99.3: 0.7. For Scheme 3.4, the product was obtained in 91% yield (18.2 mmol, 6.4 g). The % conversion of starting material = 97%. The % of minor product (reacting C−OTf site): major product (reacting C−Cl site): diborylated product (reacting both C−OTf & C−Cl site) = 0: 100: 0. Bulb-to-bulb distillation was used at 130 °C (<2 mmHg). ^{1}H NMR (400 MHz, $CDCl_3$) δ 1.37 (s, 12H), 7.29 (d, *J* = 8.6 Hz, 2H), 7.92 (d, *J* = 8.6 Hz, 2H); ^{13}C NMR (100 MHz, $CDCl_3$) δ 24.8, 84.3, 118.7 (q, *J* = 319.1 Hz), 120.5, 136.9, 151.8; ^{19}F NMR (376 MHz, $CDCl_3$) δ -72.9.

3-(4,4,5,5-Tetramethyl-1,3,2-dioxaborolan-2-yl)phenyl trifluoromethanesulfonate (Table 3.3, compound **9b**)[46]

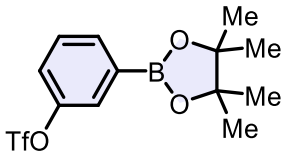

The product was obtained in 90% yield (0.901 mmol, 317 mg). The % conversion of starting material = 95%. The % of minor product (reacting C−OTf site): major product (reacting C−Cl site): diborylated product (reacting both C−OTf & C−Cl site) = 0: 100: 0. Bulb-to-bulb distillation was used at 130 °C (<1 mmHg). ^{1}H NMR (400 MHz, $CDCl_3$) δ 1.35 (s, 12H), 7.35 (d, *J* = 8.2 Hz, 1H), 7.45 (t, *J* = 8.0 Hz, 1H), 7.67 (s, 1H), 7.81 (d, *J* = 7.3 Hz, 1H); ^{13}C NMR (100 MHz, $CDCl_3$) δ 24.8, 84.4, 118.7 (q, *J* = 318.7 Hz), 123.9, 127.0, 129.7, 134.6, 149.4; ^{19}F NMR (376 MHz, $CDCl_3$) δ -73.0.

3-Methoxy-5-(4,4,5,5-tetramethyl-1,3,2-dioxaborolan-2-yl)phenyl trifluoromethanesulfonate (Table 3.3, compound **9c**)

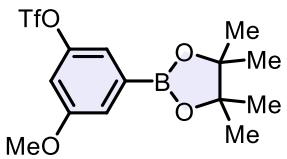

The product was obtained as a colourless liquid in 79% yield (0.791 mmol, 302 mg). The % conversion of starting material = 97%. The % of minor product (reacting C−OTf site): major

product (reacting C−Cl site): diborylated product (reacting both C−OTf & C−Cl site) = 0: 100: 0. Bulb-to-bulb distillation was used at 170 °C (<1 mmHg). ^{1}H NMR (400 MHz, $CDCl_3$) δ 1.34 (s, 12H), 3.85 (s, 3H), 6.88 (m, 1H), 7.27 (m, 1H), 7.32 (m, 1H); ^{13}C NMR (100 MHz, $CDCl_3$) δ 24.8, 55.8, 84.4, 110.7, 118.7 (q, *J* = 318.7 Hz), 119.0, 119.1, 149.9, 160.4; ^{19}F NMR (376 MHz, $CDCl_3$) δ -73.0; HRMS (EI): calculated m/z for $C_{14}H_{18}BF_3O_6S^+$ $[M]^+$: 382.0866, found 382.0880.

3-Fluoro-5-(4,4,5,5-tetramethyl-1,3,2-dioxaborolan-2-yl)phenyl trifluoromethanesulfonate (Table 3.3, compound **9d**)

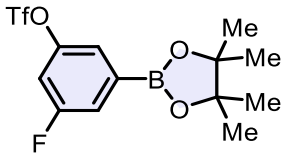

The product was obtained as a colourless liquid in 84% yield (0.838 mmol, 310 mg). The % conversion of starting material = 98%. The % of minor product (reacting C−OTf site): major product (reacting C−Cl site): diborylated product (reacting both C−OTf & C−Cl site) = 0: 100: 0. Bulb-to-bulb distillation was used at 160 °C (<1 mmHg). ^{1}H NMR (400 MHz, $CDCl_3$) δ 1.35 (s, 12H), 7.08−7.12 (m, 1H), 7.49 (s, 1H), 7.52−7.54 (m, 1H); ^{13}C NMR (100 MHz, $CDCl_3$) δ 24.8, 84.8, 112.1 (d, *J* = 25.5 Hz), 118.7 (q, *J* = 318.7 Hz), 121.3 (d, *J* = 19.1 Hz), 122.8 (d, *J* = 3.3 Hz), 149.3 (d, *J* = 10.0 Hz), 162.4 (d, *J* = 250.8 Hz); ^{19}F NMR (376 MHz, $CDCl_3$) δ -109.3 (s, 1F), -72.9 (s, 3F); HRMS (EI): calculated m/z for $C_{13}H_{15}BF_4O_5S^+$ $[M]^+$: 370.0666, found 370.0682.

2-Methyl-4-(4,4,5,5-tetramethyl-1,3,2-dioxaborolan-2-yl)phenyl trifluoromethanesulfonate (Table 3.3, compound **9e**)

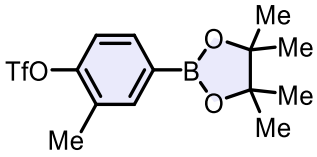

The product was obtained as a colourless liquid in 89% yield (0.886 mmol, 325 mg). The % conversion of starting material = 100%. The % of minor product (reacting C−OTf site): major product (reacting C−Cl site): diborylated product (reacting both C−OTf & C−Cl site) = 0: 100: 0. Bulb-to-bulb distillation was used at 180 °C (<1 mmHg). ^{1}H NMR (400 MHz, $CDCl_3$) δ 1.34 (s, 12H), 2.38 (s, 3H), 7.23 (d, *J* = 8.2 Hz, 1H), 7.69 (d, *J* = 8.2 Hz, 1H), 7.75 (s, 1H); ^{13}C NMR (100 MHz, $CDCl_3$) δ 16.1, 24.8, 84.2, 118.6 (q, *J* = 318.1 Hz), 120.5, 130.0, 134.2, 138.8, 150.8; ^{19}F NMR (376 MHz, $CDCl_3$) δ -73.8; HRMS (EI): calculated m/z for $C_{14}H_{18}BF_3O_5S^+$ $[M]^+$: 366.0917, found 366.0930.

2-Fluoro-4-(4,4,5,5-tetramethyl-1,3,2-dioxaborolan-2-yl)phenyl trifluoromethanesulfonate (Table 3.3, compound **9f**)

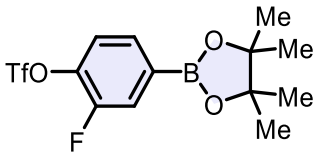

The product was obtained as a white solid in 91% yield (0.910 mmol, 337 mg). The % conversion of starting material = 100%. The % of minor product (reacting C−OTf site): major product (reacting C−Cl site): diborylated product (reacting both C−OTf & C−Cl site) = 0: 100: 0. Bulb-to-bulb distillation was used at 180 °C (<1 mmHg). The melting point was determined to be 48.7−49.9 °C. ^{1}H NMR (400 MHz, $CDCl_3$) δ 1.34 (s, 12H), 7.30−7.34 (m, 1H), 7.62−7.69 (m, 2H); ^{13}C NMR (100 MHz, $CDCl_3$) δ 24.8, 84.6, 118.7 (q, *J* = 318.7 Hz), 122.9, 123.4 (d, *J* = 16.5 Hz), 131.4 (d, *J* = 4.0 Hz), 138.9 (d, *J* = 13.5 Hz), 153.2 (d, *J* = 252.5 Hz); ^{19}F NMR (376 MHz, $CDCl_3$) δ -129.0 (m, 1F), -73.3 (m, 3F); HRMS (EI): calculated m/z for $C_{13}H_{15}BF_4O_5S^+$ $[M]^+$: 370.0666, found 370.0679.

5-(4,4,5,5-Tetramethyl-1,3,2-dioxaborolan-2-yl)pyridin-3-yl trifluoromethanesulfonate (Table 3.3, compound **9g**)

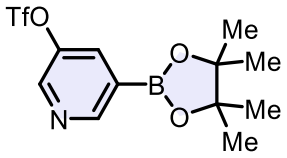

The product was obtained as a white solid in 80% yield (0.801 mmol, 283 mg). The % conversion of starting material = 97%. The % of minor product (reacting C−OTf site): major product (reacting C−Cl site): diborylated product (reacting both C−OTf & C−Cl site) = 2.2: 97.8: 0. Bulb-to-bulb distillation was used at 180 °C (<1 mmHg). The melting point was determined to be 87.8−88.9 °C. ^{1}H NMR (400 MHz, $CDCl_3$) δ 1.36 (s, 12H), 7.95 (s, 1H), 8.63 (s, 1H), 8.94 (s, 1H); ^{13}C NMR (100 MHz, $CDCl_3$) δ 24.8, 84.9, 118.6 (q, *J* = 318.8 Hz), 134.5, 144.8, 146.7, 154.9; ^{19}F NMR (376 MHz, $CDCl_3$) δ -72.7; HRMS (EI): calculated m/z for $C_{12}H_{15}BF_3NO_5S^+$ $[M]^+$: 353.0713, found 353.0700.

5-(4,4,5,5-Tetramethyl-1,3,2-dioxaborolan-2-yl)quinolin-8-yl trifluoromethanesulfonate (Table 3.3, compound **9h**)

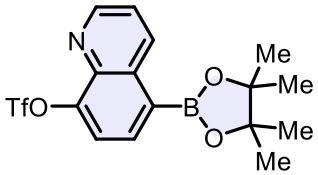

The product was obtained as white crystalline solid in 60% yield (0.596 mmol, 240 mg). The % conversion of starting material = 97%. The % of minor product (reacting C−OTf site): major product (reacting C−Cl site): diborylated product (reacting both C−OTf & C−Cl site): = 0: 100: 0. Bulb-to-bulb distillation was used at 210 °C (<2 mmHg). The melting point was determined to be

141.3−142.7 °C. ^{1}H NMR (400 MHz, $CDCl_3$) δ 1.41 (s, 12H), 7.54-7.60 (m, 2H), 8.16 (d, *J* = 7.7 Hz, 1H), 9.04 (d, *J* = 4.0 Hz, 1H), 9.18 (d, *J* = 8.6 Hz, 1H); ^{13}C NMR (100 MHz, $CDCl_3$) δ 24.9, 84.4, 118.9 (q, *J* = 318.2 Hz), 119.9, 122.7, 133.7, 135.4, 136.7, 140.7, 148.4, 151.1; ^{19}F NMR (466 MHz, $CDCl_3$) δ -73.7; HRMS (EI): calculated m/z for $C_{16}H_{17}BF_3NO_5S^+$ $[M]^+$: 403.0870, found 403.0868.

2-Methyl-5-(4,4,5,5-tetramethyl-1,3,2-dioxaborolan-2-yl)phenyl trifluoromethanesulfonate (Table 3.3, compound **9i**)

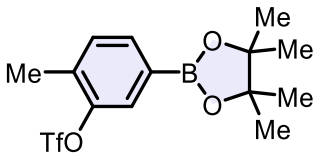

The product was obtained as a white solid in 94% yield (0.942 mmol, 345 mg). The % conversion of starting material = 99%. The % of minor product (reacting C−OTf site): major product (reacting C−Cl site): diborylated product (reacting both C−OTf & C−Cl site) = 0: 100: 0. Bulb-to-bulb distillation was used at 200 °C (<2 mmHg). The melting point was determined to be 67.8−69.2 °C. ^{1}H NMR (400 MHz, $CDCl_3$) δ 1.34 (s, 12H), 2.40 (s, 3H), 7.30 (d, *J* = 7.5 Hz, 1H), 7.64 (s, 1H), 7.70 (d, *J* = 7.5 Hz, 1H); ^{13}C NMR (100 MHz, $CDCl_3$) δ 16.6, 24.8, 84.2, 118.6 (q, *J* = 318.0 Hz), 127.1, 131.7, 134.0, 134.5, 148.4; ^{19}F NMR (376 MHz, $CDCl_3$) δ -74.0; HRMS (EI): calculated m/z for $C_{14}H_{18}BF_3O_5S^+$ $[M]^+$: 366.0917, found 366.0925.

3-Methyl-5-(4,4,5,5-tetramethyl-1,3,2-dioxaborolan-2-yl)phenyl trifluoromethanesulfonate (Table 3.3, compound **9j**)

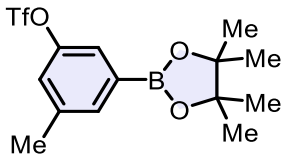

The product was obtained as a light-yellow liquid in 95% yield (0.954 mmol, 349 mg). The % conversion of starting material = 98%. The % of minor product (reacting C−OTf site): major product (reacting C−Cl site): diborylated product (reacting both C−OTf & C−Cl site) = 0: 97.8: 2.2. Bulb-to-bulb distillation was used at 180 °C (<2 mmHg). ^{1}H NMR (400 MHz, $CDCl_3$) δ 1.37 (s, 12H), 2.42 (s, 3H), 7.18 (s, 1H), 7.50 (s, 1H), 7.66 (s, 1H); ^{13}C NMR (100 MHz, $CDCl_3$) δ 21.0, 24.8, 84.3, 118.7 (q, *J* = 318.6 Hz), 123.9, 124.3, 135.3, 140.3, 149.4; ^{19}F NMR (376 MHz, $CDCl_3$) δ -73.1; HRMS (EI): calculated m/z for $C_{14}H_{18}BF_3O_5S^+$ $[M]^+$: 366.0917, found 366.0904.

2-Benzyl-4-(4,4,5,5-tetramethyl-1,3,2-dioxaborolan-2-yl)phenyl trifluoromethanesulfonate (Table 3.3, compound **9k**)

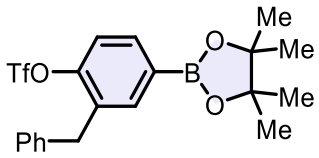

The product was obtained as a colourless liquid in 88% yield (0.876 mmol, 387 mg). The % conversion of starting material = 99%. The % of minor product (reacting C−OTf site): major product (reacting C−Cl site): diborylated product (reacting both C−OTf & C−Cl site) = 0: 100: 0. Bulb-to-bulb distillation was used at 200 °C (<2 mmHg). ^{1}H NMR (400 MHz, $CDCl_3$) δ 1.35 (s, 12H), 4.11 (s, 2H), 7.20 (d, *J* = 7.7 Hz, 2H), 7.24 (d, *J* = 7.2 Hz, 1H), 7.28−7.33 (m, 3H), 7.76−7.78 (m, 2H); ^{13}C NMR (100 MHz, $CDCl_3$) δ 24.9, 36.0, 84.3, 118.6 (q, *J* = 318.3 Hz), 120.7, 126.5, 128.6, 128.8, 132.9, 135.0, 138.7, 138.8, 150.3; ^{19}F NMR (376 MHz, $CDCl_3$) δ -73.8; HRMS (EI): calculated m/z for $C_{20}H_{22}BF_3O_5S^+$ $[M]^+$: 442.1231, found 442.1253.

2-Methoxy-4-(4,4,5,5-tetramethyl-1,3,2-dioxaborolan-2-yl)phenyl trifluoromethanesulfonate (Table 3.3 and Scheme 3.4, compound **9l**)

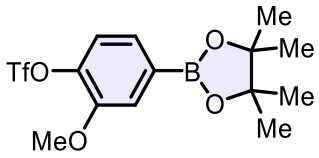

For Table 3.3, the product was obtained as a white solid in 93% yield (934 mmol, 357 mg). The % conversion of starting material = 99%. The % of minor product (reacting C−OTf site): major product (reacting C−Cl site): diborylated product (reacting both C−OTf & C−Cl site) = 0: 100: 0.

For Scheme 3.4, the product was obtained in 74% yield (14.9 mmol, 5.7 g). The % conversion of starting material = 97%. The % of minor product (reacting C−OTf site): major product (reacting C−Cl site): diborylated product (reacting both C−OTf & C−Cl site) = 0: 100: 0. Bulb-to-bulb distillation was used at 200 °C (<2 mmHg). The melting point was determined to be 87.1−88.2 °C. ^{1}H NMR (400 MHz, $CDCl_3$) δ 1.35 (s, 12H), 3.95 (s, 3H), 7.21 (d, *J* = 8.0 Hz, 1H), 7.42−7.45 (m, 2H); ^{13}C NMR (100 MHz, $CDCl_3$) δ 24.8, 56.2, 84.3, 118.7 (q, *J* = 318.4 Hz), 118.9, 121.8, 127.6, 141.0, 150.8; ^{19}F NMR (376 MHz, $CDCl_3$) δ -73.9; HRMS (EI): calculated m/z for $C_{14}H_{18}BF_3O_6S^+$ $[M]^+$: 382.0866, found 382.0859.

2-Cyano-4-(4,4,5,5-tetramethyl-1,3,2-dioxaborolan-2-yl)phenyl trifluoromethanesulfonate (Table 3.3, compound **9m**)

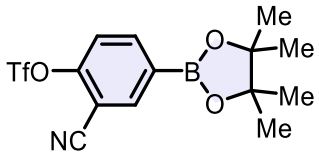

The product was obtained as a colourless liquid in 65% yield (0.646 mmol, 244 mg). The % conversion of starting material = 93%. The % of minor product (reacting C−OTf site): major

product (reacting C−Cl site): diborylated product (reacting both C−OTf & C−Cl site) = 0: 92.0: 8.0. Bulb-to-bulb distillation was used at 185 °C (<2 mmHg). ^{1}H NMR (400 MHz, $CDCl_3$) δ 1.35 (s, 12H), 7.47 (d, *J* = 8.4 Hz, 1H), 8.10 (d, *J* = 8.4 Hz, 1H), 8.18 (s, 1H); ^{13}C NMR (100 MHz, $CDCl_3$) δ 24.8, 85.0, 106.7, 113.4, 118.6 (q, *J* = 319.0 Hz), 121.7, 140.8, 140.9, 151.4; ^{19}F NMR (376 MHz, $CDCl_3$) δ -72.7; HRMS (EI): calculated m/z for $C_{14}H_{15}BF_3NO_5S^+$ $[M]^+$: 377.0713, found 377.0727.

2-Formyl-5-(4,4,5,5-tetramethyl-1,3,2-dioxaborolan-2-yl)phenyl trifluoromethanesulfonate (Table 3.3, compound **9n**)

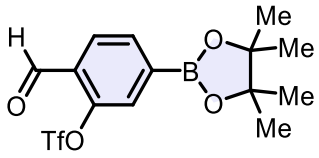

The product was obtained as a white solid in 79% yield (0.788 mmol, 300 mg). The % conversion of starting material = 99%. The % of minor product (reacting C−OTf site): major product (reacting C−Cl site): diborylated product (reacting both C−OTf & C−Cl site) = 0: 100: 0. Bulb-to-bulb distillation was used at 185 °C (<2 mmHg). The melting point was determined to be 50.5−51.7 °C. ^{1}H NMR (400 MHz, $CDCl_3$) δ 1.35 (s, 12H), 7.76 (s, 1H), 7.92−7.97 (m, 2H), 10.28 (s, 1H); ^{13}C NMR (100 MHz, $CDCl_3$) δ 24.8, 84.9, 118.6 (q, *J* = 318.6 Hz), 128.0, 129.9, 130.0, 134.9, 149.3, 186.7; ^{19}F NMR (376 MHz, $CDCl_3$) δ -73.0; HRMS (EI): calculated m/z for $C_{14}H_{16}BF_3O_6S^+$ $[M]^+$: 380.0710, found 380.0697.

2-Acetyl-5-(4,4,5,5-tetramethyl-1,3,2-dioxaborolan-2-yl)phenyl trifluoromethanesulfonate (Table 3.3, compound **9o**)

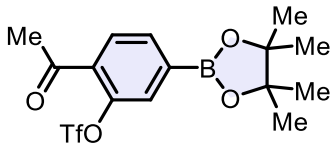

The product was obtained as a white solid in 67% yield (0.672 mmol, 265 mg). The % conversion of starting material = 90%. The % of minor product (reacting C−OTf site): major product (reacting C−Cl site): diborylated product (reacting both C−OTf & C−Cl site) = 0: 100: 0. A Bulb-to-bulb distillation was used at 190 °C (<2 mmHg). The melting point was determined to be 77.8−78.8 °C. ^{1}H NMR (400 MHz, $CDCl_3$) δ 1.35 (s, 12H), 2.63 (s, 3H), 7.70 (s, 1H), 7.76 (d, *J* = 7.6 Hz, 1H), 7.87 (d, *J* = 7.6 Hz, 1H); ^{13}C NMR (100 MHz, $CDCl_3$) δ 24.8, 29.5, 84.8, 118.6 (q, *J* = 318.6 Hz), 128.3, 129.8, 134.1, 134.6, 146.2, 197.0; ^{19}F NMR (376 MHz, $CDCl_3$) δ -73.3; HRMS (EI): calculated m/z for $C_{15}H_{18}BF_3O_6S^+$ $[M]^+$: 394.0867, found 394.0873.

3,5-Bis(4,4,5,5-tetramethyl-1,3,2-dioxaborolan-2-yl)phenyl trifluoromethanesulfonate (Table 3.3, compound **9p**)

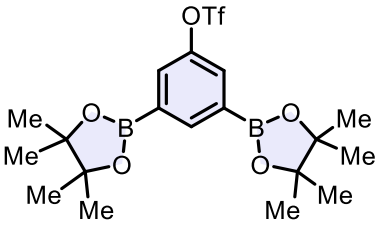

The product was obtained as a white solid in 71% yield (0.712 mmol, 340 mg). The % conversion of starting material = 100%. The % of minor product (reacting C−OTf site): major product (reacting C−Cl site): diborylated product (reacting both C−OTf & C−Cl site) = 0: 97.9: 2.1. Bulb-to-bulb distillation was used at 190 °C (<2 mmHg). The melting point was determined to be 145.7−146.9 °C. ^{1}H NMR (400 MHz, $CDCl_3$) δ 1.34 (s, 24H), 7.74 (s, 2H), 8.25 (s, 1H); ^{13}C NMR (100 MHz, $CDCl_3$) δ 24.8, 84.4, 118.7 (q, *J* = 318.4 Hz), 129.6, 140.9, 149.2; ^{19}F NMR (376 MHz, $CDCl_3$) δ -73.3; HRMS (EI): calculated m/z for $C_{19}H_{27}B_2F_3O_7S^+$ $[M]^+$: 478.1617, found 478.1615.

3-Chloro-5-(4,4,5,5-tetramethyl-1,3,2-dioxaborolan-2-yl)phenyl trifluoromethanesulfonate (Table 3.3, compound **9q**)

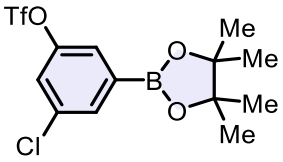

The product was obtained as a colourless liquid in 68% yield (0.680 mmol, 263 mg). The % conversion of starting material = 89%. The % of minor product (reacting C−OTf site): % of minor product (reacting C−Cl site): major product (reacting C−Br site): diborylated product (reacting both C−Br & C−Cl site): diborylated product (reacting both C−Br & C−OTf site): diborylated product (reacting both C−Cl & C−OTf site) : triborylated product (reacting both C−Br, C−Cl & C−OTf site) = 0: 0: 91.3: 8.7: 0: 0: 0. Bulb-to-bulb distillation was used at 230 °C (<2 mmHg). ^{1}H NMR (400 MHz, $CDCl_3$) δ 1.35 (s, 12H), 7.36 (s, 1H), 7.57 (s, 1H), 7.80 (s, 1H); ^{13}C NMR (100 MHz, $CDCl_3$) δ 24.8, 84.8, 118.7 (q, *J* = 318.8 Hz), 124.2, 125.2, 134.7, 135.2, 149.2; ^{19}F NMR (376 MHz, $CDCl_3$) δ -72.9; HRMS (EI): calculated m/z for $C_{13}H_{15}BClF_3O_5S^+$ $[M]^+$: 386.0371, found 386.0390.

2-Chloro-5-(4,4,5,5-tetramethyl-1,3,2-dioxaborolan-2-yl)phenyl trifluoromethanesulfonate (Table 3.3, compound **9r**)

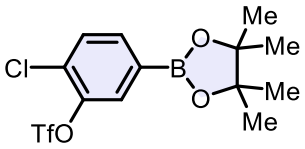

The product was obtained as a white crystalline solid in 77% yield (0.769 mmol, 297 mg). The % conversion of starting material = 95%. The % of minor product (reacting C−OTf site): % of minor product (reacting C−Cl site): major product (reacting C−Br site): diborylated product (reacting

both C−Br & C−Cl site): diborylated product (reacting both C−Br & C−OTf site): diborylated product (reacting both C−Cl & C−OTf site) : triborylated product (reacting both C−Br, C−Cl & C−OTf site) = 0: 0: 100: 0: 0: 0: 0. Bulb-to-bulb distillation was used at 200 °C (<2 mmHg). The melting point was determined to be 45.6−46.6 °C. ^{1}H NMR (400 MHz, $CDCl_3$) δ 1.34 (s, 12H), 7.51 (d, *J* = 8.2 Hz, 1H), 7.72−7.74 (m, 2H); ^{13}C NMR (100 MHz, $CDCl_3$) δ 24.8, 84.6, 118.6 (q, *J* = 318.5 Hz), 128.7, 130.1, 130.8, 135.3, 145.4; ^{19}F NMR (376 MHz, $CDCl_3$) δ -73.5; HRMS (EI): calculated m/z for $C_{13}H_{15}BClF_3O_5S^+$ $[M]^+$: 386.0371, found 386.0382.

2-Chloro-4-(4,4,5,5-tetramethyl-1,3,2-dioxaborolan-2-yl)phenyl trifluoromethanesulfonate (Table 3.3, compound **9s**)

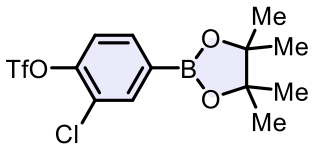

The product was obtained as an off-white solid in 84% yield (0.838 mmol, 324 mg). The % conversion of starting material = 95%. The % of minor product (reacting C−OTf site): % of minor product (reacting C−Cl site): major product (reacting C−Br site): diborylated product (reacting both C−Br & C−Cl site): diborylated product (reacting both C−Br & C−OTf site): diborylated product (reacting both C−Cl & C−OTf site) : triborylated product (reacting both C−Br, C−Cl & C−OTf site) = 0: 0: 100: 0: 0: 0: 0. Bulb-to-bulb distillation was used at 200 °C (<2 mmHg). The melting point was determined to be 47.1−48.1 °C. ^{1}H NMR (400 MHz, $CDCl_3$) δ 1.34 (s, 12H), 7.34 (d, *J* = 8.2 Hz, 1H), 7.75 (d, *J* = 8.2 Hz, 1H), 7.95 (s, 1H); ^{13}C NMR (100 MHz, $CDCl_3$) δ 24.8, 84.6, 118.6 (q, *J* = 318.6 Hz), 122.3, 126.7, 134.6, 137.5, 147.6; ^{19}F NMR (466 MHz, $CDCl_3$) δ -73.4; HRMS (EI): calculated m/z for $C_{13}H_{15}BClF_3O_5S^+$ $[M]^+$: 386.0371, found 386.0367.

4'-Benzoyl-5-methoxy-[1,1'-biphenyl]-3-yl trifluoromethanesulfonate (Table 3.4, compound **13a**)

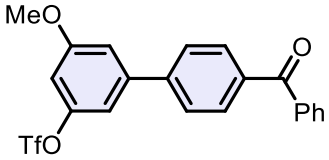

The product was obtained as a white solid in 80% yield. (0.160 mmol, 69.7 mg). Flash column chromatography was performed using ethyl acetate/hexane (1: 20) as the eluent (R_f = 0.22). The melting point was determined to be 76.3−77.3 °C. ^{1}H NMR (400 MHz, $CDCl_3$) δ 3.90 (s, 3H), 6.84 (s, 1H), 7.13 (s, 1H), 7.18 (s, 1H), 7.48−7.52 (m, 2H), 7.61 (t, *J* = 7.4 Hz, 1H), 7.66 (d, *J* = 8.4 Hz, 2H), 7.83 (d, *J* = 7.8 Hz, 2H), 7.90 (d, *J* = 8.3 Hz, 2H); ^{13}C NMR (100 MHz, $CDCl_3$) δ 55.3, 106.7, 112.3, 113.2, 118.7 (q, *J* = 318.8 Hz), 127.0, 128.3, 130.0, 130.7, 132.5, 137.3, 137.4, 142.9, 143.1, 150.5, 161.1, 196.0; ^{19}F NMR (376 MHz, $CDCl_3$) δ -72.8; HRMS (EI): calculated m/z for $C_{21}H_{15}F_3O_5S^+$ $[M]^+$: 436.0587, found 436.0593.

4'-Benzoyl-3-methyl-[1,1'-biphenyl]-4-yl trifluoromethanesulfonate (Table 3.4, compound **13b**)

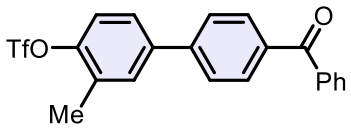

The product was obtained as a white solid in 74% yield (0.149 mmol, 62.5 mg). Flash column chromatography was performed using ethyl acetate/hexane (1: 20) as the eluent (R_f = 0.33). The melting point was determined to be 66.8−67.6 °C. ^{1}H NMR (400 MHz, $CDCl_3$) δ 2.47 (s, 3H), 7.35 (d, *J* = 8.5 Hz, 1H), 7.49−7.53 (m, 3H), 7.57 (s, 1H), 7.61 (t, *J* = 7.3 Hz, 1H), 7.66 (d, *J* = 8.2 Hz, 2H), 7.84 (d, *J* = 7.7 Hz, 2H), 7.90 (d, *J* = 8.2 Hz, 2H); ^{13}C NMR (100 MHz, $CDCl_3$) δ 16.5, 118.6 (q, *J* = 318.1 Hz), 121.8, 126.5, 127.0, 128.3, 129.9, 130.7, 131.0, 131.4, 132.5, 136.8, 137.5, 140.2, 143.3, 148.3, 196.1; ^{19}F NMR (376 MHz, $CDCl_3$) δ -73.7; HRMS (EI): calculated m/z for $C_{21}H_{15}F_3O_4S^+$ $[M]^+$: 420.0638, found 420.0645.

3-(6-Methylpyridin-2-yl)phenyl trifluoromethanesulfonate (Table 3.4, compound **13c**)

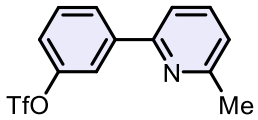

The product was obtained as a colourless liquid in 80% yield (0.160 mmol, 50.8 mg). Flash column chromatography was performed using ethyl acetate/hexane (1: 9) as the eluent (R_f = 0.42). ^{1}H NMR (400 MHz, $CDCl_3$) δ 2.63 (s, 3H), 7.15 (d, *J* = 7.6 Hz, 1H), 7.29 (d, *J* = 8.1 Hz, 1H), 7.50−7.54 (m, 2H), 7.66 (t, *J* = 7.7 Hz, 1H), 7.97−8.01 (m, 2H); ^{13}C NMR (100 MHz, $CDCl_3$) δ 24.6, 117.6, 118.8 (q, *J* = 318.8 Hz), 119.9, 121.1, 122.6, 126.6, 130.3, 137.1, 142.4, 150.1, 154.3, 158.8; ^{19}F NMR (376 MHz, $CDCl_3$) δ -72.9; HRMS (EI): calculated m/z for $C_{13}H_{10}F_3NO_3S^+$ $[M]^+$: 317.0328, found 317.0326.

5-Fluoro-3',5'-dimethoxy-[1,1'-biphenyl]-3-yl trifluoromethanesulfonate (Table 3.4, compound **13d**)

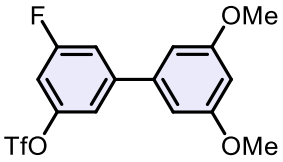

The product was obtained as a light-yellow liquid in 67% yield (0.133 mmol, 50.7 mg). Flash column chromatography was performed using ethyl acetate/hexane (1: 20) as the eluent (R_f = 0.61). ^{1}H NMR (400 MHz, $CDCl_3$) δ 3.86 (s, 6H), 6.52−6.53 (m, 1H), 6.65−6.66 (m, 2H), 7.00−7.03 (m, 1H), 7.26−7.27 (m, 1H), 7.30−7.33 (m, 1H); ^{13}C NMR (100 MHz, $CDCl_3$) δ 55.5, 100.5, 105.5, 108.3 (d, *J* = 26.1 Hz), 114.4 (d, *J* = 22.0 Hz), 116.0 (d, *J* = 3.2 Hz), 118.7 (q, *J* = 318.8 Hz), 140.1, 145.2 (d, *J* = 8.9 Hz), 149.7 (d, *J* = 12.0 Hz), 161.4, 162.8 (d, *J* = 249.1 Hz); ^{19}F NMR (376

MHz, $CDCl_3$) δ -108.2 (s, 1F), -72.7 (s, 3F); HRMS (EI): calculated m/z for $C_{15}H_{12}F_4O_5S^+$ $[M]^+$: 380.0336, found 380.0334.

3-Methyl-5-(quinolin-2-yl)phenyl trifluoromethanesulfonate (Table 3.4, compound **13e**)

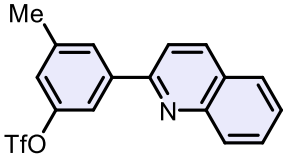

The product was obtained as a white solid in 80% yield (0.159 mmol, 58.5 mg). Flash column chromatography was performed using ethyl acetate/hexane (1: 4) as the eluent (R_f = 0.64). The melting point was determined to be 67.7−68.6 °C. ^{1}H NMR (400 MHz, $CDCl_3$) δ 2.50 (s, 3H), 7.17 (s, 1H), 7.55 (t, *J* = 7.3 Hz, 1H), 7.73−7.83 (m, 3H), 7.91 (s, 1H), 7.99 (s, 1H), 8.17 (d, *J* = 8.5 Hz, 1H), 8.21 (d, *J* = 8.6 Hz, 1H); ^{13}C NMR (100 MHz, $CDCl_3$) δ 21.4, 117.4, 118.5, 118.8 (q, *J* = 318.8 Hz), 122.2, 126.8, 127.39, 127.45, 128.0, 129.7, 129.9, 137.1, 141.2, 141.9, 148.1, 150.0, 154.9; ^{19}F NMR (376 MHz, $CDCl_3$) δ -72.9; HRMS (EI): calculated m/z for $C_{17}H_{12}F_3NO_3S^+$ $[M]^+$: 367.0485, found 368.0487.

2-Methyl-5-(6-methylpyridin-2-yl)phenyl trifluoromethanesulfonate (Table 3.4, compound **13f**)

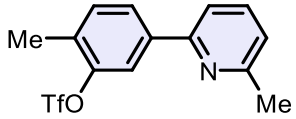

The product was obtained as a colourless liquid in 72% yield (0.145 mmol, 47.9 mg). Flash column chromatography was performed using ethyl acetate/hexane (1: 4) as the eluent (R_f = 0.65). ^{1}H NMR (400 MHz, $CDCl_3$) δ 2.42 (s, 3H), 2.62 (s, 3H), 7.12 (d, *J* = 7.6 Hz, 1H), 7.37 (d, *J* = 8.0 Hz, 1H), 7.47 (d, *J* = 7.8 Hz, 1H), 7.63 (t, *J* = 7.7 Hz, 1H), 7.89 (d, *J* = 7.9 Hz, 1H), 7.93 (s, 1H); ^{13}C NMR (100 MHz, $CDCl_3$) δ 16.2, 24.6, 117.3, 118.7 (q, *J* = 318.3 Hz), 119.8, 122.3, 126.4, 131.0, 132.2, 137.0, 139.9, 148.9, 154.5, 158.7; ^{19}F NMR (376 MHz, $CDCl_3$) δ -73.8; HRMS (EI): calculated m/z for $C_{14}H_{12}F_3NO_3S^+$ $[M]^+$: 331.0485, found 331.0480.

Methyl 4'-(4-(((trifluoromethyl)sulfonyl)oxy)benzoyl)-[1,1'-biphenyl]-4-carboxylate (Table 3.4, compound **13g**)

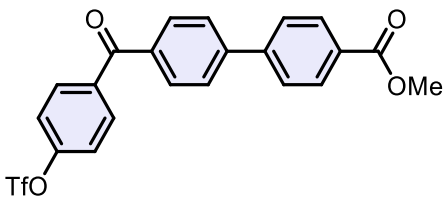

The product was obtained as a white solid in 86% yield (0.172 mmol, 80.0 mg). Flash column chromatography was performed using ethyl acetate/hexane (1: 9) as the eluent (R_f = 0.34). The melting point was determined to be 148.5−149.5 °C. ^{1}H NMR (400 MHz, $CDCl_3$) δ 3.95 (s, 3H),

7.42 (d, *J* = 8.8 Hz, 2H), 7.71 (d, *J* = 8.4 Hz, 2H), 7.75 (d, *J* = 8.4 Hz, 2H), 7.89 (d, *J* = 8.4 Hz, 2H), 7.94 (d, *J* = 8.8 Hz, 2H), 8.14 (d, *J* = 8.4 Hz, 2H); ^{13}C NMR (100 MHz, $CDCl_3$) δ 52.2, 118.7 (q, *J* = 318.7 Hz), 121.4, 127.2, 127.4, 129.9, 130.2, 130.6, 132.1, 136.0, 137.5, 144.0, 144.5, 151.9, 166.7, 194.1; ^{19}F NMR (376 MHz, $CDCl_3$) δ -72.7; HRMS (EI): calculated m/z for $C_{22}H_{15}F_3O_6S^+$ $[M]^+$: 464.0536, found 464.0526.

4'-Acetyl-3-methoxy-[1,1'-biphenyl]-4-yl trifluoromethanesulfonate (Table 3.4, compound **13h**)

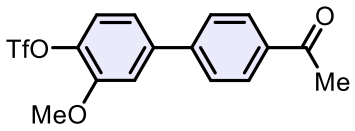

The product was obtained as a light-yellow solid in 77% yield (0.153 mmol, 57.4 mg). Flash column chromatography was performed using ethyl acetate/hexane (1: 9) as the eluent (R_f = 0.12).The melting point was determined to be 89.5−90.4 °C. ^{1}H NMR (400 MHz, $CDCl_3$) δ 2.64 (s, 3H), 3.99 (s, 3H), 7.19 (d, *J* = 8.4 Hz, 1H), 7.23 (s, 1H), 7.30 (d, *J* = 8.4 Hz, 1H), 7.64 (d, *J* = 8.4 Hz, 2H), 8.04 (d, *J* = 8.4 Hz, 2H); ^{13}C NMR (100 MHz, $CDCl_3$) δ 26.6, 56.3, 112.1, 118.7 (q, *J* = 318.7 Hz), 119.8, 122.8, 127.4, 129.0, 136.5, 138.7, 141.4, 144.2, 151.6, 197.5; ^{19}F NMR (376 MHz, $CDCl_3$) δ -73.8; HRMS (EI): calculated m/z for $C_{16}H_{13}F_3O_5S^+$ $[M]^+$: 374.0430, found 374.0432.

4-(3-Methylbenzo[*b*]thiophen-5-yl)phenyl trifluoromethanesulfonate (Table 3.4, compound **13i**)

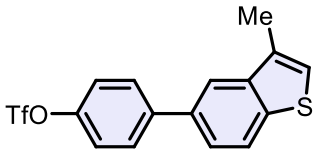

The product was obtained as a white solid in 68% yield (0.135 mmol, 50.3 mg). Flash column chromatography was performed using hexane as the eluent (R_f = 0.20). The melting point was determined to be 51.4−52.6 °C. ^{1}H NMR (400 MHz, $CDCl_3$) δ 2.50 (s, 3H), 7.16 (s, 1H), 7.38 (d, *J* = 8.8 Hz, 2H), 7.54 (d, *J* = 8.3 Hz, 1H), 7.73 (d, *J* = 8.8 Hz, 2H), 7.87 (s, 1H), 7.93 (d, *J* = 8.4 Hz, 1H); ^{13}C NMR (100 MHz, $CDCl_3$) δ 13.9, 118.8 (q, *J* = 318.8 Hz), 120.3, 121.6, 122.7, 123.2, 123.4, 129.1, 132.3, 135.4, 140.1, 140.2, 142.1, 148.8; ^{19}F NMR (376 MHz, $CDCl_3$) δ -72.7; HRMS (EI): calculated m/z for $C_{16}H_{11}F_3O_3S_2^+$ $[M]^+$: 372.0096, found 372.0099.

3'-Methyl-[1,1'-biphenyl]-4-yl trifluoromethanesulfonate (Table 3.4, compound **13j**)[37]

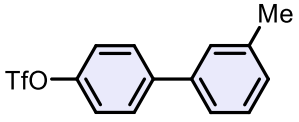

The product was obtained in 74% yield (0.149 mmol, 47.0 mg). Flash column chromatography was performed using hexane as the eluent (R_f = 0.37). ^{1}H NMR (400 MHz, $CDCl_3$) δ 2.45 (s, 3H), 7.22−7.24 (m, 1H), 7.34−7.38 (m, 5H), 7.65 (d, *J* = 8.8 Hz, 2H); ^{13}C NMR (100 MHz, $CDCl_3$) δ 21.5, 118.8 (q, *J* = 318.8 Hz), 121.5, 124.3, 128.0, 128.78, 128.85, 128.9, 138.6, 139.3, 141.8, 148.9; ^{19}F NMR (376 MHz, $CDCl_3$) δ -72.8.

4'-Formyl-[1,1'-biphenyl]-4-yl trifluoromethanesulfonate (Table 3.4, compound **13k**)

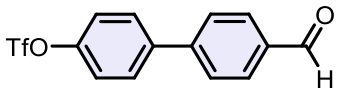

The product was obtained as a yellow solid in 74% yield (0.149 mmol, 49.1 mg). Flash column chromatography was performed using ethyl acetate/hexane (1: 9) as the eluent (R_f = 0.31). The melting point was determined to be 56.4−57.6 °C. ^{1}H NMR (400 MHz, $CDCl_3$) δ 7.40 (d, *J* = 8.8 Hz, 2H), 7.69−7.73 (m, 4H), 7.98 (d, *J* = 8.2 Hz, 2H), 10.07 (s, 1H); ^{13}C NMR (100 MHz, $CDCl_3$) δ 118.7 (q, *J* = 319.0 Hz), 121.9, 127.8, 129.2, 130.3, 135.7, 140.2, 145.0, 149.6, 191.6; ^{19}F NMR (376 MHz, $CDCl_3$) δ -72.8; HRMS (EI): calculated m/z for $C_{14}H_9F_3O_4S^+$ $[M]^+$: 330.0168, found 330.0174.

3-Benzyl-3'-methoxy-[1,1'-biphenyl]-4-yl trifluoromethanesulfonate (Table 3.4, compound **13l**)

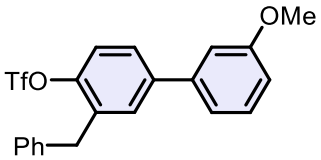

The product was obtained as a light-yellow liquid in 78% yield (0.156 mmol, 65.8 mg). Flash column chromatography was performed using ethyl acetate/hexane (1: 20) as the eluent (R_f = 0.50). ^{1}H NMR (400 MHz, $CDCl_3$) δ 3.89 (s, 3H), 4.20 (s, 2H), 6.97 (d, *J* = 8.1 Hz, 1H), 7.07 (s, 1H), 7.12 (d, *J* = 8.0 Hz, 1H), 7.27−7.32 (m, 3H), 7.36−7.42 (m, 4H), 7.47 (s, 1H), 7.54 (d, *J* = 8.5 Hz, 1H); ^{13}C NMR (100 MHz, $CDCl_3$) δ 35.9, 55.2, 113.09, 113.11, 118.6 (q, *J* = 318.1 Hz), 119.6, 121.6, 126.7, 126.8, 128.7, 129.0, 129.9, 130.5, 134.2, 138.4, 140.8, 141.5, 147.4, 160.0; ^{19}F NMR (376 MHz, $CDCl_3$) δ -73.7; HRMS (EI): calculated m/z for $C_{21}H_{17}F_3O_4S^+$ $[M]^+$: 422.0794, found 422.0803.

3.5 References

1. *Metal-Catalyzed Cross-Coupling Reactions and More*; de Meijere, A., Bräse, S., Oestreich, M., Eds.; Vol. 1−3; Wiley-VCH, 2014.

2. Lennox, A. J. J.; Lloyd-Jones, G. C. Selection of boron reagents for Suzuki−Miyaura coupling. *Chem. Soc. Rev.* **2014**, *43*, 412−443.

3. Kuehn, L.; Huang, M.; Radius, U.; Marder, T. B. Copper-Catalysed Borylation of Aryl Chlorides. *Org. Biomol. Chem.* **2019**, *17*, 6601−6606.

4. Verma, P. K.; Mandal, S.; Geetharani, K. Efficient Synthesis of Aryl Boronates via Cobalt-Catalyzed Borylation of Aryl Chlorides and Bromides. *ACS Catal.* **2018**, *8*, 4049−4054.

5. Molander, G. A.; Trice, S. L.; Tschaen, B. A Modified Procedure for the Palladium Catalyzed Borylation/Suzuki−Miyaura Cross-Coupling of Aryl and Heteroaryl Halides Utilizing Bis-Boronic Acid. *Tetrahedron* **2015**, *71*, 5758−5764.

6. Bose, S. K.; Marder, T. B. Efficient Synthesis of Aryl Boronates via Zinc-Catalyzed Cross-Coupling of Alkoxy Diboron Reagents with Aryl Halides at Room Temperature. *Org. Lett.* **2014**, *16*, 4562−4565.

7. Obligacion, J. V.; Semproni, S. P.; Chirik, P. J. Cobalt-Catalyzed C−H Borylation. *J. Am. Chem. Soc.* **2014**, *136*, 4133−4136.

8. Molander, G. A.; Trice, S. L.; Kennedy, S. M. Scope of the Two-Step, One-Pot Palladium-Catalyzed Borylation/Suzuki Cross-Coupling Reaction Utilizing Bis-Boronic Acid. *J. Org. Chem.* **2012**, *77*, 8678−8688.

9. Kleeberg, C.; Dang, L.; Lin, Z.; Marder, T. B. A Facile Route to Aryl Boronates: Room-Temperature, Copper-Catalyzed Borylation of Aryl Halides with Alkoxy Diboron Reagents. *Angew. Chem. Int. Ed.* **2009**, *48*, 5350−5354.

10. Billingsley, K. L.; Buchwald, S. L. An Improved System for the Palladium-Catalyzed Borylation of Aryl Halides with Pinacol Borane. *J. Org. Chem.* **2008**, *73*, 5589−5591.

11. Murata, M.; Sambommatsu, T.; Watanabe, S.; Masuda, Y. An Efficient Catalyst system for Palladium-Catalyzed Borylation of Aryl Halides with Pinacolborane. *Synlett* **2006**, *2006*, 1867−1870.

12. Murata, M.; Oyama, T.; Watanabe, S.; Masuda, Y. Palladium-Catalyzed Borylation of Aryl Halides or Triflates with Dialkoxyborane: A Novel and Facile Synthetic Route to Arylboronates. *J. Org. Chem.* **2000**, *65*, 164−168.

13. Ishiyama, T.; Murata, M.; Miyaura, N. Palladium(0)-Catalyzed Cross-Coupling Reaction of Alkoxydiboron with Haloarenes: A Direct Procedure for Arylboronic Esters. *J. Org. Chem.* **1995**, *60*, 7508−7510.

14. Chow, W. K.; Yuen, O. Y.; Choy, P. Y.; So, C. M.; Lau, C. P.; Wong, W. T.; Kwong, F. Y. A Decade Advancement of Transition Metal-Catalyzed Borylation of Aryl Halides and Sulfonates. *RSC Adv.* **2013**, *3*, 12518−12539.

15. He, J.; Jiang, H.; Takise, R.; Zhu, R.-Y.; Chen, G.; Dai, H.-X.; Dhar, T. G. M.; Shi, J.; Zhang, H.; Cheng, P. T. W.; Yu, J.-Q. Ligand-Promoted Borylation of C(sp^3)−H Bonds with Palladium(II) Catalysts. *Angew. Chem. Int. Ed.* **2016**, *55*, 785−789.

16. Chen, Y.; Peng, H.; Pi, Y.-X.; Meng, T.; Lian, Z.-Y.; Yan, M.-Q.; Liu, Y.; Liu, S.-H.; Yu, G.-A. Efficient Phosphine Ligands for the One-Pot Palladium-Catalyzed Borylation/Suzuki−Miyaura Cross-Coupling Reaction. *Org. Biomol. Chem.* **2015**, *13*, 3236−3242.

17. Li, P.; Fu, C.; Ma, S. Gorlos-Phos for Palladium-Catalyzed Borylation of Aryl Chlorides. *Org. Biomol. Chem.* **2014**, *12*, 3604−3610.

18. Chow, W. K.; Yuen, O. Y.; So, C. M.; Wong, W. T.; Kwong, F. Y. Carbon−Boron Bond Cross-Coupling Reaction Catalyzed by −PPh_2 Containing Palladium−Indolylphosphine Complexes. *J. Org. Chem.* **2012**, *77*, 3543−3548.

19. Vogels, C. M.; Westcott, S. A. Sterically Demanding Aryl Chlorides: No Longer a Problem for Borylations. *ChemCatChem* **2012**, *4*, 47−49.

20. Chow, W. K.; So, C. M.; Lau, C. P.; Kwong, F. Y. Palladium-Catalyzed Borylation of Aryl Mesylates and Tosylates and Their Applications in One-Pot Sequential Suzuki−Miyaura Biaryl Synthesis. *Chem. Eur. J.* **2011**, *17*, 6913−6917.

21. Varni, A. J.; Bautista, M. V.; Noonan, K. J. T. Chemoselective Rhodium-Catalyzed Borylation of Bromoiodoarenes Under Mild Conditions. *J. Org. Chem.* **2020**, *85*, 6770−6777.

22. Yoshida, H.; Kamio, S.; Osaka, I. Copper-catalyzed Borylation of Bromoaryl Triflates with Diborons: Chemoselective Replacement of an Ar−Br Bond. *Chem. Lett.* **2018**, *47*, 957−959.

23. Franco, M.; Sainz, R.; Lamsabhi, A. M.; Díaz, C.; Tortosa, M.; Cid, M. B. Evaluation of the Role of Graphene-Based Cu(I) Catalysts in Borylation Reactions. *Catal. Sci. Technol.* **2021**, *11*, 3501−3513.

24. Ratniyom, J.; Dechnarong, N.; Yotphan, S.; Kiatisevi, S. Convenient Synthesis of Arylboronates through a Synergistic Pd/Cu-Catalyzed Miyaura Borylation Reaction under Atmospheric Conditions. *Eur. J. Org. Chem.* **2014**, *2014*, 1381−1385.

25. Li, Y.; Dang, Y.; Li, D.; Pan, H.; Zhang, L.; Wang, L.; Cao, Z.; Li, Y. Zinc Complexes with an Ethylene-Bridged Bis(β-diketiminate) Ligand: Syntheses, Structures, and Applications as Catalysts in the Borylation of Aryl Iodides. *Organometallics* **2021**, *40*, 482−489.

26. Wern, C.; Ehrenreich, C.; Joosten, D.; vom Stein, T.; Buchholz, H.; König, B. Rapid Access to Bi- and Tri-Functionalized Dibenzofurans and their Application in Selective Suzuki−Miyaura Cross Coupling Reactions. *Eur. J. Org. Chem.* **2018**, *2018*, 5644−5656.

27. Herbert, J. M.; Kohler, A. D.; Le Strat, F.; Whitehead, D. Aryl Fluoroalkanesulfonate Chemistry. A New Approach to Labelled Arene Elaboration. *J. Labelled Compd. Radiopharm.* **2007**, *50*, 440−441.

28. Reeves, E. K.; Entz, E. D.; Neufeldt, S. R. Chemodivergence between Electrophiles in Cross-Coupling Reactions. *Chem. Eur. J.* **2021**, *27*, 6161−6177.

29. Almond-Thynne, J.; Blakemore, D. C.; Pryde, D. C.; Spivey, A. C. Site-Selective Suzuki−Miyaura Coupling of Heteroaryl Halides − Understanding the Trends for Pharmaceutically Important Classes. *Chem. Sci.* **2017**, *8*, 40−62.

30. Fairlamb, I. J. S. Regioselective (Site-Selective) Functionalisation of Unsaturated Halogenated Nitrogen, Oxygen and Sulfur Heterocycles by Pd-Catalysed Cross-Couplings and Direct Arylation Processes. *Chem. Soc. Rev.* **2007**, *36*, 1036−1045.

31. Kamikawa, T.; Hayashi, T. Control of Reactive Site in Palladium-Catalyzed Grignard Cross-Coupling of Arenes Containing Both Bromide and Triflate. *Tetrahedron Lett.* **1997**, *38*, 7087−7090.

32. Littke, A. F.; Dai, C.; Fu, G. C. Versatile Catalysts for the Suzuki Cross-Coupling of Arylboronic Acids with Aryl and Vinyl Halides and Triflates under Mild Conditions. *J. Am. Chem. Soc.* **2000**, *122*, 4020−4028.

33. Espino, G.; Kurbangalieva, A.; Brown, J. M. Aryl Bromide/Triflate Selectivities Reveal Mechanistic Divergence in Palladium-Catalyzed Couplings; the Suzuki−Miyaura Anomaly. *Chem. Commun.* **2007**, *2007*, 1742−1744.

34. Proutiere, F.; Schoenebeck, F. Solvent Effect on Palladium-Catalyzed Cross-Coupling Reactions and Implications on the Active Catalytic Species. *Angew. Chem. Int. Ed.* **2011**, *50*, 8192−8195.

35. Proutiere, F.; Lyngvi, E.; Aufiero, M.; Sanhueza, I. A.; Schoenebeck, F. Combining the Reactivity Properties of PCy_3 and $PtBu_3$ into a Single Ligand, P(*i*Pr)(*t*Bu)$_2$. Reaction via Mono- or Bisphosphine Palladium(0) Centers and Pd(I) Dimer Formation. *Organometallics* **2014**, *33*, 6879−6884.

36. Reeves, E. K.; Humke, J. N.; Neufeldt, S. R. *N*-Heterocyclic Carbene Ligand-Controlled Chemodivergent Suzuki−Miyaura Cross Coupling. *J. Org. Chem.* **2019**, *84*, 11799−11812.

37. So, C. M.; Yuen, O. Y.; Ng, S. S.; Chen, Z. General Chemoselective Suzuki−Miyaura Coupling of Polyhalogenated Aryl Triflates Enabled by an Alkyl-Heteroaryl-Based Phosphine Ligand. *ACS Catal.* **2021**, *11*, 7820−7827.

38. Hu, Z.; Wei, X.-J.; Handelmann, J.; Seitz, A.-K.; Rodstein, I.; Gessner, V. H.; Gooßen, L. J. Coupling of Reformatsky Reagents with Aryl Chlorides Enabled by Ylide-Functionalized Phosphine Ligands. *Angew. Chem. Int. Ed.* **2021**, *60*, 6778−6783.

39. Littke, A. F.; Schwarz, L.; Fu, G. C. Pd/P(*t*-Bu)$_3$: A Mild and General Catalyst for Stille Reactions of Aryl Chlorides and Aryl Bromides. *J. Am. Chem. Soc.* **2002**, *124*, 6343−6348.

40. Armarego, W. L. F.; Chai, C. L. L. *Purification of Laboratory Chemicals*, 6th ed.; Butterworth-Heinemann, 2009.

41. So, C. M.; Zhou, Z.; Lau, C. P.; Kwong, F. Y. Palladium-Catalyzed Amination of Aryl Mesylates. *Angew. Chem. Int. Ed.* **2008**, *47*, 6402−6406.

42. Chung, K. H.; So, C. M.; Wong, S. M.; Luk, C. H.; Zhou, Z.; Lau, C. P.; Kwong, F. Y. An Efficient Palladium−Benzimidazolyl Phosphine Complex for the Suzuki−Miyaura Coupling of Aryl Mesylates: Facile Ligand Synthesis and Metal Complex Characterization. *Chem. Commun.* **2012**, *48*, 1967−1969.

43. Aufiero, M.; Sperger, T.; Tsang, A. S.-K.; Schoenebeck, F. Highly Efficient C−$SeCF_3$ Coupling of Aryl Iodides Enabled by an Air-Stable Dinuclear Pd^{I} Catalyst. *Angew. Chem. Int. Ed.* **2015**, *54*, 10322−10326.

44. Keaveney, S. T.; Kundu, G.; Schoenebeck, F. Modular Functionalization of Arenes in a Triply Selective Sequence: Rapid C(sp^2) and C(sp^3) Coupling of C−Br, C−OTf, and C−Cl Bonds Enabled by a Single Pd(I) Dimer. *Angew. Chem. Int. Ed.* **2018**, *57*, 12573−12577.

45. Smyth, L. A.; Phillips, E. M.; Chan, V. S.; Napolitano, J. G.; Henry, R.; Shekhar, S. Pd-Catalyzed Synthesis of Aryl and Heteroaryl Triflones from Reactions of Sodium Triflinate with Aryl (Heteroaryl) Triflates. *J. Org. Chem.* **2016**, *81*, 1285−1294.

46. Wang, D.; Mück-Lichtenfeld, C.; Studer, A. Hydrogen Atom Transfer Induced Boron Retaining Coupling of Organoboronic Esters and Organolithium Reagents. *J. Am. Chem. Soc.* **2019**, *141*, 14126−14130.

4. Chapter 4: Palladium-Catalysed Chemoselective Suzuki−Miyaura Cross-Coupling Reaction of Poly(pseudo)halogenated Arenes

4.1 Introduction

The formation of carbon−carbon bonds via Pd-catalysed cross-coupling reactions, including Suzuki−Miyaura coupling, is an extremely versatile strategy in organic synthesis.[1−5] Yet, maintaining high chemoselectivity when working with polyhalogenated arenes continues to pose challenges. The preferential oxidative addition of the palladium catalyst to one of the potential electrophilic sites is a key factor that dictates the chemoselectivity. The typical reactivity order observed is Ar−I > Ar−OTf ≈ Ar−Br > Ar−Cl, with aryl iodides being the most reactive.[6−7] However, the electronic and steric attributes of the substrate can override these general patterns, resulting in unexpected or divergent chemoselectivities.[8−9]

Various strategies have been investigated to achieve the selective cross-coupling of polyhalogenated arenes.[10−11] While ligand effects can help modulate the selectivity, the optimal conditions often depend on the specific substrate.[12−14] Certain defined Pd(I) catalysts have demonstrated promise for preferential C−Br activation in Kumada and Negishi couplings.[7,15−18] Extending this approach to Suzuki coupling could potentially offer a broadly applicable and predictable protocol for the chemoselective functionalisation of polyhalogenated arenes.

Despite these developments, several unresolved limitations persist. The chemoselective cross-coupling of substrates bearing multiple (pseudo)halides typically requires a high catalyst loading (3.0−5.0 mol% Pd),[10−11] which contrasts sharply with the cross-coupling of mono(pseudo)halide reactions that only need trace amounts of the Pd-catalyst to achieve an excellent substrate scope and yield.[19−22] As a result, higher catalyst loadings, longer reaction times, and more reactive nucleophiles are necessary to compensate for the reduced reactivity and substrate scope, which also restricts their application in routine synthesis (Scheme 4.1). Therefore, the development of a generally applicable palladium catalyst system for chemoselective reactions to access polyfunctionalised arenes remains in high demand.

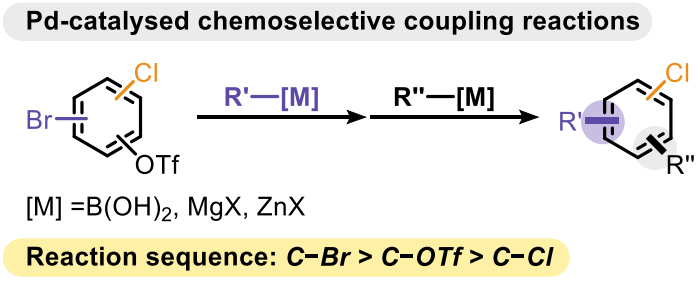

Scheme 4.1 Pd-catalysed chemoselective coupling reactions

The key to advancing cross-coupling reactions lies in the design and development of innovative ligand frameworks.[23–29] Ligands with an aryl bottom ring have exhibited several advantages in recent decades, including increased stability, enhanced reductive elimination, and enabling high reactivity.[30–31]

Our research group has recently designed and developed a series of alkyl–heteroaryl-based phosphine ligands (SelectPhos and *t*-BuPhSelectPhos) and successfully employed them in chemoselective Suzuki–Miyaura,[32] Sonogashira coupling,[33] borylation,[34] carbonyl compound α-arylation,[35] and desulfination[36] reactions, exhibiting an inverted conventional chemoselectivity order of C–Cl > C–OTf. The methine hydrogen and the steric hindrance of the C2-cyclohexyl group in SelectPhos were found to be critical factors in reactivity and chemoselectivity. Notably, the SelectPhos ligands can be readily synthesised and purified on a large scale, facilitating their practical applications.

In the field of biaryl and terphenyl derivative synthesis, the Suzuki–Miyaura coupling reaction has undoubtedly demonstrated its effectiveness for bromoaryl triflates and bromochloroaryl triflates.[32] Nonetheless, exploring a broader range of possible substrates could be beneficial, particularly considering the advantages of minimising palladium catalyst usage. This untapped potential presents an exciting opportunity to expand both the scope and applicability of the reaction.

In this study, we demonstrate a series of general examples showcasing the Pd-catalysed chemoselective Suzuki–Miyaura cross-coupling reactions of bromo(hetero)aryl triflates. Notably, these reactions display a reactivity order of C–Br > C–OTf, even with low palladium catalyst loadings as minimal as 0.020 mol% Pd. Interestingly, this selectivity is unaffected by the electronic and steric properties of the substrates, as well as the relative positioning of the competing reaction sites. Additionally, we have successfully performed one-pot sequential couplings without the need for intermediate purification, further revealing the reactivity order of C–Br > C–Cl > C–OTf (Scheme 4.2).

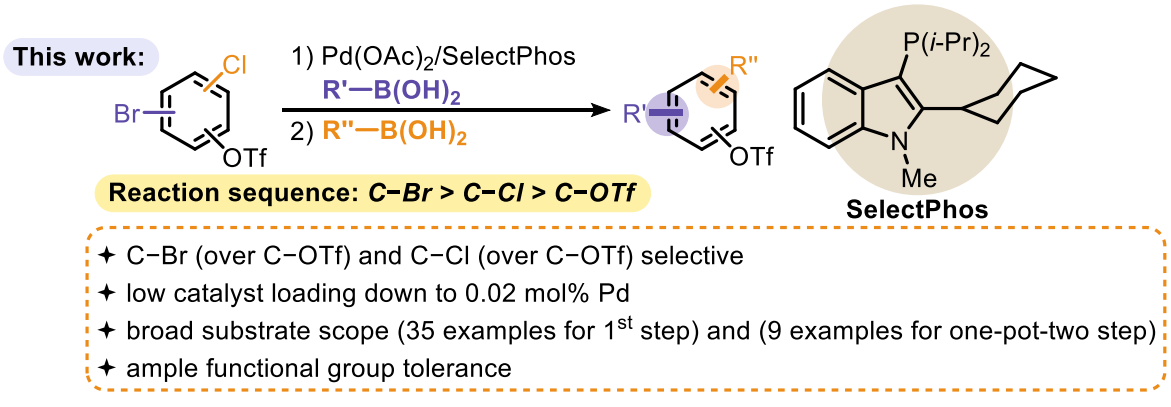

Scheme 4.2 Pd-catalysed chemoselective Suzuki–Miyaura cross-coupling reaction

4.2 Result and Discussion

4.2.1 Initial screening of ligands

Our investigation began by using 4-bromophenyl triflate **14a** and 2-tolylboronic acid **15a** as model substrates. We initially screened a range of commercially available ligands, as well as C2-alkyl-indolyl phosphines (Table 4.1). In this evaluation, **L1** emerged as a better ligand candidate than **L5**, as the former demonstrated excellent chemoselectivity by coupling exclusively at the C−Br site, while **L5** produced a small amount of the diarylated product. **L2**−**L4** exhibited inferior reactivity. Additionally, the commercially available phosphine ligands tested (**L6**−**L10**) showed poor chemoselectivity or reactivity at the C−Br site.

Table 4.1 Screening of ligands for chemoselective C−Br (over C−OTf) Suzuki−Miyaura cross-coupling reaction of 4-bromophenyl triflate **14a**[a]

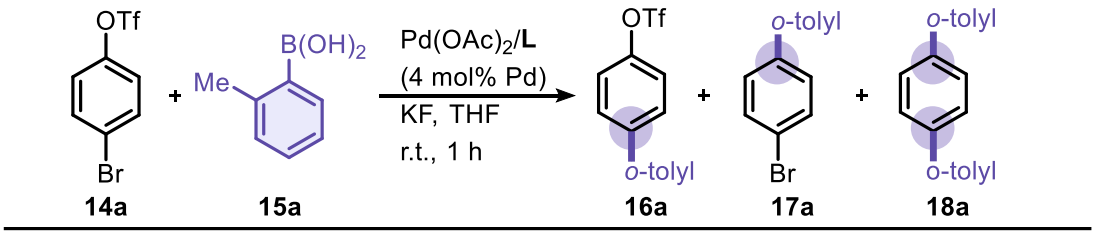

Ligands:

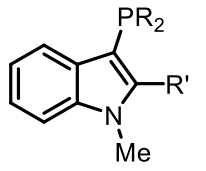

L1: R = *i*-Pr, R' = Cy (SelectPhos)
L2: R = Cy, R' = Cy (CySelectPhos)
L3: R = Ph, R' = Cy (PhSelectPhos)
L4: R = Cy, R' = 1-Ad
L5: R = *i*-Pr, R' = Ph

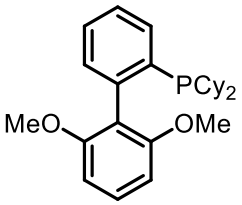

L6: SPhos

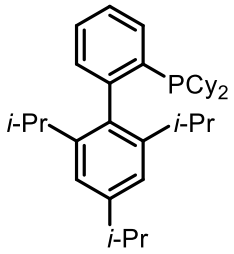

L7: XPhos

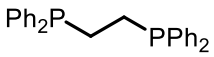

L8: dppe

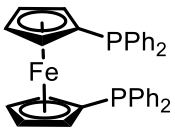

L9: dppf

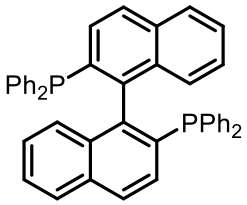

L10: BINAP

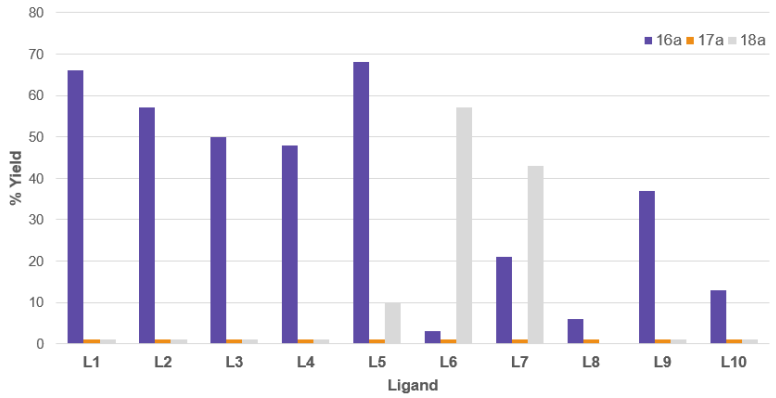

Entry	Ligands	Yield of **16a** (%)	Yield of **17a** (%)	Yield of **18a** (%)
1	**L1**	66	1	1
2	**L2**	57	1	1
3	**L3**	50	1	1
4	**L4**	48	1	1
5	**L5**	68	1	10
6	**L6**	3	1	57
7	**L7**	21	1	43
8	**L8**	6	1	0
9	**L9**	37	1	1
10	**L10**	13	1	1

[a]Reaction conditions: 4-bromophenyltriflate (0.20 mmol), 2-tolylboronic acid (0.20 mmol), $Pd(OAc)_2$ (4.0 mol%), ligand (4.0 mol%), KF (0.60 mmol), and THF (0.60 mL) were stirred under N_2 at room temperature for 1 hour. Calibrated GC yields were reported using dodecane as the internal standard.

4.2.2 Optimisation of reaction conditions

In order to enhance the effectiveness of the Pd/**L1** catalyst system, we explored the reaction conditions with different solvents and bases (Table 4.2). We screened a range of commonly used solvents (Table 4.2, entries 1−6), and found that THF and *tert*-butanol provided comparable product yields of **16a**. Upon extending the reaction time to 1 hour, *tert*-butanol emerged as the optimal solvent for this transformation (Table 4.2, entries 7−8). Furthermore, we surveyed various inorganic bases (Table 4.2, entries 5 versus 9−11), with KF exhibiting the best performance.

Table 4.2 Optimisation of reaction conditions for chemoselective C−Br (over C−OTf) Suzuki−Miyaura cross-coupling reaction of 4-bromophenyl triflate **14a**[a]

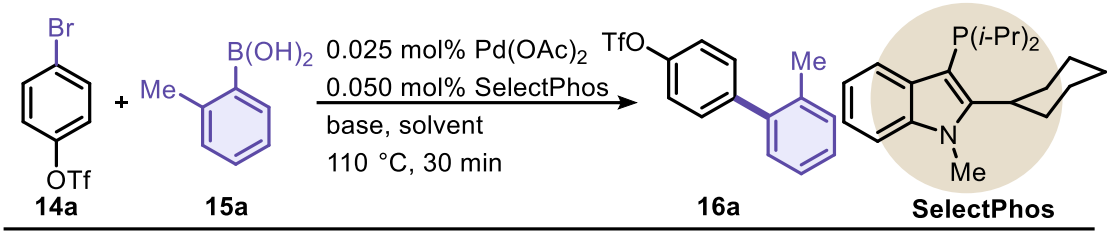

Entry	Base	Solvent	Time (min)	Yield of 16a (%)[b]
1	KF	THF	30	58
2	KF	dioxane	30	20
3	KF	toluene	30	16
4	KF	CPME	30	42
5	KF	*t*-BuOH	30	60
6	KF	DMF	30	trace
7	KF	THF	60	75
8	KF	*t*-BuOH	60	99% (90%)[c]
9	NaF	*t*-BuOH	30	trace
10	K_2CO_3	*t*-BuOH	30	51
11	Na_2CO_3	*t*-BuOH	30	47

[a]Reaction conditions: 4-bromophenyl triflate (0.20 mmol), 2-tolylboronic acid (0.20 mmol), $Pd(OAc)_2$ (0.025 mol%), **L1** (0.050 mol%), base (0.60 mmol), and solvent (0.60 mL) were stirred under N_2 at 110 °C for 30 minutes. [b] Calibrated GC yields were reported using dodecane as the internal standard. [c] Isolated yield.

4.2.3 Palladium-catalysed chemoselective Suzuki−Miyaura coupling of bromoaryl triflates

Building upon the excellent selectivity and high practicality observed in the C−Br coupling preference, we set out to explore the generality of this approach (Table 4.3). Notably, the C−Br bond was selectively arylated, regardless of the relative positioning of the competing reaction sites or the nature of the arylboronic acids. This selectivity extended to a diverse range of substrates, including heteroarylboronic acids such as 4-dibenzofuranylboronic acid, 4-dibenzothienylboronic acid, benzo[*b*]thien-2-ylboronic acid, and 2-benzofuranylboronic acid (Table 4.3, **16i**−**16l**). Furthermore, the mild reaction conditions were compatible with common functional groups like ester, aldehyde, and nitrile (Table 4.3, **16o**−**16q**). Interestingly, even sterically hindered substrates did not compromise the selectivity of C−Br over C−OTf, allowing for the synthesis of tri-*ortho*-substituted biaryl compounds (Table 4.3, **16n**−**16s**). Additionally, bromochloroaryl triflates were found to be viable cross-coupling partners, with both the C−Cl and C−OTf sites remaining untouched (Table 4.3, **16t**−**16y**). Remarkably, we achieved a high turnover frequency (average TOF > 2200) and high chemoselectivity (> 99: 1 C−Br selectivity) for a wide array of bromoaryl and bromochloroaryl triflates (Table 4.3, **16b**−**16f**, **16h**, **16i**, **16m**, **16n**, and **16u**). These results offer an efficient pathway for chemoselective coupling reactions involving electrophiles with multiple reactive sites, surpassing the limitations reported in previous studies.[37−40] With its high reactivity and exceptional chemoselectivity, the Pd/**L1** catalyst system presents great potential for further applications.

Table 4.3 Pd-catalysed chemoselective C−Br (over C−OTf) Suzuki−Miyaura cross-coupling reaction of bromo(chloro)aryl triflates[a]

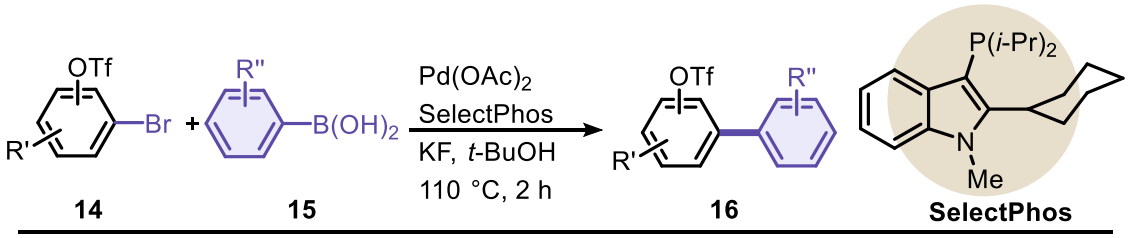

14 **15** **16** **SelectPhos**

16b
92%
(0.02 mol% Pd)

16c
97%
(0.02 mol% Pd)

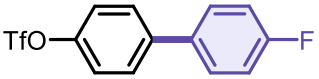

16d
97%
(0.02 mol% Pd)

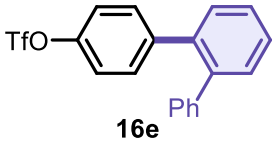

16e
85%
(0.02 mol% Pd)

16f
96%
(0.02 mol% Pd)

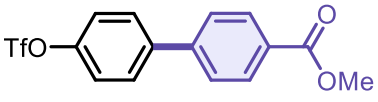

16g
85%
(0.05 mol% Pd)

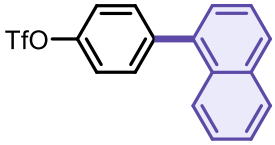

16h
97%
(0.02 mol% Pd)

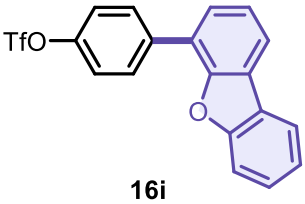

16i
96%
(0.02 mol% Pd)

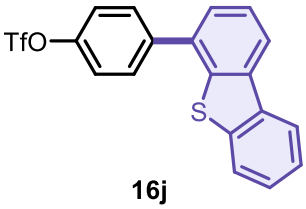

16j
98%
(0.05 mol% Pd)

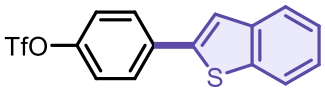

16k
85%
(0.2 mol% Pd)[b]

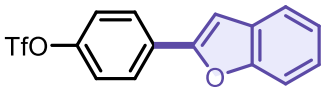

16l
92%
(0.2 mol% Pd)[b]

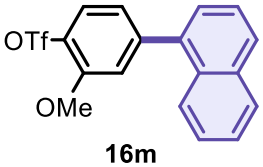

16m
99%
(0.02 mol% Pd)

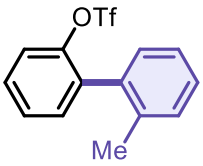

16n
77%
(0.02 mol% Pd)

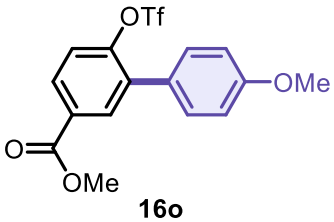

16o
83%
(0.25 mol% Pd)[c,d,e]

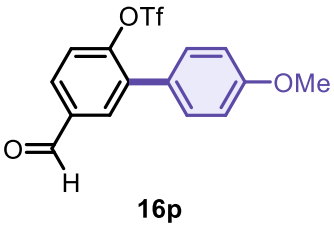

16p
50%
(0.5 mol% Pd)[c,d,e]

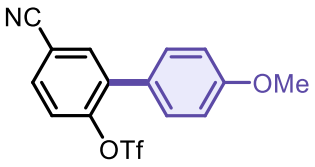

16q

87%
(0.25 mol% Pd)[c,d,e]

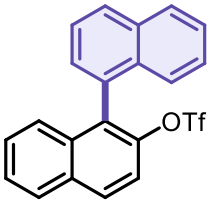

16r

50%
(0.1 mol% Pd)[c,f]

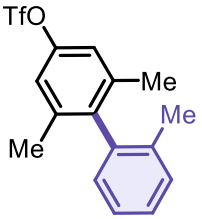

16s

96%
(0.1 mol% Pd)[c,f]

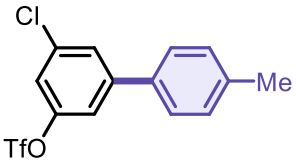

16t

82%
(0.25 mol% Pd)[d,e]

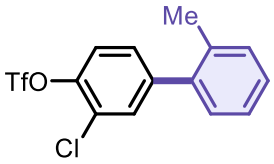

16u

79%
(0.02 mol% Pd)

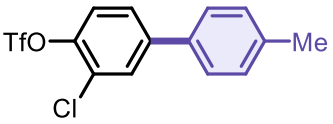

16v

94%
(0.5 mol% Pd)[d,g,h]

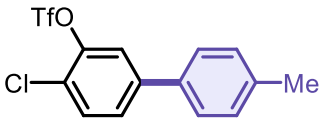

16w

90%
(0.5 mol% Pd)[d,g,h]

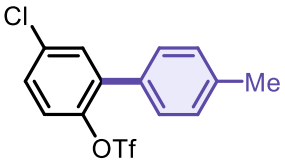

16x

77%
(0.5 mol% Pd)[c,d,h]

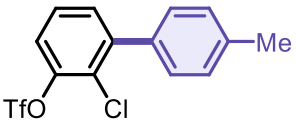

16y

85%
(0.5 mol% Pd)[c,d,h]

[a]Reaction conditions: bromo(chloro)aryl triflate (0.2 mmol), arylboronic acid (0.2 mmol), $Pd(OAc)_2$: **L1** = 1: 2, KF (0.6 mmol), and *t*-BuOH (0.6 mL) were stirred under N_2 at 110 °C for 2 hours. Isolated yields were reported. [b]Reaction time of 1 hour. [c]1.5 equiv. of arylboronic acid was used. [d]Toluene was the solvent. [e]Reaction time of 4 hours. [f]Reaction time of 3 hours. [g]1.2 equiv. arylboronic acid was used. [h]Reaction time of 1.5 hours.

4.2.4 Palladium-catalysed chemoselective Suzuki−Miyaura coupling of bromopyridyl triflates

Bromopyridyl triflates were investigated as substrates for this chemoselective Suzuki coupling reaction (Table 4.4). Generally, the reactivity of pyridine C−X bonds towards Pd(0) follows the order C2 > C4 > C3/C5.[9] In our cases, the selectivity for C−Br occurred, leaving the more activated C−OTf site untouched, especially the C2−OTf site (Table 4.4, **16aa**−**16ac**, **16ae**−**16ai**). The reaction proved to be completely selective, affording the products resulting from C−Br arylation with good-to-excellent yields. The synthesis of biheteroaryl derivatives is a challenging reaction, but in our catalyst system, bromopyridyl triflates reacted effectively with benzothienyl boronic acids at the C−Br site (Table 4.4, **16af**−**16ai**).

Table 4.4 Pd-catalysed chemoselective C−Br (over C−OTf) Suzuki−Miyaura cross-coupling reaction of bromopyridyl triflates[a]

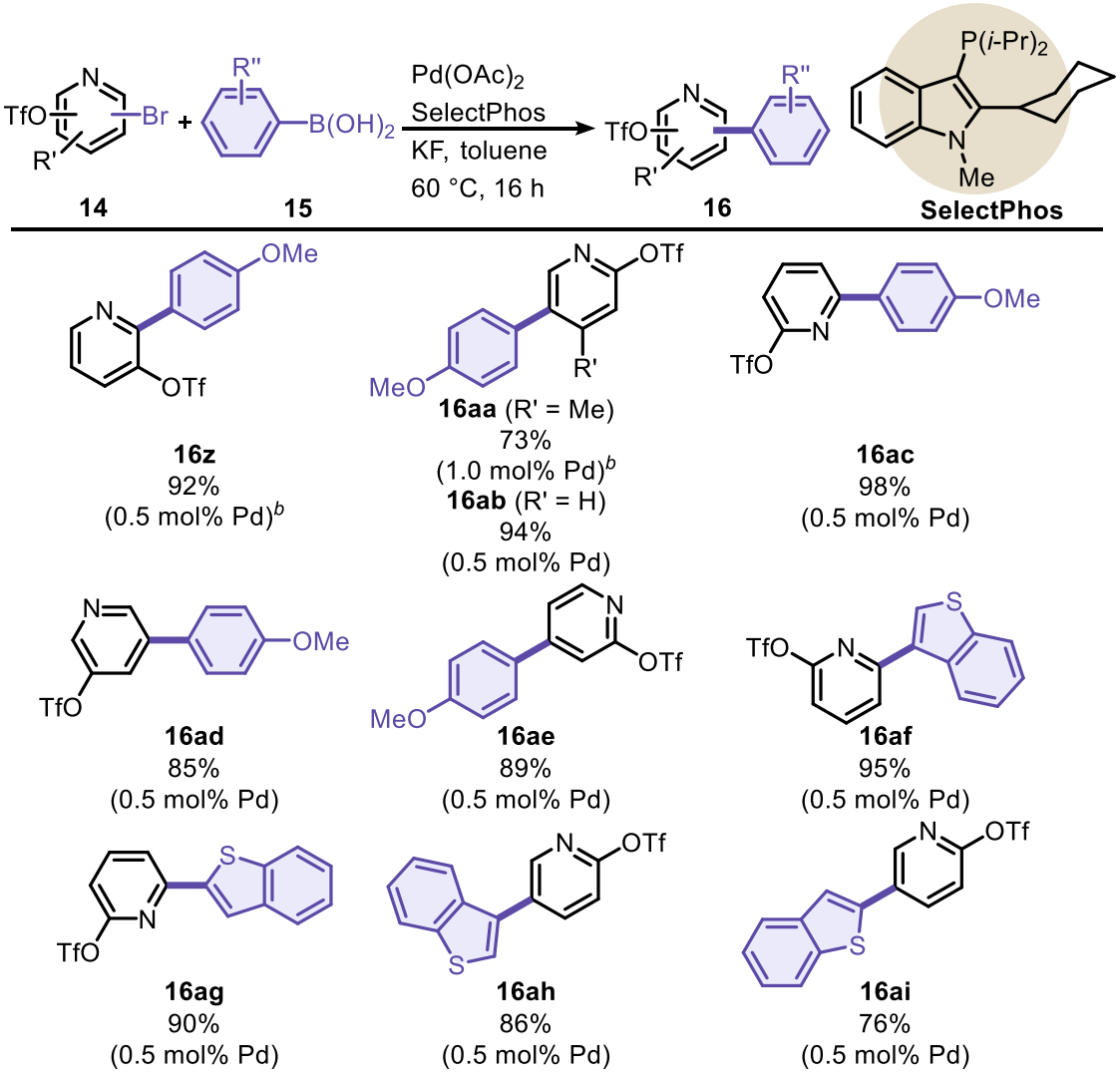

[a] Reaction condition: bromo(chloro)aryl triflate (0.20 mmol), arylboronic acid (0.30 mmol), $Pd(OAc)_2$: **L1** = 1: 2, KF (0.6 mmol), and toluene (0.60 mL) were stirred under N_2 at 60 °C for 16 hours. Isolated yields were reported. [b]Reaction time of 18 hours.

4.2.5 Palladium-catalysed sequential double functionalisation of bromochloroaryl triflates

An unconventional chemoselective sequence of C−Br > C−Cl > C−OTf was achieved through a one-pot process involving C−Br reaction followed by C−Cl functionalisation, without purifying the intermediate (Table 4.5). This sequence enabled the synthesis of disubstituted products in good-to-excellent yields using a single catalyst comprising $Pd(OAc)_2$ and **L1**. Remarkably, the C−OTf site remained intact throughout the process. Importantly, no additional catalyst was added before the second chemoselective C−Cl Suzuki−Miyaura step. This precise selectivity control permits the use of bromochloroaryl triflates for the unsymmetrical synthesis of structurally complex molecules in sequential cross-coupling strategies, as the C−OTf site is preserved for further functionalisation.

Table 4.5 Sequential two-stage functionalisation of bromochloroaryl triflates[a]

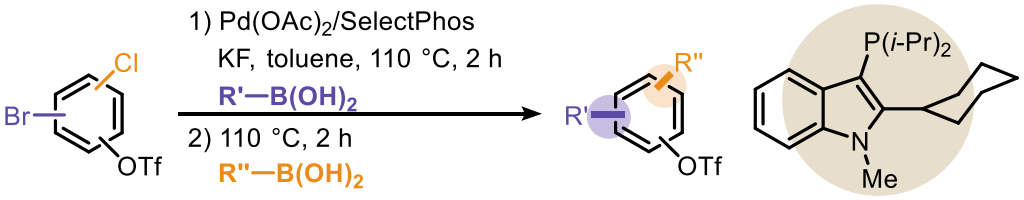

19 **20** **SelectPhos**

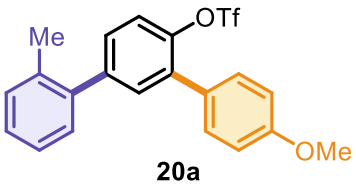

20a
80%
(0.5 mol% Pd)

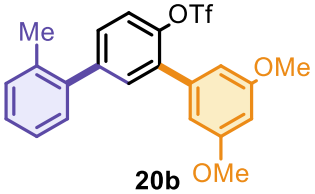

20b
80%
(0.5 mol% Pd)

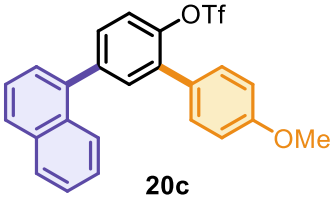

20c
71%
(0.5 mol% Pd)

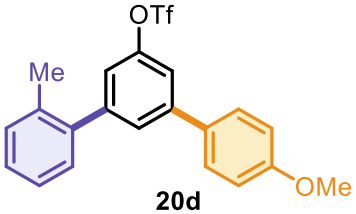

20d
88%
(0.5 mol% Pd)[b]

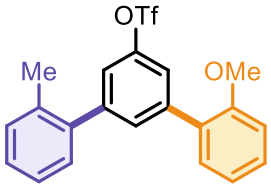

20e
93%
(0.5 mol% Pd)[b,c]

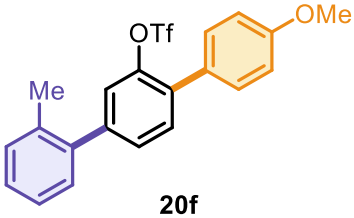

20f
90%
(0.5 mol% Pd)

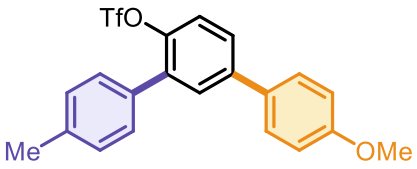

20g
71%
(0.5 mol% Pd)[b]

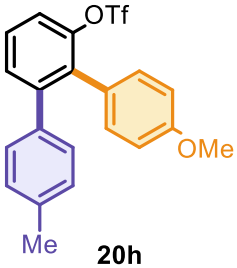

20h
82%
(0.5 mol% Pd)[b]

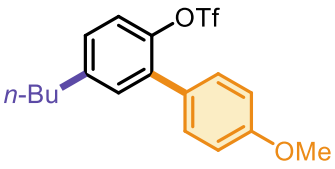

20i
61%
(0.5 mol% Pd)

[a]1st Step: bromochloroaryl triflate (0.20 mmol), arylboronic acid (0.20 mmol), $Pd(OAc)_2$ (0.50 mol%), **L1** (1.0 mol%), KF (1.2 mmol), and toluene (0.60 mL) were stirred under N_2 at 110 °C for 2 hours. 2nd Step: An additional arylboronic acid (0.40 mmol) was then added, and the reaction mixture was stirred under N_2 at 110 °C for 2 hours. Isolated yields were reported. [b]1.2 equiv. of arylboronic acid was used in the first step. [c]1.5 equiv. of arylboronic acid was used in the second step.

4.3 Summary

In summary, a Pd-catalysed Suzuki−Miyaura cross-coupling reaction has been developed, involving polyhalogenated aryl triflates and (hetero)arylboronic acids. This reaction exhibits an unconventional reactivity order of C−Br > C−Cl > C−OTf, and utilises a catalyst system comprising $Pd(OAc)_2$ and SelectPhos (**L1**). The catalyst loading is as low as 0.020 mol% Pd, and a wide range of bromo/bromochloro(hetero)aryl triflates and (hetero)arylboronic acids are coupled with excellent yield, chemoselectivity, and functional group compatibility. Remarkably, the one-pot process successfully carries out both C−Br and C−Cl functionalisation without requiring intermediate purification. Given the good reactivity and chemoselectivity of this approach, it is anticipated to provide a new platform for constructing complex molecules for pharmaceuticals, materials, and other applications.

4.4 Experimental Section

4.4.1 General considerations

All reagents used in the study were purchased from commercial suppliers and employed without further purification, unless otherwise noted. Suzuki coupling reactions were carried out in resealable screw cap Schlenk tubes (approximately 20 mL volume) containing a Teflon-coated magnetic stirrer bar (5 mm × 10 mm). Solvents such as dioxane, cyclopentyl methyl ether (CPME), and toluene were freshly distilled from sodium under nitrogen.[41] THF was freshly distilled from sodium benzophenone ketyl under nitrogen.[41] *tert*-Butanol (*t*-BuOH) was freshly distilled from anhydrous CaH_2 under nitrogen.[41] Anhydrous *N*,*N*-dimethylacetamide (DMF) was purchased in Sure/Seal bottles from Dieckmann and used as received. Inorganic bases, including KF, NaF, K_2CO_3, and Na_2CO_3, were obtained from Dieckmann and used without further treatment. Ligands **L1**−**L5** were prepared according to literature procedures,[32] while ligands **L6**−**L10** were acquired from commercial suppliers. A fresh bottle of *n*-BuLi was used, and its concentration was determined by titration prior to use. Thin layer chromatography was performed on pre-coated silica gel 60 F_{254} plates, and silica gel (Grace, 60 Å, 40−63 μm) was utilised for column chromatography. Melting points were recorded on an uncorrected Stuart Melting Point SMP30 instrument. The NMR spectra were collected using a Brüker spectrometer operating at 400 MHz for ^{1}H NMR, 100 MHz for ^{13}C NMR, 376 MHz for ^{19}F NMR, and 162 MHz for ^{31}P NMR. The spectra were internally referenced to the residual proton resonance in $CDCl_3$ (δ 7.26 ppm). Chemical shifts (δ) are reported in parts per million (ppm) downfield from the tetramethylsilane (TMS) standard. The ^{13}C NMR spectra were referenced to the middle peak of $CDCl_3$ (δ 77.0 ppm). The ^{19}F NMR chemical shifts were determined relative to $CFCl_3$ as the external standard, with low field being positive. The ^{31}P NMR spectra were referenced to 85% H_3PO_4 externally. Coupling constants (J) are reported in Hertz (Hz). Mass spectra were recorded using an HP 5977A MSD Mass Spectrometer in the electron ionisation (EI-MS) mode. High-resolution mass spectra (HRMS) were obtained on an Agilent 6540 ESI-QToF-MS or APPI-QToF-MS, and a Waters GCT Premier EI-ToF-MS. GC-MS analysis was conducted on an HP 7890B GC system using an HP5MS column (30 m × 0.25 mm). The GC yields reported refer to the isolated yields of compounds estimated to be greater than 95% pure, as determined by capillary gas chromatography (GC) or ^{1}H NMR. Compounds described in the literature were characterised by comparing their ^{1}H, ^{13}C and/or ^{19}F NMR spectra to the previously reported data. The procedures described in this section are representative, and therefore the yields may differ from those reported in the tables.

4.4.2 Polyhalogenated aryl triflate synthesis and characterisation

The polyhalogenated aryl triflates were synthesised from their respective phenol precursors. This was done by reacting the phenols with triflyl chloride, in the presence of triethylamine, in dry dichloromethane. The procedure follows the method described in the literature.[32]

General procedure

The phenol precursor (20 mmol, 1.0 equiv.) was dissolved in freshly distilled dichloromethane (50 mL) at room temperature under a nitrogen atmosphere. Triethylamine (28 mmol, 1.4 equiv.) was then added to the solution. The reaction mixture was cooled to -78 °C using a dry ice/acetone bath. Triflyl chloride (19 mmol, 0.95 equiv.) was then added dropwise using a syringe. The reaction was allowed to warm to room temperature and stirred for 1 hour. Ethyl acetate and water were added, and the organic phase was separated. The organic layer was washed with water several times, dried over Na_2SO_4, and then concentrated. The concentrated solution was subjected to column chromatography and eluted with a mixture of ethyl acetate and hexane. The solution was then evaporated to yield the product.

The characterisation data for the new polyhalogenated aryl triflates are provided below.

2-Bromo-4-formylphenyl trifluoromethanesulfonate

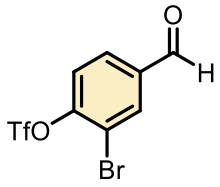

The product was obtained as a white solid in 91% yield (6.06 g). Flash column chromatography was performed using ethyl acetate/hexane (1: 9) as the eluent (R_f = 0.27). The melting point was determined to be 28.4−29.4 °C. ^{1}H NMR (400 MHz, $CDCl_3$) δ 7.53 (d, *J* = 8.4 Hz, 1H), 7.91 (dd, *J* = 8.4, 2.0 Hz, 1H), 8.18 (s, 1H), 9.97 (s, 1H); ^{13}C NMR (100 MHz, $CDCl_3$) δ 117.1, 118.5 (q, *J* = 318.8 Hz), 123.6, 130.1, 135.2, 136.6, 150.6, 188.8; ^{19}F NMR (376 MHz, $CDCl_3$) δ -73.2; HRMS (EI): calculated m/z for $C_8H_4BrF_3O_4S^+$: 331.8966, found 331.8968.

6-Bromopyridin-2-yl trifluoromethanesulfonate

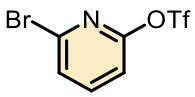

The product was obtained as a colourless liquid in 87% yield (5.29 g). Flash column chromatography was performed using ethyl acetate/hexane (1: 9) as the eluent (R_f = 0.48). ^{1}H NMR (400 MHz, $CDCl_3$) δ 7.17 (d, *J* = 8.0 Hz, 1H), 7.59 (d, *J* = 7.8 Hz, 1H), 7.76 (t, *J* = 7.9 Hz, 1H); ^{13}C NMR (100 MHz, $CDCl_3$) δ 114.0, 118.6 (q, *J* = 318.9 Hz), 128.8, 139.7, 142.4, 154.1; ^{19}F

NMR (376 MHz, $CDCl_3$) δ -72.9; HRMS (APPI): calculated m/z for $C_6H_4BrF_3NO_3S^+$: 305.9042, found 305.9051.

4.4.3 General procedure for ligand and reaction condition screenings

General procedure for the initial ligand screening of the chemoselective Suzuki−Miyaura coupling of 4-bromophenyltriflate with 4.0 mol% Pd catalyst loading

A Schlenk tube equipped with a Teflon-coated magnetic stir bar (5 mm × 10 mm) and a screw cap was carefully evacuated and flushed with nitrogen (3 cycles). The following reagents were then added to the tube: Pd source (0.0080 mmol), ligand (0.0080 mmol), 2-tolylboronic acid (0.20 mmol), and KF (0.60 mmol). 4-Bromophenyltriflate (0.20 mmol) and freshly distilled THF (0.60 mL) were added to the tube via syringe. The sealed tube was then magnetically stirred at room temperature for 1 hour. After the reaction, ethyl acetate (~4.0 mL), dodecane (45.2 µL, internal standard), and water (~2.0 mL) were added. The organic layer was subjected to GC analysis, with the GC yield previously calibrated using an authentic sample and a dodecane calibration curve.

General procedure for the reaction conditions screening of the chemoselective Suzuki−Miyaura coupling of 4-bromophenyltriflate with 0.025 mol% Pd catalyst loading

A stock solution of $Pd(OAc)_2$ (0.010 mmol) with ligand **L1** (Pd: L =1: 2) in freshly distilled THF (20 mL) was initially prepared by stirring at room temperature for 1 minute. An array of Schlenk tubes were charged with magnetic stirrer bars (5 mm × 10 mm) and were evacuated and backfilled with nitrogen (3 cycles). The stock solution (0.10 mL, 0.025 mol% Pd) was then added to the Schlenk tubes via syringe, and the solvent was removed under reduced pressure. The Schlenk tubes were then charged with 2-tolylboronic acid (0.20 mmol) and bases (0.60 mmol), and were again evacuated and backfilled with nitrogen (3 cycles). 4-Bromophenyltriflate (0.20 mmol) and freshly distilled solvent (0.60 mL) were added to the Schlenk tubes via syringe. The tubes were then resealed and magnetically stirred in a preheated oil bath (110°C) for 30 minutes to 1 hour. After the reaction, the mixtures were allowed to cool to room temperature. Ethyl acetate (~4.0 mL), dodecane (45.2 µL, internal standard), and water (~2.0 mL) were then added. The organic layer was subjected to GC analysis, with the GC yield previously calibrated using an authentic sample and a dodecane calibration curve.

4.4.4 General procedure for chemoselective Suzuki−Miyaura coupling of polyhalogenated aryl triflates

A stock solution of $Pd(OAc)_2$ (2.3 mg, 0.010 mmol) with ligand **L1** (6.6 mg, 0.020 mmol) in freshly distilled 25 mL THF (0.20 mol% Pd per 1.0 mL stock solution) was initially prepared by continuous stirring at room temperature for 1 minute. A Schlenk tube was charged with a magnetic stirrer bar (5 mm × 10 mm) and was evacuated and backfilled with nitrogen (3 cycles). The corresponding volume of the stock solution was then added to the tube via syringe, and the solvent was removed under reduced pressure. Aryl boronic acids (0.20−0.30 mmol), polyhalogenated aryl triflates (0.20 mmol, if solid), and potassium fluoride (0.60 mmol) were added to the tube, which was again evacuated and backfilled with nitrogen (3 cycles). Polyhalogenated aryl triflates (0.20 mmol, if liquid) and freshly distilled *t*-BuOH or toluene (0.60 mL) were then added to the tube via syringe. The tube was resealed and magnetically stirred in a preheated oil bath (60 °C or 110 °C) for 1.5−18 hours. After the reaction, the mixture was allowed to cool to room temperature. Ethyl acetate (~4.0 mL) and water (~2.0 mL) were added, and the organic layer was subjected to GC analysis. The aqueous layer was washed with ethyl acetate, and the combined organic layers were concentrated. The crude products were then purified by column chromatography on silica gel (230−400 mesh) to afford the desired product.

4.4.5 General procedure for sequential double functionalisation of bromochloroaryl triflates

A stock solution was initially prepared by combining $Pd(OAc)_2$ (2.3 mg, 0.010 mmol) and ligand **L1** (6.6 mg, 0.020 mmol) in freshly distilled 25 mL THF (0.20 mol% Pd per 1 mL stock solution), with continuous stirring at room temperature for 1 minute. A Schlenk tube was charged with a magnetic stirrer bar (5 mm × 10 mm) and was evacuated and backfilled with nitrogen (3 cycles). The corresponding volume of the stock solution was then added to the tube via syringe, and the solvent was removed under reduced pressure. Aryl or alkyl boronic acids (0.20−0.24 mmol), polyhalogenated aryl triflates (0.20 mmol, if solid), and KF (1.2 mmol) were added to the tube, which was again evacuated and backfilled with nitrogen (3 cycles). Polyhalogenated aryl triflates (0.20 mmol, if liquid) and toluene (0.60 mL) were then added to the tube via syringe. The tube was resealed and magnetically stirred in a preheated oil bath (110 °C) for 2 hours. After the reaction was complete, the reaction tube was allowed to cool to room temperature. The second aryl boronic acids (0.30−0.40 mmol) were then loaded into the tube under nitrogen. The tube was placed back into the preheated oil bath (110 °C) for an additional 2 hours. After the second reaction was complete, the reaction tube was allowed to cool to room temperature. Ethyl acetate (~4.0 mL) and water (~2.0 mL) were added, and the organic layer was subjected to GC analysis. The crude product in the organic layer was then extracted, and the aqueous layer was washed with ethyl acetate. The filtrate was concentrated under reduced pressure, and the crude products were purified by flash column chromatography on silica gel (230−400 mesh) to afford the desired product.

4.4.6 Characterisation data for coupling products

2'-Methyl-[1,1'-biphenyl]-4-yl trifluoromethanesulfonate (Table 4.2, entry 8, compound **16a**)[42]

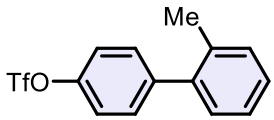

Flash column chromatography was performed using hexane as the eluent (R_f = 0.24). ^{1}H NMR (400 MHz, $CDCl_3$) δ 2.29 (s, 3H), 7.23 (d, *J* = 7.2 Hz, 1H), 7.29−7.36 (m, 5H), 7.42 (d, *J* = 8.5 Hz, 2H); ^{13}C NMR (100 MHz, $CDCl_3$) δ 20.3, 118.8 (q, *J* = 318.7 Hz), 121.0, 126.0, 127.9, 129.6, 130.5, 131.0, 135.2, 139.9, 142.4, 148.5; ^{19}F NMR (376 MHz, $CDCl_3$) δ -72.9.

4'-Methyl-[1,1'-biphenyl]-4-yl trifluoromethanesulfonate (Table 4.3, compound **16b**)[42]

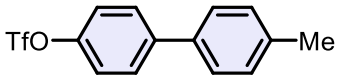

Flash column chromatography was performed using hexane as the eluent (R_f = 0.24). ^{1}H NMR (400 MHz, $CDCl_3$) δ 2.42 (s, 3H), 7.28 (d, *J* = 7.9 Hz, 2H), 7.34 (d, *J* = 8.8 Hz, 2H), 7.47 (d, *J* = 8.1 Hz, 2H), 7.64 (d, *J* = 8.8 Hz, 2H); ^{13}C NMR (100 MHz, $CDCl_3$) δ 21.1, 118.8 (q, *J* = 318.8 Hz), 121.5, 127.0, 128.6, 129.5, 136.4, 138.0, 141.6, 148.7; ^{19}F NMR (376 MHz, $CDCl_3$) δ -72.8.

4'-(*tert*-Butyl)-[1,1'-biphenyl]-4-yl trifluoromethanesulfonate (Table 4.3, compound **16c**)[36]

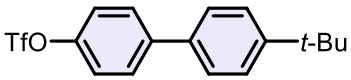

Flash column chromatography was performed using hexane as the eluent (R_f = 0.40). ^{1}H NMR (400 MHz, $CDCl_3$) δ 1.38 (s, 9H), 7.34 (d, *J* = 8.8 Hz, 2H), 7.46−7.56 (m, 4H), 7.65 (d, *J* = 8.8 Hz, 2H); ^{13}C NMR (100 MHz, $CDCl_3$) δ 31.3, 34.6, 118.8 (q, *J* = 318.9 Hz), 121.5, 125.9, 126.8, 128.7, 136.4, 141.5, 148.7, 151.2; ^{19}F NMR (376 MHz, $CDCl_3$) δ -72.8.

4'-Fluoro-[1,1'-biphenyl]-4-yl trifluoromethanesulfonate (Table 4.3, compound **16d**)[42]

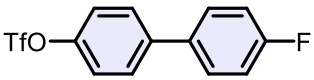

Flash column chromatography was performed using hexane as the eluent (R_f = 0.40). ^{1}H NMR (400 MHz, $CDCl_3$) δ 7.13−7.18 (m, 2H), 7.35 (d, *J* = 8.8 Hz, 2H), 7.50−7.54 (m, 2H), 7.56−7.62 (m, 2H); ^{13}C NMR (100 MHz, $CDCl_3$) δ 115.9 (d, *J* = 21.6 Hz), 118.8 (q, *J* = 318.9 Hz), 121.7, 128.7, 128.8 (d, *J* = 8.1 Hz), 135.4 (d, *J* = 3.2 Hz), 140.7, 148.9, 162.9 (d, *J* = 246.3 Hz); ^{19}F NMR (376 MHz, $CDCl_3$) δ -114.3 (s, 1F), -72.8 (s, 3F).

[1,1':2',1''-Terphenyl]-4-yl trifluoromethanesulfonate (Table 4.3, compound **16e**)[32]

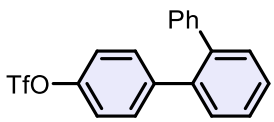

Flash column chromatography was performed using hexane as the eluent (R_f = 0.52). ^{1}H NMR (400 MHz, $CDCl_3$) δ 7.36−7.41 (m, 4H), 7.46−7.51 (m, 5H), 7.67−7.73 (m, 4H); ^{13}C NMR (100 MHz, $CDCl_3$) δ 118.7 (q, *J* = 318.9 Hz), 120.7, 126.8, 127.7, 128.0, 128.2, 129.8, 130.3, 130.7, 131.6, 138.6, 140.7, 140.8, 142.0, 148.3; ^{19}F NMR (376 MHz, $CDCl_3$) δ -72.8.

4'-Methoxy-[1,1'-biphenyl]-4-yl trifluoromethanesulfonate (Table 4.3, compound **16f**)[42]

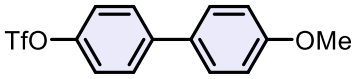

Flash column chromatography was performed using ethyl acetate/hexane (1: 20) as the eluent (R_f = 0.28). ^{1}H NMR (400 MHz, $CDCl_3$) δ 3.86 (s, 3H), 7.00 (d, *J* = 8.8 Hz, 2H), 7.32 (d, *J* = 8.8 Hz, 2H), 7.50 (d, *J* = 8.8 Hz, 2H), 7.60 (d, *J* = 8.8 Hz, 2H); ^{13}C NMR (100 MHz, $CDCl_3$) δ 55.3, 114.4, 118.8 (q, *J* = 318.8 Hz), 121.5, 128.2, 128.3, 131.7, 141.3, 148.5, 159.7; ^{19}F NMR (376 MHz, $CDCl_3$) δ -72.8.

Methyl 4'-(((trifluoromethyl)sulfonyl)oxy)-[1,1'-biphenyl]-4-carboxylate (Table 4.3, compound **16g**)[42]

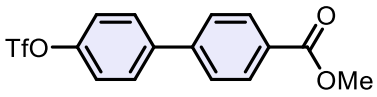

Flash column chromatography was performed using ethyl acetate/hexane (1: 9) as the eluent (R_f = 0.46). ^{1}H NMR (400 MHz, $CDCl_3$) δ 3.95 (s, 3H), 7.37 (d, *J* = 8.7 Hz, 2H), 7.62 (d, *J* = 8.4 Hz, 2H), 7.68 (d, *J* = 8.8 Hz, 2H), 8.12 (d, *J* = 8.4 Hz, 2H); ^{13}C NMR (100 MHz, $CDCl_3$) δ 52.2, 118.7 (q, *J* = 318.9 Hz), 121.8, 127.1, 129.1, 129.7, 130.2, 140.4, 143.5, 149.4, 166.7; ^{19}F NMR (376 MHz, $CDCl_3$) δ -72.8.

4-(Naphthalen-1-yl)phenyl trifluoromethanesulfonate (Table 4.3, compound **16h**)[32]

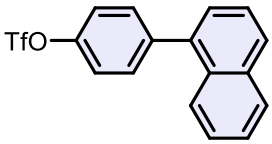

Flash column chromatography was performed using hexane as the eluent (R_f = 0.38). ^{1}H NMR (400 MHz, $CDCl_3$) δ 7.41−7.43 (m, 3H), 7.46−7.59 (m, 5H), 7.81 (d, *J* = 8.3 Hz, 1H), 7.91−7.95 (m, 2H); ^{13}C NMR (100 MHz, $CDCl_3$) δ 118.8 (q, *J* = 318.9 Hz), 121.2, 125.3, 125.4, 126.0, 126.5, 127.1, 128.40, 128.44, 131.3, 131.8, 133.8, 138.1, 141.2, 148.8; ^{19}F NMR (376 MHz, $CDCl_3$) δ -72.8.

4-(Dibenzo[*b*,*d*]furan-4-yl)phenyl trifluoromethanesulfonate (Table 4.3, compound **16i**)[32]

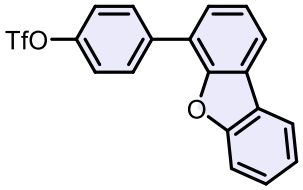

Flash column chromatography was performed using ethyl acetate/hexane (1: 9) as the eluent (R_f = 0.62). ^{1}H NMR (400 MHz, $CDCl_3$) δ 7.37−7.52 (m, 5H), 7.56 (d, *J* = 7.5 Hz, 1H), 7.61 (d, *J* = 8.1 Hz, 1H), 7.96−8.01 (m, 4H); ^{13}C NMR (100 MHz, $CDCl_3$) δ 111.8, 118.8 (q, *J* = 318.8 Hz), 120.5, 120.7, 121.5, 123.0, 123.3, 123.7, 123.9, 125.1, 126.6, 127.5, 130.5, 136.8, 149.0, 153.1, 156.1; ^{19}F NMR (376 MHz, $CDCl_3$) δ -72.7.

4-(Dibenzo[*b*,*d*]thiophen-4-yl)phenyl trifluoromethanesulfonate (Table 4.3, compound **16j**)[32]

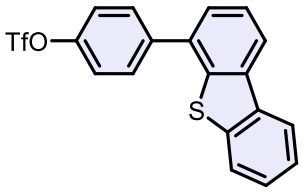

Flash column chromatography was performed using ethyl acetate/hexane (1: 9) as the eluent (R_f = 0.67). ^{1}H NMR (600 MHz, $CDCl_3$) δ 7.42−7.45 (m, 3H), 7.49−7.50 (m, 2H), 7.56 (t, *J* = 7.5 Hz, 1H), 7.80 (d, *J* = 8.3 Hz, 2H), 7.84 (d, *J* = 7.1 Hz, 1H), 8.17−8.20 (m, 2H); ^{13}C NMR (151 MHz, $CDCl_3$) δ 118.8 (q, *J* = 321.3 Hz), 121.1, 121.7, 121.8, 122.6, 124.6, 125.2, 126.9, 127.0, 130.1, 134.9, 135.5, 136.4, 138.3, 139.2, 140.9, 149.1; ^{19}F NMR (565 MHz, $CDCl_3$) δ -72.7.

4-(Benzo[*b*]thiophen-2-yl)phenyl trifluoromethanesulfonate (Table 4.3, compound **16k**)[32]

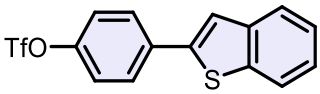

Flash column chromatography was performed using ethyl acetate/hexane (1: 9) as the eluent (R_f = 0.67). ^{1}H NMR (600 MHz, $CDCl_3$) δ 7.33 (d, *J* = 8.2 Hz, 2H), 7.35−7.40 (m, 2H), 7.54 (s, 1H), 7.75 (d, *J* = 8.2 Hz, 2H), 7.80 (d, *J* = 7.6 Hz, 1H), 7.84 (d, *J* = 7.7 Hz, 1H); ^{13}C NMR (151 MHz, $CDCl_3$) δ 118.7 (q, *J* = 321.4 Hz), 120.8, 121.9, 122.3, 123.9, 124.8, 124.9, 128.0, 134.7, 139.7, 140.4, 141.7, 149.1; ^{19}F NMR (565 MHz, $CDCl_3$) δ -72.7.

4-(Benzofuran-2-yl)phenyl trifluoromethanesulfonate (Table 4.3, compound **16l**)[33]

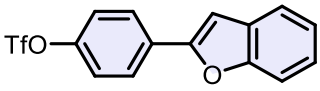

Flash column chromatography was performed using ethyl acetate/hexane (1: 9) as the eluent (R_f = 0.63). ^{1}H NMR (600 MHz, $CDCl_3$) δ 7.03 (s, 1H), 7.25 (t, *J* = 7.2 Hz, 1H), 7.30−7.34 (m, 3H), 7.52 (d, *J* = 8.2 Hz, 1H), 7.59 (d, *J* = 7.6 Hz, 1H), 7.89 (d, *J* = 8.0 Hz, 2H); ^{13}C NMR (151 MHz, $CDCl_3$) δ 102.7, 111.3, 118.7 (q, *J* = 321.3 Hz), 121.2, 121.8, 123.2, 125.0, 126.5, 128.8, 130.8, 149.1, 153.7, 155.0; ^{19}F NMR (565 MHz, $CDCl_3$) δ -72.7.

2-Methoxy-4-(naphthalen-1-yl)phenyl trifluoromethanesulfonate (Table 4.3, compound **16m**)

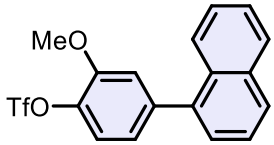

The product was obtained as a colourless liquid. Flash column chromatography was performed using ethyl acetate/hexane (1: 50) as the eluent (R_f = 0.33). ^{1}H NMR (400 MHz, $CDCl_3$) δ 3.94 (s, 3H), 7.11 (d, *J* = 8.3 Hz, 1H), 7.18 (s, 1H), 7.36 (d, *J* = 8.2 Hz, 1H), 7.44 (d, *J* = 7.0 Hz, 1H), 7.48−7.58 (m, 3H), 7.88 (d, *J* = 8.4 Hz, 1H), 7.93 (d, *J* = 8.4 Hz, 1H), 7.95 (d, *J* = 8.7 Hz, 1H); ^{13}C NMR (100 MHz, $CDCl_3$) δ 56.2, 114.9, 118.8 (q, *J* = 318.5 Hz), 122.1, 122.4, 125.2, 125.5, 126.0, 126.4, 126.9, 128.3, 128.4, 131.2, 133.7, 138.0, 138.5, 142.2, 151.1; ^{19}F NMR (376 MHz, $CDCl_3$) δ -73.8; HRMS: calculated m/z for $C_{18}H_{13}F_3O_4S$: 382.0487, found 382.0487.

2'-Methyl-[1,1'-biphenyl]-2-yl trifluoromethanesulfonate (Table 4.3, compound **16n**)[7]

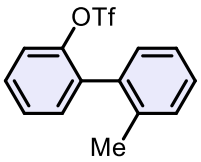

Flash column chromatography was performed using hexane as the eluent (R_f = 0.21). ^{1}H NMR (400 MHz, $CDCl_3$) δ 2.18 (s, 3H), 7.22−7.35 (m, 4H), 7.36−7.41 (m, 2H), 7.43−7.47 (m, 2H); ^{13}C NMR (100 MHz, $CDCl_3$) δ 19.8, 118.3 (q, *J* = 318.4 Hz), 121.6, 125.6, 128.2, 128.6, 129.1, 130.1, 130.3, 132.3, 135.0, 135.5, 136.4, 147.0; ^{19}F NMR (376 MHz, $CDCl_3$) δ -74.4.

Methyl 4'-methoxy-6-(((trifluoromethyl)sulfonyl)oxy)-[1,1'-biphenyl]-3-carboxylate (Table 4.3, compound **16o**)

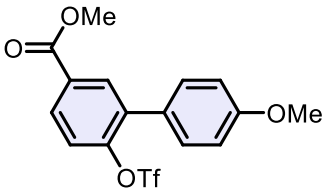

The product was obtained as a colourless liquid. Flash column chromatography was performed using ethyl acetate/hexane (1: 9) as the eluent (R_f = 0.46). ^{1}H NMR (400 MHz, $CDCl_3$) δ 3.86 (s, 3H), 3.94 (s, 3H), 7.00 (d, *J* = 8.8 Hz, 2H), 7.39−7.44 (m, 3H), 8.05 (d, *J* = 8.6 Hz, 1H), 8.15 (s, 1H); ^{13}C NMR (100 MHz, $CDCl_3$) δ 52.5, 55.3, 113.5, 118.3 (q, *J* = 318.7 Hz), 122.2, 126.9, 129.7, 130.3, 130.6, 133.3, 135.5, 149.7, 160.0, 165.6; ^{19}F NMR (376 MHz, $CDCl_3$) δ -73.9; HRMS (APPI): calculated m/z for $C_{16}H_{13}F_3O_6S^+$: 390.0385, found 390.0388.

5-Formyl-4'-methoxy-[1,1'-biphenyl]-2-yl trifluoromethanesulfonate (Table 4.3, compound **16p**)[42]

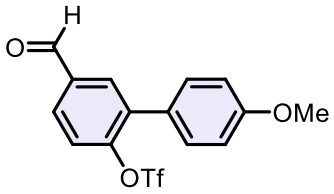

Flash column chromatography was performed using ethyl acetate/hexane (1: 9) as the eluent (R_f = 0.36). ^{1}H NMR (400 MHz, $CDCl_3$) δ 3.87 (s, 3H), 7.01 (d, *J* = 8.8 Hz, 2H), 7.42 (d, *J* = 8.8 Hz, 2H), 7.54 (d, *J* = 8.4 Hz, 1H), 7.91 (dd, *J* = 8.4, 2.1 Hz, 1H), 7.98 (s, 1H), 10.06 (s, 1H); ^{13}C NMR (100 MHz, $CDCl_3$) δ 55.3, 114.2, 118.3 (q, *J* = 318.8 Hz), 123.0, 126.5, 129.4, 130.5, 133.1, 135.9, 136.3, 150.4, 160.1, 190.3; ^{19}F NMR (376 MHz, $CDCl_3$) δ -73.9.

5-Cyano-4'-methoxy-[1,1'-biphenyl]-2-yl trifluoromethanesulfonate (Table 4.3, compound **16q**)

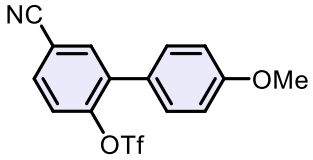

The product was obtained as a light-yellow liquid. Flash column chromatography was performed using ethyl acetate/hexane (1: 9) as the eluent (R_f = 0.37). ^{1}H NMR (400 MHz, $CDCl_3$) δ 3.86 (s, 3H), 7.01 (d, *J* = 8.8 Hz, 2H), 7.38 (d, *J* = 8.8 Hz, 2H), 7.49 (d, *J* = 8.5 Hz, 1H), 7.67−7.69 (m, 1H), 7.77 (s, 1H); ^{13}C NMR (100 MHz, $CDCl_3$) δ 55.3, 112.9, 114.3, 117.1, 118.2 (q, *J* = 318.9 Hz), 123.3, 125.5, 130.4, 132.0, 135.6, 136.8, 149.2, 160.4; ^{19}F NMR (376 MHz, $CDCl_3$) δ -73.8; HRMS (APPI): calculated m/z for $C_{15}H_{10}F_3NO_4S^+$: 357.0277, found 357.0286.

[1,1'-Binaphthalen]-2-yl trifluoromethanesulfonate (Table 4.3, compound **16r**)[43]

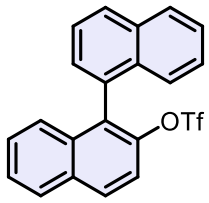

Flash column chromatography was performed using hexane as the eluent (R_f = 0.18). ^{1}H NMR (400 MHz, $CDCl_3$) δ 7.43−7.46 (m, 2H), 7.60−7.65 (m, 2H), 7.68−7.72 (m, 2H), 7.84−7.91 (m, 5H), 8.32 (d, *J* = 8.5 Hz, 2H); ^{13}C NMR (100 MHz, $CDCl_3$) δ 116.2, 118.7 (q, *J* = 318.7 Hz), 119.9, 120.3, 124.5, 124.9, 127.7, 127.76, 127.78, 128.31, 128.33, 128.5, 128.7, 128.8, 129.7, 131.3, 132.7, 132.9, 133.0, 143.3, 145.0; ^{19}F NMR (376 MHz, $CDCl_3$) δ -73.4.

2,2',6-Trimethyl-[1,1'-biphenyl]-4-yl trifluoromethanesulfonate (Table 4.3, compound **16s**)[32]

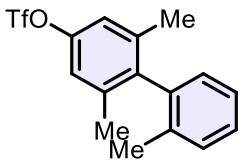

Flash column chromatography was performed using hexane as the eluent (R_f = 0.56). ^{1}H NMR (400 MHz, $CDCl_3$) δ 1.96 (s, 3H), 1.98 (s, 6H), 6.98 (d, *J* = 7.0 Hz, 1H), 7.03 (s, 2H), 7.27−7.31 (m, 3H); ^{13}C NMR (100 MHz, $CDCl_3$) δ 19.2, 20.4, 118.7 (q, *J* = 318.7 Hz), 119.6, 126.3, 127.6, 128.6, 130.2, 135.4, 138.68, 138.74, 141.4, 148.2; ^{19}F NMR (376 MHz, $CDCl_3$) δ -73.1.

5-Chloro-4'-methyl-[1,1'-biphenyl]-3-yl trifluoromethanesulfonate (Table 4.3, compound **16t**)

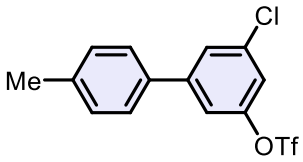

The product was obtained as a colourless liquid. Flash column chromatography was performed using hexane as the eluent (R_f = 0.45). ^{1}H NMR (400 MHz, $CDCl_3$) δ 2.42 (s, 3H), 7.25 (s, 1H), 7.29 (d, *J* = 7.9 Hz, 2H), 7.37 (s, 1H), 7.44 (d, *J* = 8.0 Hz, 2H), 7.59 (s, 1H); ^{13}C NMR (100 MHz, $CDCl_3$) δ 21.1, 118.1, 118.7 (q, *J* = 318.8 Hz), 119.9, 126.9, 127.1, 129.9, 134.9, 135.7, 139.0, 144.9, 149.7; ^{19}F NMR (376 MHz, $CDCl_3$) δ -72.7; HRMS (APPI): calcd. for $C_{14}H_{10}ClF_3O_3S^+$: 349.9991, found 349.9994.

3-Chloro-2'-methyl-[1,1'-biphenyl]-4-yl trifluoromethanesulfonate (Table 4.3, compound **16u**)[7]

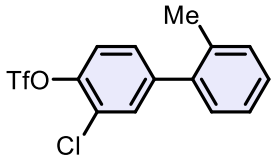

Flash column chromatography was performed using hexane as the eluent (R_f = 0.36). ^{1}H NMR (400 MHz, $CDCl_3$) δ 2.28 (s, 3H), 7.20 (d, *J* = 7.2 Hz, 1H), 7.27−7.31 (m, 4H), 7.41 (d, *J* = 8.4 Hz, 1H), 7.49 (s, 1H); ^{13}C NMR (100 MHz, $CDCl_3$) δ 20.3, 118.7 (q, *J* = 318.6 Hz), 122.5, 126.1, 126.8, 128.4, 129.1, 129.5, 130.6, 131.8, 135.1, 138.8, 143.5, 144.5; ^{19}F NMR (376 MHz, $CDCl_3$) δ -73.4.

3-Chloro-4'-methyl-[1,1'-biphenyl]-4-yl trifluoromethanesulfonate (Table 4.3, compound **16v**)[36]

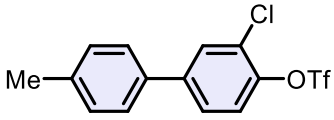

Flash column chromatography was performed using hexane as the eluent (R_f = 0.48). ^{1}H NMR (400 MHz, $CDCl_3$) δ 2.42 (s, 3H), 7.28 (d, *J* = 8.0 Hz, 2H), 7.39−7.45 (m, 3H), 7.51 (d, *J* = 8.6 Hz, 1H), 7.71 (s, 1H); ^{13}C NMR (100 MHz, $CDCl_3$) δ 21.1, 118.6 (q, *J* = 318.7 Hz), 123.1, 126.6, 126.9, 127.4, 129.4, 129.8, 135.2, 138.6, 142.7, 144.5; ^{19}F NMR (376 MHz, $CDCl_3$) δ -73.4.

4-Chloro-4'-methyl-[1,1'-biphenyl]-3-yl trifluoromethanesulfonate (Table 4.3, compound **16w**)

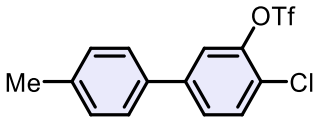

The product was obtained as a colourless liquid. Flash column chromatography was performed using hexane as the eluent (R_f = 0.38). ^{1}H NMR (400 MHz, $CDCl_3$) δ 2.42 (s, 3H), 7.29 (d, *J* = 7.9 Hz, 2H), 7.44 (d, *J* = 8.1 Hz, 2H), 7.52−7.57 (m, 3H); ^{13}C NMR (100 MHz, $CDCl_3$) δ 21.1, 118.7 (q, *J* = 318.6 Hz), 121.2, 125.4, 126.8, 127.4, 129.9, 131.3, 135.2, 138.6, 142.1, 145.9; ^{19}F NMR (376 MHz, $CDCl_3$) δ -73.3; HRMS (APPI): calculated m/z for $C_{14}H_{10}ClF_3O_3S^+$: 349.9991, found 349.9993.

5-Chloro-4'-methyl-[1,1'-biphenyl]-2-yl trifluoromethanesulfonate (Table 4.3, compound **16x**)[36]

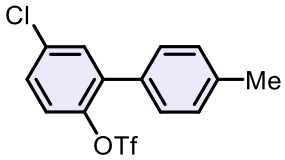

Flash column chromatography was performed using hexane as the eluent (R_f = 0.50). ^{1}H NMR (400 MHz, $CDCl_3$) δ 2.42 (s, 3H), 7.27−7.39 (m, 6H), 7.46 (s, 1H); ^{13}C NMR (100 MHz, $CDCl_3$) δ 21.2, 118.3 (q, *J* = 318.8 Hz), 123.3, 128.5, 129.0, 129.4, 131.5, 131.7, 134.1, 137.2, 138.8, 145.2; ^{19}F NMR (376 MHz, $CDCl_3$) δ-73.9.

2-Chloro-4'-methyl-[1,1'-biphenyl]-3-yl trifluoromethanesulfonate (Table 4.3, compound **16y**)

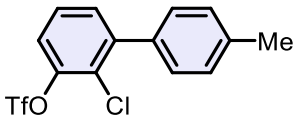

The product was obtained as a colourless liquid. Flash column chromatography was performed using hexane as the eluent (R_f = 0.57). ^{1}H NMR (400 MHz, $CDCl_3$) δ 2.44 (s, 3H), 7.28 (d, *J* = 8.0 Hz, 2H), 7.33−7.39 (m, 5H); ^{13}C NMR (100 MHz, $CDCl_3$) δ 21.2, 118.6 (q, *J* = 318.5 Hz), 121.4, 126.1, 127.5, 129.0, 129.2, 130.8, 134.9, 138.3, 143.6, 146.2; ^{19}F NMR (376 MHz, $CDCl_3$) δ -73.4; HRMS (APPI): calculated m/z for $C_{14}H_{10}ClF_3O_3S^+$: 349.9991, found 349.9995.

2-(4-Methoxyphenyl)pyridin-3-yl trifluoromethanesulfonate (Table 4.4, compound **16z**)

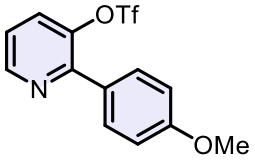

The product was obtained as an orange liquid. Flash column chromatography was performed using ethyl acetate/hexane (1: 2) as the eluent (R_f = 0.61). ^{1}H NMR (400 MHz, $CDCl_3$) δ 3.86 (s, 3H), 7.01 (d, *J* = 8.9 Hz, 2H), 7.28−7.32 (m, 1H), 7.70 (d, *J* = 8.2 Hz, 1H), 7.76 (d, *J* = 8.9 Hz, 2H), 6.67 (d, *J* = 4.6 Hz, 1H); ^{13}C NMR (100 MHz, $CDCl_3$) δ 55.3, 113.9, 118.3 (q, *J* = 318.8 Hz), 122.6, 127.5, 130.2, 130.7, 144.3, 149.0, 151.7, 160.8; ^{19}F NMR (376 MHz, $CDCl_3$) δ -73.8; HRMS (APPI): calculated m/z for $C_{13}H_{11}F_3NO_4S^+$: 334.0355, found 334.0358.

5-(4-Methoxyphenyl)-4-methylpyridin-2-yl trifluoromethanesulfonate (Table 4.4, compound **16aa**)[44]

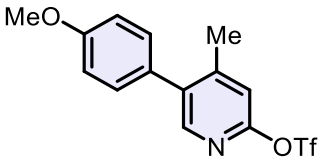

Flash column chromatography was performed using ethyl acetate/hexane (1: 9) as the eluent (R_f = 0.28). ^{1}H NMR (400 MHz, $CDCl_3$) δ 2.36 (s, 3H), 3.87 (s, 3H), 7.00 (d, *J* = 8.7 Hz, 2H), 7.07 (s, 1H), 7.23 (d, *J* = 8.7 Hz, 2H), 8.18 (s, 1H); ^{13}C NMR (100 MHz, $CDCl_3$) δ 20.4, 55.3, 114.1, 115.8, 118.6 (q, *J* = 318.5 Hz), 128.1, 130.3, 138.5, 148.3, 150.7, 154.8, 159.6; ^{19}F NMR (376 MHz, $CDCl_3$) δ -73.2.

5-(4-Methoxyphenyl)pyridin-2-yl trifluoromethanesulfonate (Table 4.4, compound **16ab**)[32]

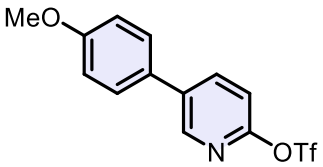

Flash column chromatography was performed using ethyl acetate/hexane (1: 9) as the eluent (R_f = 0.47). ^{1}H NMR (400 MHz, $CDCl_3$) δ 3.87 (s, 3H), 7.02 (d, *J* = 8.8 Hz, 2H), 7.22 (d, *J* = 8.5 Hz, 1H), 7.50 (d, *J* = 8.8 Hz, 2H), 8.00 (dd, *J* = 8.4, 2.6 Hz, 1H), 8.53 (s, 1H); ^{13}C NMR (100 MHz, $CDCl_3$) δ 55.3, 114.7, 115.0, 118.6 (q, *J* = 318.5 Hz), 128.1, 128.3, 137.4, 138.7, 146.2, 154.5, 160.3; ^{19}F NMR (376 MHz, $CDCl_3$) δ -73.1.

6-(4-Methoxyphenyl)pyridin-2-yl trifluoromethanesulfonate (Table 4.4, compound **16ac**)

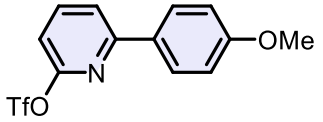

The product was obtained as a yellow liquid. Flash column chromatography was performed using ethyl acetate/hexane (1: 9) as the eluent (R_f = 0.32). ^{1}H NMR (400 MHz, $CDCl_3$) δ 3.86 (s, 3H), 6.98−7.00 (m, 3H), 7.70 (d, *J* = 7.8 Hz, 1H), 7.85 (t, *J* = 7.9 Hz, 1H), 7.97 (d, *J* = 8.8 Hz, 2H); ^{13}C NMR (100 MHz, $CDCl_3$) δ 55.3, 111.8, 114.0, 114.3, 118.7 (q, *J* = 318.5 Hz), 119.1, 128.4, 141.4,

155.7, 156.8, 161.3; ^{19}F NMR (376 MHz, $CDCl_3$) δ -72.9; HRMS: calculated m/z for $C_{13}H_{11}F_3NO_4S^+$: 334.0355, found 334.0363.

5-(4-Methoxyphenyl)pyridin-3-yl trifluoromethanesulfonate (Table 4.4, compound **16ad**)[32]

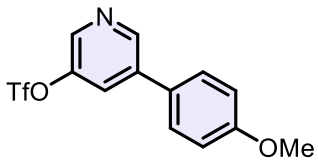

Flash column chromatography was performed using ethyl acetate/hexane (1: 9) as the eluent (R_f = 0.33). ^{1}H NMR (400 MHz, $CDCl_3$) δ 3.86 (s, 3H), 7.03 (d, *J* = 8.8 Hz, 2H), 7.52 (t, *J* = 8.8 Hz, 2H), 7.74 (s, 1H), 8.51 (s, 1H), 8.83 (s, 1H); ^{13}C NMR (100 MHz, $CDCl_3$) δ 55.3, 114.8, 118.7 (q, *J* = 319.1 Hz), 126.4, 127.7, 128.4, 138.3, 140.2, 146.9, 147.5, 160.5; ^{19}F NMR (376 MHz, $CDCl_3$) δ -72.5.

4-(4-Methoxyphenyl)pyridin-2-yl trifluoromethanesulfonate (Table 4.4, compound **16ae**)[32]

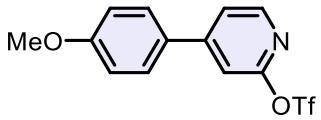

Flash column chromatography was performed using ethyl acetate/hexane (1: 9) as the eluent (R_f = 0.33). ^{1}H NMR (400 MHz, $CDCl_3$) δ 3.87 (s, 3H), 7.02 (d, *J* = 8.8 Hz, 2H), 7.30 (s, 1H), 7.53 (dd, *J* = 5.2, 1.4 Hz, 1H), 7.59 (d, *J* = 8.8 Hz, 2H), 8.36 (d, *J* = 5.2 Hz, 1H); ^{13}C NMR (100 MHz, $CDCl_3$) δ 55.4, 111.8, 114.8, 118.6 (q, *J* = 318.5 Hz), 121.5, 128.31, 128.34, 148.7, 153.6, 156.8, 161.4; ^{19}F NMR (376 MHz, $CDCl_3$) δ -73.2.

6-(Benzo[*b*]thiophen-3-yl)pyridin-2-yl trifluoromethanesulfonate (Table 4.4, compound **16af**)

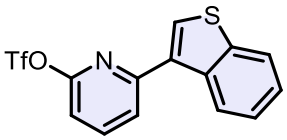

The product was obtained as a colourless liquid. Flash column chromatography was performed using ethyl acetate/hexane (1: 9) as the eluent (R_f = 0.33). ^{1}H NMR (600 MHz, $CDCl_3$) δ 7.10 (d, *J* = 8.0 Hz, 1H), 7.43 (t, *J* = 7.4 Hz, 1H), 7.50 (t, *J* = 7.6 Hz, 1H), 7.74 (d, *J* = 7.6 Hz, 1H), 7.90−7.91 (m, 3H), 8.59 (d, *J* = 8.2 Hz, 1H); ^{13}C NMR (151 MHz, $CDCl_3$) δ 112.5, 118.6 (q, *J* = 320.8 Hz), 122.1, 122.7, 124.1, 124.9, 125.0, 128.5, 133.9, 136.4, 140.7, 141.3, 154.0, 155.3; ^{19}F NMR (565 MHz, $CDCl_3$) δ -73.1; HRMS (EI): calculated m/z for $C_{14}H_8F_3NO_3S_2^+$: 358.9892, found 358.9900.

6-(Benzo[*b*]thiophen-2-yl)pyridin-2-yl trifluoromethanesulfonate (Table 4.4, compound **16ag**)

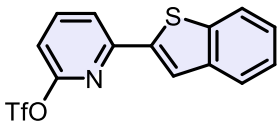

The product was obtained as a white solid. Flash column chromatography was performed using ethyl acetate/hexane (1: 9) as the eluent (R_f = 0.30). The melting point was determined to be 106.2−107.1 °C. ^{1}H NMR (600 MHz, $CDCl_3$) δ 7.01 (d, *J* = 7.9 Hz, 1H), 7.37−7.38 (m, 2H), 7.72 (d, *J* = 7.6 Hz, 1H), 7.80−7.87 (m, 4H); ^{13}C NMR (151 MHz, $CDCl_3$) δ 113.1, 118.7 (q, *J* = 321.2 Hz), 119.5, 122.5, 123.3, 124.5, 124.7, 125.7, 140.0, 140.9, 141.4, 141.6, 152.3, 155.3; ^{19}F NMR (565 MHz, $CDCl_3$) δ -72.6; HRMS (EI): calculated m/z for $C_{14}H_8F_3NO_3S_2^+$: 358.9892, found 358.9883.

5-(Benzo[*b*]thiophen-3-yl)pyridin-2-yl trifluoromethanesulfonate (Table 4.4, compound **16ah**)

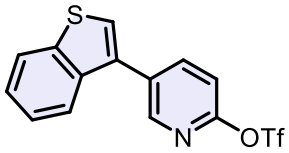

The product was obtained as a colourless liquid. Flash column chromatography was performed using dichloromerthane/hexane (1: 20) as the eluent (R_f = 0.25). ^{1}H NMR (600 MHz, $CDCl_3$) δ 7.32 (d, *J* = 8.3 Hz, 1H), 7.45−7.46 (m, 2H), 7.52 (s, 1H), 7.80 (d, *J* = 4.3 Hz, 1H), 7.96 (d, *J* = 5.7 Hz, 1H), 8.09 (d, *J* = 8.3 Hz, 1H), 8.60 (s, 1H); ^{13}C NMR (151 MHz, $CDCl_3$) δ 115.2, 118.6 (q, *J* = 321.0 Hz), 121.9, 123.2, 124.97, 125.03, 125.8, 132.1, 132.8, 137.0, 140.6, 147.9, 154.9; ^{19}F NMR (565 MHz, $CDCl_3$) δ -73.0; HRMS (EI): calculated m/z for $C_{14}H_8F_3NO_3S_2^+$: 358.9892, found 358.9891.

5-(Benzo[*b*]thiophen-2-yl)pyridin-2-yl trifluoromethanesulfonate (Table 4.4, compound **16ai**)

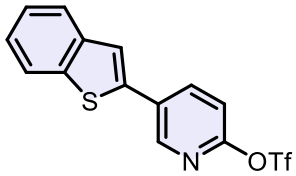

The product was obtained as a white solid. Flash column chromatography was performed using dichloromethane/hexane (1: 20) as the eluent (R_f = 0.25). The melting point was determined to be 141.4−142.4 °C. ^{1}H NMR (600 MHz, $CDCl_3$) δ 7.23 (d, *J* = 8.4 Hz, 1H), 7.38−7.42 (m, 2H), 7.59 (s, 1H), 7.82 (d, *J* = 7.4 Hz, 1H), 7.85 (d, *J* = 7.4 Hz, 1H), 8.11 (d, *J* = 8.4 Hz, 1H), 8.70 (s, 1H); ^{13}C NMR (151 MHz, $CDCl_3$) δ 115.3, 118.6 (q, *J* = 321.1 Hz), 121.9, 122.4, 124.1, 125.1, 125.4, 131.4, 137.7, 138.2, 139.8, 140.1, 145.8, 155.0; ^{19}F NMR (565 MHz, $CDCl_3$) δ -73.0; HRMS (EI): calculated m/z for $C_{14}H_8F_3NO_3S_2^+$: 358.9892, found 358.9885.

4''-Methoxy-2-methyl-[1,1':3',1''-terphenyl]-4'-yl trifluoromethanesulfonate (Table 4.5, compound **20a**)

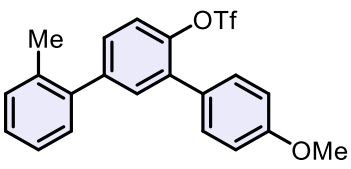

The product was obtained as a colourless gel. Flash column chromatography was performed using ethyl acetate/hexane (1: 20) as the eluent (R_f = 0.40). ^{1}H NMR (400 MHz, $CDCl_3$) δ 2.33 (s, 3H), 3.87 (s, 3H), 7.01 (d, *J* = 8.7 Hz, 2H), 7.26−7.36 (m, 5H), 7.41−7.47 (m, 4H); ^{13}C NMR (100 MHz, $CDCl_3$) δ 20.4, 55.3, 114.0, 118.4 (q, *J* = 318.7 Hz), 121.8, 126.0, 127.9, 128.0, 129.2, 129.7, 130.56, 130.6, 132.6, 134.8, 135.3, 140.0, 142.4, 145.8, 159.8; ^{19}F NMR (376 MHz, $CDCl_3$) δ -73.9; HRMS (APPI): calculated m/z for $C_{21}H_{17}F_3O_4S^+$: 422.0800, found 422.0803.

3'',5''-Dimethoxy-2-methyl-[1,1':3',1''-terphenyl]-4'-yl trifluoromethanesulfonate (Table 4.5, compound **20b**)

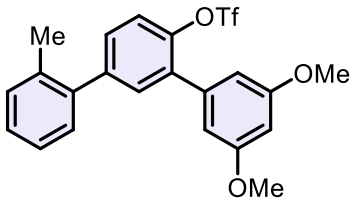

The product was obtained as a colourless liquid. Flash column chromatography was performed using ethyl acetate/hexane (1: 20) as the eluent (R_f = 0.24). ^{1}H NMR (400 MHz, $CDCl_3$) δ 2.34 (s, 3H), 3.86 (s, 6H), 6.56 (s, 1H), 6.69 (s, 2H), 7.26−7.32 (m, 4H), 7.38−7.50 (m, 3H); ^{13}C NMR (100 MHz, $CDCl_3$) δ 20.4, 55.4, 100.6, 107.5, 118.4 (q, *J* = 318.5 Hz), 121.7, 126.0, 128.0, 129.66, 129.72, 130.5, 132.5, 135.0, 135.2, 137.3, 139.8, 142.4, 145.6, 160.7; ^{19}F NMR (376 MHz, $CDCl_3$) δ -74.0; HRMS (APPI): calculated m/z for $C_{22}H_{20}F_3O_5S^+$: 453.0978, found 453.0984.

4'-Methoxy-5-(naphthalen-1-yl)-[1,1'-biphenyl]-2-yl trifluoromethanesulfonate (Table 4.5, compound **20c**)

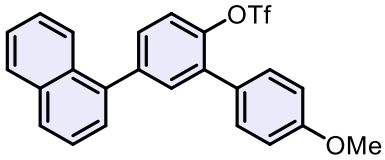

The product was obtained as a white gel. Flash column chromatography was performed using ethyl acetate/hexane (1: 20) as the eluent (R_f = 0.32). ^{1}H NMR (400 MHz, $CDCl_3$) δ 3.87 (s, 3H), 7.03 (d, *J* = 8.7 Hz, 2H), 7.46−7.58 (m, 8H), 7.62 (s, 1H), 7.92−7.96 (m, 3H); ^{13}C NMR (100 MHz, $CDCl_3$) δ 55.2, 114.0, 118.4 (q, *J* = 318.8 Hz), 121.9, 125.3, 125.5, 126.0, 126.5, 127.1, 127.7, 128.37, 128.44, 129.9, 130.6, 131.3, 133.3, 133.8, 135.1, 138.1, 141.3, 146.1, 159.7; ^{19}F NMR (376 MHz, $CDCl_3$) δ -73.9; HRMS (APPI): calculated m/z for $C_{24}H_{17}F_3O_4S^+$: 458.0794, found 458.0802.

4''-Methoxy-2-methyl-[1,1':3',1''-terphenyl]-5'-yl trifluoromethanesulfonate (Table 4.5, compound **20d**)

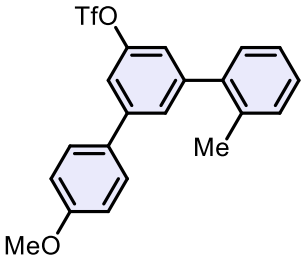

The product was obtained as a colourless liquid. Flash column chromatography was performed using ethyl acetate/hexane (1: 20) as the eluent (R_f = 0.32). ^{1}H NMR (400 MHz, $CDCl_3$) δ 2.35 (s, 3H), 3.88 (s, 3H), 7.03 (d, *J* = 8.8 Hz, 2H), 7.21 (s, 1H), 7.30−7.36 (m, 4H), 7.46 (s, 1H), 7.56−7.59 (m, 3H); ^{13}C NMR (100 MHz, $CDCl_3$) δ 20.3, 55.4, 114.5, 117.7, 118.9 (q, *J* = 318.8 Hz), 119.9, 126.1, 127.4, 128.2, 128.3, 129.6, 130.7, 131.4, 135.3, 139.9, 143.2, 144.7, 149.8, 160.2; ^{19}F NMR (376 MHz, $CDCl_3$) δ -72.7; HRMS (APPI): calculated m/z for $C_{21}H_{17}F_3O_4S^+$: 422.0800, found 422.0803.

2-Methoxy-2''-methyl-[1,1':3',1''-terphenyl]-5'-yl trifluoromethanesulfonate (Table 4.5, compound **20e**)

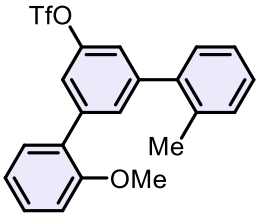

The product was obtained as a colourless liquid. Flash column chromatography was performed using ethyl acetate/hexane (1: 20) as the eluent (R_f = 0.40). ^{1}H NMR (400 MHz, $CDCl_3$) δ 2.39 (s, 3H), 3.89 (s, 3H), 7.05−7.12 (m, 2H), 7.26−7.43 (m, 7H), 7.56 (s, 1H), 7.60 (s, 1H); ^{13}C NMR (100 MHz, $CDCl_3$) δ 20.3, 55.5, 111.3, 118.8 (q, *J* = 319.1 Hz), 120.2, 120.7, 121.0, 126.0, 128.0, 128.2, 129.67, 129.69, 130.3, 130.59, 130.65, 135.3, 139.9, 140.5, 143.7, 149.0, 156.4; ^{19}F NMR (376 MHz, $CDCl_3$) δ -72.7; HRMS (APPI): calculated m/z for $C_{21}H_{17}F_3O_4S^+$: 422.0794, found 422.0800.

4-Methoxy-2''-methyl-[1,1':4',1''-terphenyl]-2'-yl trifluoromethanesulfonate (Table 4.5, compound **20f**)[32]

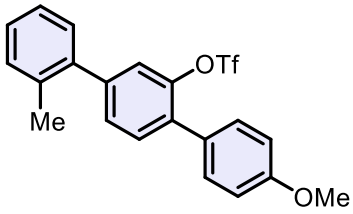

Flash column chromatography was performed using ethyl acetate/hexane (1: 20) as the eluent (R_f = 0.36). ^{1}H NMR (400 MHz, $CDCl_3$) δ 2.37 (s, 3H), 3.90 (s, 3H), 7.05 (d, *J* = 8.7 Hz, 2H), 7.29−7.34 (m, 4H), 7.39−7.43 (m, 2H), 7.49−7.54 (m, 3H); ^{13}C NMR (100 MHz, $CDCl_3$) δ 20.3,

55.2, 114.0, 118.4 (q, J = 318.7 Hz), 122.8, 126.1, 127.7, 128.1, 129.3, 129.6, 130.55, 130.64, 131.4, 133.4, 135.3, 139.5, 142.6, 146.5, 159.7; ^{19}F NMR (376 MHz, $CDCl_3$) δ -74.0.

4-Methoxy-4''-methyl-[1,1':3',1''-terphenyl]-4'-yl trifluoromethanesulfonate (Table 4.5, compound **20g**)

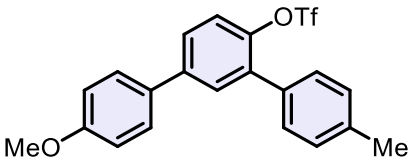

The product was obtained as a colourless liquid. Flash column chromatography was performed using ethyl acetate/hexane (1: 20) as the eluent (R_f = 0.44). ^{1}H NMR (400 MHz, $CDCl_3$) δ 2.44 (s, 3H), 3.87 (s, 3H), 7.00 (d, J = 8.7 Hz, 2H), 7.31 (d, J = 7.9 Hz, 2H), 7.41−7.44 (m, 3H), 7.53−7.57 (m, 3H), 7.64 (s, 1H); ^{13}C NMR (100 MHz, $CDCl_3$) δ 21.2, 55.3, 114.4, 118.4 (q, J = 318.6 Hz), 122.2, 126.7, 128.2, 129.18, 129.21, 130.0, 131.7, 132.8, 135.7, 138.2, 141.3, 145.7, 159.7; ^{19}F NMR (376 MHz, $CDCl_3$) δ -73.9; HRMS (APPI): calculated m/z for $C_{21}H_{17}F_3O_4S^+$: 422.0800, found 422.0803.

4''-Methoxy-4-methyl-[1,1':2',1''-terphenyl]-3'-yl trifluoromethanesulfonate (Table 4.5, compound **20h**)

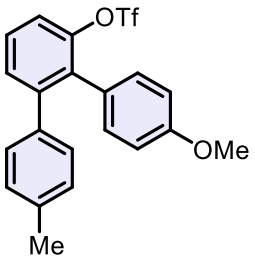

The product was obtained as a colourless liquid. Flash column chromatography was performed using ethyl acetate/hexane (1: 20) as the eluent (R_f = 0.30). ^{1}H NMR (400 MHz, $CDCl_3$) δ 2.31 (s, 3H), 3.80 (s, 3H), 6.82 (d, J = 8.7 Hz, 2H), 6.97−7.06 (m, 6H), 7.36−7.39 (m, 1H), 7.45 (d, J = 4.7 Hz, 2H); ^{13}C NMR (100 MHz, $CDCl_3$) δ 21.0, 55.1, 113.4, 118.3 (q, J = 318.3 Hz), 120.1, 126.0, 128.4, 128.6, 129.5, 130.2, 132.1, 134.0, 136.6, 136.9, 144.4, 147.8, 159.0; ^{19}F NMR (376 MHz, $CDCl_3$) δ -74.3; HRMS (APPI): calculated m/z for $C_{21}H_{17}F_3O_4S^+$: 422.0800, found 422.0800.

5-Butyl-4'-methoxy-[1,1'-biphenyl]-2-yl trifluoromethanesulfonate (Table 4.5, compound **20i**)

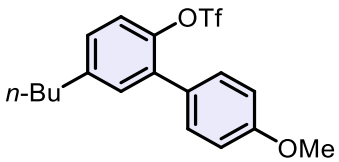

The product was obtained as a colourless liquid. Flash column chromatography was performed using ethyl acetate/hexane (1: 20) as the eluent (R_f = 0.43). ^{1}H NMR (400 MHz, $CDCl_3$) δ 0.95 (t, J = 7.3 Hz, 3H), 1.34−1.44 (m, 2H), 1.60−1.68 (m, 2H), 2.67 (t, J = 7.8 Hz, 2H), 3.86 (s, 3H), 6.99

(d, *J* = 8.7 Hz, 2H), 7.17−7.27 (m, 3H), 7.40 (d, *J* = 8.7 Hz, 2H); ^{13}C NMR (100 MHz, $CDCl_3$) δ 13.9, 22.3, 33.4, 35.0, 55.3, 113.9, 118.4 (q, *J* = 318.7 Hz), 121.7, 128.2, 128.3, 130.5, 131.7, 134.8, 143.5, 144.9, 159.9; ^{19}F NMR (376 MHz, $CDCl_3$) δ -74.1; HRMS (APPI): calculated m/z for $C_{18}H_{19}F_3O_4S^+$: 388.0956, found 388.0958.

4.5 References

1. *Metal-Catalyzed Cross-Coupling Reactions and More*; de Meijere, A., Bräse, S., Oestreich, M., Eds.; Vol. 1−3; Wiley-VCH, 2014.

2. Miyaura, N.; Suzuki, A. Palladium-Catalyzed Cross-Coupling Reactions of Organoboron Compounds. *Chem. Rev.* **1995**, *95*, 2457−2483.

3. Suzuki, A. Recent Advances in the Cross-Coupling Reactions of Organoboron Derivatives with Organic Electrophiles, 1995−1998. *J. Organomet. Chem.* **1999**, *576*, 147−168.

4. Kadu, B. S. Suzuki−Miyaura Cross Coupling Reaction: Recent Advancements in Catalysis and Organic Synthesis. *Catal. Sci. Technol.* **2021**, *11*, 1186−1221.

5. D'Alterio, M. C.; Casals-Cruañas, È.; Tzouras, N. V.; Talarico, G.; Nolan, S. P.; Poater, A. Mechanistic Aspects of the Palladium-Catalyzed Suzuki−Miyaura Cross-Coupling Reaction. *Chem. Eur. J.* **2021**, *27*, 13481−13493.

6. Fitton, P.; Rick, E. A. The Addition of Aryl Halides to Tetrakis(triphenylphosphine)palladium(0). *J. Organomet. Chem.* **1971**, *28*, 287−291.

7. Kalvet, I.; Magnin, G.; Schoenebeck, F. Rapid Room-Temperature, Chemoselective Csp^2-Csp^2 Coupling of Poly(pseudo)halogenated Arenes Enabled by Pd(I) Catalysis in Air. *Angew. Chem. Int. Ed.* **2017**, *56*, 1581−1585.

8. Fairlamb, I. J. S. Regioselective (Site-Selective) Functionalisation of Unsaturated Halogenated Nitrogen, Oxygen and Sulfur Heterocycles by Pd-Catalysed Cross-Couplings and Direct Arylation Processes. *Chem. Soc. Rev.* **2007**, *36*, 1036−1045.

9. Almond-Thynne, J.; Blakemore, D. C.; Pryde, D. C.; Spivey, A. C. Site-Selective Suzuki−Miyaura Coupling of Heteroaryl Halides − Understanding the Trends for Pharmaceutically Important Classes. *Chem. Sci.* **2017**, *8*, 40−62.

10. Reeves, E. K.; Entz, E. D.; Neufeldt, S. R. Chemodivergence between Electrophiles in Cross-Coupling Reactions. *Chem. Eur. J.* **2021**, *27*, 6161−6177.

11. Ng, S. S.; Pang, W. H.; Yuen, O. Y.; So, C. M. Recent Advances in the Application of Ligands in Palladium-Catalyzed Chemoselective Coupling Reactions at C−Br, C−OTf, and C−Cl sites. *Org. Chem. Front.* **2023**, *10*, 4408−4436.

12. Kamikawa, T.; Hayashi, T. Control of Reactive Site in Palladium-Catalyzed Grignard Cross-Coupling of Arenes Containing Both Bromide and Triflate. *Tetrahedron Lett.* **1997**, *38*, 7087−7090.

13. Wang, J.; Seefeld, M. A.; Luengo, J. Unusual Ligand-Dependent Chemoselective Suzuki−Miyaura Cross-Coupling Reactions of 3-Bromo-4-trifloyl-thiophenes. *Tetrahedron Lett.* **2011**, *52*, 6346−6348.

14. Khaddour, Z.; Akrawi, O. A.; Hamdy, A. M.; Suleiman, A. Jamous, K.; Villinger, A.; Langer, P. Chemoselective Suzuki-Cross Coupling Reactions of 5-Bromoquinolin-8-yl Trifluoromethanesulfonate. *Tetrahedron Lett.* **2015**, *56*, 554−557.

15. Kundu, G.; Sperger, T.; Rissanen, K.; Schoenebeck, F. A Next-Generation Air-Stable Pd(I) Dimer Enables Olefin Migration and Selective C−C Coupling in Air. *Angew. Chem. Int. Ed.* **2020**, *59*, 21930−21934.

16. Kalvet, I.; Deckers, K.; Funes-Ardoiz, I.; Magnin, G.; Sperger, T.; Kremer, M.; Schoenebeck, F. Selective *ortho*-Functionalization of Adamantylarenes Enabled by Dispersion and an Air-Stable Pd(I) Dimer. *Angew. Chem. Int. Ed.* **2020**, *59*, 7721−7725.

17. Keaveney, S. T.; Kundu, G.; Schoenebeck, F. Modular Functionalization of Arenes in a Triply Selective Sequence: Rapid C(sp^2) and C(sp^3) Coupling of C−Br, C−OTf, and C−Cl Bonds Enabled by a Single Pd(I) Dimer. *Angew. Chem. Int. Ed.* **2018**, *57*, 12573−12577.

18. Kalvet, I.; Sperger, T.; Scattolin, T.; Magnin, G.; Schoenebeck, F. Pd(I) Dimer Enabled Extremely Rapid and Chemoselective Alkylation of Aryl Bromides over Triflates and Chlorides in Air. *Angew. Chem. Int. Ed.* **2017**, *56*, 7078−7082.

19. Wong, S. M.; So, C. M.; Chung, K. H.; Lau, C. P.; Kwong, F. Y. An Efficient Class of P, N-Type “PhMezole-phos” Ligands: Applications in Palladium-Catalyzed Suzuki Coupling of Aryl Chlorides. *Eur. J. Org. Chem.* **2012**, 4172−4177.

20. Handa, S.; Andersson, M. P.; Gallou, F.; Reilly, J.; Lipshutz, B. H. HandaPhos: A General Ligand Enabling Sustainable Ppm Levels of Palladium-Catalyzed Cross-Couplings in Water at Room Temperature. *Angew. Chem. Int. Ed.* **2016**, *55*, 4914−4918.

21. Roy, D.; Uozumi, Y. Recent Advances in Palladium-Catalyzed Cross-Coupling Reactions at Ppm to Ppb Molar Catalyst Loadings. *Adv. Synth. Catal.* **2018**, *360*, 602−625.

22. Akporji, N.; Thakore, R. R.; Cortes-Clerget, M.; Andersen, J.; Landstrom, E.; Aue, D. H.; Gallou, F.; Lipshutz, B. H. N_2Phos − An Easily Made, Highly Effective Ligand Designed for Ppm Level Pd-Catalyzed Suzuki−Miyaura Cross Couplings in Water. *Chem. Sci.* **2020**, *11*, 5205−5212.

23. Zapf, A.; Beller, M. The Development of Efficient Catalysts for Palladium-Catalyzed Coupling Reactions of Aryl Halides. *Chem. Commun.* **2005**, 431−440.

24. Hartwig, J. F. Evolution of a Fourth Generation Catalyst for the Amination and Thioetherification of Aryl Halides. *Acc. Chem. Res.* **2008**, *41*, 1534−1544.

25. Martin, R.; Buchwald, S. L. Palladium-Catalyzed Suzuki−Miyaura Cross-Coupling Reactions Employing Dialkylbiaryl Phosphine Ligands. *Acc. Chem. Res.* **2008**, *41*, 1461−1473.

26. Lundgren, R. J.; Stradiotto, M. Addressing Challenges in Palladium-Catalyzed Cross-Coupling Reactions Through Ligand Design. *Chem. Eur. J.* **2012**, *18*, 9758−9769.

27. Gildner, P. G.; Colacot, T. J. Reactions of the 21st Century: Two Decades of Innovative Catalyst Design for Palladium-Catalyzed Cross-Couplings. *Organometallics* **2015**, *34*, 5497−5508.

28. Wong, S. M.; Yuen, O. Y.; Choy, P. Y.; Kwong, F. Y. When Cross-Coupling Partners Meet Indolylphosphines. *Coord. Chem. Rev.* **2015**, *293−294*, 158−186.

29. Tse, M. H.; Choy, P. Y.; Kwong, F. Y. Facile Assembly of Modular-Type Phosphines for Tackling Modern Arylation Processes. *Acc. Chem. Res.* **2022**, *55*, 3688−3705.

30. Surry, D. S.; Buchwald, S. L. Biaryl Phosphane Ligands in Palladium-Catalyzed Amination. *Angew. Chem. Int. Ed.* **2008**, *47*, 6338−6361.

31. Surry, D. S.; Buchwald, S. L. Dialkylbiaryl Phosphines in Pd-Catalyzed Amination: A User's Guide. *Chem. Sci.* **2011**, *2*, 27−50.

32. So, C. M.; Yuen, O. Y.; Ng, S. S.; Chen, Z. General Chemoselective Suzuki−Miyaura Coupling of Polyhalogenated Aryl Triflates Enabled by an Alkyl-Heteroaryl-Based Phosphine Ligand. *ACS Catal.* **2021**, *11*, 7820−7827.

33. Wang, M.; So, C. M. Inverting Conventional Chemoselectivity in the Sonogashira Coupling Reaction of Polyhalogenated Aryl Triflates with TMS-Arylalkynes. *Org. Lett.* **2022**, *24*, 681−685.

34. Ng, S. S.; Chen, Z.; Yuen, O. Y.; So, C. M. Palladium-Catalyzed Chemoselective Borylation of (Poly)halogenated Aryl Triflates and Their Application in Consecutive Reactions. *Adv. Synth. Catal.* **2022**, *364*, 1596−1601.

35. Chen, Z.; Gu, C.; Yuen, O. Y.; So, C. M. Palladium-Catalyzed Chemoselective Direct α-Arylation of Carbonyl Compounds with Chloroaryl Triflates at the C−Cl site. *Chem. Sci.* **2022**, *13*, 4762−4769.

36. Wang, M.; Yuen, O. Y.; So, C. M. Palladium-Catalyzed Desulfinative Cross-Coupling of Polyhalogenated Aryl Triflates with Aryl Sulfinate Salts: Inversion of Traditional Chemoselectivity. *Chin. J. Chem.* **2023**, *41*, 909−914.

37. Littke, A. F.; Dai, C.; Fu, G. C. Versatile Catalysts for the Suzuki Cross-Coupling of Arylboronic Acids with Aryl and Vinyl Halides and Triflates under Mild Conditions. *J. Am. Chem. Soc.* **2000**, *122*, 4020−4028.

38. Espino, G.; Kurbangalieva, A.; Brown, J. M. Aryl Bromide/Triflate Selectivities Reveal Mechanistic Divergence in Palladium-Catalyzed Couplings; the Suzuki−Miyaura Anomaly. *Chem. Commun.* **2007**, *2007*, 1742−1744.

39. Jopp, S.; Wallaschkowski, T.; Ehlers, P.; Frank, E.; Schneider, G.; Wölfling, J.; Mernyák, E.; Villinger, A.; Langer, P. Chemoselective Suzuki−Miyaura Reactions of 4-Bromo-3-*O*-triflyl-estrone. Synthesis and Atropisomerism of Arylated Estrones. *Tetrahedron* **2018**, *74*, 2825−2836.

40. Hassan, Z.; Hussain, M.; Villinger, A.; Langer, P. Synthesis of Aryl-Substituted Naphthalenes by Chemoselective Suzuki−Miyaura Reactions of Bromo-trifluoromethanesulfonyloxy-naphthalenes. Influence of Steric and Electronic Parameters. *Tetrahedron* **2012**, *68*, 6305−6313.

41. Armarego, W. L. F. *Purification of Laboratory Chemicals*, 8th ed.; Butterworth-Heinemann, 2017.

42. Reeves, E. K.; Humke, J. N.; Neufeldt, S. R. *N*-Heterocyclic Carbene Ligand-Controlled Chemodivergent Suzuki−Miyaura Cross Coupling. *J. Org. Chem.* **2019**, *84*, 11799−11812.

43. Ramírez-López, P.; Ros, A.; Estepa, B.; Fernández, R.; Fiser, B.; Gómez-Bengoa, E.; Lassaletta, J. M. A Dynamic Kinetic C−P Cross-Coupling for the Asymmetric Synthesis of Axially Chiral P,N Ligands. *ACS Catal.* **2016**, *6*, 3955−3964.

44. Daab, J. C.; Bracher, F. Total Syntheses of the Alkaloids Ipalbidinium and Clathryimine B. *Monatsh. Chem.* **2003**, *134*, 573−583.

5. Chapter 5: Conclusion

5

This dissertation presents the design and synthesis of two classes of novel phosphine ligands: indole-amide-based phosphine ligands and C2-alkylated indole-based phosphine ligands. The research focuses on applying these ligands in Pd-catalysed cross-coupling reactions, underscoring their significance in achieving high reactivity and chemoselectivity under low palladium catalyst loading conditions, thereby addressing long-standing challenges in transition metal catalysis.

Chapter 2 presents a significant advancement in constructing sterically hindered biaryls using a catalytic system composed of $Pd_2(dba)_3$ and indole-amide-based phosphine ligands. The developed methodology enables Suzuki−Miyaura cross-coupling reactions, delivering excellent results in as little as 10 minutes with exceptionally low palladium catalyst loadings, as low as 50 ppm. However, this work is limited to the synthesis of tetra-*ortho*-substituted biaryls. This suggests that ligand design still requires improvement to achieve highly sterically hindered Suzuki−Miyaura cross-coupling reactions.

Chapter 3 details the unconventional chemoselectivity exhibited by a C2-alkylated indole-based phosphine ligand, SelectPhos, in the Pd-catalysed borylation of polyhalogenated aryl triflates. Traditionally, the general reactivity order of C−Br > C−OTf > C−Cl is observed. However, this research demonstrates a new reactivity order of C−Cl > C−OTf, achieved through the specifically designed structural features of the ligand. This finding is significant as it challenges existing paradigms and highlights the potential to drastically alter reaction pathways through ligand design. Due to the difficulty in purifying the target pinacol arylboronic ester via chromatography, bulb-to-bulb distillation was employed to isolate the pure product. Unfortunately, this method is unsuitable for thermally labile pinacol heteroaryl esters, resulting in a limited substrate scope due to challenges in isolation. Notably, a one-pot, two-step sequence combining chemoselective borylation with subsequent intermolecular Suzuki−Miyaura coupling, facilitating the efficient synthesis of asymmetric biaryls bearing triflate moieties. This approach opens new avenues for the synthesis of complex terphenyl structures, which are crucial in various advanced applications.

Building on the insights from Chapter 3, Chapter 4 focuses on the application of SelectPhos in Suzuki−Miyaura cross-coupling reactions. In this chapter, the observed reactivity order is C−Br > C−Cl > C−OTf, consistent with the previous finding but achieved with exceptional reactivity and chemoselectivity. The successful coupling of various bromo(hetero)aryl triflates with (hetero)arylboronic acids, along with the catalyst's efficacy at a mere 0.02 mol% palladium loading, underscores the robustness and efficiency of SelectPhos. Additionally, the demonstration of sequential dual functionalisation of bromochloroaryl triflates further expands the

synthetic utility and facilitate the construction of triphenyl derivatives by showcasing the versatility of SelectPhos.

The findings in this thesis have profound implications for palladium catalysis. The novel phosphine ligands developed exhibit exceptional performance, providing new avenues for reaction optimisation and challenging traditional reactivity paradigms. The ability of these ligands to function under mild conditions with minimal catalyst loadings paves the way for more sustainable and cost-effective synthetic processes. The efficient synthesis of biaryls and terphenyls demonstrated in Chapter 2 and Chapter 4 holds significant promise for pharmaceutical and materials science applications. The mild reaction conditions and high selectivity can lead to more straightforward, scalable production of complex molecules, potentially accelerating drug discovery and the development of advanced materials. In pharmaceutical chemistry, these biaryls serve as core structures in many bioactive compounds, making the presented synthetic methods invaluable for the rapid and efficient protocol of drug candidates. In materials science, the ability to construct intricate biaryl frameworks with precision opens new possibilities for designing novel materials with unique electronic, optical, or mechanical properties.

The success of indole-based phosphine ligands in this thesis suggests that exploring other heterocyclic frameworks could yield additional promising candidates, offering solutions to an even broader array of synthetic challenges. The unconventional reactivity order observed in Chapter 3 and Chapter 4 highlights the importance of ligand design in influencing reaction pathways. These findings suggest that a structurally fine-tuned ligand can achieve desired reactivity and selectivity, offering a powerful tool for chemists. Understanding how specific ligand features impact chemoselectivity and reactivity could unlock new possibilities for tailor-made catalysts for a wide range of reactions, guiding the design of even more effective catalysts.

Future research could focus on expanding the ligand toolbox with diverse structures by synthesising and evaluating ligands based on different heterocyclic backbones, optimising their structures for specific applications, and enhancing the versatility of Pd-catalysed reactions. Such efforts could lead to the discovery of new catalyst systems with unprecedented reactivity and selectivity, further broadening the scope of palladium catalysis.

6. Appendix

NMR and HRMS Spectra of Chapter 2

^{1}H NMR of *N*,*N*-diisopropyl-1-methyl-1*H*-indole-2-carboxamide (**P1**)

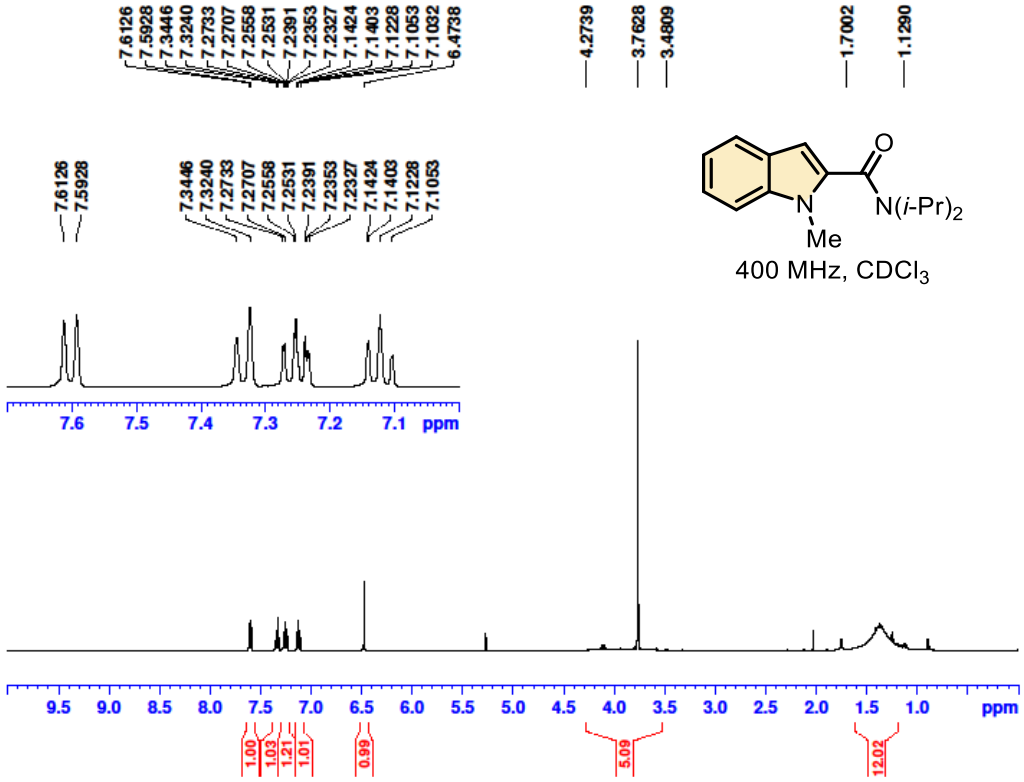

^{13}C NMR of *N*,*N*-diisopropyl-1-methyl-1*H*-indole-2-carboxamide (**P1**)

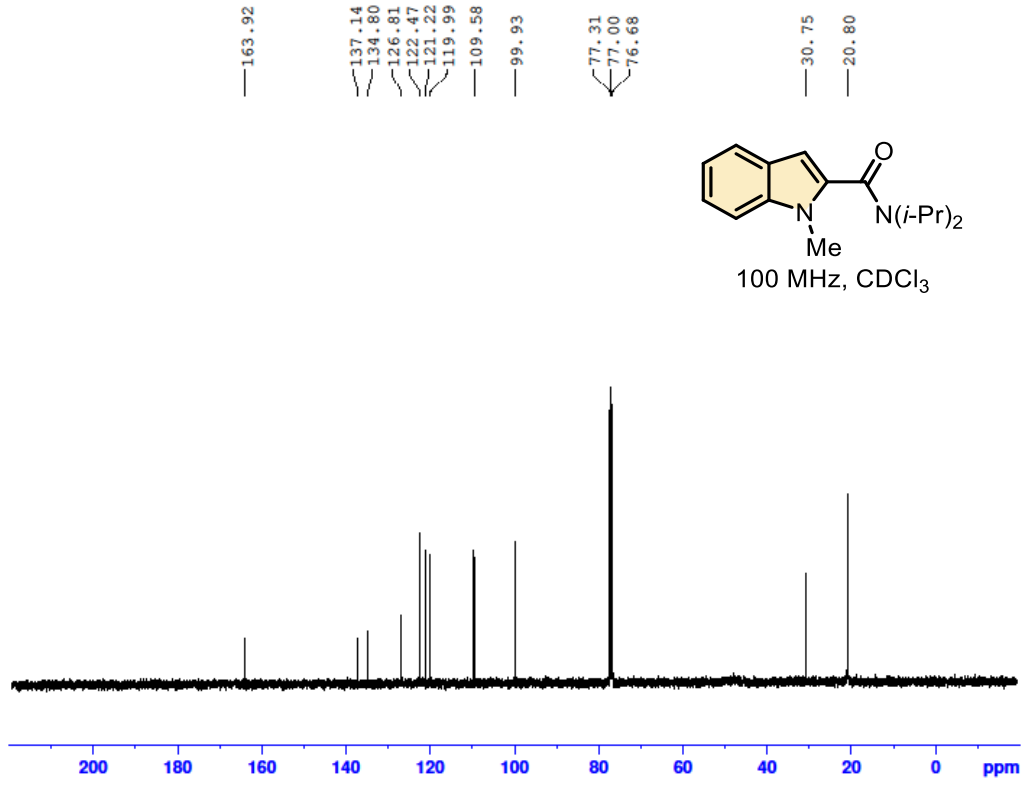

^{1}H NMR of 3-bromo-*N*,*N*-diisopropyl-1-methyl-1*H*-indole-2-carboxamide (**P1'**)

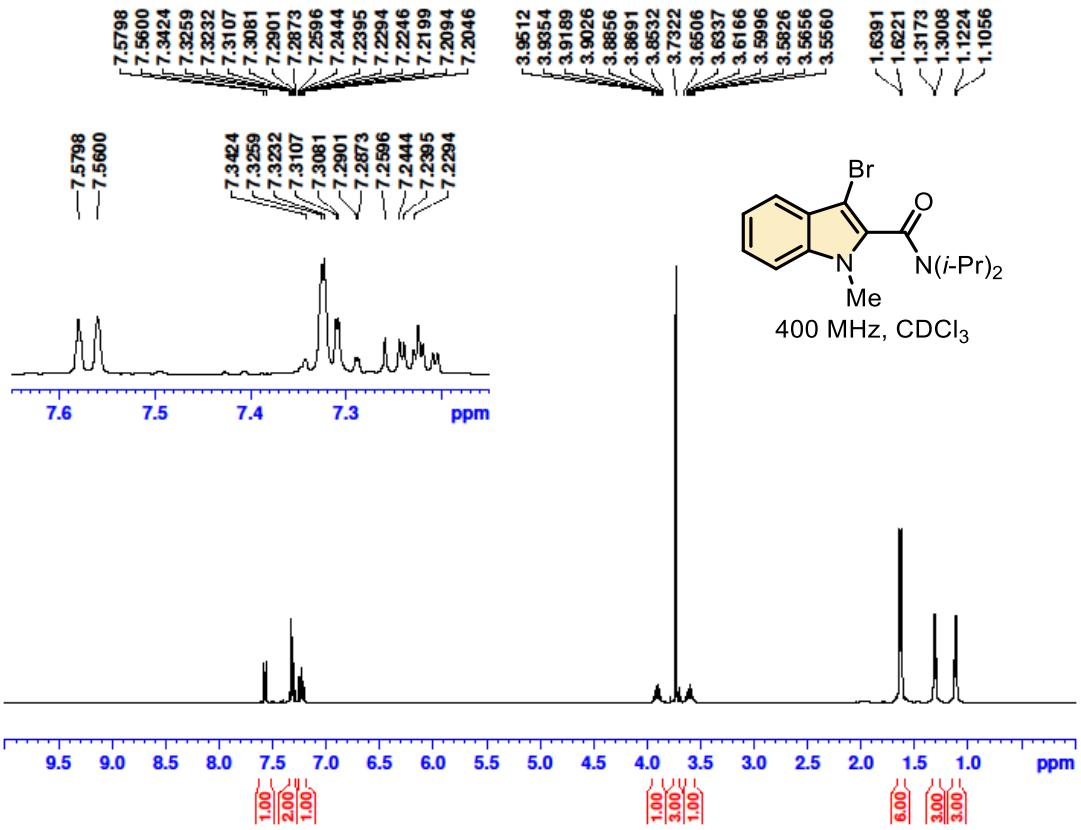

^{13}C NMR of 3-bromo-*N*,*N*-diisopropyl-1-methyl-1*H*-indole-2-carboxamide (**P1'**)

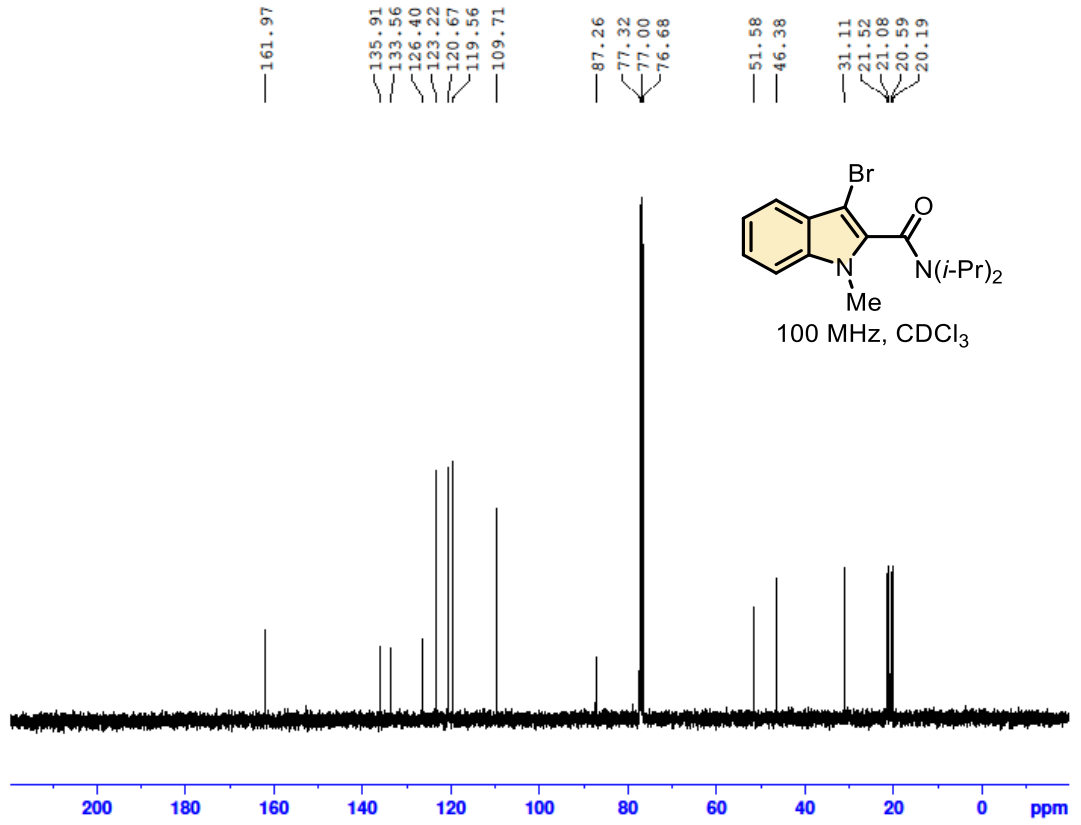

HRMS of 3-bromo-*N*,*N*-diisopropyl-1-methyl-1*H*-indole-2-carboxamide (**P1'**)

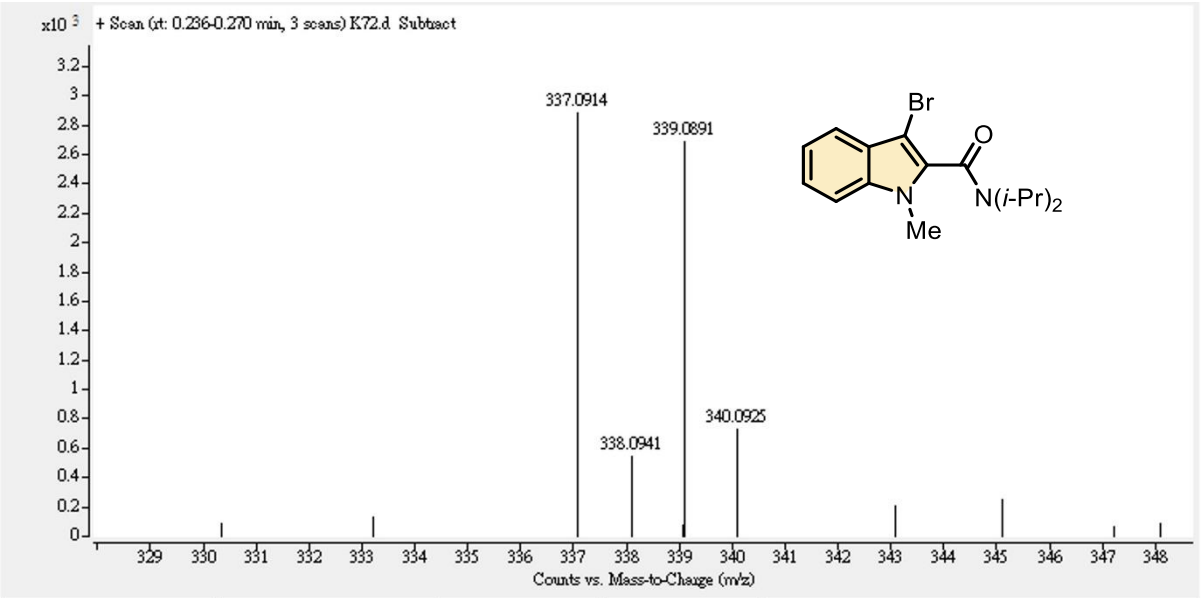

Mass	Calc. Mass	mDa	PPM	Formula
337.0914	337.0910	-0.40	-1.18	C16 H22 Br N2 O

^{1}H NMR of 3-(dicyclohexylphosphanyl)-*N*,*N*-diisopropyl-1-methyl-1*H*-indole-2-carboxamide (**L1**)

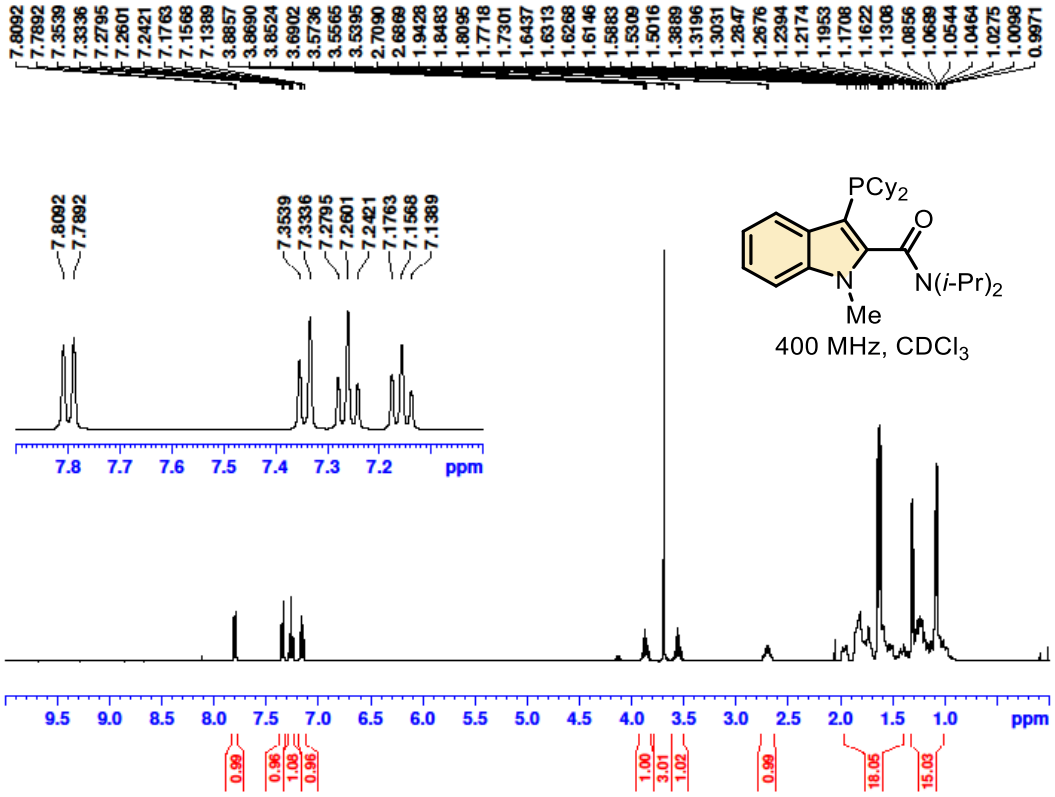

^{13}C NMR of 3-(dicyclohexylphosphanyl)-*N*,*N*-diisopropyl-1-methyl-1*H*-indole-2-carboxamide (**L1**)

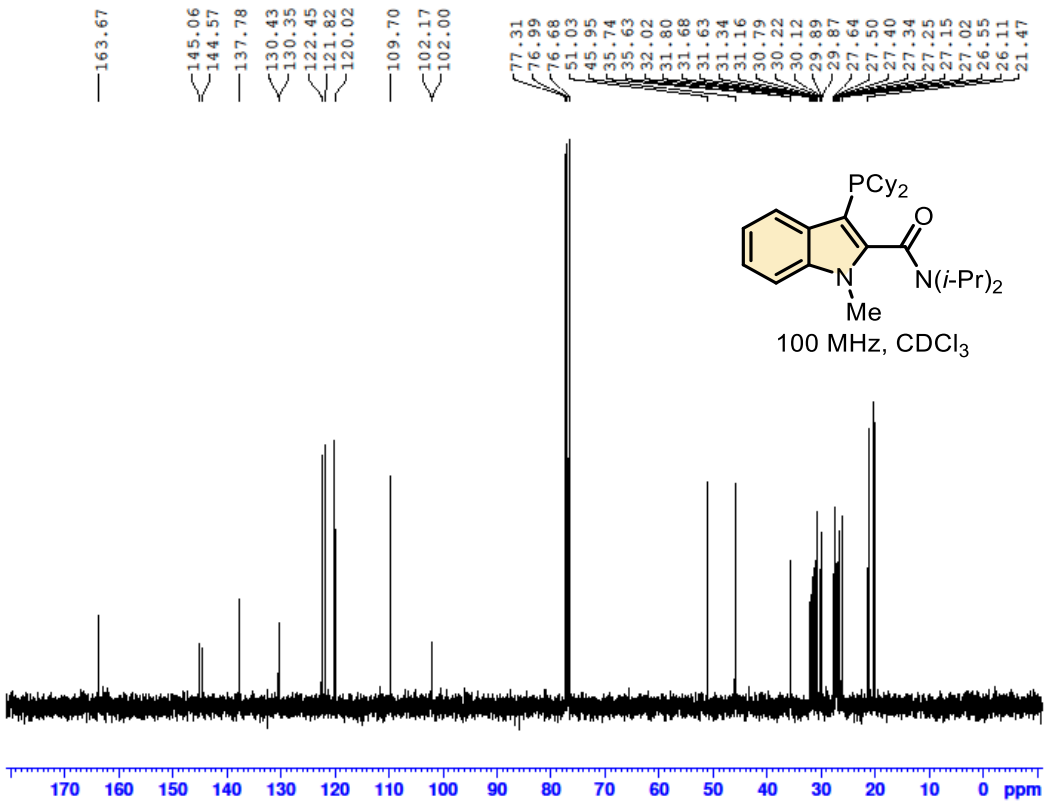

^{31}P NMR of 3-(dicyclohexylphosphanyl)-*N*,*N*-diisopropyl-1-methyl-1*H*-indole-2-carboxamide (**L1**)

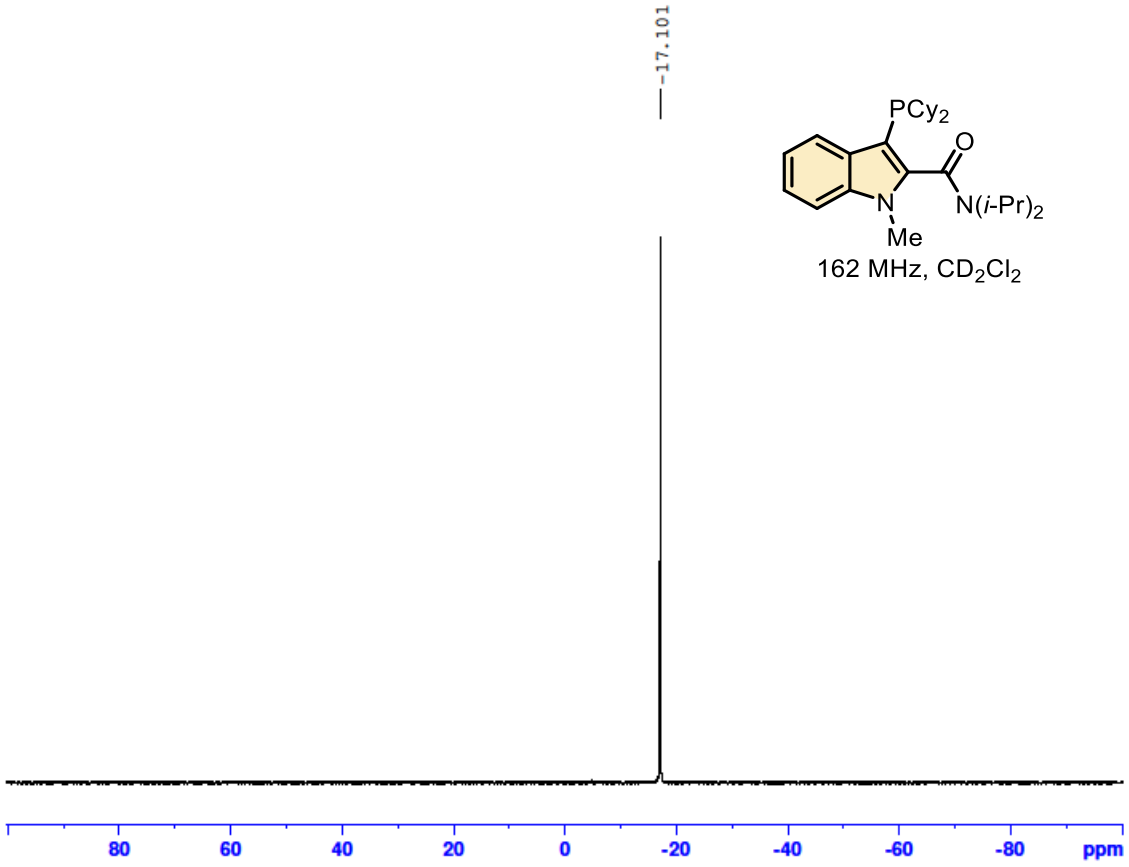

HRMS of 3-(dicyclohexylphosphanyl)-*N*,*N*-diisopropyl-1-methyl-1*H*-indole-2-carboxamide (**L1**)

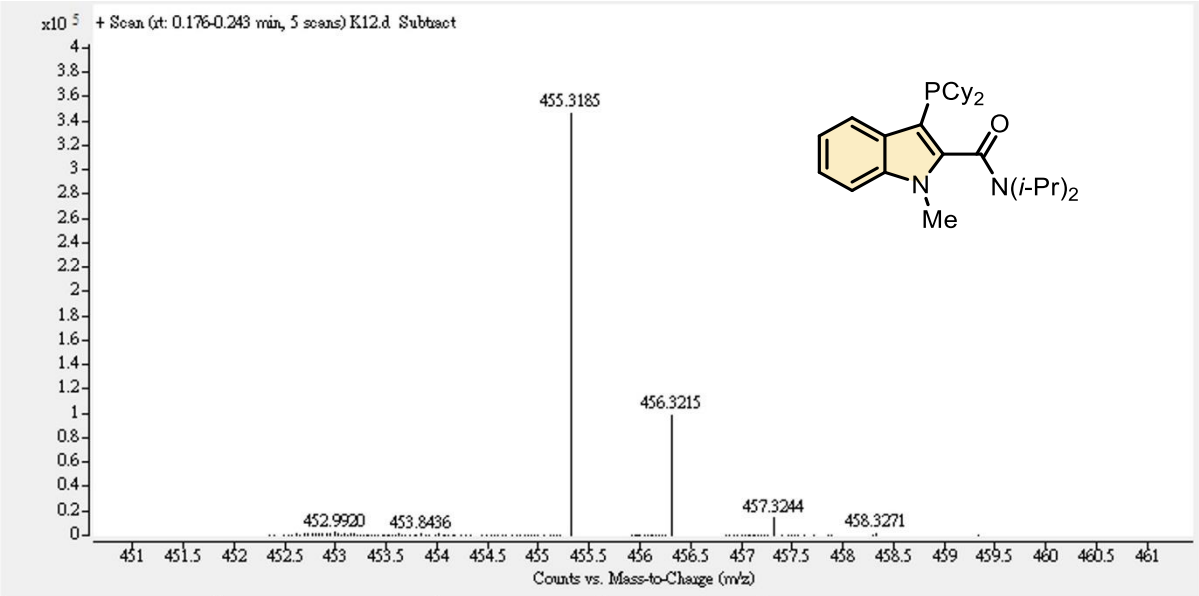

Mass	Calc. Mass	mDa	PPM	Formula
455.3185	455.3186	0.08	0.17	C28 H44 N2 O P

^{1}H NMR of *N*,*N*,1-trimethyl-1*H*-indole-2-carboxamide (**P2**)

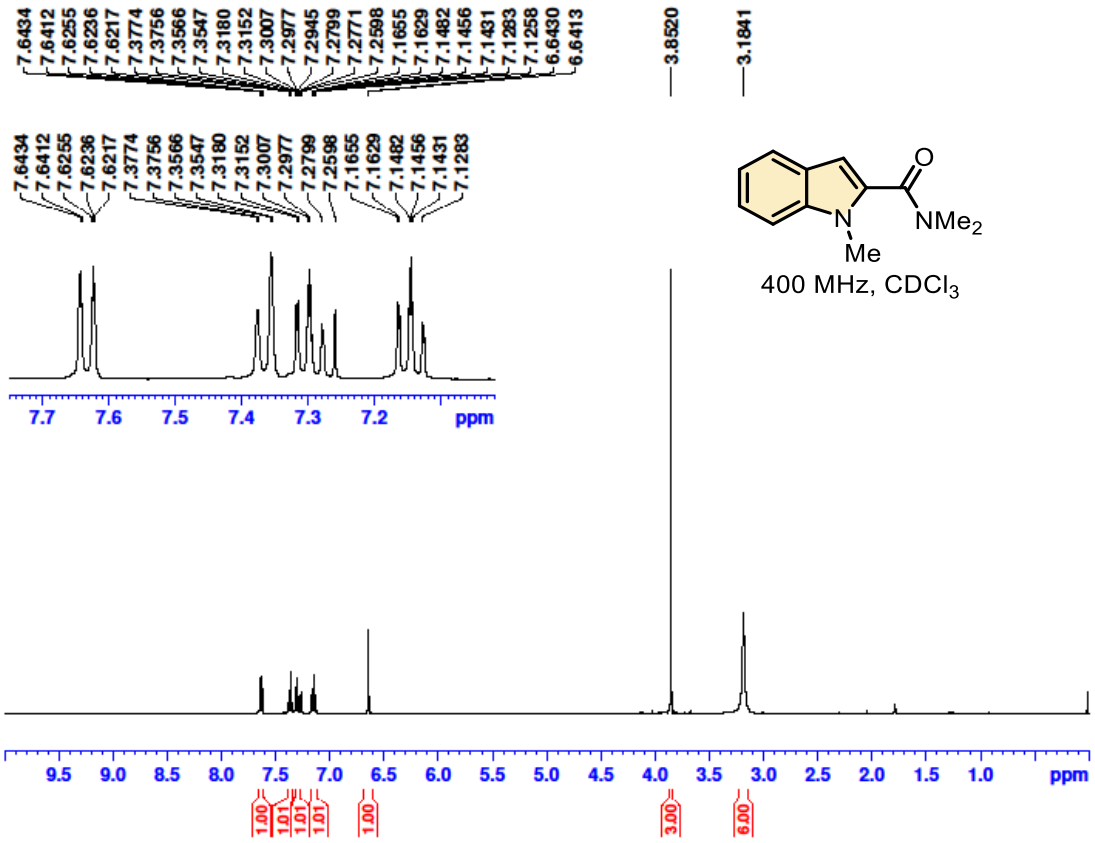

^{13}C NMR of *N*,*N*,1-trimethyl-1*H*-indole-2-carboxamide (**P2**)

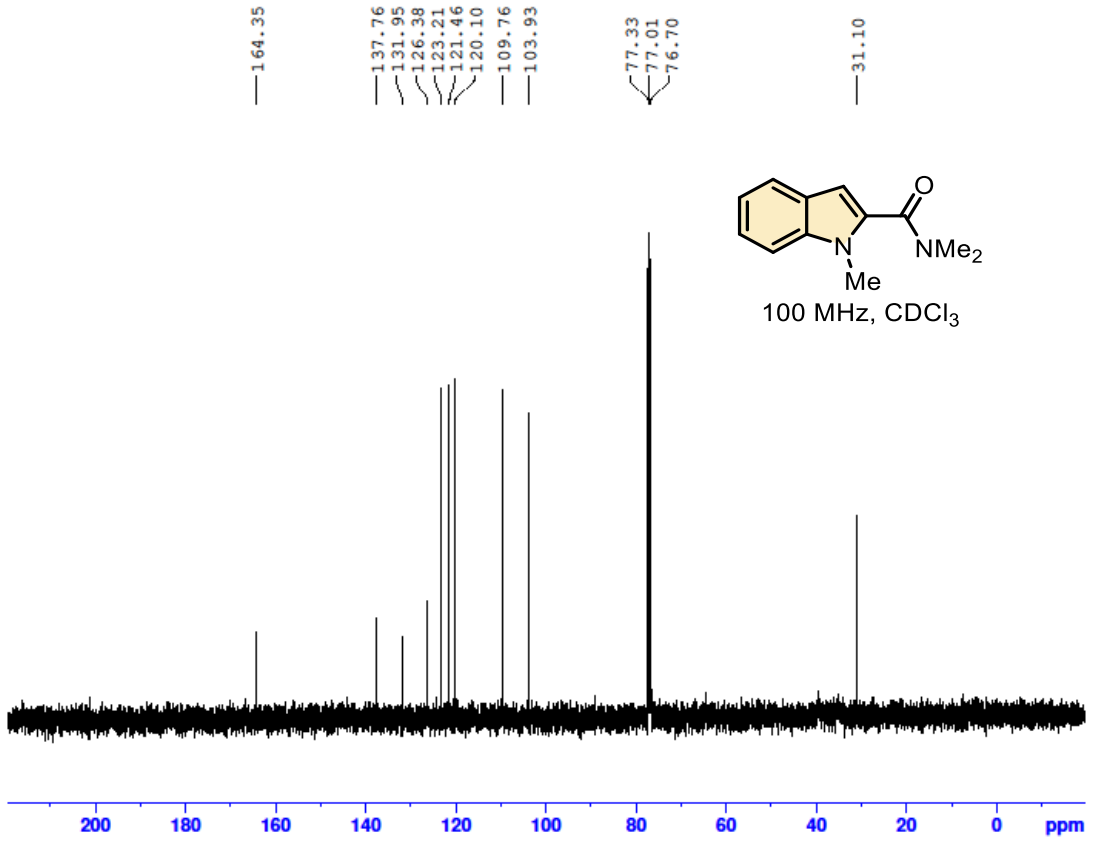

^{1}H NMR of 3-bromo-*N*,*N*,1-trimethyl-1*H*-indole-2-carboxamide (**P2'**)

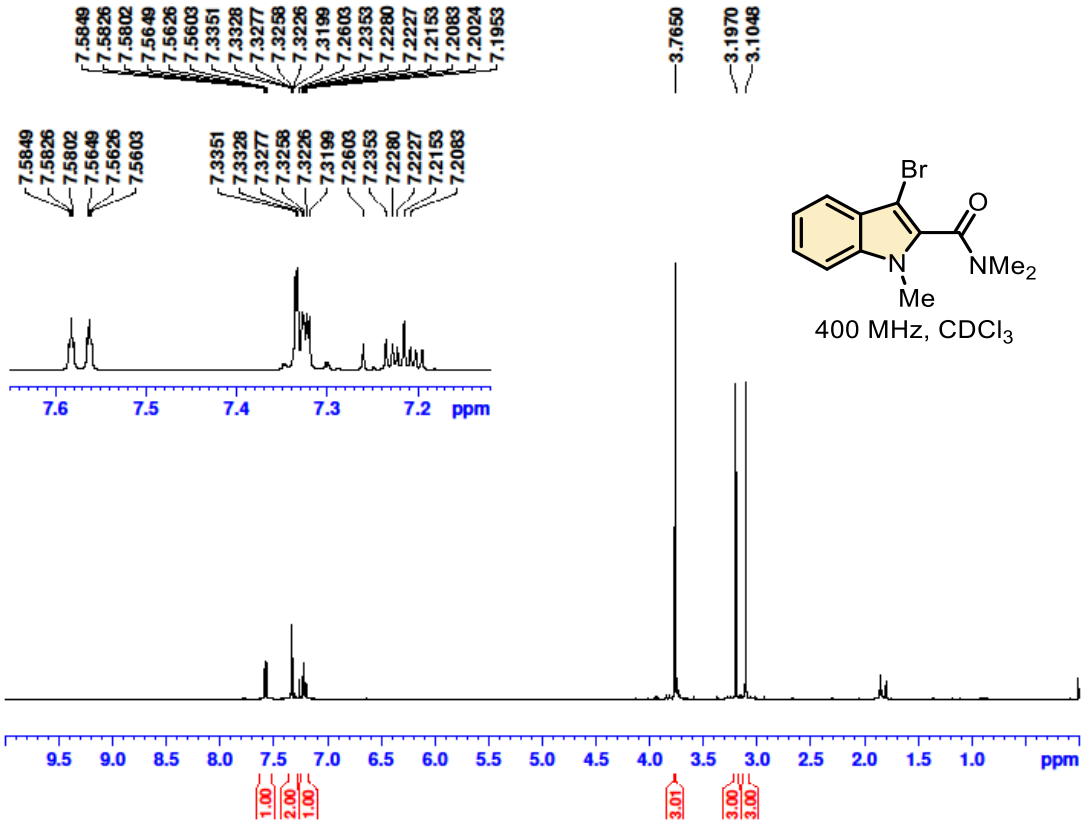

^{13}C NMR of 3-bromo-*N*,*N*,1-trimethyl-1*H*-indole-2-carboxamide (**P2'**)

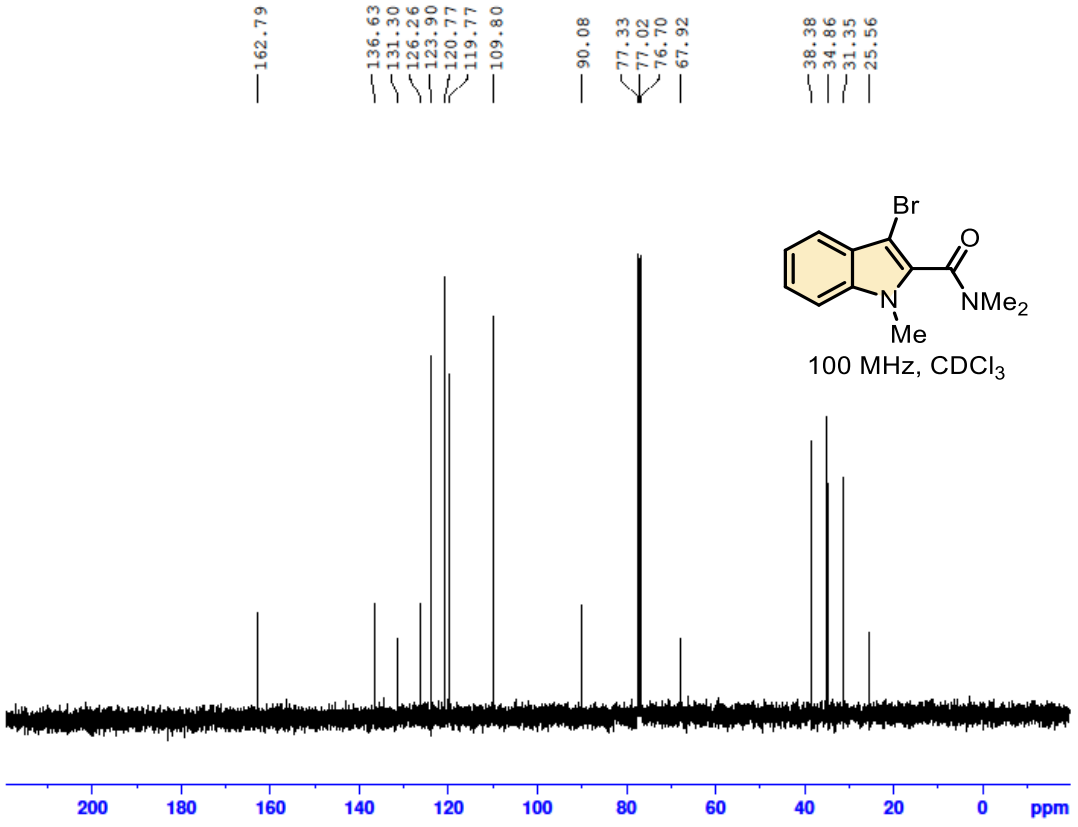

HRMS of 3-bromo-*N*,*N*,1-trimethyl-1*H*-indole-2-carboxamide (**P2'**)

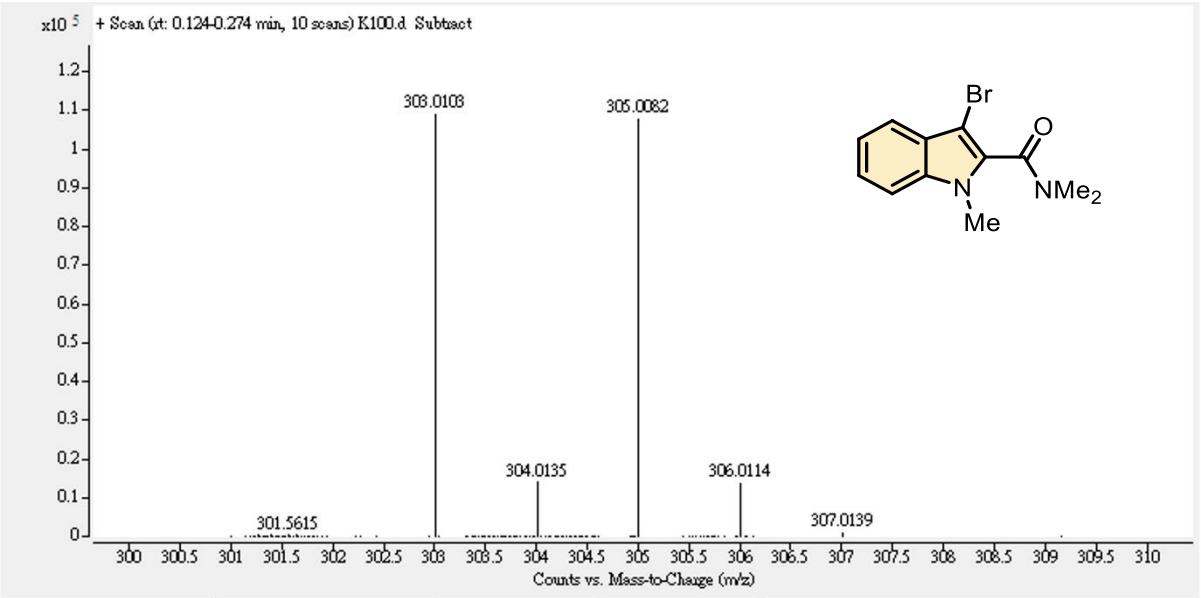

Mass	Calc. Mass	mDa	PPM	Formula
303.0103	303.0103	0.05	0.17	C12 H13 Br N2 Na O

^{1}H NMR of 3-(dicyclohexylphosphanyl)-*N*,*N*,1-trimethyl-1*H*-indole-2-carboxamide (**L2**)

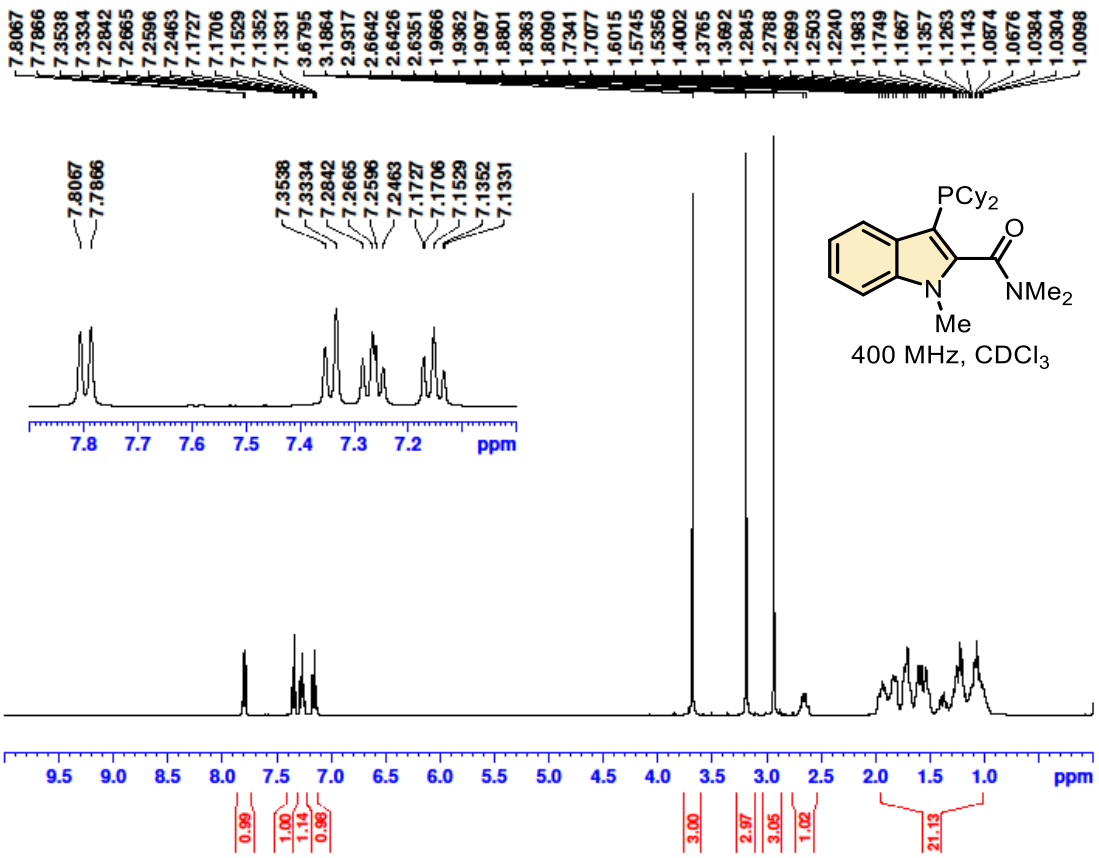

^{13}C NMR of 3-(dicyclohexylphosphanyl)-*N*,*N*,1-trimethyl-1*H*-indole-2-carboxamide (**L2**)

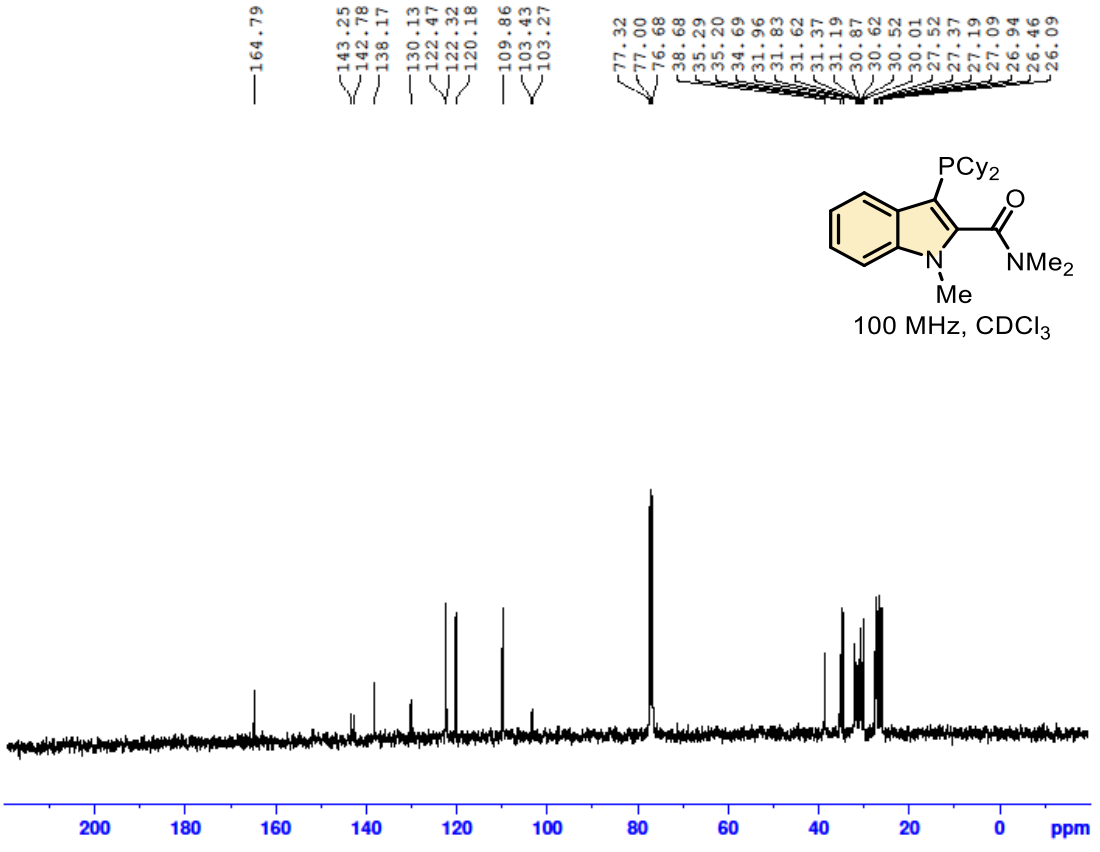

^{31}P NMR of 3-(dicyclohexylphosphanyl)-*N*,*N*,1-trimethyl-1*H*-indole-2-carboxamide (**L2**)

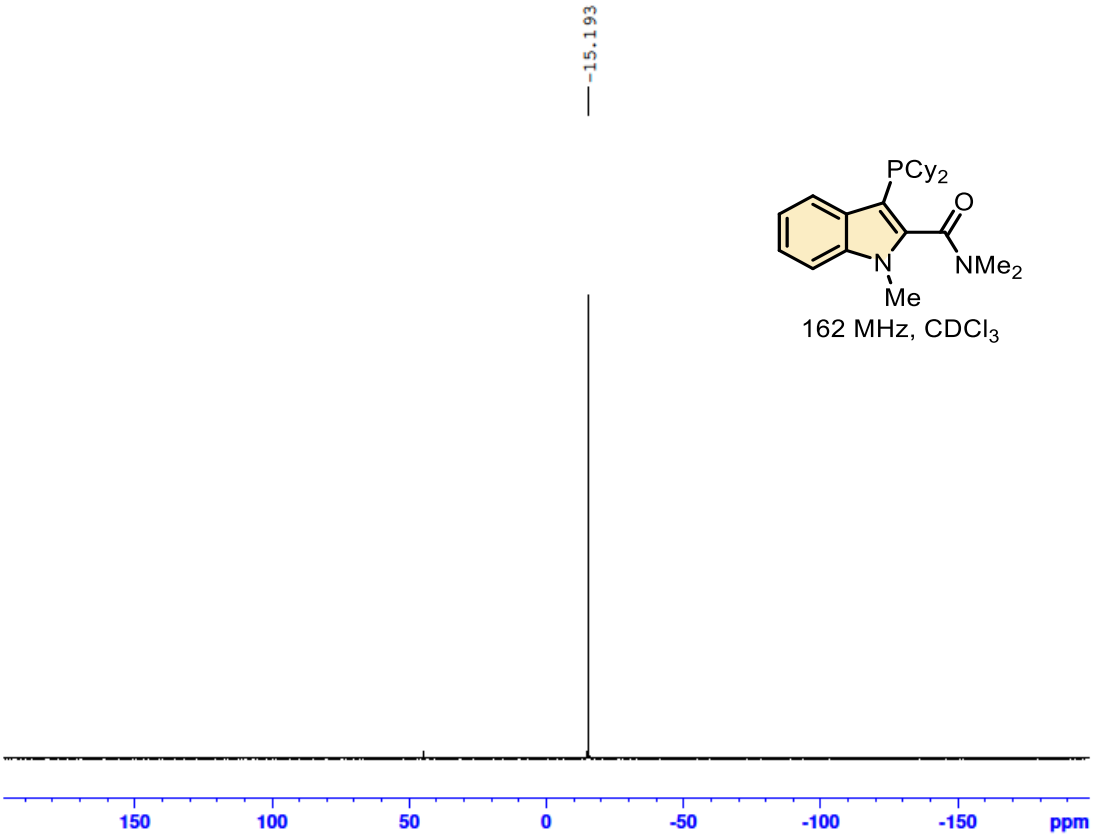

HRMS of 3-(dicyclohexylphosphanyl)-*N*,*N*,1-trimethyl-1*H*-indole-2-carboxamide (**L2**)

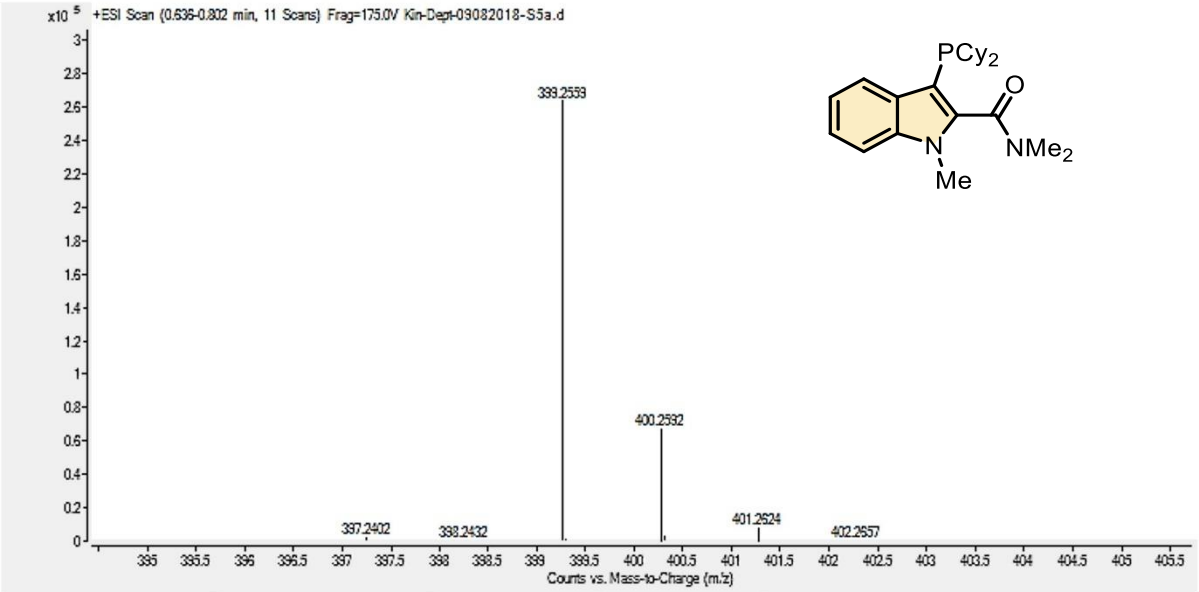

Mass	Calc. Mass	mDa	PPM	Formula
399.2559	399.2560	0.08	0.19	C24 H36 N2 O P

^{1}H NMR of 3-(diisopropylphosphanyl)-*N*,*N*,1-trimethyl-1*H*-indole-2-carboxamide (**L8**)

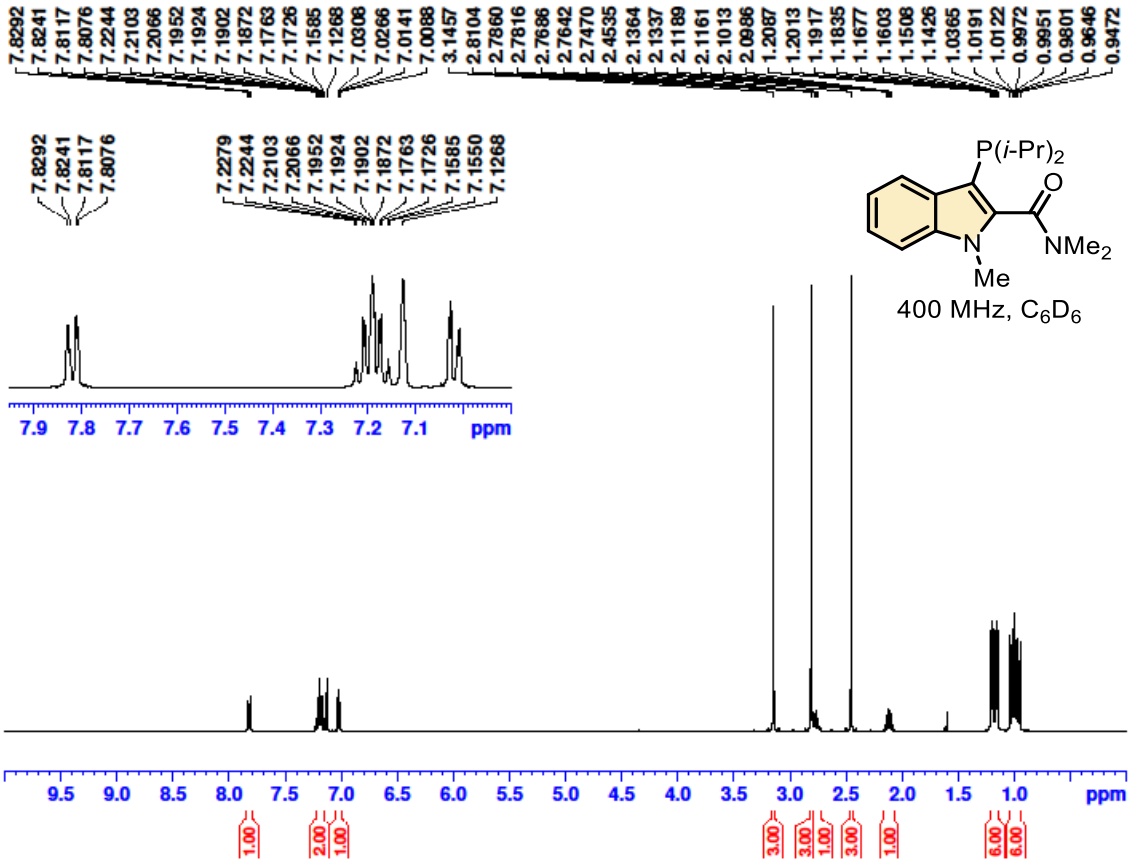

^{13}C NMR of 3-(diisopropylphosphanyl)-*N*,*N*,1-trimethyl-1*H*-indole-2-carboxamide (**L8**)

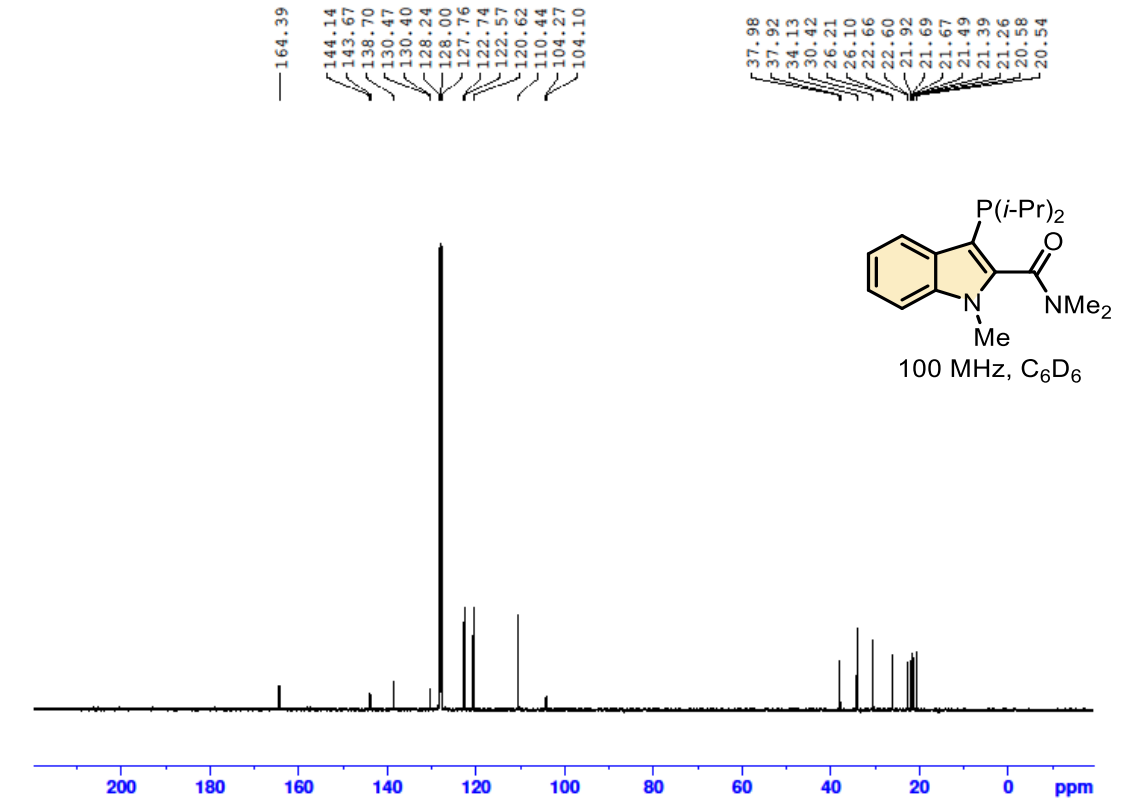

^{31}P NMR of 3-(diisopropylphosphanyl)-*N*,*N*,1-trimethyl-1*H*-indole-2-carboxamide (**L8**)

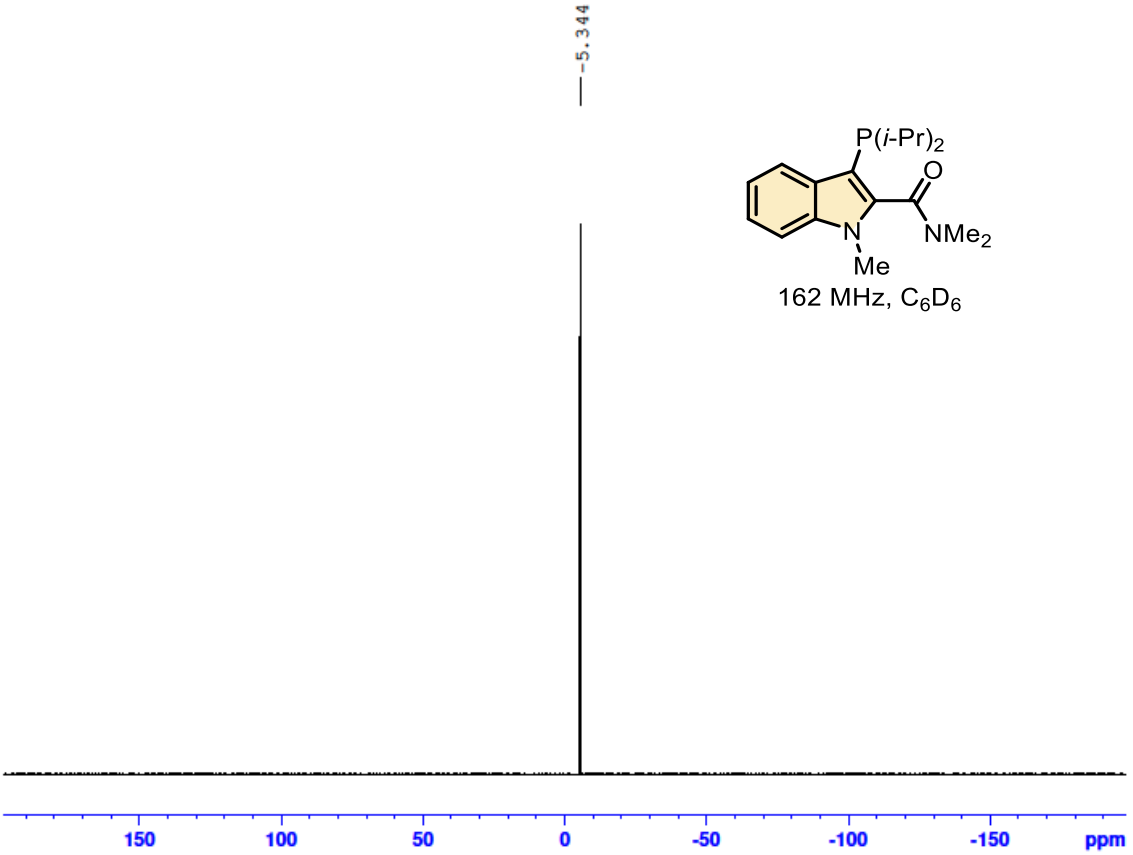

HRMS of 3-(diisopropylphosphanyl)-*N*,*N*,1-trimethyl-1*H*-indole-2-carboxamide (**L8**)

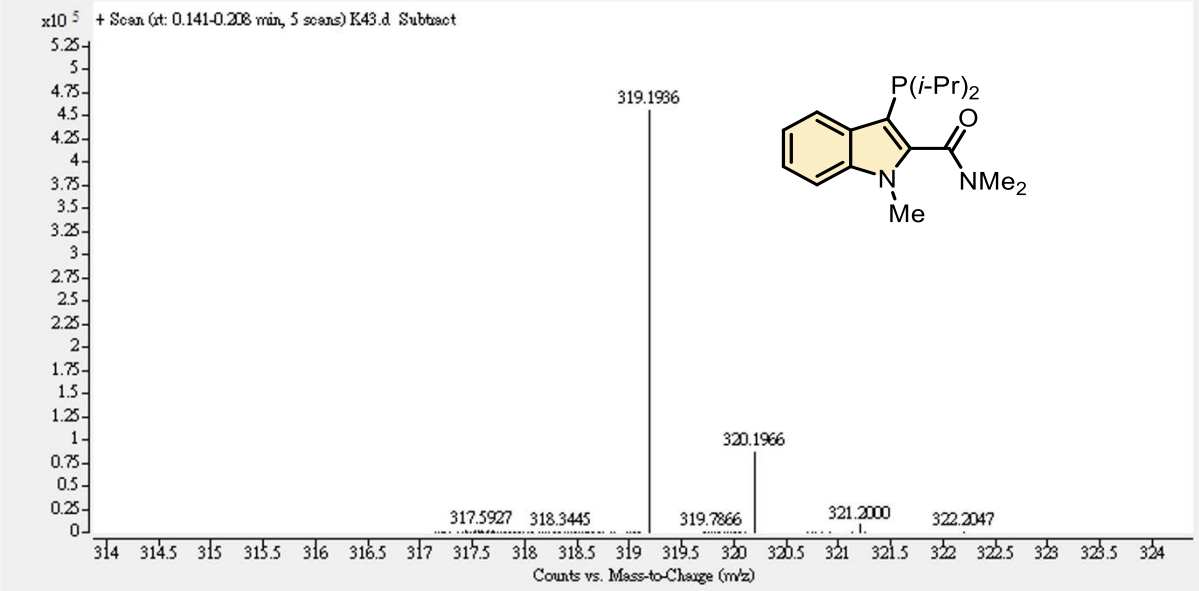

Mass	Calc. Mass	mDa	PPM	Formula
319.1936	319.1934	-0.22	-0.70	C18 H28 N2 O P

^{1}H NMR of 3-(diphenylphosphanyl)-*N*,*N*,1-trimethyl-1*H*-indole-2-carboxamide (**L9**)

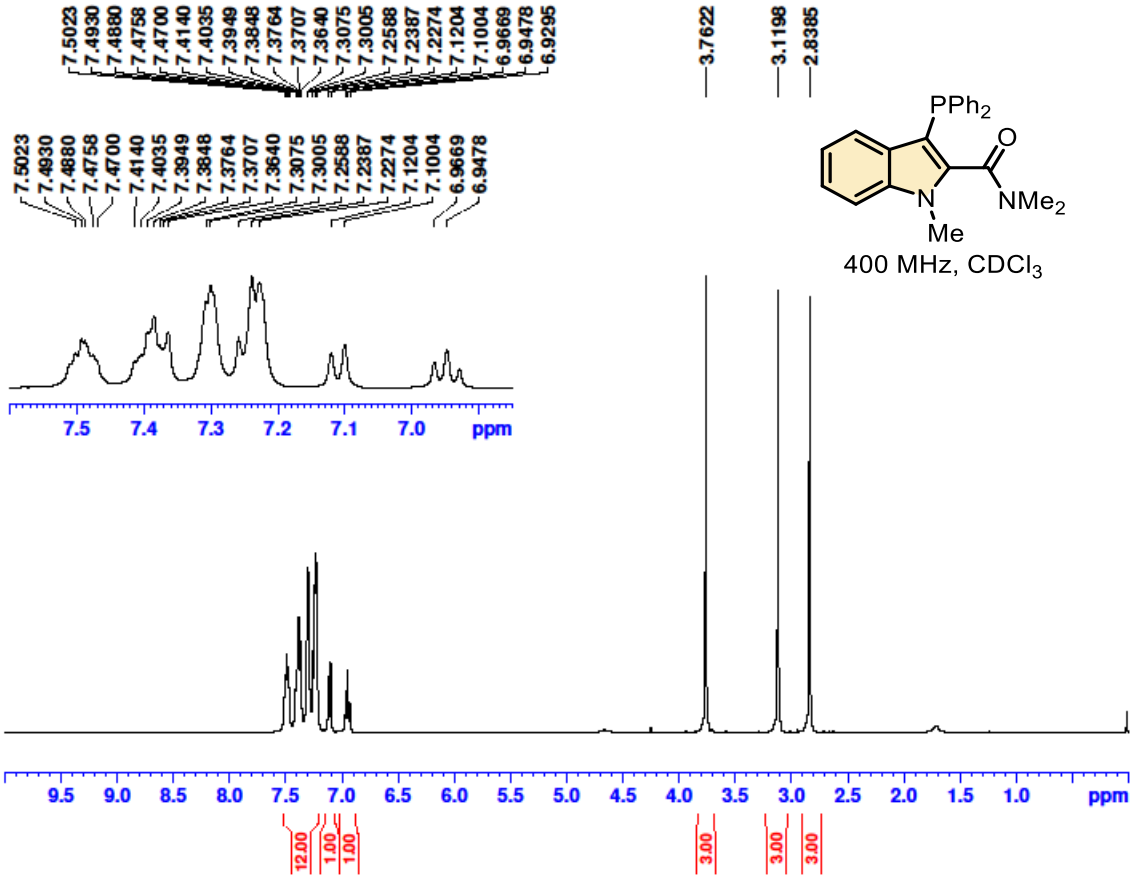

^{13}C NMR of 3-(diphenylphosphanyl)-*N*,*N*,1-trimethyl-1*H*-indole-2-carboxamide (**L9**)

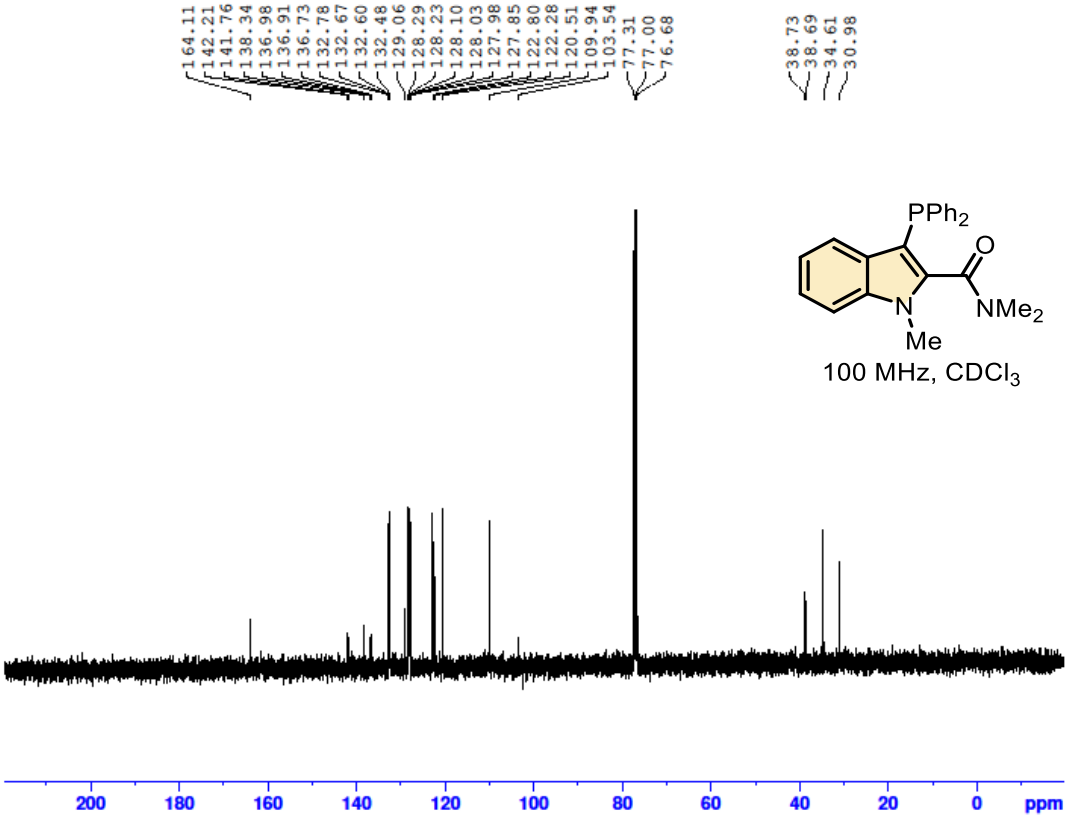

^{31}P NMR of 3-(diphenylphosphanyl)-*N*,*N*,1-trimethyl-1*H*-indole-2-carboxamide (**L9**)

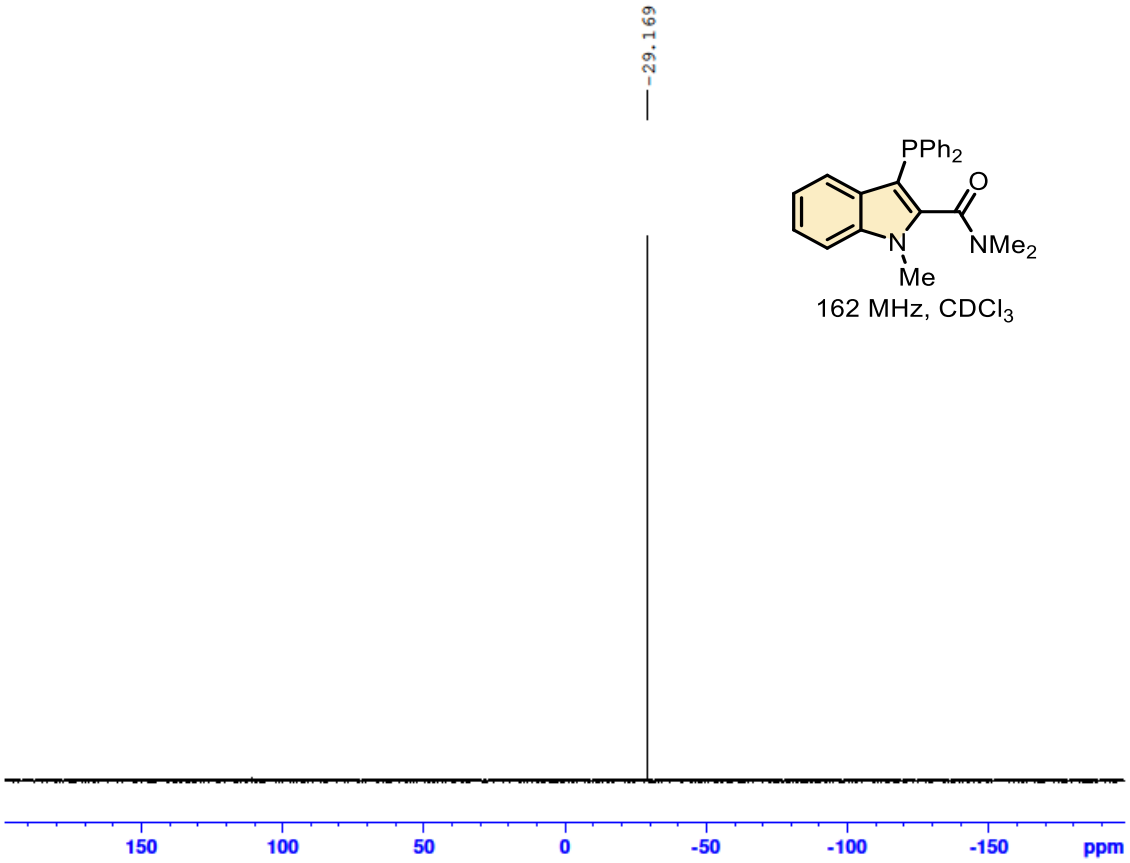

HRMS of 3-(diphenylphosphanyl)-*N*,*N*,1-trimethyl-1*H*-indole-2-carboxamide (**L9**)

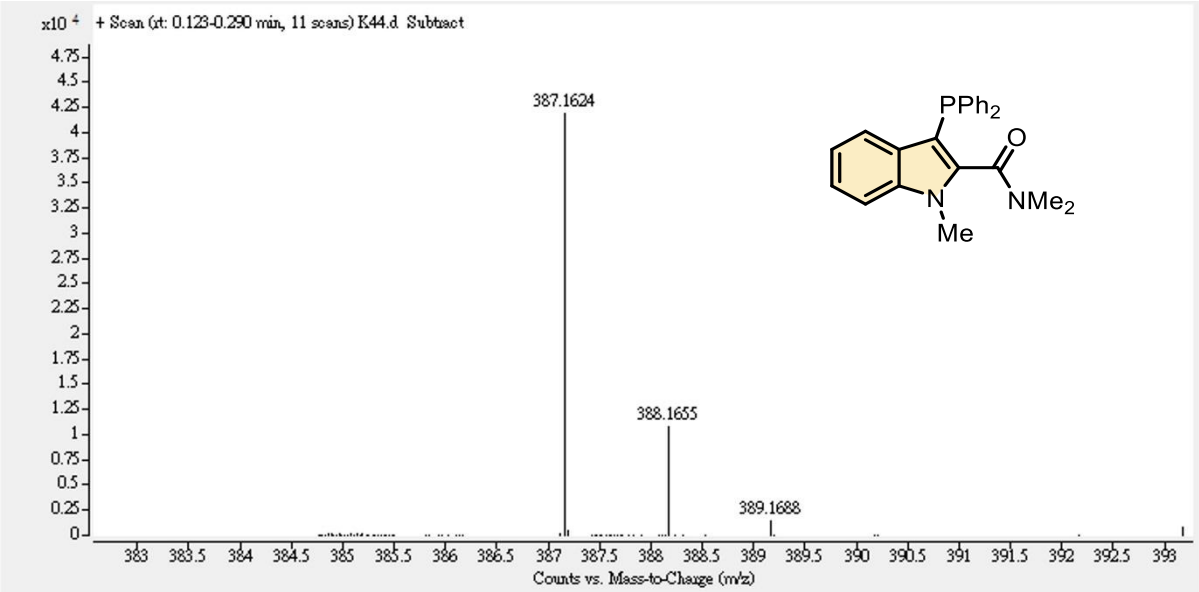

Mass	Calc. Mass	mDa	PPM	Formula
387.1624	387.1621	-0.32	-0.84	C24 H24 N2 O P

^{1}H NMR of (1-methyl-1*H*-indol-2-yl)(morpholino)methanone (**P3**)

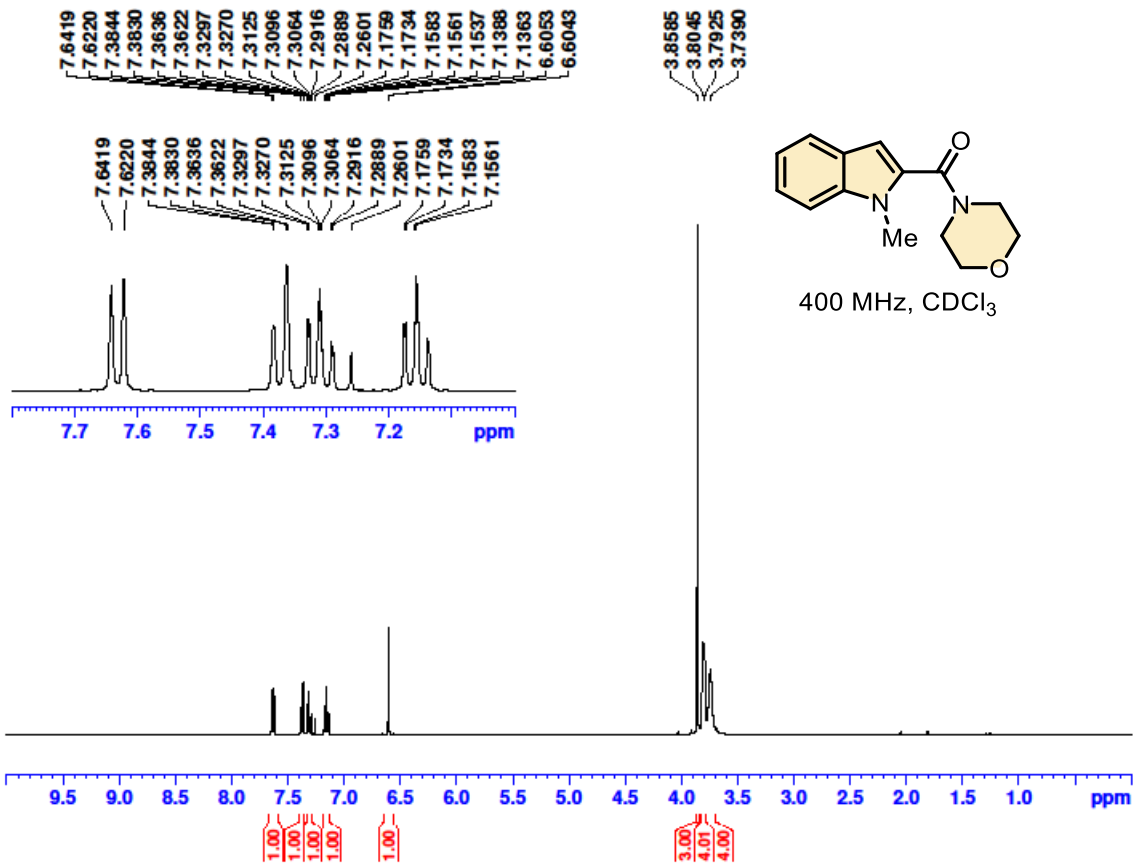

^{13}C NMR of (1-methyl-1*H*-indol-2-yl)(morpholino)methanone (**P3**)

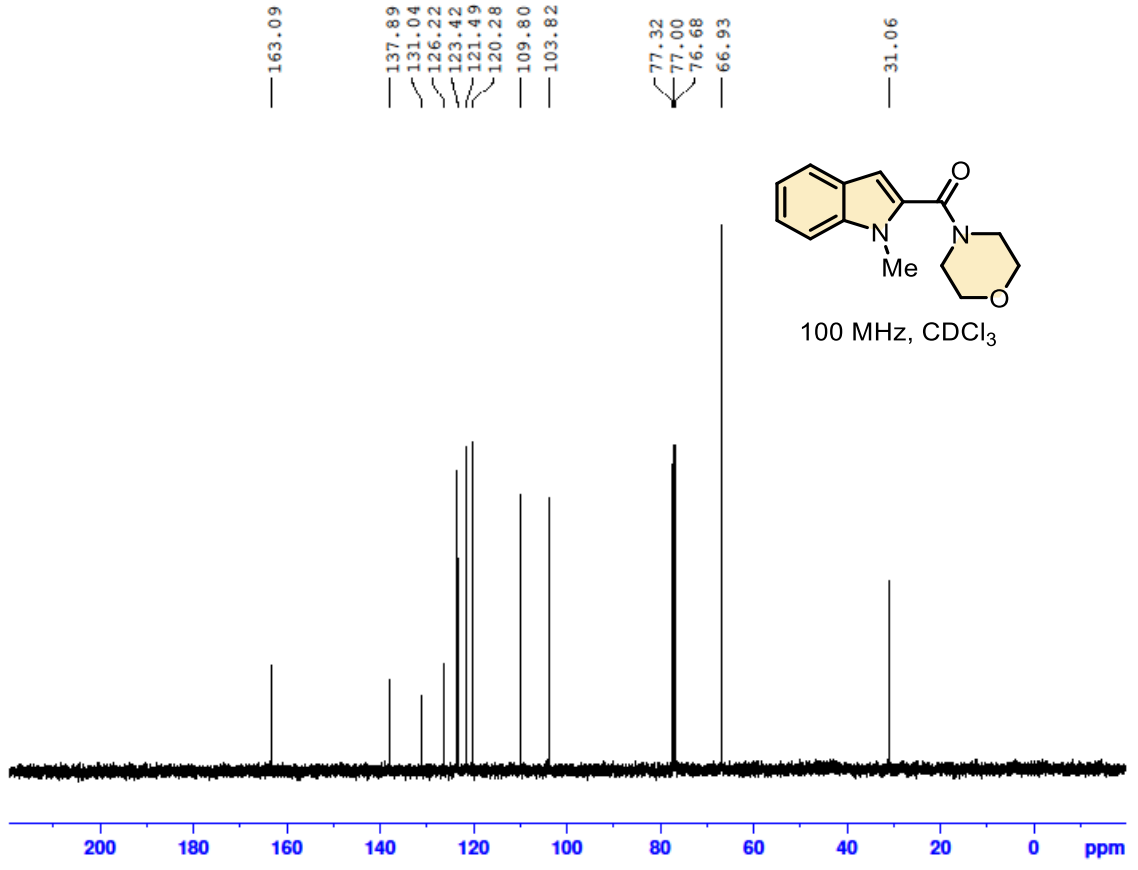

^{1}H NMR of (3-bromo-1-methyl-1*H*-indol-2-yl)(morpholino)methanone (**P3'**)

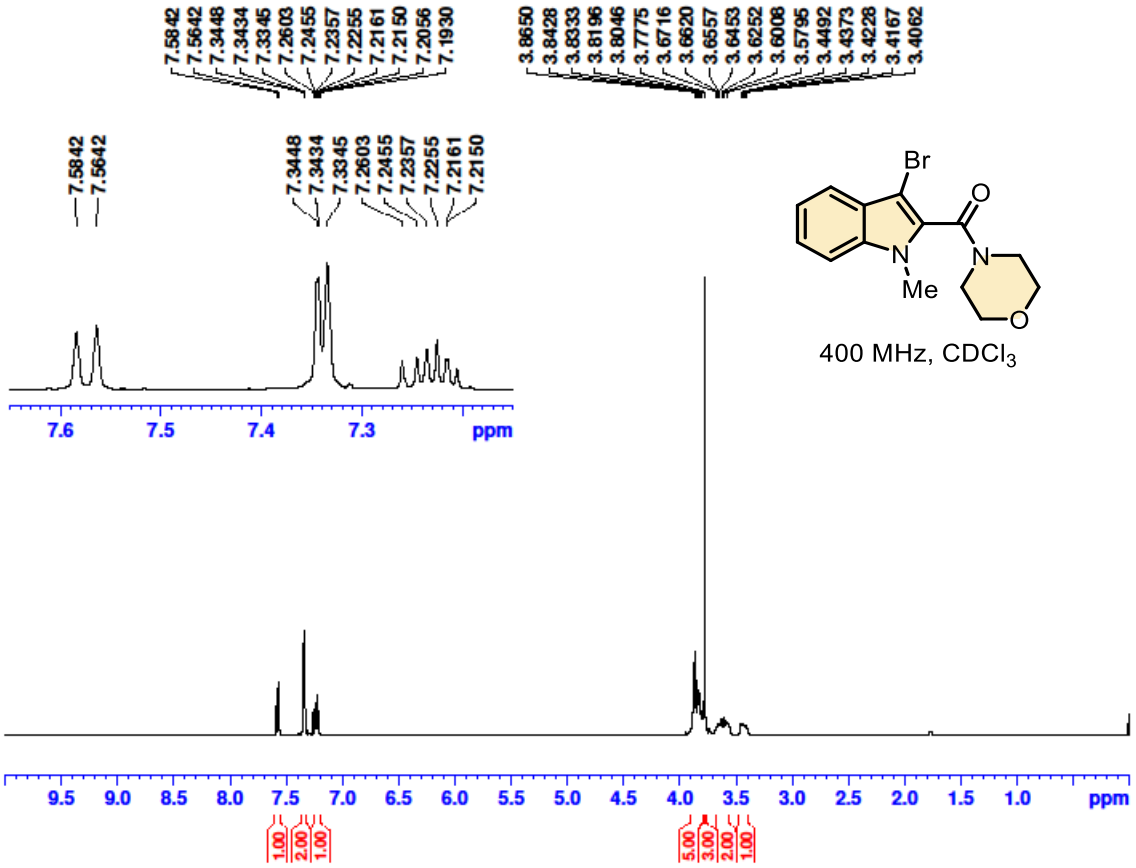

^{13}C NMR of (3-bromo-1-methyl-1*H*-indol-2-yl)(morpholino)methanone (**P3'**)

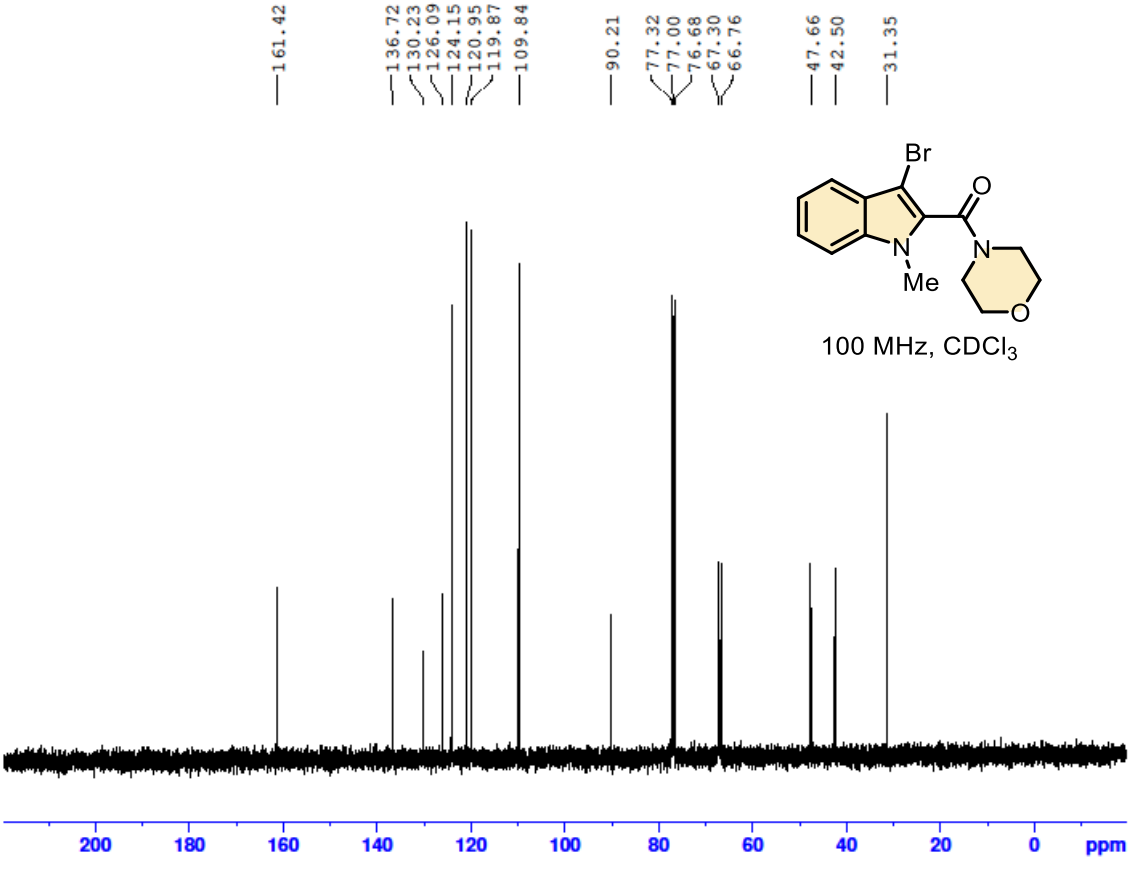

HRMS of (3-bromo-1-methyl-1*H*-indol-2-yl)(morpholino)methanone (**P3'**)

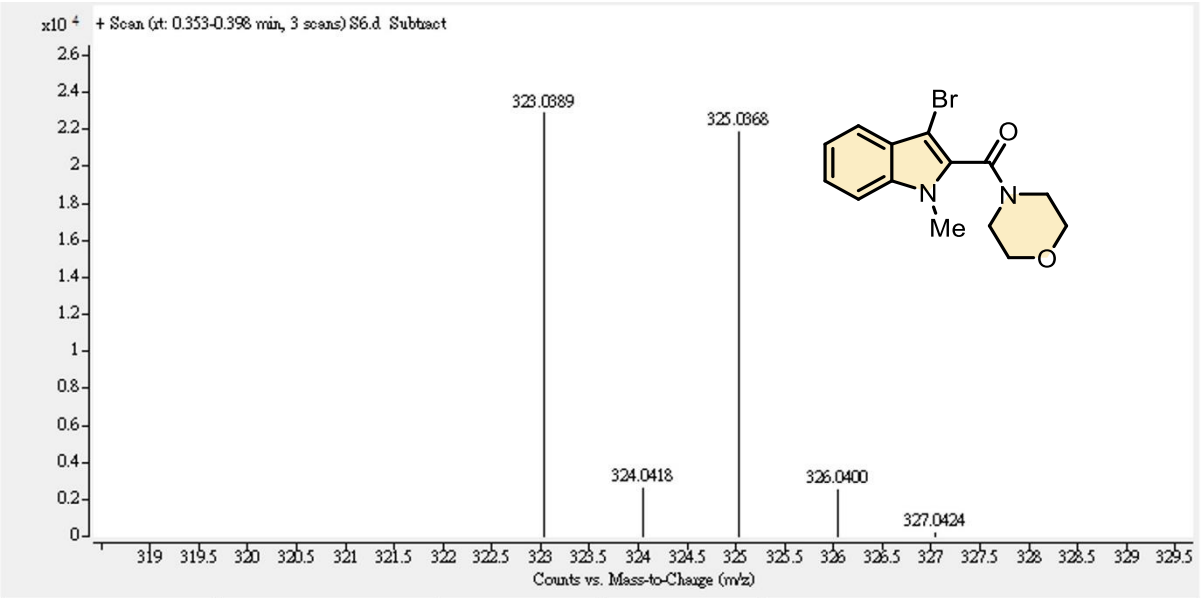

Mass	Calc. Mass	mDa	PPM	Formula
323.0389	323.0390	0.07	0.21	C14 H16 Br N2 O2

^{1}H NMR of (3-(dicyclohexylphosphanyl)-1-methyl-1*H*-indol-2-yl)(morpholino)methanone (**L3**)

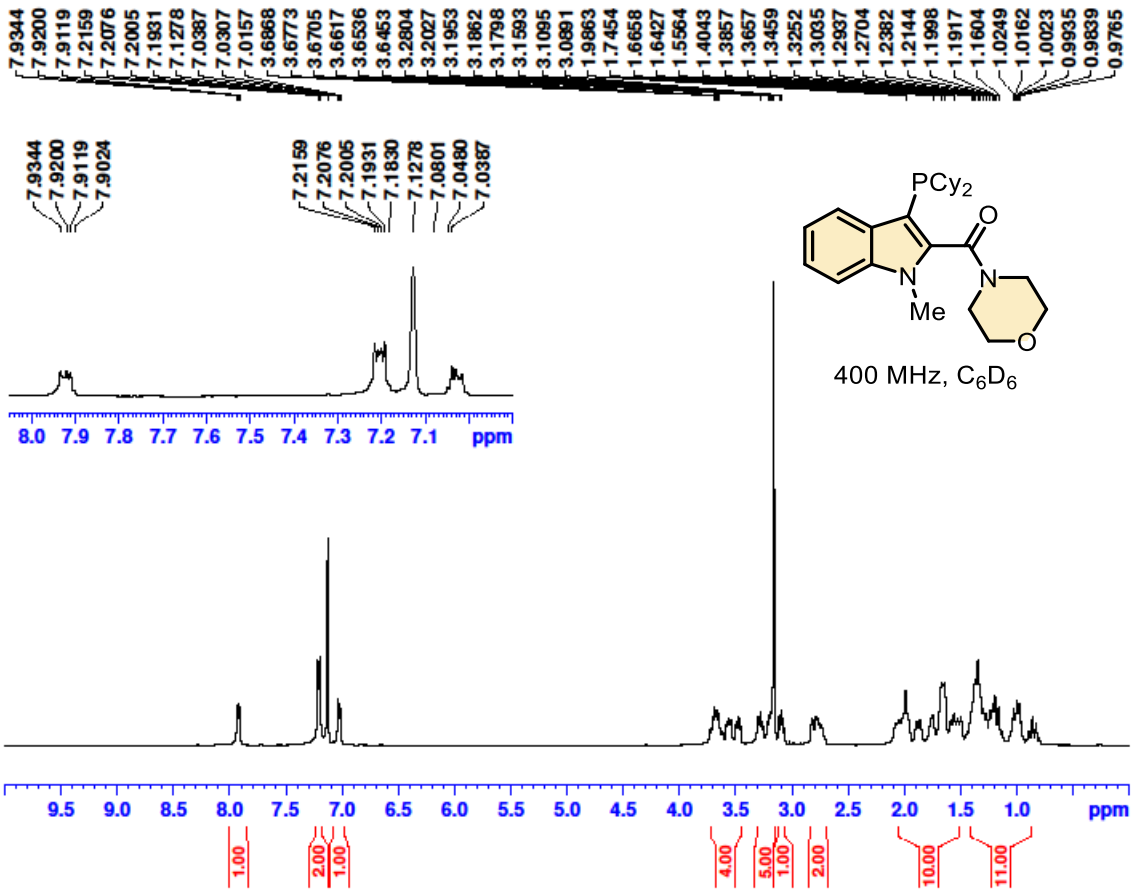

^{13}C NMR of (3-(dicyclohexylphosphanyl)-1-methyl-1*H*-indol-2-yl)(morpholino)methanone (**L3**)

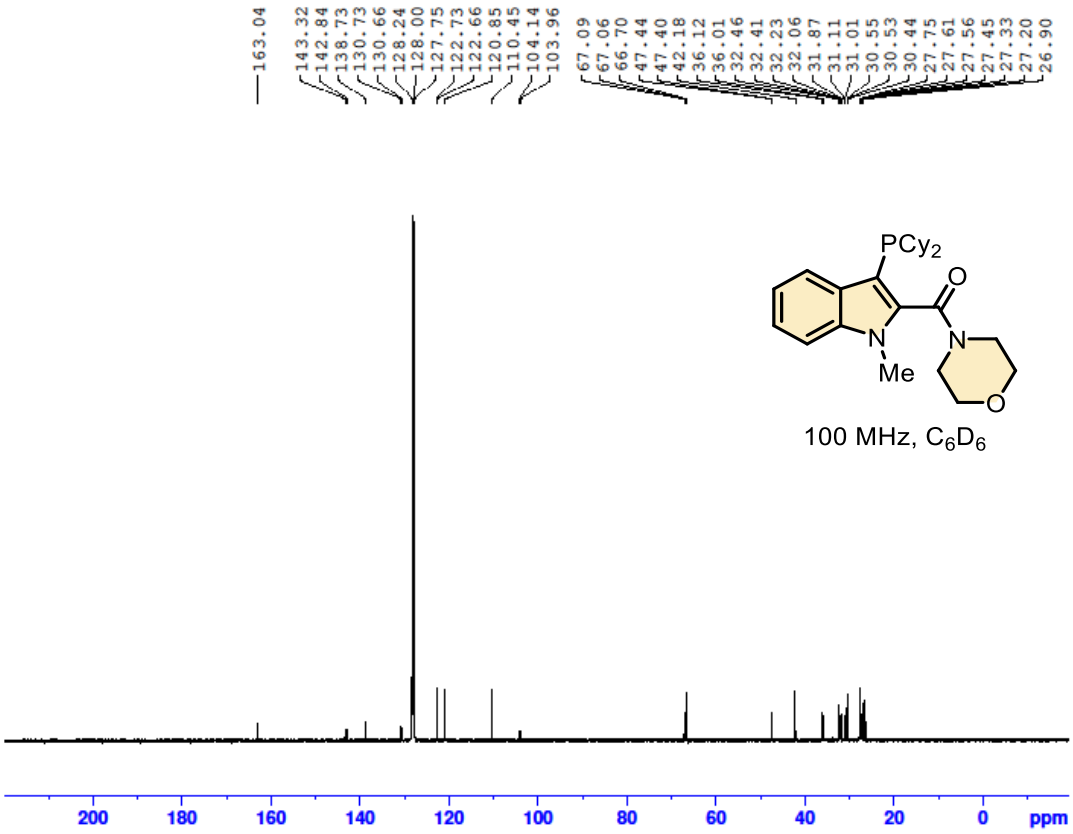

^{31}P NMR of (3-(dicyclohexylphosphanyl)-1-methyl-1*H*-indol-2-yl)(morpholino)methanone (**L3**)

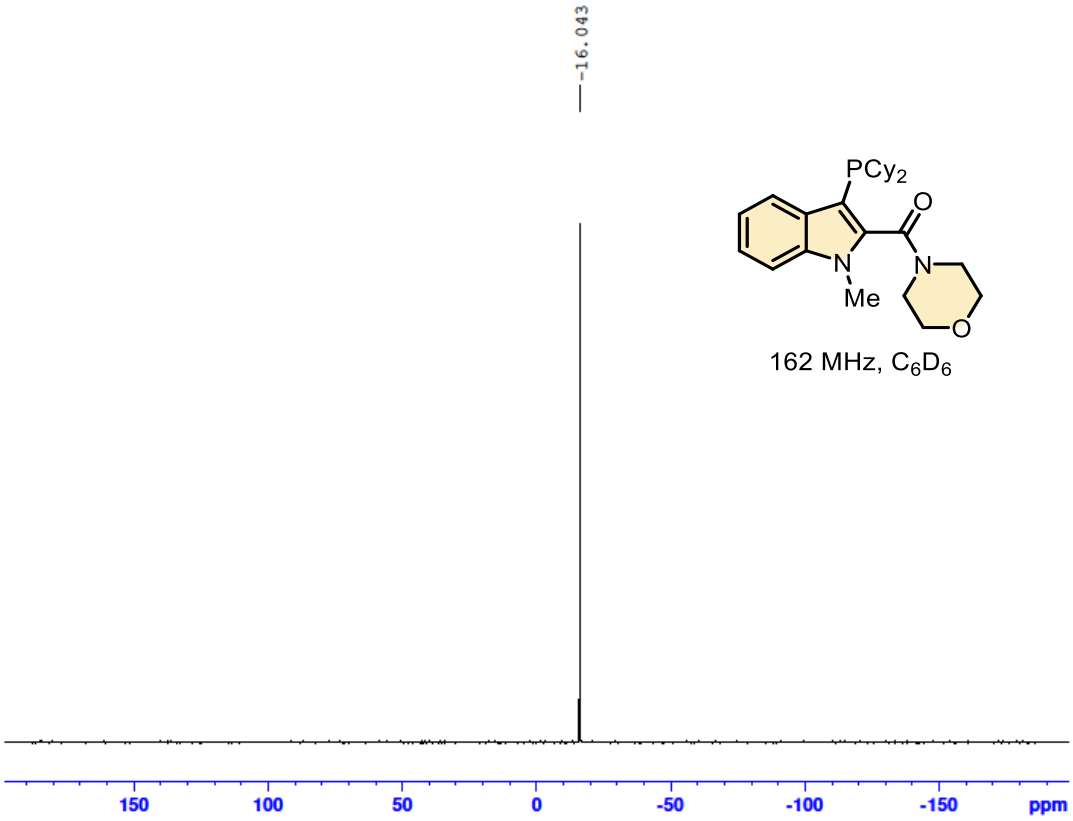

HRMS of (3-(dicyclohexylphosphanyl)-1-methyl-1*H*-indol-2-yl)(morpholino)methanone (**L3**)

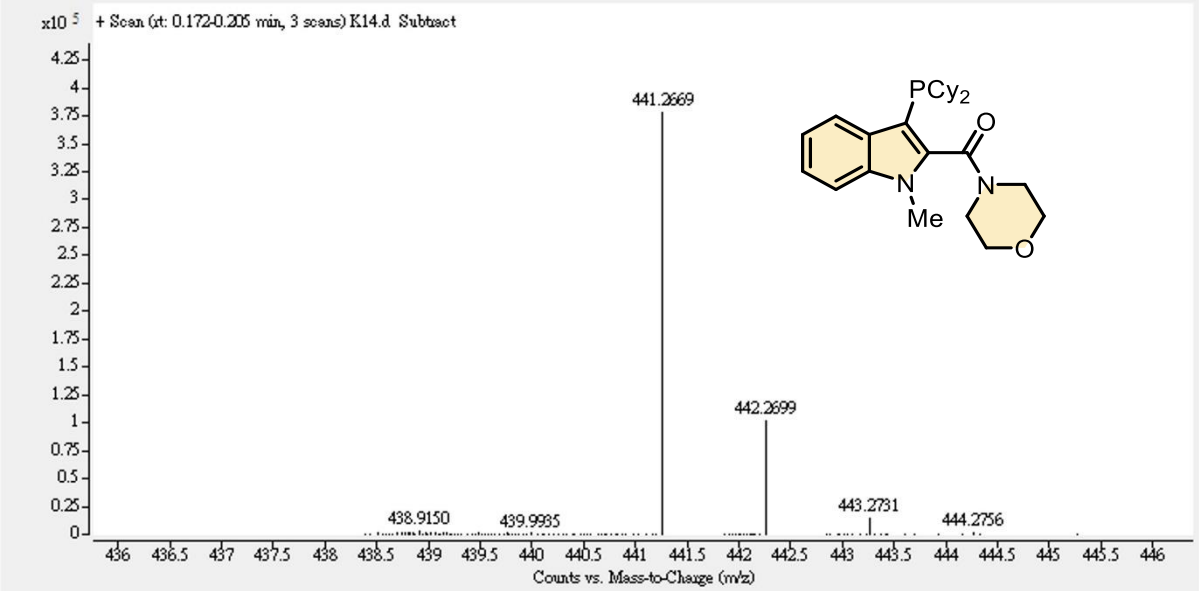

Mass	Calc. Mass	mDa	PPM	Formula
441.2669	441.2665	-0.36	-0.81	C26 H38 N2 O2 P

^{1}H NMR of (3-(diphenylphosphanyl)-1-methyl-1*H*-indol-2-yl)(morpholino)methanone (**L10**)

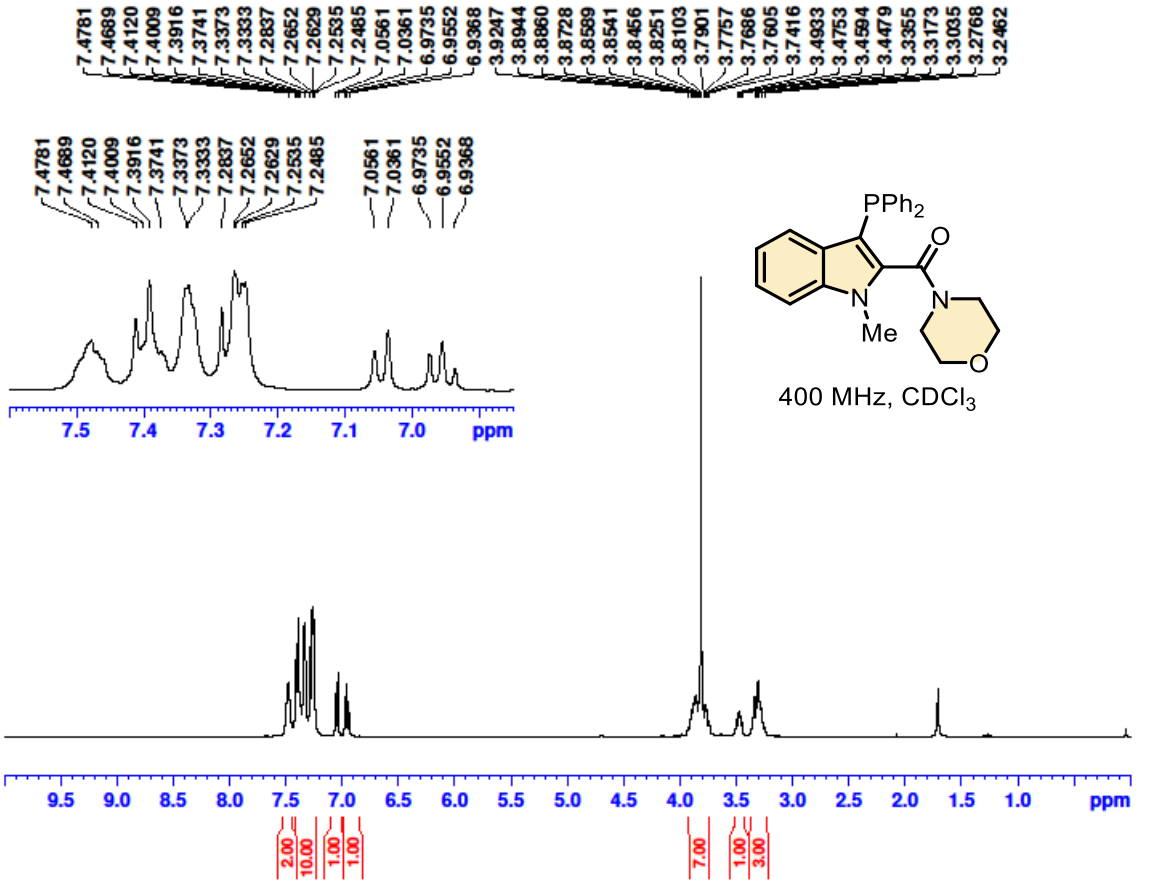

^{13}C NMR of (3-(diphenylphosphanyl)-1-methyl-1*H*-indol-2-yl)(morpholino)methanone (**L10**)

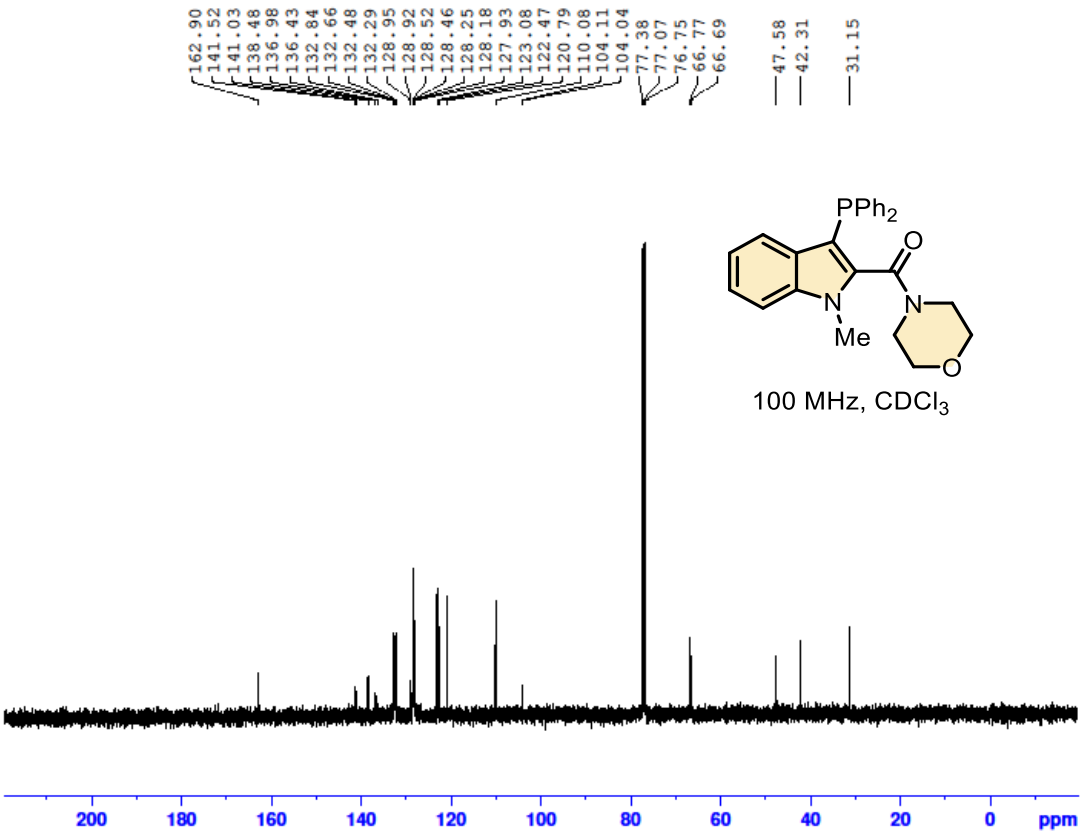

^{31}P NMR of (3-(diphenylphosphanyl)-1-methyl-1*H*-indol-2-yl)(morpholino)methanone (**L10**)

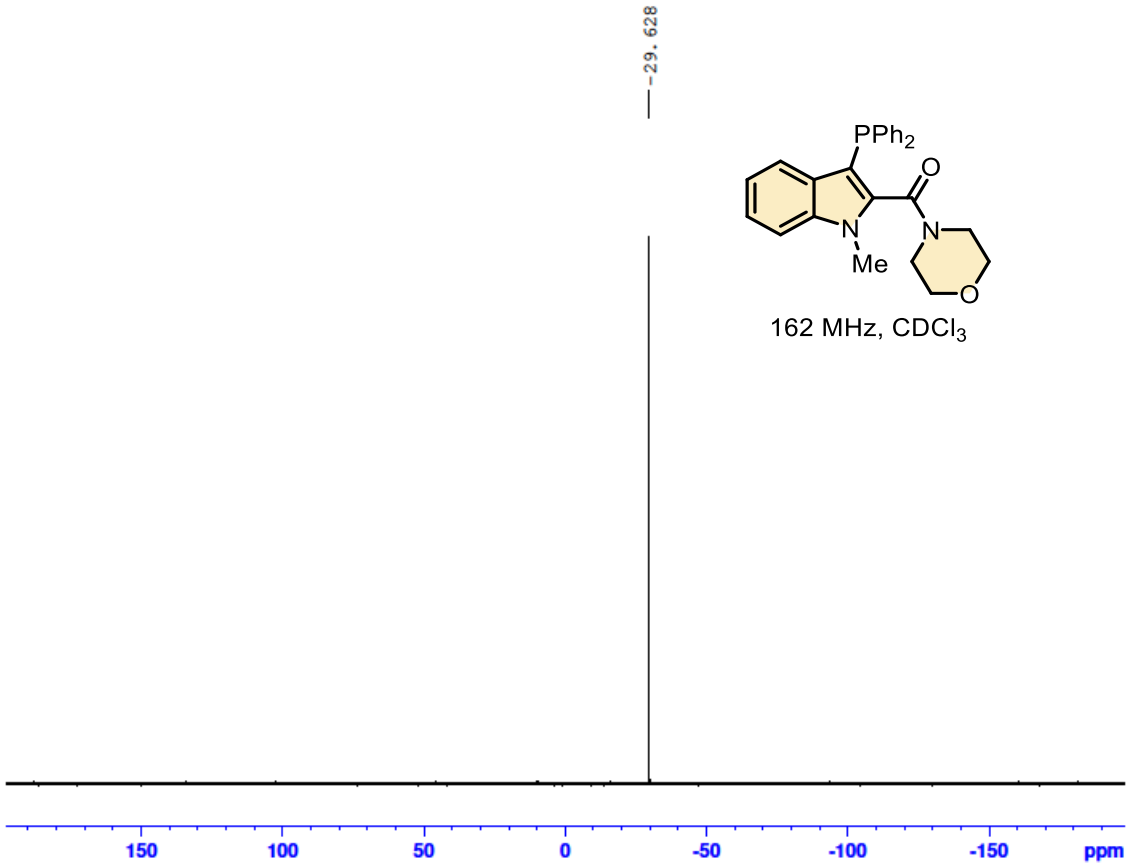

HRMS of (3-(diphenylphosphanyl)-1-methyl-1*H*-indol-2-yl)(morpholino)methanone (**L10**)

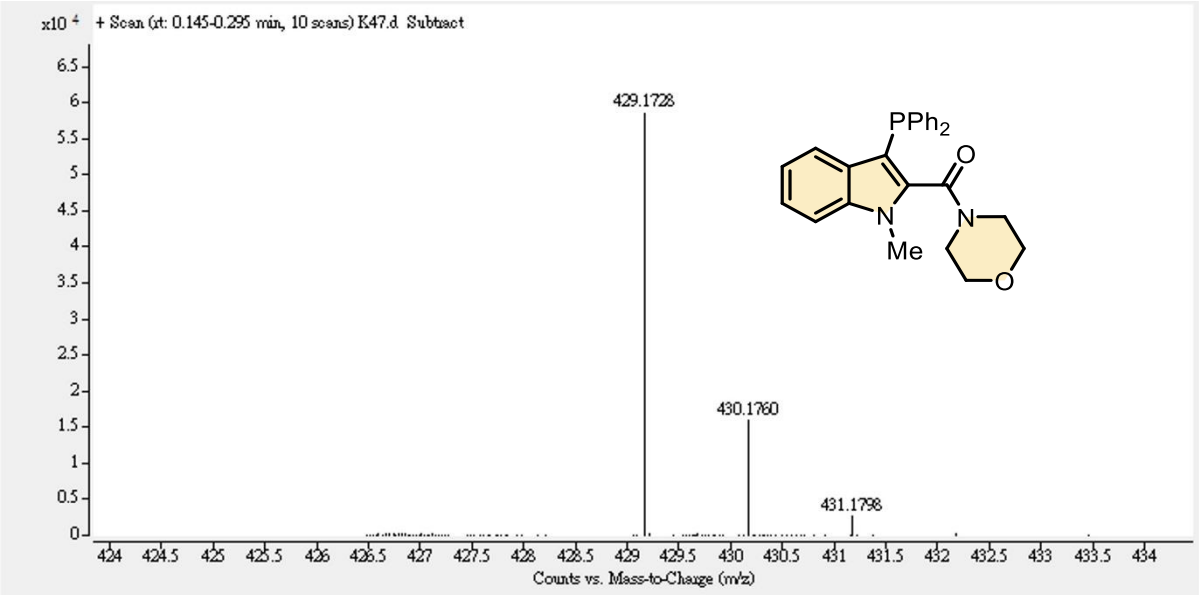

Mass	Calc. Mass	mDa	PPM	Formula
429.1728	429.1726	-0.16	-0.37	C26 H26 N2 O2 P

^{1}H NMR of 1-methyl-*N*,*N*-diphenyl-1*H*-indole-2-carboxamide (**P4**)

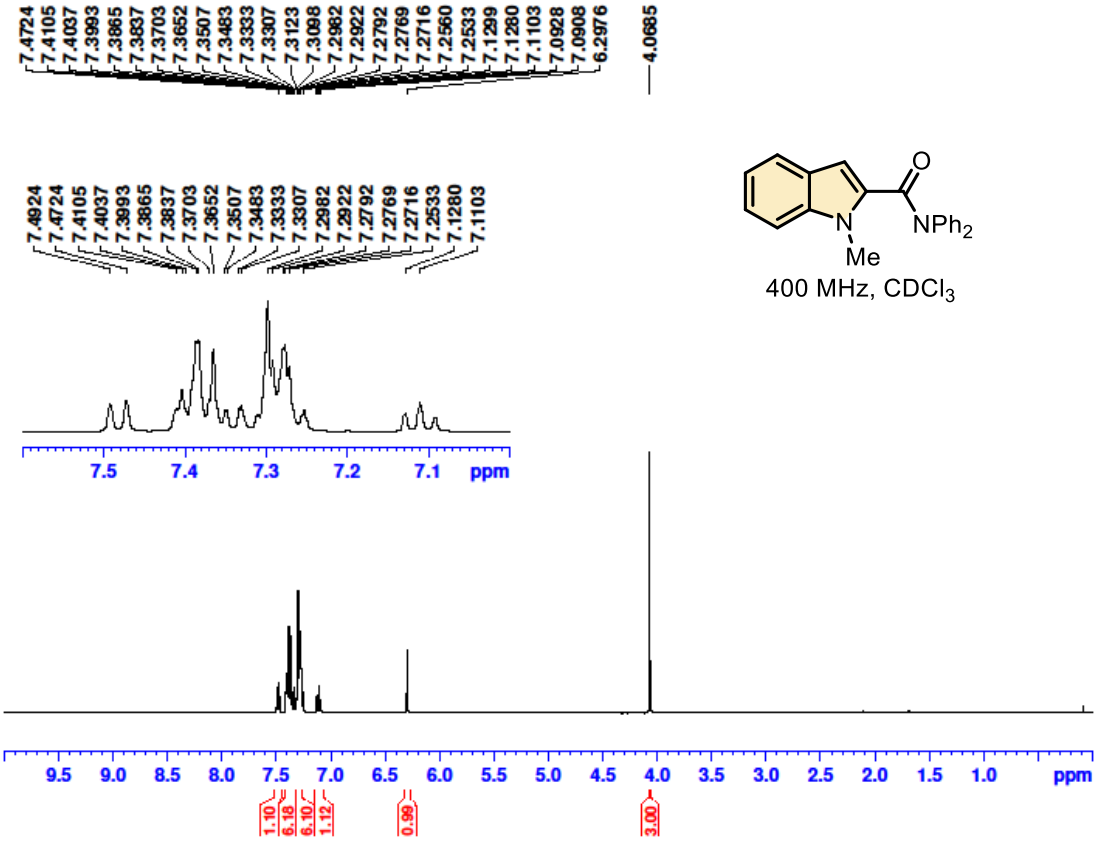

^{13}C NMR of 1-methyl-*N*,*N*-diphenyl-1*H*-indole-2-carboxamide (**P4**)

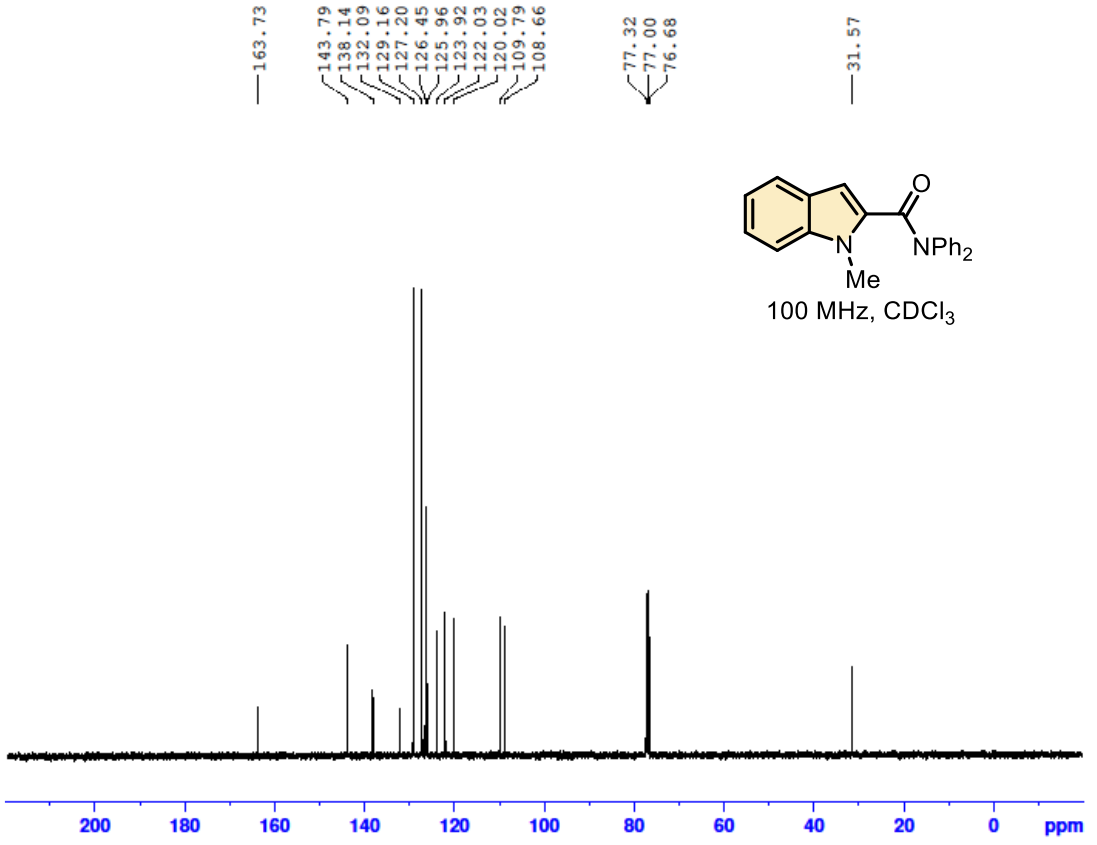

HRMS of 1-methyl-*N*,*N*-diphenyl-1*H*-indole-2-carboxamide (**P4**)

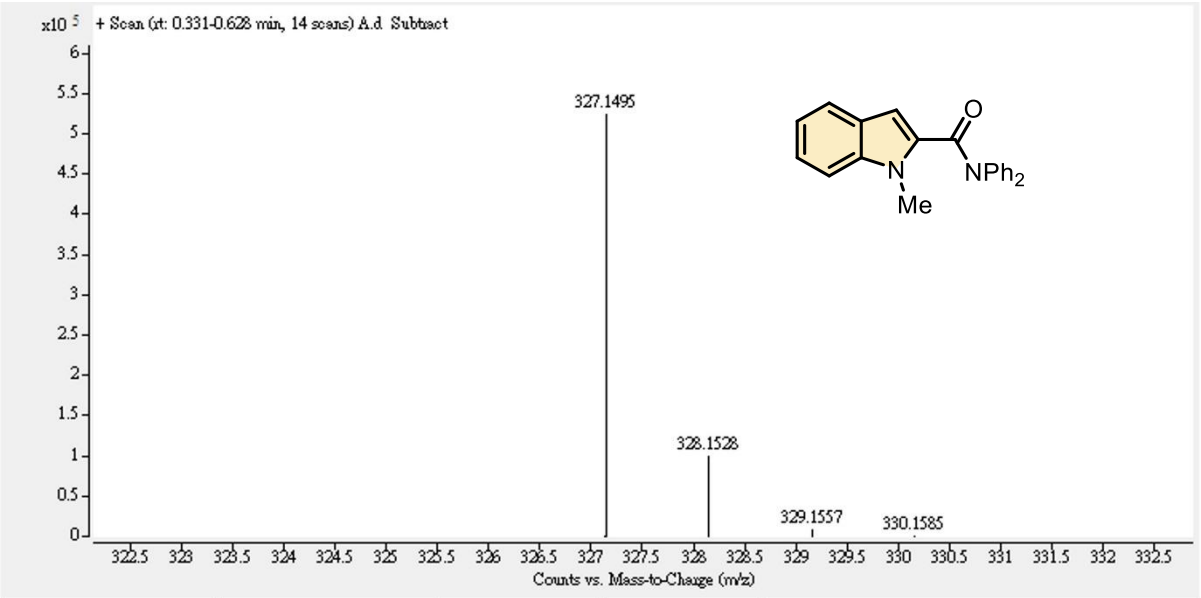

Mass	Calc. Mass	mDa	PPM	Formula
327.1495	327.1492	-0.31	-0.95	C22 H19 N2 O

^{1}H NMR of 3-bromo-1-methyl-*N*,*N*-diphenyl-1*H*-indole-2-carboxamide (**P4'**)

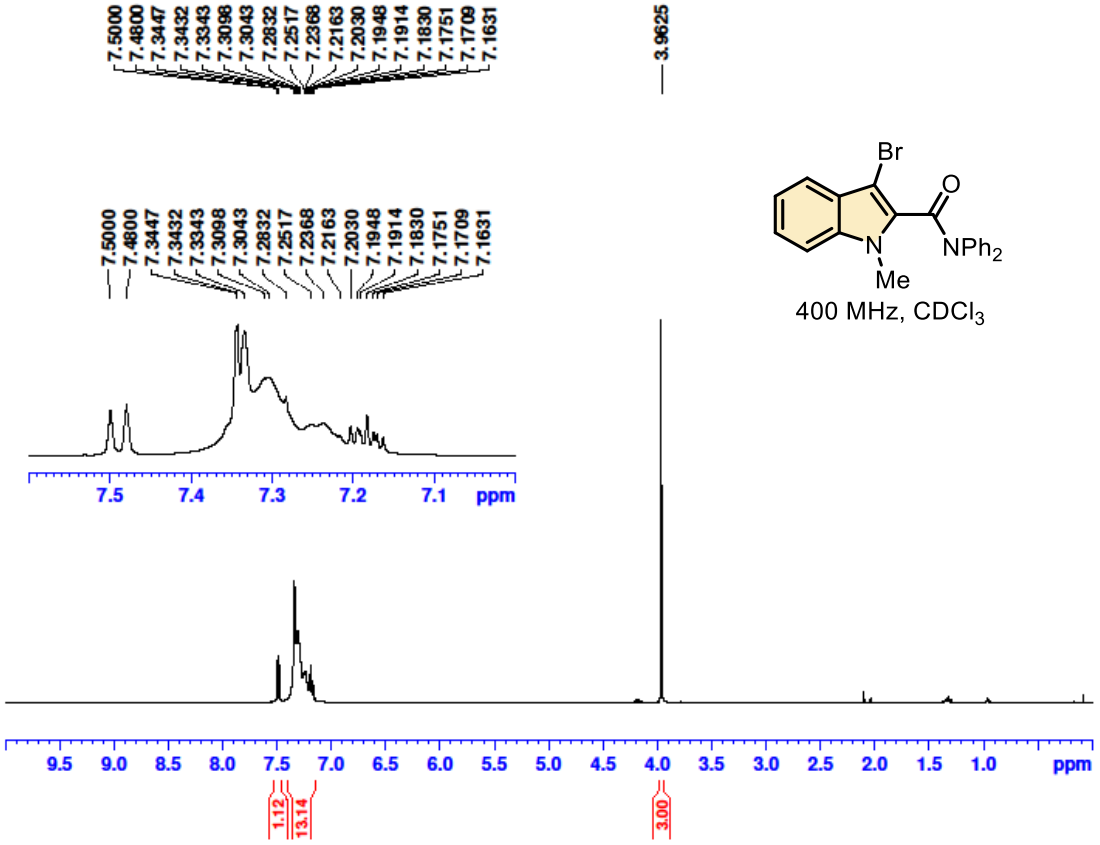

^{13}C of NMR of 3-bromo-1-methyl-*N*,*N*-diphenyl-1*H*-indole-2-carboxamide (**P4'**)

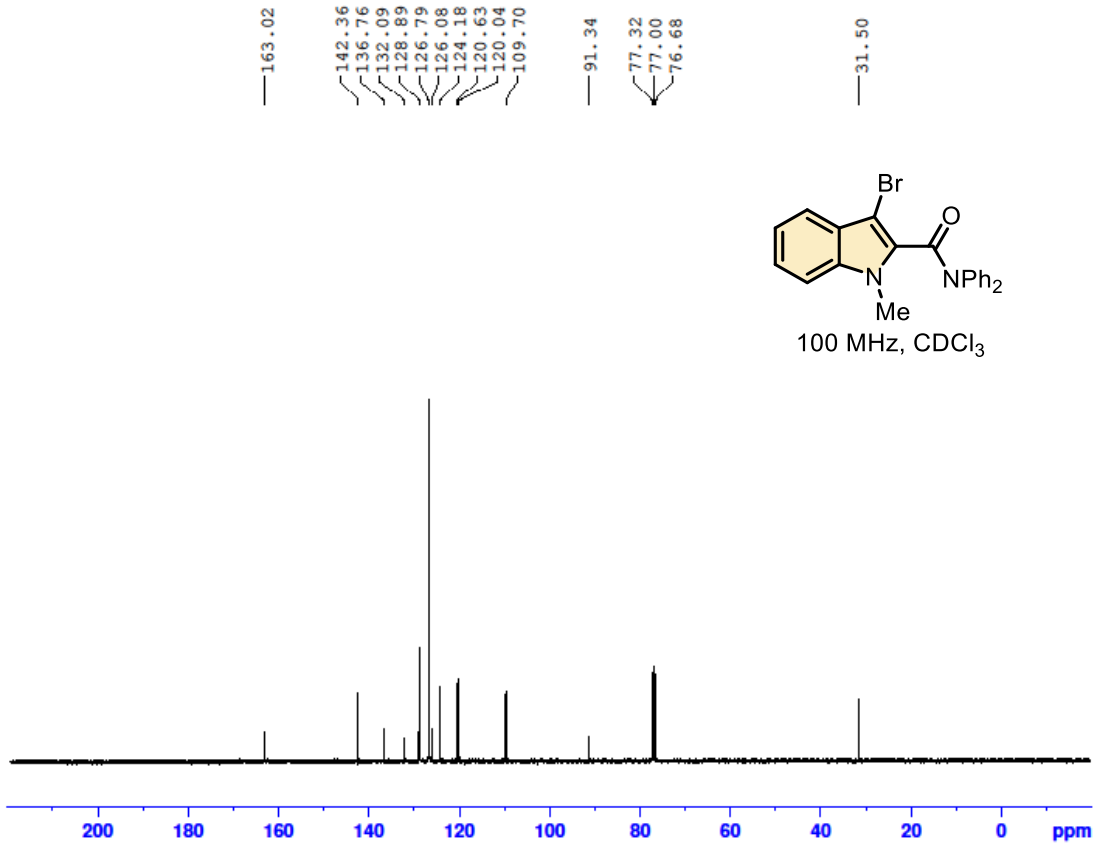

HRMS of 3-bromo-1-methyl-*N*,*N*-diphenyl-1*H*-indole-2-carboxamide (**P4'**)

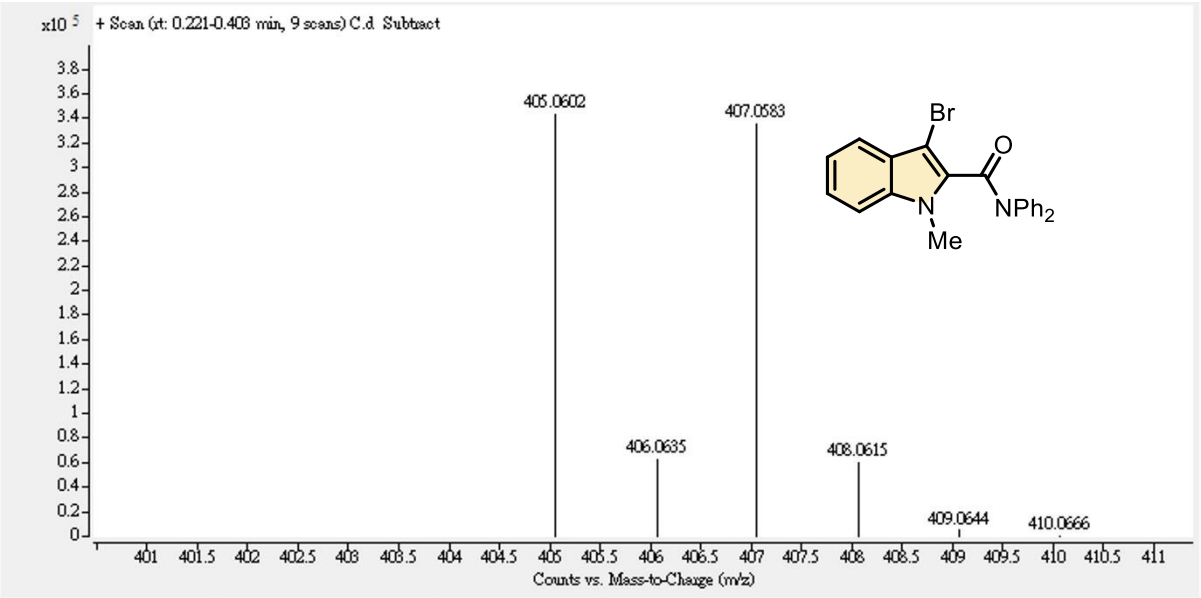

Mass	Calc. Mass	mDa	PPM	Formula
405.0602	405.0597	-0.50	-1.23	C22 H18 Br N2 O

^{1}H NMR of 3-(dicyclohexylphosphanyl)-1-methyl-*N*,*N*-diphenyl-1*H*-indole-2-carboxamide (**L4**)

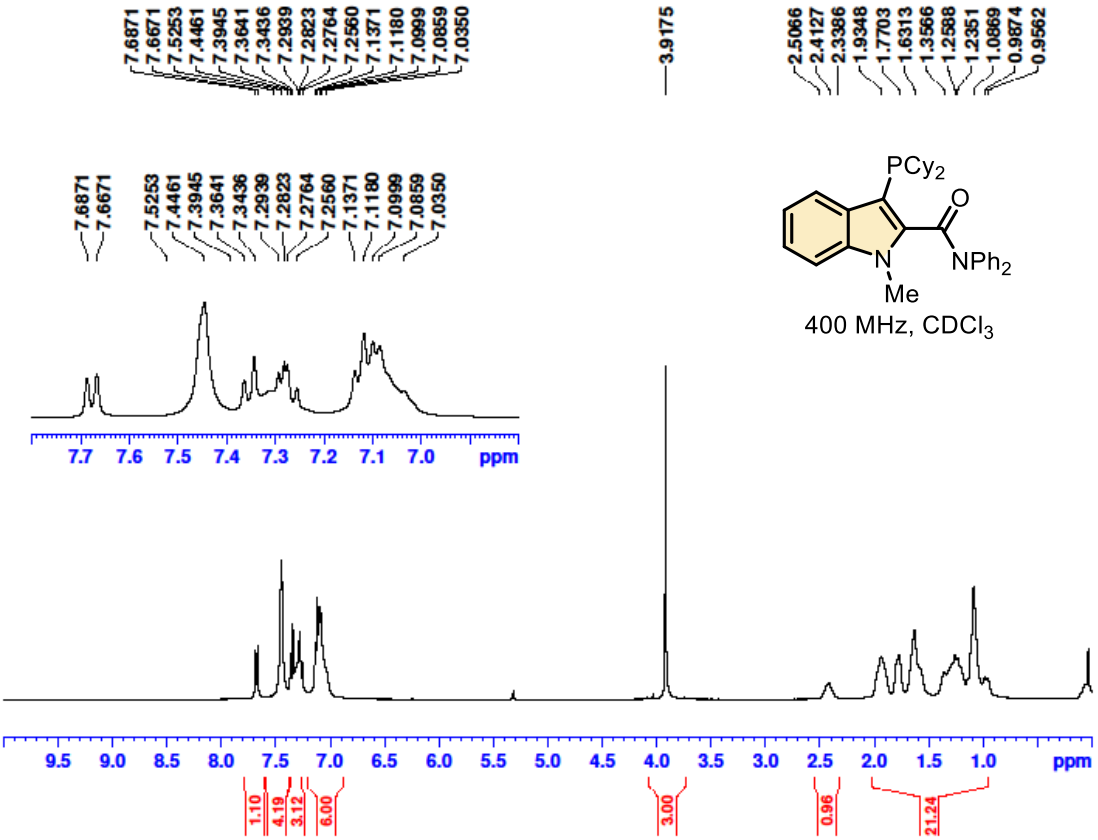

^{13}C NMR of 3-(dicyclohexylphosphanyl)-1-methyl-*N*,*N*-diphenyl-1*H*-indole-2-carboxamide (**L4**)

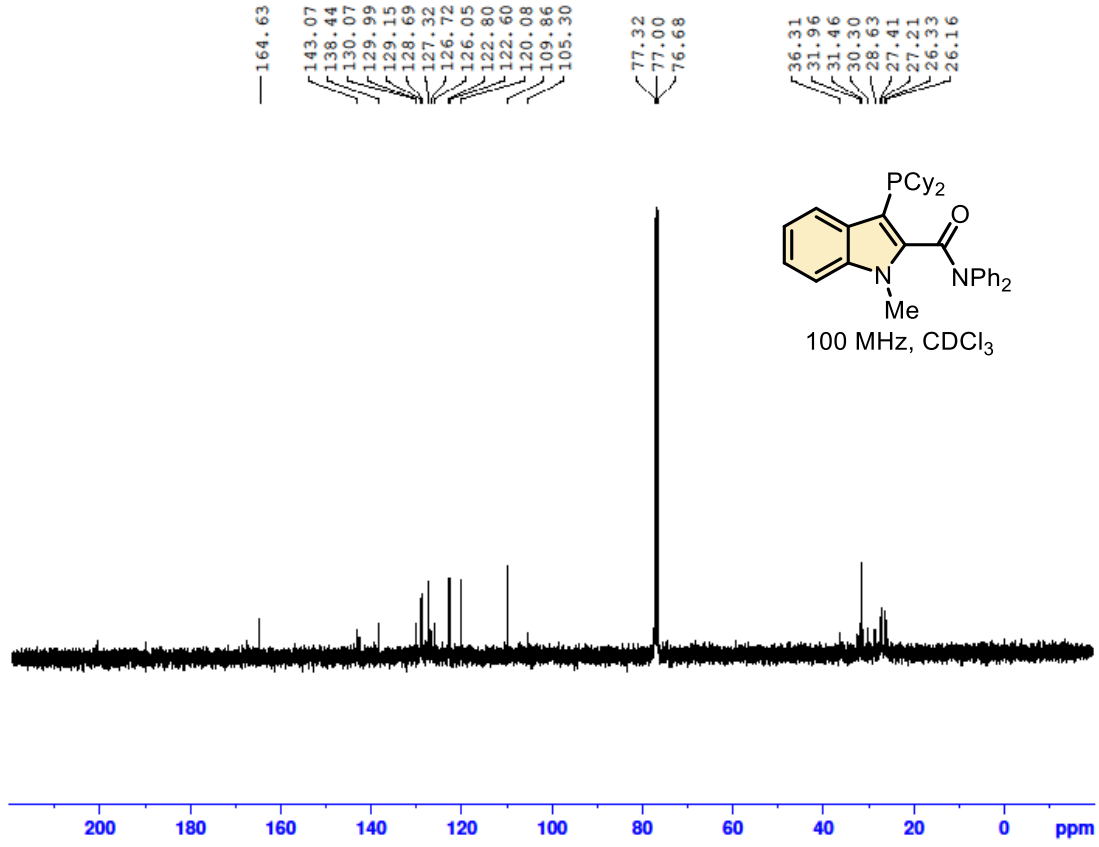

^{31}P NMR of 3-(dicyclohexylphosphanyl)-1-methyl-*N*,*N*-diphenyl-1*H*-indole-2-carboxamide (**L4**)

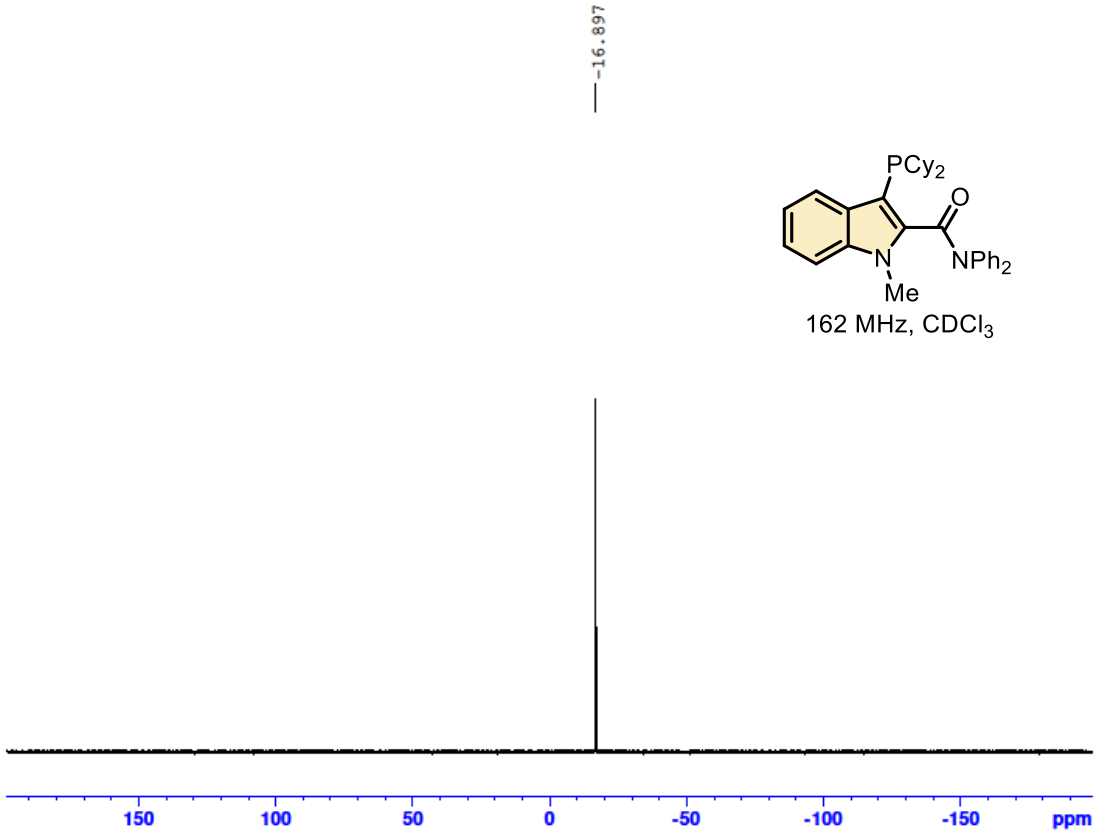

HRMS of 3-(dicyclohexylphosphanyl)-1-methyl-*N*,*N*-diphenyl-1*H*-indole-2-carboxamide (**L4**)

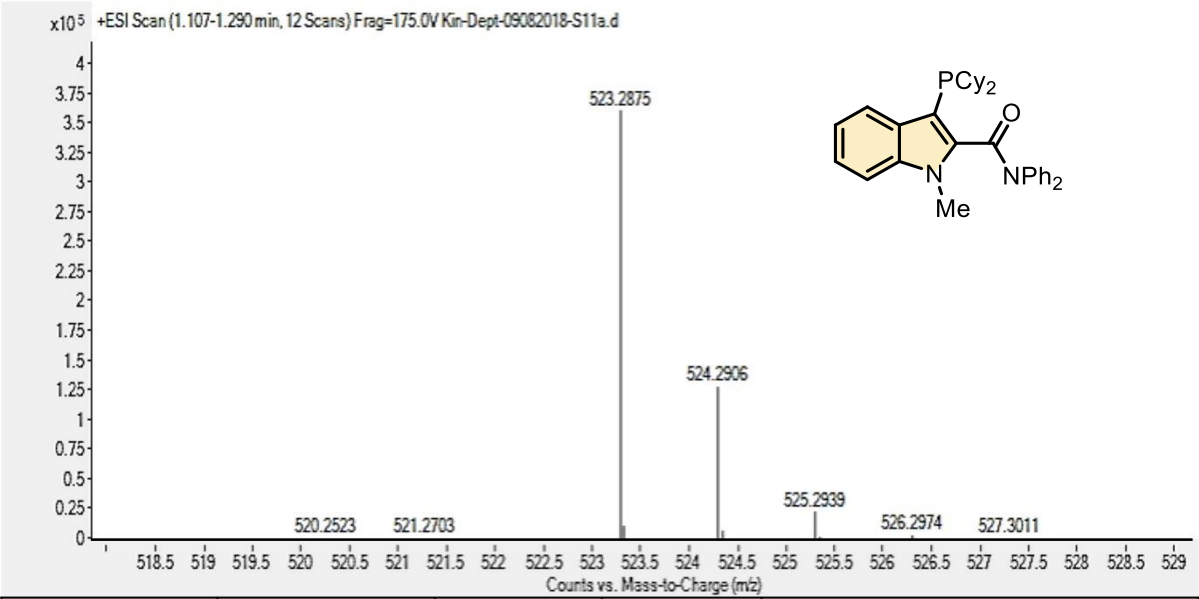

Mass	Calc. Mass	mDa	PPM	Formula
523.2875	523.2873	0.22	0.43	C34 H40 N2 O P

^{1}H NMR of *N*,*N*-dicyclohexyl-1*H*-indole-2-carboxamide (**P5**)

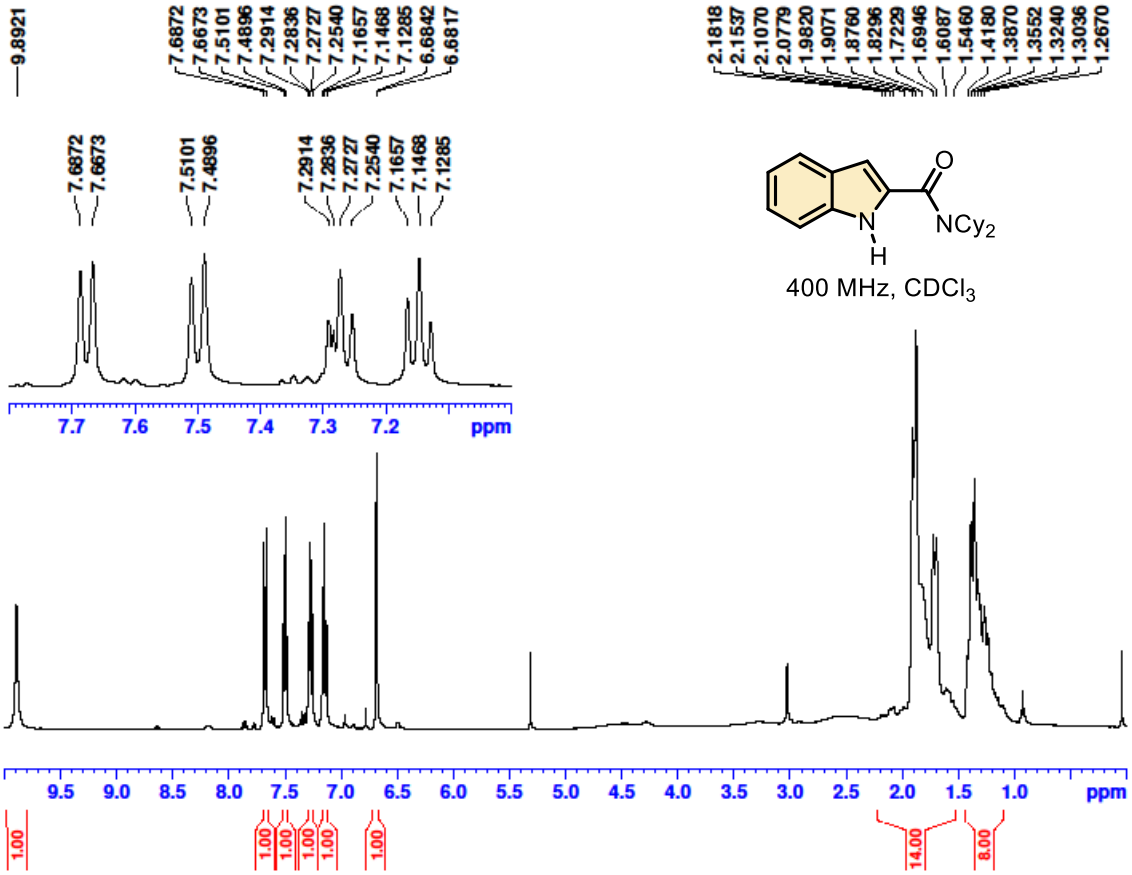

^{13}C NMR of *N*,*N*-dicyclohexyl-1*H*-indole-2-carboxamide (**P5**)

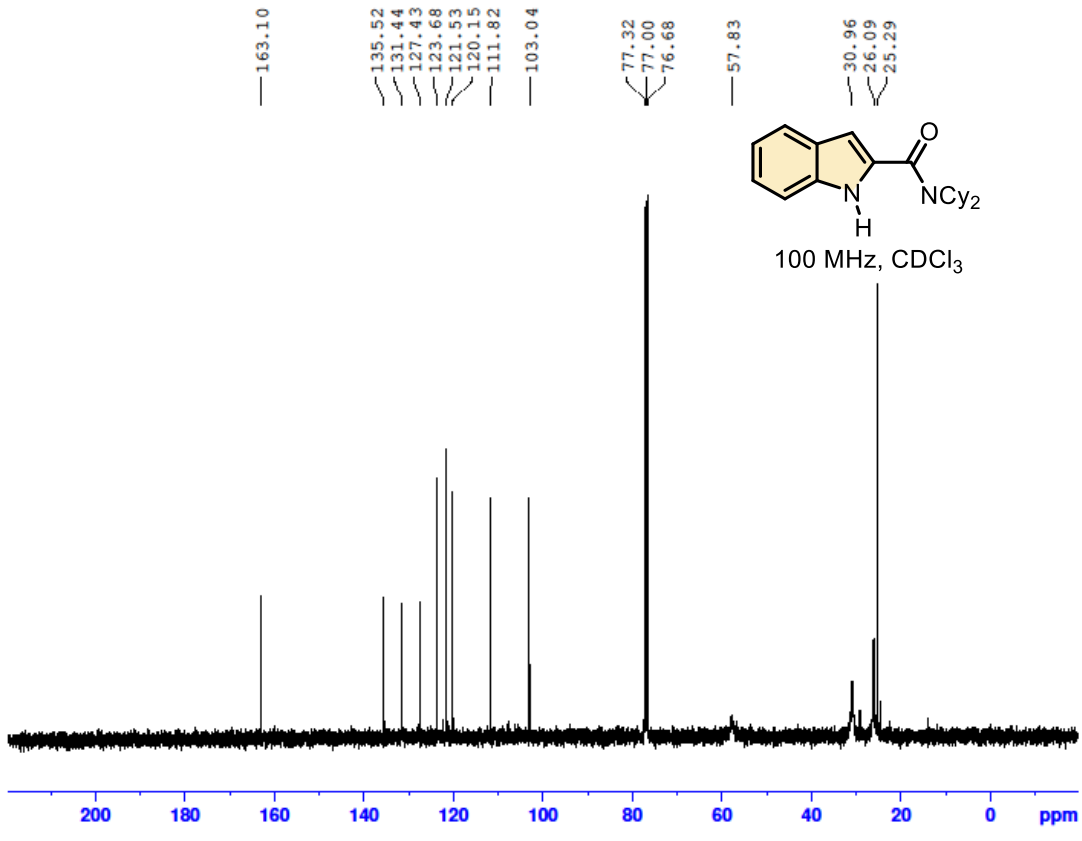

HRMS of *N*,*N*-dicyclohexyl-1*H*-indole-2-carboxamide (**P5**)

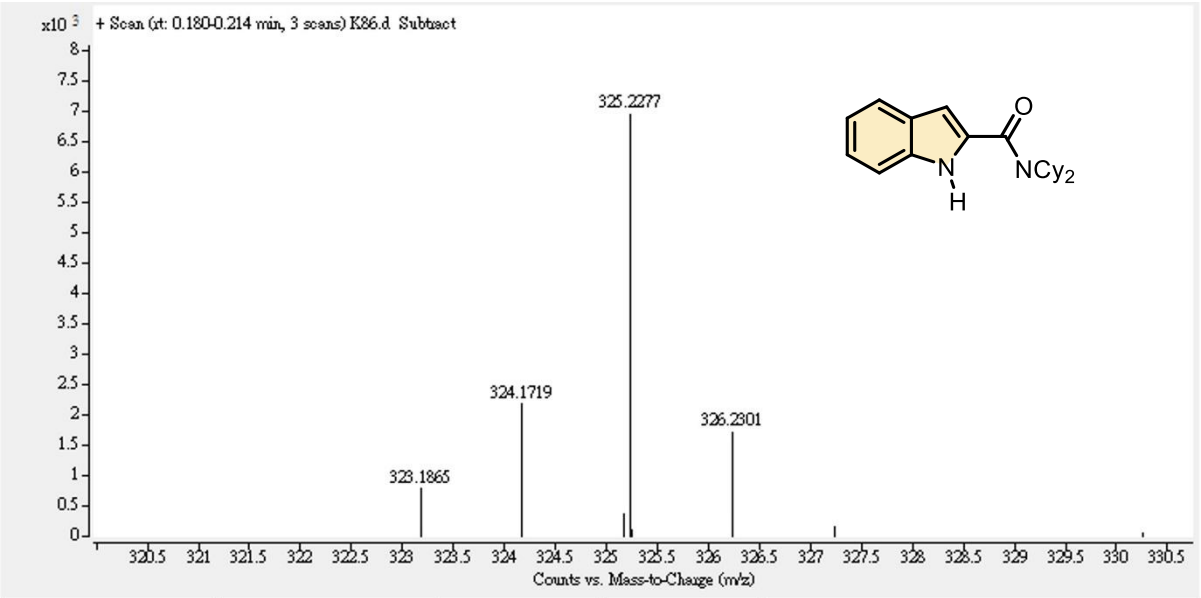

Mass	Calc. Mass	mDa	PPM	Formula
325.2277	325.2274	-0.26	-0.80	C21 H29 N2 O

^{1}H NMR of *N*,*N*-dicyclohexyl-1-methyl-1*H*-indole-2-carboxamide (**P5'**)

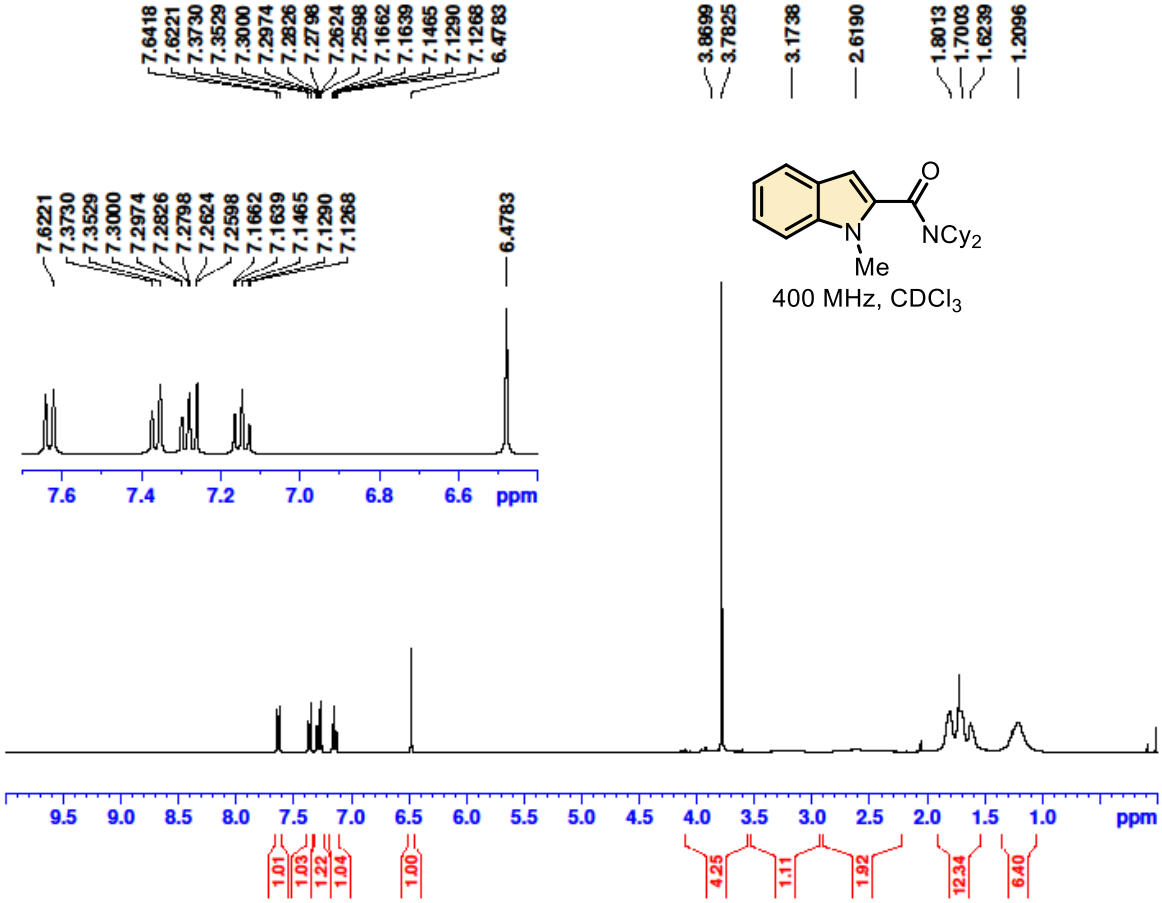

^{13}C NMR of *N*,*N*-dicyclohexyl-1-methyl-1*H*-indole-2-carboxamide (**P5'**)

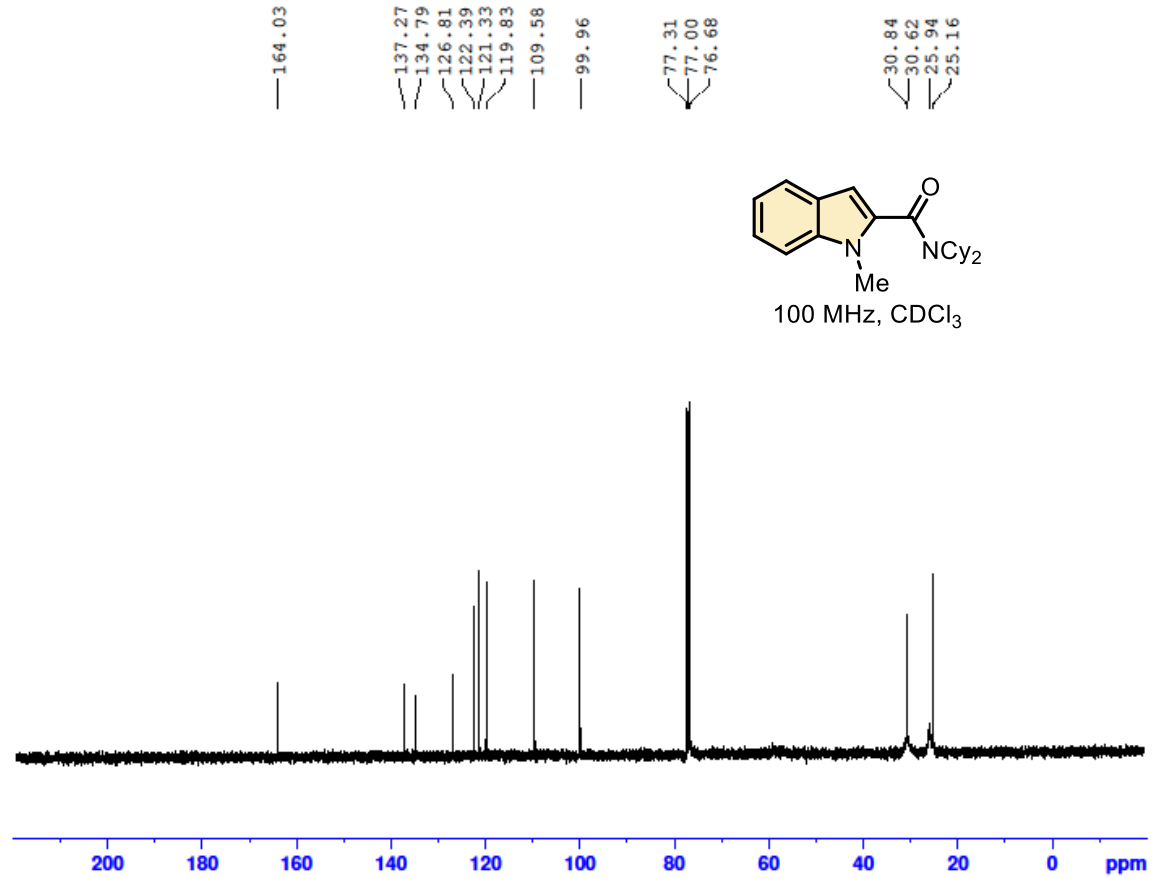

HRMS of *N*,*N*-dicyclohexyl-1-methyl-1*H*-indole-2-carboxamide (**P5'**)

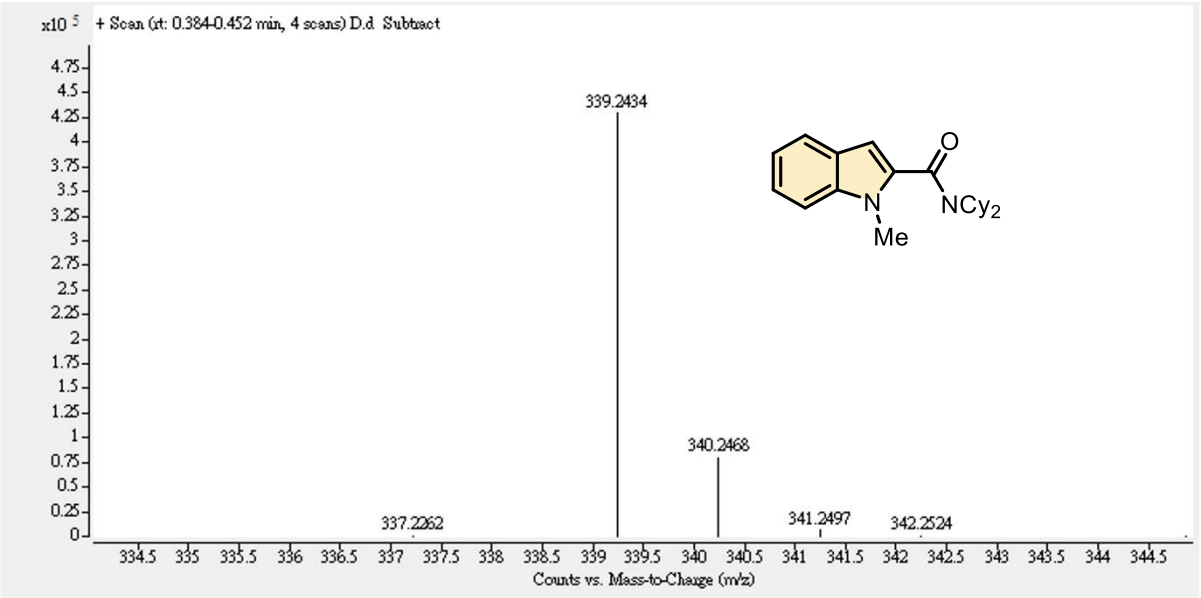

Mass	Calc. Mass	mDa	PPM	Formula
339.2434	339.2431	-0.31	-0.92	C22 H31 N2 O

^{1}H NMR of 3-bromo-*N*,*N*-dicyclohexyl-1-methyl-1*H*-indole-2-carboxamide (**P5''**)

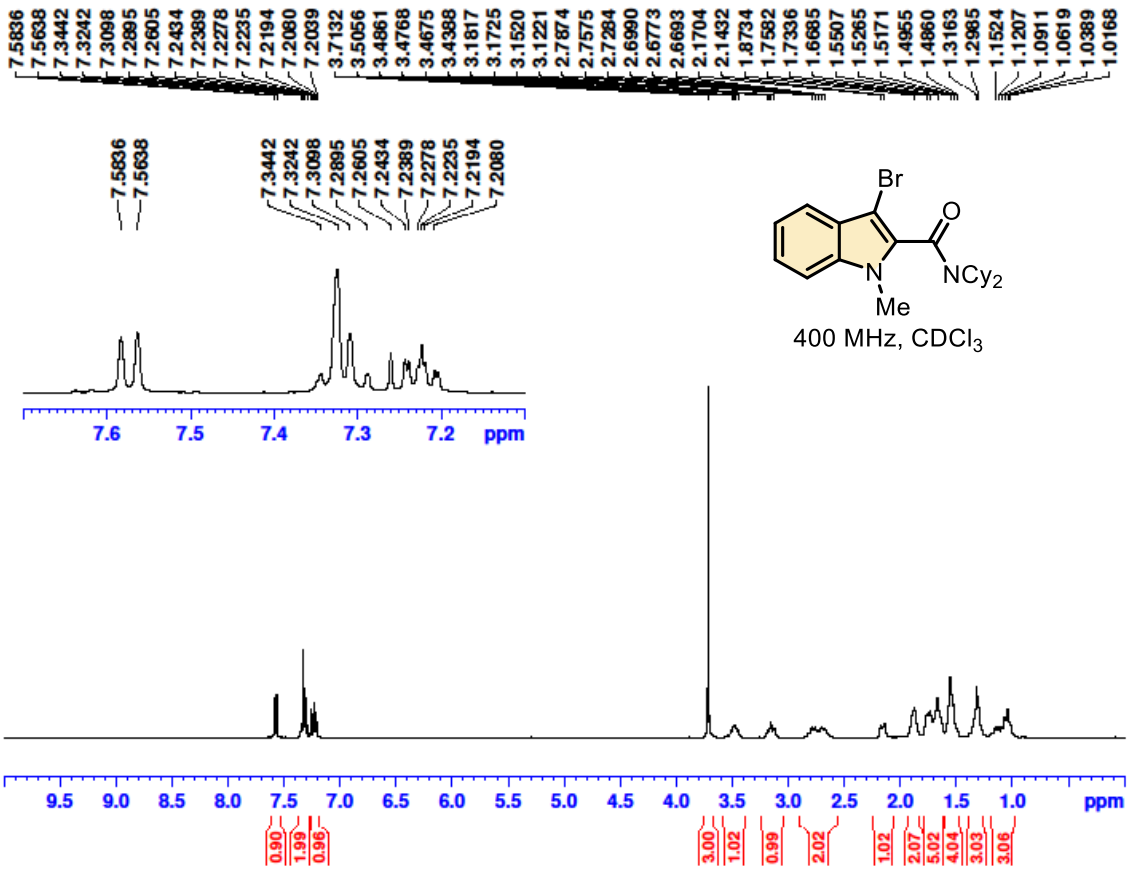

^{13}C NMR of 3-bromo-*N*,*N*-dicyclohexyl-1-methyl-1*H*-indole-2-carboxamide (**P5''**)

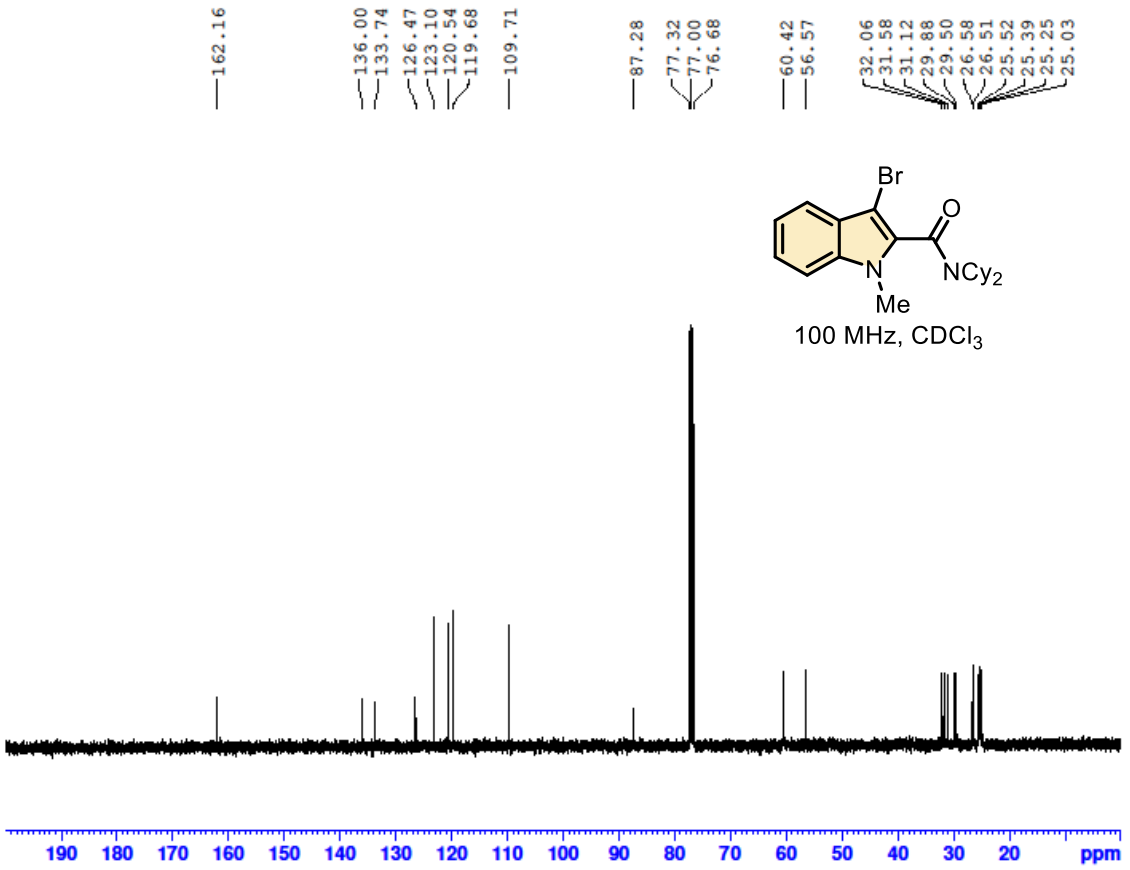

HRMS of 3-bromo-*N*,*N*-dicyclohexyl-1-methyl-1*H*-indole-2-carboxamide (**P5''**)

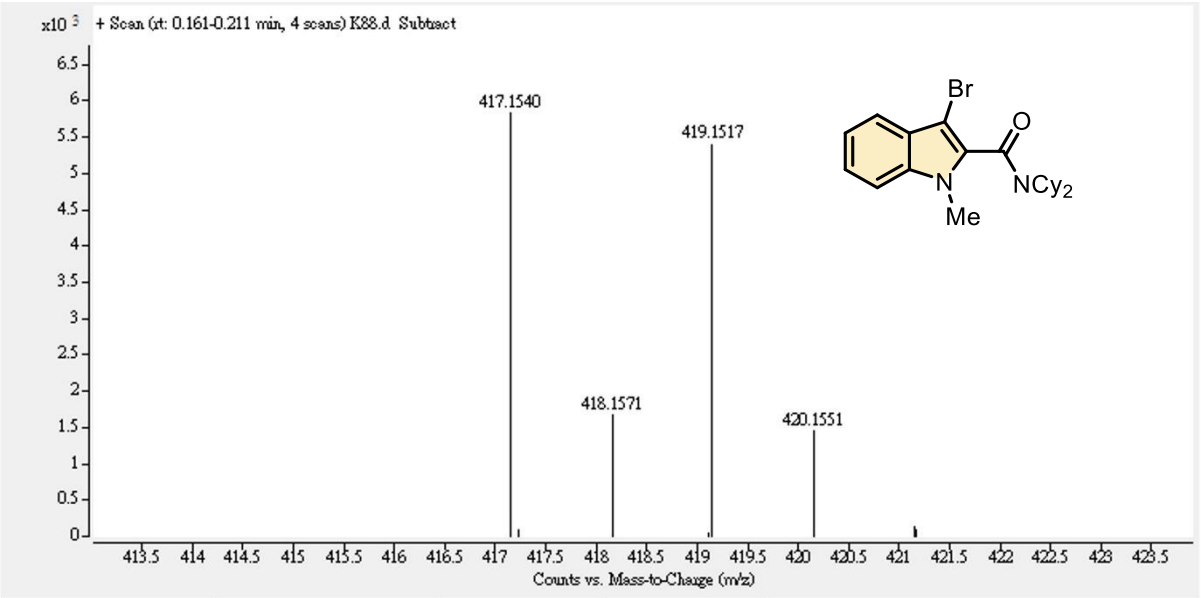

Mass	Calc. Mass	mDa	PPM	Formula
417.1540	417.1536	-0.40	-0.95	C22 H30 Br N2 O

^{1}H NMR of *N*,*N*-dicyclohexyl-3-(dicyclohexylphosphanyl)-1-methyl-1*H*-indole-2-carboxamide (**L5**)

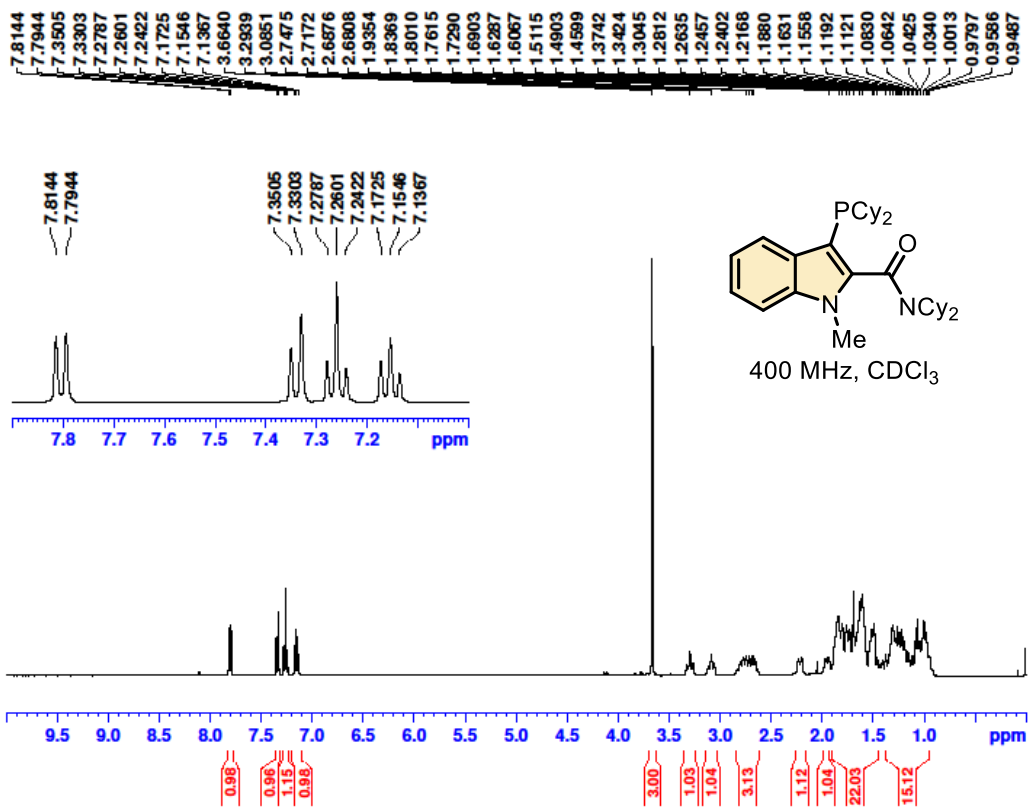

^{13}C NMR of *N*,*N*-dicyclohexyl-3-(dicyclohexylphosphanyl)-1-methyl-1*H*-indole-2-carboxamide (**L5**)

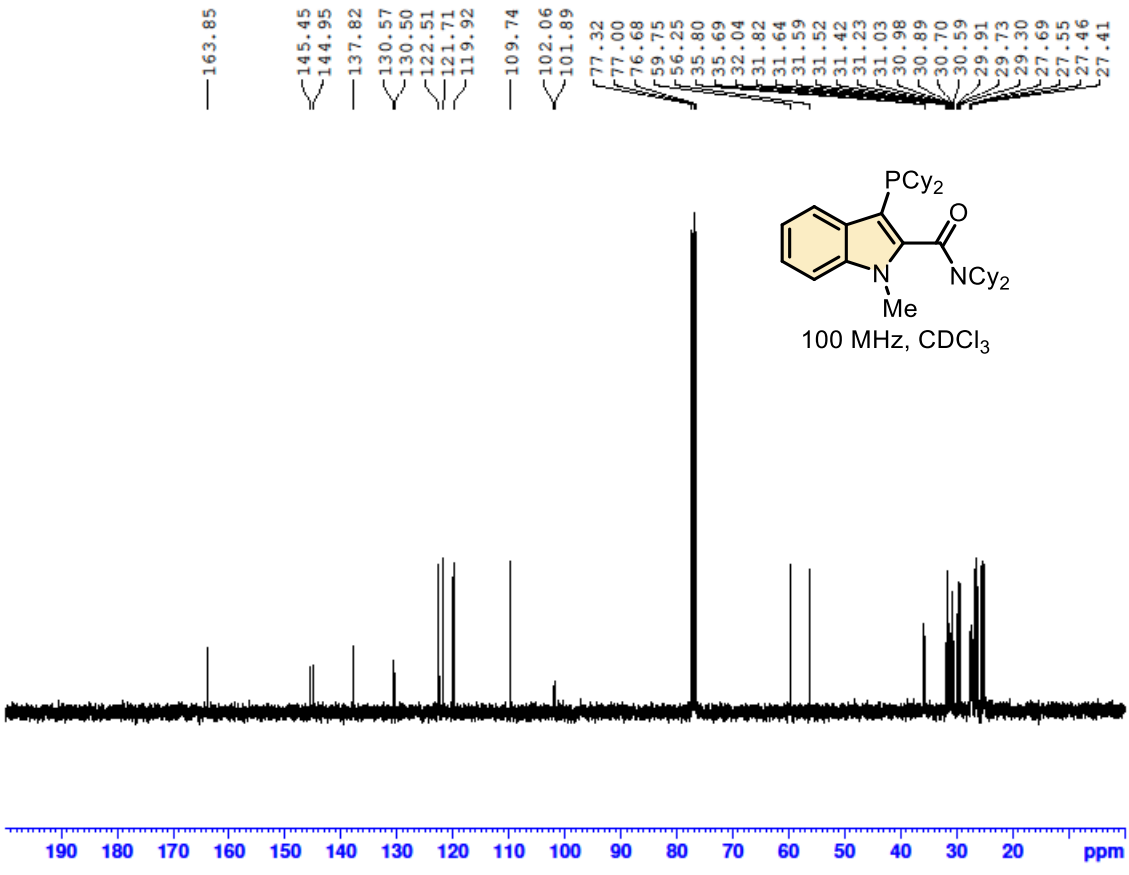

^{31}P NMR of *N*,*N*-dicyclohexyl-3-(dicyclohexylphosphanyl)-1-methyl-1*H*-indole-2-carboxamide (**L5**)

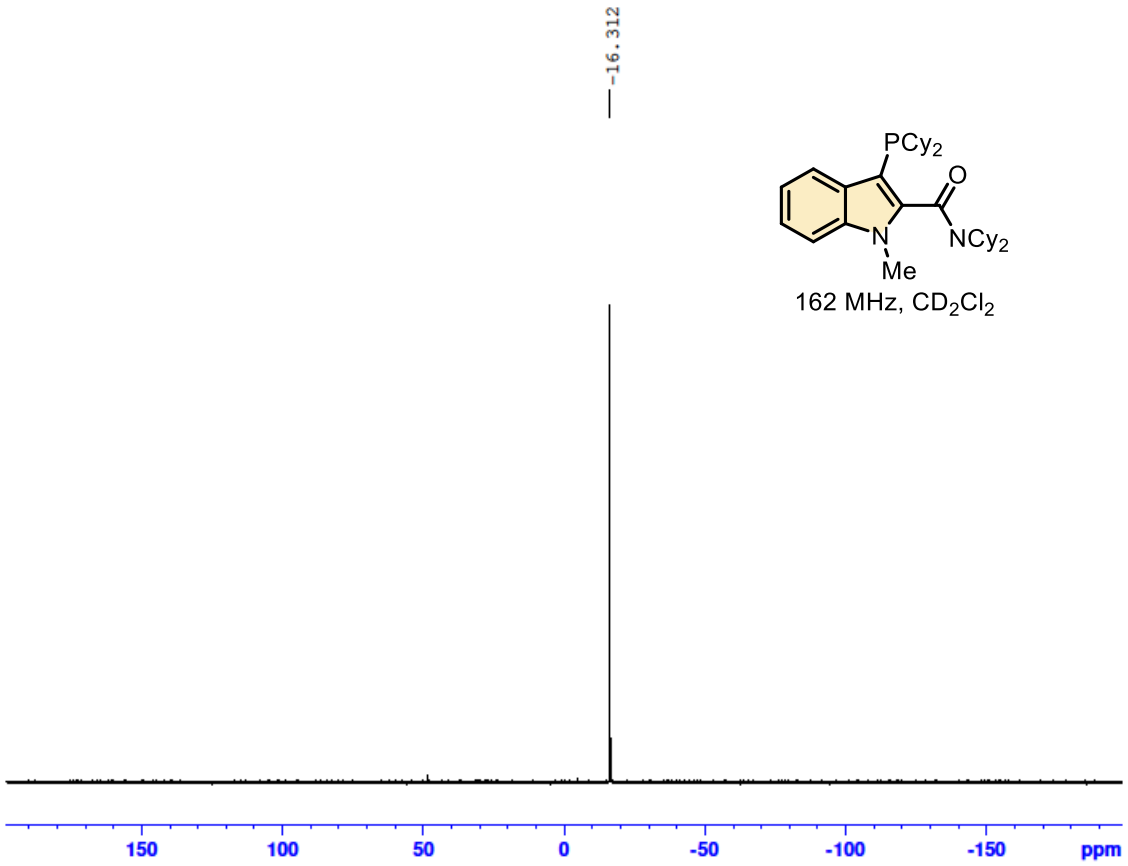

HRMS of *N*,*N*-dicyclohexyl-3-(dicyclohexylphosphanyl)-1-methyl-1*H*-indole-2-carboxamide (**L5**)

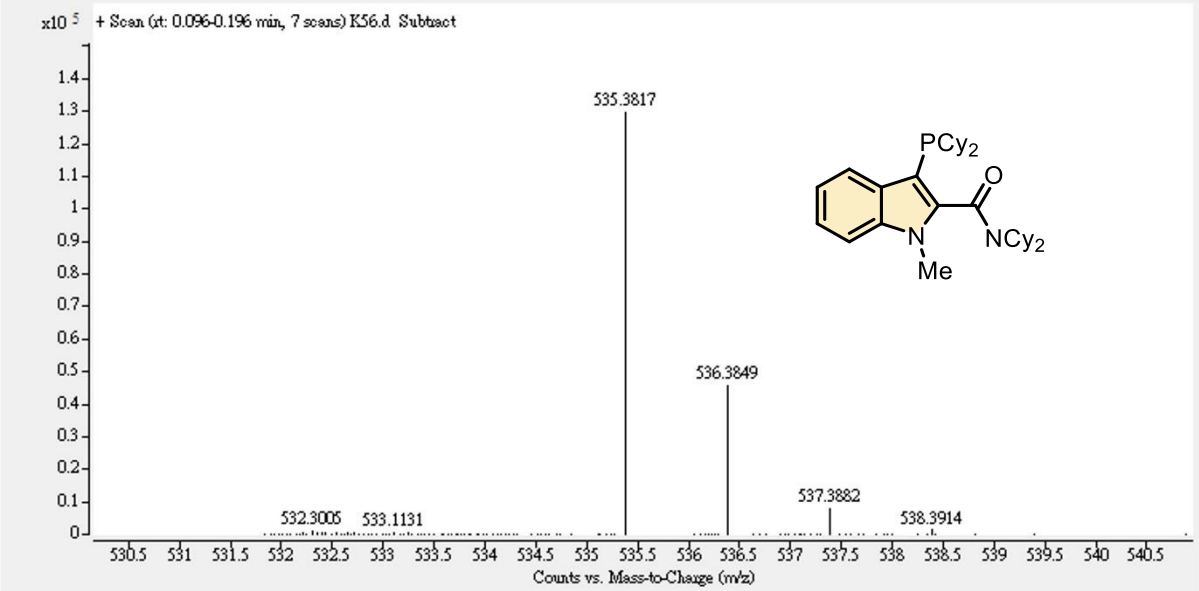

Mass	Calc. Mass	mDa	PPM	Formula
535.3817	535.3812	-0.52	-0.98	C34 H52 N2 O P

^{1}H NMR of *N*,*N*-diisopropyl-1*H*-indole-2-carboxamide (**P6**)

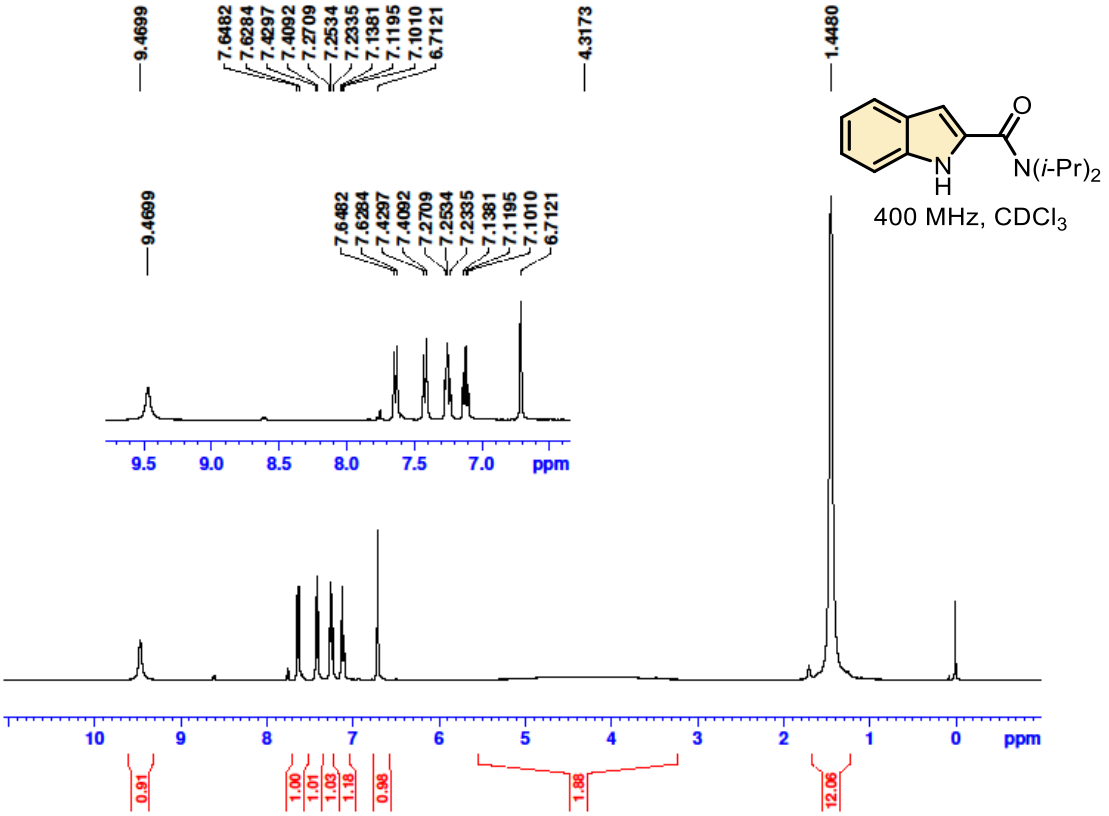

^{13}C NMR of *N*,*N*-diisopropyl-1*H*-indole-2-carboxamide (**P6**)

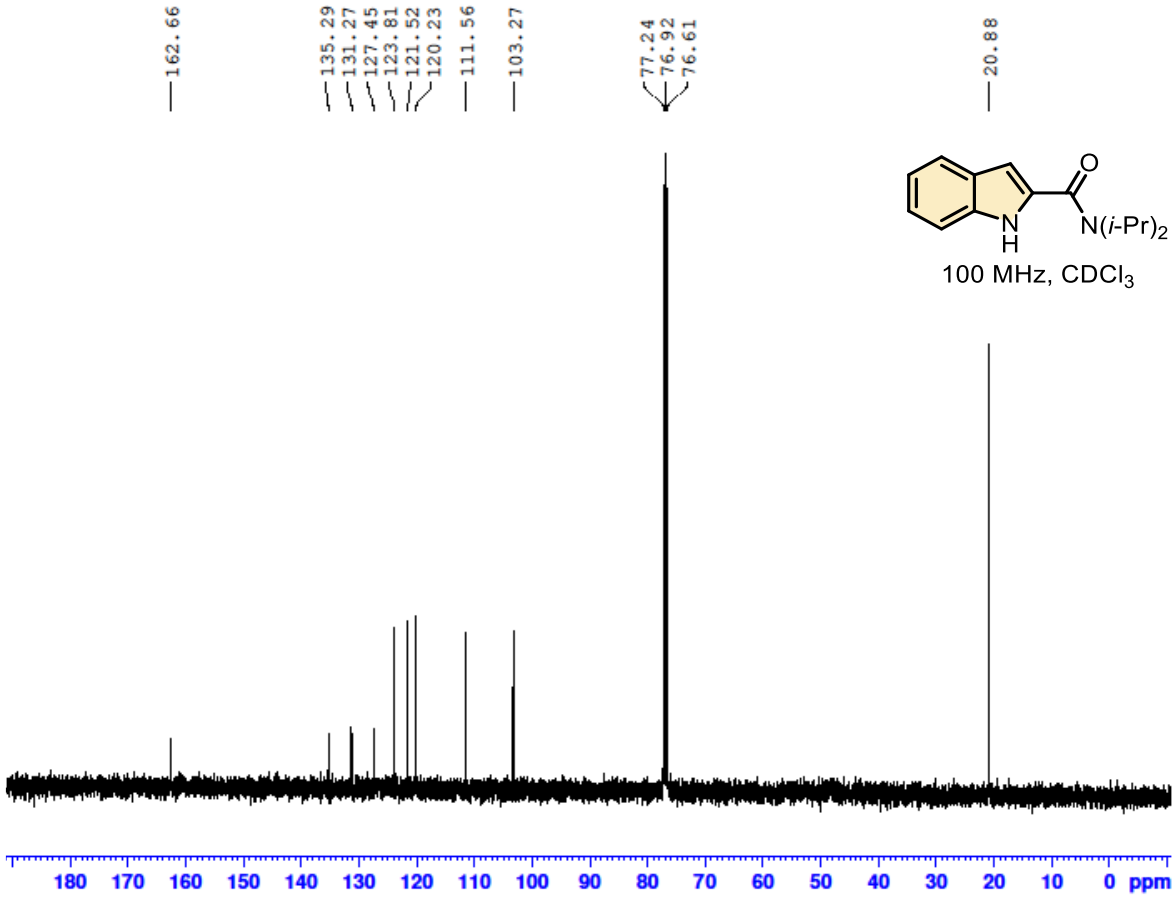

^{1}H NMR of *N*,*N*-diisopropyl-1-isopropyl-1*H*-indole-2-carboxamide (**P6'**)

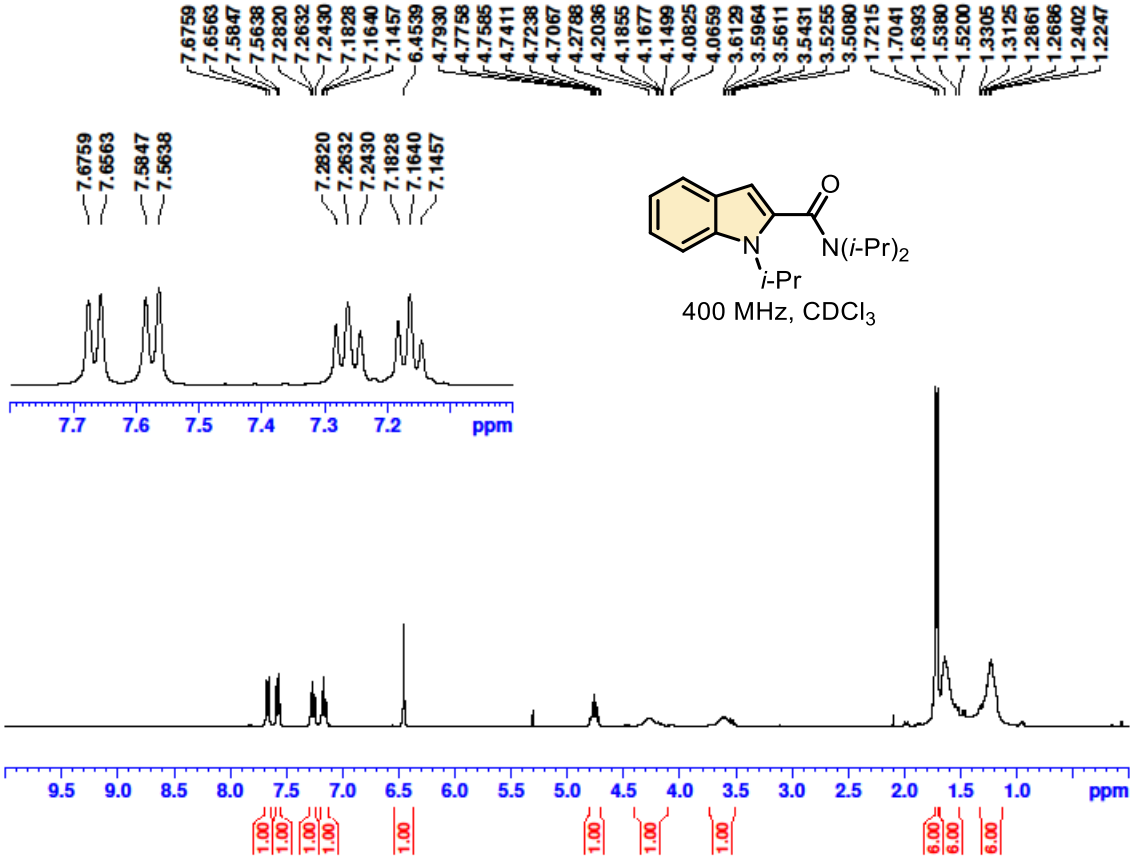

^{13}C NMR of *N*,*N*-diisopropyl-1-isopropyl-1*H*-indole-2-carboxamide (**P6'**)

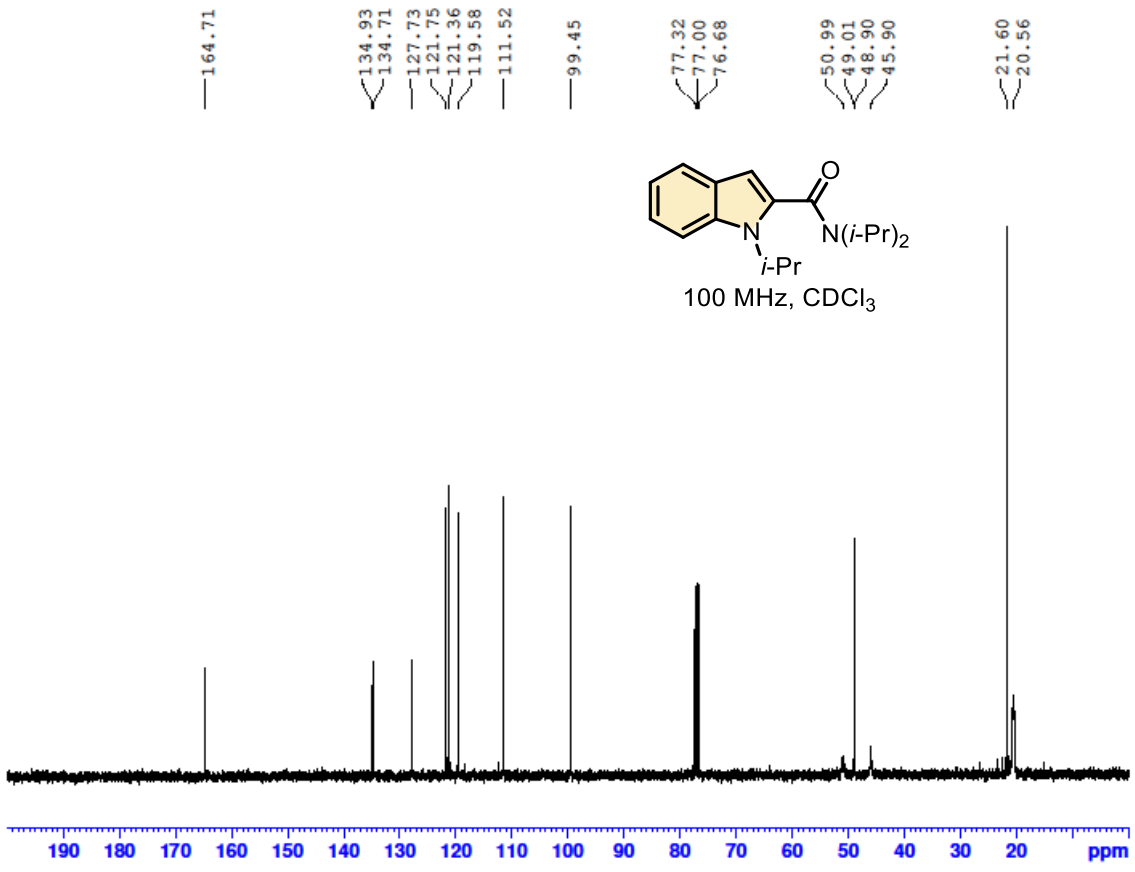

HRMS of *N*,*N*-diisopropyl-1-isopropyl-1*H*-indole-2-carboxamide (**P6'**)

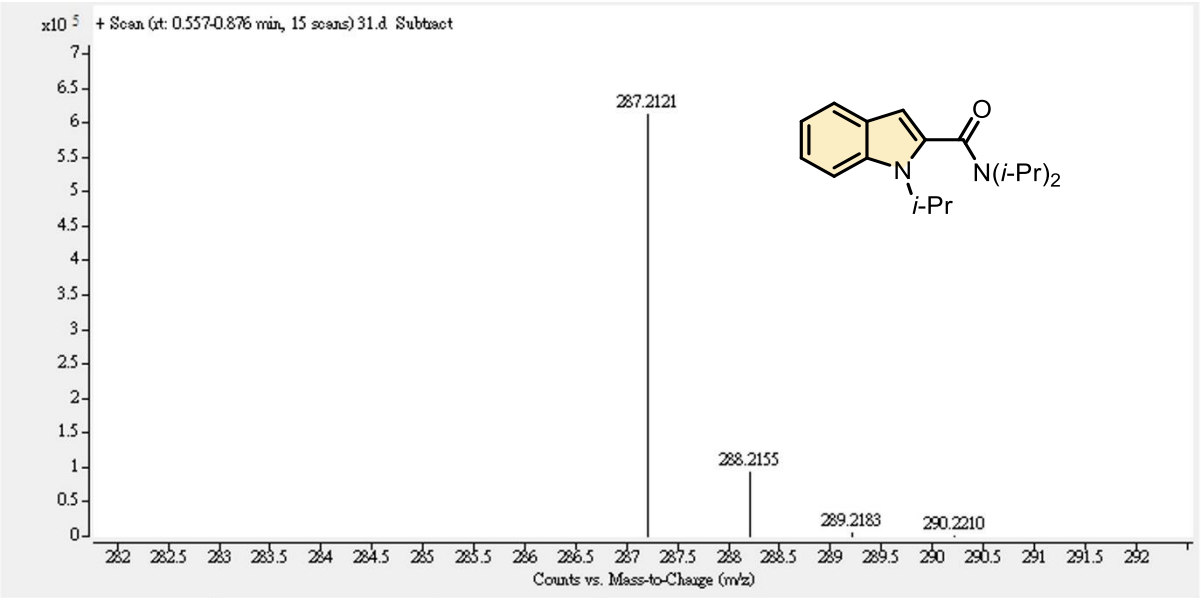

Mass	Calc. Mass	mDa	PPM	Formula
287.2121	287.2118	-0.31	-1.08	C18 H27 N2 O

^{1}H NMR of 3-bromo-*N*,*N*,1-triisopropyl-1*H*-indole-2-carboxamide (**P6''**)

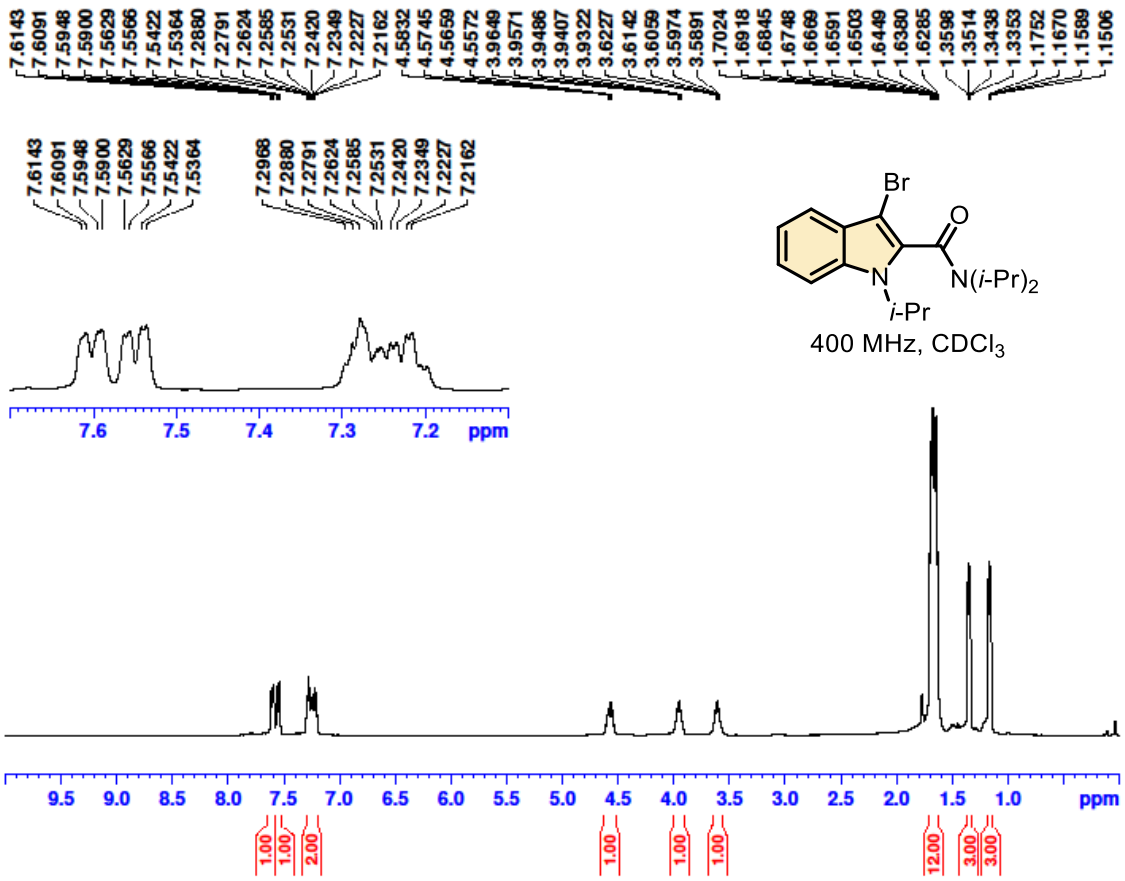

^{13}C NMR of 3-bromo-*N*,*N*,1-triisopropyl-1*H*-indole-2-carboxamide (**P6''**)

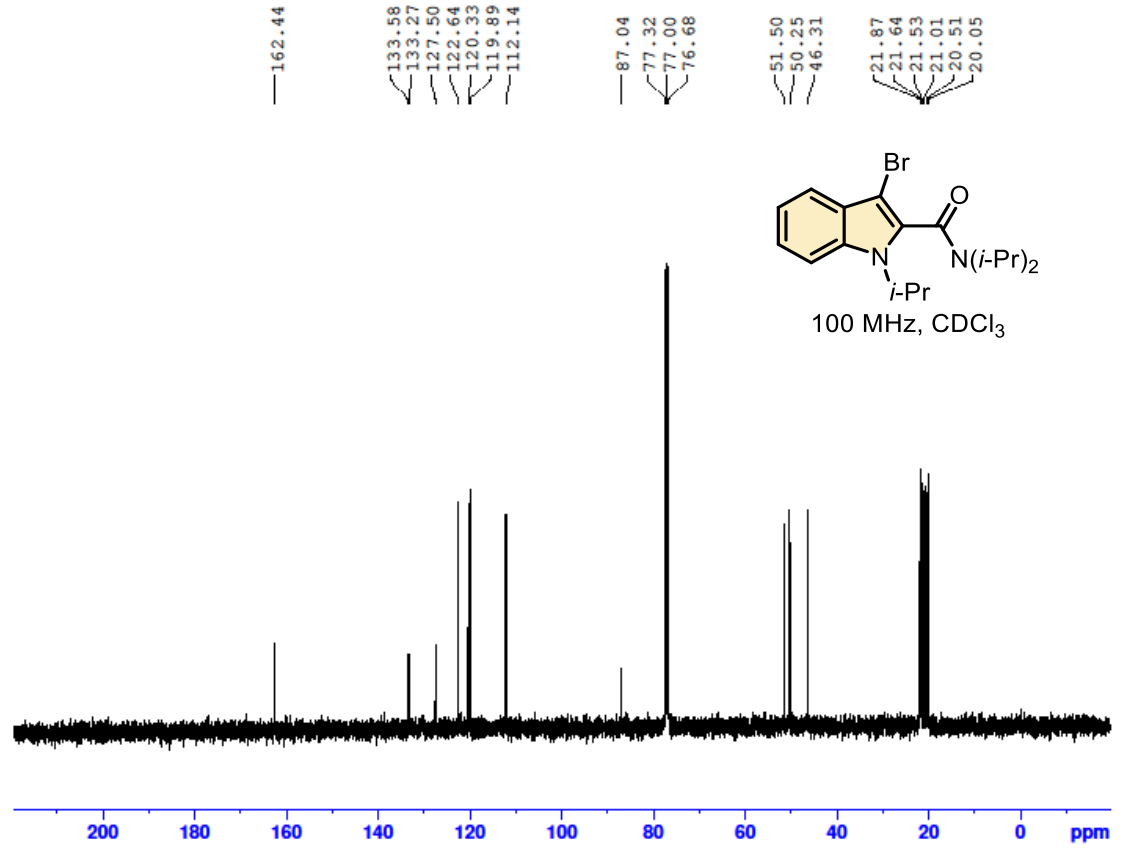

HRMS of 3-bromo-*N*,*N*,1-triisopropyl-1*H*-indole-2-carboxamide (**P6''**)

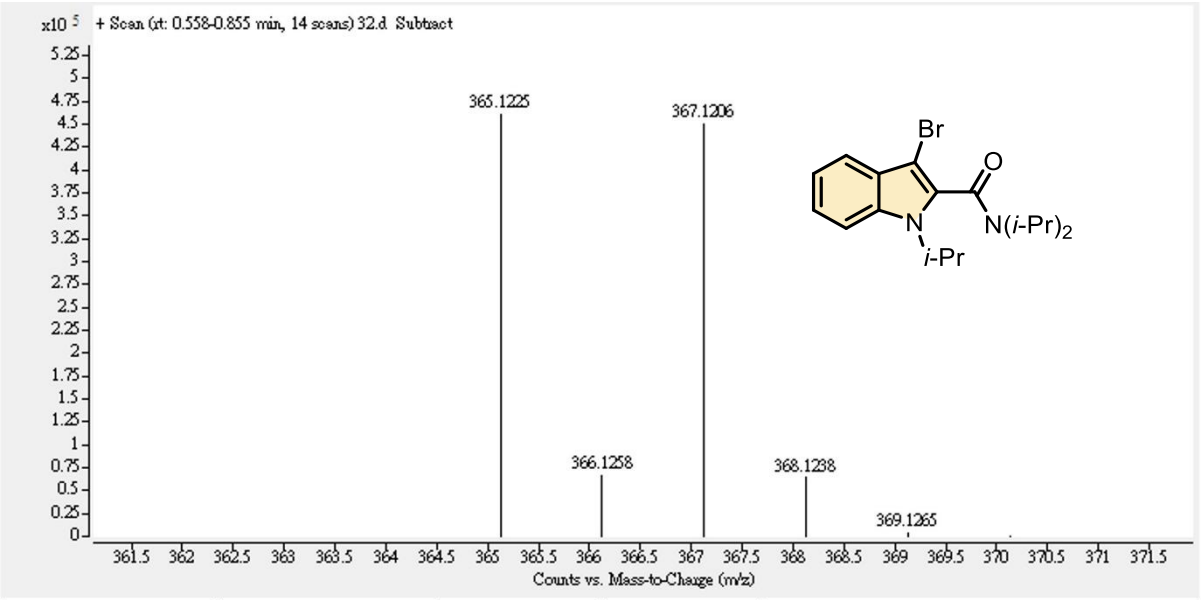

Mass	Calc. Mass	mDa	PPM	Formula
365.1225	365.1223	-0.20	-0.54	C18 H26 Br N2 O

^{1}H NMR of 3-(dicyclohexylphosphanyl)-*N*,*N*,1-triisopropyl-1*H*-indole-2-carboxamide (**L6**)

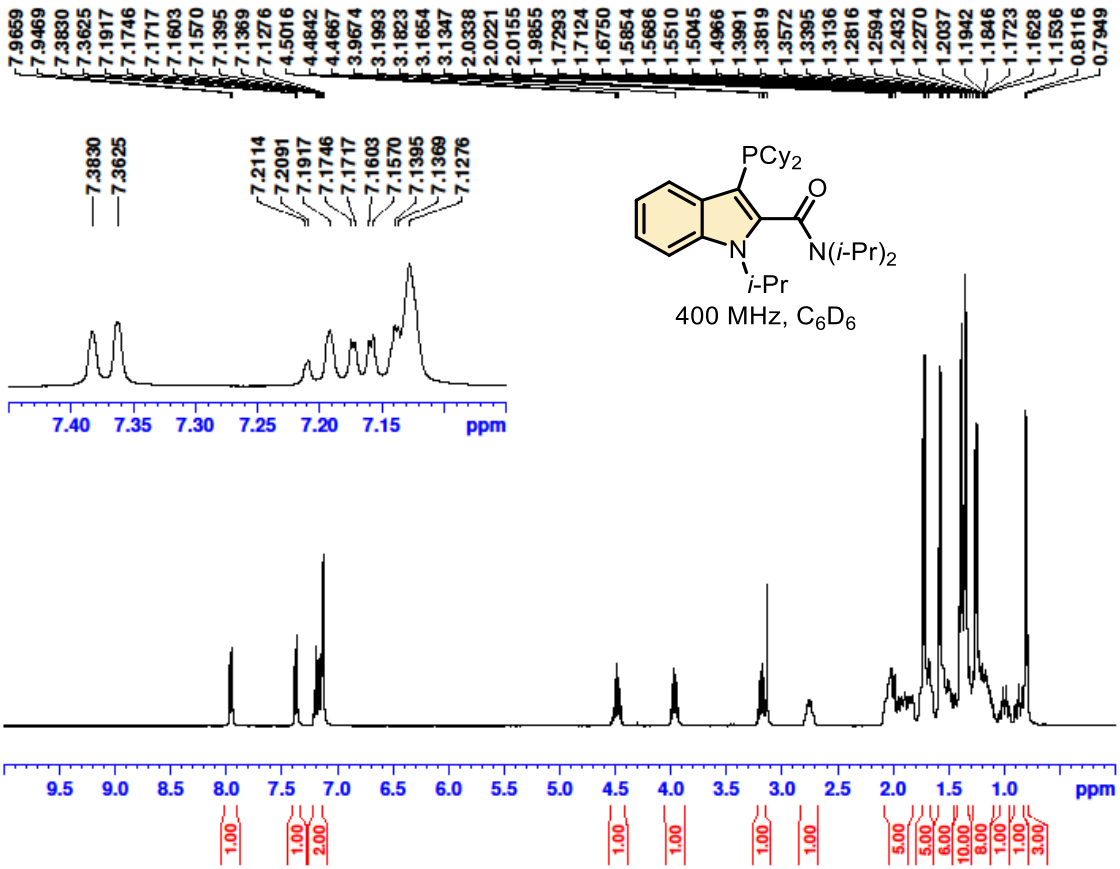

^{13}C NMR of 3-(dicyclohexylphosphanyl)-*N*,*N*,1-triisopropyl-1*H*-indole-2-carboxamide (**L6**)

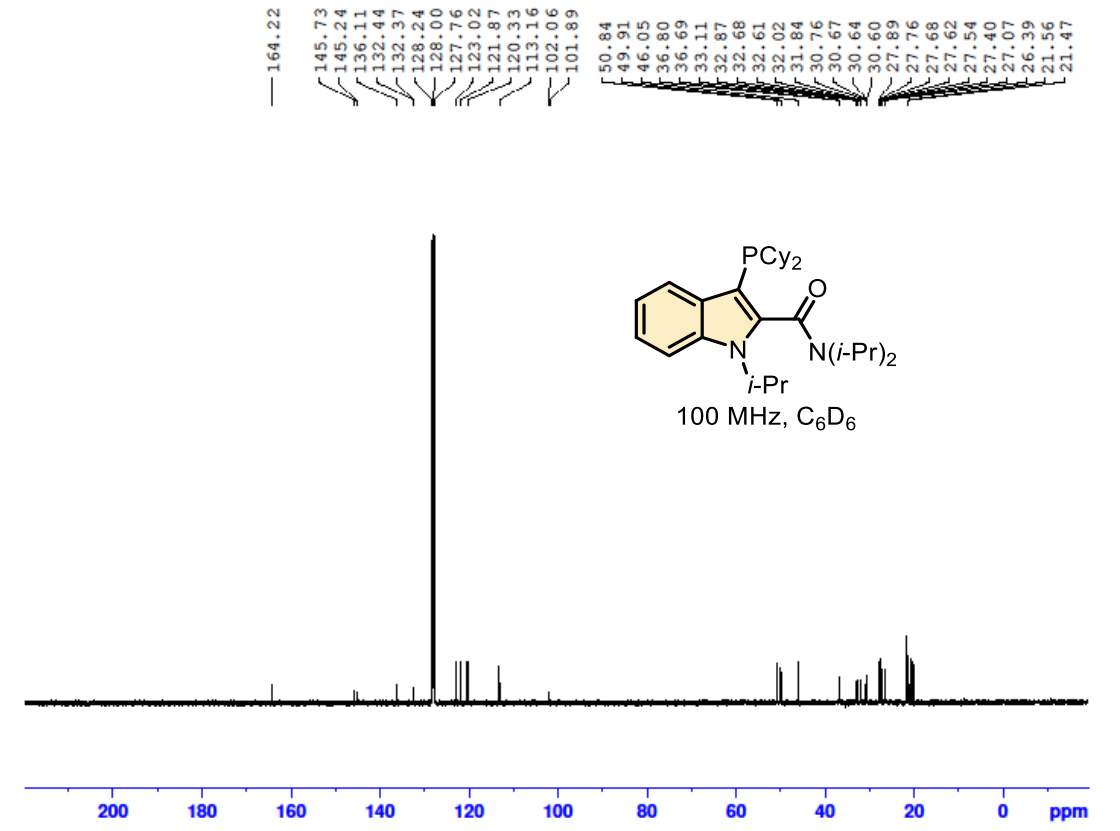

^{31}P NMR of 3-(dicyclohexylphosphanyl)-*N*,*N*,1-triisopropyl-1*H*-indole-2-carboxamide (**L6**)

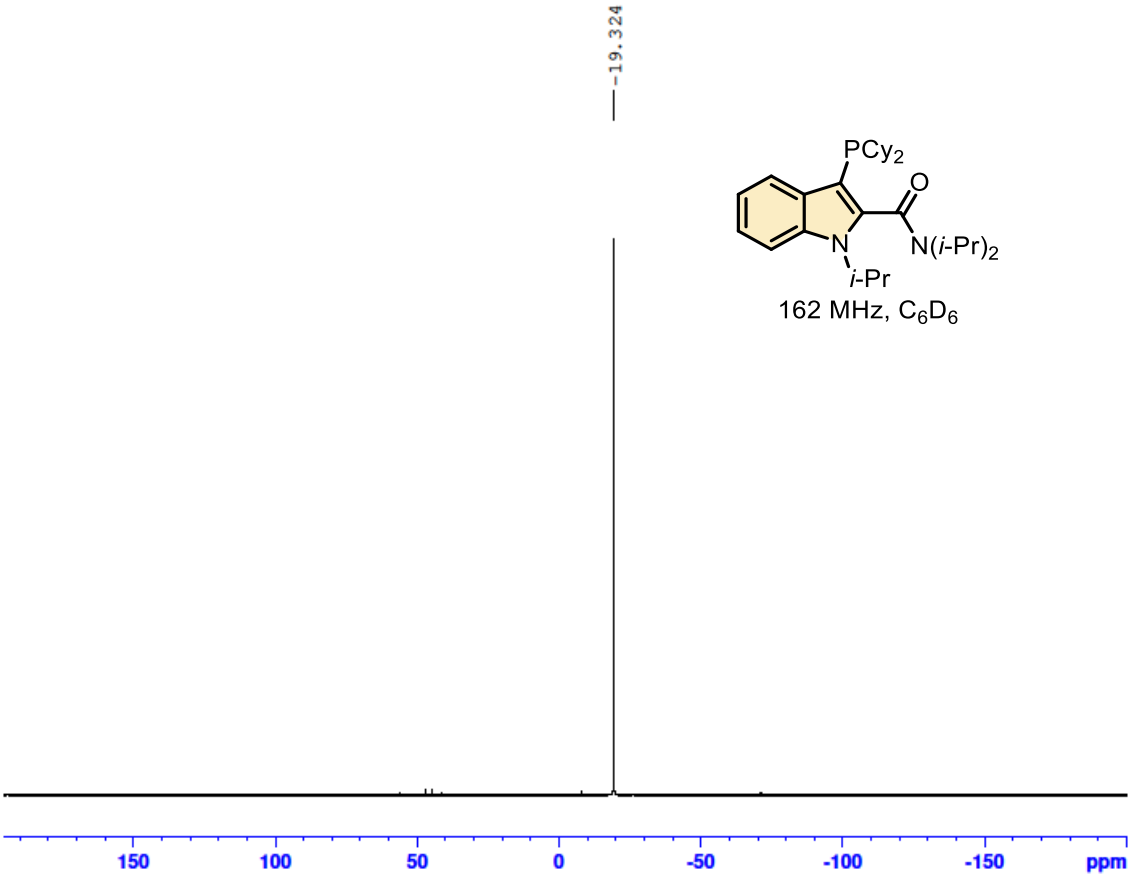

HRMS of 3-(dicyclohexylphosphanyl)-*N*,*N*,1-triisopropyl-1*H*-indole-2-carboxamide (**L6**)

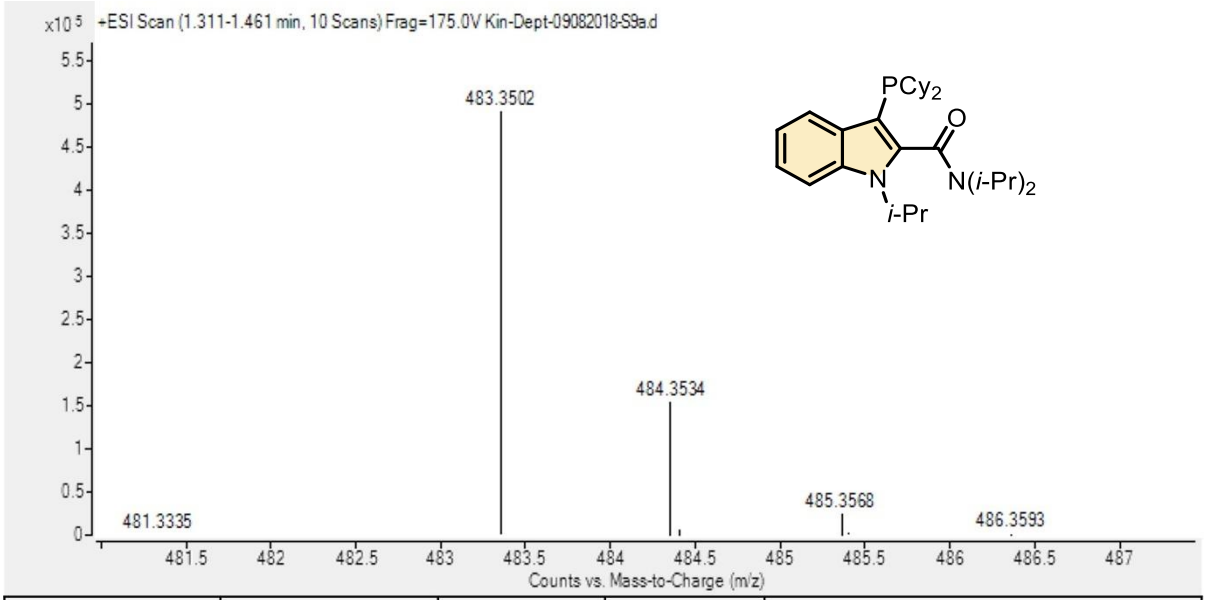

Mass	Calc. Mass	mDa	PPM	Formula
483.3502	483.3499	0.35	0.67	C30 H48 N2 O P

^{1}H NMR of *N*,*N*-dicyclohexyl-1-isopropyl-1*H*-indole-2-carboxamide (**P7**)

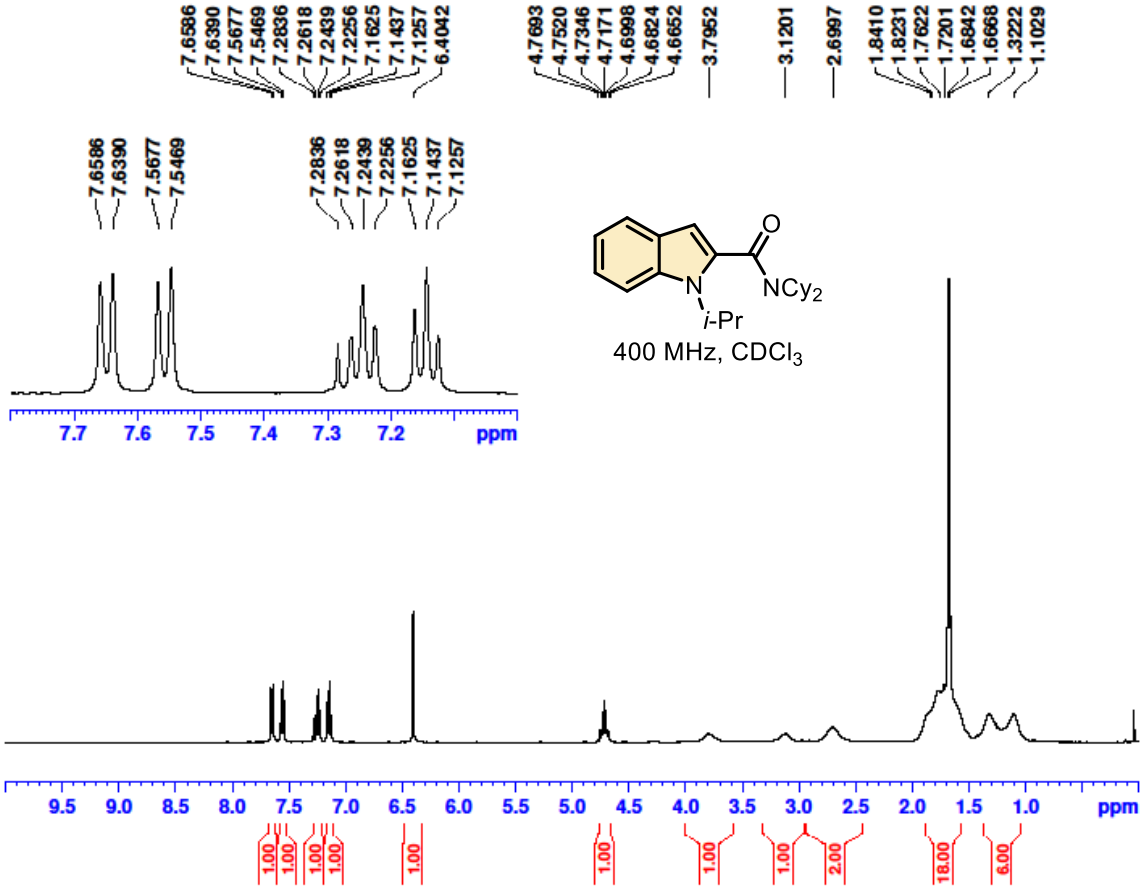

^{13}C NMR of *N*,*N*-dicyclohexyl-1-isopropyl-1*H*-indole-2-carboxamide (**P7**)

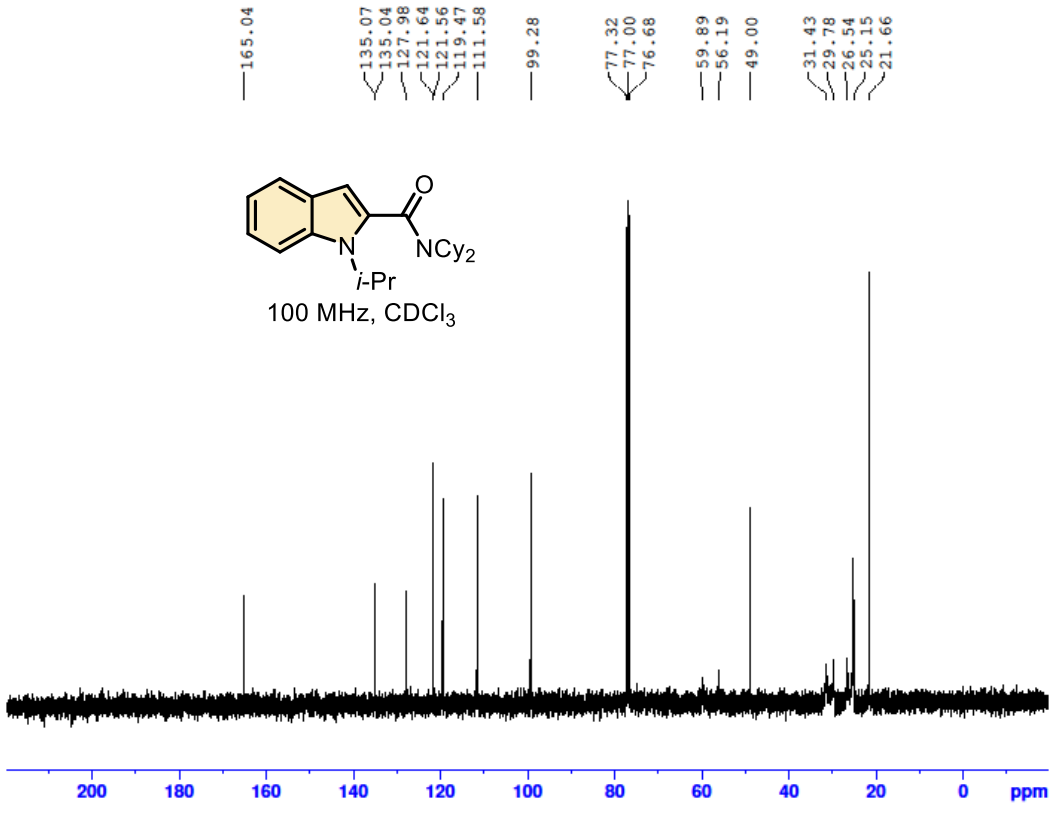

HRMS of *N*,*N*-dicyclohexyl-1-isopropyl-1*H*-indole-2-carboxamide (**P7**)

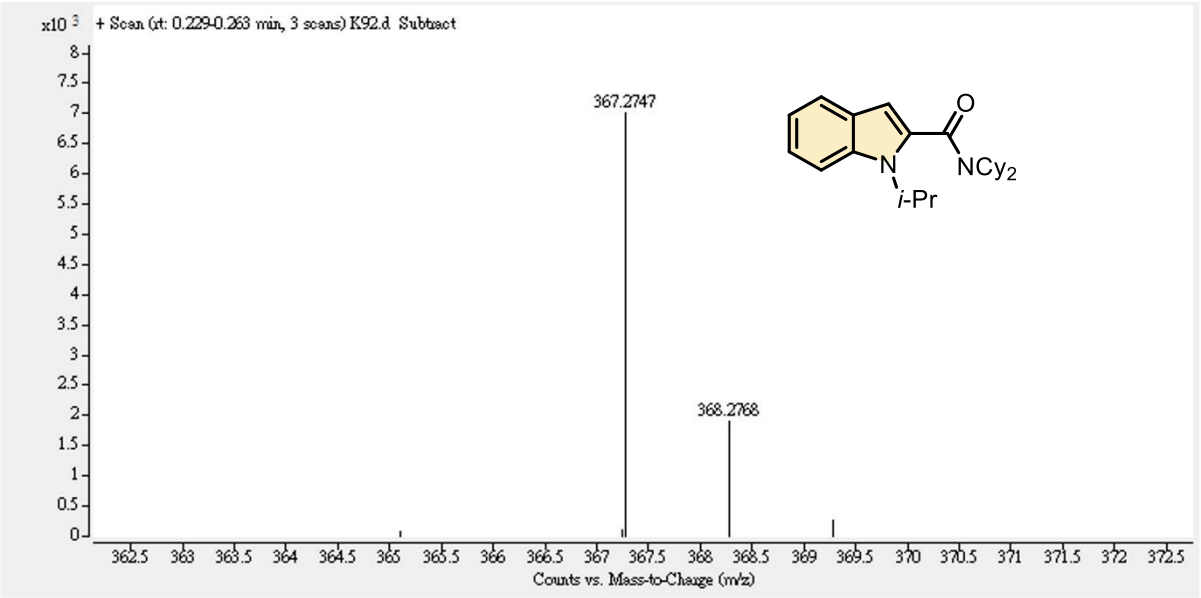

Mass	Calc. Mass	mDa	PPM	Formula
367.2747	367.2744	-0.31	-0.85	C24 H35 N2 O

^{1}H NMR of 3-bromo-*N*,*N*-dicyclohexyl-1-isopropyl-1*H*-indole-2-carboxamide (**P7'**)

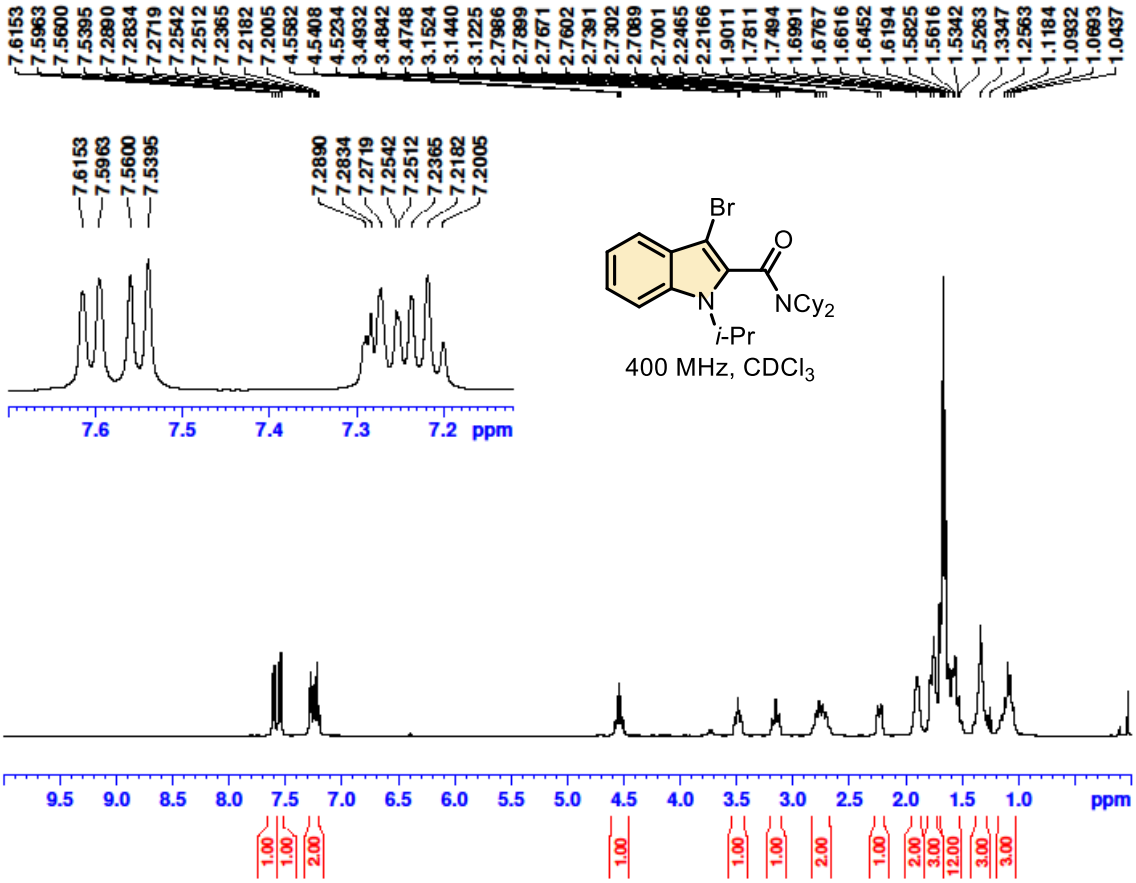

^{13}C NMR of 3-bromo-*N*,*N*-dicyclohexyl-1-isopropyl-1*H*-indole-2-carboxamide (**P7'**)

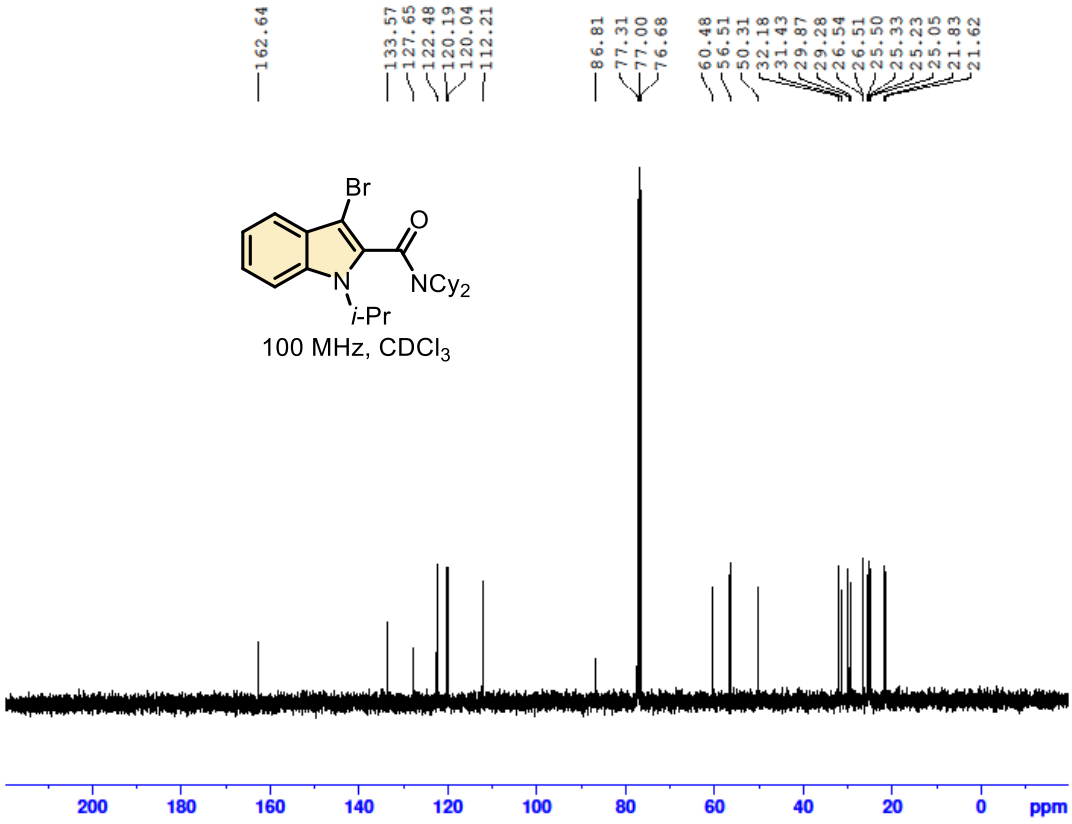

HRMS of 3-bromo-*N*,*N*-dicyclohexyl-1-isopropyl-1*H*-indole-2-carboxamide (**P7'**)

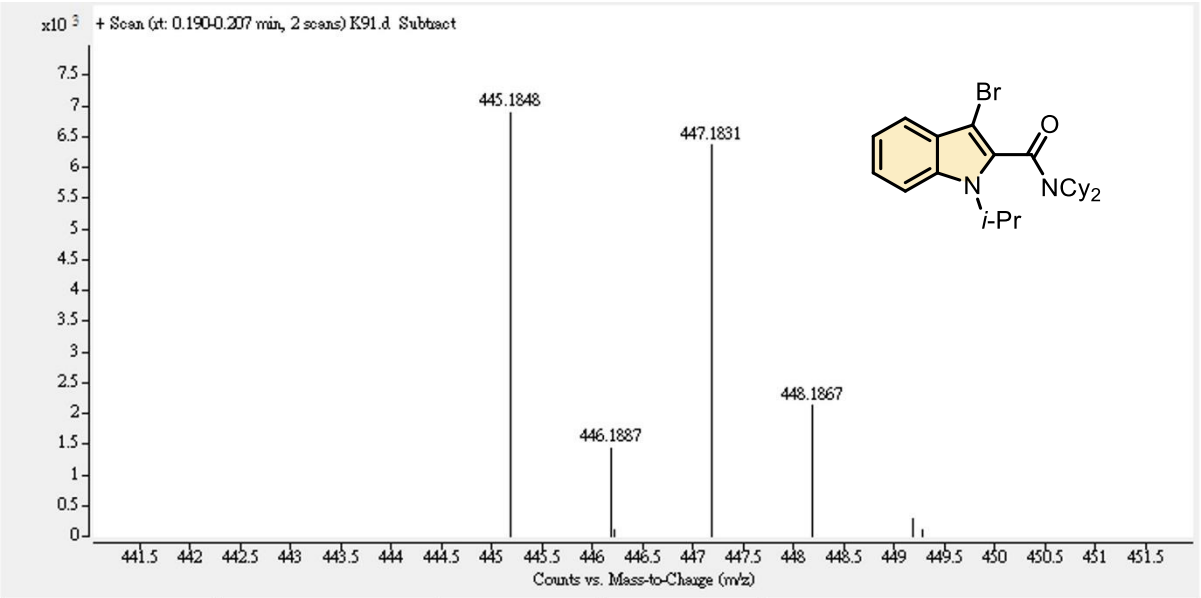

Mass	Calc. Mass	mDa	PPM	Formula
445.1848	445.1849	0.10	0.23	C24 H34 Br N2 O

^{1}H NMR of *N*,*N*-dicyclohexyl-3-(dicyclohexylphosphanyl)-1-isopropyl-1*H*-indole-2-carboxamide (**L7**)

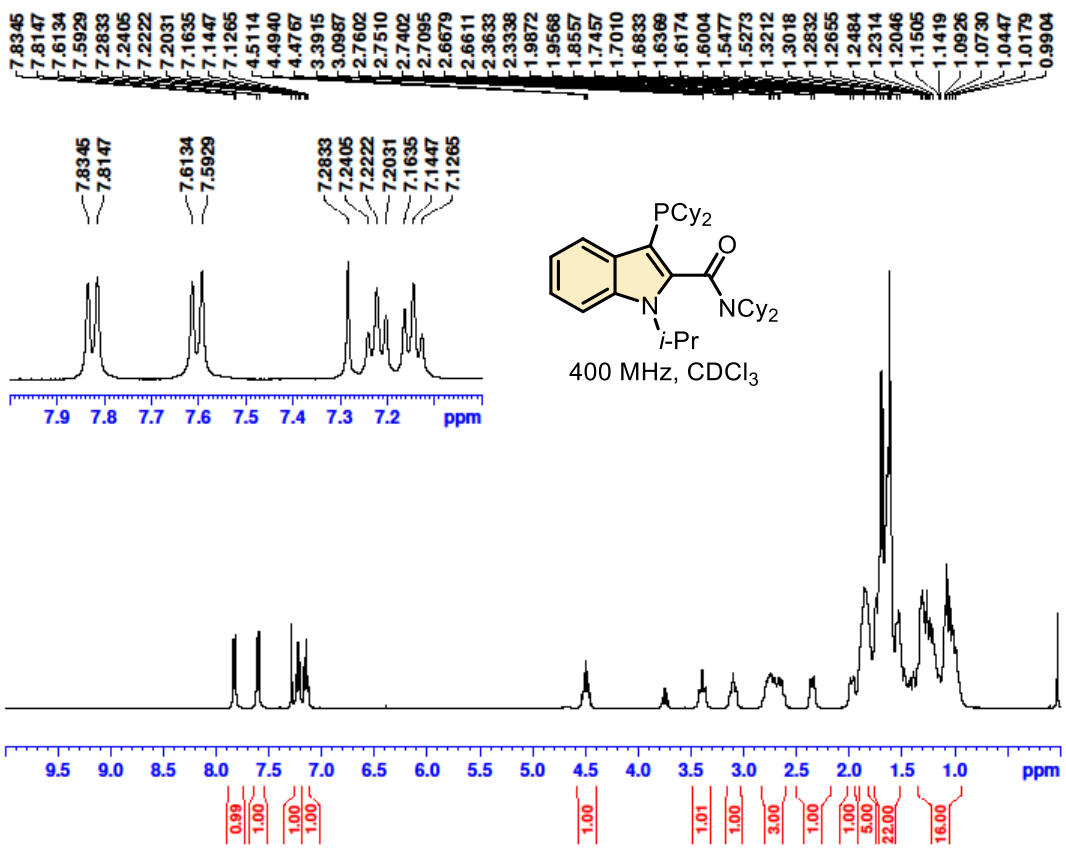

^{13}C NMR of *N*,*N*-dicyclohexyl-3-(dicyclohexylphosphanyl)-1-isopropyl-1*H*-indole-2-carboxamide (**L7**)

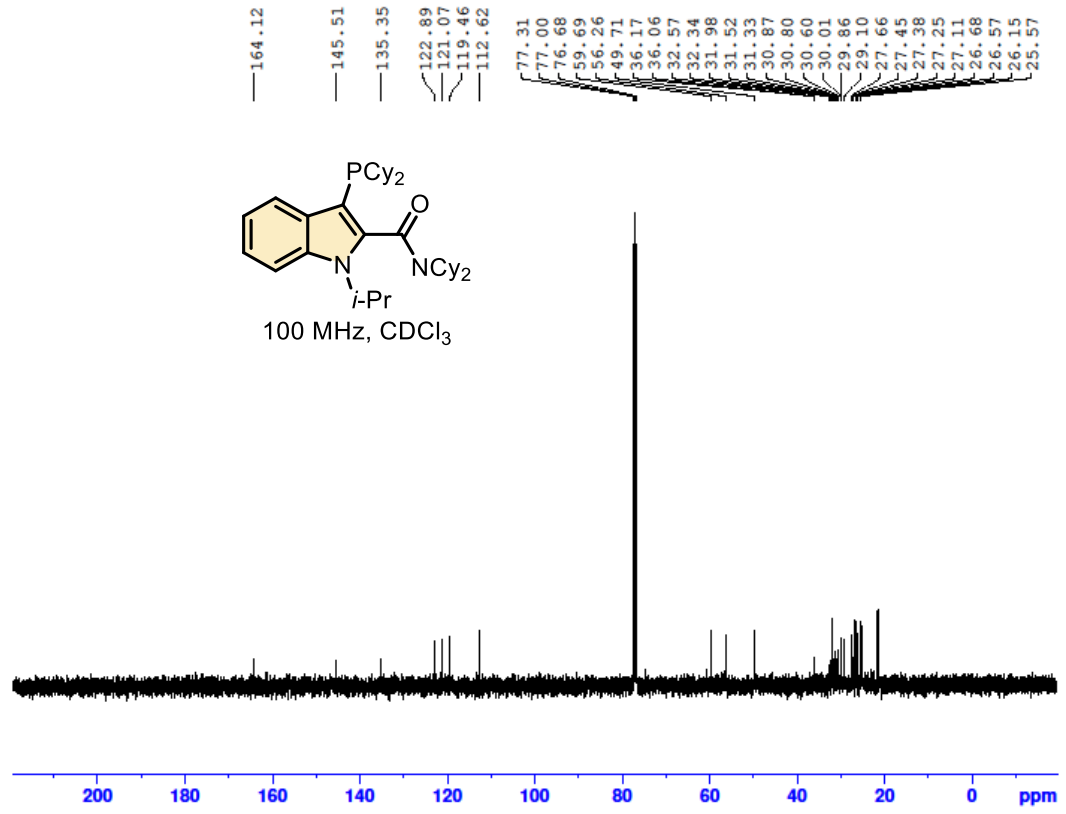

^{31}P NMR of *N*,*N*-dicyclohexyl-3-(dicyclohexylphosphanyl)-1-isopropyl-1*H*-indole-2-carboxamide (**L7**)

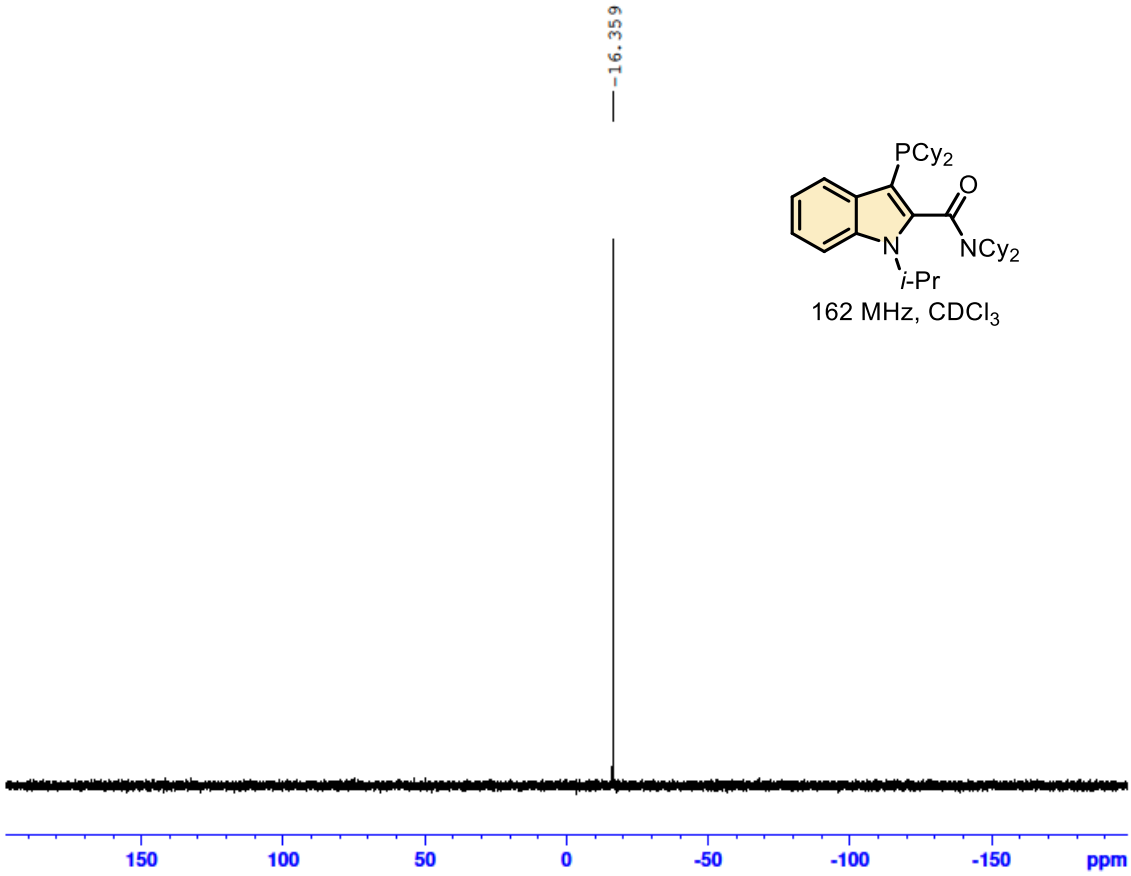

HRMS of *N*,*N*-dicyclohexyl-3-(dicyclohexylphosphanyl)-1-isopropyl-1*H*-indole-2-carboxamide (**L7**)

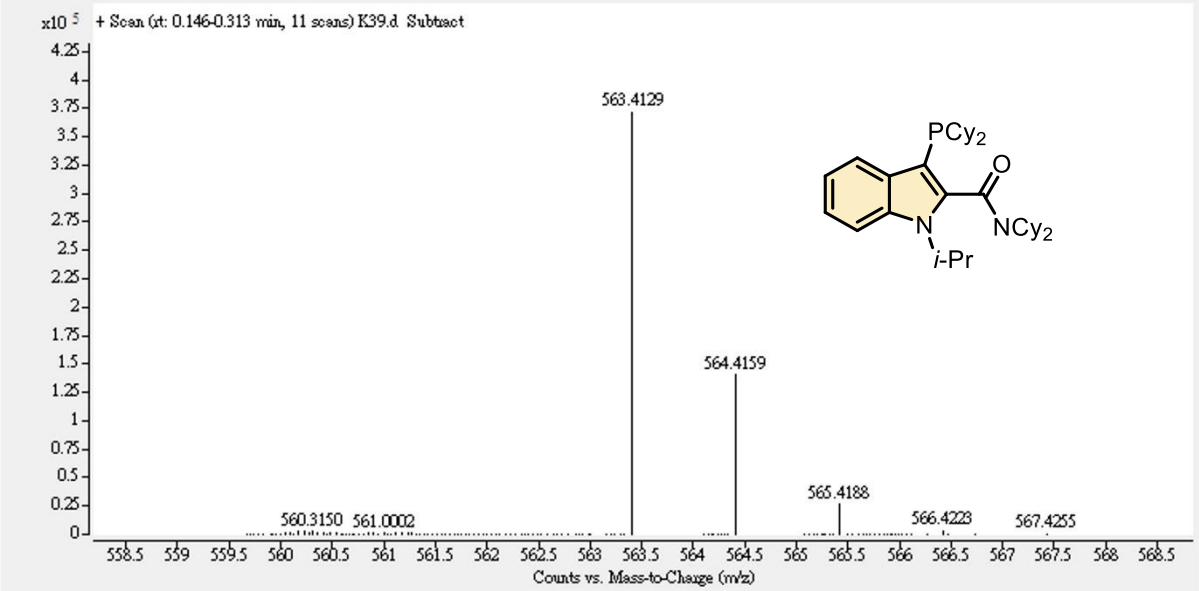

Mass	Calc. Mass	mDa	PPM	Formula
563.4129	563.4125	-0.41	-0.75	C36 H56 N2 O P

^{1}H NMR of 2,2',6-trimethyl-1,1'-biphenyl (Table 2.3, 2.4, and 2.5, compound **3a**)

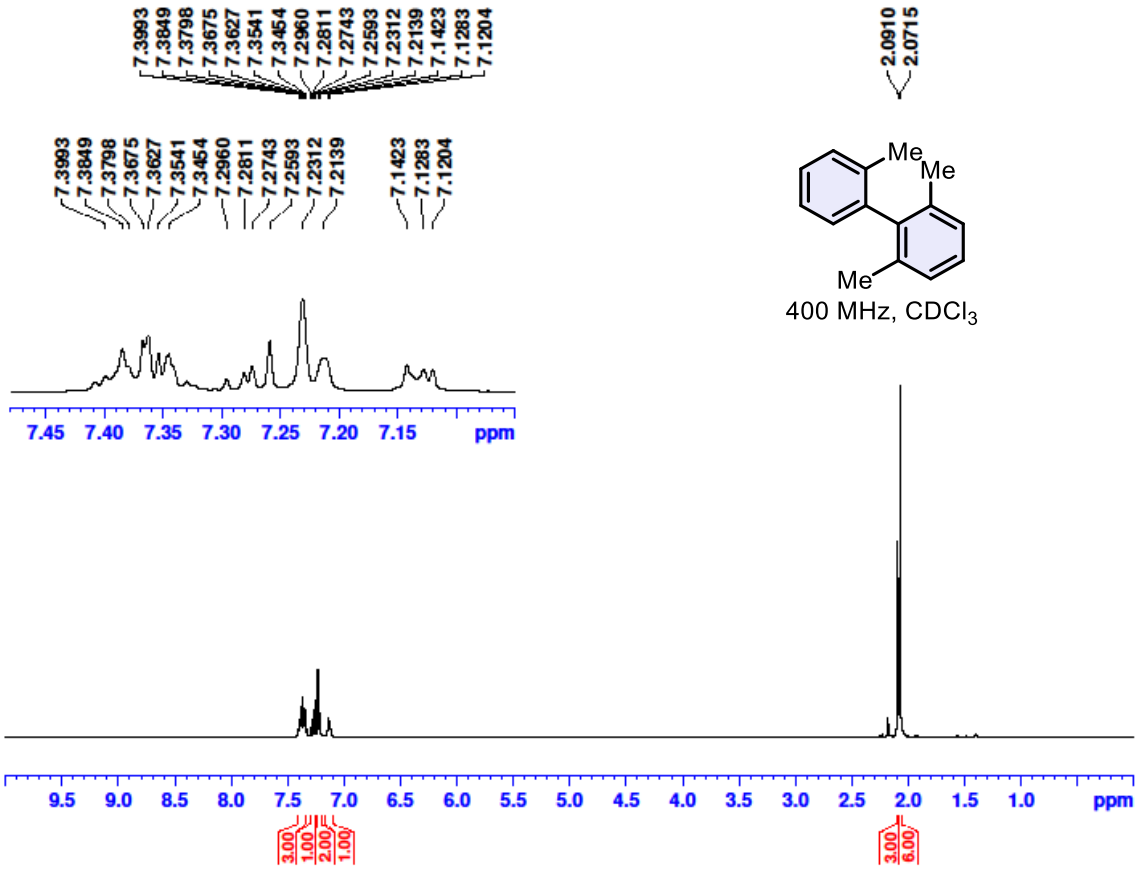

^{13}C NMR of 2,2',6-trimethyl-1,1'-biphenyl (Table 2.3, 2.4, and 2.5, compound **3a**)

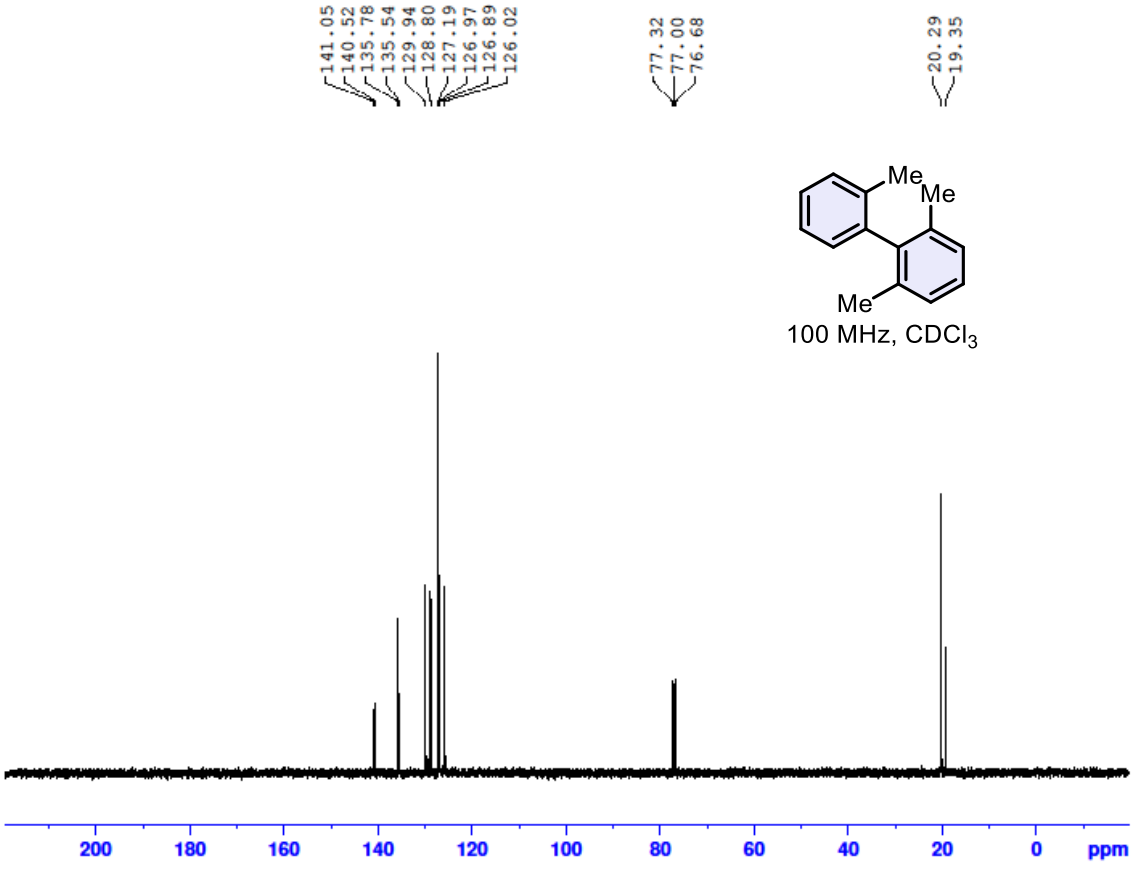

^{1}H NMR of 2'-methoxy-2,6-dimethyl-1,1'-biphenyl (Table 2.3 and 2.4, compound **3b**)

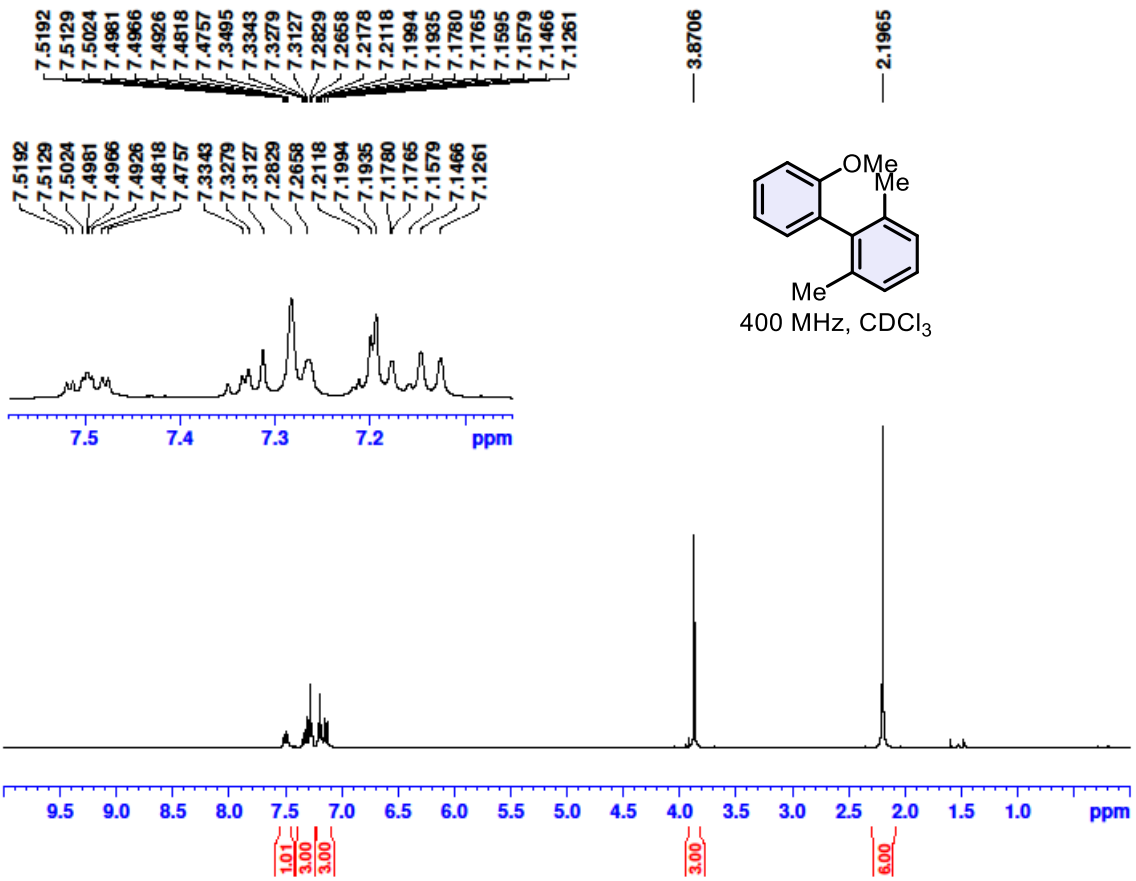

^{13}C NMR of 2'-methoxy-2,6-dimethyl-1,1'-biphenyl (Table 2.3 and 2.4, compound **3b**)

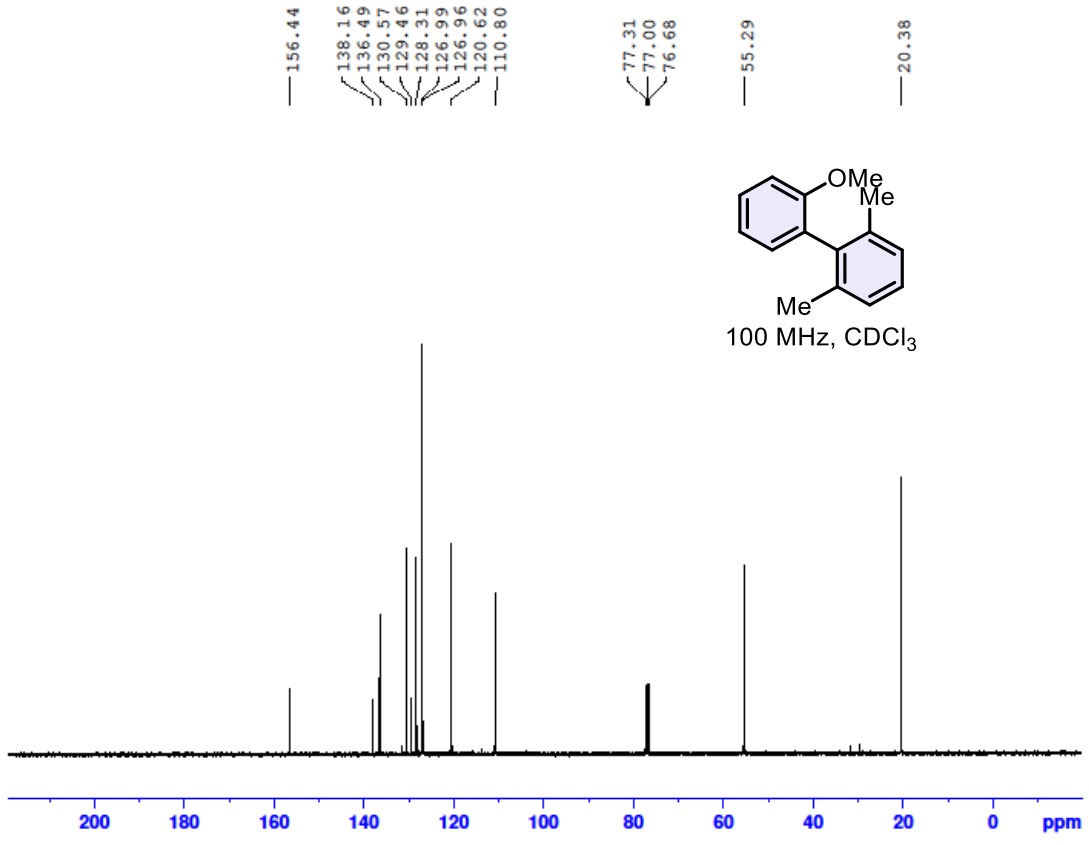

^{1}H NMR of 2,2',4,6-tetramethyl-1,1'-biphenyl (Table 2.3 and 2.4, compound **3c**)

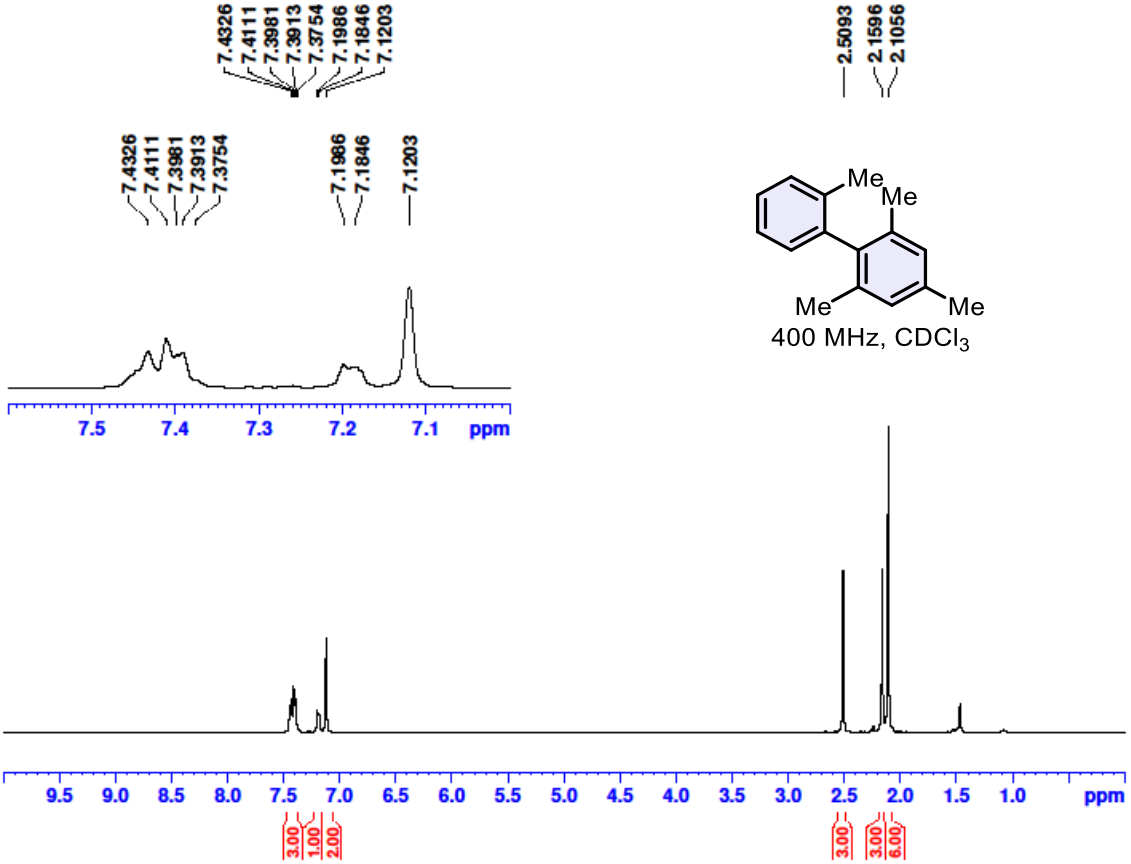

^{13}C NMR of 2,2',4,6-tetramethyl-1,1'-biphenyl (Table 2.3 and 2.4, compound **3c**)

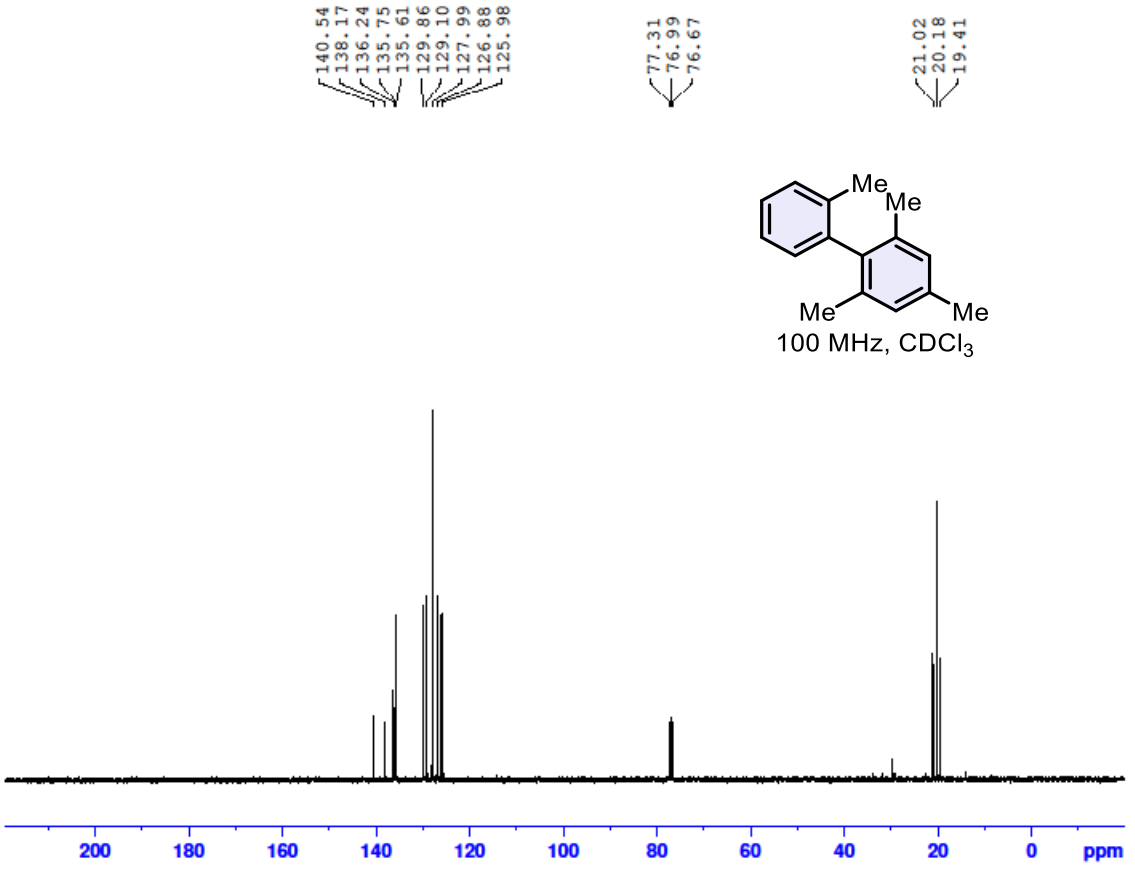

^{1}H NMR of 2'-fluoro-2,6-dimethyl-1,1'-biphenyl (Table 2.3, compound **3d**)

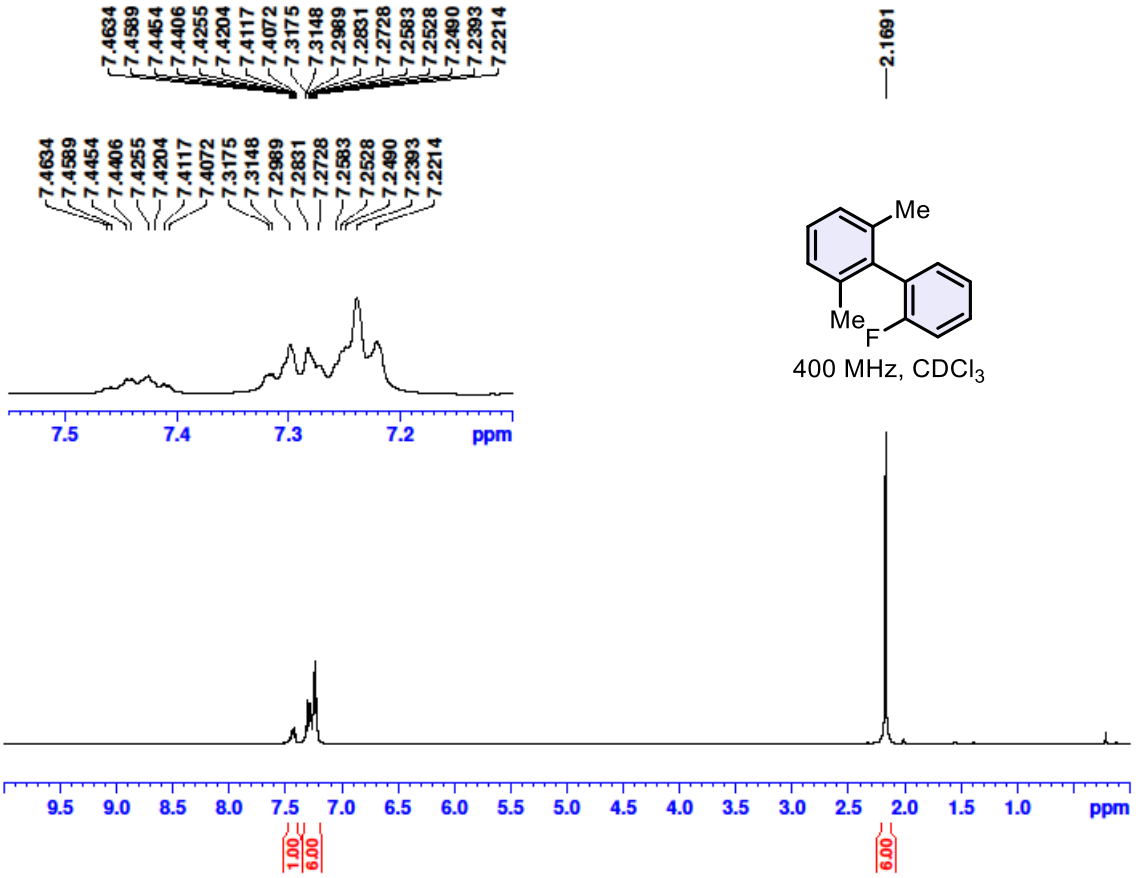

^{13}C NMR of 2'-fluoro-2,6-dimethyl-1,1'-biphenyl (Table 2.3, compound **3d**)

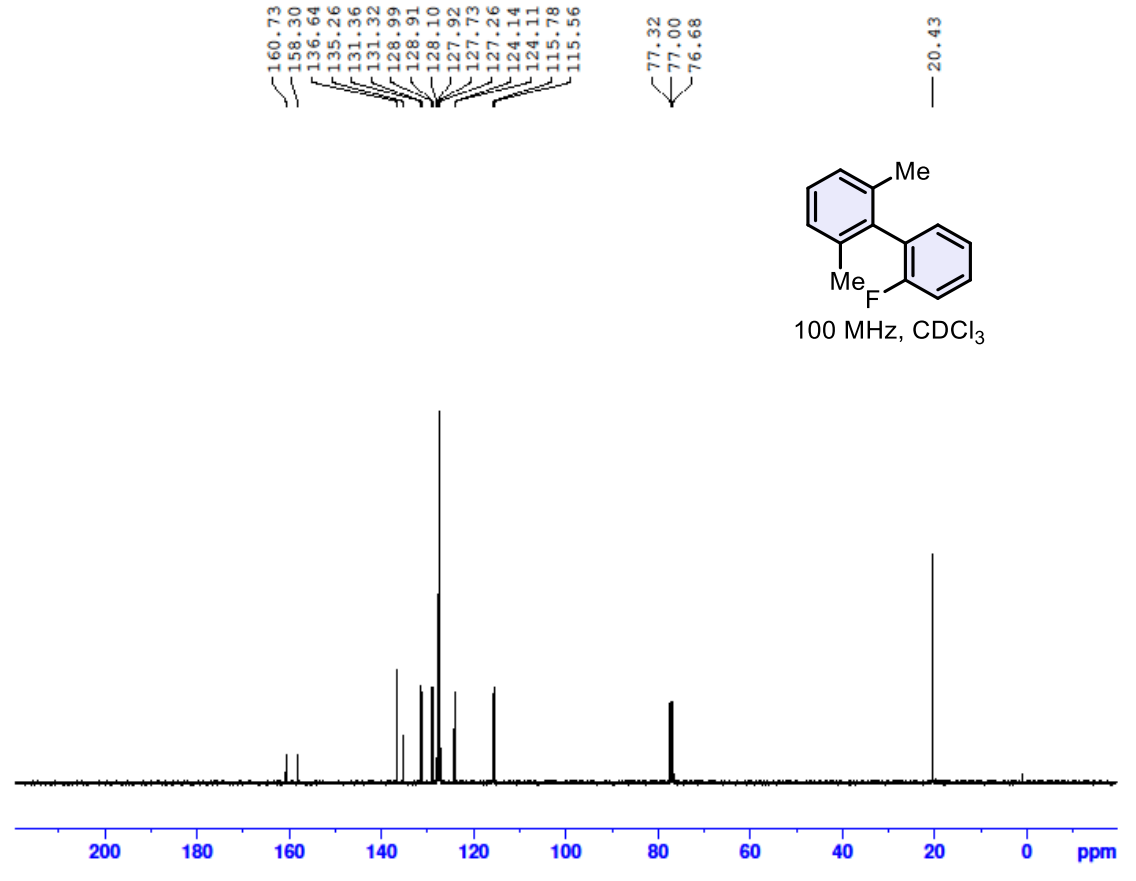

^{19}F NMR of 2'-fluoro-2,6-dimethyl-1,1'-biphenyl (Table 2.3, compound **3d**)

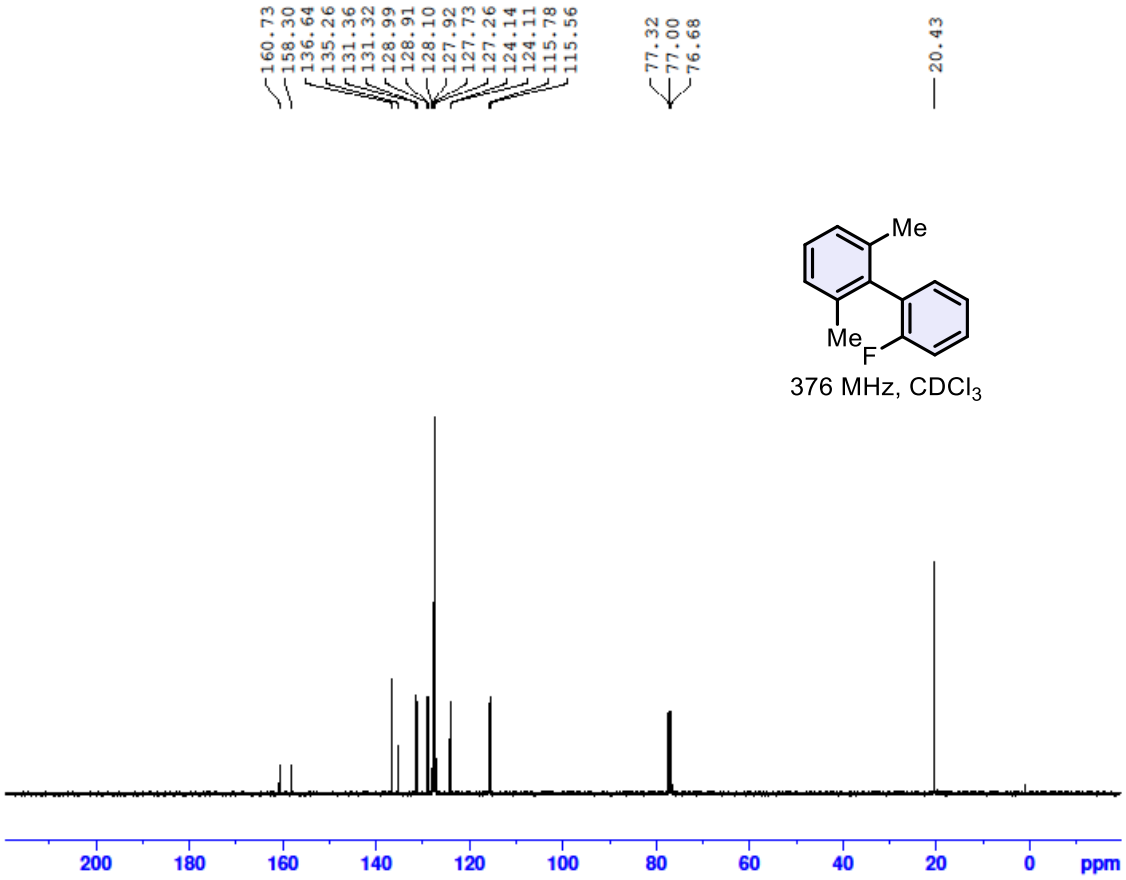

^{1}H NMR of 2,4-difluoro-2',6'-dimethyl-1,1'-biphenyl (Table 2.3, compound **3e**)

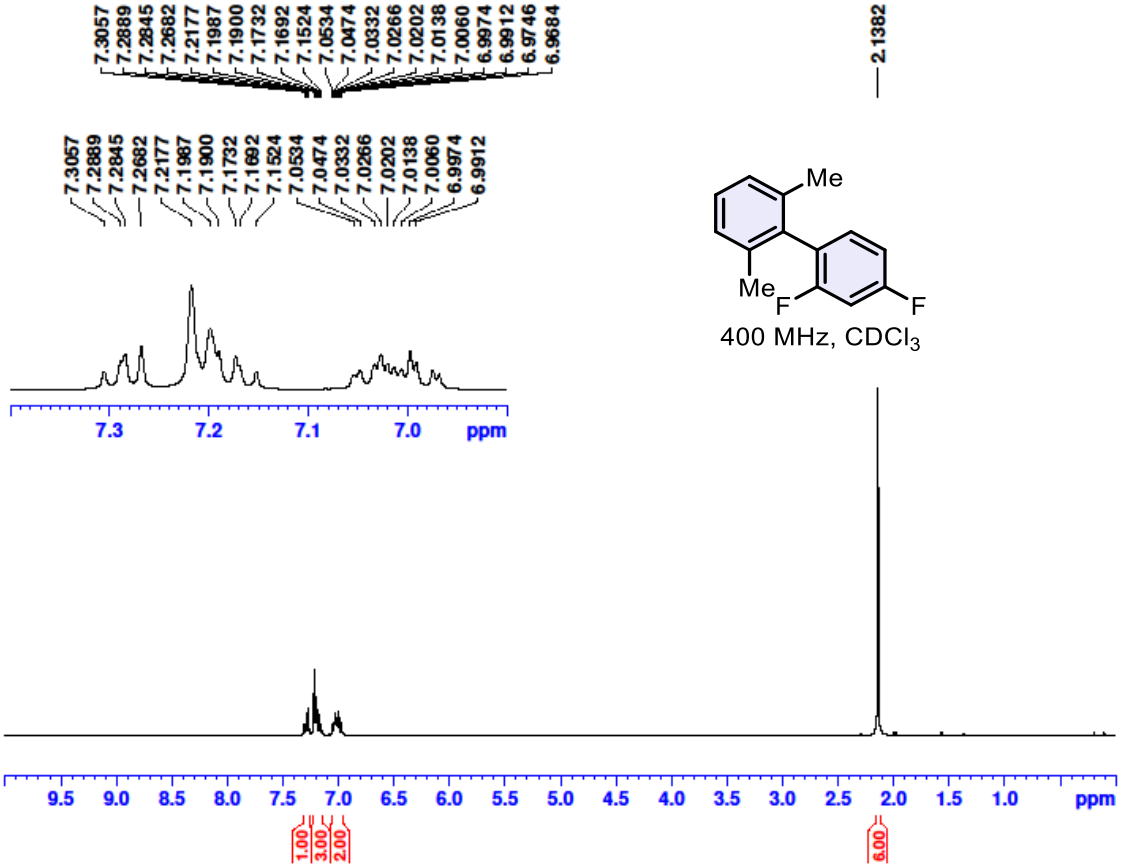

^{13}C NMR of 2,4-difluoro-2',6'-dimethyl-1,1'-biphenyl (Table 2.3, compound **3e**)

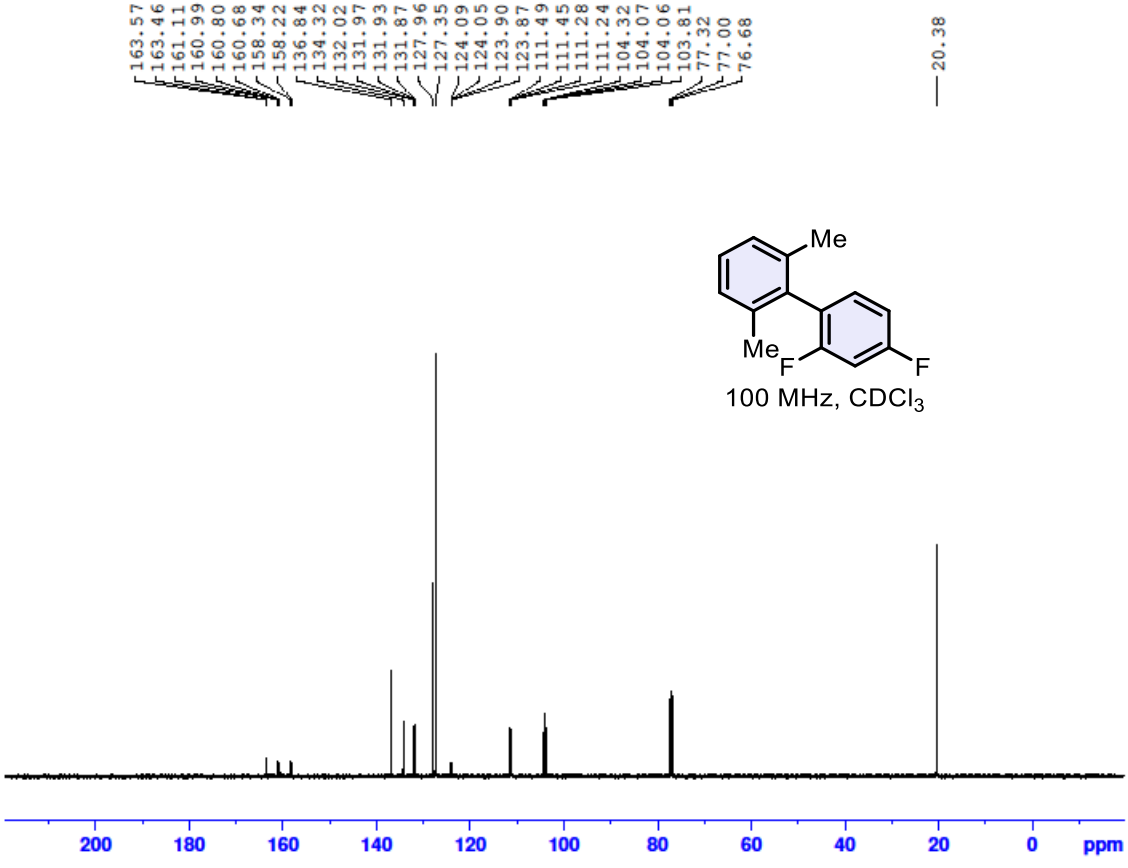

^{19}F NMR of 2,4-difluoro-2',6'-dimethyl-1,1'-biphenyl (Table 2.3, compound **3e**)

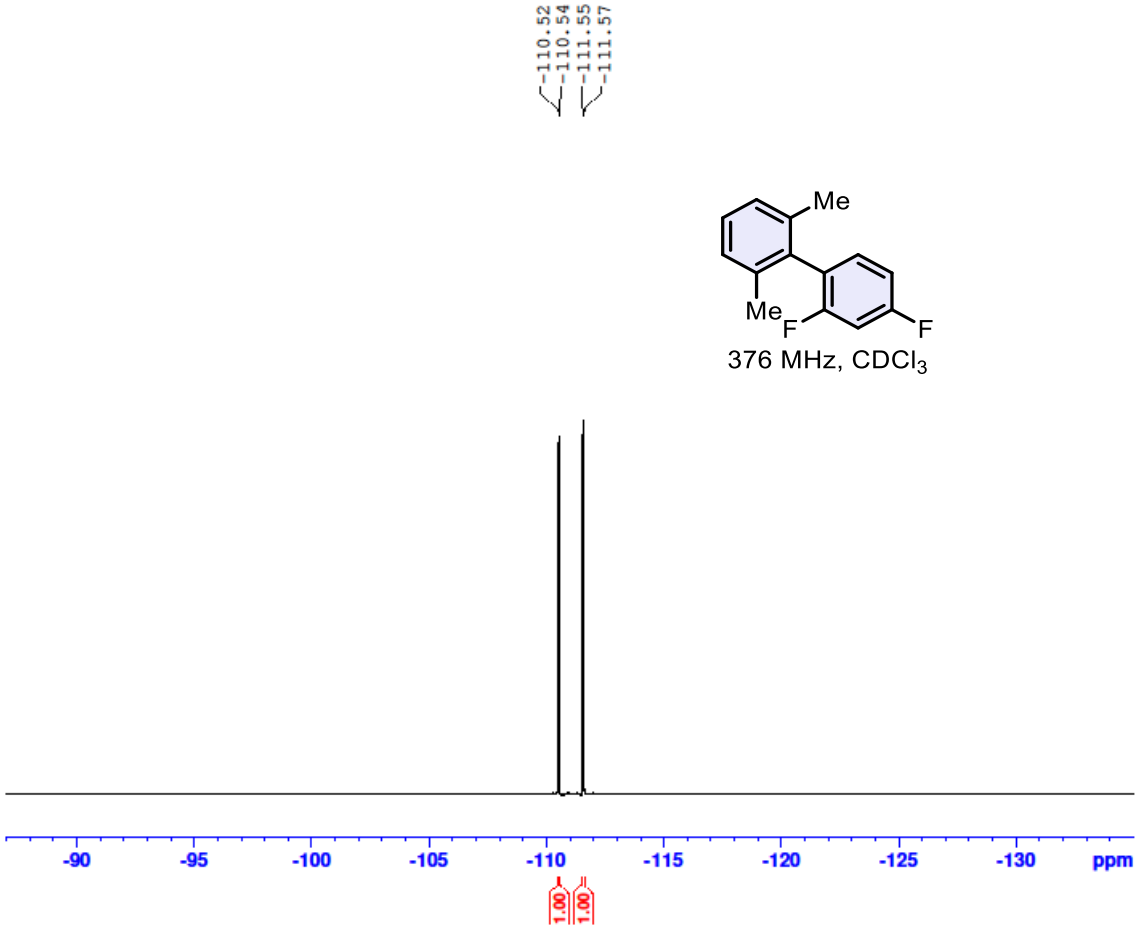

^{1}H NMR of 2'-methoxy-2,4,6-trimethyl-1,1'-biphenyl (Table 2.3, compound **3f**)

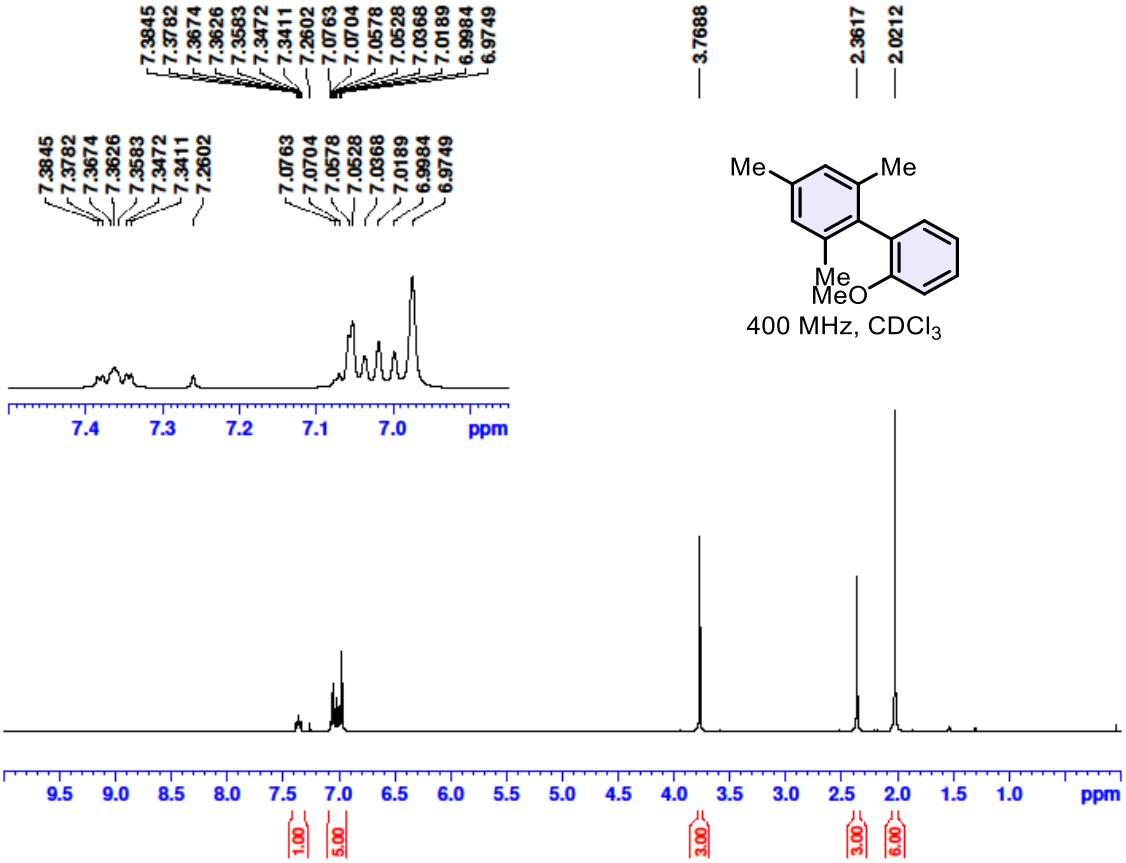

^{13}C NMR of 2'-methoxy-2,4,6-trimethyl-1,1'-biphenyl (Table 2.3, compound **3f**)

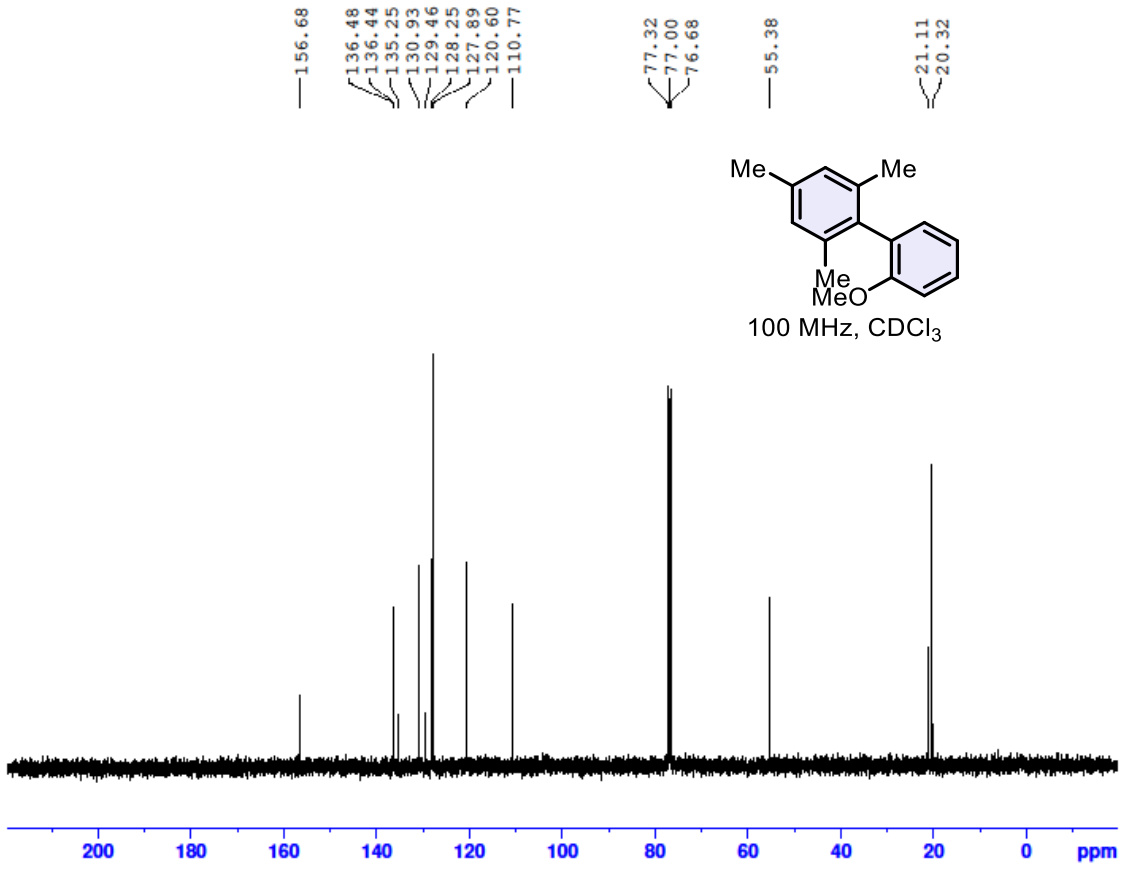

^{1}H NMR of 2',6'-dimethyl-[1,1'-biphenyl]-2-amine (Table 2.3, compound **3g**)

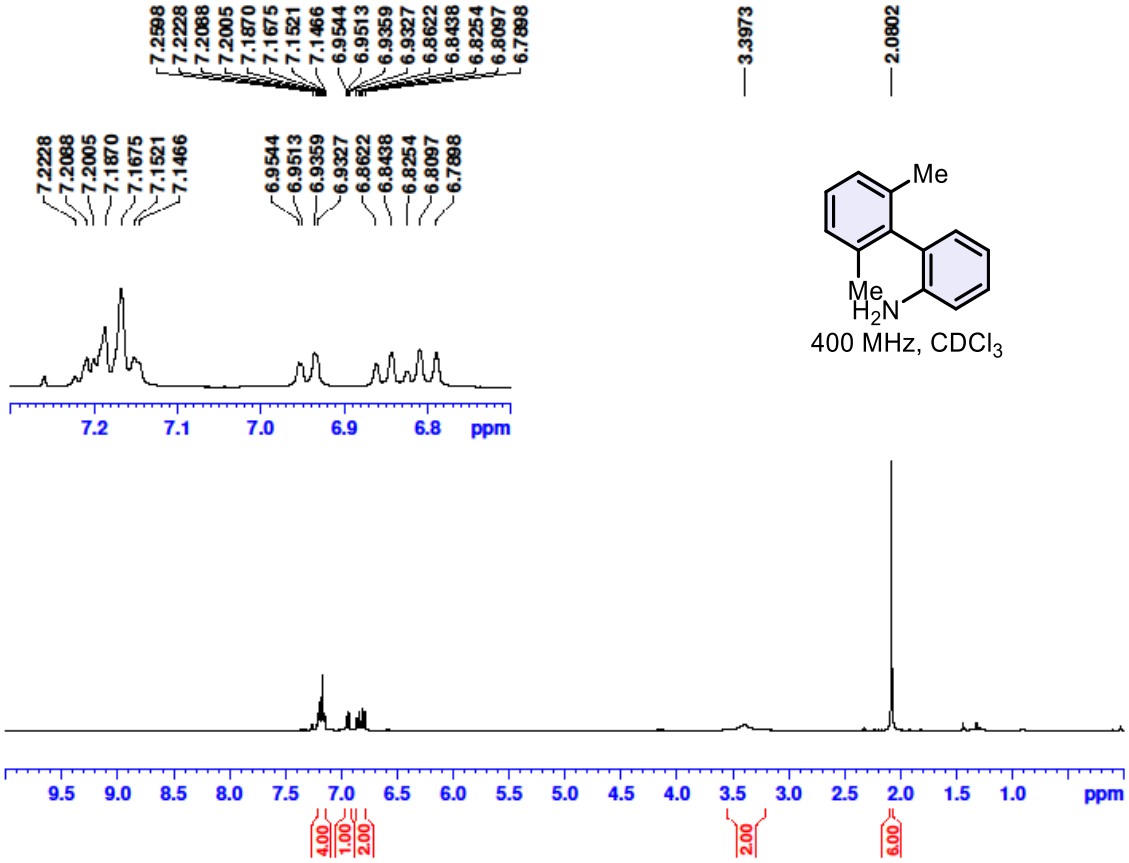

^{13}C NMR of 2',6'-dimethyl-[1,1'-biphenyl]-2-amine (Table 2.3, compound **3g**)

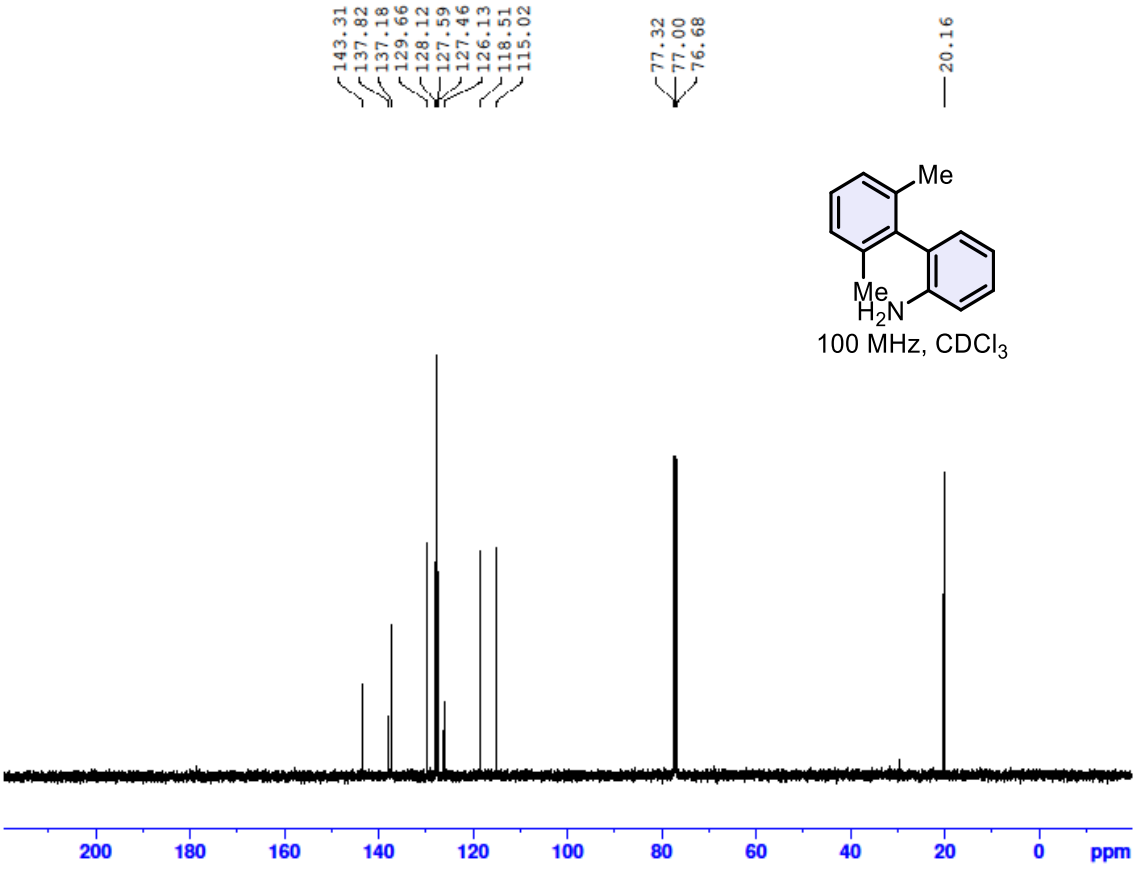

^{1}H NMR of 4-(2,6-dimethylphenyl)quinoline (Table 2.3, compound **3h**)

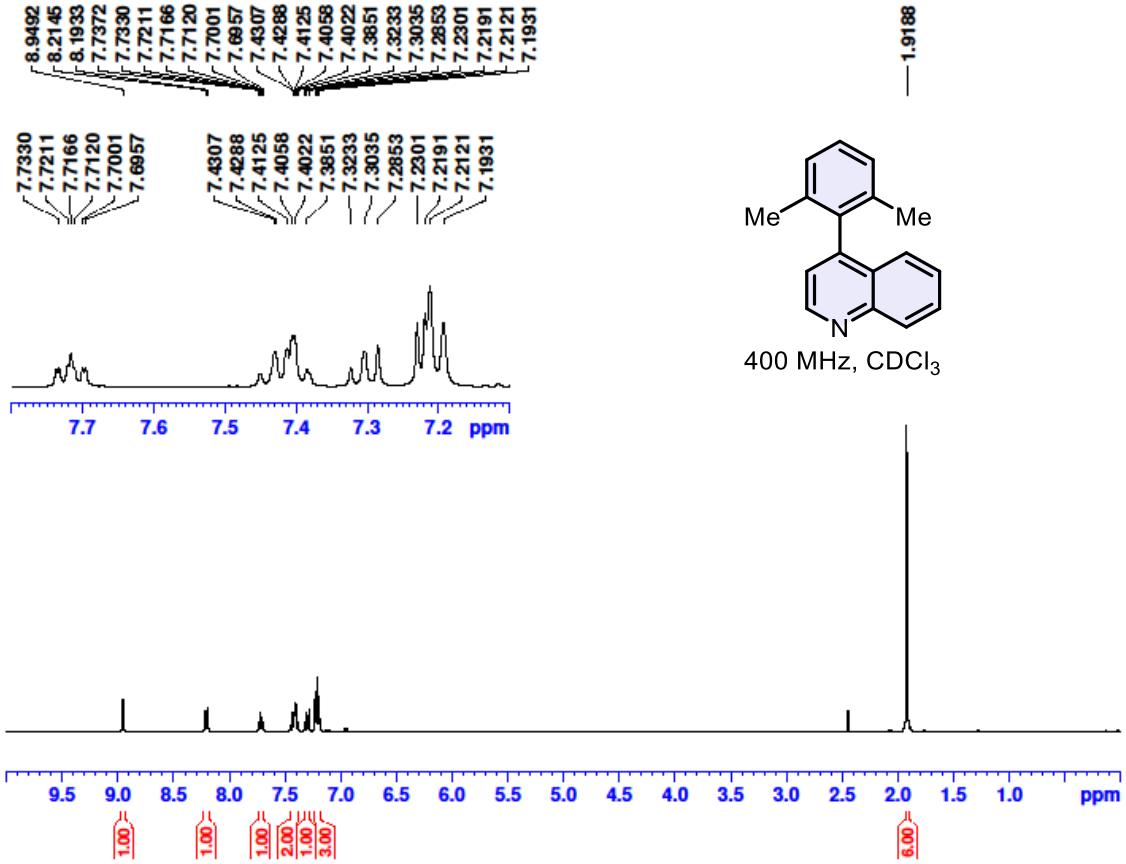

^{13}C NMR of 4-(2,6-dimethylphenyl)quinoline (Table 2.3, compound **3h**)

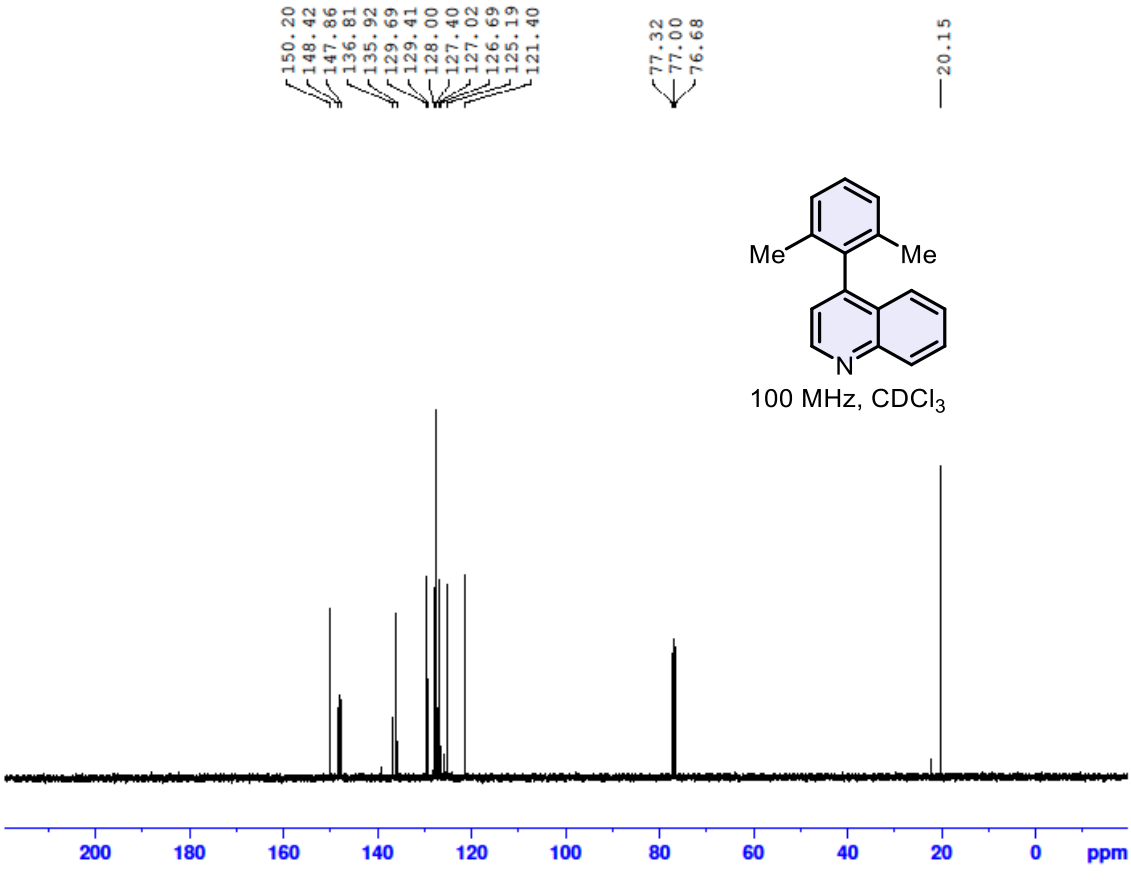

HRMS of 4-(2,6-dimethylphenyl)quinoline (Table 2.3, compound **3h**)

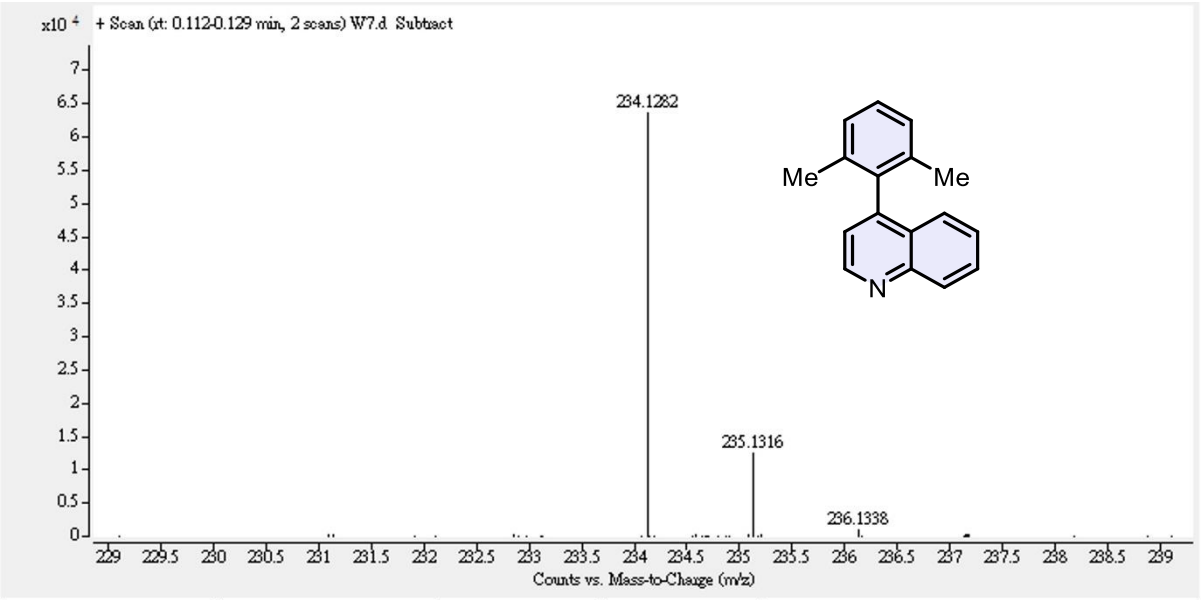

Mass	Calc. Mass	mDa	PPM	Formula
234.1282	234.1277	-0.47	-2.03	C17 H16 N

^{1}H NMR of ethyl 6-ethoxy-2',6'-dimethyl-[1,1'-biphenyl]-3-carboxylate (Table 2.3, compound **3i**)

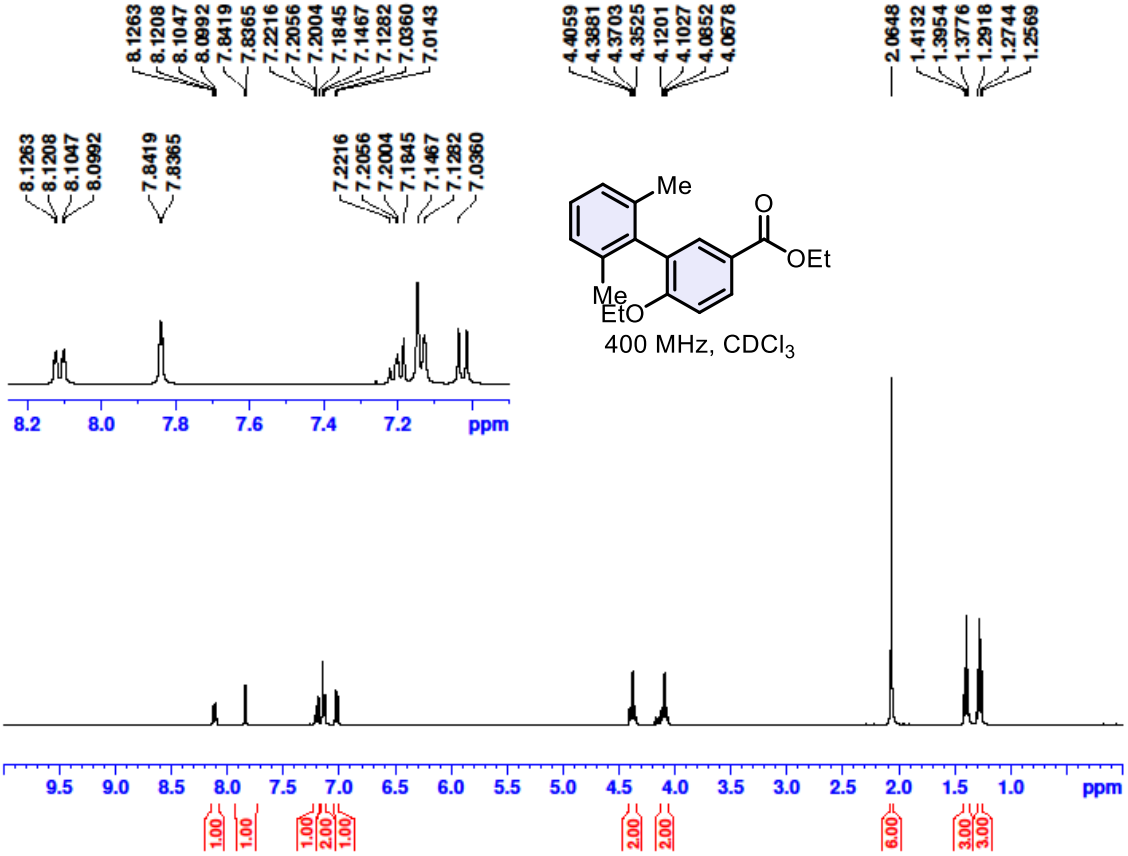

^{13}C NMR of ethyl 6-ethoxy-2',6'-dimethyl-[1,1'-biphenyl]-3-carboxylate (Table 2.3, compound **3i**)

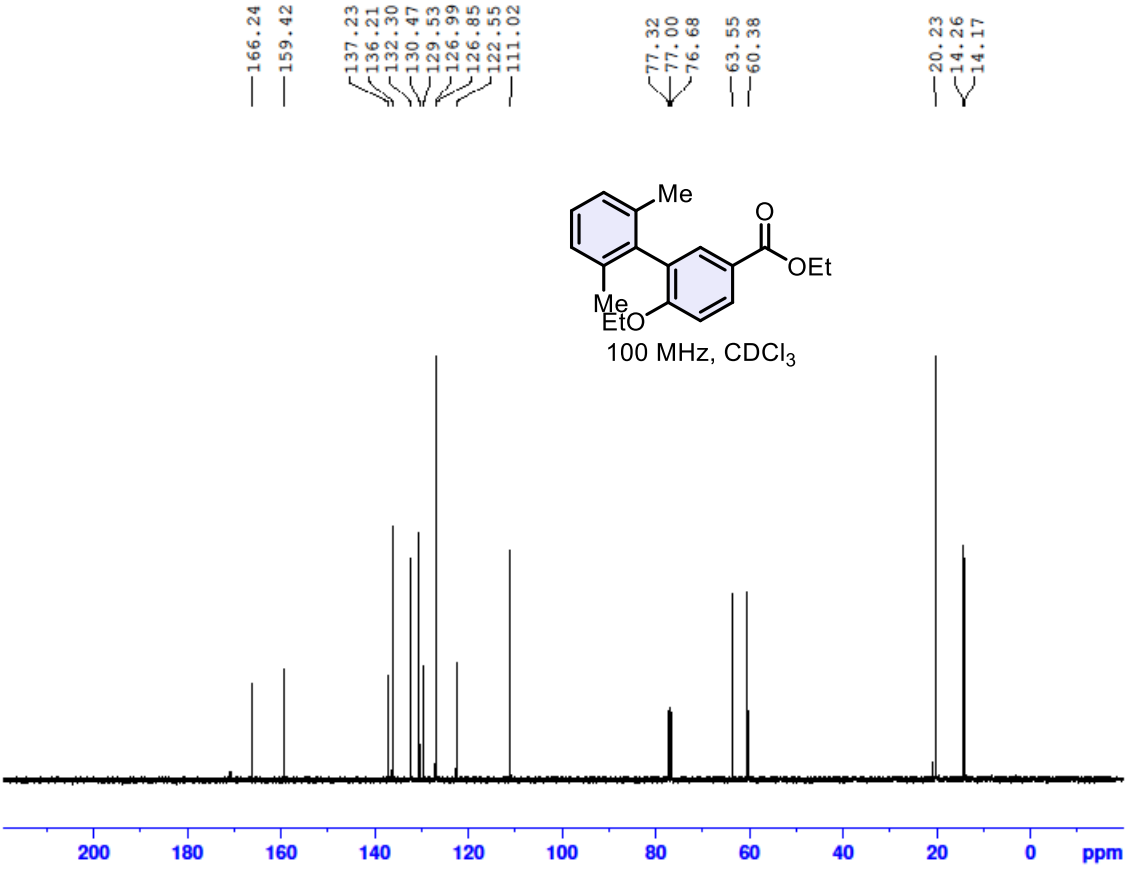

HRMS of ethyl 6-ethoxy-2’,6’-dimethyl-[1,1’-biphenyl]-3-carboxylate (Table 2.3, compound **3i**)

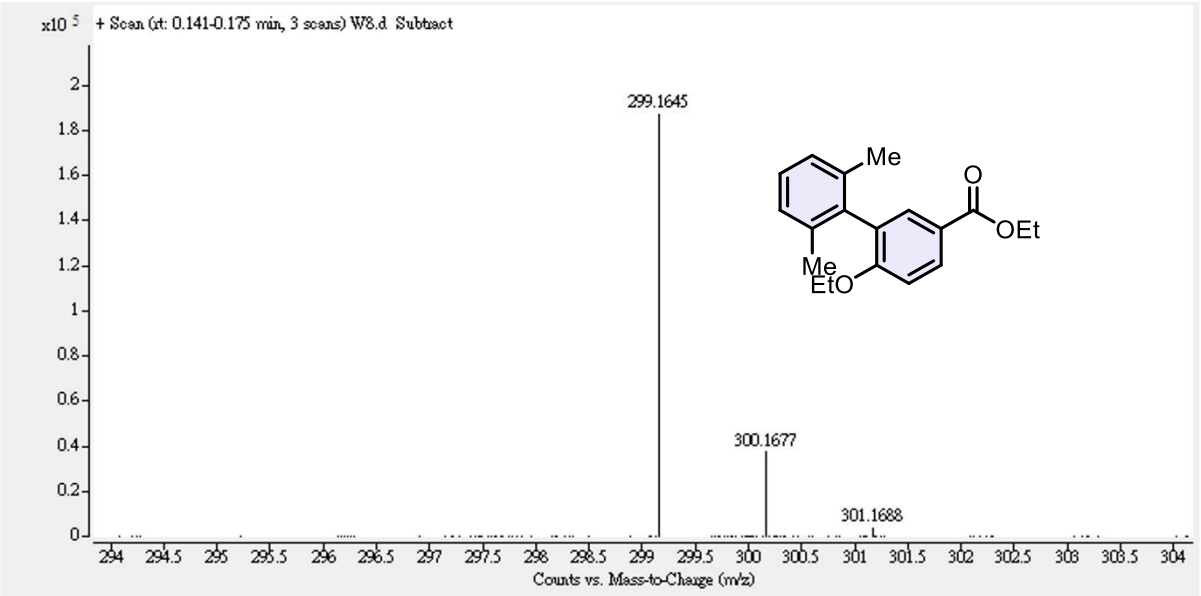

Mass	Calc. Mass	mDa	PPM	Formula
299.1645	299.1642	-0.33	-1.10	C19 H23 O3

^{1}H NMR of 5-methoxy-2,2',6'-trimethyl-1,1'-biphenyl (Table 2.3, compound **3j**)

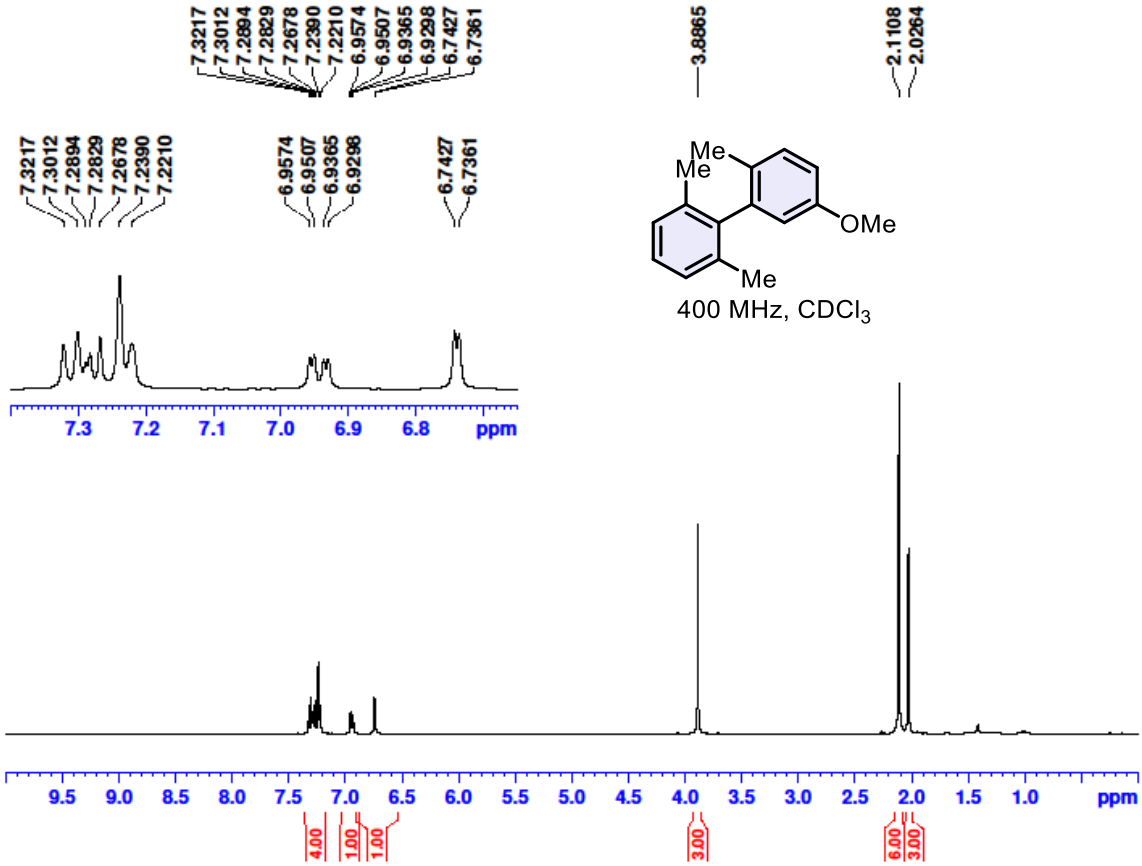

^{13}C NMR of 5-methoxy-2,2',6'-trimethyl-1,1'-biphenyl (Table 2.3, compound **3j**)

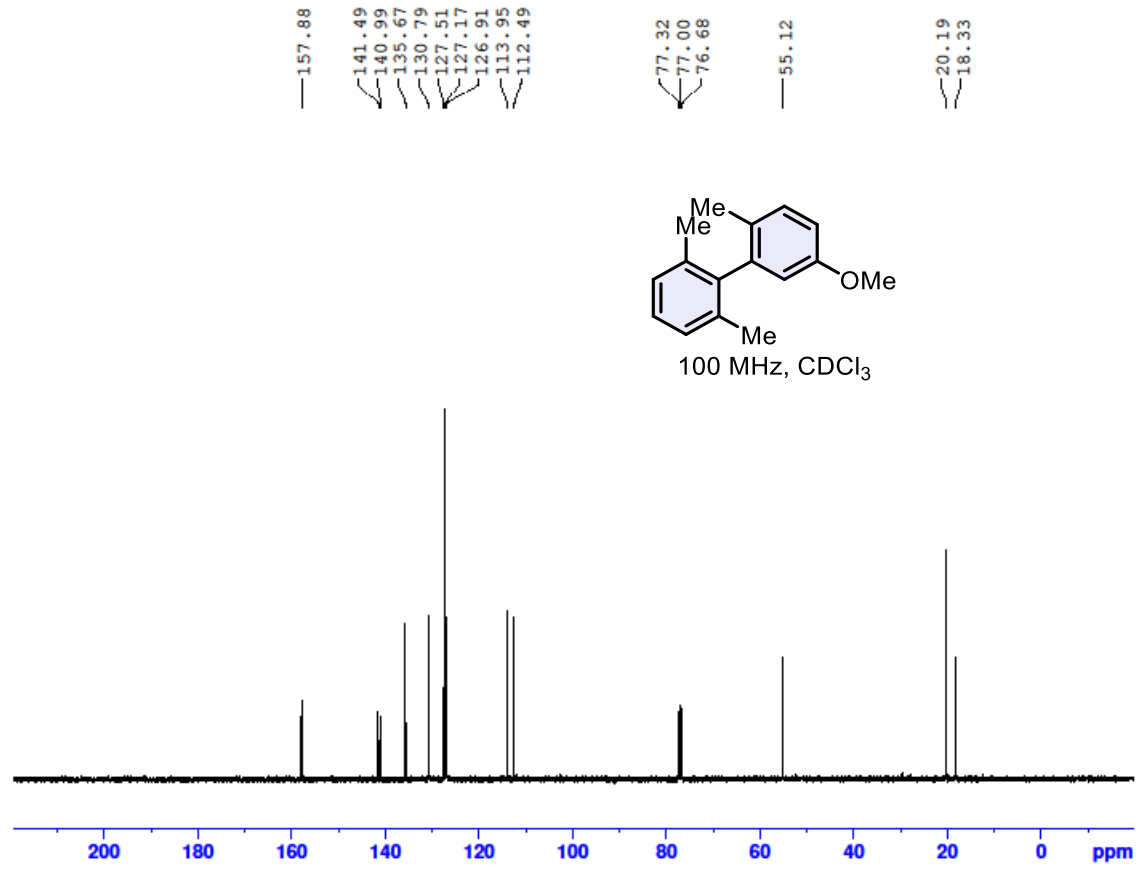

HRMS of 5-Methoxy-2,2',6'-trimethyl-1,1'-biphenyl (Table 2.3, compound **3j**)

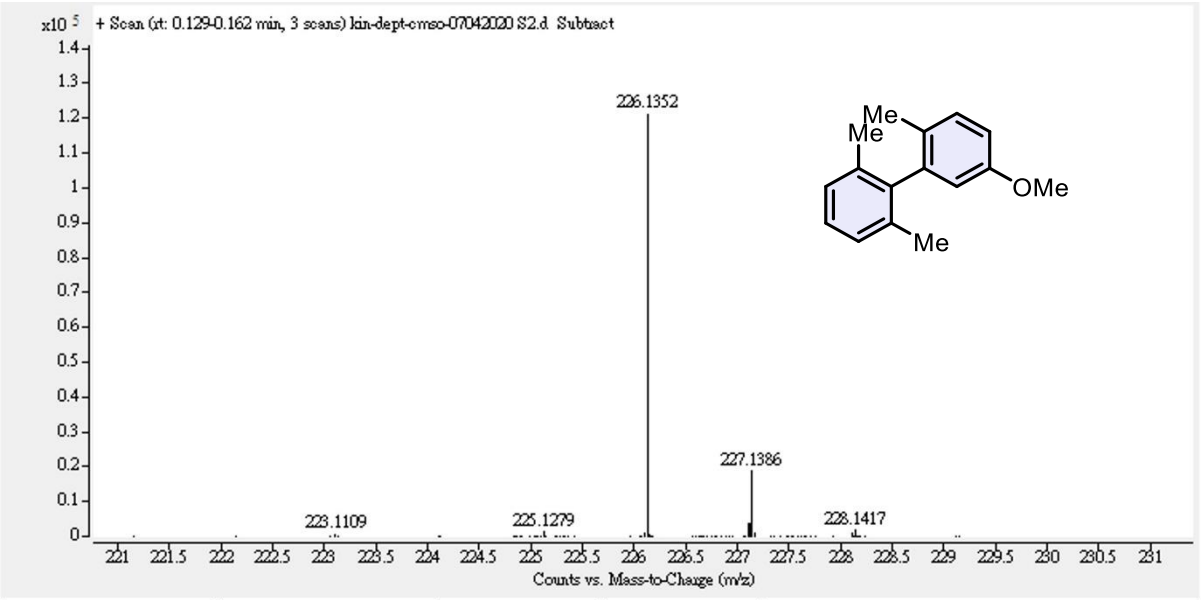

Mass	Calc. Mass	mDa	PPM	Formula
226.1352	226.1352	0.02	0.07	C16 H18 O

^{1}H NMR of 2-methoxy-2',6'-dimethyl-[1,1'-biphenyl]-4-carbaldehyde (Table 2.3, compound **3k**)

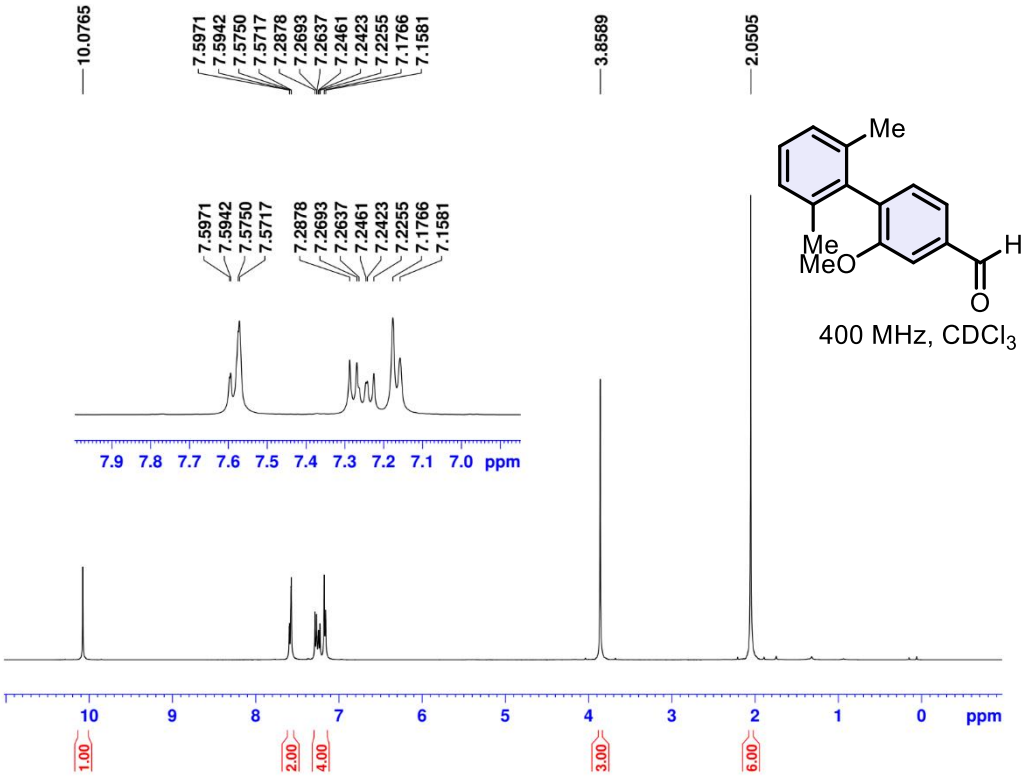

^{13}C NMR of 2-methoxy-2',6'-dimethyl-[1,1'-biphenyl]-4-carbaldehyde (Table 2.3, compound **3k**)

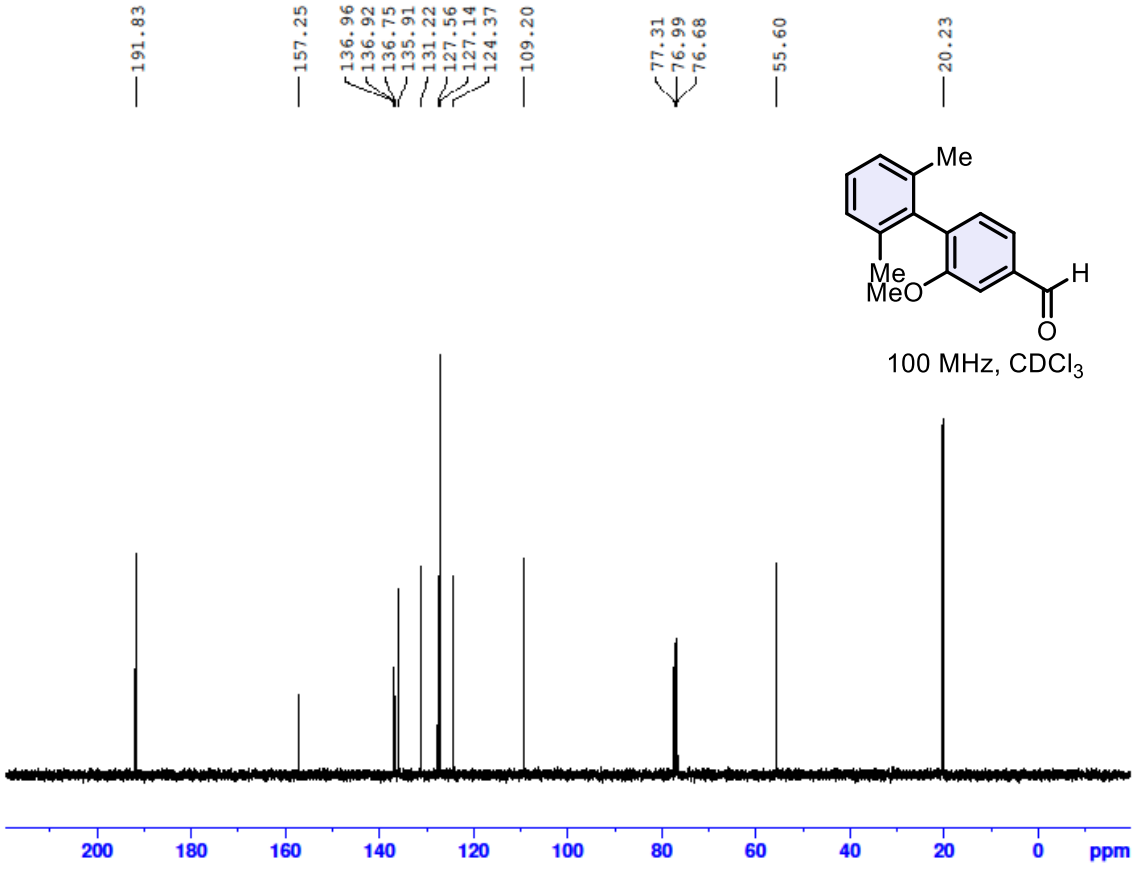

HRMS of 2-methoxy-2’,6’-dimethyl-[1,1’-biphenyl]-4-carbaldehyde (Table 2.3, compound **3k**)

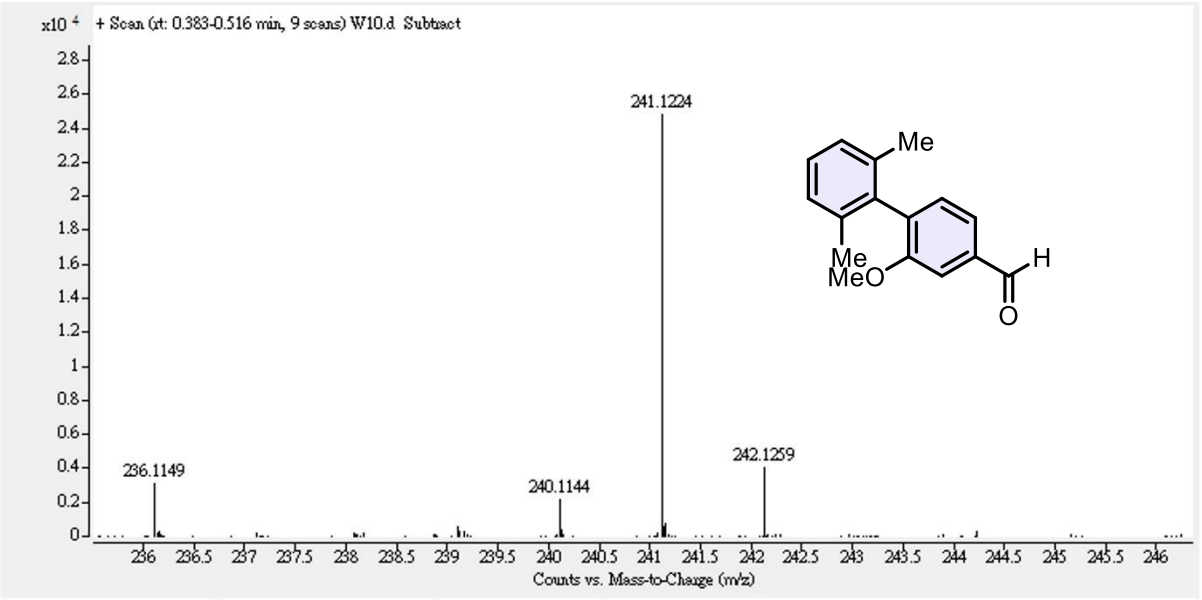

Mass	Calc. Mass	mDa	PPM	Formula
241.1224	241.1223	-0.09	-0.39	C16 H17 O2

^{1}H NMR of 4-methoxy-2,2',6-trimethyl-1,1'-biphenyl (Table 2.3, compound **3l**)

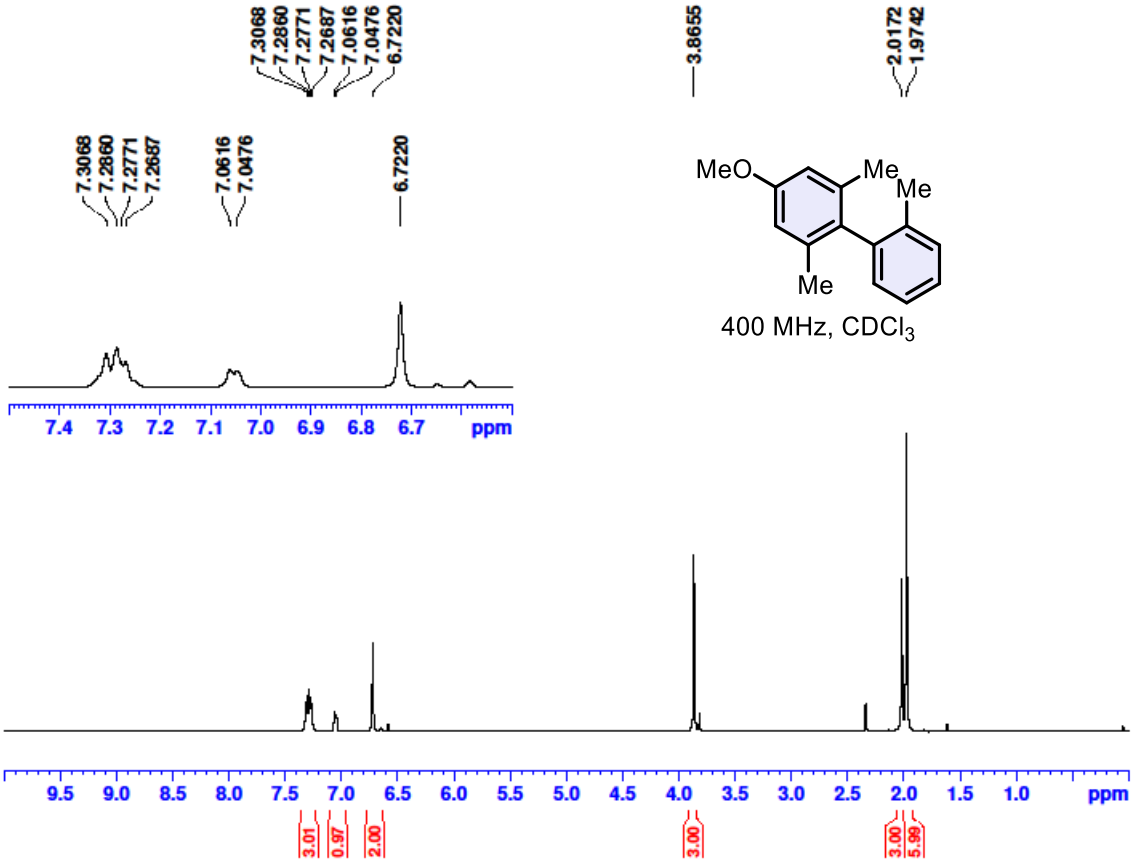

^{13}C NMR of 4-methoxy-2,2',6-trimethyl-1,1'-biphenyl (Table 2.3, compound **3l**)

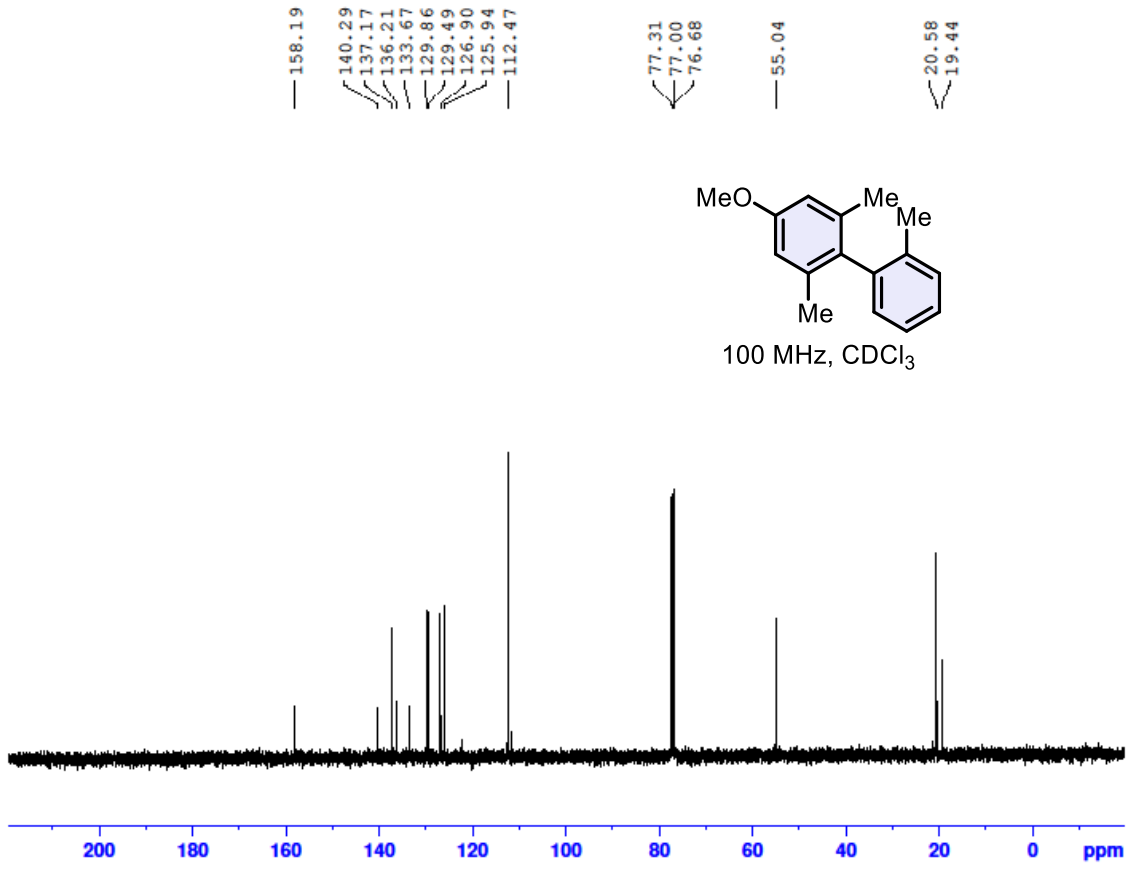

^{1}H NMR of 2-fluoro-2',6'-dimethyl-4-(trifluoromethyl)-1,1'-biphenyl (Table 2.4, compound **3m**)

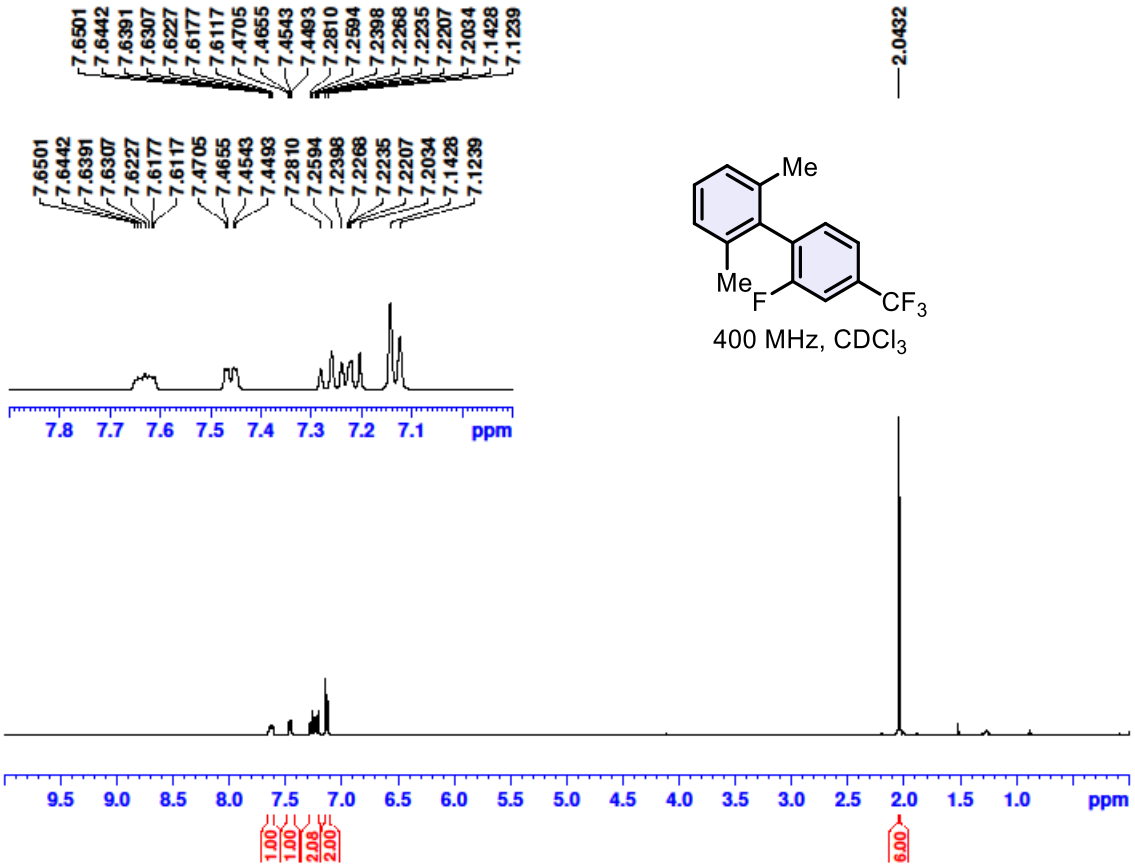

^{13}C NMR of 2-fluoro-2',6'-dimethyl-4-(trifluoromethyl)-1,1'-biphenyl (Table 2.4, compound **3m**)

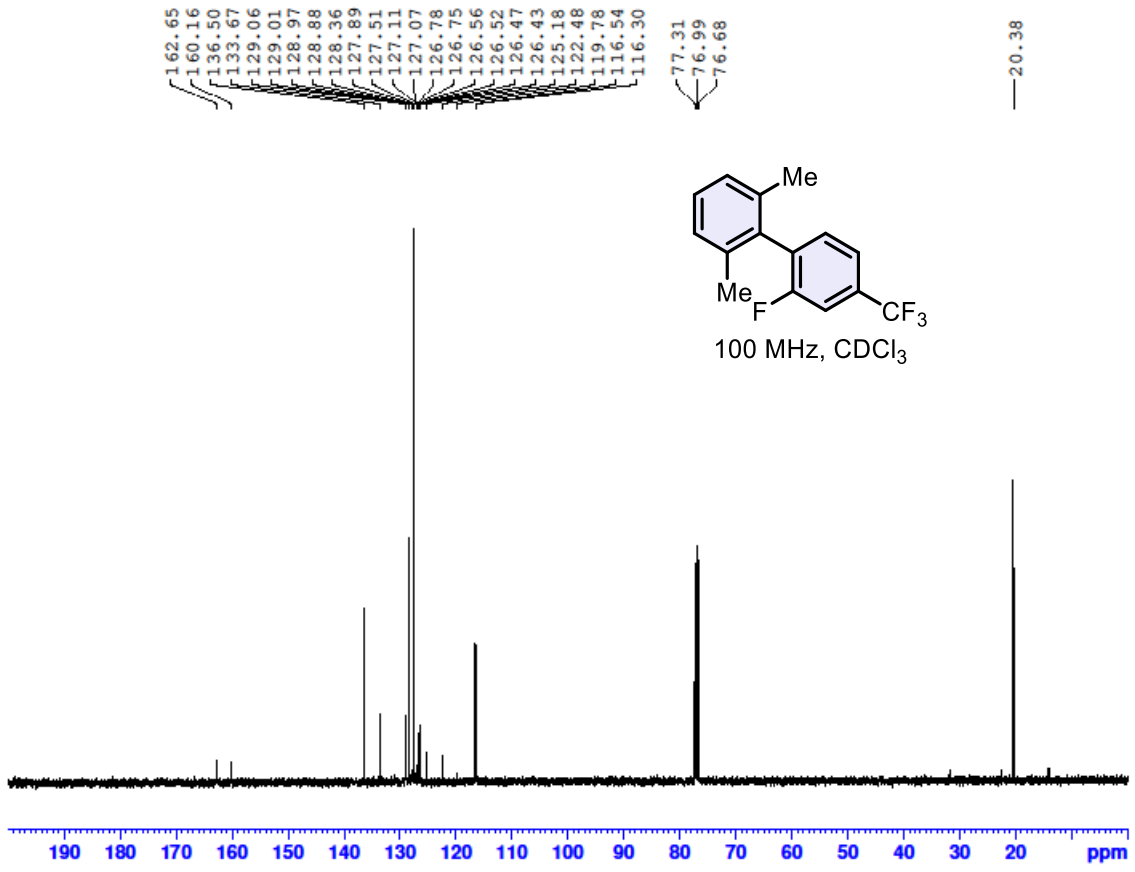

^{19}F NMR of 2-fluoro-2',6'-dimethyl-4-(trifluoromethyl)-1,1'-biphenyl (Table 2.4, compound **3m**)

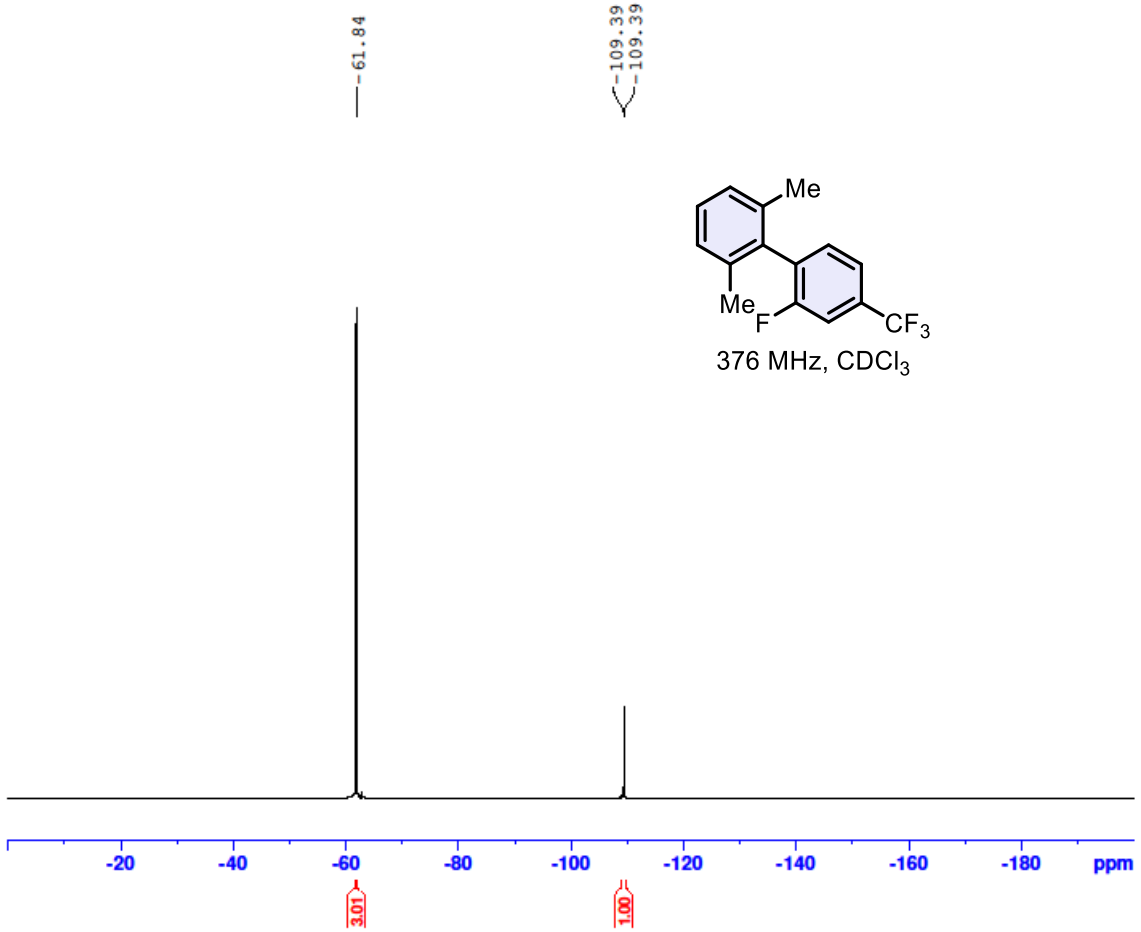

HRMS of 2-fluoro-2',6'-dimethyl-4-(trifluoromethyl)-1,1'-biphenyl (Table 2.4, compound **3m**)

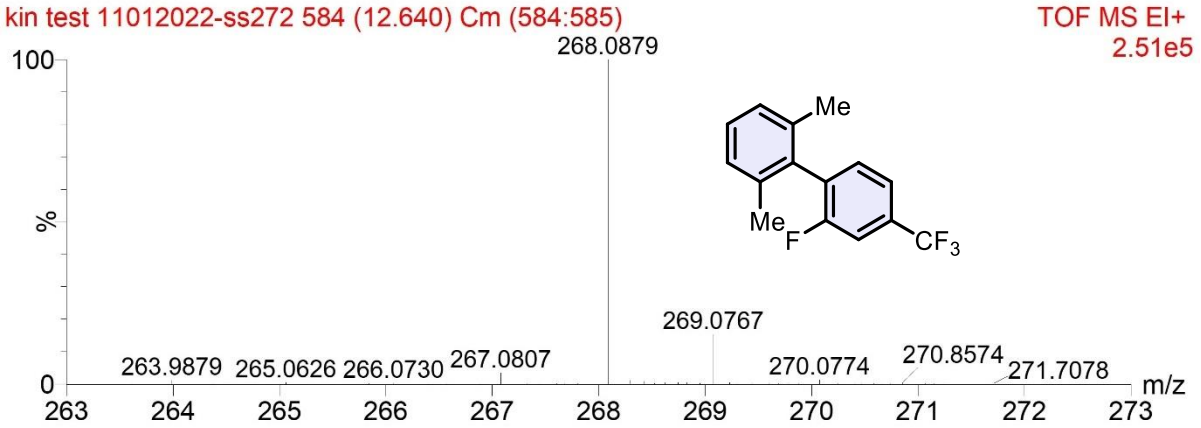

Mass	Calc. Mass	mDa	PPM	Formula
268.0879	268.0870	-0.94	-3.49	C15 H12 F4

^{1}H NMR of 2,2',5,6'-tetramethyl-1,1'-biphenyl (Table 2.4, compound **3n**)

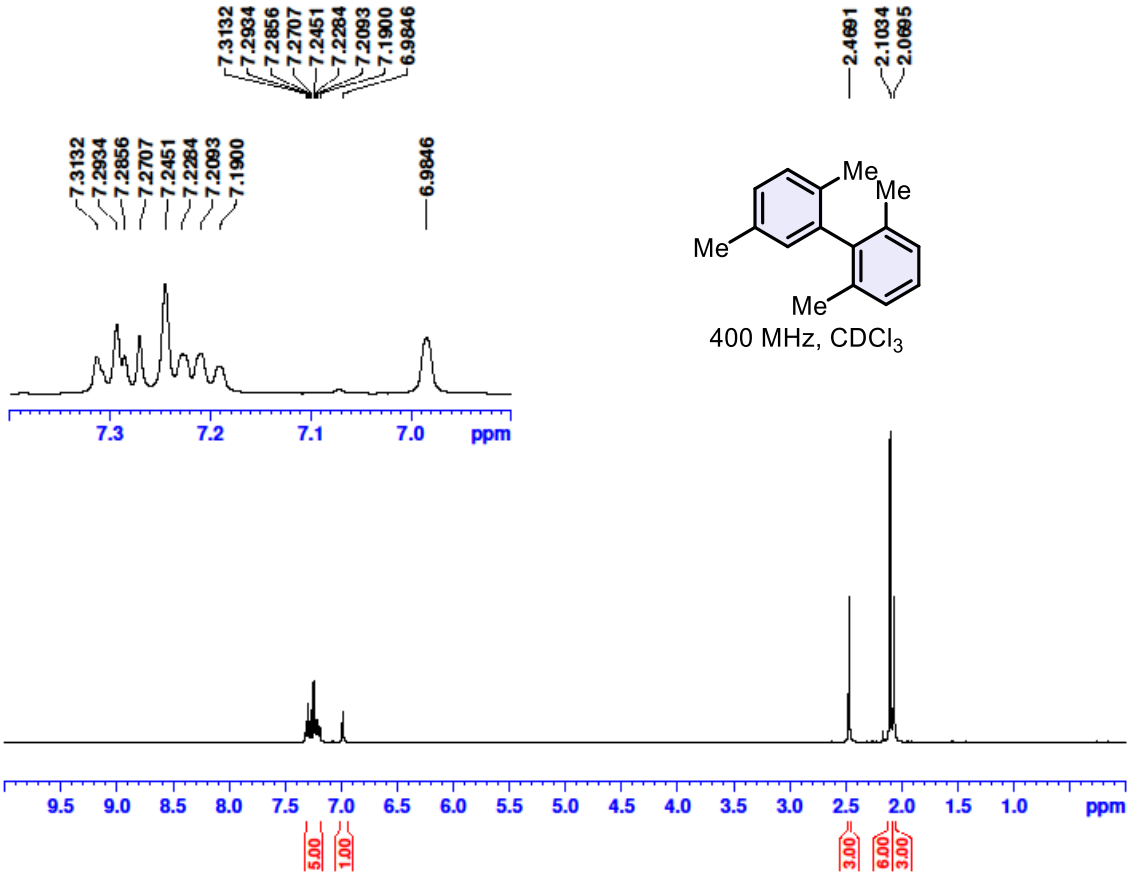

^{13}C NMR of 2,2',5,6'-tetramethyl-1,1'-biphenyl (Table 2.4, compound **3n**)

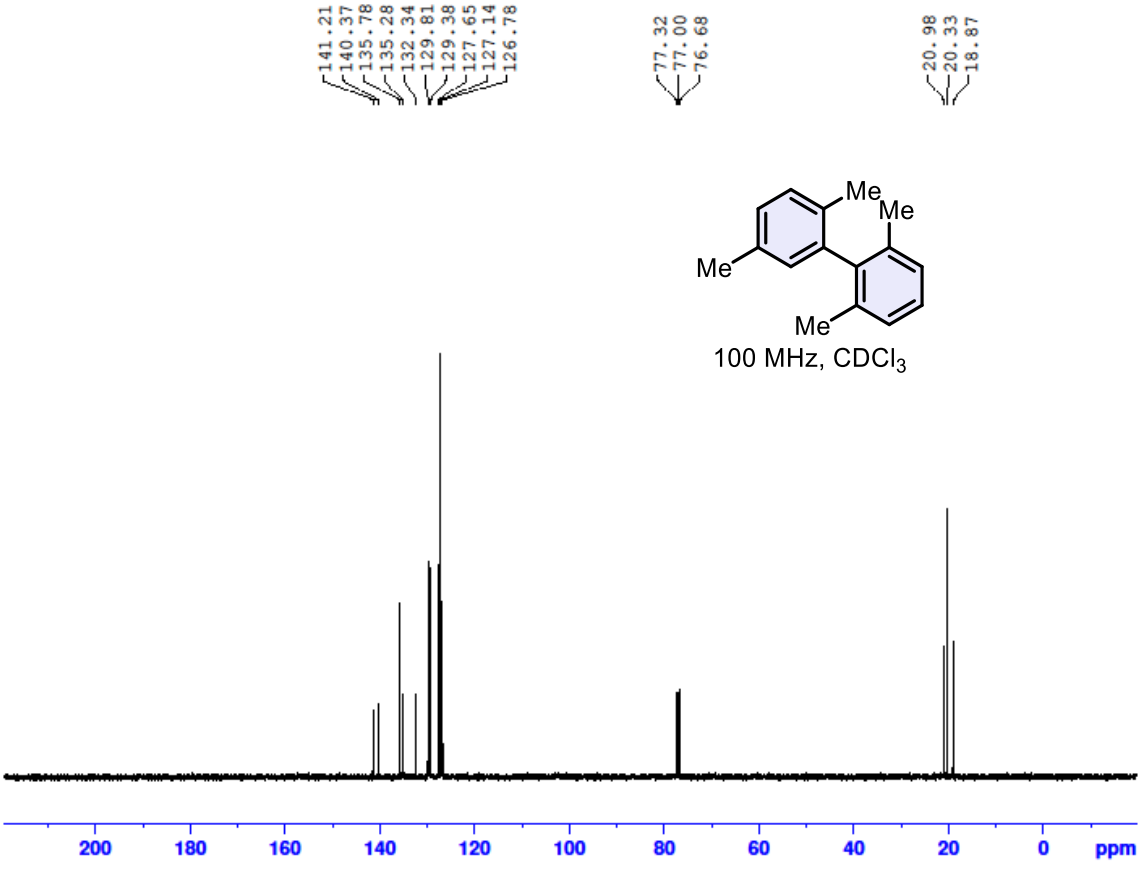

^{1}H NMR of 2,6-dimethyl-1,1':2',1''-terphenyl (Table 2.4, compound **3o**)

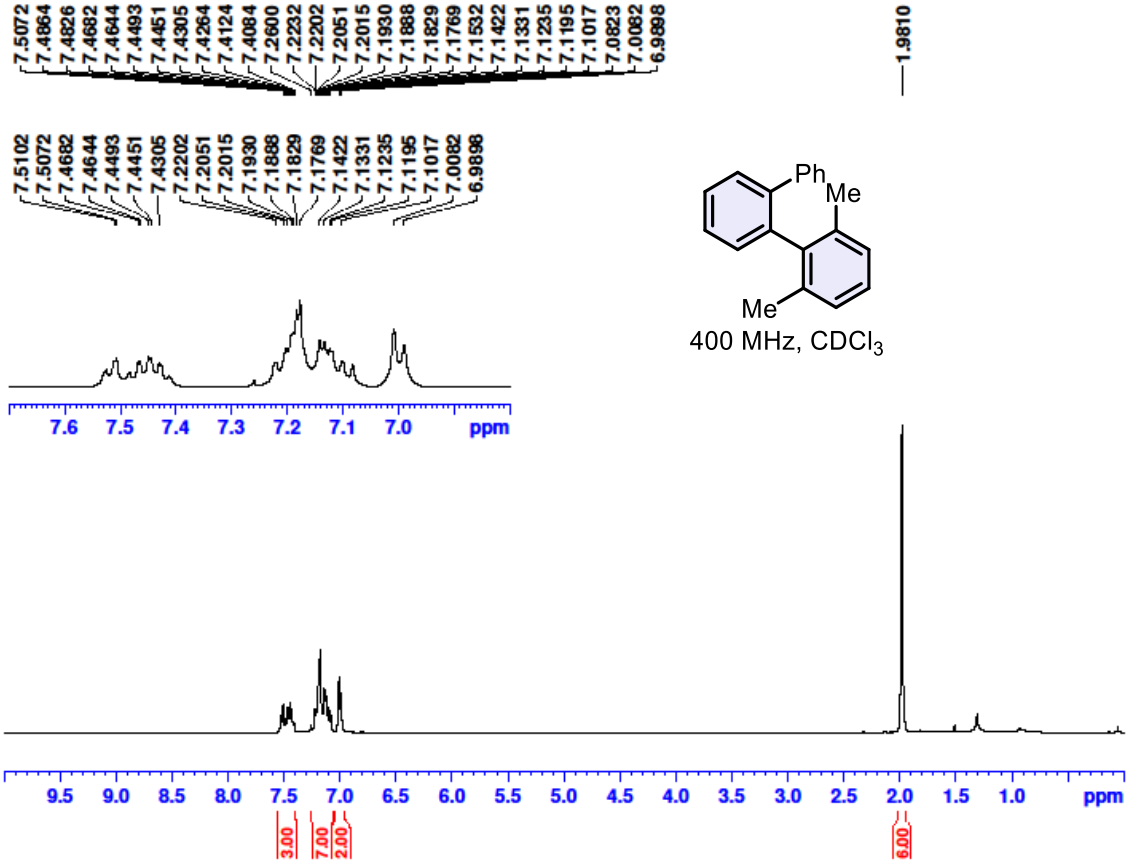

^{13}C NMR of 2,6-dimethyl-1,1':2',1''-terphenyl (Table 2.4, compound **3o**)

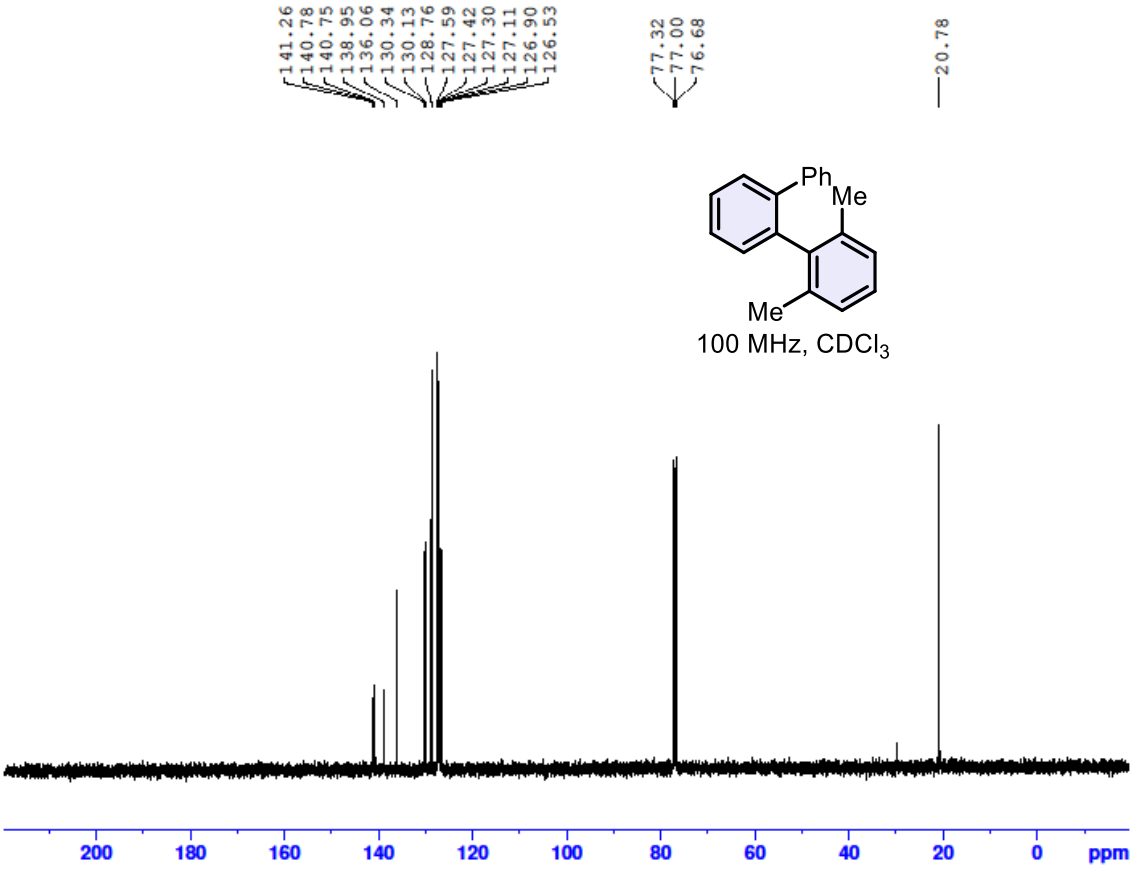

^{1}H NMR of 2,6-difluoro-2'-methyl-1,1'-biphenyl (Table 2.4 and 2.5, compound **3p**)

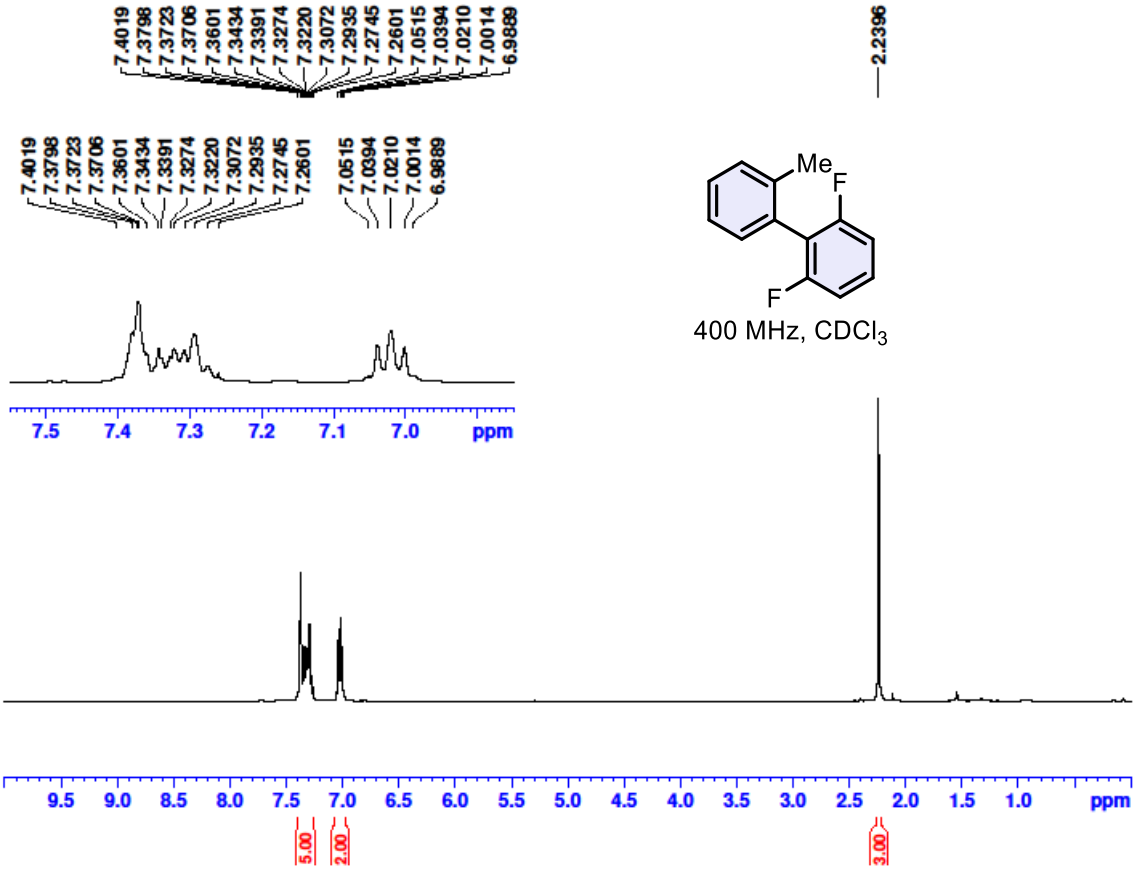

^{13}C NMR of 2,6-difluoro-2'-methyl-1,1'-biphenyl (Table 2.4 and 2.5, compound **3p**)

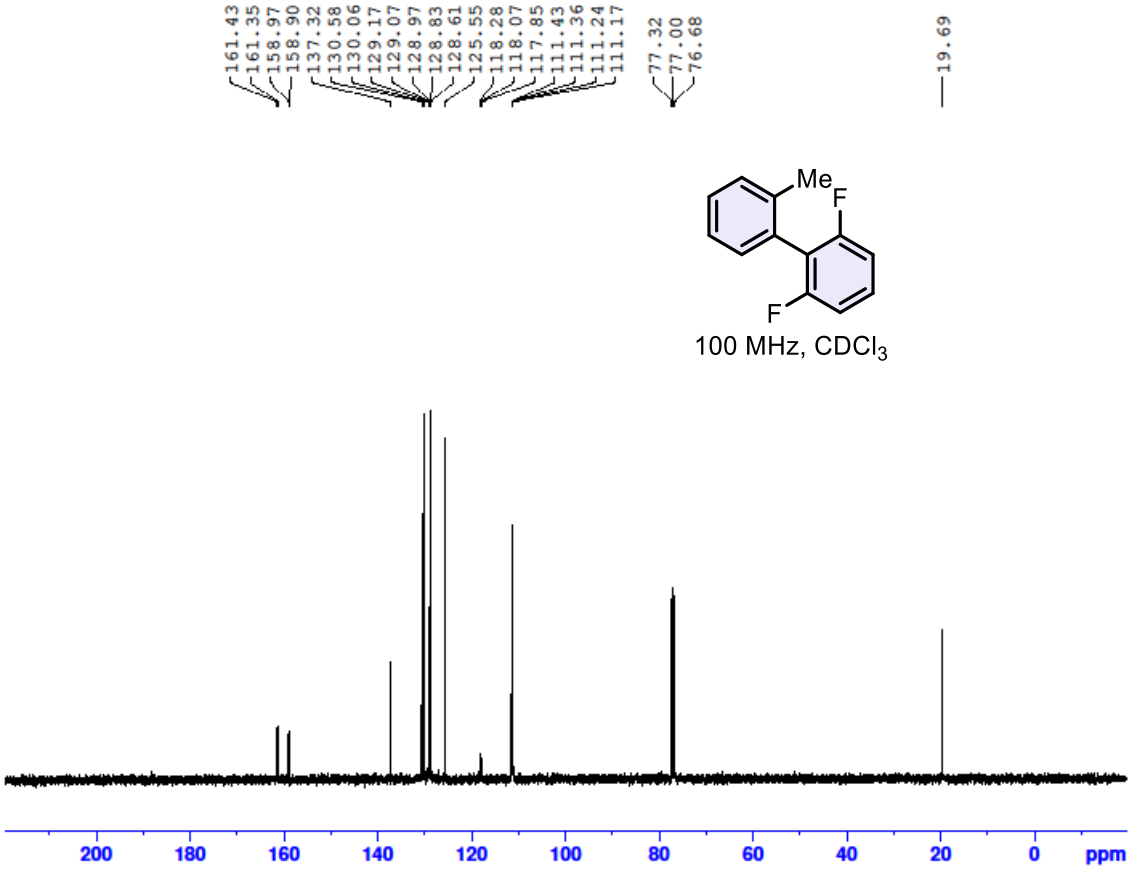

^{19}F NMR of 2,6-difluoro-2'-methyl-1,1'-biphenyl (Table 2.4 and 2.5, compound **3p**)

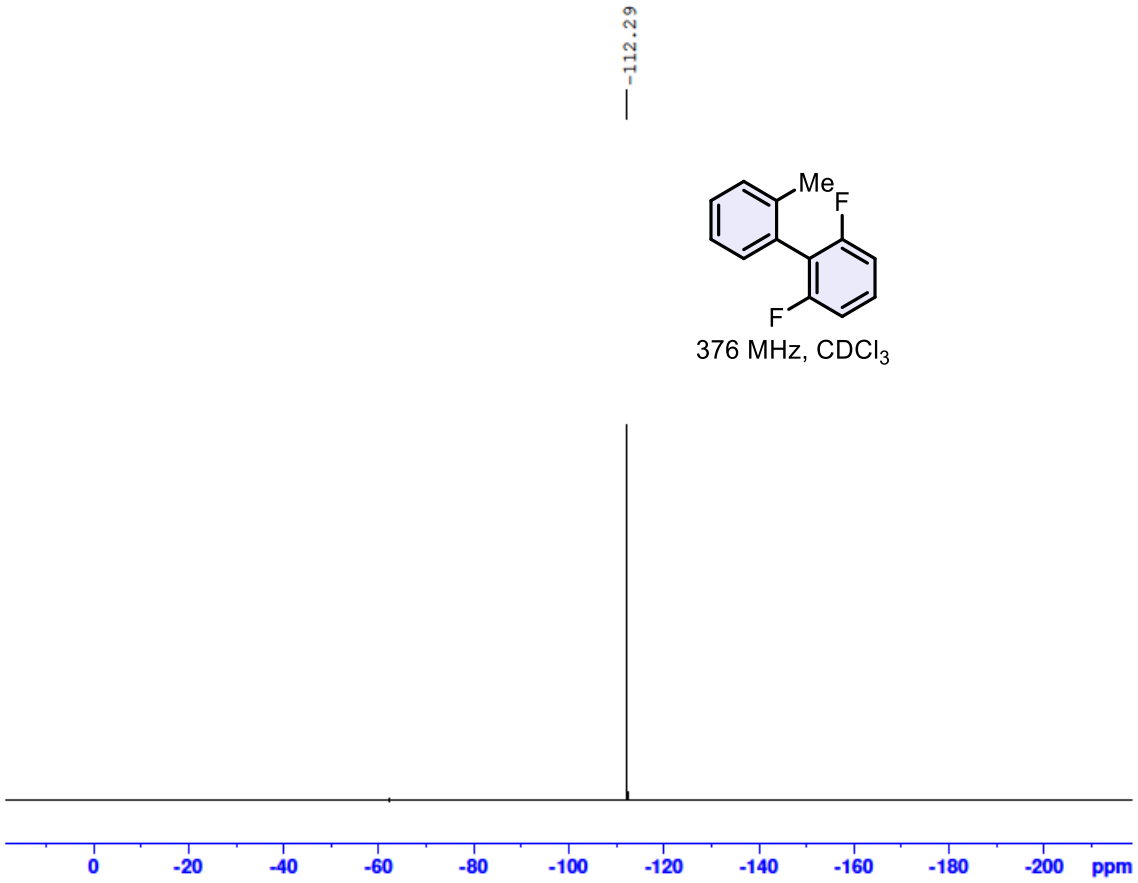

^{1}H NMR of 1-(2,6-dimethylphenyl)naphthalene (Table 2.4, compound **3q**)

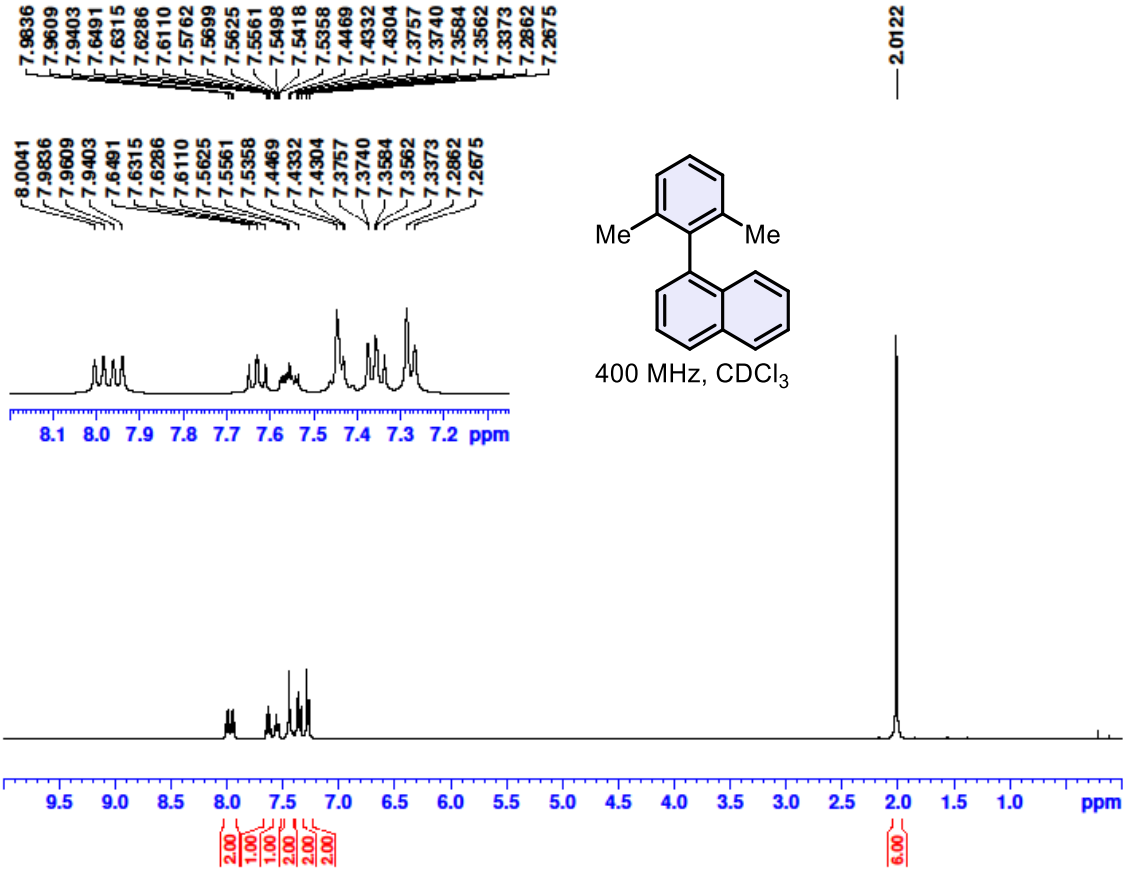

^{13}C NMR of 1-(2,6-dimethylphenyl)naphthalene (Table 2.4, compound **3q**)

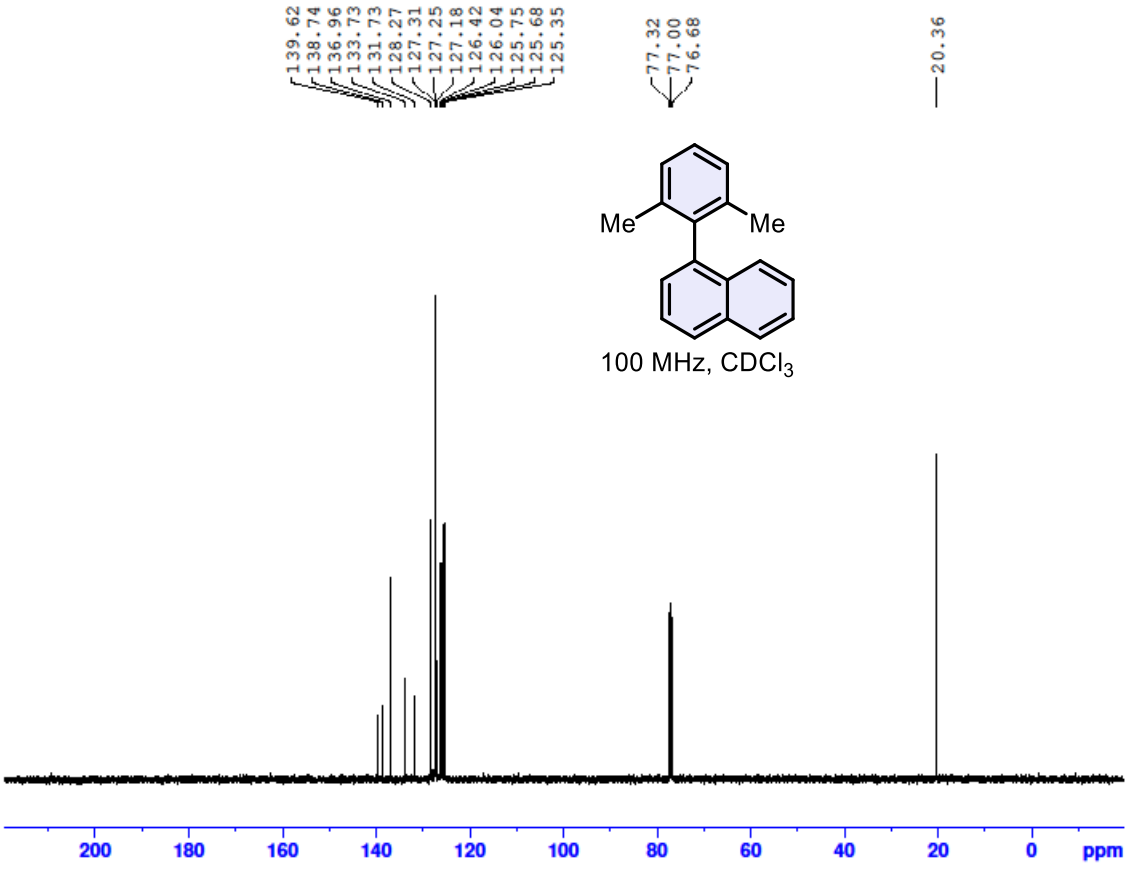

^{1}H NMR of 3-methyl-4-(*o*-tolyl)quinoline (Table 2.4, compound **3r**)

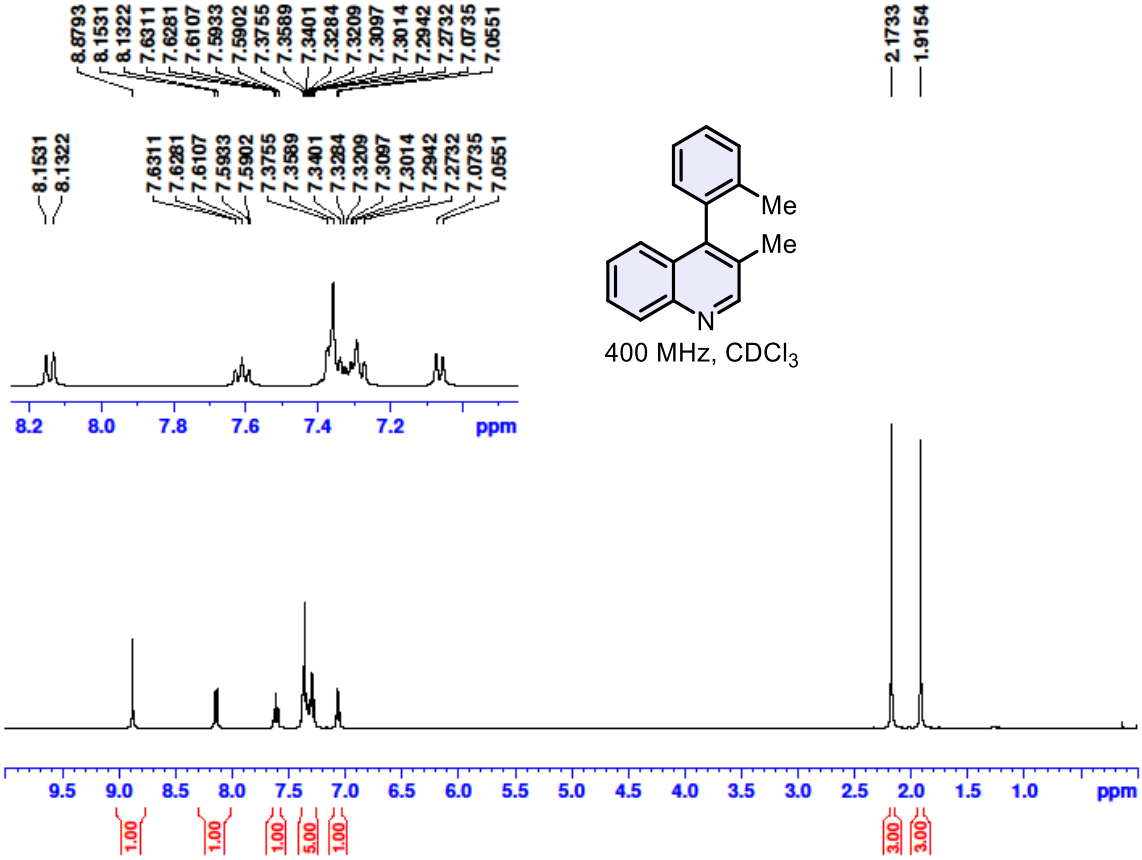

^{13}C NMR of 3-methyl-4-(*o*-tolyl)quinoline (Table 2.4, compound **3r**)

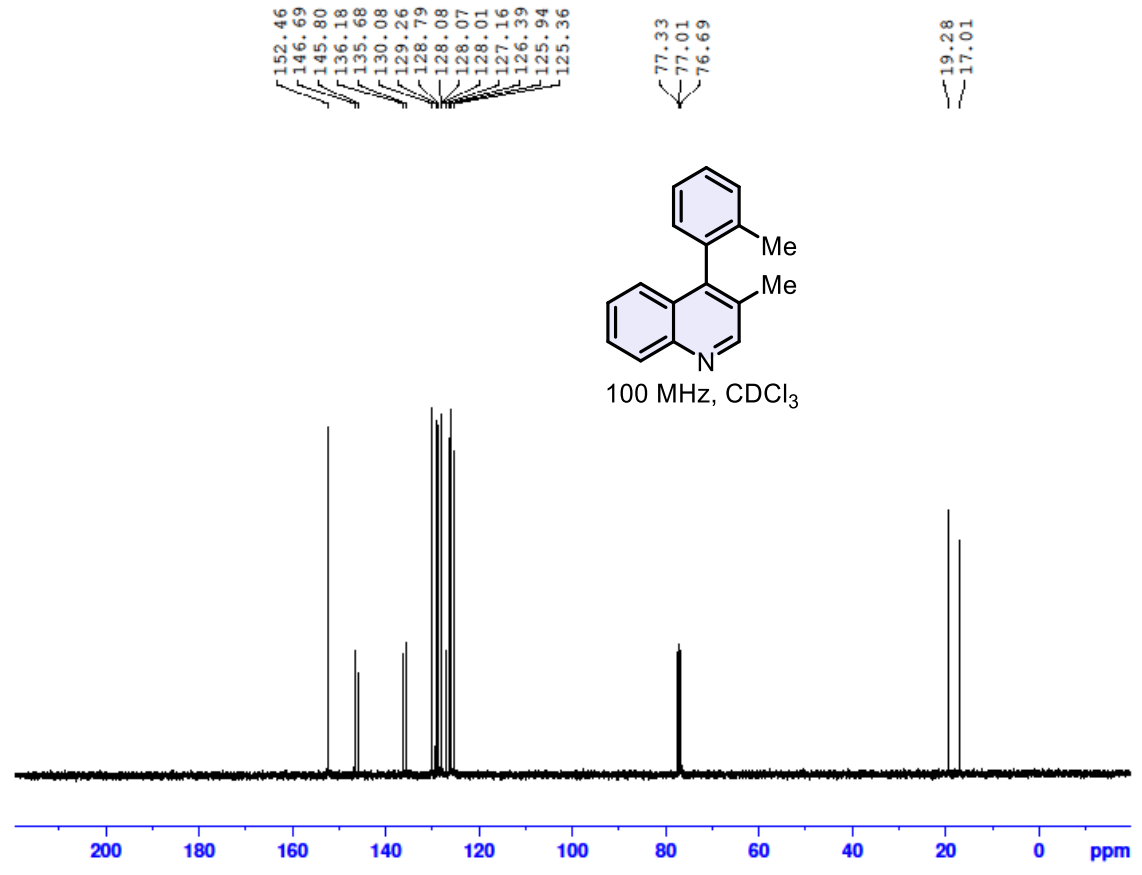

^{1}H NMR of 6-methoxy-2'-methyl-[1,1'-biphenyl]-2-carbonitrile (Table 2.4, compound **3s**)

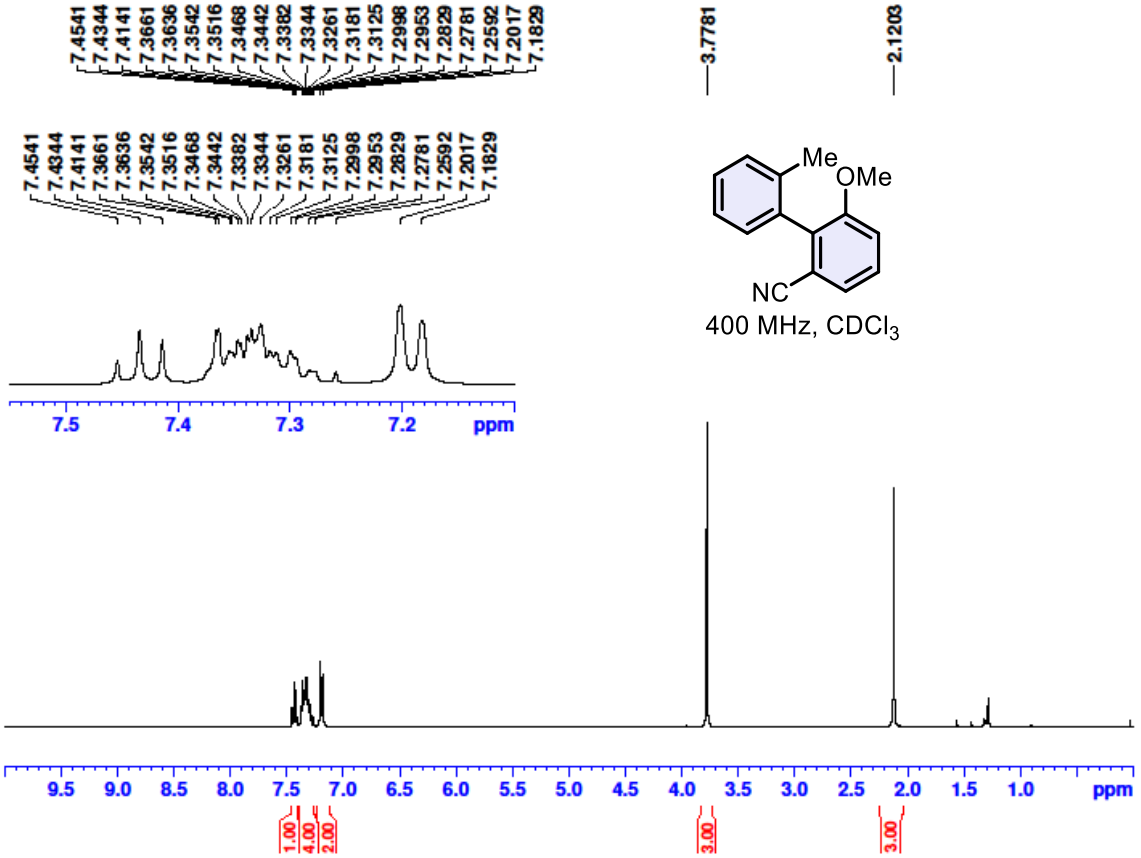

^{13}C NMR of 6-methoxy-2'-methyl-[1,1'-biphenyl]-2-carbonitrile (Table 2.4, compound **3s**)

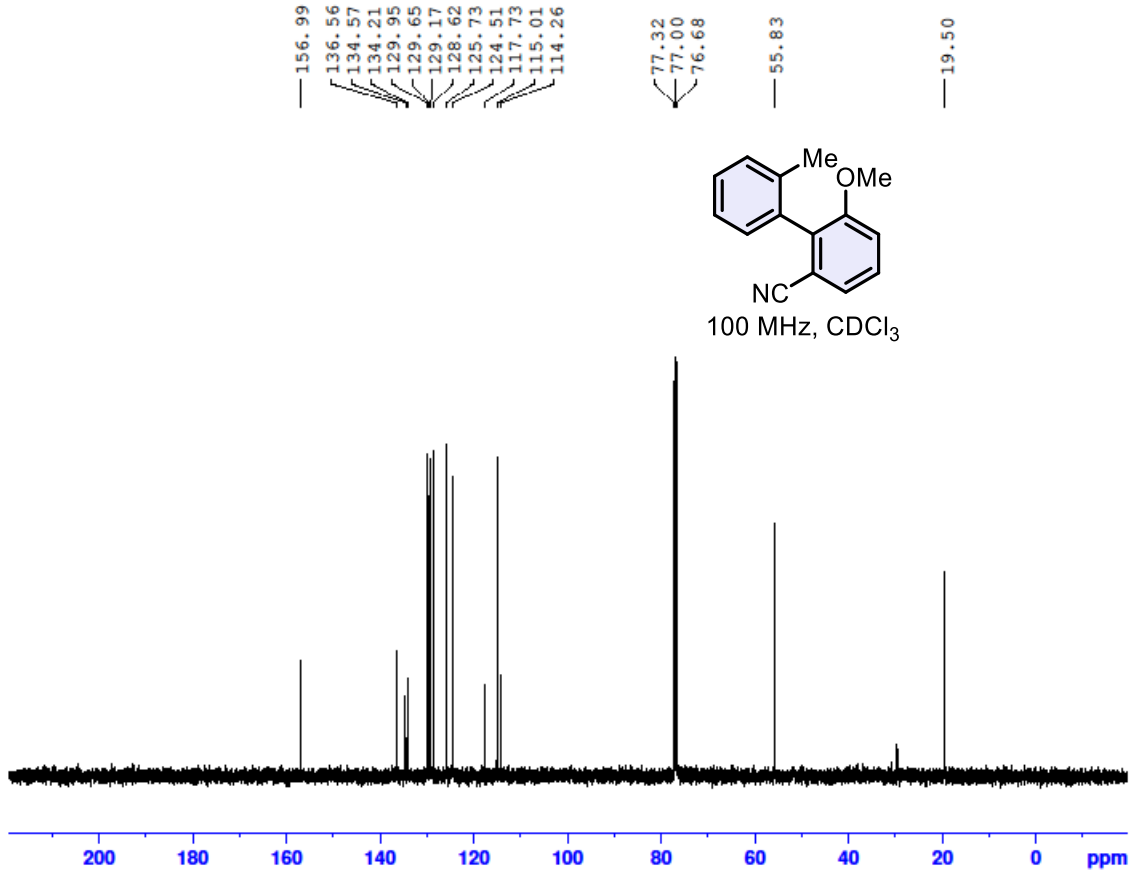

^{1}H NMR of 2,4,6-triethyl-2'-methyl-1,1'-biphenyl (Table 2.4, compound **3t**)

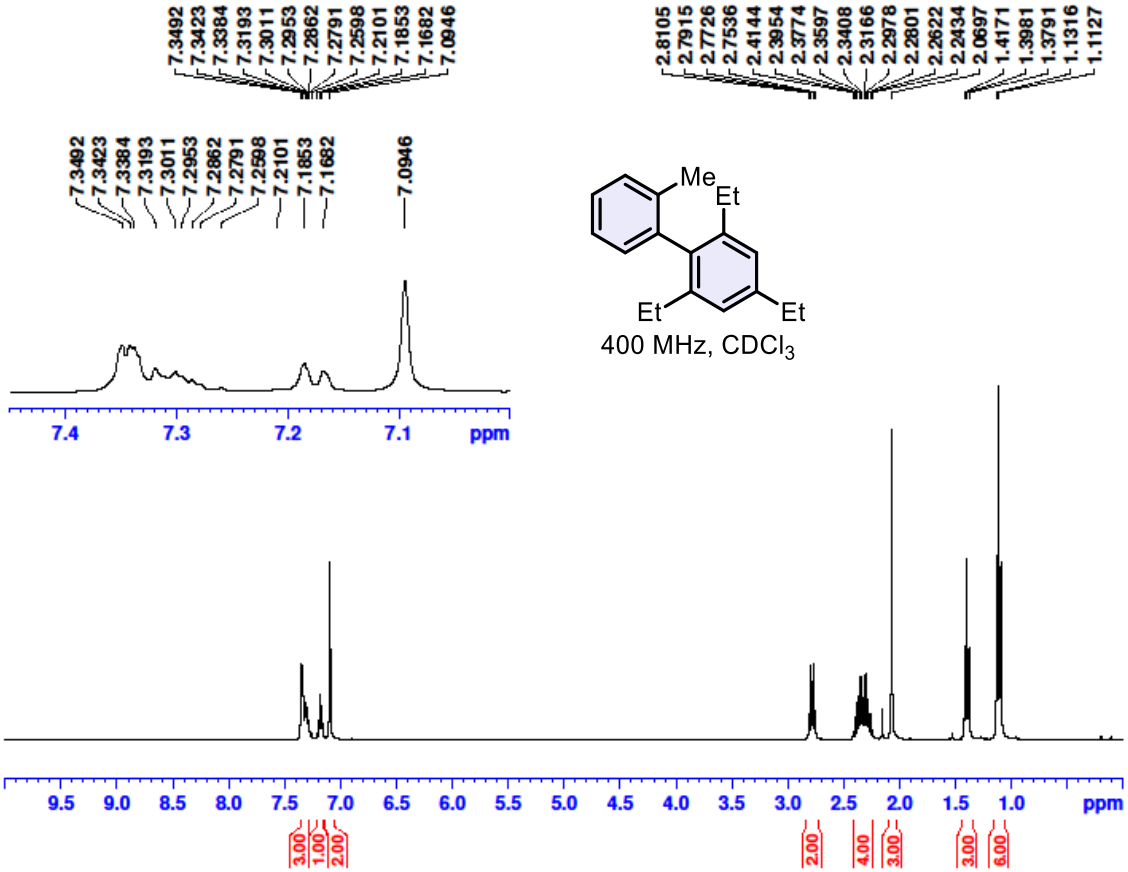

^{13}C NMR of 2,4,6-triethyl-2'-methyl-1,1'-biphenyl (Table 2.4, compound **3t**)

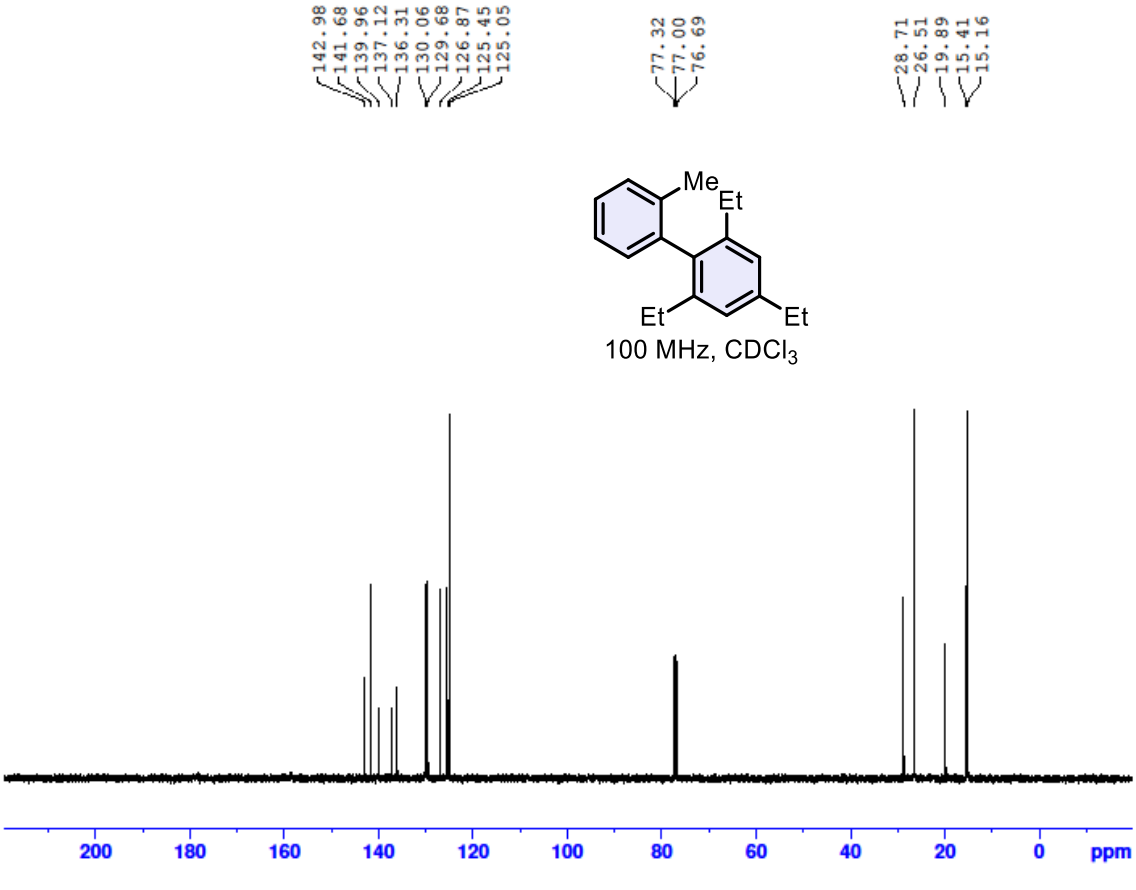

^{1}H NMR of 4’-methoxy-2,2’,4,5,6’-pentamethyl-1,1’-biphenyl (Table 2.4, compound **3u**)

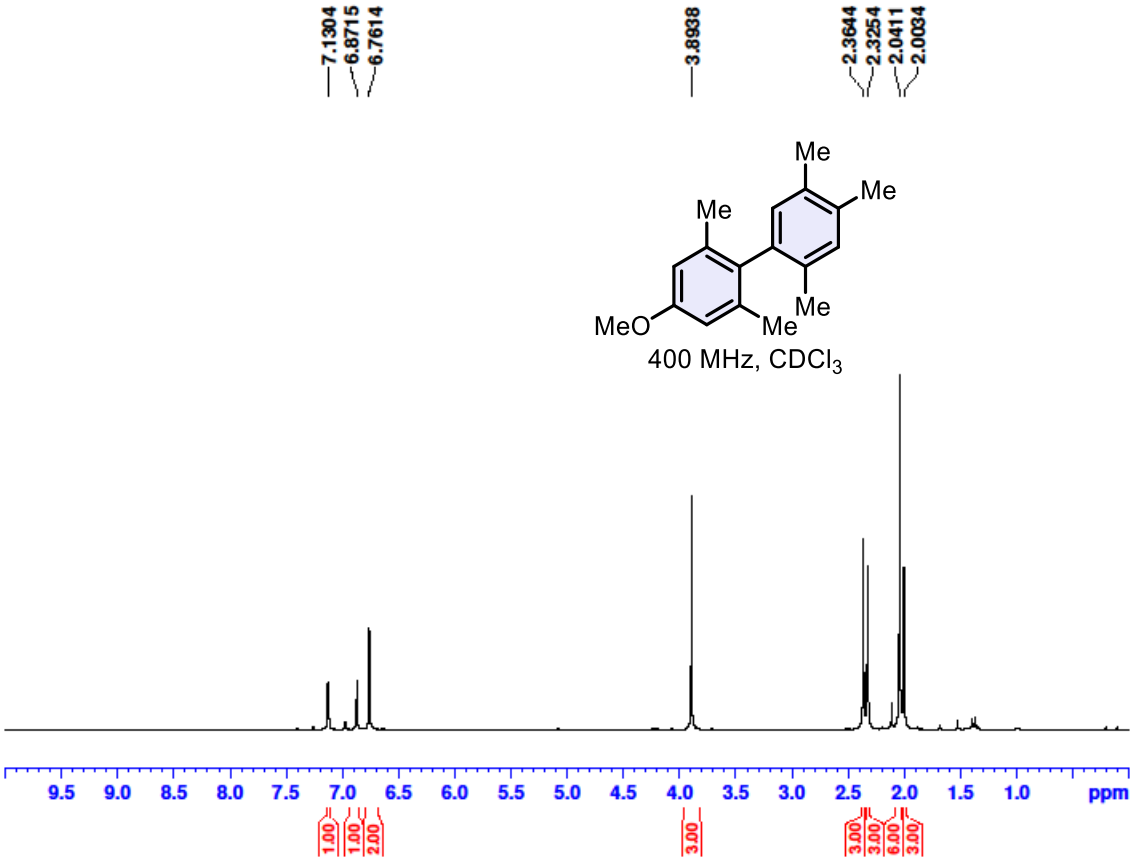

^{13}C NMR of 4’-methoxy-2,2’,4,5,6’-pentamethyl-1,1’-biphenyl (Table 2.4, compound **3u**)

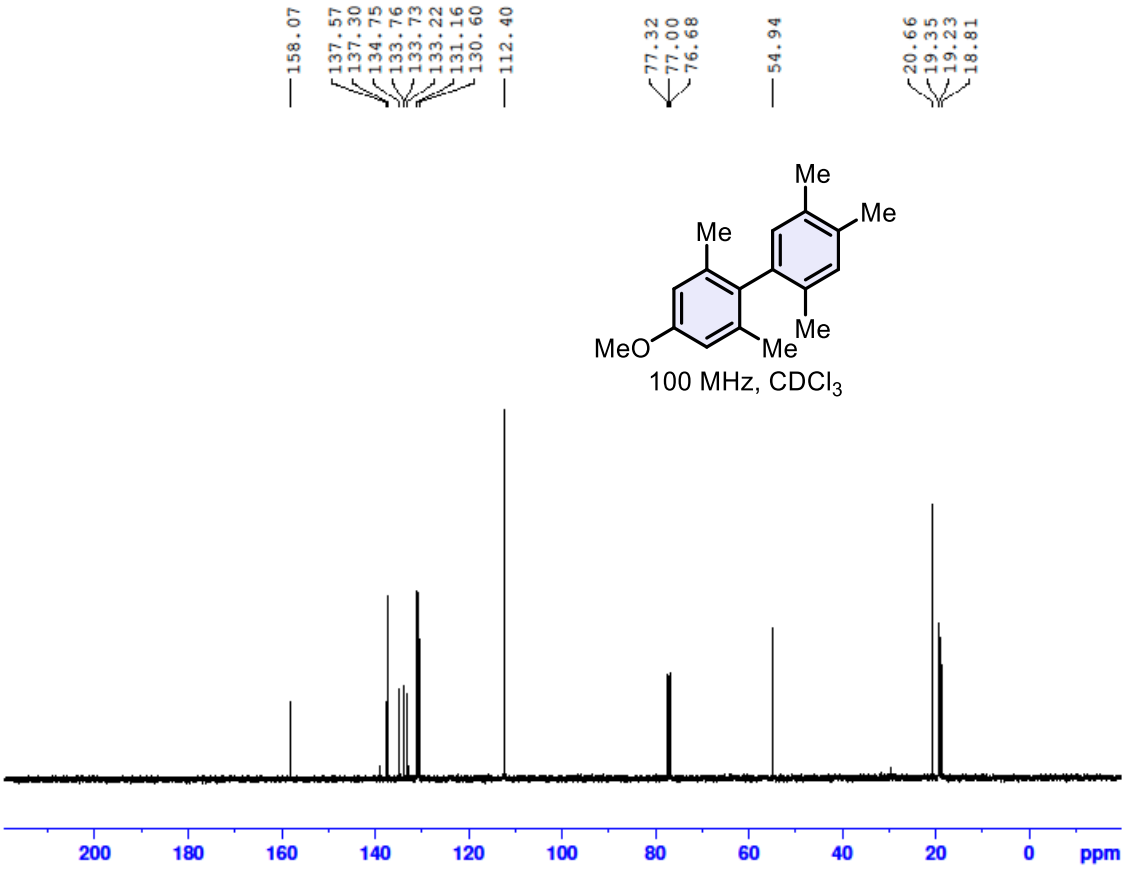

HRMS of 4’-methoxy-2,2’,4,5,6’-pentamethyl-1,1’-biphenyl (Table 2.4, compound **3u**)

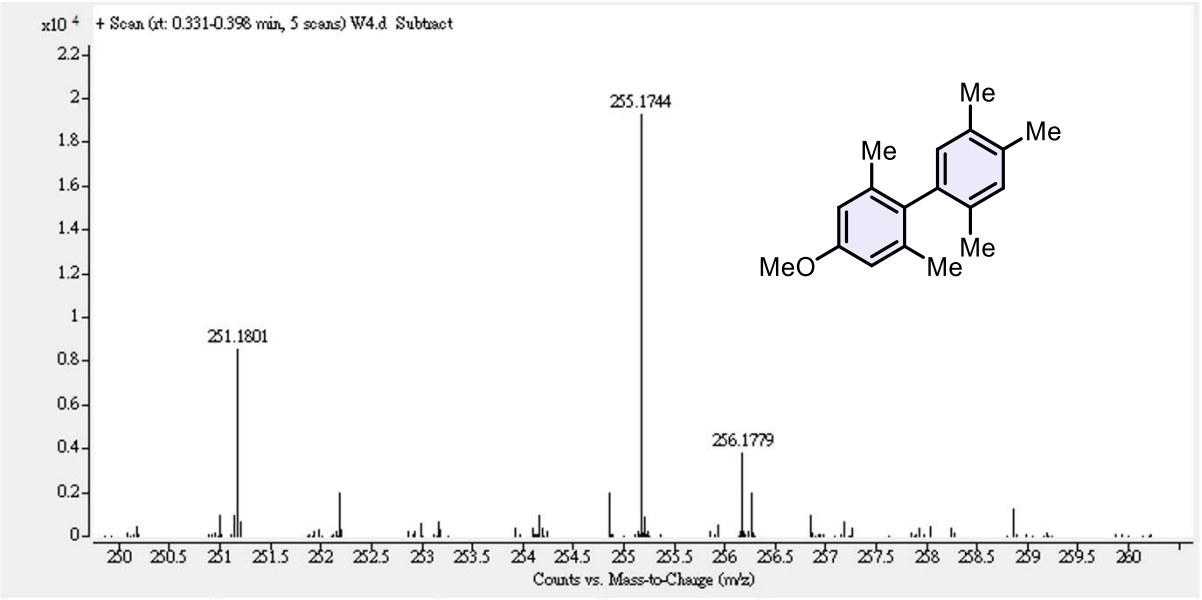

Mass	Calc. Mass	mDa	PPM	Formula
255.1744	255.1743	-0.06	-0.23	C18 H23 O

^{1}H NMR of 4,4'-dimethoxy-2,2',6-trimethyl-1,1'-biphenyl (Table 2.4, compound **3v**)

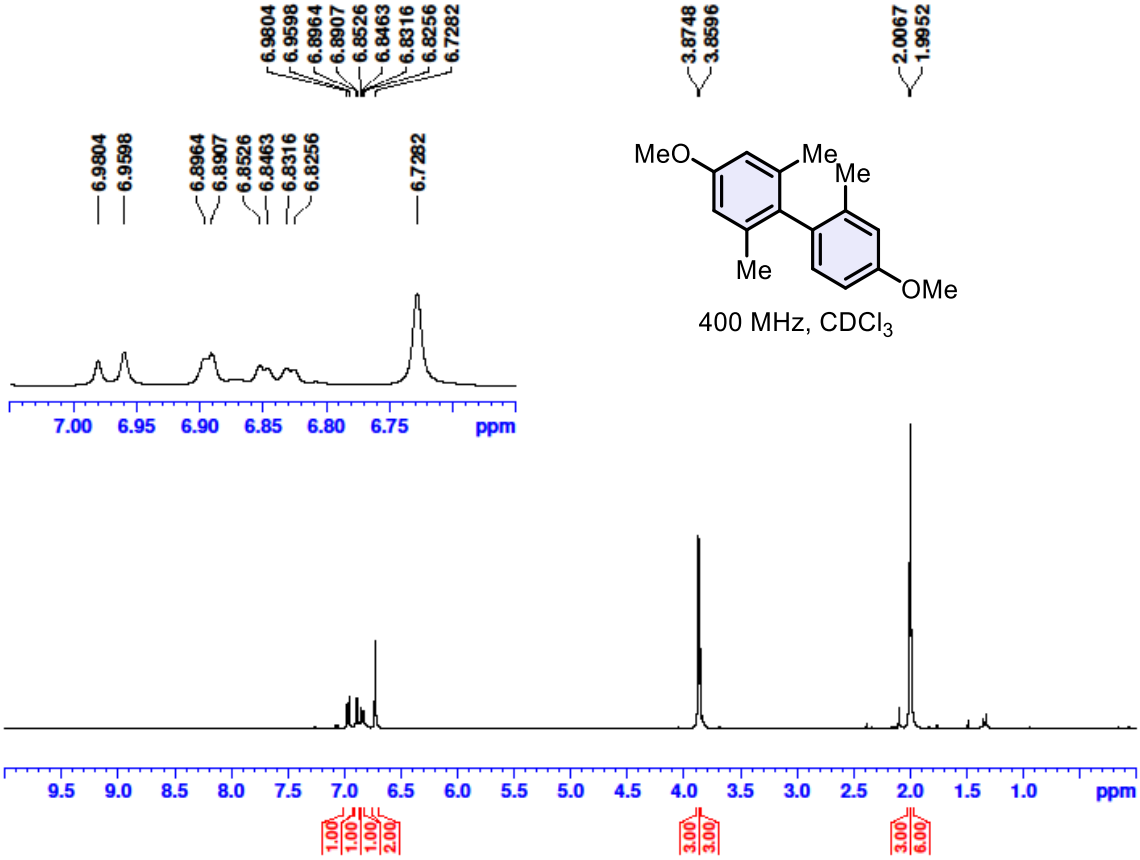

^{13}C NMR of 4,4'-dimethoxy-2,2',6-trimethyl-1,1'-biphenyl (Table 2.4, compound **3v**)

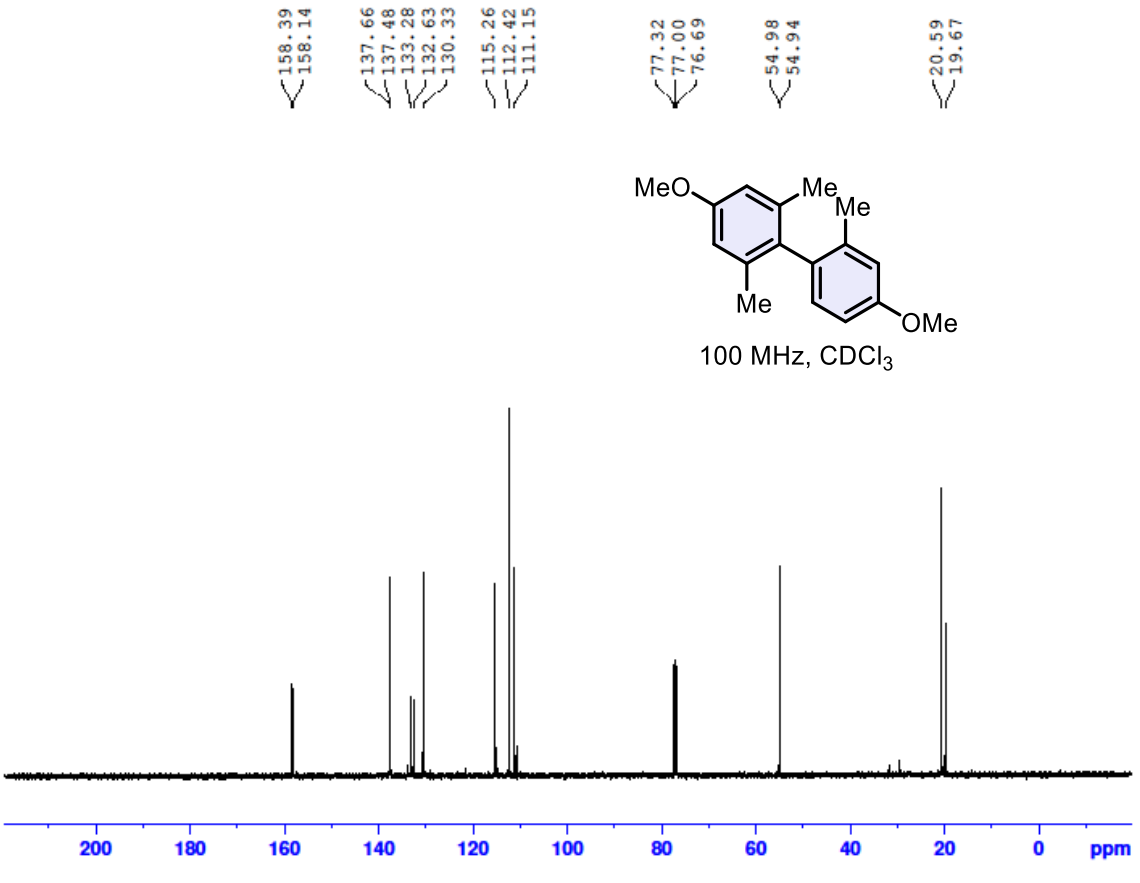

HRMS of 4,4’-dimethoxy-2,2’,6-trimethyl-1,1’-biphenyl (Table 2.4, compound **3v**)

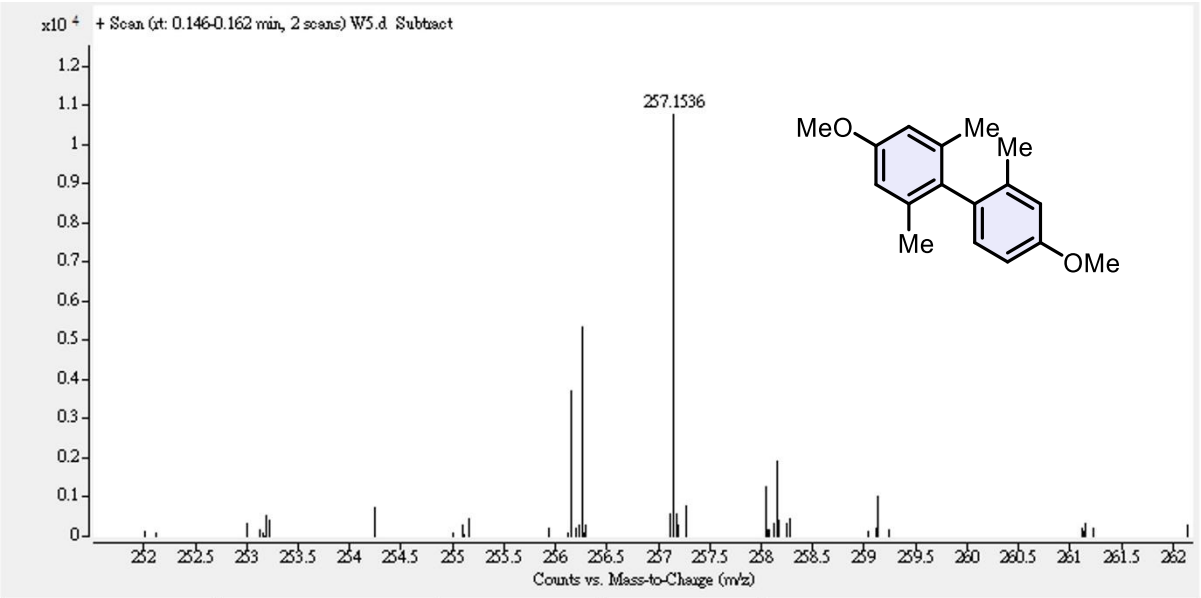

Mass	Calc. Mass	mDa	PPM	Formula
257.1536	257.1536	0.01	0.02	C17 H21 O2

^{1}H NMR of 2,2',6-trimethyl-[1,1'-biphenyl]-4-yl dimethylsulfamate (Table 2.4, compound **3w**)

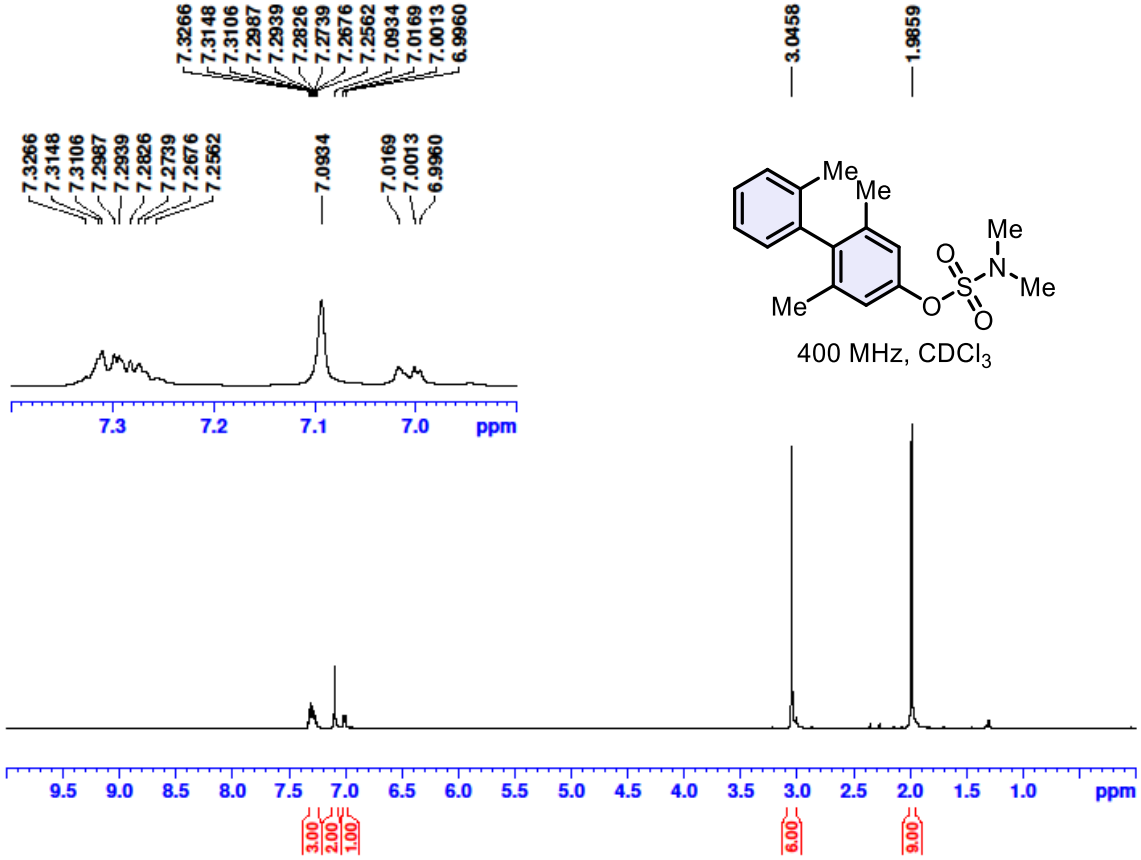

^{13}C NMR of 2,2',6-trimethyl-[1,1'-biphenyl]-4-yl dimethylsulfamate (Table 2.4, compound **3w**)

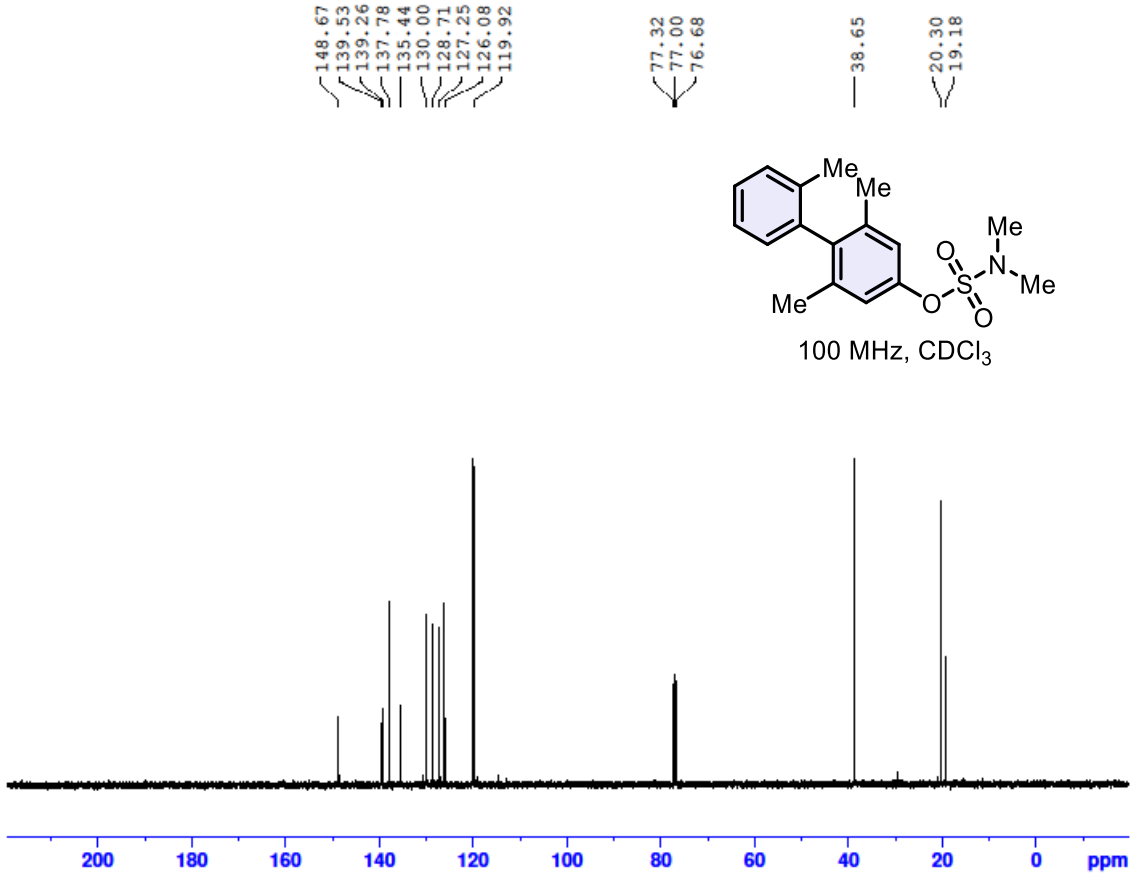

HRMS of 2,2',6-trimethyl-[1,1'-biphenyl]-4-yl dimethylsulfamate (Table 2.4, compound **3w**)

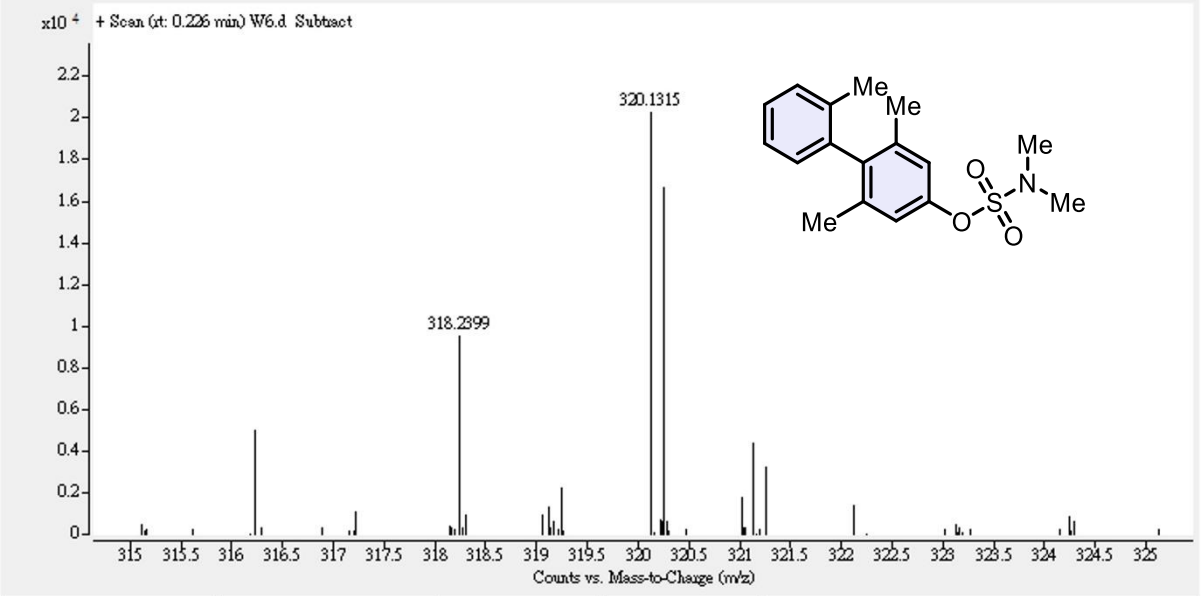

Mass	Calc. Mass	mDa	PPM	Formula
320.1315	320.1315	-0.01	-0.03	C17 H22 N O3 S

^{1}H NMR of 4-(2,6-dimethylphenyl)dibenzo[*b*,*d*]furan (Table 2.4, compound **3x**)

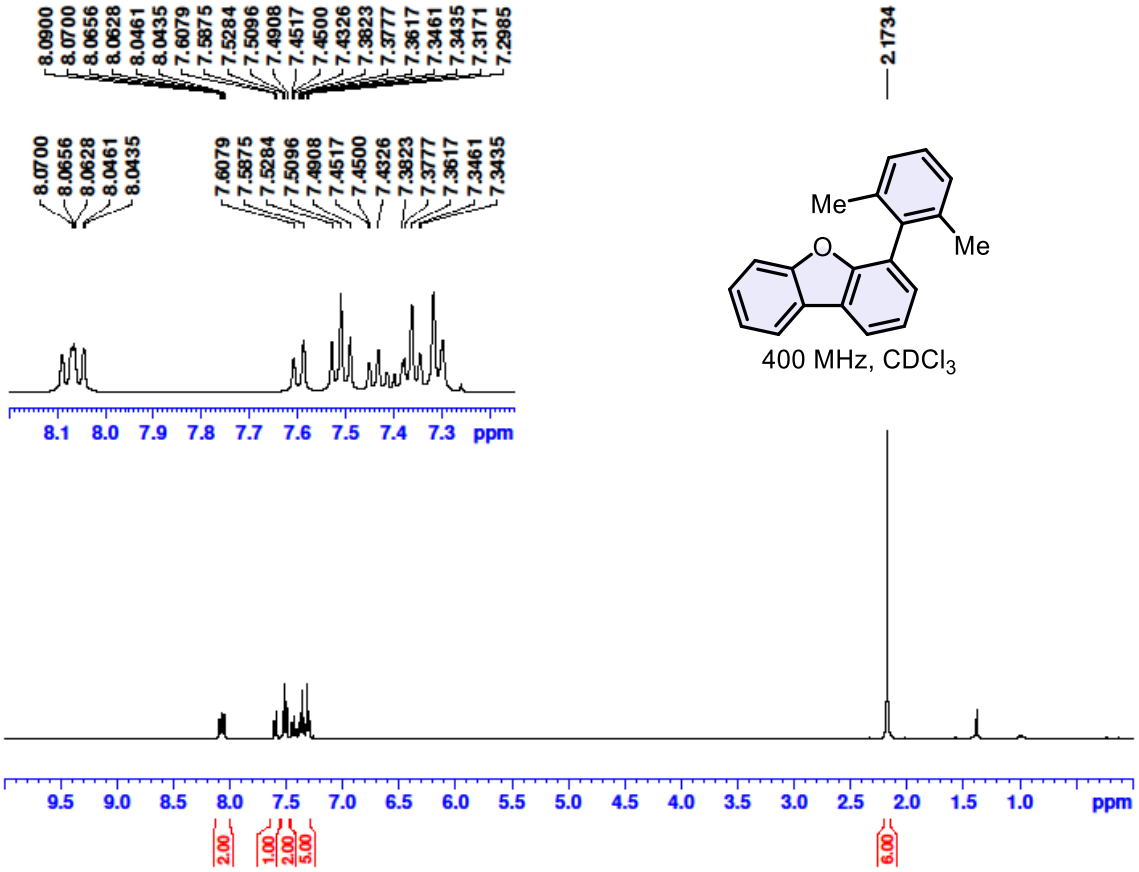

^{13}C NMR of 4-(2,6-dimethylphenyl)dibenzo[*b*,*d*]furan (Table 2.4, compound **3x**)

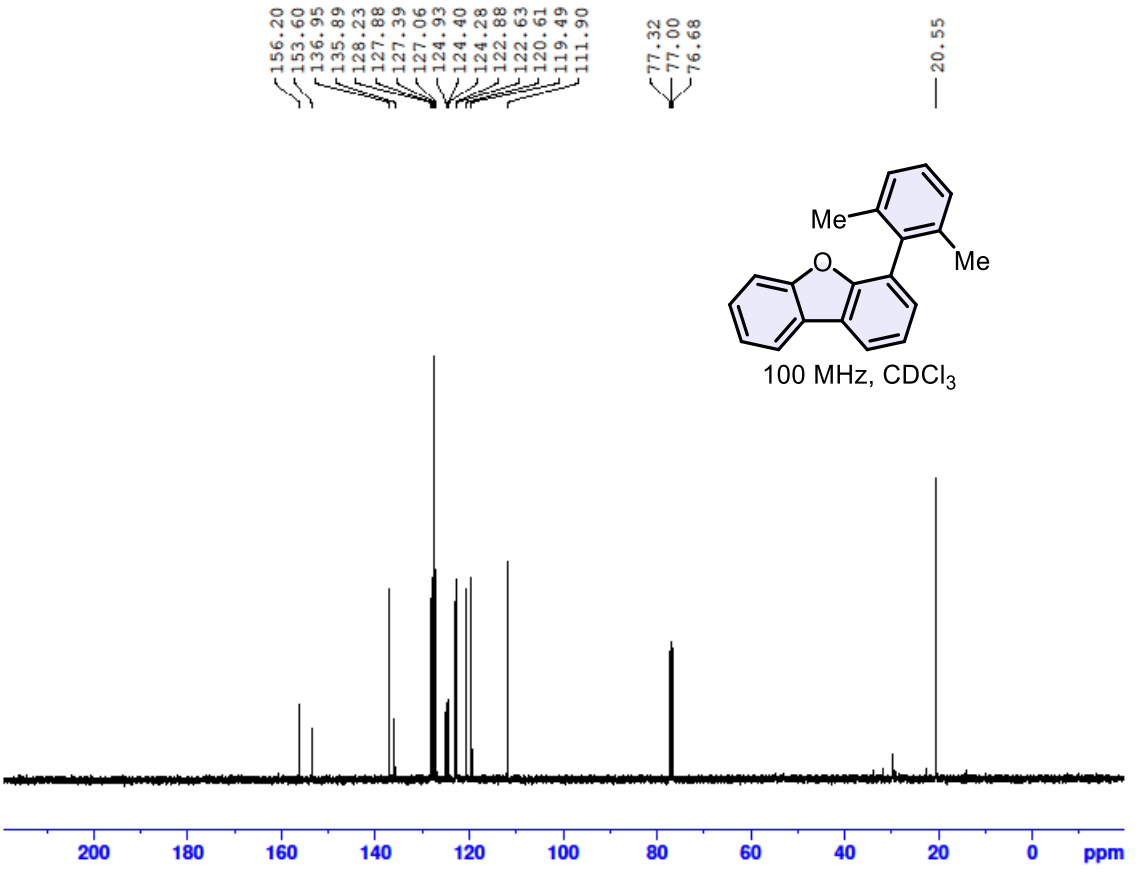

HRMS of 4-(2,6-dimethylphenyl)dibenzo[*b*,*d*]furan (Table 2.4, compound **3x**)

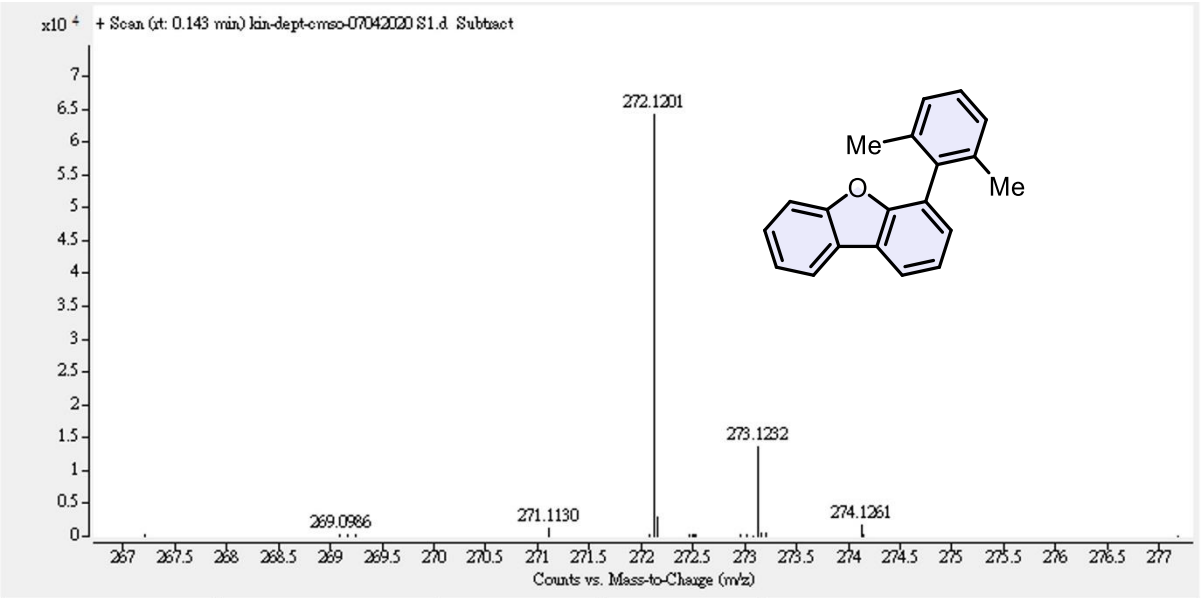

Mass	Calc. Mass	mDa	PPM	Formula
272.1201	272.1196	-0.53	-1.97	C20 H16 O

^{1}H NMR of 4-(2,6-dimethylphenyl)dibenzo[*b*,*d*]thiophene (Table 2.4, compound **3y**)

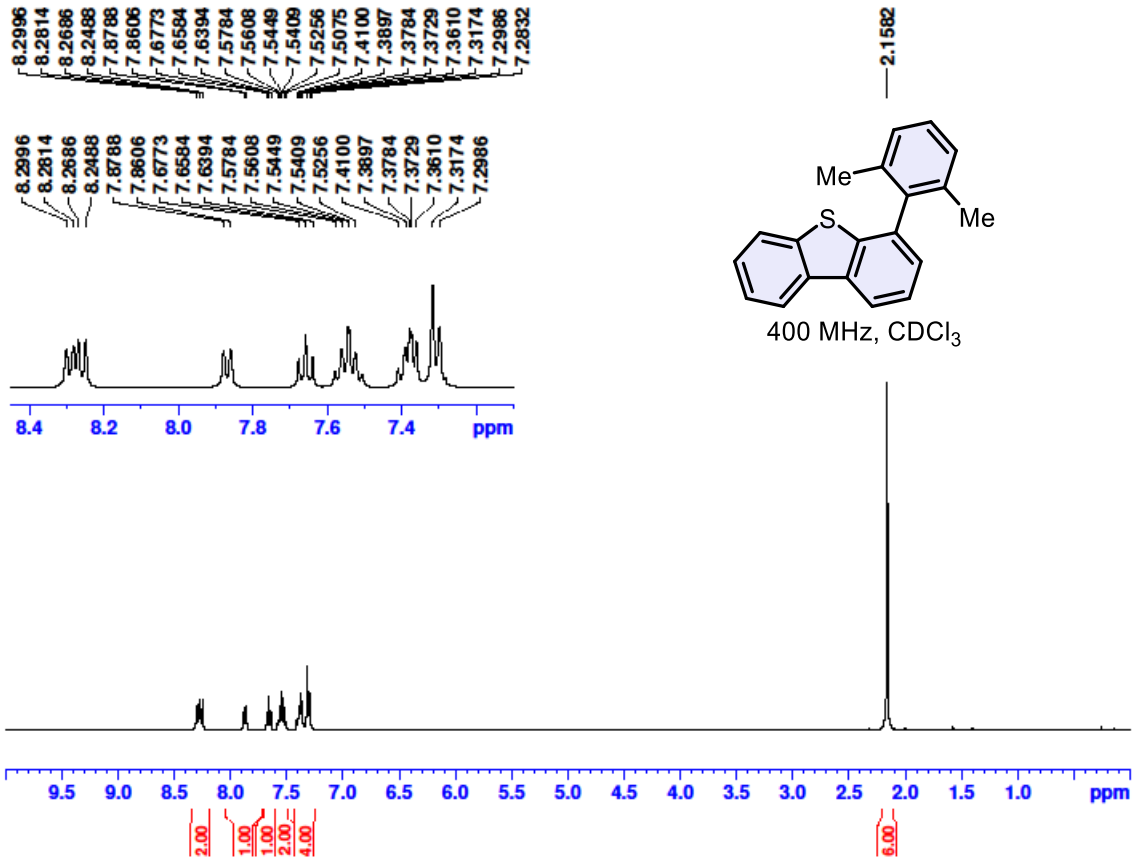

^{13}C NMR of 4-(2,6-dimethylphenyl)dibenzo[*b*,*d*]thiophene (Table 2.4, compound **3y**)

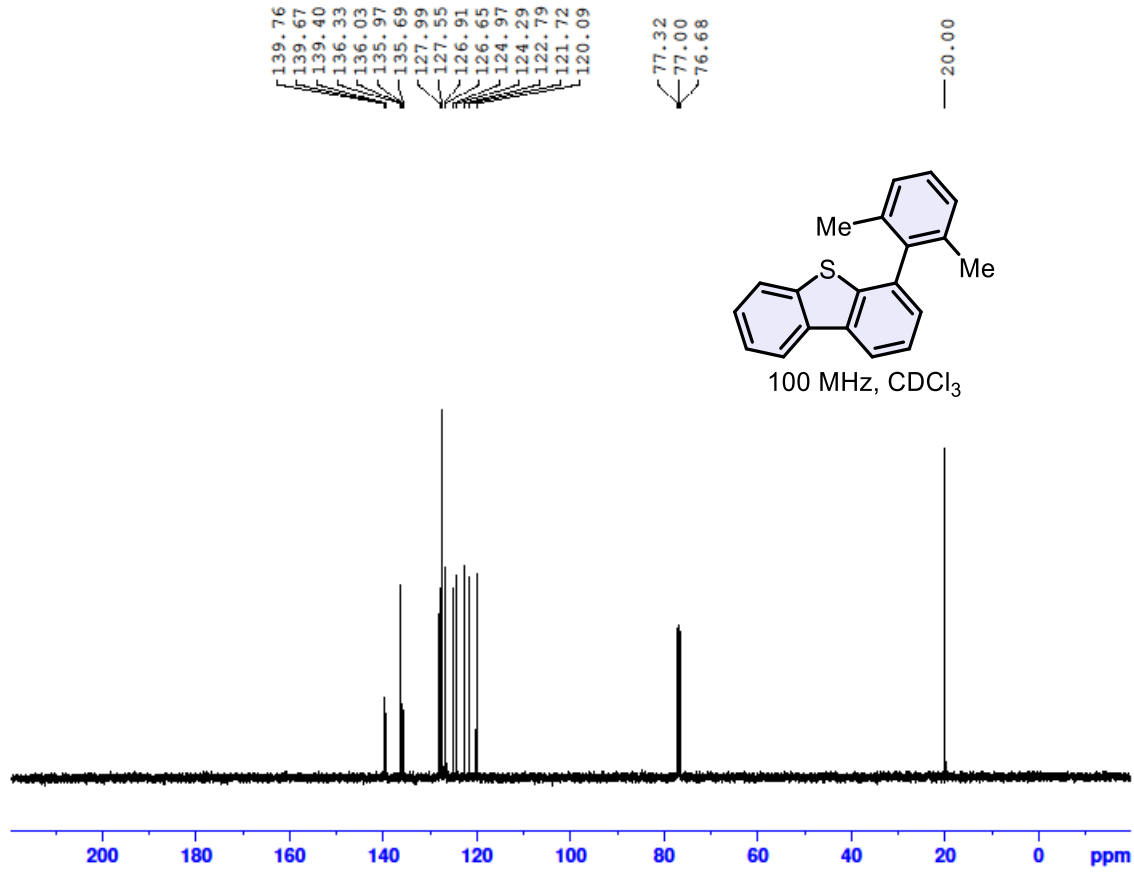

HRMS of 4-(2,6-dimethylphenyl)dibenzo[*b*,*d*]thiophene (Table 2.4, compound **3y**)

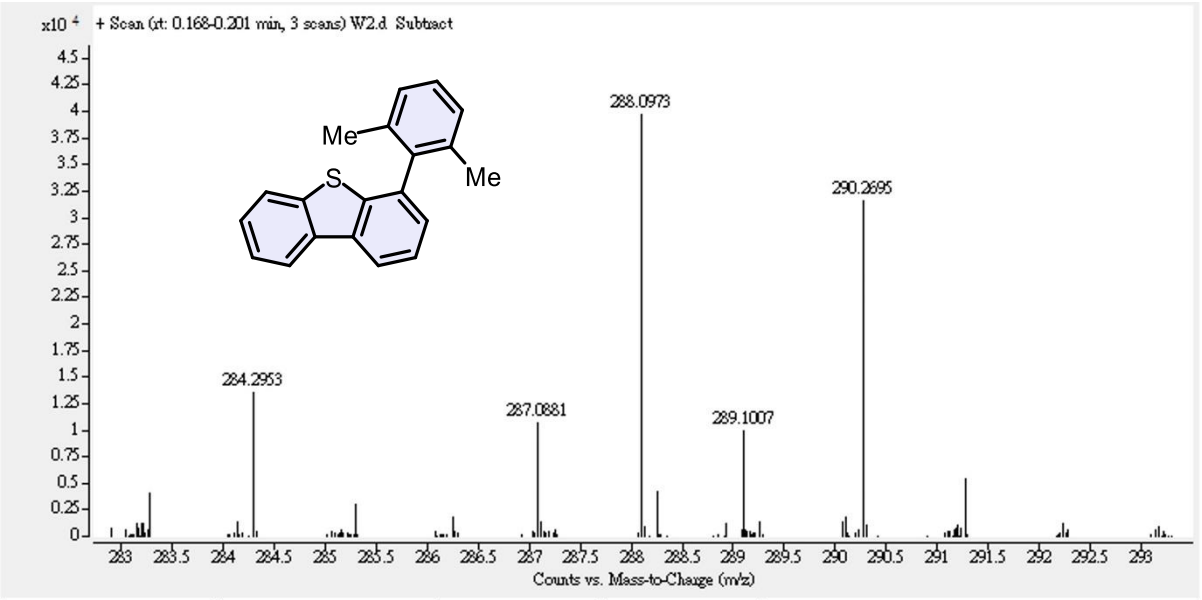

Mass	Calc. Mass	mDa	PPM	Formula
288.0973	288.0973	-0.03	-0.10	C20 H16 S

^{1}H NMR of 1-mesitylpyrene (Table 2.4, compound **3z**)

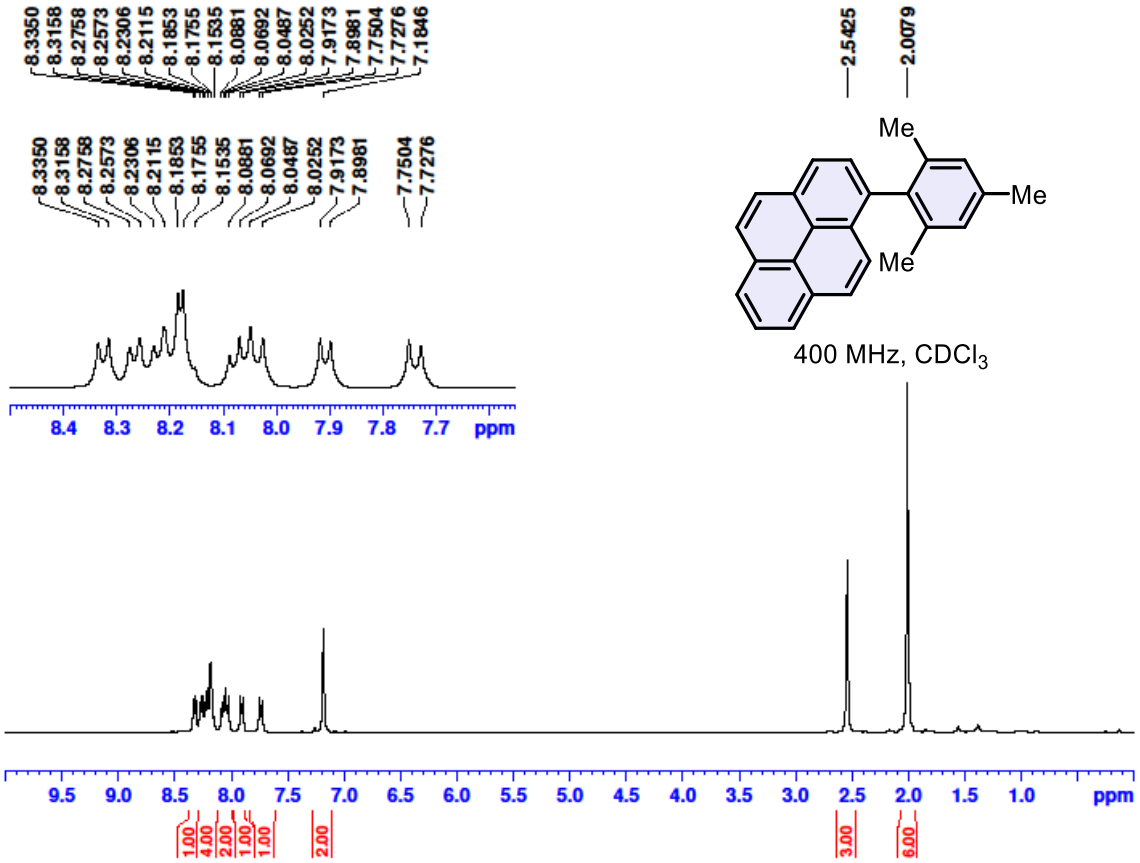

^{13}C NMR of 1-mesitylpyrene (Table 2.4, compound **3z**)

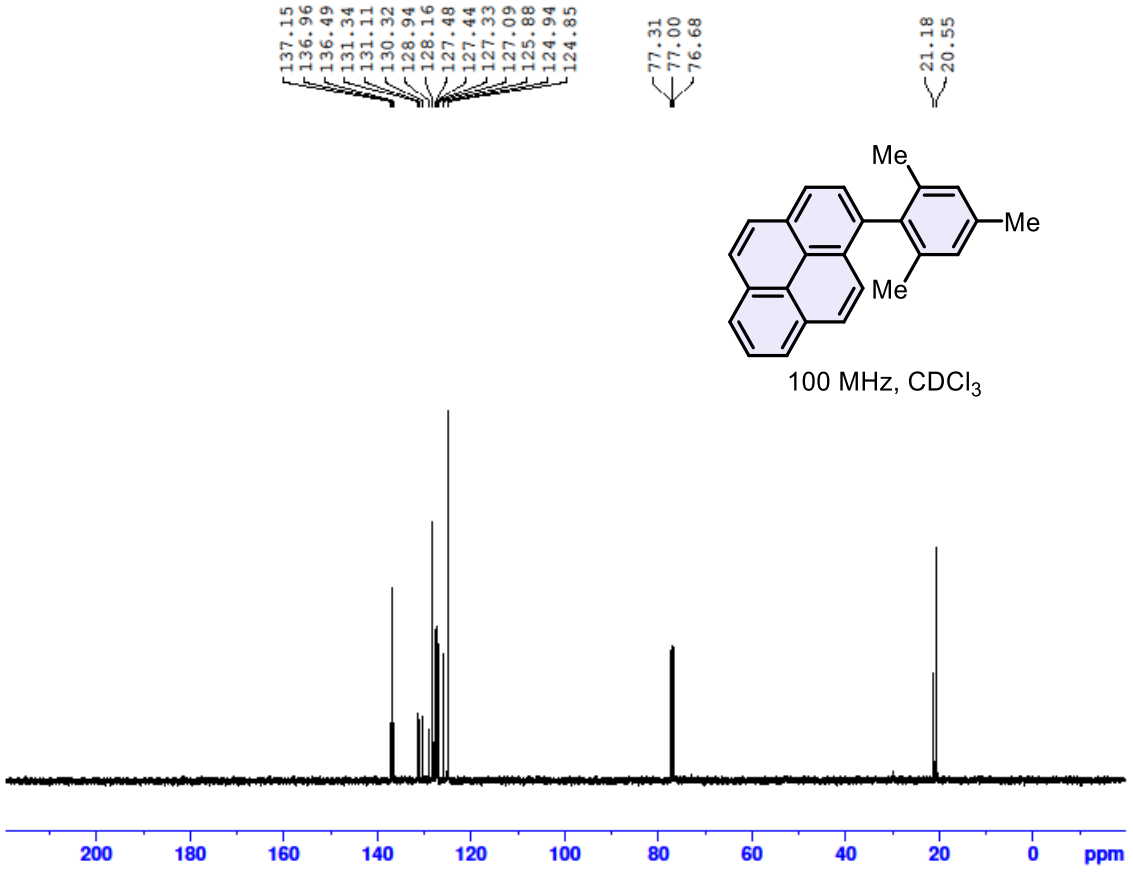

HRMS of 1-mesitylpyrene (Table 2.4, compound **3z**)

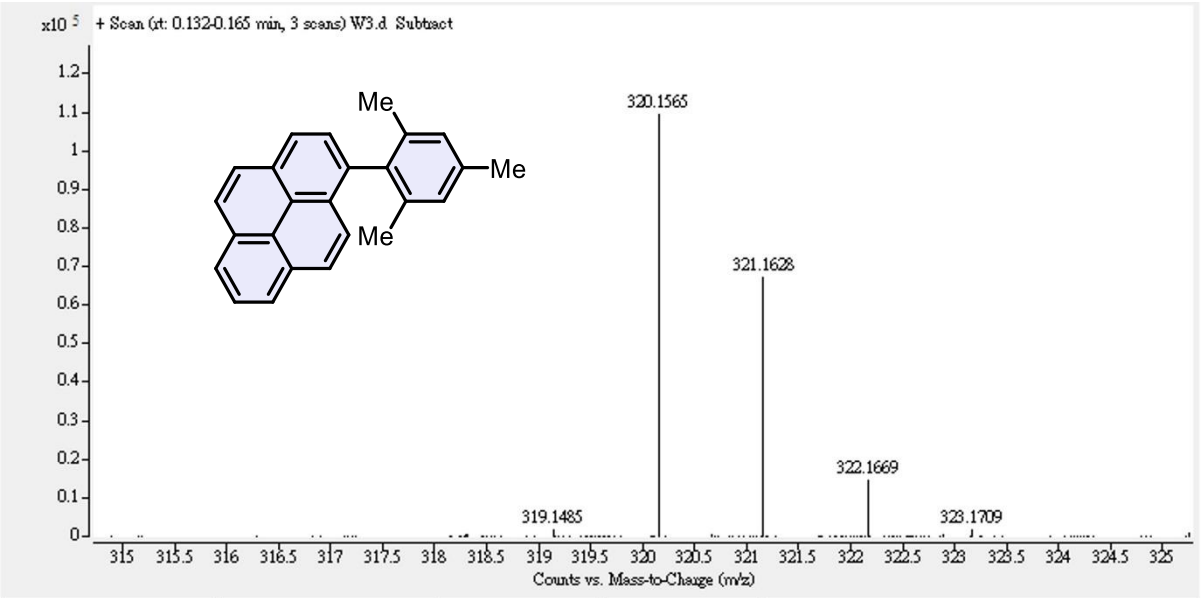

Mass	Calc. Mass	mDa	PPM	Formula
320.1565	320.1565	0.00	0.00	C25 H20

^{1}H NMR of 1-(4-methoxy-2,6-dimethylphenyl)pyrene (Table 2.4, compound **3aa**)

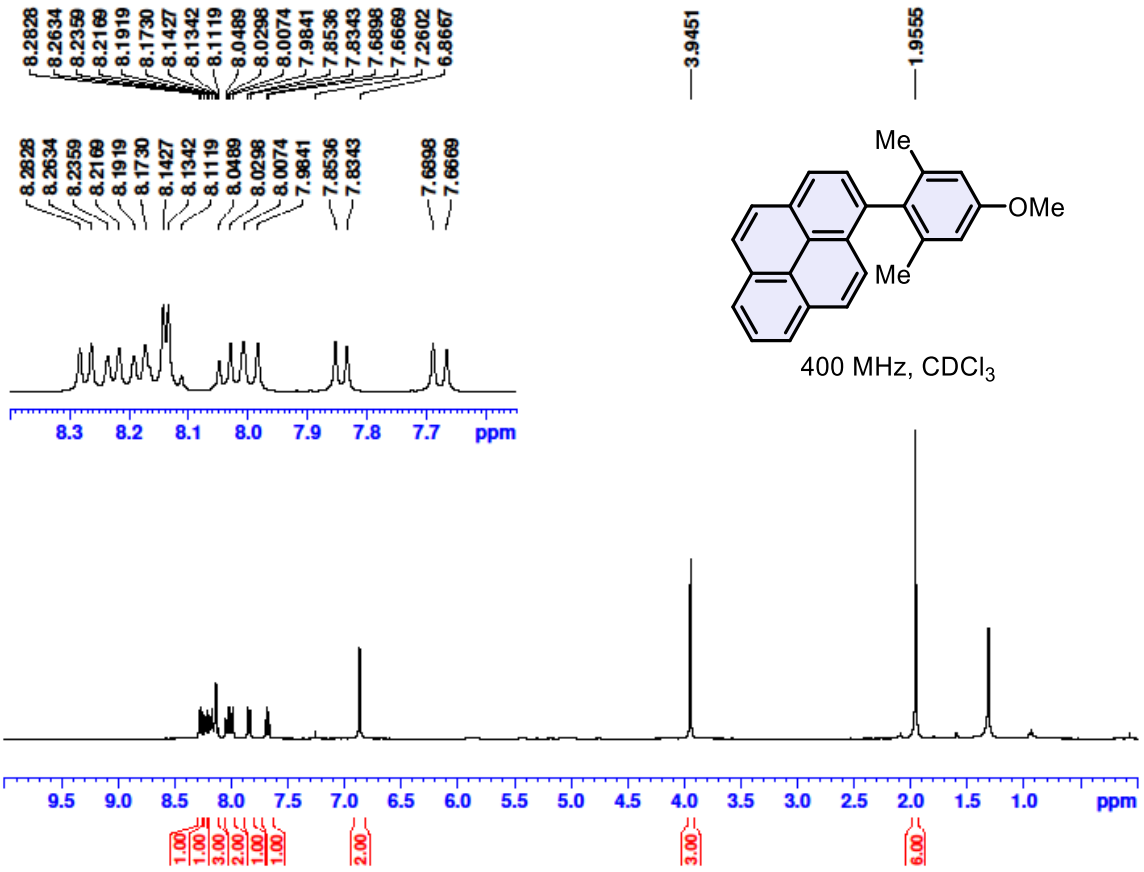

^{13}C NMR of 1-(4-methoxy-2,6-dimethylphenyl)pyrene (Table 2.4, compound **3aa**)

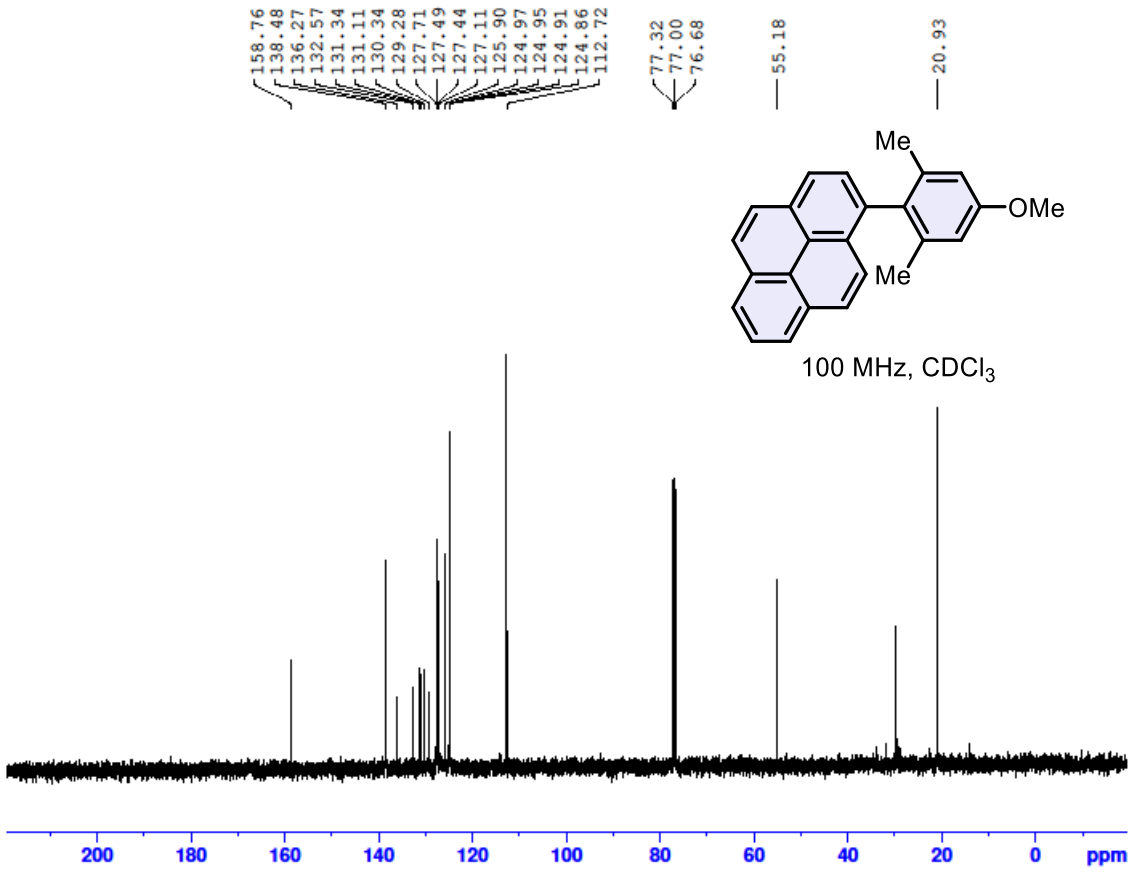

^{1}H NMR of 9-(*o*-tolyl)anthracene (Table 2.4 and 2.5, compound **3ab**)

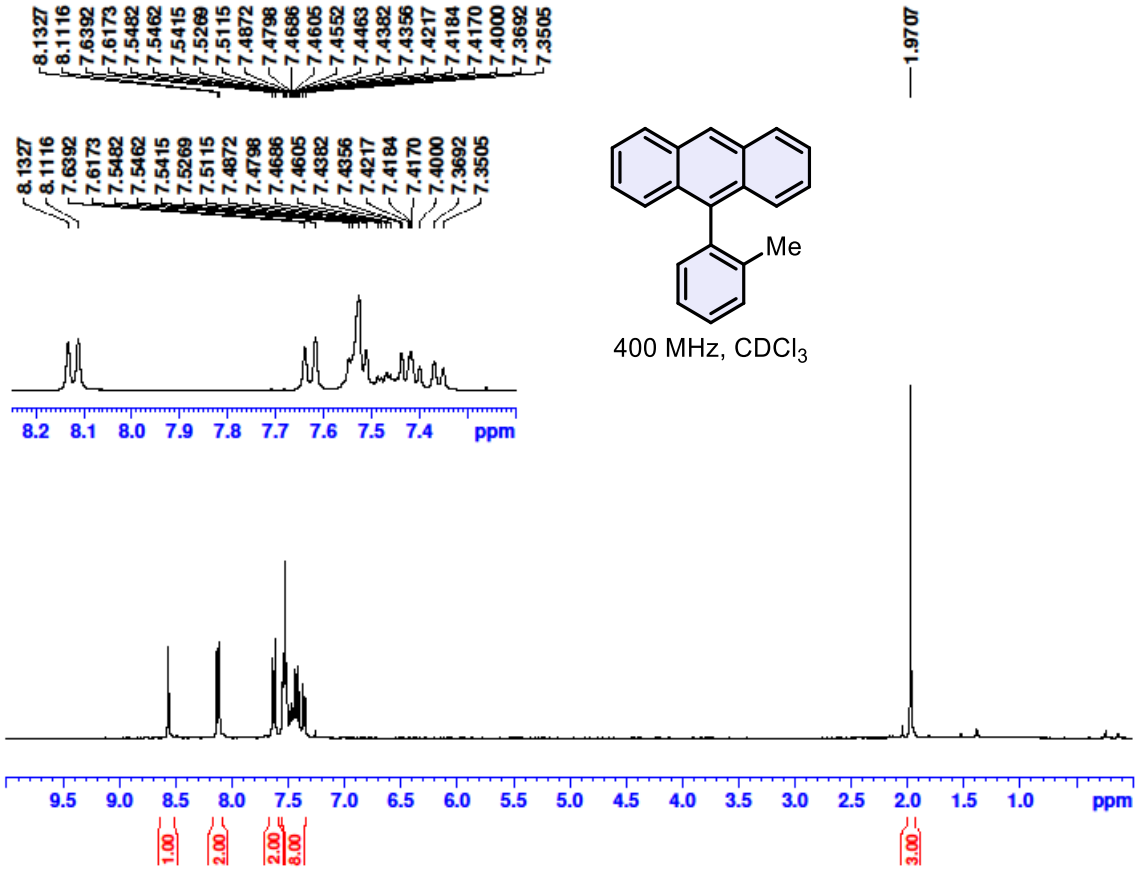

^{13}C NMR of 9-(*o*-tolyl)anthracene (Table 2.4 and 2.5, compound **3ab**)

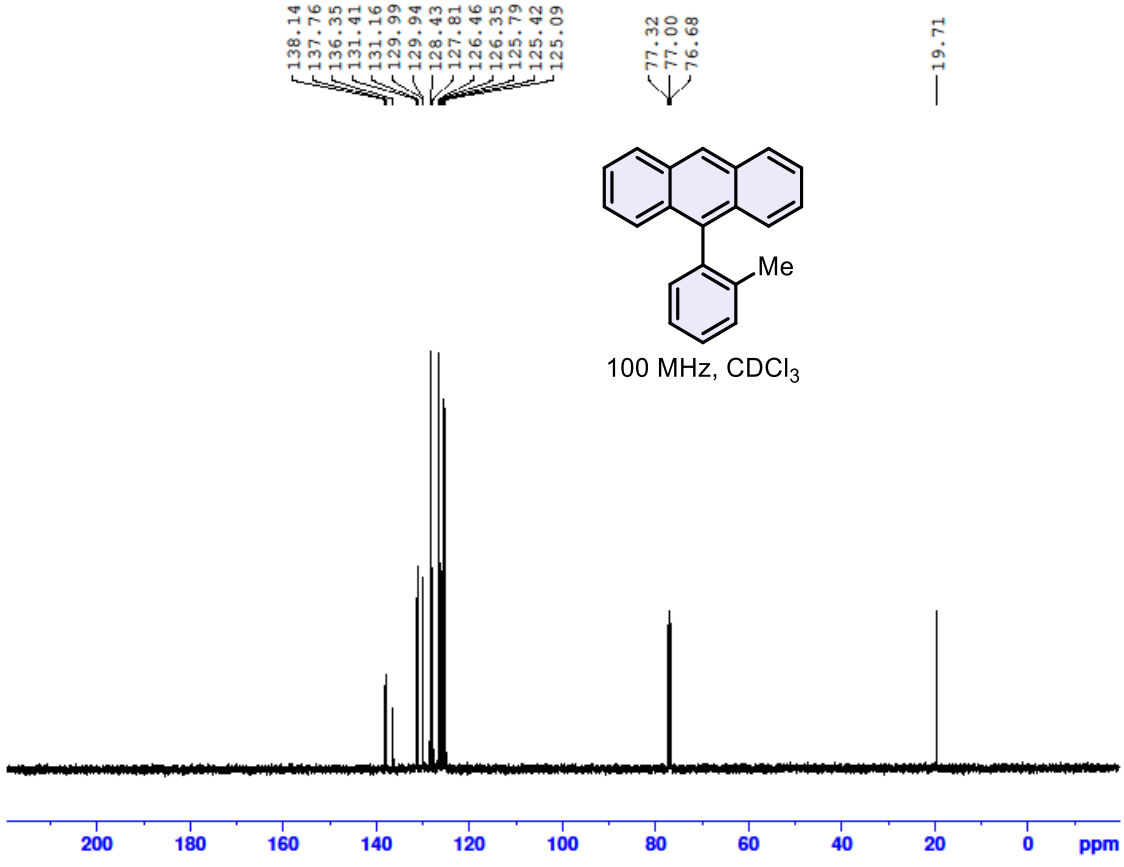

^{1}H NMR of 9-(4-methoxy-2-methylphenyl)anthracene (Table 2.4, compound **3ac**)

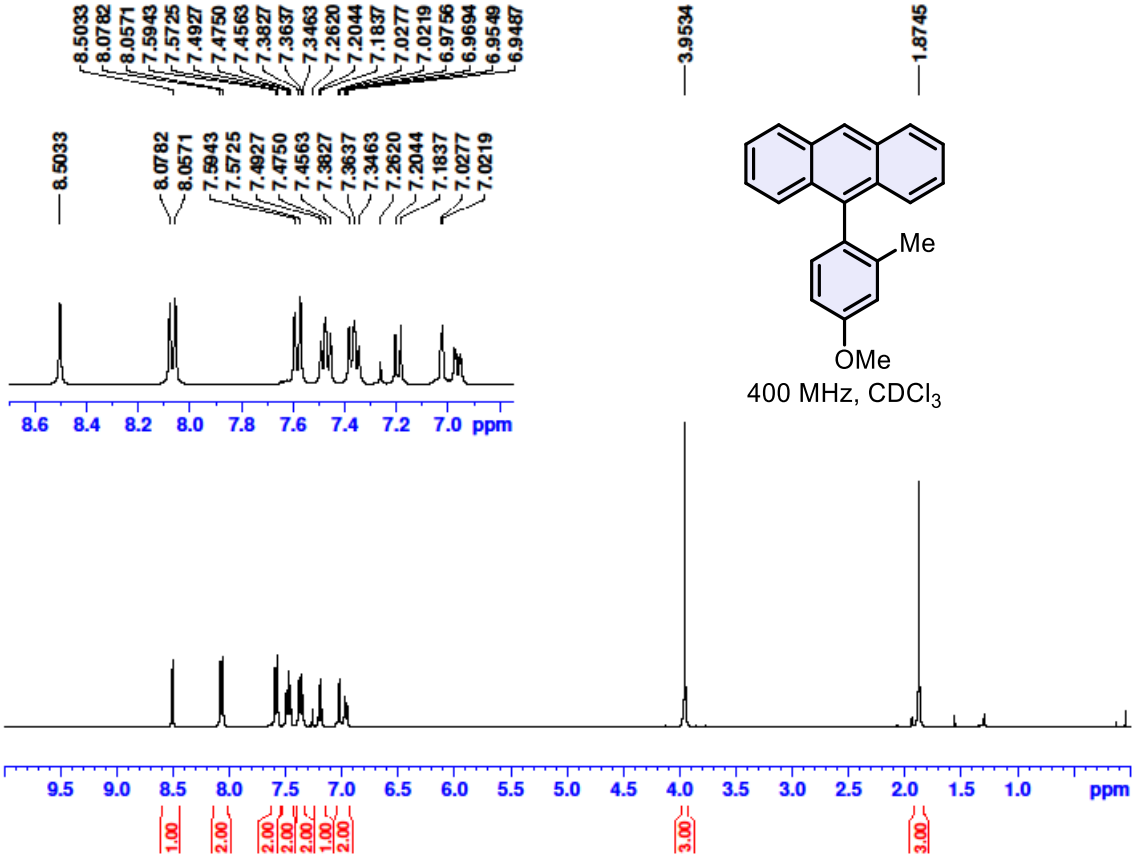

^{13}C NMR of 9-(4-methoxy-2-methylphenyl)anthracene (Table 2.4, compound **3ac**)

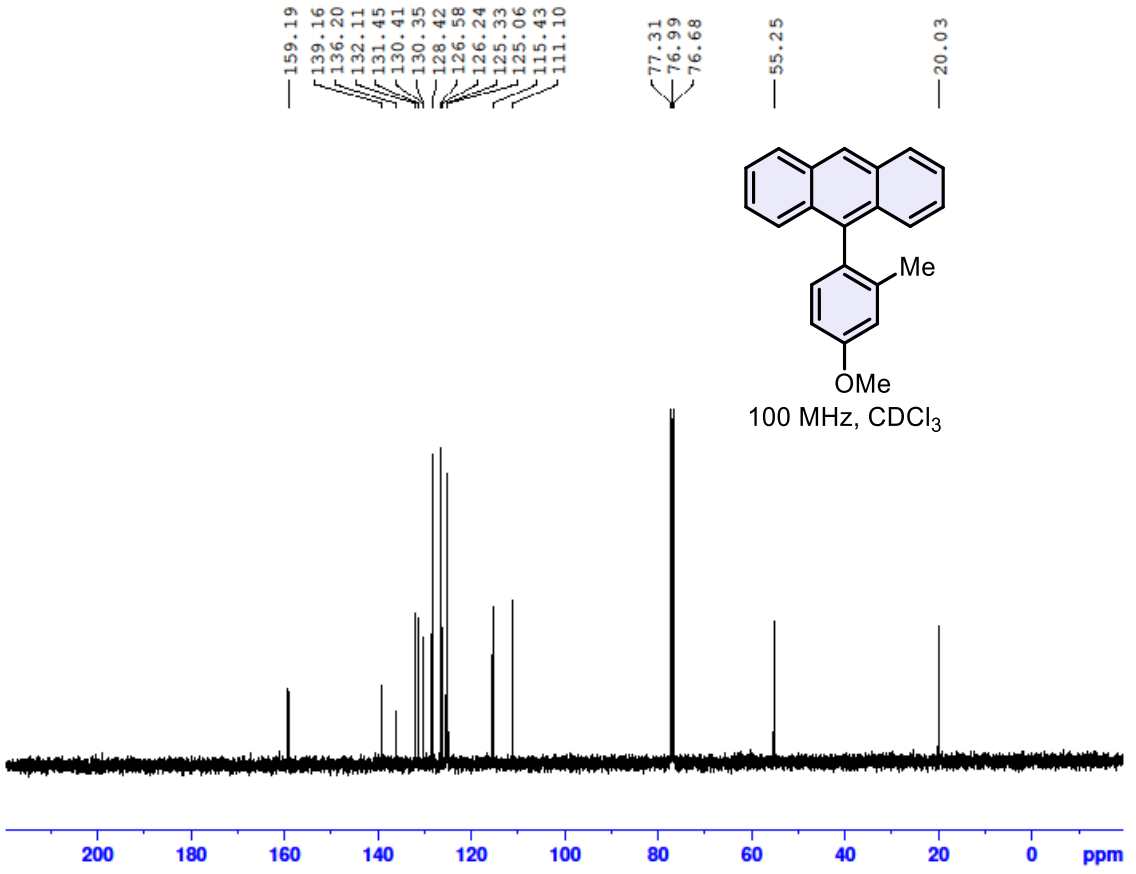

^{1}H NMR of 9-(naphthalen-1-yl)anthracene (Table 2.4, compound **3ad**)

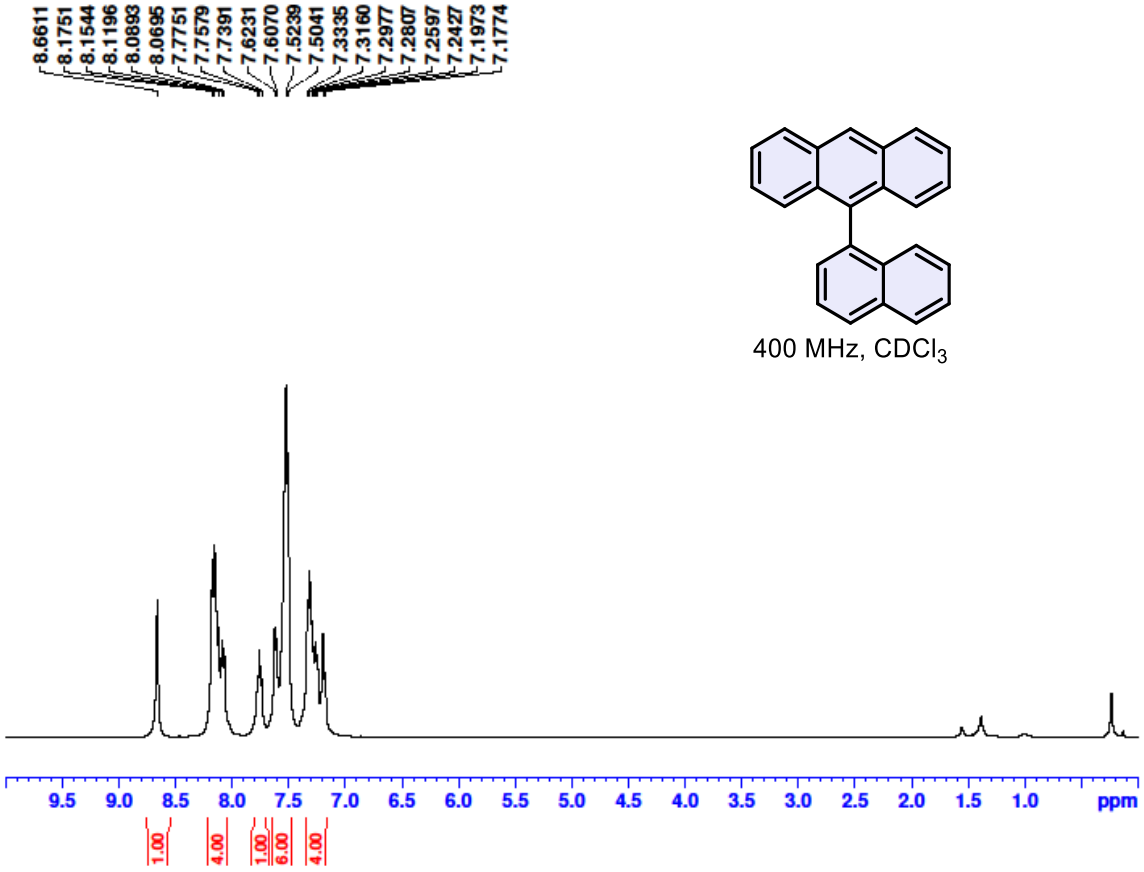

^{13}C NMR of 9-(naphthalen-1-yl)anthracene (Table 2.4, compound **3ad**)

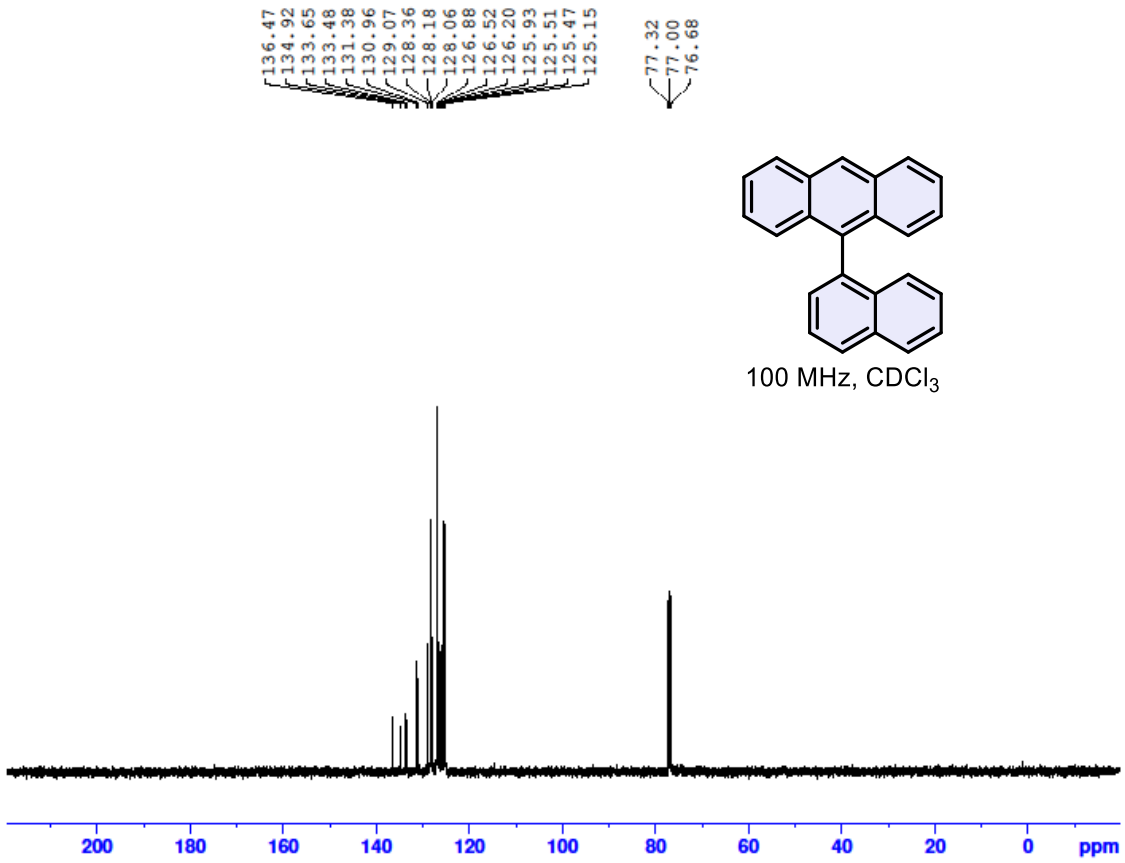

^{1}H NMR of 10-(*o*-tolyl)anthracene-9-carbaldehyde (Table 2.4 and 2.5, compound **3ae**)

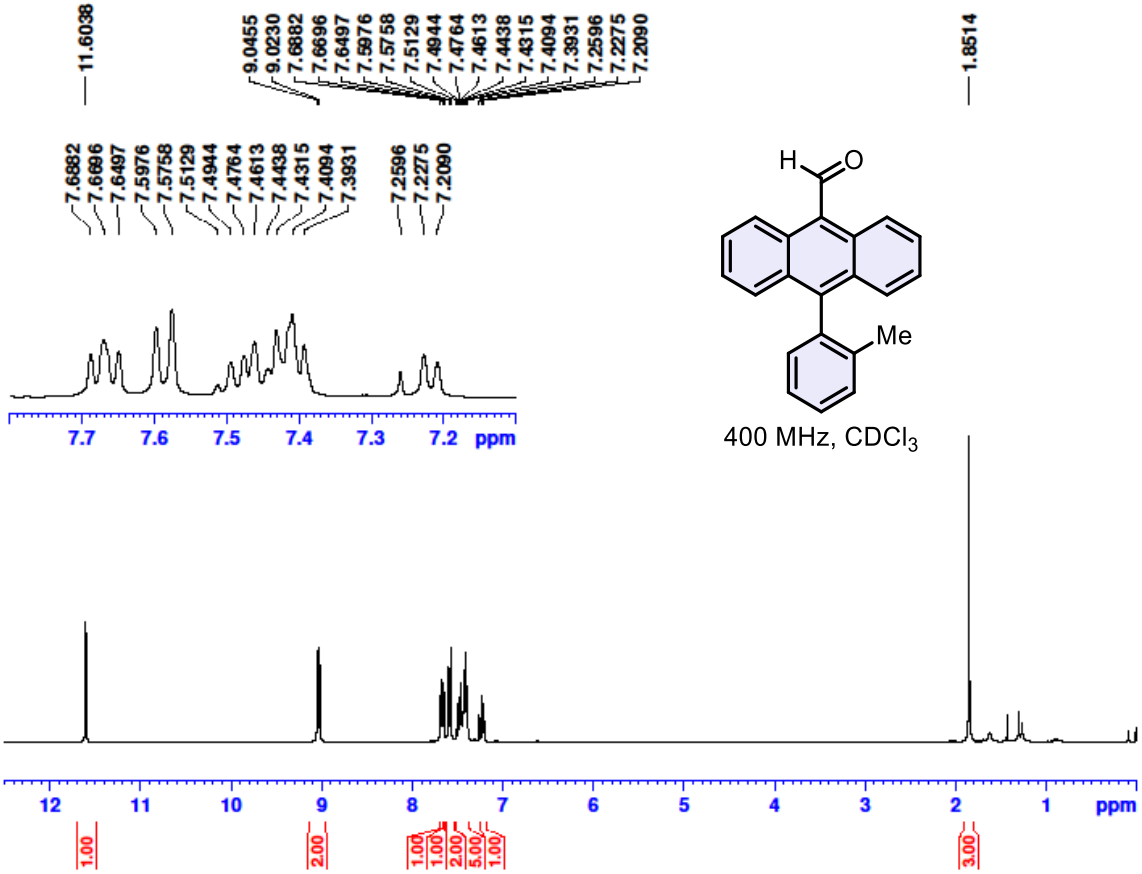

^{13}C NMR of 10-(*o*-tolyl)anthracene-9-carbaldehyde (Table 2.4 and 2.5, compound **3ae**)

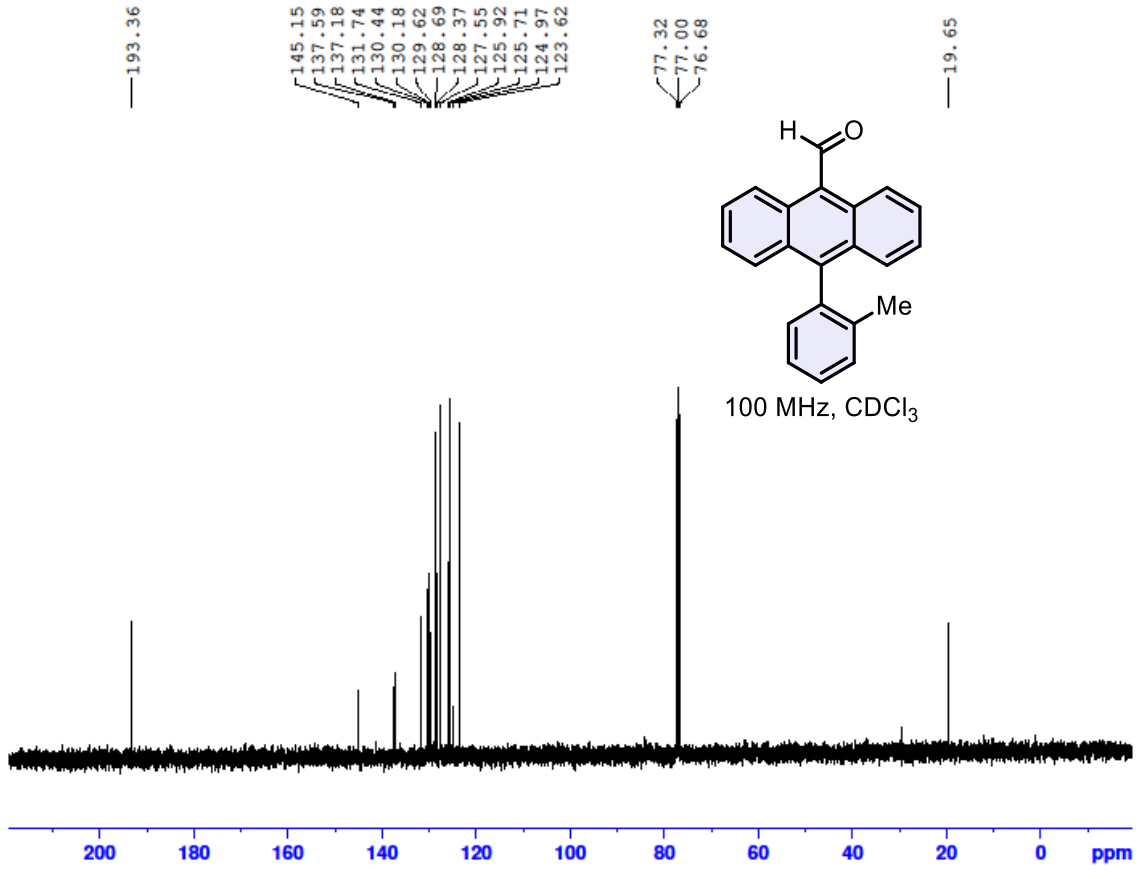

^{1}H NMR of 9-(4-methoxy-2,6-dimethylphenyl)phenanthrene (Table 2.4, compound **3af**)

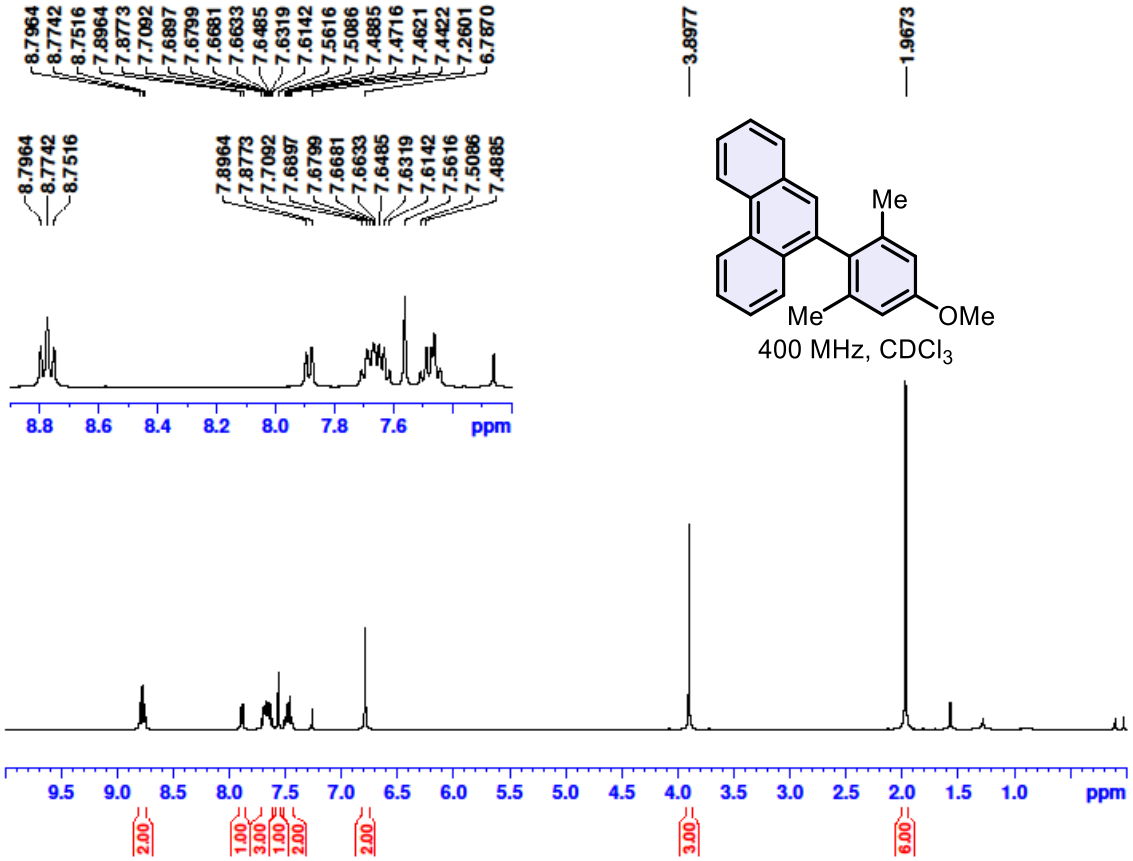

^{13}C NMR of 9-(4-methoxy-2,6-dimethylphenyl)phenanthrene (Table 2.4, compound **3af**)

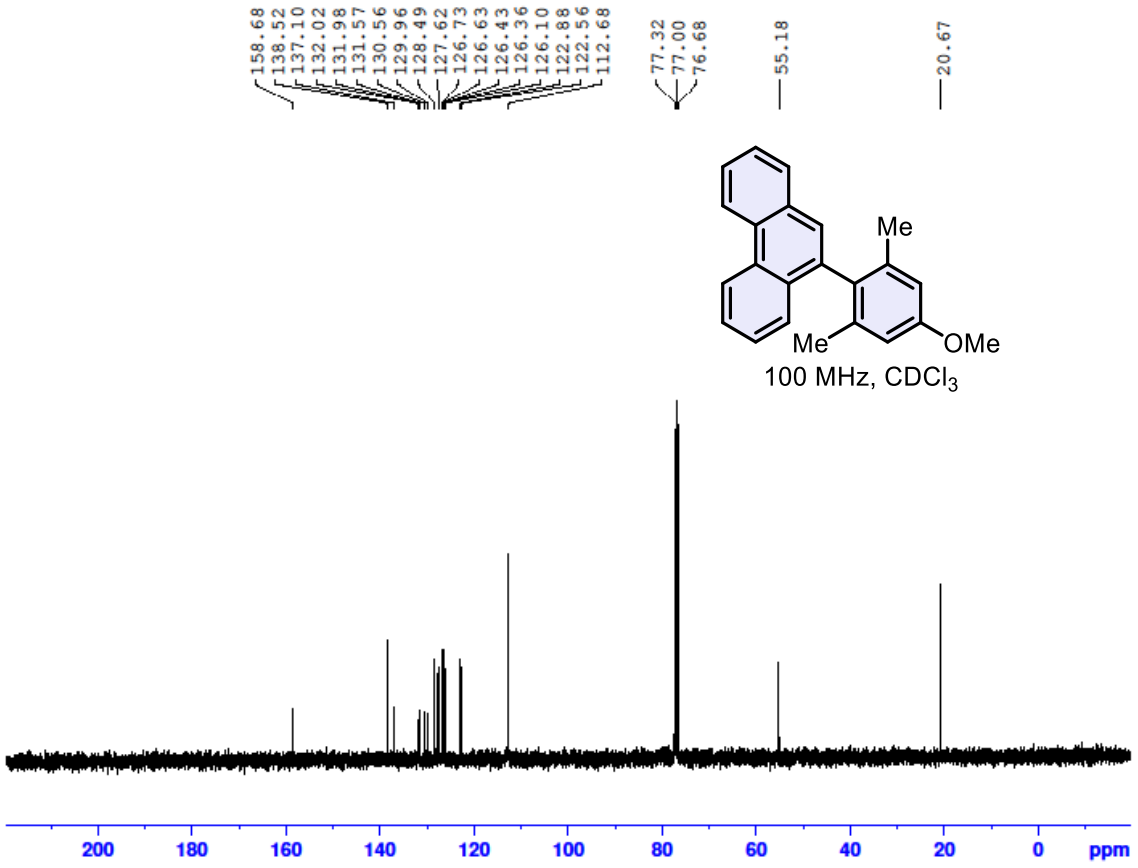

^{1}H NMR of 3-chloro-5-methylphenyl trifluoromethanesulfonate

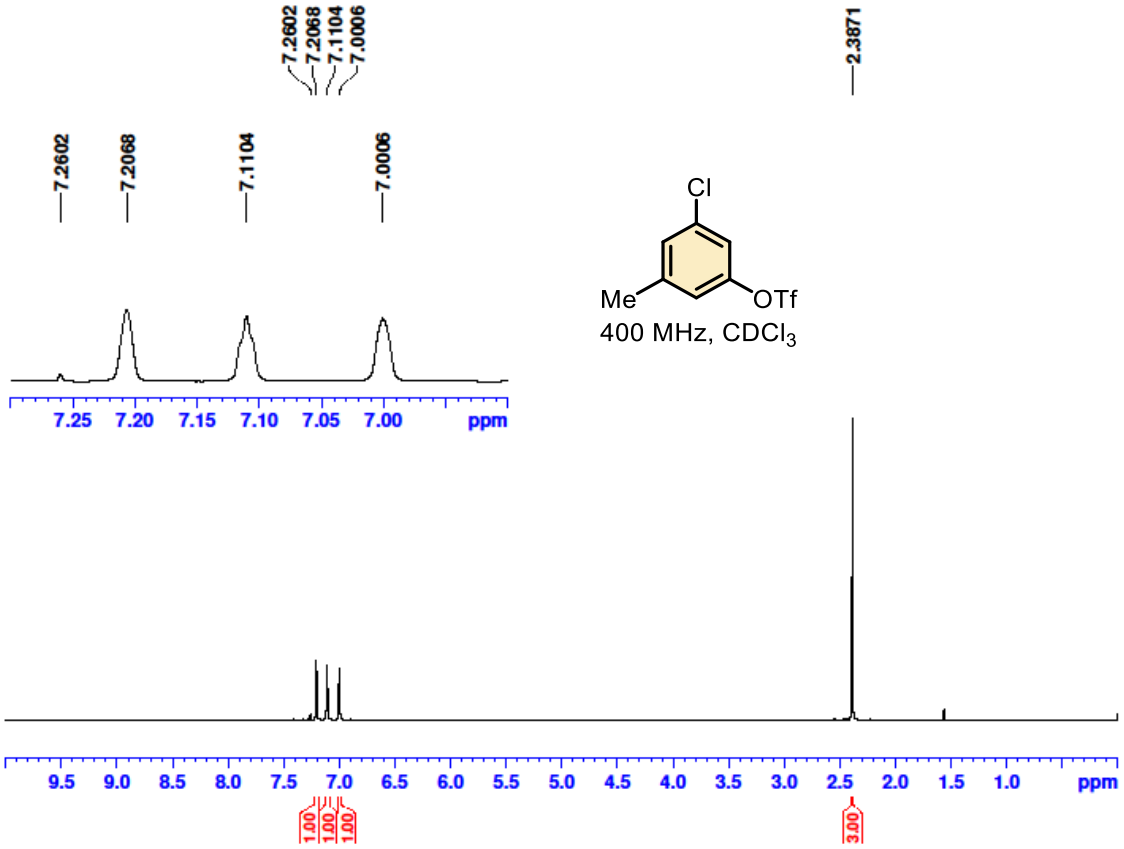

^{13}C NMR of 3-chloro-5-methylphenyl trifluoromethanesulfonate

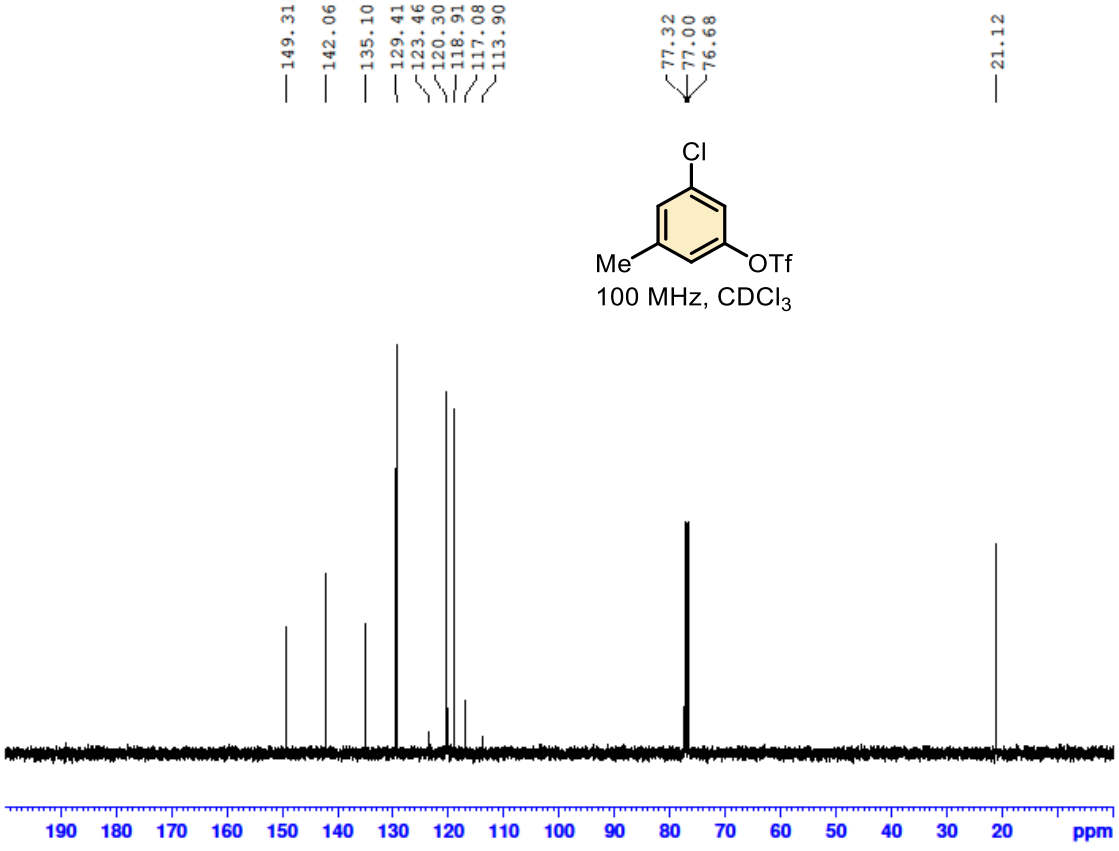

^{19}F NMR of 3-chloro-5-methylphenyl trifluoromethanesulfonate

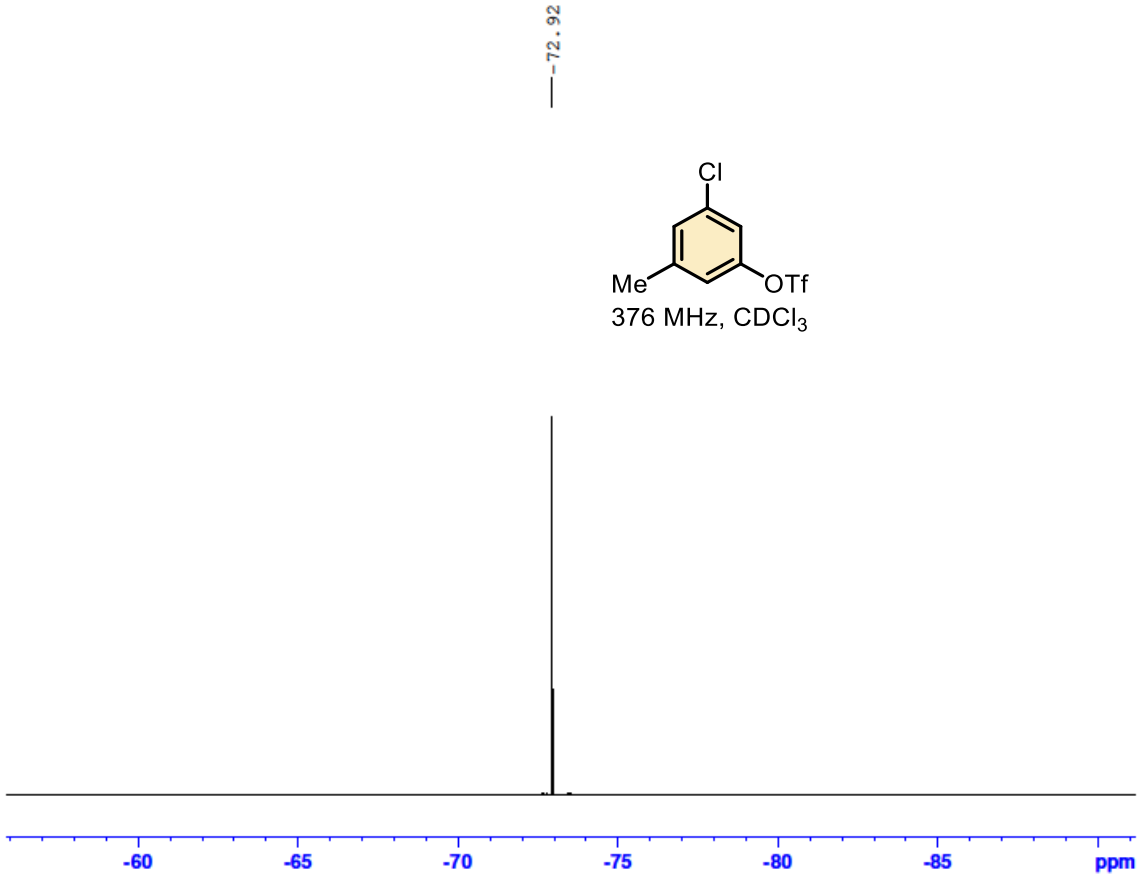

HRMS of 3-chloro-5-methylphenyl trifluoromethanesulfonate

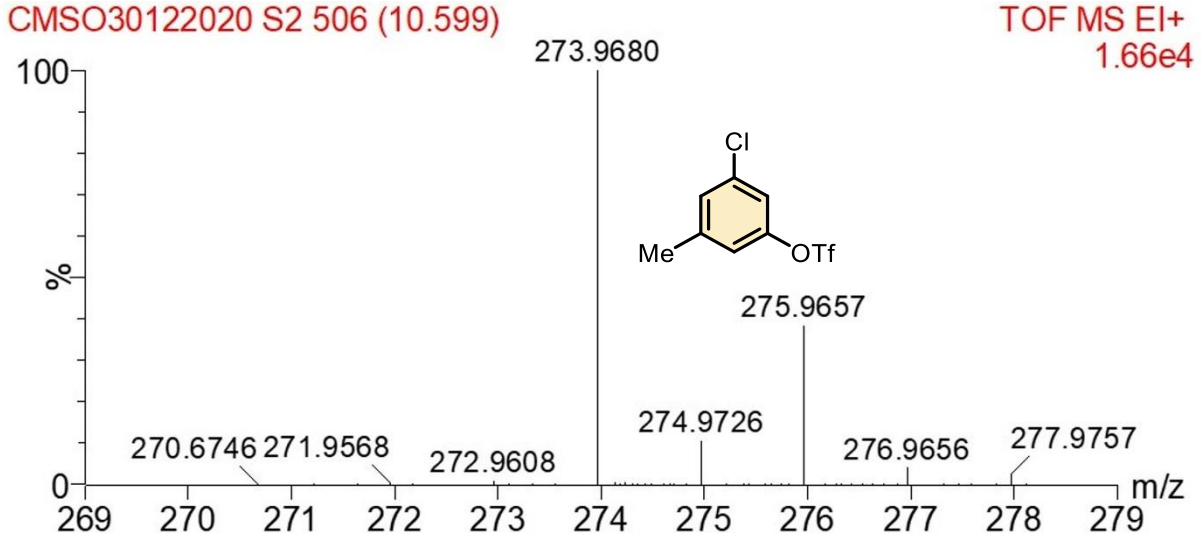

Mass	Calc. Mass	mDa	PPM	Formula
273.9680	273.9673	-0.72	-2.63	C8 H6 Cl F3 O3 S

^{1}H NMR of 2-benzyl-4-chlorophenyl trifluoromethanesulfonate

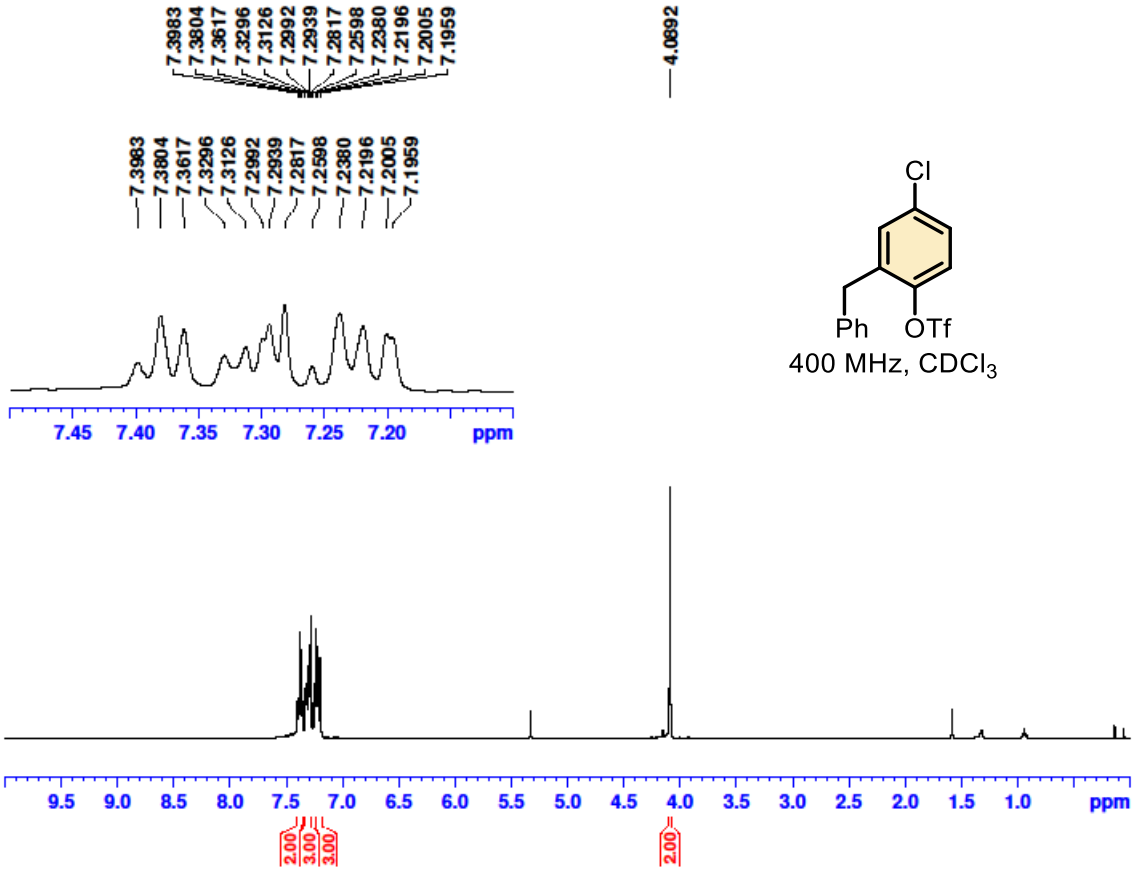

^{13}C NMR of 2-benzyl-4-chlorophenyl trifluoromethanesulfonate

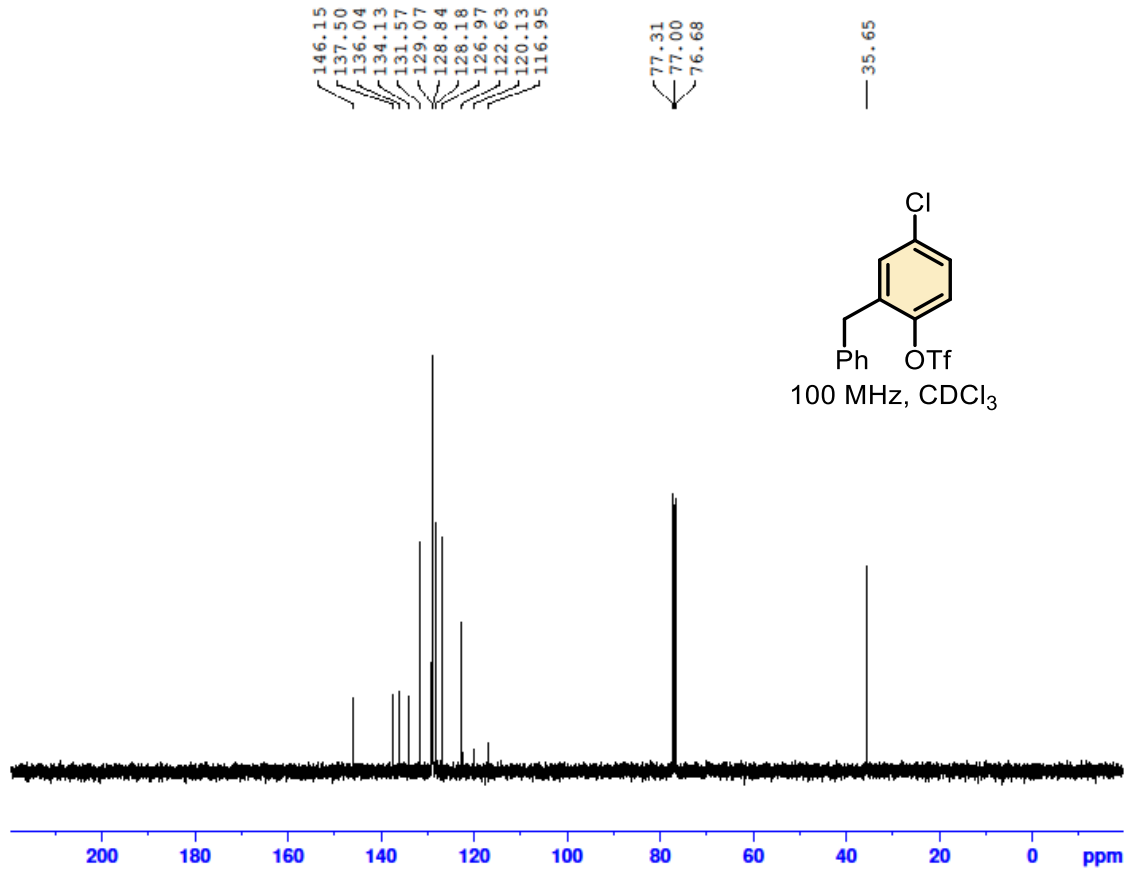

^{19}F NMR of 2-benzyl-4-chlorophenyl trifluoromethanesulfonate

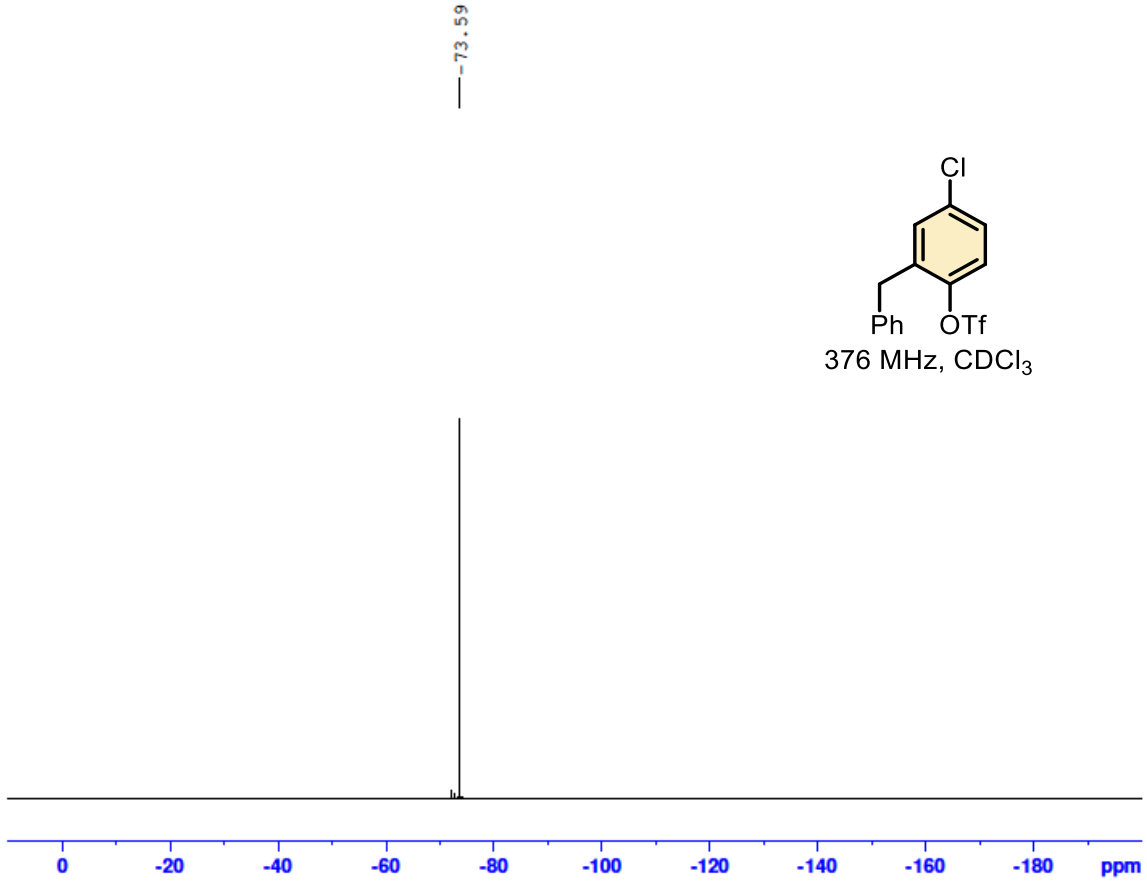

HRMS of 2-benzyl-4-chlorophenyl trifluoromethanesulfonate

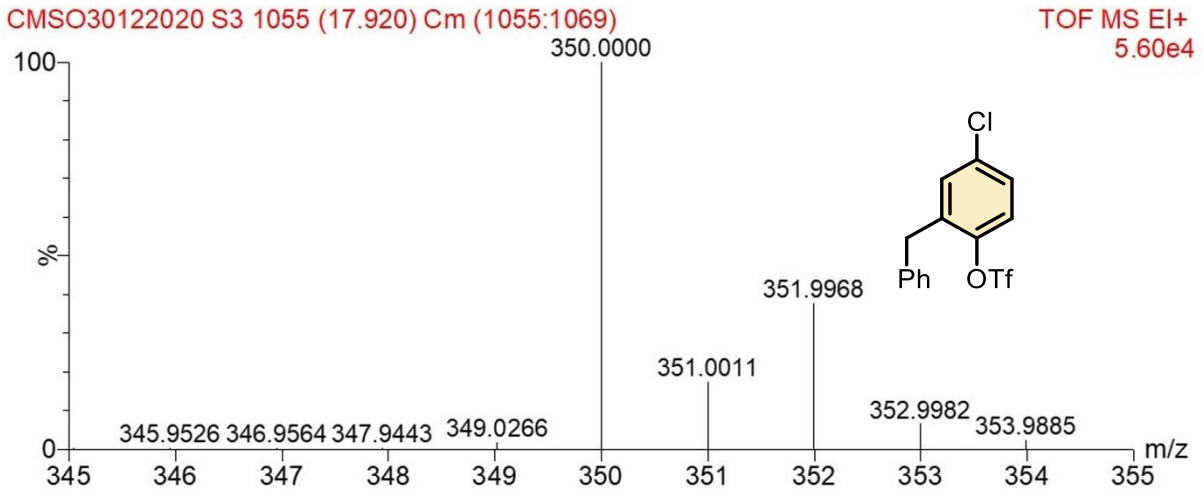

Mass	Calc. Mass	mDa	PPM	Formula
350.0000	349.9986	-1.42	-4.06	C14 H10 Cl F3 O3 S

^{1}H NMR of 2-acetyl-5-chlorophenyl trifluoromethanesulfonate

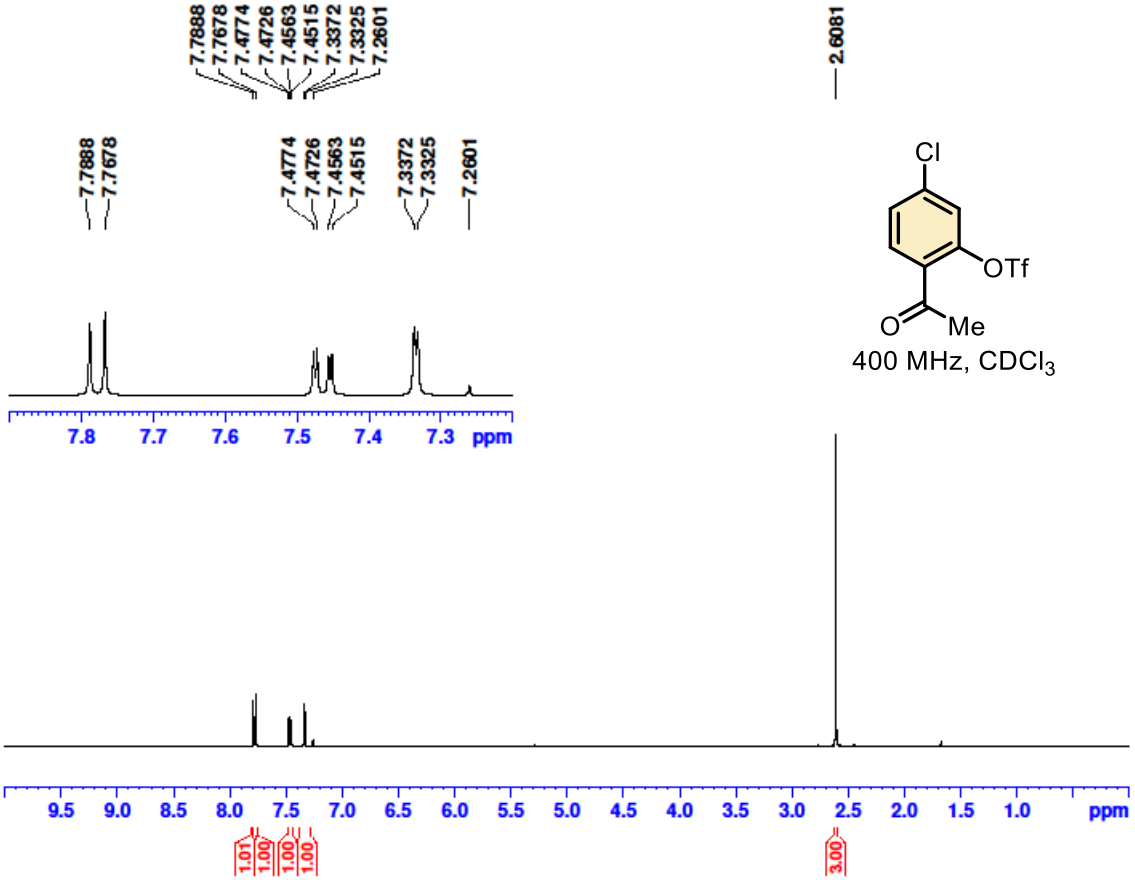

^{13}C NMR of 2-acetyl-5-chlorophenyl trifluoromethanesulfonate

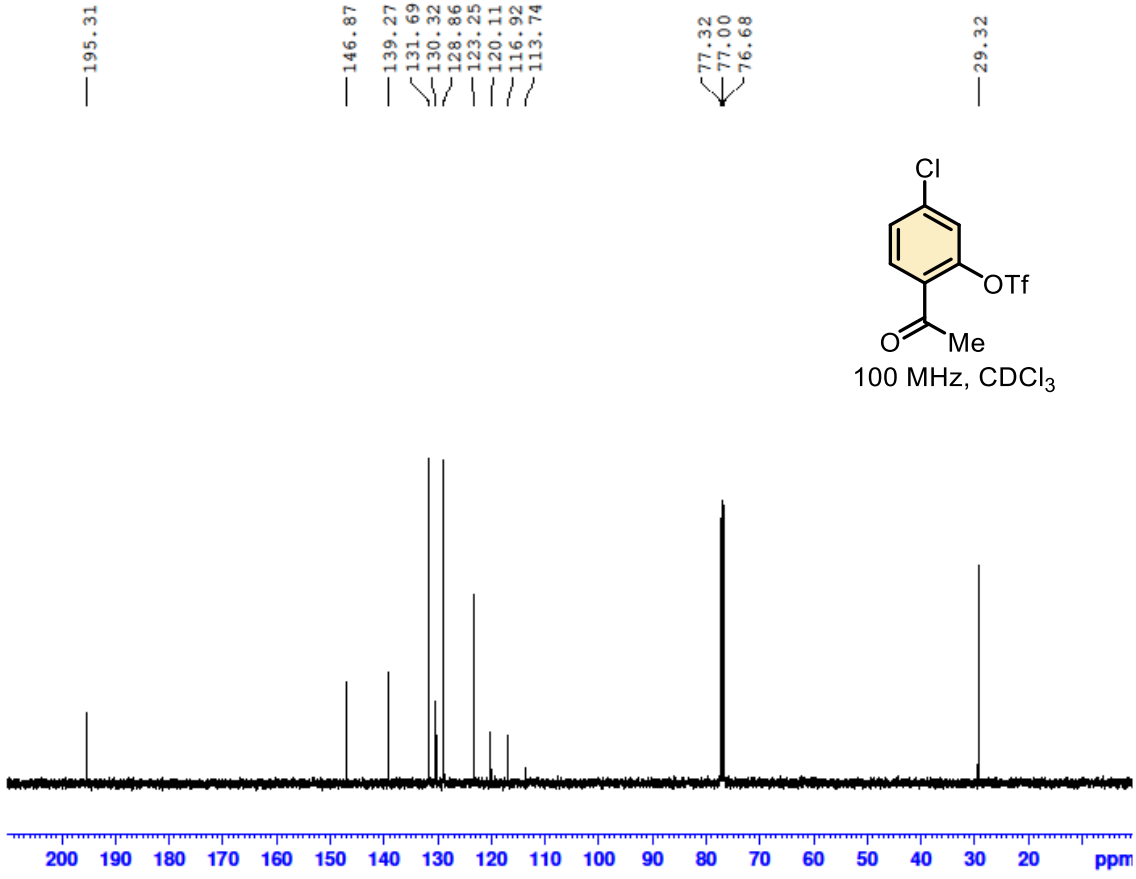

^{19}F NMR of 2-acetyl-5-chlorophenyl trifluoromethanesulfonate

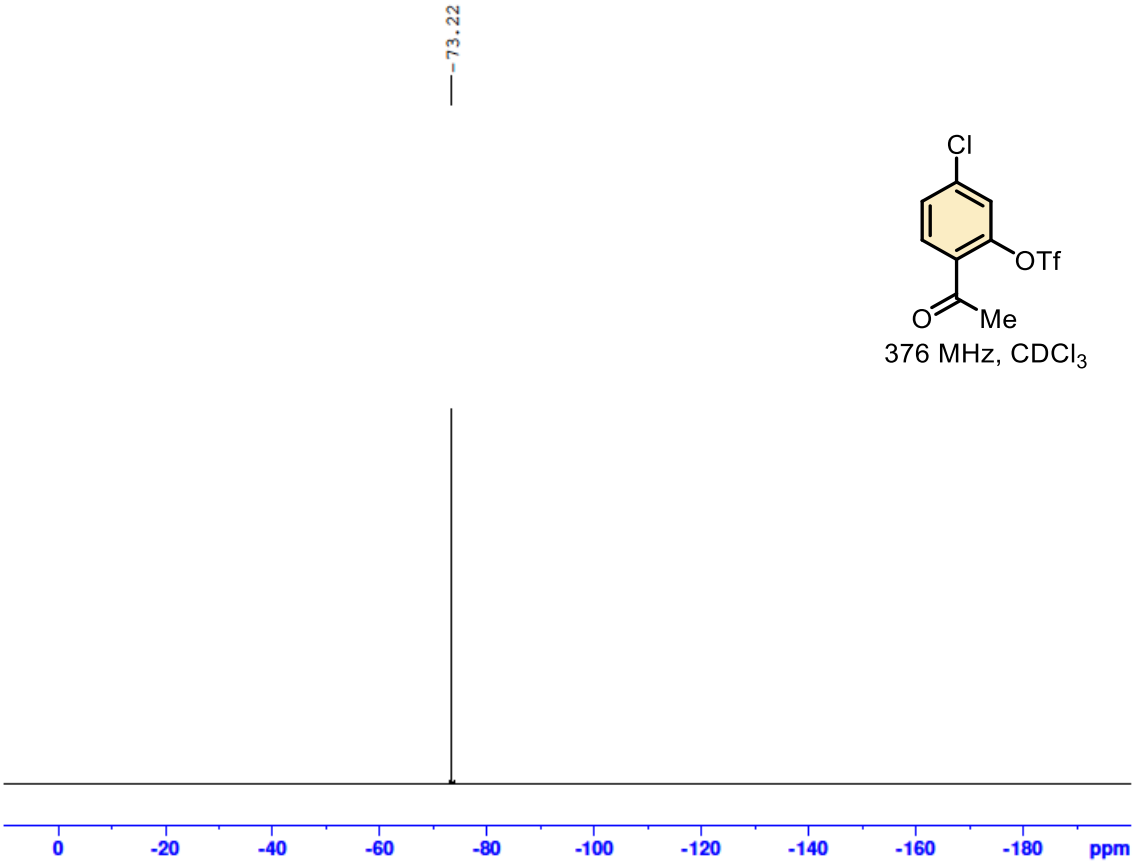

HRMS of 2-acetyl-5-chlorophenyl trifluoromethanesulfonate

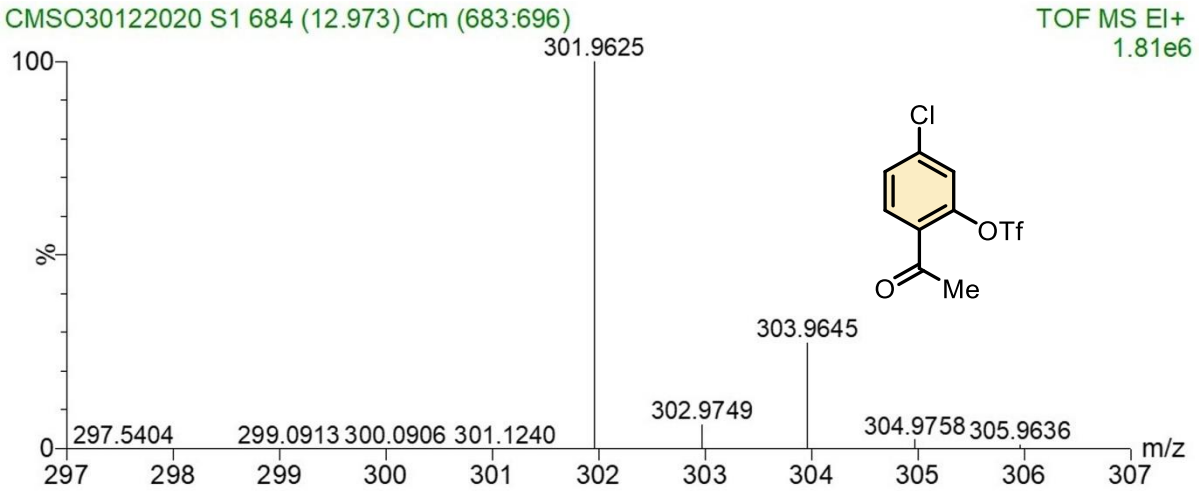

Mass	Calc. Mass	mDa	PPM	Formula
301.9625	301.9622	-0.31	-1.02	C9 H6 Cl F3 O4 S

^{1}H NMR of 4-(4,4,5,5-tetramethyl-1,3,2-dioxaborolan-2-yl)phenyl trifluoromethanesulfonate

(Table 3.3 and Scheme 3.4, compound **9a**)

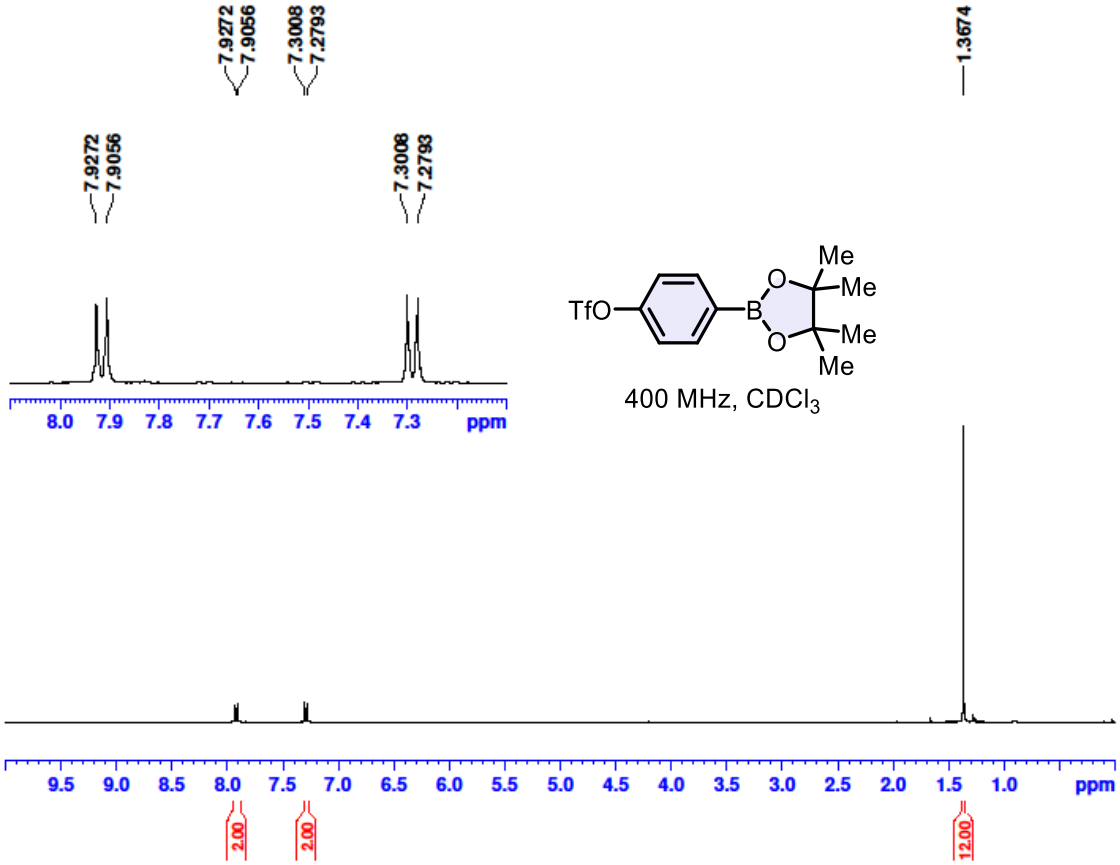

^{13}C NMR of 4-(4,4,5,5-tetramethyl-1,3,2-dioxaborolan-2-yl)phenyl trifluoromethanesulfonate

(Table 3.3 and Scheme 3.4, compound **9a**)

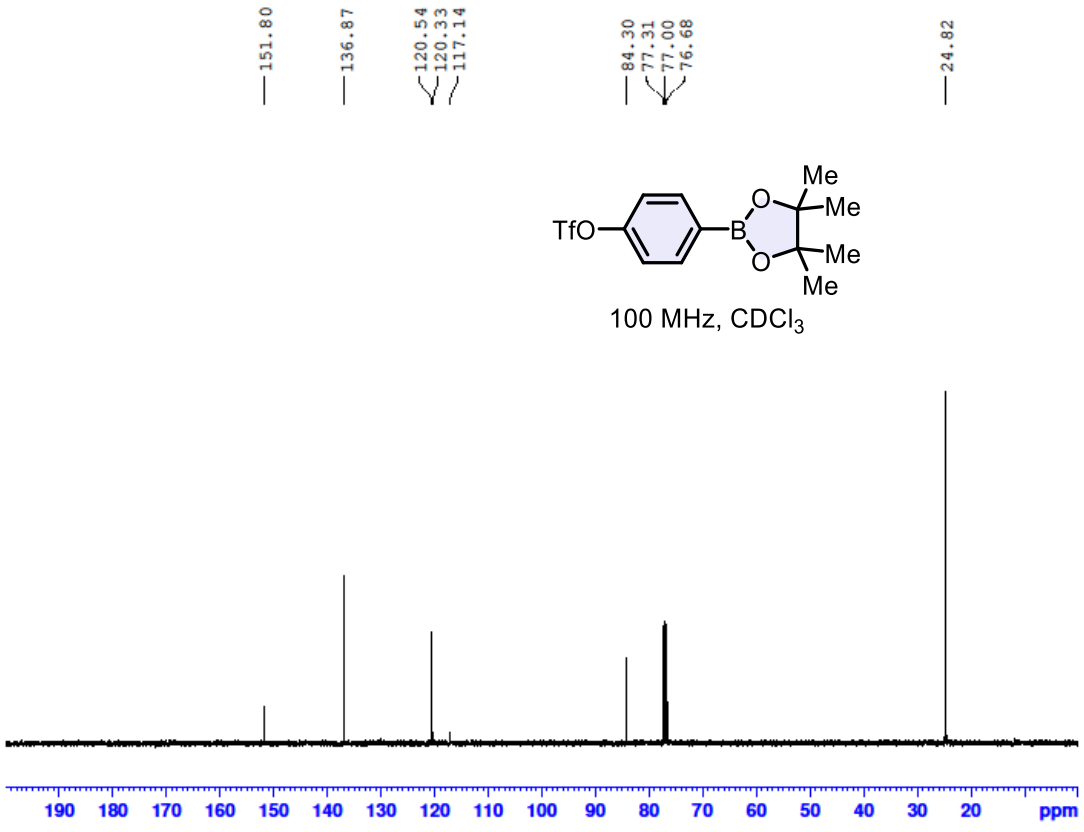

^{19}F NMR of 4-(4,4,5,5-tetramethyl-1,3,2-dioxaborolan-2-yl)phenyl trifluoromethanesulfonate (Table 3.3 and Scheme 3.4, compound **9a**)

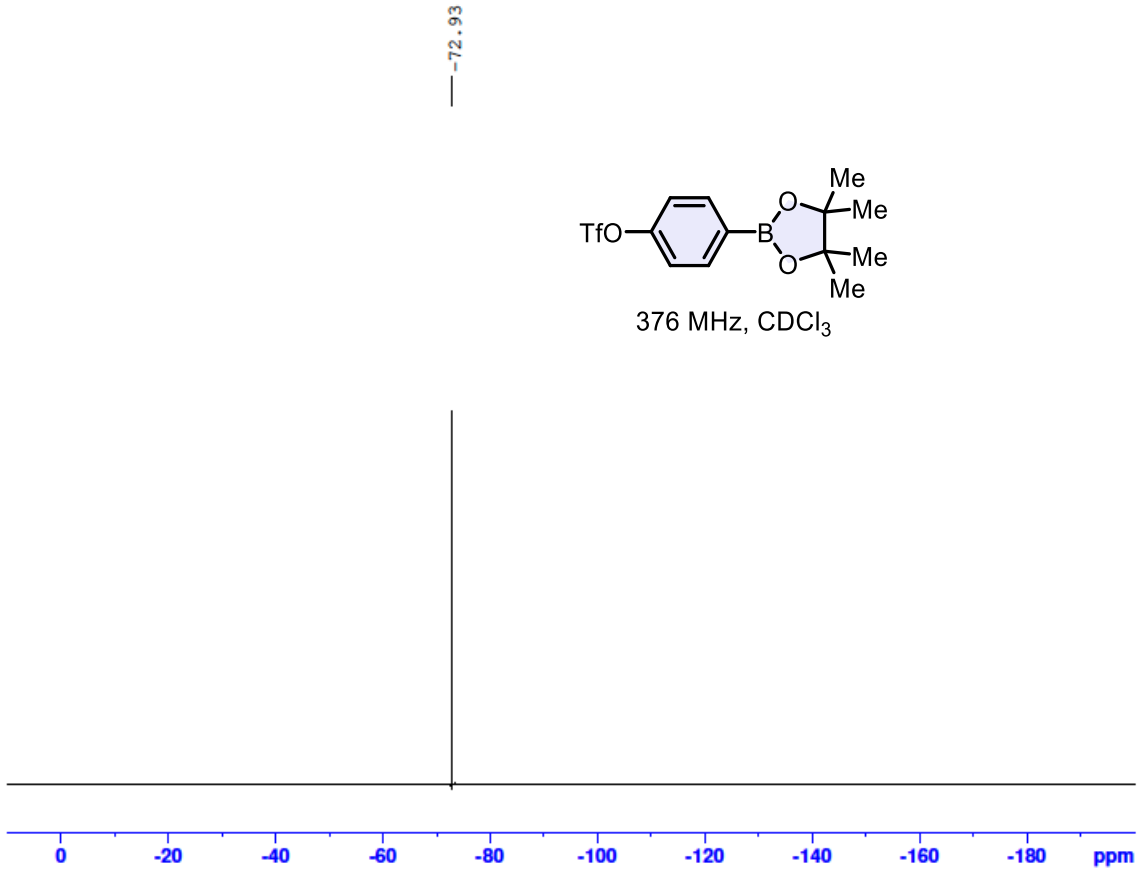

^{1}H NMR of 3-(4,4,5,5-tetramethyl-1,3,2-dioxaborolan-2-yl)phenyl trifluoromethanesulfonate (Table 3.3, compound **9b**)

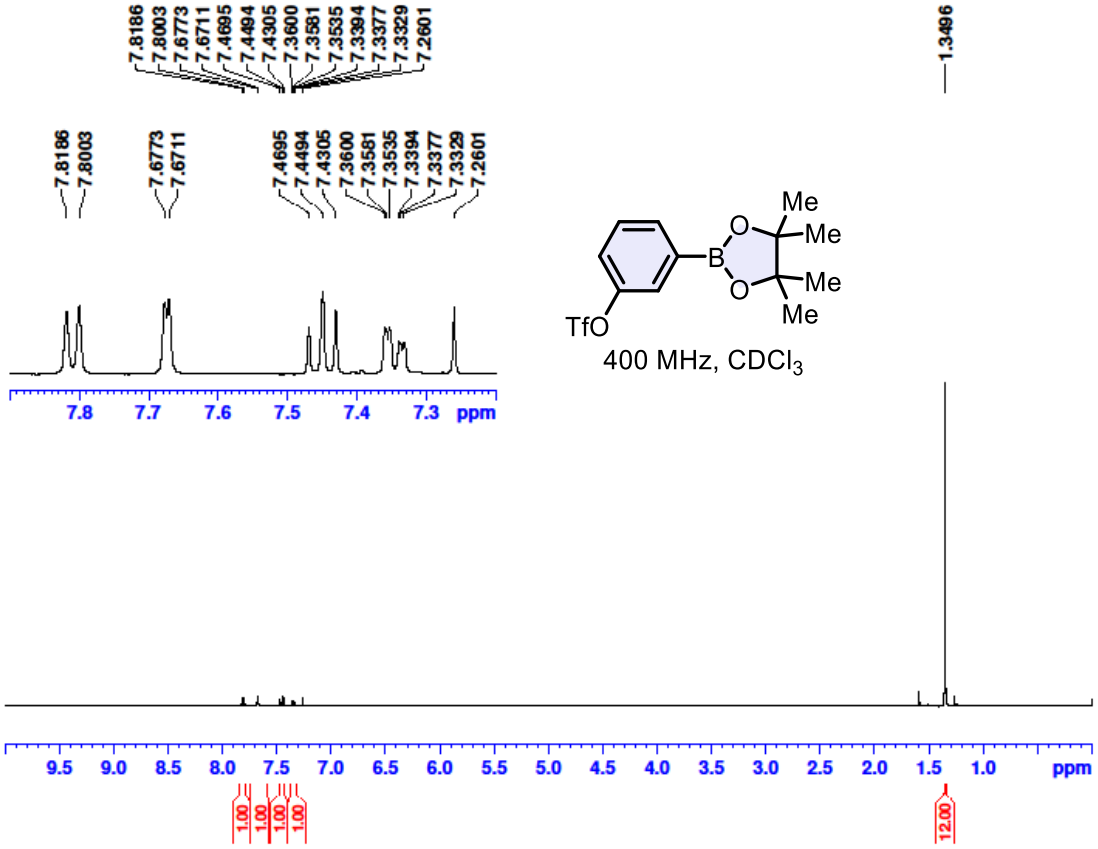

^{13}C NMR of 3-(4,4,5,5-tetramethyl-1,3,2-dioxaborolan-2-yl)phenyl trifluoromethanesulfonate (Table 3.3, compound **9b**)

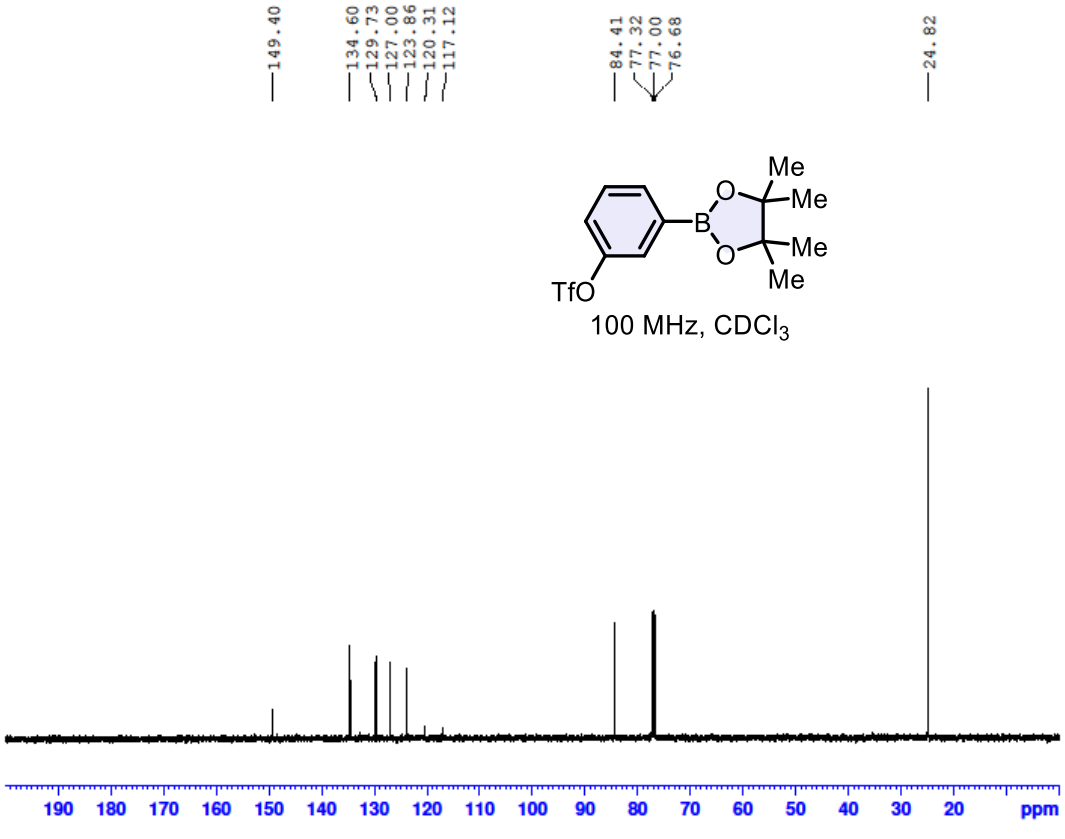

^{19}F NMR of 3-(4,4,5,5-tetramethyl-1,3,2-dioxaborolan-2-yl)phenyl trifluoromethanesulfonate (Table 3.3, compound **9b**)

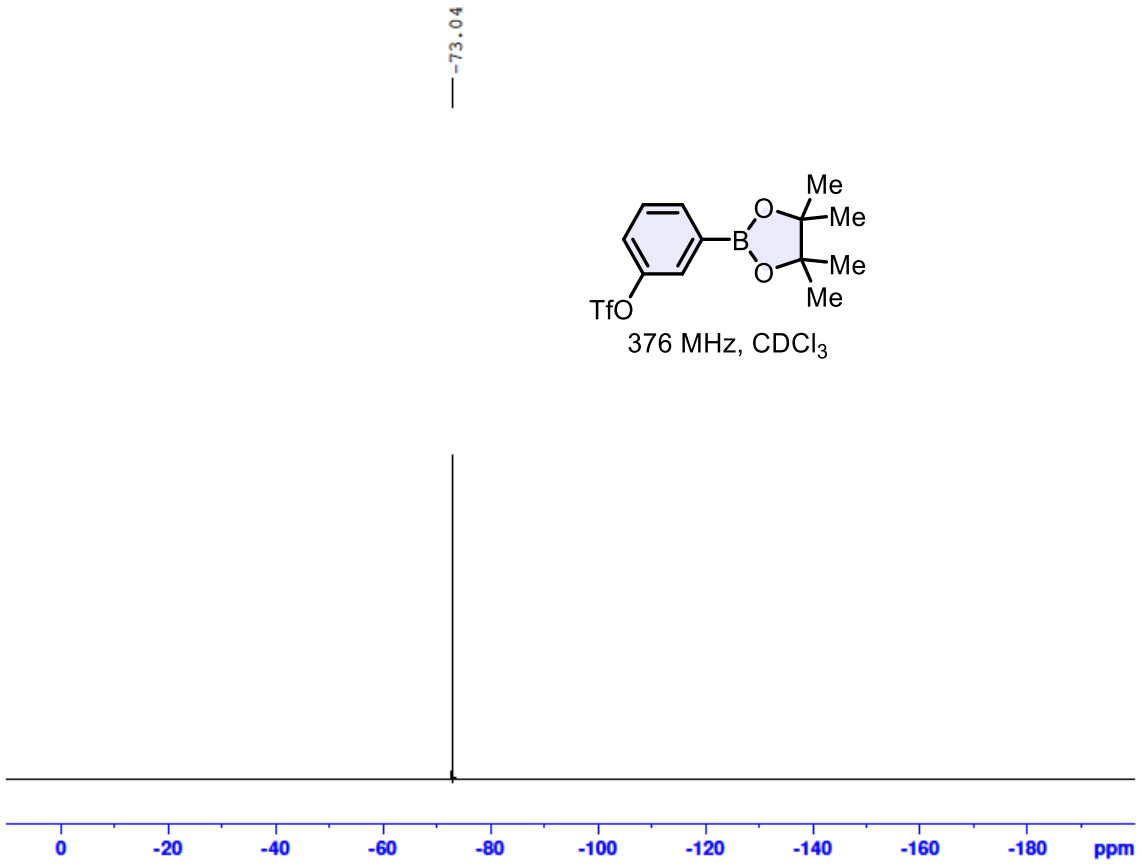

^{1}H NMR of 3-methoxy-5-(4,4,5,5-tetramethyl-1,3,2-dioxaborolan-2-yl)phenyl trifluoromethanesulfonate (Table 3.3, compound **9c**)

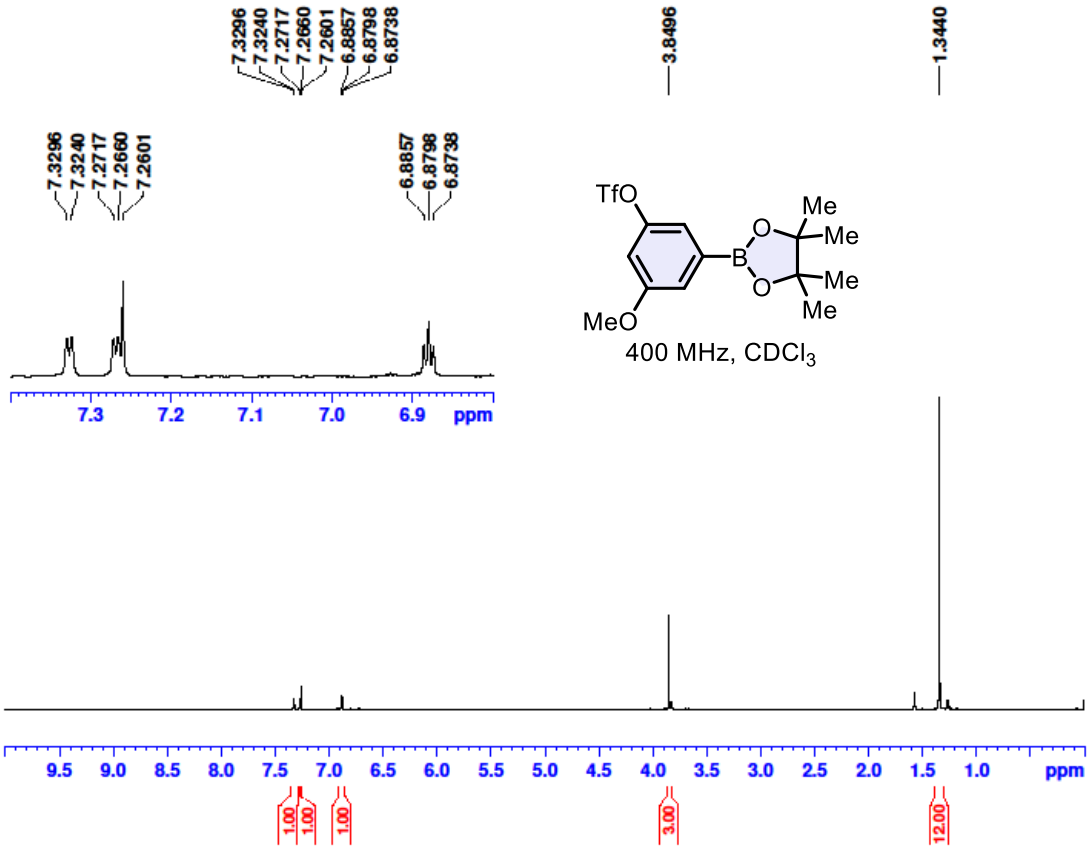

^{13}C NMR of 3-methoxy-5-(4,4,5,5-tetramethyl-1,3,2-dioxaborolan-2-yl)phenyl trifluoromethanesulfonate (Table 3.3, compound **9c**)

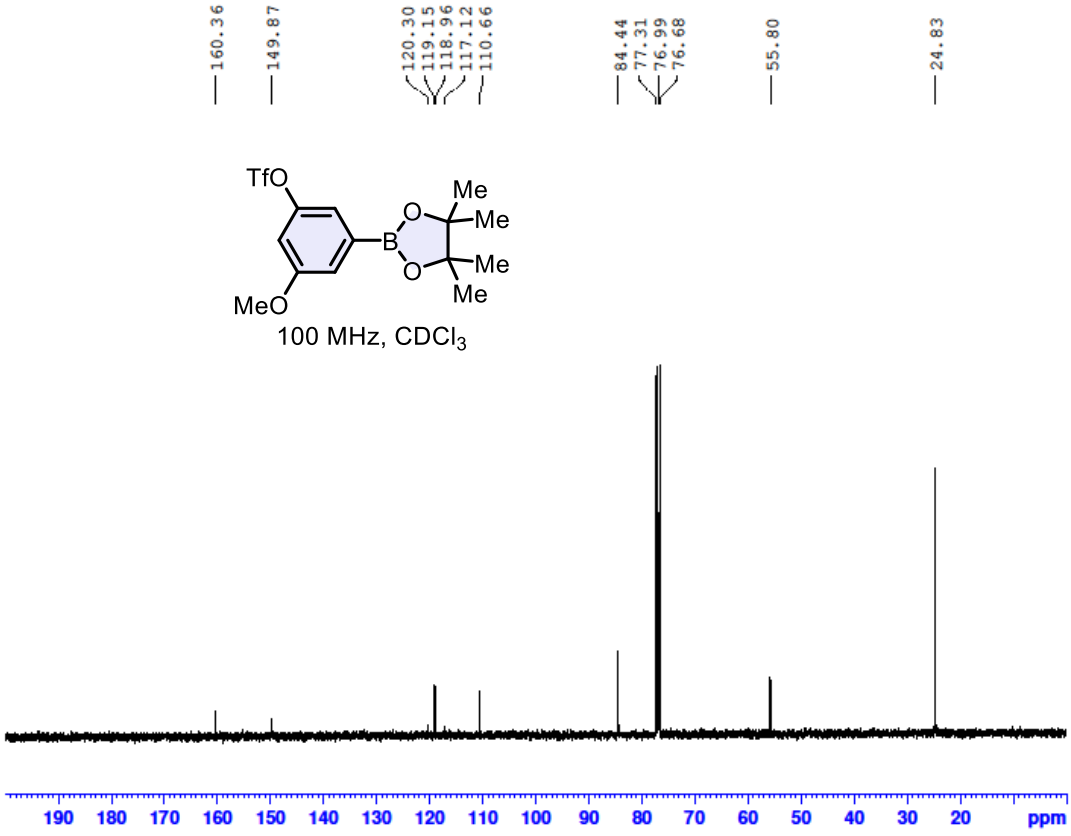

^{19}F NMR of 3-methoxy-5-(4,4,5,5-tetramethyl-1,3,2-dioxaborolan-2-yl)phenyl trifluoromethanesulfonate (Table 3.3, compound **9c**)

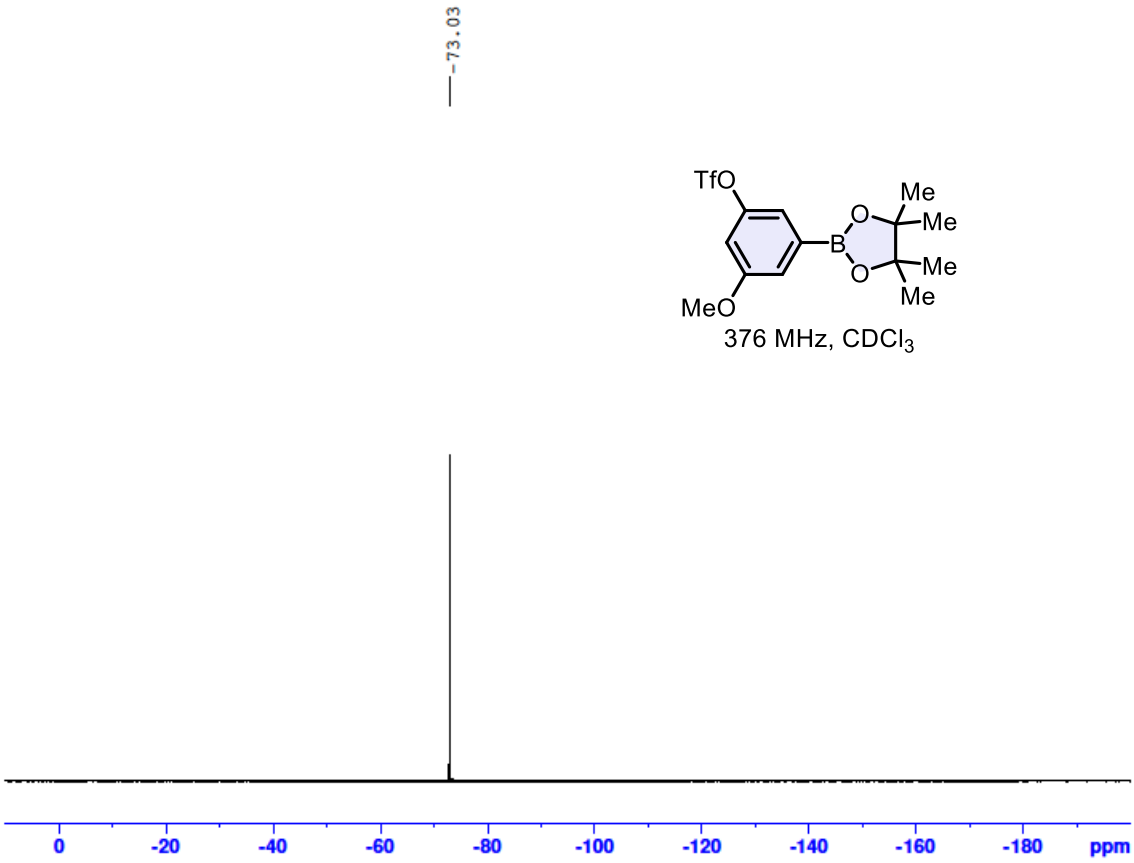

HRMS of3-methoxy-5-(4,4,5,5-tetramethyl-1,3,2-dioxaborolan-2-yl)phenyl trifluoromethanesulfonate (Table 3.3, compound **9c**)

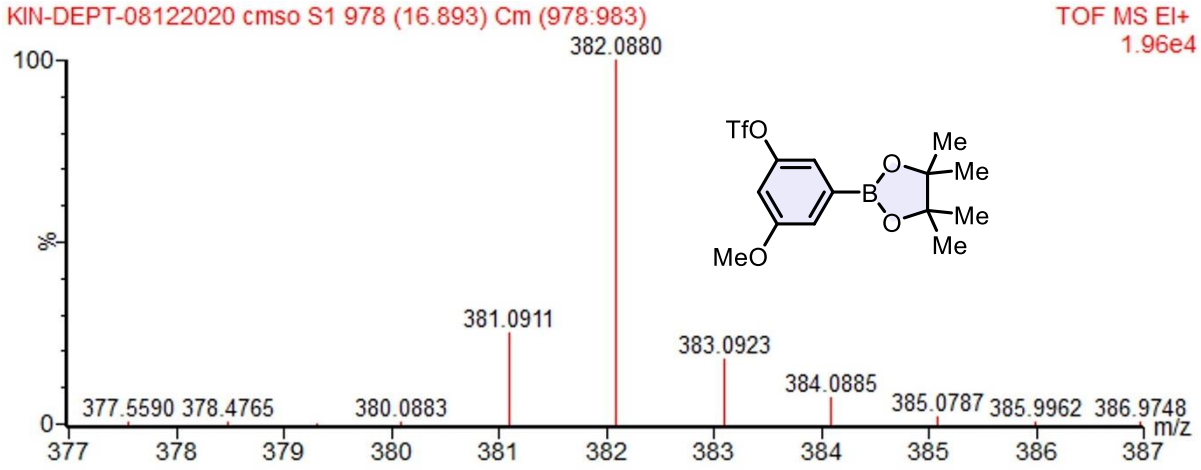

Mass	Calc. Mass	mDa	PPM	Formula
382.0880	382.0866	-1.36	-3.55	C14 H18 B F3 O6 S

^{1}H NMR of 3-fluoro-5-(4,4,5,5-tetramethyl-1,3,2-dioxaborolan-2-yl)phenyl trifluoromethanesulfonate (Table 3.3, compound **9d**)

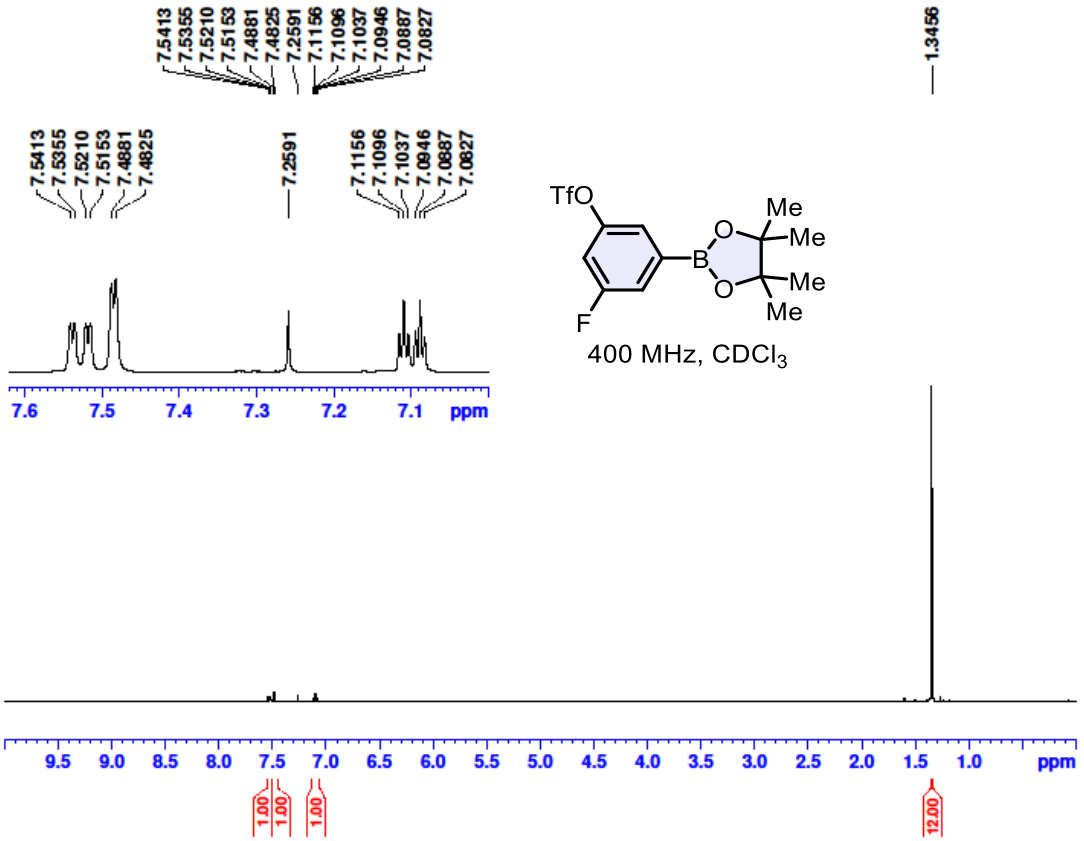

^{13}C NMR of 3-fluoro-5-(4,4,5,5-tetramethyl-1,3,2-dioxaborolan-2-yl)phenyl trifluoromethanesulfonate (Table 3.3, compound **9d**)

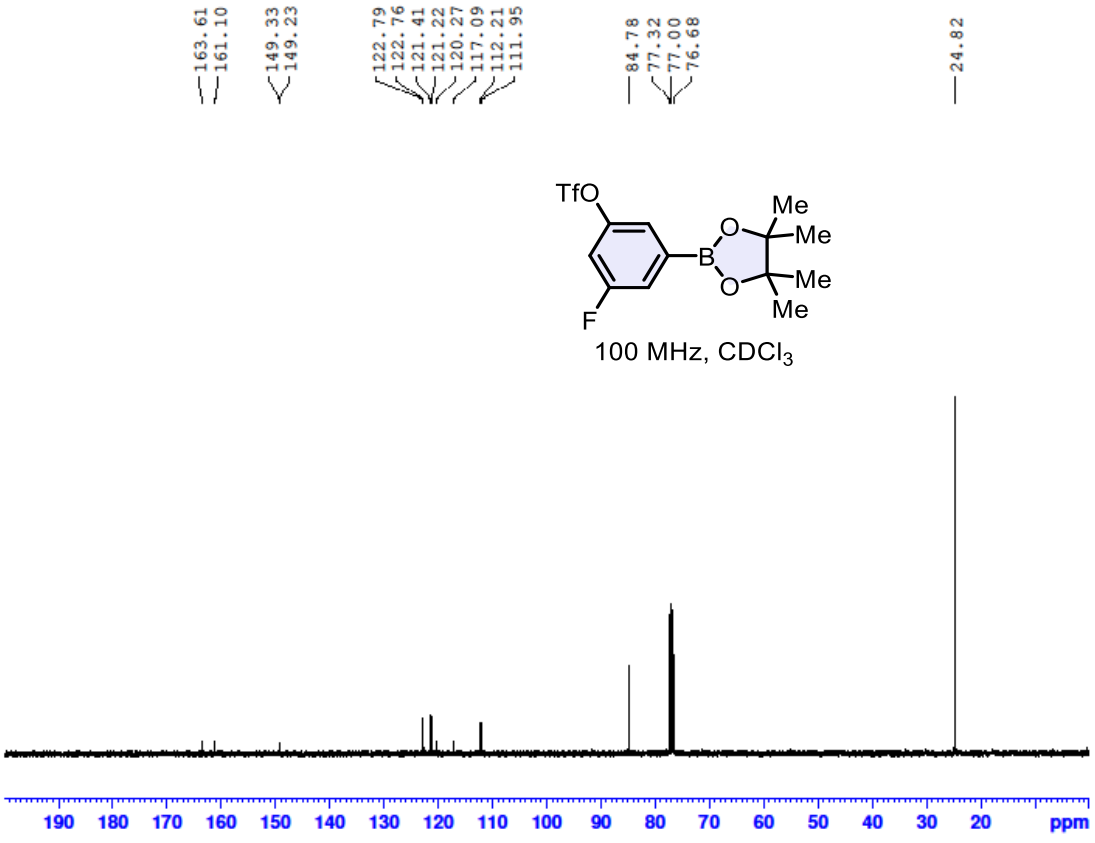

^{19}F NMR of 3-fluoro-5-(4,4,5,5-tetramethyl-1,3,2-dioxaborolan-2-yl)phenyl trifluoromethanesulfonate (Table 3.3, compound **9d**)

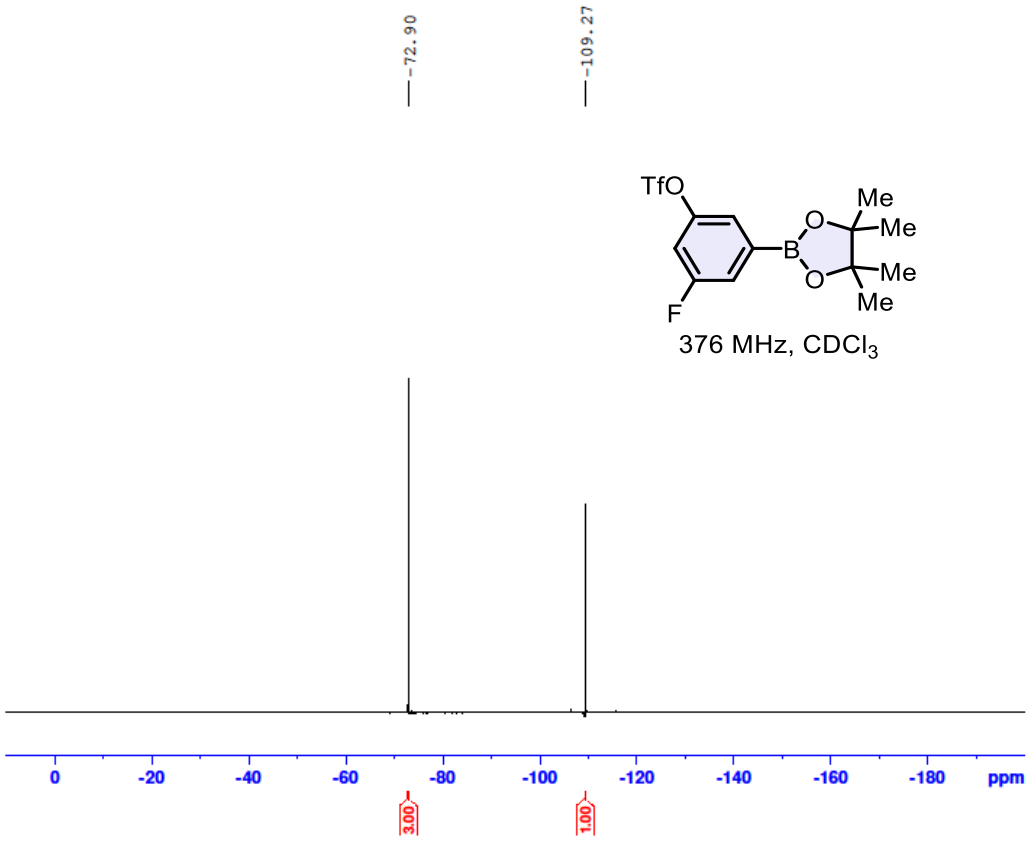

HRMS of 3-fluoro-5-(4,4,5,5-tetramethyl-1,3,2-dioxaborolan-2-yl)phenyl trifluoromethanesulfonate (Table 3.3, compound **9d**)

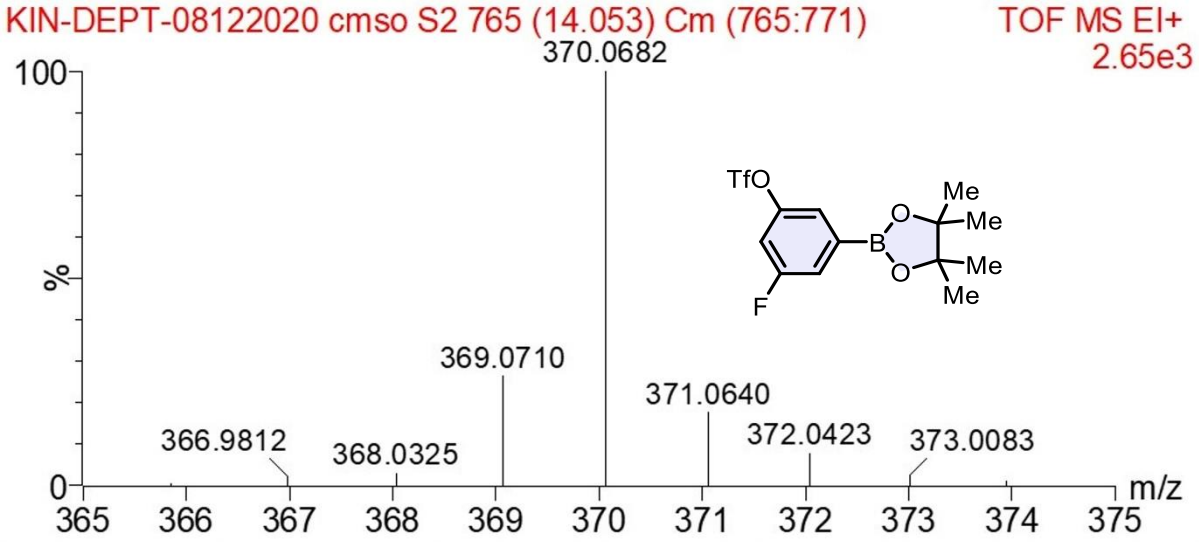

Mass	Calc. Mass	mDa	PPM	Formula
370.0682	370.0666	-1.56	-4.22	C13 H15 B F4 O5 S

^{1}H NMR of 2-methyl-4-(4,4,5,5-tetramethyl-1,3,2-dioxaborolan-2-yl)phenyl trifluoromethanesulfonate (Table 3.3, compound **9e**)

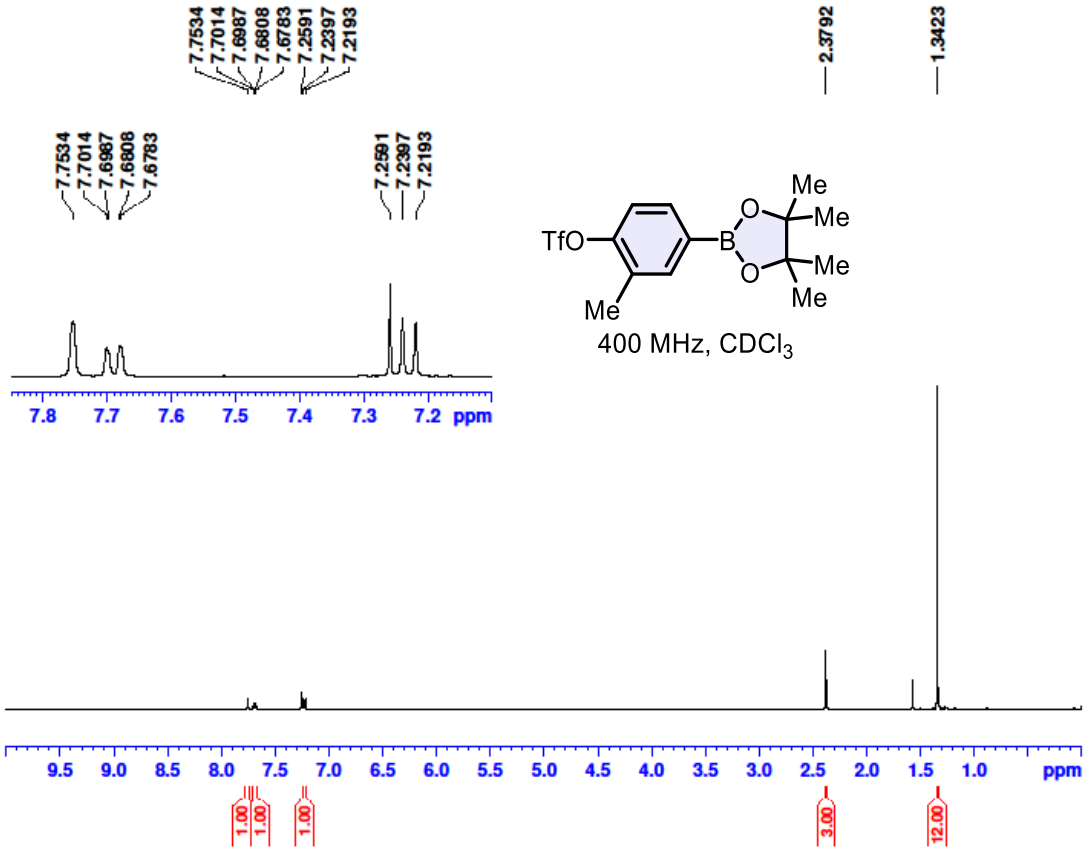

^{13}C NMR of 2-methyl-4-(4,4,5,5-tetramethyl-1,3,2-dioxaborolan-2-yl)phenyl trifluoromethanesulfonate (Table 3.3, compound **9e**)

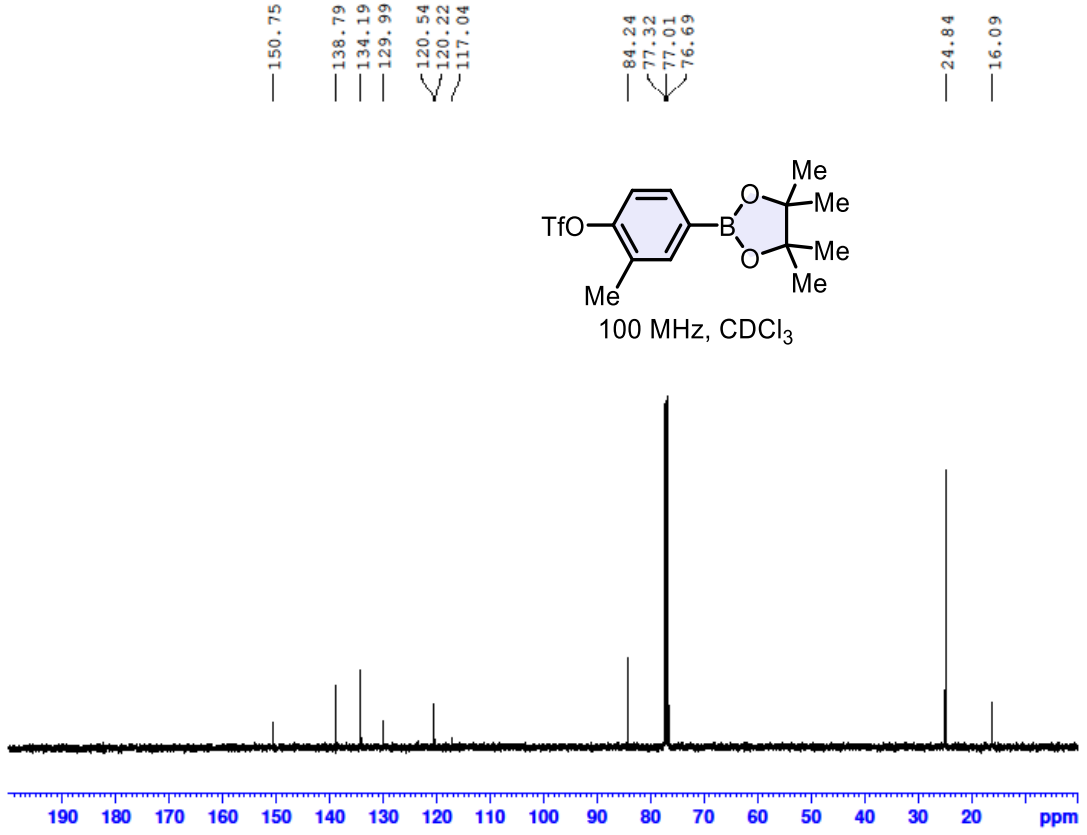

^{19}F NMR of 2-methyl-4-(4,4,5,5-tetramethyl-1,3,2-dioxaborolan-2-yl)phenyl trifluoromethanesulfonate (Table 3.3, compound **9e**)

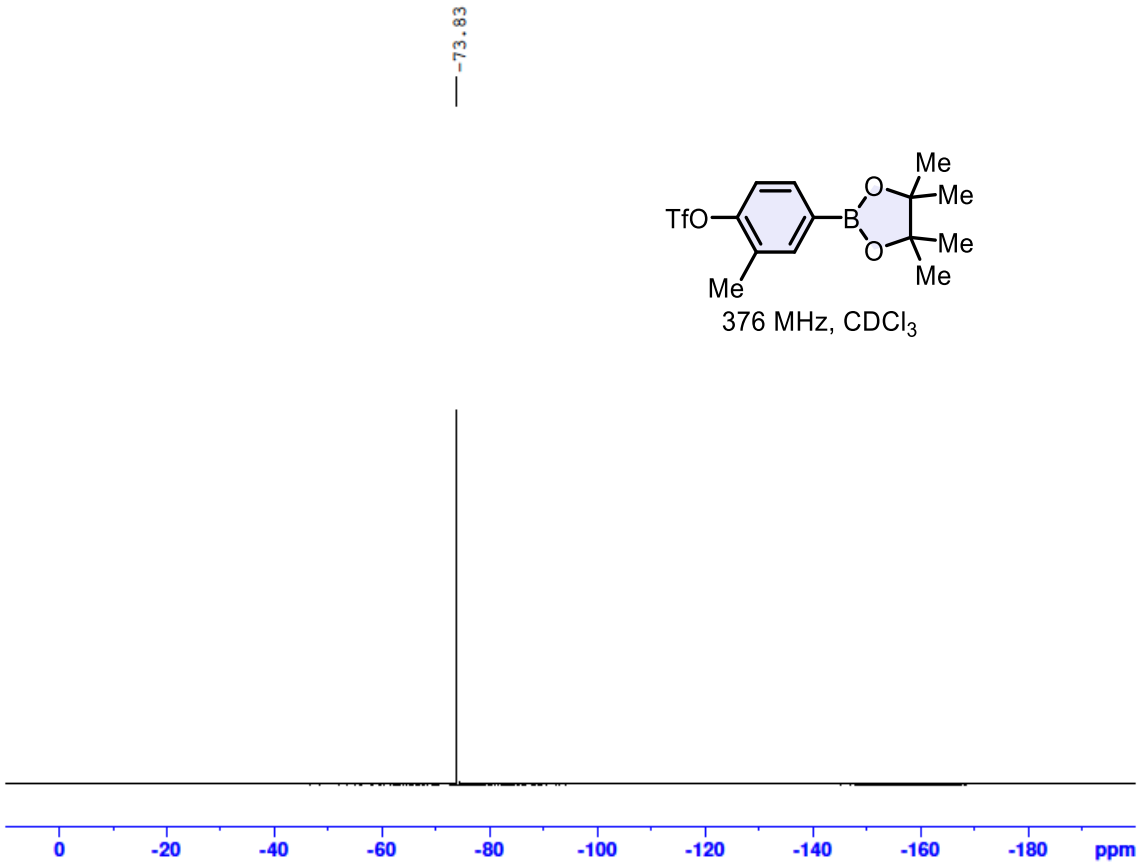

HRMS of 2-methyl-4-(4,4,5,5-tetramethyl-1,3,2-dioxaborolan-2-yl)phenyl trifluoromethanesulfonate (Table 3.3, compound **9e**)

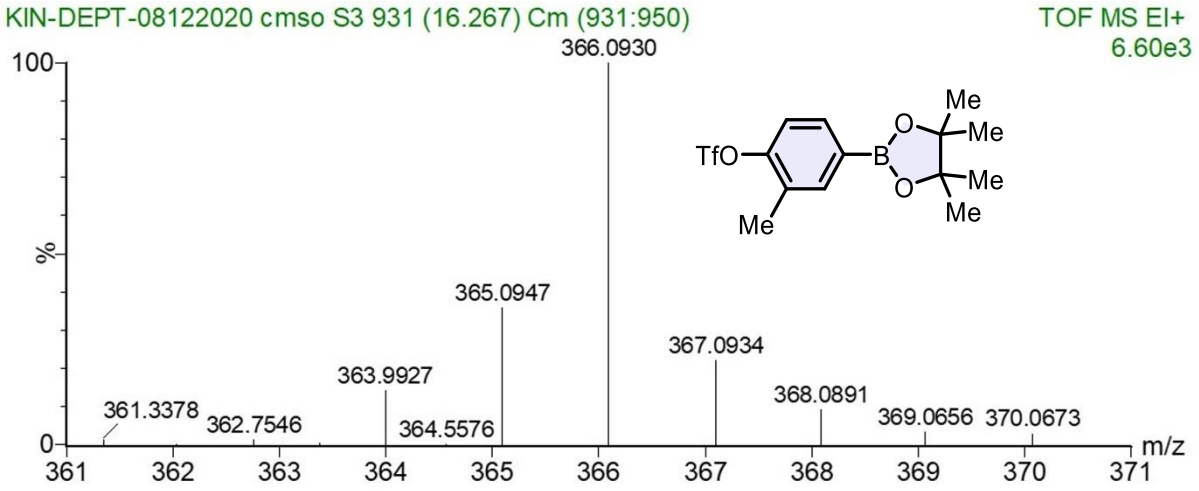

Mass	Calc. Mass	mDa	PPM	Formula
366.0930	366.0917	-1.27	-3.48	C14 H18 B F3 O5 S

^{1}H NMR of 2-fluoro-4-(4,4,5,5-tetramethyl-1,3,2-dioxaborolan-2-yl)phenyl trifluoromethanesulfonate (Table 3.3, compound **9f**)

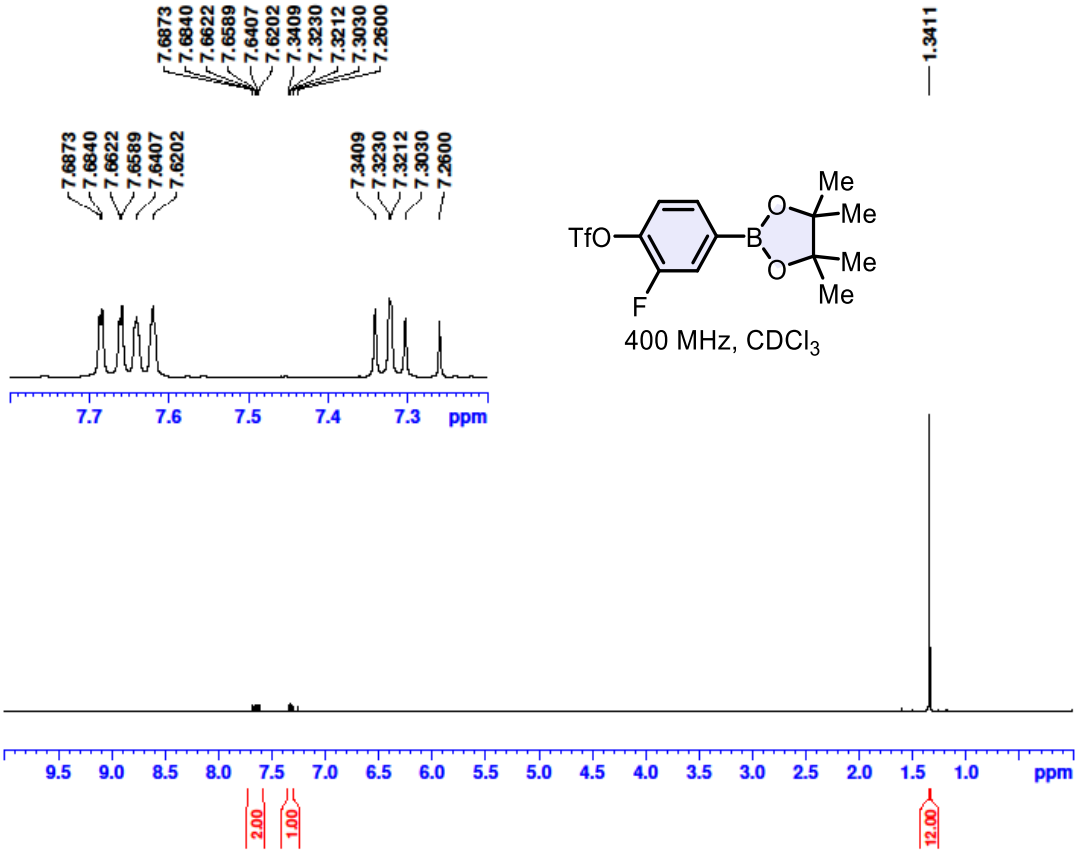

^{13}C NMR of 2-fluoro-4-(4,4,5,5-tetramethyl-1,3,2-dioxaborolan-2-yl)phenyl trifluoromethanesulfonate (Table 3.3, compound **9f**)

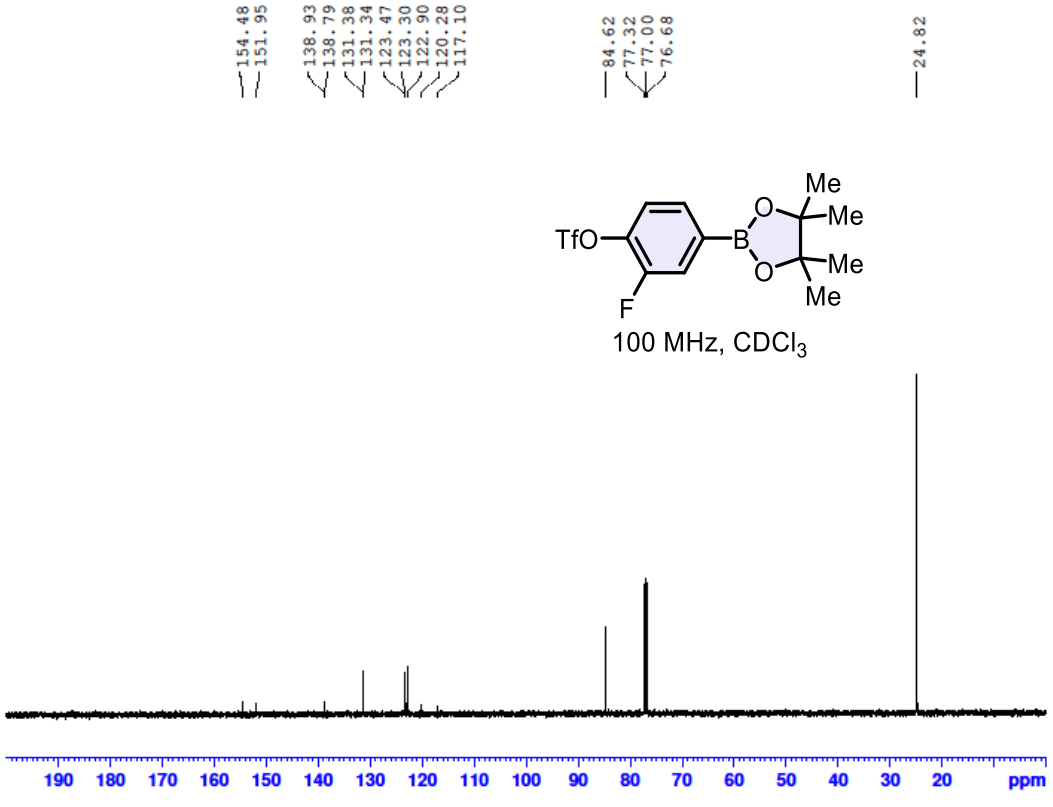

^{19}F NMR of 2-fluoro-4-(4,4,5,5-tetramethyl-1,3,2-dioxaborolan-2-yl)phenyl trifluoromethanesulfonate (Table 3.3, compound **9f**)

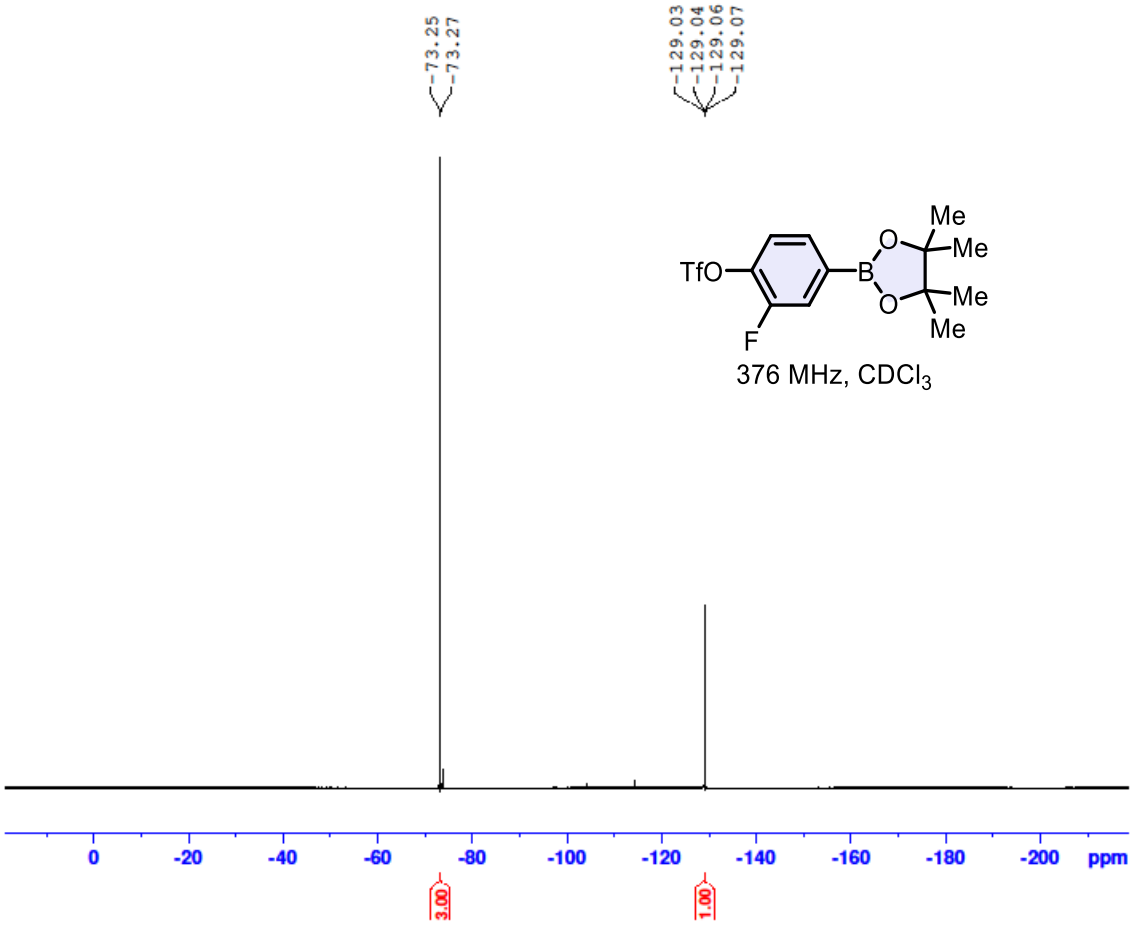

HRMS of 2-fluoro-4-(4,4,5,5-tetramethyl-1,3,2-dioxaborolan-2-yl)phenyl trifluoromethanesulfonate (Table 3.3, compound **9f**)

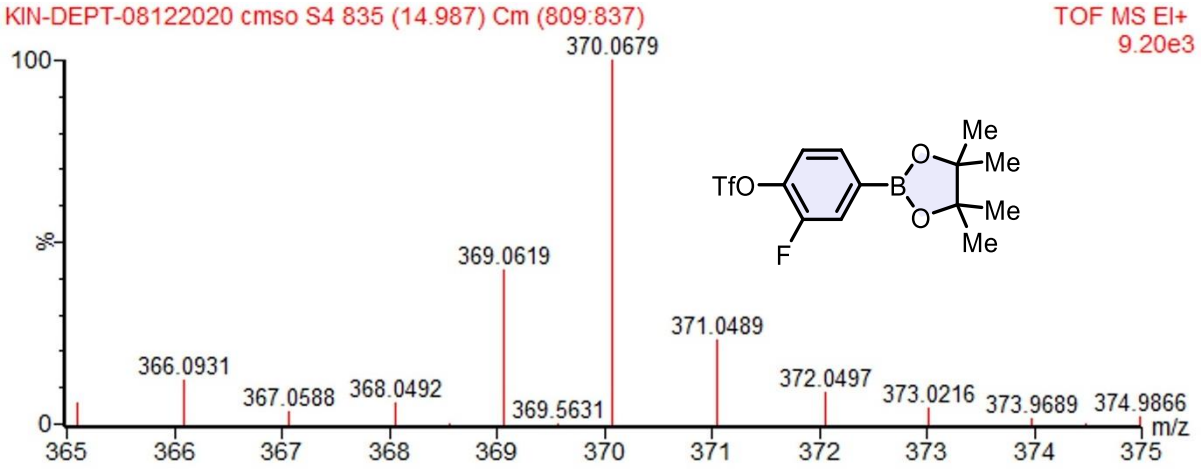

Mass	Calc. Mass	mDa	PPM	Formula
370.0679	370.0666	-1.26	-3.41	C13 H15 B F4 O5 S

^{1}H NMR of 5-(4,4,5,5-tetramethyl-1,3,2-dioxaborolan-2-yl)pyridin-3-yl trifluoromethanesulfonate (Table 3.3, compound **9g**)

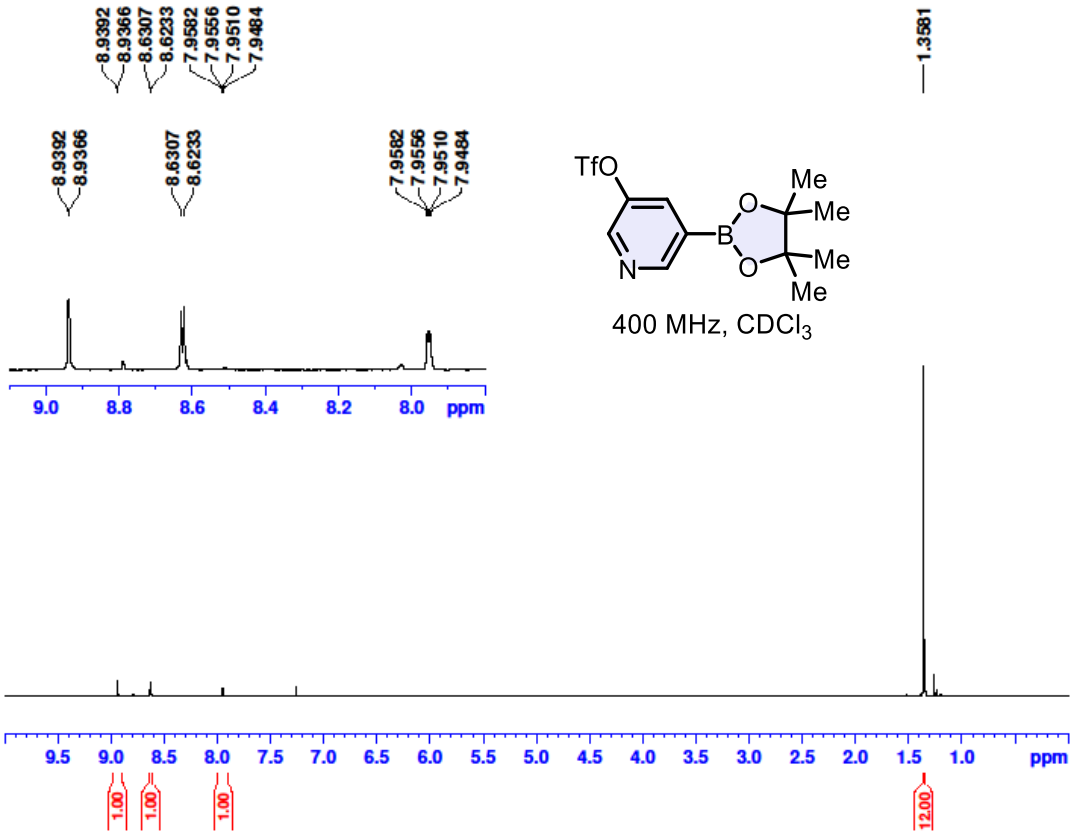

^{13}C NMR of 5-(4,4,5,5-tetramethyl-1,3,2-dioxaborolan-2-yl)pyridin-3-yl trifluoromethanesulfonate (Table 3.3, compound **9g**)

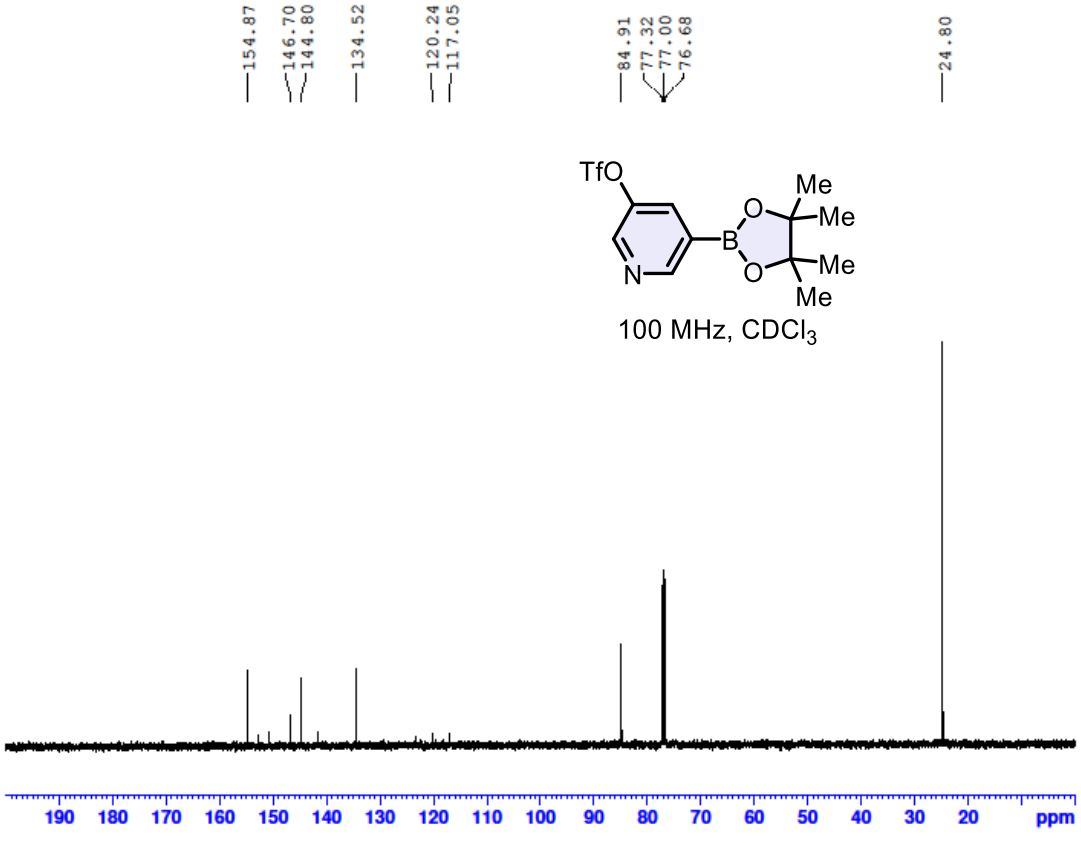

^{19}F NMR of 5-(4,4,5,5-tetramethyl-1,3,2-dioxaborolan-2-yl)pyridin-3-yl trifluoromethanesulfonate (Table 3.3, compound **9g**)

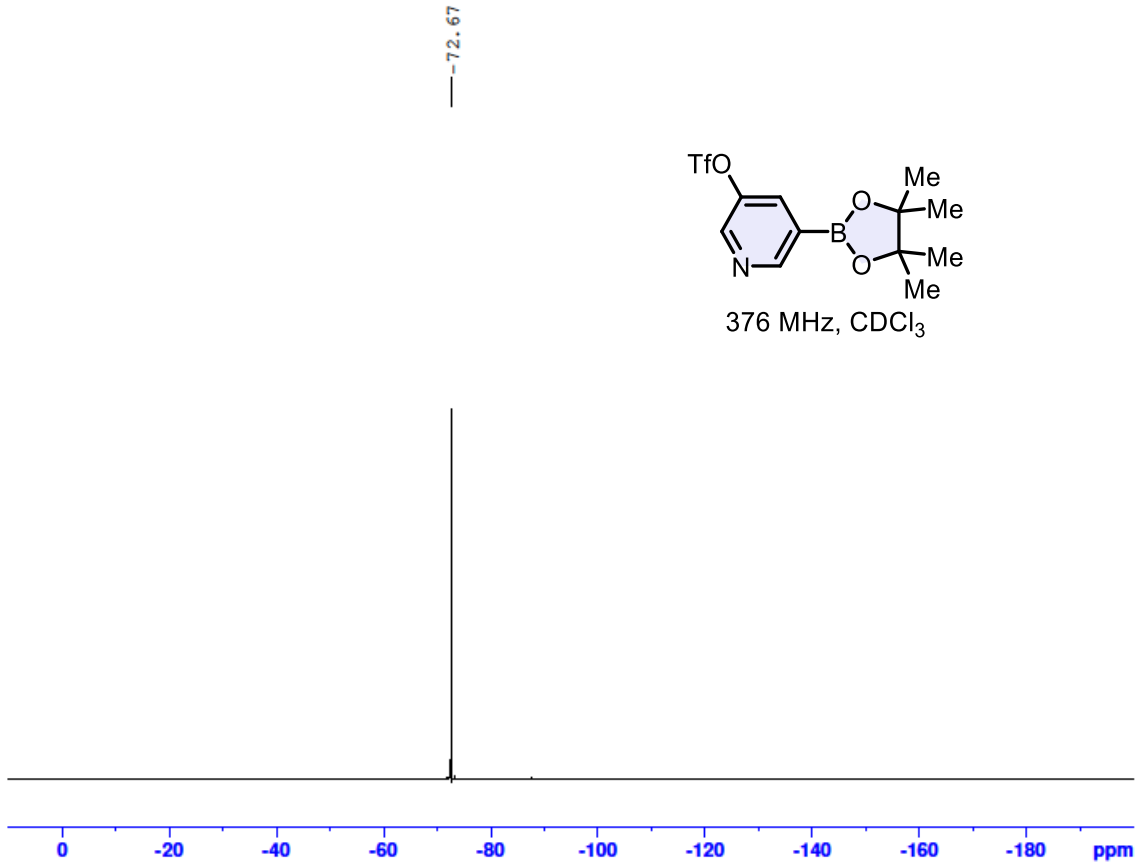

HRMS of 5-(4,4,5,5-tetramethyl-1,3,2-dioxaborolan-2-yl)pyridin-3-yl trifluoromethanesulfonate (Table 3.3, compound **9g**)

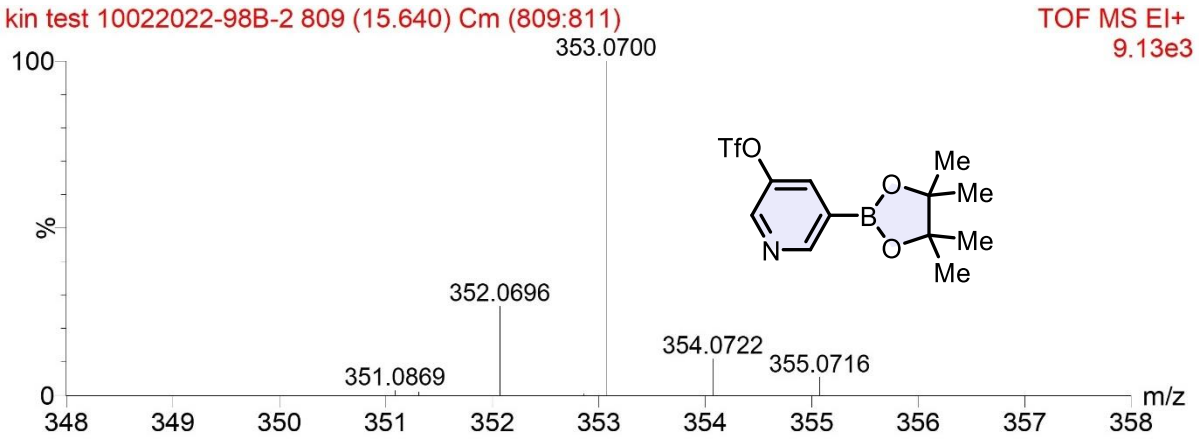

Mass	Calc. Mass	mDa	PPM	Formula
353.0700	353.0713	-1.29	-3.65	C12 H15 B F3 O5 S

^{1}H NMR of 5-(4,4,5,5-tetramethyl-1,3,2-dioxaborolan-2-yl)quinolin-8-yl trifluoromethanesulfonate (Table 3.3, compound **9h**)

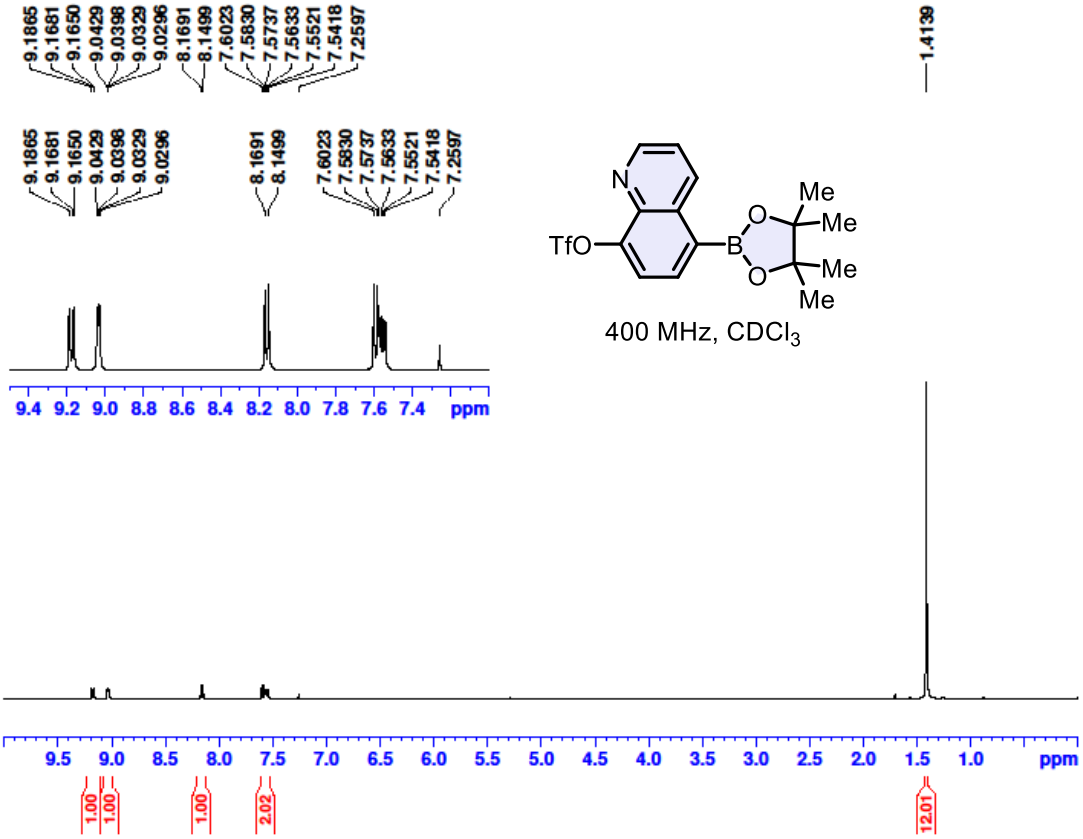

^{13}C NMR of 5-(4,4,5,5-tetramethyl-1,3,2-dioxaborolan-2-yl)quinolin-8-yl trifluoromethanesulfonate (Table 3.3, compound **9h**)

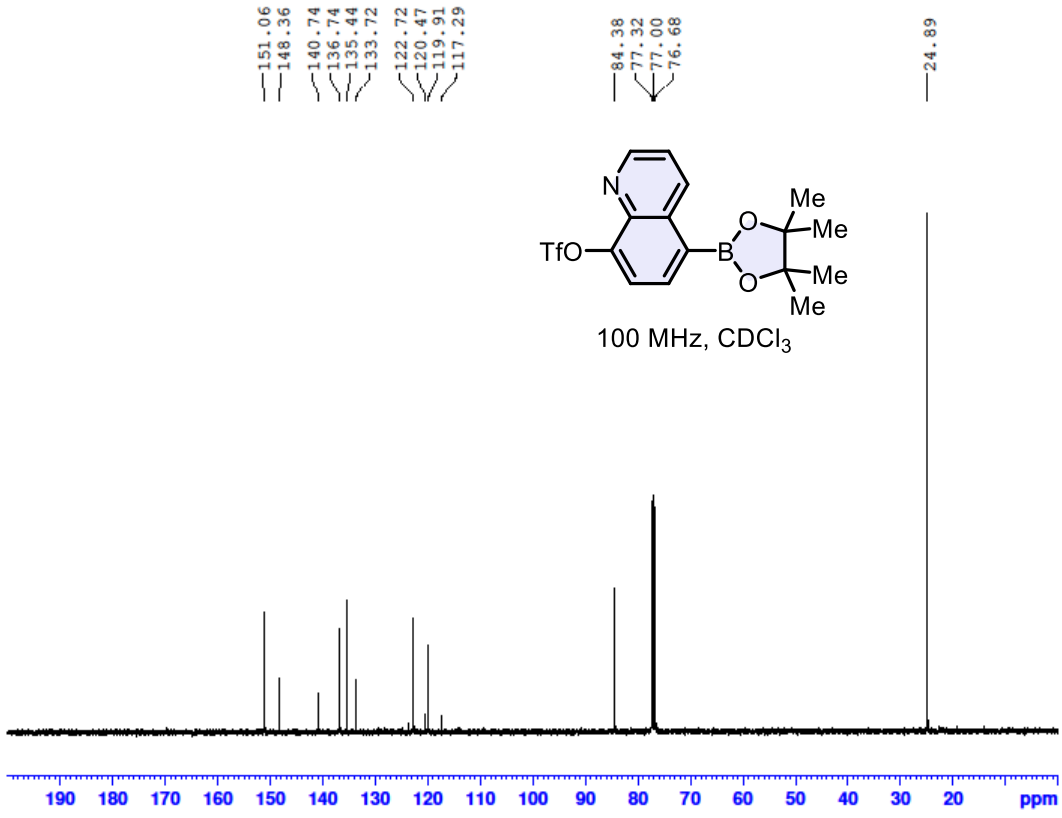

^{19}F NMR of 5-(4,4,5,5-tetramethyl-1,3,2-dioxaborolan-2-yl)quinolin-8-yl trifluoromethanesulfonate (Table 3.3, compound **9h**)

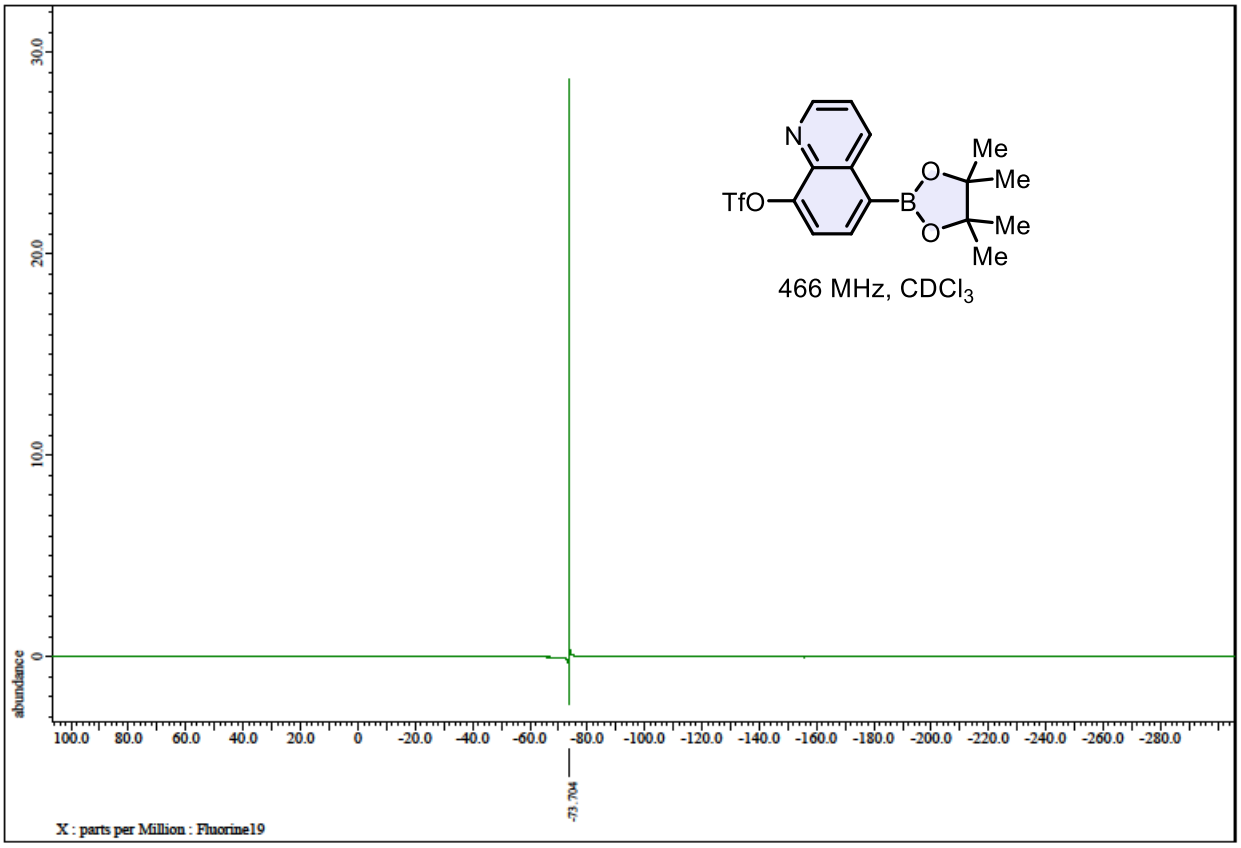

HRMS of 5-(4,4,5,5-tetramethyl-1,3,2-dioxaborolan-2-yl)quinolin-8-yl trifluoromethanesulfonate (Table 3.3, compound **9h**)

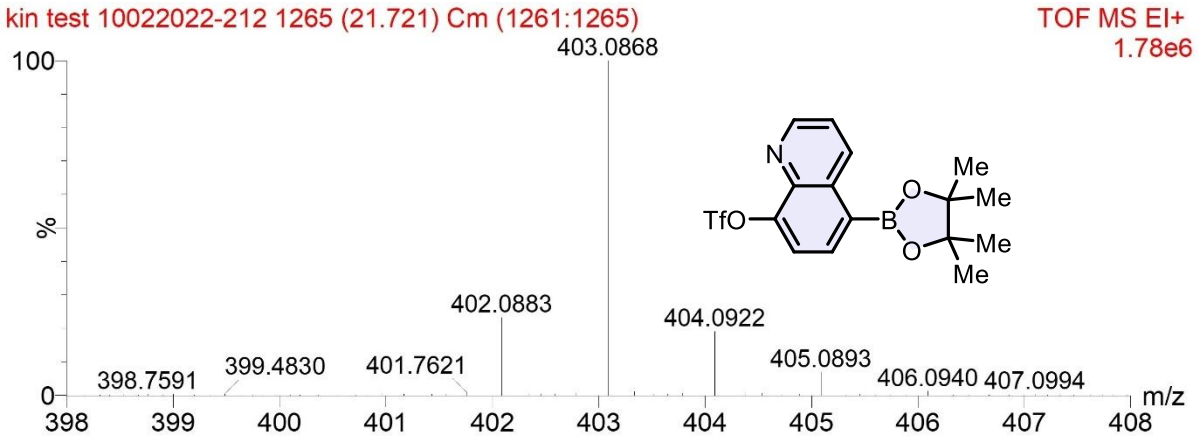

Mass	Calc. Mass	mDa	PPM	Formula
403.0868	403.0870	-0.21	-0.52	C16 H17 B F3 O5 S

^{1}H NMR of 2-methyl-5-(4,4,5,5-tetramethyl-1,3,2-dioxaborolan-2-yl)phenyl trifluoromethanesulfonate (Table 3.3, compound **9i**)

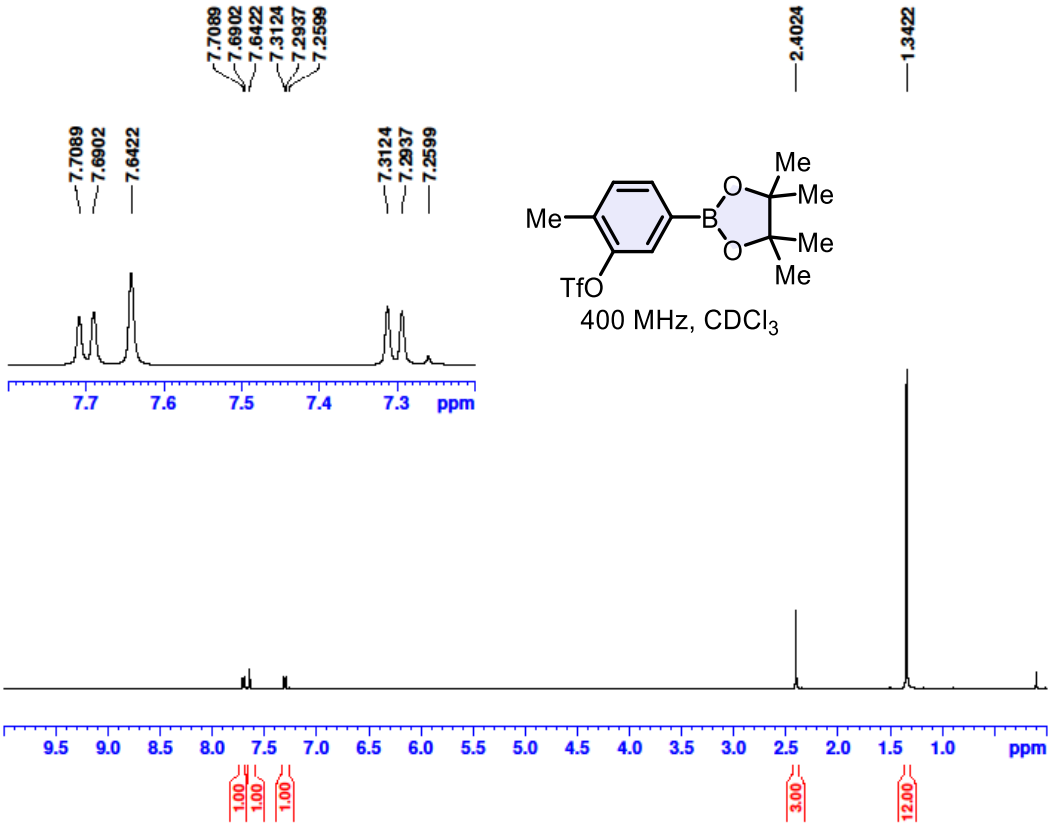

^{13}C NMR of 2-methyl-5-(4,4,5,5-tetramethyl-1,3,2-dioxaborolan-2-yl)phenyl trifluoromethanesulfonate (Table 3.3, compound **9i**)

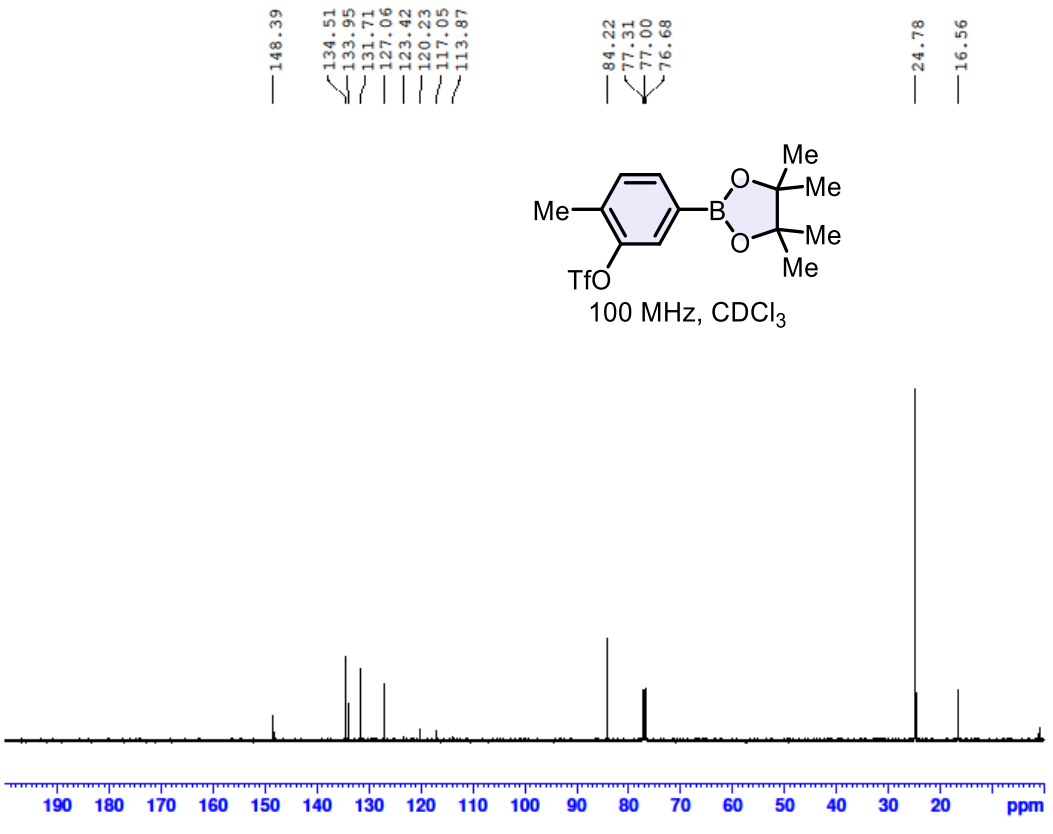

^{19}F NMR of 2-methyl-5-(4,4,5,5-tetramethyl-1,3,2-dioxaborolan-2-yl)phenyl trifluoromethanesulfonate (Table 3.3, compound **9i**)

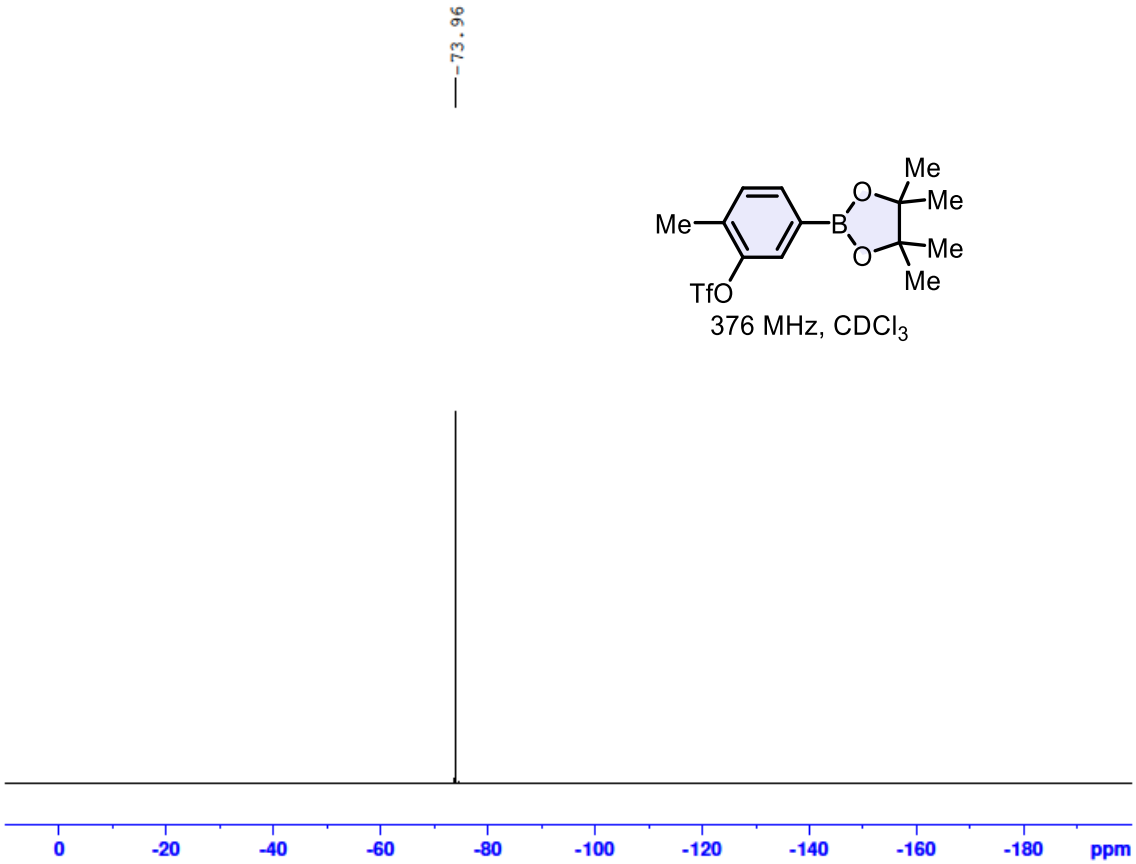

HRMS of 2-methyl-5-(4,4,5,5-tetramethyl-1,3,2-dioxaborolan-2-yl)phenyl trifluoromethanesulfonate (Table 3.3, compound **9i**)

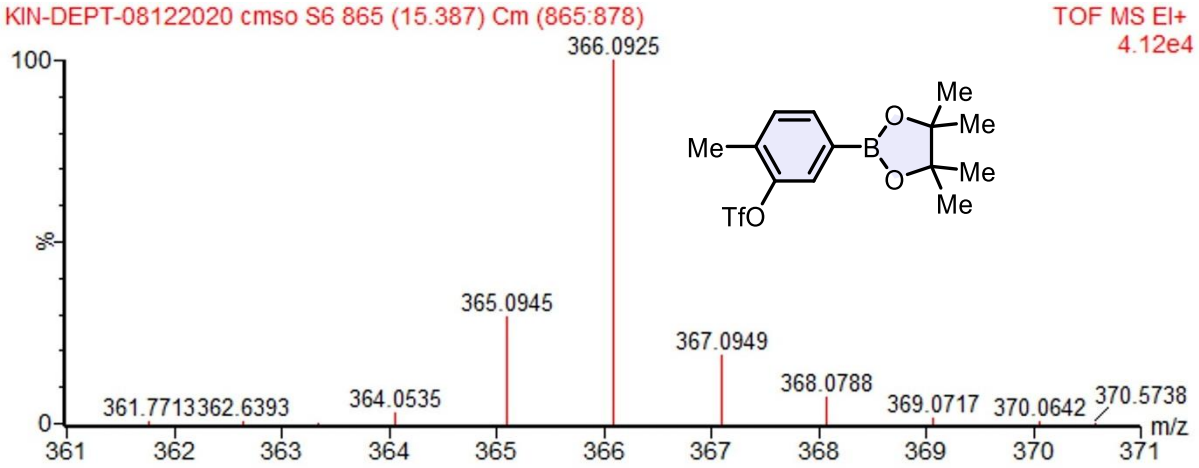

Mass	Calc. Mass	mDa	PPM	Formula
366.0925	366.0917	-0.77	-2.11	C14 H18 B F3 O5 S

^{1}H NMR of 3-methyl-5-(4,4,5,5-tetramethyl-1,3,2-dioxaborolan-2-yl)phenyl trifluoromethanesulfonate (Table 3.3, compound **9j**)

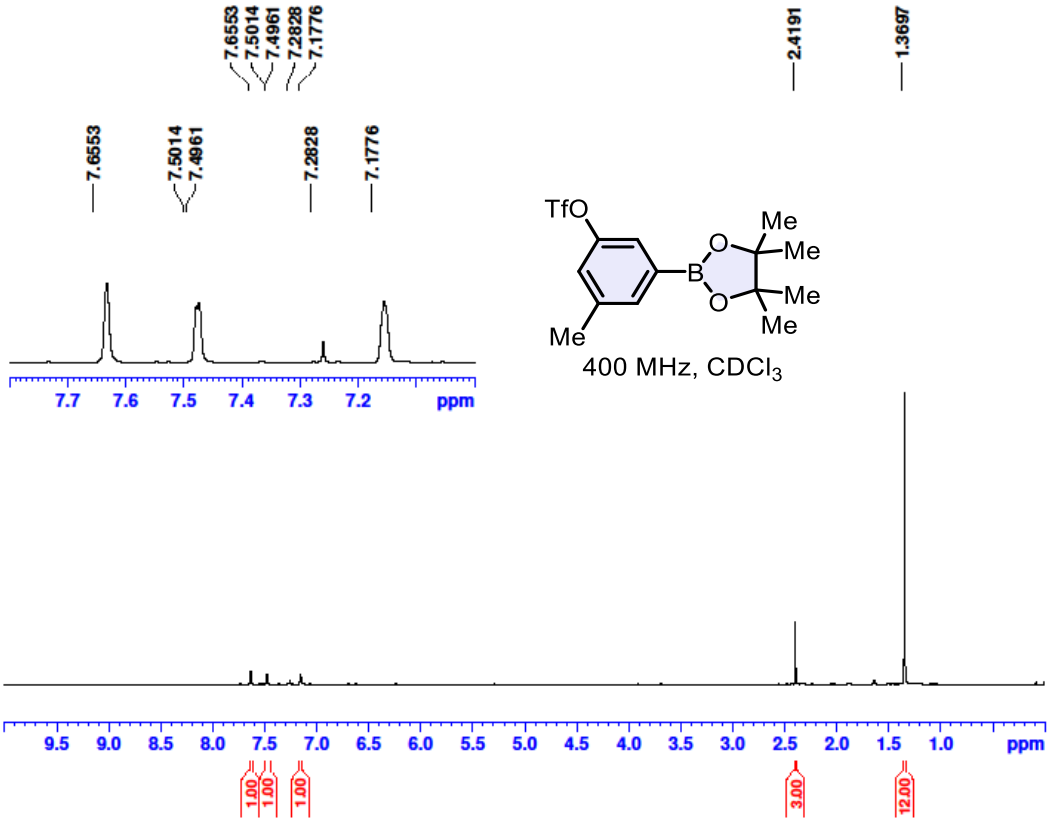

^{13}C NMR of 3-methyl-5-(4,4,5,5-tetramethyl-1,3,2-dioxaborolan-2-yl)phenyl trifluoromethanesulfonate (Table 3.3, compound **9j**)

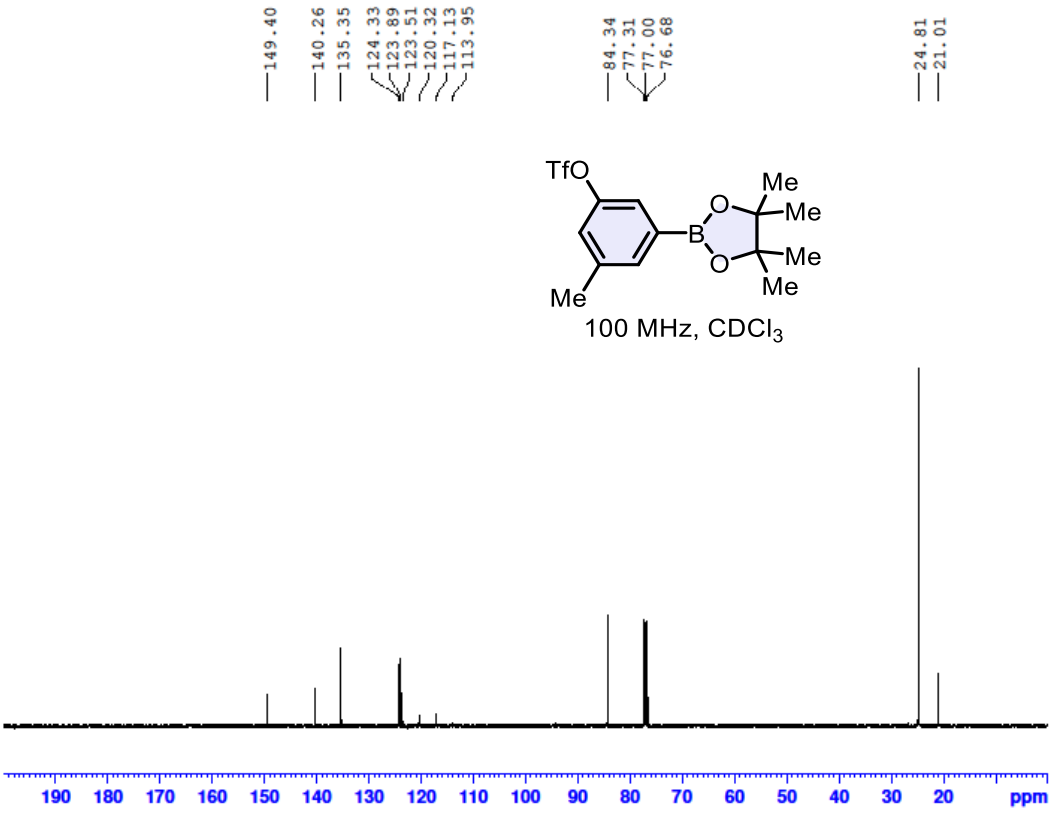

^{19}F NMR of 3-methyl-5-(4,4,5,5-tetramethyl-1,3,2-dioxaborolan-2-yl)phenyl trifluoromethanesulfonate (Table 3.3, compound **9j**)

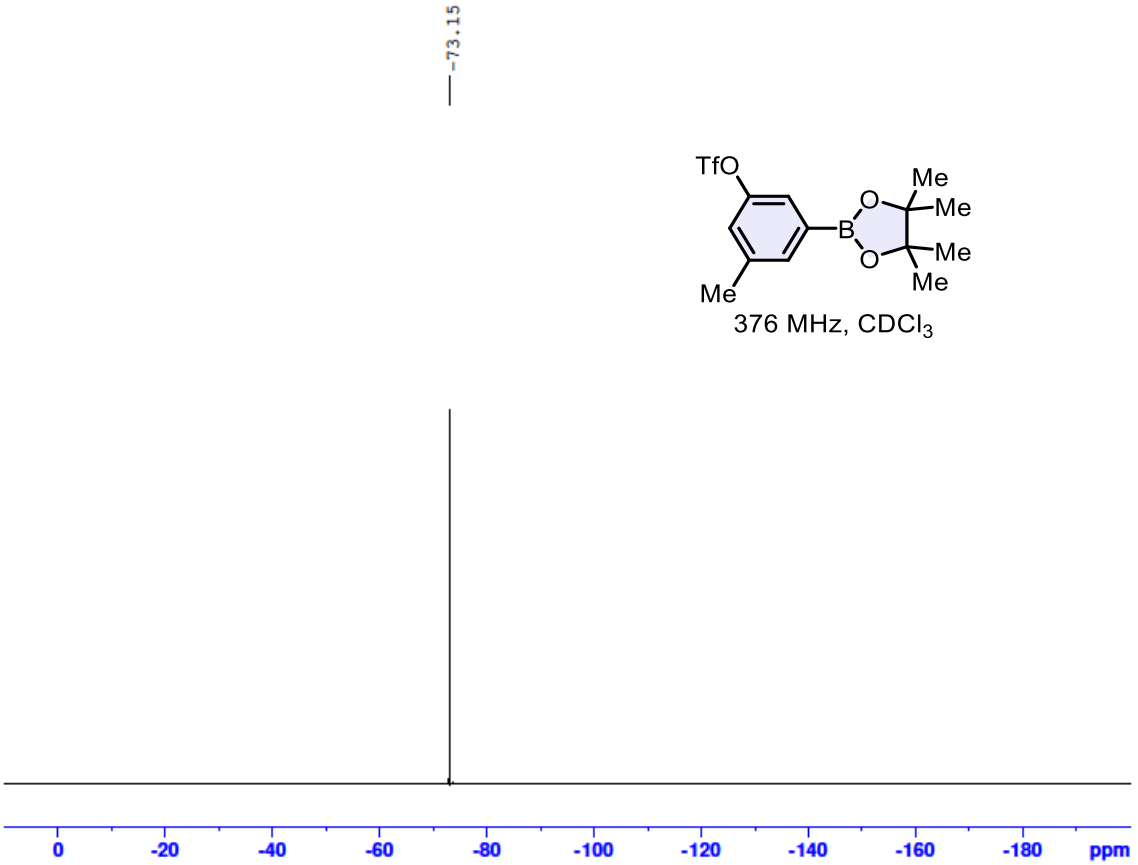

HRMS of 3-methyl-5-(4,4,5,5-tetramethyl-1,3,2-dioxaborolan-2-yl)phenyl trifluoromethanesulfonate (Table 3.3, compound **9j**)

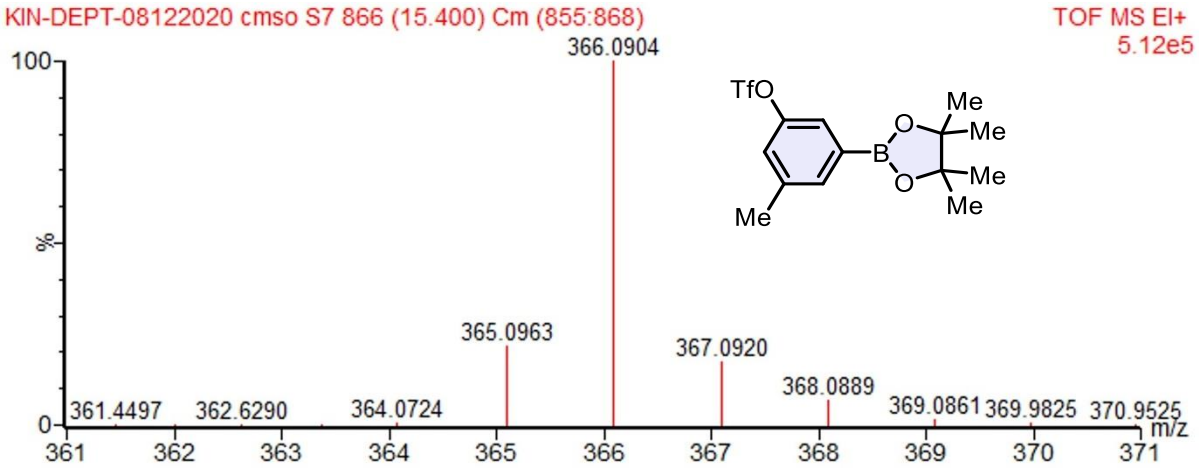

Mass	Calc. Mass	mDa	PPM	Formula
366.0904	366.0917	1.33	3.63	C14 H18 B F3 O5 S

^{1}H NMR of 2-benzyl-4-(4,4,5,5-tetramethyl-1,3,2-dioxaborolan-2-yl)phenyl trifluoromethanesulfonate (Table 3.3, compound **9k**)

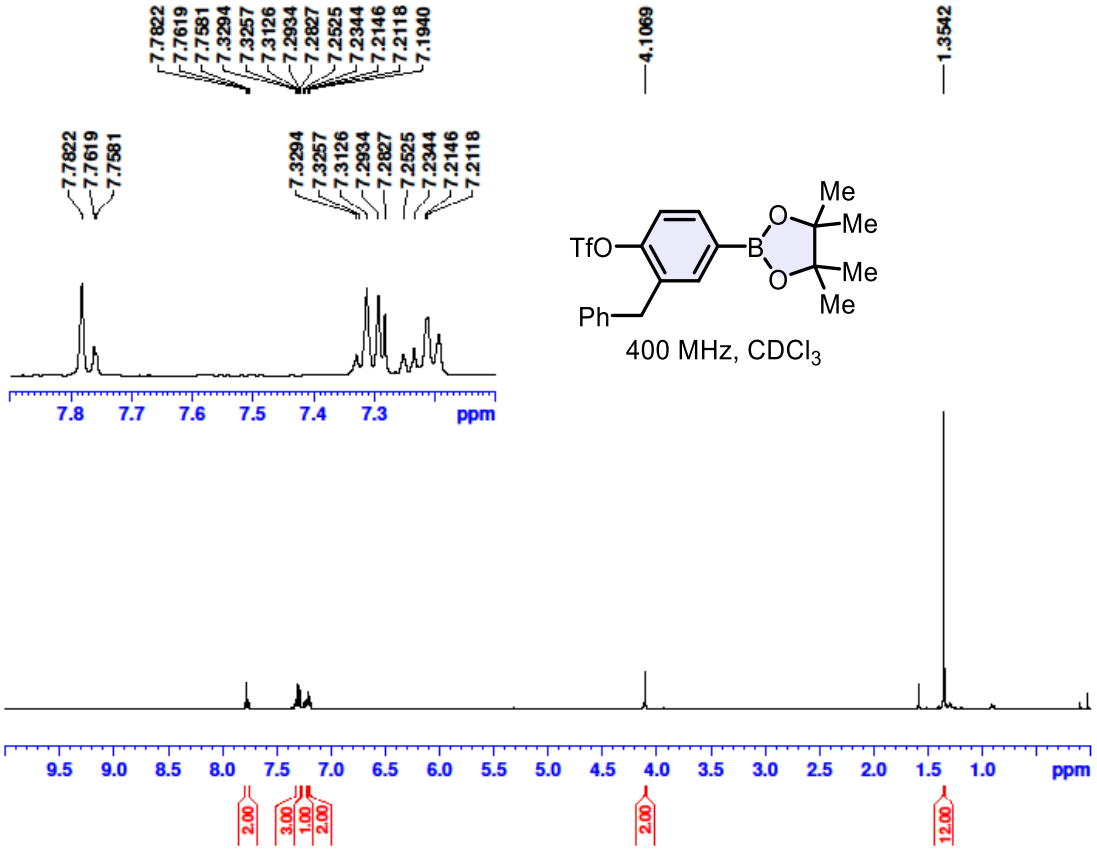

^{13}C NMR of 2-benzyl-4-(4,4,5,5-tetramethyl-1,3,2-dioxaborolan-2-yl)phenyl trifluoromethanesulfonate (Table 3.3, compound **9k**)

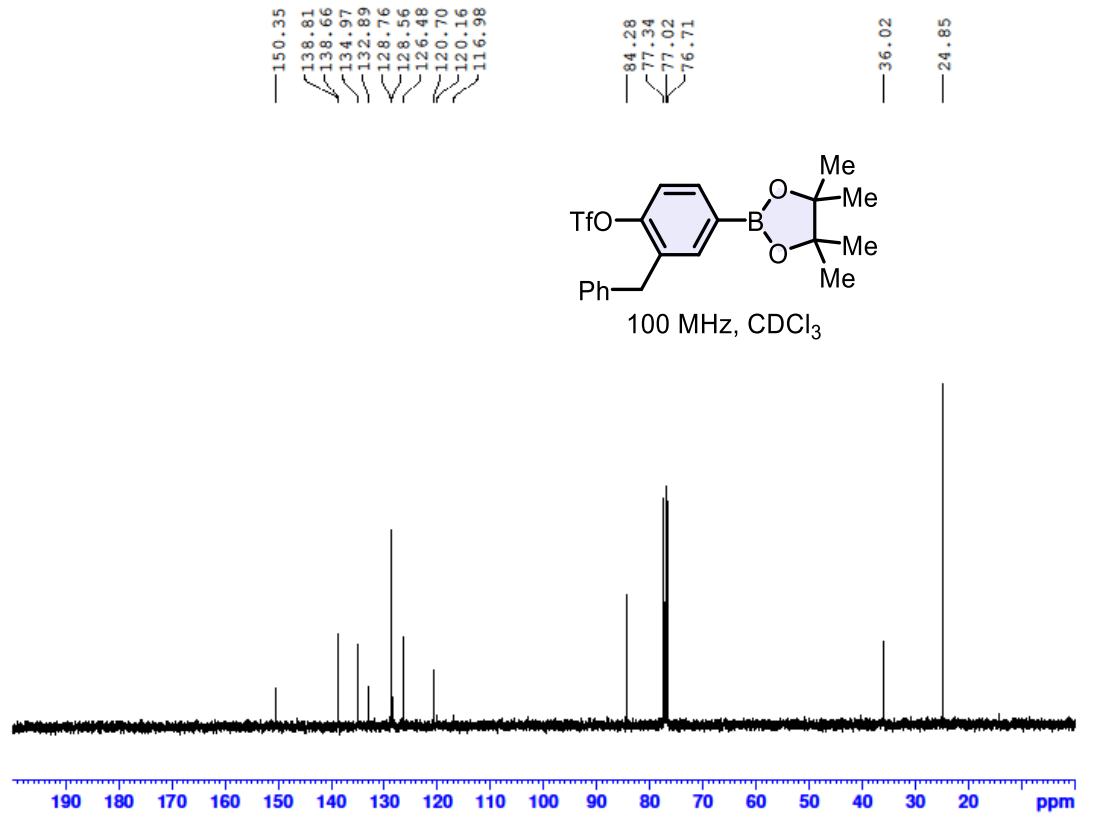

^{19}F NMR of 2-benzyl-4-(4,4,5,5-tetramethyl-1,3,2-dioxaborolan-2-yl)phenyl trifluoromethanesulfonate (Table 3.3, compound **9k**)

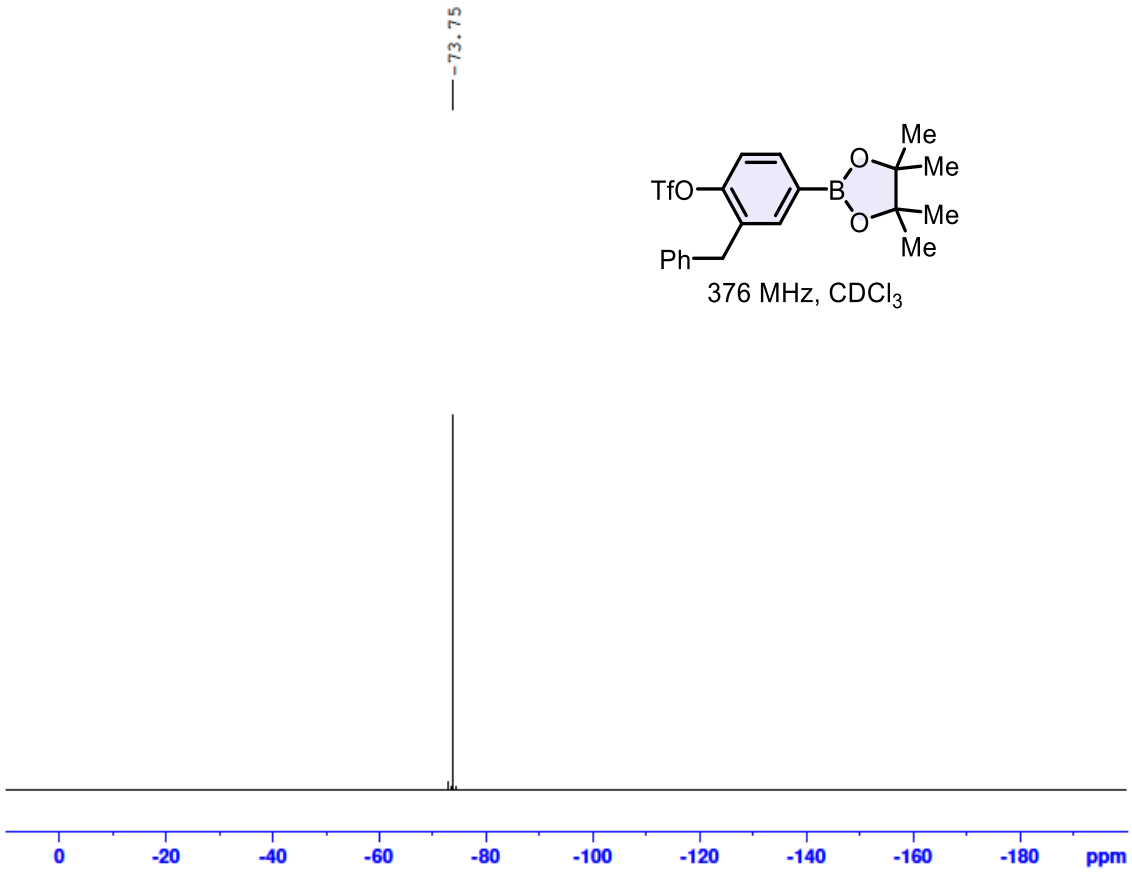

HRMS of 2-benzyl-4-(4,4,5,5-tetramethyl-1,3,2-dioxaborolan-2-yl)phenyl trifluoromethanesulfonate (Table 3.3, compound **9k**)

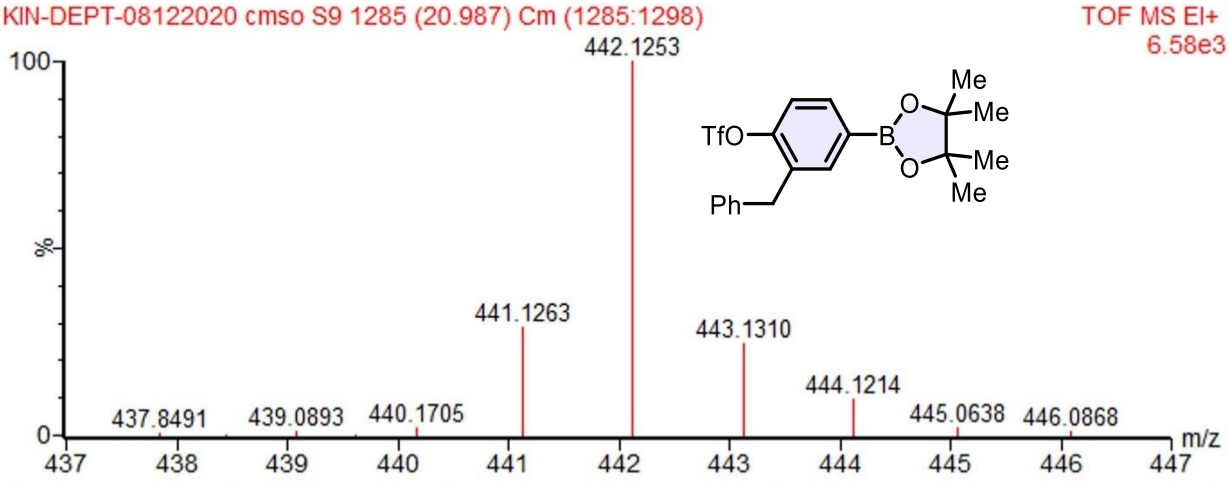

Mass	Calc. Mass	mDa	PPM	Formula
442.1253	442.1231	-2.17	-4.90	C20 H22 B F3 O5 S

^{1}H NMR of 2-methoxy-4-(4,4,5,5-tetramethyl-1,3,2-dioxaborolan-2-yl)phenyl trifluoromethanesulfonate (Table 3.3 and Scheme 3.4, compound **9l**)

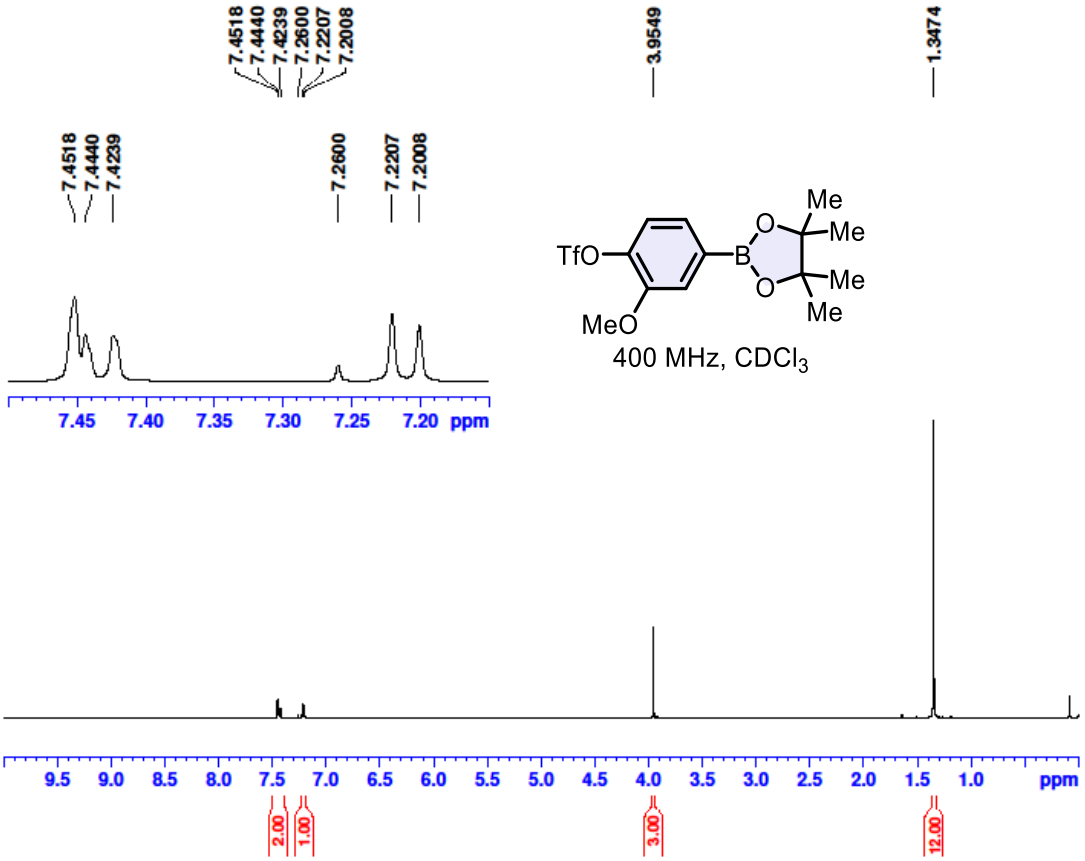

^{13}C NMR of 2-methoxy-4-(4,4,5,5-tetramethyl-1,3,2-dioxaborolan-2-yl)phenyl trifluoromethanesulfonate (Table 3.3 and Scheme 3.4, compound **9l**)

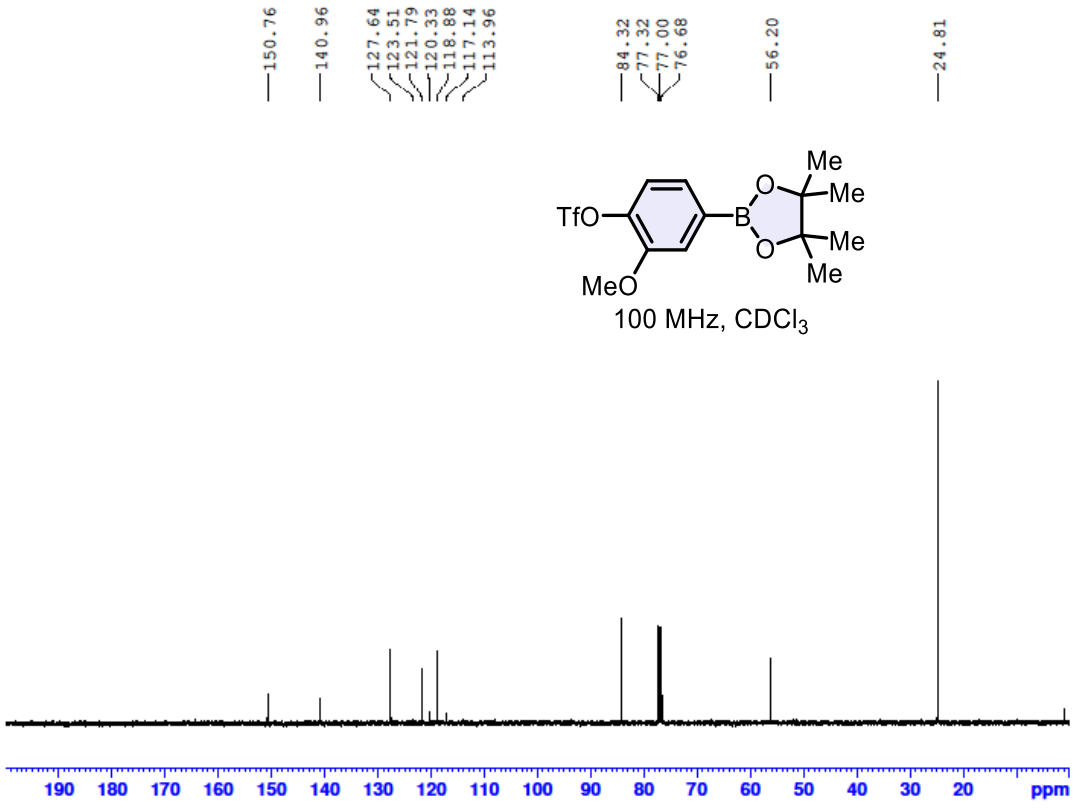

^{19}F NMR of 2-methoxy-4-(4,4,5,5-tetramethyl-1,3,2-dioxaborolan-2-yl)phenyl trifluoromethanesulfonate (Table 3.3 and Scheme 3.4, compound **9l**)

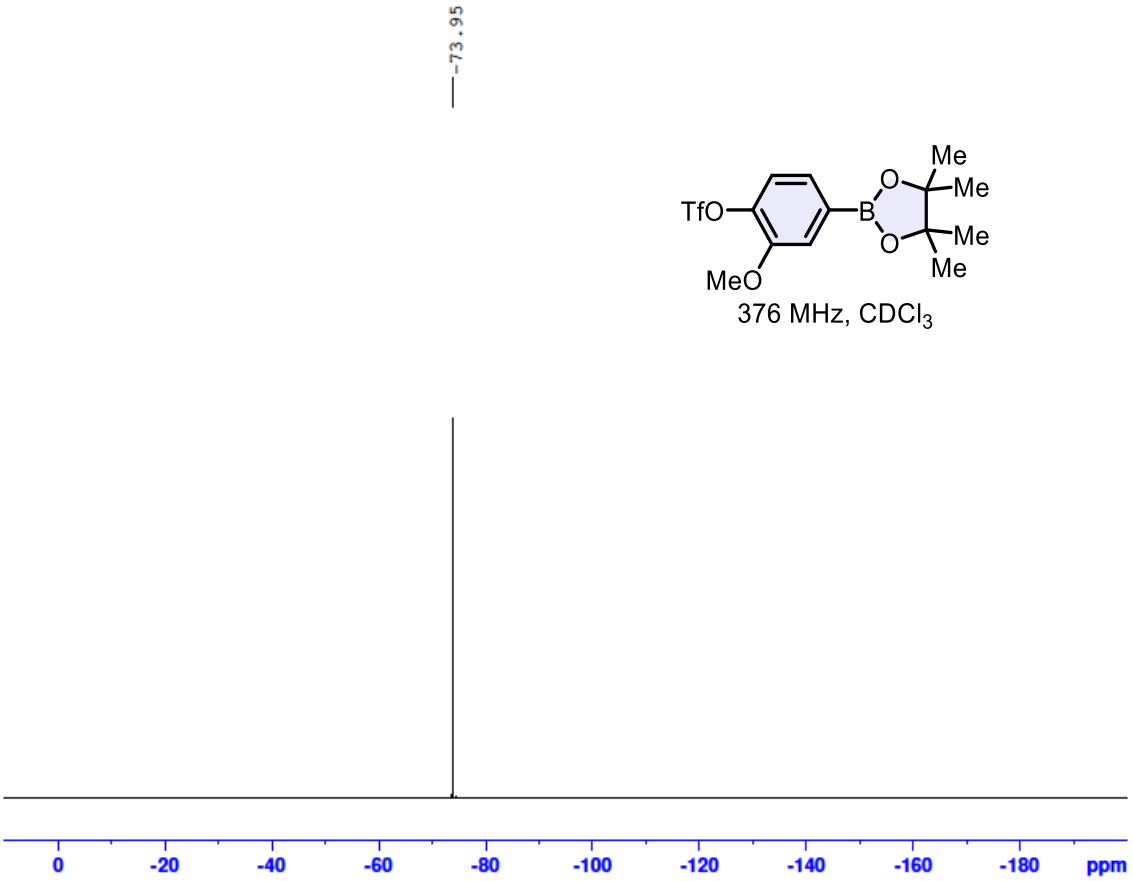

HRMS of 2-methoxy-4-(4,4,5,5-tetramethyl-1,3,2-dioxaborolan-2-yl)phenyl trifluoromethanesulfonate (Table 3.3 and Scheme 3.4, compound **9l**)

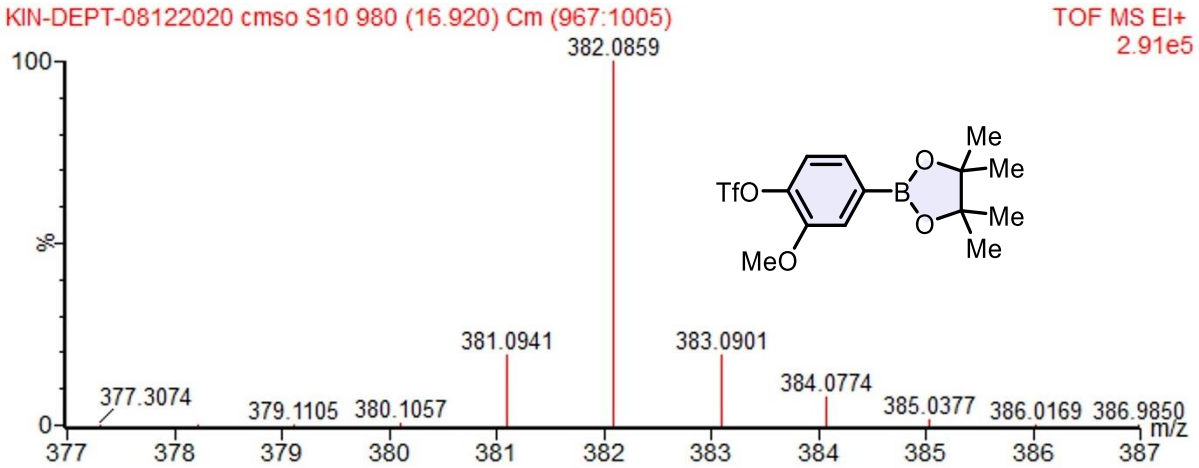

Mass	Calc. Mass	mDa	PPM	Formula
382.0859	382.0866	0.74	1.94	C14 H18 B F3 O6 S

^{1}H NMR of 2-cyano-4-(4,4,5,5-tetramethyl-1,3,2-dioxaborolan-2-yl)phenyl trifluoromethanesulfonate (Table 3.3, compound **9m**)

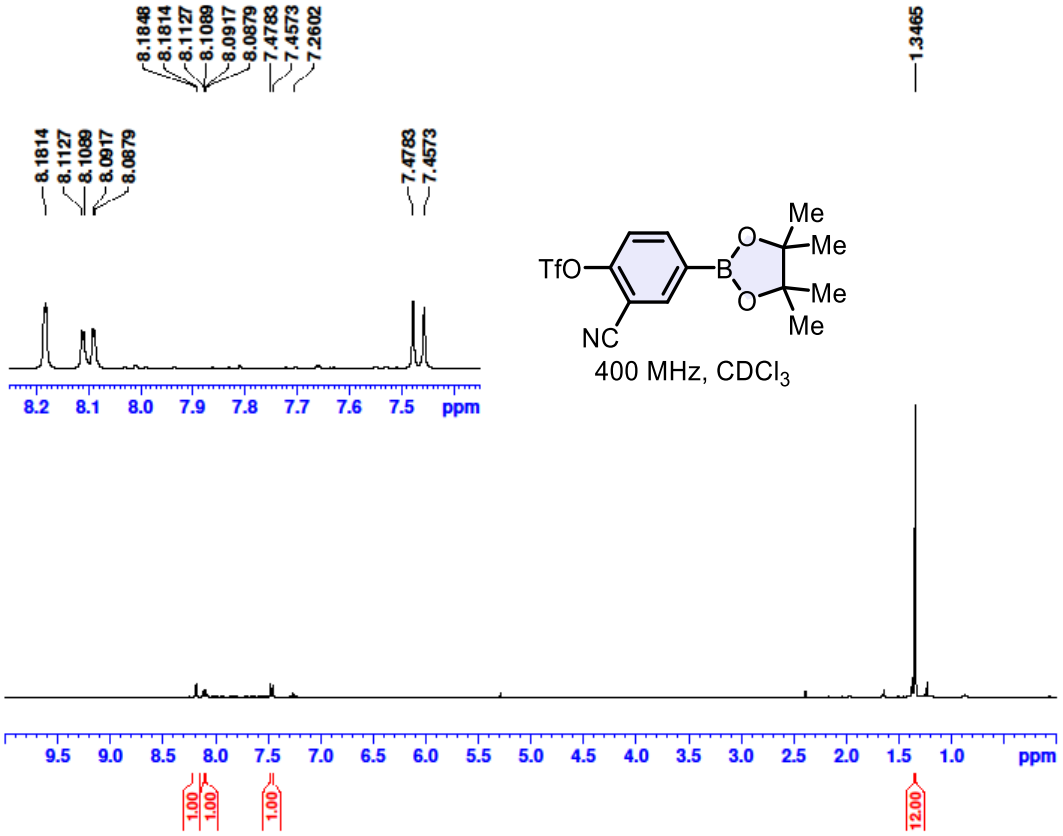

^{13}C NMR of 2-cyano-4-(4,4,5,5-tetramethyl-1,3,2-dioxaborolan-2-yl)phenyl trifluoromethanesulfonate (Table 3.3, compound **9m**)

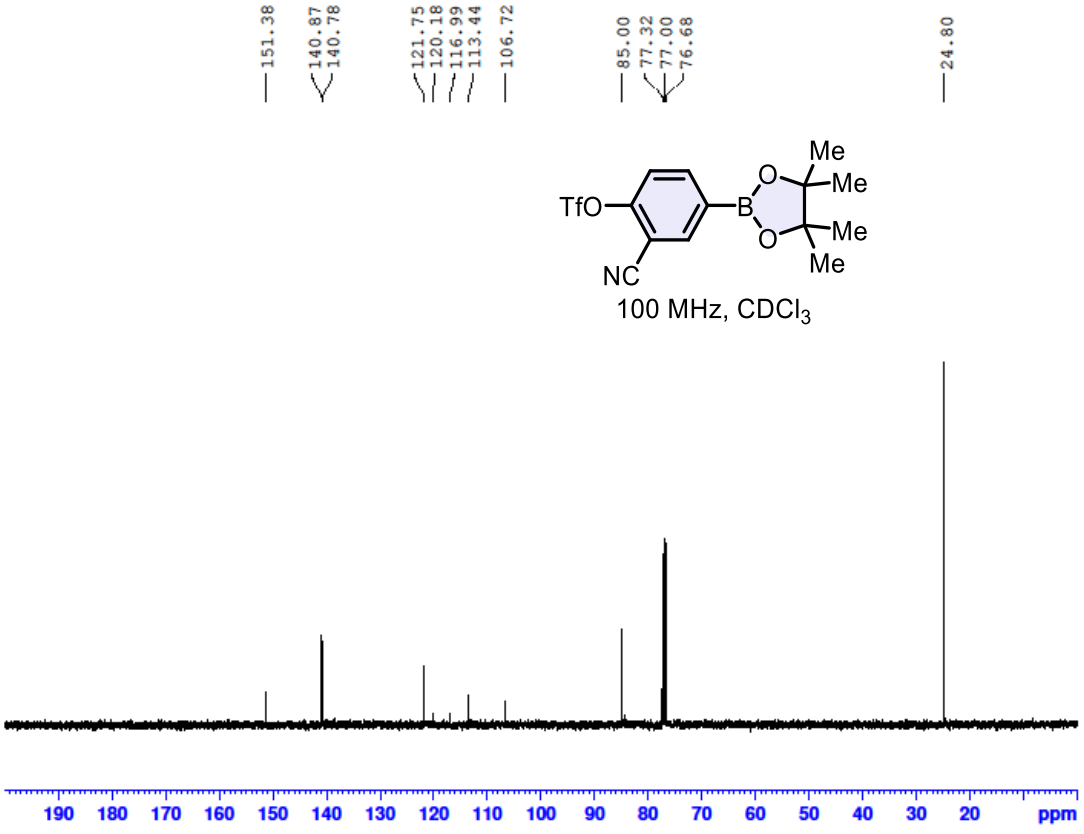

^{19}F NMR of 2-cyano-4-(4,4,5,5-tetramethyl-1,3,2-dioxaborolan-2-yl)phenyl trifluoromethanesulfonate (Table 3.3, compound **9m**)

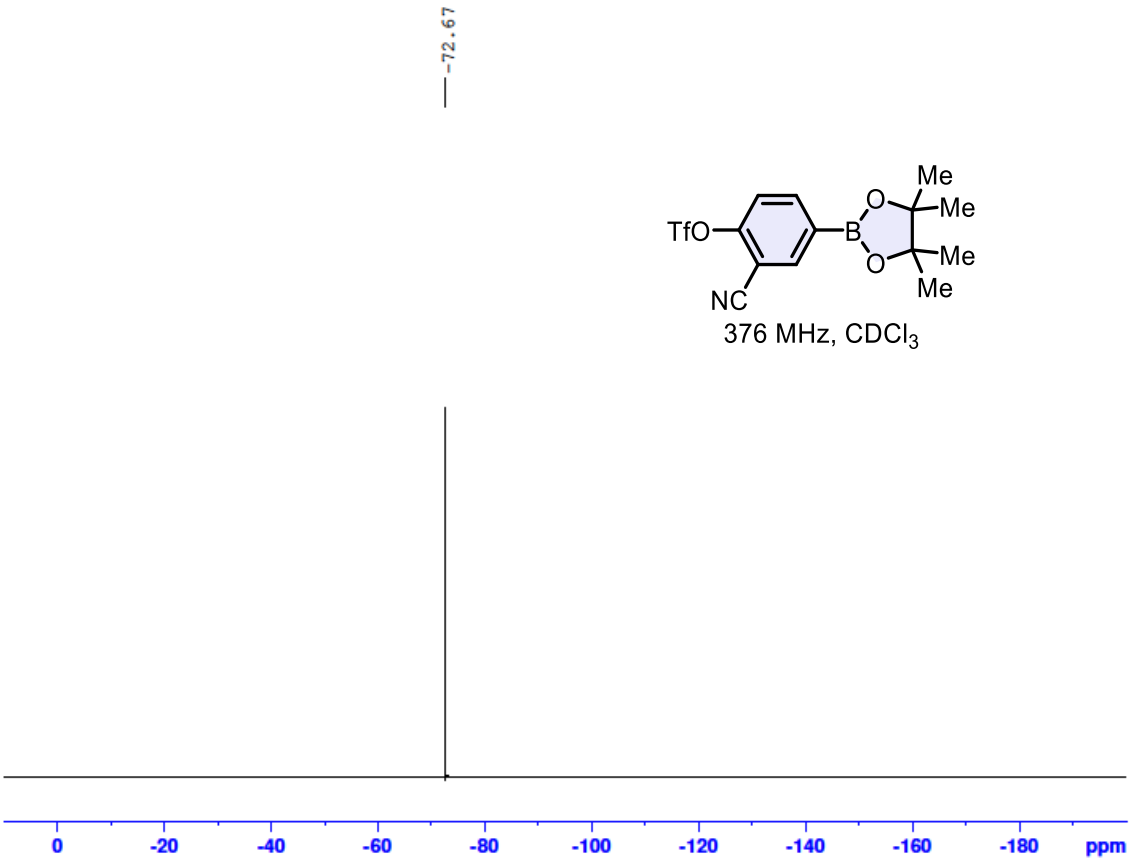

HRMS of 2-cyano-4-(4,4,5,5-tetramethyl-1,3,2-dioxaborolan-2-yl)phenyl trifluoromethanesulfonate (Table 3.3, compound **9m**)

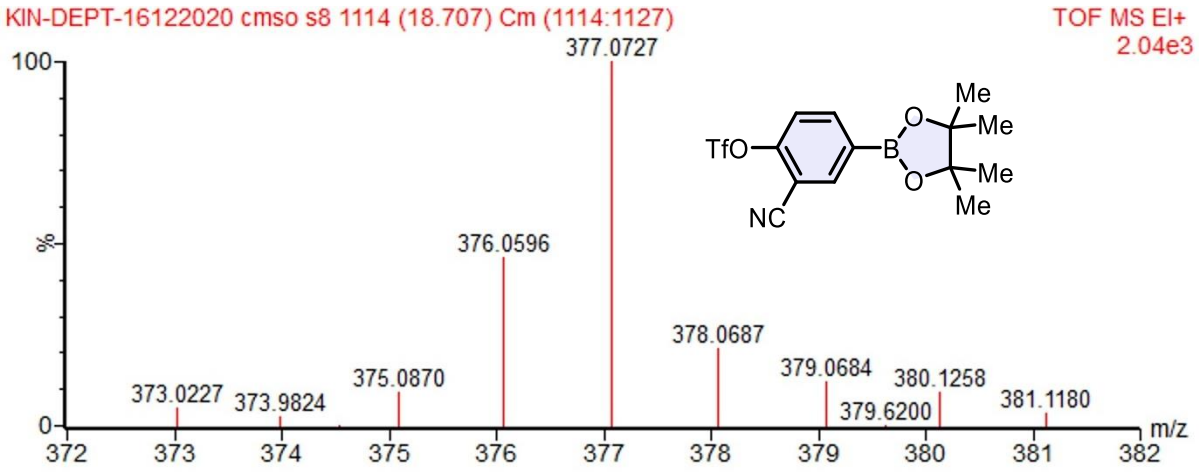

Mass	Calc. Mass	mDa	PPM	Formula
377.0727	377.0713	-1.37	-3.64	C14 H15 B F3 N O5 S

^{1}H NMR of 2-formyl-5-(4,4,5,5-tetramethyl-1,3,2-dioxaborolan-2-yl)phenyl trifluoromethanesulfonate (Table 3.3, compound **9n**)

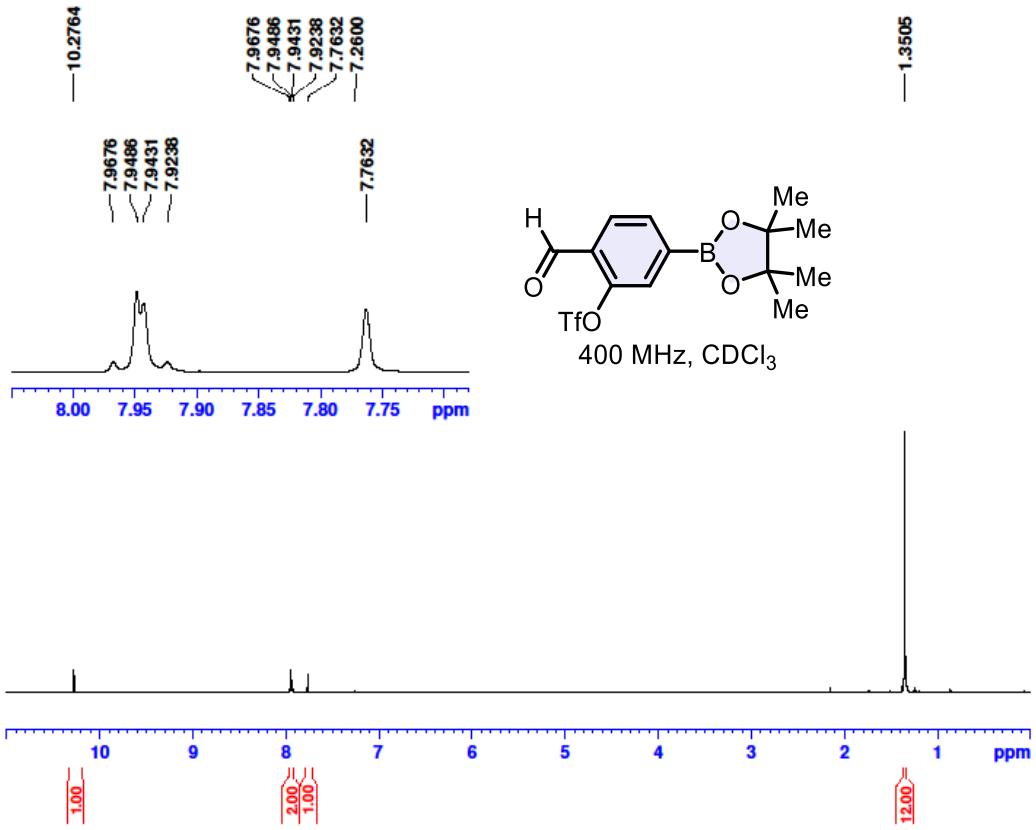

^{13}C NMR of 2-formyl-5-(4,4,5,5-tetramethyl-1,3,2-dioxaborolan-2-yl)phenyl trifluoromethanesulfonate (Table 3.3, compound **9n**)

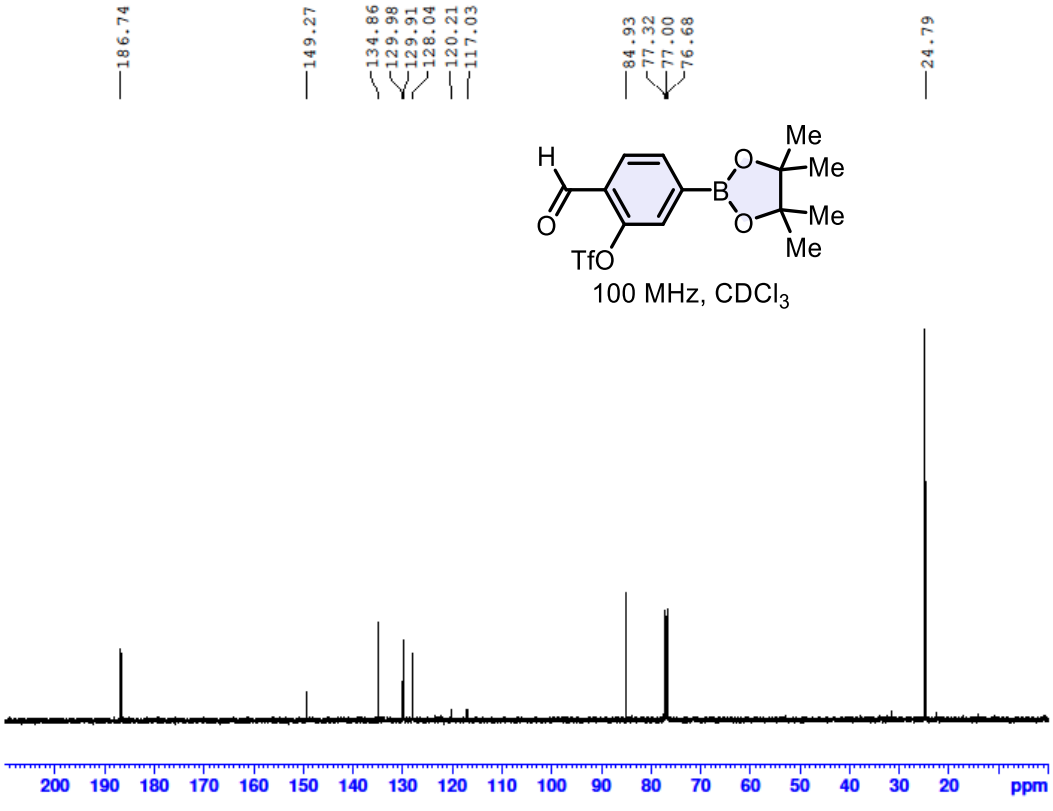

^{19}F NMR of 2-formyl-5-(4,4,5,5-tetramethyl-1,3,2-dioxaborolan-2-yl)phenyl trifluoromethanesulfonate (Table 3.3, compound **9n**)

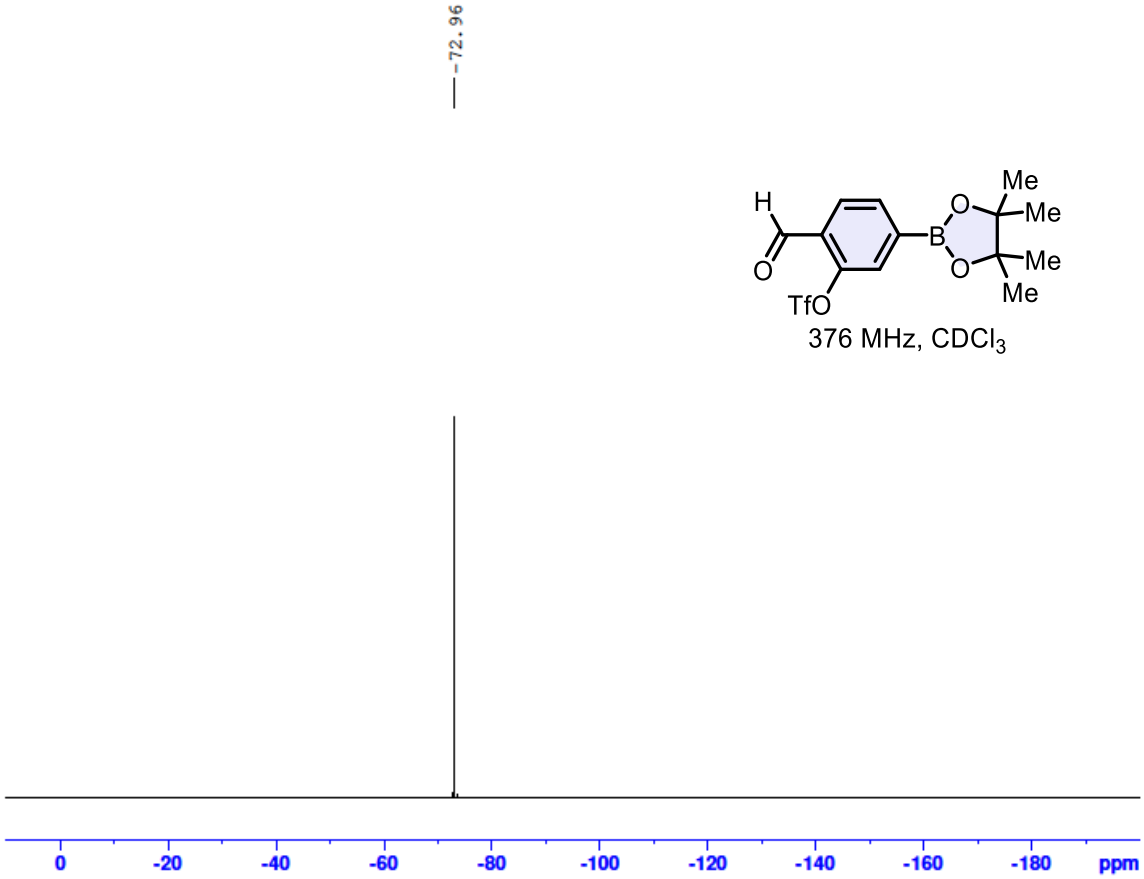

HRMS of 2-formyl-5-(4,4,5,5-tetramethyl-1,3,2-dioxaborolan-2-yl)phenyl trifluoromethanesulfonate (Table 3.3, compound **9n**)

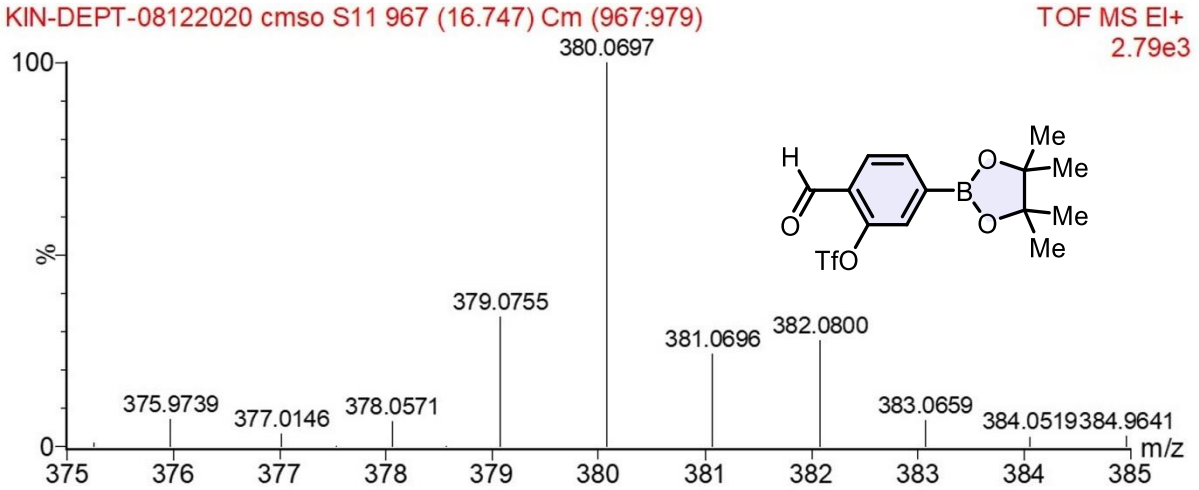

Mass	Calc. Mass	mDa	PPM	Formula
380.0697	380.0710	1.29	3.40	C14 H16 B F3 O6 S

^{1}H NMR of 2-acetyl-5-(4,4,5,5-tetramethyl-1,3,2-dioxaborolan-2-yl)phenyl trifluoromethanesulfonate (Table 3.3, compound **9o**)

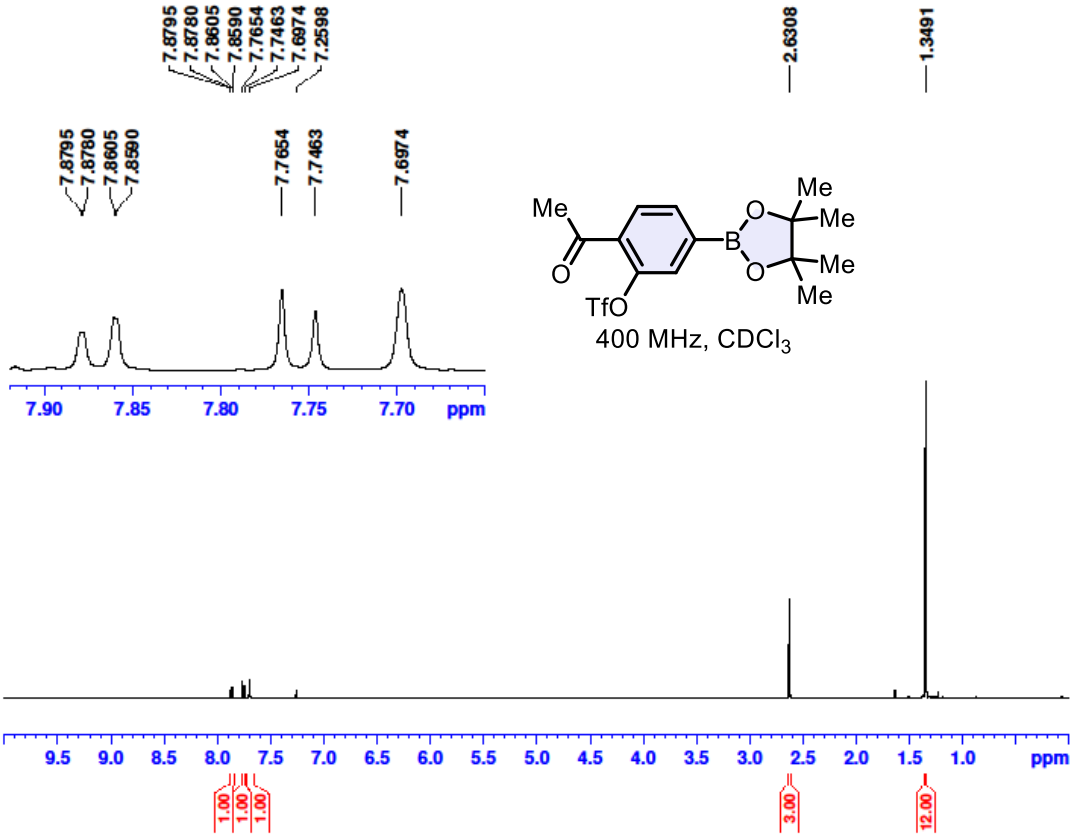

^{13}C NMR of 2-acetyl-5-(4,4,5,5-tetramethyl-1,3,2-dioxaborolan-2-yl)phenyl trifluoromethanesulfonate (Table 3.3, compound **9o**)

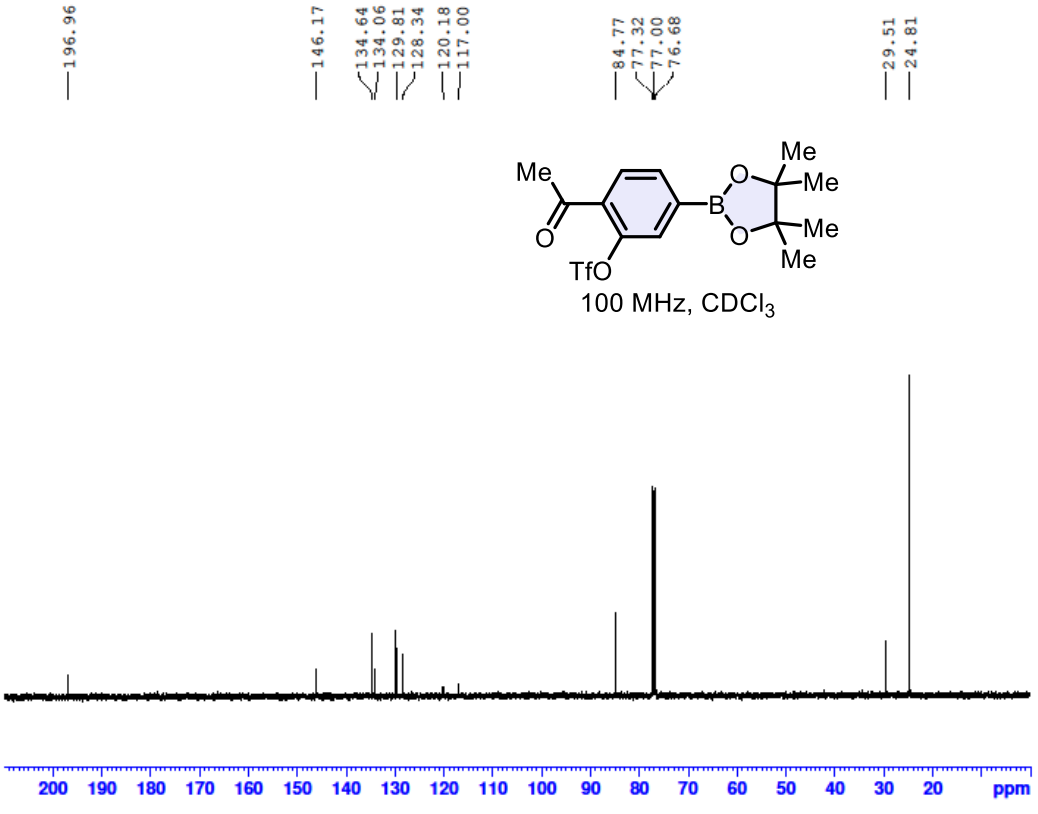

^{19}F NMR of 2-acetyl-5-(4,4,5,5-tetramethyl-1,3,2-dioxaborolan-2-yl)phenyl trifluoromethanesulfonate (Table 3.3, compound **9o**)

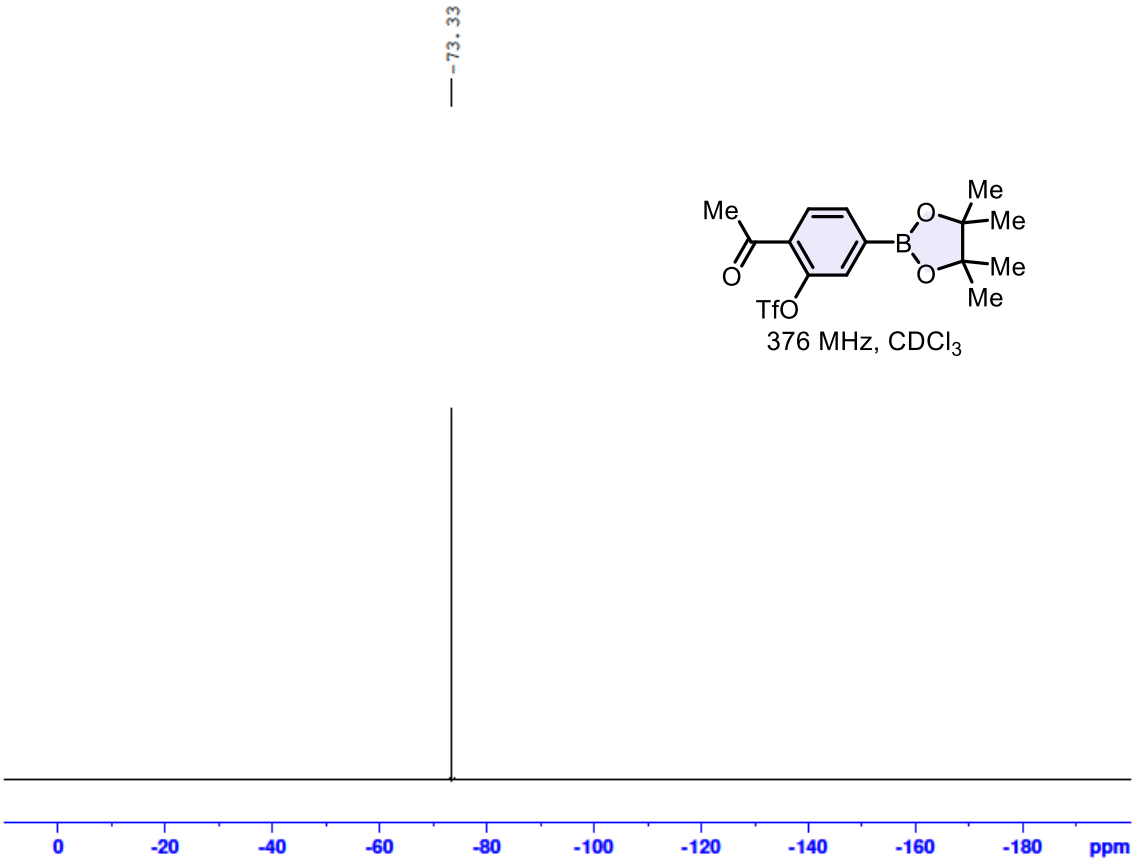

HRMS of 2-acetyl-5-(4,4,5,5-tetramethyl-1,3,2-dioxaborolan-2-yl)phenyl trifluoromethanesulfonate (Table 3.3, compound **9o**)

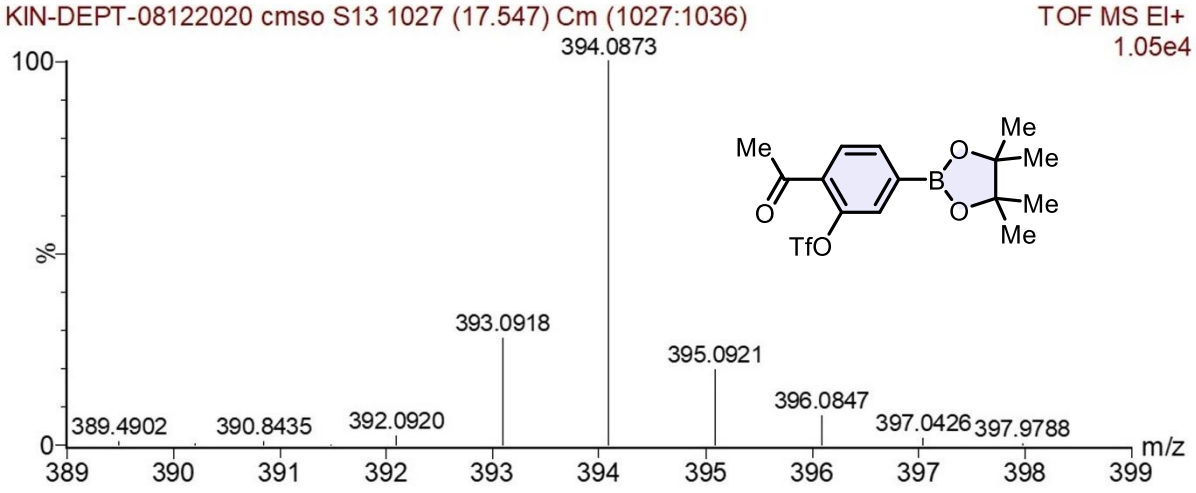

Mass	Calc. Mass	mDa	PPM	Formula
394.0873	394.0867	-0.64	-1.62	C15 H18 B F3 O6 S

^{1}H NMR of 3,5-bis(4,4,5,5-tetramethyl-1,3,2-dioxaborolan-2-yl)phenyl trifluoromethanesulfonate (Table 3.3, compound **9p**)

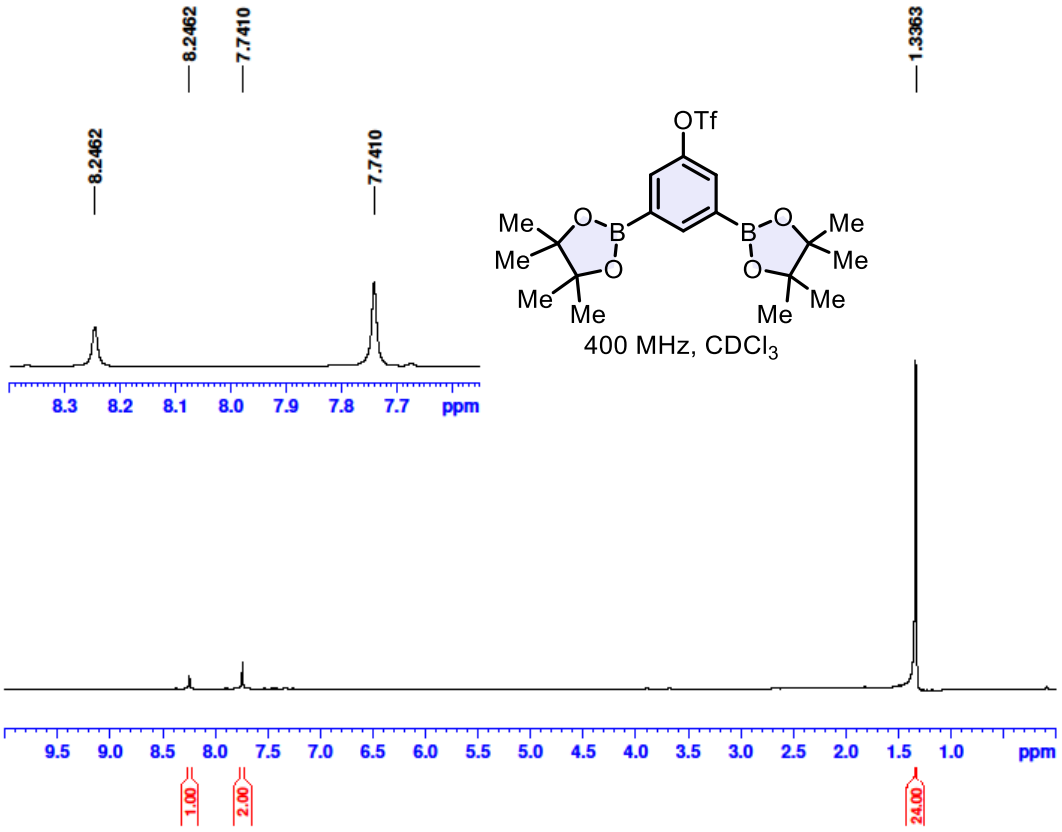

^{13}C NMR of 3,5-bis(4,4,5,5-tetramethyl-1,3,2-dioxaborolan-2-yl)phenyl trifluoromethanesulfonate (Table 3.3, compound **9p**)

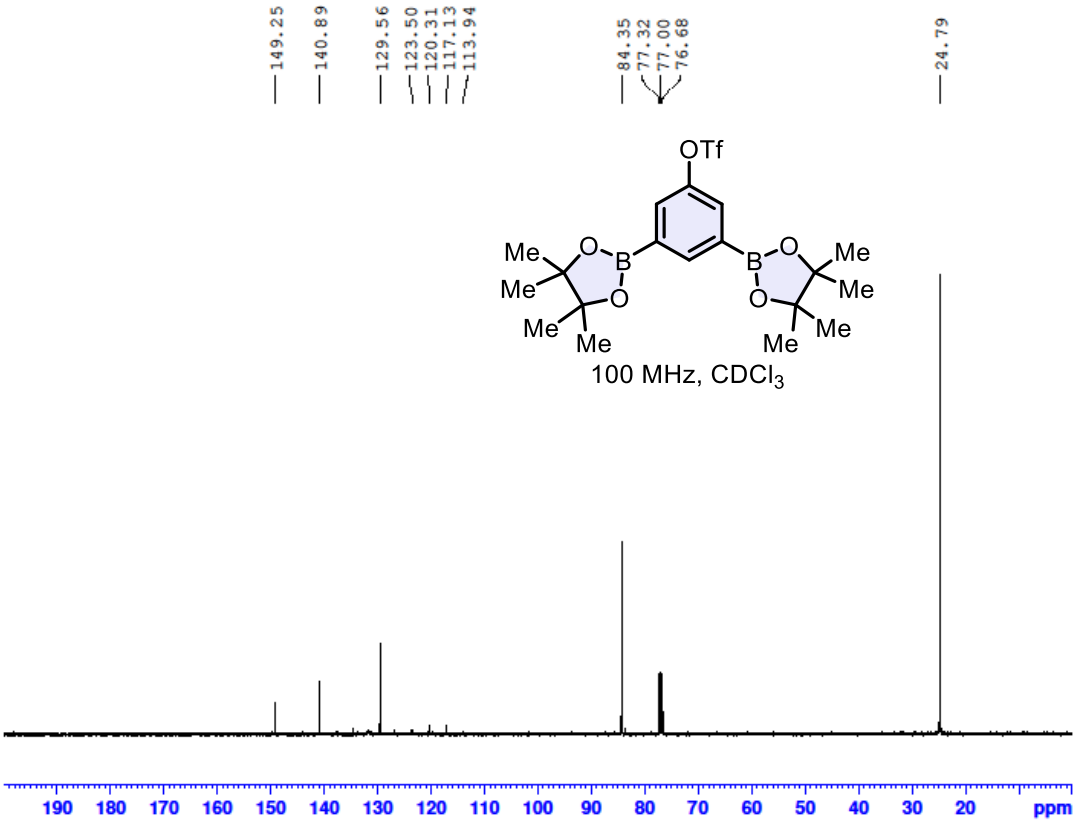

^{19}F NMR of 3,5-bis(4,4,5,5-tetramethyl-1,3,2-dioxaborolan-2-yl)phenyl trifluoromethanesulfonate (Table 3.3, compound **9p**)

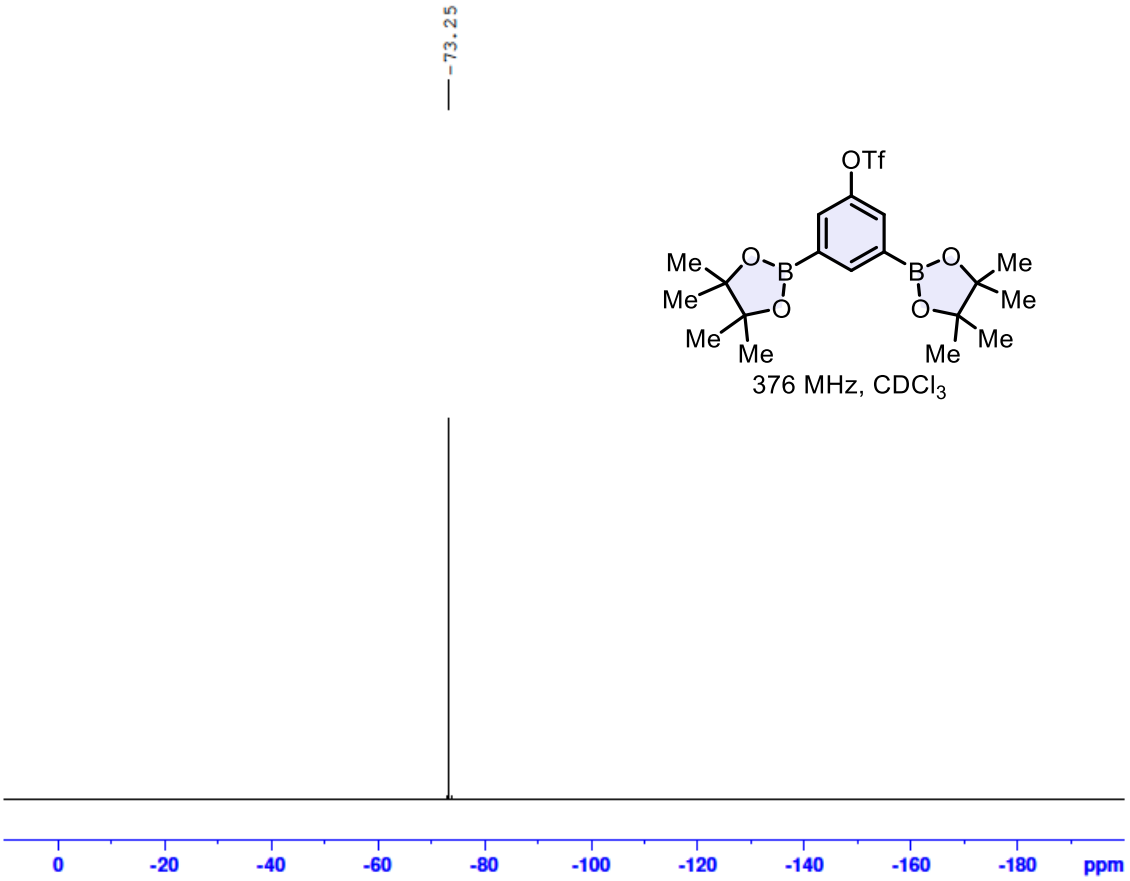

HRMS of 3,5-bis(4,4,5,5-tetramethyl-1,3,2-dioxaborolan-2-yl)phenyl trifluoromethanesulfonate (Table 3.3, compound **9p**)

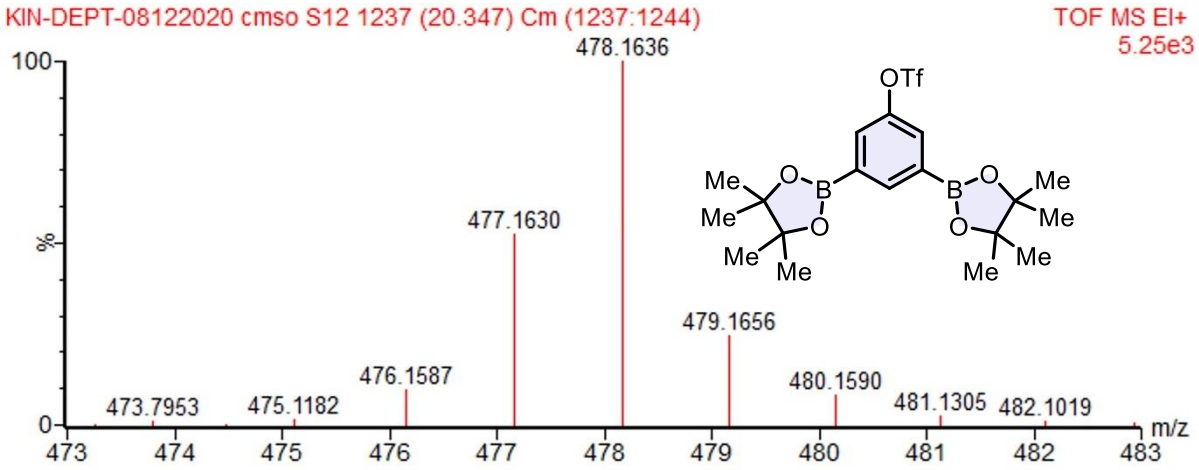

Mass	Calc. Mass	mDa	PPM	Formula
478.1636	478.1617	-1.87	-3.91	C19 H27 B2 F3 O7 S

^{1}H NMR of 3-chloro-5-(4,4,5,5-tetramethyl-1,3,2-dioxaborolan-2-yl)phenyl trifluoromethanesulfonate (Table 3.3, compound **9q**)

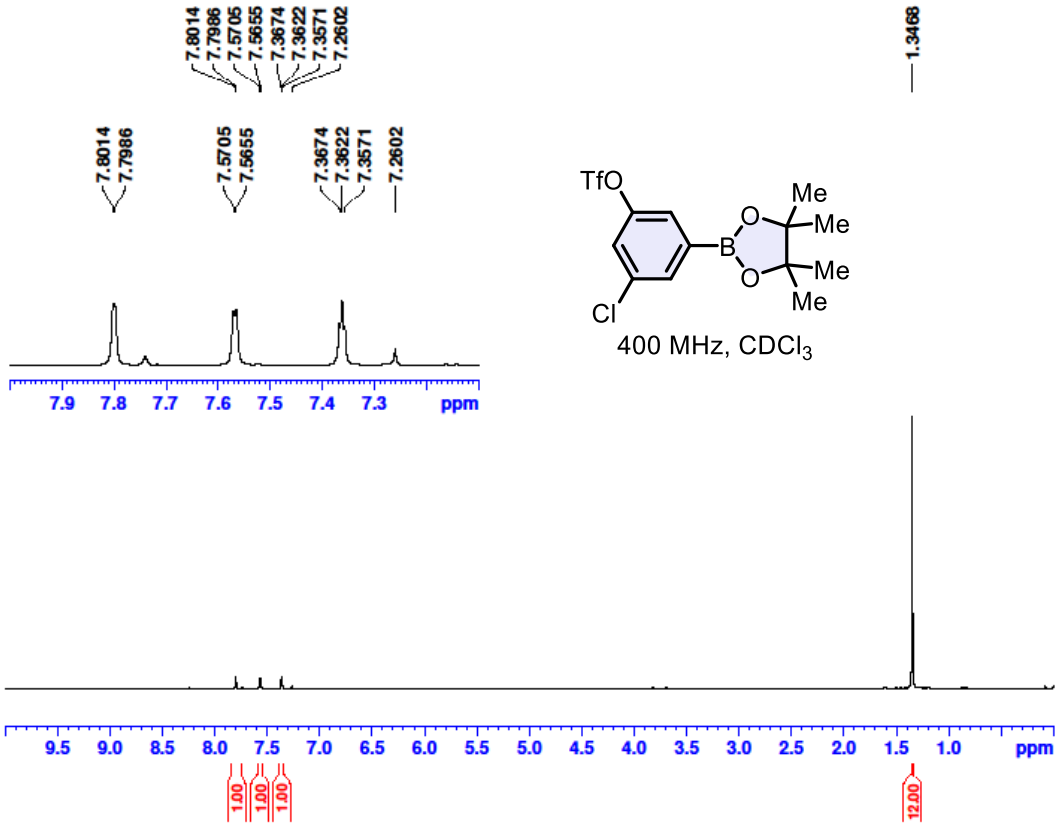

^{13}C NMR of 3-chloro-5-(4,4,5,5-tetramethyl-1,3,2-dioxaborolan-2-yl)phenyl trifluoromethanesulfonate (Table 3.3, compound **9q**)

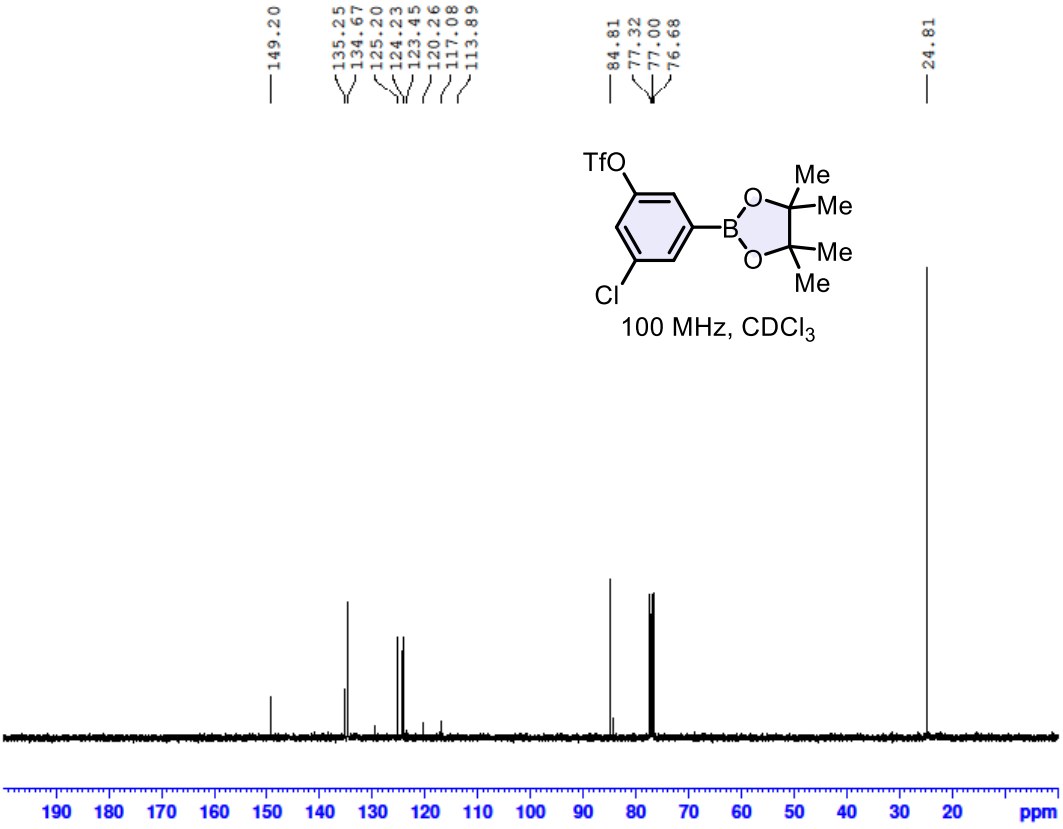

^{19}F NMR of 3-chloro-5-(4,4,5,5-tetramethyl-1,3,2-dioxaborolan-2-yl)phenyl trifluoromethanesulfonate (Table 3.3, compound **9q**)

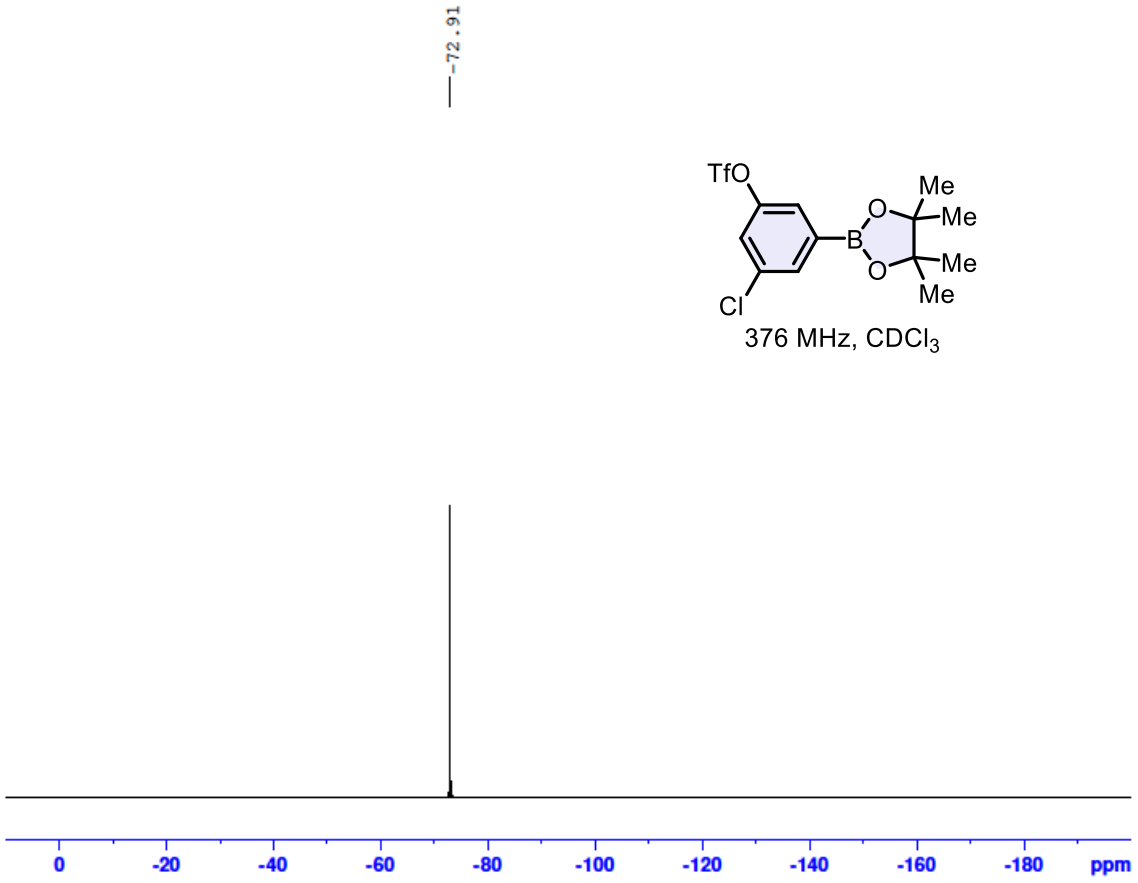

HRMS of 3-chloro-5-(4,4,5,5-tetramethyl-1,3,2-dioxaborolan-2-yl)phenyl trifluoromethanesulfonate (Table 3.3, compound **9q**)

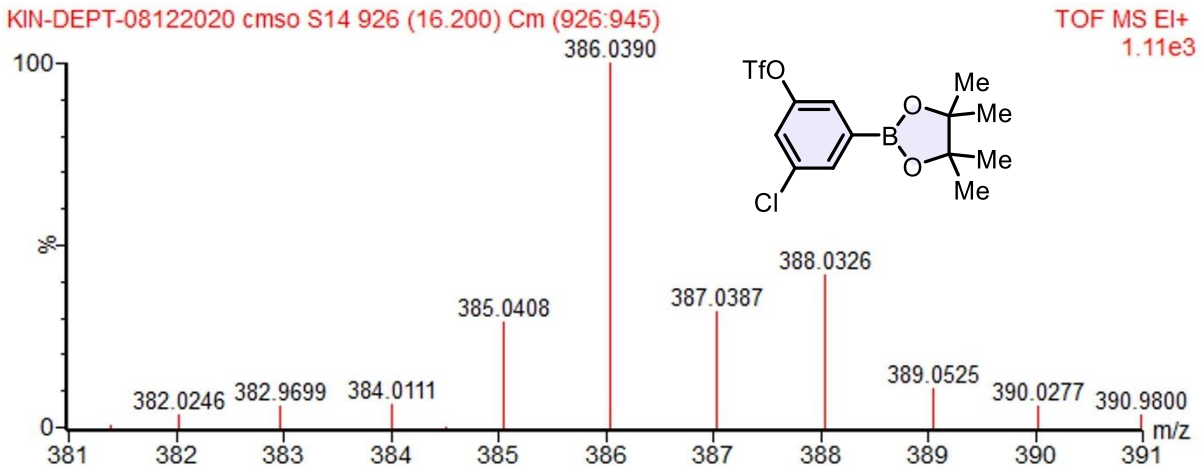

Mass	Calc. Mass	mDa	PPM	Formula
386.0390	386.0371	-1.91	-4.96	C13 H15 B Cl F3 O5 S

^{1}H NMR of 2-chloro-5-(4,4,5,5-tetramethyl-1,3,2-dioxaborolan-2-yl)phenyl trifluoromethanesulfonate (Table 3.3, compound **9r**)

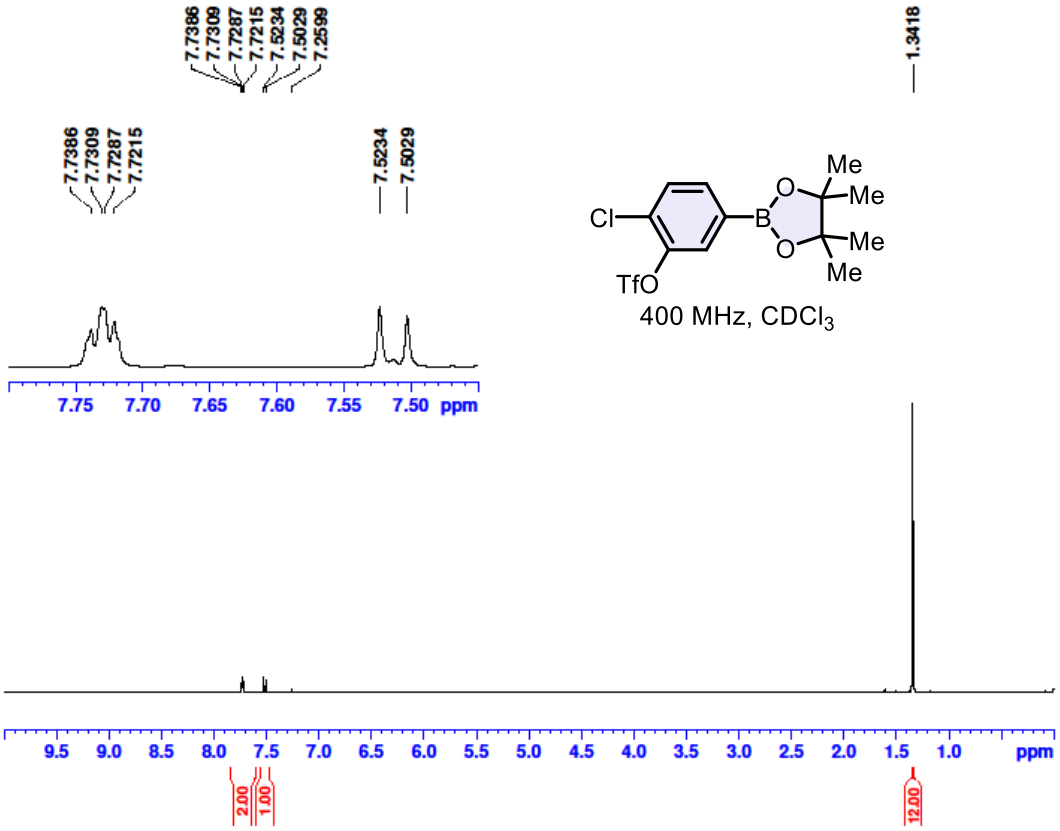

^{13}C NMR of 2-chloro-5-(4,4,5,5-tetramethyl-1,3,2-dioxaborolan-2-yl)phenyl trifluoromethanesulfonate (Table 3.3, compound **9r**)

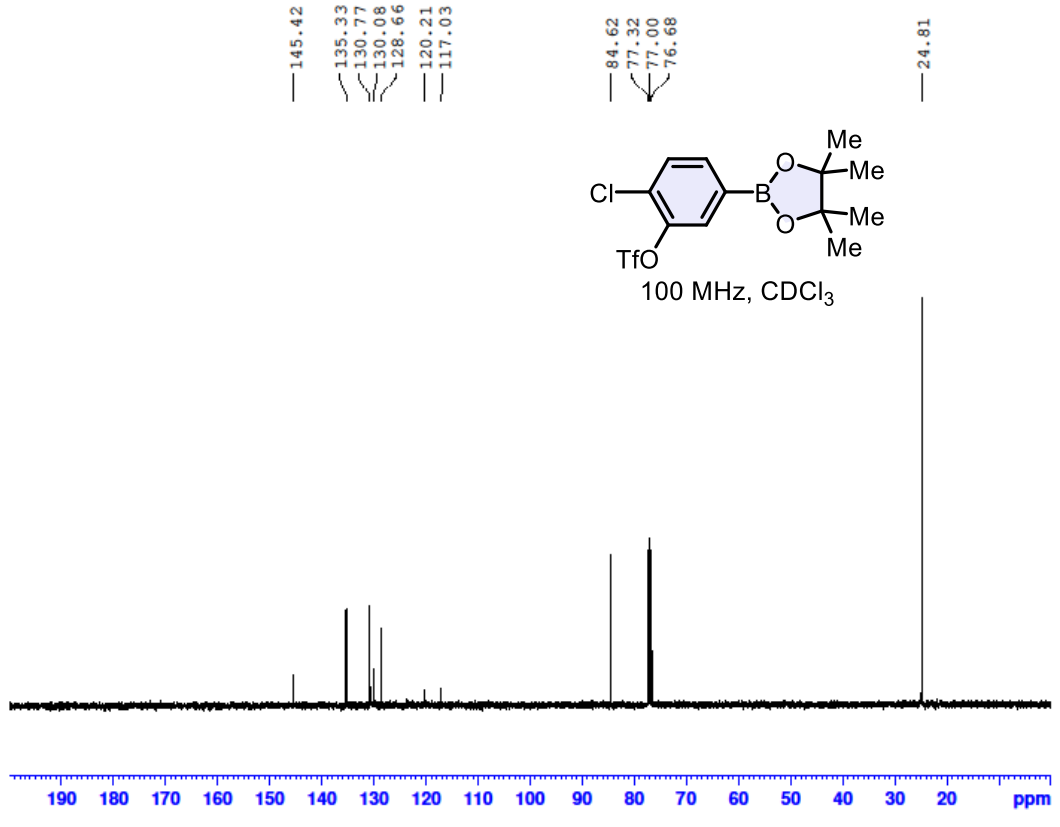

^{19}F NMR of 2-chloro-5-(4,4,5,5-tetramethyl-1,3,2-dioxaborolan-2-yl)phenyl trifluoromethanesulfonate (Table 3.3, compound **9r**)

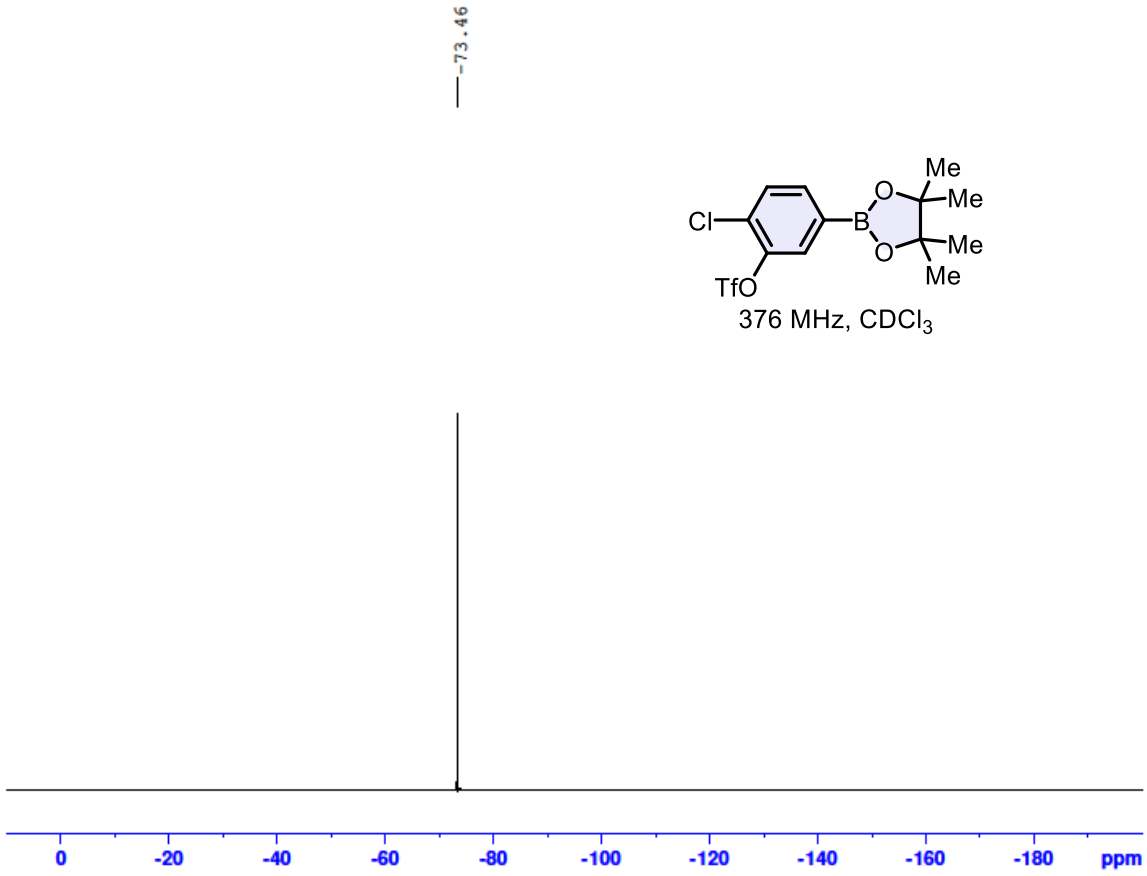

HRMS of 2-chloro-5-(4,4,5,5-tetramethyl-1,3,2-dioxaborolan-2-yl)phenyl trifluoromethanesulfonate (Table 3.3, compound **9r**)

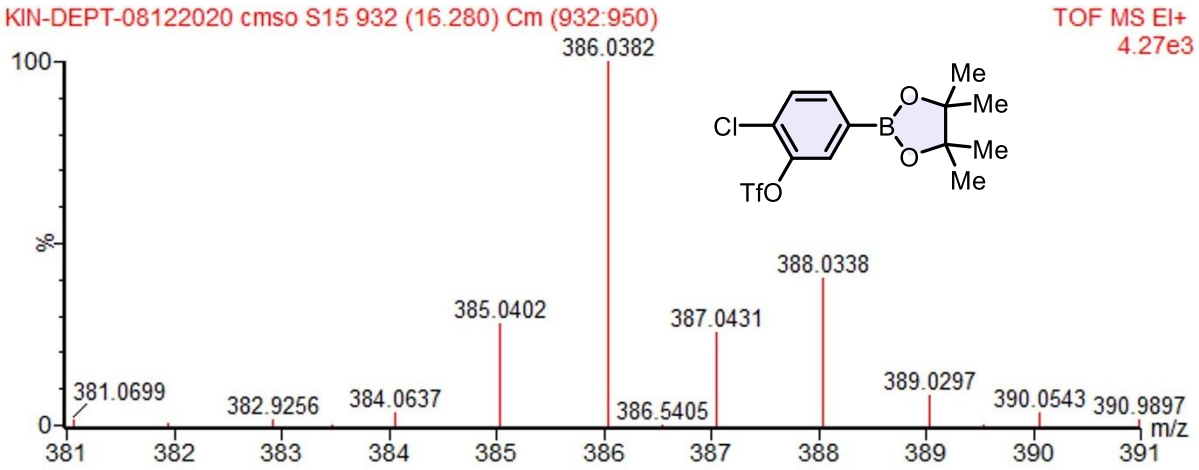

Mass	Calc. Mass	mDa	PPM	Formula
386.0382	386.0371	-1.11	-2.88	C13 H15 B Cl F3 O5 S

^{1}H NMR of 2-chloro-4-(4,4,5,5-tetramethyl-1,3,2-dioxaborolan-2-yl)phenyl trifluoromethanesulfonate (Table 3.3, compound **9s**)

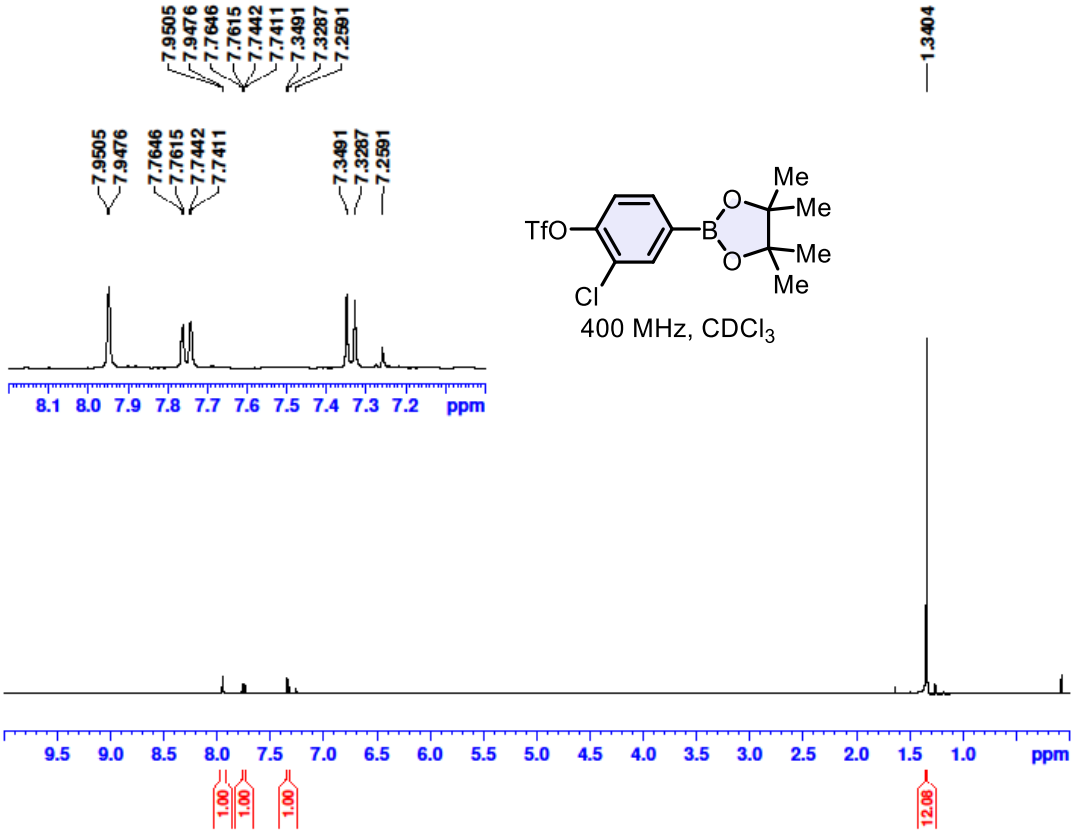

^{13}C NMR of 2-chloro-4-(4,4,5,5-tetramethyl-1,3,2-dioxaborolan-2-yl)phenyl trifluoromethanesulfonate (Table 3.3, compound **9s**)

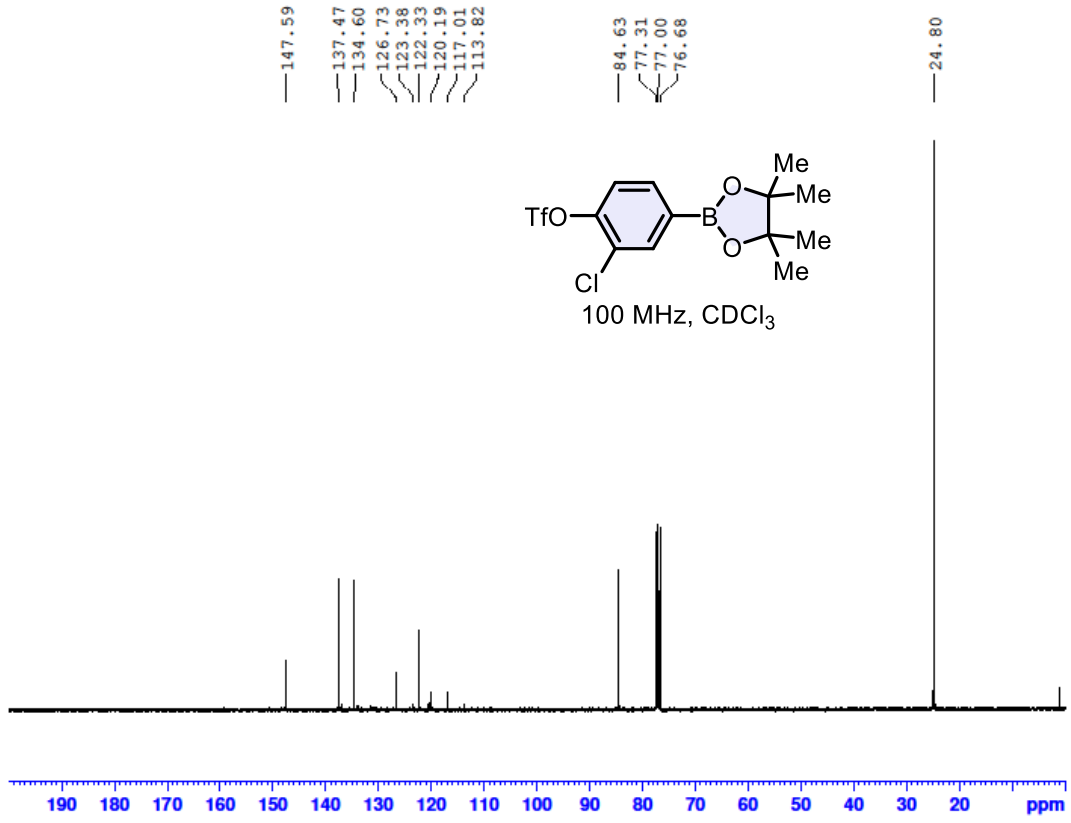

^{19}F NMR of 2-chloro-4-(4,4,5,5-tetramethyl-1,3,2-dioxaborolan-2-yl)phenyl trifluoromethanesulfonate (Table 3.3, compound **9s**)

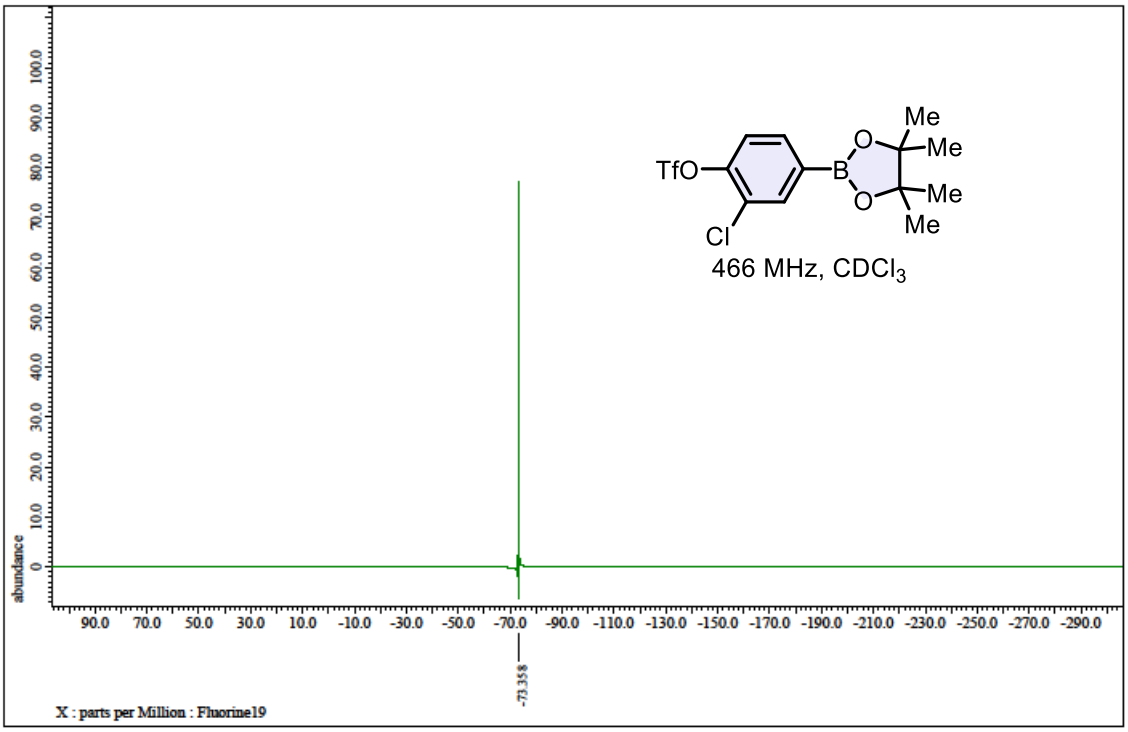

HRMS of 2-chloro-4-(4,4,5,5-tetramethyl-1,3,2-dioxaborolan-2-yl)phenyl trifluoromethanesulfonate (Table 3.3, compound **9s**)

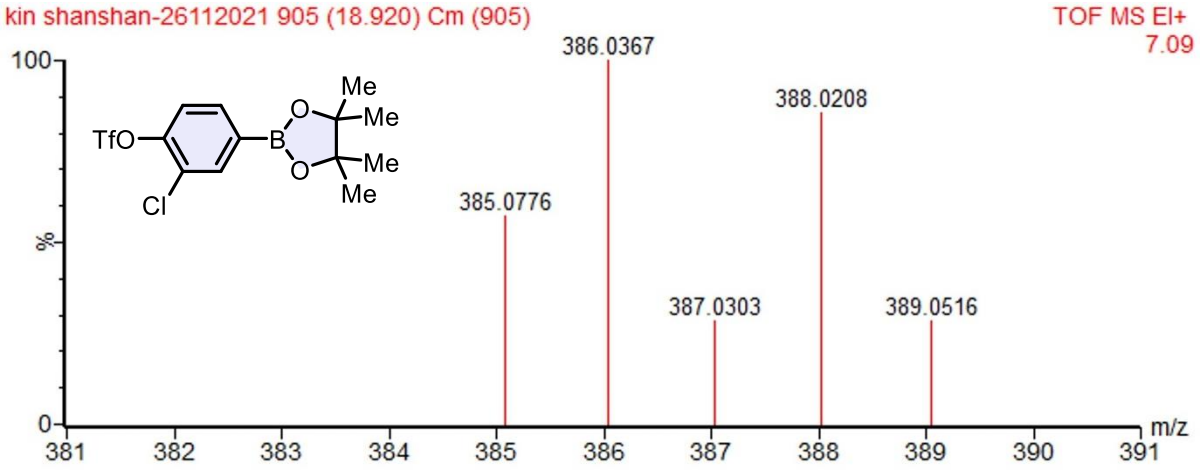

Mass	Calc. Mass	mDa	PPM	Formula
386.0367	386.0371	-0.39	-1.00	C13 H15 B Cl F3 O5 S

^{1}H NMR of 4'-benzoyl-5-methoxy-[1,1'-biphenyl]-3-yl trifluoromethanesulfonate (Table 3.4, compound **13a**)

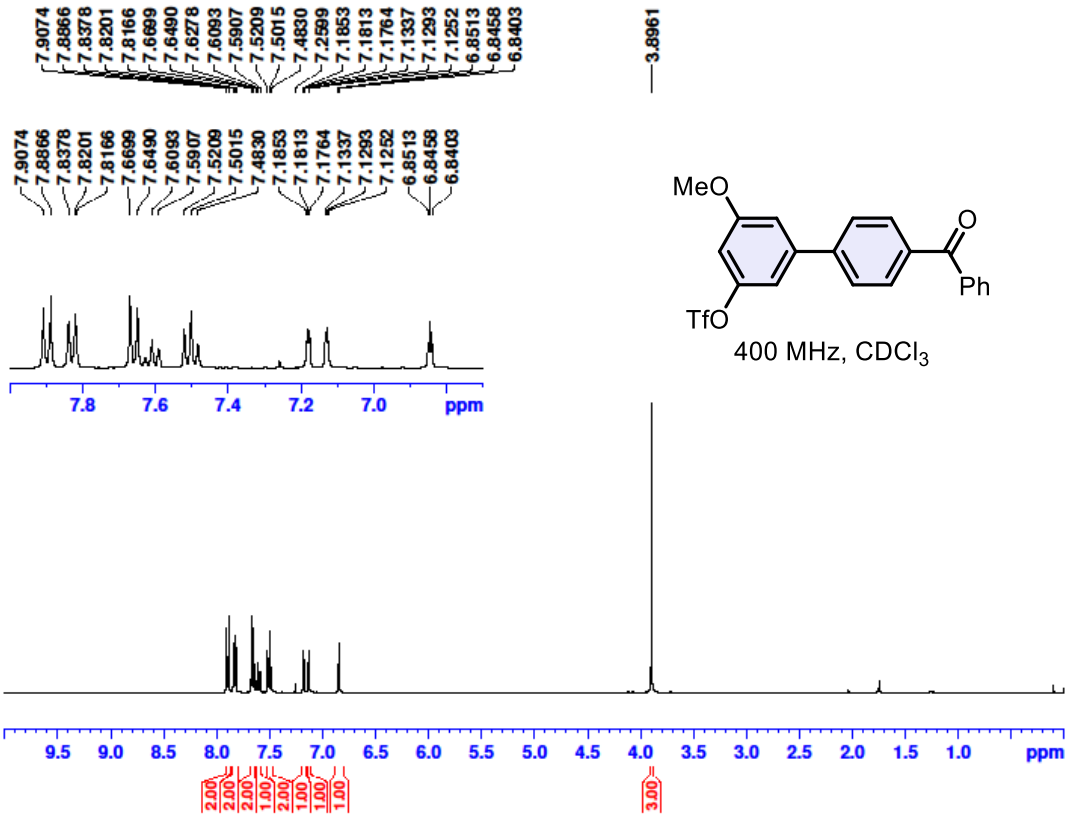

^{13}C NMR of 4'-benzoyl-5-methoxy-[1,1'-biphenyl]-3-yl trifluoromethanesulfonate (Table 3.4, compound **13a**)

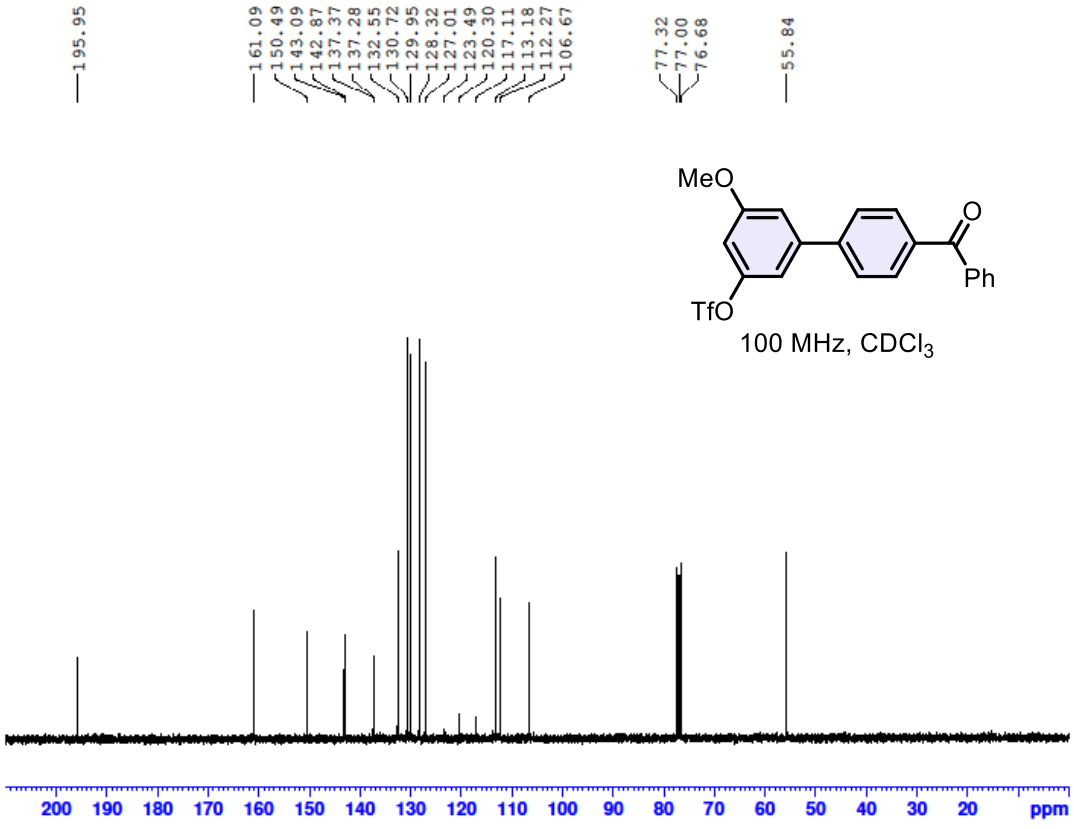

^{19}F NMR of 4'-benzoyl-5-methoxy-[1,1'-biphenyl]-3-yl trifluoromethanesulfonate (Table 3.4, compound **13a**)

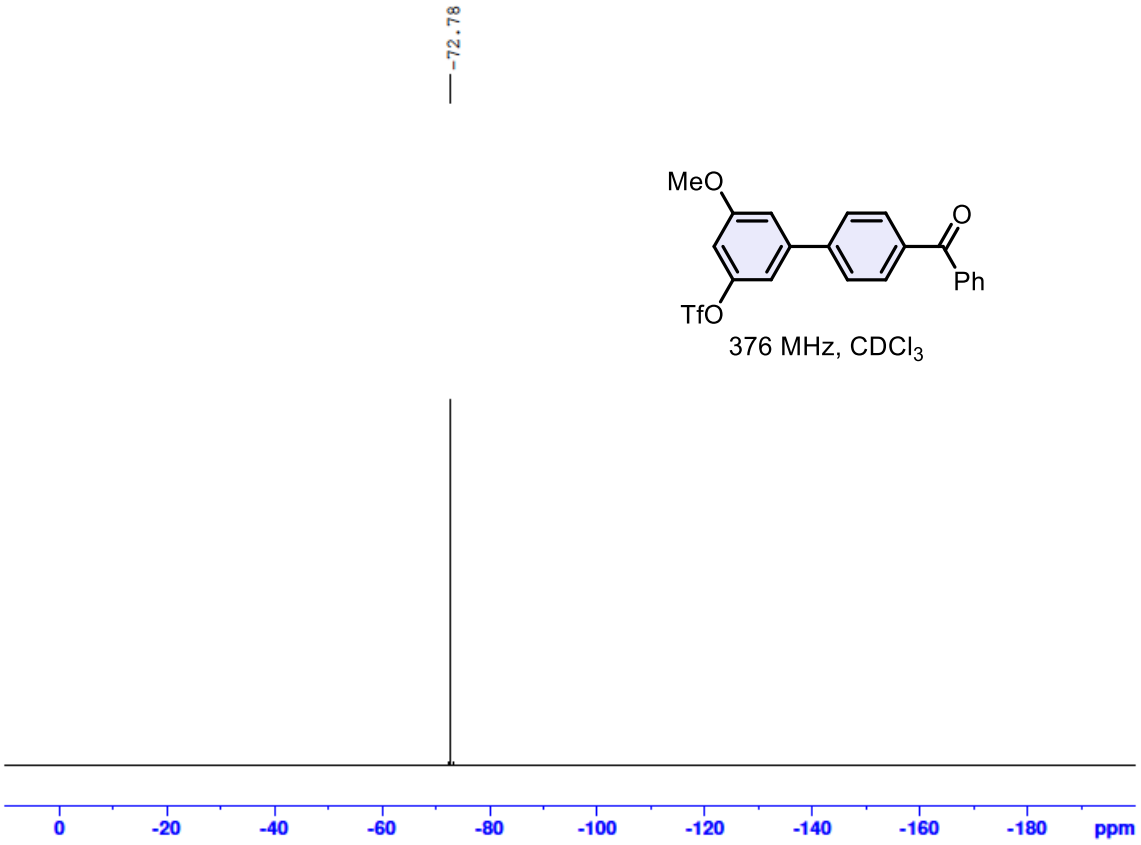

HRMS of 4'-benzoyl-5-methoxy-[1,1'-biphenyl]-3-yl trifluoromethanesulfonate (Table 3.4, compound **13a**)

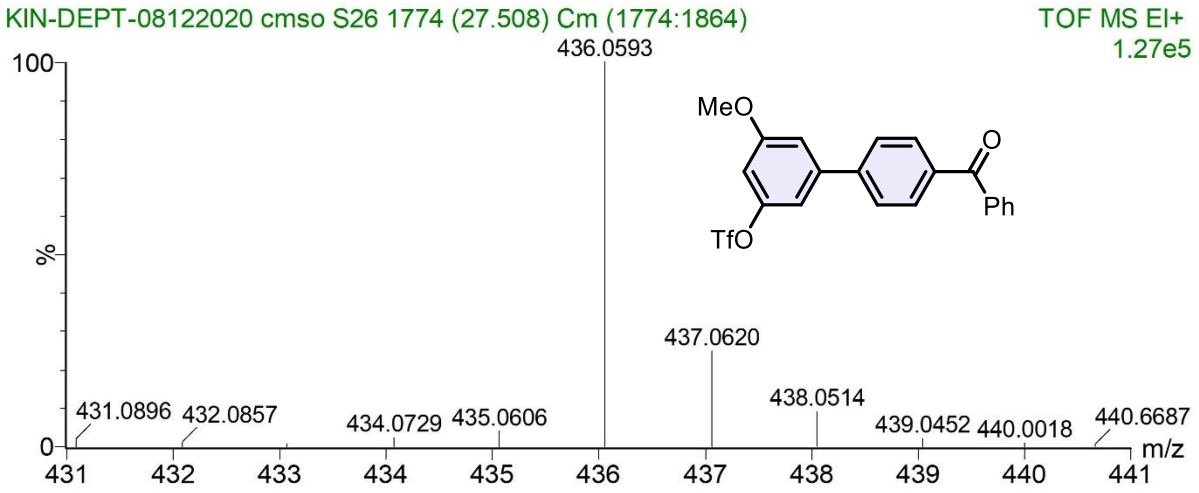

Mass	Calc. Mass	mDa	PPM	Formula
436.0593	436.0587	-0.62	-1.42	C12 H15 F3 O5 S

^{1}H NMR of 4'-benzoyl-3-methyl-[1,1'-biphenyl]-4-yl trifluoromethanesulfonate (Table 3.4, compound **13b**)

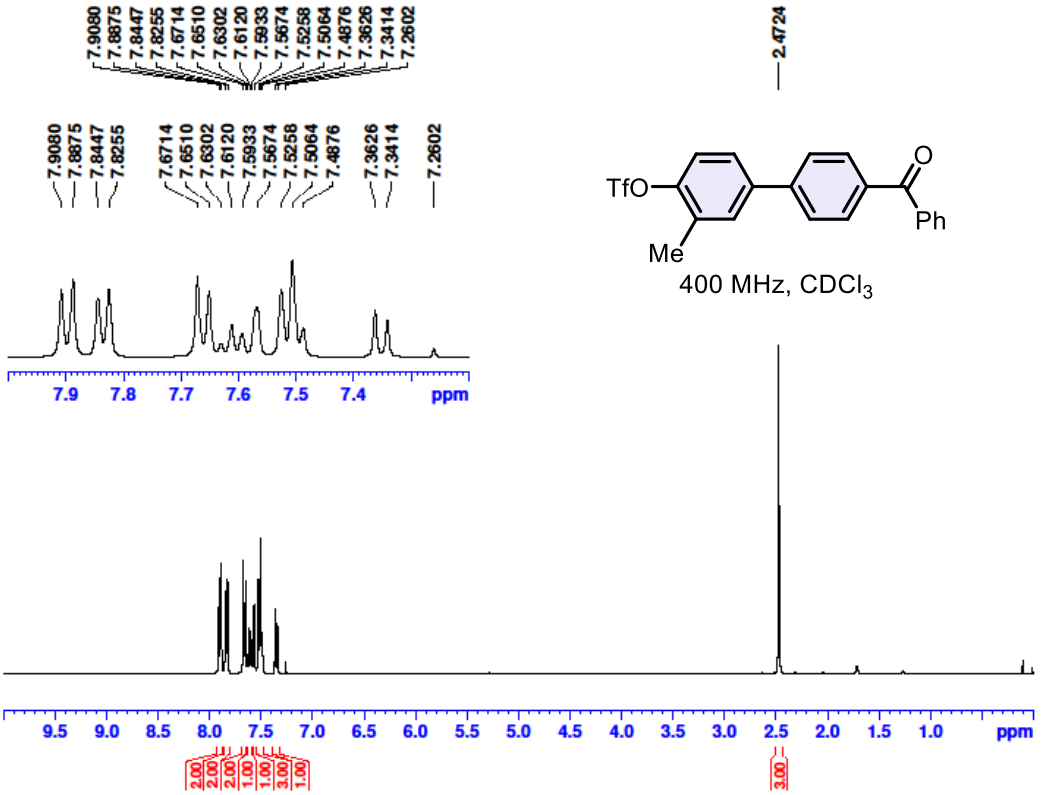

^{13}C NMR of 4'-benzoyl-3-methyl-[1,1'-biphenyl]-4-yl trifluoromethanesulfonate (Table 3.4, compound **13b**)

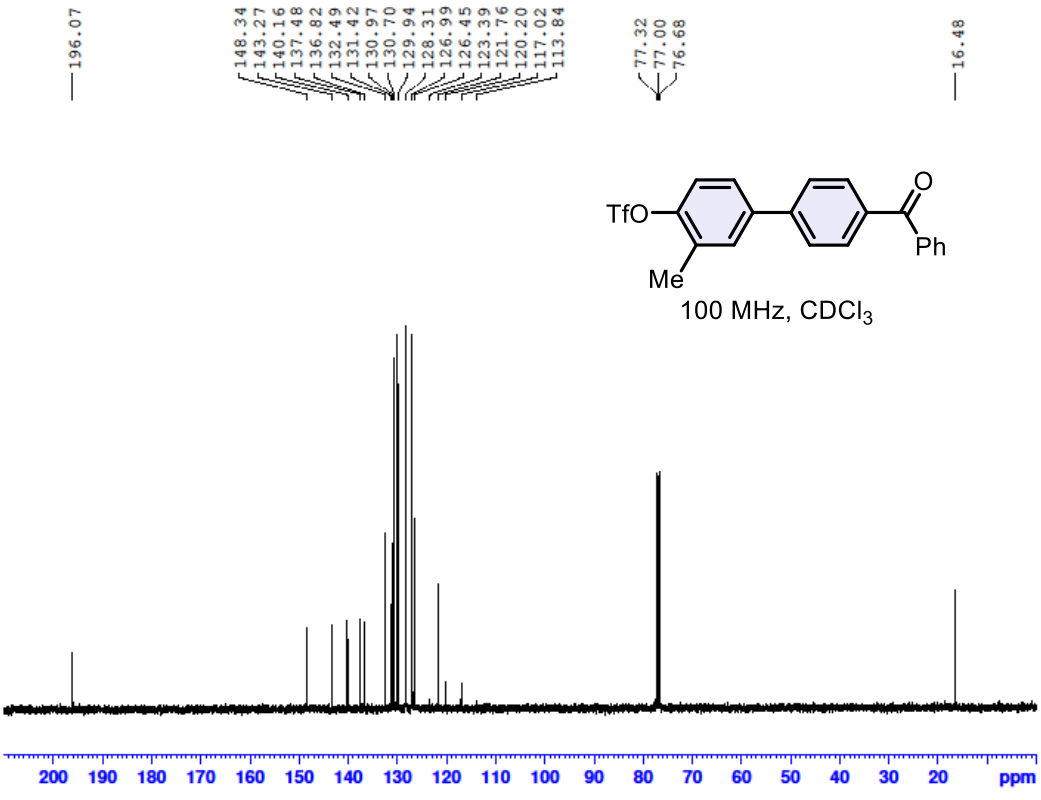

^{19}F NMR of 4’-benzoyl-3-methyl-[1,1’-biphenyl]-4-yl trifluoromethanesulfonate (Table 3.4, compound **13b**)

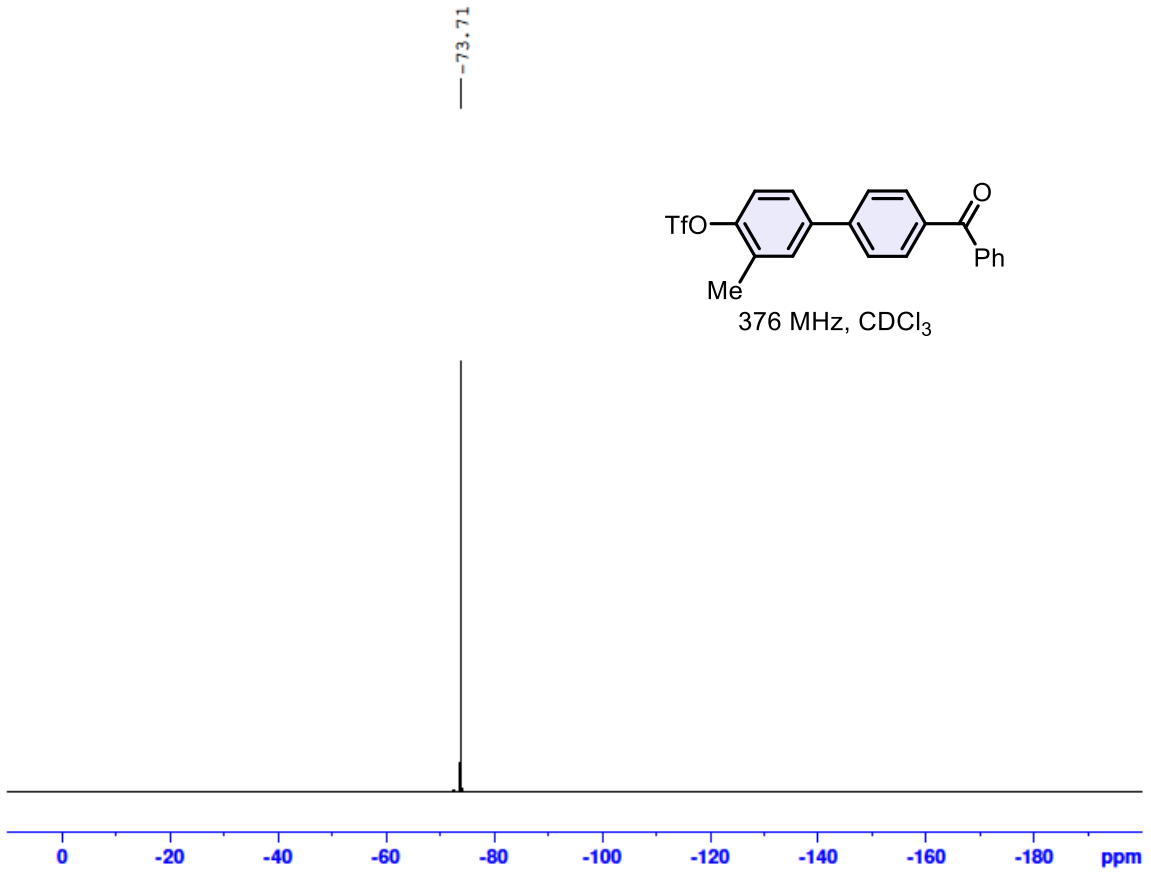

HRMS of 4’-benzoyl-3-methyl-[1,1’-biphenyl]-4-yl trifluoromethanesulfonate (Table 3.4, compound **13b**)

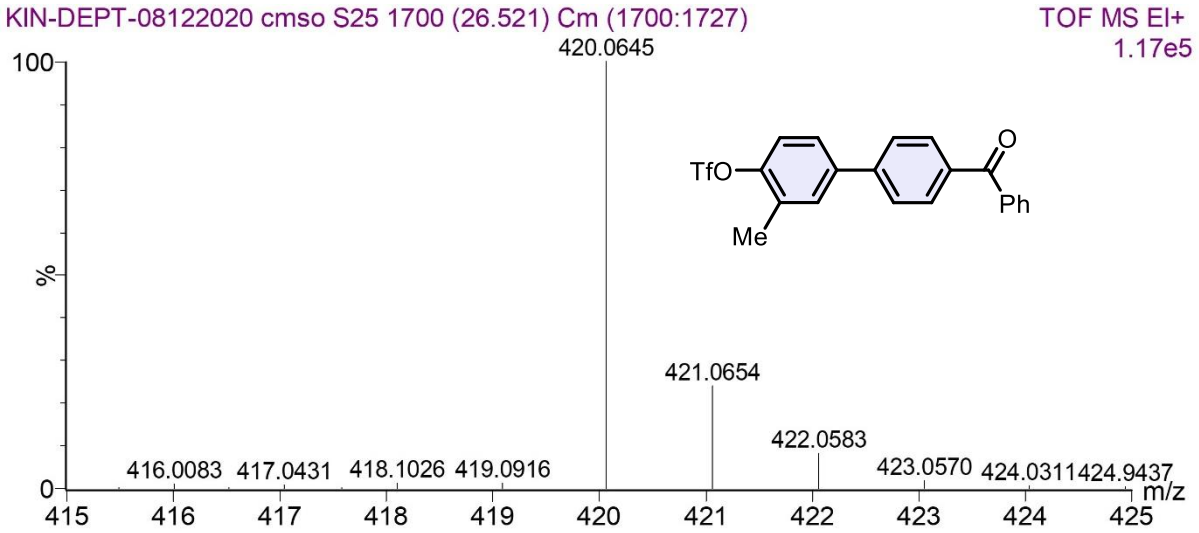

Mass	Calc. Mass	mDa	PPM	Formula
420.0645	420.0638	-0.73	-1.75	C21 H15 F3 O4 S

^{1}H NMR of 3-(6-methylpyridin-2-yl)phenyl trifluoromethanesulfonate (Table 3.4, compound **13c**)

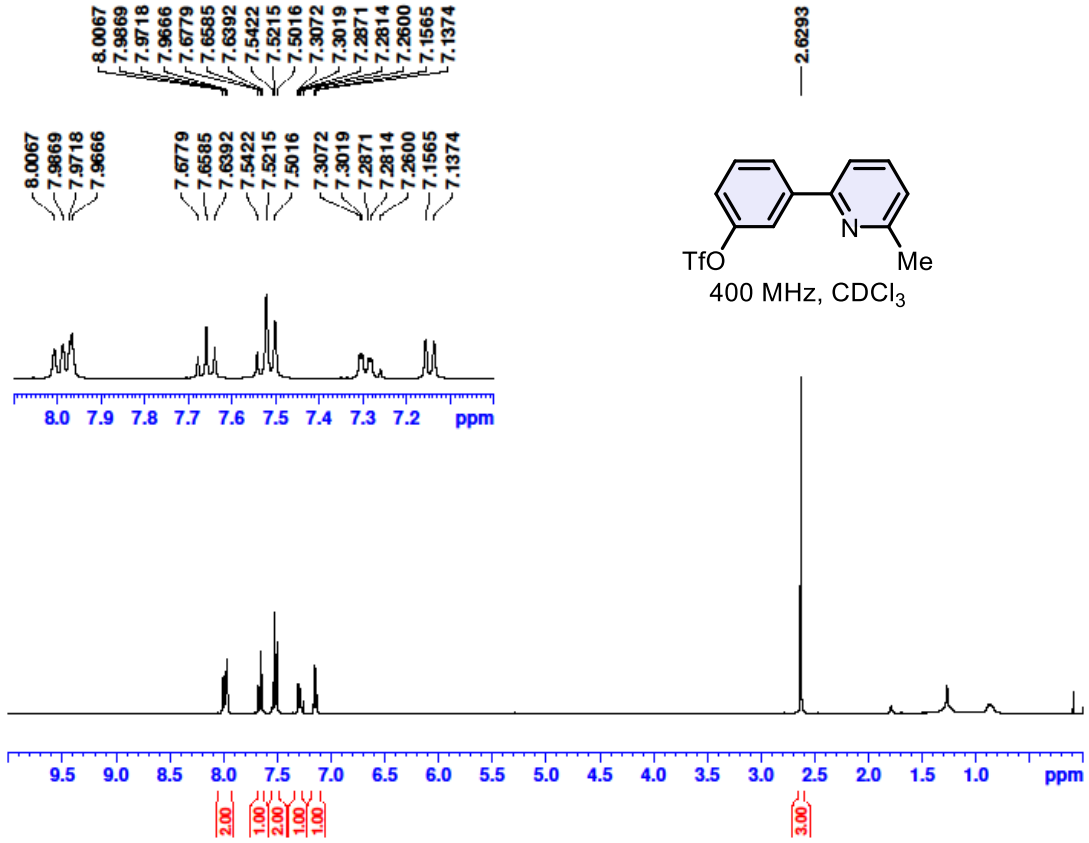

^{13}C NMR of 3-(6-methylpyridin-2-yl)phenyl trifluoromethanesulfonate (Table 3.4, compound **13c**)

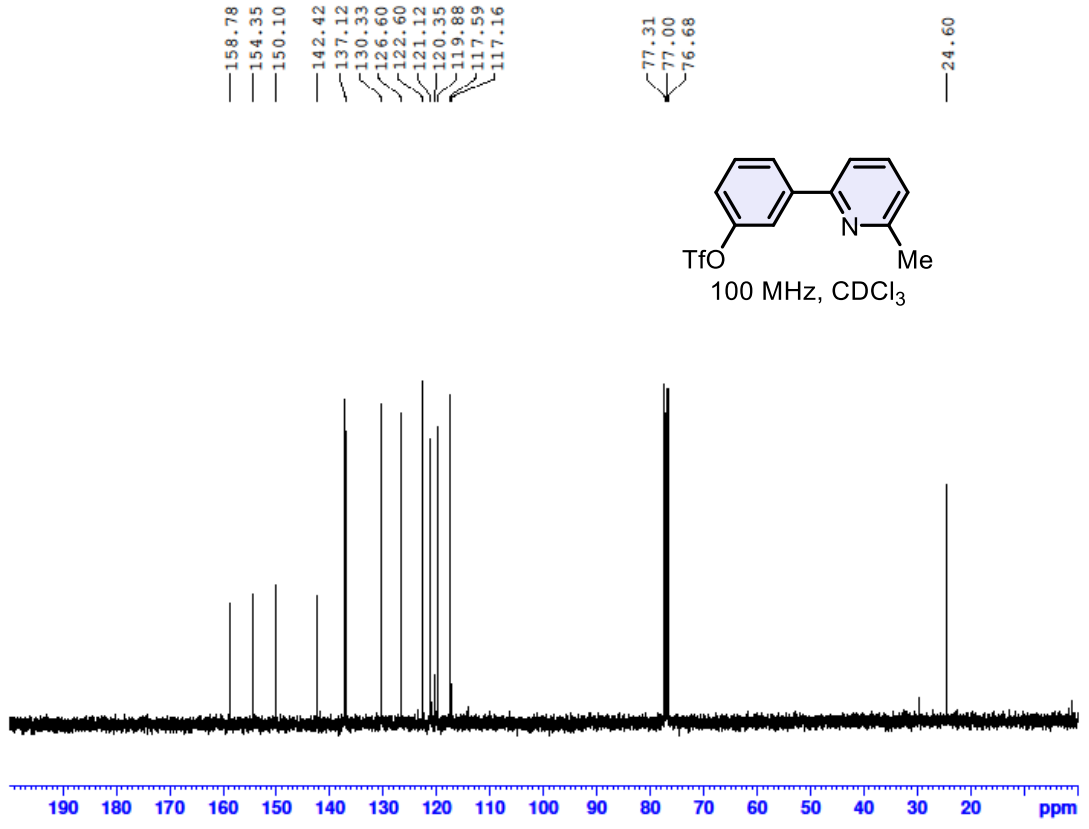

^{19}F NMR of 3-(6-methylpyridin-2-yl)phenyl trifluoromethanesulfonate (Table 3.4, compound **13c**)

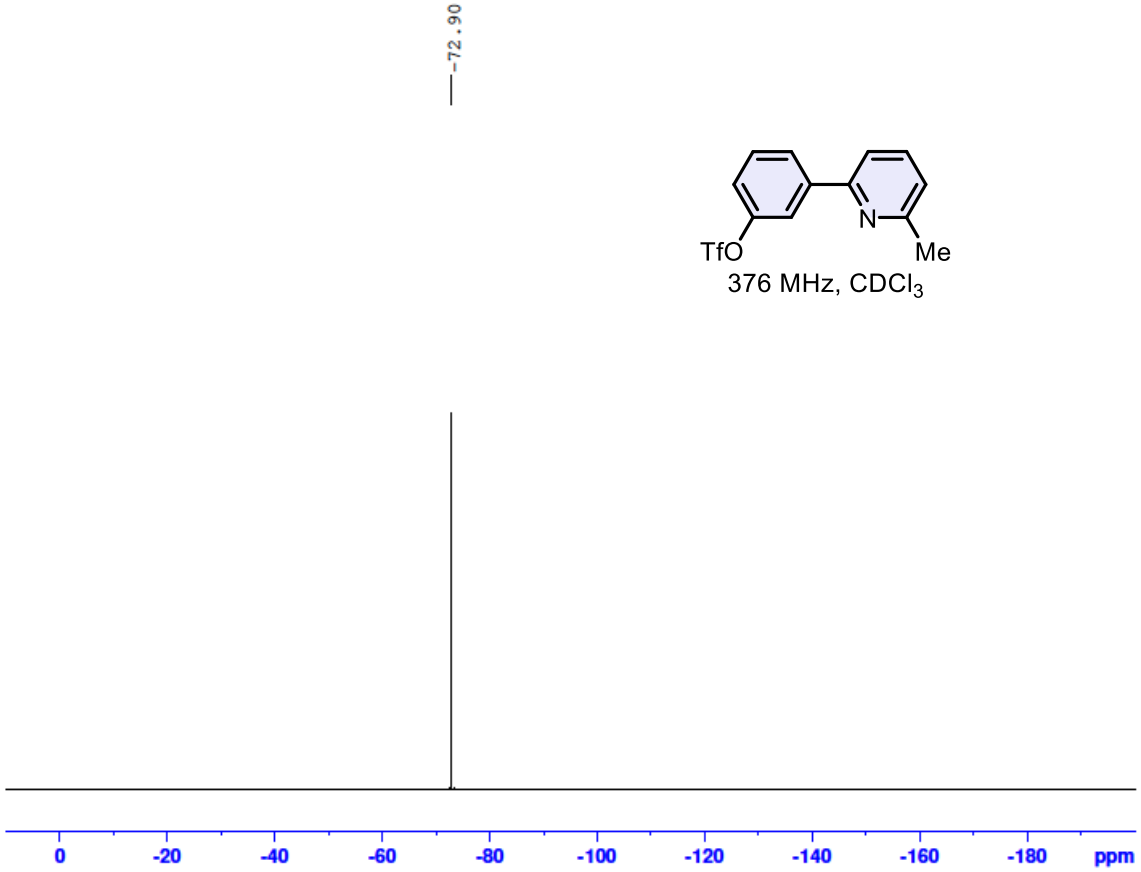

HRMS of 3-(6-methylpyridin-2-yl)phenyl trifluoromethanesulfonate (Table 3.4, compound **13c**)

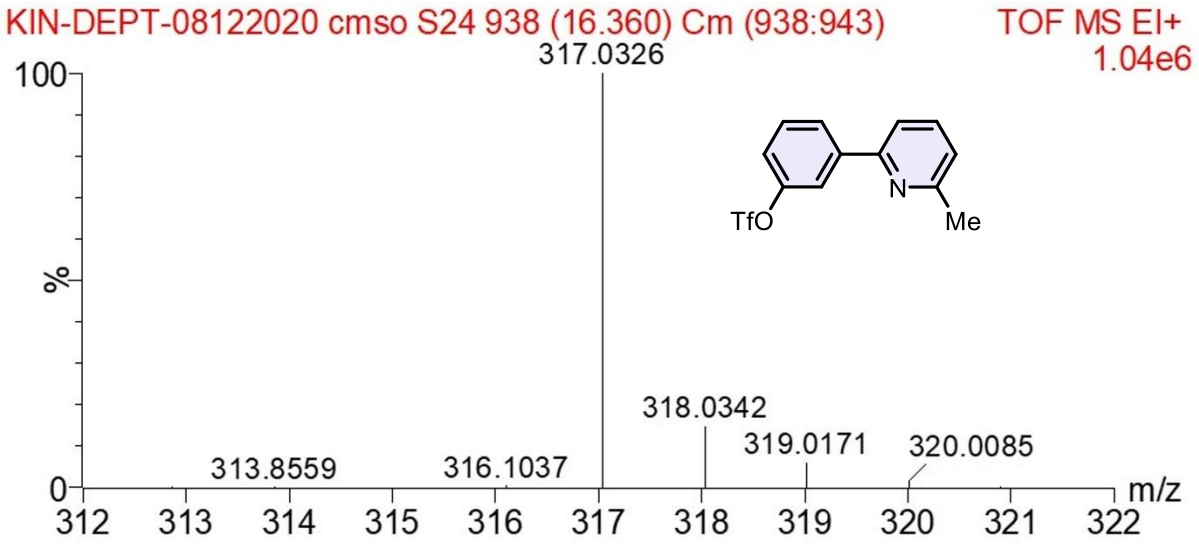

Mass	Calc. Mass	mDa	PPM	Formula
317.0326	317.0328	0.20	0.63	C13 H10 F3 N O3 S

^{1}H NMR of 5-fluoro-3',5'-dimethoxy-[1,1'-biphenyl]-3-yl trifluoromethanesulfonate (Table 3.4, compound **13d**)

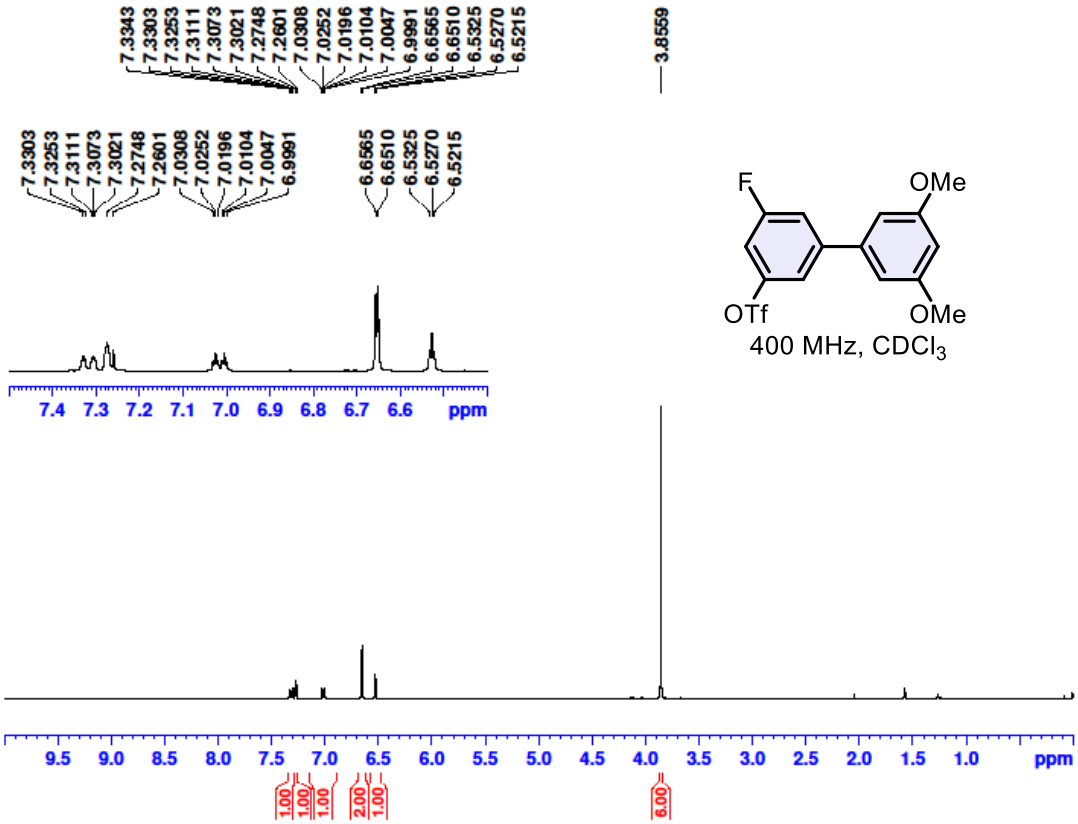

^{13}C NMR of 5-fluoro-3',5'-dimethoxy-[1,1'-biphenyl]-3-yl trifluoromethanesulfonate (Table 3.4, compound **13d**)

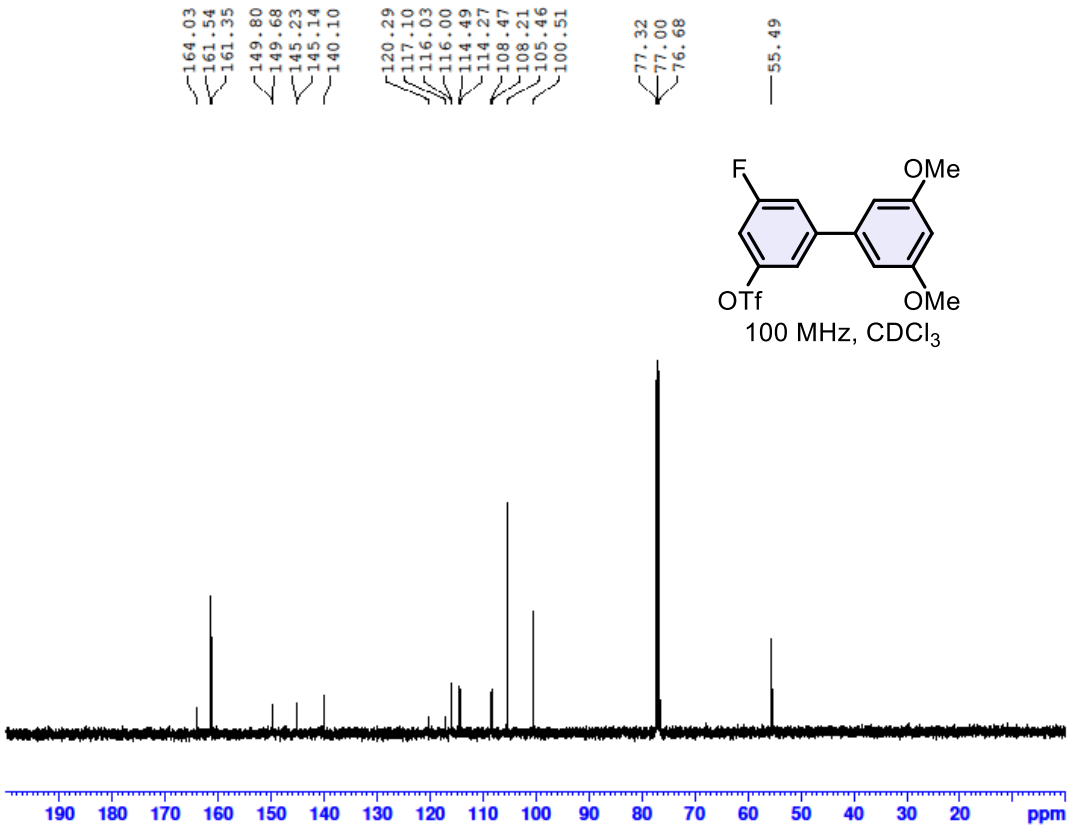

^{19}F NMR of 5-fluoro-3',5'-dimethoxy-[1,1'-biphenyl]-3-yl trifluoromethanesulfonate (Table 3.4, compound **13d**)

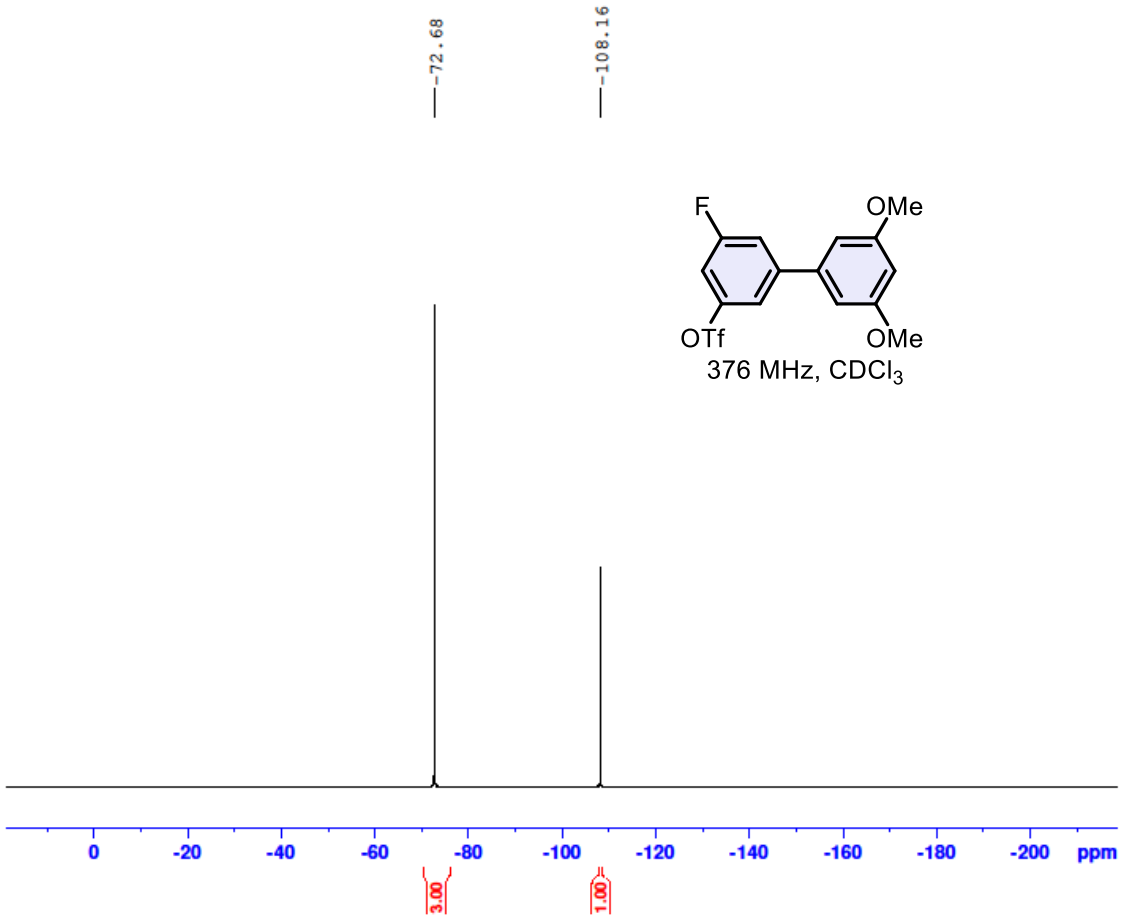

HRMS of 5-fluoro-3',5'-dimethoxy-[1,1'-biphenyl]-3-yl trifluoromethanesulfonate (Table 3.4, compound **13d**)

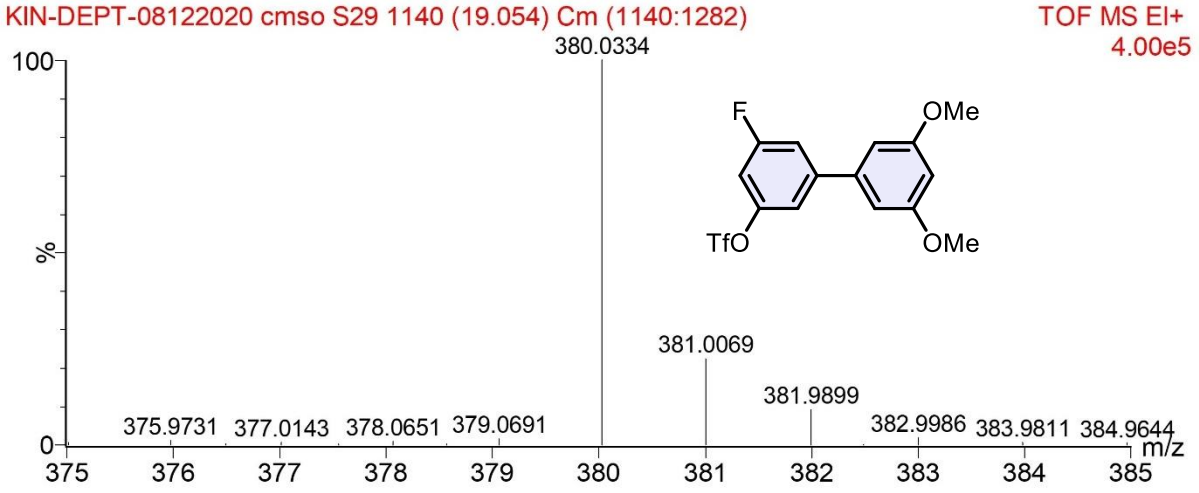

Mass	Calc. Mass	mDa	PPM	Formula
380.0334	380.0336	0.21	0.55	C15 H12 F4 O5 S

^{1}H NMR of 3-methyl-5-(quinolin-2-yl)phenyl trifluoromethanesulfonate (Table 3.4, compound **13e**)

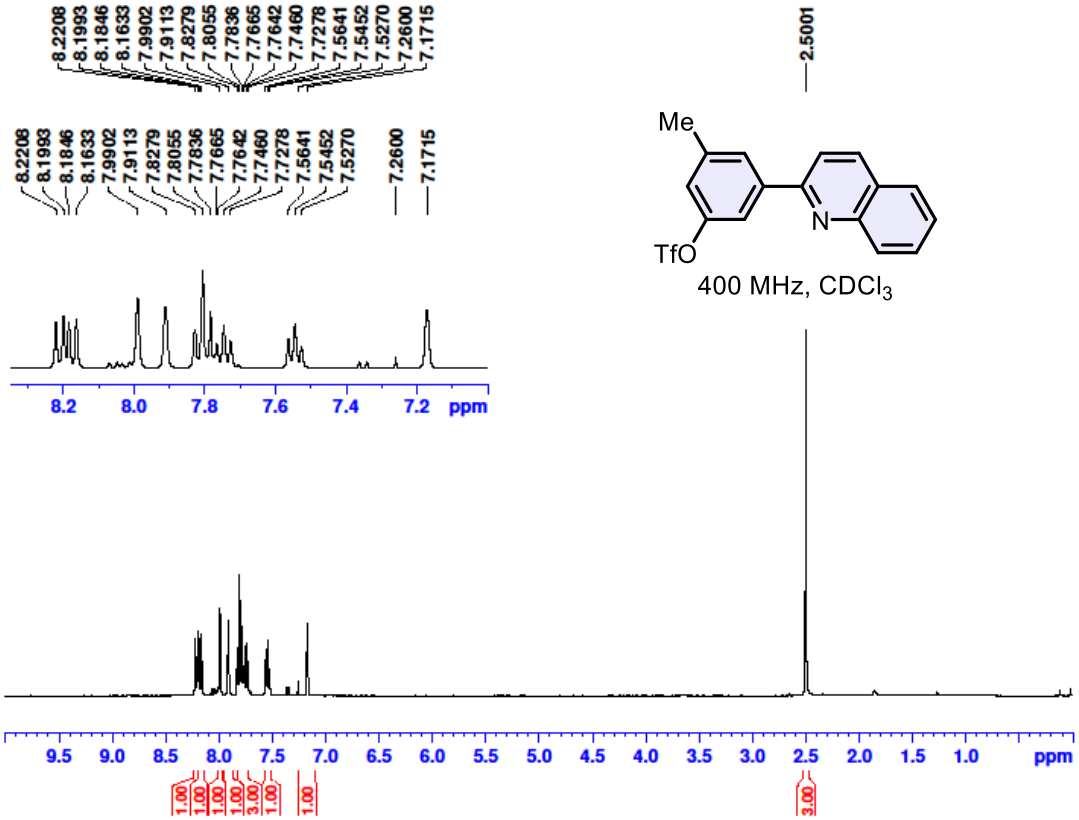

^{13}C NMR of 3-methyl-5-(quinolin-2-yl)phenyl trifluoromethanesulfonate (Table 3.4, compound **13e**)

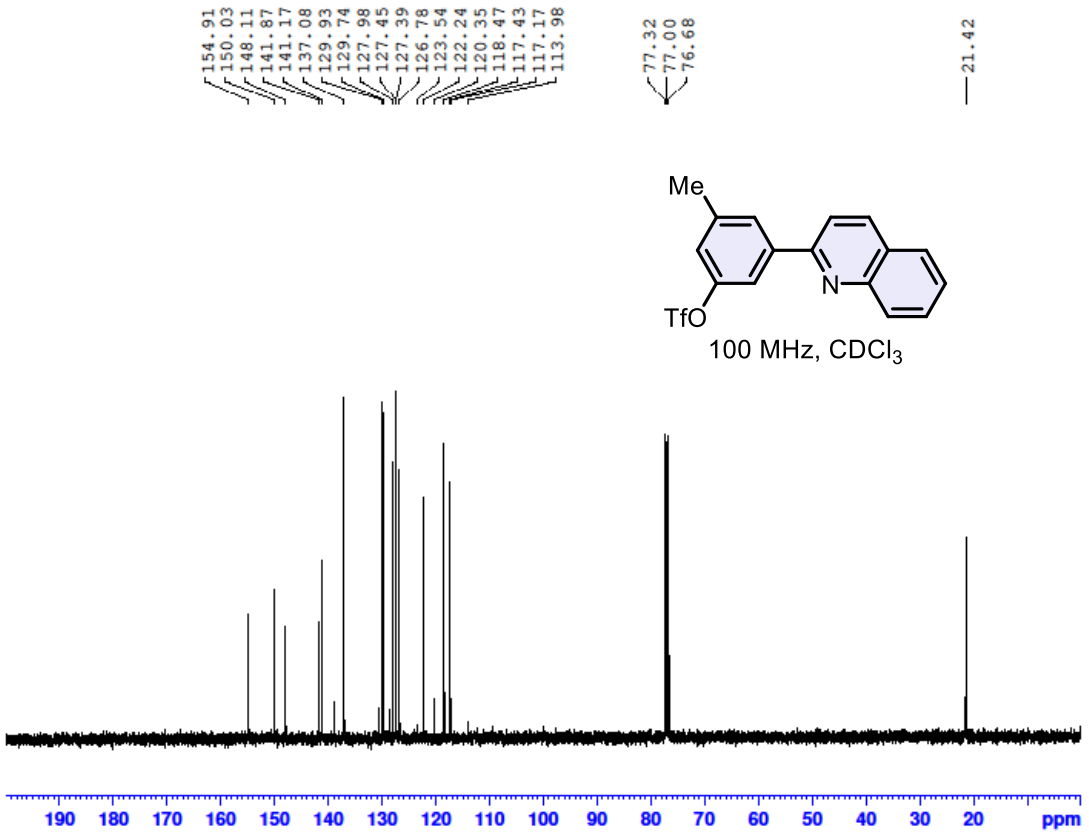

^{19}F NMR of 3-methyl-5-(quinolin-2-yl)phenyl trifluoromethanesulfonate (Table 3.4, compound **13e**)

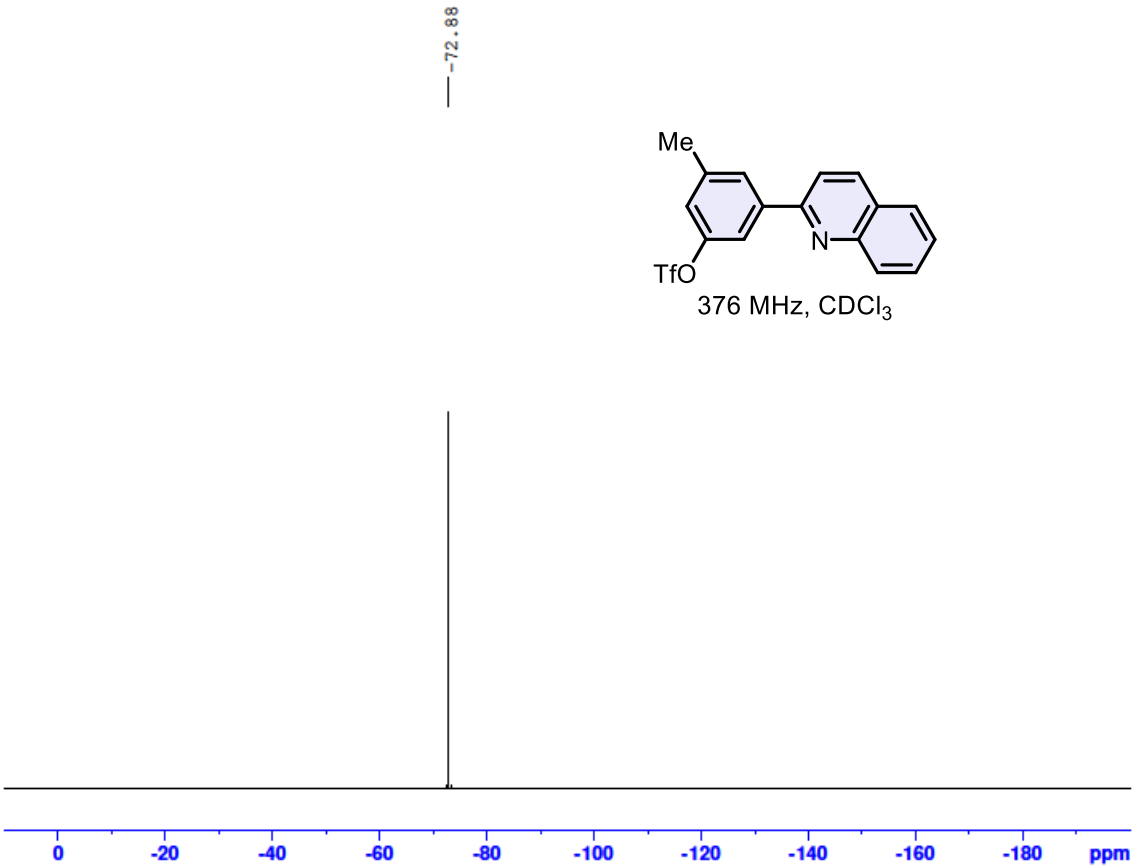

HRMS of 3-methyl-5-(quinolin-2-yl)phenyl trifluoromethanesulfonate (Table 3.4, compound **13e**)

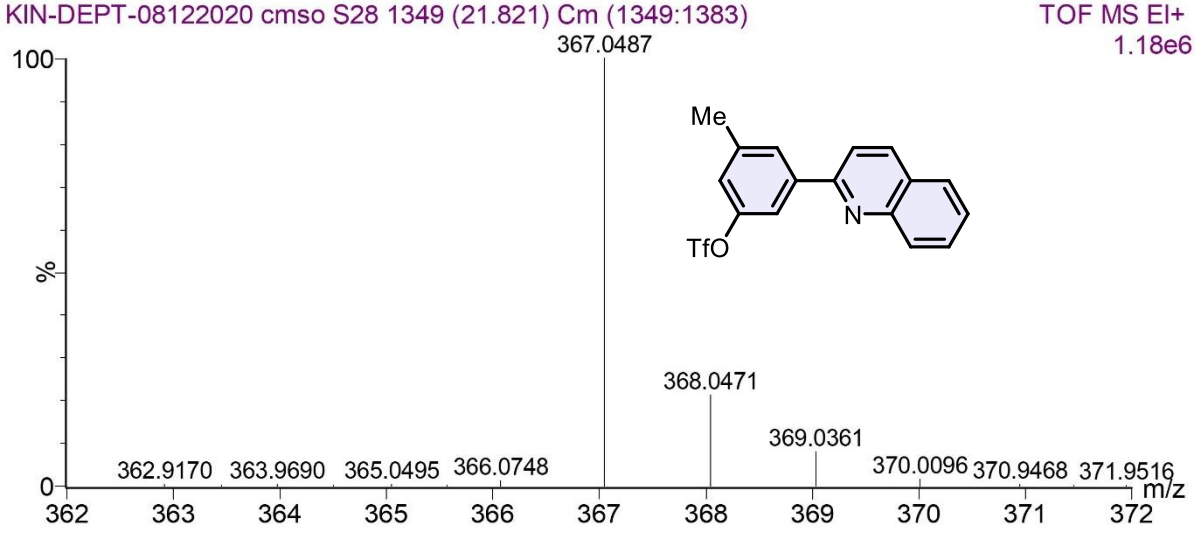

Mass	Calc. Mass	mDa	PPM	Formula
367.0487	367.0485	-0.25	-0.68	C17 H12 F3 N O3 S

^{1}H NMR of 2-methyl-5-(6-methylpyridin-2-yl)phenyl trifluoromethanesulfonate (Table 3.4, compound **13f**)

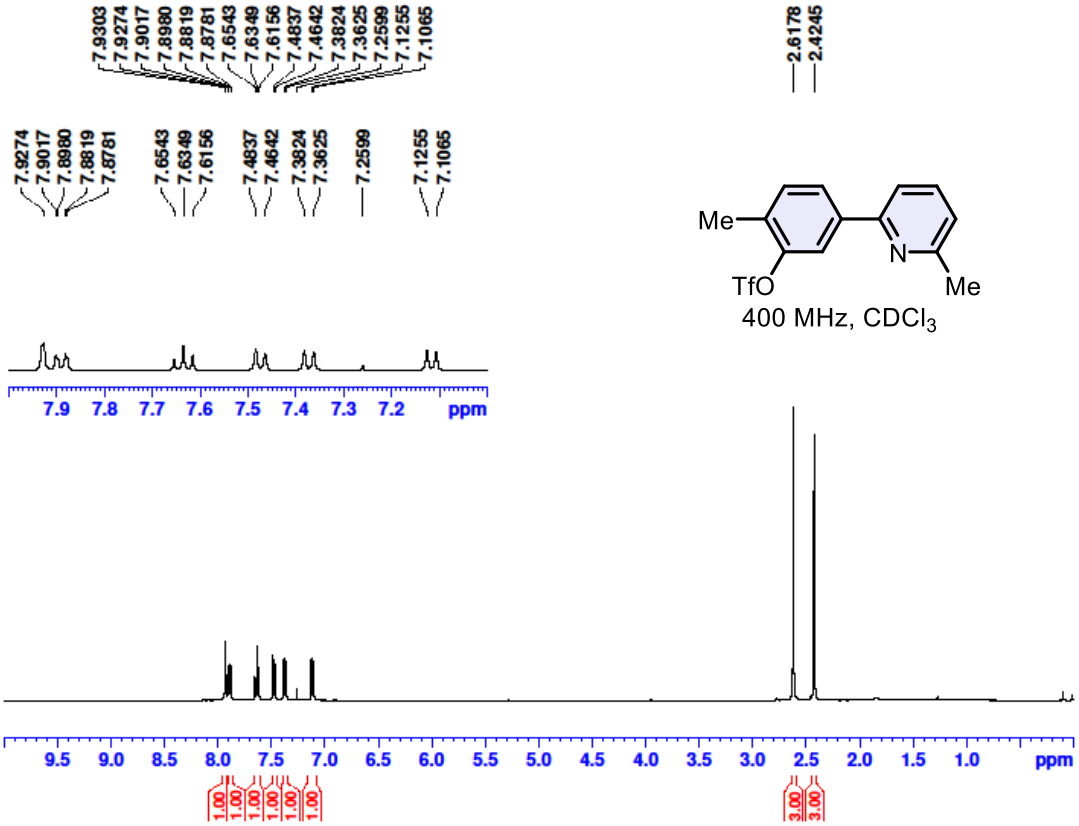

^{13}C NMR of 2-methyl-5-(6-methylpyridin-2-yl)phenyl trifluoromethanesulfonate (Table 3.4, compound **13f**)

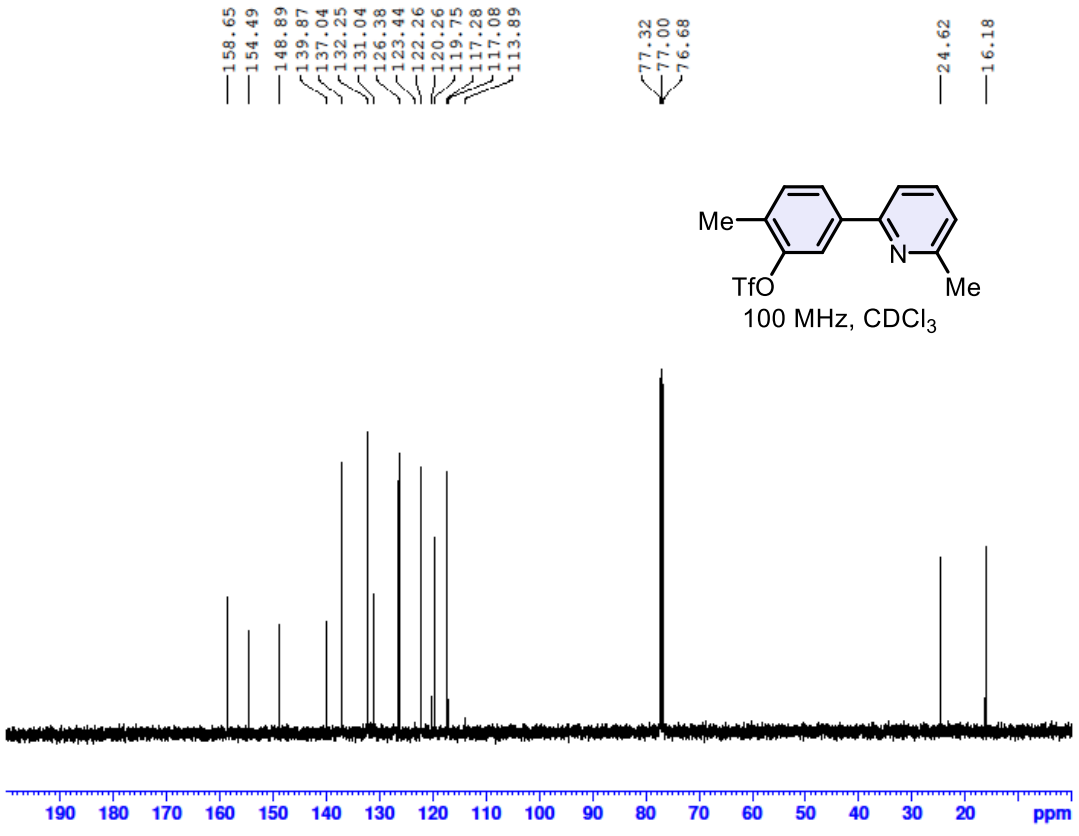

^{19}F NMR of 2-methyl-5-(6-methylpyridin-2-yl)phenyl trifluoromethanesulfonate (Table 3.4, compound **13f**)

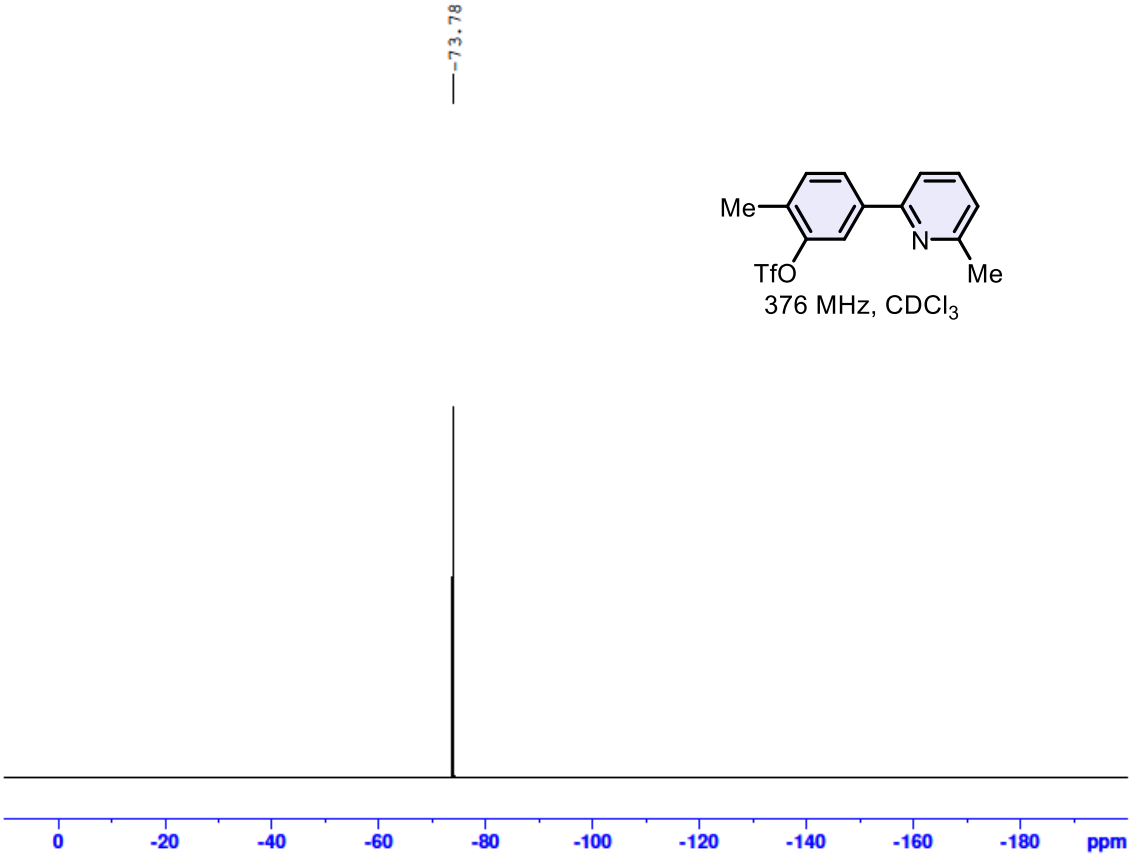

HRMS of 2-methyl-5-(6-methylpyridin-2-yl)phenyl trifluoromethanesulfonate (Table 3.4, compound **13f**)

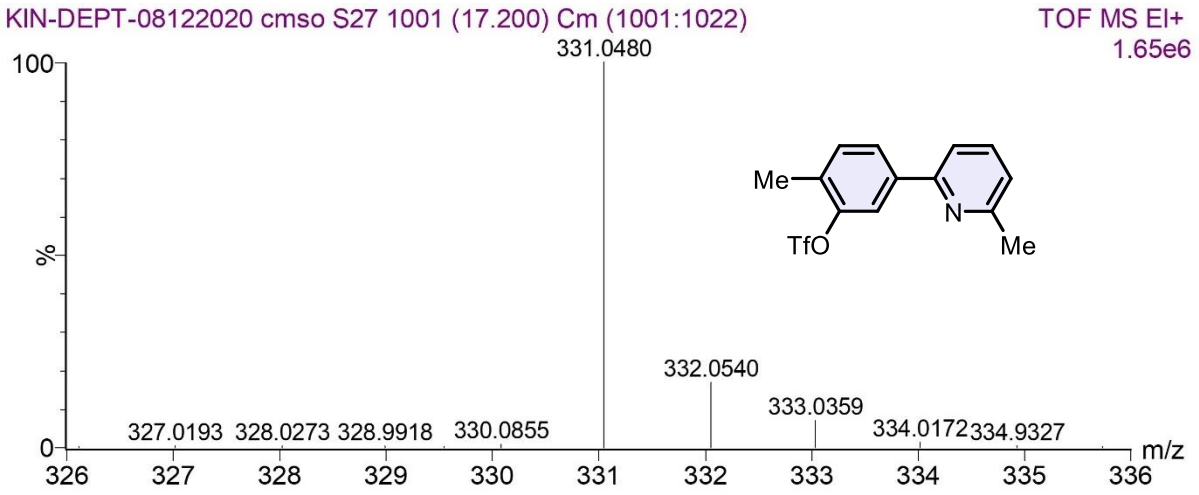

Mass	Calc. Mass	mDa	PPM	Formula
331.0480	331.0485	0.45	1.36	C14 H12 F3 N O3 S

^{1}H NMR of methyl 4'-(4-(((trifluoromethyl)sulfonyl)oxy)benzoyl)-[1,1'-biphenyl]-4-carboxylate (Table 3.4, compound **13g**)

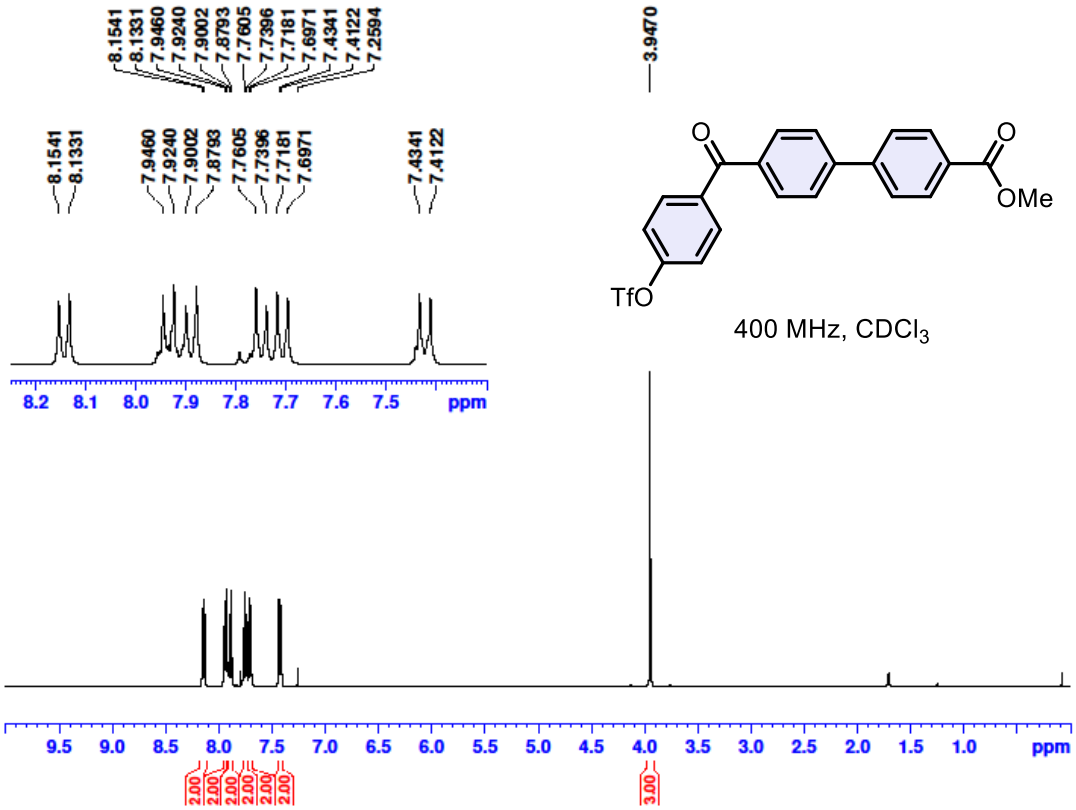

^{13}C NMR of methyl 4'-(4-(((trifluoromethyl)sulfonyl)oxy)benzoyl)-[1,1'-biphenyl]-4-carboxylate (Table 3.4, compound **13g**)

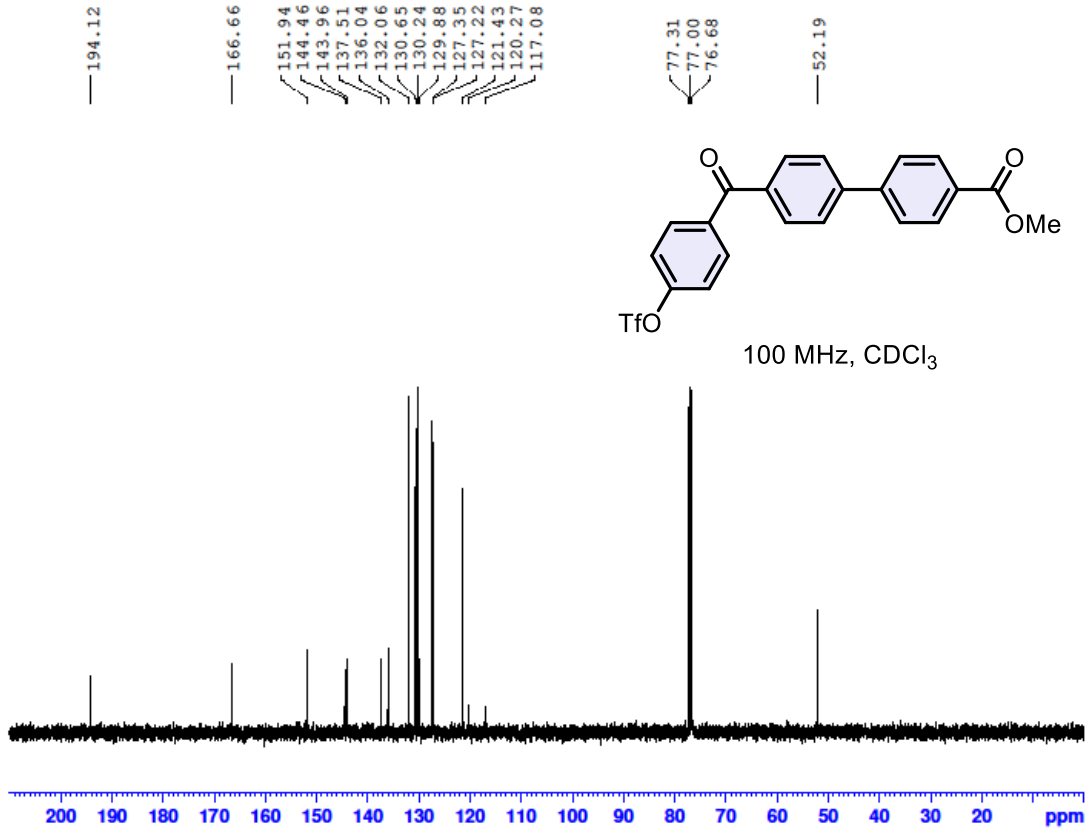

^{19}F NMR of methyl 4'-(4-(((trifluoromethyl)sulfonyl)oxy)benzoyl)-[1,1'-biphenyl]-4-carboxylate (Table 3.4, compound **13g**)

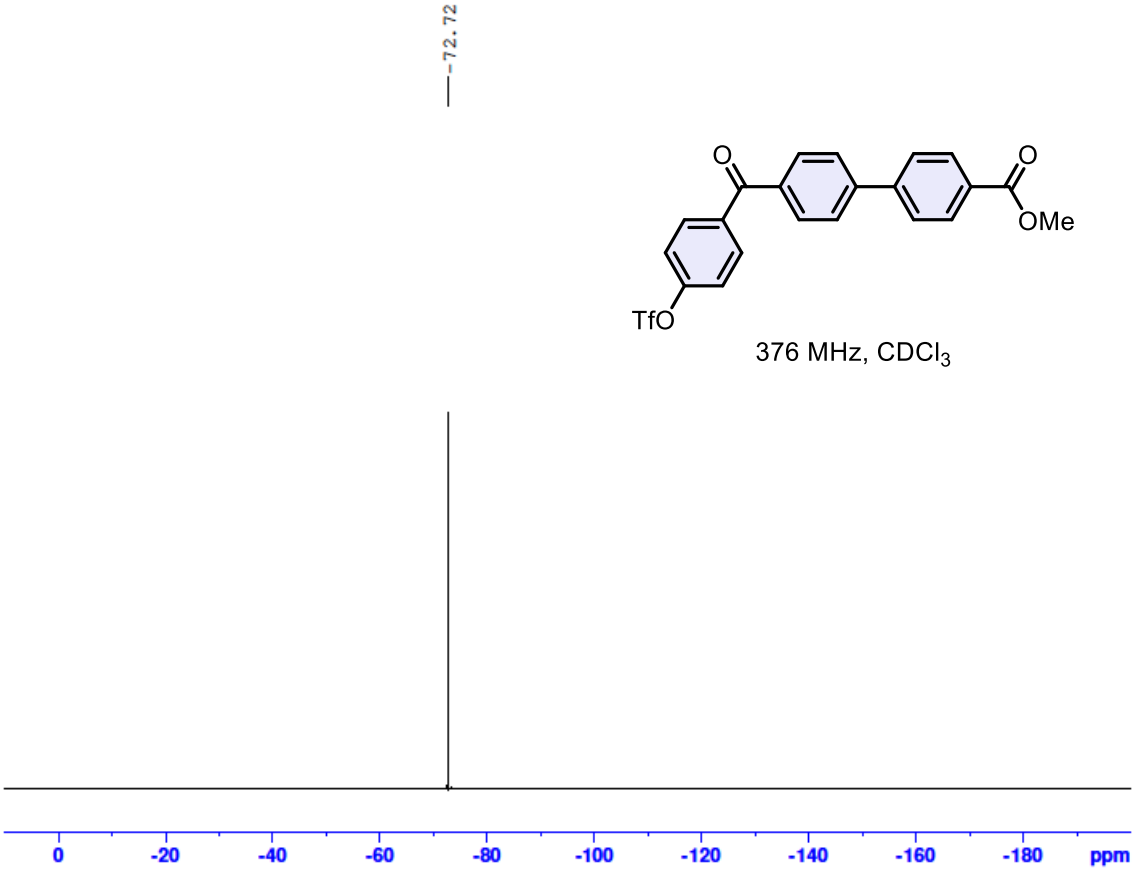

HRMS of methyl 4'-(4-(((trifluoromethyl)sulfonyl)oxy)benzoyl)-[1,1'-biphenyl]-4-carboxylate (Table 3.4, compound **13g**)

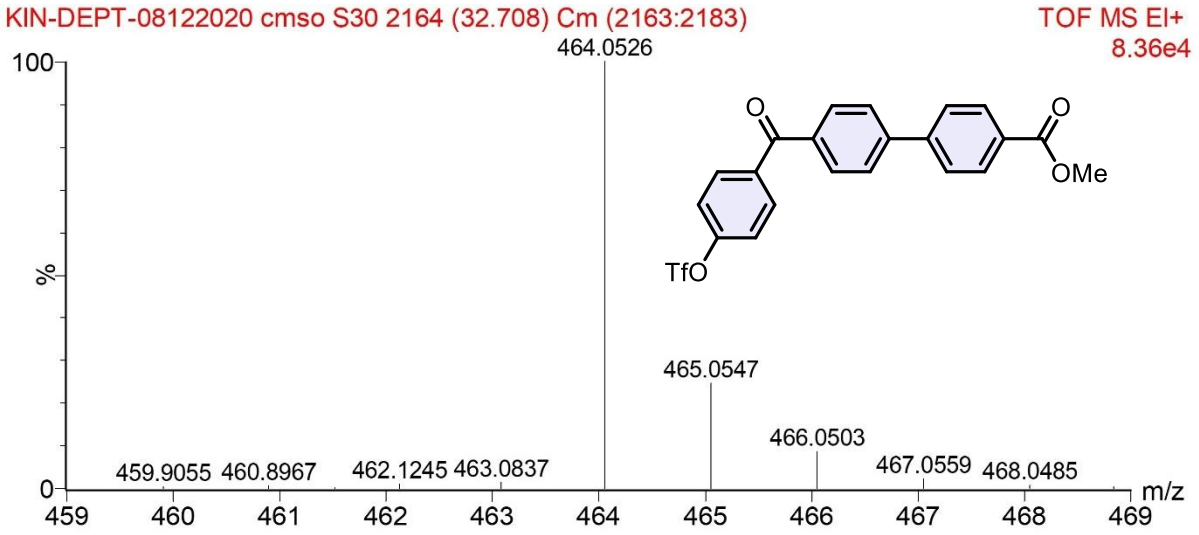

Mass	Calc. Mass	mDa	PPM	Formula
464.0526	464.0536	0.99	2.14	C22 H15 F3 O6 S

^{1}H NMR of 4'-acetyl-3-methoxy-[1,1'-biphenyl]-4-yl trifluoromethanesulfonate (Table 3.4, compound **13h**)

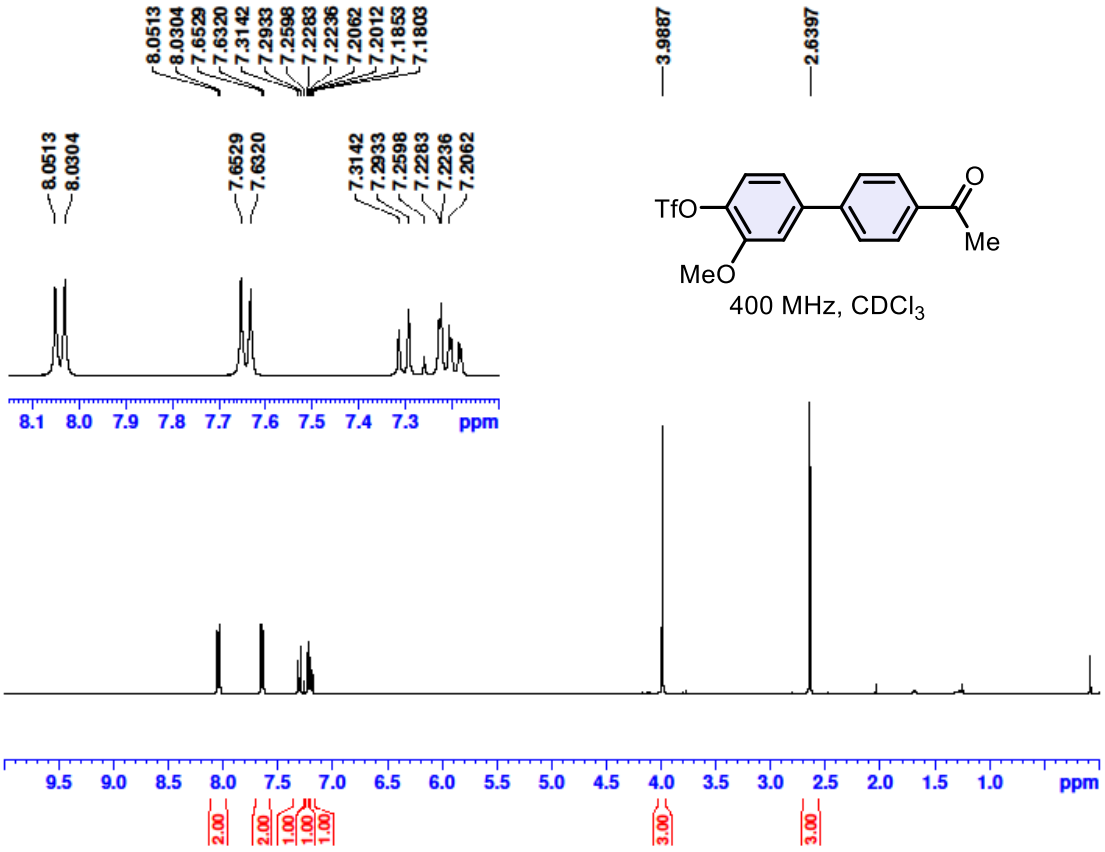

^{13}C NMR of 4'-acetyl-3-methoxy-[1,1'-biphenyl]-4-yl trifluoromethanesulfonate (Table 3.4, compound **13h**)

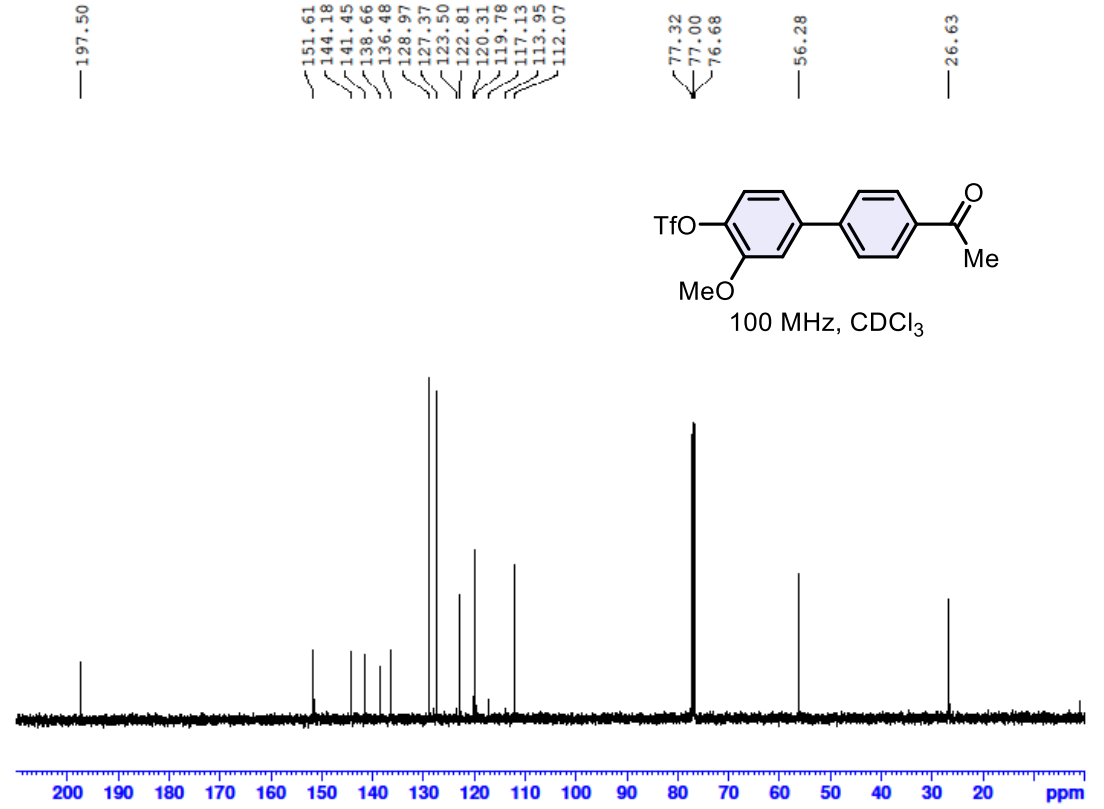

^{19}F NMR of 4’-acetyl-3-methoxy-[1,1’-biphenyl]-4-yl trifluoromethanesulfonate (Table 3.4, compound **13h**)

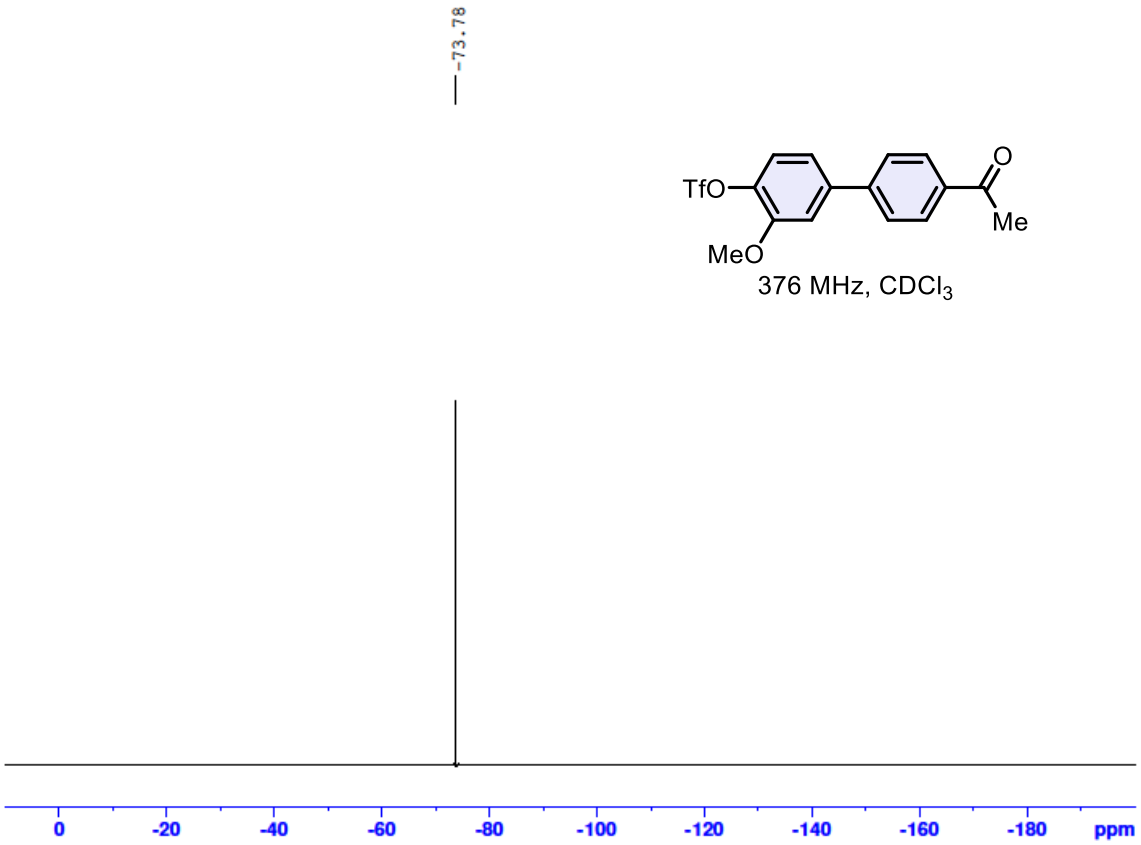

HRMS of 4’-acetyl-3-methoxy-[1,1’-biphenyl]-4-yl trifluoromethanesulfonate (Table 3.4, compound **13h**)

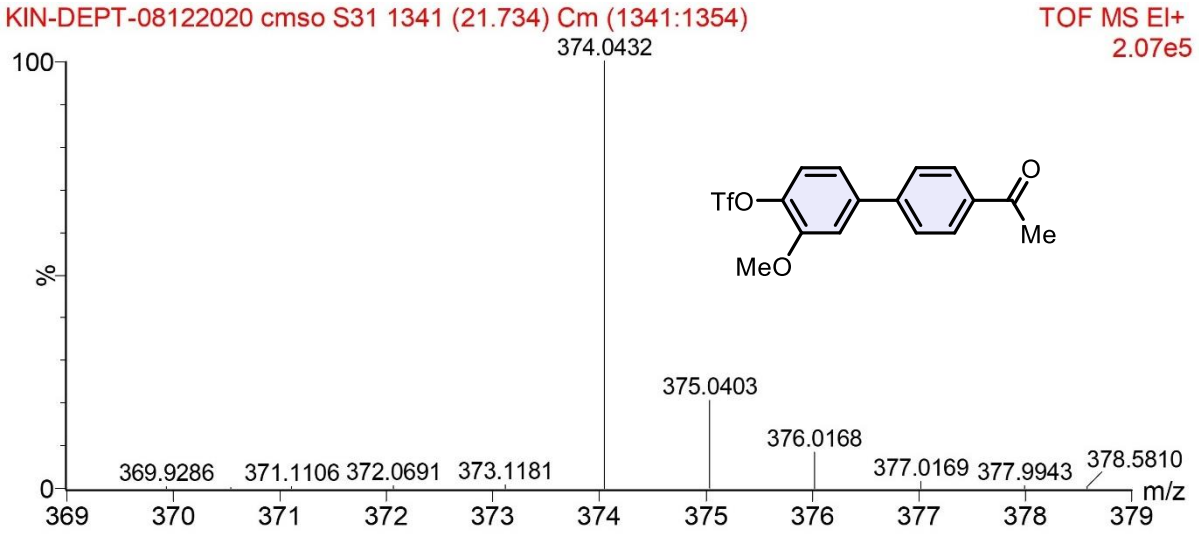

Mass	Calc. Mass	mDa	PPM	Formula
374.0432	374.0430	-0.17	-0.45	C16 H13 F3 O5 S

^{1}H NMR of 4-(3-methylbenzo[*b*]thiophen-5-yl)phenyl trifluoromethanesulfonate (Table 3.4, compound **13i**)

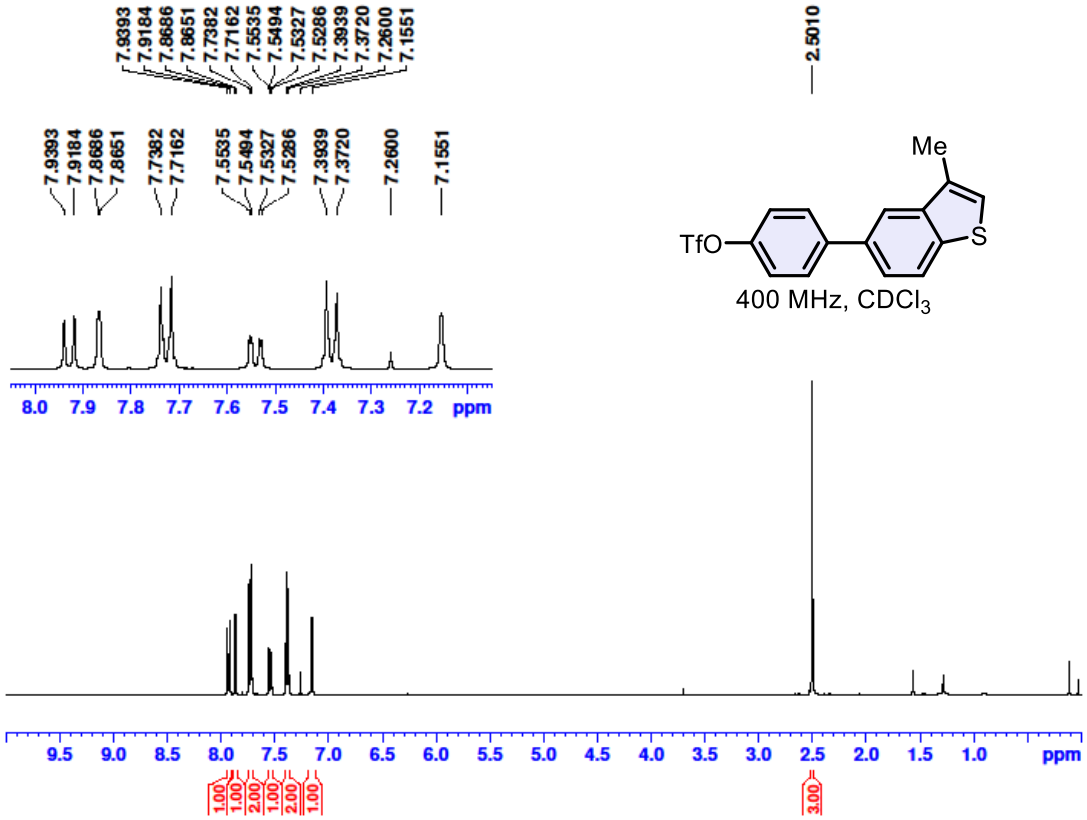

^{13}C NMR of 4-(3-methylbenzo[*b*]thiophen-5-yl)phenyl trifluoromethanesulfonate (Table 3.4, compound **13i**)

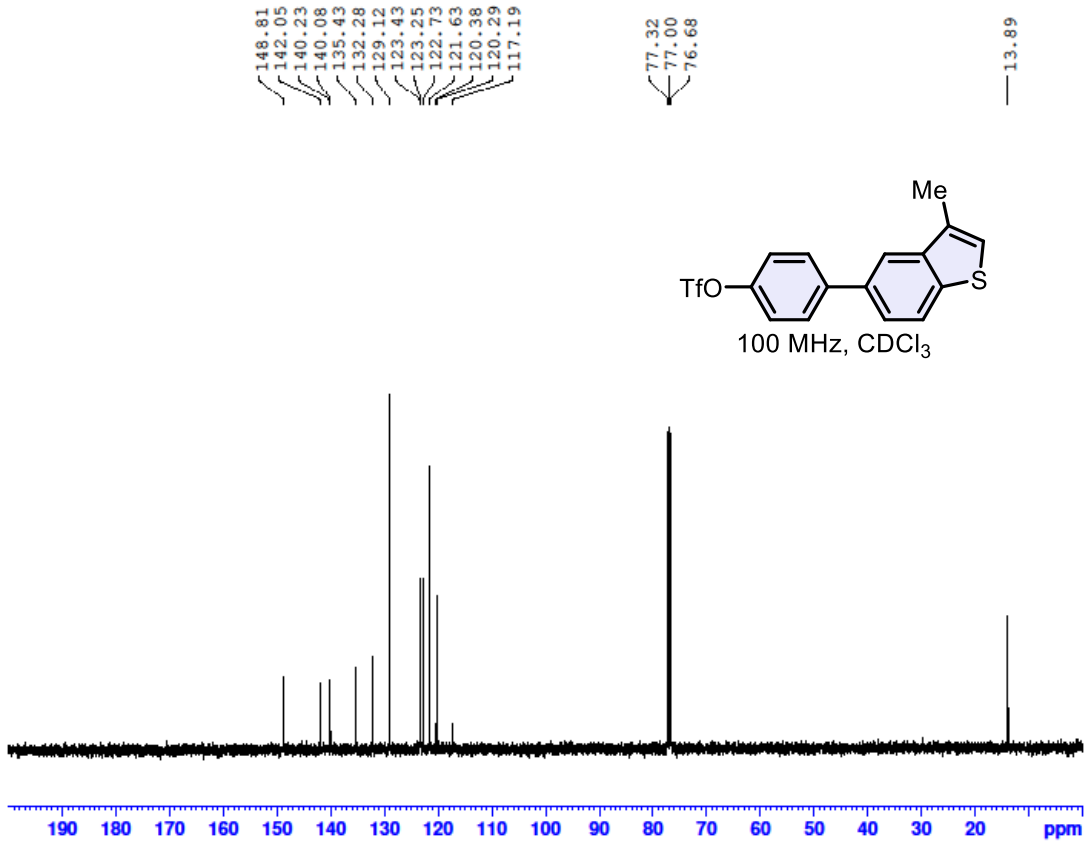

^{19}F NMR of 4-(3-methylbenzo[*b*]thiophen-5-yl)phenyl trifluoromethanesulfonate (Table 3.4, compound **13i**)

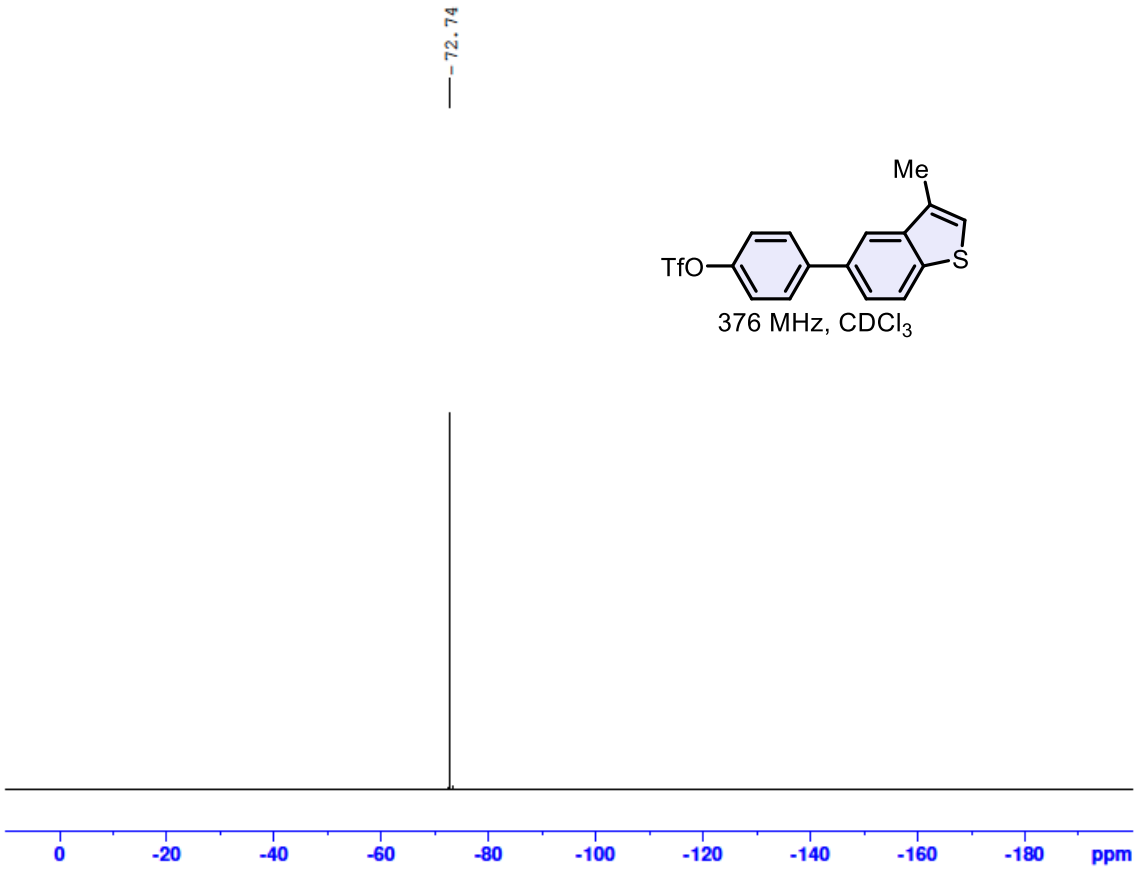

HRMS of 4-(3-methylbenzo[*b*]thiophen-5-yl)phenyl trifluoromethanesulfonate (Table 3.4, compound **13i**)

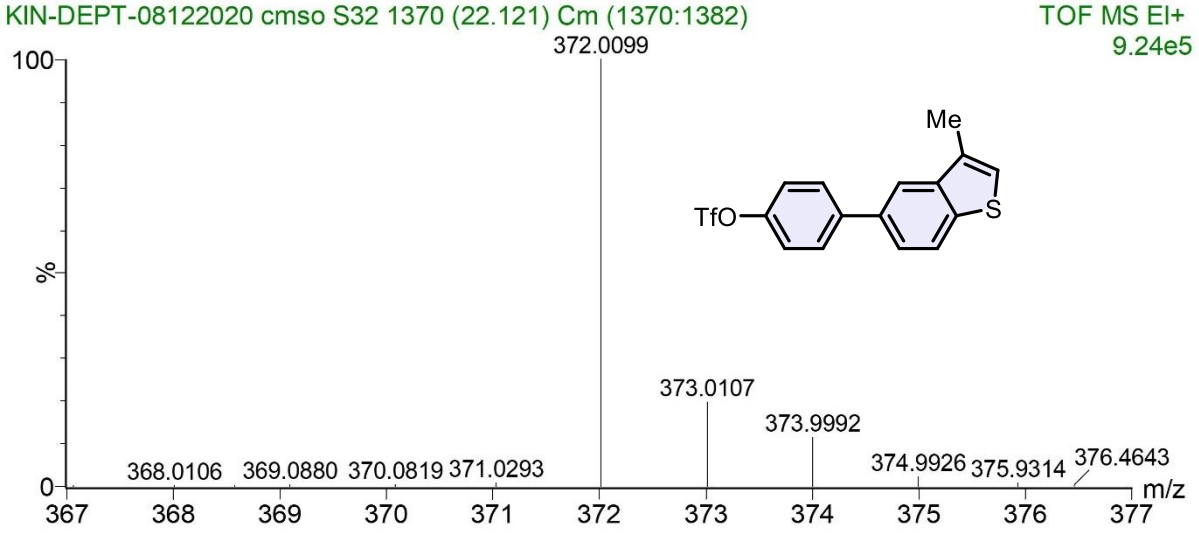

Mass	Calc. Mass	mDa	PPM	Formula
372.0099	372.0096	-0.28	-0.75	C16 H11 F3 O3 S2

^{1}H NMR of 3'-methyl-[1,1'-biphenyl]-4-yl trifluoromethanesulfonate (Table 3.4, compound **13j**)

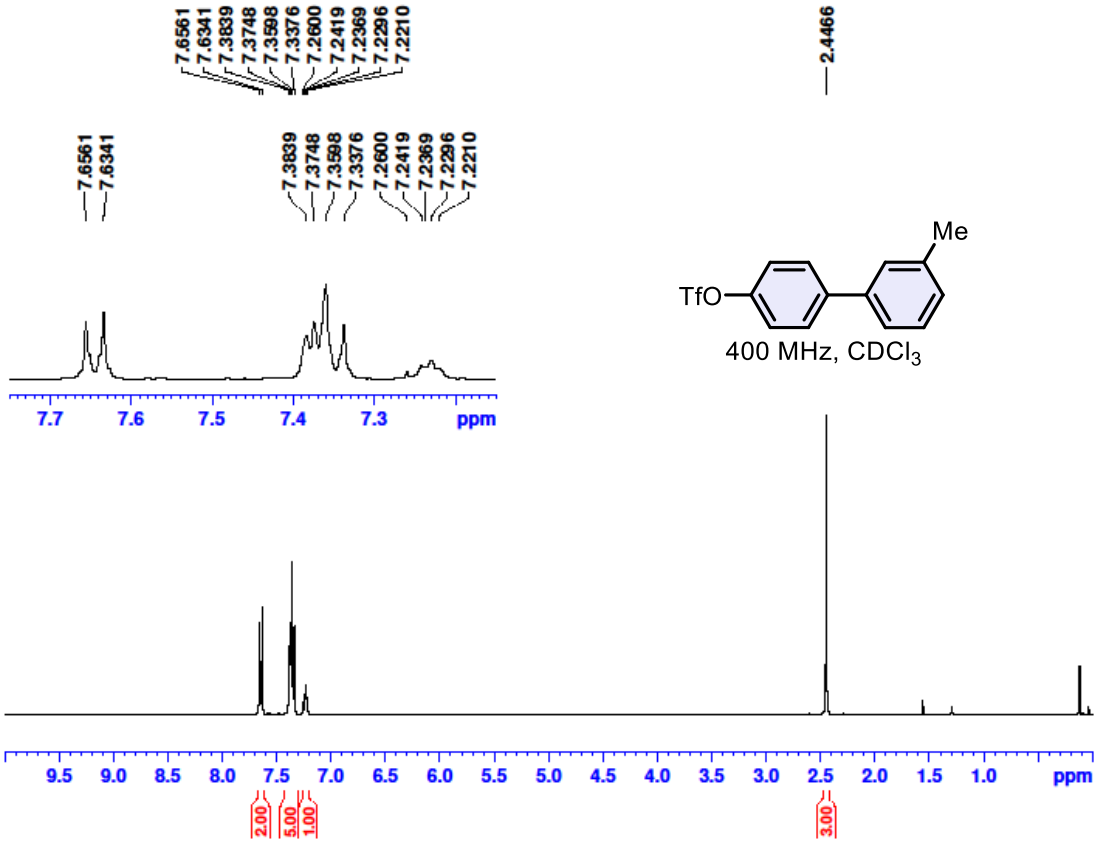

^{13}C NMR of 3'-methyl-[1,1'-biphenyl]-4-yl trifluoromethanesulfonate (Table 3.4, compound **13j**)

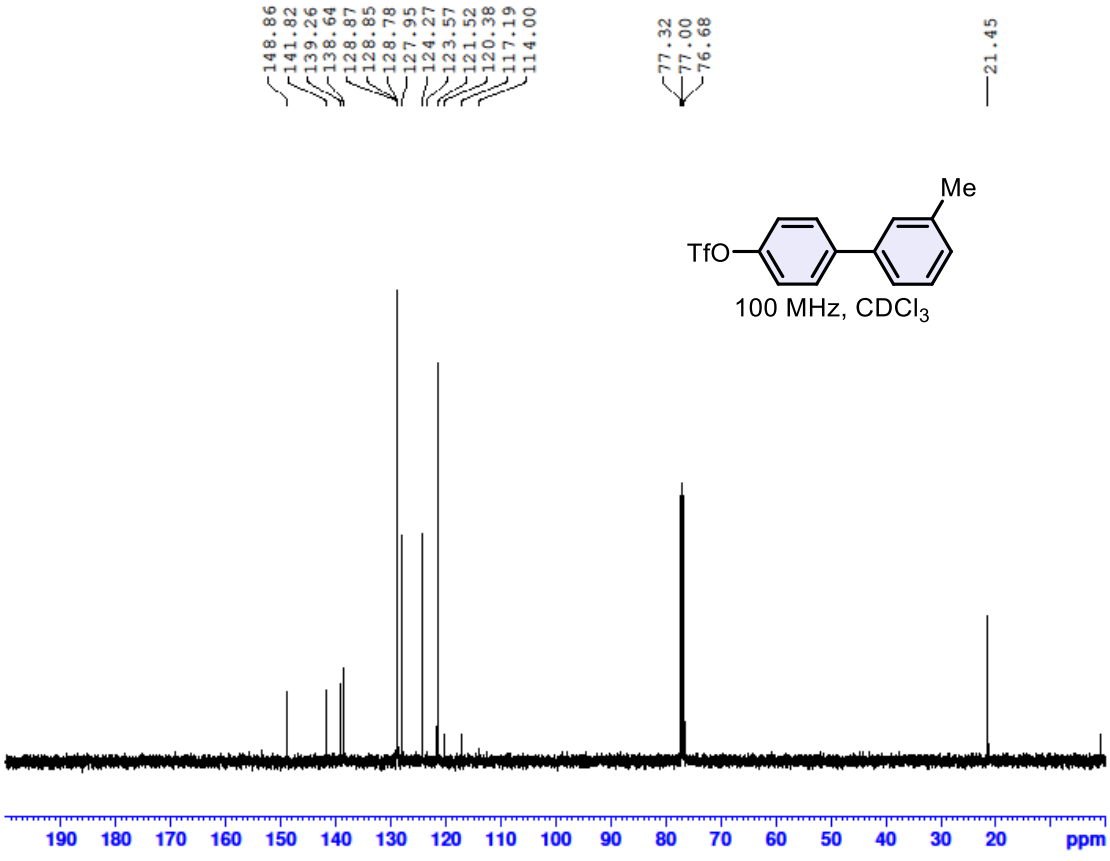

^{19}F NMR of 3'-methyl-[1,1'-biphenyl]-4-yl trifluoromethanesulfonate (Table 3.4, compound **13j**)

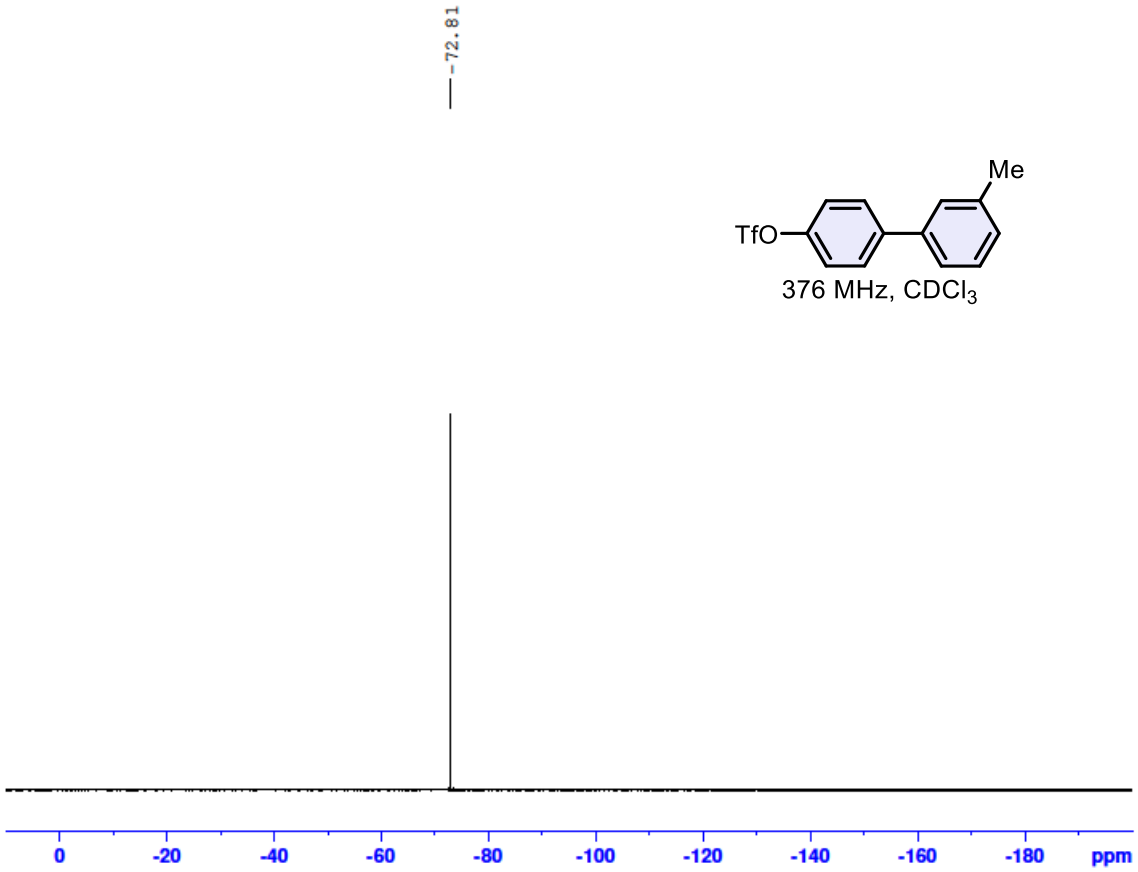

^{1}H NMR of 4'-formyl-[1,1'-biphenyl]-4-yl trifluoromethanesulfonate (Table 3.4, compound **13k**)

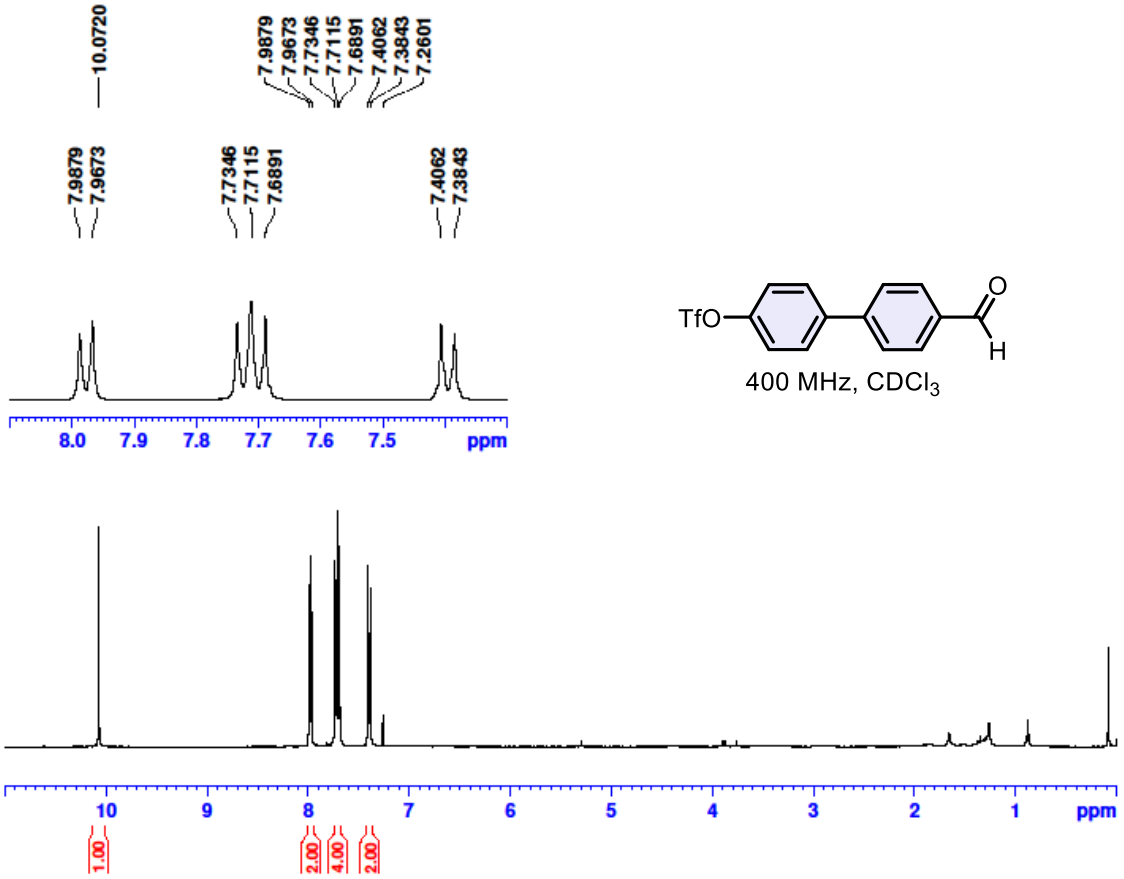

^{13}C NMR of 4'-formyl-[1,1'-biphenyl]-4-yl trifluoromethanesulfonate (Table 3.4, compound **13k**)

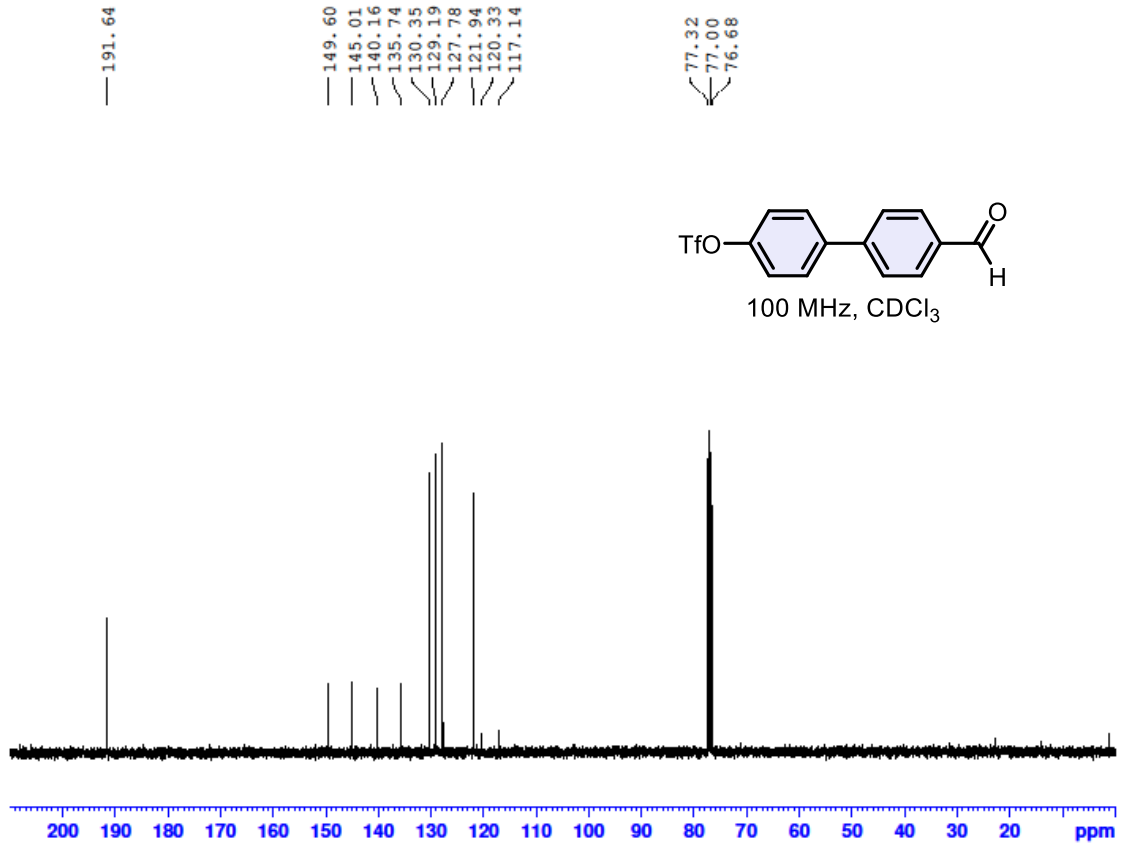

^{19}F NMR of 4’-formyl-[1,1’-biphenyl]-4-yl trifluoromethanesulfonate (Table 3.4, compound **13k**)

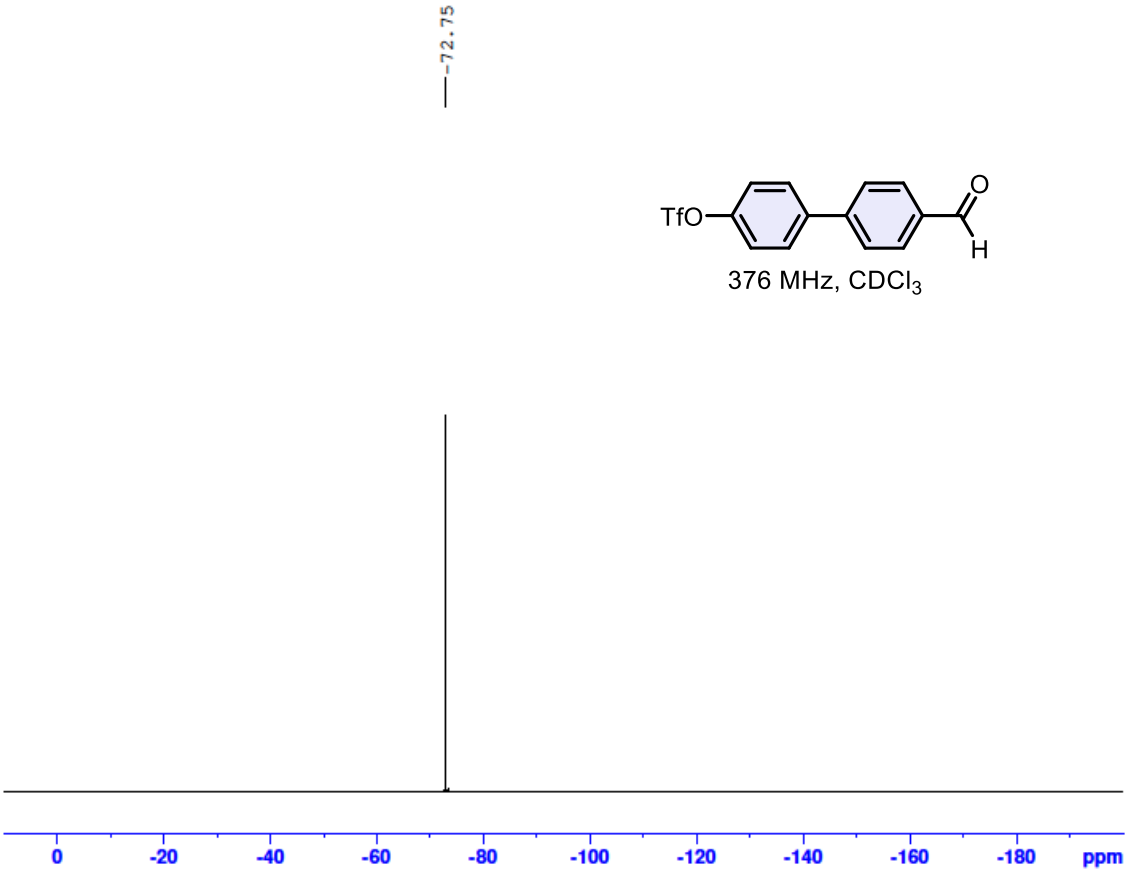

HRMS of 4’-formyl-[1,1’-biphenyl]-4-yl trifluoromethanesulfonate (Table 3.4, compound **13k**)

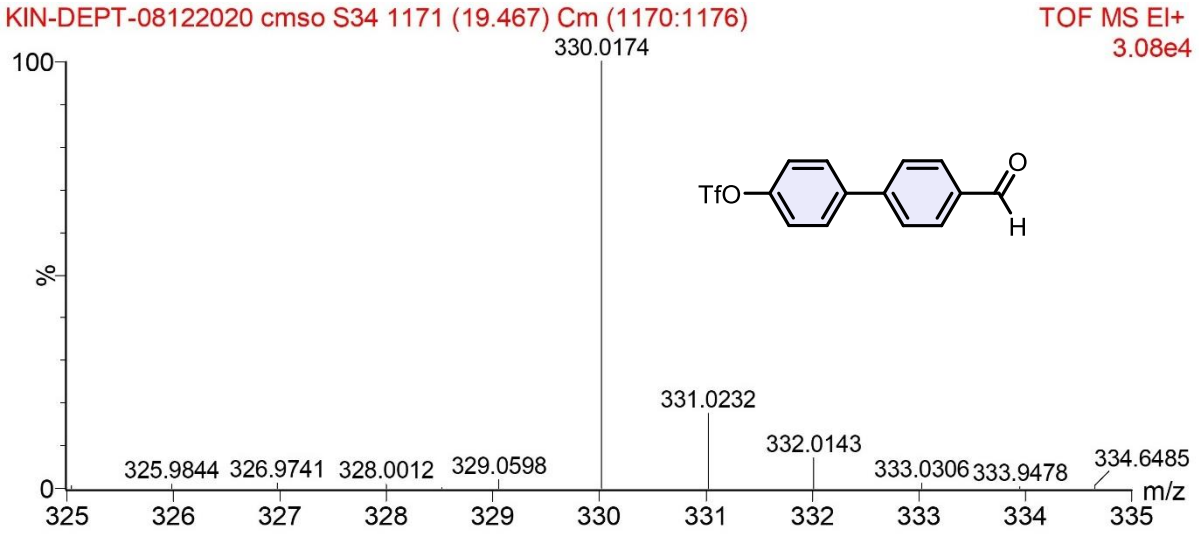

Mass	Calc. Mass	mDa	PPM	Formula
330.1074	330.0168	-0.58	-1.77	C14 H9 F3 O4 S

^{1}H NMR of 3-benzyl-3'-methoxy-[1,1'-biphenyl]-4-yl trifluoromethanesulfonate (Table 3.4, compound **13l**)

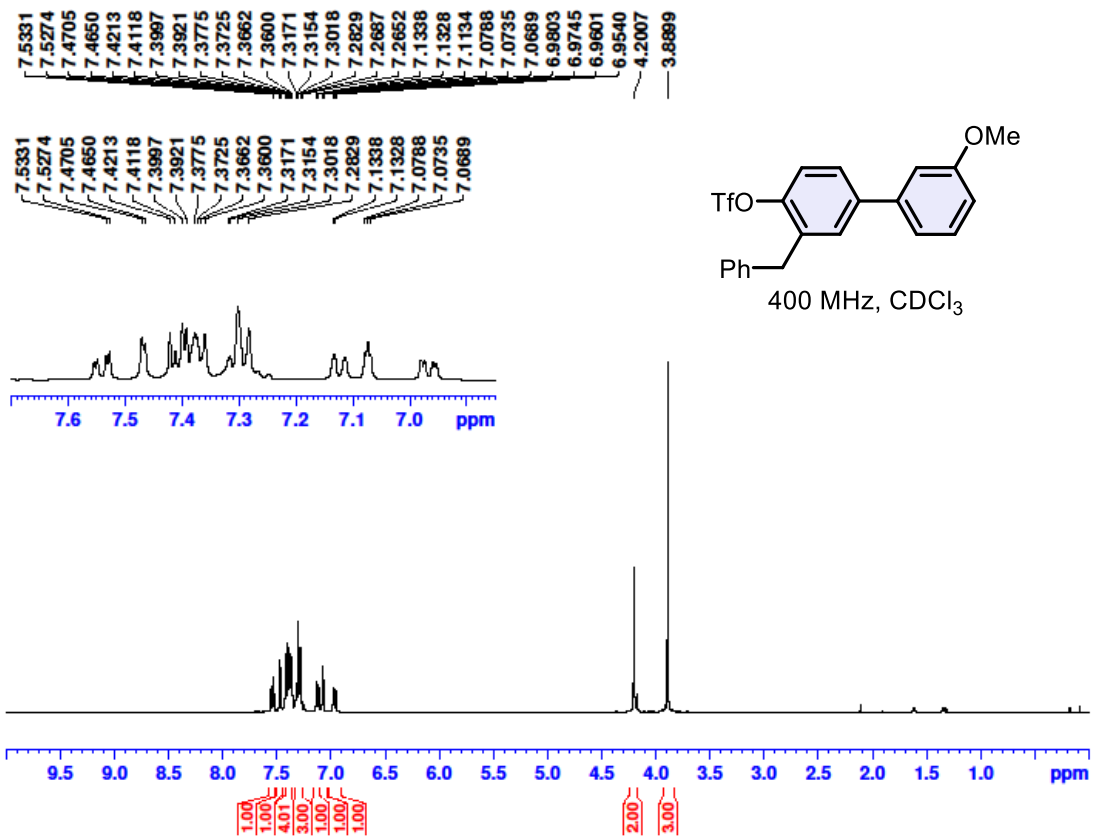

^{13}C NMR of 3-benzyl-3'-methoxy-[1,1'-biphenyl]-4-yl trifluoromethanesulfonate (Table 3.4, compound **13l**)

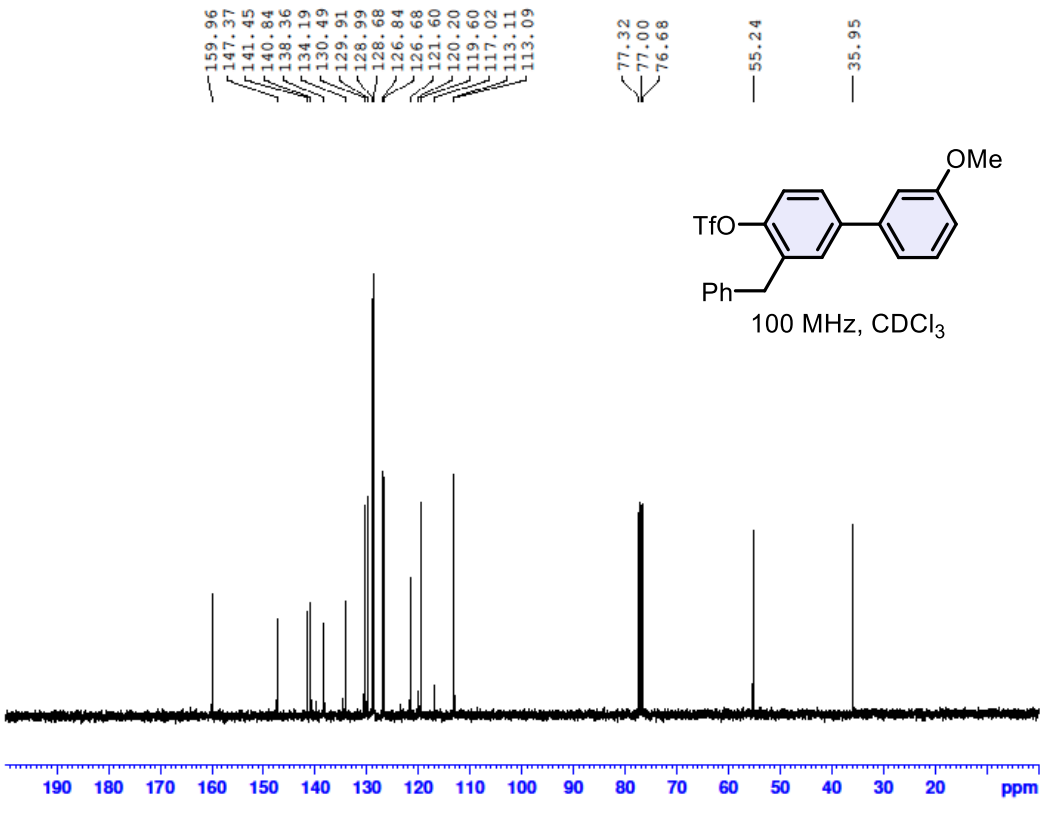

^{19}F NMR of 3-benzyl-3'-methoxy-[1,1'-biphenyl]-4-yl trifluoromethanesulfonate (Table 3.4, compound **13l**)

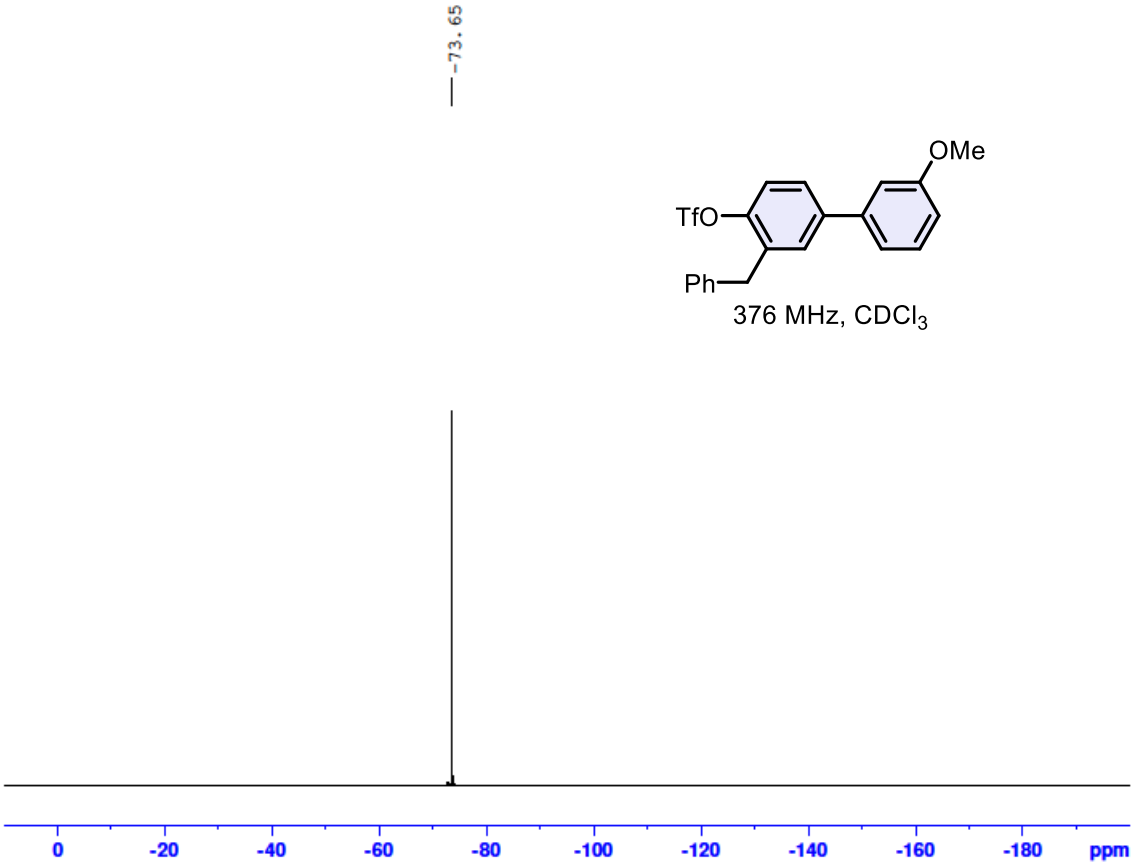

HRMS of 3-benzyl-3'-methoxy-[1,1'-biphenyl]-4-yl trifluoromethanesulfonate (Table 3.4, compound **13l**)

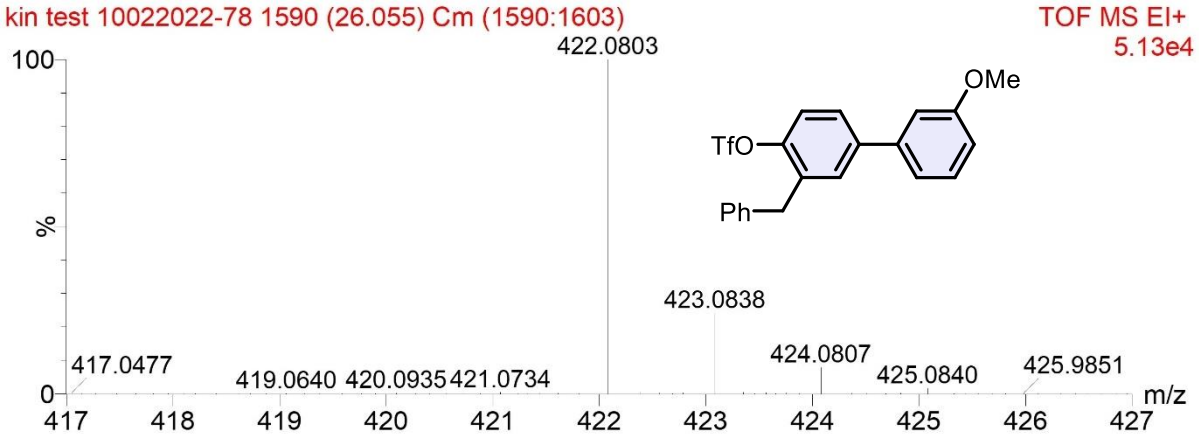

Mass	Calc. Mass	mDa	PPM	Formula
422.0803	422.0794	0.88	2.08	C21 H17 F3 O4 S

^{1}H NMR of 2-bromo-4-formylphenyl trifluoromethanesulfonate

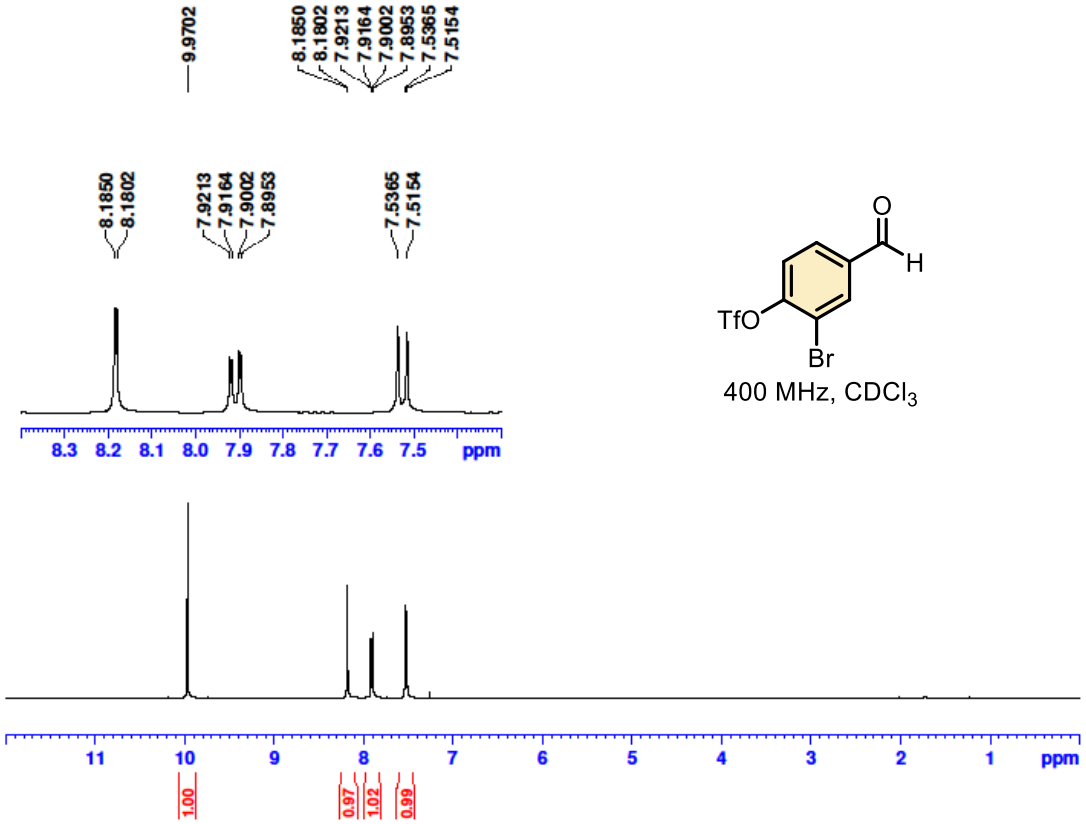

400 MHz, $CDCl_3$

^{13}C NMR of 2-bromo-4-formylphenyl trifluoromethanesulfonate

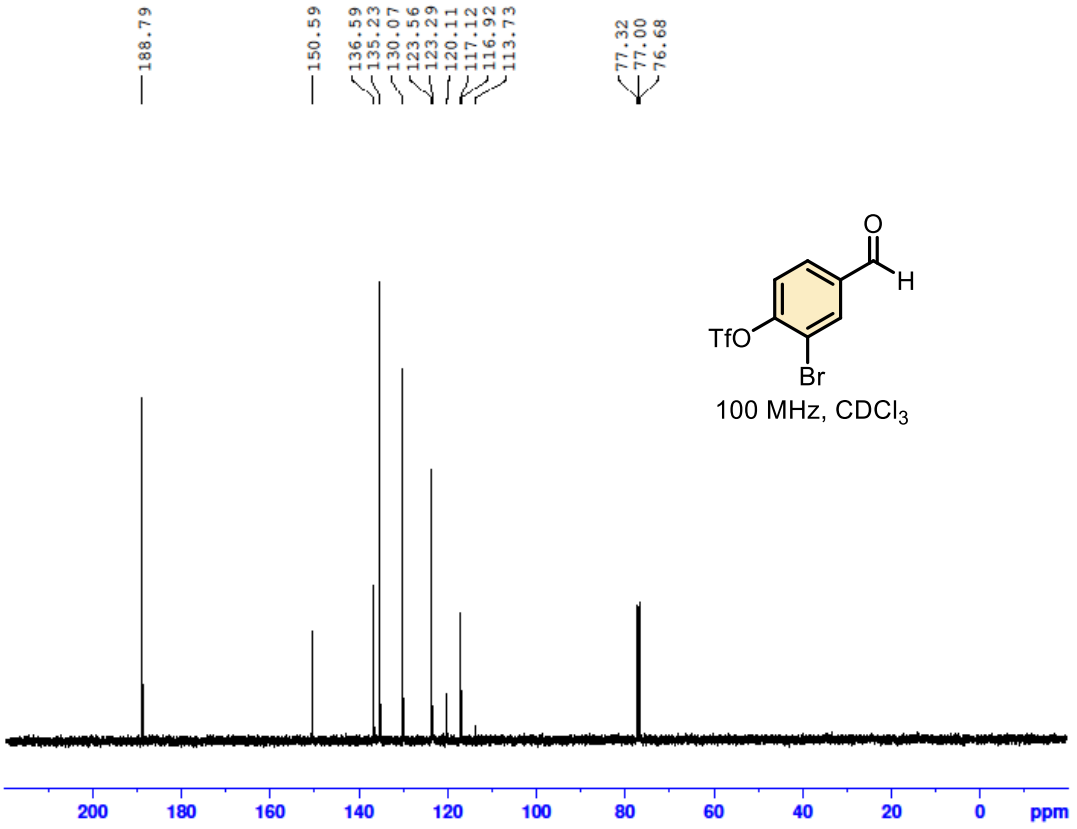

100 MHz, $CDCl_3$

^{19}F NMR of 2-bromo-4-formylphenyl trifluoromethanesulfonate

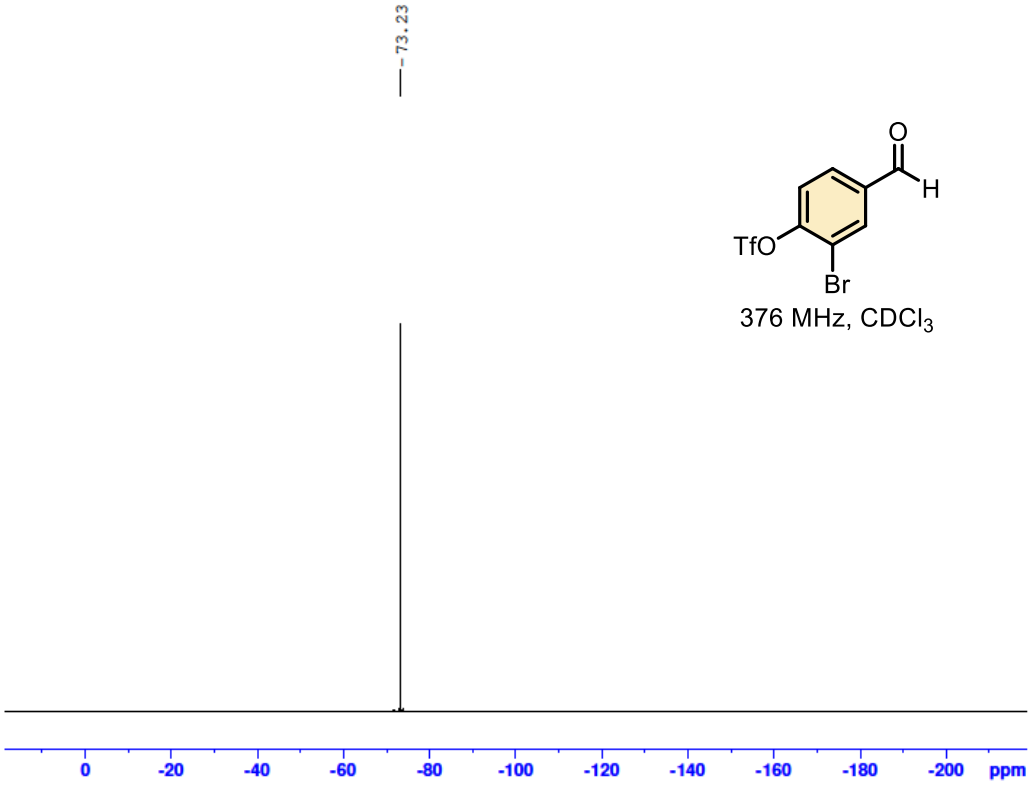

HRMS of 2-bromo-4-formylphenyl trifluoromethanesulfonate

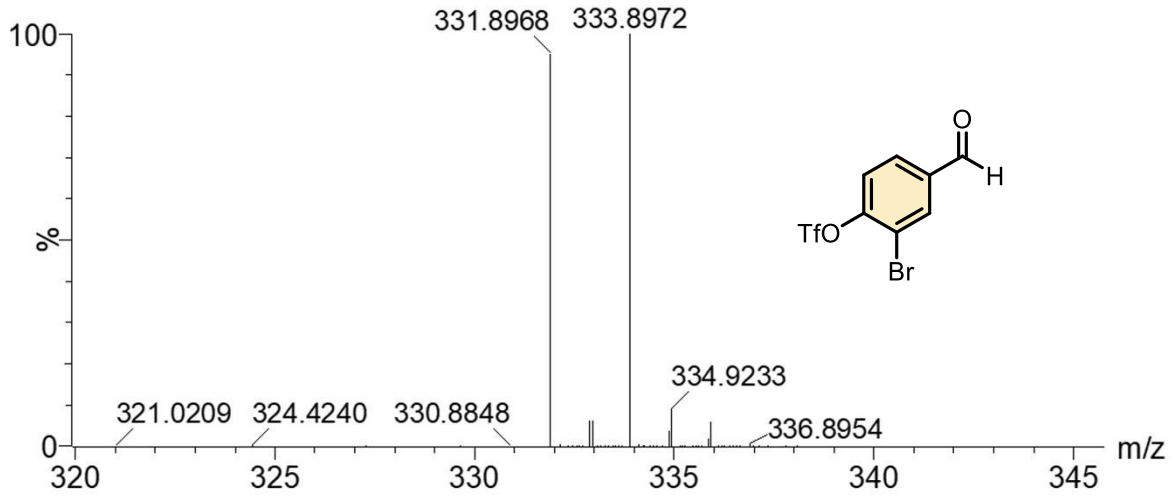

Mass	Calc. Mass	mDa	PPM	Formula
331.8968	331.8966	-0.22	-0.67	C8 H4 Br F3 O4 S

^{1}H NMR of 6-bromopyridin-2-yl trifluoromethanesulfonate

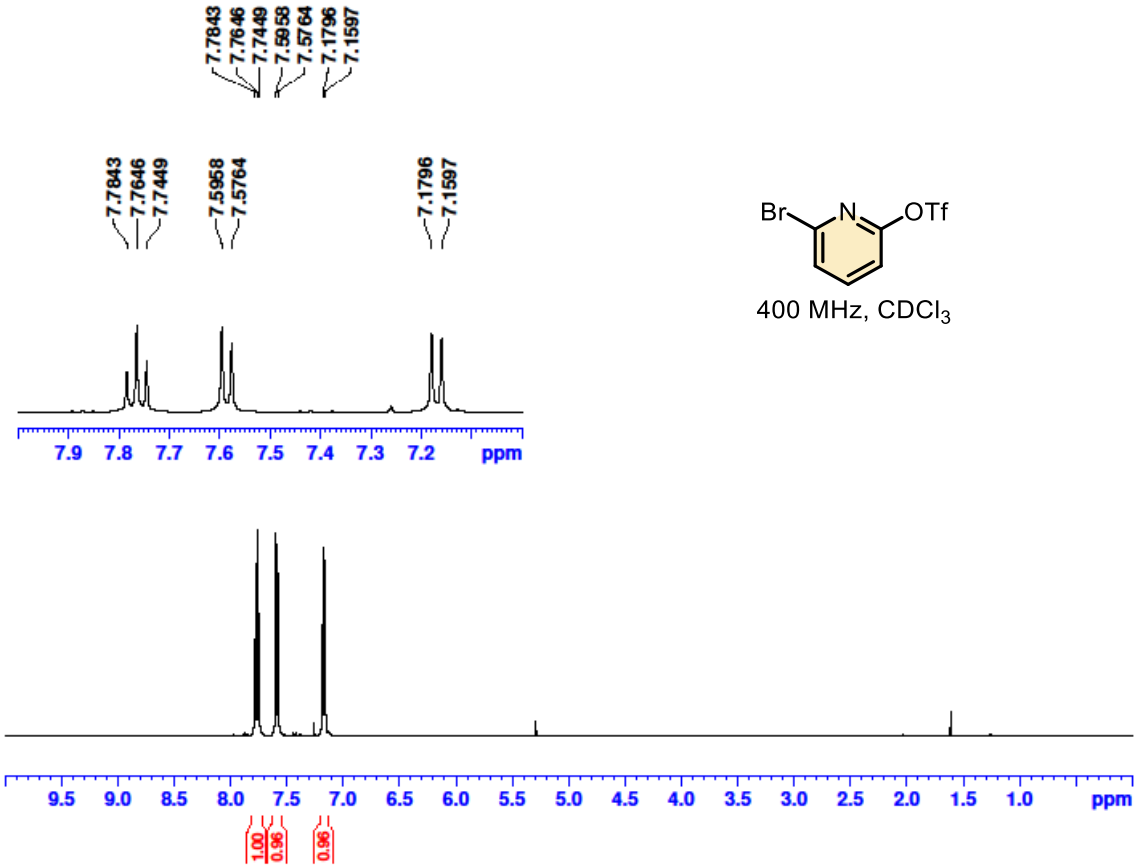

^{13}C NMR of 6-bromopyridin-2-yl trifluoromethanesulfonate

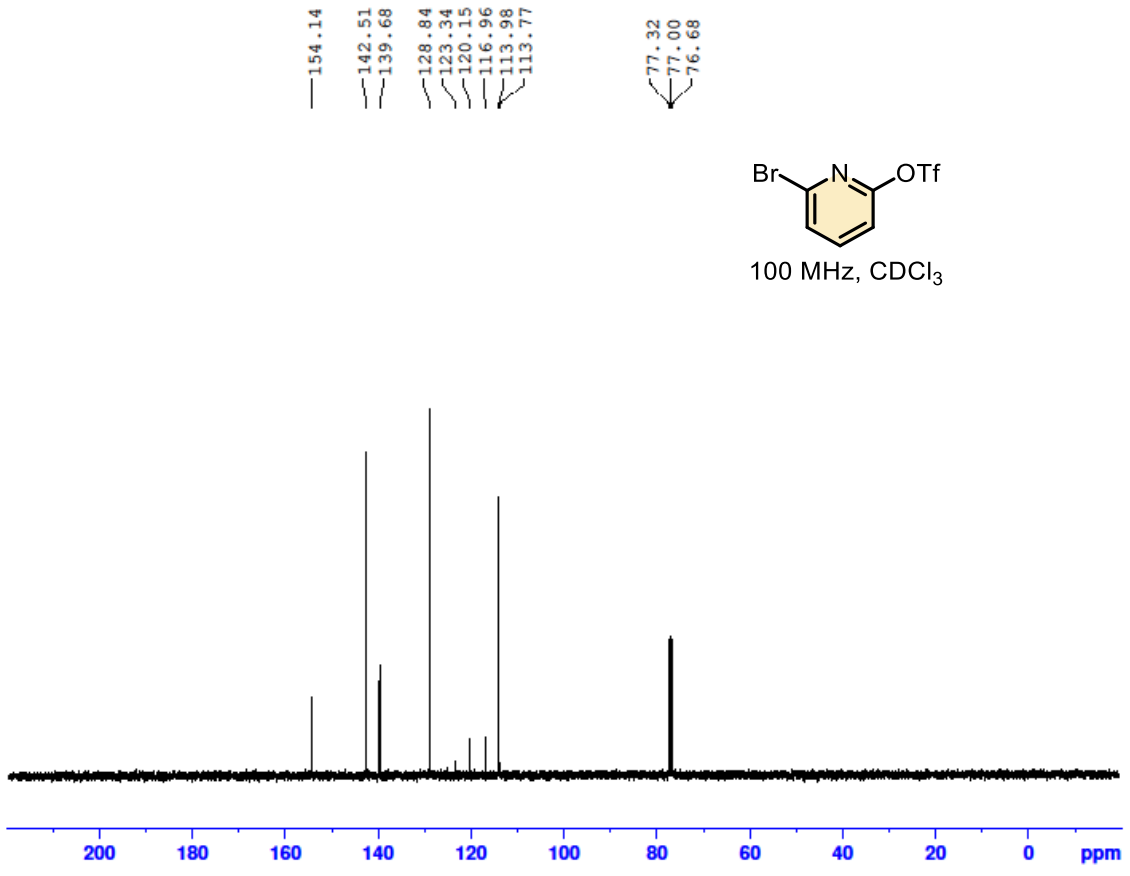

^{19}F NMR of 6-bromopyridin-2-yl trifluoromethanesulfonate

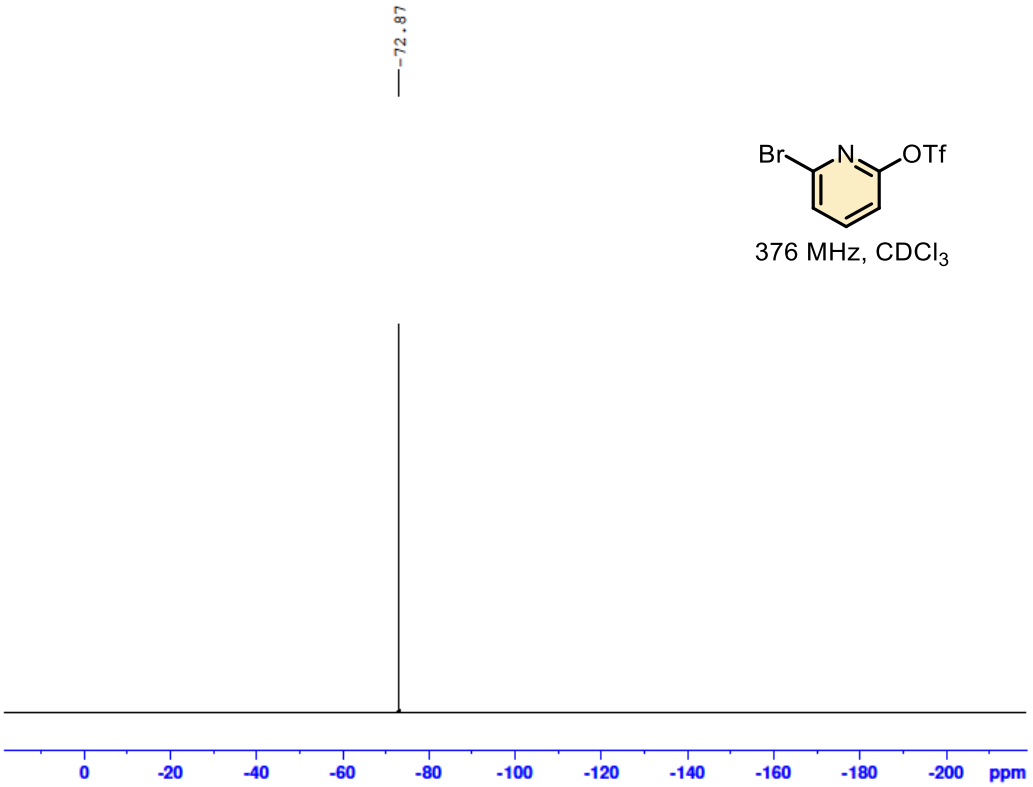

HRMS of 6-bromopyridin-2-yl trifluoromethanesulfonate

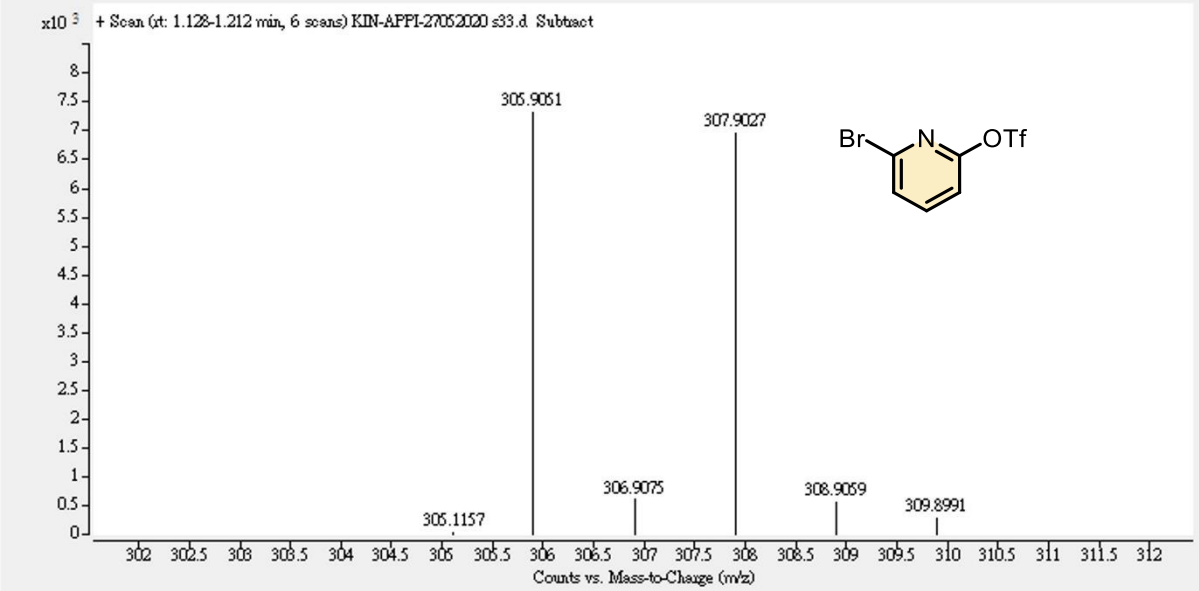

Mass	Calc. Mass	mDa	PPM	Formula
305.9051	305.9042	-0.91	-2.99	C6 H4 Br F3 N O3 S

^{1}H NMR of 2'-methyl-[1,1'-biphenyl]-4-yl trifluoromethanesulfonate (Table 4.2, entry 8, compound **16a**)

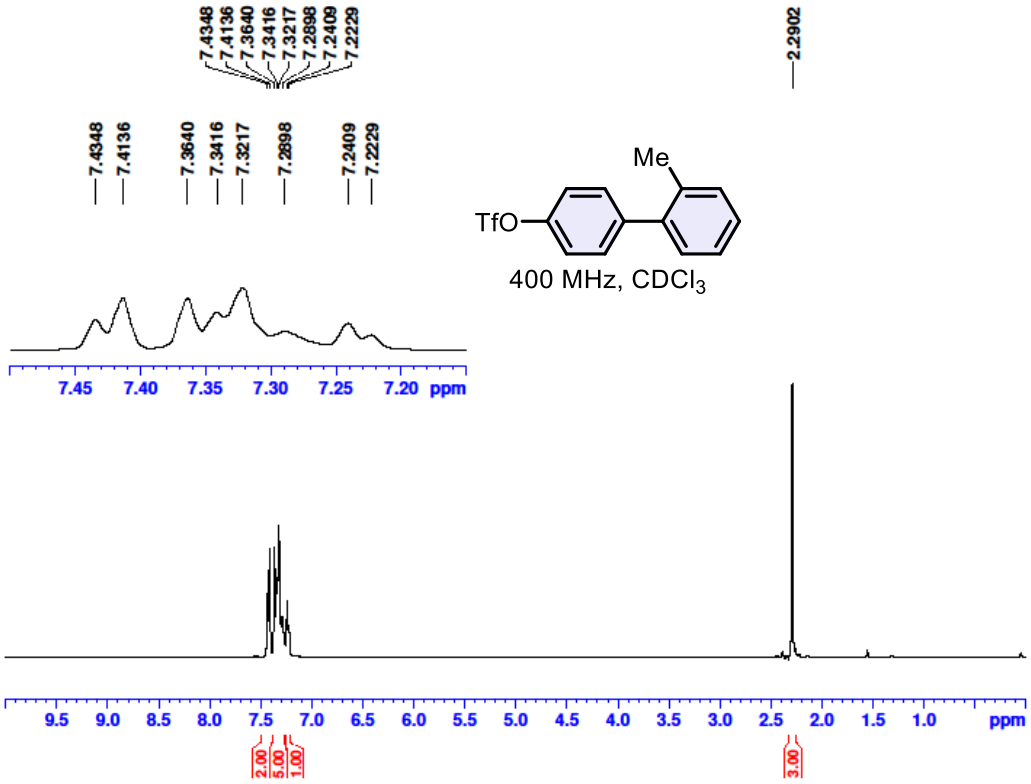

^{13}C NMR of 2'-methyl-[1,1'-biphenyl]-4-yl trifluoromethanesulfonate (Table 4.2, entry 8, compound **16a**)

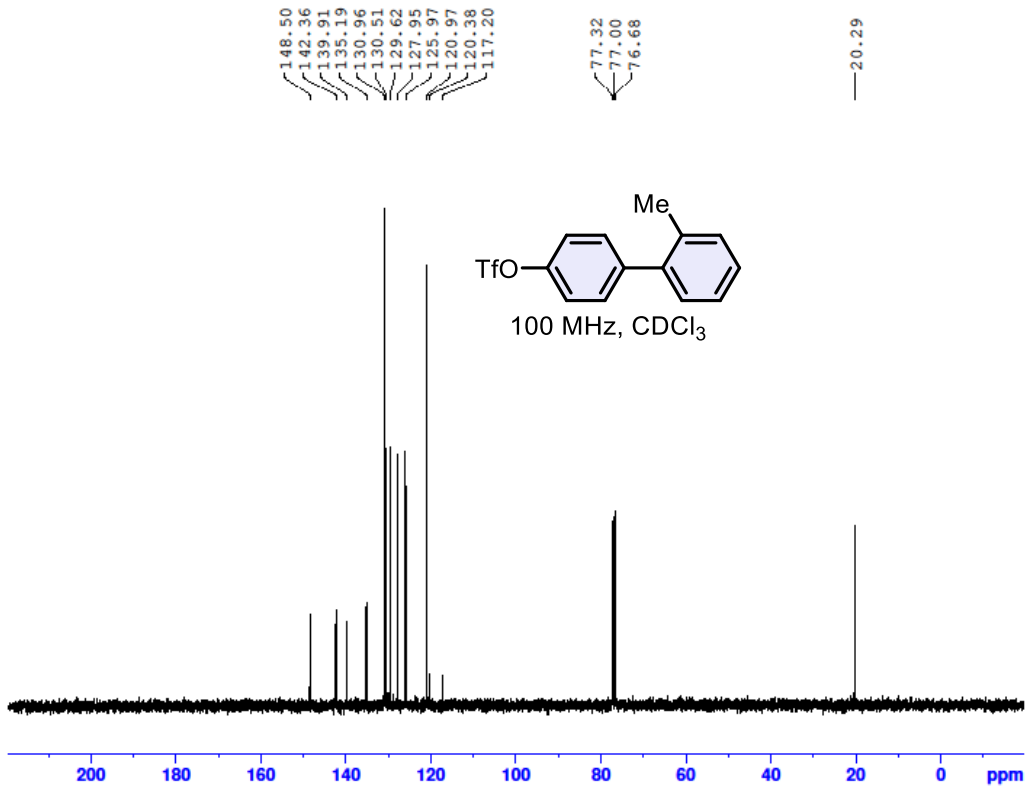

^{19}F NMR of 2'-methyl-[1,1'-biphenyl]-4-yl trifluoromethanesulfonate (Table 4.2, entry 8, compound **16a**)

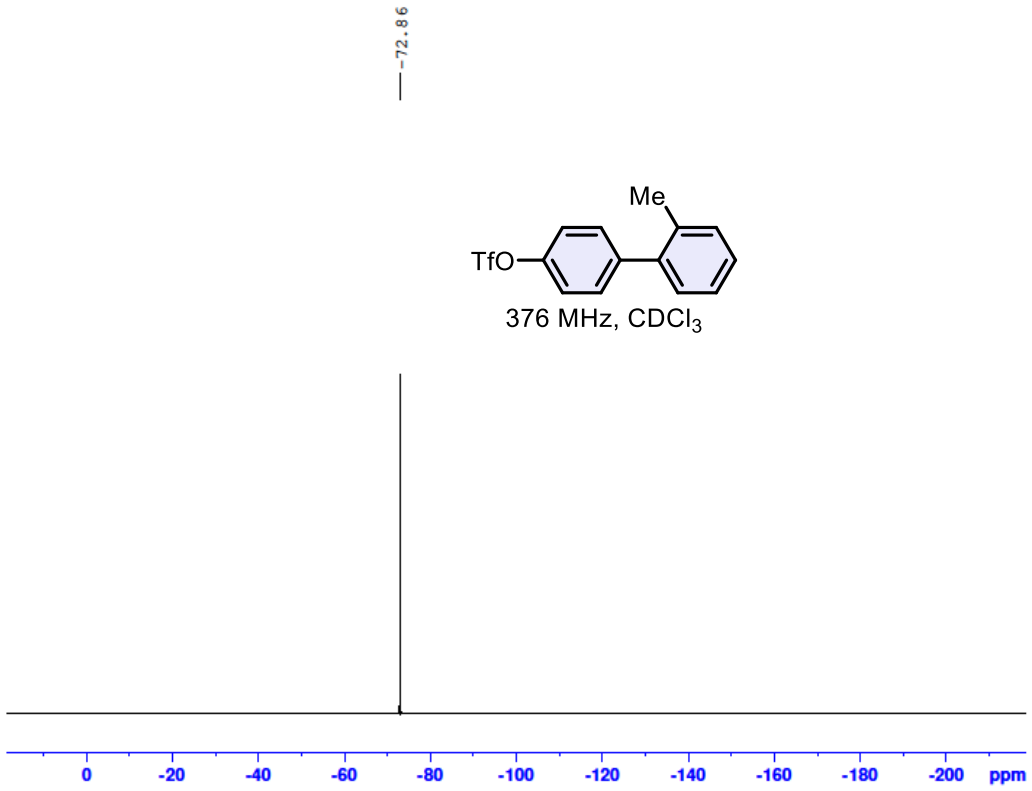

^{1}H NMR of 4'-methyl-[1,1'-biphenyl]-4-yl trifluoromethanesulfonate (Table 4.3, compound **16b**)

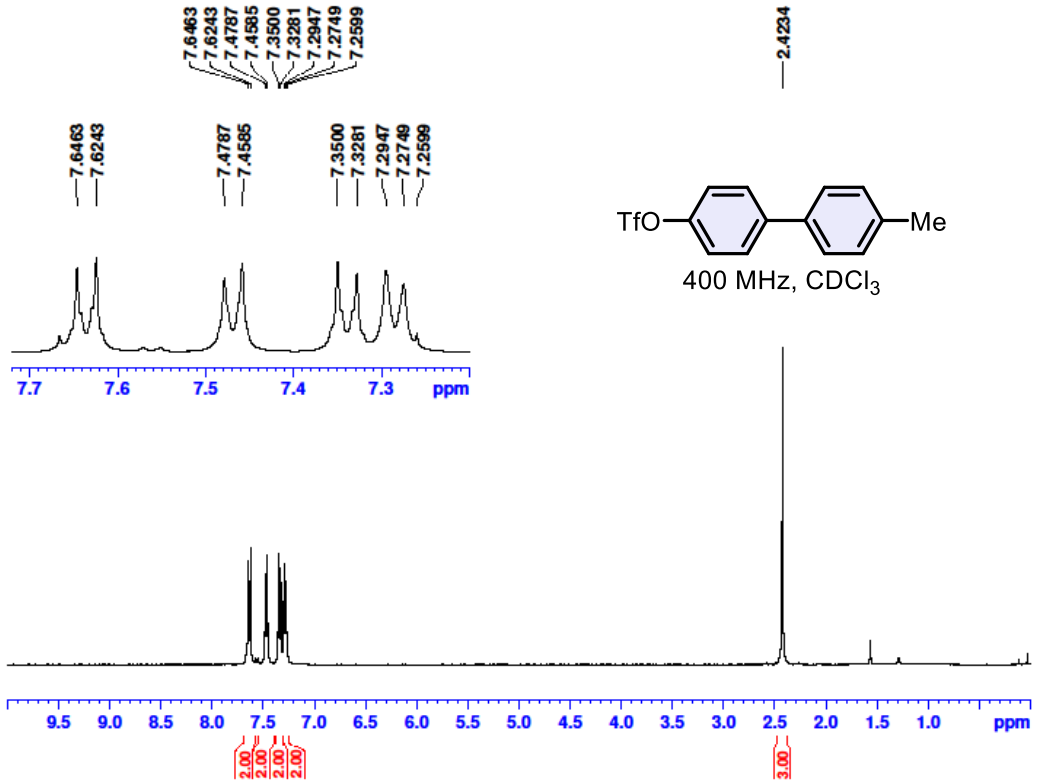

^{13}C NMR of 4'-methyl-[1,1'-biphenyl]-4-yl trifluoromethanesulfonate (Table 4.3, compound **16b**)

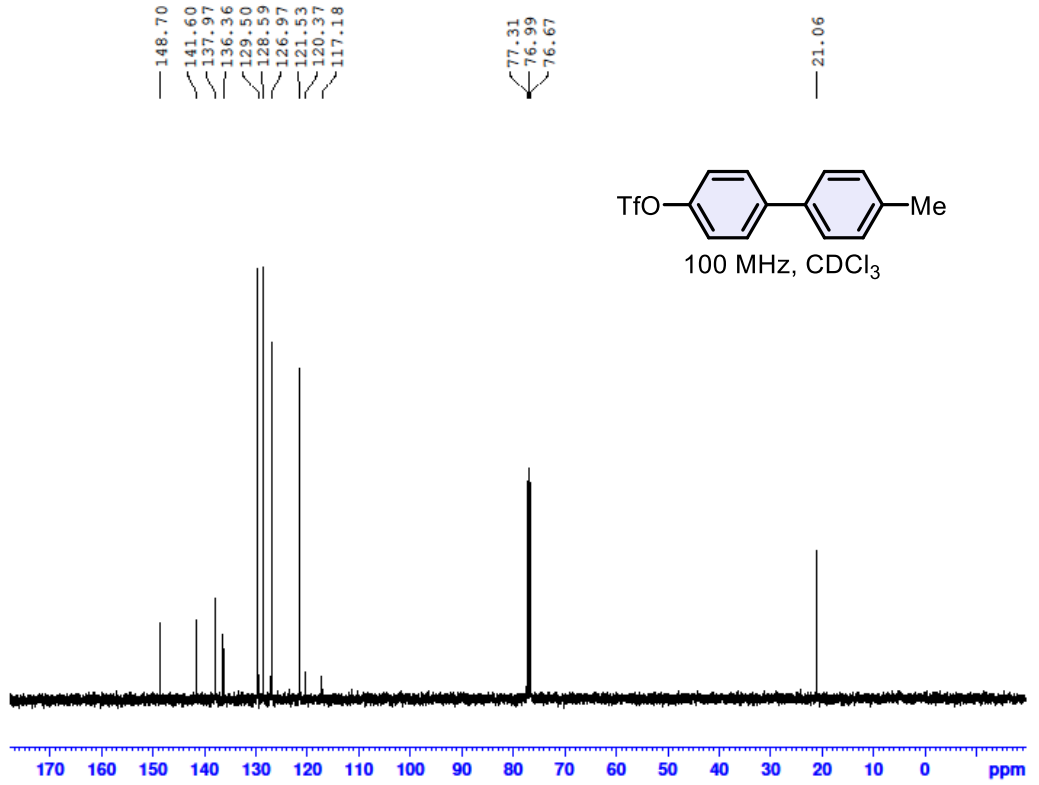

^{19}F NMR of 4'-methyl-[1,1'-biphenyl]-4-yl trifluoromethanesulfonate (Table 4.3, compound **16b**)

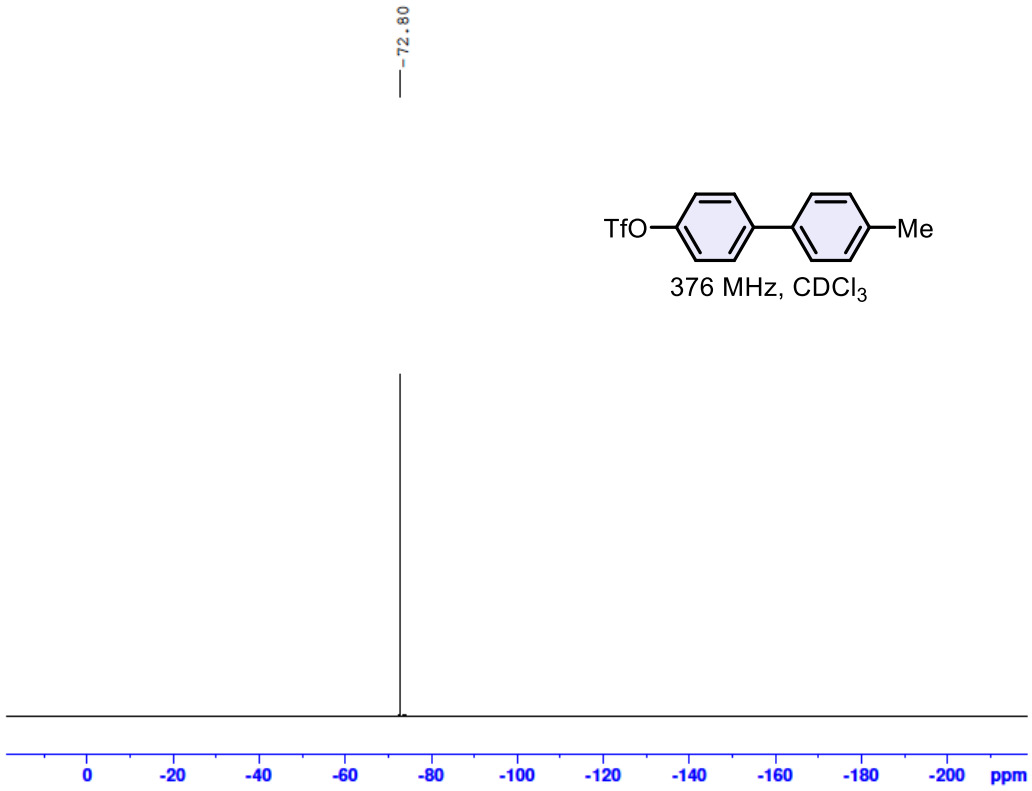

^{1}H NMR of 4'-(*tert*-butyl)-[1,1'-biphenyl]-4-yl trifluoromethanesulfonate (Table 4.3, compound **16c**)

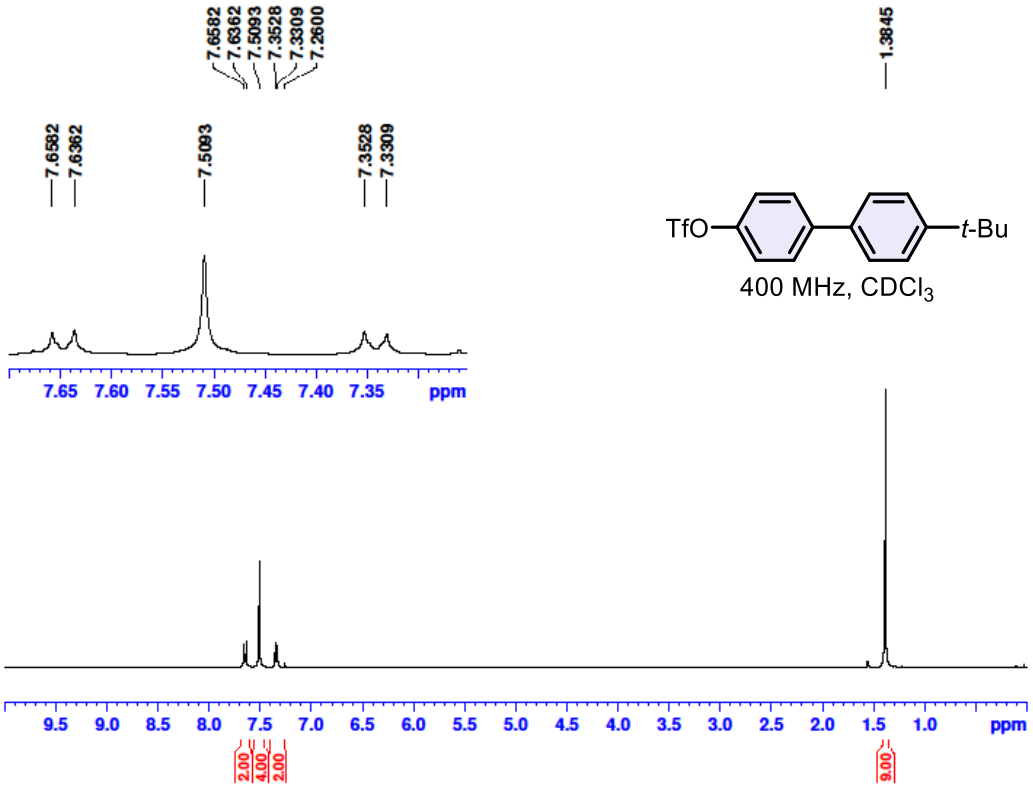

^{13}C NMR of 4'-(*tert*-butyl)-[1,1'-biphenyl]-4-yl trifluoromethanesulfonate (Table 4.3, compound **16c**)

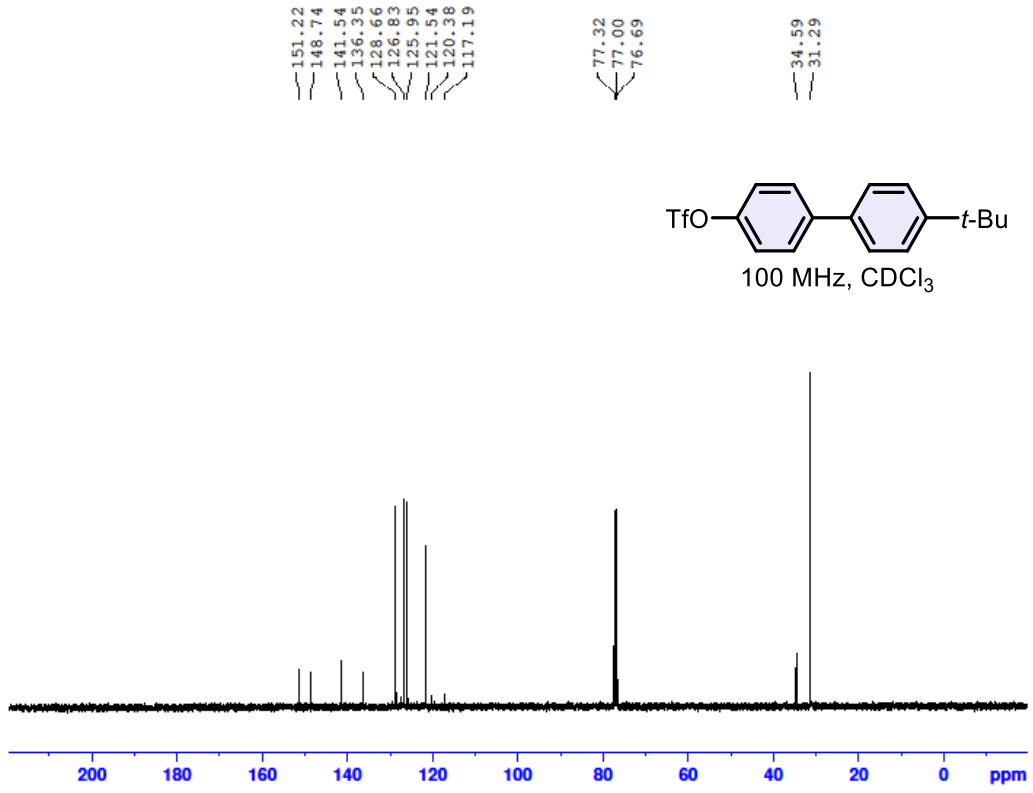

^{19}F NMR of 4'-(*tert*-butyl)-[1,1'-biphenyl]-4-yl trifluoromethanesulfonate (Table 4.3, compound **16c**)

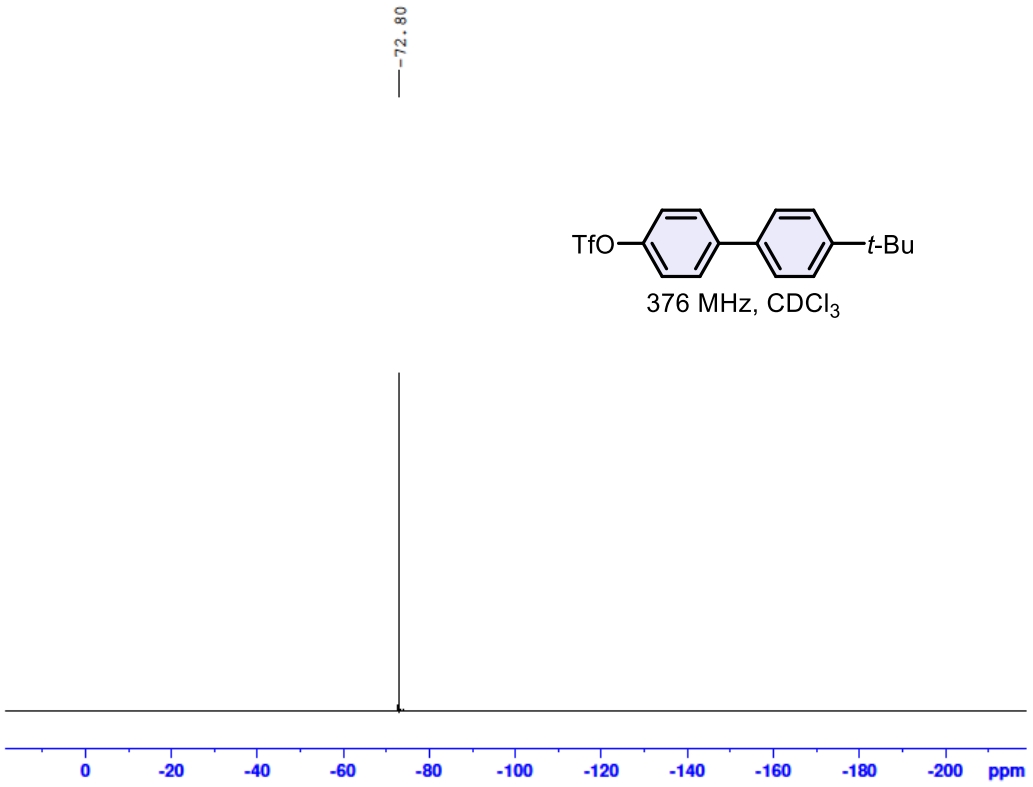

^{1}H NMR of 4'-fluoro-[1,1'-biphenyl]-4-yl trifluoromethanesulfonate (Table 4.3, compound **16d**)

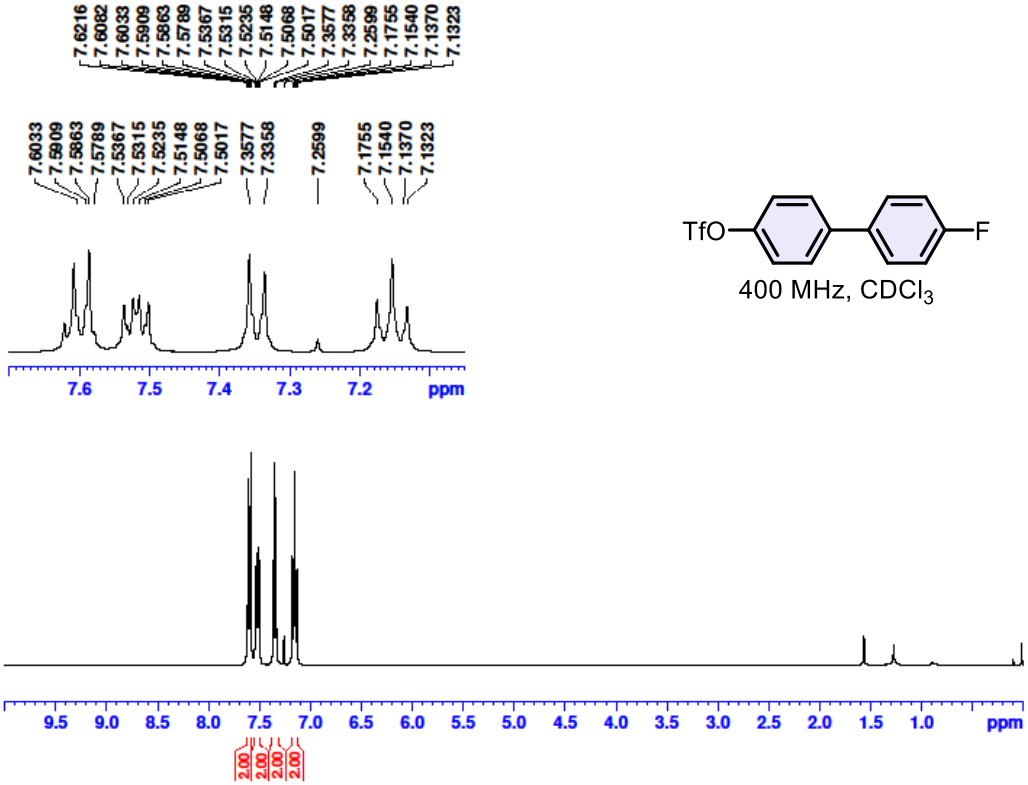

^{13}C NMR of 4'-fluoro-[1,1'-biphenyl]-4-yl trifluoromethanesulfonate (Table 4.3, compound **16d**)

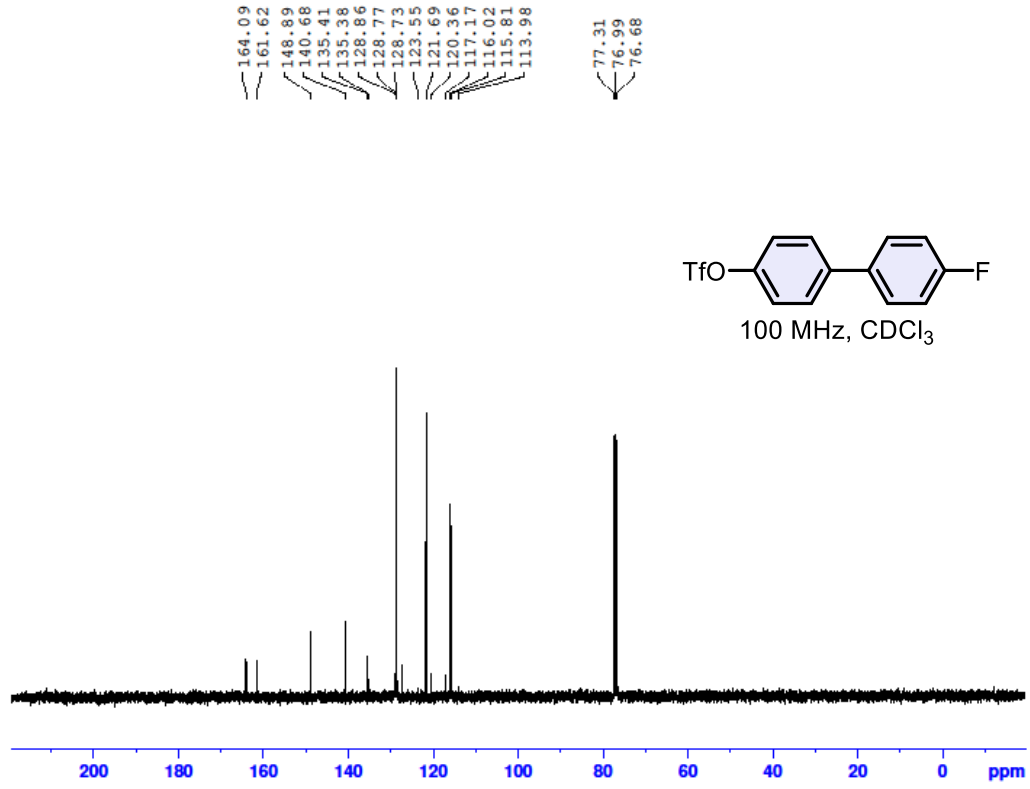

^{19}F NMR of 4'-fluoro-[1,1'-biphenyl]-4-yl trifluoromethanesulfonate (Table 4.3, compound **16d**)

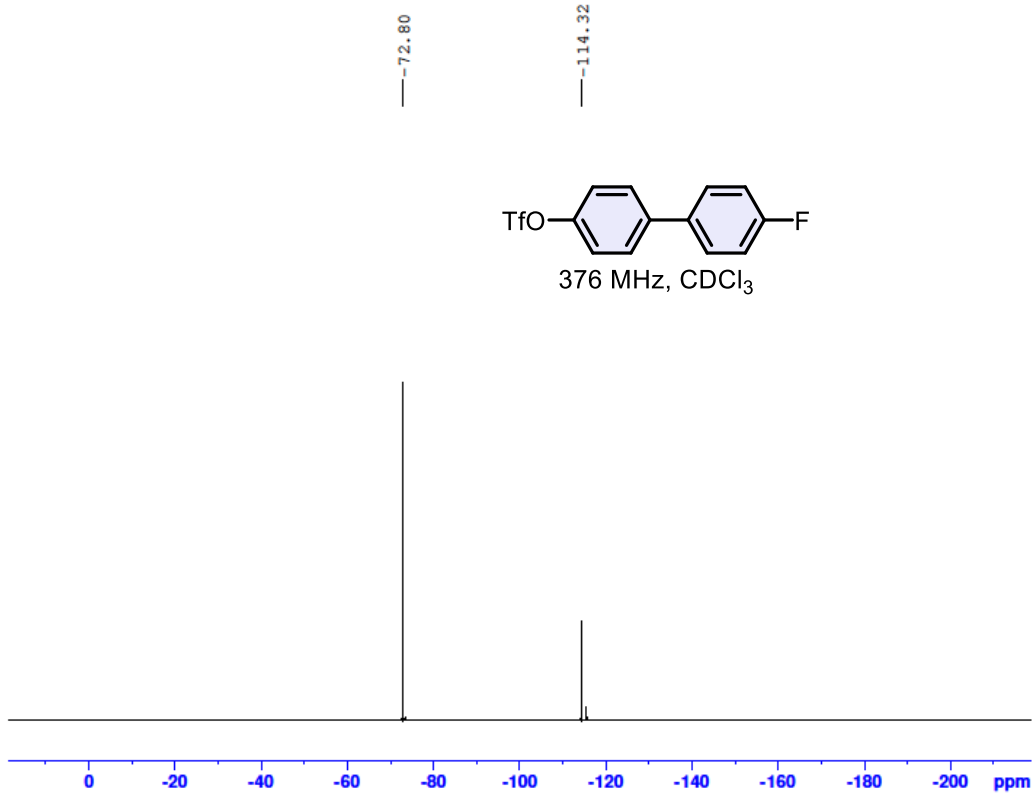

^{1}H NMR of [1,1':2',1''-terphenyl]-4-yl trifluoromethanesulfonate (Table 4.3, compound **16e**)

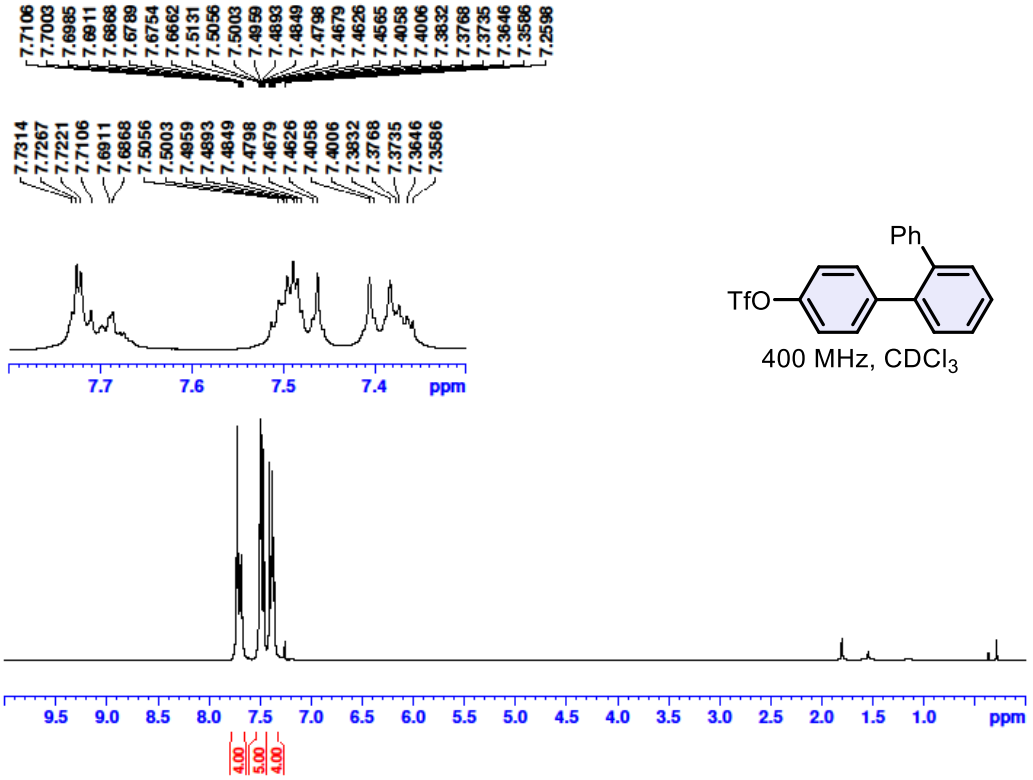

^{13}C NMR of [1,1':2',1''-terphenyl]-4-yl trifluoromethanesulfonate (Table 4.3, compound **16e**)

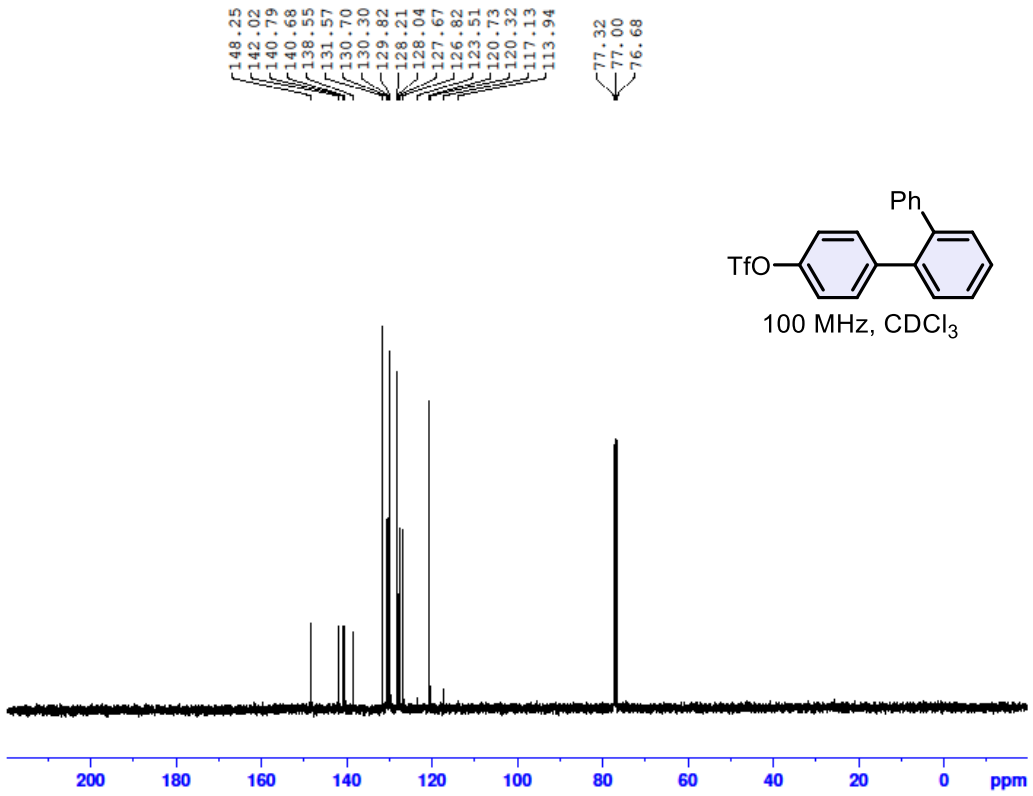

^{19}F NMR of [1,1':2',1''-terphenyl]-4-yl trifluoromethanesulfonate (Table 4.3, compound **16e**)

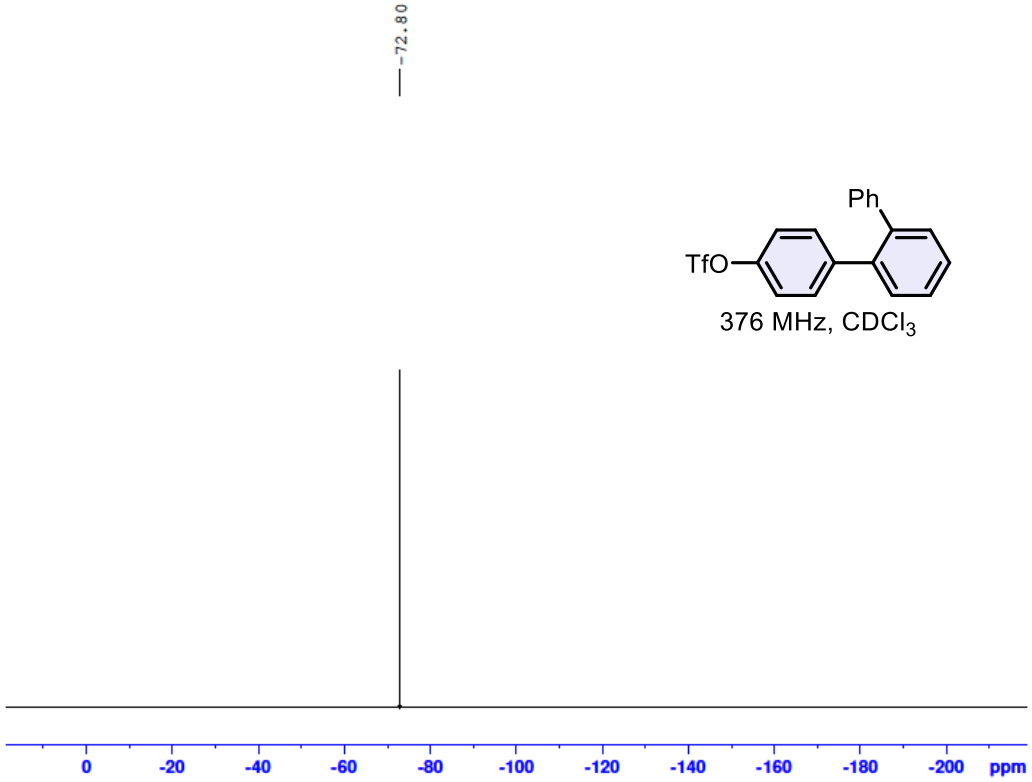

^{1}H NMR of 4'-methoxy-[1,1'-biphenyl]-4-yl trifluoromethanesulfonate (Table 4.3, compound **16f**)

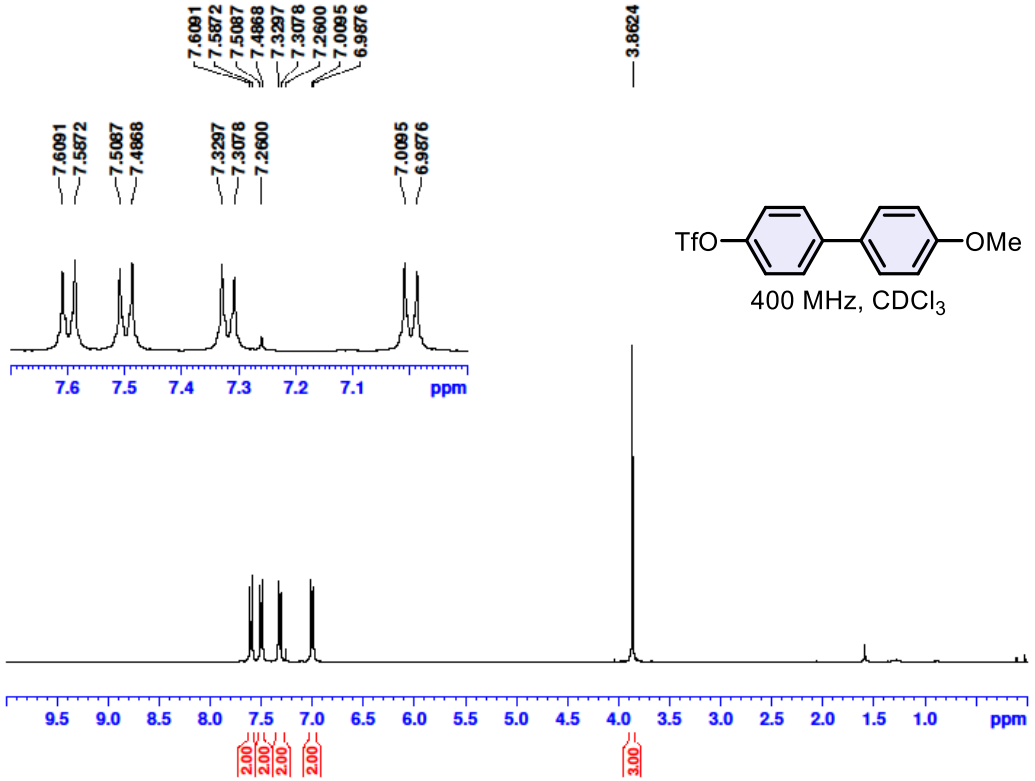

^{13}C NMR of 4'-methoxy-[1,1'-biphenyl]-4-yl trifluoromethanesulfonate (Table 4.3, compound **16f**)

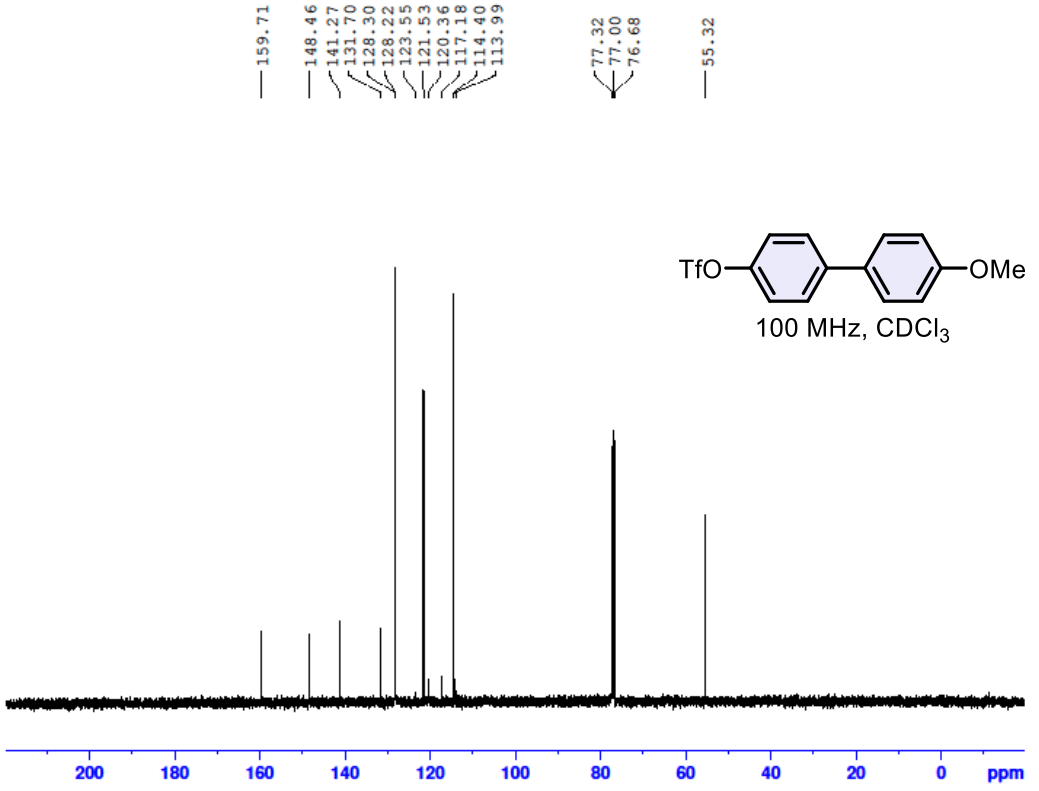

^{19}F NMR of 4'-methoxy-[1,1'-biphenyl]-4-yl trifluoromethanesulfonate (Table 4.3, compound **16f**)

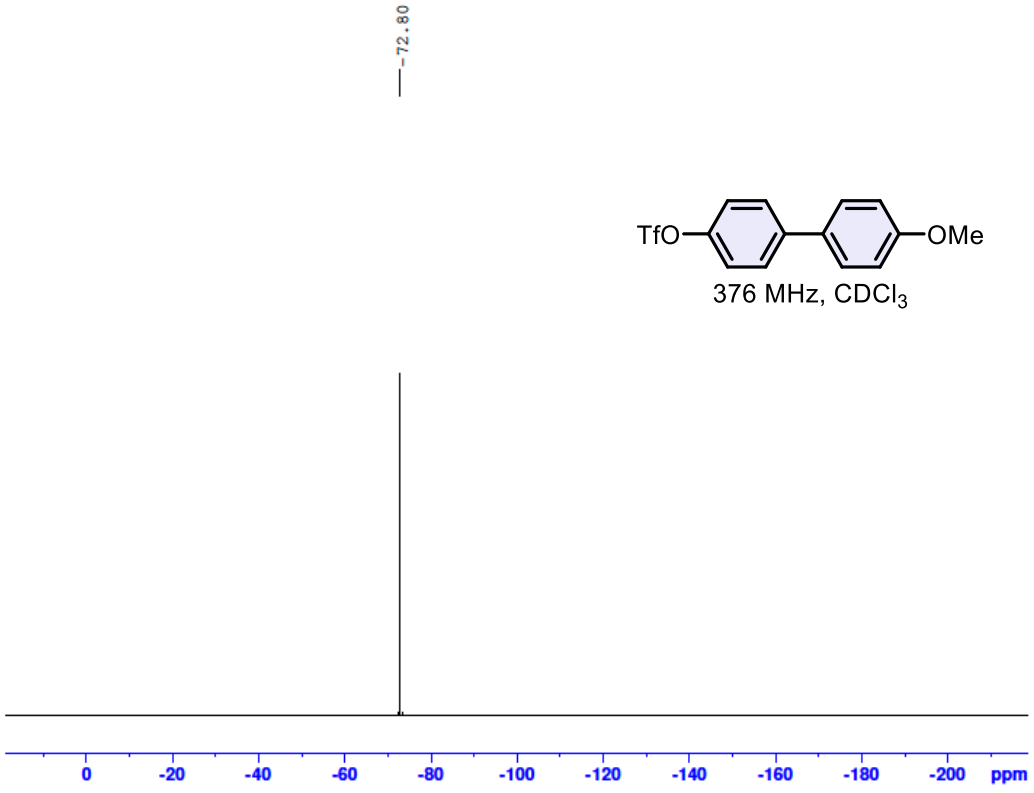

[1]H NMR of methyl 4'-(((trifluoromethyl)sulfonyl)oxy)-[1,1'-biphenyl]-4-carboxylat**e** (Table 4.3, compound **16g**)

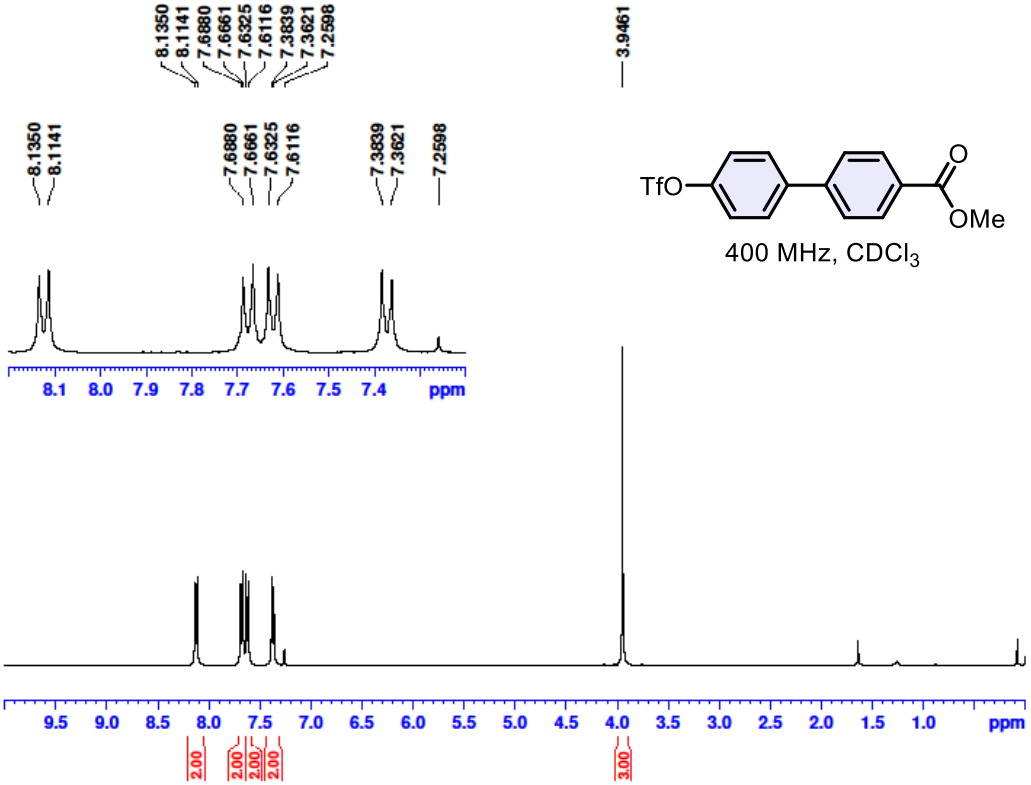

[13]C NMR of methyl 4'-(((trifluoromethyl)sulfonyl)oxy)-[1,1'-biphenyl]-4-carboxylat**e** (Table 4.3, compound **16g**)

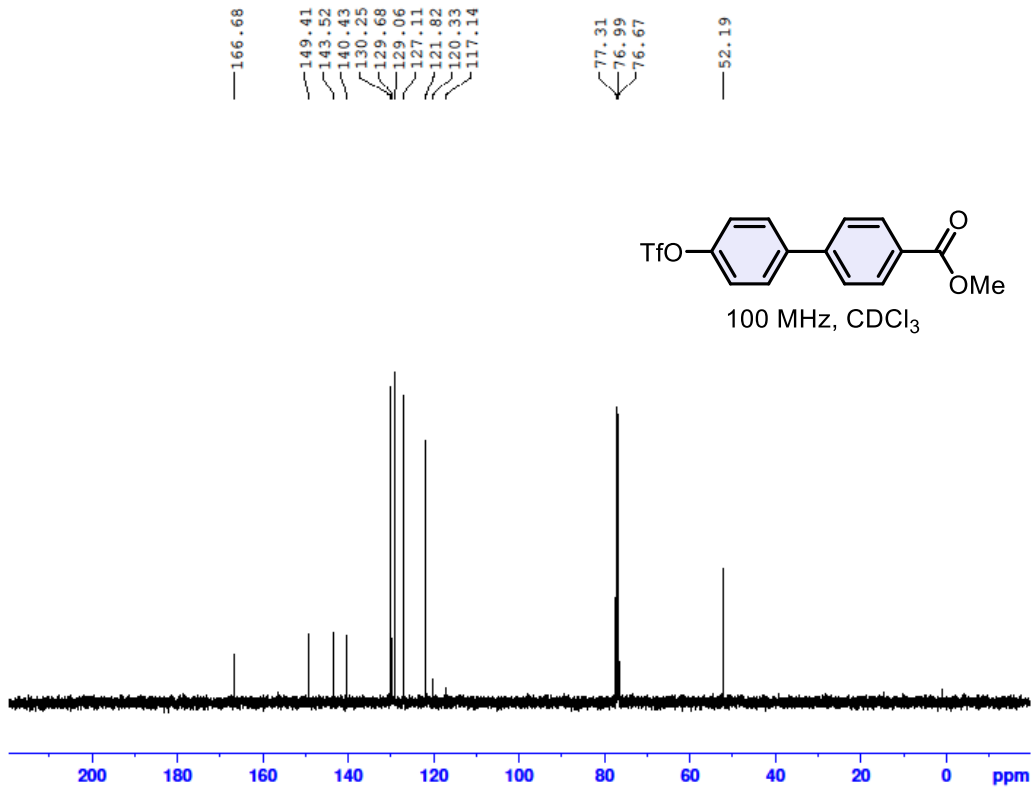

^{19}F NMR of methyl 4'-(((trifluoromethyl)sulfonyl)oxy)-[1,1'-biphenyl]-4-carboxylat**e** (Table 4.3, compound **16g**)

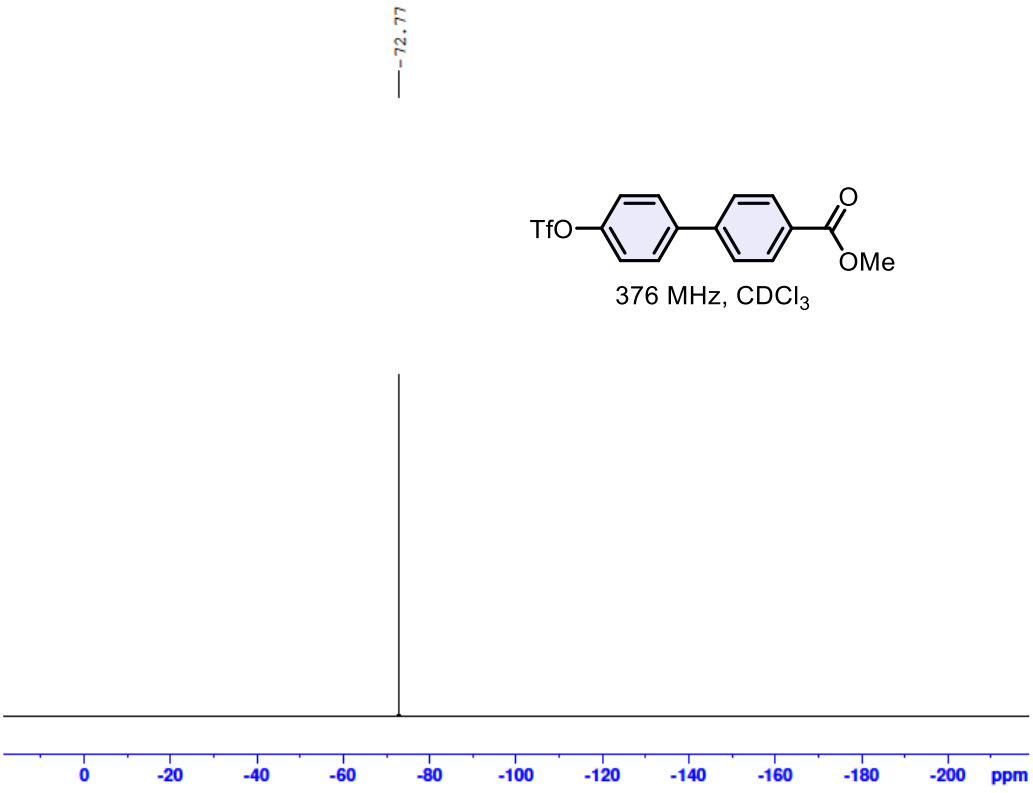

^{1}H NMR of 4-(naphthalen-1-yl)phenyl trifluoromethanesulfonate (Table 4.3, compound **16h**)

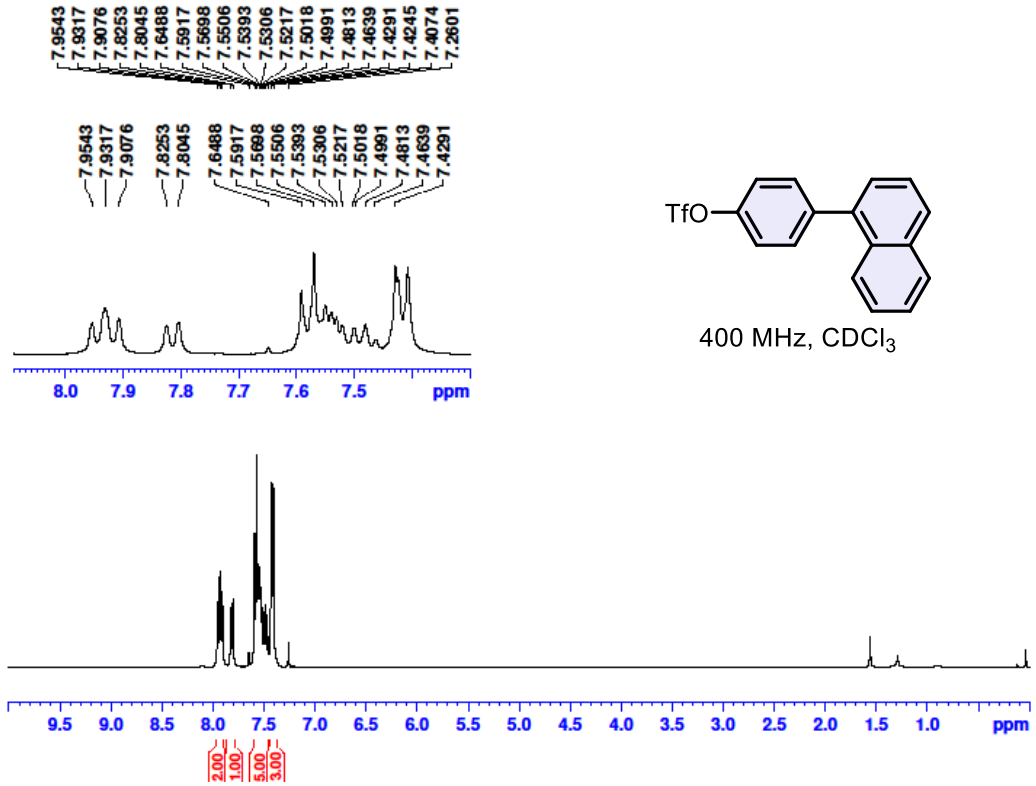

^{13}C NMR of 4-(naphthalen-1-yl)phenyl trifluoromethanesulfonate (Table 4.3, compound **16h**)

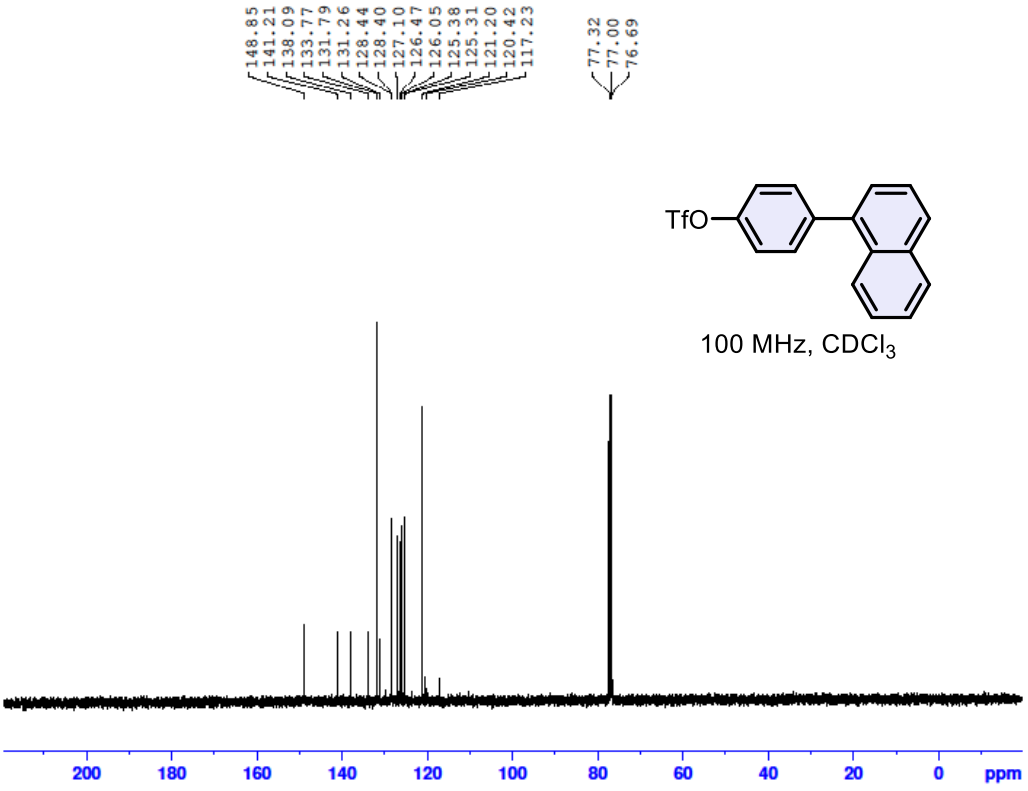

^{19}F NMR of 4-(naphthalen-1-yl)phenyl trifluoromethanesulfonate (Table 4.3, compound **16h**)

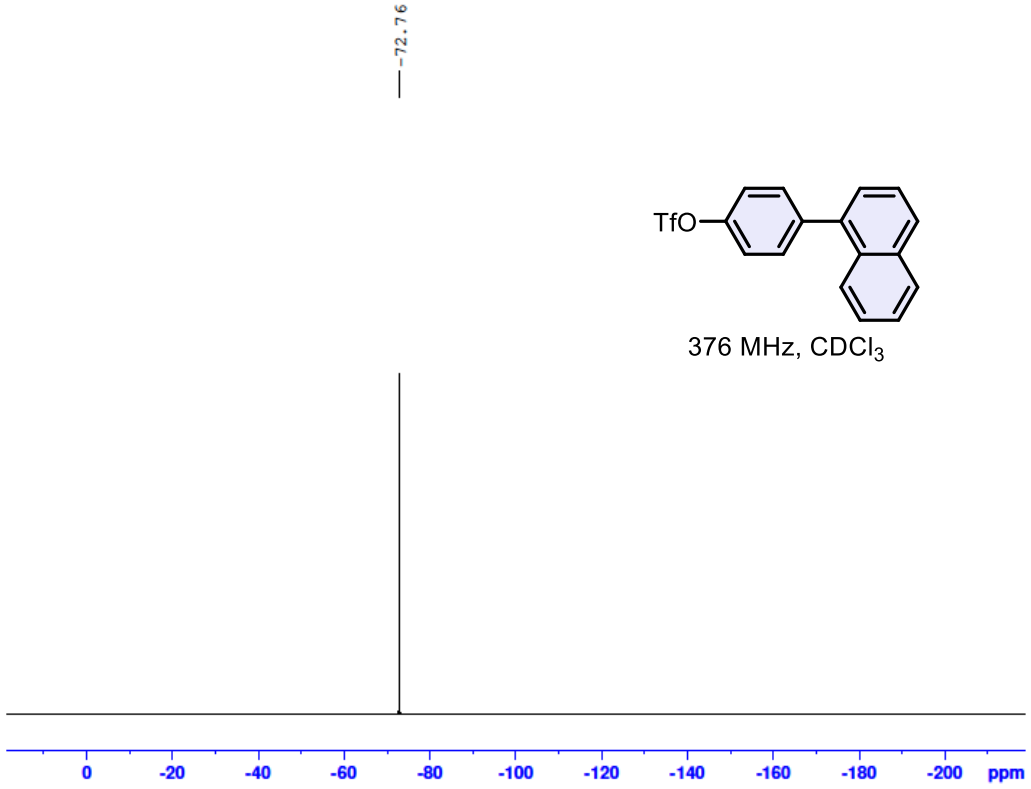

^{1}H NMR of 4-(dibenzo[*b*,*d*]furan-4-yl)phenyl trifluoromethanesulfonate (Table 4.3, compound **16i**)

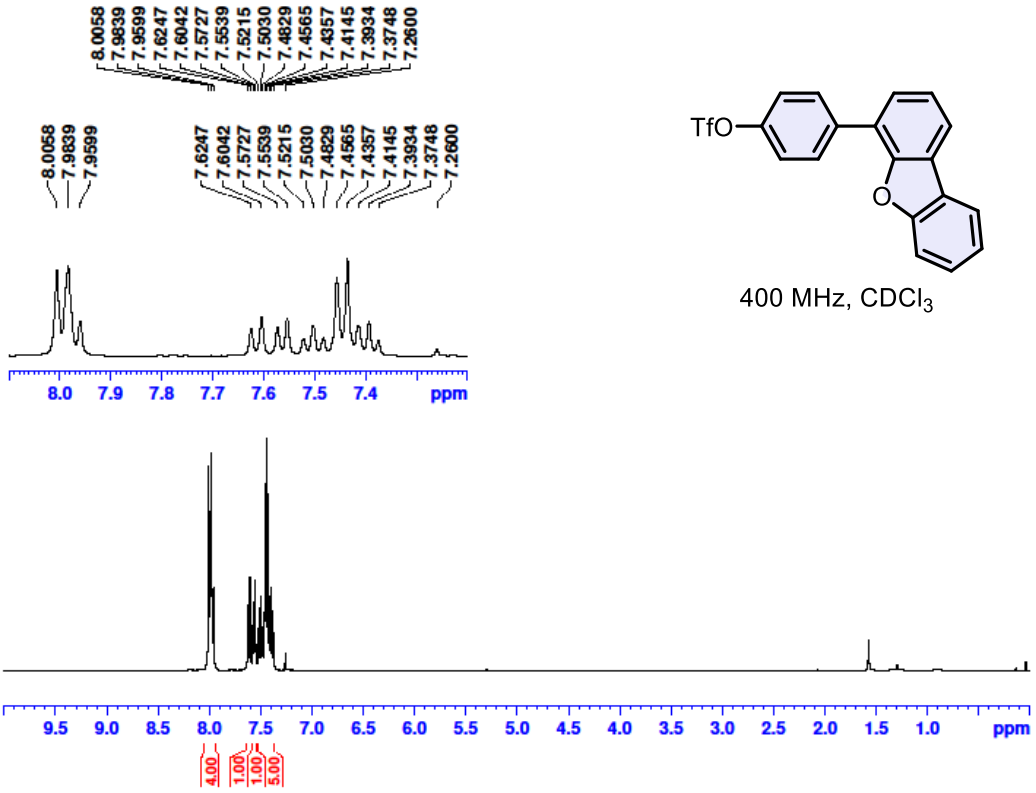

^{13}C NMR of 4-(dibenzo[*b*,*d*]furan-4-yl)phenyl trifluoromethanesulfonate (Table 4.3, compound **16i**)

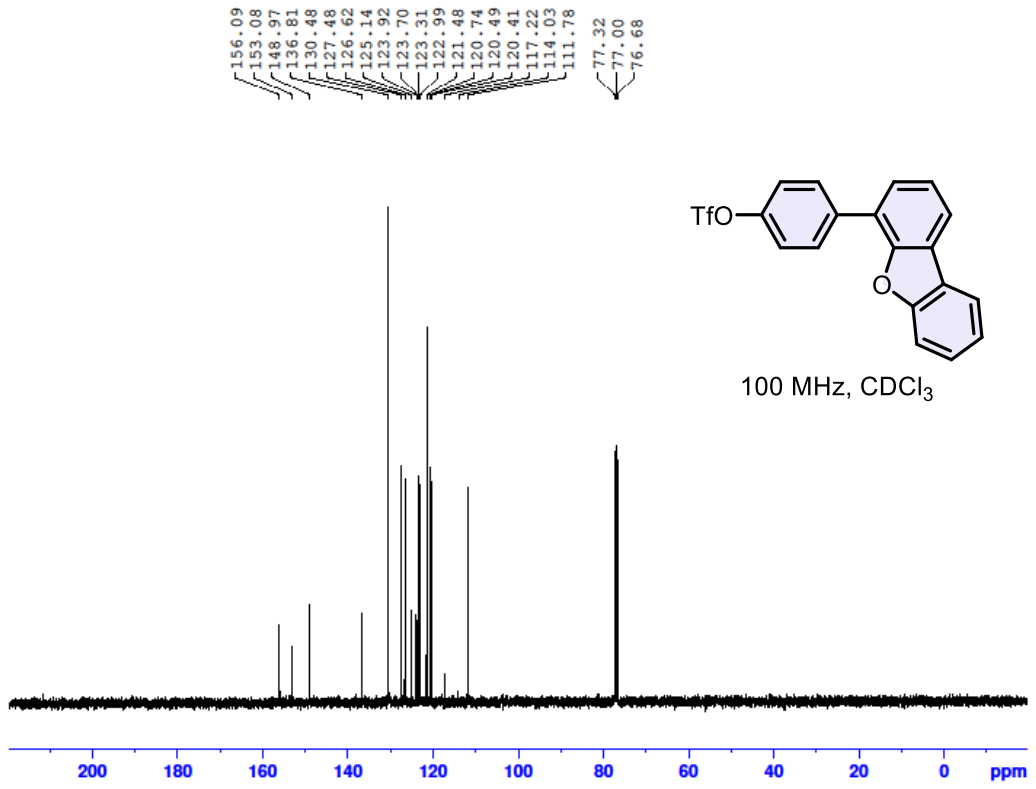

^{19}F NMR of 4-(dibenzo[*b*,*d*]furan-4-yl)phenyl trifluoromethanesulfonate (Table 4.3, compound **16i**)

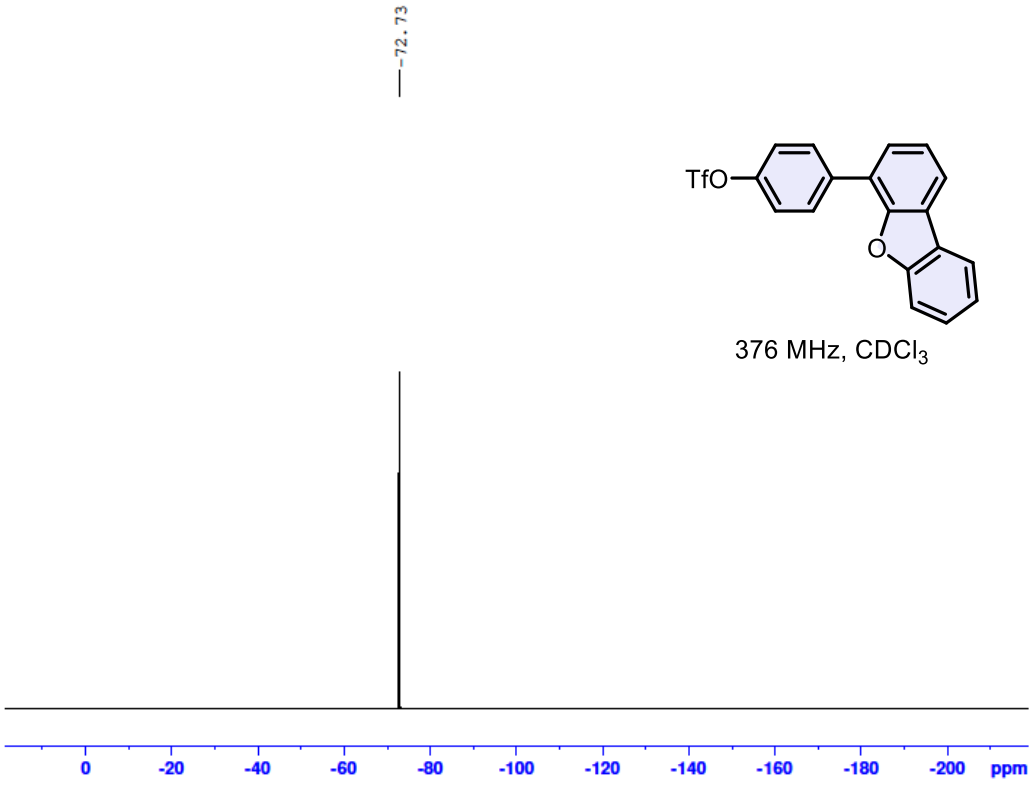

^{1}H NMR of 4-(dibenzo[*b*,*d*]thiophen-4-yl)phenyl trifluoromethanesulfonate (Table 4.3, compound **16j**)

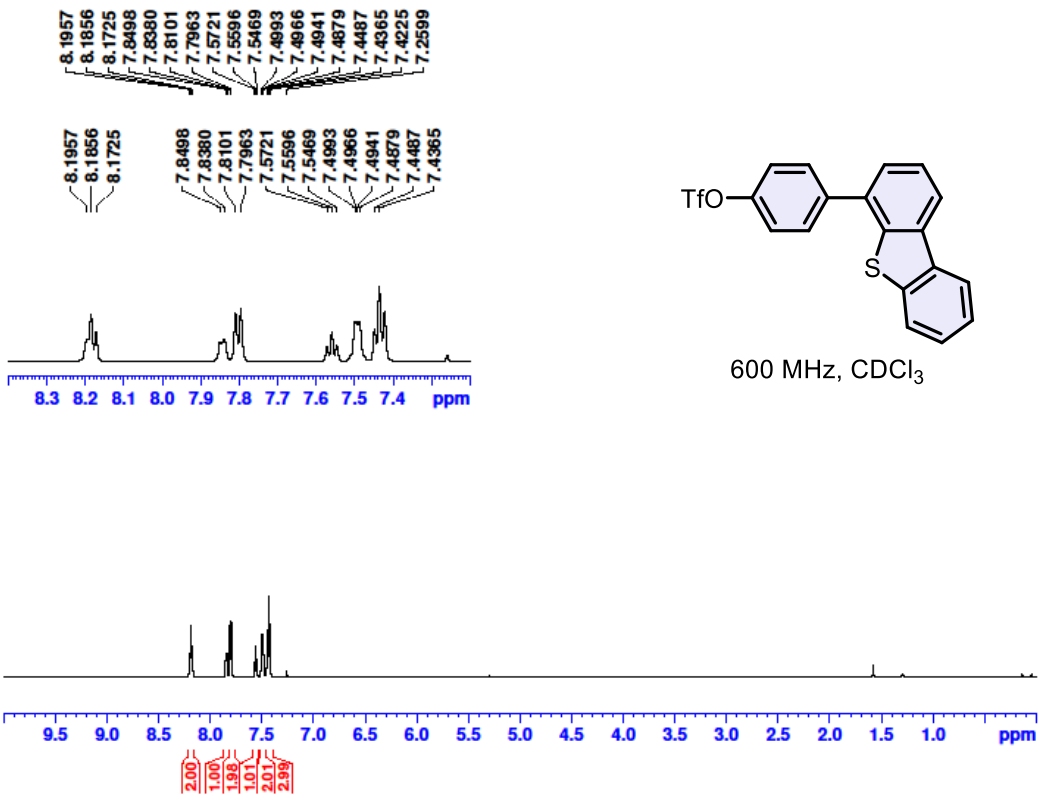

^{13}C NMR of 4-(dibenzo[*b*,*d*]thiophen-4-yl)phenyl trifluoromethanesulfonate (Table 4.3, compound **16j**)

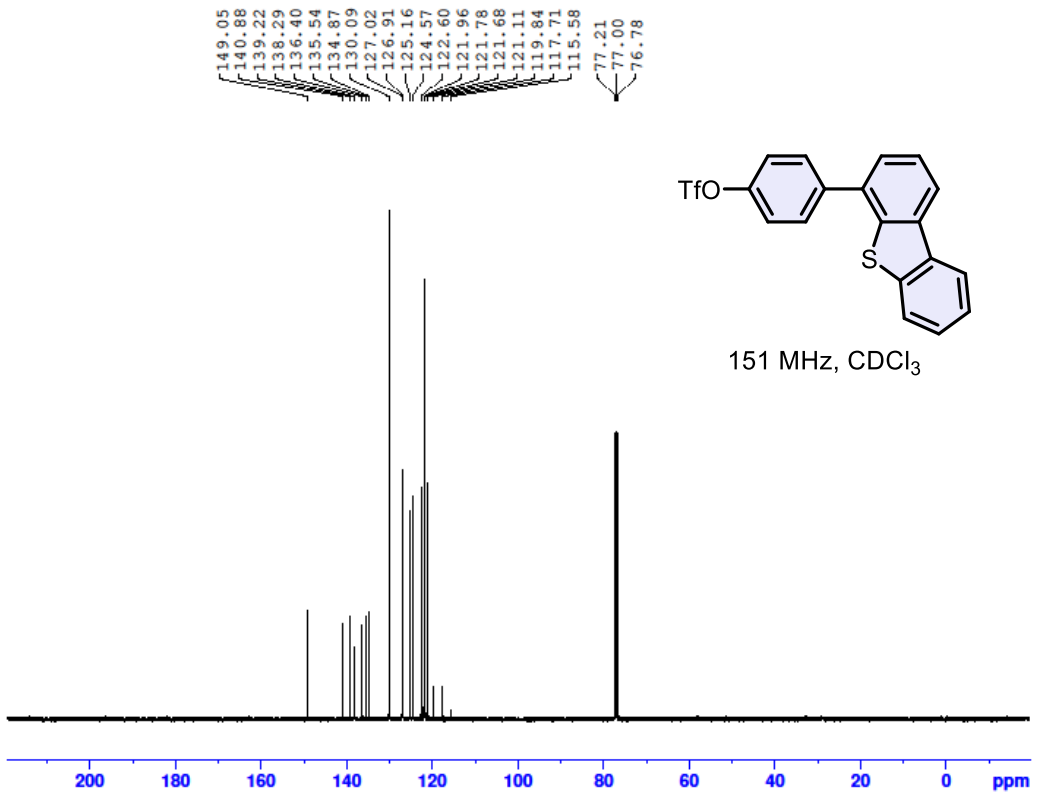

^{19}F NMR of 4-(dibenzo[*b*,*d*]thiophen-4-yl)phenyl trifluoromethanesulfonate (Table 4.3, compound **16j**)

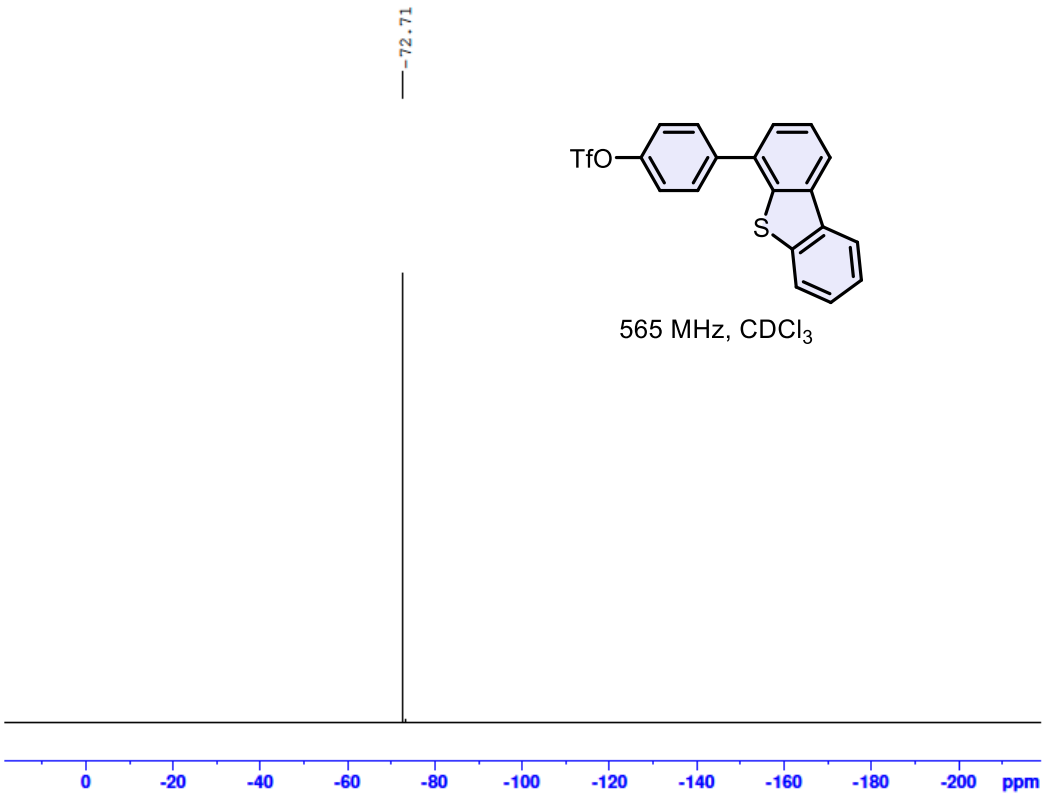

^{1}H NMR of 4-(benzo[*b*]thiophen-2-yl)phenyl trifluoromethanesulfonate (Table 4.3, compound **16k**)

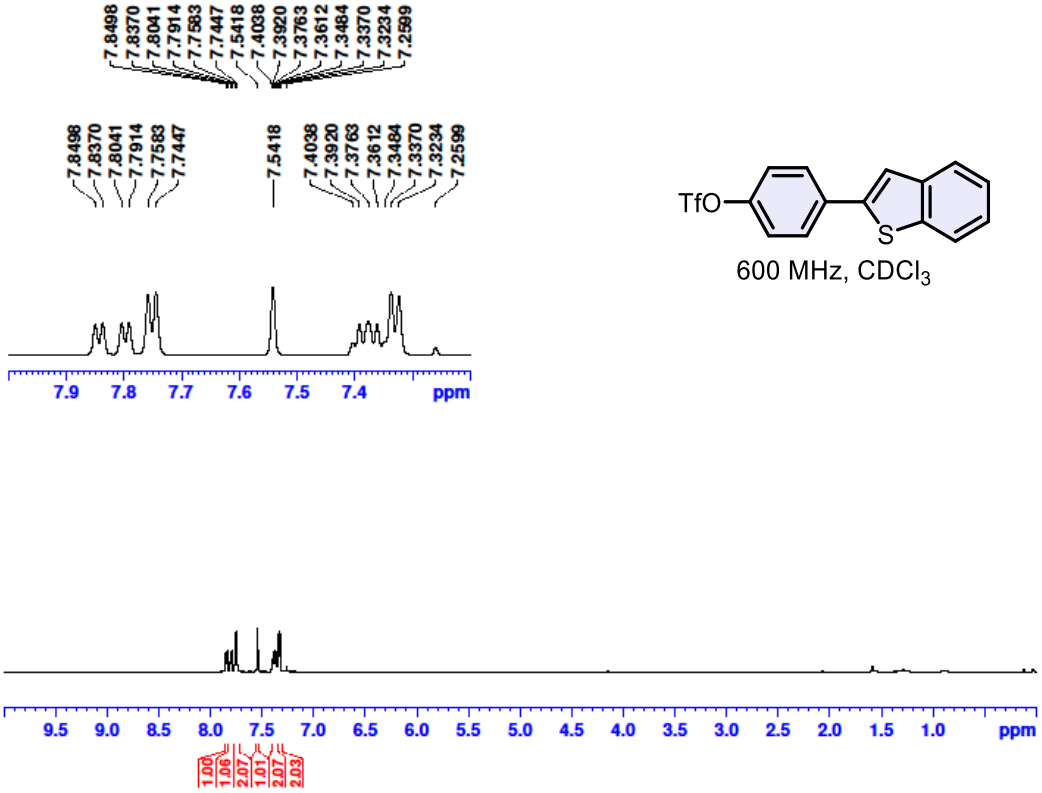

^{13}C NMR of 4-(benzo[*b*]thiophen-2-yl)phenyl trifluoromethanesulfonate (Table 4.3, compound **16k**)

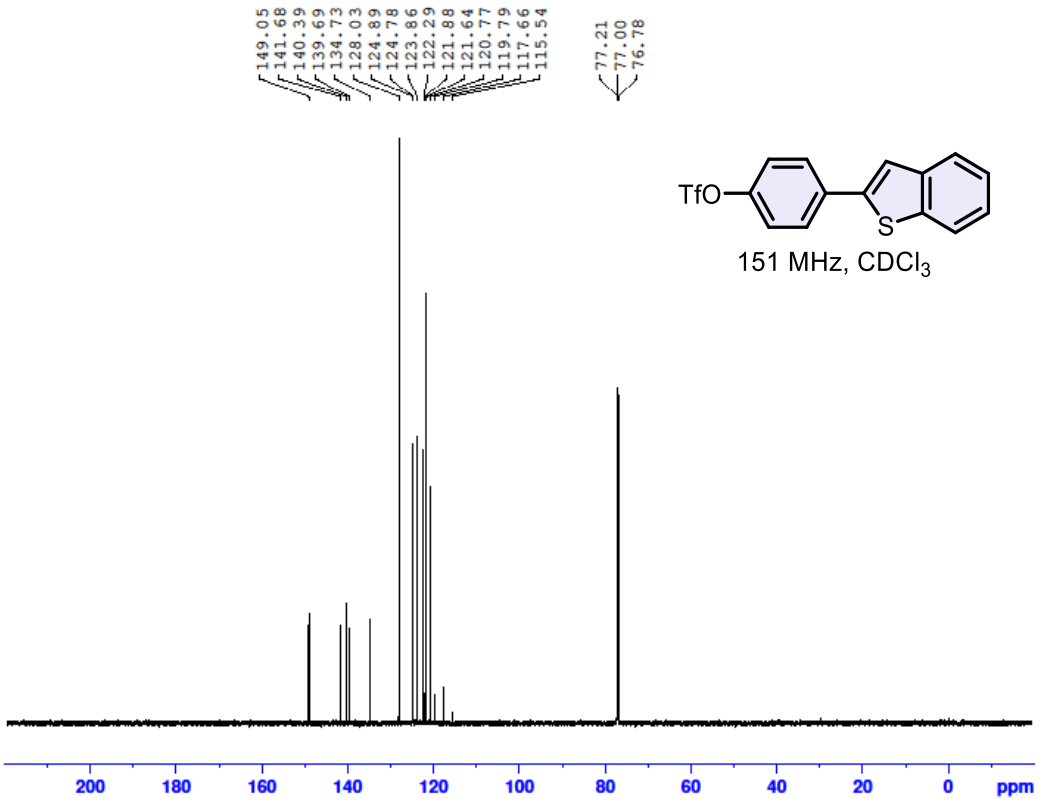

^{19}F NMR of 4-(benzo[*b*]thiophen-2-yl)phenyl trifluoromethanesulfonate (Table 4.3, compound **16k**)

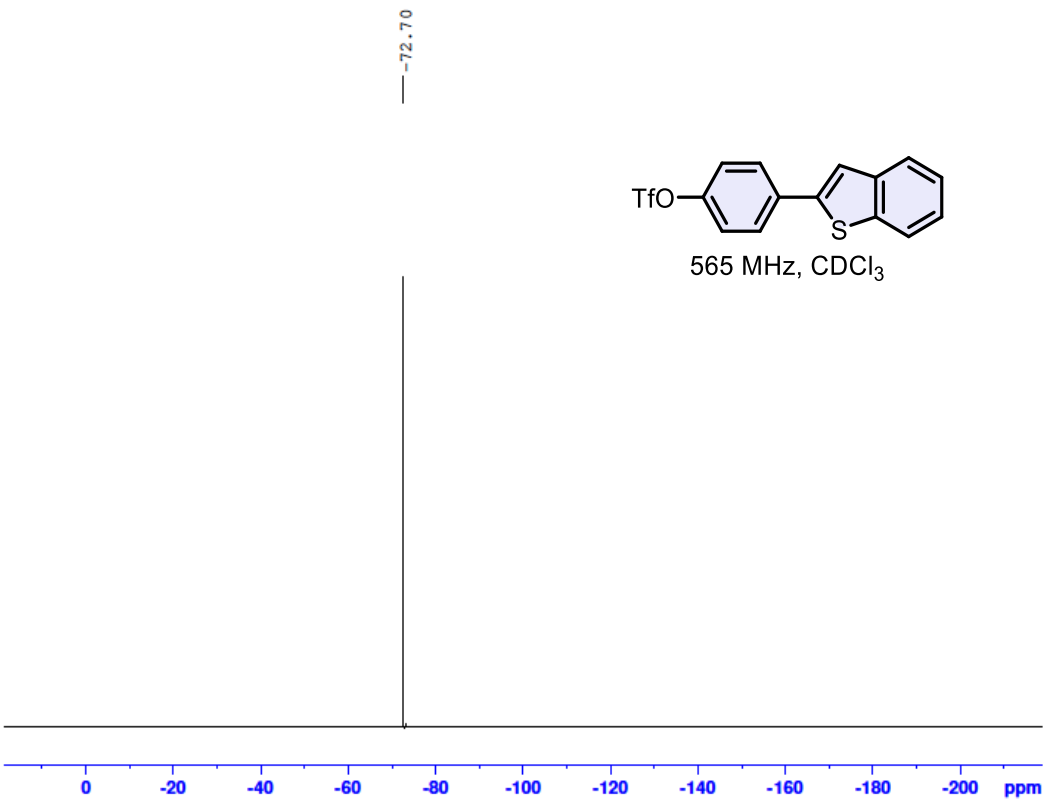

^{1}H NMR of 4-(benzofuran-2-yl)phenyl trifluoromethanesulfonate (Table 4.3, compound **16l**)

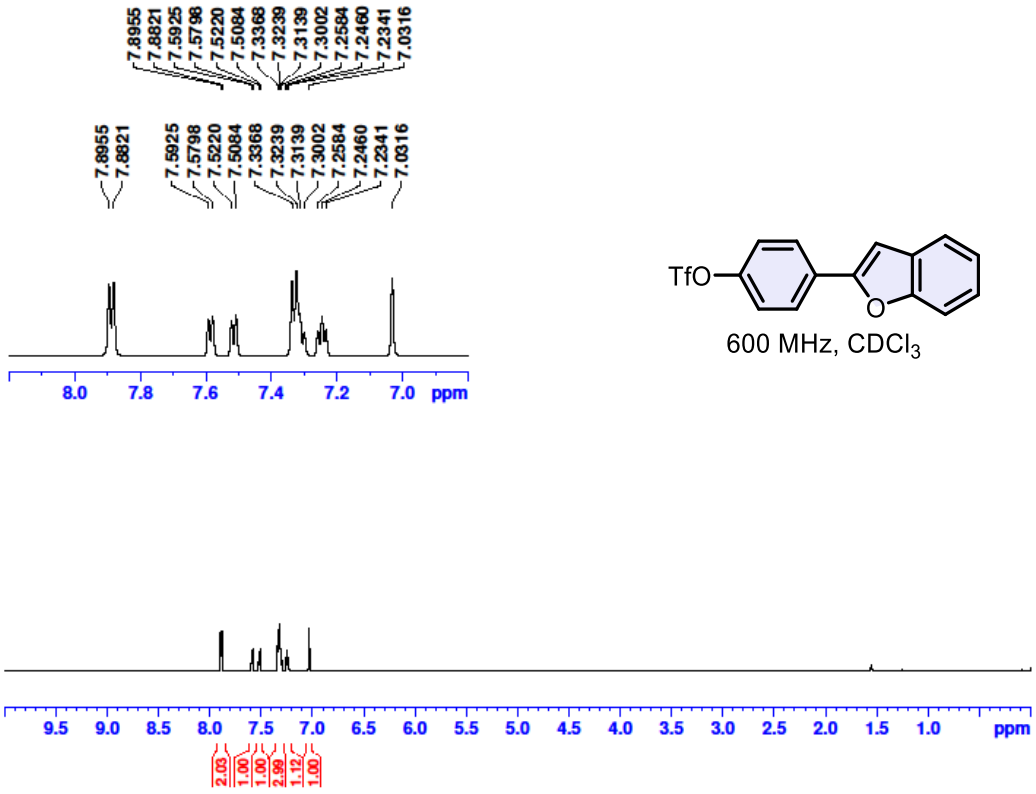

^{13}C NMR of 4-(benzofuran-2-yl)phenyl trifluoromethanesulfonate (Table 4.3, compound **16l**)

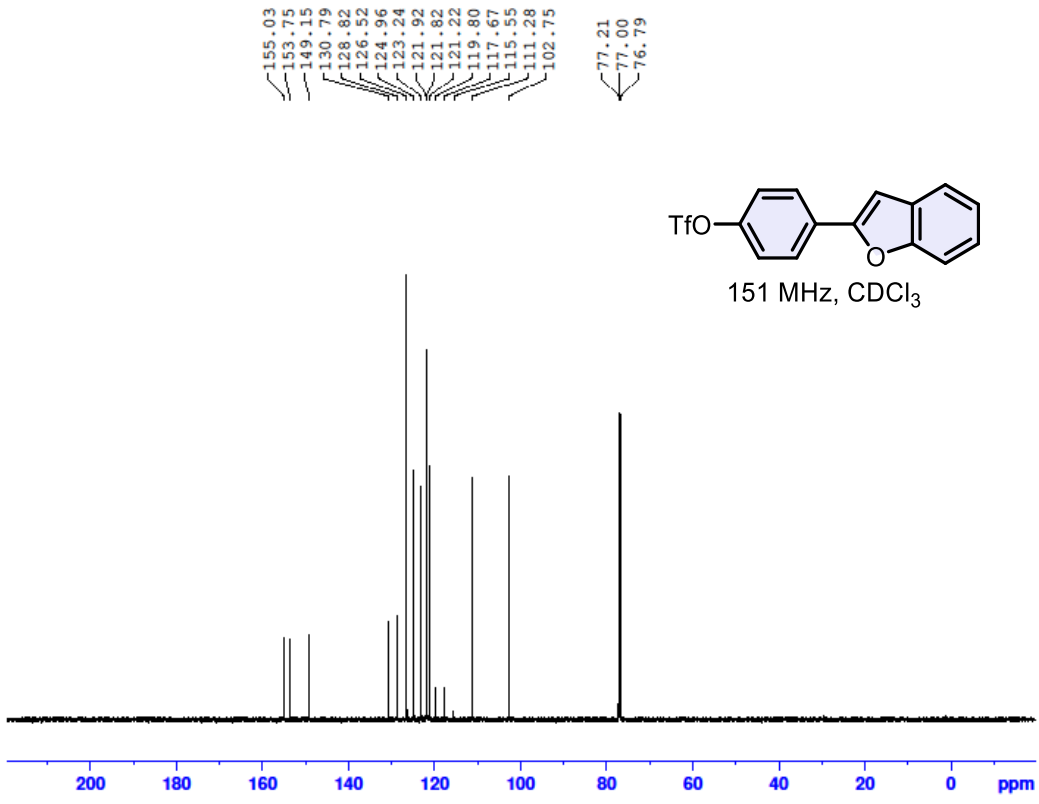

^{19}F NMR of 4-(benzofuran-2-yl)phenyl trifluoromethanesulfonate (Table 4.3, compound **16l**)

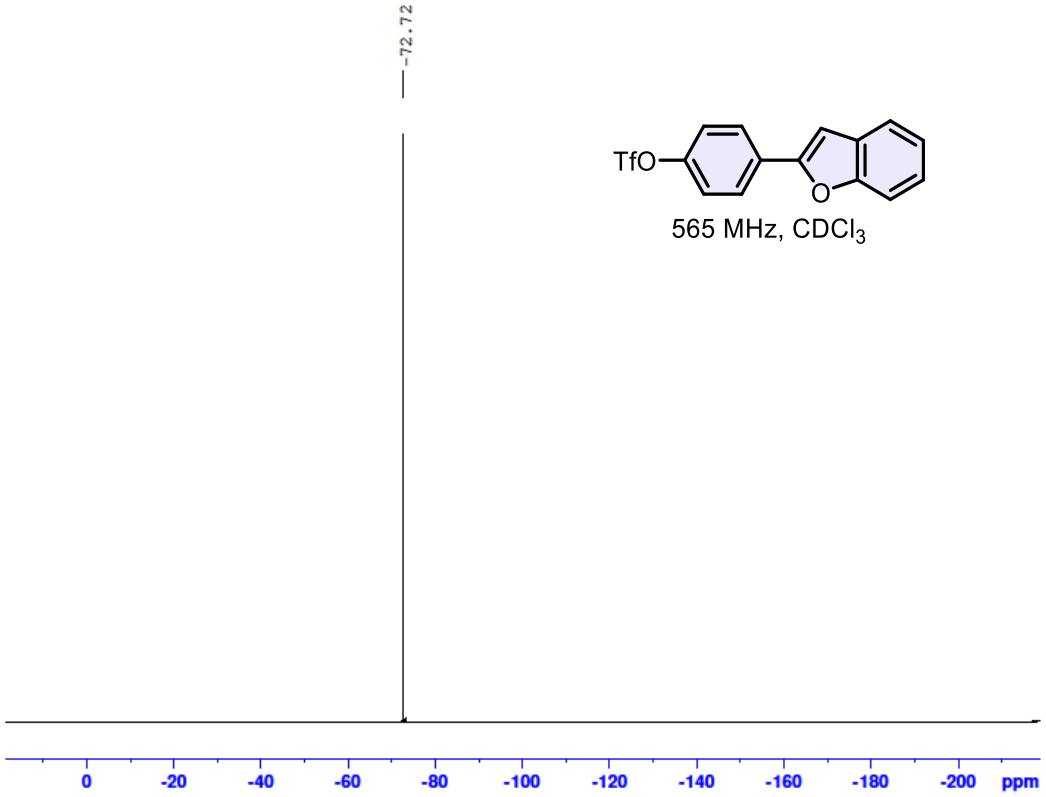

^{1}H NMR of 2-methoxy-4-(naphthalen-1-yl)phenyl trifluoromethanesulfonate (Table 4.3, compound **16m**)

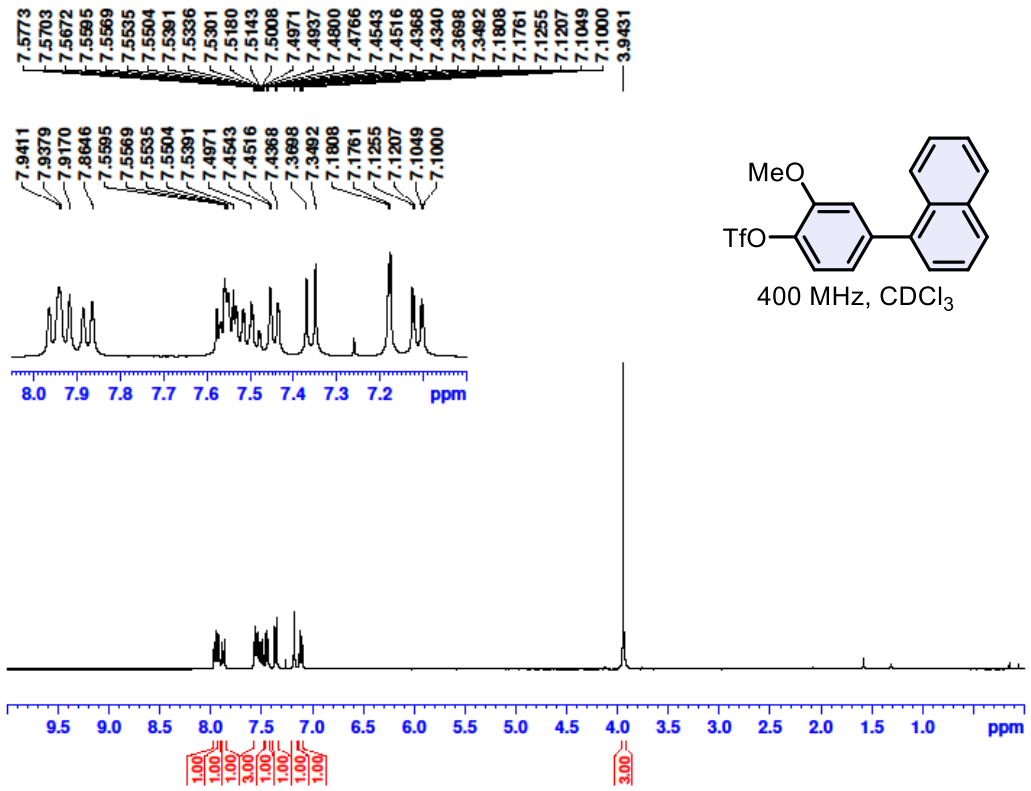

^{13}C NMR of 2-methoxy-4-(naphthalen-1-yl)phenyl trifluoromethanesulfonate (Table 4.3, compound **16m**)

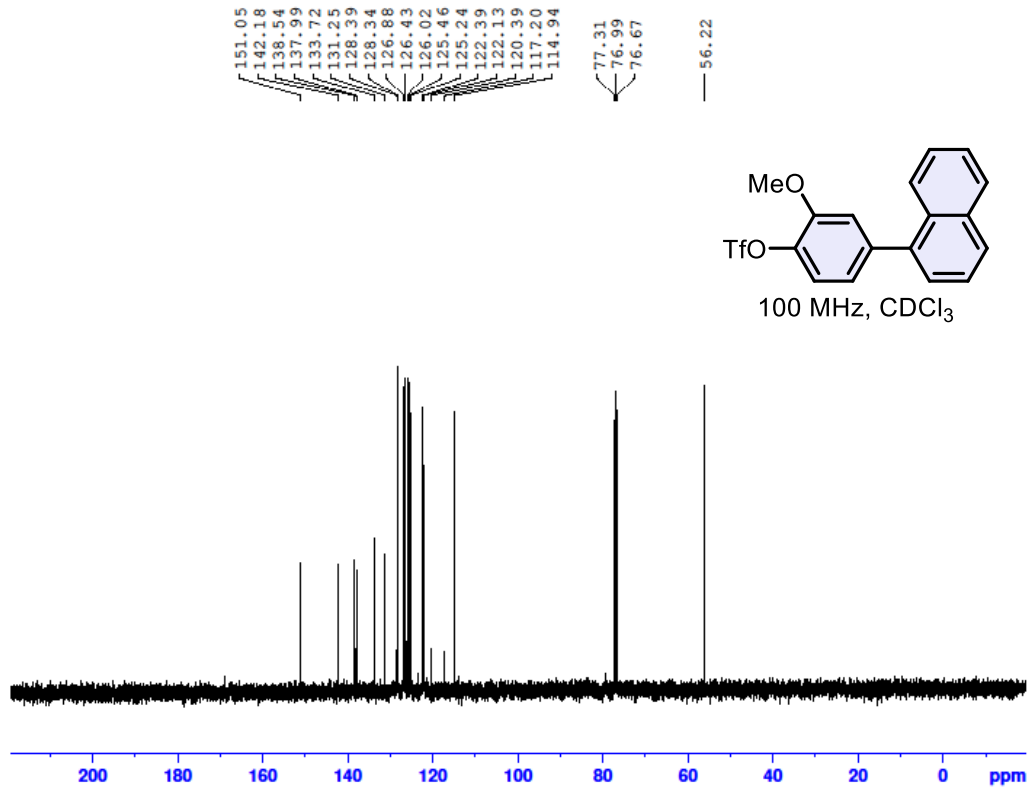

^{19}F NMR of 2-methoxy-4-(naphthalen-1-yl)phenyl trifluoromethanesulfonate (Table 4.3, compound **16m**)

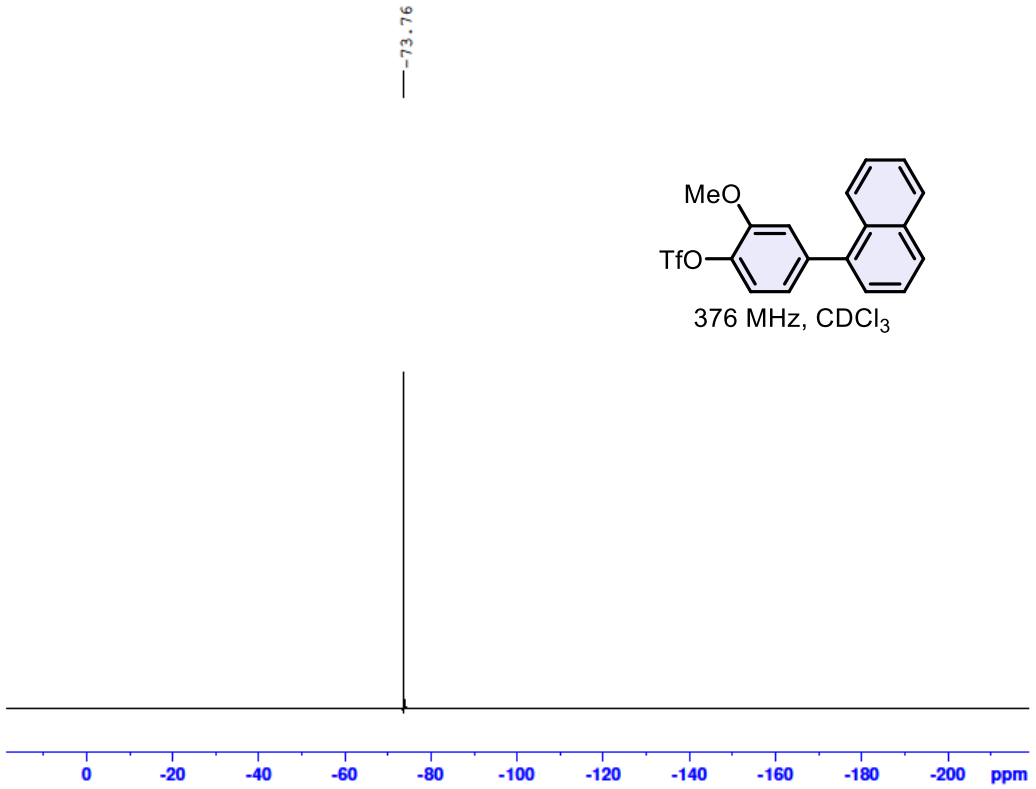

HRMS of 2-methoxy-4-(naphthalen-1-yl)phenyl trifluoromethanesulfonate (Table 4.3, compound **16m**)

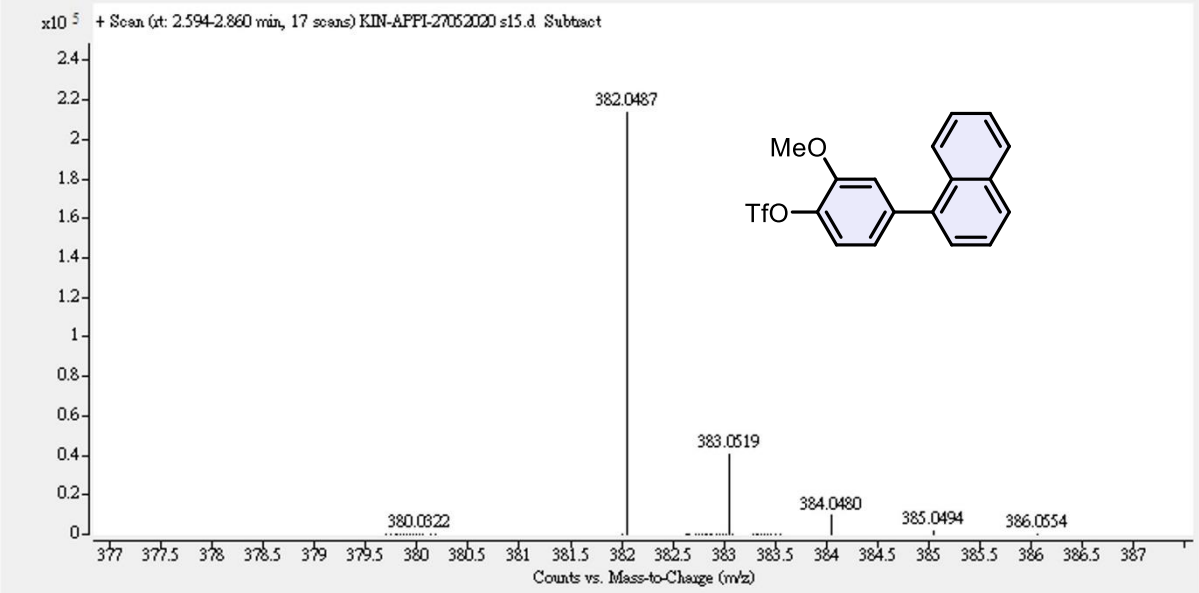

Mass	Calc. Mass	mDa	PPM	Formula
382.0487	382.0487	-0.04	-0.09	C18 H13 F3 O4 S

^{1}H NMR of 2'-methyl-[1,1'-biphenyl]-2-yl trifluoromethanesulfonate (Table 4.3, compound **16n**)

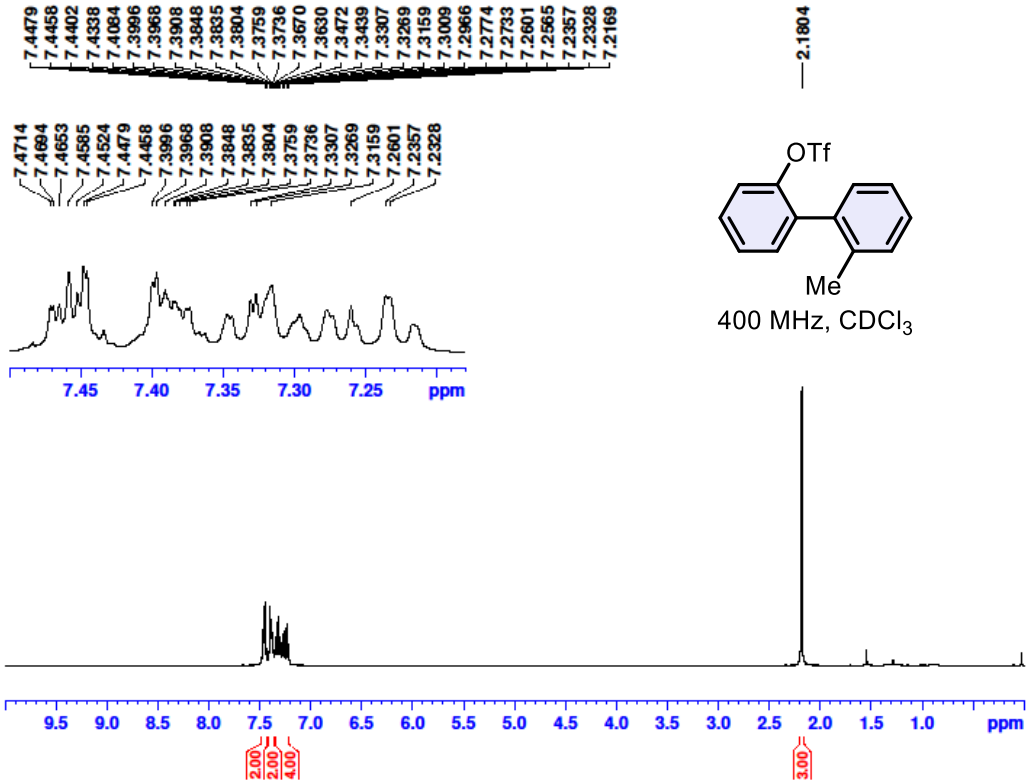

^{13}C NMR of 2'-methyl-[1,1'-biphenyl]-2-yl trifluoromethanesulfonate (Table 4.3, compound **16n**)

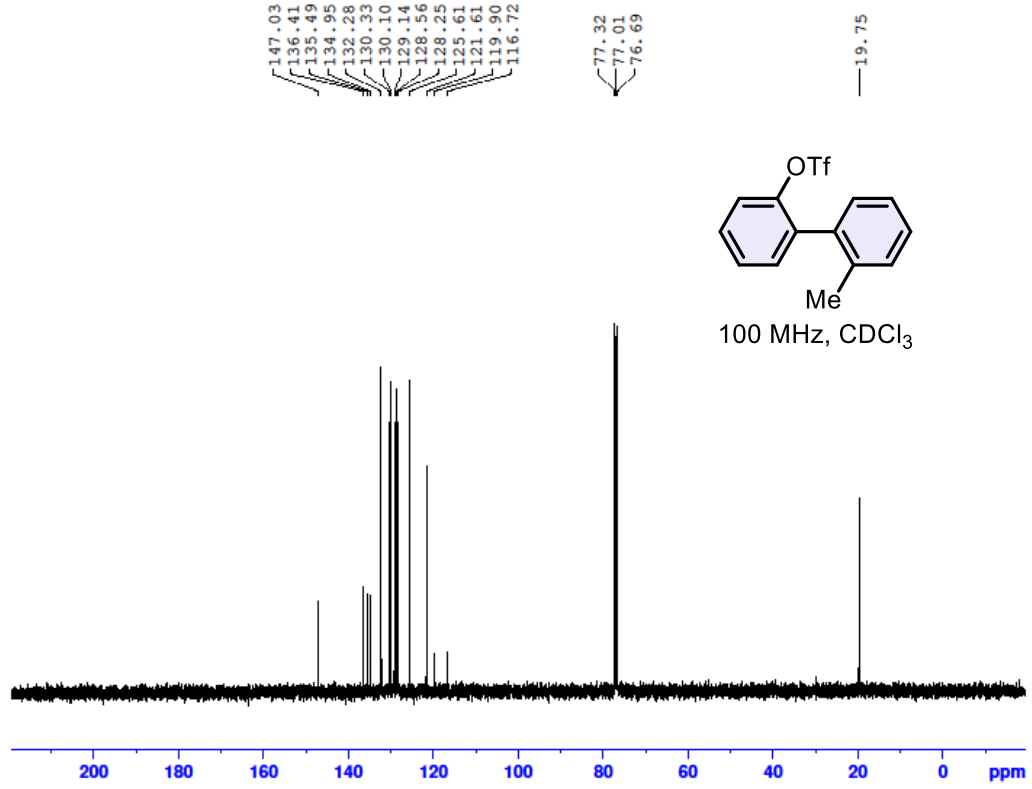

^{19}F NMR of 2'-methyl-[1,1'-biphenyl]-2-yl trifluoromethanesulfonate (Table 4.3, compound **16n**)

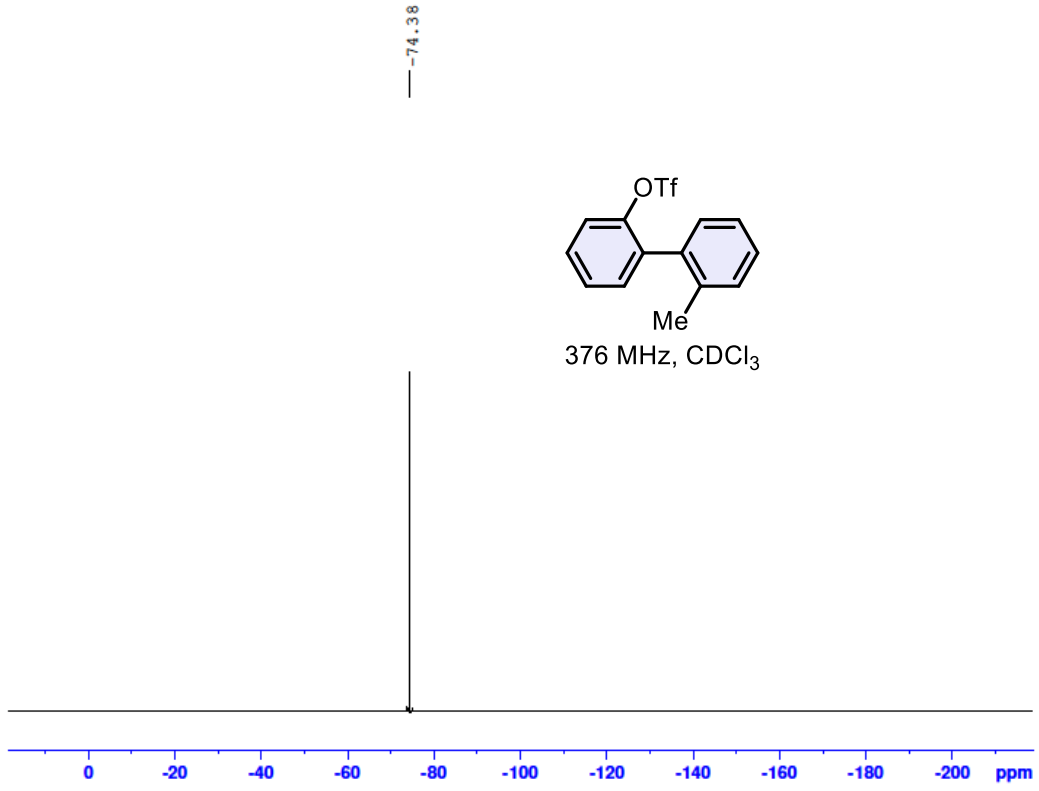

^{1}H NMR of methyl 4'-methoxy-6-(((trifluoromethyl)sulfonyl)oxy)-[1,1'-biphenyl]-3-carboxylate (Table 4.3, compound **16o**)

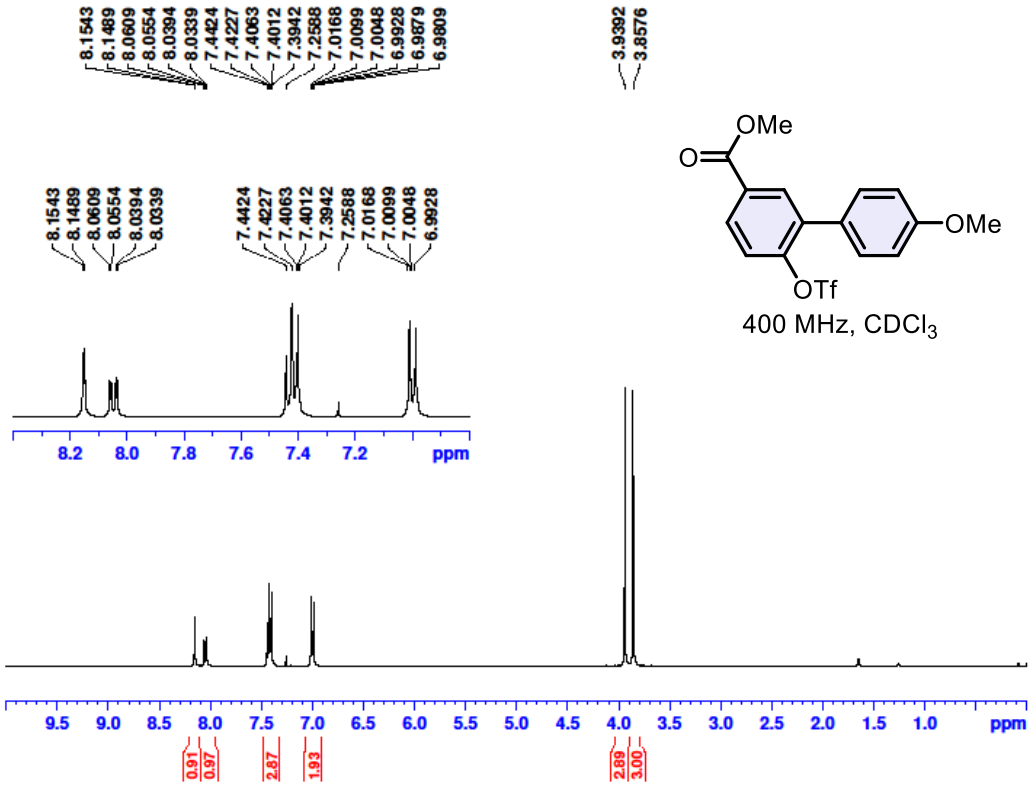

^{13}C NMR of methyl 4'-methoxy-6-(((trifluoromethyl)sulfonyl)oxy)-[1,1'-biphenyl]-3-carboxylate (Table 4.3, compound **16o**)

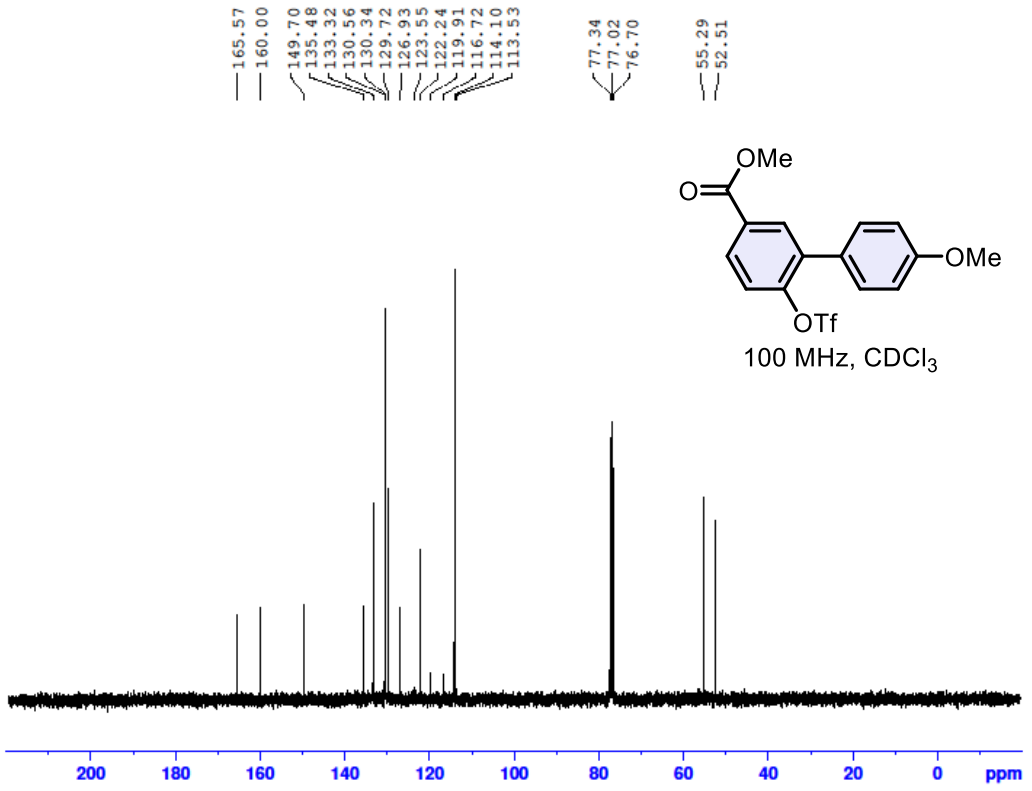

^{19}F NMR of methyl 4’-methoxy-6-(((trifluoromethyl)sulfonyl)oxy)-[1,1’-biphenyl]-3-carboxylate (Table 4.3, compound **16o**)

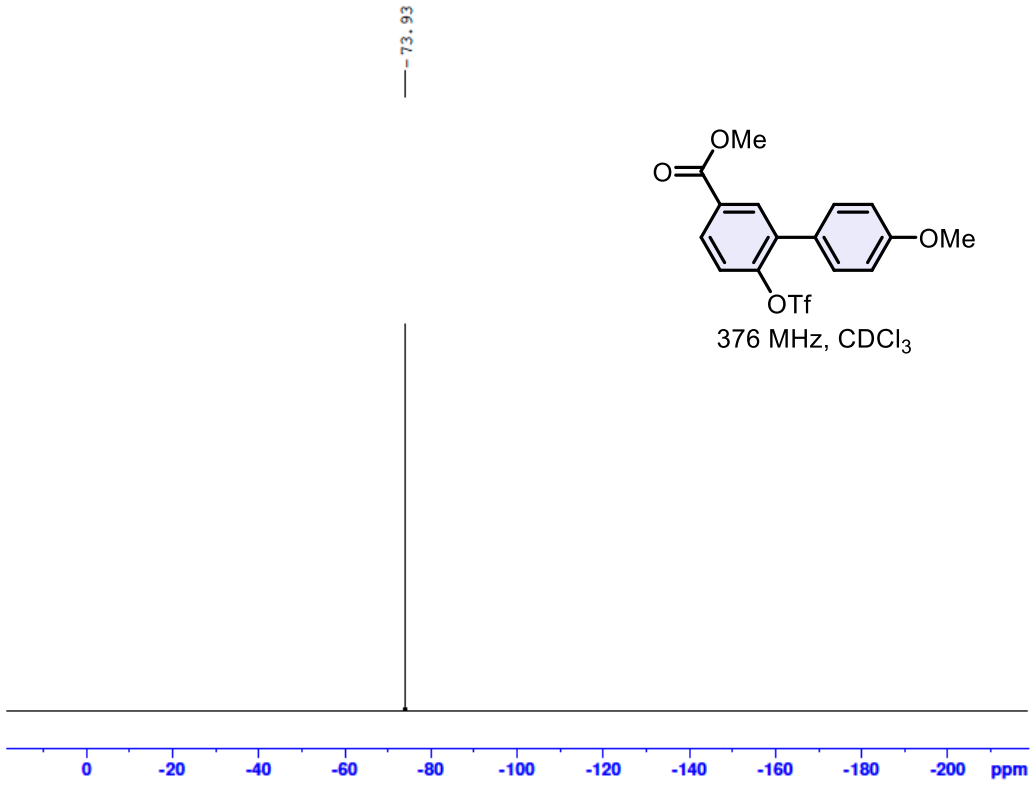

HRMS of methyl 4’-methoxy-6-(((trifluoromethyl)sulfonyl)oxy)-[1,1’-biphenyl]-3-carboxylate (Table 4.3, compound **16o**)

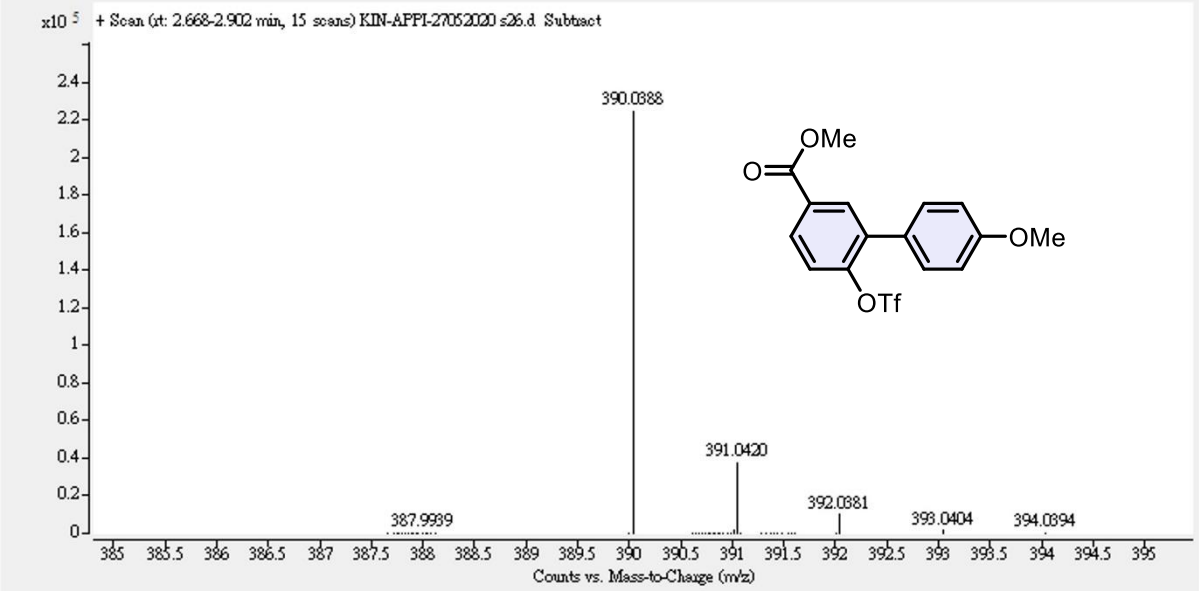

Mass	Calc. Mass	mDa	PPM	Formula
390.0388	390.0385	-0.31	-0.79	C16 H13 F3 O6 S

^{1}H NMR of 5-formyl-4'-methoxy-[1,1'-biphenyl]-2-yl trifluoromethanesulfonate (Table 4.3, compound **16p**)

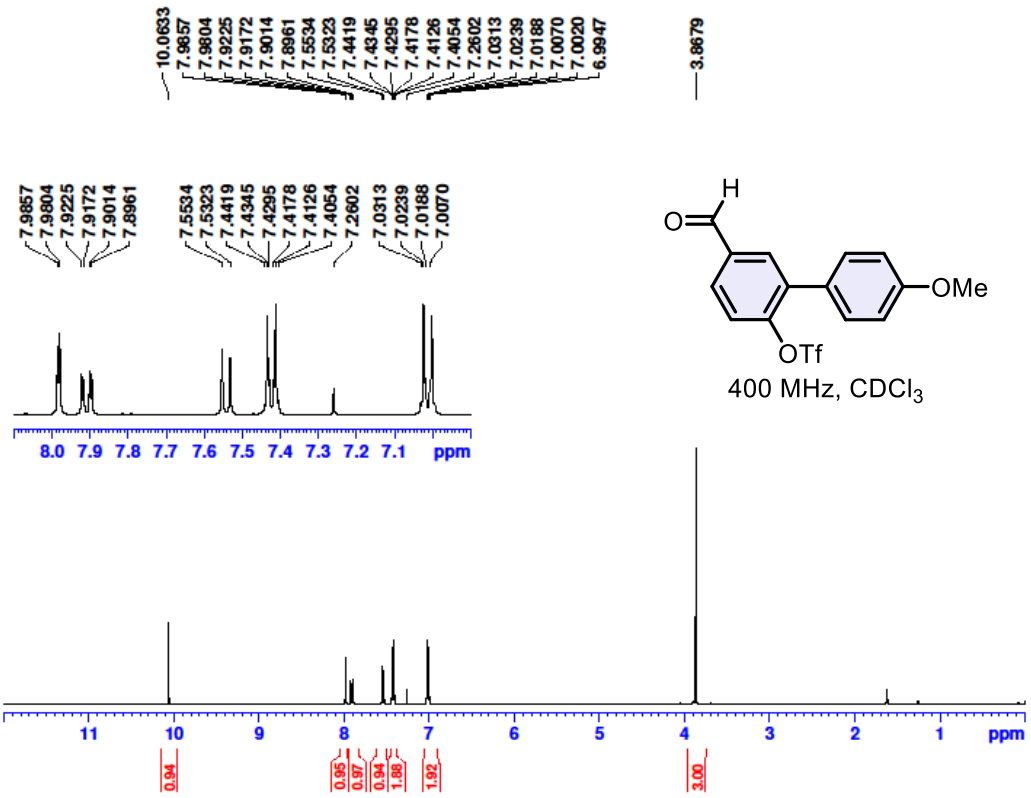

^{13}C NMR of 5-formyl-4'-methoxy-[1,1'-biphenyl]-2-yl trifluoromethanesulfonate (Table 4.3, compound **16p**)

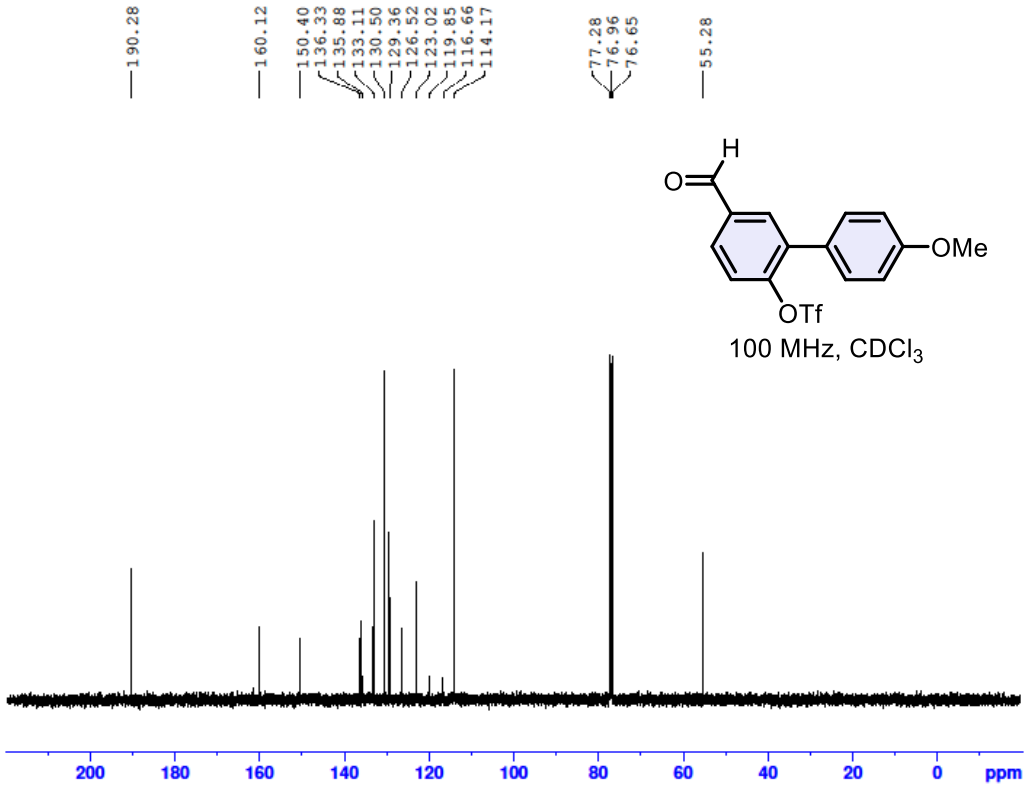

^{19}F NMR of 5-formyl-4'-methoxy-[1,1'-biphenyl]-2-yl trifluoromethanesulfonate (Table 4.3, compound **16p**)

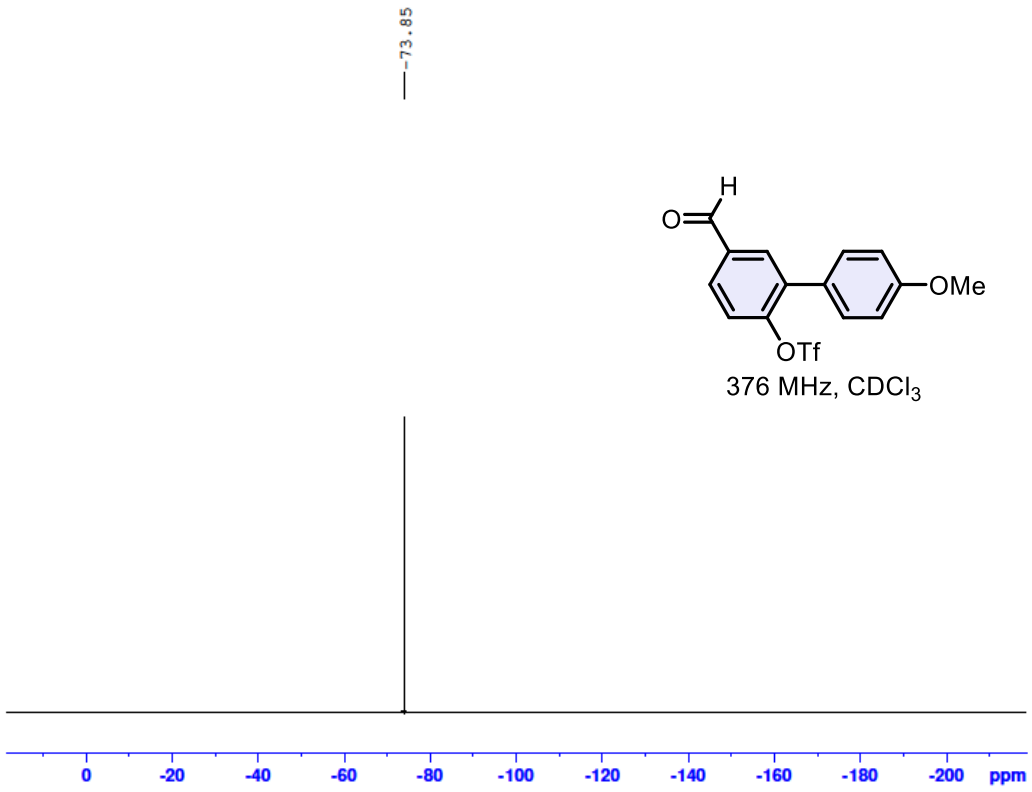

^{1}H NMR of 5-cyano-4'-methoxy-[1,1'-biphenyl]-2-yl trifluoromethanesulfonate (Table 4.3, compound **16q**)

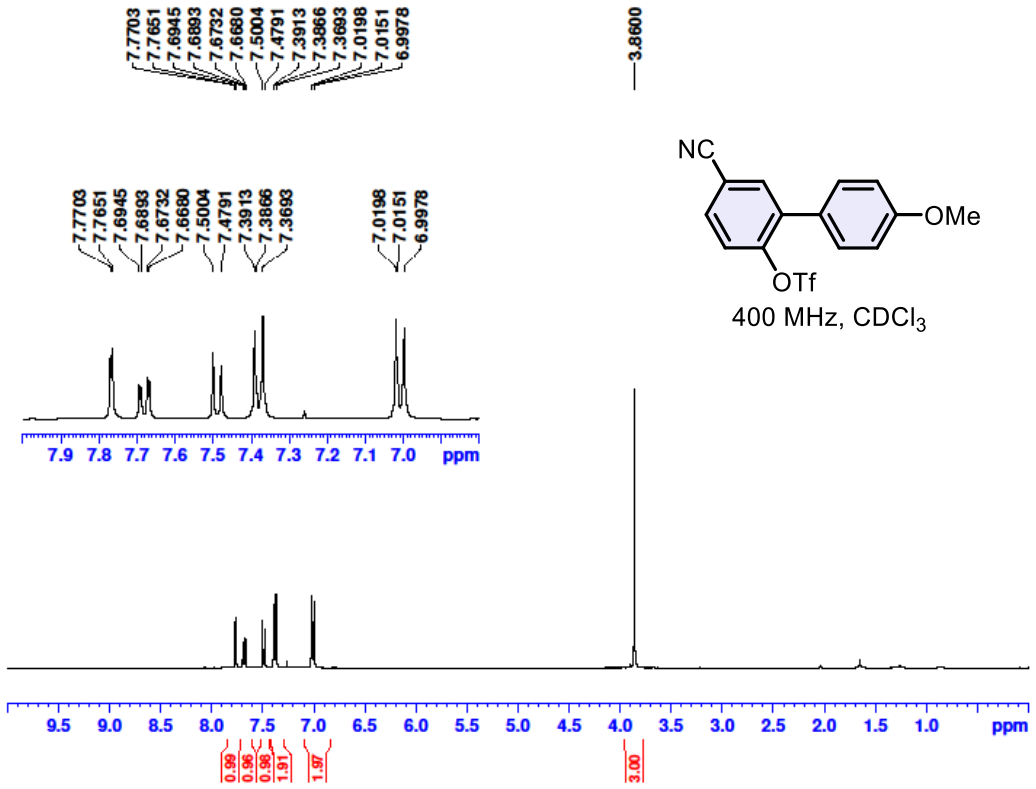

^{13}C NMR of 5-cyano-4'-methoxy-[1,1'-biphenyl]-2-yl trifluoromethanesulfonate (Table 4.3, compound **16q**)

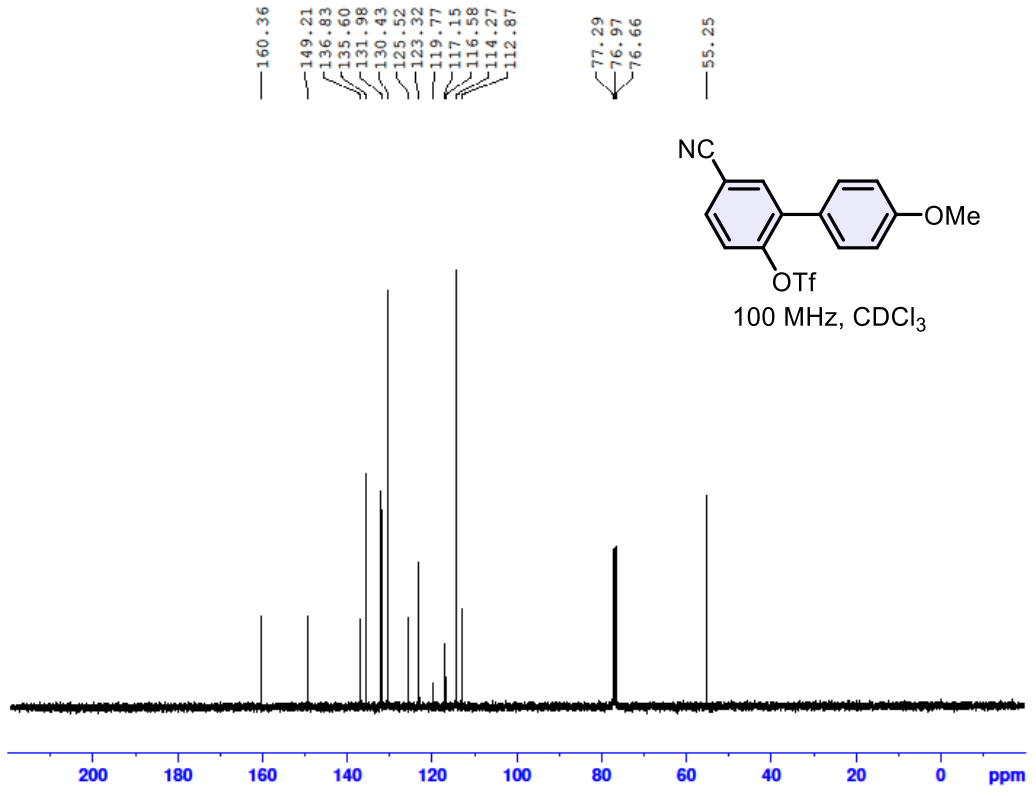

^{19}F NMR of 5-cyano-4'-methoxy-[1,1'-biphenyl]-2-yl trifluoromethanesulfonate (Table 4.3, compound **16q**)

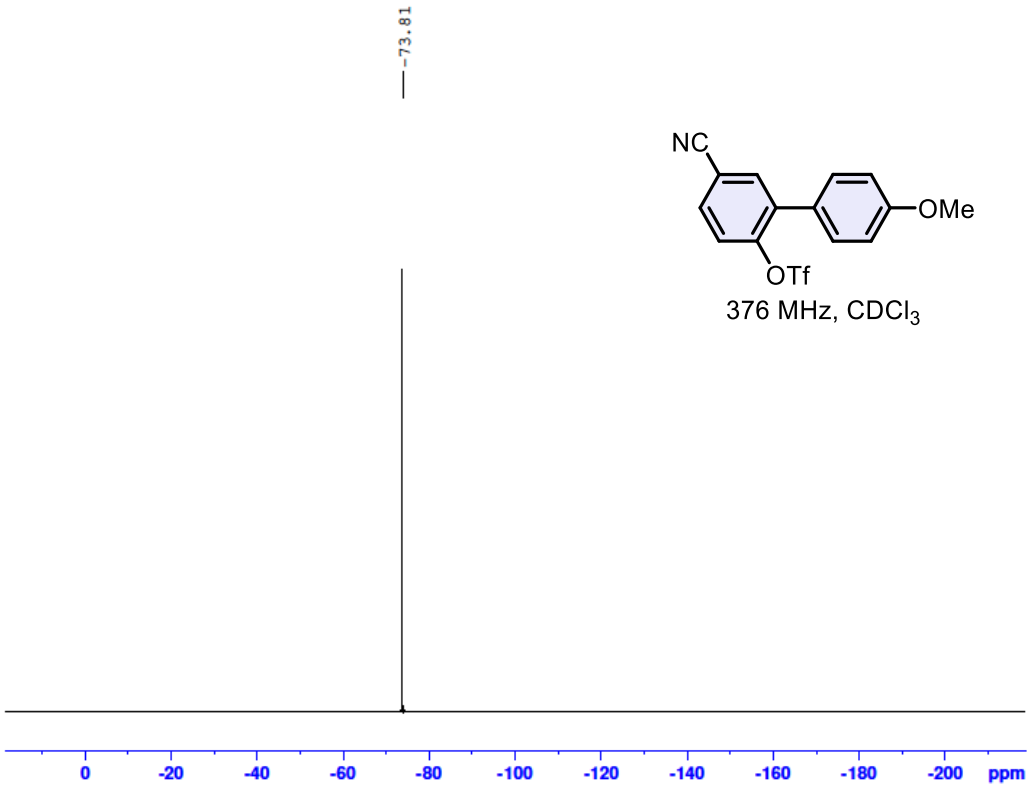

HRMS of 5-cyano-4'-methoxy-[1,1'-biphenyl]-2-yl trifluoromethanesulfonate (Table 4.3, compound **16q**)

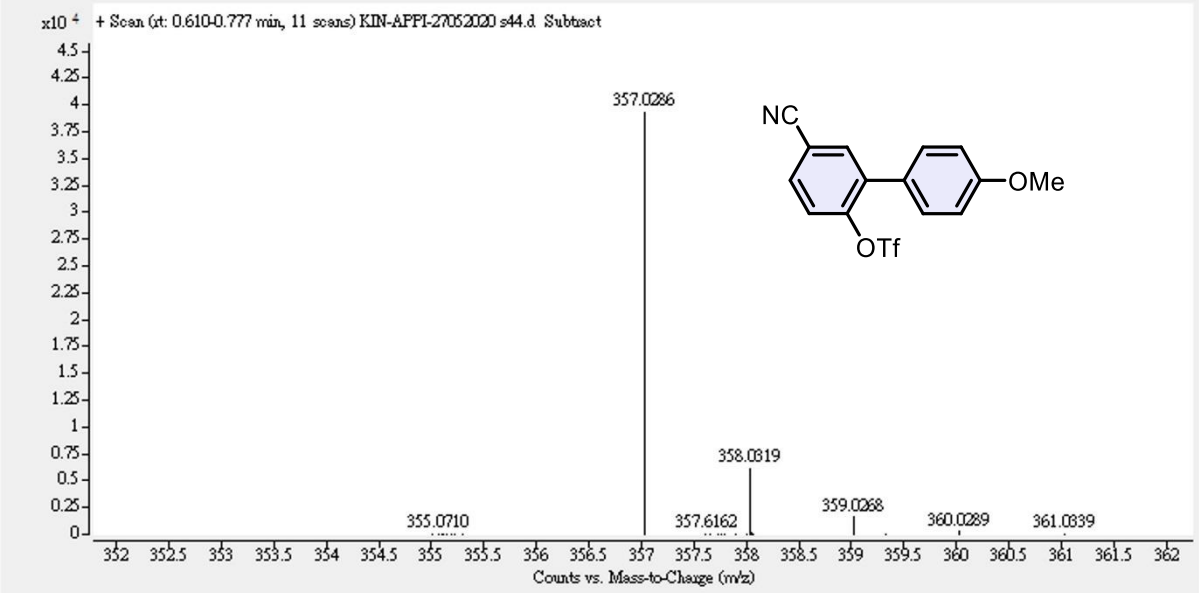

Mass	Calc. Mass	mDa	PPM	Formula
357.0286	357.0277	-0.89	-2.49	C15 H10 F3 N O4 S

^{1}H NMR of [1,1'-binaphthalen]-2-yl trifluoromethanesulfonate (Table 4.3, compound **16r**)

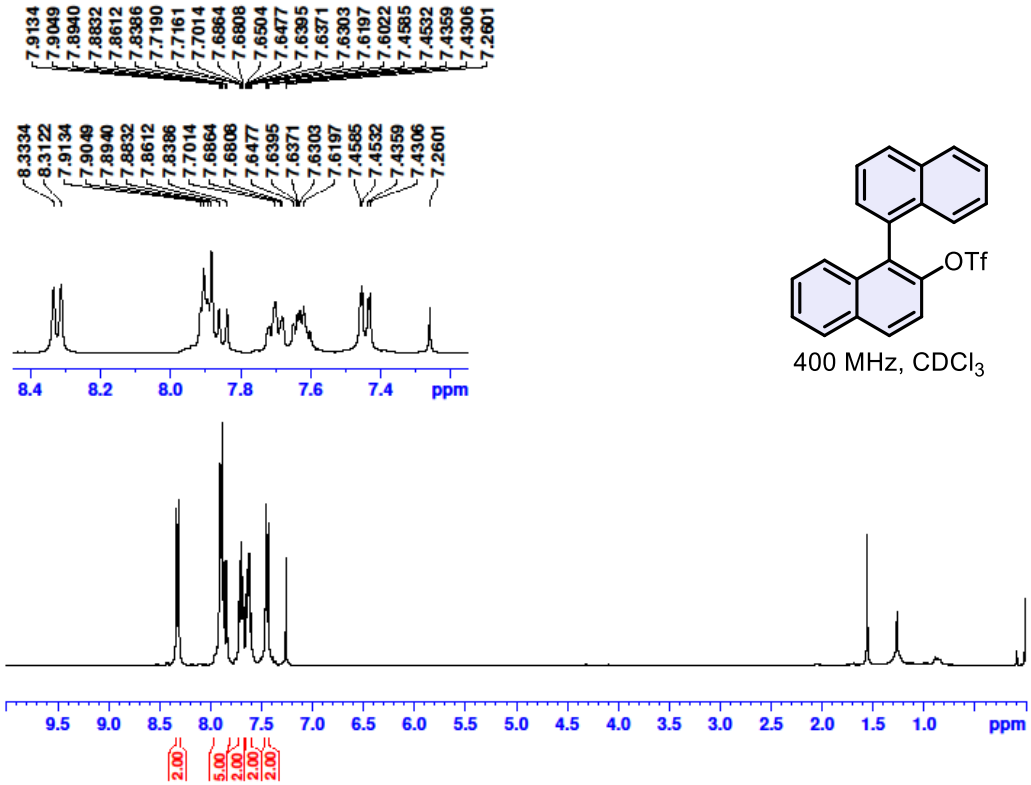

^{13}C NMR of [1,1'-binaphthalen]-2-yl trifluoromethanesulfonate (Table 4.3, compound **16r**)

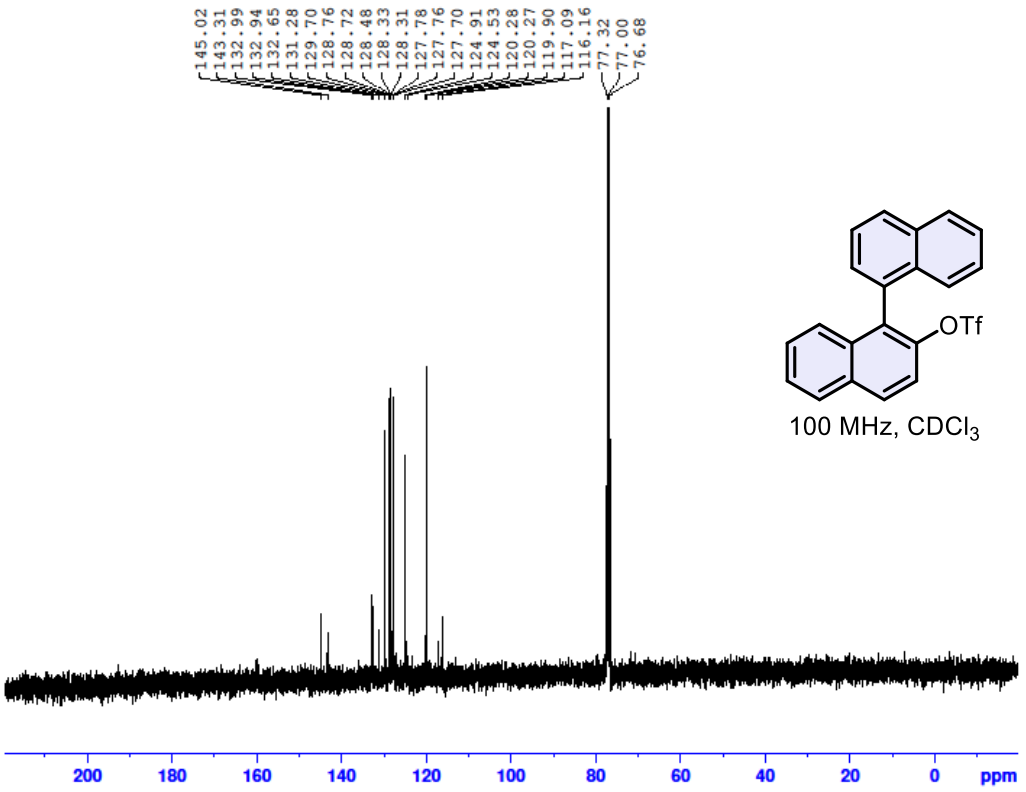

^{19}F NMR of [1,1'-binaphthalen]-2-yl trifluoromethanesulfonate (Table 4.3, compound **16r**)

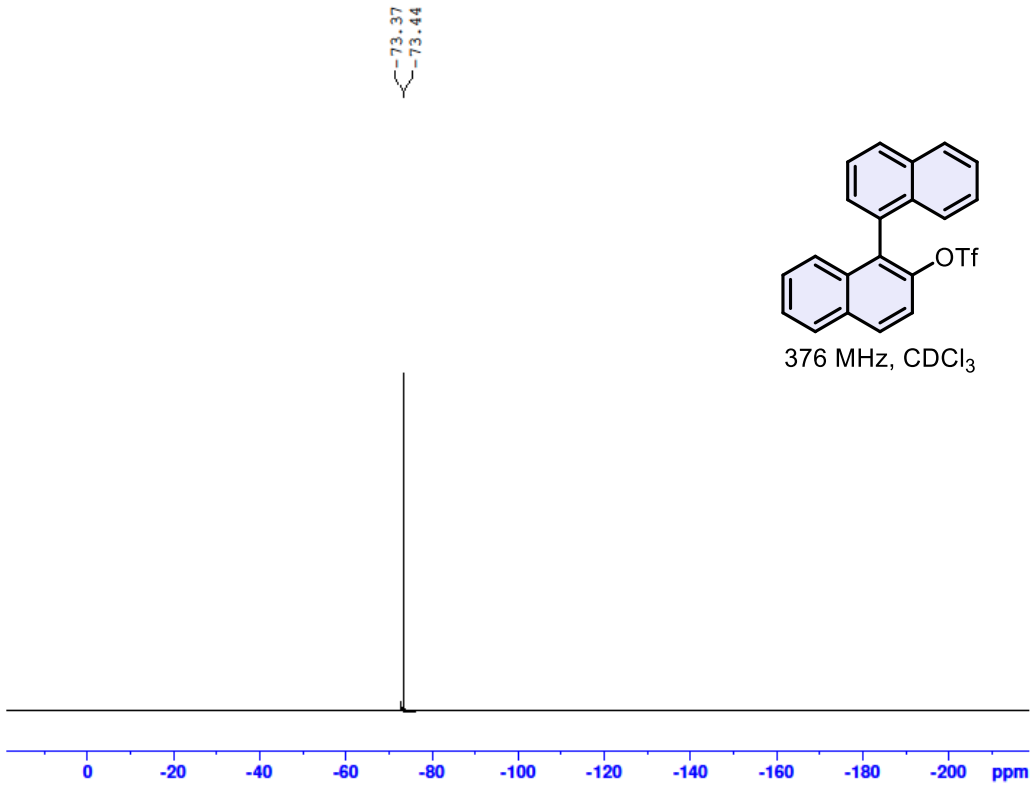

^{1}H NMR of 2,2',6-trimethyl-[1,1'-biphenyl]-4-yl trifluoromethanesulfonate (Table 4.3, compound **16s**)

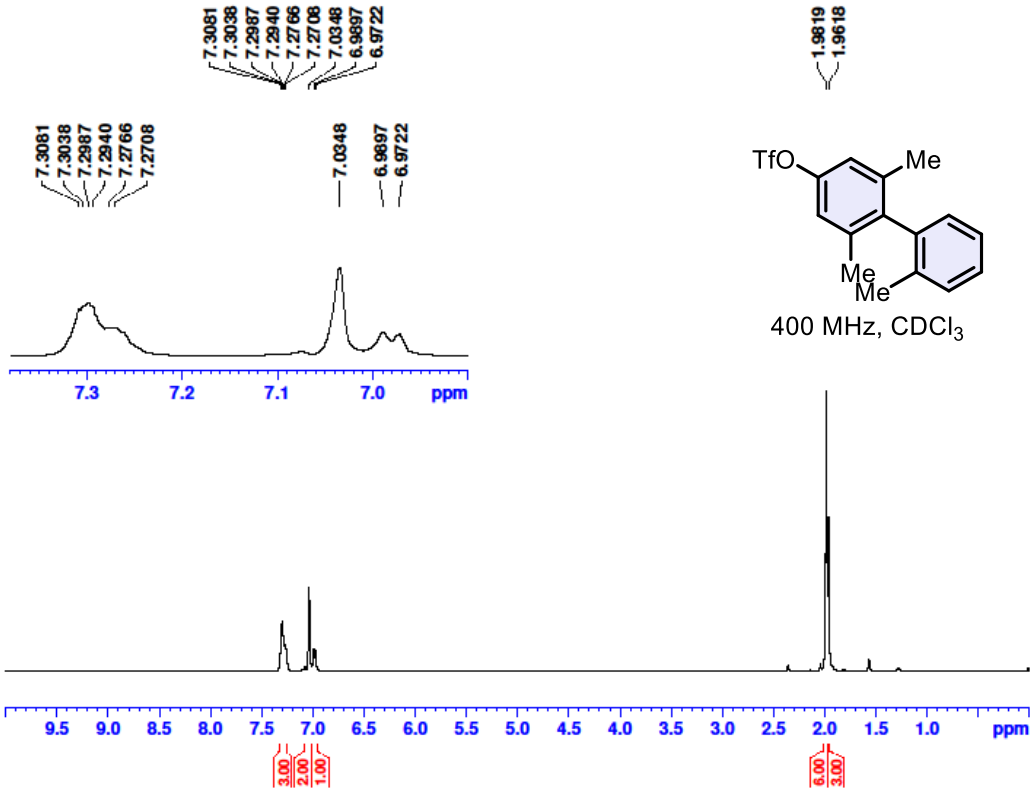

^{13}C NMR of 2,2',6-trimethyl-[1,1'-biphenyl]-4-yl trifluoromethanesulfonate (Table 4.3, compound **16s**)

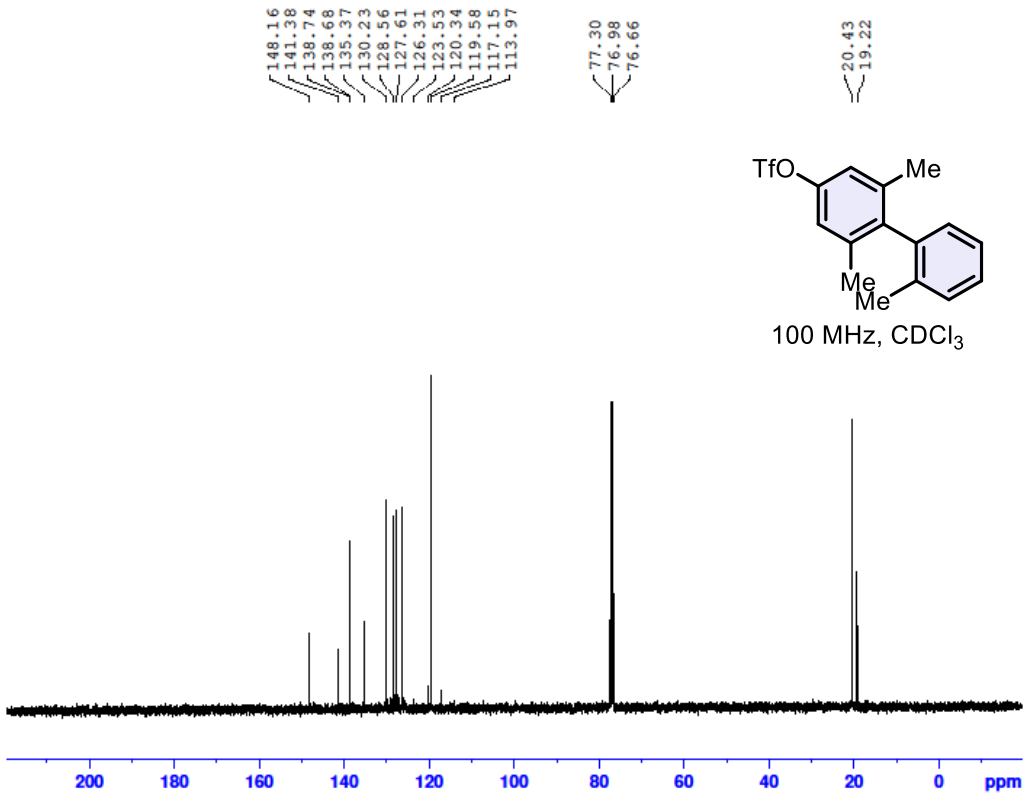

^{19}F NMR of 2,2',6-trimethyl-[1,1'-biphenyl]-4-yl trifluoromethanesulfonate (Table 4.3, compound **16s**)

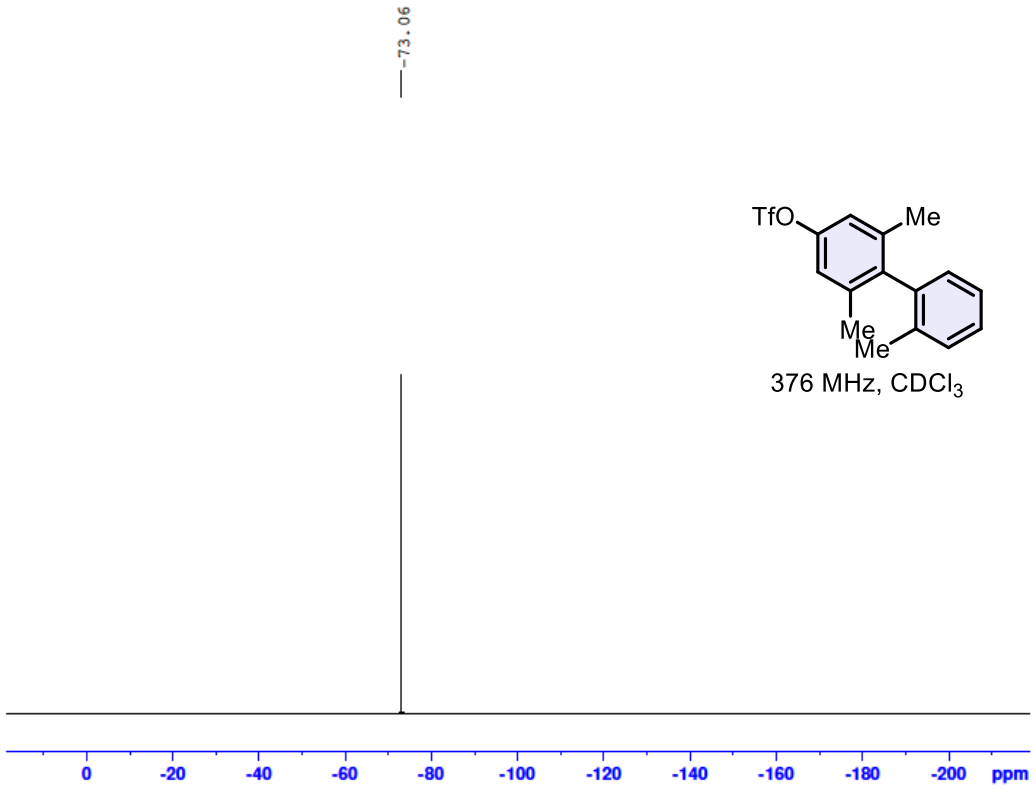

^{1}H NMR of 5-chloro-4'-methyl-[1,1'-biphenyl]-3-yl trifluoromethanesulfonate (Table 4.3, compound **16t**)

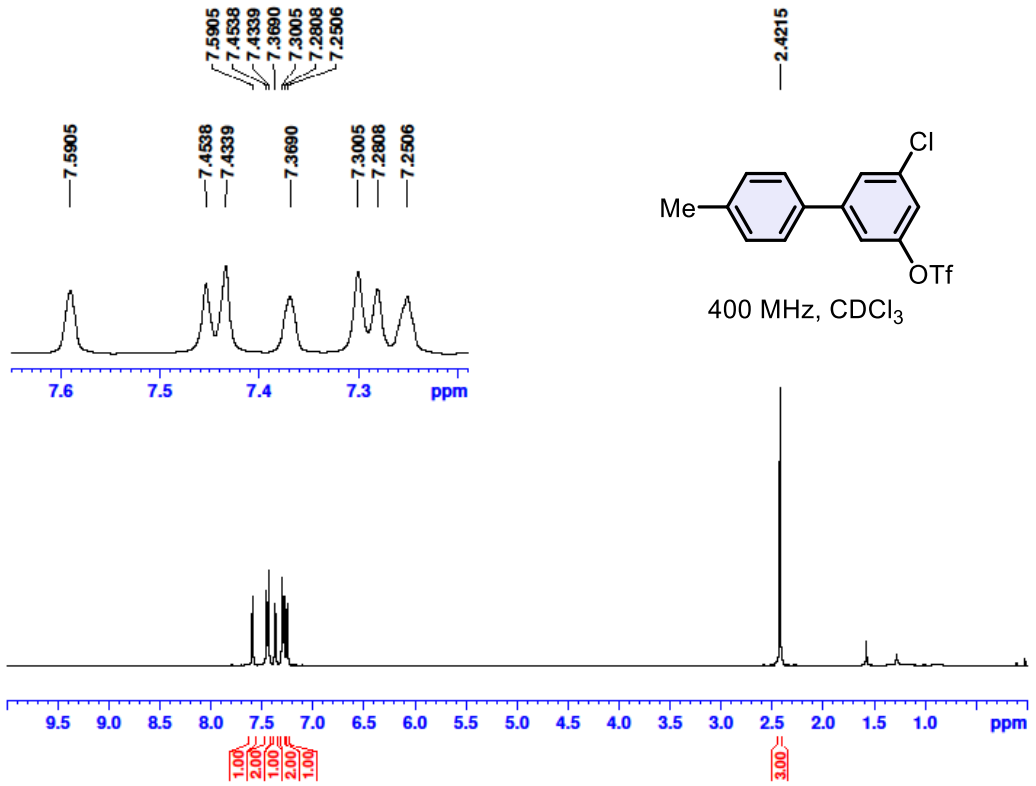

^{13}C NMR of 5-chloro-4'-methyl-[1,1'-biphenyl]-3-yl trifluoromethanesulfonate (Table 4.3, compound **16t**)

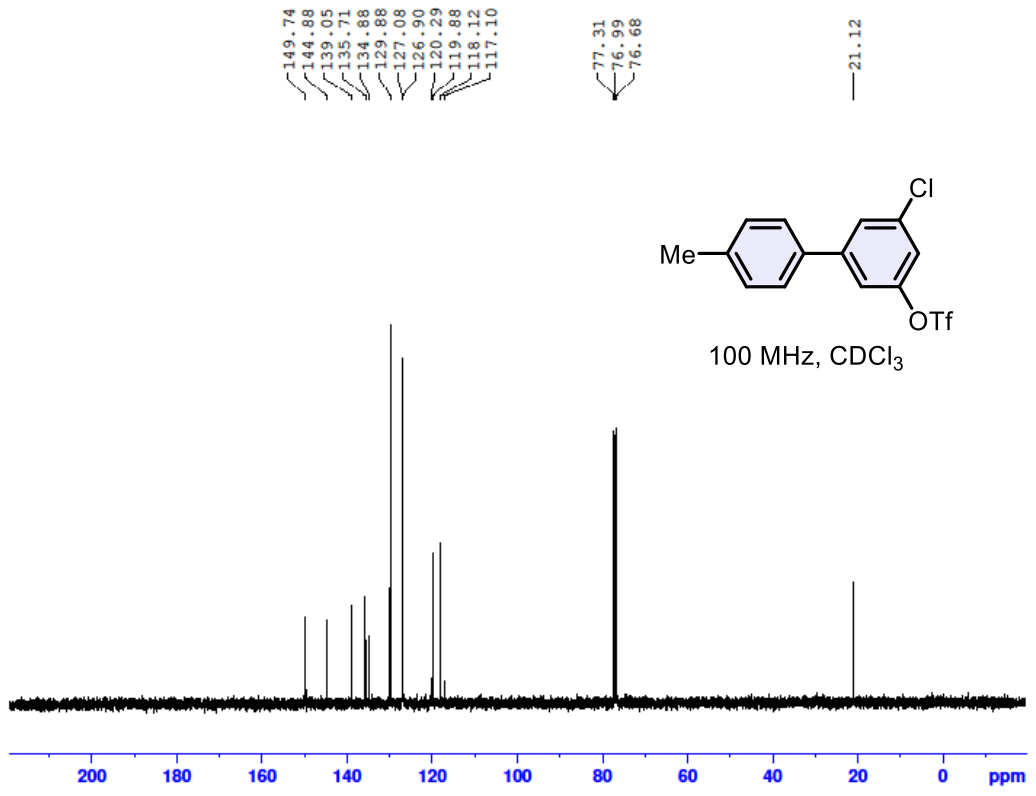

^{19}F NMR of 5-chloro-4’-methyl-[1,1’-biphenyl]-3-yl trifluoromethanesulfonate (Table 4.3, compound **16t**)

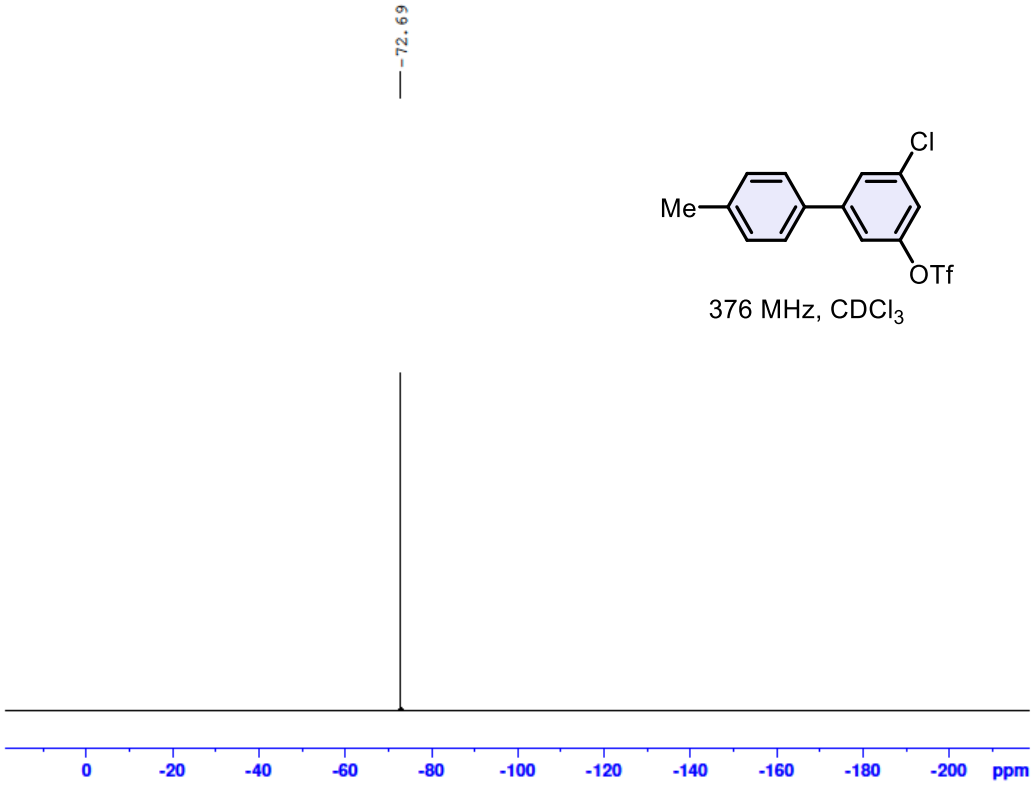

HRMS of 5-chloro-4’-methyl-[1,1’-biphenyl]-3-yl trifluoromethanesulfonate (Table 4.3, compound **16t**)

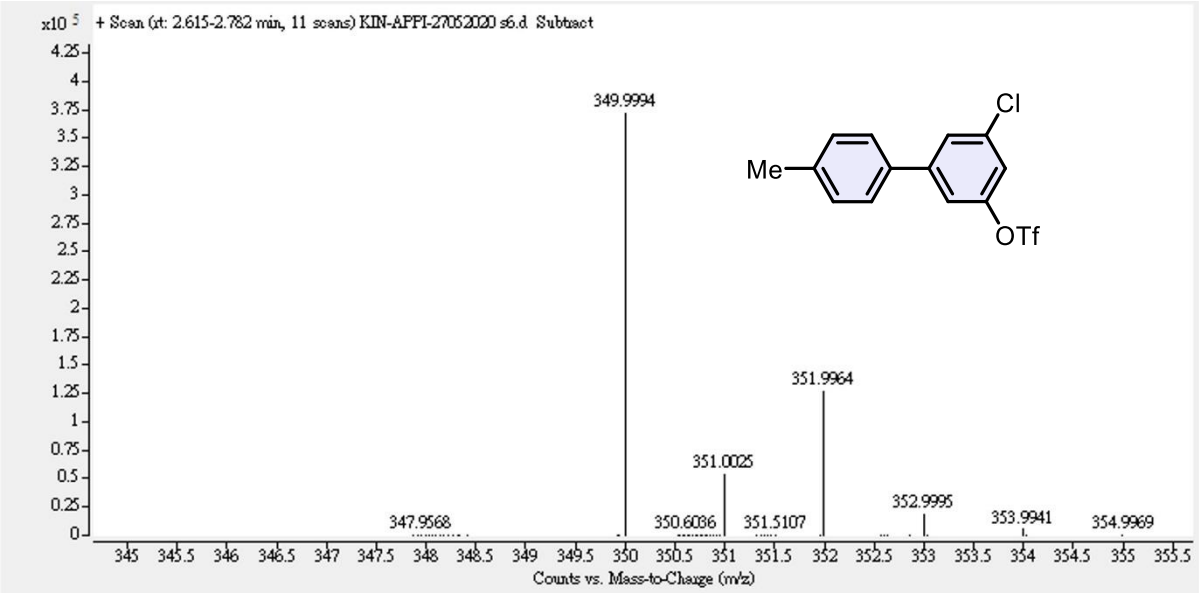

Mass	Calc. Mass	mDa	PPM	Formula
349.9994	349.9991	-0.27	-0.78	C14 H10 Cl F3 O3 S

^{1}H NMR of 3-chloro-2'-methyl-[1,1'-biphenyl]-4-yl trifluoromethanesulfonate (Table 4.3, compound **16u**)

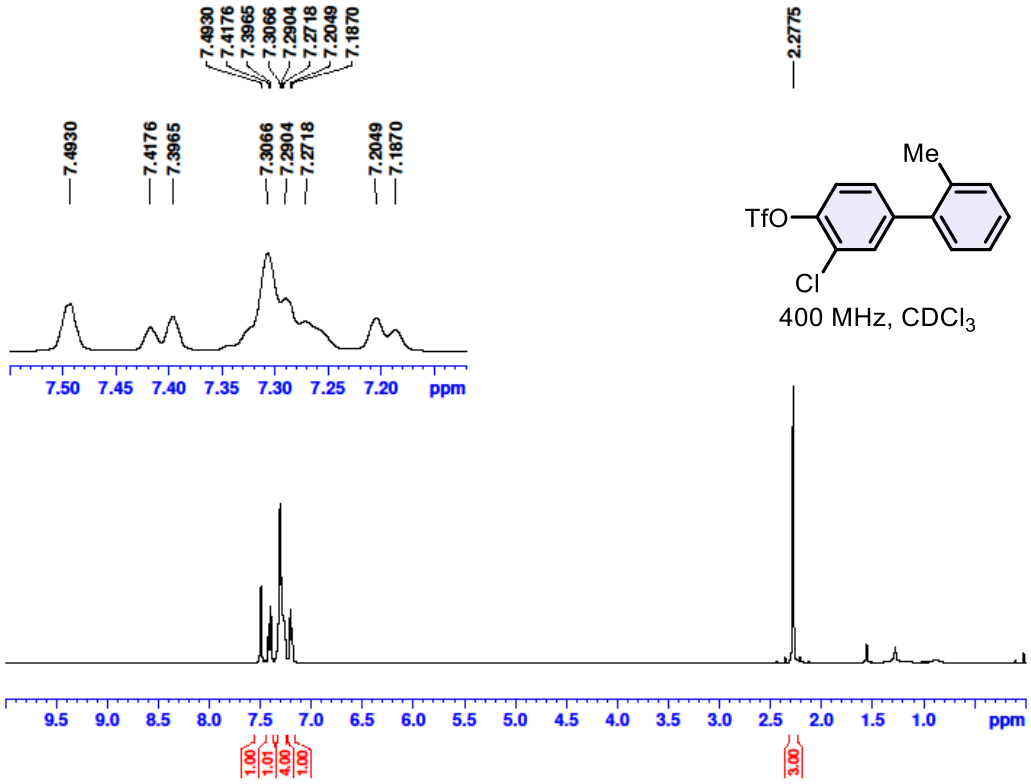

^{13}C NMR of 3-chloro-2'-methyl-[1,1'-biphenyl]-4-yl trifluoromethanesulfonate (Table 4.3, compound **16u**)

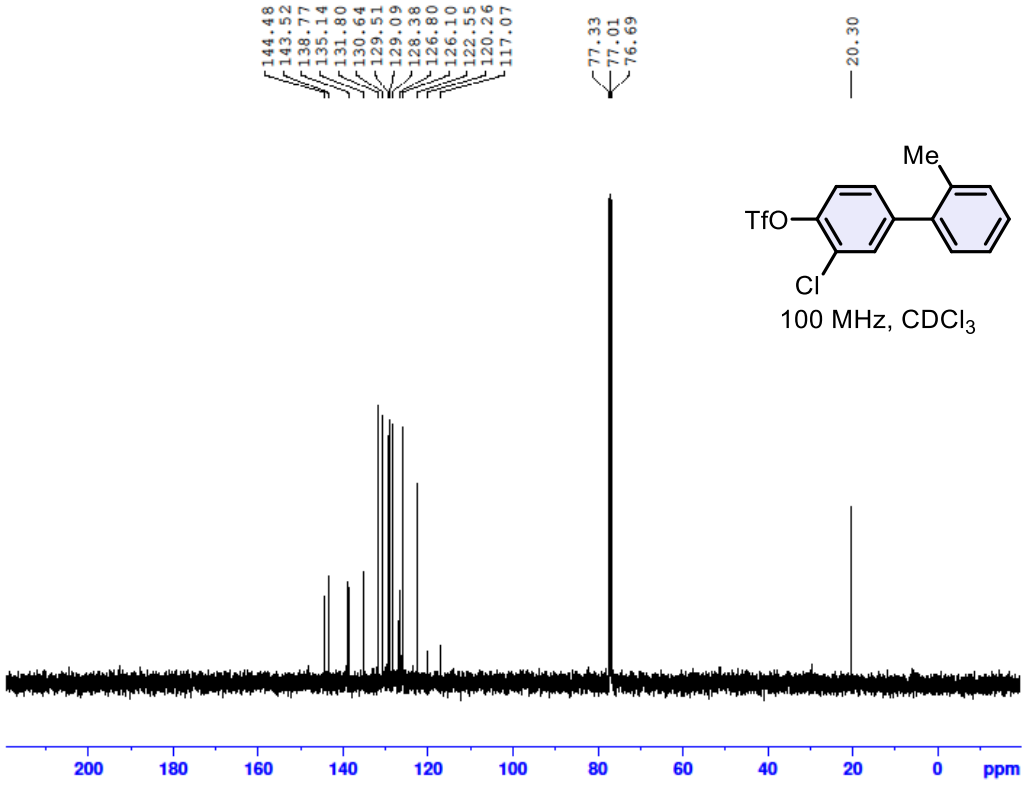

^{19}F NMR of 3-chloro-2'-methyl-[1,1'-biphenyl]-4-yl trifluoromethanesulfonate (Table 4.3, compound **16u**)

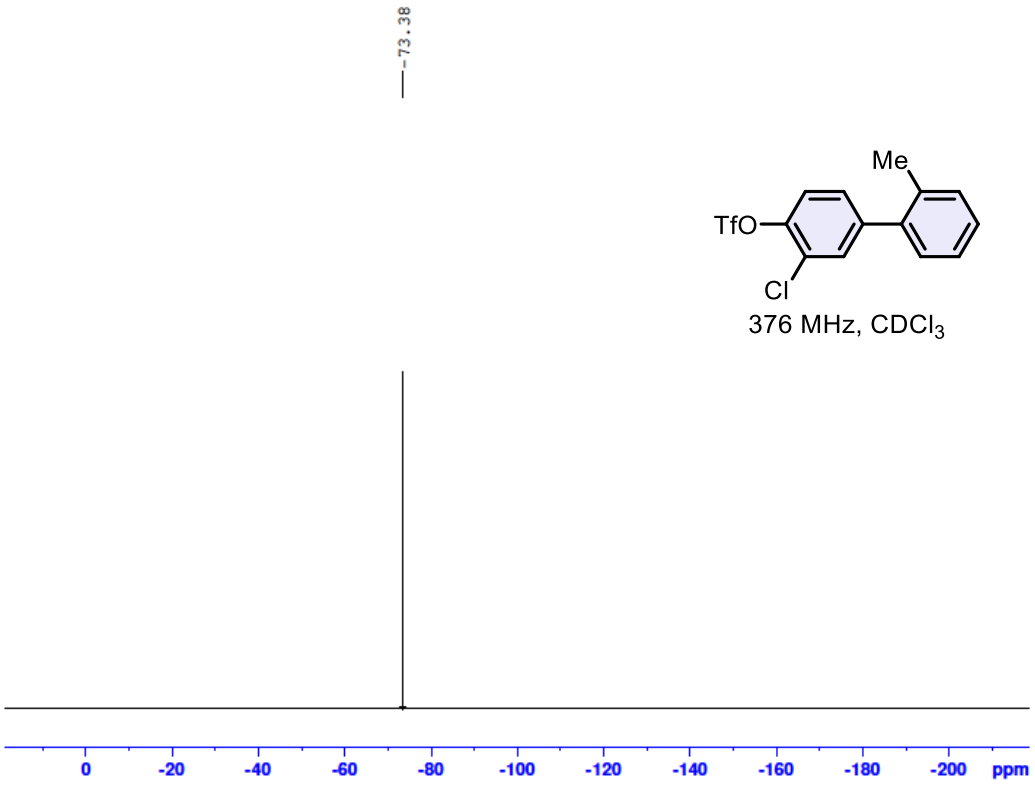

^{1}H NMR of 3-chloro-4'-methyl-[1,1'-biphenyl]-4-yl trifluoromethanesulfonate (Table 4.3, compound **16v**)

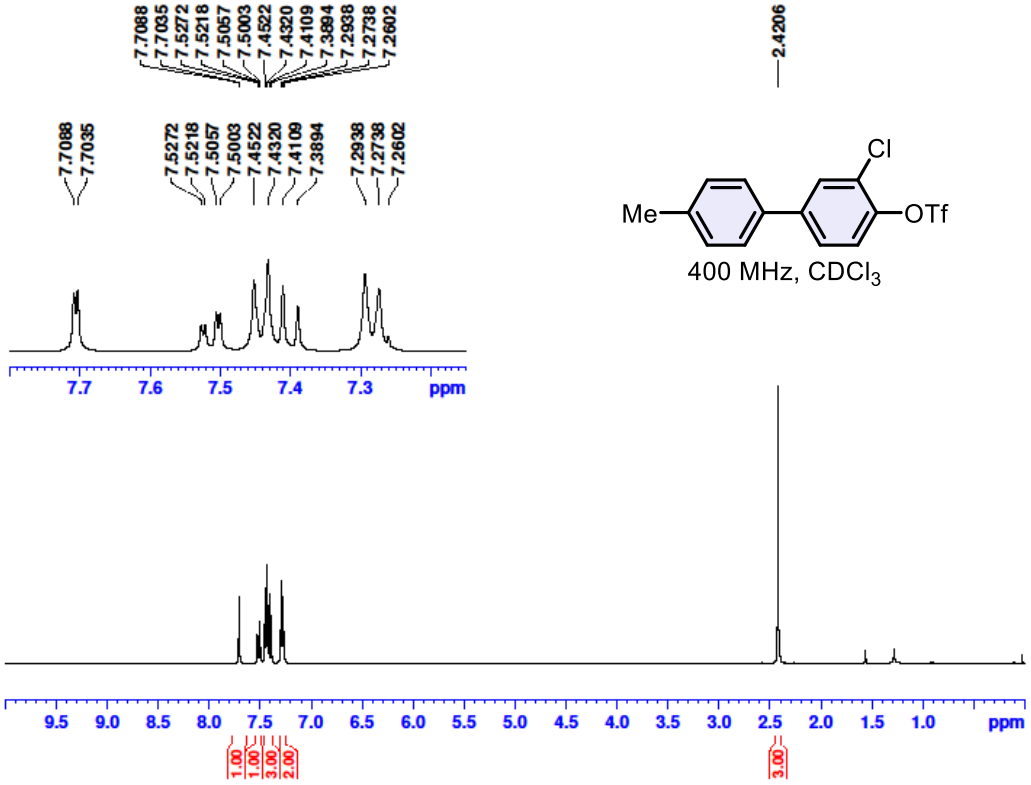

^{13}C NMR of 3-chloro-4'-methyl-[1,1'-biphenyl]-4-yl trifluoromethanesulfonate (Table 4.3, compound **16v**)

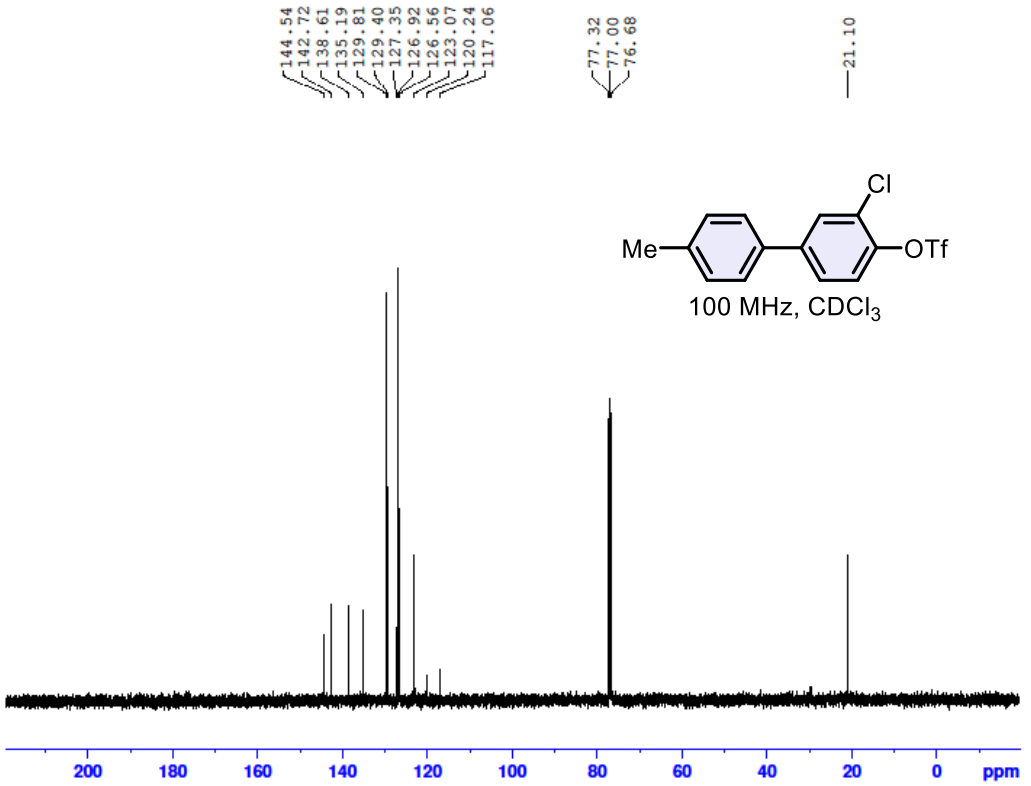

^{19}F NMR of 3-chloro-4'-methyl-[1,1'-biphenyl]-4-yl trifluoromethanesulfonate (Table 4.3, compound **16v**)

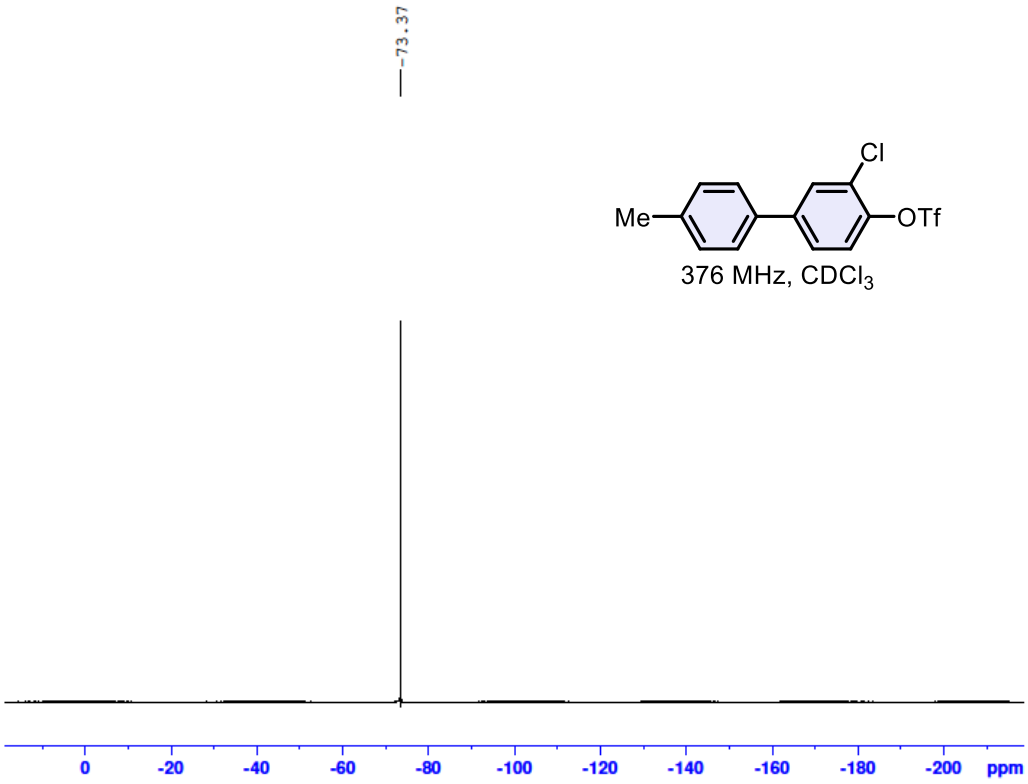

^{1}H NMR of 4-chloro-4'-methyl-[1,1'-biphenyl]-3-yl trifluoromethanesulfonate (Table 4.3, compound **16w**)

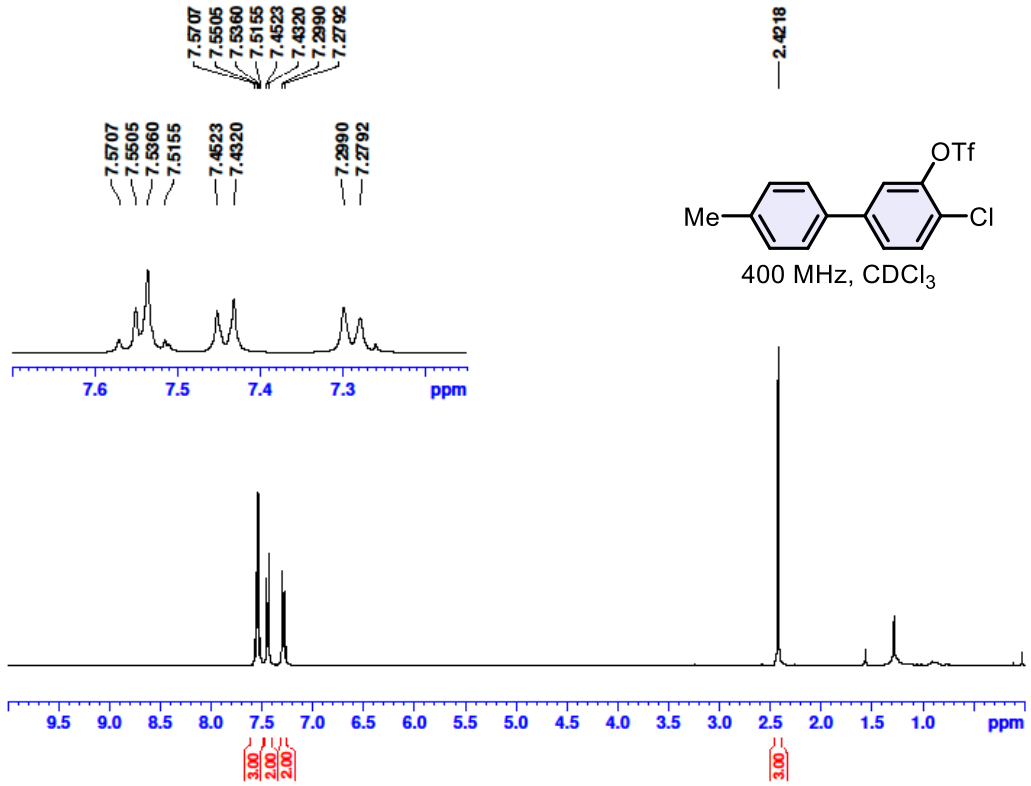

^{13}C NMR of 4-chloro-4'-methyl-[1,1'-biphenyl]-3-yl trifluoromethanesulfonate (Table 4.3, compound **16w**)

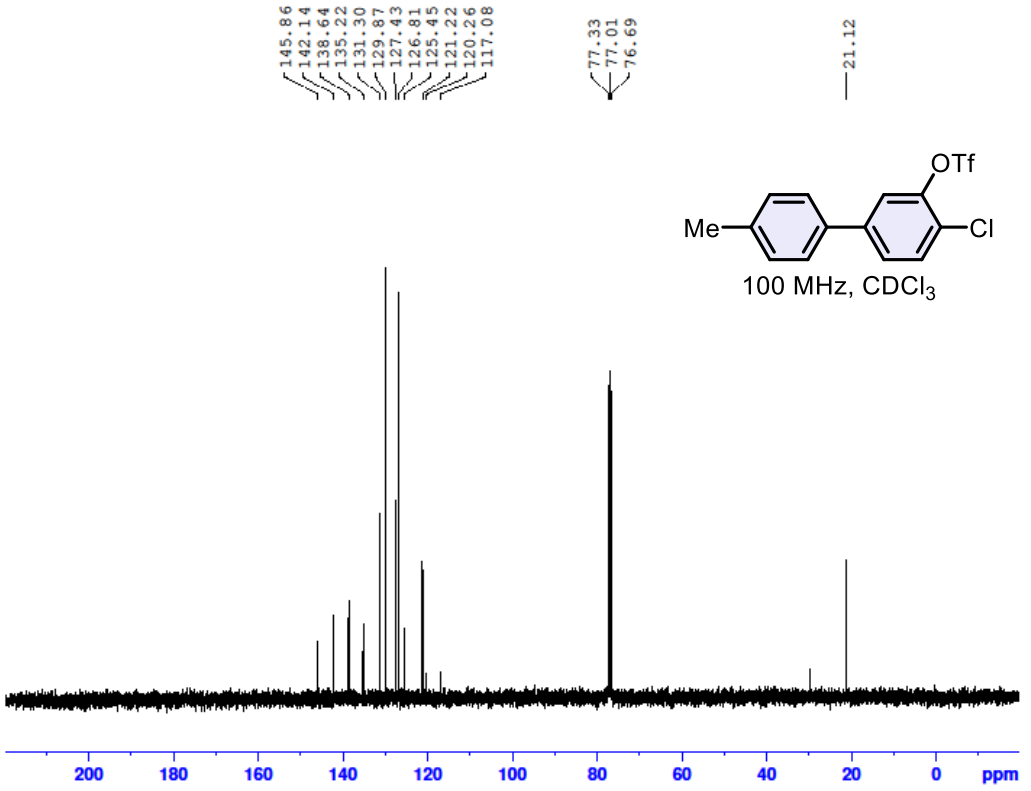

^{19}F NMR of 4-chloro-4’-methyl-[1,1’-biphenyl]-3-yl trifluoromethanesulfonate (Table 4.3, compound **16w**)

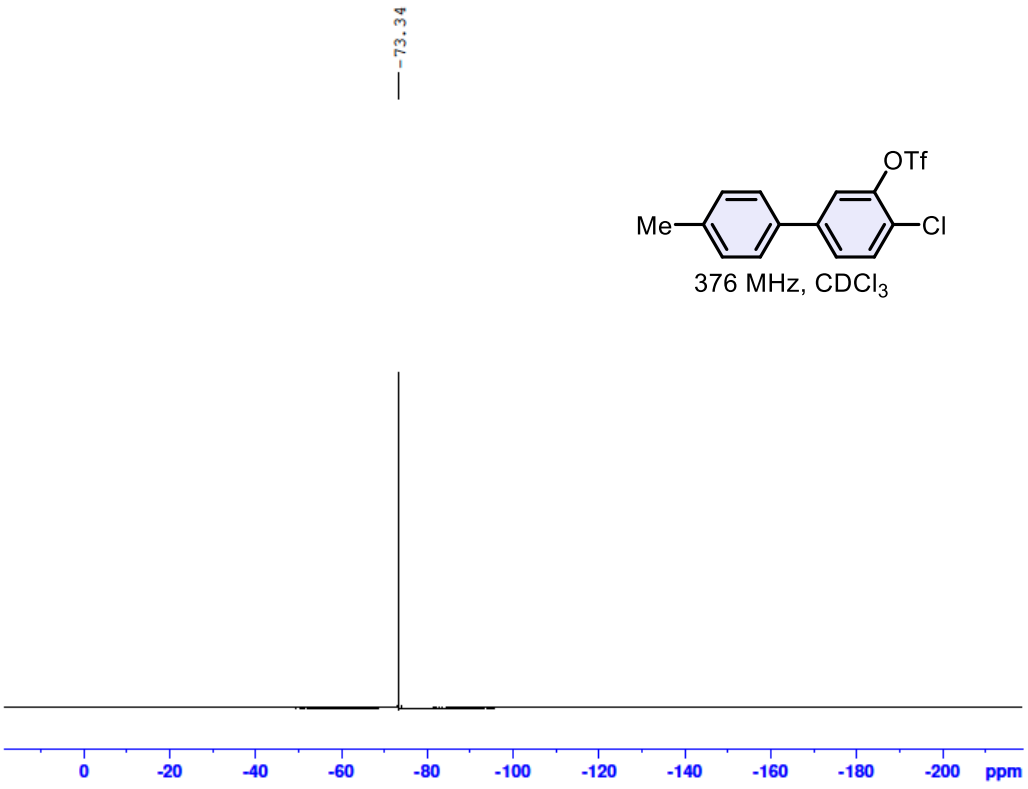

HRMS of 4-chloro-4’-methyl-[1,1’-biphenyl]-3-yl trifluoromethanesulfonate (Table 4.3, compound **16w**)

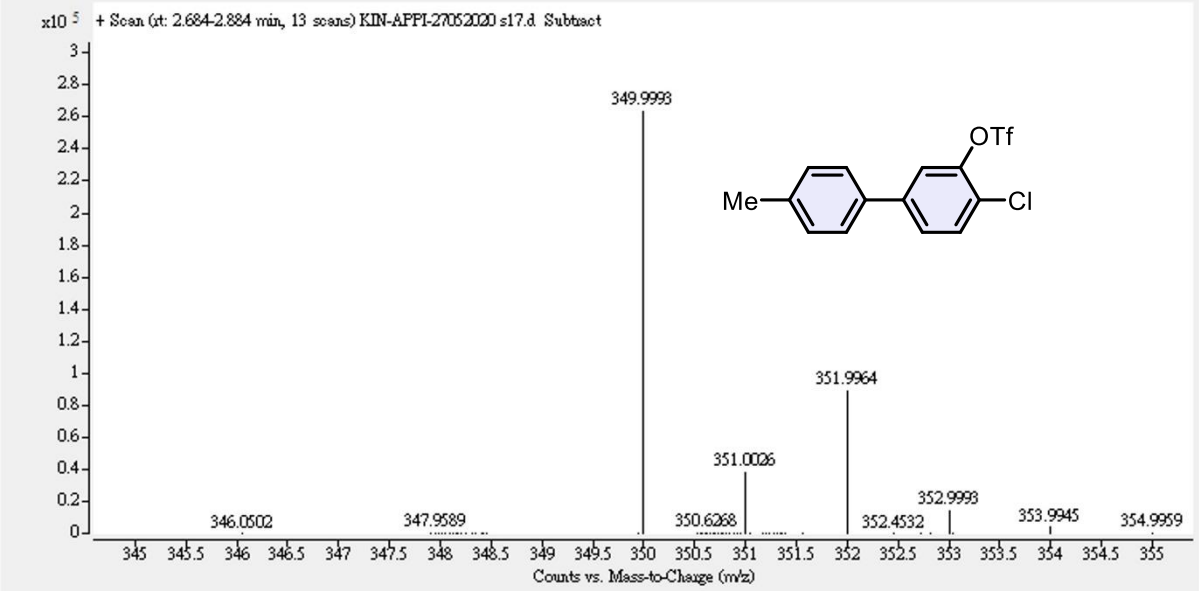

Mass	Calc. Mass	mDa	PPM	Formula
349.9993	349.9991	-0.17	-0.49	C14 H10 Cl F3 O3 S

^{1}H NMR of 5-chloro-4'-methyl-[1,1'-biphenyl]-2-yl trifluoromethanesulfonate (Table 4.3, compound **16x**)

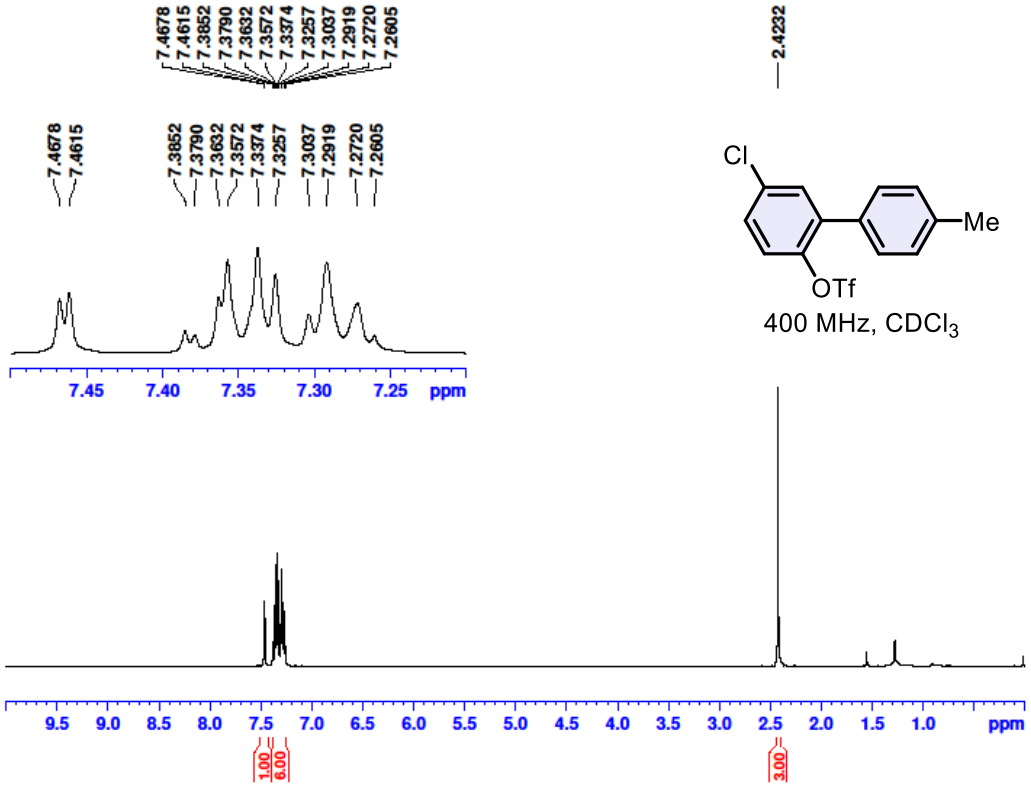

^{13}C NMR of 5-chloro-4'-methyl-[1,1'-biphenyl]-2-yl trifluoromethanesulfonate (Table 4.3, compound **16x**)

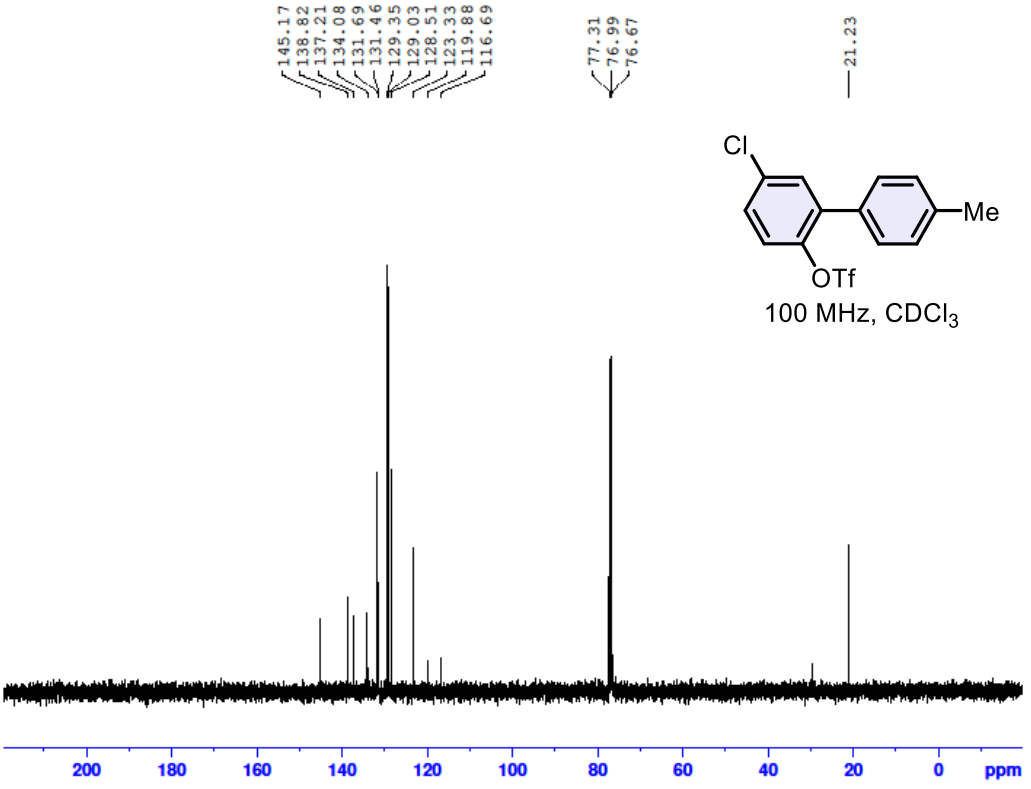

^{19}F NMR of 5-chloro-4'-methyl-[1,1'-biphenyl]-2-yl trifluoromethanesulfonate (Table 4.3, compound **16x**)

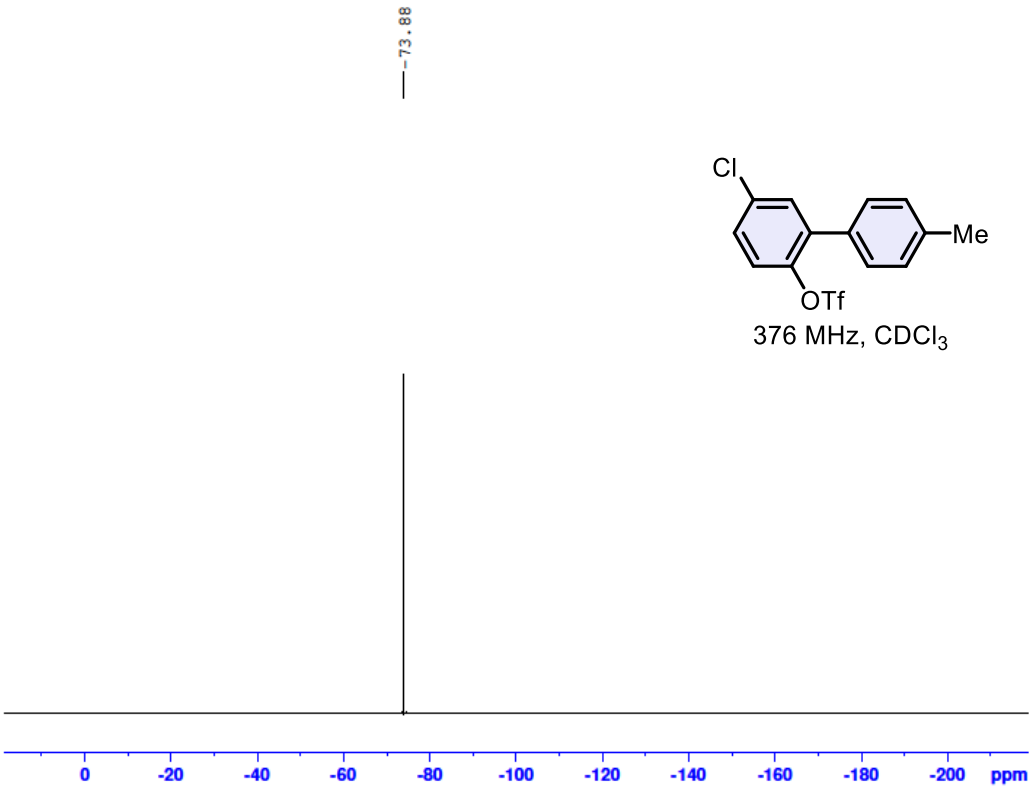

^{1}H NMR of 2-chloro-4'-methyl-[1,1'-biphenyl]-3-yl trifluoromethanesulfonate (Table 4.3, compound **16y**)

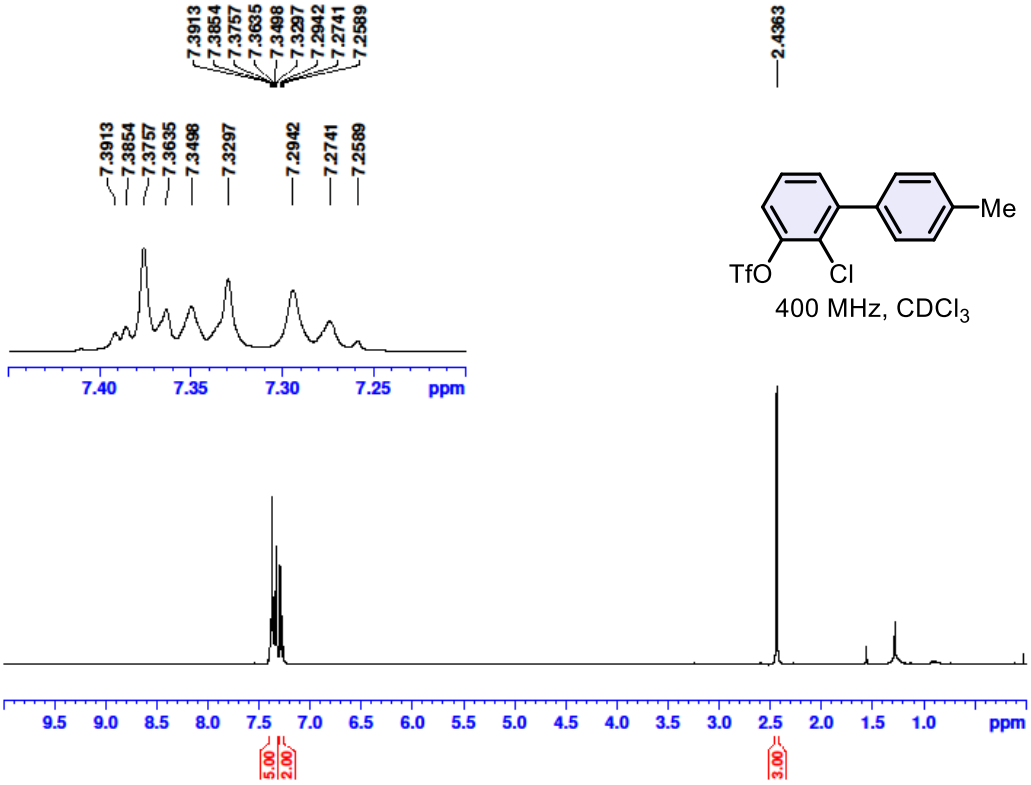

^{13}C NMR of 2-chloro-4'-methyl-[1,1'-biphenyl]-3-yl trifluoromethanesulfonate (Table 4.3, compound **16y**)

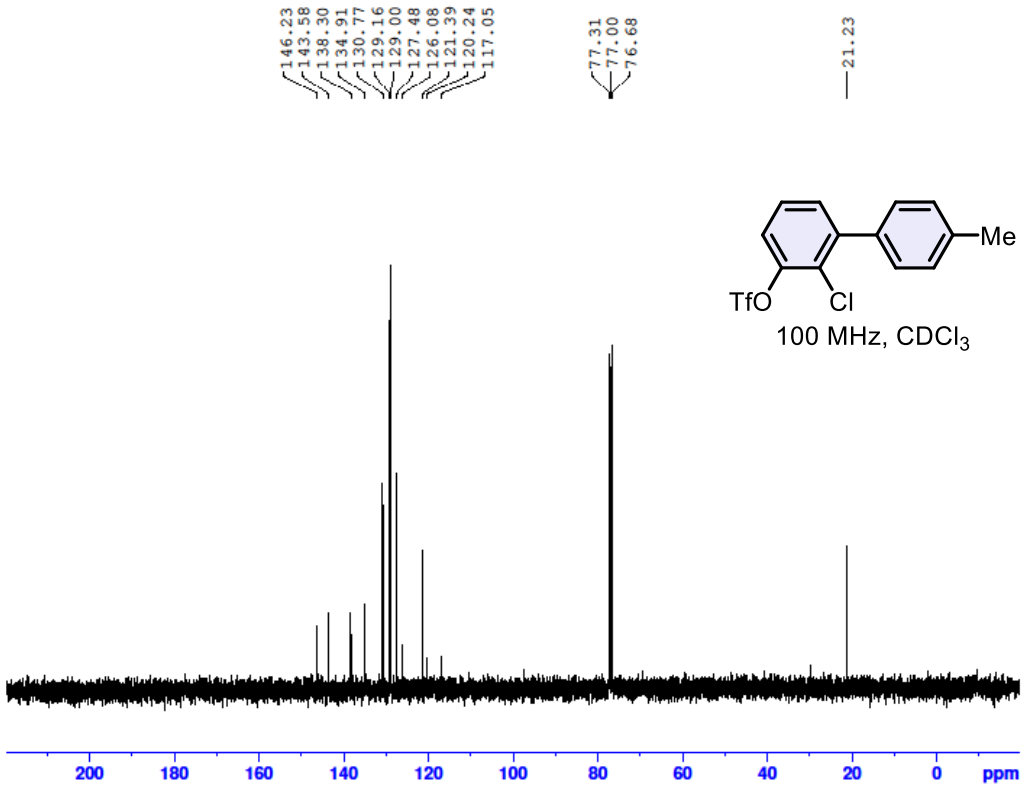

^{19}F NMR of 2-chloro-4'-methyl-[1,1'-biphenyl]-3-yl trifluoromethanesulfonate (Table 4.3, compound **16y**)

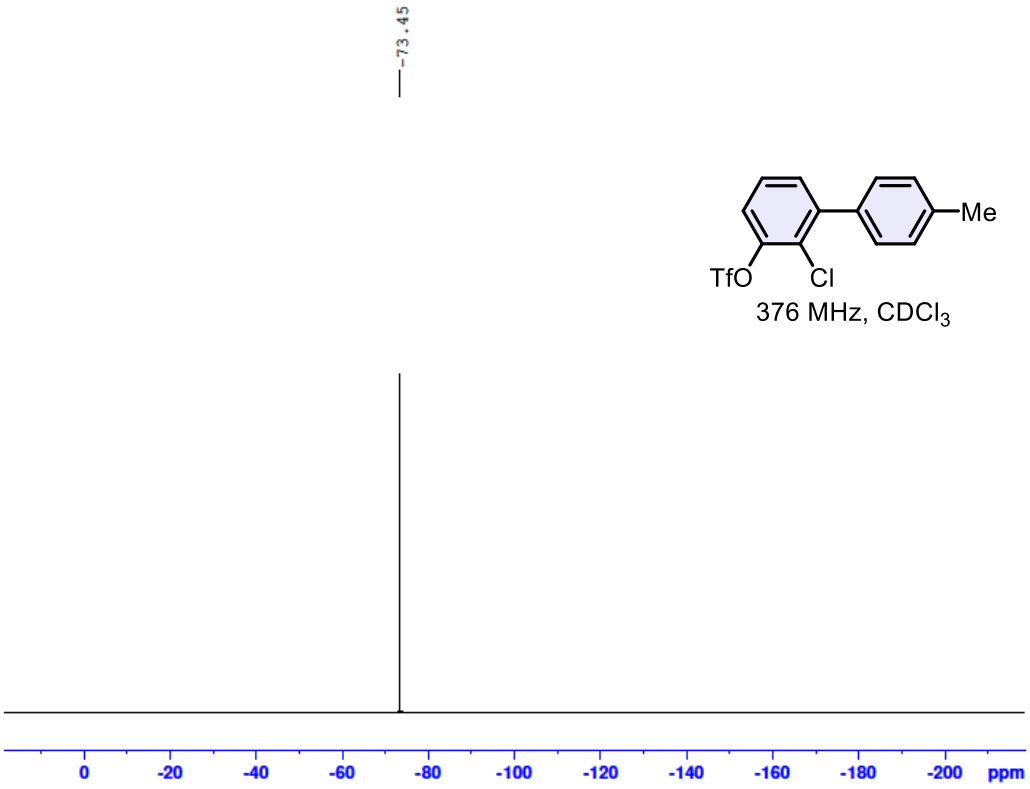

HRMS of 2-chloro-4'-methyl-[1,1'-biphenyl]-3-yl trifluoromethanesulfonate (Table 4.3, compound **16y**)

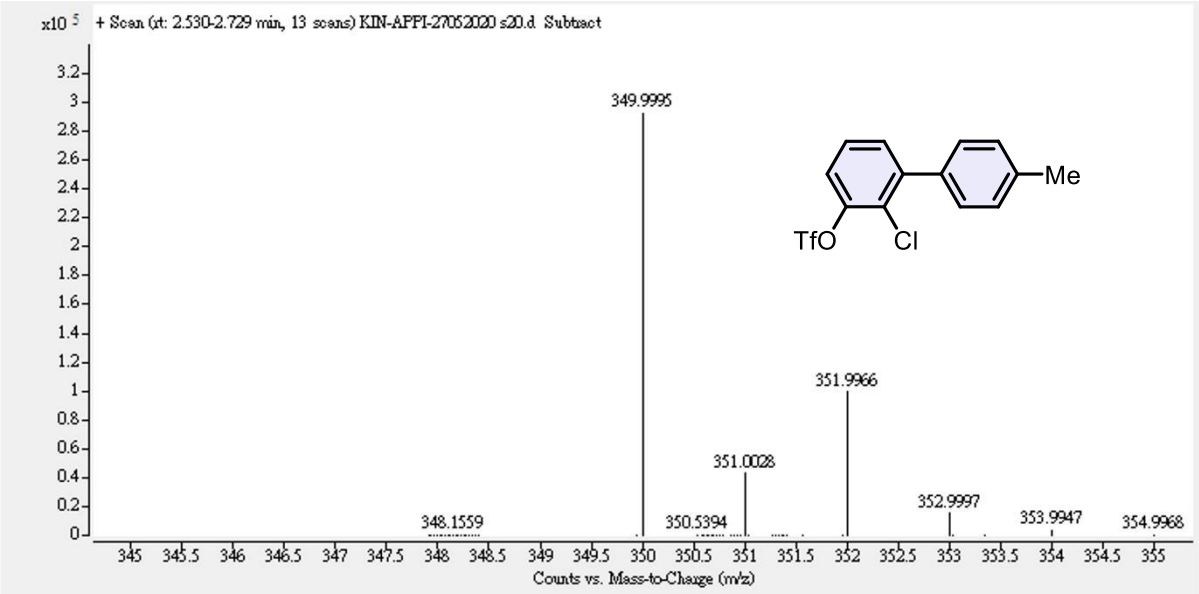

Mass	Calc. Mass	mDa	PPM	Formula
349.9995	349.9991	-0.37	-1.07	C14 H10 Cl F3 O3 S

^{1}H NMR of 2-(4-methoxyphenyl)pyridin-3-yl trifluoromethanesulfonate (Table 4.4, compound **16z**)

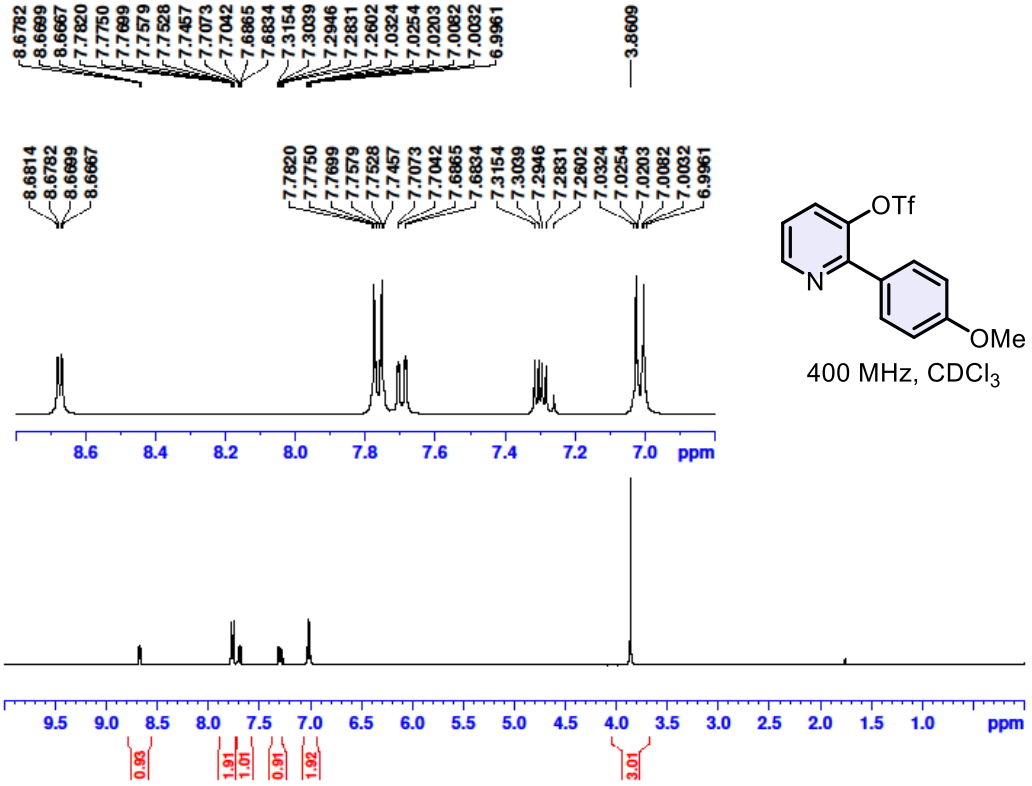

^{13}C NMR of 2-(4-methoxyphenyl)pyridin-3-yl trifluoromethanesulfonate (Table 4.4, compound **16z**)

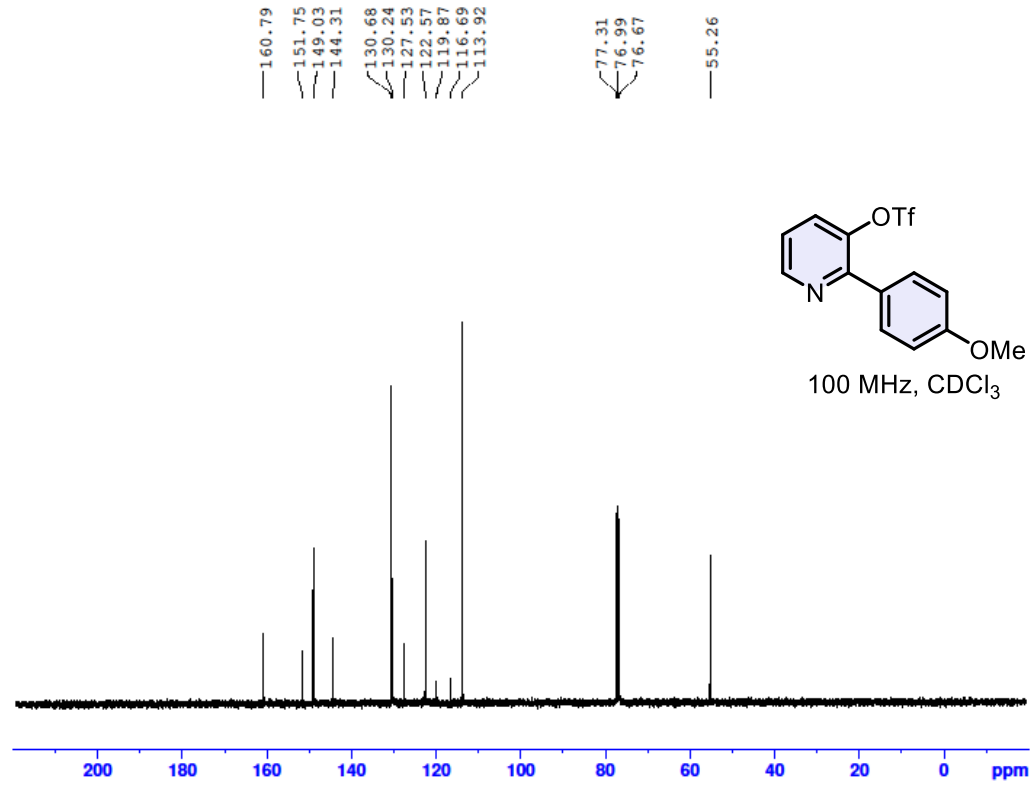

^{19}F NMR of 2-(4-methoxyphenyl)pyridin-3-yl trifluoromethanesulfonate (Table 4.4, compound **16z**)

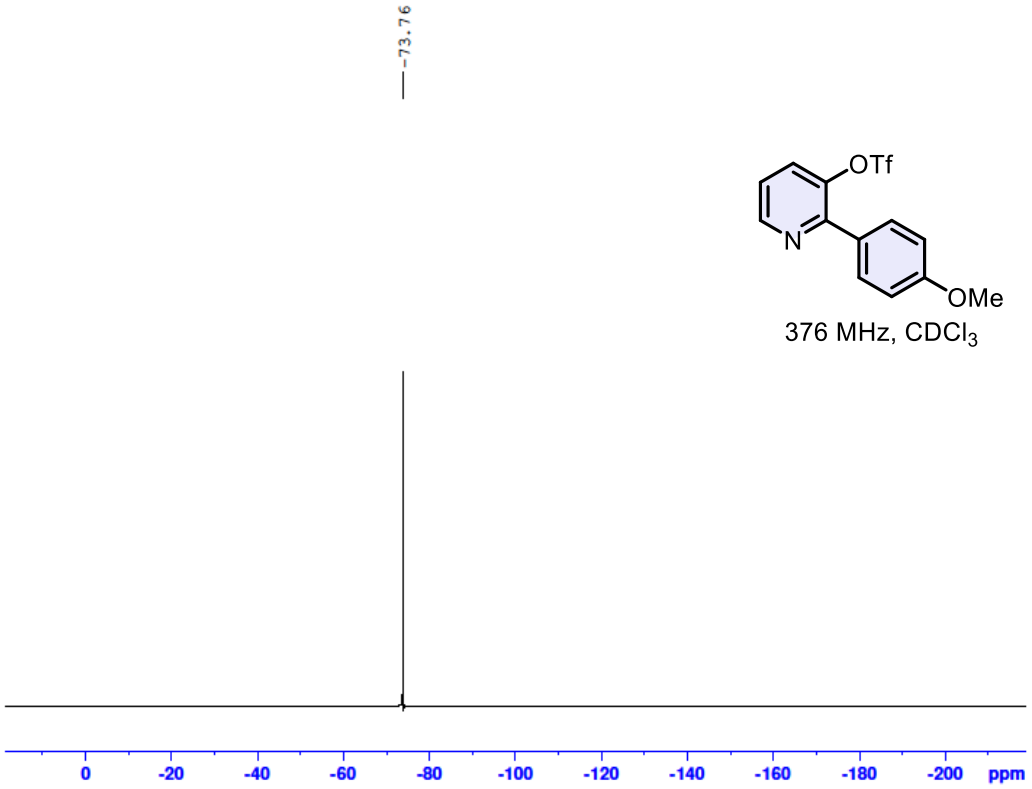

HRMS of 2-(4-methoxyphenyl)pyridin-3-yl trifluoromethanesulfonate (Table 4.4, compound **16z**)

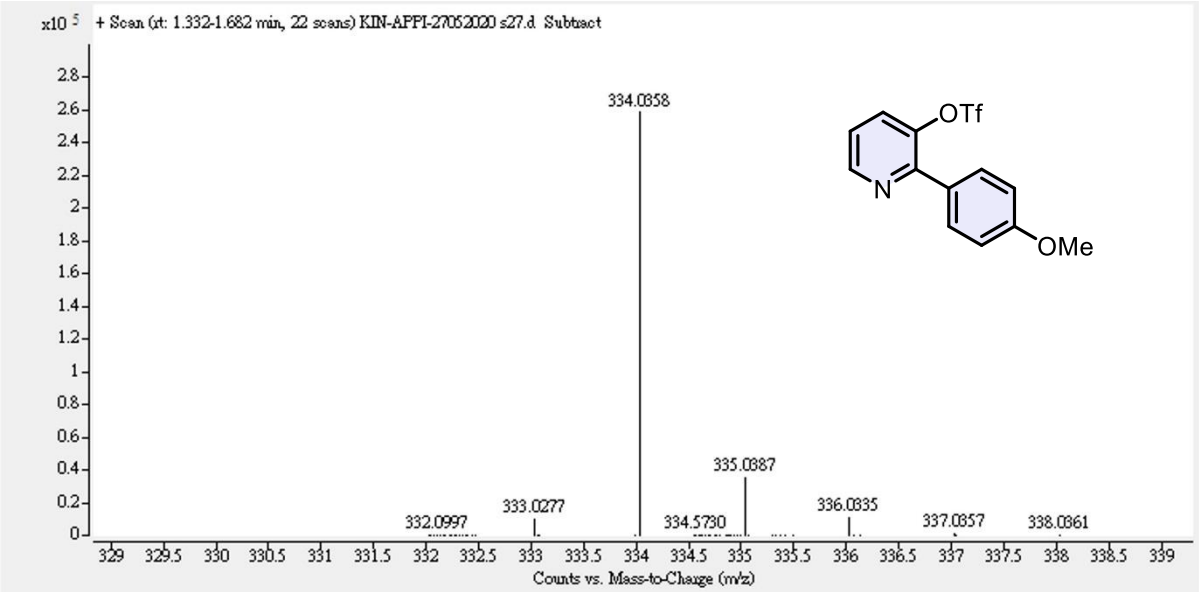

Mass	Calc. Mass	mDa	PPM	Formula
334.0358	334.0355	-0.26	-0.78	C13 H11 F3 N O4 S

^{1}H NMR of 5-(4-methoxyphenyl)-4-methylpyridin-2-yl trifluoromethanesulfonate (Table 4.4, compound **16aa**)

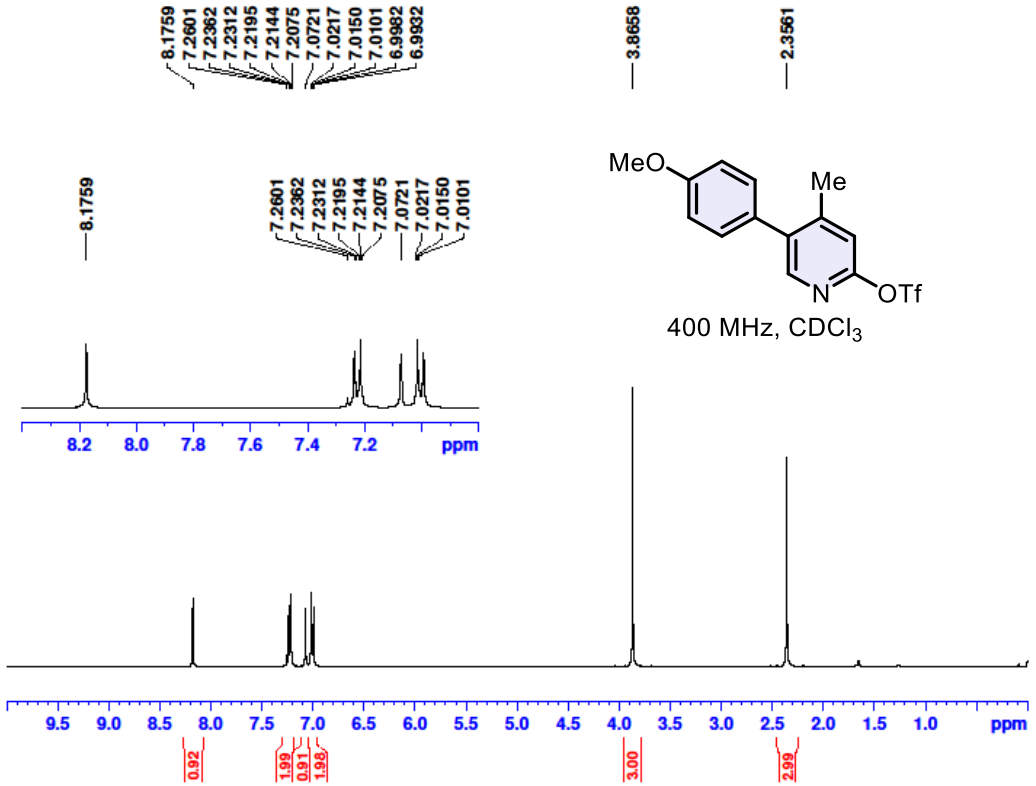

^{13}C NMR of 5-(4-methoxyphenyl)-4-methylpyridin-2-yl trifluoromethanesulfonate (Table 4.4, compound **16aa**)

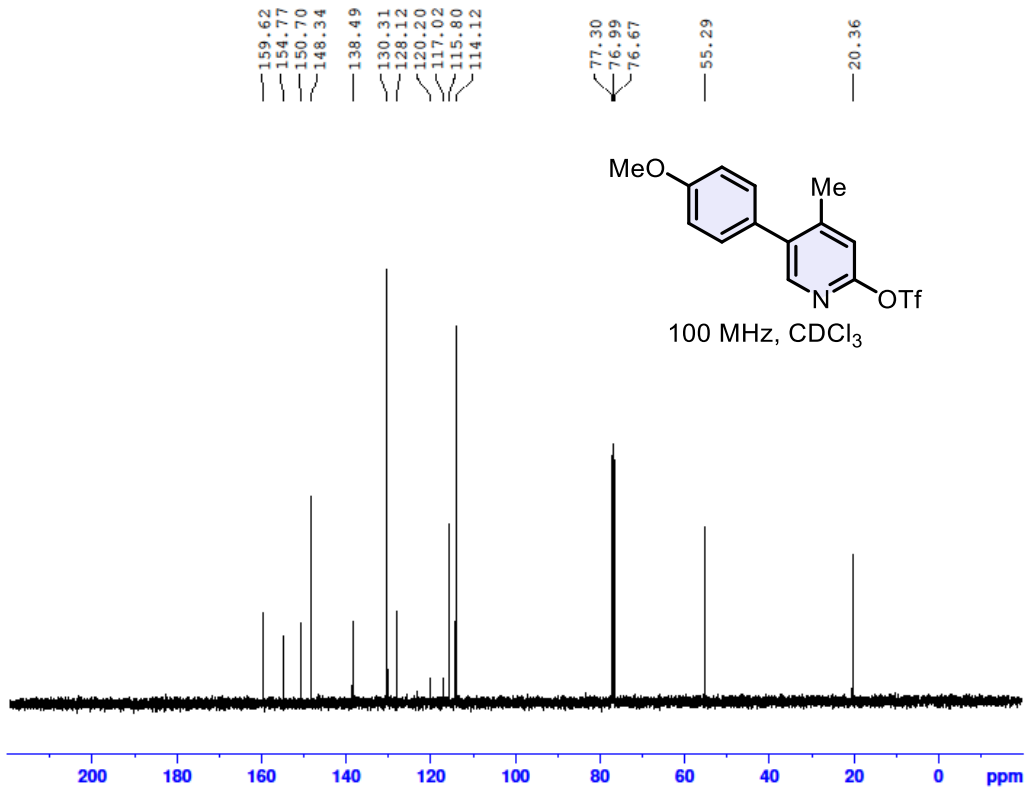

^{19}F NMR of 5-(4-methoxyphenyl)-4-methylpyridin-2-yl trifluoromethanesulfonate (Table 4.4, compound **16aa**)

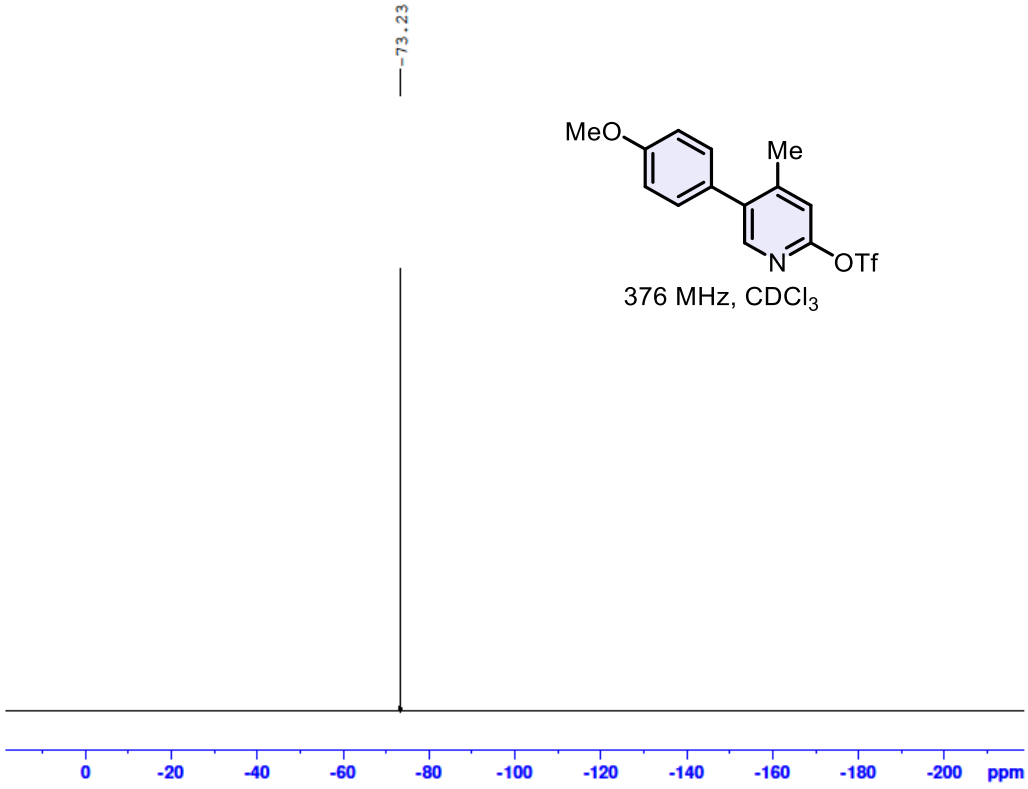

^{1}H NMR of 5-(4-methoxyphenyl)pyridin-2-yl trifluoromethanesulfonate (Table 4.4, compound **16ab**)

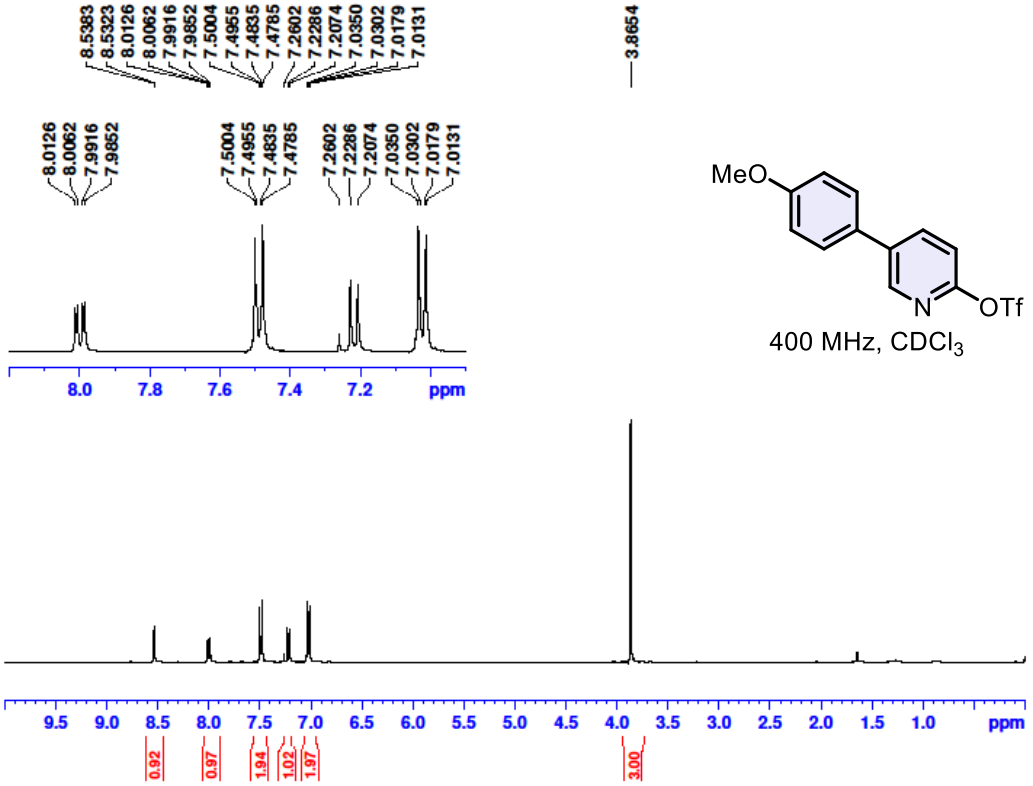

^{13}C NMR of 5-(4-methoxyphenyl)pyridin-2-yl trifluoromethanesulfonate (Table 4.4, compound **16ab**)

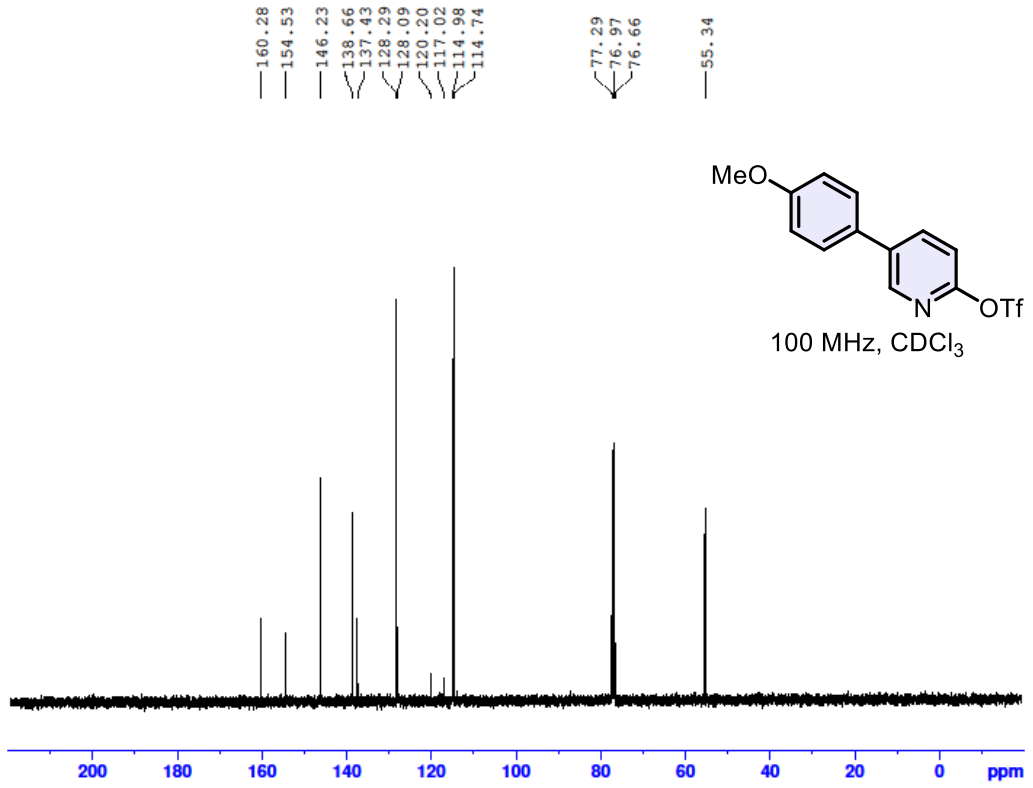

^{19}F NMR of 5-(4-methoxyphenyl)pyridin-2-yl trifluoromethanesulfonate (Table 4.4, compound **16ab**)

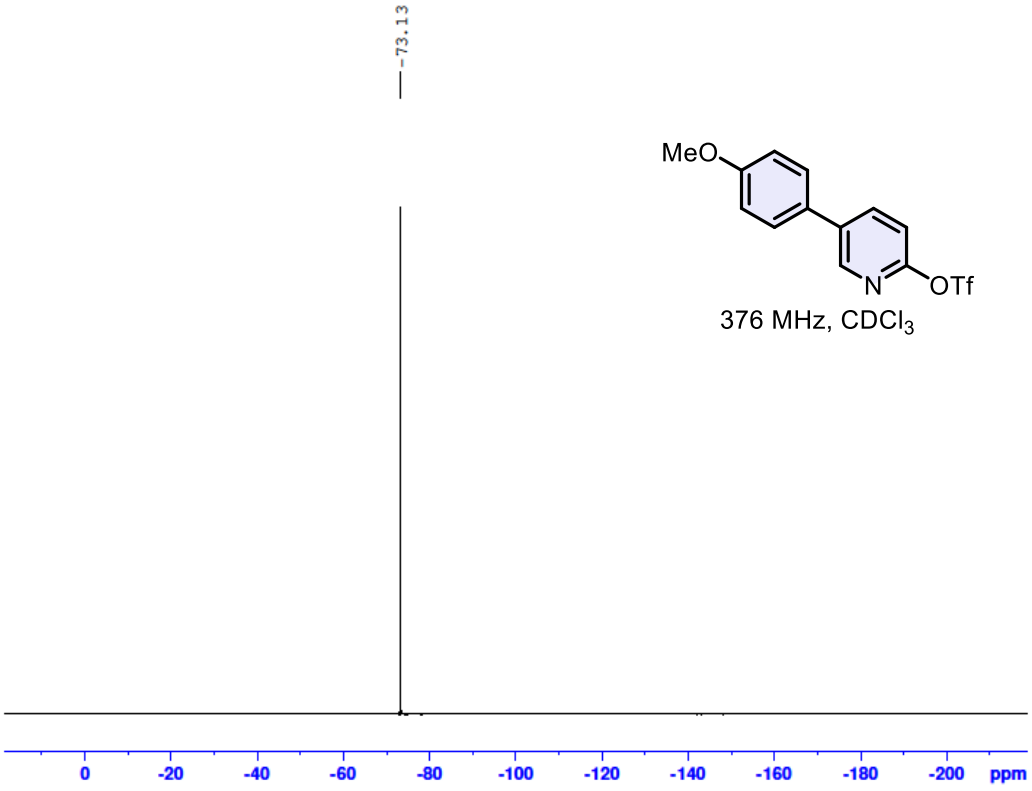

^{1}H NMR of 6-(4-methoxyphenyl)pyridin-2-yl trifluoromethanesulfonate (Table 4.4, compound **16ac**)

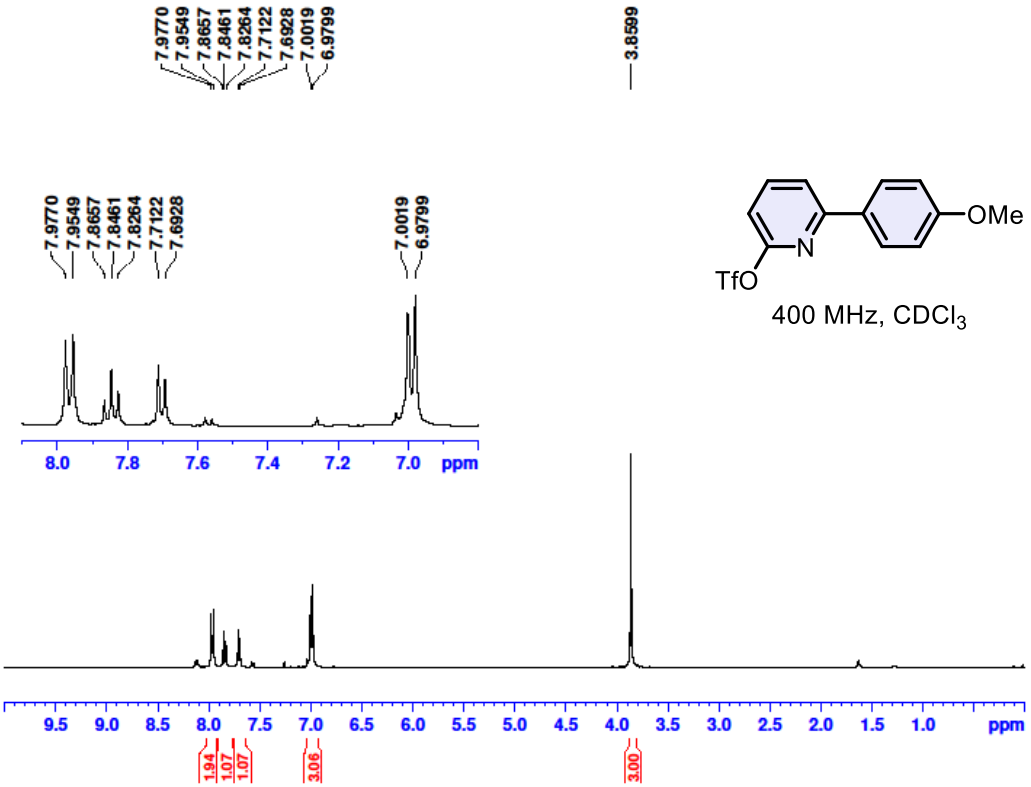

^{13}C NMR of 6-(4-methoxyphenyl)pyridin-2-yl trifluoromethanesulfonate (Table 4.4, compound **16ac**)

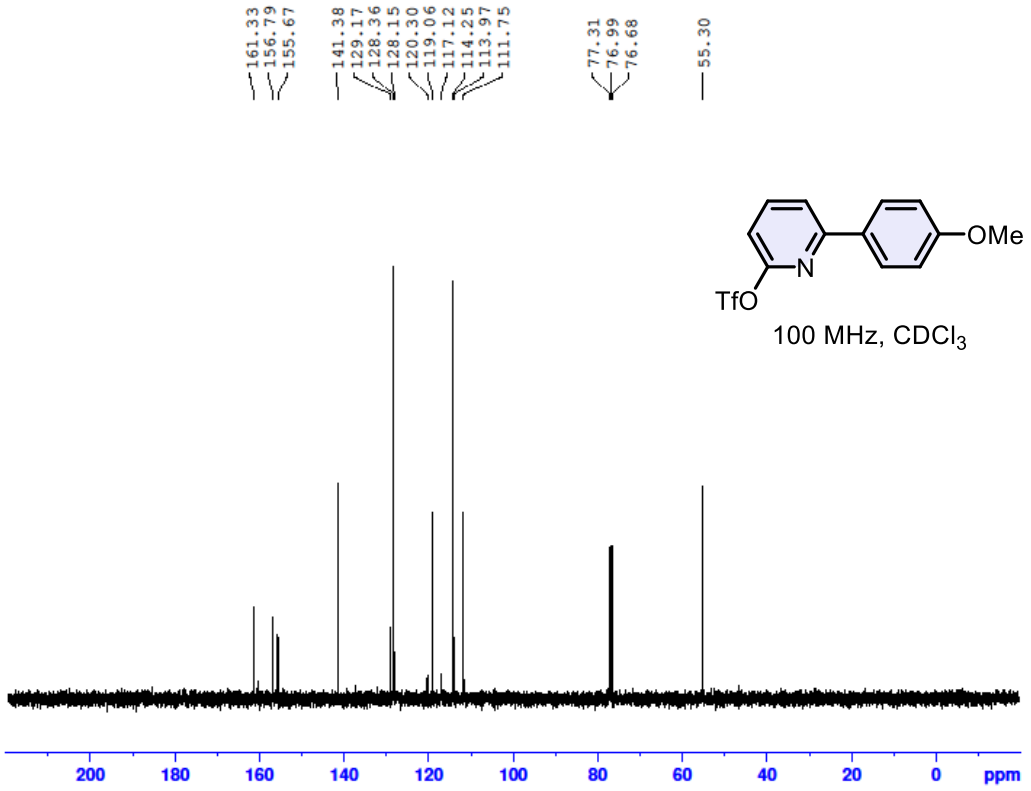

^{19}F NMR of 6-(4-methoxyphenyl)pyridin-2-yl trifluoromethanesulfonate (Table 4.4, compound **16ac**)

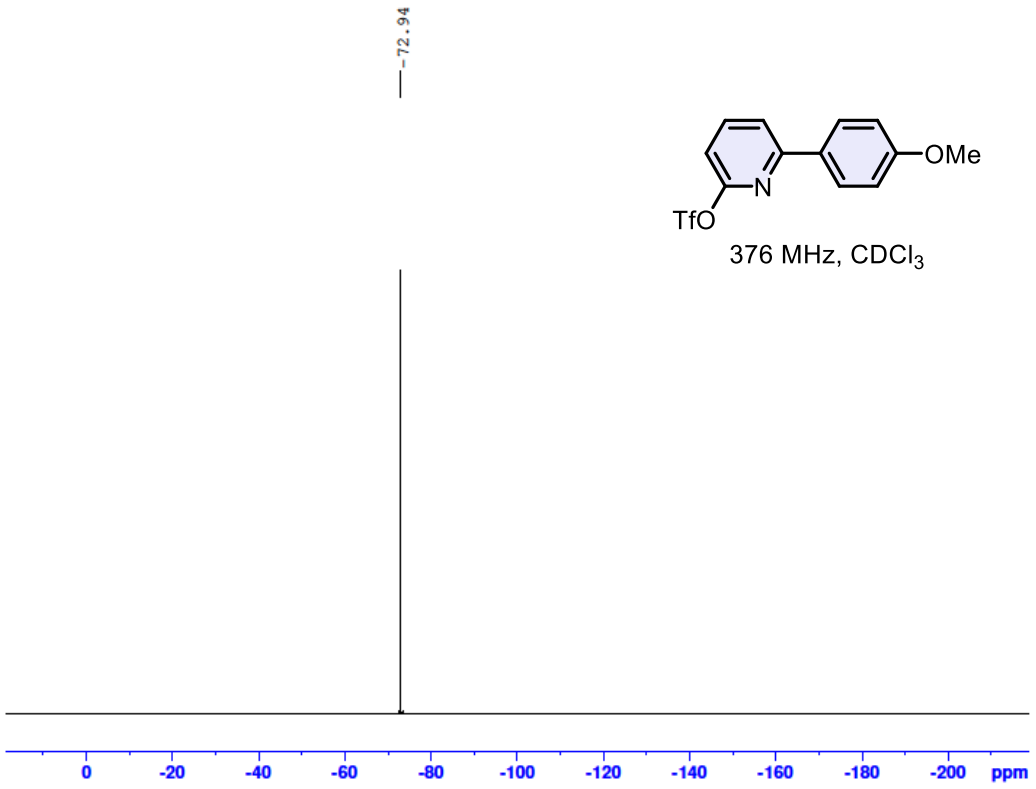

HRMS of 6-(4-methoxyphenyl)pyridin-2-yl trifluoromethanesulfonate (Table 4.4, compound **16ac**)

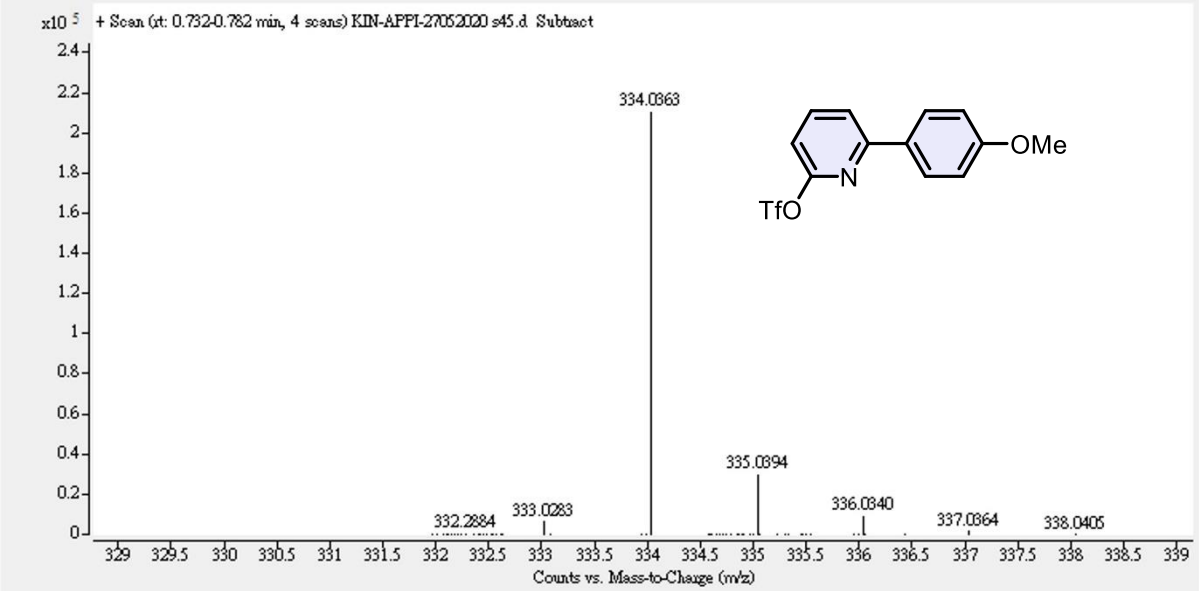

Mass	Calc. Mass	mDa	PPM	Formula
334.0363	334.0355	-0.76	-2.28	C13 H11 F3 N O4 S

^{1}H NMR of 5-(4-methoxyphenyl)pyridin-3-yl trifluoromethanesulfonate (Table 4.4, compound **16ad**)

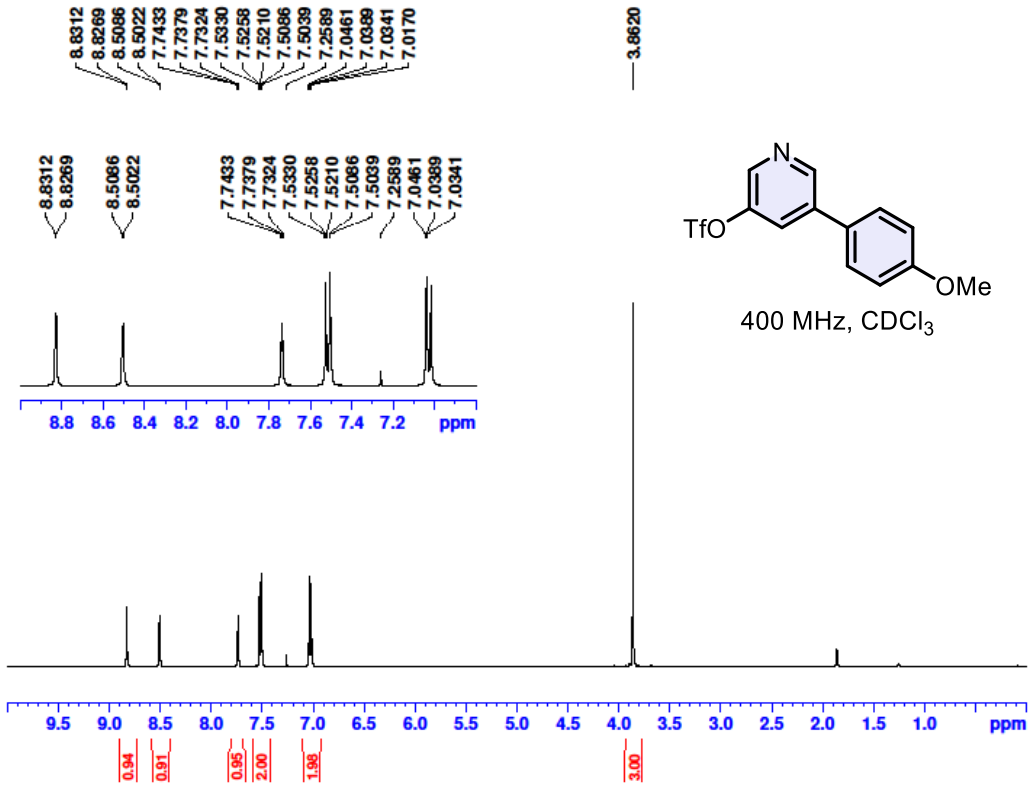

^{13}C NMR of 5-(4-methoxyphenyl)pyridin-3-yl trifluoromethanesulfonate (Table 4.4, compound **16ad**)

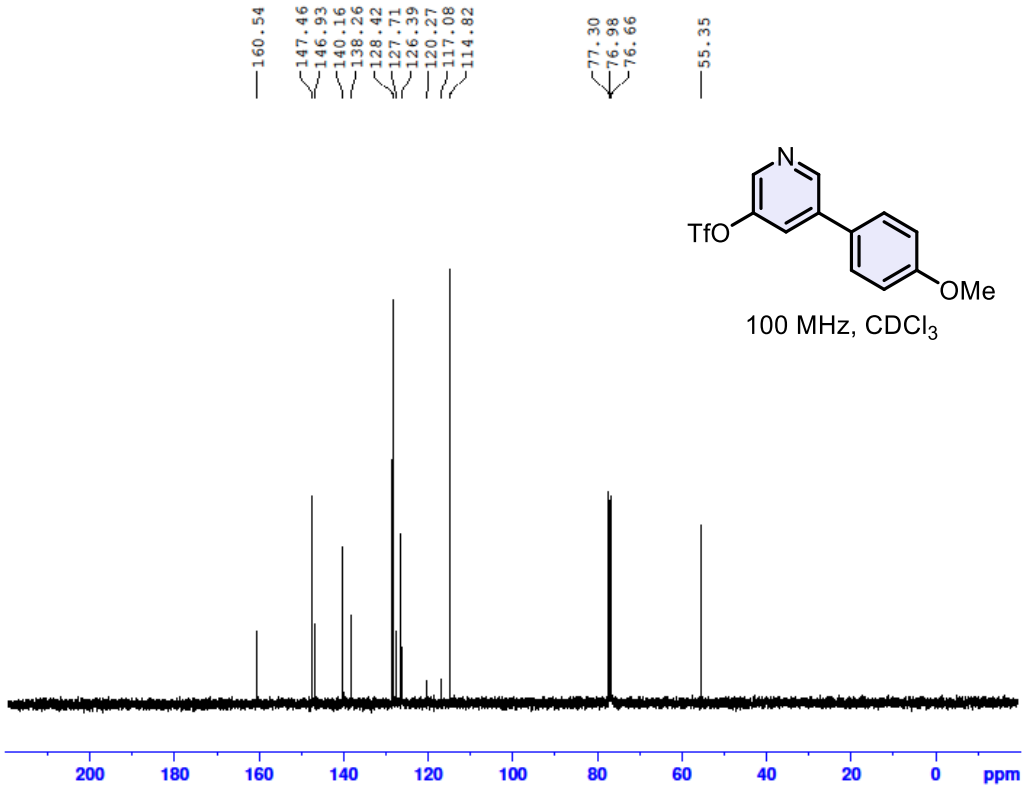

^{19}F NMR of 5-(4-methoxyphenyl)pyridin-3-yl trifluoromethanesulfonate (Table 4.4, compound **16ad**)

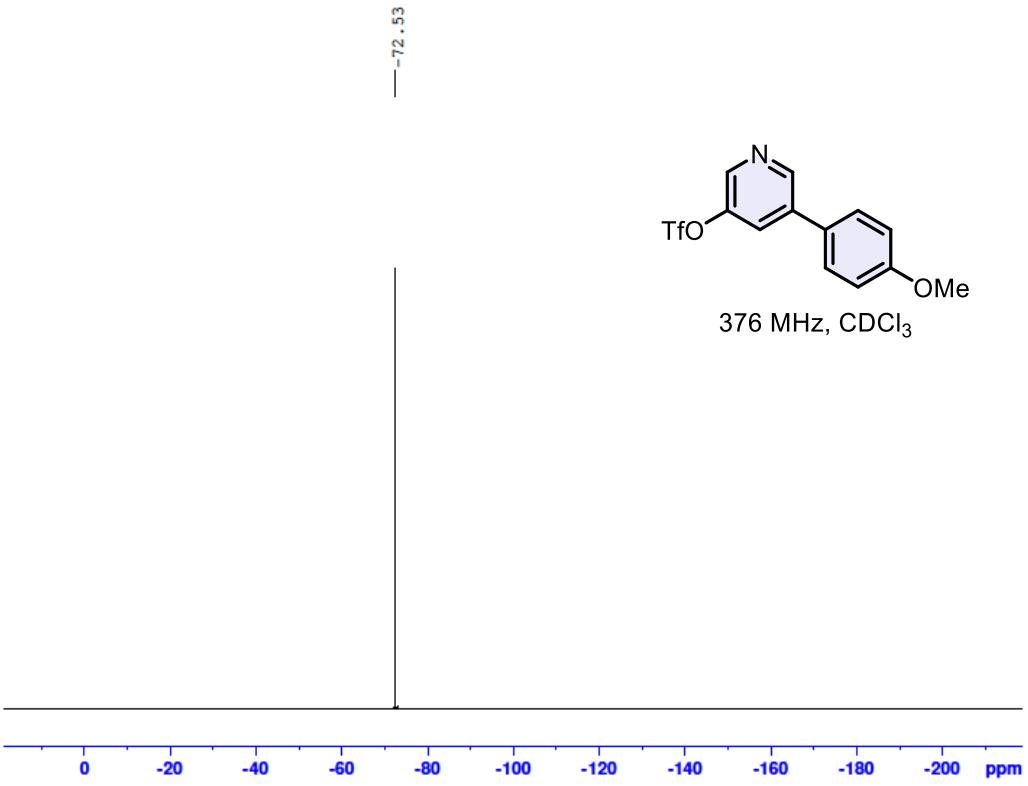

^{1}H NMR of 4-(4-methoxyphenyl)pyridin-2-yl trifluoromethanesulfonate (Table 4.4, compound **16ae**)

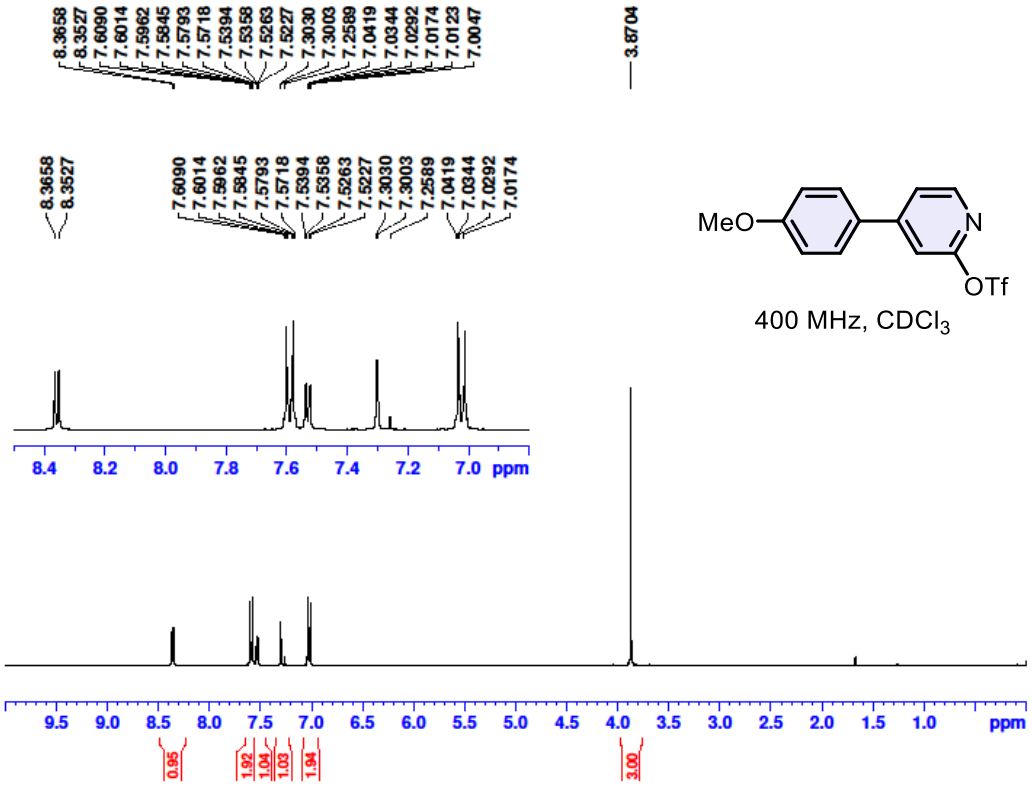

^{13}C NMR of 4-(4-methoxyphenyl)pyridin-2-yl trifluoromethanesulfonate (Table 4.4, compound **16ae**)

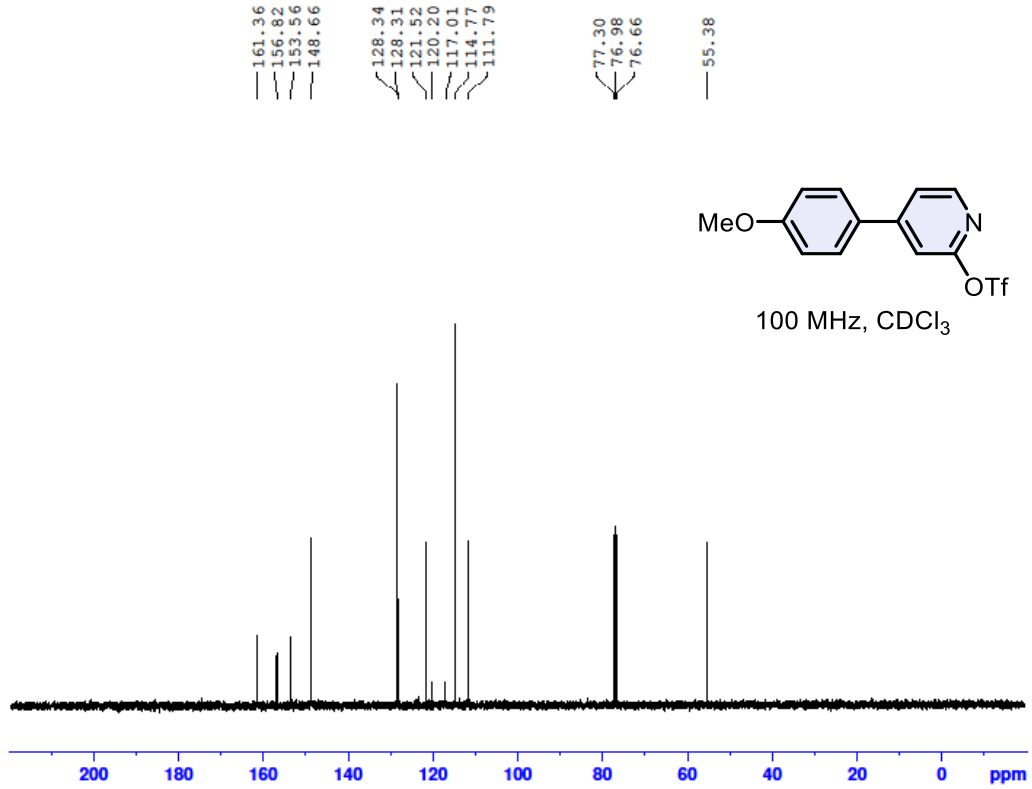

^{19}F NMR of 4-(4-methoxyphenyl)pyridin-2-yl trifluoromethanesulfonate (Table 4.4, compound **16ae**)

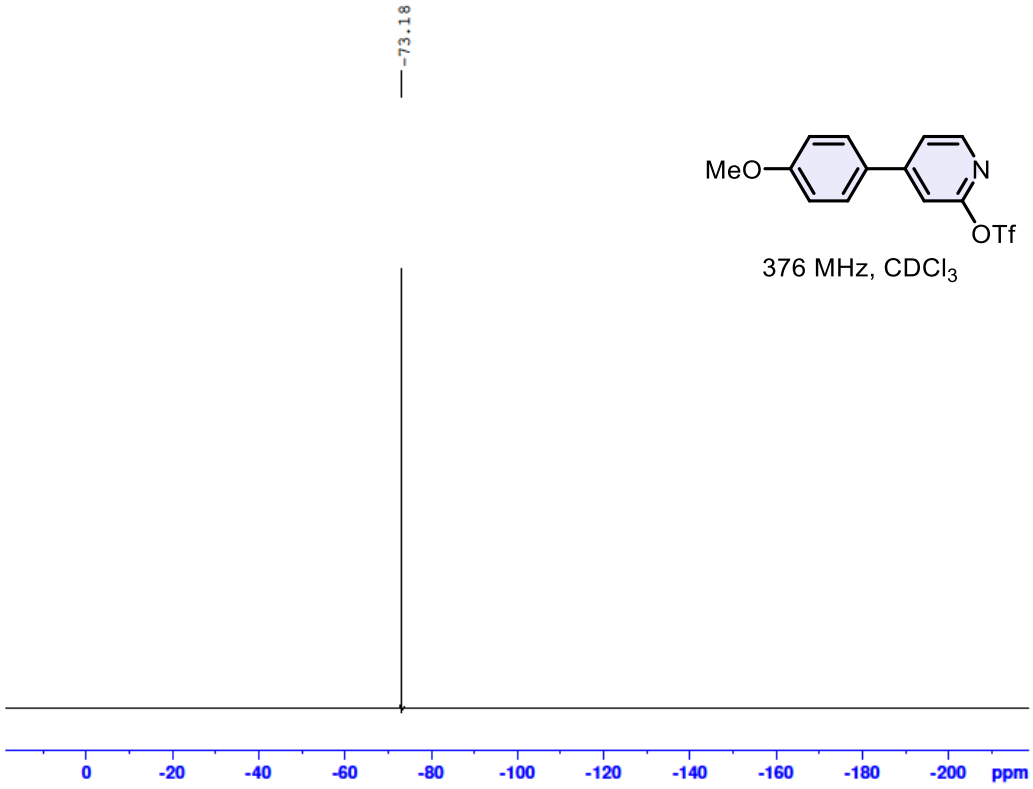

^{1}H NMR of 6-(benzo[*b*]thiophen-3-yl)pyridin-2-yl trifluoromethanesulfonate (Table 4.4, compound **16af**)

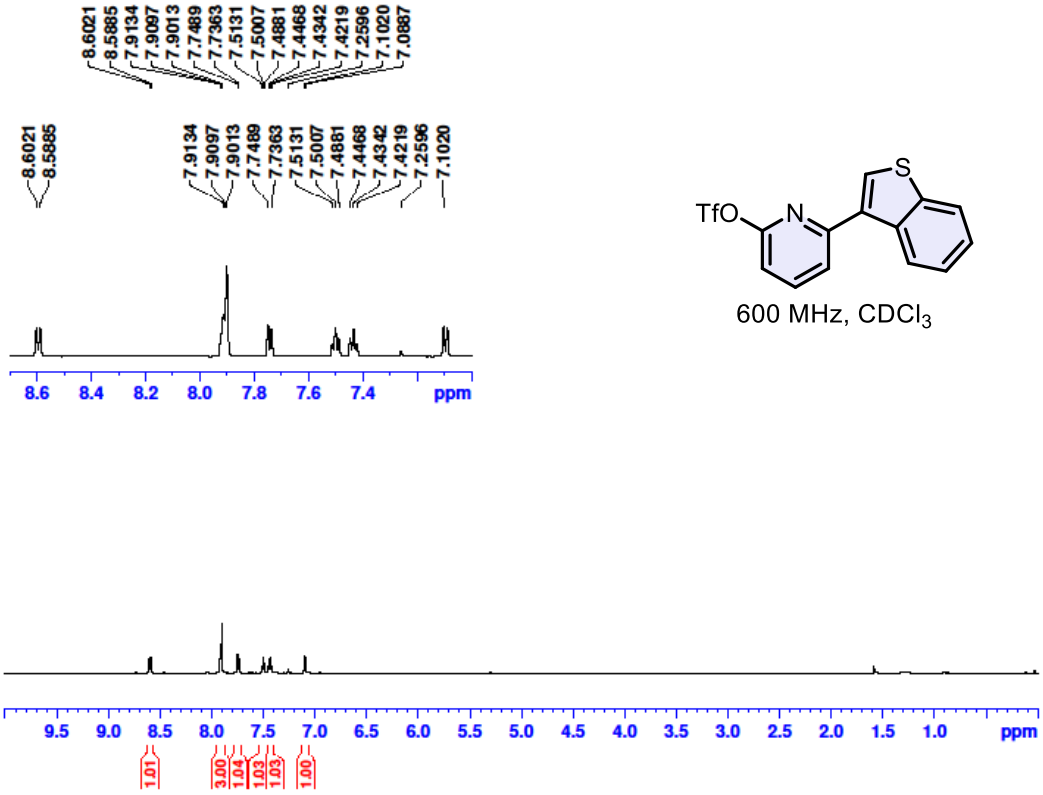

^{13}C NMR of 6-(benzo[*b*]thiophen-3-yl)pyridin-2-yl trifluoromethanesulfonate (Table 4.4, compound **16af**)

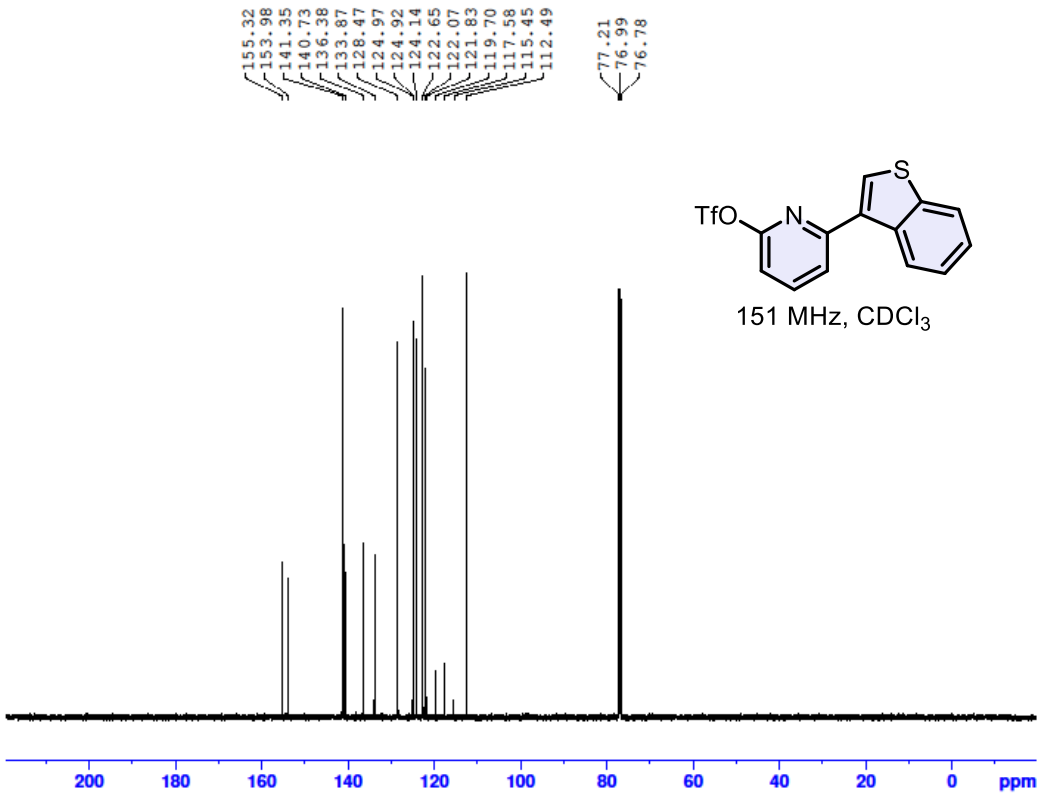

^{19}F NMR of 6-(benzo[*b*]thiophen-3-yl)pyridin-2-yl trifluoromethanesulfonate (Table 4.4, compound **16af**)

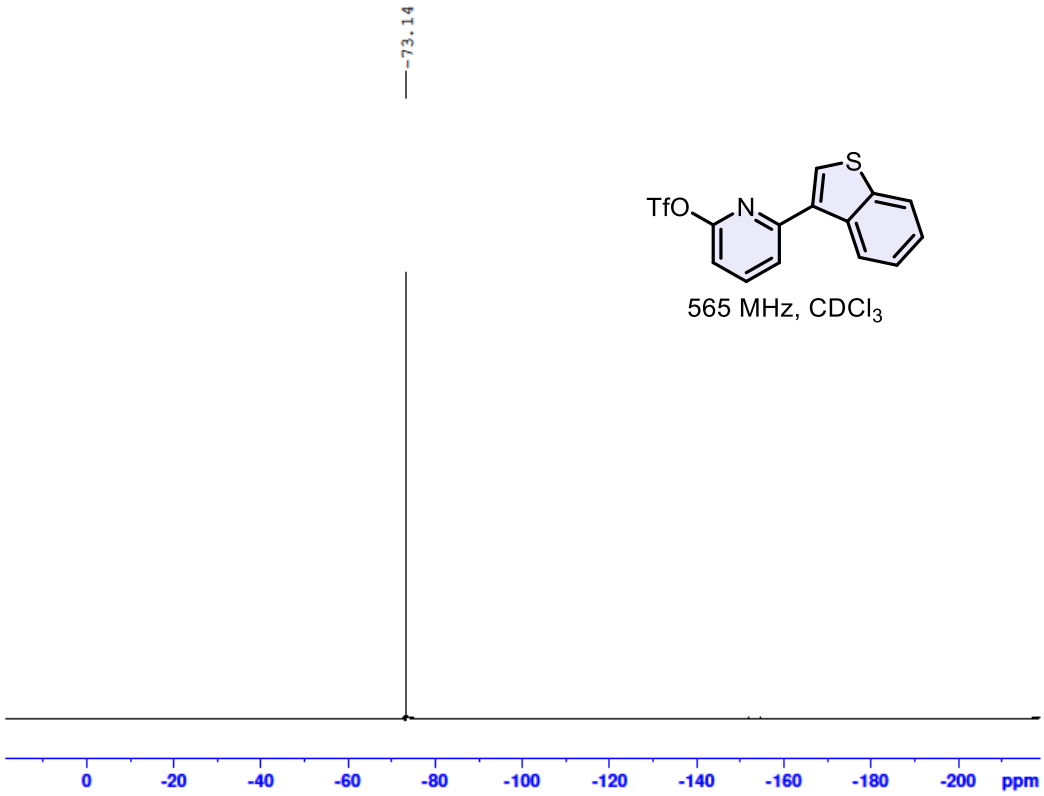

HRMS of 6-(benzo[*b*]thiophen-3-yl)pyridin-2-yl trifluoromethanesulfonate (Table 4.4, compound **16af**)

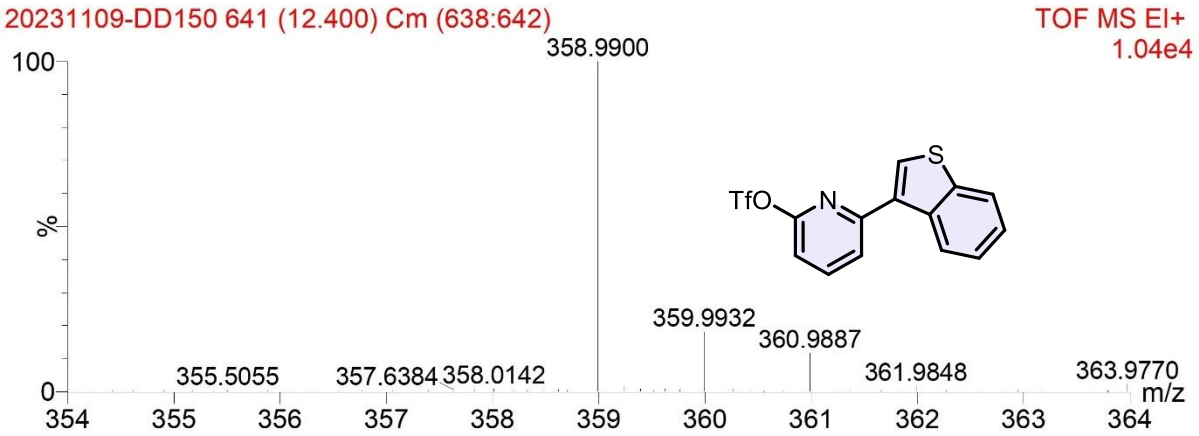

Mass	Calc. Mass	mDa	PPM	Formula
358.9900	358.9892	-0.78	-2.17	C14 H8 F3 N O3 S2

^{1}H NMR of 6-(benzo[*b*]thiophen-2-yl)pyridin-2-yl trifluoromethanesulfonate (Table 4.4, compound **16ag**)

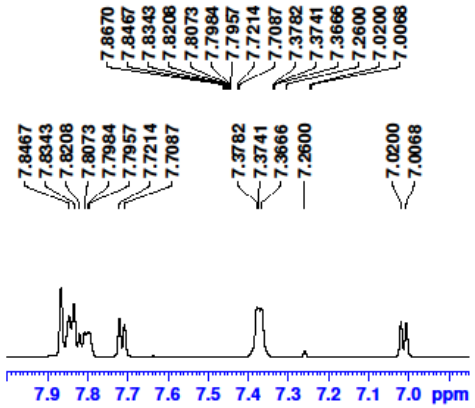

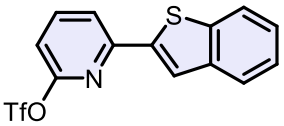

600 MHz, $CDCl_3$

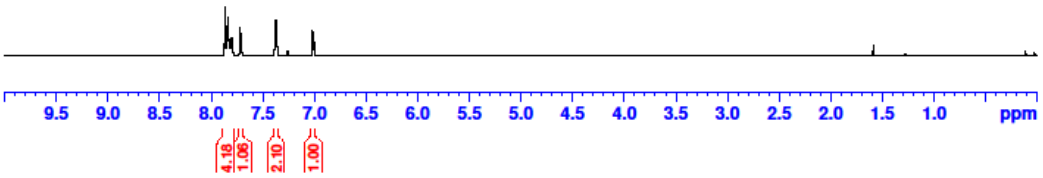

^{13}C NMR of 6-(benzo[*b*]thiophen-2-yl)pyridin-2-yl trifluoromethanesulfonate (Table 4.4, compound **16ag**)

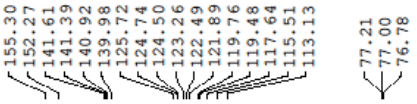

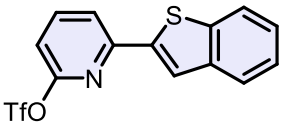

151 MHz, $CDCl_3$

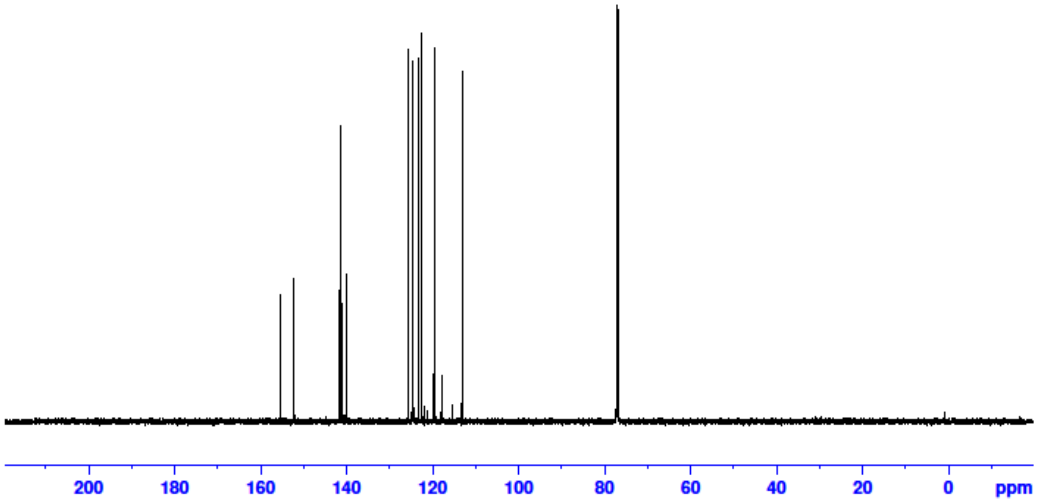

^{19}F NMR of 6-(benzo[*b*]thiophen-2-yl)pyridin-2-yl trifluoromethanesulfonate (Table 4.4, compound **16ag**)

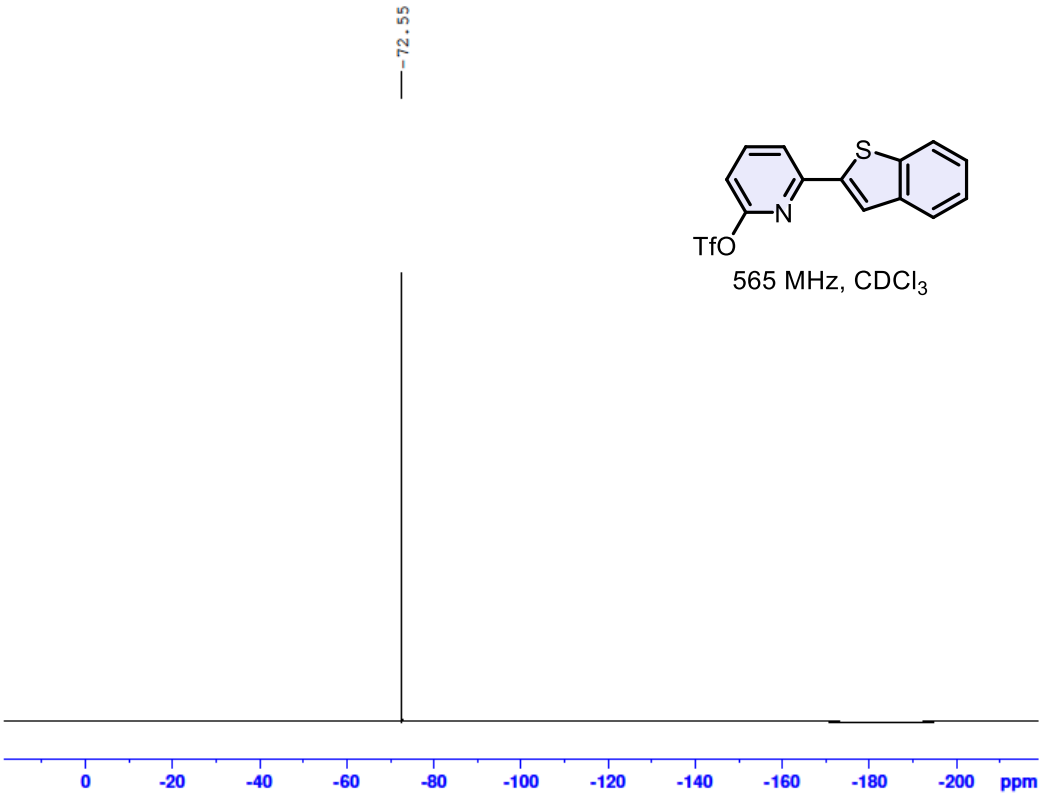

HRMS of 6-(benzo[*b*]thiophen-2-yl)pyridin-2-yl trifluoromethanesulfonate (Table 4.4, compound **16ag**)

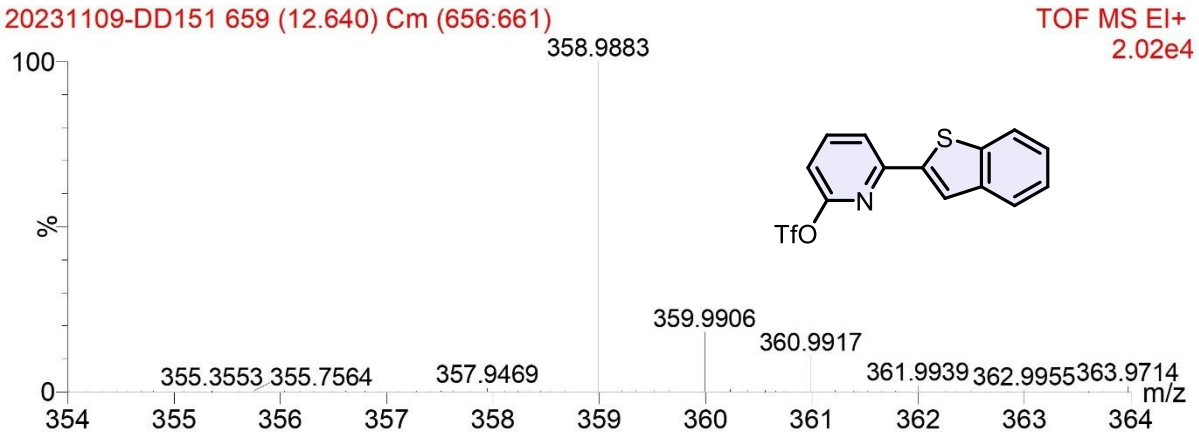

Mass	Calc. Mass	mDa	PPM	Formula
358.9883	358.9892	0.92	2.56	C14 H8 F3 N O3 S2

^{1}H NMR of 5-(benzo[*b*]thiophen-3-yl)pyridin-2-yl trifluoromethanesulfonate (Table 4.4, compound **16ah**)

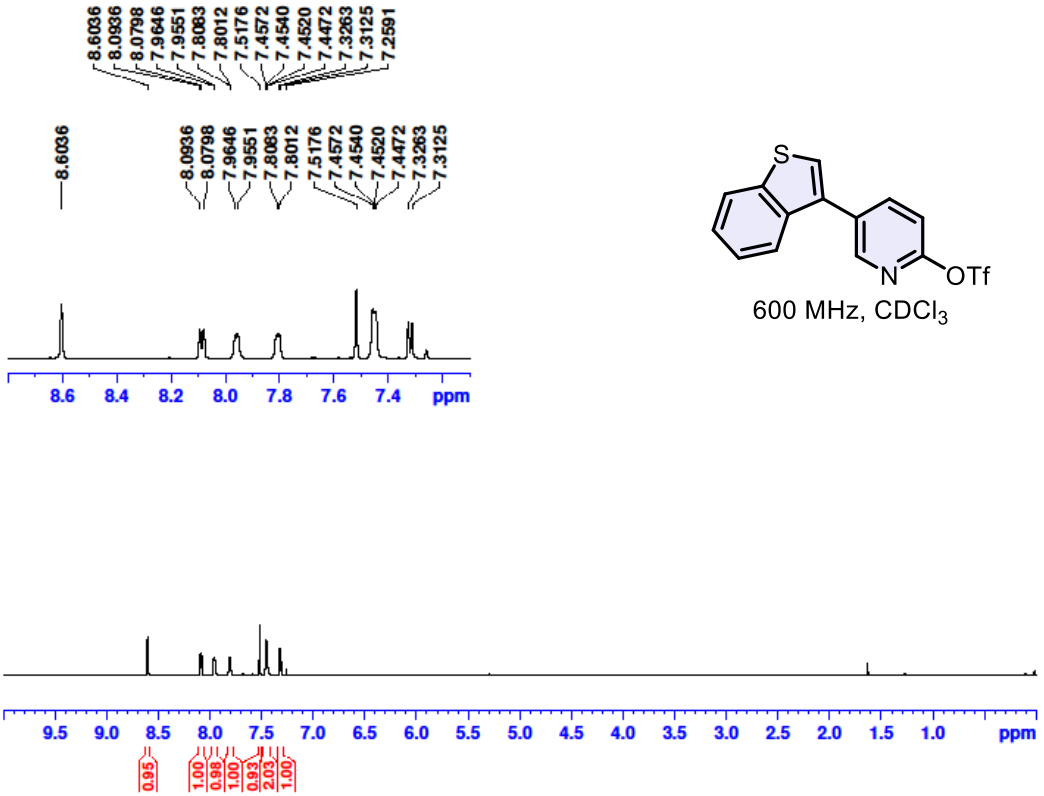

^{13}C NMR of 5-(benzo[*b*]thiophen-3-yl)pyridin-2-yl trifluoromethanesulfonate (Table 4.4, compound **16ah**)

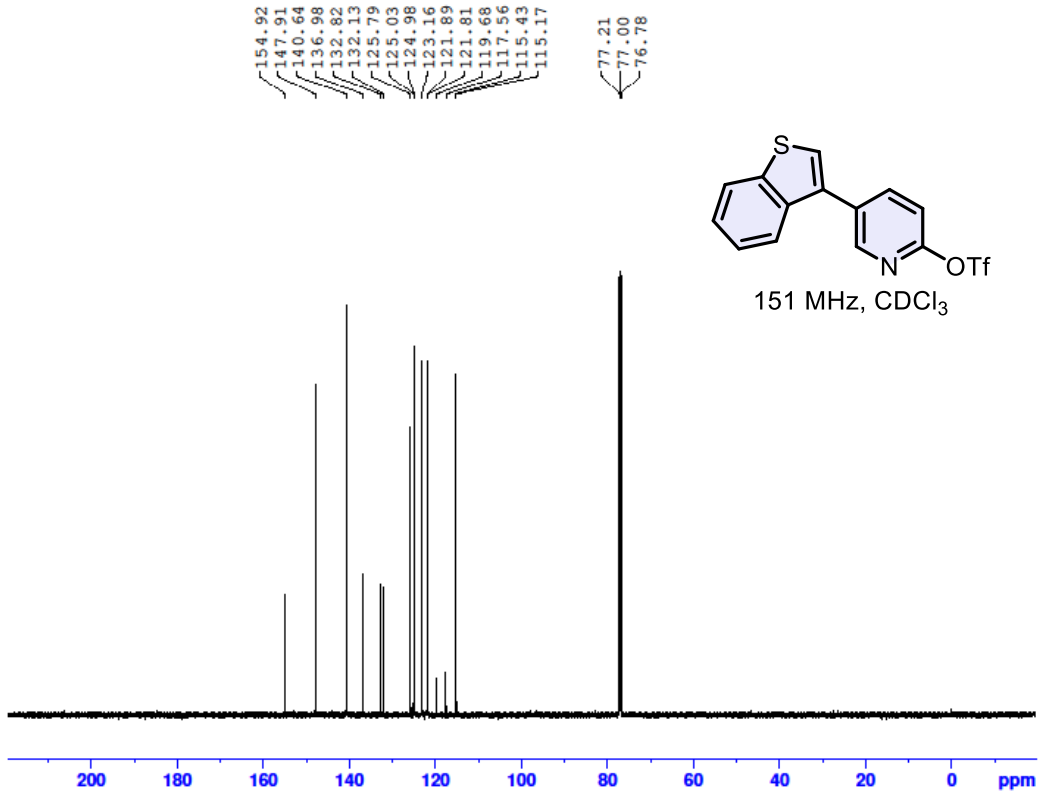

^{19}F NMR of 5-(benzo[*b*]thiophen-3-yl)pyridin-2-yl trifluoromethanesulfonate (Table 4.4, compound **16ah**)

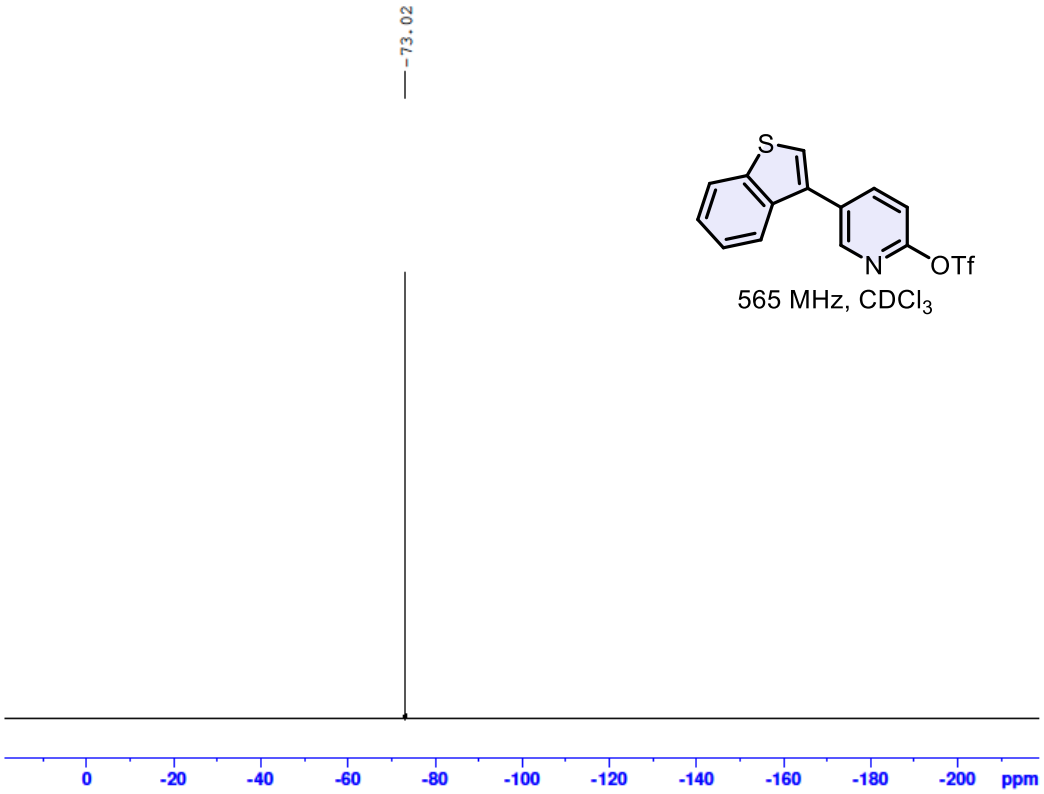

HRMS of 5-(benzo[*b*]thiophen-3-yl)pyridin-2-yl trifluoromethanesulfonate (Table 4.4, compound **16ah**)

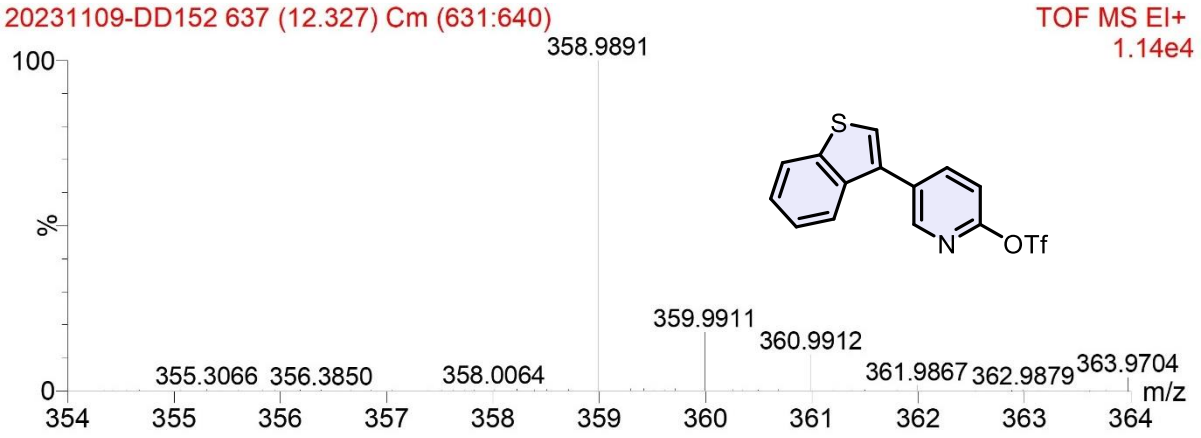

Mass	Calc. Mass	mDa	PPM	Formula
358.9891	358.9892	0.12	0.34	C14 H8 F3 N O3 S2

^{1}H NMR of 5-(benzo[*b*]thiophen-2-yl)pyridin-2-yl trifluoromethanesulfonate (Table 4.4, compound **16ai**)

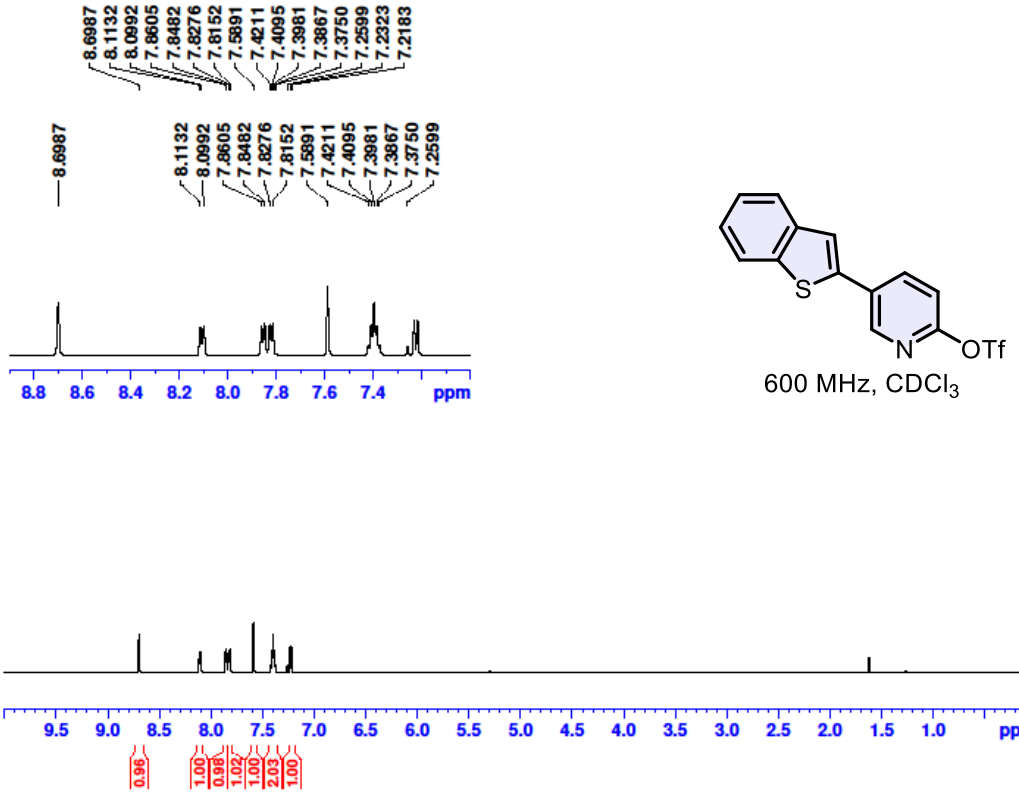

^{13}C NMR of 5-(benzo[*b*]thiophen-2-yl)pyridin-2-yl trifluoromethanesulfonate (Table 4.4, compound **16ai**)

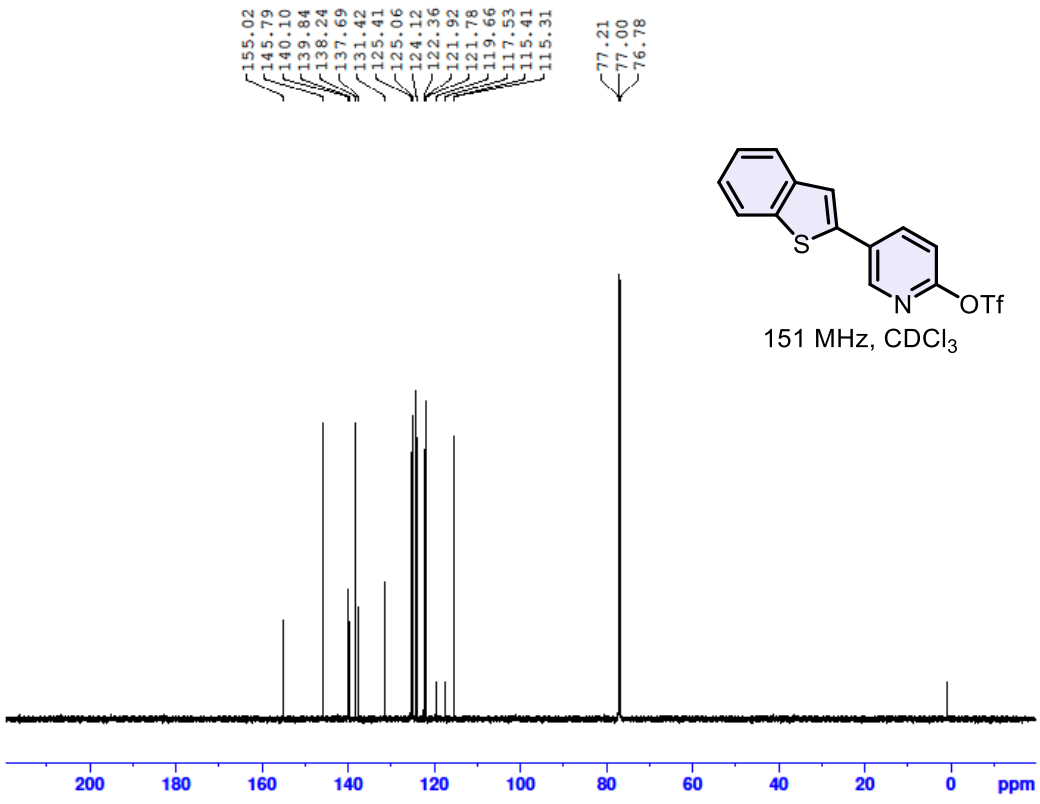

^{19}F NMR of 5-(benzo[*b*]thiophen-2-yl)pyridin-2-yl trifluoromethanesulfonate (Table 4.4, compound **16ai**)

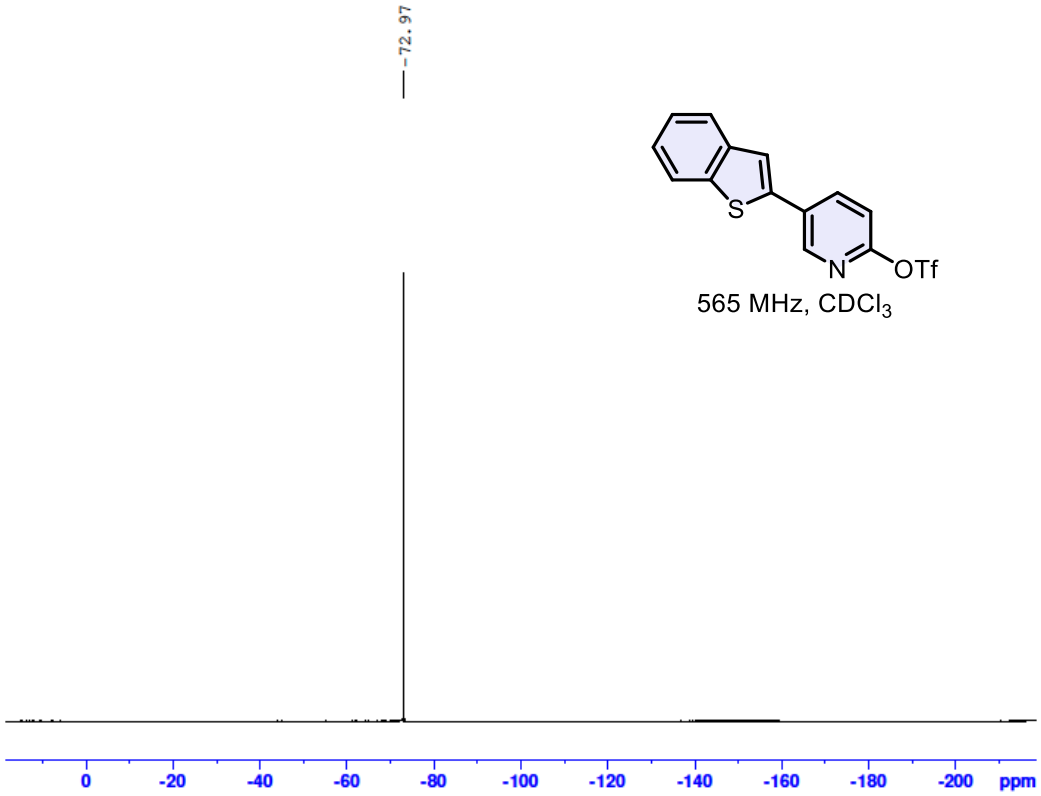

HRMS of 5-(benzo[*b*]thiophen-2-yl)pyridin-2-yl trifluoromethanesulfonate (Table 4.4, compound **16ai**)

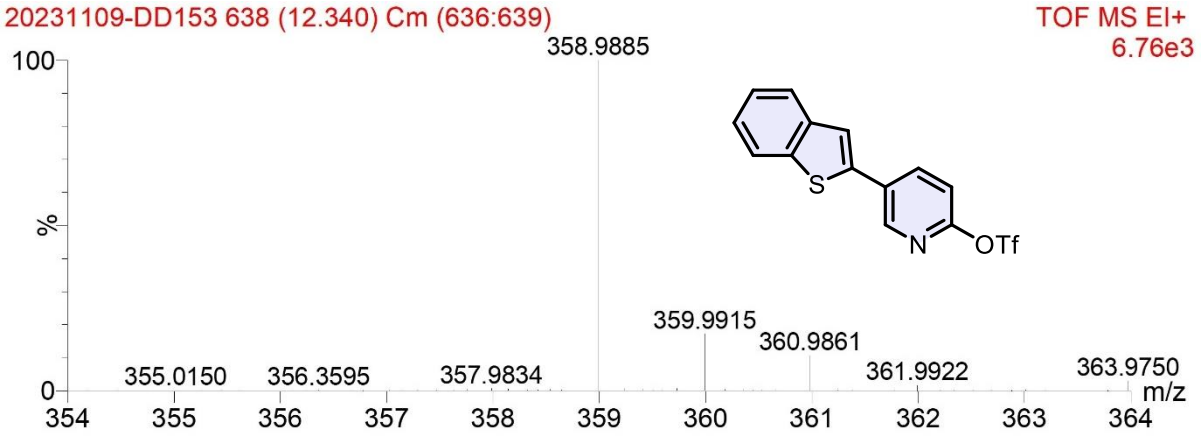

Mass	Calc. Mass	mDa	PPM	Formula
358.9885	358.9892	0.72	2.01	C14 H8 F3 N O3 S2

^{1}H NMR of 4''-methoxy-2-methyl-[1,1':3',1''-terphenyl]-4'-yl trifluoromethanesulfonate (Table 4.5, compound **20a**)

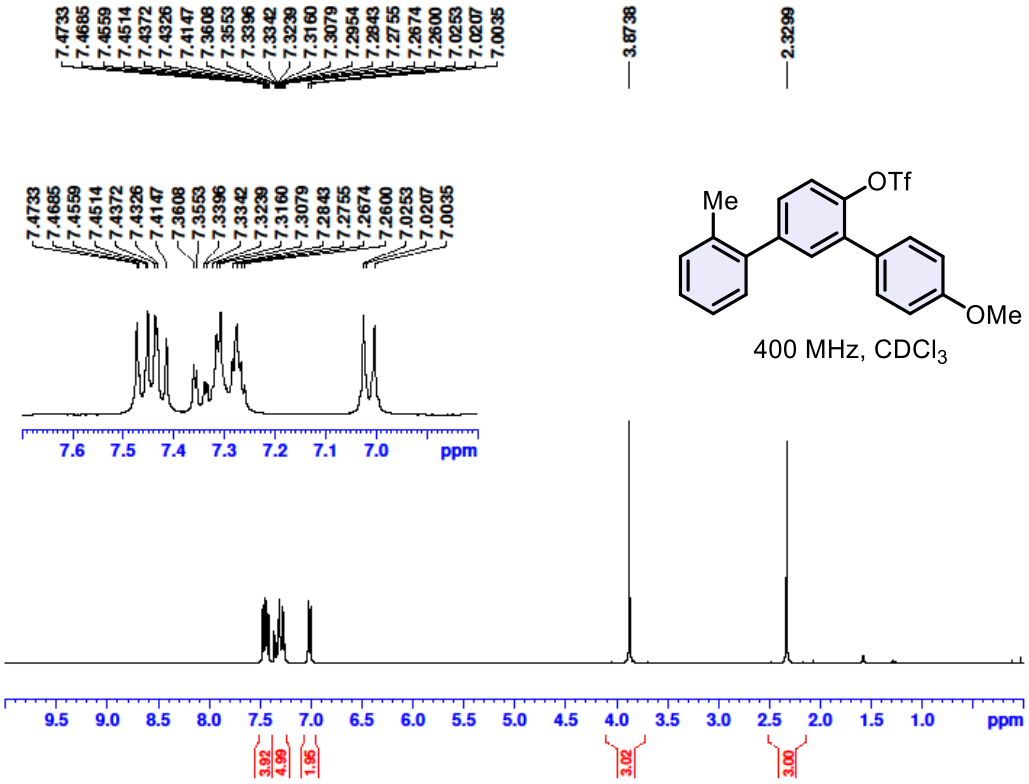

^{13}C NMR of 4''-methoxy-2-methyl-[1,1':3',1''-terphenyl]-4'-yl trifluoromethanesulfonate (Table 4.5, compound **20a**)

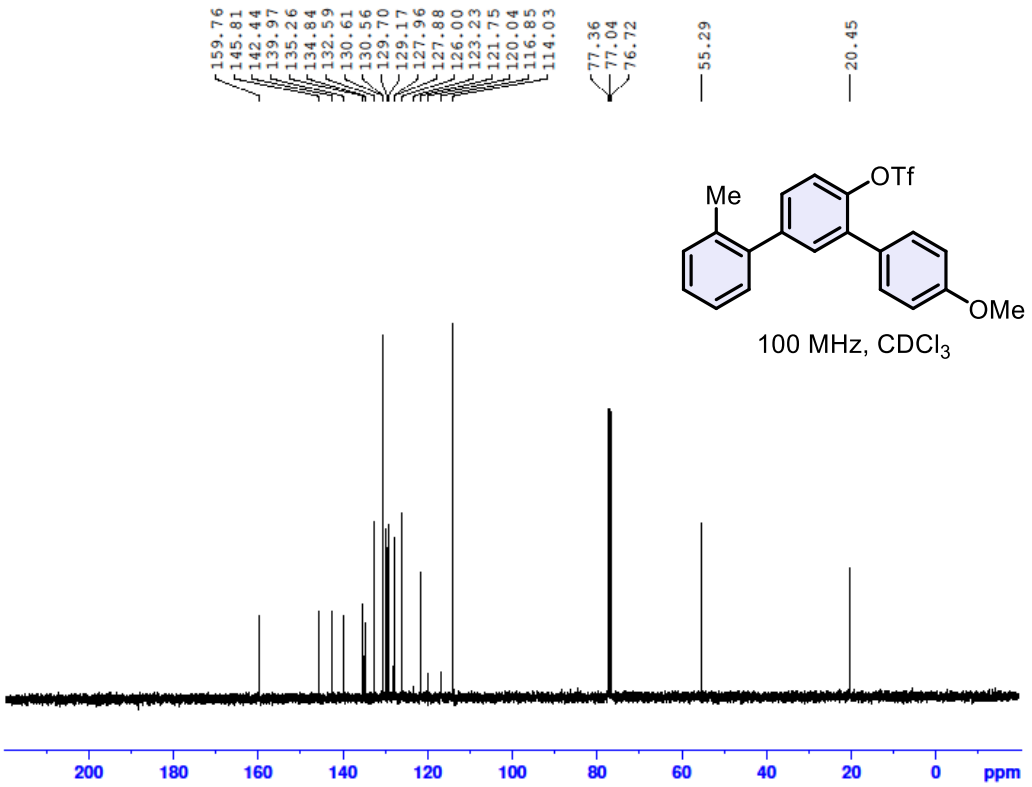

^{19}F NMR of 4''-methoxy-2-methyl-[1,1':3',1''-terphenyl]-4'-yl trifluoromethanesulfonate (Table 4.5, compound **20a**)

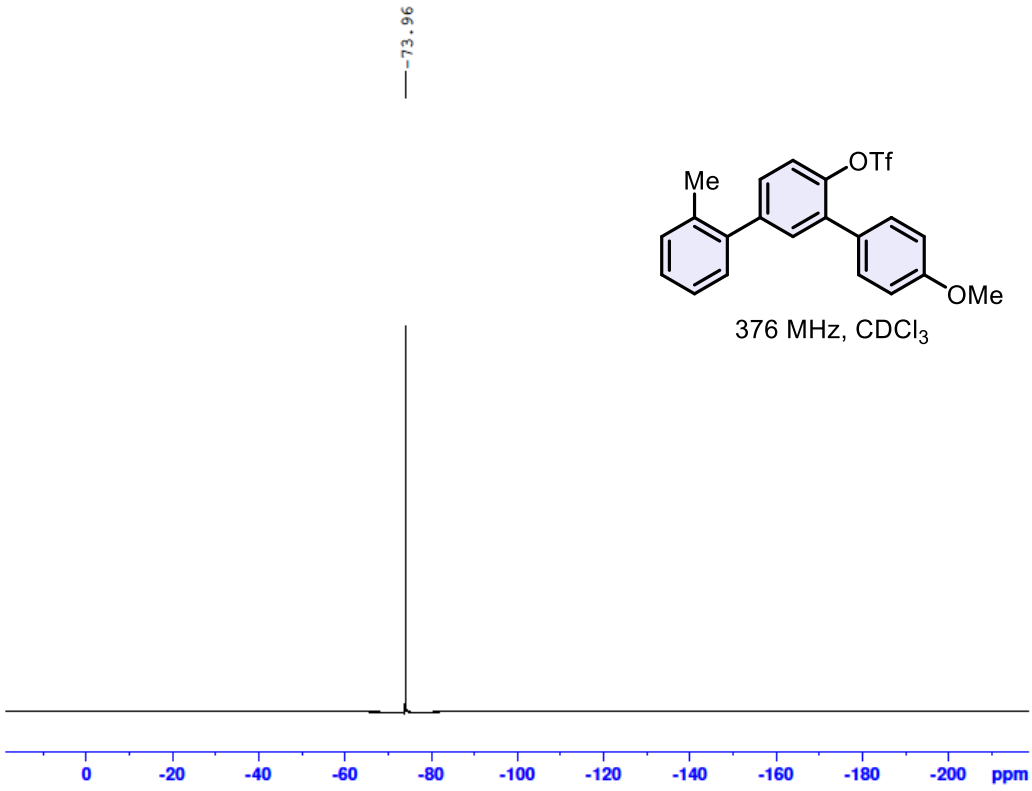

HRMS of 4''-methoxy-2-methyl-[1,1':3',1''-terphenyl]-4'-yl trifluoromethanesulfonate (Table 4.5, compound **20a**)

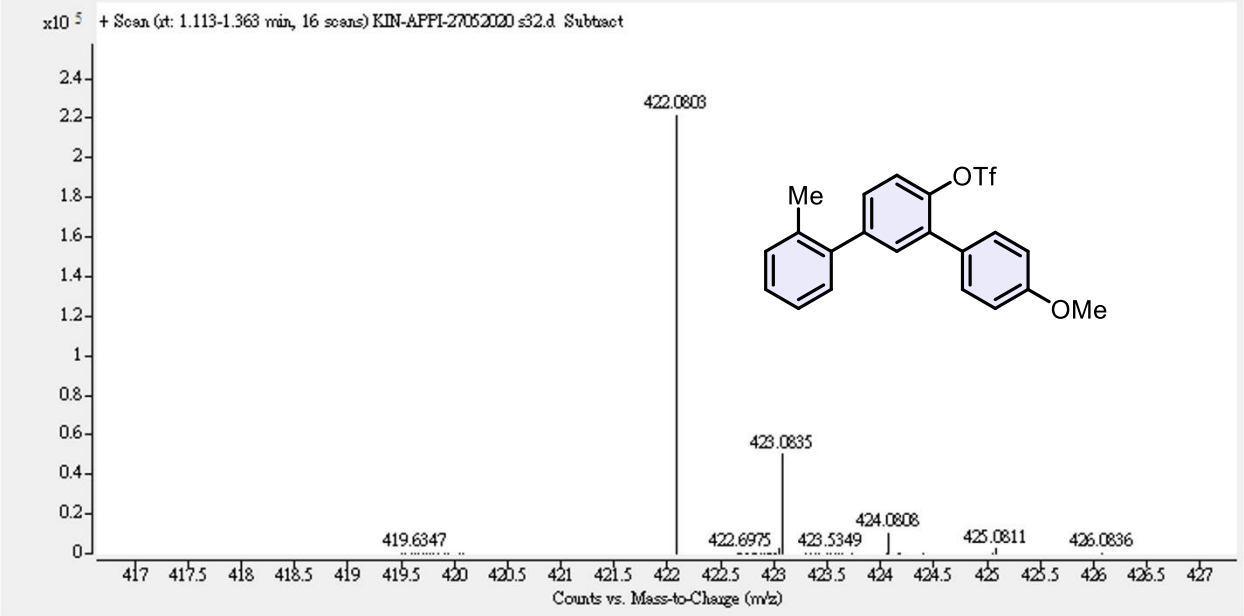

Mass	Calc. Mass	mDa	PPM	Formula
422.0803	422.0800	-0.34	-0.80	C14 H10 Cl F3 O3 S

^{1}H NMR of 3'',5''-dimethoxy-2-methyl-[1,1':3',1''-terphenyl]-4'-yl trifluoromethanesulfonate

(Table 4.5, compound **20b**)

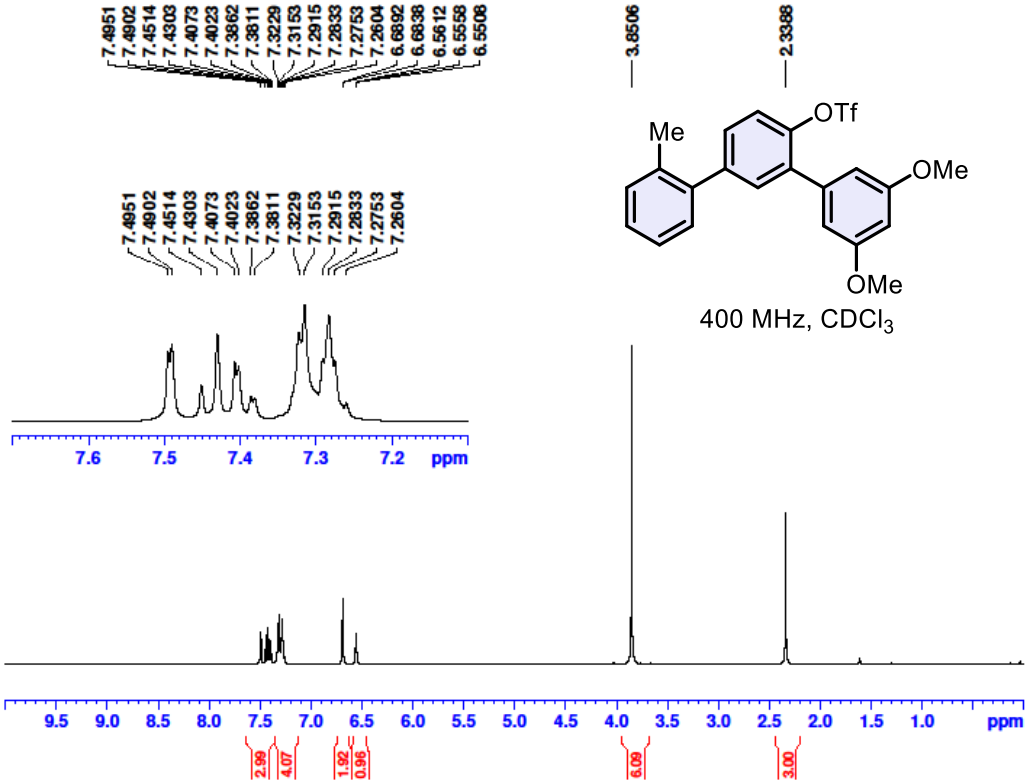

^{13}C NMR of 3'',5''-dimethoxy-2-methyl-[1,1':3',1''-terphenyl]-4'-yl trifluoromethanesulfonate

(Table 4.5, compound **20b**)

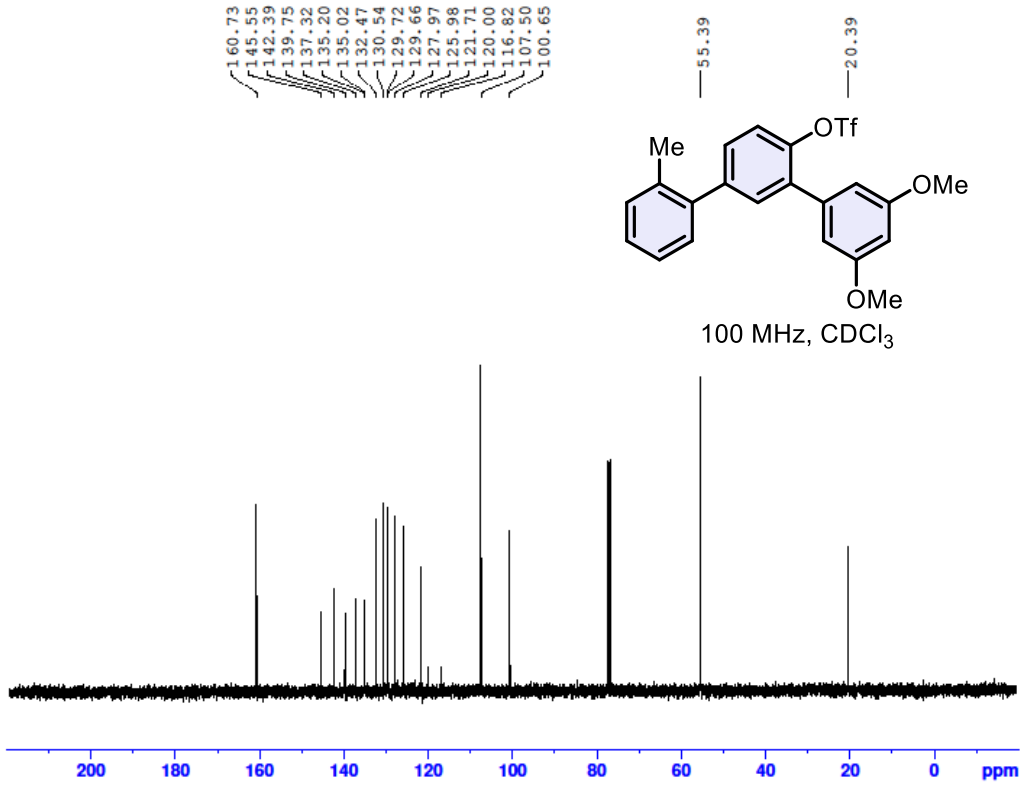

^{19}F NMR of 3’’,5’’-dimethoxy-2-methyl-[1,1’:3’,1’’-terphenyl]-4’-yl trifluoromethanesulfonate (Table 4.5, compound **20b**)

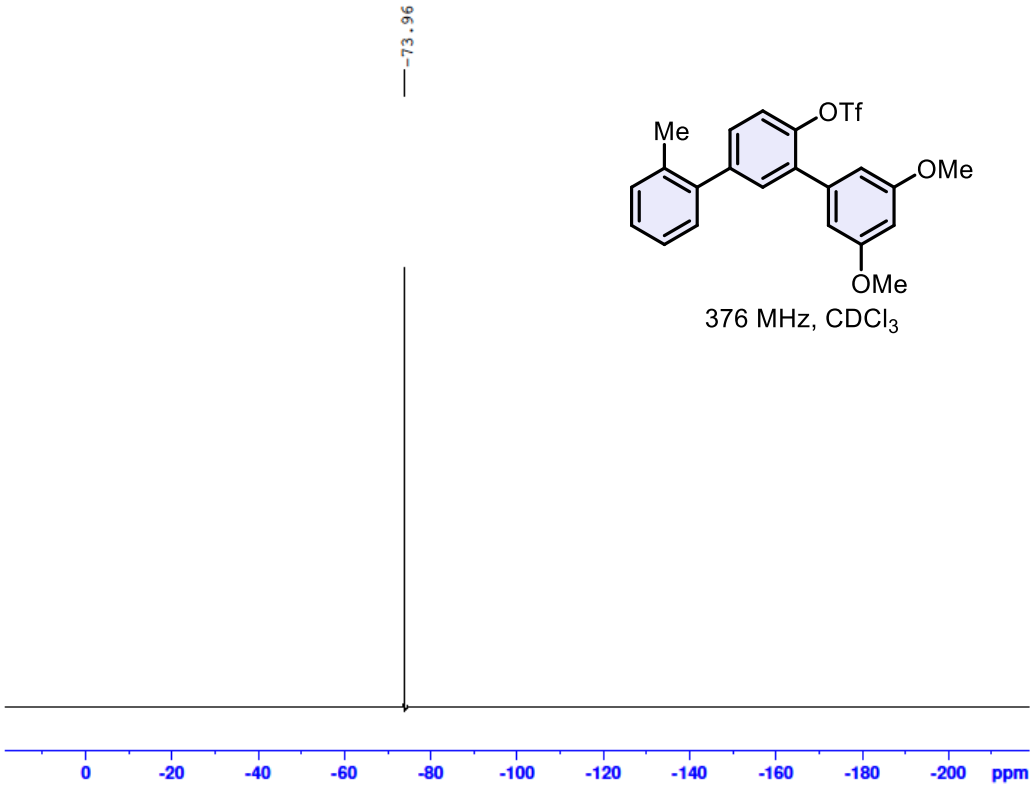

HRMS of 3’’,5’’-dimethoxy-2-methyl-[1,1’:3’,1’’-terphenyl]-4’-yl trifluoromethanesulfonate (Table 4.5, compound **20b**)

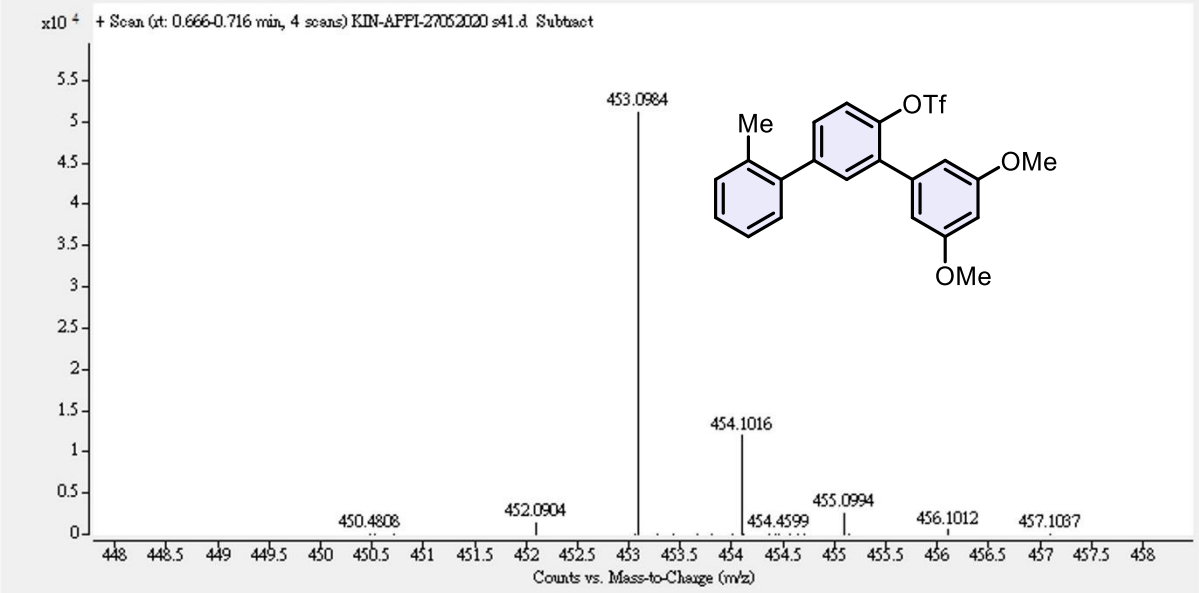

Mass	Calc. Mass	mDa	PPM	Formula
453.0984	453.0978	-0.59	-1.32	C22 H20 F3 O5 S

^{1}H NMR of 4’-methoxy-5-(naphthalen-1-yl)-[1,1’-biphenyl]-2-yl trifluoromethanesulfonate (Table 4.5, compound **20c**)

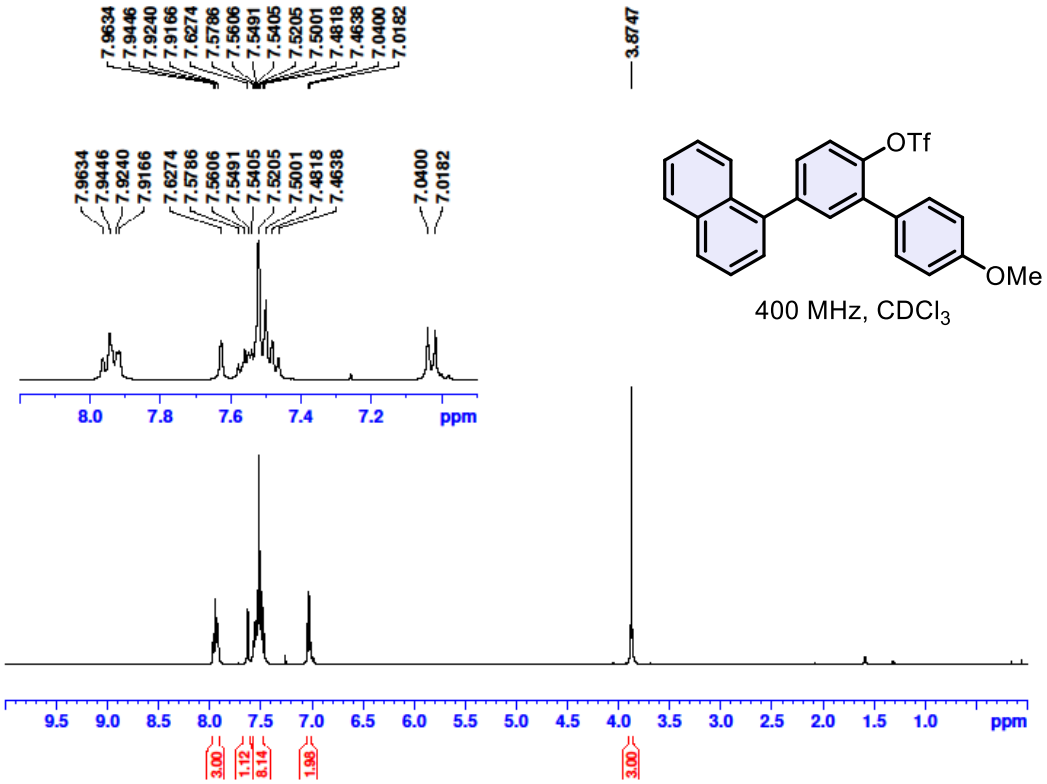

^{13}C NMR of 4’-methoxy-5-(naphthalen-1-yl)-[1,1’-biphenyl]-2-yl trifluoromethanesulfonate (Table 4.5, compound **20c**)

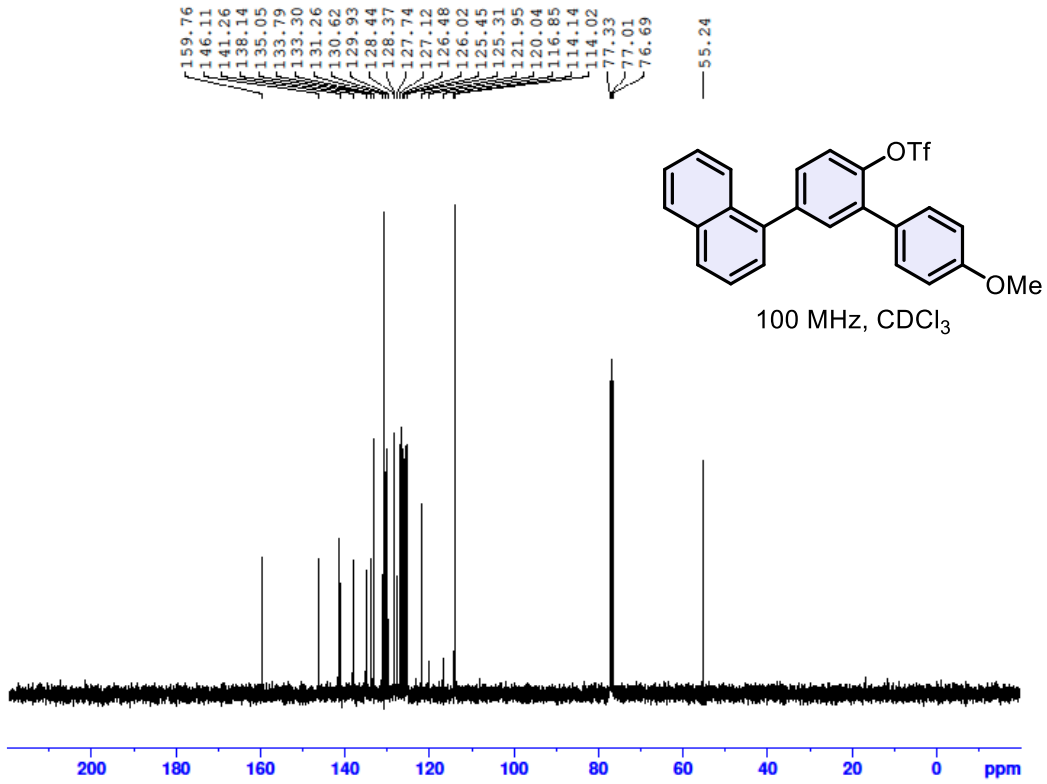

^{19}F NMR of 4’-methoxy-5-(naphthalen-1-yl)-[1,1’-biphenyl]-2-yl trifluoromethanesulfonate (Table 4.5, compound **20c**)

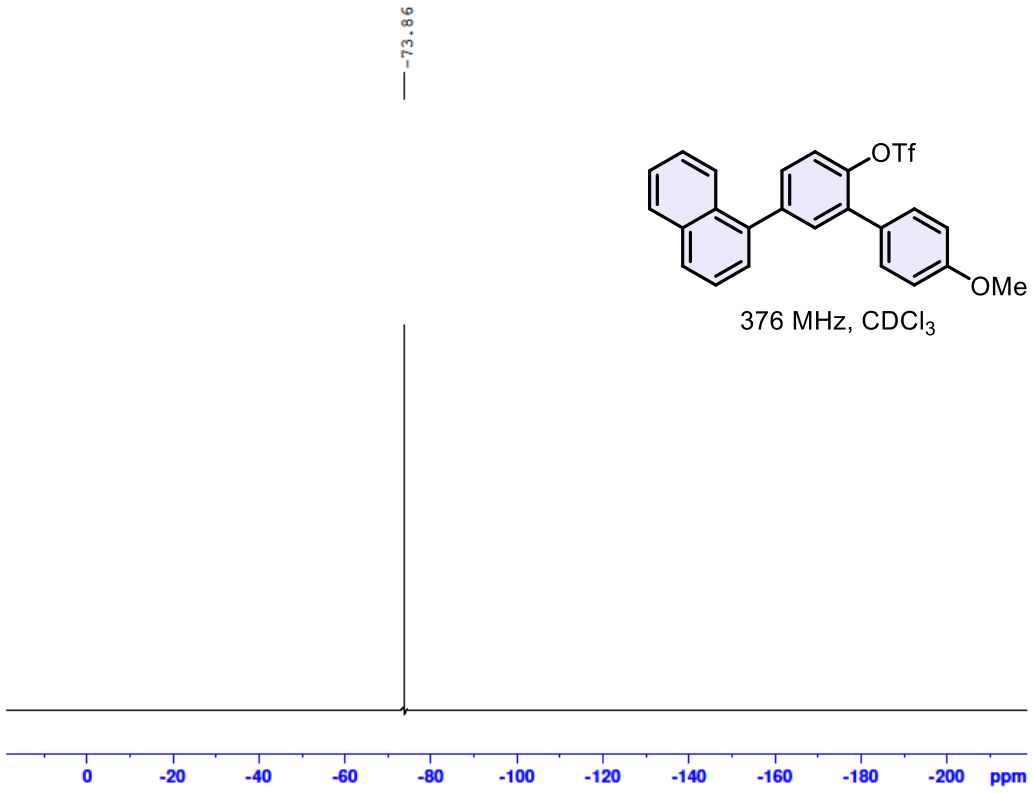

HRMS of 4’-methoxy-5-(naphthalen-1-yl)-[1,1’-biphenyl]-2-yl trifluoromethanesulfonate (Table 4.5, compound **20c**)

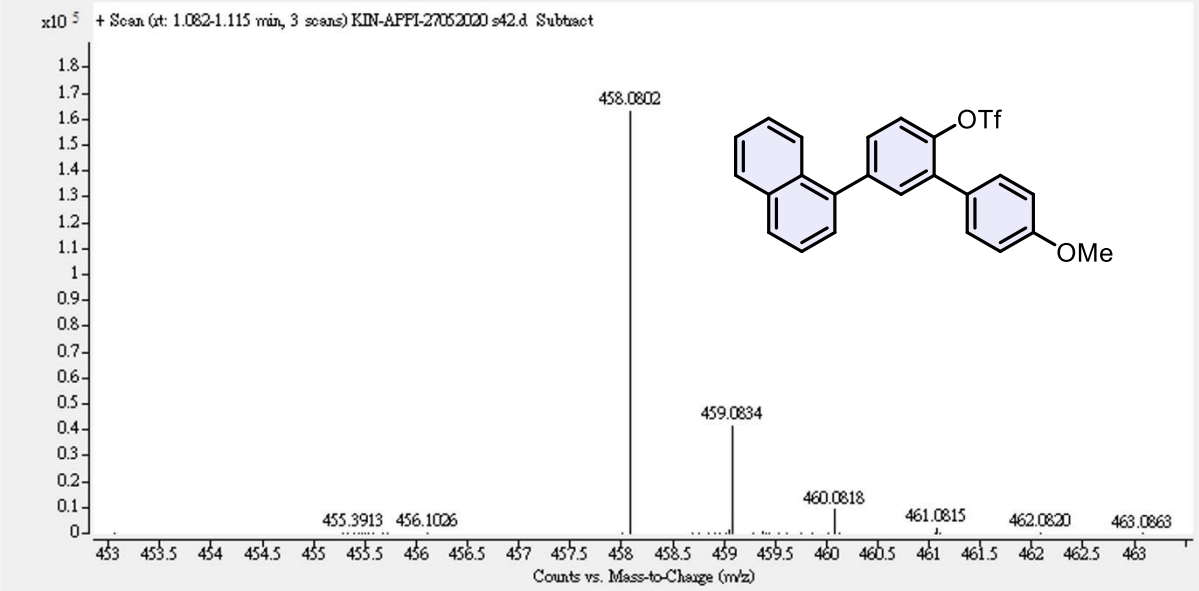

Mass	Calc. Mass	mDa	PPM	Formula
458.0802	458.0794	-0.78	-1.72	C24 H17 F3 F3 O4 S

^{1}H NMR of 4''-methoxy-2-methyl-[1,1':3',1''-terphenyl]-5'-yl trifluoromethanesulfonate (Table 4.5, compound **20d**)

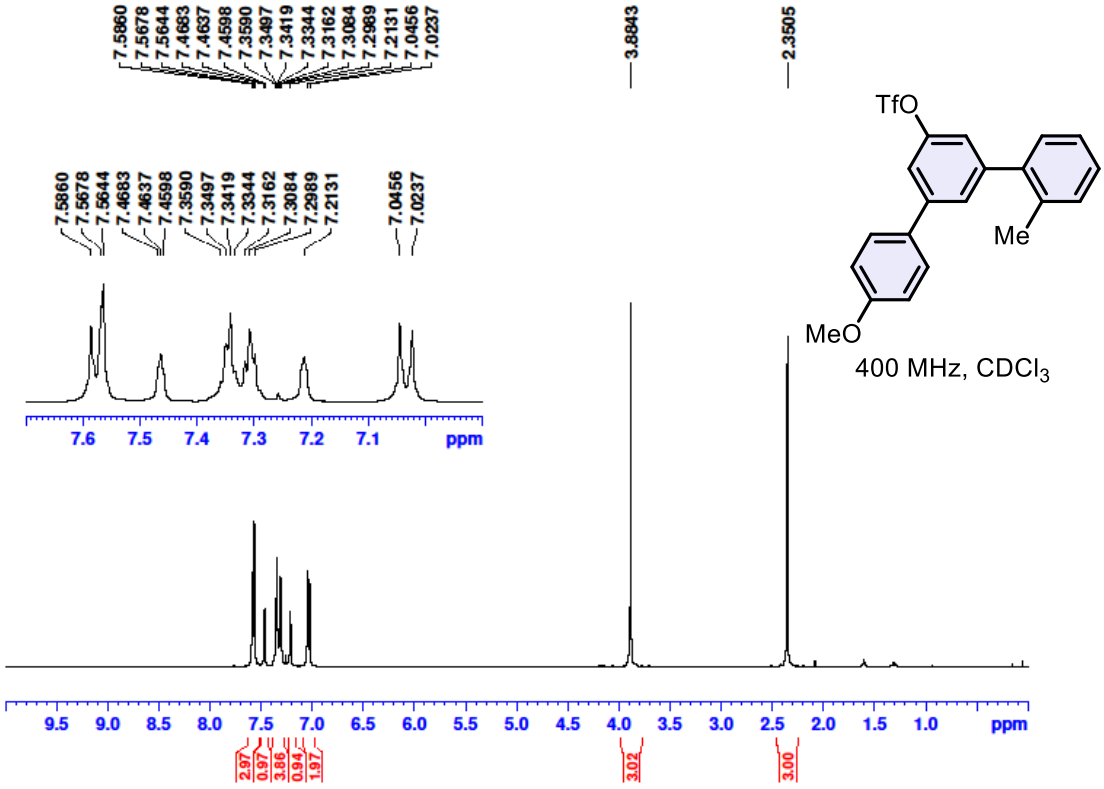

^{13}C NMR of 4''-methoxy-2-methyl-[1,1':3',1''-terphenyl]-5'-yl trifluoromethanesulfonate (Table 4.5, compound **20d**)

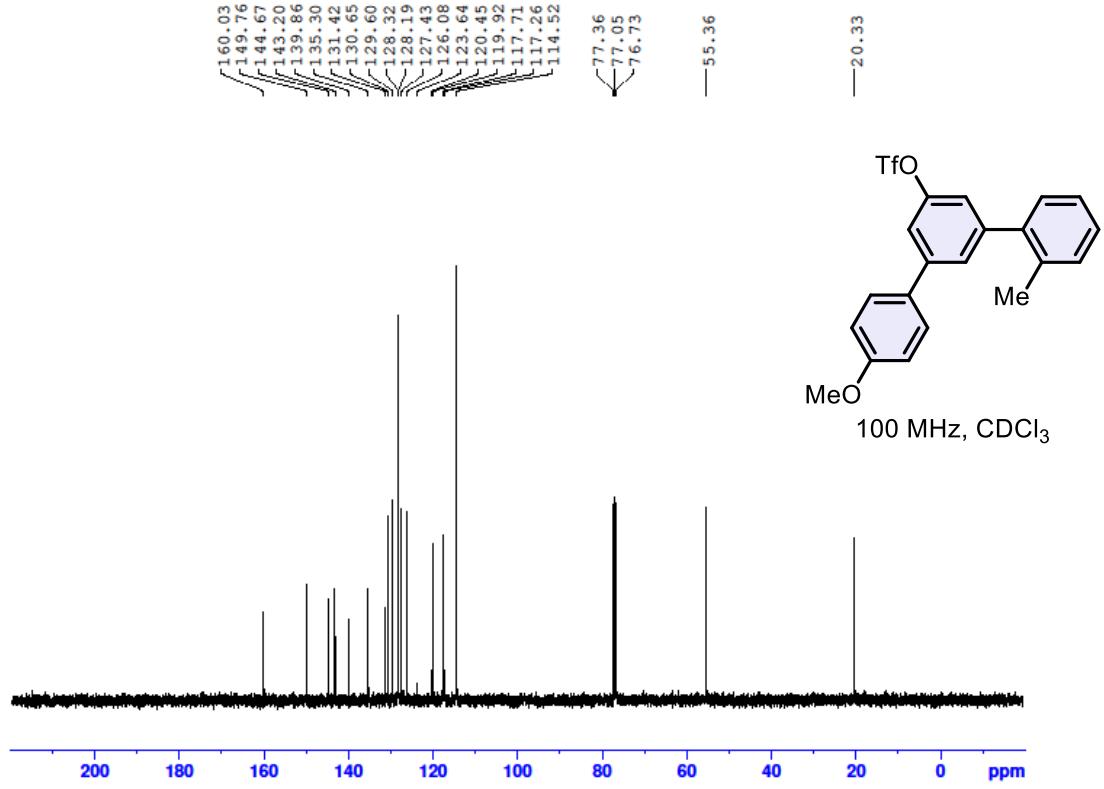

^{19}F NMR of 4''-methoxy-2-methyl-[1,1':3',1''-terphenyl]-5'-yl trifluoromethanesulfonate (Table 4.5, compound **20d**)

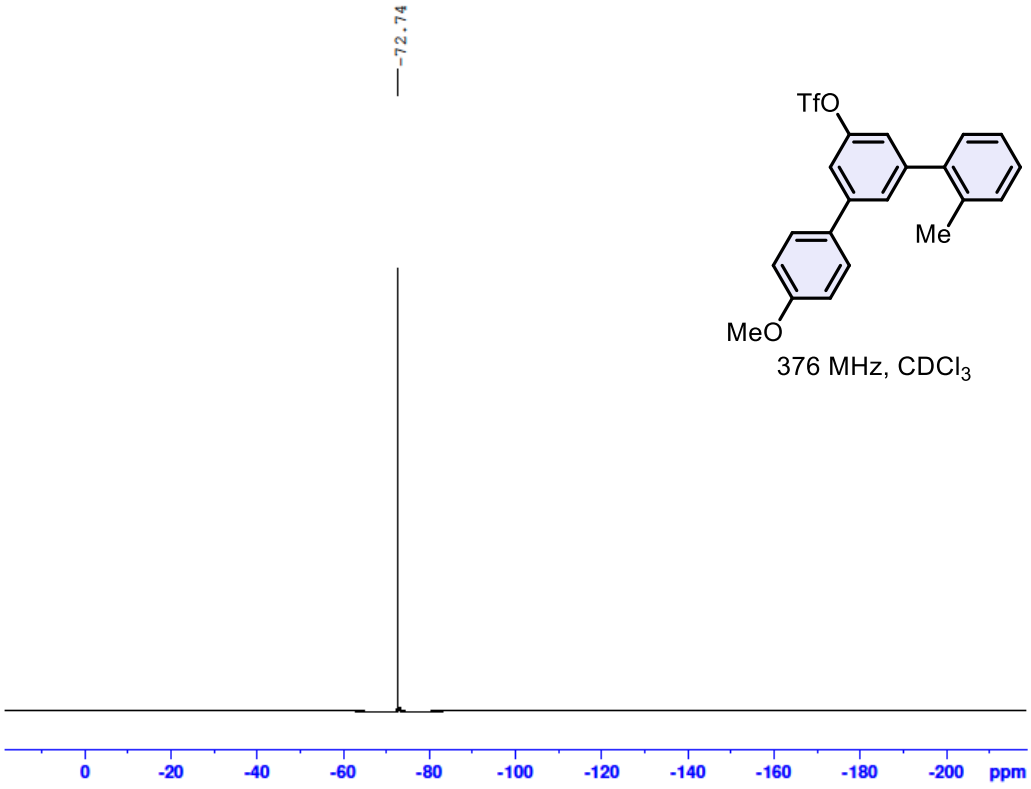

HRMS of 4''-methoxy-2-methyl-[1,1':3',1''-terphenyl]-5'-yl trifluoromethanesulfonate (Table 4.5, compound **20d**)

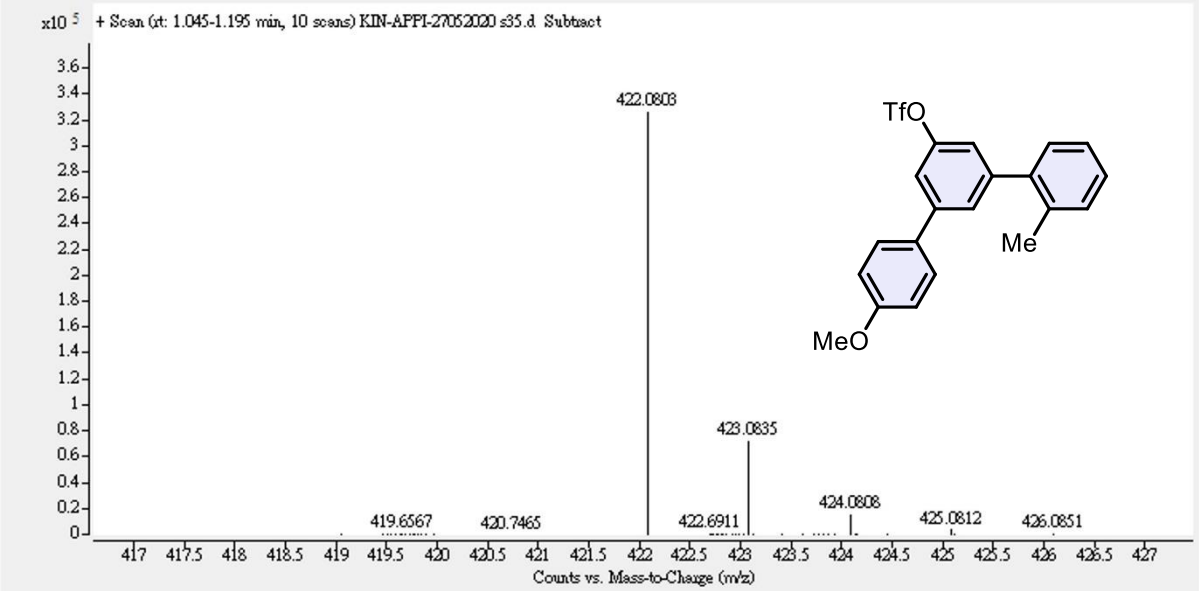

Mass	Calc. Mass	mDa	PPM	Formula
422.0803	422.0800	-0.34	-0.80	C21 H17 F3 O4 S

^{1}H NMR of 2-methoxy-2''-methyl-[1,1':3',1''-terphenyl]-5'-yl trifluoromethanesulfonate (Table 4.5, compound **20e**)

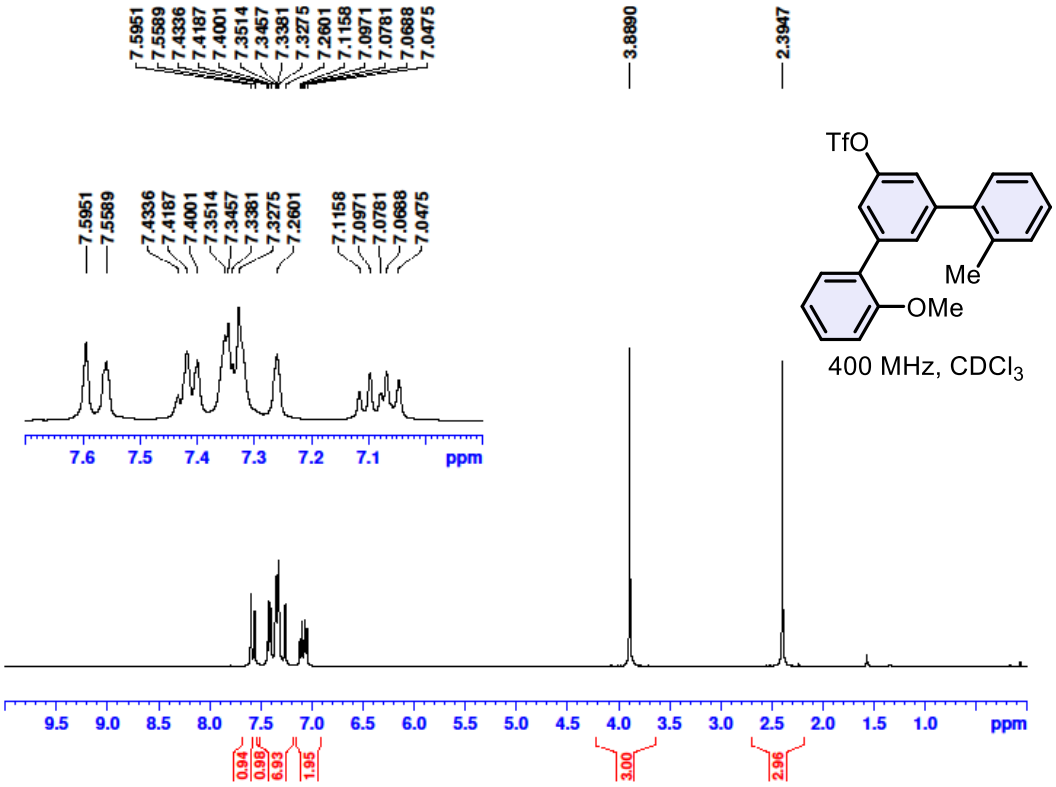

^{13}C NMR of 2-methoxy-2''-methyl-[1,1':3',1''-terphenyl]-5'-yl trifluoromethanesulfonate (Table 4.5, compound **20e**)

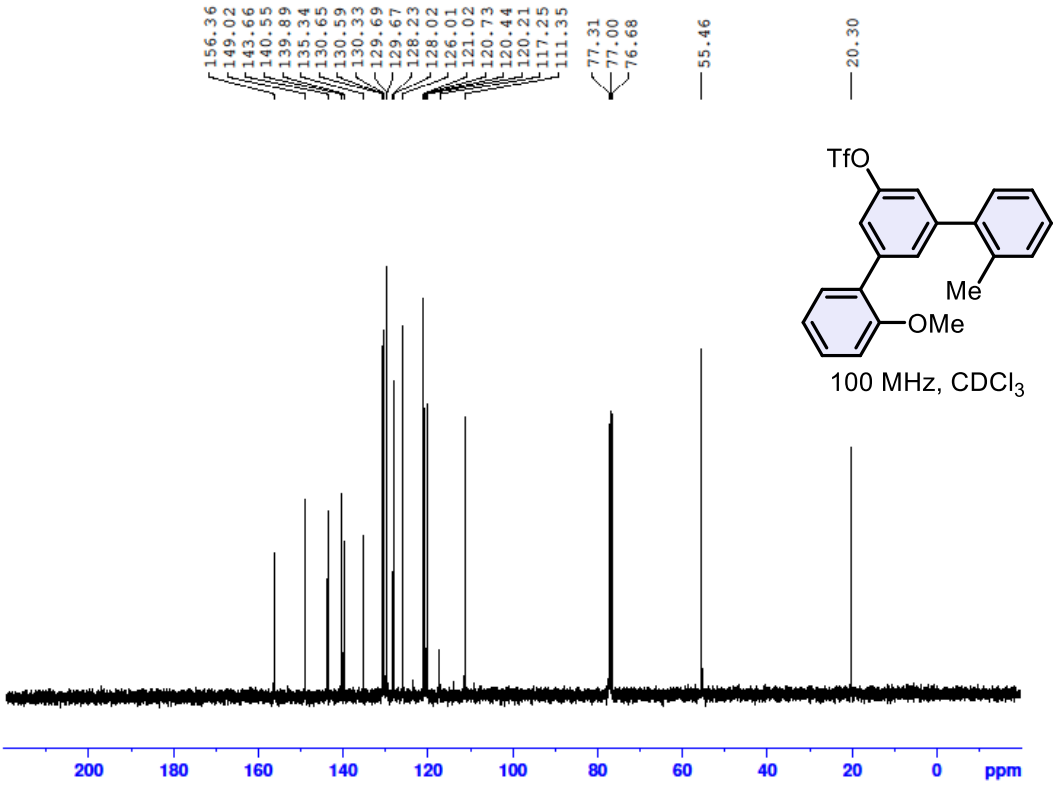

^{19}F NMR of 2-methoxy-2''-methyl-[1,1':3',1''-terphenyl]-5'-yl trifluoromethanesulfonate (Table 4.5, compound **20e**)

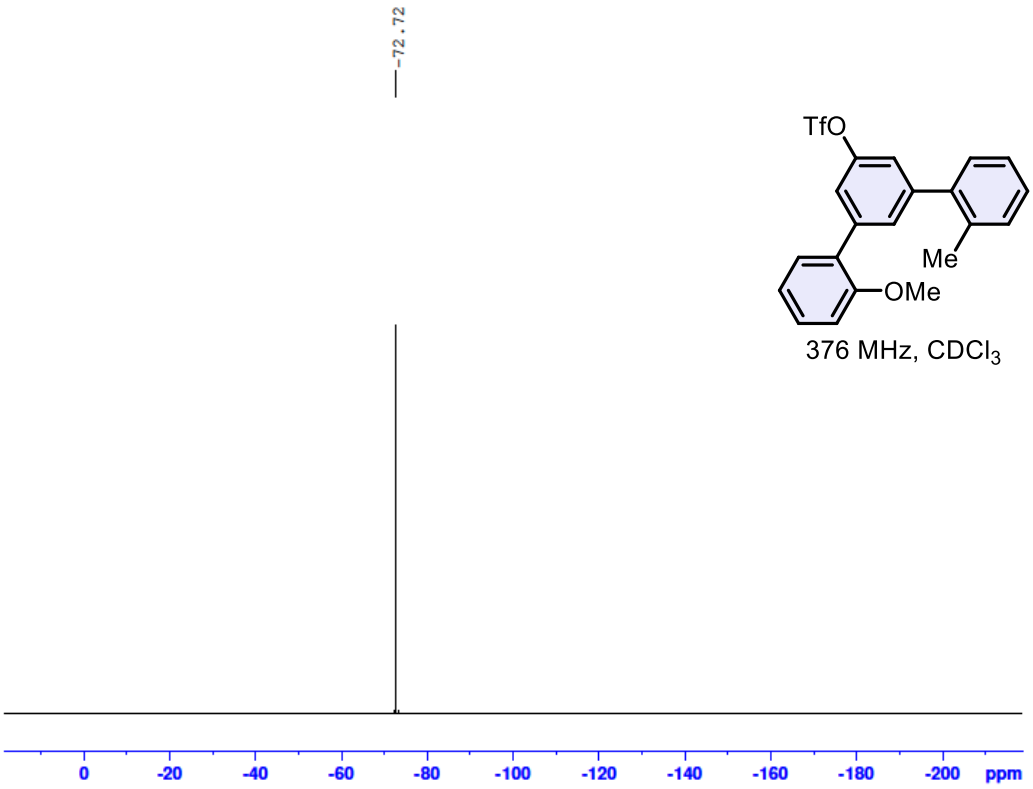

HRMS of 2-methoxy-2''-methyl-[1,1':3',1''-terphenyl]-5'-yl trifluoromethanesulfonate (Table 4.5, compound **20e**)

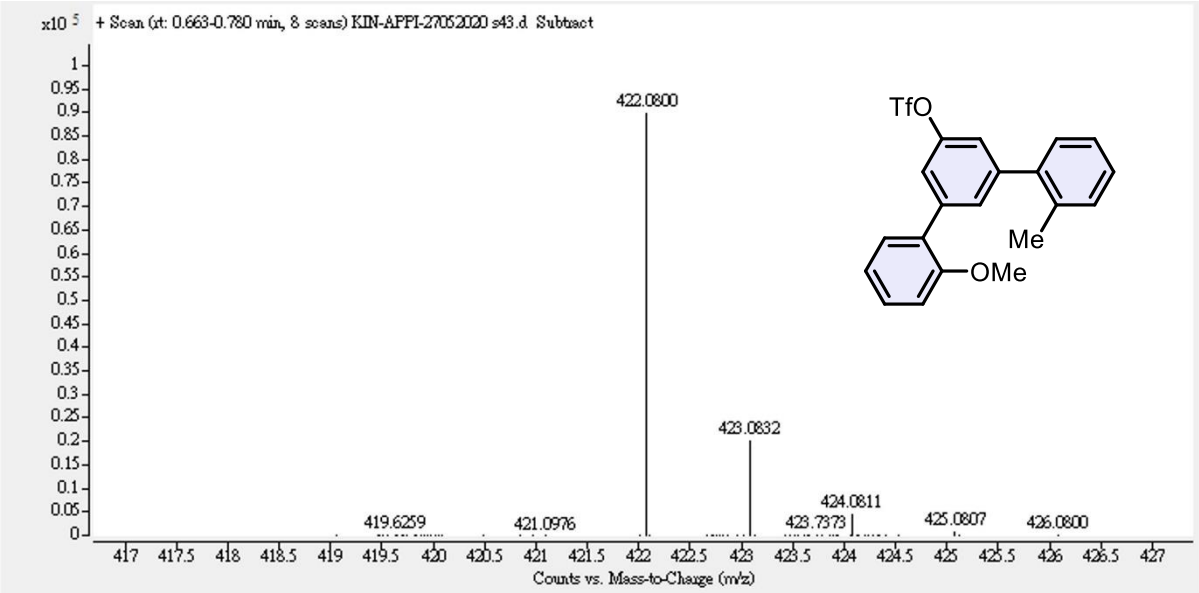

Mass	Calc. Mass	mDa	PPM	Formula
422.0800	422.0794	-0.58	-1.39	C21 H17 F3 O4 S

^{1}H NMR of 4-methoxy-2''-methyl-[1,1':4',1''-terphenyl]-2'-yl trifluoromethanesulfonate (Table 4.5, compound **20f**)

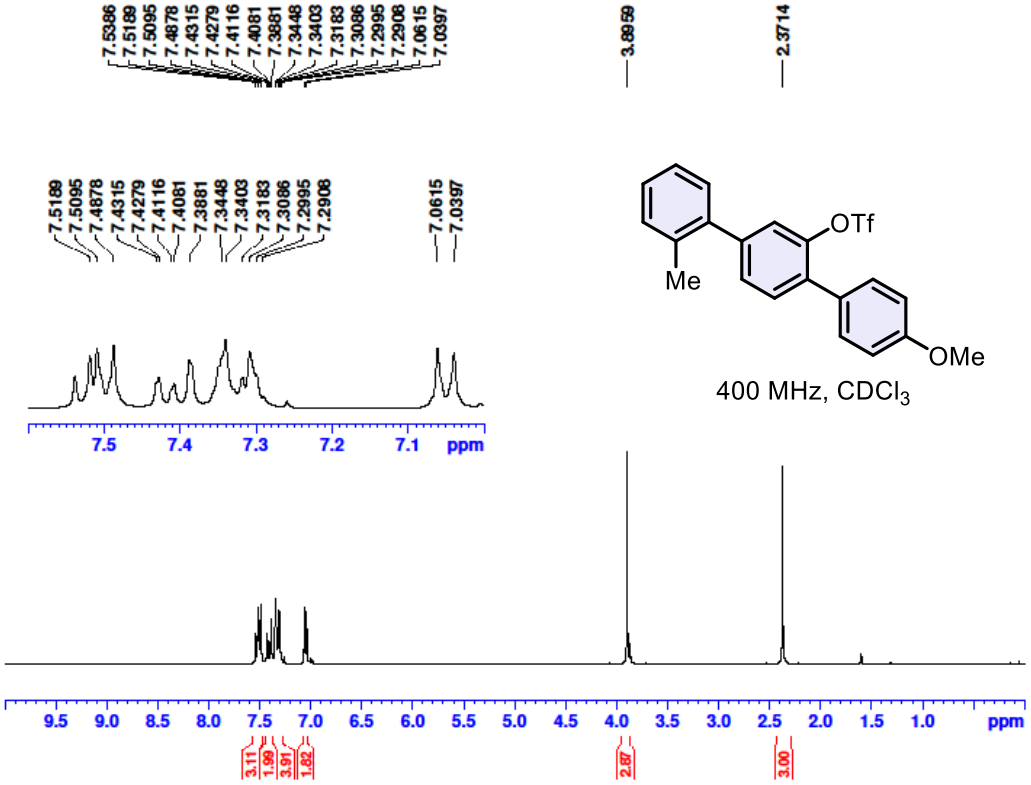

^{13}C NMR of 4-methoxy-2''-methyl-[1,1':4',1''-terphenyl]-2'-yl trifluoromethanesulfonate (Table 4.5, compound **20f**)

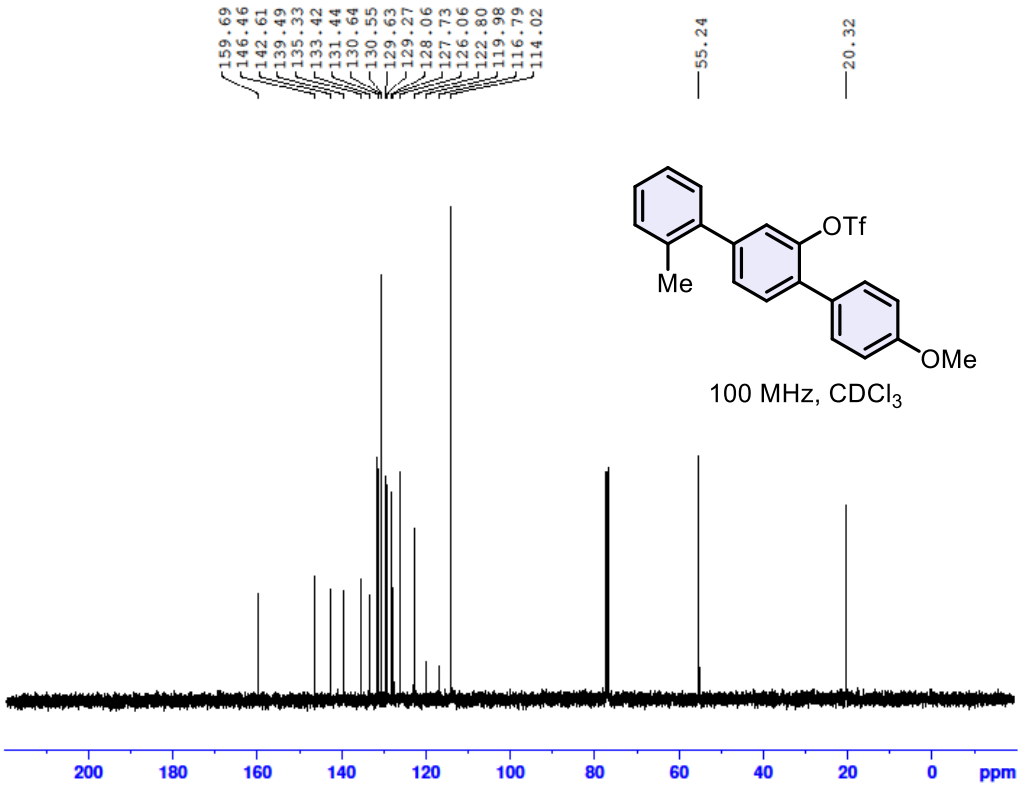

^{19}F NMR of 4-methoxy-2''-methyl-[1,1':4',1''-terphenyl]-2'-yl trifluoromethanesulfonate (Table 4.5, compound **20f**)

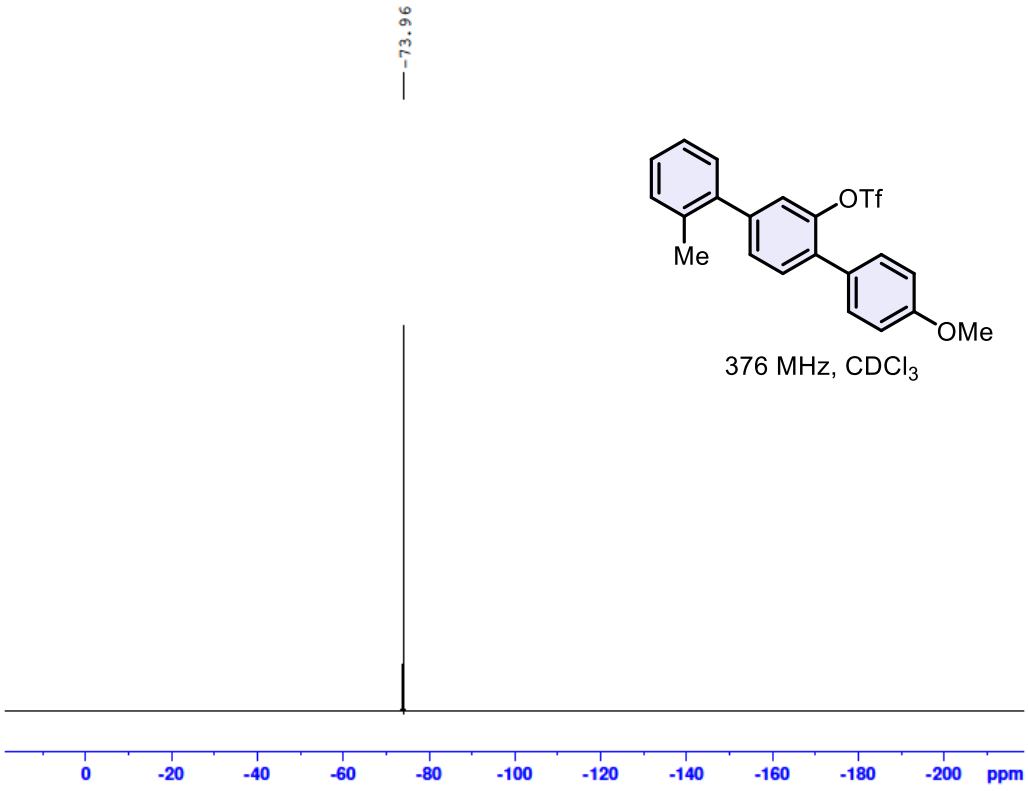

^{1}H NMR of 4-methoxy-4''-methyl-[1,1':3',1''-terphenyl]-4'-yl trifluoromethanesulfonate (Table 4.5, compound **20g**)

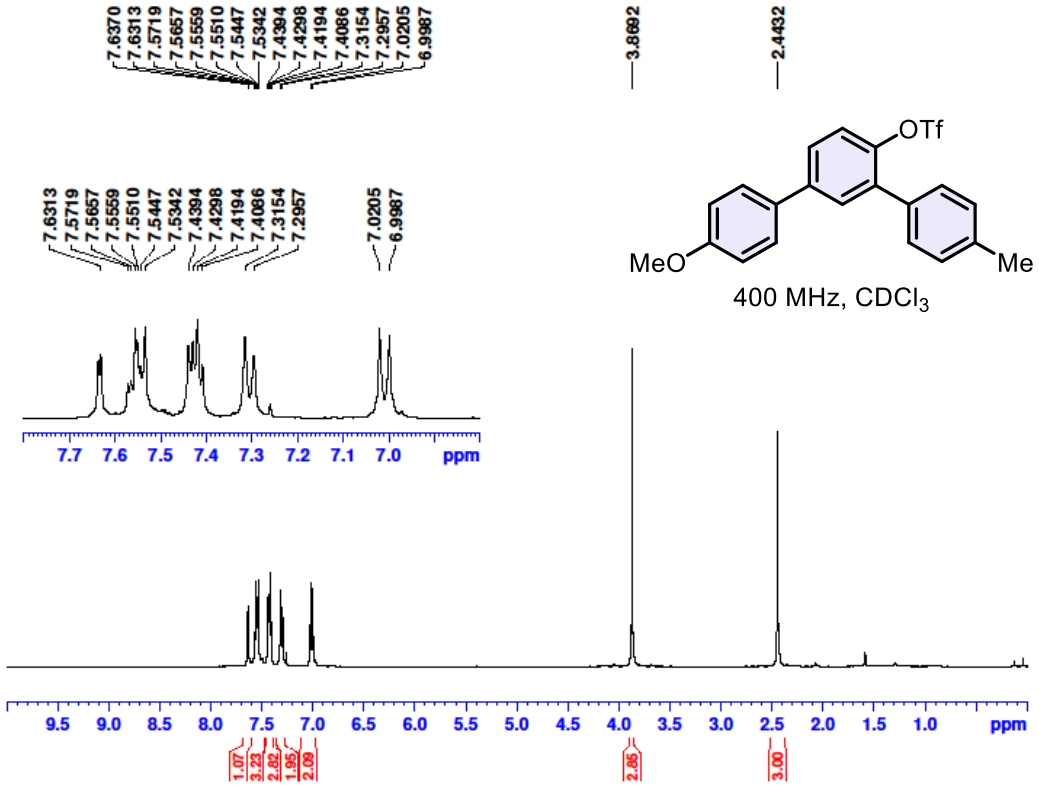

^{13}C NMR of 4-methoxy-4''-methyl-[1,1':3',1''-terphenyl]-4'-yl trifluoromethanesulfonate (Table 4.5, compound **20g**)

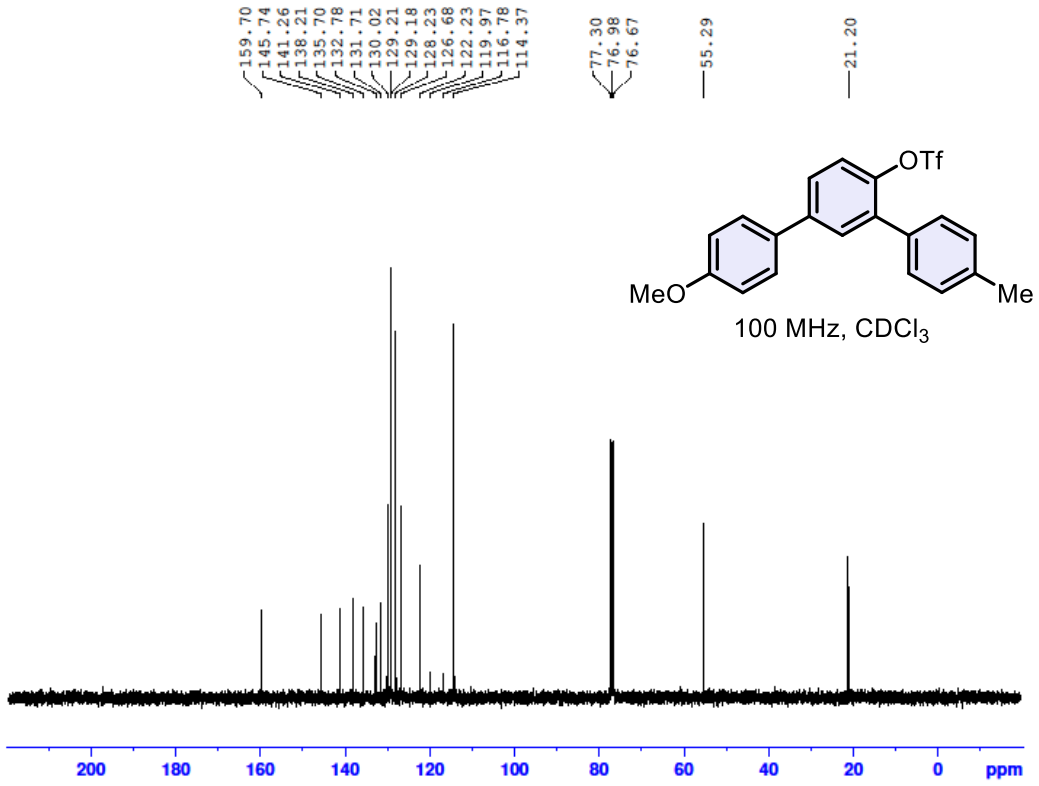

^{19}F NMR of 4-methoxy-4''-methyl-[1,1':3',1''-terphenyl]-4'-yl trifluoromethanesulfonate (Table 4.5, compound **20g**)

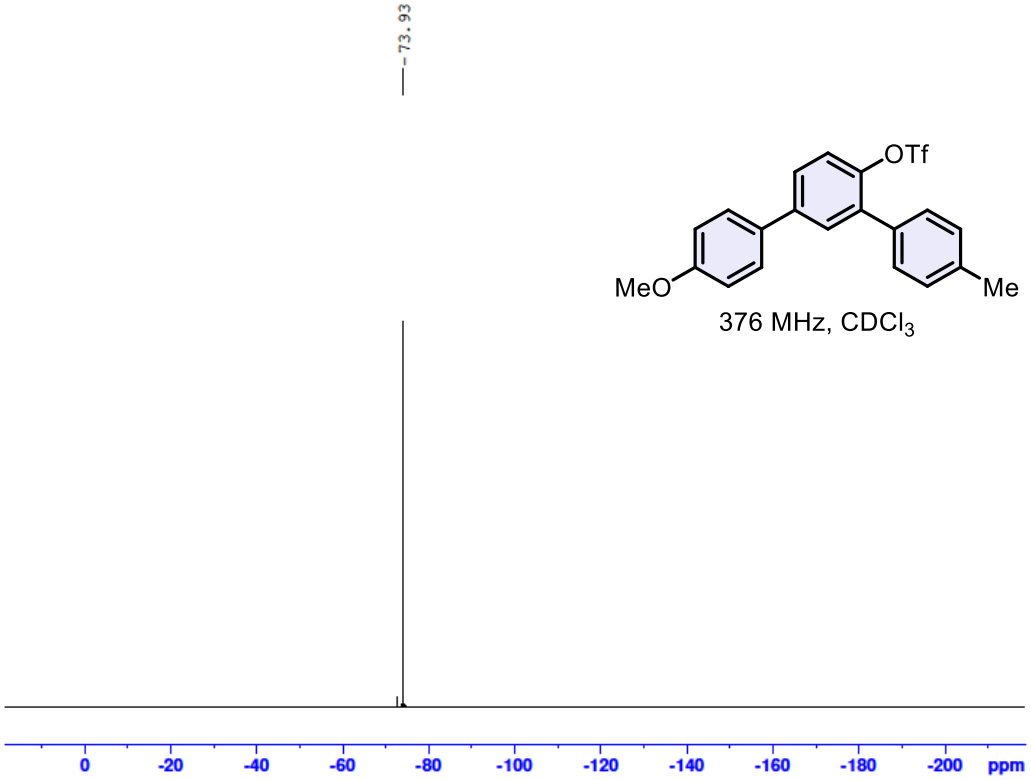

HRMS of 4-methoxy-4''-methyl-[1,1':3',1''-terphenyl]-4'-yl trifluoromethanesulfonate (Table 4.5, compound **20g**)

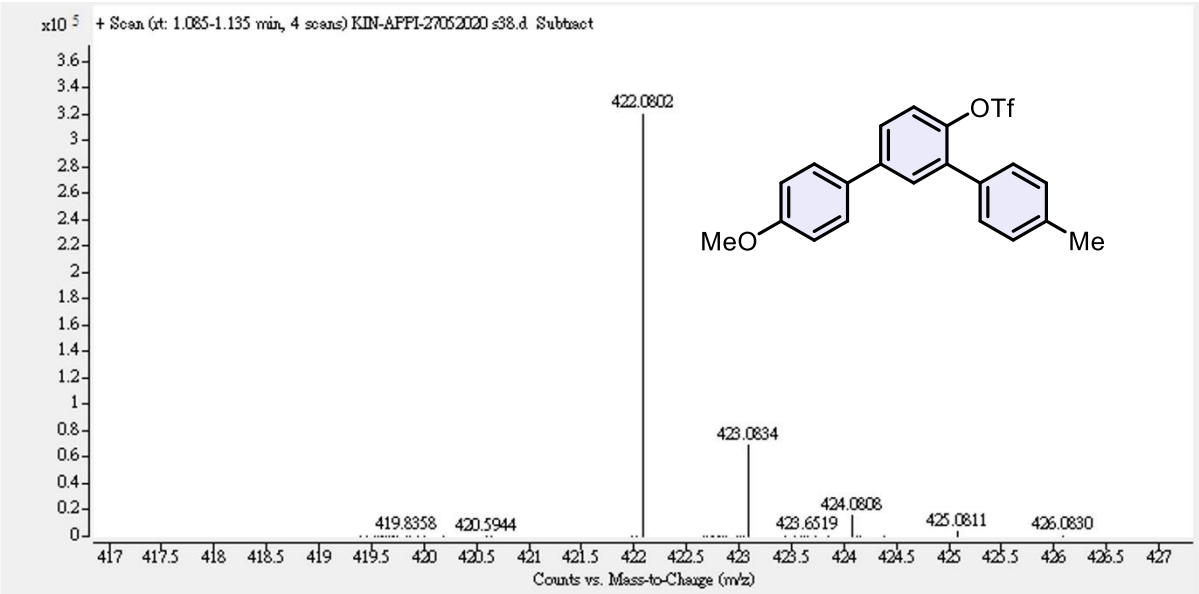

Mass	Calc. Mass	mDa	PPM	Formula
422.0803	422.0800	-0.34	-0.80	C21 H17 F3 O4 S

^{1}H NMR of 4''-methoxy-4-methyl-[1,1':2',1''-terphenyl]-3'-yl trifluoromethanesulfonate (Table 4.5, compound **20h**)

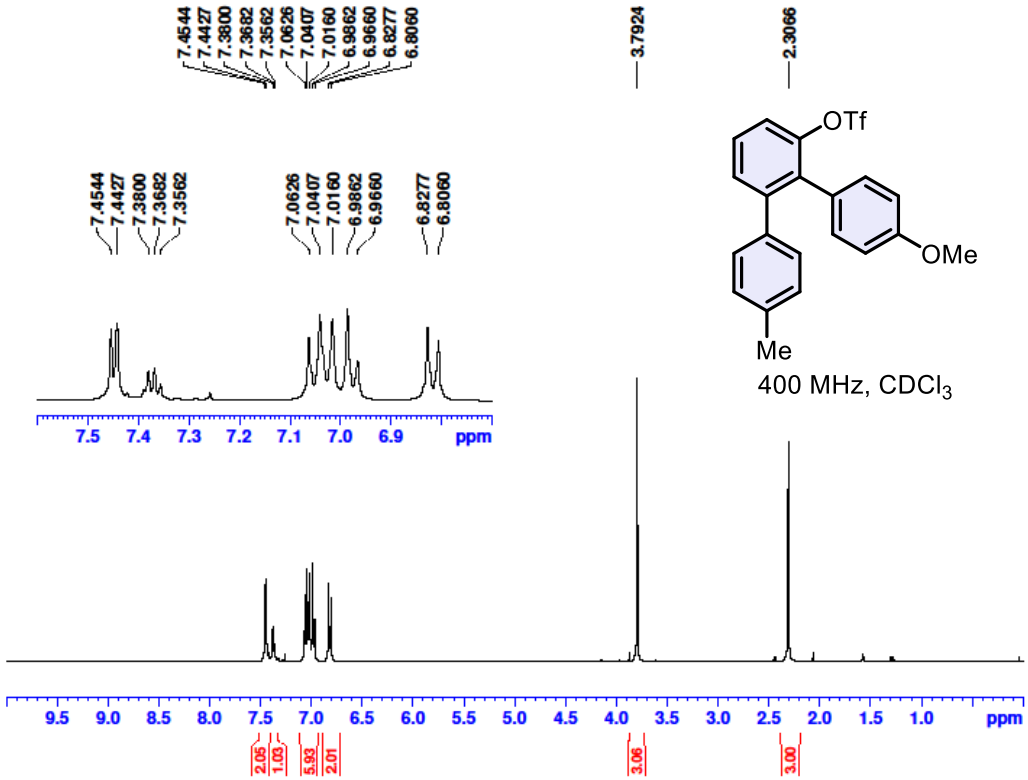

^{13}C NMR of 4''-methoxy-4-methyl-[1,1':2',1''-terphenyl]-3'-yl trifluoromethanesulfonate (Table 4.5, compound **20h**)

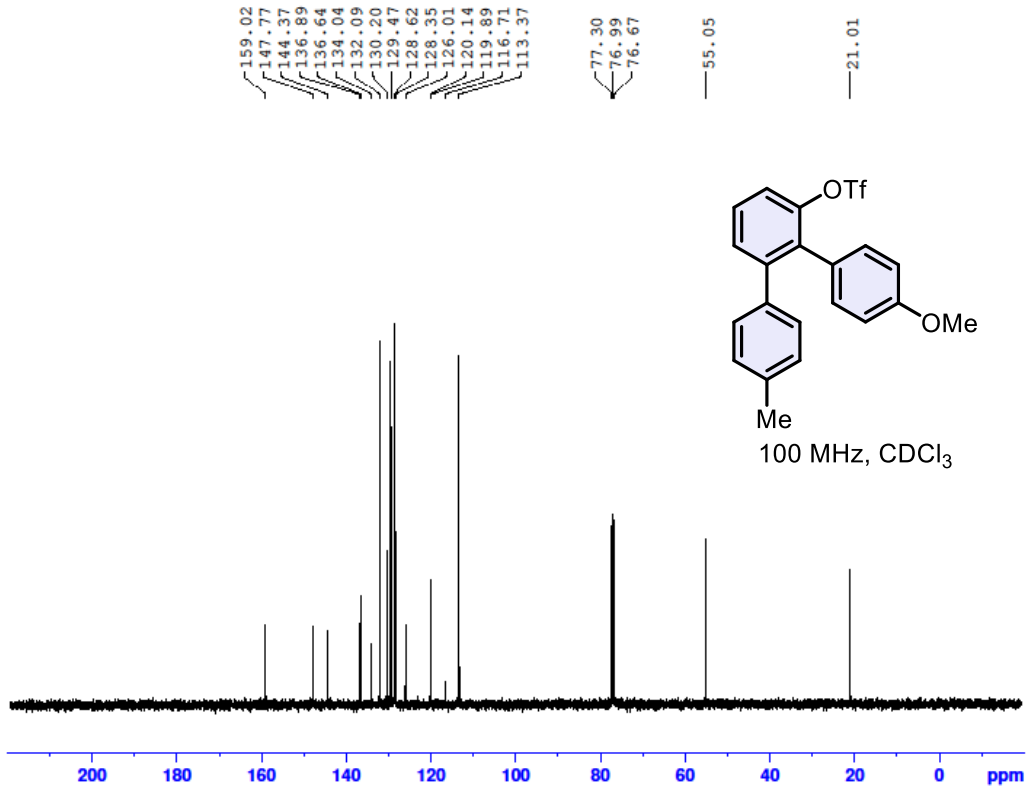

^{19}F NMR of 4''-methoxy-4-methyl-[1,1':2',1''-terphenyl]-3'-yl trifluoromethanesulfonate (Table 4.5, compound **20h**)

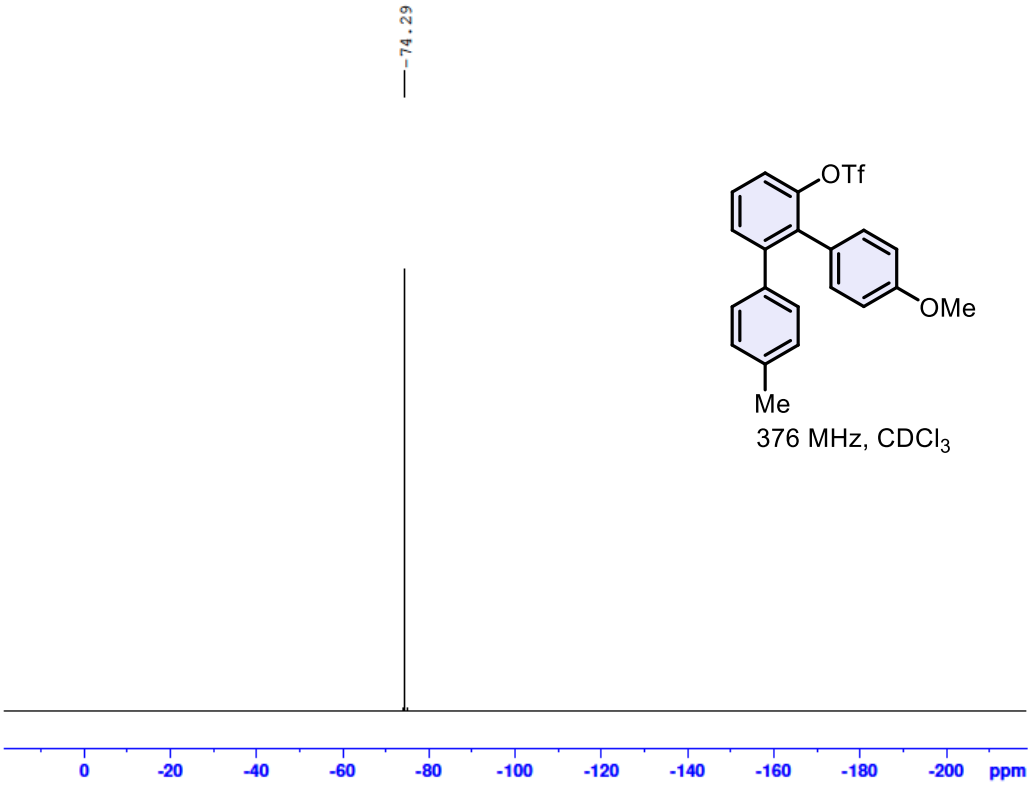

HRMS of 4''-methoxy-4-methyl-[1,1':2',1''-terphenyl]-3'-yl trifluoromethanesulfonate (Table 4.5, compound **20h**)

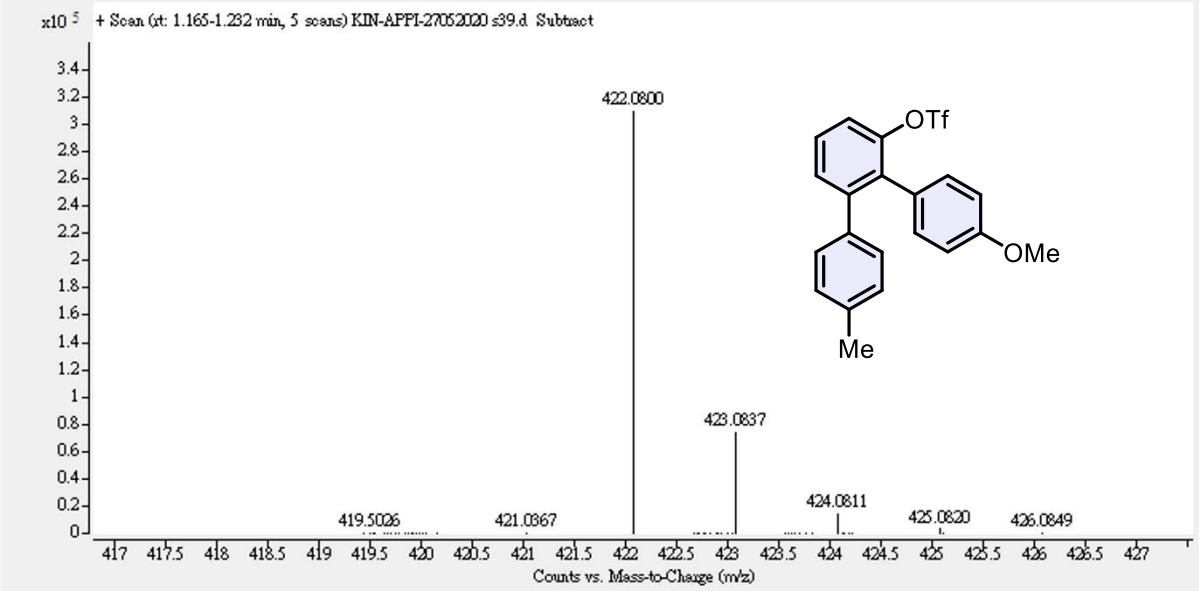

Mass	Calc. Mass	mDa	PPM	Formula
422.0800	422.0800	-0.04	-0.08	C21 H17 F3 O4 S

^{1}H NMR of 5-butyl-4'-methoxy-[1,1'-biphenyl]-2-yl trifluoromethanesulfonate (Table 4.5, compound **20i**)

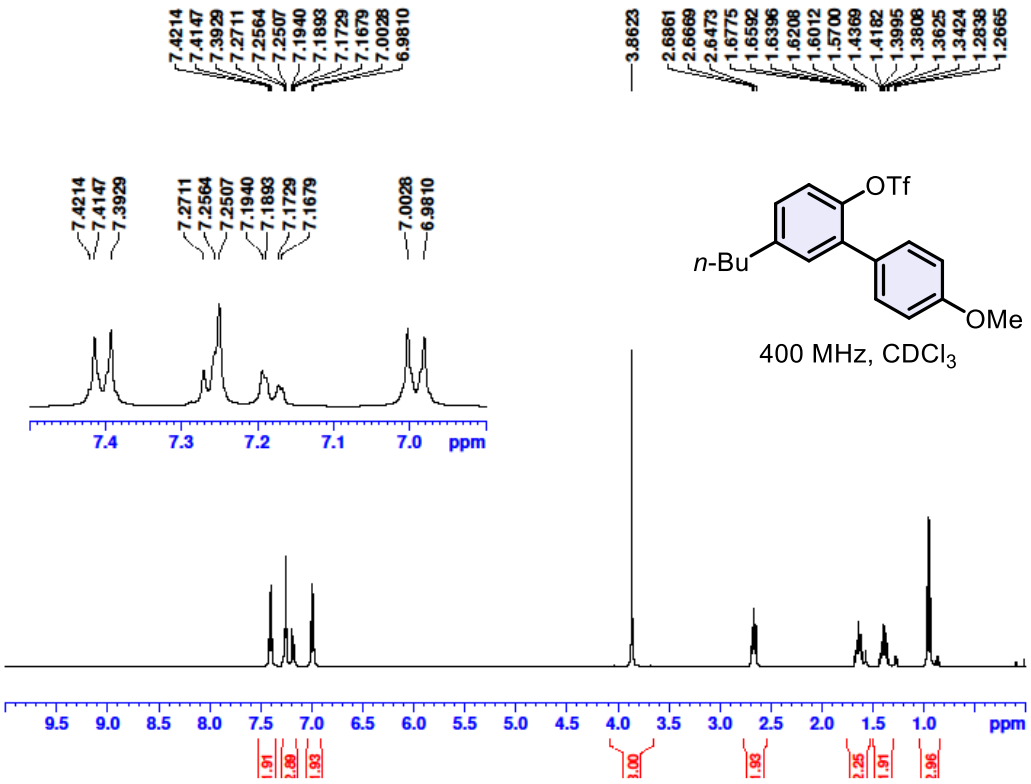

^{13}C NMR of 5-butyl-4'-methoxy-[1,1'-biphenyl]-2-yl trifluoromethanesulfonate (Table 4.5, compound **20i**)

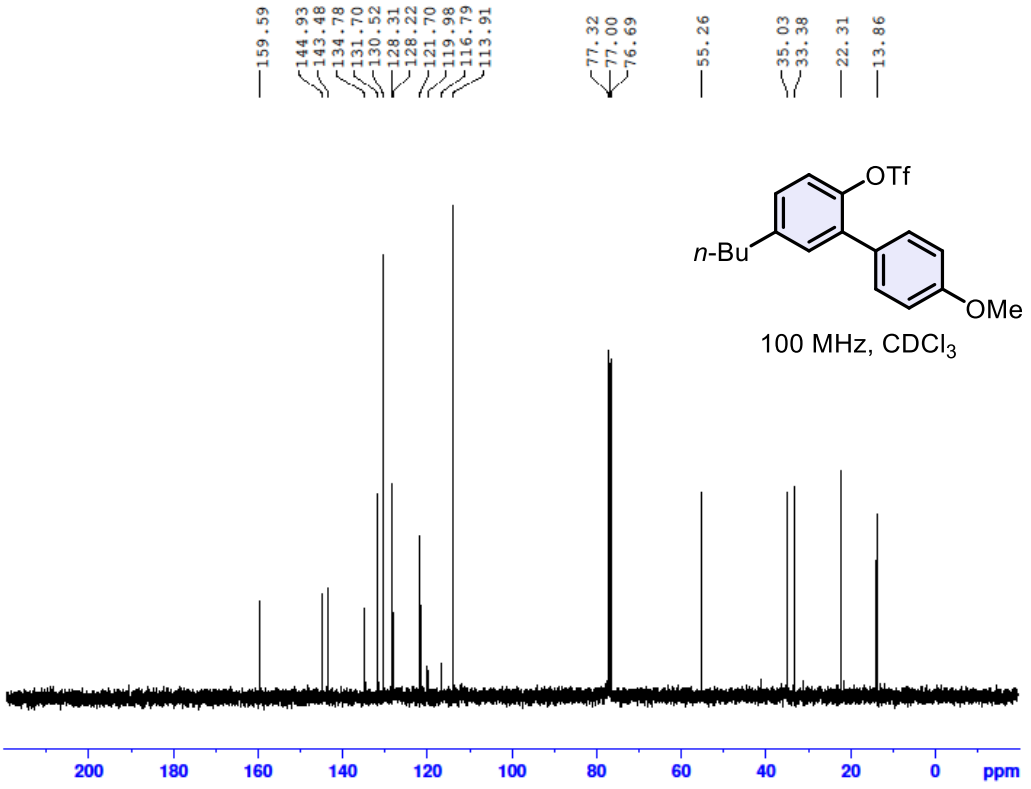

^{19}F NMR of 5-butyl-4'-methoxy-[1,1'-biphenyl]-2-yl trifluoromethanesulfonate (Table 4.5, compound **20i**)

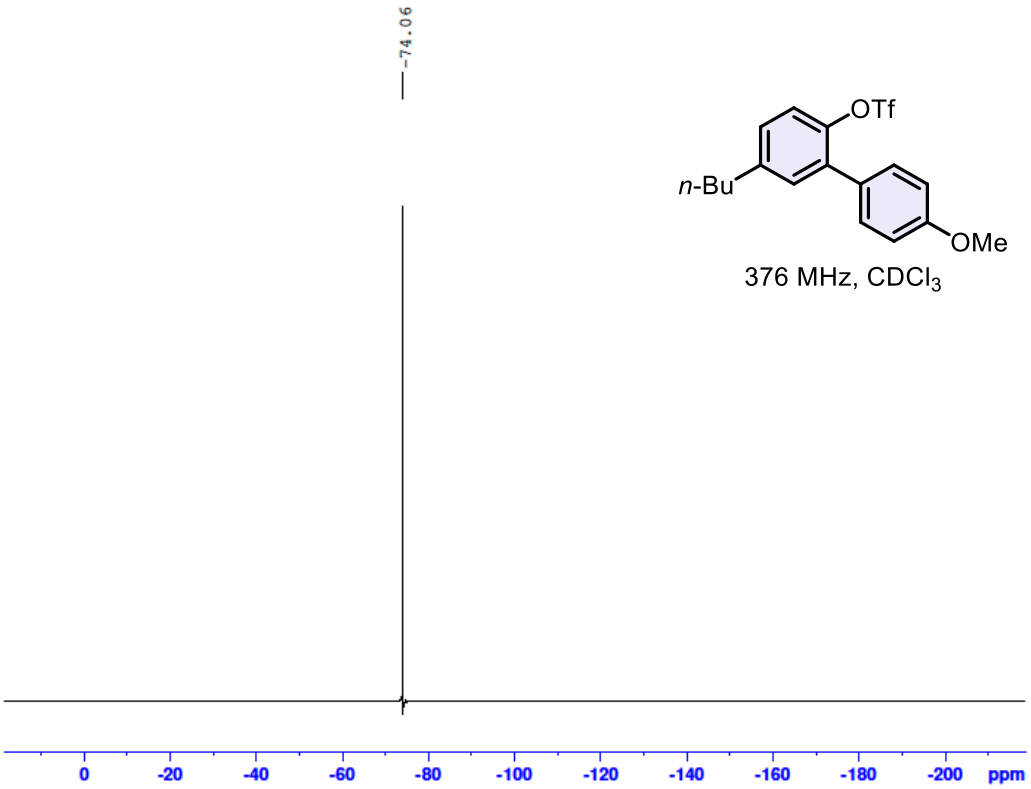

HRMS of 5-butyl-4'-methoxy-[1,1'-biphenyl]-2-yl trifluoromethanesulfonate (Table 4.5, compound **20i**)

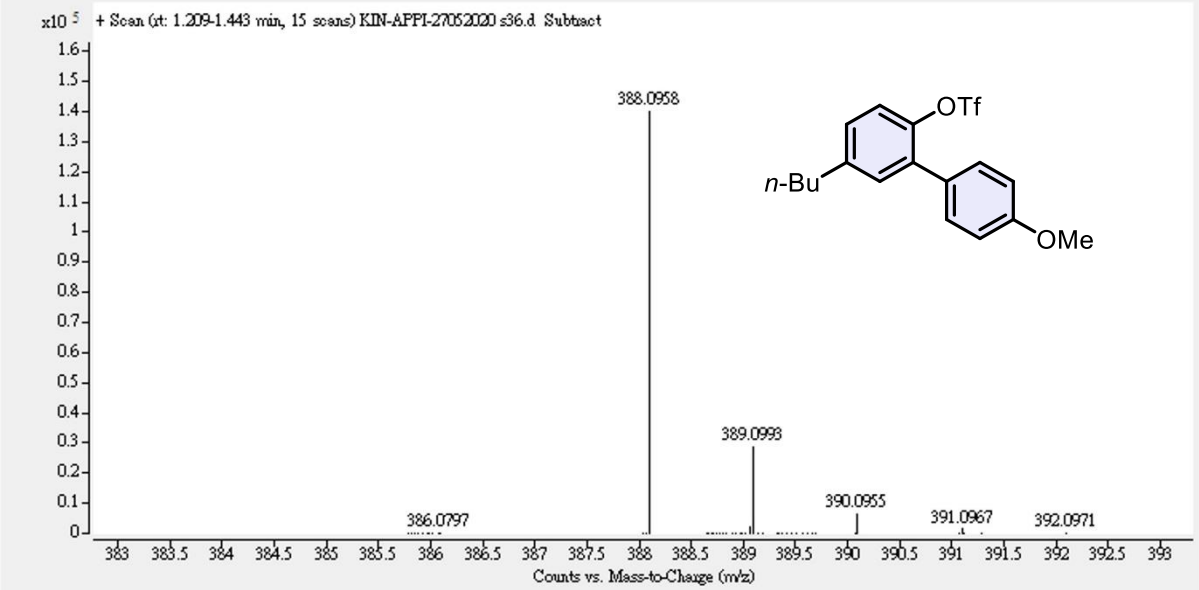

Mass	Calc. Mass	mDa	PPM	Formula
388.0958	388.0956	-0.19	-0.48	C18 H19 F3 O4 S